

# REGULATORY INFORMATION DISTRIBUTION SYSTEM (RIDS)

ACCESSION: N3R:81112502751 DOC. DATE: 81/11/06 NOTARIZED: NO DOCKET #  
 FACIL: 50-397 WPPSS Nuclear Project, Unit 2, Washington Public Powe 05000397  
 AUTH: NAME: AUTHOR AFFILIATION  
 SATIR, J. Burns & Roe Co.  
 RECIP: NAME: RECIPIENT AFFILIATION  
 AULUCK, R. Office of Nuclear Reactor Regulation, Director

SUBJECT: Forwards draft Sept 1981 Amend 18 to FSAR, Section 2.5, re: geology, seismology & geotechnical engineering, per request.

DISTRIBUTION CODE: B001S COPIES RECEIVED: LTR 0 ENCL 60 SIZE: 1.700  
 TITLE: PSAR/FSAR AMDTs and Related Correspondence

NOTES: 2 copies all matl: PM.

05000397

see RPT  
2 columns

ACTION:	RECIPIENT ID CODE/NAME		COPIES LTR ENCL		ACTION:	RECIPIENT ID CODE/NAME		COPIES LTR ENCL	
ACTION:	A/D. LICEVSN		1	0	ACTION:	LIC BR #2 BC		1	0
	LIC BR #2 LA		7	7		AULUCK, R.	01	1	1
INTERNAL:	ELOI		1	0	INTERNAL:	IEI	06	3	3
	IEV/DEP/EPDB	35	1	1		IEV/DEP/EPLB	36	3	3
	MPAI		1	0		NRR/DE/CEB	11	1	1
	NRR/DE/ESB	13	3	3		NRR/DE/GB	28	2	2
	NRR/DE/HGB	30	2	2		NRR/DE/MEB	18	1	1
	NRR/DE/MTEB	17	1	1		NRR/DE/QAB	21	1	1
	NRR/DE/SAB	24	1	1		NRR/DE/SEB	25	1	1
	NRR/DHFS/HFE	40	1	1		NRR/DHFS/LQB	32	1	1
	NRR/DHFS/DLB	34	1	1		NRR/DHFS/PTR	20	1	1
	NRR/DSI/AEB	26	1	1		NRR/DSI/ASB	27	1	1
	NRR/DSI/CPB	10	1	1		NRR/DSI/CSB	09	1	1
	NRR/DSI/ETSB	12	1	1		NRR/DSI/ICSB	16	1	1
	NRR/DSI/PSB	19	1	1		NRR/DSI/RAB	22	1	1
	NRR/DSI/RSEB	23	1	1		NRR/DST/LGB	33	1	1
	REG. FILE	04	1	1					
EXTERNAL:	ACRS	41	1	16	EXTERNAL:	BNL(CAMDTs ONLY)		1	1
	FEMA-REP DIV	39	1	1		LPDR	03	2	2
	NRCI PDR	02	1	1		VSIC	05	1	1
	NTIS		1	1					

DEC 03 1981

MD

TOTAL NUMBER OF COPIES REQUIRED: LTR

0  
70 ENCL 68  
68





R. Auluck  
NRR

50-397

8111250276 811106  
PDR ADDCK 05000397  
K PDR

Forwards 40 Cys of  
Enclosure as per your Request



J. Satir  
Burns & Roe

Boal  
50/60



8111250276 |

**Appendix 2.5J**  
**Analysis of the Instrumental**  
**Seismicity of the Columbia Plateau**

Prepared for  
Washington Public Power Supply System  
under the Direction of  
United Engineers and Constructors, Inc.  
Philadelphia, Pennsylvania

by

W. Foxall, W.U. Savage, M.R. Schnapp, and L.C. Seekins  
Woodward-Clyde Consultants  
Three Embarcadero Center, Suite 700  
San Francisco, CA 94111

## TABLE OF CONTENTS

	<u>Page</u>
LIST OF TABLES	2.5J-iii
LIST OF FIGURES	2.5J-iv
2.5J.0 SUMMARY	2.5J-1
2.5J.1 INTRODUCTION	2.5J-1
2.5J.2 EARTHQUAKE DETECTION LEVEL AND LOCATION ACCURACY	2.5J-6
2.5J.2.1 <u>Earthquake Monitoring and Data Analysis</u>	2.5J-6
2.5J.2.2 <u>Magnitude Detection and Location Thresholds</u>	2.5J-7
2.5J.2.3 <u>Location Accuracy</u>	2.5J-10
2.5J.3. CHARACTERISTICS OF COLUMBIA PLATEAU INSTRUMENTAL SEISMICITY	2.5J-12
2.5J.3.1 <u>Spatial Distribution of Seismicity</u>	2.5J-12
2.5J.3.2 <u>Columbia Plateau Seismic Zone Features</u>	2.5J-16
2.5J.3.2.1 <u>Shallow Crustal Zone (0 to 3 km)</u>	2.5J-16
2.5J.3.2.2 <u>Intermediate Crustal Zone (3 to 8 km)</u>	2.5J-17
2.5J.3.2.3 <u>Deeper Crustal Zone (8 to 25± km)</u>	2.5J-17
2.5J.4. SWARMS AND SHALLOW SEISMICITY	2.5J-18
2.5J.4.1 <u>Earthquake Swarms</u>	2.5J-18
2.5J.4.2 <u>Previous Studies of Columbia Plateau Earthquake Swarms</u>	2.5J-20
2.5J.4.3 <u>Definition of Earthquake Swarms in the Columbia Plateau</u>	2.5J-23
2.5J.4.4 <u>Characteristics of Columbia Plateau Swarms</u>	2.5J-25
2.5J.4.5 <u>Non-Swarm Shallow Seismicity</u>	2.5J-28
2.5J.5. SOURCES OF SHALLOW EARTHQUAKES	2.5J-28
2.5J.5.1 <u>Fractures in the Columbia River Basalts</u>	2.5J-29
2.5J.5.2 <u>Larger Earthquakes</u>	2.5J-33
2.5J.5.3 <u>Focal Mechanisms for the Shallow Crustal Zone</u>	2.5J-36
2.5J.5.4 <u>Spatial Patterns of Shallow Seismicity</u>	2.5J-37
2.5J.6. ASSOCIATION OF SHALLOW EARTHQUAKE ACTIVITY WITH IRRIGATED AREAS	2.5J-38
2.5J.6.1 <u>Hydrogeology of the Central Columbia Plateau</u>	2.5J-38
2.5J.6.2 <u>Mechanisms of Fluid-Induced Seismicity</u>	2.5J-40
2.5J.6.3 <u>Spatial Distributions of Earthquake Activity and Irrigation Within the Pasco Basin Area</u>	2.5J-42



## TABLE OF CONTENTS

	<u>Page</u>
2.5J.6.4 <u>Analysis of the Temporal Association of</u> <u>Ground-Water Level Changes and Earthquake</u> <u>Activity</u>	2.5J-44
2.5J.6.5 <u>Physical Parameters for Irrigation-Induced</u> <u>Seismicity</u>	2.5J-46
2.5J.7. EVALUATION OF MAXIMUM EARTHQUAKE MAGNITUDE	2.5J-47
2.5J.7.1 <u>Shallow Crustal Sources</u>	2.5J-48
2.5J.7.2 <u>Intermediate and Deep Crustal Sources</u>	2.5J-50
2.5J.8 REFERENCES	
TABLES	
FIGURES	

## LIST OF TABLES

<u>Table No.</u>	<u>Title</u>
2.5J-1	Magnitude Detection Thresholds for Eastern Washington
2.5J-2	University of Washington Swarm Areas
2.5J-3	Alterations to Swarm Boundaries
2.5J-4	New Swarm Areas Defined in this Study
2.5J-5	Swarms Defined in this Study
2.5J-6	Estimates of Annual Irrigation Water Uses in the Pasco Basin Area by County
2.5J-7	Comparison of Observed Earthquake Distribution with a Random Distribution
2.5J-8	Summary of Well Data





## LIST OF FIGURES

<u>Figure No.</u>	<u>Title</u>
2.5J-0	Location Map of Columbia Plateau
2.5J-1	Eastern Washington Seismograph Stations, 3/69 - 6/75
2.5J-2	Eastern Washington Seismograph Stations, 7/75 - 12/80
2.5J-3	Cumulative Number of Earthquakes Versus Magnitude for Area I: 7/75 - 12/80 $\leq$ 3 km
2.5J-4	Cumulative Number of Earthquakes Versus Magnitude for Area II: 7/75 - 12/80, All Depths
2.5J-5	Cumulative Number of Earthquakes Versus Magnitude for Area I: 7/75 - 12/80, Depth $>$ 3 km
2.5J-6	Cumulative Number of Earthquakes Versus Magnitude for Area I: 6/71 - 6/75, Depth $\leq$ 3km
2.5J-7	Detection and Location Limits for Magnitude $M_C$ 1.5 and 2.0 Earthquakes during 1975 and 1976
2.5J-8	Epicenters of Earthquakes with $M_C \geq 1.0$ , 3/69 - 12/80
2.5J-9	Epicenters of Earthquakes with $M_C \geq 2.0$ , 3/69 - 6/75
2.5J-10	Epicenters of Earthquakes with $M_C \geq 2.0$ , 7/75 - 12/80
2.5J-11	East-West Cross-Section: Better-Located Earthquakes
2.5J-12	North-South Cross-Section: Better-Located Earthquakes
2.5J-13	East-West Cross-Section: All Earthquakes
2.5J-14	North-South Cross-Section: All Earthquakes
2.5J-15	Number of Events and Maximum Magnitude Versus Depth
2.5J-16	Cumulative Number of Earthquakes Versus Magnitude: All Depths

- 2.5J-17 Cumulative Number of Earthquakes Versus Magnitude, Depth  $> 3$  km
- 2.5J-18 Cumulative Number of Earthquakes Versus Magnitude,  $Z \leq 3$  km
- 2.5J-19 Epicenters of Earthquakes with  $M_C \geq 1.0$ , Depth  $\leq 3$  km
- 2.5J-20 Epicenters of Earthquakes with  $M_C \geq 1.0$ ,  $3 \text{ km} < \text{Depth} \leq 8 \text{ km}$
- 2.5J-21 Epicenters of Earthquakes with  $M_C > 10$ , Depth  $> 8$  km
- 2.5J-22 Magnitude Versus Occurrence Date, Wooded Island Earthquakes, 3/69 - 12/80
- 2.5J-23 Swarm Area Boundaries
- 2.5J-24 Epicenters of Swarm Earthquakes: All Depths, 3/69 - 12/80
- 2.5J-25 Epicenters of Non-Swarm Earthquakes: All Depths, 3/69 - 12/80
- 2.5J-26 Epicenters of Earthquakes in Selected Swarms
- 2.5J-27 Distribution of Maximum Observed Swarm Earthquake Magnitudes
- 2.5J-28 Magnitude Time History for Selected Swarms
- 2.5J-29 Cumulative Number of Swarm Earthquakes Versus Magnitude
- 2.5J-30 Fault Plane Solution for the 20 December 1973,  $M_L$  4.4 Royal Slope Earthquake
- 2.5J-31 Location of the November 1, 1918 Earthquake
- 2.5J-32 Fault Plane Solution for the 15 February 1973, Scooteney D Swarm Earthquake
- 2.5J-33 Fault Plane Solutions for Selected Wahlake D Swarm Earthquakes

## LIST OF FIGURES (continued)

- 2.5J-34      Fault Plane Solution for the 4 September 1974,  
              Royal E Swarm Earthquake
- 2.5J-35      Fault Plane Solution for the 22 September 1972  
              Smyrna C Swarm Earthquake
- 2.5J-36      Areas of Irrigation and Epicenter of Shallow  
              Earthquakes (Depth  $\times$  3 km)
- 2.5J-37      Selected Water Well Locations and Epicenters of  
              Earthquakes (Depth  $\leq$  5 km)
- 2.5J-38      Hydrograph Record Well No. 49
- 2.5J-39      Hydrograph Record Well No. 56
- 2.5J-40      Hydrograph Record Well No. 75
- 2.5J-41      Water Well Areas and Water Table Rise 1944-1978
- 2.5J-42      Amount of Irrigation Water Used Versus Time in the  
              Columbia Basin Irrigation Project
- 2.5J-43      Number of Earthquakes per Month, Depth  $\leq$  5 km,  
              3/69 - 12/80
- 2.5J-44      Principal Stresses and Coulomb-Navier Failure  
              Criterion



## APPENDIX 2.5J

ANALYSIS OF THE INSTRUMENTAL  
SEISMICITY OF THE COLUMBIA PLATEAU

## 2.5J.0 SUMMARY

In this appendix, earthquake characteristics within the Columbia Plateau, Washington, are analyzed using instrumentally recorded earthquake data. The infrequent occurrence of earthquakes in this area has been recorded by a network of seismograph stations that have provided a 11.3-year data set of high quality.

Earthquake activity is more concentrated within the central Columbia Plateau (which is defined by latitudes  $46^{\circ}$  to  $47^{\circ}$ N and longitudes  $118.75^{\circ}$  to  $120^{\circ}$ W and which contains the Hanford Reservation and the WNP-2 and -1/4 sites) than in surrounding areas. Magnitude detection and location thresholds have been sufficiently low (coda length magnitude  $M_C$  2.0 or less) to conclude that the apparent concentration is not an artifact of the seismograph station distribution. The earthquake activity within the central Plateau is distinctly zoned by focal depth as follows:

Shallow crustal zone (0- to 3-km depth): This zone is the most active, containing 68 percent of the total recorded activity (excluding events whose focal depth are fixed at 3.00 km). The shallow zone is dominated by the occurrence of earthquake swarms. This shallow seismicity appears to be related geologically and spatially to the Columbia River basalt flows and older volcanics. The basalts appear to be a tectonic-stress, low strain-rate environment.

Intermediate crustal zone (3 to 8 km depth): Earthquake activity in this zone is distinct from the shallow zone in that swarm activity essentially ceases below 3 km. There is also a notable decrease in the frequency of occurrence of earthquakes below 8 km, which is the approximate depth (constrained geophysically) to the top of basement. The intermediate-depth zone is considered to consist mostly of sediments.

Deep crustal zone (8 to 25 + km): The scattered earthquakes in this zone (10 percent of the total activity) describe a bowl-like shape within the basement, with the deepest region (15 to 25 km) occurring under the central Columbia Plateau. Focal mechanisms suggest that the deep zone, as well as the shallower zones, is undergoing regional north-south compression.



AMENDMENT NO. 18  
September 1981

The earthquake swarms that dominate the shallow zone in the Columbia Plateau exhibit a variety of characteristics:

- o Long durations (a few days to a few months) and long cluster time-lengths (approximately 10 days) compared to swarms that occur in other geologic environments.
- o Spatially restricted to focal regions that are a few kilometers in extent and above a depth of about 3 km.
- o Spatial patterns suggestive of earthquake occurrence on several or many fault planes.
- o Focal mechanisms that generally exhibit a variety of fault plane orientations within an individual swarm.
- o Shallow seismicity in general and swarms in particular having a high frequency-magnitude slope (1.00 or greater), compared to deeper Columbia Plateau earthquakes.
- o Frequency of occurrence of shallow earthquakes that is statistically correlated with and appears directly related to the occurrence of irrigation and/or groundwater-level increases.

Tectonic fractures (deformation-related shear surfaces within the basalt flows) are identified as a reasonable physical source for small-magnitude shallow earthquakes. Cooling joints are less likely to be seismic slip surfaces than tectonic fractures. Observations of the dimensions of these fractures and joints suggest a maximum magnitude value of  $M_L$  3.0 for earthquakes that would rupture the maximum available fracture surface.

Subsequent to the installation of the Spokane seismograph in 1909, the largest earthquakes observed during the past 70 within the central Columbia Plateau years are the 1918 Corfu ( $M_S$  4.4) and the 1973 Royal Slope ( $M_C$  4.4). Both of these events occurred at a shallow depth north of the Saddle Mountains in a broadly constrained seismic zone that trends parallel to the Saddle Mountains. However, no correlations between earthquake activity and specific mapped faults or postulated faults associated with mapped folds are observed within this zone of seismic activity or elsewhere in the central Columbia Plateau. The earthquake activity that occurs between the Gable Mountain structural trend and the Rattlesnake-Wallula alignment exhibits a lower rate of occurrence and appears to have a lower maximum magnitude.

Based on the observations and analyses of this appendix, the maximum magnitude expected to occur within the Columbia River

AMENDMENT NO. 18  
September 1981

basalts in close proximity to the site is  $M_C$  3.0. Due to limitations and uncertainties in these observations and analyses, a reasonable conservative maximum magnitude value is  $M_C$  4.0. Potential earthquakes of  $M_S$  5.0 and larger can be reasonably associated with the significant deformation of identified surface geologic structures, the nearest of which to the site is the Umtanum Ridge-Gable Mountain structural trend.





APPENDIX 2.5J  
ANALYSIS OF THE INSTRUMENTAL  
SEISMICITY OF THE COLUMBIA PLATEAU

## 2.5J.1. INTRODUCTION

In this appendix, instrumentally recorded earthquake data are used to analyze the spatial, temporal, and source characteristics of seismic activity in the Columbia Plateau of eastern Washington (Figure 2.5J-0). Two primary factors influence the detailed study of seismicity in the Columbia Plateau; these are: (1) the low level of that seismicity, and (2) the time period of operation of seismographs in the region. The Columbia Plateau is characterized by infrequent moderate-magnitude earthquakes, as compared to more active areas in western Washington or California (see discussion of regional historical seismicity in Washington Public Power Supply System, 1981, Section 2.5.2.1). For example, during the past 70 years, only one earthquake of magnitude ( $M_S$  or  $M_L$ ) greater than 5 has occurred in the Plateau, while at least 10 events of magnitude 5 or larger have occurred in a similar-sized area of Puget Sound (see Section 2.5.2.1 and Table 2.5-5 of Washington Public Power Supply System, 1981). The occurrence of smaller-magnitude events is also lower in the Plateau than in western Washington, and the events have been less frequently recorded on seismographs.

In regards to the period of operation of seismographs the first seismograph installed in eastern Washington was at Spokane in 1909 (Poppe, 1979). This seismograph was a Wiechert low-gain, long-period instrument, and it recorded several of the felt earthquakes in the Columbia Plateau, such as the 1 November 1918 ( $M_S$  4.4) Corfu and the 16 July 1936 ( $M_S$  5-3/4) Milton-Freewater earthquakes; however, data from other stations for these events were limited (Woodward-Clyde Consultants, 1980b; Section 2.5J.5.2 of this appendix). Additional seismographs were installed by Geotech in central Washington in 1962 through 1964 (Poppe, 1979) in association with the VELA-uniform project (Racine, 1979), and these detected some small ( $M_S$  2 to 3.2) earthquakes in the Columbia Plateau. Additional stations include a high-gain station at Newport, Washington, beginning operation in 1966, and the Blue Mountain Observatory array in northern Oregon, operating from 1962 through 1975. In spite of these additional stations, however, detailed seismicity data in the Columbia Plateau, and particularly in the vicinity of the Hanford Reservation, have been available only since the inception of microearthquake network operations in March 1969. This appendix is the product of studies that used the seismicity data from this

network, and it also includes other seismologic, geologic, and geophysical data.

#### Data

The use of an instrumental data set to study characteristics of earthquake occurrence depends greatly on the quality of the data. The data used in this study are a compilation of data that were used to produce the eastern Washington seismicity catalogs spanning the 11.3-year period from March 1969 through December 1979 and June through December 1980. These catalogs have been published by the University of Washington (UW) in their Annual Technical Reports on Earthquake Monitoring of the Hanford Region, Eastern Washington (Malone, 1975, 1977, 1978, 1979, 1980). Earthquake locations for the period 1969 through December 1974, when the U.S. Geological Survey operated the eastern Washington network, were recomputed by the UW in 1979 (Appendix A of Malone, 1979). These recomputations used the same crustal velocity models, hypocenter location program, and earthquake magnitude formula as have been used for subsequent periods. The hypocentral solutions and magnitude determinations presently available for the period June through December 1980 are preliminary; however, Dr. S.D. Malone (1981, personal communication) believes that these data are consistent with previous data. With the exception of magnitude determinations for the period March 1969 through June 1971, which are discussed in Section 2.5J.2.1 below, the entire catalog represents a homogeneously processed data base for the plateau.

In addition to compiling the data base, the UW Technical Reports (Malone, 1977-1980) have also reported the results of topical studies of crustal structure, seismic attenuation, and seismicity in the region. Additional studies of Columbia Plateau seismicity that use the 11.3-year data base have focused on the deeper (focal depths greater than 9 km) earthquakes (Woodward-Clyde Consultants, 1980a); on three shallow earthquake swarms (Malone et al., 1975); and on the Wooded Island earthquake swarms (Pitt, 1971; Rothe, 1979).

During the past decade, additional geologic and geophysical data have contributed to the further understanding of the regional tectonic environment and on possible earthquake source structures. Extensive hydrogeologic data on changes in the local and regional ground-water regime that resulted from ground-water pumping and from irrigation projects in the Columbia Basin and Yakima Basin have also been collected. These geologic, geophysical, and hydrogeologic data are used in the present study to aid in the interpretation of the seismologic data.

## 2.5J.2. EARTHQUAKE DETECTION LEVEL AND LOCATION ACCURACY

2.5J.2.1 Earthquake Monitoring and Data Analysis

The locations of high-gain seismograph stations in the vicinity of the Hanford Reservation are shown in Figure 2.5J-1 for the USGS operation period (1969-1975) and in Figure 2.5J-2 for the UW operation period (1975 to the present). Details of the development of the eastern Washington network are given in Malone (1979, Appendix A). In this reference, the routine network operation and data analysis carried out by the USGS are also discussed. The UW network operations and data analysis are discussed in Malone (1977-1980).

At the end of 1980, 43 seismograph stations were in operation in eastern Washington (Figure 2.5J-2), including the three stations (ALD, RPK, FMC) of the Portland General Electric Pebble Springs array and the station at Newport (NEW) operated by the USGS. The density of station coverage has varied throughout the period. In the vicinity of the Hanford Reservation, the average spacing between stations has varied from approximately 40 km in 1969, 20 km from 1972 through 1975 (Figure 2.5J-1), to the present 25 km (Figure 2.5J-2). For the remainder of the region, station spacing north to Ephrata and Odessa and west to Vantage was about 30 km during the period 1972 through 1975 (Figure 2.5J-1). After 1975, coverage was expanded to include the region shown by Figure 2.5J-2 and has an average spacing outside of the Hanford Reservation vicinity of approximately 25 km in the Chelan area and 50 to 70 km elsewhere.

For the period 1969 through 1979, earthquake data were recorded on Develocorder film; the achievable precision of the arrival-times read from these records is 0.05 second. Since the beginning of 1980, data have been recorded on a triggered digital system that permits an achievable reading precision of 0.01 second. The hypocentral locations of earthquakes have been determined using the computer program HYP071 (Lee and Lahr, 1975) and regional velocity models and station delays derived by Eaton (1976) and Malone (1977) (See Section 2.5J.1.1).

Magnitudes of eastern Washington earthquakes are calculated at UW using the coda-length formula:

$$M_C = 2.82 (\log_{10} C) - 2.46$$

where  $M_C$  is the coda-length magnitude and  $C$  the coda-length.

Coda-length magnitudes are commonly used to express the relative sizes of small-magnitude earthquakes recorded by



AMENDMENT NO. 18  
September 1981

local and regional networks (see, for example, Lee et al., 1972; Crosson, 1972; Lee and Wetmiller, 1978). However, the definition of coda length used by different organizations and in different regions varies. For eastern Washington, coda-length is defined as the interval (in seconds) from the time of the first P-wave onset on a seismogram until the trace amplitude returns to twice the background noise level (Malone, 1979). Malone (1979) investigated the relationship of coda length to  $M_L$  (local magnitude as defined by Richter, 1958). The preliminary result of these investigations suggests that coda-length magnitudes computed for earthquakes in the eastern Washington region are approximately 0.3 higher than the corresponding Richter  $M_L$  magnitudes over the magnitude range from 1.3 to 5.1 (Malone, 1979). An inconsistency such as this might be expected because the magnitude formula was originally derived for the Puget Sound region (Crosson, 1972) and subsequently adopted for eastern Washington (Malone, 1979). This calculation, however, is preliminary since it is strongly influenced by the relatively sparse data (6 events) above magnitude  $M_L$  3 (Malone, 1979).

As noted in Section 2.5J.1.1, magnitudes for the period March 1969 through June 1971 were not recomputed by Malone (1979) because the USGS did not read coda-lengths for earthquakes that occurred during this period. The magnitudes for this period appearing in the seismicity catalog are the original values reported by the USGS, which were computed using an amplitude-based magnitude scale. Malone (1979, Appendix A) considers that such magnitudes are questionable. Therefore, because the relationship between the amplitude-based magnitude scale and the coda-length magnitudes subsequently computed has not been established, magnitude data for earthquakes that occurred prior to July 1971 have not been used in this study.

#### 2.5J.2.2 Magnitude Detection and Location Thresholds

Because the area of coverage of the eastern Washington network has not been uniform, it is possible that some of the observed patterns of seismicity may be artifacts of the station distributions. To investigate this possibility, the threshold magnitudes above which all earthquakes should have been detected and located by the network were estimated for different time periods and for different areas within the region. The effects of detection on the seismicity patterns are discussed in Section 2.5J.3.1.

Each of the numbered areas shown in Figures 2.5J-1 and 2.5J-2 has a station distribution history that is different from the other areas. Threshold magnitudes within each area are dependent upon the station distribution and upon the sensitivity of the recording instruments. Table 2.5J-1 shows

AMENDMENT NO. 18  
September 1981

the magnitude detection and location thresholds for each area. In order to assess the influence of focal depth on earthquake detection, Area I is divided into two depth ranges: greater than and less than 3 km. (The choice of this depth division is discussed in Section 2.5J.3.2). Seismicity data for the other areas are insufficient to permit a similar depth division.

Earthquakes have generally been observed to occur within a region according to the log-normal frequency distribution expressed by  $\log N = A - bM$  (Richter, 1958), where  $N$  is the cumulative number of events that have occurred per unit time with magnitudes equal to or greater than  $M$ , and  $A$  and  $b$  are constants that are characteristic of the regional seismicity. Assuming that all earthquakes occurring in the region during the time period under consideration have been detected, a plot of  $\log N$  versus  $M$  should be linear, with slope  $b$  and intercept  $A$  on the  $\log N$  axis. In reality, such frequency-magnitude plots usually have a well-defined linear segment within a discrete magnitude range. At lower magnitudes, the number of events falls below the straight line, which indicates that not all earthquakes within the lower-magnitude range have been detected. Therefore, the magnitude at which the plot "rolls off" can be considered to be the detection threshold magnitude for the region and for the time period under consideration.

Frequency-magnitude plots for each of the areas, depth ranges, and time periods given in Table 2.5J-1 were constructed. Threshold magnitudes were estimated from each of these plots and are also shown in Table 2.5J-1. Because this analysis is based on the published UW seismicity catalogs, the threshold estimates presented in Table 2.5J-1 represent the minimum magnitudes above which all earthquakes are estimated to have been recorded sufficiently well to be located. However, the numerical threshold magnitude estimates presented in Table 2.5J-1 are not considered to be final, because of the limited data available to construct several of the frequency-magnitude plots and the ambiguous interpretation of some of the plots. Specific uncertainties in the results are discussed below.

#### Area I

The results for Area I are somewhat anomalous. It seems unlikely that the threshold magnitude estimate of  $M_C$  1.7 for Area I (depths less than or equal to 3 km) for the period July 1975 through December 1980 is the same as for Area II for the same period, since the density of stations in Area I is significantly greater than in Area II. Although these estimates appear to be well constrained, as shown in Figures 2.5J-3 and 2.5J-4, it is possible that the threshold magnitude estimate





for Area I represents a break in the slope of the frequency-magnitude plot at  $M_C$  1.7 rather than a true "roll-off." That this value may be a characteristic of the data for Area I is suggested by the plot for the period July 1975 through December 1980 (depths greater than 3 km) shown in Figure 2.5J-5 and, to a lesser extent, by the plot for the period October 1971 through June 1975 (depths less than or equal to 3 km) shown in Figure 2.5J-6. Both of these plots (Figures 2.5J-5 and 2.5J-6) appear to have a linear segment, indicated by a dashed line between approximately  $M_C$  1.8 and  $M_C$  1, that has a more gentle slope than the linear segment for higher magnitudes. The "roll-off" in these plots appears to be at about  $M_C$  1.0. A similar break in slope was discussed by Rothe (1978) for frequency-magnitude plots for the Wooded Island swarm area. Such breaks in slope could represent a characteristic of the mode of earthquake occurrence in the area, as suggested by Rothe (1978), or a non-linearity in the magnitude relationship used. The breaks in the slopes in Figures 2.5J-5 and 2.5J-6 are not sufficiently well defined by the data to resolve whether they are due to the above causes or whether they do, in fact, represent location and detection thresholds. Therefore, the threshold magnitudes for Area I for all periods could either be close to magnitude  $M_C$  1 or about  $M_C$  1.8.

Based on the above discussion, the earthquake data for Area I, for the period October 1971 through December 1980, are considered to be complete for magnitudes at least as low as  $M_C$  1.8. This is a conservative estimate, and the data set may be complete down to approximately magnitude  $M_C$  1.25.

#### Areas II, III, IV, and V

Earthquake detection and location for Areas II and IV appear to be complete for magnitude  $M_C$  2.0 and above for the period June 1971 through December 1980. There are insufficient data to estimate threshold magnitudes for Area V. The threshold magnitude estimate of  $M_C$  2.0 for Area IV for the period June 1971 through June 1979 appears to be well defined. Because instruments were installed in Area IV in July 1979 (Figure 2.5J-2), it is most probable that the threshold magnitude for this area has been considerably less than  $M_C$  2.0 since that date. Area III appears complete above  $M_C$  1.5 after July 1975.

The estimates in Table 2.5J-1 are in general agreement with Malone's (1977) results for the detection capability of the eastern Washington network as it existed in 1975 and 1976. Based on the data recorded at any particular station for that period, Malone estimated that the maximum epicentral distances that earthquakes of magnitude  $M_C$  1.5 and 2.0 would be detected by that station and by at least three other stations. These

distances were then plotted as radii from each station to produce contours of the limits of detectability and locatability of earthquakes of magnitude  $M_C$  1.5 to 2.0, as shown in Figure 2.5J-7 (reproduced from Malone, 1977). The contours shown in Figure 2.5J-7 represent the limits of detectability of magnitude  $M_C$  1.5 and 2.0 earthquakes under optimal conditions. Therefore, not all earthquakes with magnitudes  $M_C$  1.5 or less had been located during 1975 and 1976 within the  $M_C$  1.5 contour. However, based on frequency-magnitude plots similar to those used in the present study, Malone feels that all events larger than  $M_C$  2.0 had been located within the  $M_C$  1.5 contour (Malone, 1979), which encompasses Area I and most of Areas II and IV. Malone also estimated that all events greater than  $M_C$  1.7 had been located within the immediate Hanford area shown in Figure 2.5J-7, which is roughly the same as Area I. This estimate is based on a frequency-magnitude plot for the Hanford area. Therefore, the ambiguities in interpreting the Area I plots discussed above also apply to Malone's results.

#### 2.5J.2.3 Location Accuracy

An assessment of the accuracy with which earthquakes comprising the data set have been located is of importance when the spatial patterns of the seismicity and its relationships to tectonic structures and other features are investigated. The accuracy of a location is measured by the difference between the computed location and the true location of the earthquake. The precision of a location is expressed by the error estimates computed by the location program. It is an expression of how well the location (computed using a given crustal-velocity model and set of station delays) fits the arrival times that were input to the program, and it depends in great part on the precision with which arrival times can be read from the seismograms of the event. The accuracy, therefore, depends not only on the precision of the location but also on how well the given velocity model approximates the actual crustal velocity structure, on how well the station delays compensate for inhomogeneities in the crust, and on the accuracy of arrival times.

Two studies have been conducted to estimate the location accuracy of earthquakes in the region. The most definitive study was carried out by Weston Geophysical Corporation (1981). This study used explosions of known locations within the Hanford Reservation to estimate the accuracy of UW-computed hypocentral locations of shallow earthquakes within this area. Two sets of explosions were used: the first set consisting of 20 explosions had known locations; the second set consisting of 9 explosions had known locations and known origin times. The first set was located by the UW using P-

AMENDMENT NO. 18  
September 1981

and S-wave arrival time data from the eastern Washington network and standard procedures, but without having an experienced seismologist check the arrival time picks, as is normally done for microearthquake data processing. The second set was also located using standard procedures after Dr. S.D. Malone had checked the picks. The results for the first set indicate that the computed locations of nine of the 20 explosions had horizontal mislocations of less than 1 km. Ten locations had depth mislocations of less than 1 km, and only one had a depth mislocation greater than 2 km. In the second set, seven of the nine locations had horizontal mislocations less than 1 km, and all the computed epicenters were within 1.5 km of the true locations. The depth mislocations were greater for the second set: only two computed focal depths were within 1 km of the surface, while the rest were within approximately 6 km. Computed arrival times were usually within 0.1 second of the true arrival times.

These results indicate that epicentral locations routinely calculated for the Hanford Reservation area are accurate and that the velocity models and station delays closely approximate the true velocity structure, at least in this area. The accuracy of earthquake focal depths is not reliably estimated by using surface blasts. However, because the results for epicentral locations and for arrival times indicate that the crustal velocity model is appropriate, earthquakes that occur less than 1 or 2 focal depths distant from a station should have good focal depth constraint. Also, based on the depth accuracies discussed above, the likelihood is fairly high that valid shallow focal depths (0 to 3 km) would be computed by the routine UW data analysis.

The second study, by Systems, Science, and Software (1981), was conducted in two phases: (1) an estimation of the three-dimensional velocity structure to a depth of 60 km in Eastern Washington that is consistent with a combination of both local travel times and gravity data; and (2) the computation (based upon UW locations) of revised hypocentral locations incorporating the three-dimensional velocity structure. A total of 68 events (including 6 known and 11 probable blasts) distributed throughout the study area were used in both phases. The average number of recording stations was 14, and the depths ranged from 0 to 15 km. The revised epicenters of the 6 known explosions were within 2 km of the UW locations, and the original focal depths were generally less than 0.5 km, while the largest revision was 1.3 km. This result suggests that, for shallow events within the array, the UW location procedures and the procedure using the three-dimensional velocity model are of equivalent accuracy.

AMENDMENT NO. 18  
September 1981

For the remainder of the events (earthquakes and probable blasts), the revised hypocenters were generally within 1 km for events located near the center of the array and increased to 15 km for events near the periphery of the network. The increase in hypocenter deviation with distance from the center of the array is not unexpected, but it is difficult to give an unambiguous interpretation of this pattern. The error in locations is expected to increase for events outside the array. In addition, the resolution of the three-dimensional velocity structure must necessarily decrease near the edges due to less complete raypath sampling. The combination of these edge effects, then, is probably responsible for the observed pattern of increased hypocenter deviation toward the fringes of the net.

The results of these two studies indicate that hypocentral locations computed by the UW are accurate within about 1 km for events that occur within the central Columbia Plateau and within a distance of one or two focal depths from a station. The locations for the remainder of the region are less well constrained, but epicenter locations should be more accurate than focal depths.

### 2.5J.3. CHARACTERISTICS OF COLUMBIA PLATEAU INSTRUMENTAL SEISMICITY

This section presents a summary of the general characteristics of the seismicity within the Columbia Plateau. Section 2.5J.4 contains more detailed analyses of the characteristics of shallow-crustal (focal depths less than or equal to 3 km) and intermediate-depth (focal depths between 3 and 8 km) seismicity. In Section 2.5J.5, the characteristics of the seismicity are interpreted in terms of earthquake source models.

#### 2.5J.3.1 Spatial Distribution of Seismicity

A plot of the epicenters of all earthquakes that had magnitudes greater than  $M_C$  1.0 and that were located between latitudes  $45.5^\circ\text{N}$  and  $48^\circ\text{N}$ , and longitudes  $118^\circ\text{W}$  and  $121^\circ\text{W}$  during the period March 1969 through December 1980 is shown in Figure 2.5J-8. Earthquake activity is broadly scattered within the region. Two areas within this region exhibit concentrated activity. The first area is the central Columbia Plateau, which is defined for this study as the area bounded by latitudes  $46^\circ\text{N}$  and  $47^\circ\text{N}$  and by longitudes  $118.75^\circ\text{W}$  and  $120^\circ\text{W}$ . From Figures 2.5J-0 and 2.5J-8, it can be seen that the northern and southern boundaries of this area roughly correspond to the Frenchman Hills anticline and the Horse Heaven Hills anticline, respectively. The area encompasses the eastern portions of Saddle Mountains, Umtanum Ridge,



Yakima Ridge, and Rattlesnake Hills, and includes Gable Mountain and Gable Butte. All of these are anticlines of the Yakima Fold Belt. The Hanford Reservation, within which the site is located, occupies the center of this area (Figure 2.5J-8). Because the central Columbia Plateau (as defined here) contains the site, it is the main focus of this study.

The second area of concentrated activity is near Lake Chelan (Figure 2.5J-8). The seismicity of the Chelan area has been studied by Malone (1977, 1978, 1979), Bor (1977), and Woodward-Clyde Consultants (1978) and is discussed in Washington Public Power Supply System (1981, Appendix 2.5I). These studies have shown that the seismicity of this area is distinctly different from the central Columbia Plateau and from the rest of the region in several important respects, as summarized here. Nearly all of the earthquakes in the Chelan area have occurred within the depth range 3 to 8 km, with the majority near 5 and 6 km (Malone, 1977). As discussed by Malone (1977), because the basalt layer in this area appears to be thin (less than a few kilometers), these earthquakes appear to have occurred within the basement. As discussed later in Section 2.5J.3.2.1, the majority of the central Columbia Plateau earthquakes occurs in the upper 3 km of the crust, apparently within the Columbia River basalt flows and older volcanoes. The Chelan seismicity does not show the dominant swarming characteristics (Malone, 1978) that are noted later in this section for the central Columbia Plateau and in Section 4. The level of activity in the Chelan region has also been observed as a low-level seismic source throughout the period covered by the historical seismicity record (Rasmussen, 1967; Malone, 1977; Washington Public Power Supply System, 1981, Section 2.5.2.1).

Much of the analysis discussed in the remainder of this report is concerned with characterizing the seismicity of the Columbia Plateau region as a whole, and the central Columbia Plateau in particular. Therefore, in view of the apparent differences between the seismicity of the Chelan area and the seismicity of the central Columbia Plateau, and the distance of the Chelan Area from the site, this area has not been included in subsequent analyses of the central Columbia Plateau.

Because detection and location magnitude thresholds have been consistently lower for the central Plateau (approximately Area I in Figures 2.5J-1 and 2.5J-2) than for the surrounding region (as discussed in Section 2.5J.2.2), the possibility was considered that the concentration of activity in the central Plateau area could be an artifact of the seismograph station configuration. To test this, the spatial distributions of earthquakes having magnitudes greater than or equal to  $M_C$  2.0



September 1981

were compared for the region for the time period March 1969 through June 1975 (Figure 2.5J-9) and for July 1975 through December 1980 (Figure 2.5J-10). From Section 2.5J.2.2, magnitude  $M_C$  2.0 is estimated to be the minimum detection threshold for the entire region for both of the above periods. Therefore, if the concentration of events in the central Plateau is an artifact of station distribution, then it should not be apparent on either of these plots. However, Figure 2.5J-9 does show a definite concentration of earthquakes in the central Plateau area. Figure 2.5J-10 also shows relatively more events in this area, but the contrast with the rest of the region is not so marked. Furthermore, the overall distribution of activity throughout the region shown on Figures 2.5J-9 and 2.5J-10 is not significantly different for the period 1969 through June 1975 (when most of the stations were located within the central Columbia Plateau) than for the period July 1975 through 1980 (after the network had been extended). The greater number of events on Figure 2.5J-10 in the Yakima-Ellensburg region (identified in Figure 2.5J-2) does not appear to be related to station distribution since, as shown in Table 2.5J-1, the coverage of this area (Area IV) was uniform until June 1979 when local stations were installed and only two events have been located since that date. Therefore, it is concluded that the distribution of events in the central Columbia Plateau is real, and not an artifact of the station array geometry. However, the concentrated appearance of the seismicity in the central Plateau in Figure 2.5J-8, which includes magnitudes as low as  $M_C$  1.0, is undoubtedly enhanced by the lower detection threshold there.

Within the central Columbia Plateau, the regions of greatest seismicity (Figure 2.5J-8) lie between Saddle Mountains and Frenchman Hills and between Saddle Mountains and Gable Mountain-Gable Butte. The interior of the Hanford Reservation is markedly lower in activity, particularly the eastern part. Scattered earthquakes occur south and southeast of the Reservation. A prominent feature of the total seismicity of the central Columbia Plateau is the numerous, dense-clustered groups of epicenters that provide a contrast to the more scattered events surrounding the central Plateau. Most of these groups are found to cluster both in space and time, and are termed "earthquake swarms" (discussed in detail in Section 2.5J.4).

Figures 2.5J-11 and 2.5J-12, which are vertical cross-sections through the region along the projection axes shown on Figure 2.5J-8, and include all hypocenters within 60 km of the lines plotted. Only better quality data, selected according to the following criteria, were used to plot these cross-sections:





AMENDMENT NO. 18  
September 1981

Standard error in epicenter:  $< 2.5$  km  
Standard error in focal depth:  $< 5$  km  
RMS of travel time residuals:  $< 0.3$  second  
Station coverage ( $360^\circ$ -Gap):  $> 160^\circ$  in azimuth

These quality estimates are those computed by the HYPO 71 location program (Lee and Lahr, 1975). In addition to the above criteria, hypocentral solutions with a focal depth of 3.00 km were not plotted. This is the trial starting depth for all the HYPO 71 runs (Malone, 1979), and a final solution that has this depth implies that the focal depth cannot be controlled by the data and has been arbitrarily constrained.

For comparison with Figures 2.5J-11 and 2.5J-12, the cross-sections using all hypocenters are presented in Figures 2.5J-13 and 2.5J-14. Although some loss of resolution occurs with this data set due to the inclusion of statistically less well-located events, it is important to include the more regional framework of the central Plateau. The earthquakes with focal depth fixed at 3.00 km form distinct horizontal lineations in these two figures.

To aid interpretation of the depth distribution of seismicity in terms of the deep structure of the Plateau, available crustal structure interpretations from regional geophysical studies are included in Figures 2.5J-11 to 2.5J-14. These data consist of the top of basement as defined by time-term analyses (Eaton, 1976; Malone, 1977), the depth to the Moho as defined by long-range seismic refraction (Hill, 1972, 1978), and the modelled cross-section of a deeper, older basalt body underlying the Columbia River basalts interpreted from gravity data (Washington Public Power Supply System, 1981, Appendix 2.5.L). The three-dimensional model developed by Systems, Science and Software (1980), although not shown here, is generally compatible with these geophysical interpretations.

A prominent feature of the seismicity seen in all four cross-sections is the apparent zonation according to depth. With few exceptions, the events that tend to occur in clusters are limited to the depth range 0 to 3 km and are underlain by a more diffuse zone of activity. Few clusters of events are in this intermediate zone, but not nearly of the pronounced level as in the uppermost 3 km. At about 8 km, this middle zone is replaced by a zone of very diffuse activity that continues down to approximately 25 km. This zone contains no prominent clusters, and the distribution of events within it is sparse compared to the overlying activity.

These depth divisions are similarly evident in a plot of the number of events versus depth (Figure 2.5J-15). As discussed earlier, the concentration at 3 to 4 km is due to the fixed



depth of 3.00 km; the portion of events of depth 3.00 km is shown by the dotted bar in Figure 2.5J-15. It is likely that the events fixed at the 3.00-km lower depth are actually similarly distributed; they are generally included in subsequent analyses of seismicity patterns in this appendix. The decrease in level of activity with increasing depth is not produced by poorer detection with depth. As noted in Table 2.5J-1, the detection threshold appears to be lower for earthquakes deeper than 3 km. Excluding the fixed-depth events, 68 percent of the activity occurs in the top 3 km, 22 percent in the 3- to 8-km range, and 10 percent is deeper than 8 km. The size of the largest earthquake in each depth zone (Figure 2.5J-15) also decreases with increasing depth, but not in so pronounced a fashion as the number of events. Based on these distinctions in seismicity with depth, these three zones are defined as the shallow crustal zone (0 to 3 km), the intermediate crustal zone (3 to 8 km), and the deep crustal zone (8 to 25 km+). Each of these zones is discussed in more detail below.

Frequency-magnitude plots were examined to establish regional seismicity characteristics within the Columbia Plateau. The data set used is for the period July 1971 through December 1980, thus excluding the period of anomalous magnitudes prior to June 1971 (Section 2.5J.2.1). In Figure 2.5J-16, the frequency-magnitude data set for the area of longitudes 45.5°N to 47.5°N by latitudes 118°W to 121°W is plotted. The slope defined by the range  $2.0 < M_c < 4.0$  is linear and has the value of 0.85. The magnitude range is above the region's cutoff magnitude (2.0) and excludes the two largest events in order to establish a definitive slope. When the shallow crustal events are excluded from this data set, the slope of 0.72 is obtained (Figure 2.5J-17). The shallow data set alone is examined for the central Columbia Plateau, where focal depths are more accurately defined, and the cutoff magnitude of 1.75 is used. The shallow crustal zone has a slope of 1.00 (Figure 2.5J-18), distinctly higher than the previous two values that represented or included the deeper earthquakes.

### 2.5J.3.2 Columbia Plateau Seismic Zone Features

#### 2.5J.3.2.1 Shallow Crustal Zone (0 to 3 km)

The shallow zone is dominated by swarm-like activity that appears to be restricted to a depth of about 3 km (Figure 2.5J-19). The swarm activity is concentrated within the central Columbia Plateau in several zones following the trend of the Saddle Mountains. The shallow seismicity exhibits a relatively high ratio of small- to large-magnitude earthquakes (slope of 1.00 in Figure 2.5J-18). Swarms and other features



of the shallow seismicity are discussed in Sections 2.5J.4, 2.5J.5, and 2.5J.6.

The distinct shallow crustal zone suggests a possible geologic association. Depth modeling of gravity data (Washington Public Power Supply System, 1981, Appendix 2.5.L), the deep basalt well near Rattlesnake Hills (Raymond and Tillson, 1968) (located on Figure 2.5J-19), and regional geologic investigations (Swanson et al., 1979) suggest that the Columbia River basalt flows and older volcanics form a distinct zone above about 3 km thick. This spatial association with the volcanic sequence provides an important means to further examine the possible geologic origin of the shallow seismicity, as discussed in Section 2.5J.5.

#### 2.5J.3.2.2 Intermediate Crustal Zone (3 to 8 km)

Most of the activity in the intermediate depth range occurs under the central Columbia Plateau (Figure 2.5J-20). The change between the intermediate zone and the deep zone coincides fairly well with the basement boundary defined by Eaton (1976) and Malone (1979). This is best seen in Figure 2.5J-12, the north-south cross-section. The basement contours from gravity and seismic refraction do not match very closely in Figure 2.5J-11, but are associated with the change in level of activity. The swarm pattern of activity seen in the shallow zone does not appear to extend to the intermediate depths. As noted in Section 2.5J.4.4, a few of the shallow swarms appear to extend to depths greater than 3 km; the deeper events, however, are generally less well-located in terms of numbers of readings, azimuthal gap between stations, and distance to the closest station in the hypocentral location. Thus, a portion of the intermediate activity may be mislocated in depths and may more correctly belong with the shallow zone.

The intermediate zone appears to correspond to a region interpreted to be mostly sediments (Myers and Price, 1979) lying above the basement and below the Columbia River basalts. The zone is also restricted laterally (Figures 2.5J-13 and 2.5J-14) and seems to be confined to a basin in the basement centered on the central Columbia Plateau.

#### 2.5J.3.2.3 Deep Crustal Zone (8 to 25 km+)

The events with depths greater than about 8 km are apparently basement events, as noted in earlier studies (Woodward-Clyde Consultants, 1980). A map view (Figure 2.5J-21) shows essentially none of the clustering that is characteristic of the shallow events. As with the intermediate events, the events generally underlie the central Columbia Plateau.



The cross-sections (Figures 2.5J-13 and 2.5J-14) reveal a bowl-like shape at the base of the deep events. The deepest events (depths 15 to 25 km) occur under the center of the central Columbia Plateau, and the earthquakes become shallower toward the edges. Because this slope occurs well within the area of good station distribution and is also apparent in the better-located data (Figures 2.5J-11 and 2.5J-12), it is not considered to be a function of the station array.

Composite focal mechanisms suggest that the basement beneath the central Columbia Plateau is undergoing regional north-south compression. The details of the focal mechanism and other aspects of deeper seismicity are discussed in Woodward-Clyde Consultants (1980).

#### 2.5J.4.. SWARMS AND SHALLOW SEISMICITY

##### 2.5J.4.1 Earthquake Swarms

In most regions of the world, the overall temporal occurrence of earthquakes may be characterized as a random process combined with occasional increases in the normally observed frequency of earthquake occurrences that last for varying periods of time. Occurrences of earthquakes within these spatially and temporally defined increases in activity behave according to some non-random relationship. The following three main types of earthquake sequences have been identified (see, for example, Richter, 1958, and Mogi, 1963): mainshock-aftershock sequences, foreshock-mainshock-aftershock sequences, and earthquake swarms. Earthquake swarms are defined by Mogi (1963) as sequences of earthquakes in which the number and magnitude of events gradually increase with time and then decrease, with no single predominating event that can be identified as a mainshock. Richter's (1958) definition of a swarm as being "a long series of large and small shocks with no one outstanding principal event" is less restrictive in that the activity is not required to increase and decay with time. Swarms can be composed of tens to thousands of events occurring within periods from a few hours to many days.

Earthquake swarms, as defined above, have been observed in many tectonic and geologic environments and occur over widely different scales of energy release. They occur in regions of high seismic activity, where the other types of sequences are also common. In Japan and California, for example, swarms frequently include earthquakes in the magnitude range 5 to 6 (Utsu, 1970; Richter, 1958). The seismicity of volcanic regions commonly exhibits swarm characteristics, especially in association with active volcanoes. Swarms are often observed in geothermal areas, usually at the microearthquake level.



Richter (1958) observes that swarms often occur in areas of recent, but not active volcanism, such as the Owens Valley in California, where the swarms occurred in areas underlain by volcanic tuff and basalt flows. Sykes (1970) discussed swarms associated with the mid-Atlantic ridge. Sequences of small- to moderate-sized earthquakes that are induced by the filling of reservoirs (Talwani et al., 1979), by the injection of fluids into wells (Hermann et al., 1981; Hsieh and Bredehoeff, 1981), and by fluid extraction (Yerkes and Castle, 1976) often exhibit swarm characteristics. Many such cases of induced seismicity have been reported from areas in which the normal level of seismicity is relatively low.

The occurrences of certain swarms in California, such as those in the Imperial Valley, and in Japan are associated with known active fault zones. Swarms associated with active volcanoes and geothermal reservoirs are caused by the intrusion of magma or high pressure hot water and steam. Artificially induced swarms are sometimes localized on pre-existing fault zones, which may have been seismically quiet. In other cases swarms cannot be associated with structures. Therefore, considering the variety of geologic and tectonic environments in which swarms are observed, an all-encompassing theory to explain their occurrence would not be likely. However, certain geologic conditions may favor the occurrence of swarms in preference to other types of sequences.

Mogi (1963) broadly classified the areas where swarms would be the characteristic mode of strain release as those where the crust is extremely heterogeneous or fractured or where stress is locally concentrated. Both of these conditions exist in active volcanic and geothermal areas, and they often exist in areas of recent volcanism. The predominance of swarms in areas where the crust is heterogeneous has been noted in several cases. For example, in a study of three earthquake sequences that occurred between 1968 and 1971 near Hollister, California (in the San Andreas fault zone), Udias (1977) found that there were two mainshock-aftershock sequences and one swarm sequence. He postulated that the swarm occurred on the same fault system as the other two sequences but in an area where the crust is less homogeneous. The large swarm of activity that occurred near Denver between 1962 and 1967 was caused by the injection of fluid into highly fractured Precambrian basement rock (Hsieh and Bredehoeff, 1981). Talwani et al. (1979) observed that the swarm activity associated with Lake Keowee in South Carolina is associated with an orthogonal set of joints within a 2-km-wide zone.



#### 2.5J.4.3 Previous Studies of Columbia Plateau Earthquake Swarms

Earthquake swarms, as generally defined above, have been observed in the central Columbia Plateau since microearthquake monitoring began in 1969. Swarms have been routinely reported by the UW (Malone, 1977, 1978, 1979, 1980) and have been the subject of three detailed investigations.

Pitt (1971). The first of these, by Pitt (1971), dealt with the 1969-1970 swarm at Wooded Island. Pitt describes the general features of the swarm, including the limited extent of the zone of activity (5 km east-west, 3 km north-south), the shallow focal depths (less than 5 km), and the apparent migration of activity with time. His study is superceded by that of Rothe (1978), as discussed later.

Malone et al. (1975). The second study was carried out by Malone et al. (1975), who investigated the 1972 swarm on the Wahluke Slope, the 1973 Eltopia swarm, and the 1973-1974 Royal Slope sequence. Each of these sequences was investigated in detail using earthquake data recorded by a closely spaced network of portable seismograph stations deployed around the swarm zone. Therefore, the investigation was based on relatively accurate hypocentral solutions. Both the Wahluke and Eltopia sequences followed the swarm pattern as defined by Mogi (1963). The Royal sequence, however, began with a magnitude  $M_C$  4.4 earthquake followed by a large number of smaller shocks and could be described as a mainshock-aftershock sequence rather than a swarm. All of the sequences were confined to small areas of less than 10 km<sup>2</sup>, and all earthquakes occurred at depths of less than 2 km.

To investigate possible causative mechanisms, Malone et al. (1975) constructed composite fault-plane solutions for the Eltopia and Royal sequences. Of the events in the Eltopia swarm, 85 percent fit into one of three mechanisms. The three mechanisms all indicate northeast- or east-striking, steeply dipping reverse faulting; two of the mechanisms have a significant strike-slip component. Earthquakes in the Royal sequence fit into either one of two mechanisms, both of which indicate reverse faulting on steeply dipping, east-striking planes. The authors conclude that, in both cases, slip took place on a number of planes having different orientations but in response to a uniform stress field having north-south, horizontal maximum compression and vertical minimum compression. The hypocenters of each subset of Eltopia events fall into an individual focal category mechanism and roughly define a steeply dipping plane that agrees in strike and dip with one of the planes interpreted from the focal mechanism. The three planes thus defined intersect near the main cluster of



AMENDMENT NO. 18  
September 1981

epicenters in the swarm area. Migration of activity of the Royal sequence from the center of activity, first to the west and then to the northeast, was observed. Based on the observation that the earthquakes appear to have occurred on several slip planes and based on the restricted depth range involved, Malone et al. (1975) conclude that perhaps only one competent basalt flow (or at most a few) is involved in any one event and that large-scale, through-going faulting is unlikely.

Rothe (1978). Rothe (1978) investigated the 1975 earthquake swarm at Wooded Island in detail and also dealt with possible causative mechanisms of Columbia Plateau swarms in general. The 1975 Wooded Island swarm began in April of that year and continued until November. The swarm was monitored using the eastern Washington network, which included station WIW located at Wooded Island. The UW installed a portable network of up to seven stations directly above the swarm zone in June 1975, with an average station spacing of less than 1 km. The detection threshold of the portable network was very low ( $M_c - 0.1$ ). A total of 365 events were detected during the three months of operation of the local network, of which 192 were locatable. The dense local network also enabled the calculation of very precise hypocentral locations (estimated error less than 150 m). The shallow crustal-velocity model used was based on Eaton's (1976) time-term model, and station delays were calculated from local stratigraphic and cross-hole velocity data. Rothe also studied the effects of the potential velocity anisotropy of the basalts on Wooded Island hypocentral locations. He found that locations computed using an anisotropic model were not significantly different from those computed using a layered half-space model, although the anisotropic model tended to increase focal depths slightly.

The swarm earthquakes all occurred within an area of 2-1/2 km east-west by 2 km north-south, which is roughly the same area within which the 1969-1970 swarms occurred. All but four of the events were located at depths less than 2.5 km. Time-lapse studies of the entire swarm indicated that the earthquakes migrated from the center of activity, first to the north and then to the north and northwest. During the period of local network operation, the migration had the effect of establishing southeast-northwest and east-west linear trends of epicenters.

Rothe devotes particular attention to identification of apparent linear trends in the distribution of hypocenters. The epicentral plot of the 1975 swarm reveals two rather poorly defined trends: one northwest-southeast, the other west-east. Rothe notes that a "hotspot" of activity is localized near the intersection of the two trends and that the



AMENDMENT NO. 18  
September 1981

largest event ( $M_C$  2.83) occurred near the spatial and temporal center of the swarm. Similar migration of about a kilometer was observed for the 1969-70 swarm (Pitt, 1971) to establish, in this case, an east-west trend of epicenters. Relocation by Rothe of the better-determined hypocenters of the 1969-70 swarm using the time-term velocity model results in the 3-km-long, east-west trend of epicenters being more pronounced than originally shown by Pitt.

Vertical cross-sections through the zone of hypocenters suggest that the northwest and west linear trends of epicenters are the expressions of steeply dipping (almost vertical) linear concentrations of hypocenters in the depth range 0.5 to 2.5 km. These linear trends are poorly defined, however.

Rothe found that almost all the energy release during the 1975 swarm occurred in the depth range 0.3 to 2.0 km. Based on the well cuttings and E-logs obtained from the Rattlesnake No. 1 Deep Well (Raymond and Tillson, 1968), this depth range is likely to correspond to a zone of basalt flows. Therefore, in support of the conclusion drawn by Malone et al. (1975), Rothe suggests that the earthquakes occur only in basalt, which is capable of storing strain energy, and not in interflow zones.

Magnitude-frequency plots that were constructed for the 1975 swarm using both eastern Washington and local network data, show distinct breaks in the b-slope at about  $M_C$  1.7. Rothe interprets the break in b-slope as being indicative of a "characteristic" swarm-earthquake magnitude. He identifies this characteristic, preferentially occurring earthquake "size" as approximately  $M_C$  1.5. The possibility that the break in slope may be an artifact of the method of computing magnitudes is noted in Section 2.5J.2.2.

Rothe, in agreement with the results of Malone et al. (1975), found that no one focal mechanism would fit the data for all events. Ten rather poorly constrained composite mechanisms were required to fit all the events. (No event had sufficient data with which to construct an individual focal mechanism.) However, about 60 percent of the events fit one of three mechanisms, all of which indicate high-angle (greater than about 45 degrees) thrust faulting on planes striking north-northeast, east, or southeast. Rothe concludes that, as for the Royal and Eltopia swarms, slip took place on several planes of varying orientations, rather than on a single fault plane.

D

#### 2.5J.4.3 Definition of Earthquake Swarms in the Columbia Plateau

In order to treat the occurrence of swarms in the Columbia Plateau in a systematic fashion, a statistical definition of an earthquake swarm is needed. Techniques for quantifying earthquake clustering have been developed by several investigators (Vere-Jones and Davies, 1966; Shlien and Toksoz, 1970; Savage, 1972 and 1976; Udias and Rice, 1975; McNally, 1976). These studies consisted of searching for appropriate cluster time-lengths (between associated events) and then testing, using relatively sophisticated statistical techniques, for non-Poissonian (non-independent) behaviour within the clusters and Poissonian (independent) behavior in the residual data set. The choice of cluster time-lengths appropriate to an area or region determines the efficiency and success of the approach. Previously reported cluster time-lengths vary widely, from a few minutes to a few days. Spatial definition of the clusters has also been important to most of these studies.

Because the swarm occurrences are so prominent in the Columbia Plateau, relatively simple observational criteria are used to define swarms. Although this may not result in a statistically thorough identification of the non-random seismicity, it will suffice to identify the major features of the more readily identified swarms.

Previous investigations in the central Columbia Plateau (Malone, 1979) have defined areas in which swarms appear to be the dominant characteristic of the seismicity. To initially define swarms, boundaries were drawn around these areas, and all the seismicity within the boundaries were defined as swarm activity. However, this definition includes only the spatial aspect of swarms and ignores the possibility that, in a temporal sense, non-swarm, background seismicity might also occur within the swarm areas and time windows. The temporal distribution of seismicity within the previously defined swarm areas was examined using several cluster time-lengths. This examination was accomplished by manually searching the Hanford earthquake catalog and testing for those cluster time-lengths that appeared to be successful in separating occasional, apparently randomly occurring events from those that occurred during periods of high activity. The appropriate cluster time-length was refined through several iterations of this process. The cluster time-length thus defined was then used to identify swarms in time, to refine the boundaries of previously identified swarm areas, and to identify new swarm areas.

U



AMENDMENT NO. 18  
September 1981

Cluster time-lengths ranging from 2 to 15 days were examined. A 10-day cluster time-length was found to perform relatively well in defining previously identified swarms, although cluster time-lengths varying up to several days around this value could be equally appropriate. Therefore, using the 10-day cluster time-length, a swarm is defined for this study as a group of four or more events that occur within a small volume having defined boundaries and within which no event is separated from the events immediately preceding and succeeding it by more than 10 days. According to this definition, a four-event swarm could occur over a maximum period of 30 days. Characteristic cluster time-lengths and cluster durations for Columbia Plateau swarms appear to be much longer than have been reported for non-Poisson seismicity in other areas.

It must be pointed out that any temporal cluster definition may be arbitrary to some degree. While some sequences fall easily into either the cluster or background categories, a gradational boundary between the categories may vary from area to area and perhaps even from year to year within each area in the central Plateau. An example is the time history of Wooded Island seismicity, shown in Figure 2.5J-22. Occasional events, such as those at 39, 60, and 121 months, stand alone in time and must be considered random background events. Other episodes, such as the those starting at 6 and 76 months, are clearly clusters. However, other events are not so obviously categorized. The pair of events at 26 months may be associated with the 1969-70 series of swarms or may be in the background. In the Wooded Island area, a longer cluster time-length might be appropriate, but a wider time window applied to the more consistently active region in the Saddle Mountains area would cause activity that appears to be random background to be included in the swarms. While this problem may be inherent in choosing a single cluster time-length for all of the swarms, all of the prominent and most of the less obvious swarms can be selected by using the criteria herein defined.

The swarm areas identified by the UW are listed in Table 2.5J-2. Swarm and non-swarm events in each area were separated using the swarm definition described above. The seismicity in the immediate vicinity of each area was examined to see if any of the temporally defined swarms extends outside the previously defined boundaries. In four cases, listed in Table 2.5J-3(a), it was found that the swarm areas should be slightly larger. Instances occurred where a swarm in one area included events from one in an adjacent area; these are listed in Table 2.5J-3(b). As noted in Table 2.5J-3(c), in four cases, a combination of events in two adjacent areas revealed small swarms where none was apparent when the individual areas were used.

The data that remained after the previously defined swarm areas (Tables 2.5J-2 and 2.5J-3) had been studied were examined for spatial and temporal associations using a moving 10-day window. All the swarm area boundaries are shown in Figure 2.5J-23. Thirty-four additional swarms were found in 28 new swarm areas. The newly defined swarm areas are listed in Table 2.5J-4. Several of the new areas overlap, and several of them could be combined into larger areas. Table 2.5J-5 lists all the swarms identified, their dates of occurrence, number of events, and the largest magnitude recorded. Figures 2.5J-24 and 2.5J-25 show plots of swarm and non-swarm seismicity, respectively.

Noteworthy from Table 2.5J-5 is that some of the UW-defined sequences in the swarm areas that had previously been identified as single swarms are now split up into two or more swarms. Therefore, it appears that the temporal aspect of swarm activity is more fully reflected in the new swarm definition. For certain cases, such as the 1970 to 1971 Scootenev Reservoir Swarms B and C, strict adherence to the 10-day cluster time-length has resulted in two swarms being defined when perhaps one might be appropriate.

#### 2.5J.4.4 Characteristics of Columbia Plateau Swarms

Epicentral plots of larger swarms (i.e., those containing 10 or more earthquakes) were examined for indications of spatial trends. Most of the earthquakes in each swarm are clustered within an area that has dimensions of less than 3 to 4 km. Linear trends of epicenters are apparent, to varying degrees, within some of the swarms. The best defined of these are the northwest-southeast trend of the Eltopia A swarm (Figure 2.5J-26a) and the east-northeast/west-southwest trends of the Scootenev Reservoir B and C swarms (Figures 2.5J-26b and 2.5J-26c). Well-defined, but relatively short, east-west trends are evident for the Wooded Island B and E swarms (Figures 2.5J-26d and 2.5J-26e) similar to those noted by Rothe (1978). Apart from the Eltopia and Scootenev Reservoir swarms, the linear trends discussed above are rather short, not greatly different than the 1- to 2-km uncertainty in event locations. Thus, no general or consistent spatial patterns are revealed by the swarms.

The patterns of spatial occurrence of successive swarms vary within the swarm areas. In Wooded Island and Berg Ranch, successive swarms have been centered in about the same location. The Smyrna C and F swarms also occurred at about the same place, although Smyrna G occurred well to the west of this location. In all of the other areas, the tendency has been for successive swarms to migrate away from earlier swarm



AMENDMENT NO. 18  
September 1981

locations. For the majority of cases, successive swarms overlap, and migration has extended the activity in a particular direction.

Focal depths of the earthquakes comprising most of the swarms are confined to the range 0 km to approximately 5 km. Maximum focal depths for several of the swarms, including Eltopia A, Wooded Island G, Corfu B and H, Wahluke F, and Royal D are less than 3 km. These very shallow focal depths are in agreement with those reported by Malone et al. (1975) for the Royal D, Wahluke D, and Eltopia A swarms, and by Rothe (1978) for the Wooded Island I swarm. Malone et al. (1975) reported depths of less than 2 km for the three swarms they studied, based on relatively accurate hypocenters computed using data from local networks (see Section 2.5J.5.1.2). Therefore, since the focal depths of some shallow earthquakes that were located using regional network data are likely to be in error by up to a few kilometers (see Section 2.5J.2.3), it is probable that virtually all of the earthquakes comprising the swarms in the central Columbia Plateau occurred at depths less than about 3 km.

Three swarms, namely Scooteney Reservoir B and C and Connell G, contain earthquakes that appear to be anomalously deep compared with the other swarms. These swarms occurred close to each other, near the eastern end of Saddle Mountains. Approximately half of the Scooteney Reservoir B earthquakes were located in the depth range of 6 to 12 km. These deeper earthquakes form parts of both the east-northeast linear trend and the east linear trend (Figure 2.5J-26). Scooteney Reservoir C contains fewer deep earthquakes in the same depth range. All four of the earthquakes in the Connell G swarm have focal depths in the range 5.9 to 10.2 km. Because it is possible for microearthquake swarms to occur as a small component of seismicity in any seismic environment, the occurrence of an occasional swarm in the intermediate crustal zone or deeper crustal zone is not surprising. However, this occasional swarm occurrence at depth does not require that the shallow crustal zone be causally related (in a seismologic sense) to the deeper zones.

Figure 2.5J-27 shows the observed distribution of maximum swarm earthquake magnitudes for the swarms having more than 10 events, as well as for all the swarms listed in Table 2.5J-5. The distribution is considered complete above  $M_C$  2.0 (Section 2.5J.2.2) and shows a flattening and decrease due to incomplete detection below  $M_C$  2.0. For maximum magnitudes above  $M_C$  2.0, there is a steep decrease in the number of swarms to the sequence containing the largest event, the  $M_C$  4.4 Royal Slope earthquake.

According to the generally accepted definitions of earthquake swarms given in Section 2.5J.4.1, the primary criterion used in differentiating a swarm from foreshock-mainshock-aftershock sequences or mainshock-aftershock sequences is whether the sequence includes an event that can be considered a "mainshock." However, there is no universally accepted definition of how large the mainshock should be relative to the other events in the sequence. Arbitrary definitions have been used in previous investigations. For example, Tryggvason (1973) used the following criteria to define earthquake swarms in Iceland: (1) the magnitude difference between the first and second largest-magnitude earthquakes in a sequence is less than 1.0; and (2) the magnitude difference between the largest and fifth largest-magnitude earthquakes is less than 1.5. A similar criterion was adopted for a preliminary assessment of whether any of the Columbia Plateau swarms could in fact be considered to be other types of sequences.

Figure 2.5J-28 shows magnitude versus time plots of all seven sequences in the vicinity of the central Columbia Plateau within which one event, or a pair of events, have magnitudes at least 1.0 greater than the other events. Eltopia A (Figure 2.5J-28[a]), West Saddle Mountains C (Figure 2.5J-28[f]), and Area 18A (Figure 2.5J-28[g]) are sequences within which the largest-magnitude events did not occur near the beginning of the sequence. There are too few events in the West Saddle Mountains and Area 18A plots for patterns to be discerned. The Eltopia sequence does not appear to be a foreshock-mainshock-aftershock sequence but rather two relatively large-magnitude events superimposed on an essentially constant level of swarm activity.

The remaining two sequences have the largest magnitude event occurring close to the beginning of the sequence. The Royal D sequence (Figure 2.5J-28[b]) can be regarded as a non-swarm type of sequence according to the definition given in Section 2.5J.4.1 and could be viewed as a mainshock-aftershock sequence. As discussed earlier in this section, this sequence also seems to be an unusual occurrence (compared with the rest of the observed shallow seismicity) because of the size of its maximum earthquake magnitude. However, the Royal D sequence does not exhibit the characteristics of a classic mainshock-aftershock sequence. The rate of aftershock activity in such sequences decays with time according to an inverse-power law (Utsu, 1970), and the magnitudes of the aftershocks become progressively smaller. This general type of behavior is observed even for complex aftershock sequences (Utsu, 1970). The Royal D sequence does not exhibit these decay characteristics. The level of activity after the "mainshock" drops almost immediately to a relatively low level and remains essentially constant for the duration of the sequence. The

Royal E and Coyote Rapids B and F sequences all have an apparent "mainshock," but subsequent events are too few for examining the possibility of these being mainshock-aftershock sequences.

Figure 2.5J-29 shows the cumulative number versus magnitude plot for swarm earthquakes within the Columbia Plateau (latitudes  $46^{\circ}10'N$  to  $47^{\circ}10'N$ ; longitudes  $118^{\circ}30'W$  to  $120^{\circ}W$ ). This plot shows essentially the same features as Figure 2.5J-18, which includes all the shallow seismicity in this area, namely, a steep slope (1.15) for magnitudes greater than  $M_C 2.0$  and the apparent break in slope at approximately  $M_C 2.0$ . Individual plots for those swarms that have sufficient data generally show similar characteristics.

#### 2.5J.4.5 Non-Swarm Shallow Seismicity

Shallow earthquakes remaining after the removal of the swarms are shown in Figure 2.5J-25. It can be seen that much of this non-swarm activity is concentrated in the defined swarm areas. This concentration is partly due to incomplete separation of the swarm activity using the 10-day cluster time-length, as discussed in Section 2.5J.4.3. Because the spatial distributions of low-magnitude swarm and non-swarm shallow activity in the Pasco Basin area are essentially the same, this similarity suggests that the nature and causes of both categories of earthquakes are the same and that clustering in time is only one characteristic of the total Pasco Basin shallow seismicity. This conclusion is further supported by the similarity of the frequency-magnitude plot for shallow non-swarm earthquakes to the plot for swarm earthquakes (Figure 2.5J-29).

#### 2.5J.5. SOURCES OF SHALLOW EARTHQUAKES

As discussed in Sections 2.5J.3 and 2.5J.4, the shallow microearthquakes that have occurred in the central Columbia Plateau appear to represent a process of crustal deformation that is distinct from the commonly observed crustal earthquake mechanisms. This distinction is suggested (1) by the narrow range of shallow depths within which most of the earthquakes have occurred; (2) by the frequency-magnitude slopes of 1.00 or more; and (3) by the predominance of earthquake swarms. Therefore, based on these occurrence patterns, the geological features of the central Columbia Plateau were evaluated to assess their physical capability as sources for shallow seismicity and their spatial correlation with the areas of shallow seismicity.

### 2.5J.5.1 Fractures in the Columbia River Basalts

Mogi's (1963) suggestion that earthquake swarms tend to be characteristic of heterogeneous or highly fractured rock fits the central Columbia Plateau, where the basalts of the Columbia River Group at or near the surface are known to be highly jointed. The primary jointing in the Columbia River basalts appears to be a response to tensional stresses that develop during the cooling of a flow. The results are characteristic primary fractures, among them vertical columns and horizontal fractures. The descriptive terminology in the following paragraphs, based on classical architectural format, was proposed by Tomkeieff (1940) to describe basalt flows of the Giant's Causeway and was refined by Spry (1962). Basalt flows from various parts of the Columbia Plateau are described in Mackin (1961), Schmincke (1967), Myers (1973), Reidel (1978), Ross (1978), and Myers and Price (1979). A detailed investigation of primary or cooling flow features at limited localities may be found in Long (1978).

Ideally, a basalt flow consists of an upper and lower colonnade, a central entablature, a flow top, and a basal pillow-palagonite zone. Colonnade and entablature comprise the major portion of a flow, but flow tops have been known to comprise nearly half a flow's width (Long, 1978). Columns are polygonal, usually six-sided, and have interlocking straight faces, although wavy "pinch and swell" faces are common. Colonnade columns are most often normal to the flow width and range in diameter from 0.5 to 3 m (average 1 to 2 m). Horizontal and oblique fractures in the colonnade are usually spaced 0.25 to 1 m apart and may shape the columns into stubby, hackly, and/or rubbly forms. Entablature columns are generally slender (a few centimeters to 0.5 m in diameter) and are often arranged in seemingly chaotic patterns that are combinations of fan, rosette, and chevron arrangements. Other primary flow interior features are horizontal "platy joint" zones and vesicular zones (Spry, 1962; Long, 1978). Flow tops are usually vesicular and may consist of a rubbly breccia, or they may be tightly welded (Long, 1978). Basal pillow-palagonite zones are more rare, occurring only where a flow entered a pre-existing body of water.

Columnar joints within the colonnade are roughly vertical, while in the entablature, they commonly exhibit the more diverse patterns described above. The joints are usually narrow bands (less than 1 mm wide) and may be filled and/or mineralized, presumably by montmorillonite clays (Long, 1978). These features are extensional and rarely, if ever, show relative displacement between columns (P. Long, 1981, personal communication). Within either colonnade or entablature, joints may often extend through the width of the





section. In some cases, joints extend through both sections, but this is the exception rather than the rule.

In addition to the primary cooling features described above, other types of fracture zones have been observed in basalt flows. Some of these may have originated during cooling and were probably enhanced by subsequent deformation. Other fractures, are clearly tectonic in origin, such as in the Sentinel Bluffs and Schwana stratigraphic sections in the Saddle Mountains (Long, 1978) and in the Emerson Nipple stratigraphic section in the Umtanum Ridge anticline (Myers and Price, 1979).

Tectonic fractures (as studied at the above localities) differ from cooling joints in that the fractures are wider zones of breakage (up to several centimeters across) and consist of bands of fractures or, in places, breccia. The tectonic fractures are faults along which shear failure has occurred. They are oriented at angles to the primary cooling features, either steeply vertical (Long, 1978) but more commonly as low-angle conjugate shears (Price, 1981), and often displace primary cooling features. Tectonic fractures have been observed to extend several tens of meters in the plane of a flow and may extend an unknown distance into the flow. Several low-angle fractures in the Umtanum Flow and the B flow of the Schwana sequence; for example, measured up to 90 m.

Tectonic fractures, are often sinuous and may, in cases, coincide with the plane of primary cooling. They may transect more than one flow, but such a situation is difficult to observe and may not be common (P. Long, 1981, personal communication). Finally, tectonic fractures have been observed most often in basalt sections near the hinges of anticlinal folds (Long, 1978; Myers and Price, 1979; Price, 1981). Fewer such fractures have been reported in relatively flat basalt sections (E. Price, 1981, personal communication), such as borehole DC-7 (Myers and Price, 1979), although this may reflect the lack of data from such areas.

Based on his studies of the Wooded Island swarm, Rothe (1978) speculates on the causative mechanisms for shallow seismic activity in the central Columbia Plateau as a whole. Rothe proposes columnar joints within the basalts as the most likely pre-existing zones of weakness along which slip would occur. He suggests that the "characteristic size" swarm earthquake is related to the characteristic dimensions of the basalt columns. Assuming that the earthquakes do occur on columnar joints, this theory implies that the occurrence of each earthquake involves only one basalt flow. The variety of focal mechanisms observed is cited as further evidence supporting slip along columnar joints. Rothe states that such

AMENDMENT NO. 18  
September 1981

variety indicates slip on a "random collection of shear planes." He also states that, because only a few mechanisms fit the majority of events, slip is preferred along those planes that are favorably oriented with respect to the north-south direction of maximum compressive stress.

Rothe's (1978) proposed seismic source--slip on columnar joints--does not fit the available seismological observations nor the slips along the tectonic fractures described above. Malone et al. (1975) and Rothe (1978) suggest that shallow earthquakes within a particular swarm occur on a variety of planes, rather than on a single fault. The limited number of fault plane solutions that describe most of the events studied by Malone et al. (1975) suggests that slip preferentially occurs on non-vertical fractures that are favorably oriented with respect to the regional stress direction. Tectonic fractures agree with this, since they are most often oriented as conjugated shears to the observed regional compressive stress (Price, 1981). Columnar joints are generally near-vertical and oriented independent of the regional stress field. However, localized stress concentrations within the highly heterogeneous basalt are also likely and could cause slip on planes having other orientations. In this fashion, slip might occur on cooling joints (not necessarily columnar joints) that were optimally oriented so as to move when stressed

As suggested by Rothe (1978), it seems likely that earthquakes would occur only in basalt and not in interflow zones, because inflow zones appear to be less capable of storing sufficient strain energy. If slip occurs primarily on tectonic fractures, then each earthquake would probably involve one or possibly two adjacent basalt flows, although this does not preclude the possibility of successive earthquakes occurring in adjacent flows.

In the case of either slip on existing tectonic fractures (faults) or slip on cooling joints, a characteristic limiting dimension is implied. For cooling joints, this limiting dimension would be the width of cooling zones in a single basalt flow--on the order of 10's of meters (Myers and Price, 1979). For tectonic fractures, the limiting dimension would be the equivalent of the width of one or two flows--in the range of 100 to 150 m. These dimensions are consistent with the limited field observations of tectonic fractures discussed

It is not known what the lateral extent of tectonic fractures may be. It is reasonable to assume that, since these fractures are related to folding and other deformation processes within the basalt sequence, it is likely that they have greater extent laterally than vertically.. For purposes of estimating earthquake source dimensions, the occurrence of an individual earthquake is assumed to be associated with an approximately equidimensional slip surface. Seismic sources with fault rupture length much greater than width are usually those involving faulting through the entire crust. For example, in central California smaller earthquakes ( $M_L < 5$ ) studied, using aftershock, exhibit generally equidimensional source areas, while earthquakes larger than about  $M_L 6$  have fault lengths in excess of thickness of the brittle crust.

The maximum source dimensions of this earthquake model are comparable with source dimensions that have been derived for earthquakes in the magnitude range  $M_L 0$  to  $M_L 3$  in other areas (Smith et al., 1974; Bakun and Bufe, 1975; Majer and McEvilly, 1979; McGarr et al., 1981).. These studies used Brune's (1970, 1971) formulation to derive seismic moment, source dimensions, fault displacements, and stress drops from long-period spectral levels and corner frequencies of observed microearthquake displacement spectra. Unfortunately, minimal spectral data presently exist for Columbia Plateau earthquakes. Malone (personal communication, July 1981) has estimated that the seismic moment of zero-magnitude earthquakes that occurred as part of the Eltopia C and Royal D sequences is approximately  $5 \times 10^{15}$  dyne-cm. The corner frequencies of these events were apparently higher than the upper frequency response of the recording systems used and, thus, are probably greater than 25 Hz.. This seismic moment is in good agreement with those observed for zero magnitude earthquakes in the Geysers geothermal field by Majer and McEvilly (1979), who also observed corner frequencies greater than 20 Hz. Although both the structure and rock type for the Geysers (hydrothermally altered Franciscan graywacke) are different than those of the central Columbia Plateau and the seismicity of the Geysers is related to fluid removal, the swarm-like seismicity of the

Geysers appears to have features similar to those exhibited by earthquakes in the central Columbia Plateau. The  $b$  values calculated for the Geysers area and for the surrounding region are similar to those calculated for central Columbia Plateau swarm earthquakes and the Columbia Plateau. Such high  $b$ -values suggest a low stress in a fractured medium (Scholz, 1968a). Microearthquakes at the Geysers are concentrated at focal depths of less than 5 km, and the reservoir rock in this area is highly fractured. Calculated source dimensions for  $M_L$  0 to 2 earthquakes at the Geysers are in the range 50 to 100 m, which is similar to the observed range of fracture lengths in the Columbia River basalts noted earlier in this section. Associated estimated stress drops and fault displacements are on the order of 0.1 to 1 bar and 0.01 to 1 mm, respectively.

Using the relationship between  $M_L$  and seismic moment empirically derived by Majer and McEvilly (1979) and assuming an upper bound source dimension of 150 m for a tectonic basalt fracture, a displacement of about 0.5 cm and a stress drop of about 10 bars would be associated with an earthquake of  $M_L$  3.0. These values are within the ranges commonly observed for microearthquakes and are compatible with fractures observed in the Columbia Plateau basalt flows. The average displacement for a magnitude  $M_L$  4.0 earthquake, on the other hand, would be about 1 m, which is unreasonably high for these fractures of such small dimensions. In locations where surface fault displacements have been mapped (summarized in Washington Public Power Supply System, 1981), the dimensions of fault length and displacement exceed the values discussed here and larger earthquakes might be postulated. However, based on the observations and inferred occurrence of tectonic fractures within basalt flows, it appears that a reasonable upper-bound magnitude for earthquakes occurring on the tectonic fractures should be about  $M_L$  3.0.

#### 2.5J.5.2 Larger Earthquakes

The earthquakes within the central Columbia Plateau that are most likely to be associated with large-scale structures are the largest historical events, namely the 1973 Royal Slope and the 1918 Corfu earthquakes, summarized below:

##### 20 December 1973 Royal Slope

The  $M_C$  4.4 Royal Slope earthquake is the largest instrumentally located event to have occurred in the central Columbia Plateau. The focal depth of this event, based on the eastern Washington network, was 2.5 km. This event did not exhibit aftershock behavior in a classic sense (see Section 2.5J.4.4), but the associated microearthquake sequence behaved like a Columbia Plateau earthquake swarm. The spatial distri-

AMENDMENT NO. 18  
September 1981

bution of epicenters for the Royal D sequence does not define any obvious lineation suggestive of a large fault. The plot of Malone et al. (1975, Figure 2), which is based on data recorded by a dense, temporary local network, does indicate an alignment of epicenters that trends S60° from near the center of activity for approximately 2 km. Malone et al. (1975) noted that most of the events that occurred within a few days of the mainshock fit into a single fault-plane solution, whereas most events that occurred some weeks later fit a different solution. The fault-plane solution for the initial aftershocks is similar to the solution determined for the  $M_C$  4.4 event (Figure 2.5J-30) and indicates almost pure reverse-slip movement on a plane striking east or slightly south of east. It appears, therefore, that the mainshock occurred on an east- or east-southeast-striking reverse fault and was followed by low-level activity on the fault; however, the mainshock also triggered swarm activity on structures having different orientations.

The orientation and style of faulting indicated by the focal mechanisms agree with the generally observed north-south horizontal compressive regional stress field. However, based on available geologic mapping, no specific fault is known to occur in the vicinity of the 1973 epicenter. The epicenter was located north of the central anticlinal fold of the Saddle Mountains (Figure 2.5J-31) and lies along the band of relatively high, shallow activity between Saddle Mountains and Frenchman Hills (Section 2.5J-3.1, Figure 2.5J-19).

#### 1 November 1918 Corfu Earthquake

The only other magnitude 4+ earthquake located in the central Columbia Plateau was the 1 November 1918 Corfu earthquake. The magnitude of this event has been estimated as  $M_S$  4.4, based on a seismic moment computed from the seismogram recorded at Spokane (SPO), and employing an  $M_S$ -moment relationship calibrated using the SPO record of the 1936 earthquake ( $M_S$  5-3/4) near Walla Walla. The Earth Physics Branch in Canada reported an  $M_L$  4.3 event, although this magnitude may be based on maximum intensity (Woodward-Consultants, 1978).

The epicenter of the 1918 earthquake has been reported at 46.7°N, 119.5°W (Rasmussen, 1967; Coffman and von Hake, 1970). However, it is not clear how this location was determined, since the event was recorded at only one station (SPO). This location is 15 km southeast of the area of maximum intensity (MM V) at Corfu, Washington (Figure 2.5J-31), which was originally reported in the Bulletin of the Seismological Society of America (BSSA, 1918). Fifer (1966) concluded that the intensity at White Bluffs, only 2 km from

AMENDMENT NO. 18  
September 1981

the quoted epicenter, was probably MM IV.. The earthquake, therefore, probably occurred in the vicinity of Corfu,, north of the quoted epicenter. Based on the value of the maximum intensity, the small felt area, and the small magnitude, the earthquake was likely shallow and is assumed to have occurred in the shallow crustal zone.

The location of the 1918 event was further investigated using the seismogram from SPO. The P- and S-wave arrivals on the records are well defined for both horizontal components and give an estimated S-P time interval of 21.7 seconds at SPO. The Newport (NEW) Wood-Anderson seismogram for the 20 December 1973 event was used to calibrate an S-P versus distance relationship. Because NEW is at about the same azimuth and distance from the 1973 epicenter as is SPO from the epicentral area of the 1918 event and because, at these distances, P- and S-waves refracted from the top of the mantle are the first arrivals, this calibration should be valid for the 1918 event, given the depth assumption made above. The relationship found is 1 sec (S-P) = 7.95 km. Using this relationship, a best estimate distance of the 1918 epicenter from SPO is 173 km, which is shown by the solid arc in Figure 2.5J-31. Uncertainty in the estimates of the S-P time interval range from 20.7 to 22.5 seconds, which correspond to distances of 164 and 179 km, respectively, shown as dashed arcs on Figure 2.5J-31.

The epicenter of the 1973 earthquake falls very close to the best estimate of the distance of the 1918 event from SPO. This proximity suggests that the events may have occurred near the same location, north of the Saddle Mountains, which is supported by the similarity in the intensity data for the events. The 1918 event was reported as having "shook goods from the shelves" at Corfu (BSSA, 1918); during the 1973 event "objects fell from shelves and pictures fell from walls" in Othello and vicinity (Coffman and von Hake, 1975). The reports of landslides associated with the 1918 event are not considered to be a good measure of intensity, since landslides in the vicinity of the Saddle Mountains are common and could be unrelated to earthquakes. Because Corfu and Othello are approximately the same distance from the 1973 Royal Slope epicenter, the intensity data also suggest that the events occurred in the same vicinity. The 1918 earthquake apparently occurred within the cross-hatched area shown in Figure 2.5J-31, and the most likely epicenter is close to the position plotted on this figure.

The similarity of the 1918 and 1973 events suggests that both events could have occurred in the same geologic environment to the north of the Saddle Mountains anticlinal axis.



### 2.5J.5.3 Focal Mechanisms for the Shallow Crustal Zone

Single-event fault plane solutions were computed for those earthquakes for which at least 15 first motion readings were reported and that are surrounded by stations through at least 230 degrees in azimuth. About 10 events were examined, and the 8 solutions shown in Figures 2.5J-32 through 2.5J-35 are those for which fault planes can be drawn that are at least moderately consistent with the first motion patterns.

The alignments of epicenters for the Scooteney B and C swarms, shown in Figure 2.5J-26 (see Section 2.5J.4.4), are in an east-northeast direction. The fault plane solution of the only earthquake from these sequences that fits the criteria described above is shown in Figure 2.5J-32. This solution is only moderately constrained and suggests high-angle thrust faulting with a minor strike-slip component on planes striking either north or N30°E. An alternative pure thrust solution is indicated by the dashed curves in Figure 2.5J-32. None of the possible fault planes strike close to the trend of the alignment, which suggests that this earthquake, at least, did not occur on an east-northeast-striking fault plane.

The 1973 Eltopia C swarm (maximum magnitude  $M_C$  2.5) was included in the study by Malone et al. (1975). Using their local network, they located 42 events in the period June through July 1973. Composite focal mechanisms for the latter sequence are well constrained (see Malone et al., 1975, Figure 3). None of the shear planes indicates a northwest-striking fault. Rather, three classes of mechanisms are suggested that strike between northeast and east. This was cited by Malone et al. as the strongest evidence in favor of slip on several planes having different orientations. Therefore, the data for the Eltopia swarm area appear to argue against a single, through-going fault as the source of the earthquakes.

Five single-event fault plane solutions are constructed for events in the Wahluke D sequence (maximum magnitude  $M_L$  2.1) shown in Figure 2.5J-33(a through e). Three of the solutions indicate pure or predominant reverse faulting on planes striking east-west or northeast-southwest. The remaining two solutions indicate reverse faulting on north-northeast-striking planes. The epicentral trends for the Wahluke D swarm are poorly defined, and no correlation with the focal mechanisms is convincing.

The only other single-event fault plane solutions for the swarm areas that could be moderately well constrained are for events of the Royal E and Smyrna C swarms, shown in Figures 2.5J-34 and 2.5J-35, respectively. Neither of these swarms exhibit discernable epicentral alignments.



The focal mechanisms for shallow crustal events discussed here exhibit generally consistent high-angle, predominantly reverse faulting, with varied orientation of the maximum compressive stress axis. While north-south maximum compression is usually observed in each sequence of earthquakes, other directions are observed as well. This suggests that a generally pervasive, horizontal, roughly north-south maximum compressive stress system exists. However, if the difference between maximum and minimum stress (deviatoric stress) were low, local variations in stress combined with the existence of fractures and joints of many orientations would allow the observed rotations in the apparent maximum stress axis orientation. The occurrence of stress release at the shallow depths of 3 km or less, where the confining pressure is low, also favors variations in mechanisms due to local effects.

Based on geodetic measurements for the period 1972-1979, Savage et al. (1981) noted that the strain rate in the central Columbia Plateau was so low as to be marginally significant with respect to random and possible systematic errors, if strain had accumulated at all during the observation period. Such a low strain rate would be consistent with the low level of tectonic stress in the central Plateau.

#### 2.5J.5.4 Spatial Patterns of Shallow Seismicity

A detailed examination was conducted at a map scale of 1:62,500 to investigate possible correlations of seismicity with mapped structures in the Gable Mountain-Saddle Mountains-Frenchman Hills area. For this examination, a three-dimensional model, constructed from Mylar epicentral plots for a series of depths and viewed in a plastic layer model, was used. No correlations and no well-defined planar trends of earthquakes that might define active faults were observed. Most events in this area larger than  $M_L$  3.0 have occurred between Saddle Mountains and Frenchman Hills, at an appreciable distance from the axis of either structure and from mapped faults. However, the pattern of seismicity between and following the trend of the anticline suggests that the occurrence of potential seismic sources may be influenced or controlled by the major anticlines within the central Columbia Plateau.

The detailed examination of the epicentral plots and cross-sections shown in this report and of the three-dimensional model did reveal numerous apparent alignments of hypocenters. None of these clearly occurred along mapped structures or projections at depth of such structures. The available focal mechanism data do not confirm or support the

coherence of such alignments. Based on the available data, these alignments appear to be fortuitous and do not indicate potentially significant earthquake sources.

#### 2.5J.6 ASSOCIATION OF SHALLOW EARTHQUAKE ACTIVITY WITH IRRIGATED AREAS

The observed tendency for earthquakes to be concentrated within portions of the central Columbia Plateau has been discussed in Sections 2.5J.3, 2.5J.4, and 2.5J.5. Previous investigators (Turcotte, 1975; Rothe, 1978) have suggested that changes in ground-water levels may be at least partially responsible for differences in seismicity between areas within the Hanford Reservation and the surrounding areas. Land usage in and surrounding the Pasco Basin can be divided, in a general sense, into agriculture and the Hanford Reservation operations. The agricultural land is north, east, and southwest of the Columbia River, outside the Hanford Reservation, and is used primarily for crops requiring irrigation. It has been proposed that the differences in the earthquake occurrence patterns observed within the Hanford Reservation and the areas surrounding the Reservation are spatially correlated with, and in some way related to, irrigation (Turcotte, 1975). This section analyzes this possibility and is divided into four parts:

- (1) A summary of the hydrogeology of the Columbia Basin (the term "hydrogeology" is used to refer to ground-water characteristics);
- (2) A discussion of fluid-induced earthquakes and the mechanisms proposed for earthquake occurrence;
- (3) An analysis of the spatial and temporal characteristics of the earthquake activity and irrigation in the central Columbia Plateau;
- (4) A discussion of the effect that ground-water changes have on earthquake activity and the physical mechanisms that are responsible.

##### 2.5J.6.1 Hydrogeology of the Central Columbia Plateau

Hydrogeology within the central Columbia Plateau area has been extensively studied by Gephart et al. (1979). The features of the hydrogeologic system relevant to this study are summarized below.

In general, the hydrogeologic system of the central Columbia Plateau can be characterized as unsaturated and saturated. The unsaturated zone occurs at shallow depths within the

AMENDMENT NO. 18  
September 1981

Hanford and Ringold Formations and ranges in thickness from 1 to 350 feet on the Hanford Site to over 450 feet outside the Reservation. The water table lies below the unsaturated zone in the Ringold Formation. The unconfined aquifer, which lies at the top of the saturated zone, attains a thickness of over 200 feet in some parts of the central Plateau, with the bottom considered to be either the top of the basalt or a thick unit of low-permeability silts and clays comprising the base of the Ringold Formation.

Recharge comes from both natural and artificial sources. Natural recharge is due primarily to precipitation occurring in the Cascade Mountains, from surface runoff and from the Columbia River during its high stages. Artificial recharge within the Hanford Reservation has come from the disposal of liquid wastes in ponds, which has raised the water table locally as much as 85 feet. Outside the Reservation, artificial recharge comes from irrigation, primarily in the areas to the north and east. The Columbia River acts as the major discharge area and, in general, dictates the direction of ground-water flow.

The confined aquifer system is below the water table and is found principally within the Columbia River Basalt Group. These basalts are composed of flows overlying one another, separated by more permeable interflow and interbed zones (Gephart et al., 1979). In general, the interflow zones usually lie between zones composed of dense, relatively impermeable basalt flows.

A large percentage of the land in the central Columbia Plateau area is irrigated by surface water transported through a canal system built and operated by the Bureau of Reclamation's Columbia Basin Irrigation Project. The Columbia Basin Irrigation Project began delivering water in 1952. The areas under irrigation have increased gradually since that time. The project covers about 10,000 km<sup>2</sup> and distributes water from the area just below Grand Coulee Dam in the north to the confluence of the Snake and Columbia Rivers near Pasco. To a lesser extent, portions of the central Columbia Plateau are irrigated with ground water pumped from both the unconfined and confined aquifers. Irrigation from both surface-water and ground-water sources utilizes approximately 950,000 acre-feet annually. The areal extent of irrigation is shown in Figure 2.5J-36. To the south and west of the Columbia River outside the Hanford Reservation, the area under irrigation is limited. Table 2.5J-6 (reproduced from Gephart et al., 1979), summarizes the annual water use for irrigation in the area.

### 2.5J.6.2 Mechanisms of Fluid-Induced Seismicity

Several types of fluid-related occurrences have resulted in the stimulation of earthquakes: the filling of reservoirs behind dams, the rise and fall of river levels, the injection of fluid into rocks at depth, the withdrawal of fluids from underground reservoirs, and irrigation.

The list of reservoirs that have been associated with earthquakes is quite large. Numerous cases of reservoir-induced seismicity (RIS) are reviewed by Gupta et al. (1972) and Packer et al. (1979). In a summary of more than 60 of the several hundred reported cases of RIS, Packer et al. (1979) concluded that several common features encourage the occurrence of RIS. The area must be faulted, the area must have a history of seismicity (although the current level of seismicity can be extremely low), and the tectonic stress level must be close to the failure strength of the stressed material.

There are two well-documented cases of seismicity induced by fluid injection into rocks at depth: the Rocky Mountain Arsenal Well, near Denver, Colorado (Healy et al., 1968; Hsieh et al., 1981; Herman et al., 1981), and the injection of fluid into the Rangely Oil Field, Colorado (Raleigh et al., 1972). These authors have suggested that three conditions at each area were responsible for triggering the seismicity:

- (1) The area was pre-stressed to a level close to the stress necessary for failure.
- (2) The porosity resulted from a fracture system in crystalline rock that was otherwise non-porous and impermeable.
- (3) Fluid was injected at rates and pressures sufficient to increase the pore pressure.

The increased pore pressure in the fractures apparently caused these factors to propagate. Once these fractures reached a critical length, earthquakes occurred.

Fluid extraction has also induced shallow seismicity. The best documented cases of seismicity induced from fluid extraction are associated with petroleum production and ground-water withdrawal. Petroleum-production-induced seismicity has been reported in the Goose Creek, Texas oil field where earthquakes occurred coincidentally with land subsidence (Yerkes and Castle, 1976). In another incident, eight earthquakes occurred within the Wilmington, California oil field as a result of oil withdrawal. The slip associated

with these events sheared off several hundred wells over an area of approximately 2 km<sup>2</sup> (Yerkes and Castle, 1976). In the Eloy-Picacho area of Arizona, seismicity has been attributed to ground-water withdrawal (Yerkes and Castle, 1976). In this area, ground-water withdrawal had exceeded recharge for several years, and land subsidence and earth fissuring were observed coincident with the occurrence of the seismicity. Fluctuations in river levels have also induced seismicity. Such events have been noted along the Mississippi and Colorado Rivers (McGinnes, 1963; Wong and Simon, 1981). In both cases, a fall in the river level was coincident with the seismicity.

All of the above cases are similar in that they involve the perturbation of the ambient stress field by the introduction or withdrawal of fluid. Several mechanisms have been proposed to explain fluid-induced seismicity (Gough and Gough, 1970; Kisslinger, 1976; Martin, 1972): (1) changes in fluid levels cause changes in shear stresses across a fault zone; (2) changes in pore pressure cause changes in the effective stresses; (3) changes in stress levels and pore pressure may trigger the release of large pre-stresses; and (4) the acceleration of rock deformation resulting from stress-enhanced corrosion of a fracture or crack tip in the presence of a fluid. An increase in surface load alone, as in mechanism (1), has been discounted as the sole cause of seismicity because the deepest reservoirs provide surface loads of only about 20 bars, which is insufficient to be the cause of earthquakes in an unstressed environment. In general, an increase in surface loads will increase normal force across a fault and encourage a more stable condition. Therefore, present theory holds that, in order to induce seismicity, the rock must be pre-stressed to a substantial fraction of its ultimate strength. In most cases of induced seismicity, a combination of increased vertical stresses, increased pore pressure, and stress corrosion are considered to be the cause of earthquakes. (Kisslinger, 1976; Martin and Durham, 1975). Pore pressure effects on effective stress are discussed in Section 2.5J.6.4.

Stress corrosion cracking, which is the environmentally induced sub-critical crack growth under or applied stress (Anderson and Grew, 1977), is thought to be the controlling process in time dependent geologic processes such as earthquakes associated with reservoir loading and aftershocks (Scholz, 1968b; Kisslinger, 1976). Rapid crack propagation, such as an earthquake, occurs when the stress intensity near the tip of a crack equals or exceeds a critical value. In silicate rocks, stress corrosion cracking occurs in the presence of water at stress intensities above a threshold value but below that necessary for fast crack propagation. The rate of stress corrosion cracking is sensitive to factors

such as level of stress, chemistry of the crack environment, amount of water present, and temperature. In a saturated environment, stress corrosion cracking can also limit the magnitude of earthquake occurrence. It has been suggested that water reduces the stress at a crack tip necessary to cause rupture by an order of magnitude (Martin and Durham, 1965). The mechanism of stress corrosion cracking has been proposed to explain continued low-level earthquake occurrences long after the filling of a reservoir has occurred (Martin, 1972).

#### 2.5J.6.3 Spatial Distributions of Earthquake Activity and Irrigation Within the Pasco Basin Area

The spatial coincidence of seismicity and irrigation in the Hanford area was first proposed by Turcotte (1975). In this study, he analyzed the earthquake activity that occurred from March 1969 to September 1972 and compared that activity with irrigation patterns in the area. Turcotte suggested that a higher level of induced earthquake occurrence is superimposed on a low-level background occurrence of earthquakes. Turcotte (1975) statistically defined and separated these levels of earthquake occurrence, and he observed a high correlation between the remaining earthquake activity and irrigation. In this section, the spatial and temporal patterns of the earthquake activity within the central Columbia Plateau are compared with the spatial and temporal patterns of irrigation, using the techniques developed by Turcotte (1975) and the 11.3-year data set.

As in Turcotte's (1975) report, the region containing the irrigation project was partitioned by a 500-element grid (Figure 2.5J-36) that covers the area of longitudes 46°00'N to 47°15'N and latitudes 118°40'W to 120°00'W. The dimensions of each grid element are 3 minutes of latitude by 4 minutes of longitude. The size of a single grid element is about twice the uncertainty in higher-quality earthquake epicentral locations (see Section 2.5J.2.2). A grid element is considered "irrigated" if any part of it contains surface water, waste water, or ground water used for irrigation. Figure 2.5J-36 shows the distribution of grid elements with respect to irrigation.

As described by Turcotte (1975), the background earthquake activity was defined and separated. The background activity consists of those earthquakes that may be expected to occur in any given block, regardless of whether or not irrigation is present. Once the background activity is defined, the remaining earthquakes are presumed to be those events that occur in any given block due to some inducing mechanism. Using Turcotte's method, 0, 1, or 2 events per block are

assumed to represent the background activity. The probability distribution of random earthquake occurrence can be described by a Poisson distribution:

$$P(n) = \frac{\lambda^n e^{-\lambda}}{n!} \quad (2.5J-1)$$

$\lambda$  is the average number of background earthquakes per block over the entire grid, and  $n$  is number of earthquakes per block. The values  $n = 0, 1$ , and  $2$  were used to calculate  $\lambda$ ; the value  $\lambda = 0.38$  provides the best fit to the data for these values of  $n$ . Table 2.5J-7 lists the number of blocks that have  $0, 1, 2...$ etc. events per block and the observed and calculated probabilities,  $P(n)$ , of the occurrence of  $n$  earthquakes per block.

Using a  $\lambda$  of  $0.38$ , it is predicted that only 3 blocks out of 500 should contain 3 or more events due to random occurrence of the background activity instead of the observed 8. The probability that more than 3 events will occur by chance in any one block becomes progressively smaller for  $n$  greater than 3 events. As seen in Table 2.5J-7, the probability that any given block will contain greater than or equal to 6 events by chance alone is on the order of 1 in 106. Therefore, blocks containing 6 or more events are considered to be caused by a non-random mechanism and were used to examine the association of seismicity with irrigation.

Of the 500 total grid elements in the area studied, 42 grid elements contain 6 or more events. Of these, 32 grid elements lie in irrigated areas, 9 grid elements lie in areas adjacent to irrigated areas, and one grid element lies within the the Hanford Reservation and is spatially coincident with the 200W liquid waste disposal operation shown in Figure 2.5J-41. The grid elements containing six or more events were analyzed to quantify the statistical significance of this spatial association between these grid elements and the irrigated blocks. The probability that grid elements with six or more events are distributed through the irrigated and non-irrigated grids in a manner other than expected by chance was examined. A single ended binomial distribution can be used for this purpose. The distribution is:

$$P(x) = C(n,x) p^{n-x} q^x \quad (2.5J-2)$$

where

$$c(n,x) = \frac{n!}{x! (n-x)!}$$





In equation (2.5J-2),  $n$  is the number of grid elements that contain six or more events,  $x$  is the number of grid elements,  $p(x)$  is the probability of obtaining the observed distribution by chance alone;  $p$  is the fraction of grid elements under irrigation and  $q = 1 - p$  is the fraction of grid elements without irrigation. Out of a total of 500 grid elements, 252 are irrigated and 248 are not irrigated; therefore,  $p = 0.504$  and  $q = 1 - p$  or 0.496. For  $n = 42$ , the probability that 32 out of 42 blocks fall in the irrigated area purely by chance is  $5.64 \times 10^{-4}$ . Since irrigation changes the ground-water levels on a regional scale, the grids adjacent to the irrigated areas can be included in the analysis. In this case,  $p(x)$  becomes approximately  $6 \times 10^{-11}$ . Thus, the spatial relationship of seismicity to irrigation or other surface fluids appears to be statistically strongly correlated.

#### 2.5J.6.4 Analysis of the Temporal Association of Ground-Water Level Changes and Earthquake Activity

In order to evaluate the effects of irrigation on ground-water characteristics, well-level data in the central Columbia Plateau were gathered and compared with both the temporal behavior of earthquake activity and the temporal pattern of irrigation.

In 1948, in conjunction with the Bureau of Reclamation, the U.S. Geological Survey began an intensive well-level monitoring program, and have monitored several hundred wells since 1948. Eighty wells within an area bounded by longitudes  $46^{\circ}30'N$  to  $47^{\circ}15'N$ , and latitudes  $118^{\circ}40'W$  to  $120^{\circ}W$ , were chosen for analysis. This area within the central Columbia Plateau was chosen for analysis because of the large amount of well level data available. Figure 2.5J-37 depicts the study area, well locations, and the shallow earthquake seismicity for the time period 1969 through 1980. Figures 2.5J-38 through 2.5J-40 are representative plots of the water-level data gathered at all wells. Most of the wells chosen for comparison were drilled into the basalt, were uncased, and were drilled to depths such that the water levels measured are representative of water-table elevations. Table 2.5J-8 is a summary of the data.

Prior to 1952, the water levels were several hundred feet below the ground surface. With the onset of irrigation in 1952, ground-water levels began to rise. This rise was gradual, occurring over a period of several years. In general, the water levels have risen to within 30 feet of the surface throughout the central Columbia Plateau and have remained fairly constant (except for some seasonal variations). In many cases, the ground-water level reaches the surface. In

this investigation, the maximum change in ground-water level was 440 feet recorded at well No. 46.

Water-level changes within the Hanford Reservation have been monitored since 1944. Artificial recharge to the unconfined aquifer is due to liquid waste disposal operations in the 200 areas shown in Figure 2.5J-41. The discharges were confined to ponds within these areas, but the effects on the ground-water levels have extended well beyond these areas (Gephart et al., 1979). Beneath these ponds, two ground-water mounds formed. More water was being discharged to the aquifer system than could be transported away. Beneath the 200W area, the water table has risen 85 feet since the start of disposal operations in the mid-1940's. Figure 2.5J-41 shows the ground-water level changes that have occurred within the Hanford Reservation for the time period 1944 to 1978 (Gephart et al., 1979).

Several comparisons were made between ground-water level changes within the Hanford Reservation and the study region described above. In general, the changes in ground-water levels within the Reservation have been approximately 10 to 20 feet. As described above, an 85-foot change in ground-water levels was recorded in the vicinity of the 200W disposal site. While ground-water levels have changed by a hundred feet or so to the north of the Hanford Reservation, the ground-water level changes within the Reservation have been substantially less.

As a comparison of temporal patterns of seismicity with irrigation, the volume of irrigation water is plotted in Figure 2.5J-42 for the period 1969 through 1981. Water usage for irrigation peaks during the summer months and drops during the winter months. This fluctuation in water usage is also seen in Figures 2.5J-38 through 2.5J-40. The monthly occurrence of earthquakes within the Pasco Basin, plotted in Figure 2.5J-47, was compared with the temporal variation in irrigation and ground-water level variations. There does not appear to be any seasonal periodicity to the seismicity, and comparison of the temporal behavior of the seismicity with the temporal behavior of irrigation and well-level data shows no correlation. However, the lack of correlation may be due to the fact that seismic recording did not begin until 17 years after irrigation began. As the well-level data shows, most of the change in ground-water levels had occurred prior to this time. One possible case of irrigation-related seismicity prior to instrumental coverage was reported in 1955 in the vicinity of Scooteney Reservoir (Woodward-Clyde Consultants, 1978). Nearly 200 events occurred in a swarm-like sequence during January through March of 1955. Ground-water loading due to irrigation was thought to be the cause of these events.

A search was made of the available hydrogeologic literature on the central Columbia Plateau to determine if the fluctuations in ground-water levels within the shallow basalts affected the ground-water characteristics of the deeper basalts. Little data are available on the deeper basalts and no conclusions could be made. However, as discussed in Section 2.5J.5.1, fractures and joints probably traverse individual flows or series of flows, allowing for long-term vertical permeability.

#### 2.5J.6.5 Physical Mechanisms for Irrigation-Induced Seismicity

In most cases of induced seismicity, there are two common factors: (1) the state of tectonic stress is such that, on a regional scale, the rocks are stressed to a high percentage of their ultimate strength; and (2) pre-existing faults and fractures are present (Raleigh et al., 1972; Healy et al., 1968; Kisslinger, 1976). Both of these characteristics are present in the central Columbia Plateau, as evidenced by the ongoing earthquake activity and by the highly fractured nature of the basalts. It is important to understand that factor (1) does not necessarily imply that the magnitudes of the regional stresses are high. In fact, the shallow nature of the earthquakes combined with the fact that the basalts are highly fractured suggests that the ability of the material to store strain energy is limited and the ultimate strength of the basalts may be low (Section 2.5J.5.3).

The triggering process may result from three independent causes: (1) a change in the magnitude of the principal stresses; (2) a change in pore pressure; and (3) the acceleration of crack growth in the presence of water. Triggering process (1) and (2) are discussed below. Triggering process 3 has been discussed in Section 2.5J.6.2.

The Coulomb Failure criterion best describes the failure process associated with (1) and (2) above. The criterion can be expressed as

$$\tau = \tau_0 + \mu_0 \quad (3)$$

which states that the shear stress at failure,  $\tau$ , on a fault or fracture plane is equal to the sum of the intrinsic shear strength,  $\tau_0$ , and the product of the effective stress,  $\sigma_E$ , and the coefficient of shearing resistance,  $\mu$ . The effective stress is expressed as:

$$\sigma_E = \sigma - P \quad (4)$$



where  $\sigma$  is the total stress and  $P$  is the pore pressure. The strengths and compressibilities of rocks and soils are controlled by the effective stress rather than by the total stress (Brace, 1972). The Coulomb Failure criterion is represented by the straight line on Figure 2.5J-44. The state of stress in all directions at a point in the interior of a stressed body can be represented by a Mohr circle. When the circle intersects the Coulomb Failure criterion, failure occurs along the plane associated with the tangent point.

The mechanisms responsible for irrigation-induced seismicity are similar to those for reservoir-induced seismicity. Irrigation, by increasing water-table elevations, changes the stress state and pore pressure characteristics of the basalts. In the central Columbia Plateau region, a plausible mechanism for earthquake occurrence is as follows: (1) ground-water elevations rise, increasing the vertical stress acting to strengthen the basalts; (2) the increase in vertical stress serves to induce a hydraulic gradient causing fluid flow and pore pressure diffusion; (3) after a finite time period, fluid would flow to the basalts below via vertical fractures and/or permeable strata causing an increase in pore pressure and a decrease in the effective stress; (4) stress corrosion at fracture tips would be enhanced due to the change in effective stress; and (5) sub-critical crack growth would be encouraged until the fractures reach a critical length resulting in failure. These failures would tend to be limited in size because at shallow depths ( $<3$  km), the confining stresses are low and, in the presence of water, the strength of the basalts tend to decrease.

#### 2.5J.7. EVALUATION OF EARTHQUAKE MAGNITUDE

One of the more important parameters characterizing the seismicity of the central Columbia Plateau is the maximum earthquake magnitude that may be postulated to take place within the Plateau and in the vicinity of the WNP-1, -2, and -4 sites. In a probabilistic study of earthquake sources (Washington Public Power Supply System, 1981, Appendix 2.5K), known faults or faults postulated to be structurally associated with known anticlines of the central Columbia Plateau are analyzed as potential sources of earthquakes of magnitude ( $M_L$  or  $M_S$ ) larger than 4.0. A variety of techniques were used to estimate the maximum magnitudes associated with those structures; these techniques are principally based on the dimensions of the proposed causative faults. However, as noted in Section 2.5J.5, the occurrence of small-magnitude earthquakes is not directly associated with these known or postulated faults.

In this section of Appendix 2.5J, the features and characteristics of the detailed, instrumentally recorded central Columbia Plateau seismicity are evaluated to constrain the magnitudes of potential earthquakes that could occur on postulated sources within less than approximately 10 km of the site. Earthquakes that could occur in association with any of the faults or postulated faults associated with the Umtanum Ridge-Gable Mountain structural trend, and earthquakes that could occur in association with more distant seismic sources, all of which are generally more than 10 km from the site, are considered in Washington Public Power Supply System (1981, Appendix 2.5K). The potential earthquakes that are not associated with these faults or postulated faults are considered here in terms of the depth zones--shallow, intermediate, and deep (discussed in Section 2.5J.3.1).

#### 2.5J.7.1 Shallow Crustal Sources

The shallow crustal zone (depth of 0 to about 3 km) is characterized geologically, geophysically, and seismologically (see Section 2.5J.4). The larger-magnitude ( $M_C > 3.5$ ) earthquakes in this depth zone have occurred along the seismic trends related to and lying between the Frenchman Hills, Saddle Mountains, and Gable Mountain anticlines and are all associated with swarms of shallow events. Between Gable Mountain and Rattlesnake Ridge in the Hanford Reservation (where the site is located), not only is the seismicity dramatically lower but the size of the largest-magnitude shallow events is less, below  $M_C$  3.0 (see Figures 2.5J-9, 2.5J-10 and 2.5J-17).

A strong statistical correlation exists between increases in the ground-water level due to irrigation and the occurrence of shallow seismicity (see Section 2.5J.6). The causative influence of geologic structures, such as the Saddle Mountains-Frenchman Hills trends (where the  $M_S$  4.4, 1918 and the  $M_C$  4.4 1973 earthquakes occurred) cannot be easily separated from the triggering influence of significant increases in ground-water level; however, the combination of the two influences appears to be associated with both the greatest number of earthquakes and the largest-magnitude earthquakes. The influence of water-level changes appears to trigger the occurrence of earthquakes but not necessarily control their maximum size.

In areas away from the more well-defined surface faults in the Columbia River basalts, shear surfaces described as tectonic fractures or possibly cooling joints within the basalt flows (Section 2.5J.5.1) have been considered as likely source structures for seismic energy release. While the tectonic fractures are found more frequently in association with the



AMENDMENT NO. 18  
September 1981

major Plateau anticlines, they may potentially occur anywhere within the basalt. Based on observations discussed in Section 2.5J.5.1 maximum dimensions of the tectonic fractures are considered to be approximately 150 m, corresponding to earthquake magnitudes of about  $M_C$  3.0.

The following available evidence suggests that the Columbia River basalts are a low-stress environment and, thus, are not likely to be the source of significant earthquakes:

- o The frequency-magnitude slope for shallow earthquakes is high ( $\geq 1.0$ ), suggesting low stress (Scholz, 1968a);
- o The shallow depth, highly fractured medium, and regional folds act as points of compressive stress relief that leads to a limited capacity to store elastic strain energy (Mogi, 1963); and
- o The low strain rate (Savage et al., 1981) and variety of stress orientations for focal mechanisms associated with individual events or groups of events within swarms (Section 2.5J.5.3) are consistent with a low deviatoric stress regime.

Based on the observations and analyses summarized above, the maximum magnitude associated with shallow seismicity that can be expected to occur within the Columbia River basalts in close proximity to the site is approximately  $M_C$  3.0.

However, specific limitations and uncertainties have affected the analyses leading to this value:

- o This instrumental historical record is short (11.3 years)
- o This record of felt earthquakes is also short (approximately 150 years) and incomplete for lower intensities
- o The frequency of occurrence of earthquakes is low
- o Detailed geologic studies of shear surfaces within basalt flows are limited in areas and depths examined.

Based on these limitations and uncertainties, a reasonably conservative maximum magnitude value is  $M_C$  4.0.

Earthquakes of magnitude  $M_C$  5.0 and larger can be reasonably associated with identified geologic structures within the central Columbia Plateau basalts. The approximate fault-plane dimension of such earthquakes, greater than about 2 km, would traverse most of the entire thickness of the basalts. The



existence of such faults would be the loci of repeated earthquakes, and the faults would be identified by significant surface deformation, such as surface faulting or folding. Earthquakes of this size, associated with surface geologic structures, are discussed in Appendix 2.5K (Washington Public Power Supply System, 1981).

The largest historical earthquakes associated with the shallow crustal zone in the Central Columbia Plateau are the  $M_S$  4.4 1918 Corfu and  $M_C$  4.4 1973 Royal Slope events. These earthquakes occurred in broadly constrained seismic zone north of Saddle Mountains (Section 2.5J.5.), approximately 40 km from the site. The frequency of occurrence of earthquakes in this zone appears to be greatly influenced by the presence of irrigation water (Section 2.5J.6).

#### 2.5J.7.2 Intermediate and Deep Crustal Sources

Within the central Columbia Plateau, the intermediate and deep crustal zones (at depths of 3 to 8 km and 8 to 25+ km, respectively) exhibit earthquake activity that is of lower frequency of occurrence and lower historical maximum magnitude, and is increasingly diffuse with depth compared to the earthquake activity of the shallow crustal zone. The diffuse spatial pattern of earthquakes and the regionally coherent north-south stress field are consistent with a broad region of very low deformation that has no identified large-magnitude earthquake sources. Thus, the intermediate and deep crustal zones appear to have less potential for significant seismic sources that might affect the site than does the shallow zone. However, in order to address alternative tectonic models for regional deformation, potential significant seismic sources within this sub-basalt zone are analyzed in Appendix 2.5K (Washington Public Power Supply System, 1981).

AMENDMENT NO. 18  
September 1981

## 2.5J.8 REFERENCES

- Anderson, O.L., and Grew, P., 1977, Stress corrosion theory of crack propagation with applications to geophysics: Reviews of Geophysics and Space Physics, 1977, v. 15, p. 77-104.
- Bakun, W.H., and Bufe, C.G., 1975, Shear-wave attenuation along the San Andreas fault zone in central California: Bulletin of the Seismological Society of America, v. 65, p. 439-460.
- Bell, M.L., and Nur, A., 1978, Strength changes due to reservoir induced seismicity and applications to Lake Oroville: Journal of Geophysical Research, v. 83, p. 4469-4484.
- Bor, S.S., 1977, Scaling for seismic source spectra and energy attenuation in the Chelan Region, eastern Washington: M.S. thesis, University of Washington, Seattle, 76 p.
- Brace, W.F., 1972, Pore pressure in geophysics: in Flow and Fracture of Rocks, Geophysical Monograph No. 16, American Geophysical Union, Washington, D.C., p. 265-274.
- Brune, J.N., 1970, Tectonic stress and the spectra of seismic shear waves from earthquakes: Journal of Geophysical Research, v. 75, p. 4997-5009.
- Brune, J.N., 1971, Tectonic stress and the spectra of seismic shear waves from earthquakes, correction: Journal of Geophysical Research, v. 76, p. 5002.
- Bulletin of the Seismological Society of America, 1918.
- Coffman, L.C., and von Hake, C.A., 1970, Earthquake history of the United States: National Oceanic and Atmospheric Administration, Publication 41-1, Boulder, CO, 208 p.
- Coffman, L.C., and von Hake, C.A., 1975, United States Earthquakes 1973: National Oceanic and Atmospheric Administration Boulder, CO.
- Crosson, R.S., 1972, Small earthquakes, structure and tectonics of the Puget Sound region: Bulletin of the Seismological Society of America, v. 62, p. 1133-1171.
- Crosson, R., 1980, Review of Seismicity in the Puget Sound region from 1970 through 1978: Unpublished report presented at the Lake Wilderness Conference, October 1980.

AMENDMENT NO. 18  
September 1981

- Eaton, J.P., 1976, Notes on the distribution of earthquakes within and near the Hanford Seismic Network, 1969-1974, and preliminary results on crustal structure of the region, obtained from an analysis (by the time-term method) of industrial explosions recorded by the network: U.S. Geological Survey, Menlo Park, CA, 22 p.
- Fifer, N.F., 1966, 1918 Corfu Earthquake: Report 1524, Douglas United Nuclear, Richland, WA, 3 p.
- Gephart, R.E., Arnett, R.C., Baca, R.G., Leonhart, L.S., and Spane, F.A., Jr., 1979 Hydrologic studies Within the Columbia Plateau, Washington: An integration of current knowledge: Report RHO-BWI-ST-5, Rockwell Hanford Operations, Richland, WA.
- Gough, D.I., and Gough, W.I., 1970, Load induced earthquakes at Lake Kariba-II: Geophysical Journal of the Royal Astronomical Society, v. 21, p. 70-101.
- Gupta, H.K., Rastogi, B.K., and Narain, H., 1972, Common features of reservoir associated seismic activities: Bulletin of the Seismological Society of America, v. 62, p. 481-492.
- Healy, J.H., Rubey, W.W., Griggs, D.T., and Raleigh, C.B., 1968, The Denver earthquakes: Science, v. 161, p. 1301-1310.
- Herman, R.B., Park, S-K, and Wang, C-Y, 1981, The Denver earthquakes of 1967-68: Bulletin of the Seismological Society of America, v. 71, p. 731-745.
- Hill, D.P., 1972, Crustal and upper mantle structure of the Columbia Plateau from long range seismic refraction measurements: Geological Society of America Bulletin, v. 83, p. 1639-1648.
- Hill, D.P., 1978, Seismic evidence for the structure and Cenozoic tectonics of the Pacific Coast States: Geologic Society of America, Memoir 152, p. 145-174.
- Hsieh, P.A., and Bredehoeff, J.D., 1981, A reservoir analysis of the Denver earthquakes: A case of induced seismicity: Journal of Geophysical Research, v. 86, no. B2, p. 903-920.
- Kisslinger, C., 1976, A review of theories of mechanisms of induced seismicity: Engineering Geology, v. 10, p. 85-98.
- Lee, W.H., Bennett, R.E., and Meagher, K.L., 1972, A method of



AMENDMENT NO. 18  
September 1981

estimating magnitude of local earthquakes from signal duration: U.S. Geological Survey Open-File Report.

- Lee, W.H., and Lahr, J.C., 1975, HYPO71 (Revised): A computer program for determining hypocenter, magnitude, and first motion pattern of local earthquakes: U.S. Geological Survey, Open-File Report 75-311, 113 p.
- Lee, W.H., and Wetmiller, R.J., 1978, Survey of practice in determining magnitudes of near earthquakes: World Data Center For Solid Earth Geophysics, Report SE-9, p. 1-102.
- Long, P.E., 1978, Characterization and recognition of intraflow structures, Grande Ronde basalt: Informal Report, RHO-BWI-LD-10, Rockwell Hanford Operations, Richland, WA, 74 p.
- Mackin, J.H., 1961, A stratigraphic section in the Yakima Basalt and the Ellensburg Formation in south-central Washington: Washington State Division of Mines and Geology Report of Investigations No. 19.
- Majer, E.L., and McEvilly, T.V., 1979, Seismological investigations at the Geysers geothermal field: Geophysics, v. 44, no. 2, p. 246-269.
- Malone, S.D., 1977-1980, Annual technical reports on earthquake monitoring of the Hanford region, eastern Washington: Reports prepared for the U.S. Department of Energy and the Washington Public Power Supply System by the Geophysics Program, University of Washington, Seattle.
- Malone, S.D., Rothe, G.H., and Smith, S.W., 1975, Details of microearthquake swarms in the Columbia Basin, Washington: Bulletin of the Seismological Society of America, v. 65, p. 855-864.
- Martin, R.J., 1972, Time-dependent crack growth in quartz and its application to the creep of rocks: Journal of Geophysical Research, v. 77, p. 1406-1419.
- Martin, R.J., III, and Durham, W.B., 1975, Mechanisms of crack growth in quartz: Journal of Geophysical Research, v. 80, p. 4837-4844.
- McGau, A., Green, R.W.E., and Spottiswoode, S.M., 1981, Strong ground motion of mine tremors: Some Implications for Near-Source Ground Motion Parameters, Bulletin of the Seismological Society of America, v. 71, p. 295-319.

AMENDMENT NO. 18  
September 1981

McGinnes, L.D., 1963, Earthquakes and crustal movement as related to water load in the Mississippi valley region: Illinois State Geological Survey, Urbana, IL, Circular 34, 20 p.

McNally, K.C., 1976, Spatial, temporal, and mechanistic character in earthquake occurrence: a segment of the San Andreas fault in central California: Ph.D. dissertation, University of California, Berkeley, 140 p.

Mogi, K., 1963, Some discussions on aftershocks, foreshocks, and earthquake swarms-the fracture of a semi-infinite body caused by an inner stress origin and its relation to the earthquake phenomena (third paper): Earthquake Research Institute Bulletin, v. 41, p. 615-658.

Myers, C.W., 1973, Yakima Basalt flows near Vantage, and from core holes in the Pasco Basin, Washington: Ph.D. dissertation, University of California, Santa Cruz.

Myers, C.W., and Price, S.M., 1979, Geological studies of the Columbia Plateau: Report RHO-BWI-ST-4, Rockwell Hanford Operations, Richland, WA.

Packer, D.R., Cluff, L.S., Knuepfer, P.L., and Withers, R.J., 1979, Study of reservoir induced seismicity: Report prepared for the U.S. Geological Survey under contract No. 14-18-0001-16809 by Woodward-Clyde Consultants, San Francisco, CA, 222 p.

Pitt, A.M., 1971, Microearthquake activity in the vicinity of Wooded Island, Hanford region, Washington: U.S. Geological Survey, Preliminary Open-File Report prepared on behalf of the Richland Operations Office, U.S. Atomic Energy Commission, 23 p.

Poppe, B.B., 1979, Historical Survey of U.S. Seismograph Stations: U.S. Geological Survey Professional Paper 1096.

Price, E.H., 1980, Strain distribution and model for formation of Eastern Umtanum Ridge anticline, south-central Washington: Report RHO-BWI-SA-30, Rockwell Hanford Operations, Richland, WA.

Price, E.H., 1981, Structural geometry, strain distribution, and tectonic evolution of East Umtanum Ridge, and a comparison with other selected localities within Yakima fold structures, south-central Washington: Ph.D. dissertation (in progress),

AMENDMENT NO. 18  
September 1981

Washington State University, Pullman.

- Racine, D., 1979, A seismicity study of the Pacific Northwest region of the United States, November 1961-August 1965: Report prepared by Teledyne-Geotech for the U.S. Nuclear Regulatory Commission, Washington, D.C., 43 p.
- Raleigh, C.B., Healy, J.H., and Bredehoeft, J.D., 9172, Faulting and crustal stress at Rangely, Colorado: in Flow and Fracture of Rock: Geophysical Monograph No. 16, American Geophysical Union, Washington, D.C., p. 273-284.
- Rasmussen, N., 1967, Washington State Earthquakes 1840 through 1965: Bulletin of the Seismological Society of America, v. 57, no. 3, p. 463-476.
- Raymond, J.R., and Tillson, D.D., 1968, Evaluation of a thick basalt sequence in south-central Washington: Geophysical and hydrological exploration of the Rattlesnake Hills deep stratigraphic test well: Report BNWL-776, Battelle Pacific Northwest Laboratory, Richland, WA, 126 p.
- Reidel, S.P., 1978, Geology of the Saddle Mountains between Sentinel Gap and 119°30' longitude: Informal Report, RHO-BWI-LD-5, Rockwell Hanford Operations, Richland, WA.
- Richter, C.F., 1958, Elementary seismology: W.H. Freeman and Company, San Francisco, CA, 768 p.
- Ross, M.E., 1978, Stratigraphy, structure, and petrology of Columbia River basalt in a portion of the Grande Ronde River-Blue Mountains area of Oregon and Washington: Report RHO-SA-58, Rockwell-Hanford Operations, Richland, WA.
- Rothe, G.H., 1978, Earthquake swarms in the Columbia River basalts: Ph.D. dissertation, University of Washington, Seattle, 181 p.
- Savage, J.C., Lisowski, M., and Prescott, W.H., 1981, Geodetic strain measurements in Washington: Journal of Geophysical Research, v. 86, no. B6, p. 4929-4940.
- Savage, W.U., 1972, Microearthquake clustering near Fairview Peak, Nevada, and in the Nevada seismic zone: Journal of Geophysical Research, v. 77, p. 7049-7056.
- Savage, W.U. 1976, Earthquake Probability Models: Recurrence Curves, Aftershock, and Cluster, Ph.D. thesis, University of Nevada, Reno.

- Schmincke, H.U., 1967, Stratigraphy and petrography of four upper Yakima Basalt flows in south-central Washington: Geological Society of America Bulletin, v. 78, no. 11, p. 1385-1422.
- Scholz, C.H., 1968a, The frequency-magnitude relation of microfracturing in rock and its relation to earthquakes: Bulletin of the Seismological Society of America, v. 58, no. 1, p. 399-415.
- Scholz, C.H., 1968b, Mechanism of creep in brittle rock: Journal of Geophysical Research, v. 73, p. 3295-3302.
- Shlien, S., and Toksoz, M.N., 1970, A clustering model for earthquake occurrences: Bulletin of the Seismological Society of America, v. 60, p. 1765-1787.
- Smith, R.B., Winkler, P.L., Anderson, J.G., and Scholz, C.H., 1974, Source mechanism of microearthquakes in eastern Utah: Bulletin of the Seismological Society of America, v. 64, p. 1295-1317.
- Spry, A., 1962, The origin of columnar jointing, particularly in basalt flows: Geological Society of Australia Journal, v. 8, p. 191-216.
- Swanson, D.A., Wright, T.L., Hooper, P.R. and Bentley, R.D., 1979, Revisions in Stratigraphic Nomenclature of the Columbia River Basalt Group, U.S. Geological Survey, Bulletin 1457-B.
- Sykes, L. R., 1970, Earthquake Swarms and Sea-Floor Spreading: Journal of Geophysical Research, v. 75, no. 32, p. 6598.
- Systems, Science and Software, 1980, Determination of three-dimensional structure of eastern Washington from the joint inclusion of gravity and earthquake travel time data: Report submitted to Weston Geophysical Corporation, Westboro, MA, by Systems, Science and Software, La Jolla, CA, 143 p.
- Systems, Science and Software, 1981, Relocation of earthquakes in eastern Washington based on a three-dimensional velocity model: Report submitted to Weston Geophysical Corporation, Westborough, MA, by Science, Systems, and Software, La Jolla, CA, 46 p.
- Talwani, P., Stevenson, D., Amick, D., and Chiang, J., 1979, An earthquake swarm at Lake Keowee, South Carolina: Bulletin of the Seismological Society of America, v. 69, p. 825-841.





- Tomkeieff, S.I., 1940, Basalt lavas of the Giant's Causeway: Bulletin of Volcanology, v. 2, p. 89-146.
- Tryggvason, E., 1973, Seismicity, earthquake swarms, and plate boundaries in the Iceland region: Bulletin of the Seismological Society of America, v. 63, p. 1327-1348.
- Turcotte, F.T., 1975, Microearthquake statistical correlation study, Hanford Reservation, Washington: Report prepared for the Washington Public Power Supply System by Weston Geophysical Research, Inc., Westborough, MA, 14 p.
- Udias, A., 1977, Time and magnitude relationships for three microearthquake series near Hollister, California: Bulletin of the Seismological Society of America, v. 67, p. 173-185.
- Udias, A., and Rice, J., 1975, Statistical Analysis of Microearthquake Activity near San Andreas Geophysical Observatory, Hollister, California: Bulletin of the Seismological Society of America, v. 65, no. 4, p. 809-827.
- Utsu, T., 1970, Aftershocks and earthquake statistics (II): Journal of the Faculty of Science, Hokkaido University, Series III (Geophysics), v. 3, p. 198-266.
- Vere-Jones, D., and Davies, R.B., 1966, A statistical survey of earthquakes in the main seismic region of New Zealand, 2, time series analysis: New Zealand Journal of Geophysics, v. 9, p. 251-284.
- Washington Public Power Supply System, 1981, Draft Section 2.5 of the WNP-2 FSAR, August 1981.
- Weston Geophysical Corporation, 1981a, Evaluation of explosion data as a source of local crustal information within the central California Plateau: Draft report prepared for the Washington Public Power Supply System, Richland, WA, 18 p.
- Woodward-Clyde Consultants, 1978a, 1872 earthquake studies, WPPSS Nuclear Project Nos. 1 & 4: Microearthquake study: Report submitted to the Washington Public Power Supply System, Richland, WA, 32 p.
- Woodward-Clyde Consultants, 1978b, Earthquake Catalog of Northwestern United States and Canada for 1841 through 1977 in the region 128°-110°W, 440-540N: Prepared for Department of Waste Isolation, Rockwell-Hanford Operations, Richland, WA, by Woodward-Clyde Consultants, San Francisco, CA.



AMENDMENT NO. 18  
September 1981

- Woodward-Clyde Consultants, 1980a, Recent seismicity of the Hanford region: Report prepared for the Washington Public Power Supply System, Richland, WA, 26 p.
- Woodward-Clyde Consultants, 1980b, Seismological review of the July 16, 1936 Milton-Freewater earthquake source region: Report prepared for the Washington Public Power Supply System, Richland, WA, 44 p.
- Wong, I.G., and Simon, R.B., 1981 (in press), Low level historical and contemporary seismicity in the Paradox Basin, Utah and its tectonic implications: Submitted to the Rocky Mountain Association of Geologists, Guidebook to the Paradox Basin.
- Yerkes, R.F., and Castle, R.O., 1976, Seismicity and faulting related to fluid extraction: Engineering Geology, v. 10, p. 151-167.



TABLE 2.5J-1

MAGNITUDE DETECTION AND LOCATION THRESHOLDS  
FOR EASTERN WASHINGTON

Area	Time Period of similar station distribution	Depth Range (km)	Total No. of Events ( $M_C > 0.0$ )	Threshold Magnitude Based on ( $M_C$ ) "Roll-off"
I	10/71-6/75	0-3	642	1.25 (a)
		>3	148	0.7
	7/75-12/80	0-3	309	1.7
		>3	149	1.25 (a,b)
II	6/71-6/75	All	30	2.0 (b)
	7/75-12/80	All	98	1.7
III	6/71-6/75	All	20	1.9 (b)
	7/75-12/80	All	234	1.5
IV	6/71-6/79	All	55	2.0
	7/79-12/80	All	2	-- (c)
V	6/71-12/76	All	21	-- (c)
	1/77-12/80	All	7	-- (c)

Notes: (a) Possible break in slope of frequency-magnitude plot; see Section 2.5J.2.2.  
 (b). Frequency-magnitude plot poorly constrained.  
 (c) Insufficient data to constrain frequency-magnitude plot.



TABLE 2.5J-2

UNIVERSITY OF WASHINGTON SWARM AREAS

Swarm	Latitude (Degrees N)		Longitude (Degrees W)	
	South	North	East	West
West Saddle Mt.	46.820	46.865	119.564	119.797
Frenchman Hills	46.865	46.960	119.514	119.600
Smyrna	46.800	46.855	119.433	119.564
Royal	46.850	46.910	119.317	119.450
Corfu	46.790	46.850	119.331	119.433
Wahluke	46.729	46.780	119.314	119.431
Berg Ranch	46.685	46.728	119.317	119.417
Othello	46.650	46.710	119.183	119.317
Scooteney Res.	46.600	46.680	119.047	119.183
Connell	46.650	46.715	118.850	118.933
Wooded Island	46.390	46.470	119.200	119.333
Eltopia	46.370	46.455	118.964	119.067
Coyote Rapids	46.635	46.730	119.483	119.650





TABLE 2.5J-3

ALTERATIONS TO SWARM BOUNDARIES

- (a) Royal: 46.85° to 46.92°,  
119.317° to 119.45°
- Frenchman Hills: 46.86° to 46.96°  
119.51° to 119.61°
- Scooteney Reservoir: 46.57° to 46.68°  
119.047° to 119.183°
- Connell: 46.63° to 46.715°  
118.80° to 118.933°
- (b) Berg Ranch contributed events to Wahluke A, B, D, F  
Wahluke contributed events to Corfu A, B, G and Berg  
Ranch  
Corfu contributed events to Wahluke A, B, D, E, Smyrna  
B, C, and Royal B, D  
Royal contributed events to Corfu A, C  
Smyrna contributed events to Corfu A
- (c) Berg-Wahluke (1 swarm)  
Corfu-Wahluke (1 swarm)  
Royal-Corfu (2 swarms)



TABLE 2.5J-4  
NEW SWARM AREAS DEFINED IN THIS STUDY

	Latitude (Degrees N)		Longitude (Degrees W)		No. of Swarms
	South	North	East	West	
1	46.00	to 46.08	119.63	to 119.72	1
2	46.08	to 46.17	119.37	to 119.50	1
3	46.08	to 46.17	119.63	to 119.72	1
5	46.25	to 46.33	119.57	to 119.65	1
8	46.47	to 46.52	119.62	to 119.67	1
12	46.67	to 46.75	119.22	to 119.30	1
13	46.67	to 46.75	119.80	to 119.97	1
14	46.70	to 46.78	119.08	to 119.17	1
15	46.08	to 46.17	119.37	to 119.50	1
16	46.80	to 46.87	119.13	to 119.22	1
17	47.07	to 47.13	119.58	to 119.65	1
18	46.87	to 46.92	119.65	to 119.70	2
19	46.29	to 46.35	119.39	to 119.44	1
20	46.73	to 46.76	119.22	to 119.27	1
21	46.59	to 46.65	119.73	to 119.80	1
22	47.03	to 47.083	120.933	to 121.0	1
25	47.6	to 47.7	120.22	to 120.33	5
29	46.5	to 46.57	119.6	to 119.68	1
31	46.34	to 46.41	119.0	to 119.1	1
32	46.8	to 46.89	119.275	to 119.375	2
33	45.6	to 45.7	119.917	to 120.017	1
34	46.25	to 46.31	119.33	to 119.43	1
37	47.63	to 47.73	120.11	to 120.267	2
38	47.817	to 47.917	120.075	to 120.15	1
40	47.61	to 47.72	120.03	to 120.183	3
41	46.78	to 46.84	119.53	to 119.60	1
42	47.65	to 47.78	119.35	to 119.44	1
S2	46.48	to 46.62	119.44	to 119.58	1



TABLE 2.5J-5  
SWARMS DEFINED IN THIS STUDY

Name of Swarm Area		Dates of Swarm	No. of Events	Largest Magnitude
Eltopia	A	72318-72363	27	2.5
	B	73035-73045	9	1.34
	C	73155-73180	8	1.80
	D	75002-75022	4	1.14
Wooded Island	A	69152-69166	4	2.51
	B	69196-69249	24	2.91
	C	69275-69279	4	2.12
	E	70015-70048	13	2.59
	F	70115-70149	6	2.38
	G	70311-70331	10	2.85
	H	73115-73121	4	1.53
	I	75100-75179	76	2.83
	J	75198-75212	5	2.23
Frenchman Hills	A	70358-70360	4	1.3
	B	71016-71046	22	3.22
	C	72056-72074	5	0.9
	D	79259-79279	10	2.1
	E	79300-79360	45	3.1
West Saddle Mountain	A	69121-69143	6	2.83
	B	71181-71191	35	1.94
	C	73242-73259	6	2.54
	D	73358-74006	4	0.88
Royal	A	70040-70072	25	2.65
	B	72026-72037	6	1.46
	B1	72059-72072	9	1.20
	C	72256-72260	5	1.05
	D	73356-74010	23	4.38
	E	74246-74274	6	2.79
Smyrna	F	80338-80347	4	1.00
	A	70265-70264	6	2.34
	B	70358-70361	7	1.6
	C	72219-72280	66	1.96
	D	74348-75022	9	2.02
	E	77185-77186	4	1.56
	F	78122-78159	39	2.02
Corfu	G	79287-78309	18	2.47
	A	70148-70159	7	2.09
	A1	70193-70222	10	1.77
	B	70331-71008	62	2.24



TABLE 2.5J-5 (Sheet 2 of 3)

Corfu (cont'd)	C	71114-71132	6	1.67
	D	72065-72073	4	1.04
	F	73164-73174	5	2.21
	G	73205-73224	8	1.76
	H	78082-78108	11	2.18
	I	78144-78161	7	1.36
Wahluke	A	70235-70315	24	3.35
	C	71187-71205	6	1.89
	D	72247-72357	64	2.11
	E	73256-73260	5	0.92
	F	74319-74365	16	1.61
Berg Ranch	A	71233-71239	8	1.78
	B	71316-71352	19	1.8
	C	74328-74342	10	1.77
Coyote Rapids	A	70329-70330	4	2.06
	B	71298-71307	5	3.82
	C	76075-76090	7	1.77
	D	77230-77236	4	1.17
	E	77252-77259	5	2.7
	F	78011-78014	6	1.77
	G	80218-80226	4	0.7
Othello	A	70063-70067	4	2.28
	B	71253-71274	13	2.59
	C	71286-71315	11	1.89
	D	72251-72269	5	1.0
	E	73256-73287	18	1.78
	F	75353-76017	11	2.7
Scooteney Reservoir	A	69119-69137	6	1.62
	B	70286-70362	33	1.96
	C	71009-71 68	34	2.38
	D	73035-73073	11	1.43
	E	73285-73291	4	1.30
	F	73302-73313	4	1.11
Connell	A	70310-70315	4	3.08
	B	70333-70335	6	2.31
	A1	70349-70353	4	1.98
	C	71 11-71 32	45	1.97
	D	71 63-71 83	9	2.79
	E	71101-71104	8	2.19
	F	71330-71339	4	1.16
	G	75284-75288	4	2.41



TABLE 2.5J-5 (Sheet 3 of 3)

Area	1	73363-73363	5	2.75
	2	70355-70356	4	1.29
	3	75179-75180	10	3.81
	5	71232-71239	6	2.13
	8	79248-79252	9	2.44
	12	69287-69307	4	2.31
	13	72296-72297	4	1.7
	14	69312-69314	6	2.47
	15	72113-72113	5	1.22
	16	74107-74113	4	1.21
	17	69111-69124	5	2.88
	18A	78267-78284	4	3.07
	B	79019-79021	8	3.93
	19	72247-72257	4	0.96
	20	74020-74026	6	1.16
	21	75242-75242	6	2.31
	22	77194-77194	4	3.83
	25A	76334-76352	4	1.75
	B	77259-77265	4	1.17
	C	77282-77308	6	1.78
	D	78057-78082	5	1.89
	E	78116-78134	5	1.23
	29	69314-69330	4	2.17
	31	71035-71049	4	1.31
	32A	72079-72098	4	0.51
	B	78063-78071	4	1.26
	33	72233-72240	4	2.56
	34	72300-72301	4	1.49
	37A	77196-77203	4	0.88
	B	80258-80270	5	0.90
	38	78018-78025	4	3.31
	40A	76335-76349	4	3.10
	B	77122-77135	4	2.13
		79030-79049	6	2.95
	41	79174-79181	5	1.95
	42	79315-79321	6	2.7
	S1	78229-78236	4	1.19
Royal and Corfu A		72130-72142	4	0.82
Royal and Corfu C		80247-80256	5	1.2
Corfu and Wahluke		72137-72142	4	0.82
Wahluke and Berg Ranch		73027-73040	4	0.73



TABLE 2.5J-6

ESTIMATES OF ANNUAL IRRIGATION WATER USE IN THE  
PASCO BASIN AREA BY COUNTY

<u>County</u>	<u>Annual Irrigation Water Use 1979</u>	
	<u>Ground Water</u>	<u>Surface Water</u>
Benton	21,300*	205,000
Franklin	26,460	559,000
Grant	<u>N.A.</u>	<u>143,600</u>
Total	47,760	907,600

---

\*All values are listed in acre-feet per year.

Reproduced from Gephart et al. (1979)



TABLE 2.5J-7

COMAPRISON OF OBSERVED EARTHQUAKE DISTRIBUTION WITH  
A RANDOM DISTRIBUTION

<u>No. of Earthquakes per Block</u>	<u>No. of Blocks Observed</u>	<u>P(n) <math>\lambda = 0.38</math></u>	<u>No. of Blocks Predicted</u>
0	364	0.684	341
1	47	0.259	130
2	25	$4.9 \times 10^{-2}$	25
3	8	$6.25 \times 10^{-3}$	3.13
4	7	$5.94 \times 10^{-4}$	$2.97 \times 10^{-1}$
5	7	$4.52 \times 10^{-5}$	$2.25 \times 10^{-2}$
6	6	$2.86 \times 10^{-6}$	$1.43 \times 10^{-3}$
7	4	$1.55 \times 10^{-7}$	$7.76 \times 10^{-5}$
$\leq 8$	3.2	negligible	negligible

WNP-2

AMENDMENT NO. 18  
September 1981TABLE 2.5J-8  
SUMMARY OF WELL DATA

<u>Well Location</u>	<u>Well No.</u>	<u>Depth of Well (feet)</u>	<u>Water Bearing Material</u>	<u>Water Level Monitoring Period</u>	<u>Maximum Change in Water Level (feet)*</u>	<u>Comments</u>
Frenchman Tunnel Vicinity	48	200	--	1940-1979	+180	Increase occurred over 8-year period
" " "	49	161	Basalt	1940-1978	+155	Increase occurred over 10-year period
Frenchman Hills Region	51	168	Basalt	1950-1979	+50	Increase occurred over 6-year period
" " "	56	315	Basalt	1942-1980	+190	Increase occurred over 10-year period
N. of Frenchman Hills	61	330	Sand Interbed	1954-1978	+180	Increase occurred over 9-year period
" " "	62	193	Basalt	1916-1978	+100	Increase occurred over 14-year period
" " "	64	168	Basalt	1954-1978	+110	Increase occurred over 14-year period
" " "	73	164	Basalt	1940-1978	+130	Increase occurred over 28-year period
" " "	74	219	Basalt	1940-1980	+160	Increase occurred over 5-year period
" " "	75	147	Basalt	1943-1980	+60	Increase occurred over 6-year period

\*+ = increase in water level  
- = decrease in water level



## WNP-2

AMENDMENT NO. 18  
September 1981

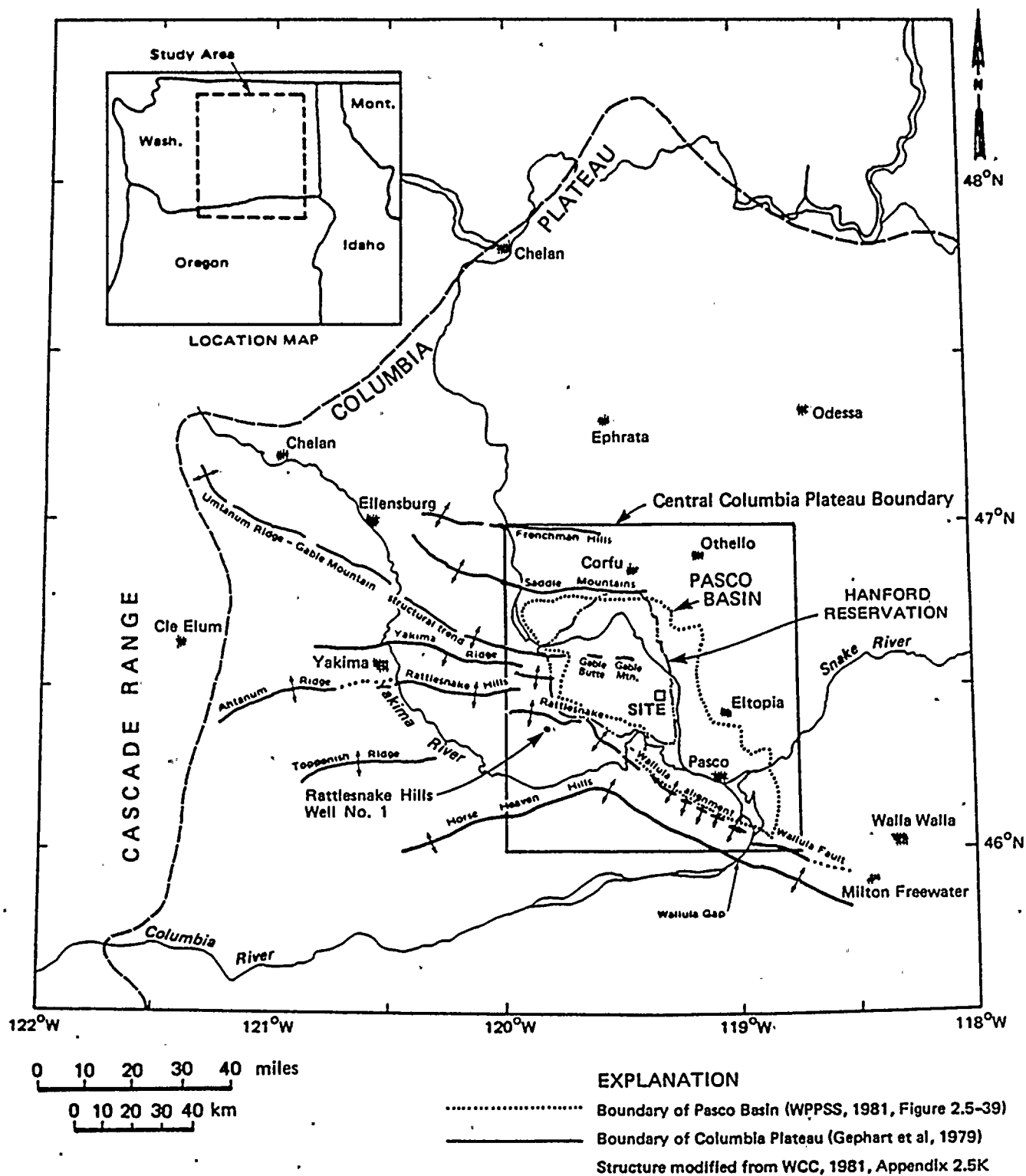
TABLE 2.5J-8 (Sheet 2 of 2)

<u>Well Location</u>	<u>Well No.</u>	<u>Depth of Well (feet)</u>	<u>Water-Bearing Material</u>	<u>Water-Level Monitoring Period</u>	<u>Maximum Change in Water Level (feet)*</u>	<u>Comments</u>
Eltopia Region	10			1961-1979	--	Average water level 125 feet; 30-foot semi-annual fluctuations due to irrigation
Scooteney Reservoir	12 1	323	Basalt	1950-1979 1958-1980	+100	Increase in water level occurred over 28-year period
Correll Region	6	--	--	1960-1978	+180	Increase in water level occurred over 22-year period
"	5			1960-1979	+140	
Taunton Vicinity	16	840	Basalt	1956-1978	+60	Increase in water level occurred over 10-year period
					+220	Increase in water level occurred over 16-year period
Frenchman Hills Region	79	840	Basalt	1949-1958	+300	
Corfu Region	81			1959-1978	+150	Increase occurred over 20-year period
"	82			1959-1978	+90	Increase occurred over 14-year period
Taunton Region	22	365	Basalt	1958-1976	+120	Increase occurred over 8-year period
" "	23	700	Basalt	1953-1978	+220	
Vicinity of Frenchman Tunnel	45	320	Basalt	1949-1963	+140	
" "	46			1961-1978	+440	Increase occurred over 17-year period

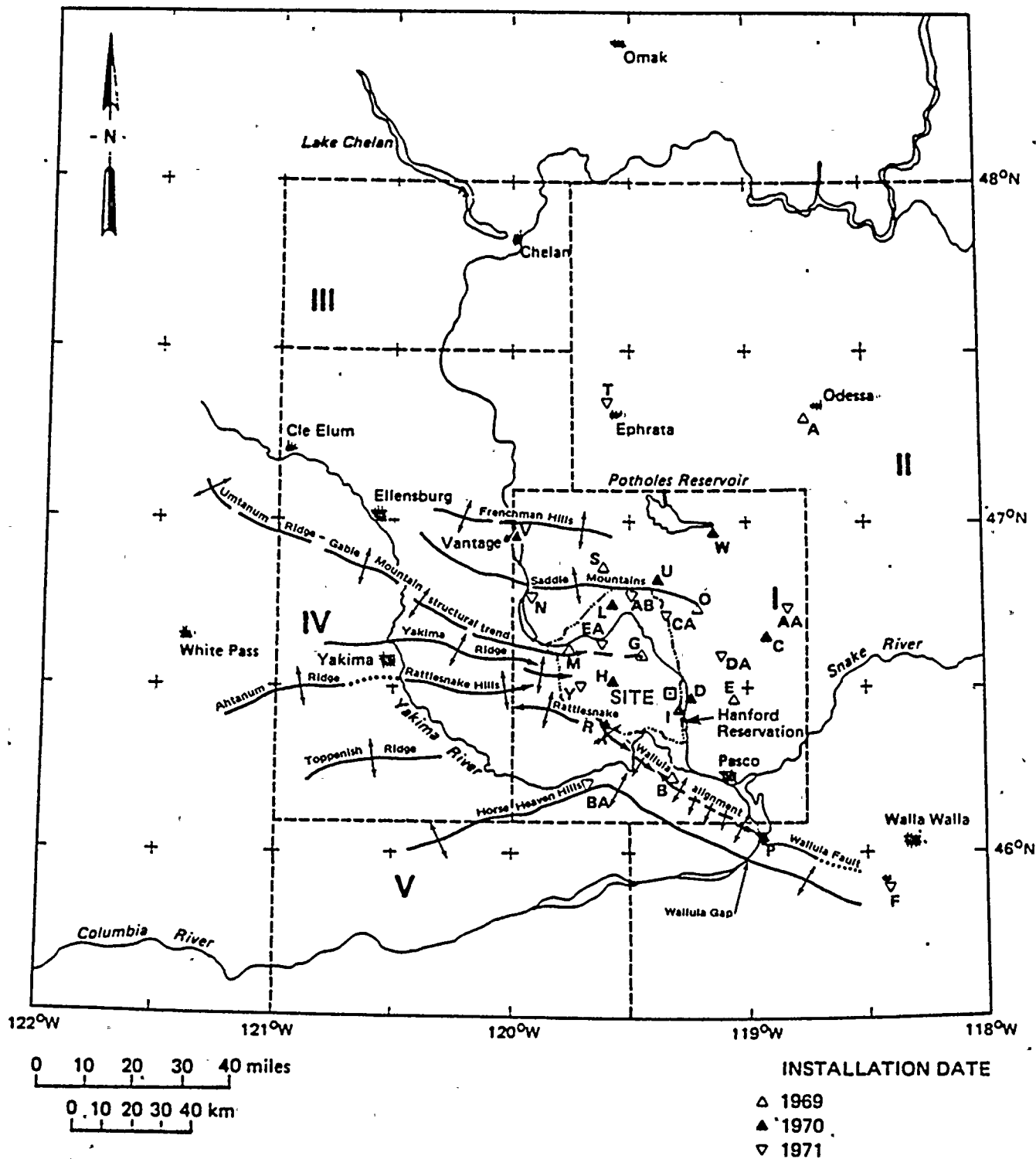
\*+ = increase in water level  
- = decrease in water level







Project No. 14940	Hanford FSAR	LOCATION MAP OF COLUMBIA PLATEAU	Figure 2.5J-0
Woodward-Clyde Consultants			



Project No.  
14940

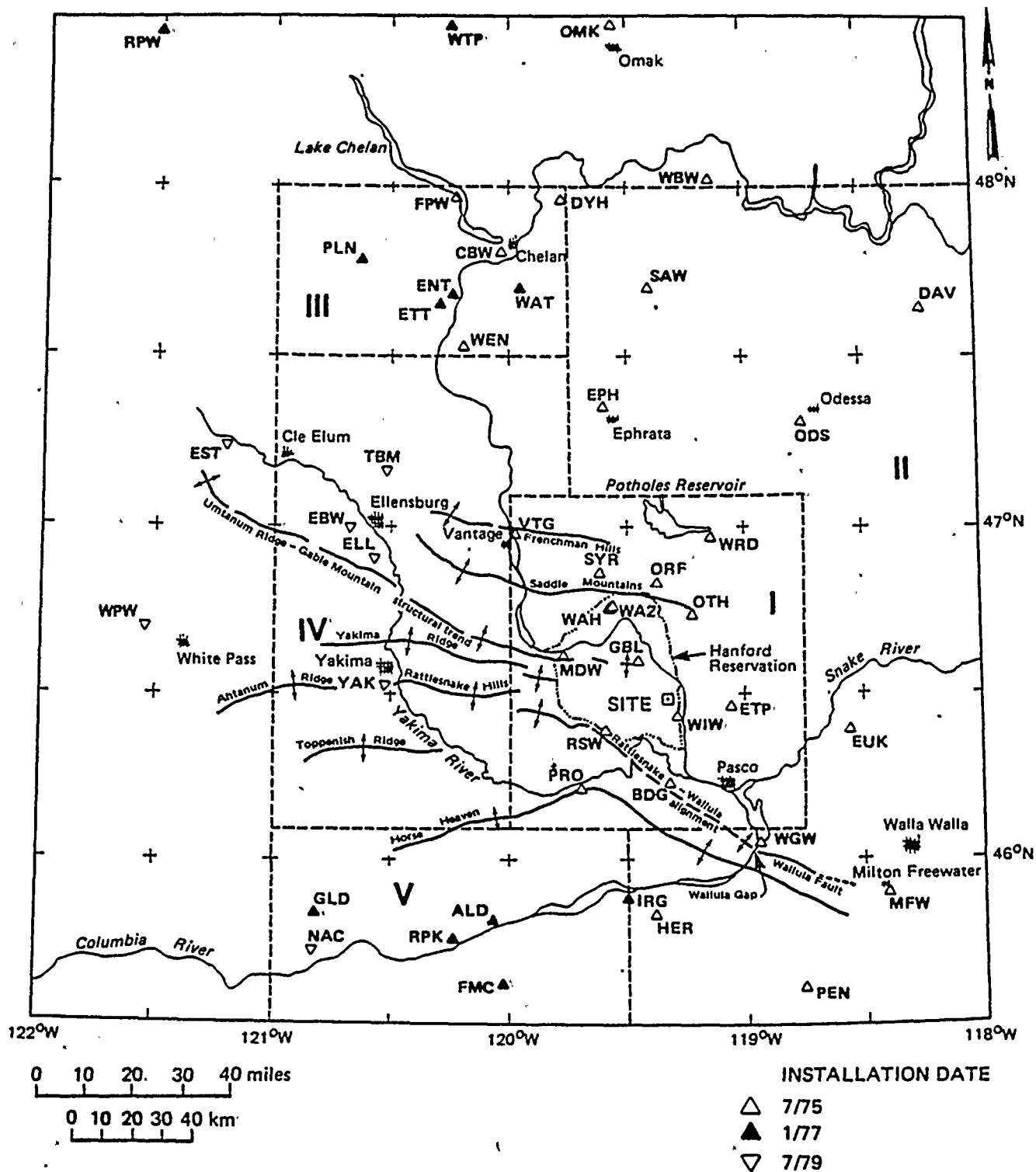
Hanford FSAR

Woodward-Clyde Consultants.

EASTERN WASHINGTON SEISMOGRAPH  
STATIONS, 3/69 - 6/75

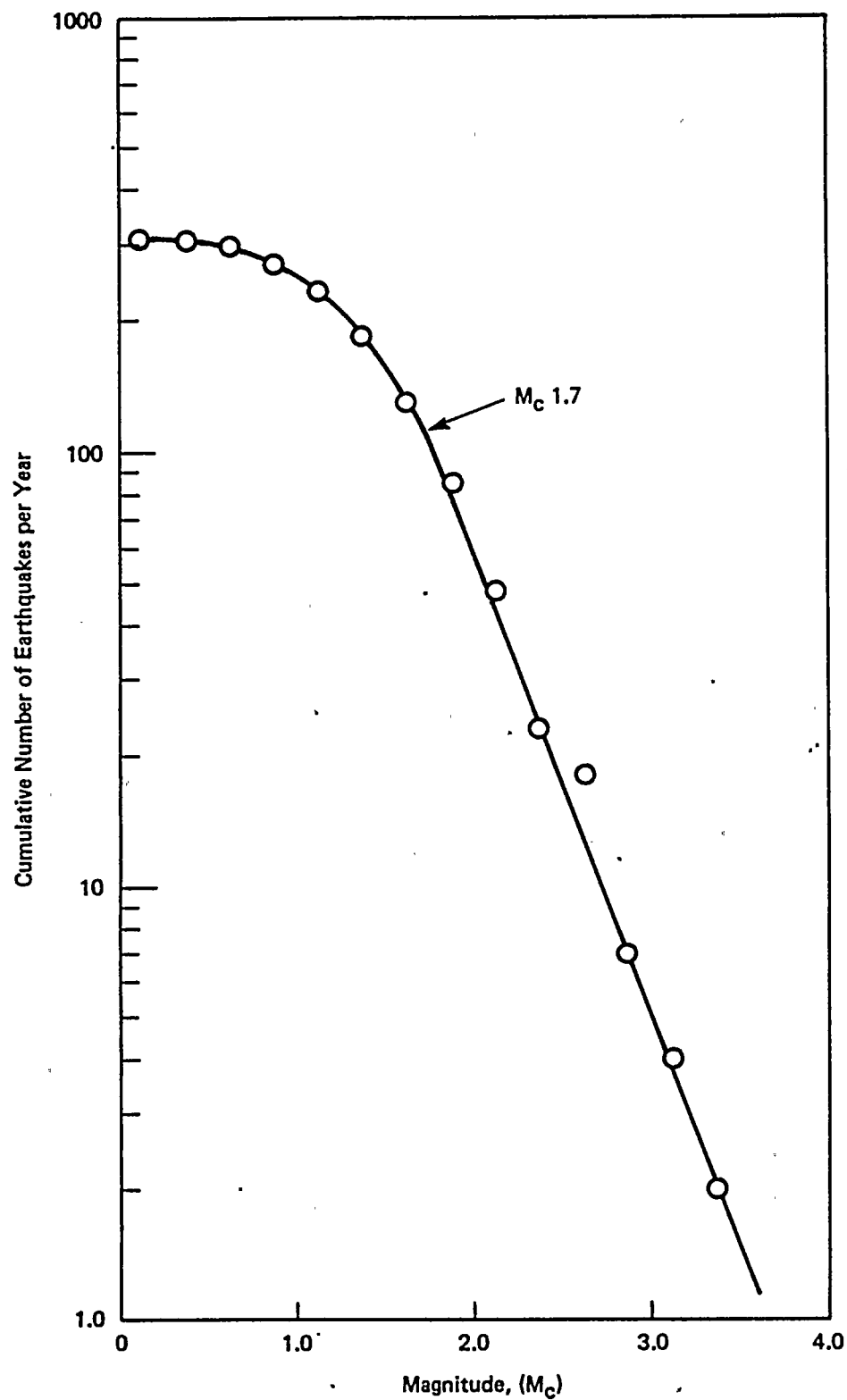
Figure  
2.5J-1





Project No. 14940	Hanford FSAR	EASTERN WASHINGTON SEISMOGRAPH STATIONS, 7/75 -12/80	Figure 2.5J-2
Woodward-Clyde Consultants			





Project No.  
14940

Hanford FSAR

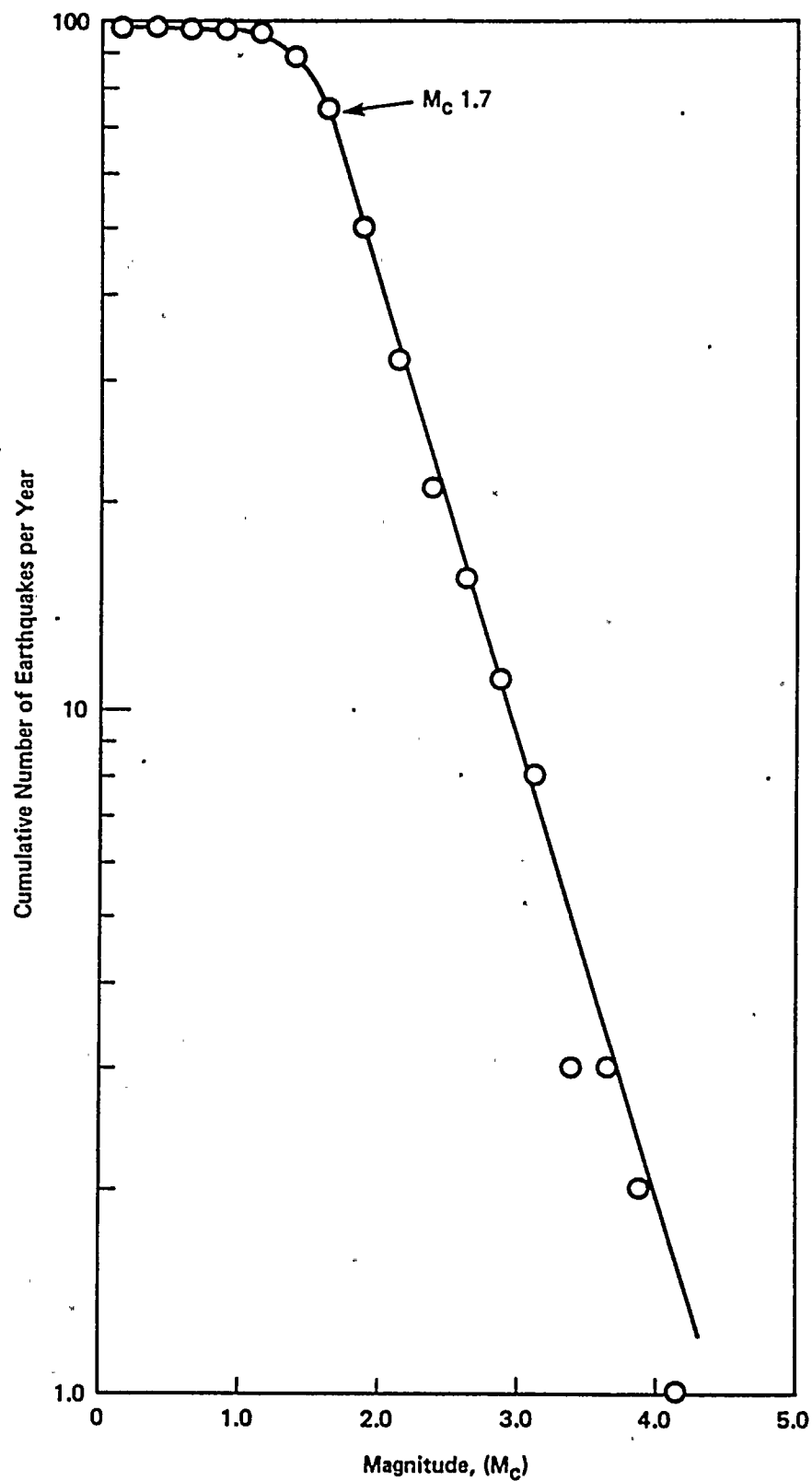
**Woodward-Clyde Consultants**

CUMULATIVE NUMBER OF EARTHQUAKES  
VERSUS MAGNITUDE FOR AREA I:  
7/75 -12/80, DEPTH  $\leq$  3 KM

Figure  
2.5J-3







Project No.  
14940

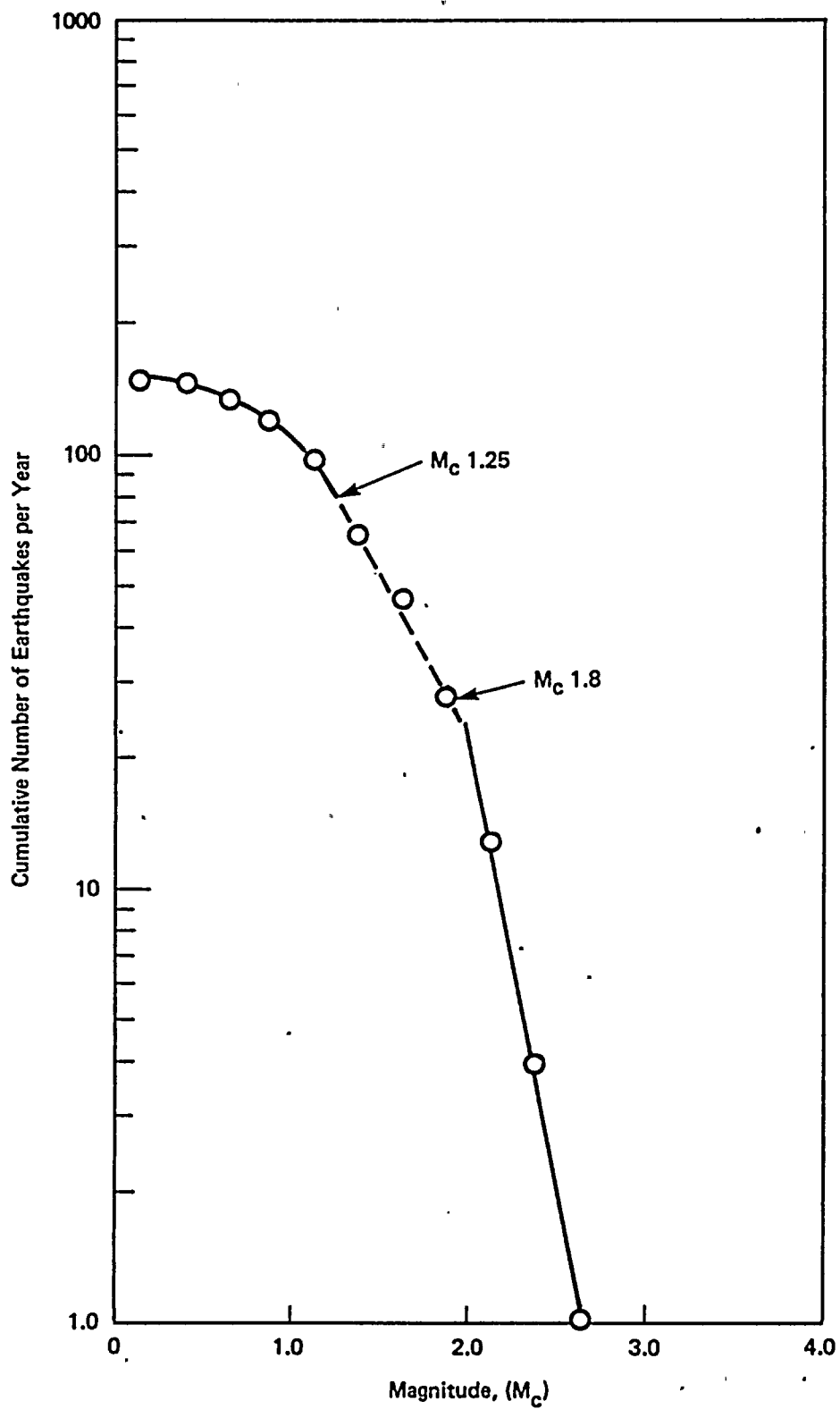
Hanford FSAR

**Woodward-Clyde Consultants**

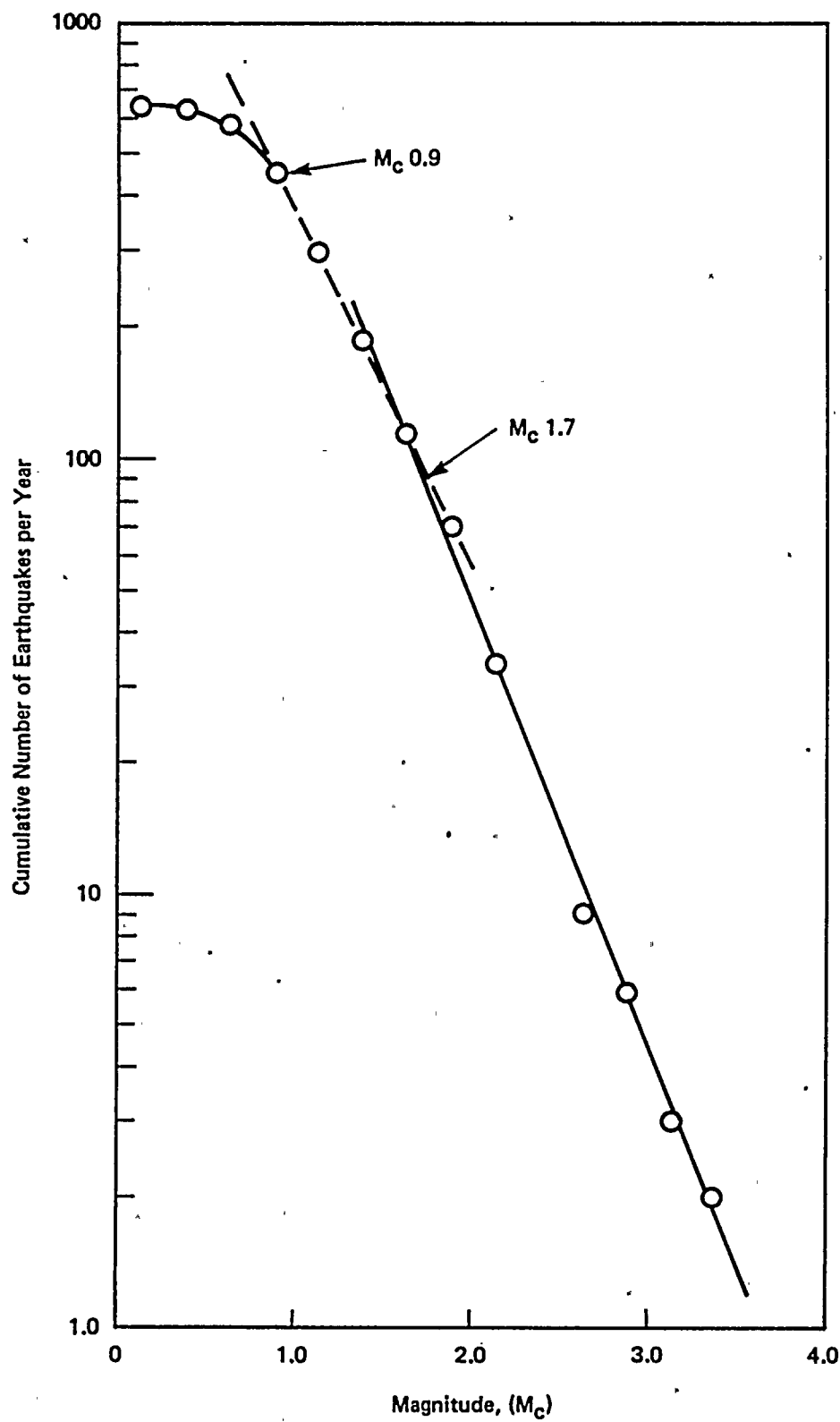
CUMULATIVE NUMBER OF EARTHQUAKES  
VERSUS MAGNITUDE FOR AREA II:  
7/75 -12/80, ALL DEPTHS

Figure  
2.5J-4





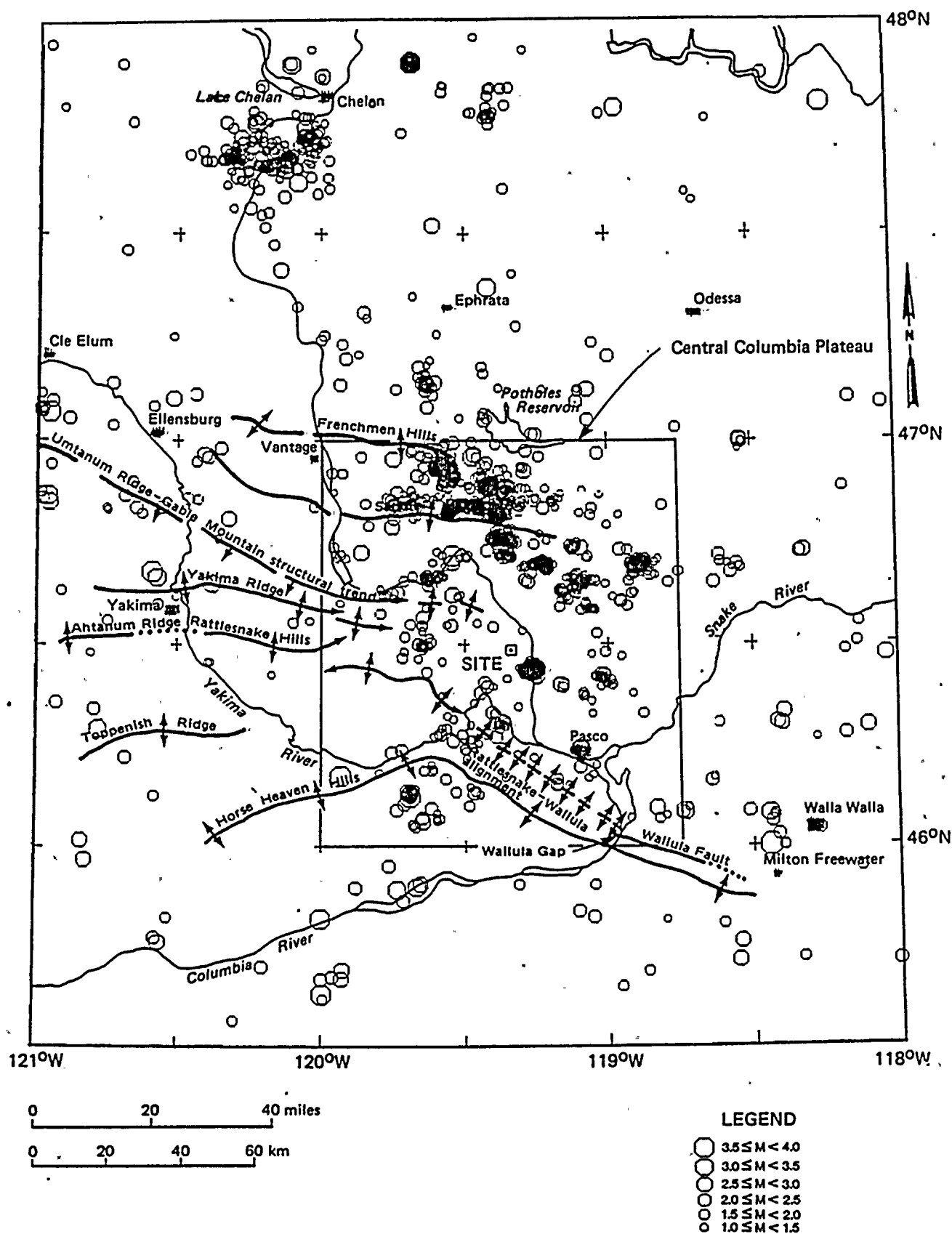
Project No. 14940	Hanford FSAR	CUMULATIVE NUMBER OF EARTHQUAKES VERSUS MAGNITUDE FOR AREA I: 7/75 -12/80, DEPTH > 3 KM	Figure 2.5J-5
Woodward-Clyde Consultants			



Project No. 14940	Hanford FSAR	CUMULATIVE NUMBER OF EARTHQUAKES VERSUS MAGNITUDE FOR AREA I: 6/71 - 6/75, DEPTH < 3 KM	Figure 2.5J-6
Woodward-Clyde Consultants			







Project No.  
14940

Hanford FSAR

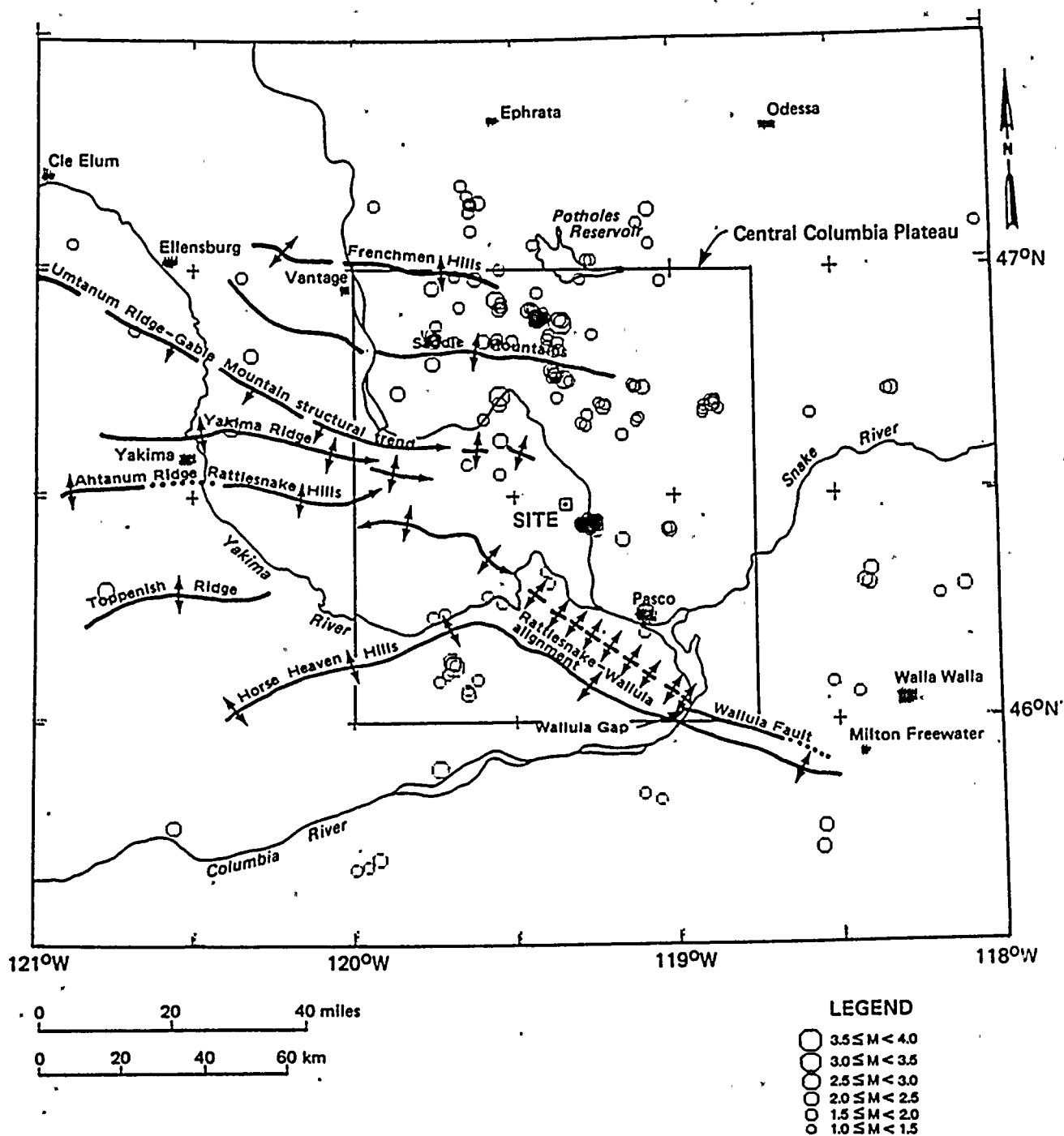
**Woodward-Clyde Consultants**

**EPICENTERS OF EARTHQUAKES  
WITH  $M_C > 1.0$ , 3/69 - 12/80**

**Figure  
2.5J-8**







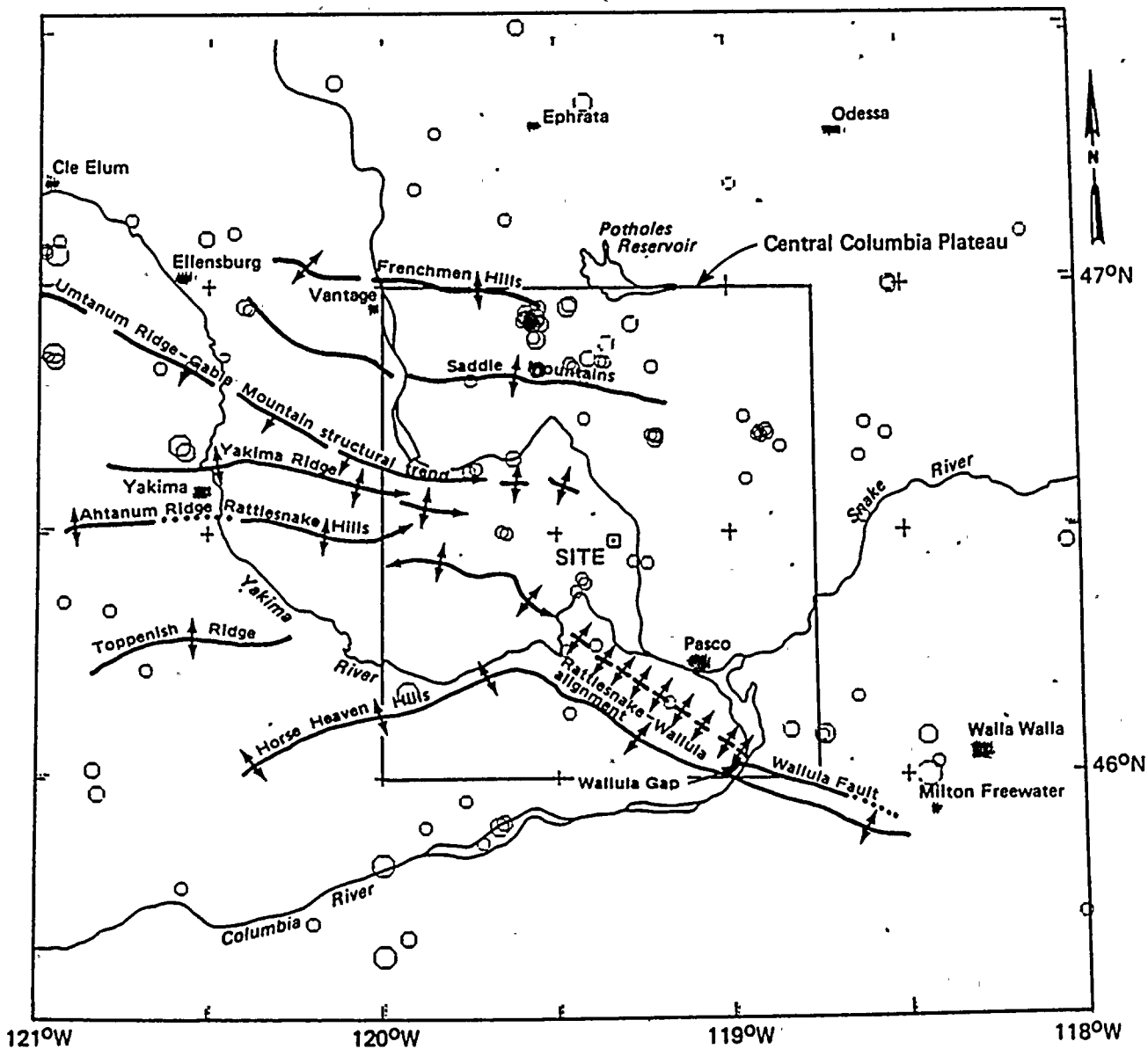
Project No.  
14940

Hanford FSAR

Woodward-Clyde Consultants

EPICENTERS OF EARTHQUAKES  
WITH  $M_C \geq 2.0$ , 3/69 - 6/75

Figure  
2.5J-9



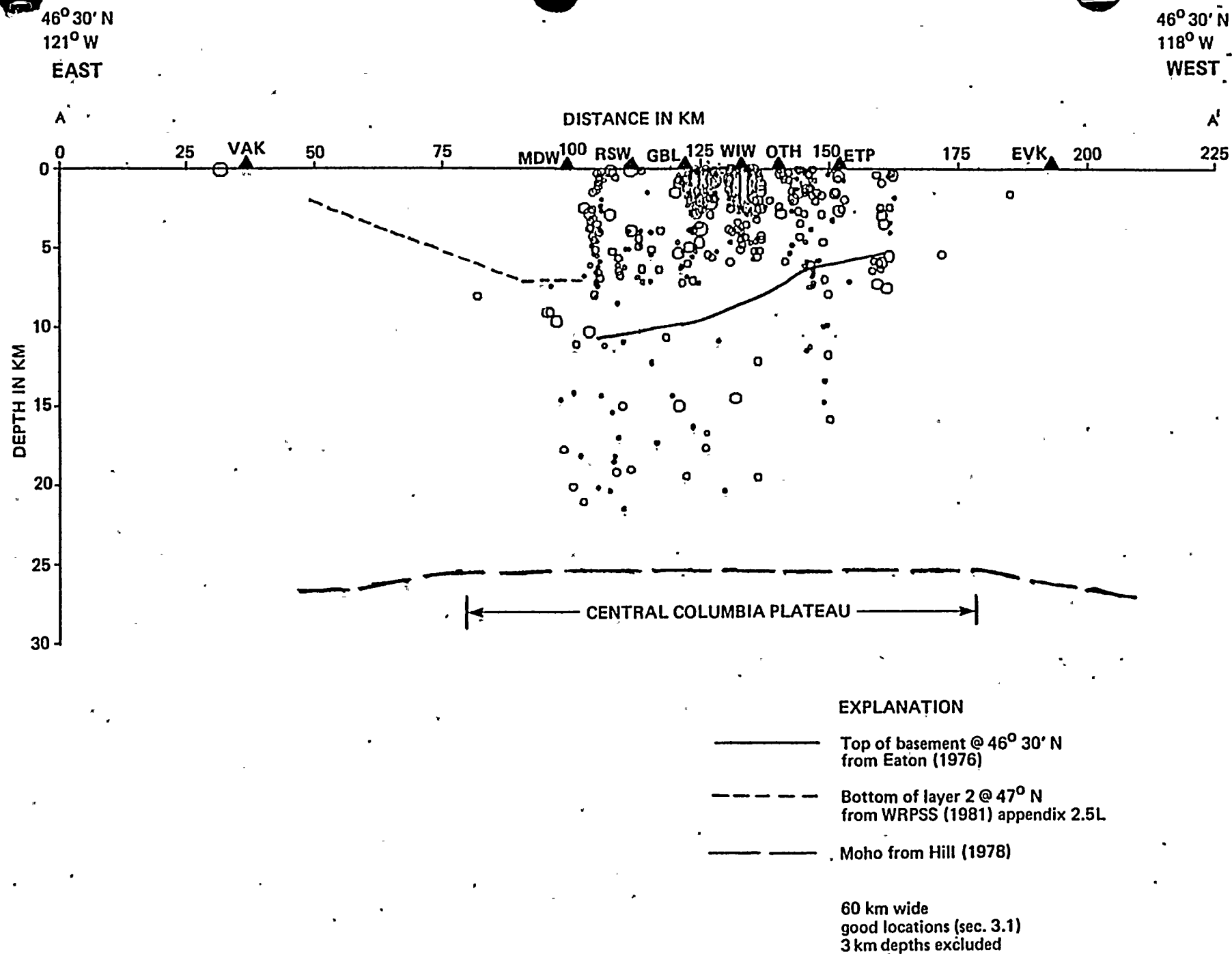
Project No.  
14940

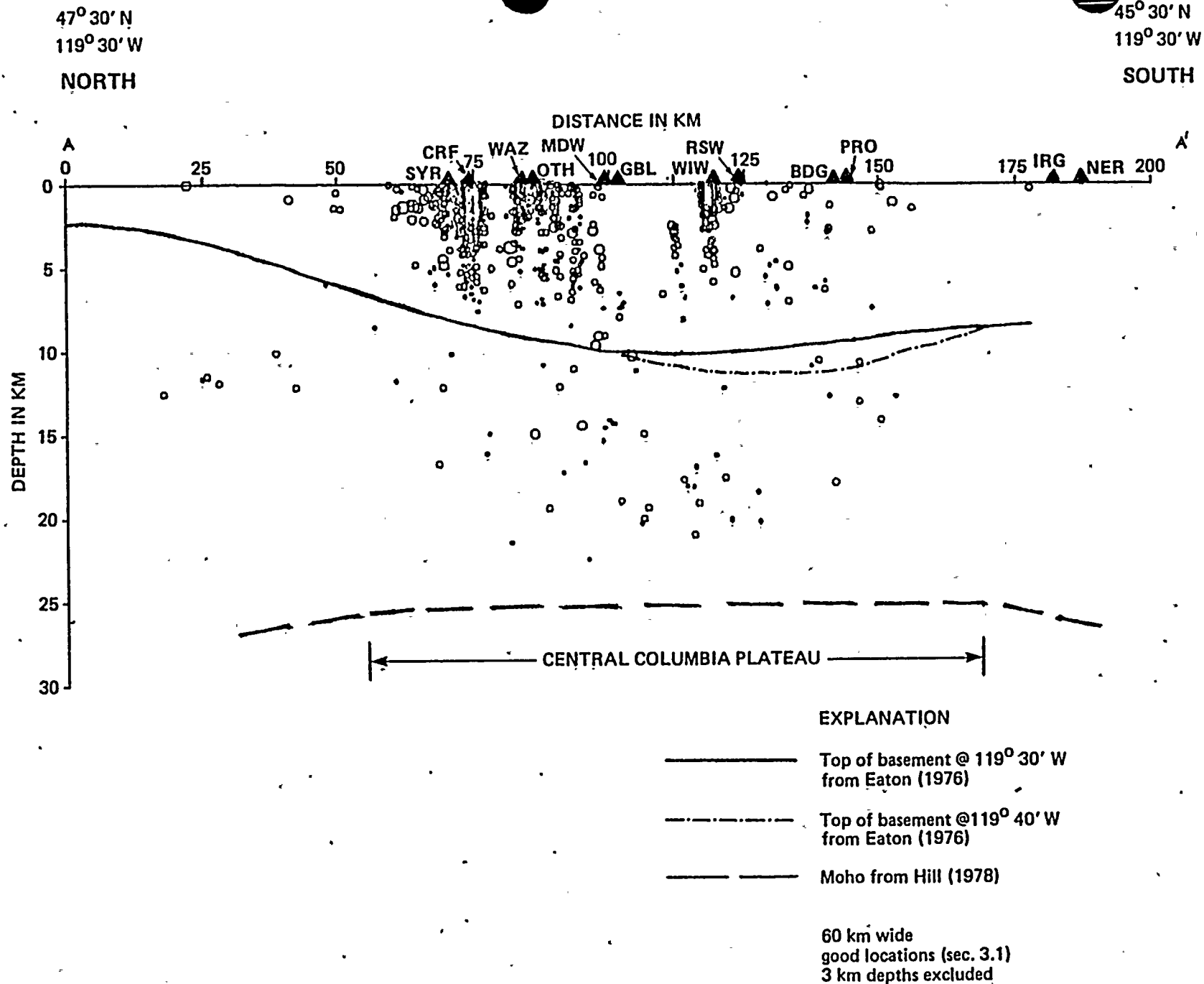
Hanford FSAR

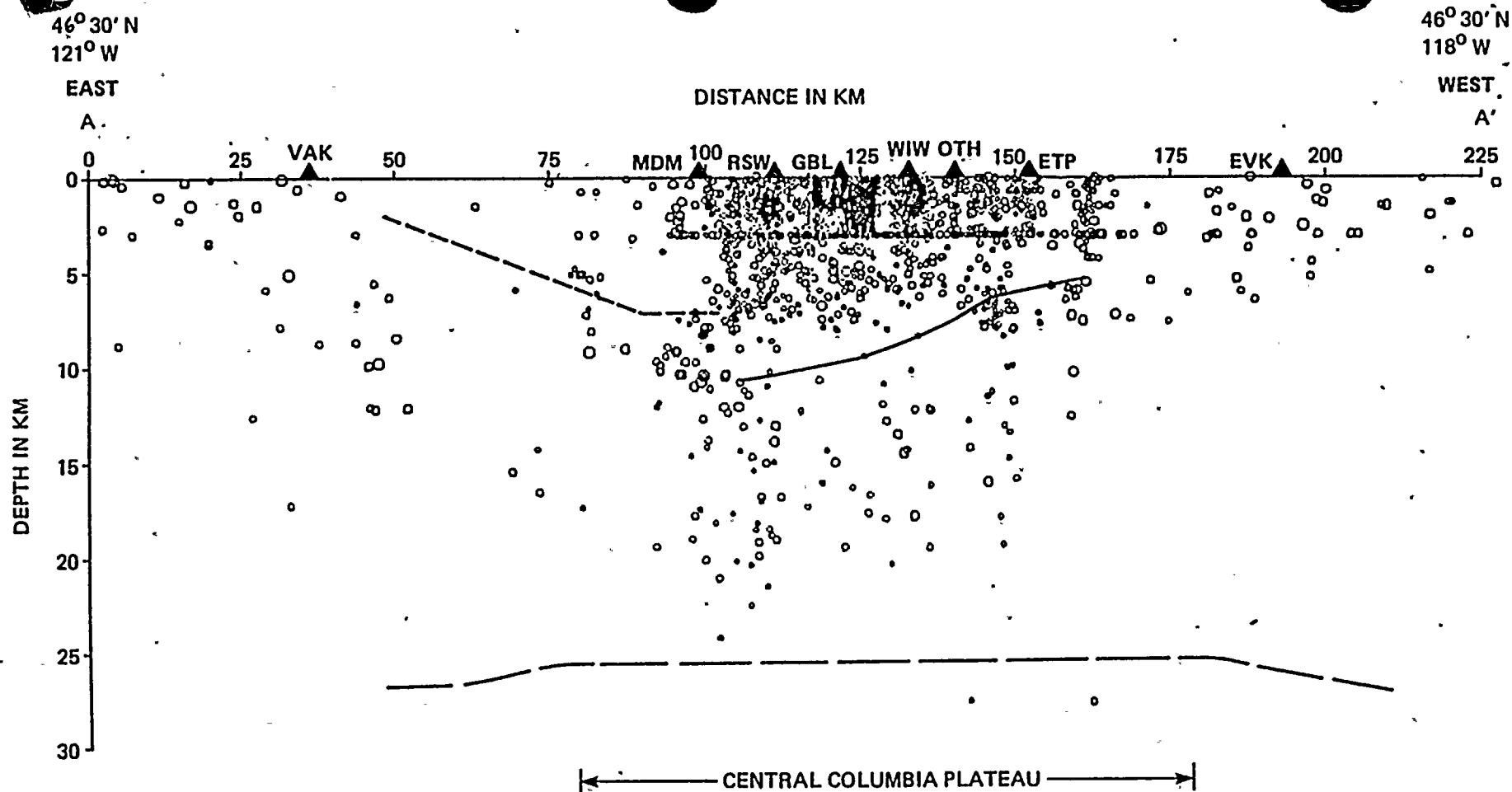
**Woodward-Clyde Consultants**

**EPICENTERS OF EARTHQUAKES  
WITH  $M_C \geq 2.0$ , 7/75 - 12/80**

**Figure  
2.5J-10**



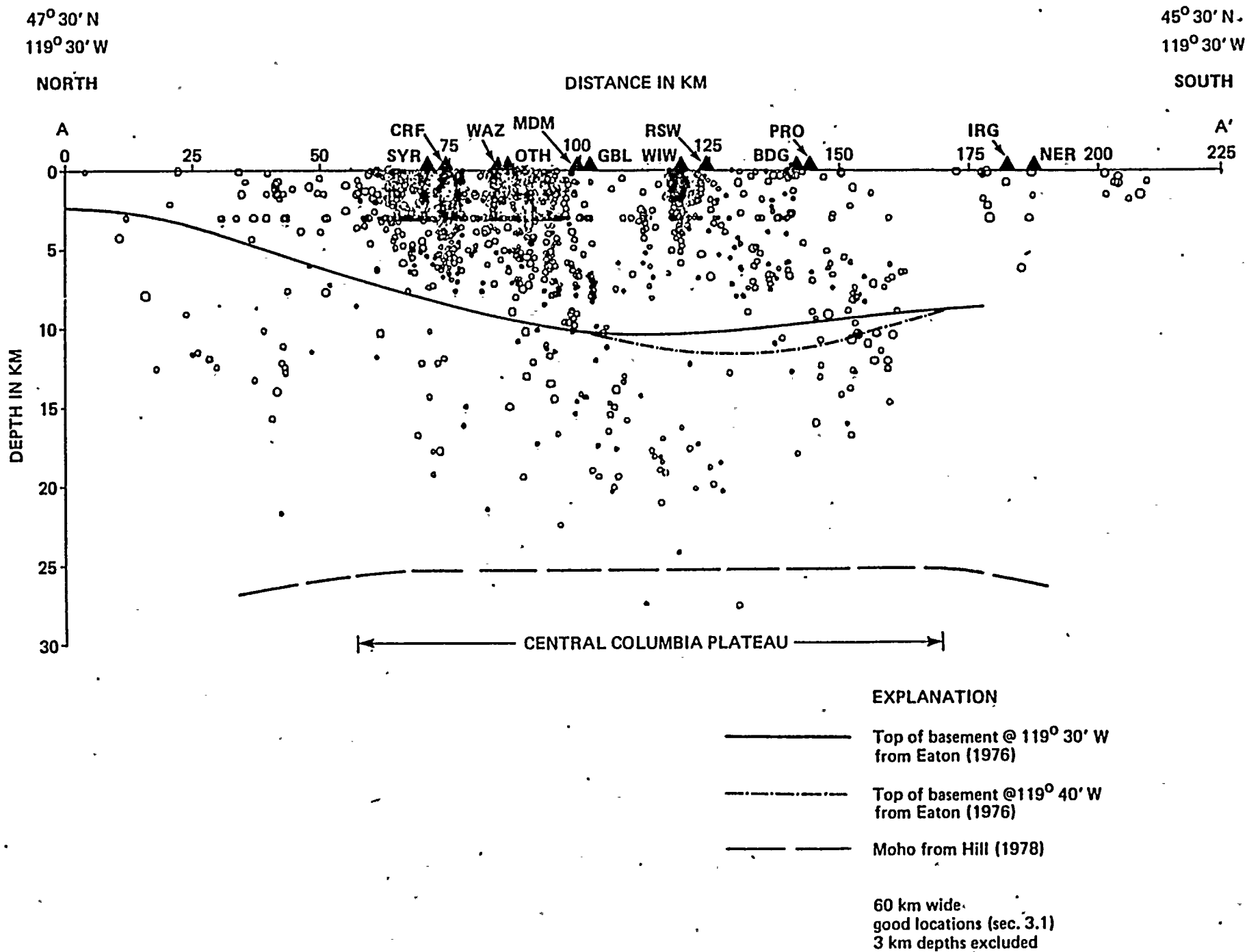




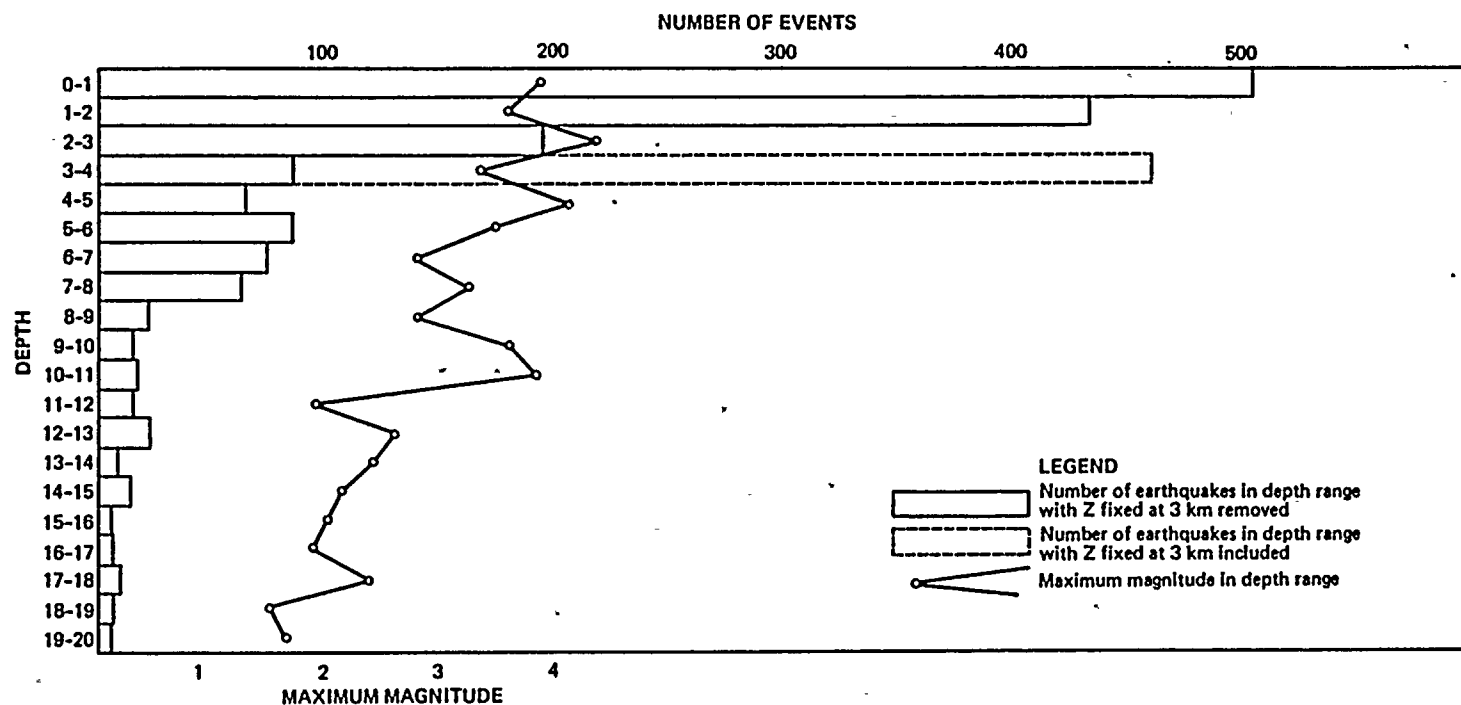
#### EXPLANATION

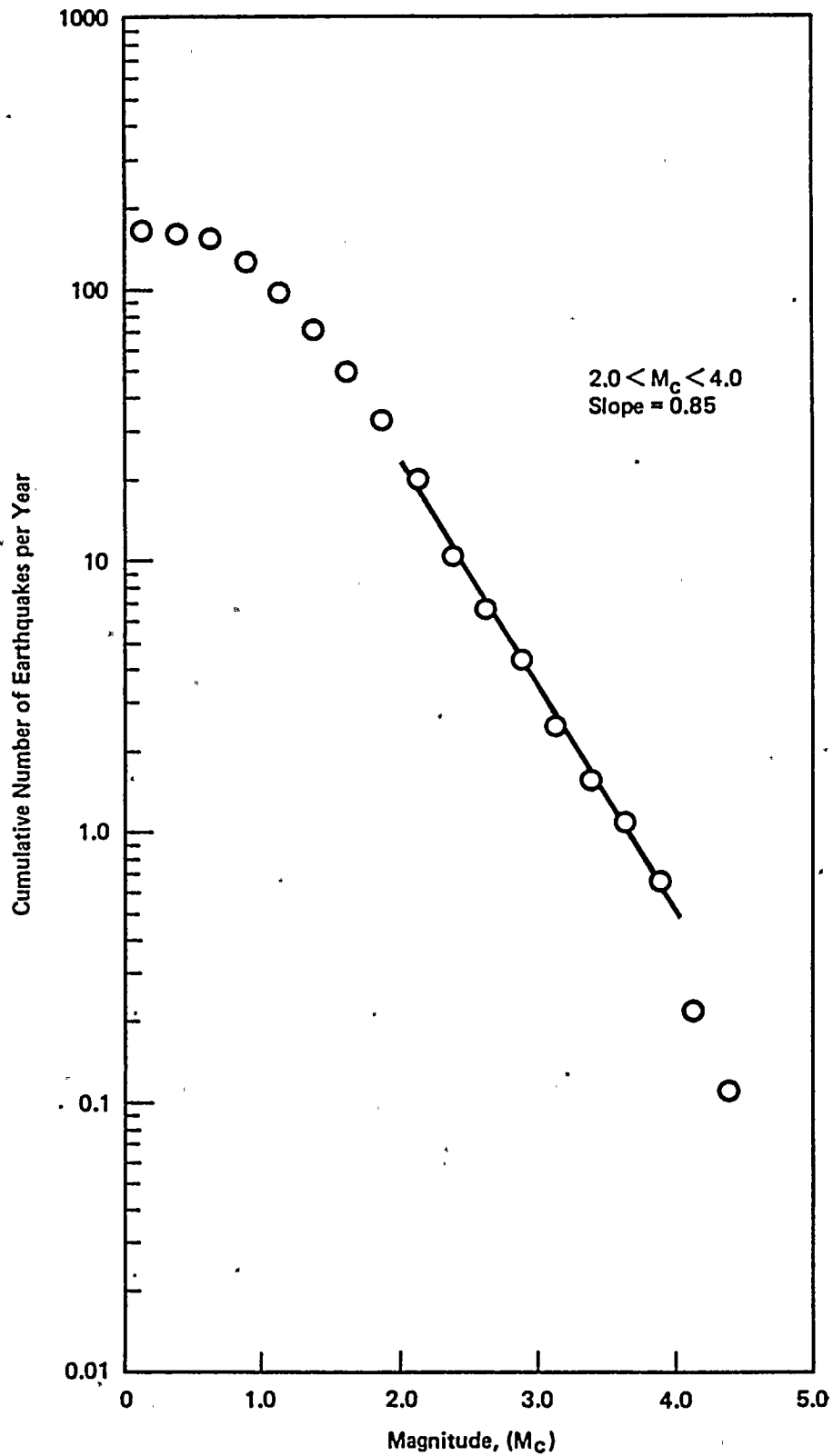
- Top of basement @ 46° 30' N  
from Eaton (1976)
- - - Bottom of layer 2 @ 47° N  
from WRPSS (1981) appendix 2.5L
- . - Moho from Hill (1978)

60 km wide  
good locations (sec. 3.1)  
3km depths excluded



45° 30' - 47° 30'  
118° - 121°

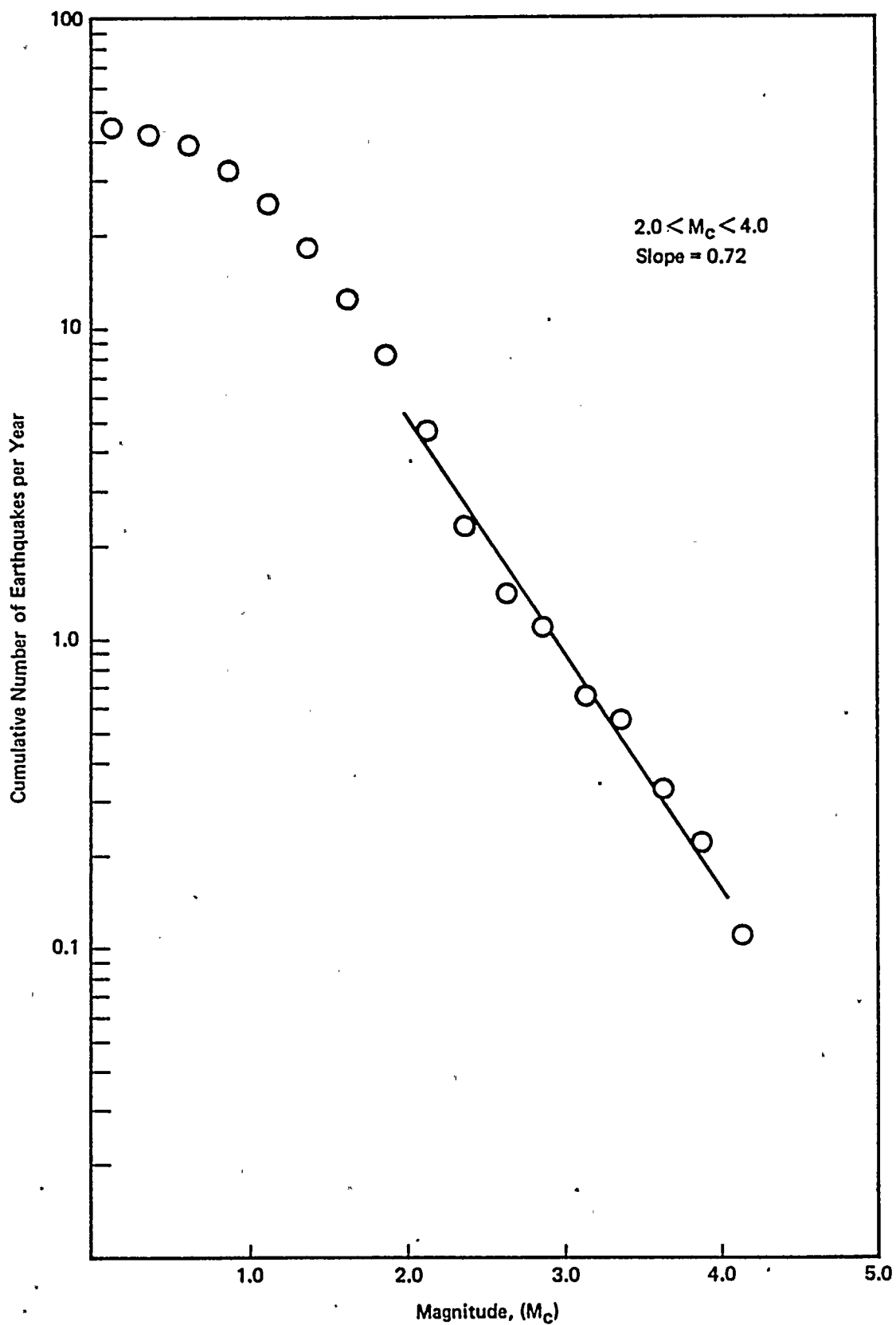




45.5°–47.5°, 118°–121°

Project No. 14940	Hanford FSAR	CUMULATIVE NUMBER OF EARTHQUAKES VERSUS MAGNITUDE, ALL DEPTHS	Figure 2.5J-16
Woodward-Clyde Consultants			





45° 30' - 47° 30' N, 118° - 121° W

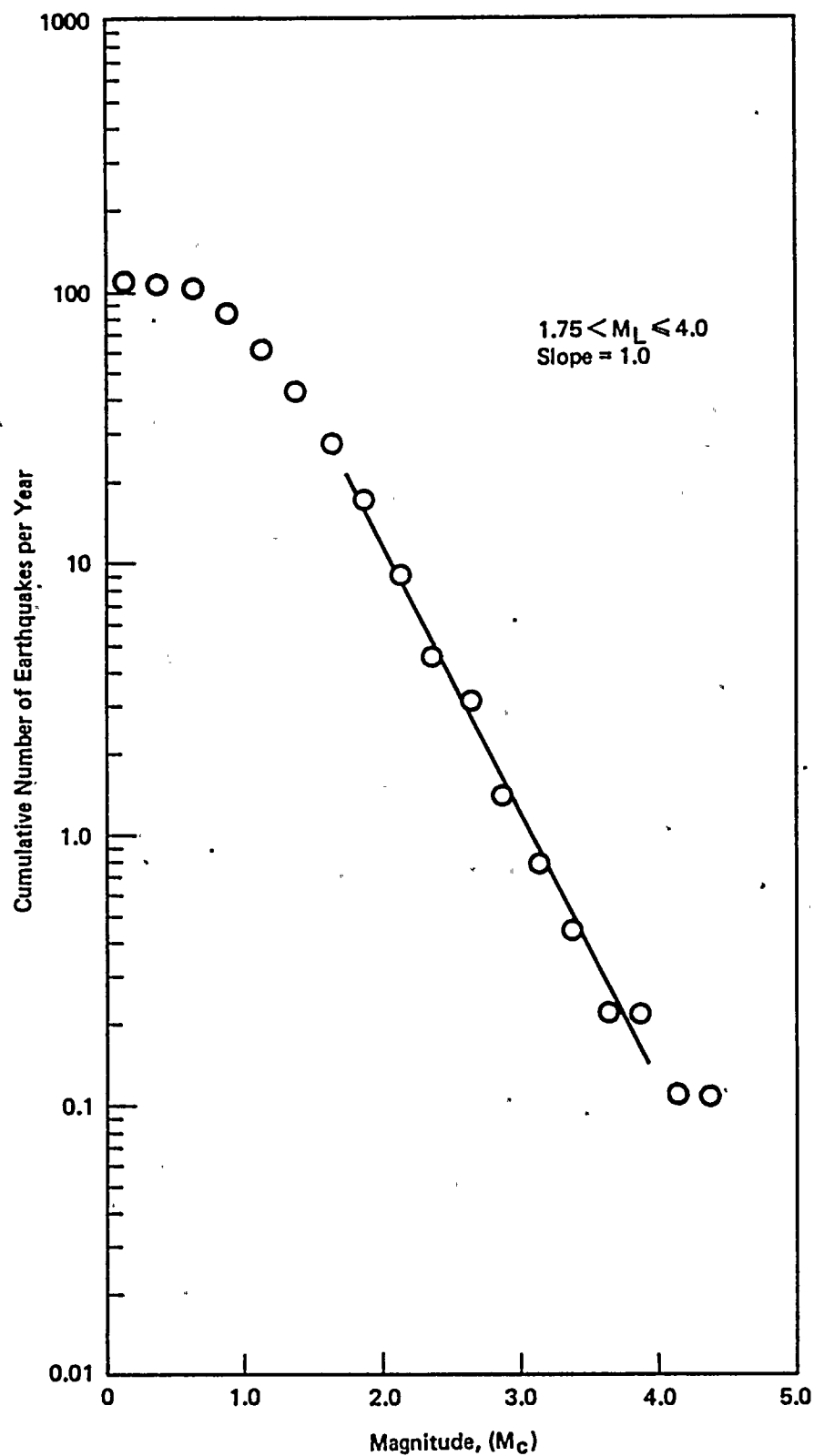
Project No.  
14940

Hanford FSAR

**Woodward-Clyde Consultants**

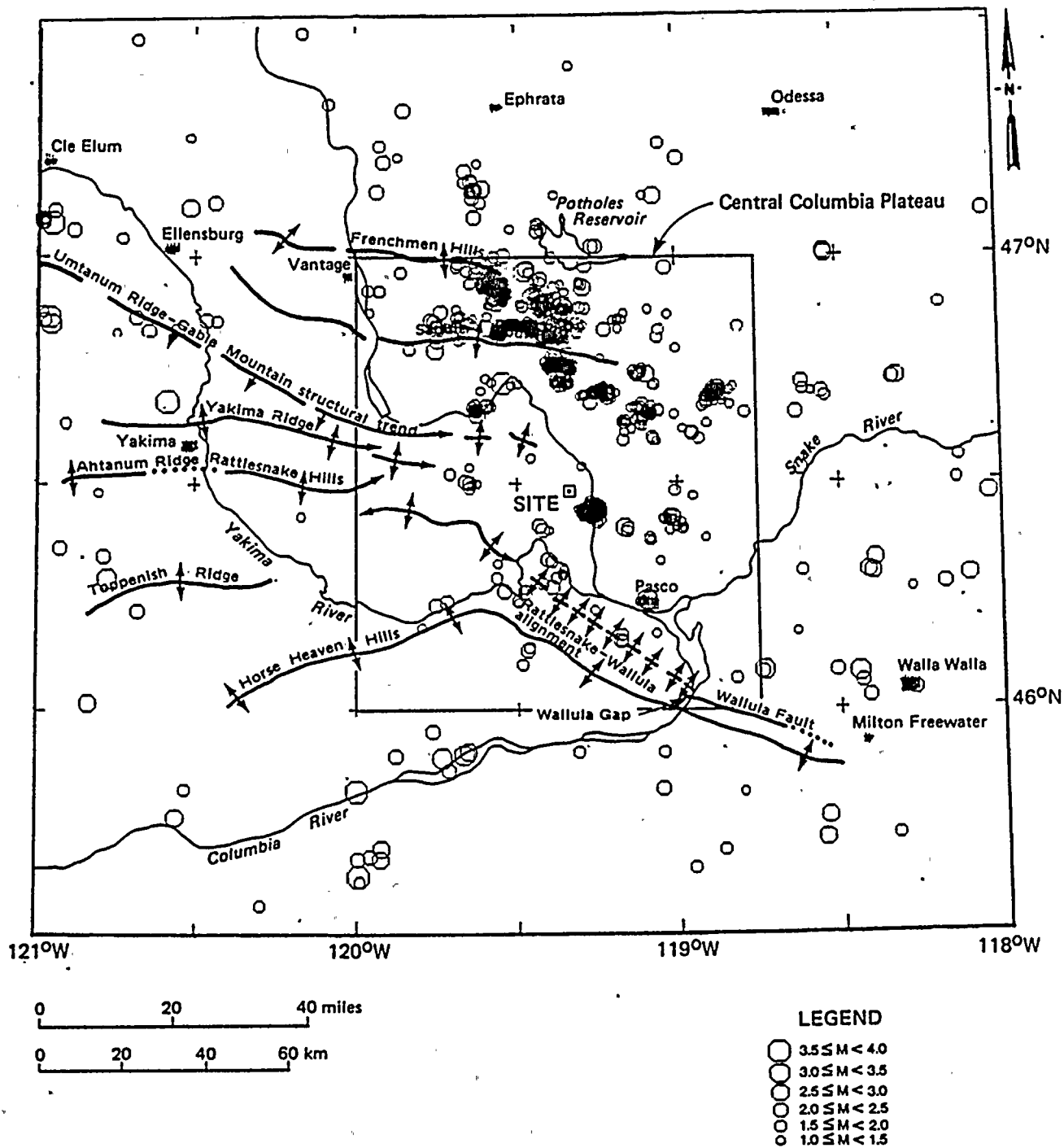
CUMULATIVE NUMBER OF EARTHQUAKES  
VERSUS MAGNITUDE, DEPTH > 3 KM

Figure  
2.5J-17

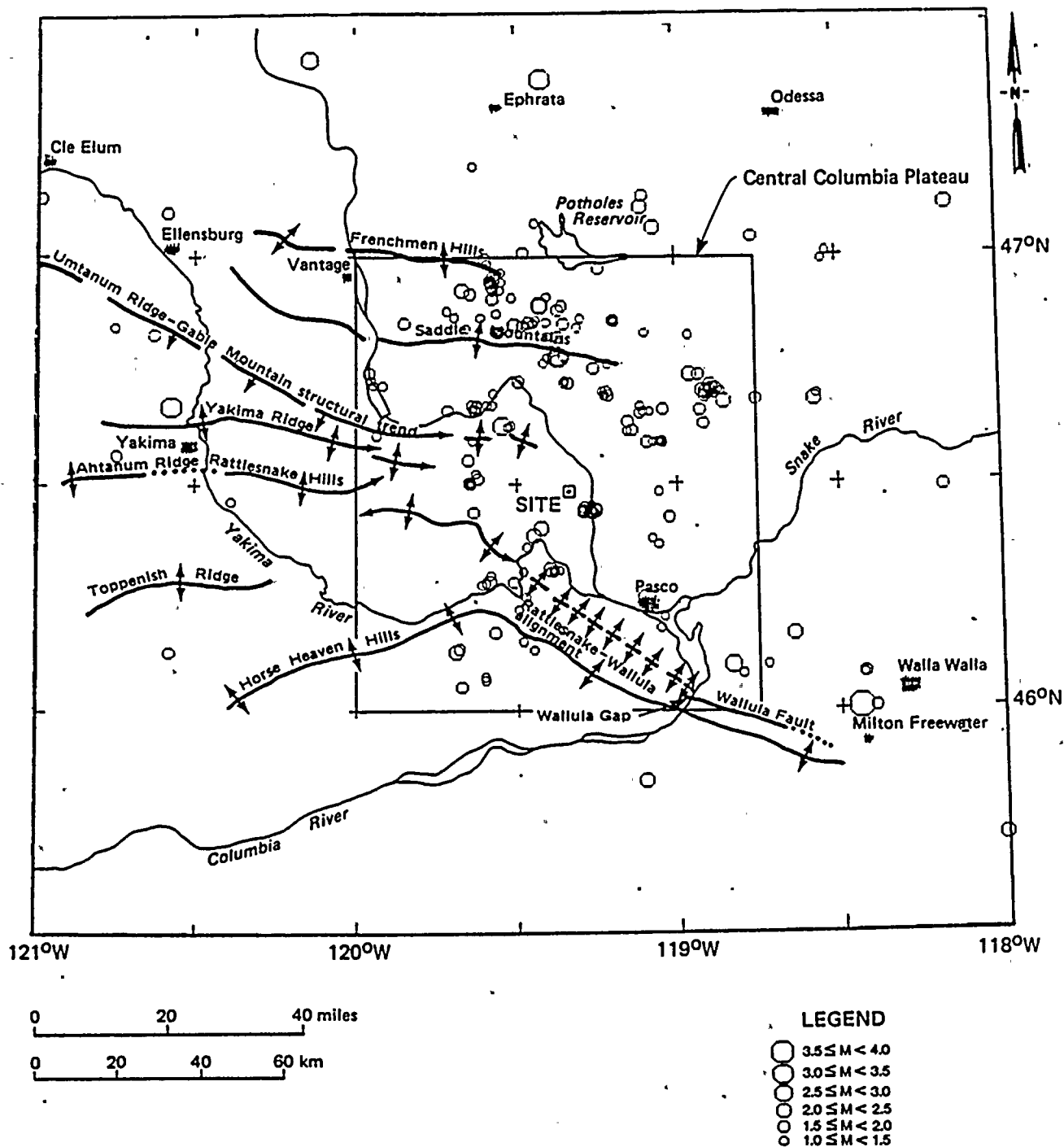


46° - 47° N, 118° 45' - 120° W

Project No. 14940	Hanford FSAR	CUMULATIVE NUMBER OF EARTHQUAKES VERSUS MAGNITUDE, Z ≤ 3 KM	Figure 2.5J-18
Woodward-Clyde Consultants			



Project No. 14940	Hanford FSAR	EPICENTERS OF EARTHQUAKES WITH $M_C \geq 1.0$ , DEPTH $\leq 3$ KM	Figure 2.5J-19
Woodward-Clyde Consultants			



Project No.  
14940

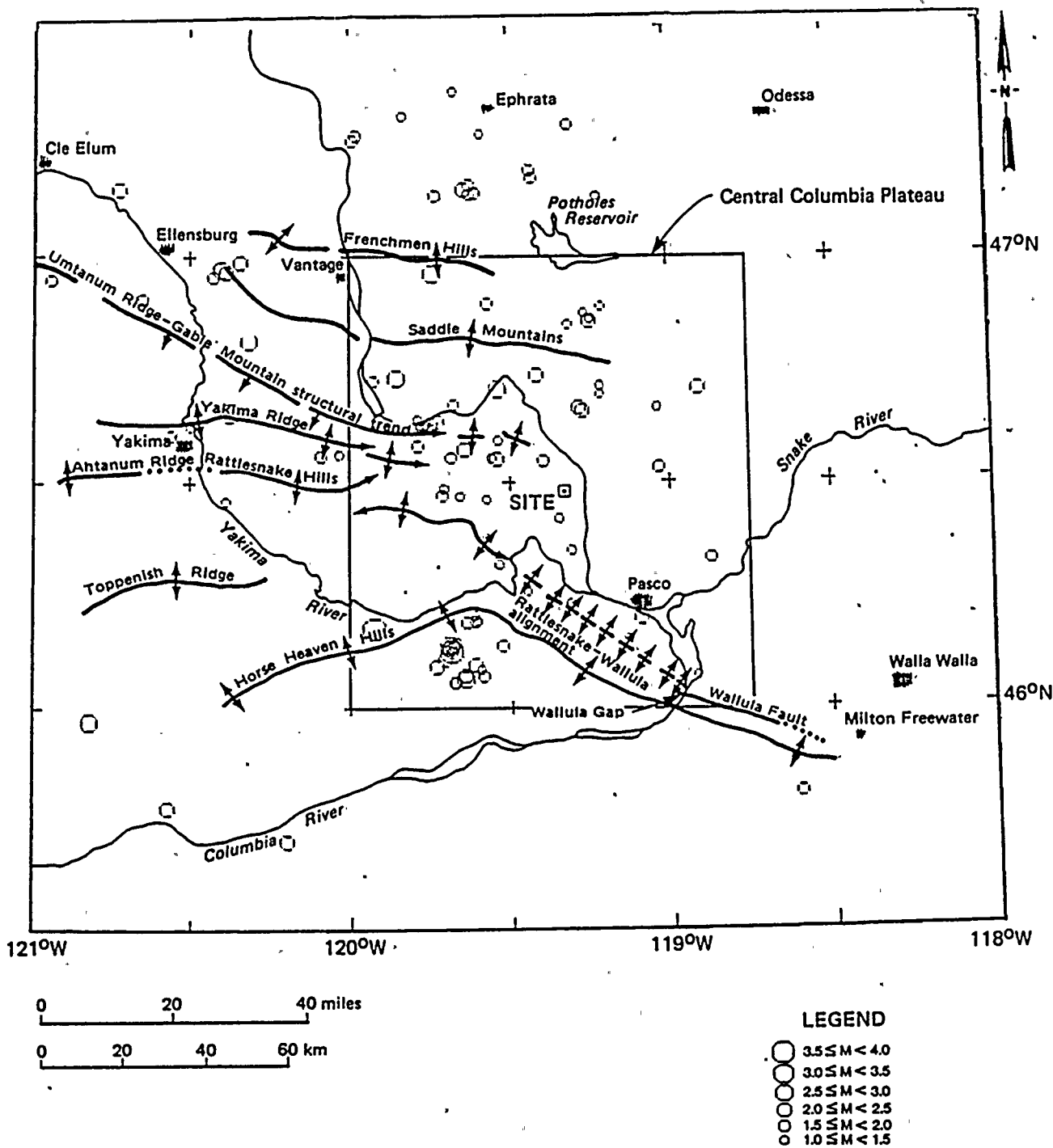
Hanford FSAR

Woodward-Clyde Consultants

EPICENTERS OF EARTHQUAKES  
WITH  $M_C \geq 1.0$ ,  $3 \text{ km} < \text{DEPTH} \leq 8 \text{ km}$

Figure  
2.5J-20





Project No.  
14940

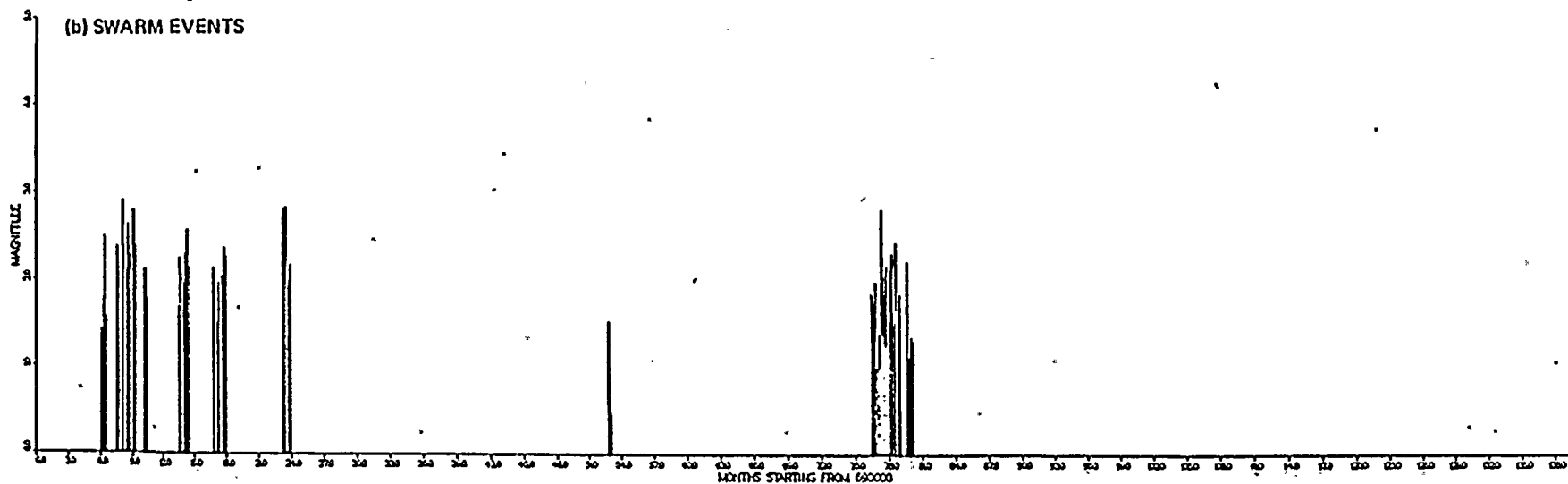
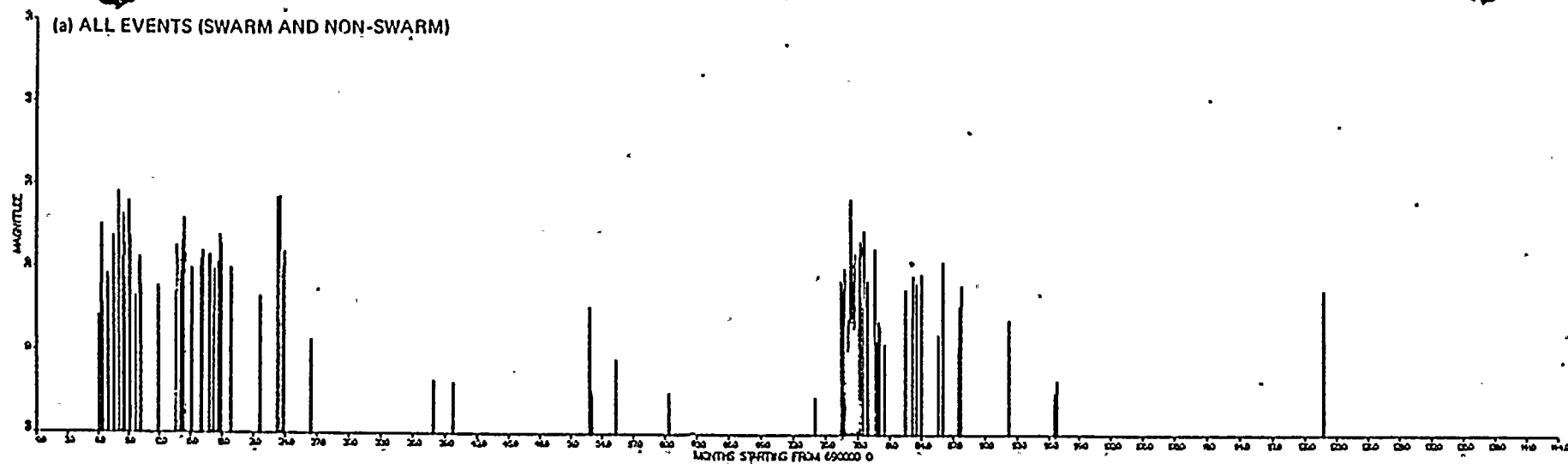
Hanford FSAR

Woodward-Clyde Consultants

EPICENTERS OF EARTHQUAKES  
WITH  $M_C \geq 1.0$ , DEPTH  $> 8$  KM

Figure  
2.5J-21

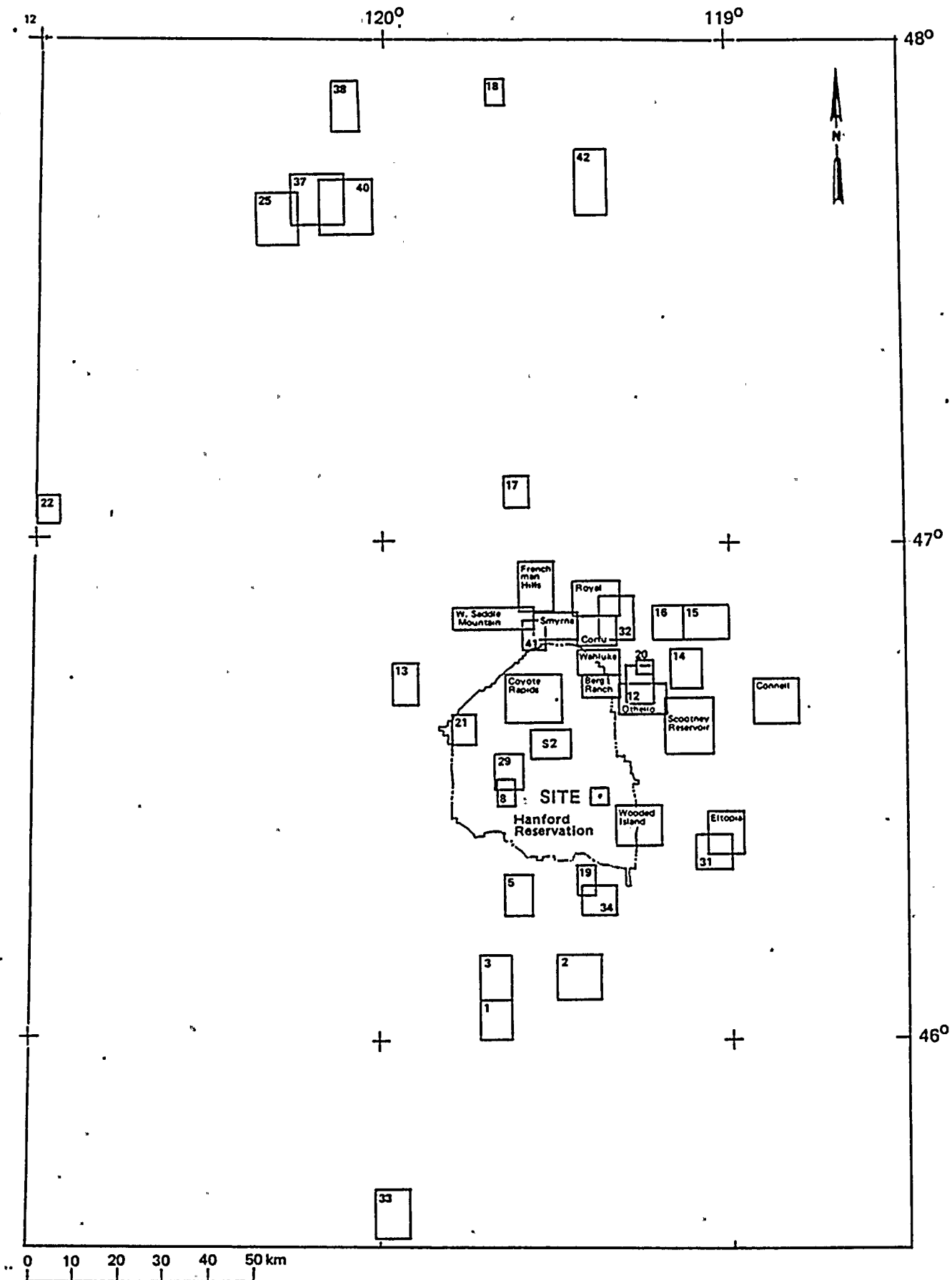




Project No. 14940	Hanford FSAR	MAGNITUDE VERSUS OCCURENCE DATE, WOODED ISLAND EARTHQUAKES, 3/69 - 12/80	Figure 2.5J-22
Woodward-Clyde Consultants			







Project No. 14940	Hanford FSAR	SWARM AREA BOUNDARIES	Figure 2.5J- 23
Woodward-Clyde Consultants			

## SWARM AREA BOUNDARIES

**Figure  
2.5J- 23**

**Woodward-Clyde Consultants**

## Hanford FSAR

**Project No.**  
**14940**

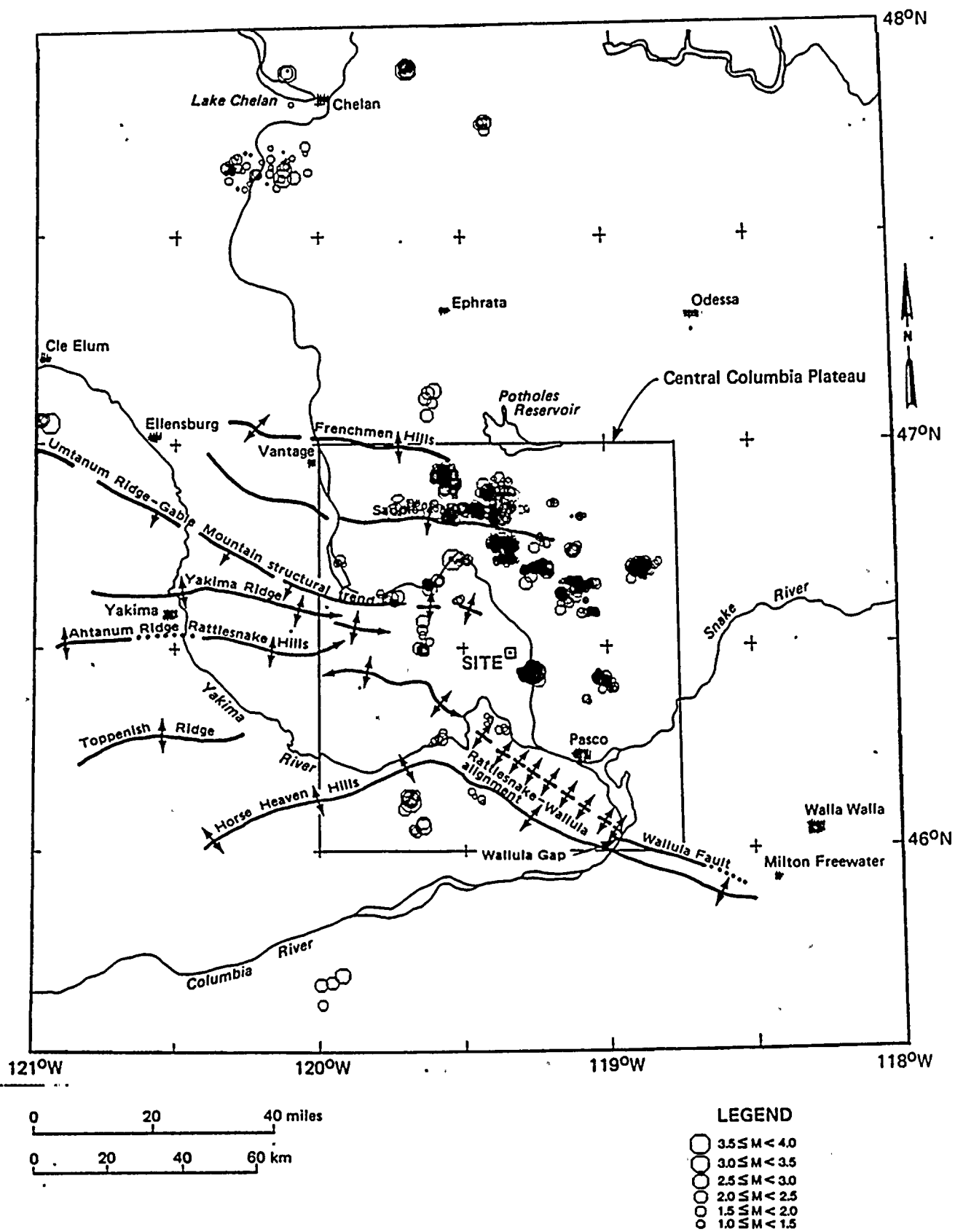
## SWARM AREA BOUNDARIES

**Figure  
2.5J- 23**

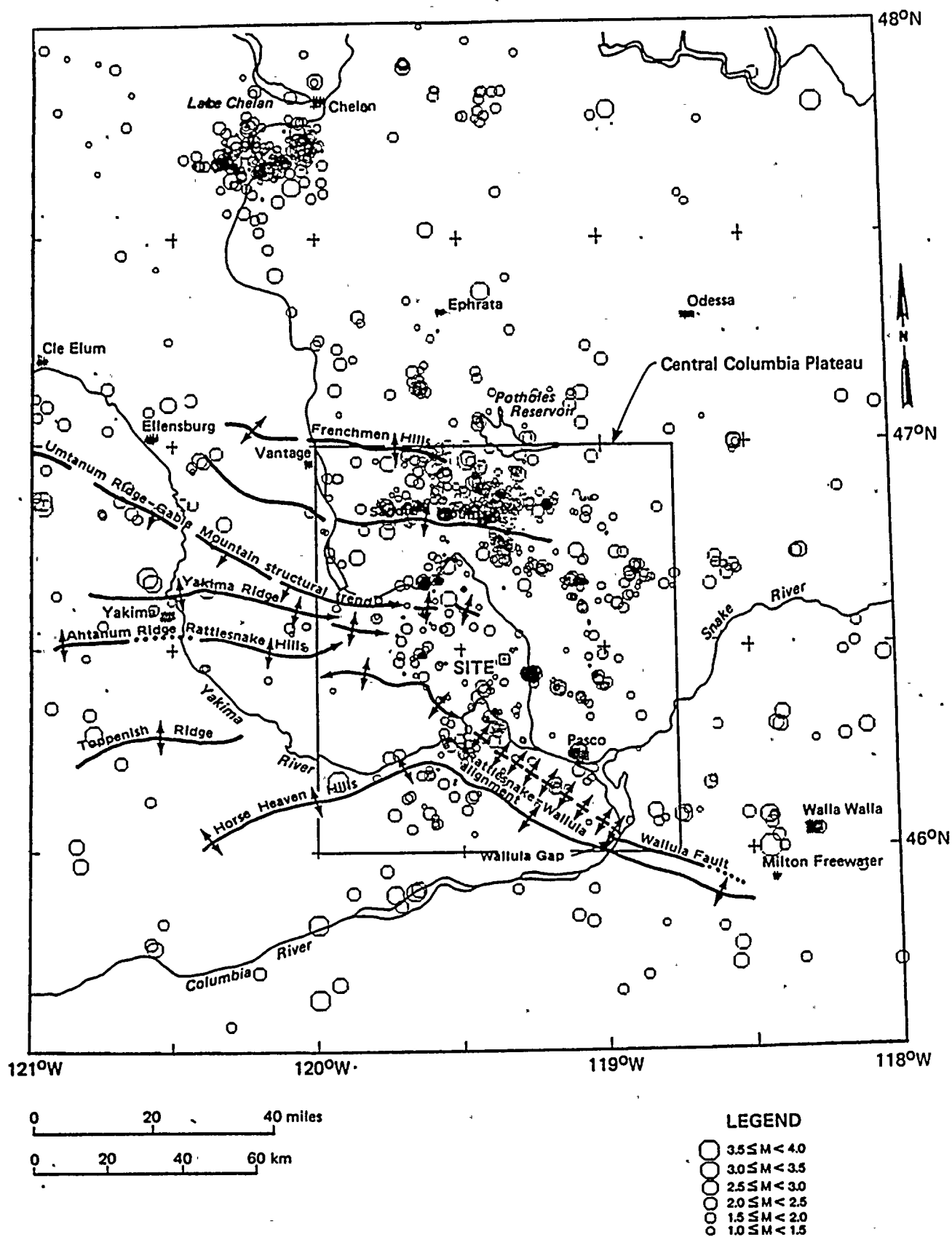
**Woodward-Clyde Consultants**

## Hanford FSAR

**Project No.**  
**14940**



Project No. 14940	Hanford FSAR	EPICENTERS OF SWARM EARTHQUAKES: ALL DEPTHS, 3/69 - 12/80	Figure 2.5J-24
Woodward-Clyde Consultants			



Project No.  
14940

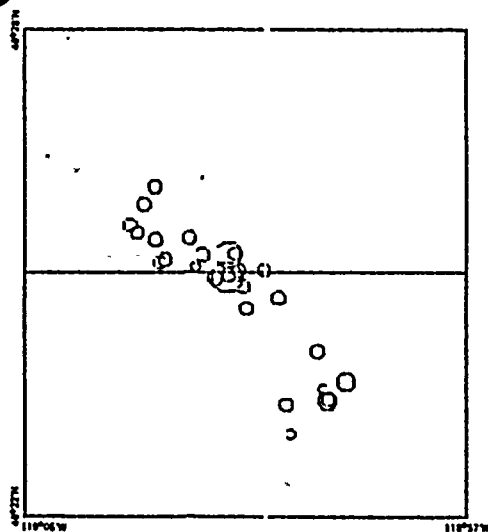
Hanford FSAR

Woodward-Clyde Consultants

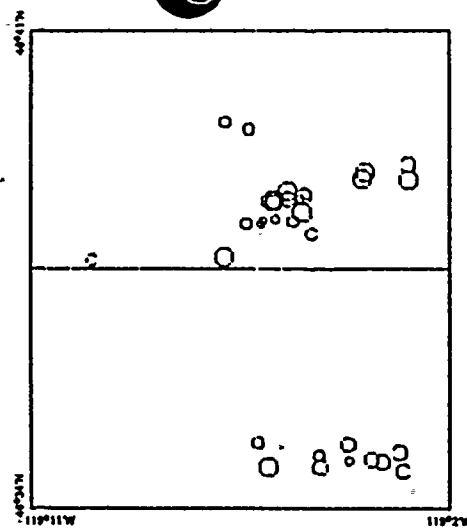
EPICENTERS OF NON-SWARM EARTHQUAKES:  
ALL DEPTHS, 3/69 -12/80

Figure  
2.5J- 25

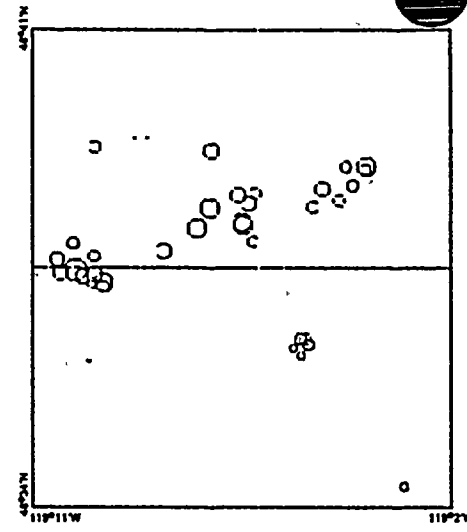
Project No. 14940	Hanford FSAR	EPICENTERS OF EARTHQUAKES IN SELECTED SWARMS	Figure 2.5J-26
Woodward-Clyde Consultants			



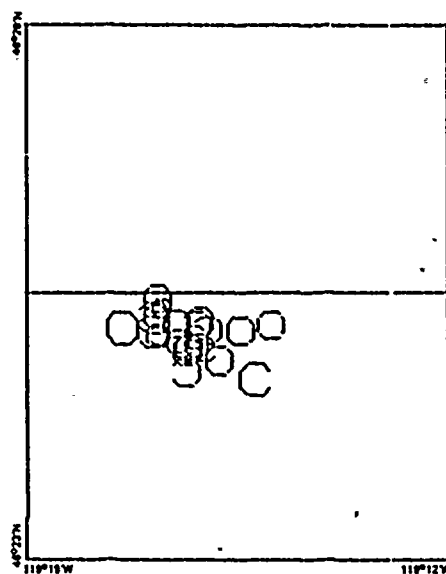
25(a) ELTOPIA SWARM A



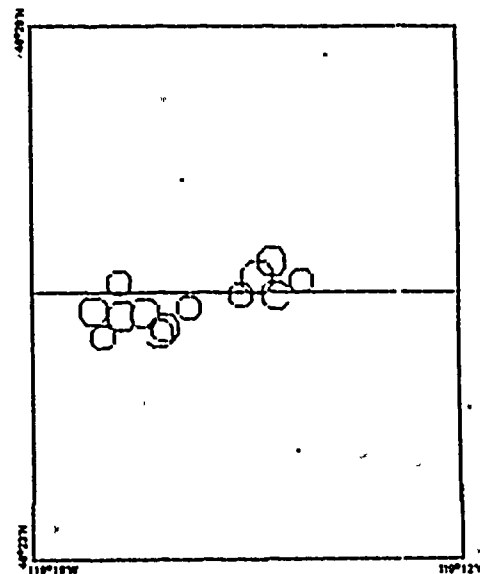
25(b) SCOOTNEY RESERVOIR  
SWARM B



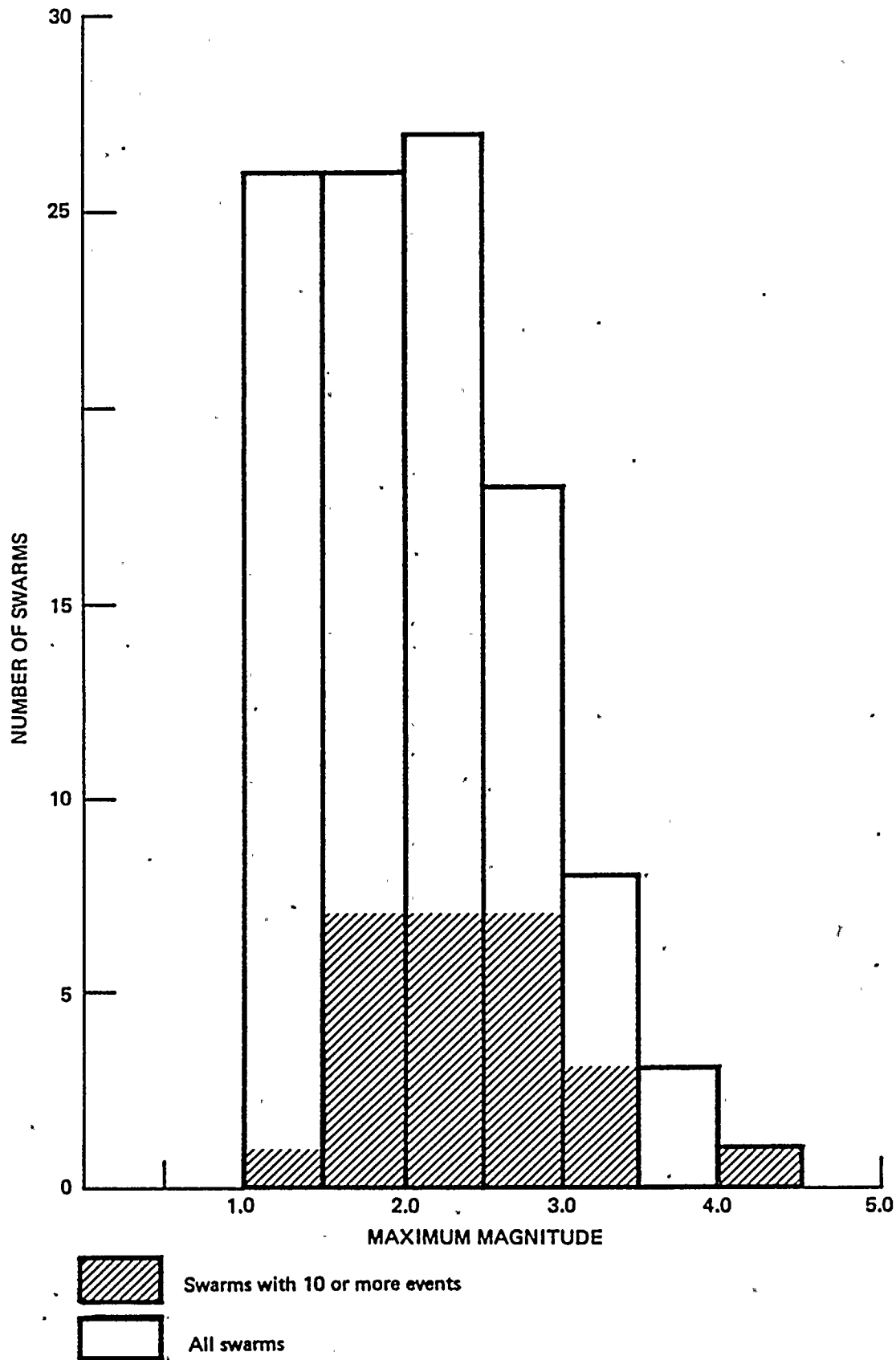
25(c) SCOOTNEY RESERVOIR  
SWARM C

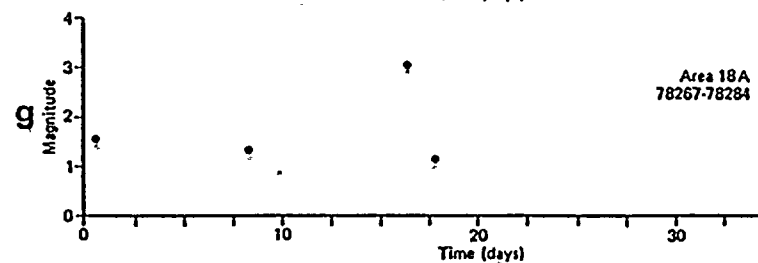
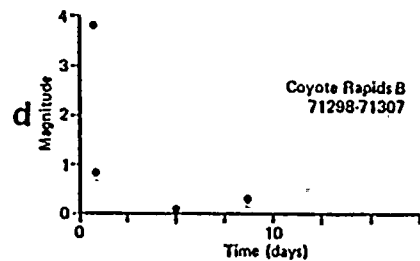
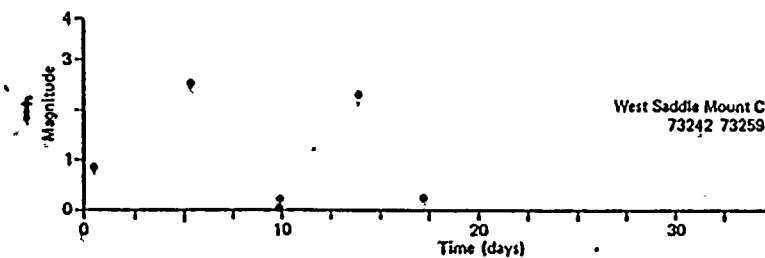
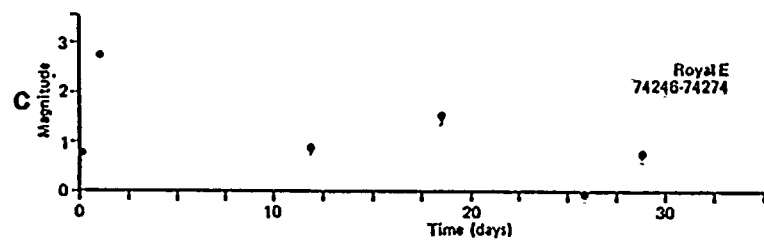
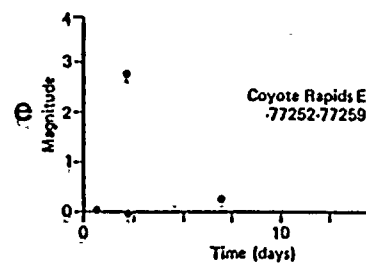
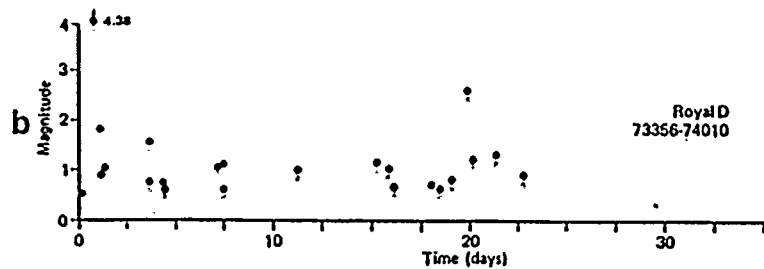
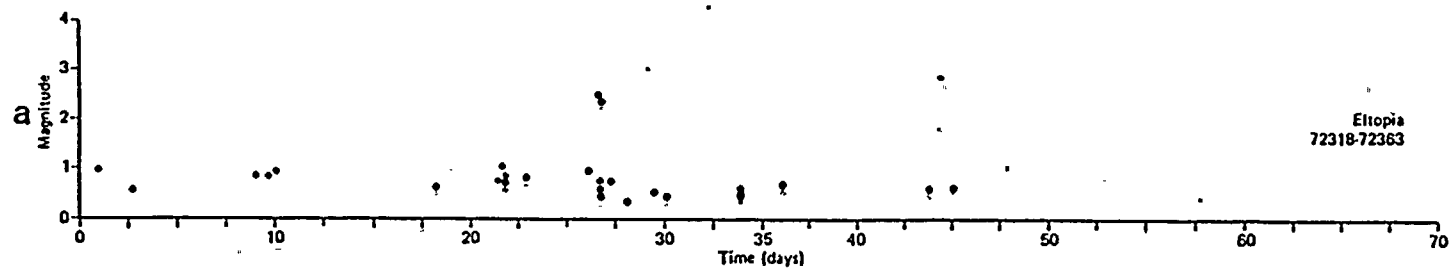


25(d) WOODIED ISLAND SWARM B

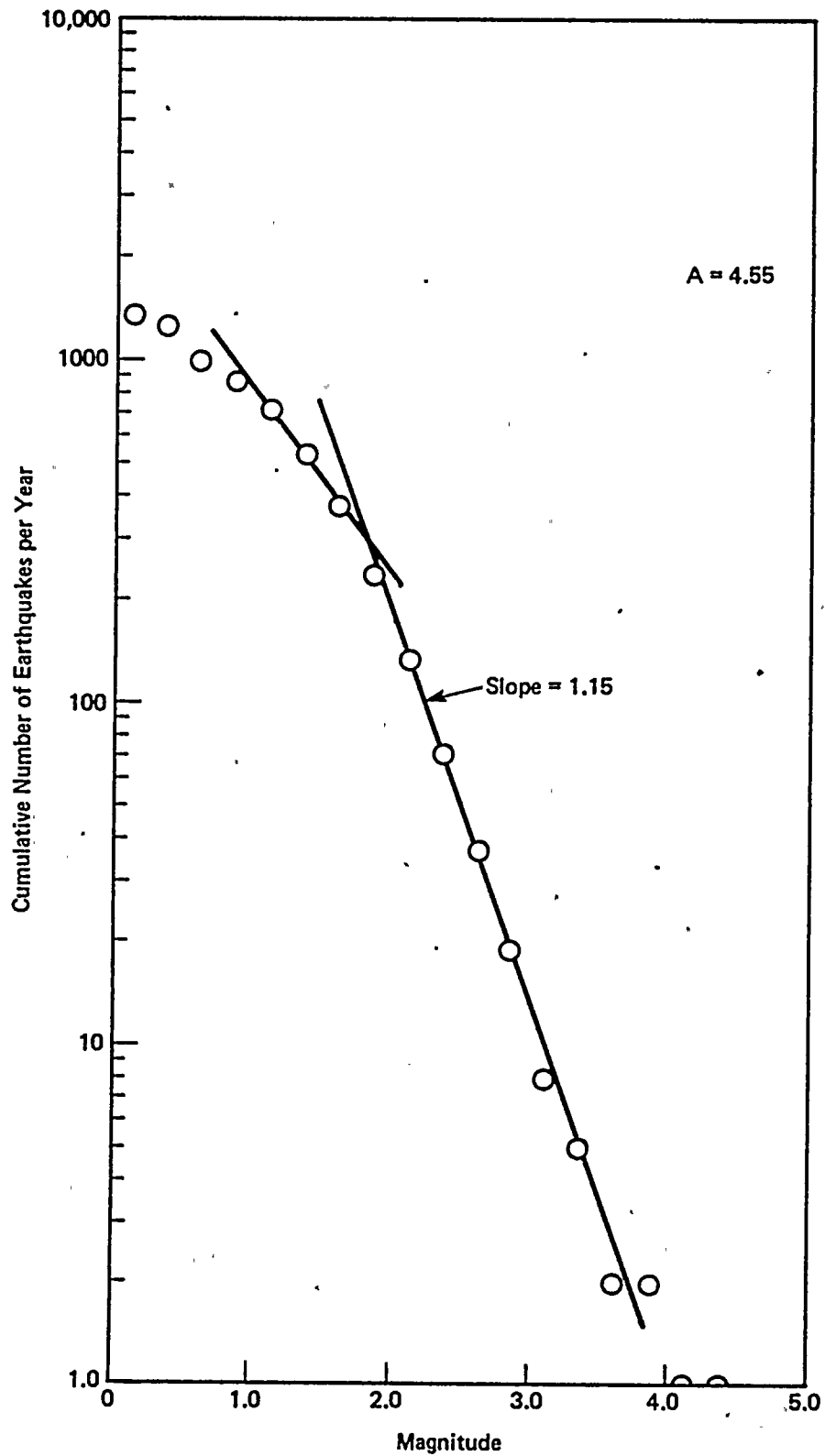


25(e) WOODIED ISLAND SWARM E



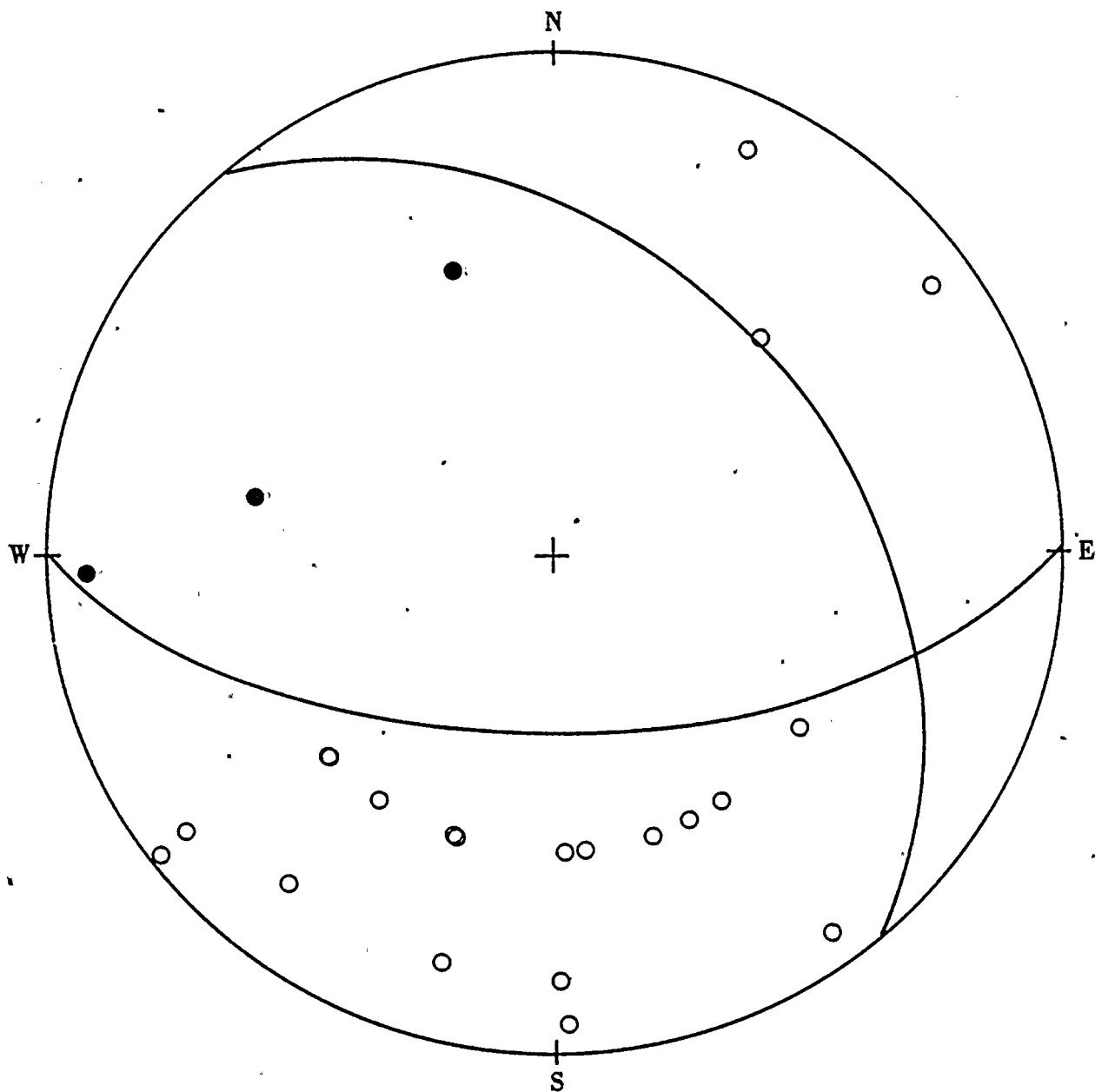


Project No. 14940	Hanford FSAR	MAGNITUDE TIME HISTORY FOR SELECTED SWARMS	Figure 2.5J- 28
Woodward-Clyde Consultants			



Project No. 14940	Hanford FSAR	CUMULATIVE NUMBER OF SWARM EARTHQUAKES VERSUS MAGNITUDE	Figure 2.5J-29
Woodward-Clyde Consultants			





EXPLANATION  
 ● Compression  
 ○ Dilatation

LOWER HEMISPHERE EQUAL AREA PROJECTION

Project No. 14940	Hanford FSAR	FAULT PLANE SOLUTION FOR THE 20 DECEMBER 1973, ML 4.4 ROYAL SLOPE EARTHQUAKE	Figure 2.5J-30
Woodward-Clyde Consultants			



dextral strain, evidenced by the northwest-trending structures, that appears to have developed synchronously with the predominant east-west trending structures. The northwestern portion of CLEW is ill defined by the fold structures. In the southeastern portion, CLEW becomes more distinctly defined by the Wallula fault zone.

The Rattlesnake-Wallula alignment is a fold dominated structural trend west of Wallula Gap. Geologic mapping has been unable to demonstrate the existence of a through-going surface fault associated with the fold structures west of Wallula Gap. Trenching across the Wallula fault zone, east of Wallula Gap, indicates non-involvement of the late Pleistocene-Holocene Touchet sediments. At Yellepit, west of Wallula Gap, a trench across the southern strand of the Wallula fault zone (Wallula Gap Fault ) shows undisturbed conglomerates of latest Pleistocene age, resting on faulted Miocene basalts. While this data limits the age of last movement, capability of the Rattlesnake-Wallula structural trend, cannot be demonstrated unequivocally on the basis of existing data.

The more southerly Columbia Plateau fold structures (e.g., Toppenish Ridge, Horse Heaven Hills, Columbia Hills) developed before extrusion of the Plio-Pleistocene Simcoe volcanics, that lie essentially undisturbed across the western traces of these structures. This relationship indicates a waning of southern plateau deformation, including CLEW, since the Pliocene. Surface ruptures of probable Quaternary age have been mapped on Toppenish Ridge. Both landslide and tectonic origins for the structure have been postulated. Woodward-Clyde Consultants (1981a) concluded that they are probably tectonic in origin.

Gable Mountain is the closest structure to the WNP 1-2-4 site, at a distance of approximately 7 kilometers to the subsurface extension of the anticlinal axis (Southeast anticline). There is evidence of faulting with probable late Pleistocene displacement of 0.2 - 0.3 feet mapped over a distance of about 1100' along strike. Golder Associates (1981a) concluded that there was "insufficient evidence to substantiate non-tectonic mechanisms for the origin of the observed displacements in glaciofluvial deposits."

No surface faulting within a distance of 8 kilometers of the WNP 1-2-4 sites is known. Approximately 5 kilometers to the east of the WNP 1-2-4 site, Pliocene Ringold sediments lie essentially horizontal with no sign of deformation, for a distance of at least 8 kilometers both north and south. No evidence was detected for faulting at depth directly



underneath the WNP 1-2-4 site on the basis of borehole geophysics. Within the limits of resolution of the gravity and aeromagnetic data there is no correlation between any known geologic features and geophysical linears suggestive of faulting within the site vicinity.

From detailed geologic and geophysical studies, there appear to be no potential hazards that will adversely affect the plant structures at the site due to natural geologic phenomena or from man's activities.

Seismicity in the vicinity of the site has been low during the historical (approximately 150 years) period, with infrequent earthquakes of low to moderate intensity or magnitude. Damage from earthquakes in the vicinity of the site has been extremely minor.

The maximum vibratory ground motion affecting the site during historic time is estimated to have been approximately 0.015 g. The maximum vibratory ground motion potential at the site from an earthquake associated either with a tectonic structure or with a tectonic province is estimated to be 0.125 g.

Vibratory acceleration levels of 0.25 g and 0.125 g are assigned as conservative design bases for the Safe Shutdown Earthquake (SSE) and the Operating Basis Earthquake (OBE), respectively.

The existing glaciofluvial sand was excavated down to the underlying, very dense Ringold gravel and replaced in a denser state by compaction (structural backfill). Groundwater was not encountered during excavation operations and appears to be stable at about elevation 380 feet (a depth of approximately 62 feet below ground surface). This is about 10 to 15 feet below the top of the Ringold gravel.

Excavated site soils were used for the structural backfill. Close control on compaction procedures was maintained to verify that specified densities (average relative density of 85 percent, with a minimum relative density of 75 percent) and uniformity of compaction were achieved during placement of backfill.

Foundations of all WNP-2 plant structures are supported in structural backfill. The backfill provides safe bearing for the structural foundations, and settlements are estimated to be minimal. Systematic monitoring and analysis of settlements of Seismic Category I foundations at the site have been continuous since the beginning of construction.



Design analysis of the structural backfill and underlying dense Ringold gravels indicates that the structural backfill would not be susceptible to loss of strength, subsidence or liquefaction resulting from potential vibratory ground motions that might be associated with the design earthquakes.

It is concluded that the site is suitable for a nuclear power plant in terms of Appendix A to 10 CFR Part 100, "Seismic and Geologic Siting Criteria for Nuclear Power Plants", and that the design basis for vibratory ground motion (Safe Shutdown Earthquake) should be 0.25 g without the need to consider surface faulting at the site. It is also concluded that subsurface materials will adequately provide vertical and lateral stability to all structures under, and dynamic conditions contemplated for, this facility at this site as constructed.

The geological, geophysical and seismological investigations performed in support of Chapter 2.5 include:

- Geologic, geophysical, and seismologic studies of the site and region for a distance of 322 kilometers;

- Remote sensing studies of the site and region for a minimum distance of 80 kilometers;

- A 40,000 line mile aeromagnetic survey centered on the site;

- Compilation of a gravity maps for the site, site province and Pacific Northwest region;

- Compilation of geologic and tectonic maps for the Pacific Northwest region;

- Detailed geologic mapping of the site and surrounding area for at least 8 kilometers and additional detailed mapping of significant structures;

- Subsurface exploration at the site and vicinity involving borings for geologic and soil engineering purposes, geologic trenching, and test pits;

- Representative penetration resistance tests and in situ deformation and density tests in boreholes, and percolation tests and in situ density test pits;

- Laboratory testing of samples taken from borings, trenches and test pits for engineering and geologic analysis;





Measurement of groundwater levels in boreholes;

Borehole geophysical surveys for stratigraphic correlation among borings;

Uphole/downhole and crosshole seismic geophysical surveys;

Surface seismic refraction to define overburden stratigraphy and to delineate depth to rock in the vicinity of the site.

The preparation of the Geology and Seismology section of the original WNP-2 PSAR was under the direction of Burns and Roe, Hempstead, New York, with assistance of the following:

Dr. Howard A. Coombs - Principal Consultant  
Dr. James W. Crosby III - Consultant for Borehole  
Geophysics  
Shannon & Wilson, Inc. - Soil Properties, Foundation  
Engineering

Dr. R. P. Miller - Project Manager  
D. Schwantes - Project Soils Engineer  
R. E. Brown - Consultant for Bedrock Stratigraphy

Weston Geophysical Research, Inc. -  
Seismic Surveys and Borehole Geophysics

T. F. Sexton - Project Manager  
E. N. Levine - Field Project Manager  
Dr. F. T. Turcotte - Seismologist

The original preparation of the Geology and Seismology section of the PSAR for project WNP-1 and WNP-4, which is utilized in the WNP-2 FSAR, was under the direction of United Engineers and Constructors, Philadelphia, Pa. with the assistance of the following:

Weston Geophysical Research, Inc. -  
Seismicity, Seismic Surveys, Borehole Geophysics,  
and Response Spectra

R. J. Holt - Project Director/Seismologist  
Dr. F. T. Turcotte - Seismologist  
Dr. H. Coombs - Consultant/Geology  
Prof. J. W. Crosby III - Consultant for Borehole  
Geophysics  
Rev. D. Linehan, S. J. - Consultant/Seismicity  
Prof. R. W. Whitman - Consultant/Response Spectra



T. F. Sexton - Project Manager  
E. N. Levine - Project Coordinator for Field  
Studies

FUGRO, Inc. - Geology

E. A. Danehy - Project Manager  
Owen Swanson - Project Geologist  
Donald Hitchcock - Assistant Project Geologist

Shannon & Wilson, Inc. -  
Soil Properties, Foundation Engineering, Soil  
Engineering

Dr. R. P. Miller - Project Supervisor  
H. H. Druebert - Project Soils Engineer  
T. L. Olmsted - Project Engineering Geologist  
Dr. I. Arango - Structure-Soil Interaction  
Evaluations  
Prof. A. J. Hendron - Consultant/Soil Dynamics  
Prof. H. B. Seed - Consultant/Structure-Soil  
Interaction  
Prof. J. Lysmer - Consultant/Structure-Soil  
Interaction

Extensive additional geologic, geophysical and seismological data were compiled for the WNP1 and WNP4 PSAR as part of studies related to the December 14, 1872 earthquake. This information was filed in October, 1977 as Amendment 23 to the WNP 1 and WNP 4 PSAR and is included herein by reference. This work was performed under the direction of United Engineers and Constructors with technical guidance provided by the following:

Dr. H. A. Coombs - Principal Consultant  
Dr. G. A. Davis - Professor Geology, USC  
Dr. Don Tocher - Chief Seismologist,  
Woodward-Clyde Consultants

The preparation of the Geology and Seismology section presented in the initial submittal of the WNP-2 FSAR was the responsibility of Burns and Roe, Woodbury, New York with assistance of the following:

Dr. H. A. Coombs - Principal Consultant

Shannon & Wilson, Inc. -  
Chapter 2.5 preparation, Regional Geology and  
Seismicity, Site Geology, Soil Properties,  
Foundation

Dr. R. P. Miller - Project Supervisor  
H. H. Druebert - Project Manager and Soils  
Engineer  
H. H. Waldron - Consultant Geologist

Weston Geophysical Research -  
Seismicity Review, Site Geophysics, and Borehole Geophysics

V. J. Murphy - Project Manager  
T. F. Sexton - Assistant Project Manager  
Andrew LaCroix - Project Coordinator/  
Seismology  
Richard Allen - Supervisor Data Processing/  
Site Geophysics

Amendment 18 to the WNP-2 FSAR integrates all of the new geological and geophysical data accumulated since the FSAR was originally docketed. It is a synthesis through 1980 based on the original FSAR and incorporates new information contained in Amendment 23 (WNP-1/4 PSAR), consultant reports, and Rockwell Hanford Operations' Basalt Waste Isolation Project reports. This amendment was prepared under the direction of the Washington Public Power Supply System by Weston Geophysical Corporation and Woodward-Clyde Consultants with the assistance of the following:

Dr. H. A. Coombs - Professor Emeritus, University of  
Washington  
Dr. G. A. Davis - Professor Geology, University of  
Southern California  
Dr. R. B. Smith - Professor Geophysics, University of  
Utah  
Mr. D. D. Tillson - Consulting Geologist

Weston Geophysical Corporation - Geophysics

Mr. V. J. Murphy - Project Manager  
Mr. J. T. Doherty - Assistant Project Manager  
Mr. J. Imse - Geophysicist  
Prof. G. Simmons - Consultant/Geophysics  
Prof. C. E. Glass - Consultant/Remote Sensing  
Prof. B. C. Burchfiel - Consultant/Geology

Prof. H. P. Laubscher - Consultant/Geology

Woodward-Clyde Consultants - Geology, Seismology,  
Earthquake Engineering

Dr. A. Patwardhan - Project Director  
Mr. D. Gross - Project Manager



Dr. F. H. Swan - Technical Coordinator  
Mr. L. Cluff - Technical Reviewer - Geology  
Dr. W. Savage - Technical Reviewer - Seismology  
Dr. I. Idriss - Technical Reviewer - Earthquake  
Engineering

Information on Gable Mountain, Gable Butte, and Umtanum Ridge was provided by Northwest Energy Services Company with assistance of the following:

Golder Associates - Geology

Mr. D. Caldwell - Project Manager  
Mr. G. Anttonen - Geologist

## 2.5.1 BASIC GEOLOGIC AND SEISMIC INFORMATION

### 2.5.1.1 Regional Geology

The WNP 1-2-4 site is located within the Pasco Basin, one of several physiographic depressions occupying the Columbia Plateau. The Columbia Plateau, a major physiographic and geologic province is surrounded by the Blue Mountains, High Lava Plains, and Snake River Plain provinces on the south, Northern Rocky Mountains and Idaho Batholith provinces on the east, the Okanogan Highlands province on the north, and the Cascade Mountains, Puget-Willamette Trough, and Washington-Oregon Coast Ranges on the west (Figure 2.5-1).

Discussions of the regional geology and tectonics of the Pacific Northwest have been presented by McKee (1972) and King (1959, 1969). Other notable treatments related to individual states and provinces have been made by Gunning and White (1966), Livingston (1969), Baldwin (1969), Ross and Savage (1967), the United States Geological Survey (1964, 1966, 1969), Rockwell (1979), Laubscher (Appendix 2.5-0), and Davis in (Washington Public Power Supply System 1977a; and Appendix 2.5-N).

The Tertiary rocks of the Columbia Plateau are bordered on the northwest, north, east, and south by pre-Cenozoic rocks. Only to the west, in the Middle Cascades, Puget-Willamette Trough, and Coast Ranges, are rock units older than Cenozoic not in evidence.

Bedrock in the Columbia Plateau consists of a thick sequence of Miocene basalt flows with minor amounts of interflow sediments. These rocks are generally mantled by younger sediments of Pliocene to Holocene age (Figure 2.5-2). The

basalts, particularly in the western parts of the Columbia Plateau, have been folded into a series of east-west anticlines.

The Pacific Northwest gravity map (Figures 2.5-9, 2.5-9a, and 2.5-9b) includes Oregon, Washington, and parts of British Columbia and Idaho. The aeromagnetic map for the central part of the area is presented in Figures 2.5-8, 2.5-8a, and 2.5-8b.

Within the Pacific northwest area, most gravity anomalies appear to correlate well with mapped rock masses and geologic structures (see Appendix 2.5L). Regional trends present in the Bouguer gravity fields are different west of the axis of the northern and central Cascade Mountains. A prominent north-south gravity gradient coincides with the Puget-Willamette Trough, whereas the Columbia Plateau is characterized by a broad northeast trending 40 mgal gravity high centered in the area of the WNP 1-2-4 site.

The total Bouguer gravity anomaly map for the central Columbia Plateau and portions of the surrounding areas is given in Appendix 2.5L (Figure 9). This discussion is based on the more extensive interpretation of that map given in Appendix 2.5L.

A relatively dense rock mass underlies the Columbia Plateau basalt. The surface layer, termed Layer 1, is relatively thin (0 to 2 kilometers), extends over a larger geographic area, and apparently completely covers the lower body termed Layer 2. The presence of several geologic structures (such as the Chiwaukum and Replublic grabens) below the upper layer and outside Layer 2 can be recognized from the gravity map. Layer 2 is much thicker than the upper Layer 1, is roughly tabular (NS dimension, 93 kilometers, and EW dimension, 47 kilometers) and has two subsurface lobes on its southern end. One lobe extends SW for approximately 31 kilometers. The other lobe extends from Wallula to Walla Walla, a distance of about 31 kilometers also. The gravity expression for Layer 2 appears to be quite uniform and the edge appears to have been unbroken by any significant strike-slip faulting or other geologic structures since the layer was formed. Layer 2 is inferred to consist of extrusive rocks that filled an elongate subsiding basin.

The western edge of Layer 2 is the source of a prominent gravity gradient that trends almost north-south for 50 kilometers, extends from south of Toppenish Ridge to north of Quincy (WA). The anomaly passes about 9 kilometers east of Yakima and is extraordinarily straight. Models have been

D used to obtain an upper bound on the horizontal displacements of any potential faults that may have occurred since the time of emplacement of Layer 2. With the present station spacing, the maximum horizontal displacement that could have occurred on any fault, or could have been distributed over any fault zone crossing the feature, is 2-3 kilometers. This conclusion is independent of the origin of the anomalies, the age of the rocks that occur in the area, and specific models of the distribution of density. Models also yield additional constraints on the timing of any horizontal displacement. The minimum time span would be 17 m.y. (the age of the oldest basalt of the area) and the maximum time span could be as old as the age of basement rocks.

The Olympic-Wallowa lineament (OWL) proposed by Skehan (1965) and others previously as a major crustal (and possibly mantle) structure is at most a very minor feature if it exists at all. Neither residual gravity anomaly nor gravity linear is associated with it. It would cross necessarily the western edge of the lower Layer 2, but does not produce any obvious disruption of that body. The maximum vertical displacement that can be discerned by this data set is 300 feet and is located in the vicinity of Pasco. Maximum horizontal displacement during the past 17 m.y. (and possibly much longer) that can be discerned with this data set is 2-3 kilometers.

#### 2.5.1.1.1 Geologic History

The tectonics and geologic history of the Pacific Northwest are the consequences of complex and poorly understood interactions among the Pacific, North American, and Juan de Fuca plates. The Juan de Fuca, a vestigial remnant of the once extensive Farallon plate, lies offshore of Oregon, Washington, and Vancouver Island. It is separated from the Pacific plate to the north, west, and south by the Explorer, Juan de Fuca, and Gorda Ridges and the transform faults (fracture zones) which bound them. The Juan de Fuca-North American plate boundary is one of past convergence and one along which subduction probably still continues at a rate of several centimeters per year (Riddihough and Hyndman, 1976).

In the Mesozoic, new oceanic crust that was generated along the East Pacific Rise, spread westward as part of the Pacific plate and eastward as part of the Farallon plate. The Farallon plate was subducted at a trench along the western margin of the North American plate. About 29 million years ago, the relative motion of the Farallon and North American plates resulted in the oblique impingement of





the East Pacific Rise along the marginal trench (Atwater, 1970). Consequently, the North American and Pacific plates were in direct contact along a right lateral transform fault system to the north and south of which remnants of the Farallon plate still separate the North American and Pacific plates. The triple junction of the Farallon, Pacific and American plates then migrated along the zone of transform shear both northward and southward. The San Andreas Fault grew in length as more of the East Pacific Rise and bordering fracture zones reached the trench along the North American plate boundary. Continued spreading in the northern and southern areas resulted in subduction of most of the Farallon plate to the extent that only a few relict pieces remain. The remaining segments of the Farallon plate interact with the North American plate as small, independent plates. The Cocos, Rivera, and Juan de Fuca plates are such small, relict plates of the Farallon plate that behave as independent plates with directions and rates of spreading different from those of the parent Farallon plate.

In the Pacific Northwest during the early Tertiary the coastline shifted from the western side of the present Cascade Mountains to the western side of the Coast Ranges with the accretion of the Siletz/Crescent volcanic assemblage. Early Tertiary deposits in the Cascade Range include thousands of feet of strata of the brackish Puget Group and continental Swauk, Ohanapecosh, Chumstick, and Roslyn Formations. In Eocene-Oligocene time, volcanism and continental sedimentation were active in much of the Cascade Volcanic Belt, the Intermontane Belt, the Omineca Crystalline Belt, and the Blue Mountains. During this early Tertiary episode of widespread volcanism and sedimentation, erosion was unroofing the Mesozoic batholiths. Granitic intrusions were emplaced in north-central Washington and northeastern Oregon during this period.

During Miocene-Pliocene time, large parts of southeastern Washington and northeastern Oregon were covered by the flood basalts of the Columbia River Basalt Group. On the Columbia Plateau the flows generally advanced from east to west from northwest trending vents. Deformation of the Columbia River Basalts commenced in the Miocene and continued into Pleistocene.

In the Cascades and Blue Mountains, minor uplifts caused the flanking and intermontane basins to receive early and middle Pliocene sediments of the Dalles and Ellensburg Formations. Throughout the Pliocene, the Cascade Volcanic Belt was

marked by local volcanism. The most recent uplift of the Cascade Range and Blue Mountains took place predominantly during the Plio-Pleistocene.

Large stratovolcanoes were formed during the early Pleistocene in the Cascade Mountains (Figure 2.5-22). Major active stratovolcanoes included Mount Baker, Glacier Peak, Mount Rainier, Mount St. Helens, Mount Adams, Mount Hood, and Mount Mazama. Some of these vents have been active into the Holocene, notably Glacier Peak, Mount St. Helens, and Mount Mazama and have erupted large volumes of ash. The ash falls from these eruptions were deposited over a large part of the region and provide time stratigraphic horizons for dating Quaternary geologic events. The latest significant eruption occurred in 1980 from Mount St. Helens.

Vast sheets of continental ice covered most of the northern part of the region during the Pleistocene. The glaciers advanced and receded several times, sculpturing the landscape and depositing till and glaciofluvial sediments. In the Columbia Plateau, the Channeled Scablands resulted from the great outpourings of floodwater after breaching of ice-dammed lakes in Montana (Pardee, 1942). Sub-basins of the Columbia Plateau, like the Pasco Basin, received glaciofluvial sediments. In eastern portions of the Columbia Plateau windblown, silty sediments (Palouse soils) were deposited over large areas. Erosion and deposition by rivers and wind continued to be significant in the Columbia Plateau in Holocene time.

The evolution of the region in light of current plate tectonics theory is discussed by Dr. G. A. Davis in Appendix 2.5-N. This discussion of late Cenozoic tectonics of the Pacific Northwest is primarily concerned with Miocene and younger events in the Columbia Plateau and adjacent geologic provinces. An earlier review (Davis in Washington Public Power Supply System, 1977a) treated evolution of the entire Pacific Northwest from Precambrian time to the present. The analysis by Davis, presented in Appendix 2.5-N, relies heavily on data and concepts developed by earth scientists since 1977, including the structural model for the Columbia Plateau developed between 1977 and 1980 by Dr. Hans P. Laubscher, University of Basel, Switzerland (Appendix 2.5-O).

Specific topics treated by Davis are: (1) the nature of the present stress state and strain patterns in the Pacific Northwest; (2) present North American-Pacific-Juan de Fuca plate relationships; (3) Quaternary and late Tertiary geometric and kinematic interrelations between the Basin-and-Range province and the Pacific Northwest; (4) the

geologic significance of the Olympic-Wallowa lineament; and (5) the implications of Quaternary deformation in the Columbia Plateau.

#### 2.5.1.1.2 Provinces

The Pacific Northwest physiographic provinces are shown on Figure 2.5-1. The source of the province boundaries and descriptions are taken from McKee (1972), Washington Public Power Supply System (1977b), and Rockwell (1979). No distinction is made between geologic and physiographic provinces due to their coincidence throughout the Pacific Northwest.

From the Pacific Ocean eastward, the first major physiographic feature is the Coast Range of Washington and Oregon. These mountains extend northward from the Klamath Mountains of southern Oregon to the Strait of Juan de Fuca. East of these mountains lies the Puget-Willamette Trough, a series of topographic lowlands that extend parallel to the Coast Range from the Willamette River valley on the south to the Strait of Georgia on the north. East of the Puget-Willamette Trough are the Cascade Mountains. The Cascade Mountains extend from northern California to southern British Columbia where they merge with the Coast Mountains. East of the Cascades, the north-south grain of the regional physiography gives way to an east-west grain. From north to south, the principal elements are the Okanogan Highlands, the Columbia Plateau, the Blue Mountains, and the High Lava Plains and Snake River Plain. To the east and north in Idaho, western Montana, and British Columbia, the north to northwest regional grain returns in the form of the Northern Rocky Mountains. A discussion of the tectonics of these provinces is contained in Section 2.5.2.2.1.

The WNP 1-2-4 site (Figure 2.5-1) lies in southeastern central Washington within the Columbia Plateau province. The site is situated near a north-south stretch of the Columbia River, the major watercourse in the region. The Pasco Basin contains the site and comprises approximately 4,144 square kilometers of undulating semiarid plain with low-lying hills, dunes, and intermittent streams. The northern and southern boundaries of the Pasco Basin (Figures 2.5-4, 2.5-6a, 2.5-6b, and 2.5-6c) are defined by the Saddle Mountains and Rattlesnake Mountain, respectively. The easterly ends of Umtanum and Yakima Ridges mark the western boundary of the basin. To the east the basin merges into a vast expanse of dunes, dissected flatlands, and coulees northwest of the Snake River. A detailed discussion of the

Columbia Plateau province is contained in Section 2.5.1.2. A detailed discussion of the Pasco Basin is contained in Section 2.5.1.2.4.

#### 2.5.1.1.2.1 Columbia Plateau

The Columbia Plateau (a physiographic and geologic province) is bounded by the Blue Mountains and High Lava Plains on the south, the northern Rocky Mountains-Idaho batholith on the east, the Okanogan Highlands on the north, and the Cascade Mountains Province on the west.

The Columbia Plateau is drained by the Columbia River which flows westward toward the Pacific Ocean. The Snake River joins the Columbia River after draining the eastern Columbia Plateau and parts of the adjoining provinces to the east and south. Most of the Plateau (see Figure 2.5-7) has gentle topographic relief. Exceptions to this gentle relief are the deep gorge of the Columbia River, the many steep-walled coulees north and east of the Columbia River, and the series of linear, generally west to northwest-trending, anticlinal ridges in the vicinity of Yakima.

The Channeled Scabland of Washington covers the Columbia Plateau from Spokane on the northeast to the Snake River on the south and to the Columbia River on the west. The scabland topography was formed in Pleistocene time by the action of glacial meltwaters and catastrophic floods due to breaching of ice-dammed lakes in western Montana.

The Columbia Plateau formed between 16.5 and 6 m.y.b.p. (Watkins and Baski, 1974; McKee and others, 1977) when large volumes of basalts were erupted from north-northwest trending linear vent systems in northeastern Oregon and southeastern Washington (see Figure 2.5N-2) (Waters, 1961; Taubeneck, 1970; Swanson and others, 1975; Fruchter and Baldwin, 1975; Price, 1977; Swanson and others, 1977).

The lavas of the Columbia Plateau cover an area of approximately 202,018 square kilometers and have an estimated volume of 170,894 cubic kilometers (Figures 2.5-3 and 2.5N-2) (Swanson and Wright, 1978). The Columbia Plateau is surrounded by topographically higher areas. The character of the pre-Tertiary rocks covered by basalt is visible only within highlands surrounding the plateau.

Individual basalt flows are voluminous, generally 8 to 25 cubic kilometers, with a maximum known volume of 604 cubic kilometers. Flows range in thickness from a few inches to more than 300 feet, with an average thickness of 90 to 120

feet (Swanson and others, 1979a). The thickest flows are interpreted as showing ponding in pre-basalt valleys, in structurally controlled basins that developed during volcanism, or in narrow canyons previously eroded into older flows (termed intracanyon flows) (Swanson and Wright, 1978).

Flows of the Columbia River Basalt Group are interbedded with and overlapped by Miocene-Pliocene epiclastic and volcanoclastic sediments, especially along the margin of the province. Invasive flows, formed when lava "burrowed" into surficial deposits of unconsolidated sediments, are also common (Byerly and Swanson, 1978). The youngest sedimentary units on the plateau are fluvial, lacustrine, glaciofluvial, and eolian deposits of Pliocene to Holocene age. Localized accumulations of Pliocene to Pleistocene lavas are also present within the western and southern portions of the province.

#### 2.5.1.1.2.2 Coast Range of Oregon and Washington

The Coast Range of Washington and Oregon lies west of the Puget-Willamette Trough. It consists of a 80 to 129 kilometers wide belt of mountains which extends more than 966 kilometers from the Klamath Mountains in southwestern Oregon to the Strait of Juan de Fuca in northwestern Washington. The Olympic Mountains are part of the Coast Range and form the highest and most rugged part of the province. Among the oldest rocks in the region are a 15,000 foot sequence of basaltic volcanics (Siletz/Crescent volcanics) that probably represent an oceanic seamount chain that was accreted to the continental margin in early Tertiary time. South of the Straits of Juan de Fuca, the principal geologic units are Eocene through Miocene marine volcanic and sedimentary rocks. Faults in the Olympic Mountains are predominantly early and middle Tertiary in age. South of the Olympic Mountains, the structure of the Coast Range can be generalized as a system of folds of Miocene and Pliocene age.

#### 2.5.1.1.2.3 Puget-Willamette Trough

The Puget-Willamette province is an elongate structural and topographic low that lies between the Cascade Mountains on the east and the Coast Range on the west. It extends from about Eugene, Oregon on the south to Vancouver, British Columbia, on the north. From south to north its major features are the Willamette Valley, the Puget Lowlands, and the Georgia depression. These troughs are the surface expressions of a large downwarp. This province is a depositional site containing thick fills of Tertiary and

Quaternary sediments. From the Puget lowlands northward, Pleistocene glacial sediments are the dominant geologic unit present. South of the Puget lowlands, the sediments are predominantly alluvial. Low hills occur in Washington between the Columbia River and the Puget Lowlands. On the north, the Puget Sound area was extensively modified during Pleistocene time by the Puget Lobe of the continental glacier.

#### 2.5.1.1.2.4. Blue Mountains

The Blue Mountains province lies immediately south of the Columbia Plateau in northeastern Oregon. This province includes the Ochoco Mountains on the west and Wallowa Mountains on the east. The overall structure can be characterized as a 322 kilometers long, northeast-trending series of anticlines with moderately steep northern flanks and gentle southern flanks. Superimposed upon these asymmetric structures is a north to northwest trend of folds and high angle faults of late Cenozoic age. Initial development of the Blue Mountains anticlinal system predates eruption of the Columbia Plateau basalts. The Blue Mountains are capped by Columbia River flood basalts which fill the Columbia Plateau to the north. Uplift and resulting erosional stripping have exposed older rock strata which do not crop out in the Columbia Plateau. These pre-Tertiary rocks consist of Paleozoic and lower Mesozoic ophiolitic rocks, and associated sedimentary and volcanic rocks that have been intruded by Mesozoic granitic plutons (Washington Public Power Supply System, 1977a).

#### 2.5.1.1.2.5 High Lava Plains Province

The High Lava Plains province, which is characterized by the presence of youthful volcanic rocks, is located south of the Blue Mountains and east of the Cascade Mountains provinces. It is a transitional province between the Blue Mountains and the Basin and Range province farther south. Most rocks exposed within the province are high-alumina basalt flows of Miocene to Pliocene age or younger. Younger basaltic and rhyolitic ash flows (as young as Holocene) were erupted from cinder cones and volcanic vents found within the topographically subdued province. The most prominent structural feature within the province is the Brothers fault zone, a diffuse northwest-trending zone of deformation first described in detail by Lawrence (1976) and discussed by Davis in Appendix 2.5-N.

#### 2.5.1.1.2.6 Northern Rocky Mountains and Idaho Batholith Provinces

The Northern Rocky Mountains are located to the east of the Okanogan Highlands province and to the northeast of the Columbia Plateau province. Major drainages flow toward the Columbia Plateau including the Spokane, Clearwater, and Salmon Rivers. Rocks of the Northern Rocky Mountains province are predominantly slates, argillites, and quartzites of the Precambrian Belt Supergroup.

Northwest-striking vertical faults and parallel folds of Tertiary age exist north of a west-northwest trending fracture belt known as the Lewis and Clark Line. The Rocky Mountain Trench is a north-south valley at least 1287 kilometers long which is formed along lines controlled by faulting. Eastward is the northwest-trending Rocky Mountain thrust belt.

The Idaho Batholith lies east of the Columbia Plateau and Blue Mountains and south of the northern Rocky Mountains. It is a major batholithic intrusion exposed over an area of approximately 41,440 square kilometers. The rocks are predominantly granodiorite and quartz monzonite of Mesozoic age. Eocene plutons and minor amounts of other granitic rocks are also present. Much of the batholith appears to have been intruded as a unit or as a number of large, related, and possibly gradational units. Within the border zone of the batholith, the sedimentary rocks have been metamorphosed to gneiss and schist, within which are bodies of igneous rocks. These marginal rocks are deformed as well as metamorphosed. The dominant types of deformation along the margins of the province are folding and thrust faulting. Internally the batholith is essentially undeformed.

#### 2.5.1.1.2.7 Okanogan Highlands

The Okanogan Highlands province lies east of the Cascade Range and north of the Columbia Plateau. The province consists of broad, rounded hills. The topography of the Okanogan Highlands has been largely molded by glacial and glaciofluvial processes active during late Pleistocene time. The major drainage in the Okanogan Highlands province is the Columbia River, which flows north-south through the province and east-west along its southern boundary. The river divides the highlands into eastern and western regions (Yates and others, 1966).



The eastern region is underlain by Precambrian Beltian rocks and by a lower Paleozoic miogeosynclinal sequence of quartzites, phyllites, and carbonates. The Kootenay Arc, a fold belt trending northward in a convex eastward arc from the Columbia Plateau to the Columbia Mountains, is the dominant structural feature of the eastern region. The folds of this belt trend approximately northeast and are cut by pre-Tertiary faults. The western region is composed of upper Paleozoic and Mesozoic rocks. These rocks constitute a eugeosynclinal assemblage of graywackes, greenstones, shales, cherts, conglomerates, and limestone. Late Mesozoic granodiorites and quartz monzonites intrude these sedimentary sequences, and lower Tertiary volcanic rocks unconformably overlie all of the older rocks. In the western region, north-trending, high-angle normal faults of Cretaceous and early Tertiary age are the most conspicuous structures.

Within the western Okanogan Highlands the major cenozoic structural element is the Republic graben, a northeast trending structure about 6 to 16 kilometers wide, that extends approximately 80 kilometers north to the Canadian Border. The graben is bounded on the west by the Bacon Creek and the Scatter Creek fault zones and to the east by the Stevens fault and several smaller faults. Apparent displacements along these bounding faults range from several hundred feet or less to over 17,000 feet (Yates and others, 1966). Geologic observations at Grand Coulee Dam and reconnaissance observations by J. A. Blume and Associates (1972) for Washington Public Power Supply System in the region between the dam and the southern most mapped exposures of the eastern border faults showed that no discernible evidence of faulting exists in the Columbia Plateau along the southern projection of the graben. Blume's reconnaissance study made this conclusion based on the following observations: no fault offset of the glacial till resting on the granitic rocks of the Colville batholith or of the granitic rocks themselves; continuity, both vertically and horizontally, of stream patterns across the projected traces of the Republic graben faults; no faulting or disturbance of the Columbia River basalts south of the Columbia River except by the Coulee and Barker Canyon monoclines; and concordance of Columbia River terraces across postulated traces of the bounding faults. These terrace surfaces and the underlying terrace deposits of the Nespelem Formation can be traced across the fault projections without interruption. The most prominent terrace surface, the Nespelem Terrace, is at least 12,000 years old and the base of the Nespelem Formation is in excess of 27,000 years old (Blume, 1972). These last two

observations have been verified by mapping and extensive exploratory drilling along the east bank of the Columbia River downstream of Grand Coulee Dam, and by geologic mapping of the Columbia River basalts in the vicinity of Banks Lake (BUREC, 1974).

The age of the Republic graben is not precisely known although Staatz (1964) felt the last movement on the bounding faults was Miocene. Muessig (1967) in his mapping of the northern Republic graben states:

The evidence for later and probably periodic movements along the marginal faults...indicates that the major movement on the Bacon Creek fault probably had terminated before the deposition of the basalt member of the Klondike Mountain Formation (late Oligocene - early Miocene). There is no limiting upper date for movement along the Stevens fault but it seems logical to suppose that the history of movement was not very much different from that of the other graben faults.

The lack of offset of glacial deposits (kame terraces and lake sediments related to Pleistocene glaciation) indicates a lack of recent fault activity (BUREC, 1974).

#### 2.5.1.1.2.8 Cascade Mountains

The Northern Cascades are separated from the Coast Mountains of British Columbia by the Fraser River Valley. Snoqualmie Pass, in west-central Washington, forms the approximate boundary between the Northern Cascades and the rest of the range.

The topographic character of the province changes progressively to the north, reflecting the increasing erosional effects of alpine glaciation at higher altitudes, and the overriding of much of the Northern Cascades by Cordilleran ice sheets.

The Northern Cascades are somewhat higher overall than comparable areas to the south of Snoqualmie Pass. Similarly, the Coast Mountains of British Columbia are somewhat higher overall than the Northern Cascades. Towering several thousand feet above the average crestline of the Cascade Mountains are the principal young strato-volcanoes: Mount Garibaldi, Mount Baker, Glacier Peak, Mount Rainier, Mount St. Helens, Mount Adams, and Mount Hood (Figure 2.5-22).

The Northern Cascades consist of a central, Precambrian crystalline basement and Paleozoic and Mesozoic marine strata that have been severely deformed, regionally metamorphosed, and invaded by numerous igneous intrusives of Cretaceous and Tertiary age. The core of the Northern Cascades is composed of metamorphosed sedimentary and volcanic rocks and granitic intrusives. These are flanked by younger sedimentary and volcanic rocks and are tightly and intricately folded along north-northwesterly trending axes. In general, the Tertiary rocks are not tightly folded, although locally they are faulted and deformed. The Central Cascades consist almost entirely of nonmarine volcanic and sedimentary rocks of Cenozoic age, and are free of large-scale granitic intrusions. Pre-Tertiary rocks in the Central Cascades are exposed in only a few locations, notably Tieton Reservoir to the west of Yakima. A thick sequence of Paleocene to Eocene volcanic and sedimentary strata comprises the core of the central Washington Cascades. These rocks are folded and faulted along a northwesterly trend. They are unconformably overlain by a series of Oligocene to Miocene volcanic rocks and associated sediments. These strata are faulted and folded, although not as strongly, along the same northwest trend as the underlying strata.

North of Mount Hood, the present Cascades were formed by late Cenozoic upwarping along a north-south axis, producing over 5,000 feet of structural relief. Late Cenozoic volcanic deposits unconformably overlie the middle Tertiary strata. Erosional remnants of Miocene to Pliocene Columbia River Basalt are found near the margins of the province, but the bulk of the late Cenozoic deposits consist of the extensive Plio-Pleistocene and Quaternary outpourings of the active stratovolcanoes Mount St. Helens, Mount Rainier, Mount Hood, and Mount Adams. These deposits were extruded from numerous vents and fissures and include pyroclastics and lavas of a variety of compositions.

These stratovolcanoes account for a large portion of the late Cenozoic volcanic rocks in the province. Quaternary glacial deposits are less abundant in the Cascade Mountain province south of Snoqualmie Pass than in that part of the province to the north. Holocene alluvial deposits mantle the older rocks in major stream drainages.

Three major structural elements are present within the northern Cascades. They are the Straight Creek-Fraser River fault system, the Methow Graben, and the Chiwaukum Graben. Each of these prominent elements is discussed separately below.

The structural trends within the Central Cascade Mountains of Washington are primarily northerly and northwesterly. They contrast with the more westerly trends to the east in the Columbia Plateau.

#### Straight Creek and Fraser River Fault Zones

The Straight Creek and Fraser River fault (Figure 2.5-3) zones are major north-northwest trending zones of faulting in northwestern Washington and southwestern British Columbia that were probably contiguous before the intrusion of tertiary plutons across them. As presently mapped, the Fraser River fault zone extends from Lillooet, British Columbia to the latitude of Chilliwack, British Columbia. The Straight Creek fault zone extends from just north of the Skagit River south to the vicinity of Snoqualmie Pass.

In British Columbia the Fraser River fault zone is dominated at its southern end by two major subparallel structures, the Hope and Yale faults. These two faults and their associated structures form a continuous zone approximately 5 kilometers wide that extends at least 257 kilometers north from the Canadian border. This zone is well-defined along most of its length by prominent alignments of hillside notches, linear talus deposits, and faceted spurs along both walls of the deep, linear canyon of the Fraser River (Woodward-Clyde Consultants, 1978a).

Although not as conspicuously defined as the Fraser River fault zone, the Straight Creek fault zone can be traced more or less continuously through pre-Oligocene rocks of the North Cascades. Along most of its length the Straight Creek fault zone separates a complex terrane of unmetamorphosed to slightly metamorphosed, pre-Tertiary volcanic and sedimentary rocks west of the fault zone from a pre-Mesozoic terrane of medium grade schist, orthogneiss, and migmatite intruded by Mesozoic granitic plutons east of the zone. Within the fault zone itself, narrow strips of downfaulted Eocene continental sediments, highly deformed blocks of the lithologies observed both east and west of the zone, and small serpentized bodies are common. The dip of the fault zone ranges from approximately 65° E to vertical. These steep dips are reflected in the linear trace of the zone (Figure 2.5-7).

The Straight Creek fault zone represents a profound structural discontinuity. West of the fault zone, rocks of low temperature, high pressure, metamorphic conditions (the Shuksan Metamorphic Suite) are involved in a series of imbricate thrust faults. East of the zone, large thrust



faults are absent and the rocks are typical of high temperature and low pressure conditions. Misch (1966) points out that only dip-slip displacements on the Straight Creek fault cannot easily explain this close juxtaposition of contrasting metamorphic facies and terranes, and that considerable strike-slip displacement is likely. He has suggested that the geology exposed west of the Fraser River fault zone near Harrison Lake in British Columbia (Lowe, 1971) is very similar to the geology in the Kachess Lake area. About 193 kilometers of right-slip displacement on the Straight Creek and Fraser River fault zones would be suggested by these relations (Misch, 1977a and b).

Although the age of latest movement of the Straight Creek and Fraser River fault zones is not precisely known, several geologic relationships put constraints on the age. The Straight Creek fault zone cuts the post-Early Cretaceous Shuksan thrust, showing that some of the displacement on the fault zone was younger than Early Cretaceous. The Kachess Lake fault, a possible southern continuation of the Straight Creek-Fraser River fault system, includes tectonic slivers of the Late Cretaceous Mount Stuart batholith, indicating that displacement occurred on it after the Late Cretaceous (Shannon and Wilson, 1977c). Several mid-Tertiary batholiths intrude the fault zone and show little or no displacement across its general trend (Misch, 1966; Washington Public Power Supply System, 1977c; Tabor and Frizzell, 1979; and Shannon and Wilson, 1977c). These intrusions are the Chilliwack and Mount Barr batholithic phases of the Chilliwack composite batholith, the Monte Cristo pluton and the Snoqualmie batholith. K-Ar age determinations of these batholiths are, respectively, 29-16 m.y., 25 m.y., and 18 m.y.b.p., indicating that extensive strike-slip displacement has not occurred along the fault zone since Miocene time.

Scattered exposures of Eocene continental sandstone, shale, and conglomerate of the Chuckanut and equivalent Swauk formations are found along the fault zone. Many of these exposures are faulted, demonstrating that displacement on the Straight Creek fault zone continued at least into Eocene time. In the Kachess Lake area, the Naches Formation of Eocene age is also involved in faulting. Also, Late Oligocene ash flow tuffs equivalent to the Stevens Ridge Formation overlie strongly deformed Naches Formation along an angular unconformity, indicating that major movement ended on the Kachess Lake fault within Oligocene time (in Washington Public Power Supply System, 1977c). These same ash flow tuff units also lie across the projection of the



Straight Creek fault in the Monte Cristo area, suggesting a similar age relationship (in Washington Public Power Supply System, 1977c).

South of the Kachess Lake the Goat Peak segment of the Straight Creek fault becomes the northwest-striking Taneum Lake fault. The Taneum Lake fault is viewed as a late dip-slip splay of the Straight Creek fault -- not the main transcurrent structure. Because the Taneum Lake reverse fault cuts only pre-Miocene units (Washington Public Power Supply System, 1977d), its age relationship to Miocene plateau basalts is unclear. However, Tabor and Frizzell (1979) conclude that Miocene or younger movement along either the southern Straight Creek fault "must be minimal or absent because the Miocene Snoqualmie batholith and its satellite stocks cut faults in the Straight Creek zone and are unmarked by structures paralleling and on strike with the fault".

#### The Methow Graben

The Methow graben is a northwest-trending structural low, lying between the Mesozoic crystalline plutonic belts of the North Cascade crest region to the west and the Okanogan Highlands to the east.

The graben is occupied by a sequence of marine and continental sedimentary and volcanic rocks of Jurassic-Cretaceous age (Barksdale, 1975). The Pasayten fault, the northeastern boundary of the graben, is a single surface that strikes N30°W. The western boundary consists of discontinuous segments interrupted by late Mesozoic and Tertiary granitic intrusions. The segments are non-colinear and have an average northwesterly trend. Both boundaries extend into the British Columbia. The Mesozoic sedimentary sequence is absent at the southern end of the graben, where the border faults converge. The continuation of the faults into the crystalline rocks bounding the graben has not been established.

The sedimentary sequence in the graben indicates several episodes of folding and internal faulting which may have been synchronous with movement on the border faults. Plutons which intrude the border faults indicate that faulting was largely completed by early Tertiary time.

The Pasayten fault, also referred to as the Chewack-Pasayten fault (Barksdale, 1975) and the Eightmile Creek fault (Lawrence, 1968; Staatz and others, 1971) is well-exposed





north of Eightmile Creek where it dips steeply westward. The southern segment of the fault is very straight, but is sinuous north of the British Columbia border.

The Pasayten fault separates crystalline plutonic rocks of the Okanogan terrane on the east from the thick supra-crustal sedimentary succession of the graben to the west. Lawrence (1968) postulates major strike-slip movement on the fault on the basis of the straightness of the fault trace. Interpretation of structural data from the rocks adjacent to the fault led him to postulate right-slip displacement. Barksdale (1975) interprets movement on the fault as largely dip-slip. Movement on the Pasayten fault predates the Island Mountain Volcanics which lie across the fault with angular unconformity just south of the Canadian border. The Island Mountain Volcanics are Tertiary, but, in the absence of radiometric dating, their precise age is not known. Attempts to trace the Pasayten fault south through the crystalline rocks toward the Columbia Plateau (Menzel and Swanberg, 1969; Washington Public Power Supply System, 1977e) have not proven successful. One point is clear: the fault does not continue directly on strike as a well-developed linear shear or mylonite zone through the crystalline rocks.

The western boundary fault system, is comprised of several irregular, non-colinear segments which collectively separate the Skagit terrane on the west from the Methow graben succession (locally, the Hozomeen Formation) on the east. The two northern segments mapped by Misch (1966) are referred to by him as the Ross Lake fault zone. The two southern segments studied by Barksdale (1975) have been called the Twisp River and Foggy Dew faults. The trend of the fault zone is approximately N45°W. Only the Twisp River segment shows strong physiographic expression. The fault zone continues north of the British Columbia border with a more northerly trend, as the Yale fault of the Fraser fault system. The southern segment, the Foggy Dew fault, is truncated by the Cooper Mountain batholith. Reconnaissance mapping by Shannon and Wilson (in Washington Public Power Supply System, 1977e) south of the Cooper Mountain batholith between Pateros and Chelan failed to identify the southern continuation of the fault in the crystalline rocks south of the graben. The Ross Lake segments of the fault zone are interrupted and separated from the Twisp River segment by several late Cretaceous and Tertiary plutons.

### The Chiwaukum Graben

The Chiwaukum graben is a major structural and geographic feature in the Cascade Mountains (Willis, 1950a and b). It extends as a topographically low region for about 100 kilometers NNW from Wenatchee, on the Columbia River, to near the crest of the Cascade Range. The graben is filled primarily by the Chumstick Formation, a thick sequence of folded and faulted continental sedimentary rocks of middle to upper Eocene age. Two major border fault systems, the Leavenworth on the west and the Entiat on the east, juxtapose the Chumstick against pre-Tertiary metamorphic and plutonic igneous rocks. Middle Miocene flows and intercalated sediments of Yakima Basalt lie unconformably across the graben at its southern end and post-date major faulting. Faults at the northern end of the graben are truncated by intrusive granitic rocks of the early Miocene Cloudy Pass batholith.

The Leavenworth fault system, at the western border of the graben, has been mapped as a zone of parallel faults at the southern end (Tabor and others, 1977) and as a single fault farther north. It trends generally north-northwest, but is irregular with several north-south segments, the longest of which is along its contact with the Mount Stuart batholith. The Entiat fault has been mapped as a single fault trace (Laravie, 1976). It is nearly straight and trends about N35°W.

An uplifted block of pre-Tertiary gneiss within the graben is bounded on the east and locally on the west by faults of the Eagle Creek system (Whetten and Laravie, 1976). These are all high-angle faults. Studies of sedimentary facies variations in the Chumstick Formation, which occupies the graben (Cashman, 1974; Laravie, 1976; and Whetten, 1977), demonstrate the coarse fanglomerates in the Chumstick were derived from local uplift of the pre-Tertiary crystalline rocks adjacent to and, in part, within the graben. These fanglomerates abut against and thin away from the contacts with the border faults, indicating that the faults were active during upper Eocene sedimentation. This early faulting was essentially tensional and probably represents a continuation of the extensional tectonic regime which led to formation of the Teanaway dike swarm in the area just to the south.

Movement on the Leavenworth and Entiat faults at the northern end of the graben was completed prior to emplacement of the Cloudy Pass batholith in early Miocene time. The latest fault movement at the southernmost end of the Entiat fault

predates the early Oligocene Wenatchee Formation, which was deposited across the fault. Movement of the southern end of the Leavenworth fault ended before deposition of the lower Yakima Basalt in middle Miocene time.

Post-lower Yakima Basalt faulting has been recognized on two structures which parallel the master boundary faults of the Chiwaukum Graben. In the area between the northern part of Table Mountain and Mission Ridge, just outside the southwestern border of the Chiwaukum graben, Rosenmeier (1968) mapped a 16 kilometers long, northwest-trending high-angle fault between Yakima Basalt on the west and Swauk Formation on the east. This fault has not been recognized within the Yakima Basalt southeast of the area of upper Nameum Creek. Shannon and Wilson (Washington Public Power Supply System, 1977c) suggest that the structure mapped by Rosenmeier fault could also result from a sharp monoclinial flexure.

Laravie (1976) recognized a 30 kilometers long fault just east of the Entiat fault along the western front of the Entiat Mountains. He initially postulated this fault, the Chumstick fault, largely on the basis of physiographic evidence. Movement on the Chumstick fault may have been related to, and synchronous with, folding of the Yakima Basalt on the Columbia Plateau to the southeast. Slip on the Chumstick fault probably represents a structural adjustment in the basement rocks which accompanied folding of the basalts in Pliocene or earliest Pleistocene time. The Chumstick fault dies out or merges with the Entiat fault both to the north and south where the bench and adjacent fault scarp disappear. The presence of a small erosional remnant of the 33 m.y. old Wenatchee Formation (Gresens, 1976) sediments at an altitude of 3,800 feet on Burch Mountain southeast of the Chumstick fault was noted above. This indicates that post-Wenatchee dip-slip movement, synchronous with movement on the Chumstick fault, has occurred on this segment of the Entiat fault. This young movement on the Entiat fault, however, dies out before the fault reaches the Columbia River where the Wenatchee Formation lies at the same elevation on both sides of the fault (Washington Public Power Supply System, 1977f).

#### 2.5.1.2 Columbia Plateau Province and Site Geology

The WNP 1-2-4 site is located within the Pasco Basin of the Columbia Plateau province. A summary discussion of the Columbia Plateau province has been previously presented in section 2.5.1.1.2.1. The discussion that follows will present an expanded version of the geologic history of the Columbia Plateau with emphasis on the major structures



surrounding the Pasco Basin. For additional detailed discussions of the geology, stratigraphy, lithology, and major folds of the Columbia Plateau refer to Washington Public Power Supply System (1977f) and Rockwell (1979).

#### 2.5.1.2.1 Geologic History of Columbia Plateau

The Columbia Plateau is underlain by a thick sequence of plateau basalt flows of Tertiary age which, in turn, are overlain locally by Pliocene fluvial and lacustrine sediments, by Pleistocene glaciofluvial and eolian sediments, and by Holocene alluvium and eolian deposits. East of the Pasco Basin, the basalt flows are essentially horizontal with only slight regional dips. To the west and south, the lava flows have been folded into a series of prominent, easterly-trending, linear, anticlinal ridges (Figure 2.5-4). The geologic history of the Columbia Plateau has been synthesized by Davis (Washington Public Power Supply System, 1977a; and Appendix 2.5-N). The following discussion is taken primarily from Davis' analysis.

##### Pre-Cenozoic

The pre-Cenozoic rocks of the Columbia Plateau are buried by the Columbia River basalts. The northern Columbia Plateau boundary area is underlain by a pre-Tertiary basement complex of plutonic and metamorphic rocks. These crystalline rocks form the mountainous highlands to the north and west of the Plateau, and are exposed below the Tertiary strata of the Plateau itself in the Columbia River canyon. These rocks include the Swakane Biotite Gneiss, Chelan Batholithic Complex, Methow Gneiss, and the Okanogan Batholithic Complex.

The absence of exposure of pre-Tertiary rocks in the plateau area has contributed to the concept of the Columbia Embayment, a convex-eastward embayment centered on the Columbia River between Oregon and Washington within which no "continental" or pre-Tertiary basement rocks should be found. The concept stems originally from deep resistivity studies in the area by Cantwell and Orange (1965), although the resistivity boundaries they drew between inferred basaltic oceanic and granitic continental crust do not coincide closely with the postulated Columbia Embayment.

The northwest-trending northern edge of the embayment was accepted by Skehan (1965) as a boundary between oceanic crust to the south and continental crust to the north, because it coincided approximately with a topographic lineament noted by Raisz (1945) and called by him the



Olympic-Wallowa lineament (OWL). The two inferred features--the surficial topographic lineament and a deeper crustal boundary--have been linked together in the literature. This is so despite the fact that regional gravity surveys across the trace of the proposed lineament do not support its existence (Danes, 1969; Appendix 2.5L); that it cannot be confirmed by regional aeromagnetic studies (Zietz and others, 1971; Washington Public Power Supply System, 1977g); and that no offsets or disruptions of any geologic units along its hypothesized trace in the bedrock areas of northeastern Oregon have been described (Shannon and Wilson, 1980; Kendall and others, 1981; Davis in Appendix 2.5-N).

Previous analyses of the Columbia Embayment and the nature of the basement beneath it and the basaltic Columbia Plateau relied almost exclusively on the geologic map distribution of pre-Tertiary units. Much can be learned, however, about the distribution of such units in Washington state when the disruptive effects of late Cretaceous strike-slip faulting in the northern part of the state are considered. The Straight Creek fault is particularly important in this regard. As previously discussed, Misch (1977b) proposed that a distinctive suite of Cascade metamorphic rocks exposed east of the fault in the Stevens Pass area has been offset 193 kilometers to the Harrison Lake area of southern British Columbia. Pre-latest Cretaceous rocks extend 225 kilometers south of Harrison Lake on the west side of the fault. If Jurassic ophiolitic rocks exposed southeast of Mount Rainier at Rimrock Lake (Tieton Reservoir) lie west of the fault as well, as seems likely, then pre-latest Cretaceous rocks extend 322 kilometers to the south of Harrison Lake.

When right-slip along the Straight Creek fault is reversed by 193 kilometers to bring the Stevens Pass and Harrison Lake areas into juxtaposition, it becomes apparent that pre-latest Cretaceous rocks on the east side of the fault must extend as far south of Stevens Pass as they do on the other side south of Harrison Lake, i.e., 140 to 322 kilometers. In other words, rocks of this age must underlie the western Columbia Plateau at least as far south as the present Columbia River, and apparently well into north-central Oregon (Washington Public Power Supply System, 1977a).

Thus the portion of the Columbia Embayment east of the Cascade Range is apparently underlain by basement oceanic crust and associated sedimentary rocks. Additional evidence for this conclusion is the widespread distribution in





western and central Washington of such rocks. Pre-Swauk Mesozoic units southeast of Stevens Pass (east side of Straight Creek fault) consist of the east-striking Ingalls "ophiolite" containing serpentinite, late Jurassic gabbro, and structurally associated chert, slate, and mafic volcanic rocks (Miller, 1977a, oral communication, and Miller, 1977b). The chert yields upper Jurassic radiolaria. This oceanic assemblage is believed to have been thrust northward (obducted) across the crystalline core of the Cascades. Structural emplacement occurred prior to intrusion of the Mount Stuart batholith, 88 m.y. ago (Miller, 1977b). Similar late Jurassic oceanic rocks occur farther south on Manastash Ridge, near Cle Elum (also probably east of the Straight Creek fault) (Hopson and Mattinson, 1973; Southwick, 1974).

On the west side of the Straight Creek fault in Snohomish, Skagit, and King Counties, assemblages of marine clastic rocks, radiolarian ribbon chert, volcanic rocks, and minor lenses of limestone yield Tithonian and lowermost Cretaceous (Neocomian) fossils (Danner, 1966). These rocks originally lay southwest of Hanford but have been offset to their present location by movement along the Straight Creek fault. Their offset counterparts east of the south-projected Straight Creek fault should now lie just north of the Columbia River in the general vicinity of Goldendale Washington. The Rimrock Lake Jurassic ophiolitic assemblage has been described by Vance and others (1980). In north-central Oregon, Jurassic argillites were encountered in Chevron's Kirkpatrick well just north of Condon. The argillites underlie a Tertiary Section (Columbia River Basalts, John Day Formation, Clarno Formation) that is approximately 2200 feet thick (S. Reber, Chevron Oil Corporation, personal communication to G. A. Davis, 1977).

Although strike-slip displacement along the Straight Creek fault appears to clarify the nature of basement beneath the Columbia Plateau, the trace of the element south of Snoqualmie Pass is unclear. In extending major right-lateral strike-slip fault zones from northern Washington southward into the Columbia Plateau, problems are encountered in north central Oregon. Here the northeastern trend of pre-Tertiary inliers and structural elements appears to be unbroken across the southern edge of the embayment. Regional gravity anomalies in central and northeastern Oregon parallel these geologic trends and also appear to be unbroken (Thiruvathukal, 1970). Because of these relations, the Columbia Embayment probably did not exist at the time of Straight Creek, Ross Lake, and related strike-slip faulting. Prior to latest Cretaceous time, the



Mesozoic continental margin in Oregon is thought to have had a more north-south trend than its present NE-SW position. Clockwise rotation of this margin is judged to have occurred after regional strike-slip faulting to the north.

#### Cenozoic

Between 40 and 20 million years ago volcanic arc activity related to eastward subduction of oceanic lithosphere beneath western North America was widespread. Such activity affected the central longitudinal third of Washington, most of Oregon with the exception of coastal and northeasternmost areas, and all of what is now the Great Basin (Snyder and others, 1976; Armstrong, 1979). Coney (1979) describes this time period, particularly in the Great Basin area, as one of (1) great ash-flow or ignimbrite eruptions from caldera centers, and (2) the development of amphibolite-grade metamorphic-mylonitic complexes at relatively shallow crustal levels (i.e. into Paleozoic and Mesozoic strata; e.g. Compton and others, 1977). Some of these complexes are now dated as Mesozoic in age, e.g. the Whipple Mountains of southeastern California (Washington Public Power Supply System, 1977a). Loring (1976) has documented widespread examples of Oligocene normal faulting of variable trend (north-south to east-west) within Utah and Nevada. Topography suggests that tectonic activity was generally subdued. A paucity of Oligocene and early Miocene sedimentary rocks in the Great Basin suggests that there were few major basins for sediment entrapment during that time (Christiansen and McKee, 1979). Sheet-like late Oligocene - early Miocene (25 to 20 m.y.b.p.) ignimbrites mantled a topography of low relief over extensive areas.

The Oligocene to early Miocene history of the Columbia Plateau is obscured by its cover of Columbia River basalts and younger units, but the history of the Blue Mountains during this time period is at least partly decipherable. The Blue Mountain province was deformed at some time after Eocene arc volcanism (Clarno Fm.), but prior to Columbia River basaltic volcanism. Before deposition of overlying Picture Gorge basalts, Clarno strata were locally folded as steeply as 60° on the northern limb of the east-west trending Aldrich Mountain anticline, the structural axis of the western Blue Mountains (Thayer & Brown, 1966). Robyn (1977) suggests that this deformation occurred between 25 and 20 m.y.b.p., but his older age limit is not well constrained. If folding was earlier, deposition of the Oligocene (36 m.y.b.p.) to Early Miocene John Day Formation may have been limited to the south by the high-standing Blue



Mountains block (Thayer and Brown, 1966), and partly controlled by synchronous folding in the basin of deposition. According to McKee (1972, p. 236-237):

The John Day Formation appears to be thickest near the centers of northwest-trending synclines. The folds are, in part, younger than the Columbia River Basalt, as that unit has been warped by the folding. The thickness data from the John Day strata suggest that the same folds existed in the Oligocene and that deformation along northwest-trending lines has been going on for at least 30 million years.

Supporting evidence for early folding (pre-Columbia River Basalt) is inferred by the occurrence of the Blue Mountains anticline along the northern edge of the John Day basin. This major fold constituted a topographic barrier in middle Miocene time and separated flows of the lower Yakima and Picture Gorge Basalts (Nathan and Fruchter, 1974), the oldest Columbia River basalts.

Plateau folds and parallel faults, usually with thrust or reverse fault geometries appear to have begun to develop during the extrusion of Miocene Columbia River basalts from fissures farther east. The best evidence for the earliest recognized deformation, that of late Grande Ronde time after nearly 85% of the basalts had been extruded (Camp and Hooper, 1980), is the work of Beeson and Moran (1979) in the northern Cascades of Oregon. They report that folds trending N 40° - 65°E began to develop during youngest Grande Ronde time. At some localities pillow lavas and sedimentary interbeds of this age are restricted to synclinal troughs and anticlinal volcanic sections are abbreviated. Similarly at the northern edge of the Columbia Plateau, in the Wenatchee Mountains of Washington, the Vantage Member of the Ellensburg Formation (post-Grande Ronde Basalt, pre-Frenchman Spring Member of Wanapum Basalt) thins toward the crest of Naneum Ridge anticline (Rockwell, 1979, p. IV-16).

Evidence for deformation during Wanapum time, approximately 14.5 to 13.6 m.y.b.p., is geographically more widespread. Again, in the northern Oregon Cascades, Beeson and Moran (1979) found evidence for uplift, northeast-southwest faulting, and erosion of the Frenchman Springs member of the Wanapum Basalt prior to deposition of Priest Rapids flows (also Wanapum Basalt). In the Pasco Basin area, stratigraphic and geochemical studies by geologists of the Rockwell Hanford group (Reidel and others, 1980; Rockwell, 1979) indicate that the Saddle Mountains structures began to



form in late-Grande Ronde time, ca. 14.5 m.y. ago. Thinning of Frenchman Springs flows has been noted across the northwest-trending Smyrna anticline on Saddle Mountain. The distribution of overlying flows of the Roza Member of the Wanapum Basalt on Saddle Mountain suggests east-west folding or arching during their deposition.

Evidence for post-Wanapum deformation is widespread. Bentley and others (1980, p. 59) state that "broad, structurally controlled basins had become noticeable at the onset of Saddle Mountain time, about 13 - 13.5 million years ago." They report that anticlinal ridges were locally high enough to confine flows of the oldest member of the Saddle Mountain Basalt, the Umatilla Member. These flows thin over the present site of the Rattlesnake Hills, suggesting that this fold structure began to form at the close of Wanapum time (Rockwell, 1979). The thinning of flow units across Saddle Mountain noted above continued to occur until Elephant Mountain time (ca. 10.5 m.y.b.p.), enabling Reidel and others (1980) to conclude that the rate of uplift of this structure between 14.5 and 10.5 m.y.b.p. was approximately 128 feet/million years.

In the latter area, just east of the Yakima River, steeply-dipping Wanapum basalts (as young as the Priest Rapids Member) are overlain with angular unconformity by flat-lying Selah conglomerates (Bentley, 1977, p. 364). The conglomerates are older than the 12 m.y. old Pomona Member of the Saddle Mountains Basalt.

Somewhat similar relations are reported by Bentley (1977, p. 377) and summarized by Rockwell, (1979, p. III-166) from the Filey Road area of eastern Umtanum Ridge. Here, 3 kilometers west of Priest Rapids Dam, Grande Ronde and Wanapum basalts, including the Priest Rapids Member of the latter, were tightly folded, overturned, reverse faulted, and eroded prior to the deposition of conglomerates across them. The conglomerates intertongue northward with fluvial sediments of Selah age that underlie the Pomona Member. The Pomona basalt in this area is described as relatively undeformed (Rockwell, 1979, p. III-166 and also their Figure III-73).

Farther east, Goff and Myers (1978) also conclude that most deformation of Umtanum Ridge occurred prior to Saddle Mountain time, but the distribution of the 10.5 m.y. old Elephant Mountain basalts around the eastern end of the structure suggests to them that some folding continued through Elephant Mountains time. Bentley (1977, p. 374)





states that more than 1200 ft. of structural relief has developed at the eastern end of Umtanum Ridge since the extrusion of Elephant Mountain lavas.

Despite some evidence for deformation of parts of the Columbia Plateau prior to extrusion of the 12 m.y. old Pomona lavas, most deformation affecting the Columbia Plateau and the adjacent Blue Mountains province is post-Pomona in age. In the Blue Mountains, strong north-south compressional deformation postdated the extrusion of Columbia River basalts, but preceded eruption of the widespread tuff member of the Rattlesnake Volcanics by 6.6 m.y.b.p. (Thayer and Brown, 1966; Robyn and others, 1977; Robyn, 1977). Robyn (1977) assigns an age of 10 to 7 m.y.b.p. for this compressional event. Renewed folding and rupturing of the north flank of the Aldrich Mountain anticline generated the east-west trending John Day fault. Northeast and northwest-striking fractures and strike-slip faults formed contemporaneously in the northern footwall of the fault as a conjugate response to north-south shortening. Only minor compression and igneous activity (silicic intrusions and basaltic volcanism) have occurred in the eastern Blue Mountains since 6.6 m.y.b.p. (Robyn, 1977).

In Washington, the widespread folding of the Elephant Mountain Member of the Saddle Mountains Basalt in the Pasco Basin area demonstrates major plateau deformation younger than the 10.5 m.y.b.p. age of the member. Rockwell (1979, p. IV-17, IV-20, 21) conclude that most deformation in the Pasco Basin area occurred between 10.5 and approximately 5. m.y.b.p., although the younger age limit is not well-controlled.

In many areas, late Quaternary deposits rest directly on deformed Miocene basalts, with a resultant hiatus in the geologic record of the region of up to 16 million years; accordingly, there is a problem in establishing an upper limit for most plateau folding and associated faulting because of the incomplete Pliocene and Quaternary stratigraphic record of the plateau area.

Pliocene stratigraphic units (ca. 5 to 1.8 m.y.b.p. old) are preserved in the northern and central Pasco Basin area (Ringold Formation), the Yakima-Ellensburg area (upper Ellensburg Formation), and in southwestern portions of the Washington plateau (Simcoe Volcanics). Geologists working on the plateau have differed on the duration of plateau deformation affecting these units, largely because of the lack of precise age controls on them. For example, in the northern Pasco Basin dips of beds in the upper part of the



Ringold Formation (5.1 - 3.3 m.y.b.p., Rockwell, 1979) are very gentle (Figures 2.5-36 and 2.5-37). This relation may indicate waning deformation (Rockwell, 1979, IV-21) since lower Ringold strata on the flanks of Saddle Mountain to the north dip as steeply as  $40^{\circ}$  (Washington Public Power Supply System, 1977h, p. 2RH 8-6). However, since basalts beneath the gently dipping Ringold sediments also dip gently, the areal differences in Ringold dips may reflect spatial rather than temporal factors.

Subsurface studies by Webster and Crosby prepared for Golder and Associates, 1981 of lower and middle Ringold sediments that lie across the buried southeastern end of the Gable Mountain anticline indicate that older Ringold sediments on the flanks of the structure dip more steeply than younger. Golder's data suggest that broad arching of Ringold sediments continued into the Pliocene.

Pliocene fanglomeratic deposits in areas between Yakima and the Kittitas Valley, e.g. the Thorp Gravel, have recently been assigned to the upper Ellensburg "Formation" (Washington Public Power Supply System, 1977h) or "group" (Bentley, 1977). Statements made in the two 1977 papers about the significance of these deposits to the dating of plateau deformation are, however, somewhat at variance. Bentley states (1977, p. 355) that "major deformation" occurred along Manastash Ridge "after some coarse basaltic fanglomerates of the Thorp (?) Gravel were deposited". Elsewhere Bentley (1977, p. 352) states that Thorp (?) conglomerates on the north flank of the Manastash structure dip only  $3 - 5^{\circ}$ . The inclined conglomerates are truncated by an early (?) Pleistocene pediment surface capped by gravels. The age of the Thorp (?) unit is not known, although tephra layers in upper Thorp Gravels in Kittitas Valley have yielded fission track and K-Ar ages of 3.7 to 4.8 m.y.b.p. (Waitt, 1979a). From such relations, Bentley (1977, p. 339) derives the conclusion that "the majority of the 'ridges' rose in Pliocene-Pleistocene times" (6 to 1.5 m.y.b.p.).

Thoms and others (in Washington Public Power Supply System, 1977h, p. 2RH 8-3) however, although favoring local deposition of upper Ellensburg deposits "during or after" ridge uplift, take a different view of the significance of these deposits:

The regional significance and age of these deposits is poorly understood. Most deposits are undeformed; only

on the west end of Smyrna Bench (Saddle Mountain) and in the Kittitas Valley do small dip slip faults cut these deposits.

Elsewhere, (Washington Public Power Supply System, 1977h, p. 2RH 8-12) Thoms and others conclude that the "age of deformation in the area of investigation is dominantly post-Elephant Mountain and pre-Thorp Gravel. Some deformation along the cores of the anticlines may be slightly older and minor tilting of pediment surfaces may be younger, but the majority of the deformation (faulting and folding) must have occurred between these two dates".

Their conclusion is, in turn, questioned by Rigby and Othberg (1979) who report that Ellensburg sedimentary rocks younger than Columbia River basalts (their "supra-basalt Ellensburg Formation") are deformed widely in the Yakima area:

The deformation exhibited by the supra-basalt Ellensburg Formation indicates that the large-scale uplift and deformation of the basalt ridges in the western Columbia Basin occurred after most, if not all, of these sediments had been deposited, or late Miocene to early (?) Pliocene in age.

Basalt terrace gravels preserved in valleys in the Yakima area are interlayered with and overlie supra-basalt Ellensburg sediments. The gravels, which according to Rigby and Othberg resemble the Thorp Gravels of the Kittitas Valley, exhibit near vertical to overturned dips at localities along Ahtanum Ridge, in the foothills of Cowiche Mountain, and in Yakima. Unfortunately, the age of these gravels is not known, although Rigby and Othberg (1979) suspect they may be broadly coeval with the Thorp gravels. They believe (p. 23) that some of the terrace gravels:

...were deposited before deformation began, while others were deposited for some time after deformation occurred. Deformation of this part of the Columbia Basin, at least, apparently came to an end sometime during deposition of this gravel unit.

Pliocene and Pleistocene lavas are widespread in the southwestern corner of the Washington portion of the Columbia Plateau. The relations of these lavas, the Simcoe volcanics, to plateau fold and fault structures are instructive. According to Bentley and others (1980, p. 60):



Eruptions of basalt and related lava began in the Simcoe volcanic field probably during early Pliocene, about 4-5 million years ago. Much of the deformation of the area had been completed before these eruptions, although some flows appear to have been tilted by later folding. The eruptions, which may have taken place over a 2-4 million year period, produced a broad continuous basalt field dotted with cinder cones.

Disagreement exists in the literature concerning the relative age of east-to-northeast-trending anticlines and northwest-striking, high angle faults in this part of the plateau. One such fault appears to cut a 4.5 m.y. old Simcoe flow, but is overlapped by a flow dated at 3.5 m.y.b.p. (Shannon and Wilson, 1973d). Shannon and Wilson (1973c) interpret the 4.5 to 3.5 m.y. old fault as being synkinematic with formation of the Columbia Hills and Horse Heaven anticlines, but studies by Anderson (1980) and Bentley and others (1980) indicate that the northwest-striking cross faults are younger than the folds (see also Rockwell, 1979, p. II-84, 85).

The Pleistocene stratigraphic record on the plateau is generally represented by poorly dated glacial deposits, flood gravels and associated sediments, and loess (Rigby and Othberg, 1979). The extent of involvement of these units in plateau folding is uncertain, in part because they tend to be best preserved in basins between major folds, and in part because of their youthfulness and the likelihood of low plateau strain rates.

All workers appear to agree that the uplift of Yakima Ridge ended prior to one million years ago, since the undeformed Tieton Andesite (K/AR age of  $1.0 \pm 0.1$  m.y.b.p.) lies in an erosional reentrant across the truncated northern flank of the anticline (Rockwell, 1979, p. II-77). Bentley (1977a, p. 354) concluded that most of the deformation along nearby Manastash Ridge occurred prior to the development of the one million year old Thrall pediment surface on its north flank.

Fault displacements of Quaternary age, unknown in 1977 at the time of submittal of Amendment 23 to the WNP 1/4 PSAR, have since been recognized in four areas of the Plateau: 1) Toppenish Ridge, approximately 85 kilometers west of the WNP 1-2-4 site (Campbell and Bentley, 1980; Woodward-Clyde Consultants, 1981a); 2) about 45 kilometers southeast of the site, from the vicinity of Wallula Gap on the Columbia River southeastward to the Walla Walla/Milton-Freewater area (Shannon and Wilson, 1980); 3) approximately 18 kilometers

north of the site on the eastern end of Gable Mountain; and  
4) approximately 93 kilometers east of the site on the  
northern flank of Ahtanum Ridge at Union Gap.

#### Quaternary

The oldest definitely Quaternary sediments, the older flood gravels at the Badger Coulee and Kennewick areas, were deposited between 605 and 130,000 years ago, and probably about 200-225,000 years ago. The contact between these older gravels and the units they overlies has not been seen, but presumably they lie on basalts. If gravels of similar age exist in the center of the Pasco Basin, they presumably lie on Ringold Formation.

Badger Coulee was formed by the ancestral Columbia River after deposition of the Columbia River basalts, according to Bunker (1980). Subsequent to its formation, flood gravels were deposited in it at least 130,000 years ago, and then it was abandoned as a regular course of the Columbia River. It is not known when the abandonment occurred, since the deposition of the gravels may have been either a catastrophic event or may have occurred over a longer depositional period.

The central part of the Pasco Basin, occupied by the Hanford works, remained as a depression filled by Ringold deposits, at least since Pliocene time.

Loess deposits were accumulating during the Bull Lake and Pinedale glaciations.

A major flood came down the Snake River when Lake Bonneville was suddenly drained between 18,000 and 30,000 years ago. So far, deposits definitely attributable to that flood have not been positively identified.

Towards the end of the Pinedale glaciation, damming of the Columbia River by the Pend Oreille ice lobe caused the formation of glacial Lake Missoula which drained catastrophically when the ice dam was breached. Massive erosion of basalt bedrock and the overlying Ringold Formation occurred as the flood spilled across the Palouse slope and through the Pasco Basin. Vast deposits of flood gravels were left in the lower parts of the flood channels, while the fine grained Touchet beds were deposited widely throughout the basin, but especially in tributary basins such as Walla Walla and Yakima.

At least two such late Pleistocene floods are known to have crossed the region between about 18,000 and 13,000 years





ago. The formation of the ubiquitous clastic dikes took place during flooding and accompanying deposition of the Touchet beds.

Volcanic activity in the Cascade Mountains has produced tephra falls from Mount Mazama, Mount St. Helens, and Glacier Peak at least during the Quaternary. The stratigraphy of the tephra units and the sources to which they are attributable has only been determined for the last 20,000-30,000 years. Eruptions from these three volcanoes has allowed the timing of the late Pleistocene flooding to be constrained.

Subsequent to the last flooding, about 13,000 years ago, severe erosion of the unconsolidated, fine-grained flood deposits took place over a period of 1,000 to 2,000 years, prior to the deposition of a Glacier Peak tephra between 11,000 and 12,500 years ago.

Deposition of loess continued from the time of the last great flood 13,000 years ago right up to the present day. Active dunes may be seen in the central part of the basin.

#### 2.5.1.2.2 Stratigraphy and Lithology

The stratigraphy of the site region is shown in Figure 2.5-10. The nomenclature is taken from Rockwell (1979). The rocks in the site region (Figure 2.5-4) consist predominantly of basalt flows but include some interflow sediments, and a sequence of fluvial, lacustrine, and eolian sediments overlying the basalts. The following is a brief lithologic description of the principal stratigraphic units. For more detailed discussion, refer to Rockwell (1979).

#### Volcanic Rocks

The Yakima Basalt subgroup (Miocene) is the principal exposed rock unit in the Columbia Plateau (Figure 2.5-2). It consists of individual flows ranging in thickness from 50 to 150 feet. The older Picture Gorge Basalt unconformably underlies the Yakima basalts in northeastern Oregon. Some Yakima basalt flows are extensive, one covering an estimated 51,800 square kilometers (Bingham and Grolier, 1966). The maximum thickness of the Columbia River Group is unknown. Only the upper 2,000 feet of Yakima Basalts have been studied in detail (Bingham and Grolier, 1966). An exploratory well near Odessa, 161 kilometers north of Richland, penetrated 4,500 feet of basalt. Raymond and



Tillson (1968) reported 10,000 feet of volcanics in the Rattlesnake Hills well on Rattlesnake Mountain, most of which may not be Columbia River basalts.

The general character of the Yakima Basalt is dark gray to black, very dense, fine-grained, and commonly vesicular or scoreaceous at the bottom and top of individual flows. Some flows have physically distinctive features but generally these features do not extend laterally for great distances. The homogeneous appearance of the individual flows and the limited areal extent of some have made correlations difficult and sometimes tenuous. However, correlation based on geophysical logging and chemical composition appears to have successfully delineated some upper flow members in the Pasco Basin.

#### Columbia River Basalt Group

This section contains a brief description of the five formations generally recognized within the Columbia River Basalt Group (Swanson and others, 1979b).

#### Imnaha Basalt and Picture Gorge Basalt

The two basal formations of the Columbia River Basalt Group, as defined by Swanson and others (1979b), are the Imnaha Basalt and Picture Gorge Basalt (Figure 2.5-10). Flows of Picture Gorge Basalt are confined to the vicinity of the John Day Basin in northcentral Oregon and were extruded from feeder dikes comprising the Monument swarm (Waters, 1961; Wilcox and Fisher, 1966; Fruchter and Baldwin, 1975). Outcrops of Imnaha Basalt are confined to southeastern Washington, northeastern Oregon, and adjacent Idaho, where known source dikes are exposed (Taubeneck, 1970; Kleck, 1976).

Flows of Imnaha Basalt are generally coarse grained and phyric. In the vicinity of the type locality (Taubeneck, 1970; Hooper, 1974; Kleck, 1976; Swanson and others, 1979b), Imnaha Basalt has a thickness of about 1,500 feet and is composed predominantly of flows of normal polarity.

#### Grande Ronde Basalt

The Grande Ronde Basalt (Figure 2.5-10), the oldest formation of the Yakima Basalt Subgroup, was extruded between 14.5 and 15.4 million years ago. Its type locality is a prominent west-trending spur ridge in the lower part of the Grande Ronde River Valley, Asotin County, extreme southeastern Washington (Camp and others, 1978; Swanson and

others, 1979b). The character of Grande Ronde Basalts at the type locality was discussed in detail by Camp (1976), Price (1977), Reidel (1978a), and Ross (1978).

The Grande Ronde Basalt is the most extensive unit of the Columbia River Basalt Group and underlies most of the Columbia Plateau. It is also the most voluminous unit, comprising 85 percent of the basalt group (Swanson and Wright, 1978). Known feeder dikes for these basalts (Taubeneck, 1970; Price, 1977; Swanson and others, 1975) are exposed in the southeastern part of the plateau. Along the plateau margin, the formation laps onto an irregular erosional surface.

The known thickness of the Grande Ronde ranges from tens of feet along the margin of the plateau to more than 3,000 feet in the Rattlesnake Hills well (Raymond and Tillson, 1968; ARHCO, 1976). Within the plateau, the thickest exposures of Grande Ronde average 2,500 feet. Sections generally comprise 30 to 40 flows (Swanson and others, 1979b).

Most Grande Ronde flows are fine grained, aphyric, black, and dense. Rarely, plagioclase and clinopyroxene phenocrysts are visible in hand specimen, and microphenocrysts of those minerals are apparent in thin section.

To date, the only consistent "regional" subdivisions of the Grande Ronde are four magnetostratigraphic units defined on the basis of dominant magnetic polarity (Swanson and Wright, 1976). These units, in ascending order are: reversed-one ( $R_1$ ), normal-one ( $N_1$ ), reversed-two ( $R_2$ ), and normal-two ( $N_2$ ). This magnetic stratigraphy, first determined from detailed and reconnaissance mapping in southeastern Washington (Swanson and others, 1977), has been found to hold throughout the area.

The contact of the Grande Ronde with the underlying Imnaha Basalt is well exposed in the Tri-state area. The contact is conformable, and there is no evidence of a major time break (Bond, 1963; Holden, 1974; Camp, 1976; Price, 1977; Reidel, 1978a; Swanson and others, 1979b).

The contact between the Grande Ronde Basalt and the older Picture Gorge Basalt is exposed only in central Oregon. The relationship between these formations has been studied in detail by Nathan and Fruchter (1974). They have shown that upper flows of the Picture Gorge Basalts interfinger with lower Grande Ronde flows of the  $N_1$  magnetic unit. Interfingering of Grande Ronde Basalt and Picture Gorge

Basalts indicates that the formations are, in part, coeval. Consistent with this interpretation, K-Ar dates indicate an age of about 16 million years for each unit (Watkins and Baski, 1974).

The contact between the Grande Ronde and the younger Wanapum Basalt commonly is marked by a zone of weathering, or by a thin sedimentary interbed (Mackin, 1961; ARHCO, 1976; Swanson and others, 1977).

#### Wanapum Basalt

The Wanapum Basalt (Figure 2.5-10) is the middle formation of the Yakima Basalt Subgroup (Swanson and others, 1979b). Its designated type locality is the nearly continuous exposure along the east side of the Columbia River near Wanapum Dam. The type Wanapum has been described by Mackin (1961) and in more detail by Myers (1973).

The Wanapum Basalt is the second most voluminous of the basalt formations, comprising about 15 percent of the Columbia River Basalt Group. Although its volume is considerably less than that of the Grande Ronde, the Wanapum is the most extensively exposed of the five formations and covers 80-90 percent of the central part of the plateau (Swanson and Wright, 1978).

The Wanapum Basalt consists mainly of medium grained, olivine-bearing, and slightly to moderately plagioclase-phyric flows. Known Wanapum feeder dikes are exposed in the southeastern part of the plateau (Price, 1977; Swanson and others, 1977).

The Wanapum currently is described in terms of four members: Eckler Mountain; Frenchman Springs; Roza; and Priest Rapids (listed oldest to youngest) (Swanson and others, 1979b). All but the Eckler Mountain Member cover large parts of the region.

#### Saddle Mountains Basalt

Saddle Mountains is the youngest formation in the Columbia River Basalt Group and comprises 10 recognized members (Figure 2.5-10). Saddle Mountains flows in the vicinity of the type locality, an anticlinal ridge located in south-central Washington, have been described by Mackin (1961), Bingham and Grolier (1966), and Schmincke (1967a).

The Saddle Mountains Basalts were extruded between 13.5 and 6 m.y. ago, predominantly from fissures in the eastern and

east-central part of the plateau (Swanson and others, 1979b). Despite the 7 m.y. accumulation period of this formation, it comprises less than one percent of the volume of the Columbia River Basalt Group. Saddle Mountains time was marked not only by waning volcanism, but by the development of thick, local, sedimentary deposits between flows, and by folding and canyon cutting (Swanson and Wright, 1978). Consequently, the contact between Saddle Mountains Basalt flows and older basalt units is generally a regional disconformity with local angular and erosional unconformities in areas of earlier ridge or basin development.

The Saddle Mountains have been subdivided into 10 members, listed from oldest to youngest as: Umatilla, Wilbur Creek, Asotin, Weissenfels Ridge, Esquatzel, Pomona, Elephant Mountain, Ward Gap, Buford, Ice Harbor, and Lower Monumental (Swanson and others, 1979b). Members of Saddle Mountains Basalt display the greatest petrographic, chemical, and paleomagnetic variability of any formation of the Columbia River Basalt Group.

#### Ellensburg Formation

The thickness and areal extent of basalt interbeds within the Columbia River Group are variable. Interbeds, which are more common in the upper portion of the group, range in thickness from 5 to 130 feet and are generally composed of tuffaceous sand, clay, or silt. Some interbeds probably represent lacustrine environments during interflow periods. Other interbeds are characterized by highly altered and weathered basalts displaying poorly developed soil profiles which reflect periods of weathering and landscape stability between succeeding flows. The Ellensburg Formation underlies and intertongues with the Yakima Basalts (Figure 2.5-10) (Bentley in Washington Public Power Supply System, 1977d).

The Ellensburg contains material derived from three distinct sources: volcanoclastic material from the Cascade volcanic range; plutonic, metamorphic, and older sedimentary material derived from the northern Cascade Range and adjacent areas north of the plateau; and basaltic material derived from within the plateau. Volcanoclastic materials are dominant in the western lithofacies and the middle and upper part of the section. Plutonic and metamorphic arkosic materials are most common in the northern and central lithofacies, and dominate the lithology of the lower part of the section. Basaltic materials dominate the lithology of the uppermost Ellensburg, and occur in middle Ellensburg





units adjacent to basalt ridges. Heavy mineral suites (Coombs, 1941) and current directions indicate a complex south and southeast drainage system involving four major system changes through time. In early Ellensburg time, marginal streams moved materials southward along the western edge of the plateau. In middle Ellensburg time, the ancestral Yakima and Columbia Rivers appear to have developed on the plateau and moved materials southward and southeastward across the plateau forming clastic wedges along their courses. In late Ellensburg time, the rising Cascades Range and Yakima Ridges trapped large volumes of locally derived materials in subsiding basins. The two later changes probably are related to continuing uplift.

Ellensburg lithologies include conglomeratic sandstone, siltstone, claystone, laharic breccia, airfall tuff, loess, and colluvial breccia. There is no evidence of a single large fan of Ellensburg materials extending over the western margin of the Columbia Plateau.

The lower Ellensburg probably is about 17 m.y. old based on K-Ar dating of lavas. The middle Ellensburg ranges in age from about 13 to 6 m.y.b.p. The age of the upper Ellensburg is Pliocene and possibly early Pleistocene. Fission-track dating methods yield ages of 4 to 2 m.y.b.p. (Waite, 1979a).

#### The Lower Ellensburg

The lower Ellensburg consists of all sedimentary material intertongued with the Wanapum Basalt (middle Yakima) and Grande Ronde Basalt (lower Yakima) and conformably underlying the Grande Ronde Basalt. Three members are well known from the work of Mackin (1961): Quincy Member, a diatomite and claystone; Squaw Creek Member, a diatomite; and Vantage Member, a coarse lithic and tuffaceous - quartz mica sandstone with interbeds of tuffaceous claystone. These members are intertongued or underlie the Wanapum Basalt. Other similar interbeds occur at several levels within the Grande Ronde in the margin area of the Grande Ronde. The dominant lithologies in the lower Ellensburg are volcanic and tuffaceous siltstones. On the plateau margin, hyaloclastites and peperite breccias are common.

#### The Middle Ellensburg

The middle Ellensburg is a sedimentary sequence intertongued with the members of Saddle Mountains Basalt (Upper Yakima). It includes the Rattlesnake Ridge, Selah, Beverly, and Mabton members (Schmincke, 1967b).

The middle Ellensburg consists of five lithofacies: volcaniclastic facies in the western basins; Columbia River facies near the ancient Columbia River; Yakima River facies near the ancient Yakima River; local sidestream and slope facies near rising ridges; and interstream or flood plain facies away from major stream channels.

#### The Upper Ellensburg

The upper Ellensburg consists of a sedimentary sequence deposited in local basins across the western plateau. It is characterized by basalt detritus derived locally from within the plateau as the Yakima Ridges reached a stage of maximum development. Each basin in the western Columbia Plateau has a different local stratigraphy with different lithofacies distributions which depend on stream size (mainstreams vs. sidestreams), local slope conditions, relative tectonic activity, and underlying rock types. Intrabasin stratigraphy has been partially established in the Kittitas, Ahtanum, and Pasco Basins.

Airfall tuffs (tephras) derived from the Cascade Range are interlayered with all facies in all basins and probably offer the best method of intra and interbasin correlation. In Kittitas Valley, the Thorp Gravel contains tuffs dated by the fission-track and K-Ar method at 3.7 to 4.8 m.y.b.p. (Porter, 1976; Waite, 1979a).

#### Ringold Formation

In the Pasco and Quincy basins, the Columbia River Basalt group is overlain by the Ringold Formation (Merriam and Buwalda, 1917; Newcomb, 1958). Sediments assigned to the Ringold Formation were deposited in a fluvial/flood plain environment and consist of stream-channel conglomerates, point-bar sandstones, fine-grained overbank flood deposits, and minor lacustrine sediments (Gustafson, 1973). In the Pasco Basin, sediments of the Ringold Formation accumulated to a maximum thickness of about 1,181 feet (Newcomb and others, 1972).

The Ringold Formation has been divided into five textural units by Tallman and others (1979): 1) basal gravity; 2) lower sand, silt, and clay; 3) middle gravel or conglomerate; 4) upper sand and silt; and 5) a local fan conglomerate facies. The middle, upper, and fan conglomerate units crop out in the Pasco Basin. Information on the nature and distribution of the basal and lower units is based only on borehole data. Brown and Brown (1961) suggest that the basal gravels may be equivalent to interbeds

beneath younger basalt flows (lower-to-middle Pliocene Ellensburg Formation) outside the north-central portion of the Pasco Basin, rather than Ringold deposits. The fanglomerates occur only along the margins of synclinal basins adjacent to the basaltic ridges that were the source for the fan deposits. The fanglomerates are included as members of the Ringold Formation on the basis of their time equivalency rather than similarity of depositional environments (Grolier and Bingham, 1978).

Based on vertebrate fossils, Merriam and Buwaldo (1917) and Strand and Hough (1952) assigned a middle to late Pleistocene age to the sediments exposed in the White Bluffs locality. Recent paleontological studies by Gustafson (1973, 1978), however, indicate that the Ringold Formation is Pliocene in age, based on the occurrence of Balnearia fauna in the upper part of the formation at White Bluffs and of Hemphillian fauna in the middle Ringold conglomerates. Woodward-Clyde Consultants (1978b) investigated the magnetostratigraphy of a 110-m section of the Ringold Formation along the White Bluffs at Parsons Canyon. The lower 66 feet of the section, which includes approximately 16 feet of middle Ringold conglomerate overlain by upper Ringold sediments, has a normal magnetic polarity. The overlying 90 m of section exhibit reversed magnetic polarity. The section is capped by calcrete and loess that are of normal magnetic polarity. Rockwell (1979) suggest that the polarity reversal and faunal evidence indicate that deposition of the upper Ringold unit took place during the Gilbert Reversed Epoch. This implies an age of 3.32 to 5.12 m.y.b.p.

In the Pasco Basin, the Ringold Formation is interpreted to be tectonically deformed (McConiga, 1955; Brown and McConiga, 1960, Grolier and Bingham, 1978; Routson and Fecht, 1979; Tallman & others, 1979). The lower units of the Ringold Formation are more deformed than the upper units, and the gradual decrease in dips upward in the Ringold section suggests syndepositional folding.

#### Basal Gravel

The basal Ringold gravel, which overlies the Columbia River Basalt, is present throughout most of the subsurface of the Pasco Basin (Rockwell, 1979). The conformability of the basal gravel and the underlying basalt is unknown in most areas, but in the Cold Creek syncline it is generally considered to be conformable (Routson and Fecht, 1979; Tallman and others, 1979). The thickness of the deposits varies from as much as 98 to 328 feet (Routson and Fecht,

1979) to less than 7 feet (Rockwell, 1979) where the desposits probably pinched out against already existing basalt highs. The relatively uniform thickness of this unit across the axis of the Cold Creek syncline suggests that the sediments were deposited on a relatively undeformed surface prior to major deformation of the syncline (Tallman and others, 1979).

The basal Ringold unit is primarily composed of gravel supported by a coarse- to fine-sand matrix. The pebble-cobble fraction is primarily composed of basalt, but also includes quartzite, metamorphic rocks, granitic rocks, and other lithologies that have sources outside the Pasco Basin (Tallman and others, 1979). The sediments were deposited by slope wash on basalt surfaces and via drainage through the Pasco Basin.

#### Lower Sand, Silt, and Clay

The basal Ringold gravel is overlain by silty coarse-to-medium sand to sandy silt containing stringers of coarse to fine pebbles. These deposits were referred to as the "blue clays" by Newcomb (1958). The sediments are composed primarily of quartz, feldspar, mica, chlorite, and smectite. Where observed in cores beneath the Hanford Site, this unit is brown to tan in color and is finely bedded to massive (Tallman and others, 1979). These sediments appear to have been deposited in a low energy floodplain or lacustrine environment.

The unit is present throughout much of the Pasco Basin, except the area around and immediately south of Gable Mountain and Gable Butte (Tallman and others, 1979; Rockwell, 1979). The unit ranges in thickness from zero, where it pinches out against the flanks of anticlinal ridges to greater than 328 feet in the Cold Creek syncline (Rockwell, 1979). The thickening of these deposits in the Cold Creek syncline suggests that deposition took place during and/or after deformation of the basin (Tallman and others, 1979). The elevation of the upper surface of this unit generally decreases toward the anticlinal ridges, which suggests that deformation continued after deposition of the lower sand, silt, and clay unit (Rockwell, 1979).

#### Middle Gravel or Conglomerate

The middle Ringold unit, which predominantly consists of silty sandy gravel, occurs in the subsurface throughout most of the Pasco Basin, except in the area north of Gable Mountain (Rockwell, 1979). Deposits of the middle Ringold



unit are also exposed along the southern part of the White Bluffs and at Coyote Rapids. This facies of the Ringold Formation appears to be limited to the Pasco Basin (Grolier and Bingham, 1978). The contact between the middle and lower Ringold units is generally clearly defined. Where the lower unit is not present, it is difficult to differentiate between the middle and basal gravel units, which are compositionally and texturally similar (Tallman and others, 1979). The thickness of the middle Ringold varies from zero at the basin margins to more than 328 feet in the central parts of Pasco Basin (Rockwell, 1979). Much of the middle Ringold unit in the western part of the Pasco Basin has been removed as the result of erosion by normal fluvial processes and by Pleistocene floods.

The middle Ringold is a conglomerate consisting of well-rounded pebbles and small cobbles supported by a relatively well sorted coarse- to medium-sand matrix. The deposits in the White Bluffs exposure have a massive appearance with minor imbrication of the larger clasts. Cross-bedding is common in sand and silt lenses. The conglomerate is generally moderately to well indurated by calcium carbonate and silica. Gravel clasts consist of basalt (derived primarily from nearby Columbia River Basalt sources), quartzite, and metamorphic, granitic, and volcanic porphyry rocks (derived from sources outside the Columbia Plateau).

The middle Ringold sediments were deposited in a high-energy fluvial environment.

#### Upper Sand, Silt, and Clay

Sand, silt, and clay of the upper Ringold overlie and interfinger with the middle Ringold conglomerate in the northern part of the White Bluffs' exposures. The deposits are best exposed in the White Bluffs, where they are more than 394 feet thick. These upper Ringold deposits underlie the 886 to 984 feet high plateau that extends throughout the eastern and northern parts of the Pasco Basin. In the subsurface of the Pasco Basin, south and west of the White Bluffs, the upper Ringold unit has been eroded, and only remnants up to 148 feet thick occur in buried topographically low areas along the Cold Creek syncline (Tallman and others, 1979).

This unit is composed of well-sorted sand and silt with minor lenses of fine pebbles. Quartz and feldspar make up more than 50 percent of the sediments (Tallman and others, 1979). Silt and clay layers are typically horizontally

bedded with fine laminations, and lack cross-bedded or other sedimentary structures that would indicate stronger currents. The sand layers are both horizontally and cross-bedded. Ripple marks are common. The sediments of the upper Ringold were deposited in lower energy fluvial and lacustrine environments. The upper Ringold unit locally contains diatomite, ash beds, and vertebrate fossils.

Where the Ringold Formation has not been channeled or otherwise dissected, its upper surface is commonly capped by a well developed calcrete. At least three other well developed calcareous soils are present within the upper Ringold unit that is exposed along the White Bluffs (Sections 11 and 14, T13N, R27E). These soils are the result of periods that lasted at least several tens of thousands of years during which the Ringold deposits were exposed to subaerial processes in a semi-arid climate, which was similar to or warmer than today's climate. A well developed calcrete horizon was also noted in wells penetrating the eroded surface of the upper Ringold unit in the central part of the Pasco Basin (Tallman and others, 1979).

#### Fanglomerate Unit

Localized occurrences of talus, alluvial fans, colluvium, and slope wash on the flanks of anticlinal ridges are included in the Ringold Formation as a fanglomerate facies (Grolier and Bingham, 1978). These deposits are best exposed along the north flank of Saddle Mountains, where they are as much as 394 feet thick. Thinner deposits, approximately 3 feet thick, are exposed on the south flank of Gable Mountain (Rockwell, 1979). In places these deposits grade into and/or interfinger with eolian and lacustrine deposits that are considered to be part of the Ringold Formation (Grolier and Bingham, 1978). The deposits consist of poorly sorted, angular to subangular pebbles, cobbles, and boulders of basalt and Ellensburg Formation sedimentary rocks. In places the deposits are capped by massive calcrete.

#### Simcoe Lavas

The Simcoe Lavas or Simcoe Mountains Volcanics cover approximately 777 square kilometers, mostly to the northwest of Goldendale, Washington. These lavas unconformably overlie the Yakima Basalt and Ellensburg Formation and predate the Pleistocene and Holocene lavas from Mount Adams and its subsidiary volcanoes. K-Ar dates of Simcoe Lavas indicate extrusion between 4.5 and 0.9 m.y. ago (Shannon and Wilson, 1973c).

Simcoe Lavas are predominantly olivine basalt, with minor amounts of pyroxene-olivine basalt, rhyolite, and dacite. Most olivine basalt occurs as thin flows erupted from northwest trending fissures or from the flanks of numerous small, shield volcanoes and spatter cones in the area. Rhyolite, dacite, and pyroxene-olivine basalts occur in a few small flows and in cinder and spatter cones (Shannon and Wilson, 1973c).

#### Tieton Andesite

The Tieton Andesite consists of several flows of hypersthene-augite andesite which were erupted from vents in the Cascade Range (Swanson, 1967). Only one flow extends into the region. This is an intracanyon flow restricted to the valleys of Cowiche Creek and the Tieton and Naches Rivers (Rigby and Othberg, 1979; Swanson and others, 1979a). A K-Ar date obtained for the Tieton Andesite by Dymond (in Shannon and Wilson, 1973c) indicates that this lava was extruded about one million years ago.

#### Fanglomerates

This unit occurs as small isolated outcrops of cemented basalt gravel on the toe of the Horse Heaven Hills near Yellepit (Washington Public Power Supply System, 1977i). The fanglomerate, up to 25 feet thick, consists mainly of rounded basalt clasts having rinds between 1/4 and 3/4 inch thick. Gravels of the Kennewick fanglomerate are compositionally distinct as compared to gravel of glaciofluvial deposits in the Pasco Basin. The latter contain up to 60 percent of non-basaltic clasts, and commonly have thinner weathering rinds or none at all.

Caliche rinds on Kennewick fanglomerate cobbles have been dated at approximately  $21,000 \pm 4,000$  years (personal communication Dr. T. L. Ku (USC) to Woodward-Clyde Consultants, 1981).

#### Older Loess Units

The fluvial and lacustrine Ringold Formation does not occur in the eastern Columbia Plateau, where late Pliocene and Pleistocene deposition was largely eolian (Baker, 1978). Here the loess sheet provides a more complete Pleistocene record that Richmond and others (1965) correlate with Richmond's (1965) Rocky Mountain glacial chronology. Richmond regarded the Bull Lake Glaciation to be early Wisconsinan, and Pinedale Glaciation to be late





Wisconsinan. Pierce and others (1976) have revised this correlation and now correlate the Bull Lake Glaciation to the Illinoian Glaciation (about 125 to 200,000 y.b.p.).

#### Pre-Palouse Loess

Baker (1978) recognized Bull Lake (Pierce and others, 1976) loess deposits at Marengo, Old Maid Coulee, Macall, and Revere. These deposits have a well-indurated petrocalcic horizon consisting of up to 2 feet of approximately horizontal carbonate laminae overlying an horizon of carbonate-plugged loess. Baker classifies this as a K horizon because it contains more than 50% carbonate.

The fluvial/lacustrine Ringold Formation does not occur in the same locations as the pre-Palouse loess and the two may, in part, be time equivalent. Baker (1978) reports at least three soils within the Palouse loess. Both Upper Ringold and Bull Lake loesses (Pierce and others, 1976) have petrocalcic cappings and both are directly overlain by pale early Pinedale (Pierce and others, 1976) loess. If the above soils may be correlated, the loesses of Baker (1978) may be as old as the 3.3 to 5.1 Ma BP age which is assigned by Rockwell (1979) to the Upper Ringold on the basis of Gustafson's (1973, 1978) faunal data and Woodward-Clyde Consultants' (1978b) paleomagnetic data.

A cliff along the Walla Walla River, southeast of Reese, at a locality referred to as Cummings Bridge by Bretz (1929) and Bjornstad (1980) exposes an older loess. The cliff at this locality (NW 1/4, NE 1/4 of Section 2, T6N, R32E, Zangar Junction quadrangle) is 82 feet high and exposes a thick sequence of late Pleistocene flood deposits. At the south end of this exposure basalt is overlain by an older loess that has a petrocalcic soil over 3 feet thick. The red-brown loess continuously underlies the late Pleistocene flood deposits along the entire length of the 500-m-long cliff.

No definite correlation has been made between this loess and the loesses described by Baker (1978). However, the presence of the thick K horizon suggests that this loess is correlative to Baker's pre-Palouse loess.

A number of bone fragments were found just below the petrocalcic cap overlying this older loess unit. Dr. E. P. Gustafson assembled the fragments into a single piece, which he identified as the rear part of a jaw bone. He was not able to identify the species, but did state that the condition of the bone suggested that it was Pleistocene and



definitely not of Ringold age. His statement suggests that correlation between the loess containing the bone fragments and Baker's (1978) pre-Palouse loess may be valid.

#### Palouse Loess

Most of the Columbia Plateau loess is correlated to Bull Lake Glaciation by Richmond and others (1965), but Pierce and others (1976) correlate it to the early Pinedale. The loess has been designated Palouse Formation by Newcomb (1961). Three separate soil horizons have been observed by Richmond and others (1965) within the Palouse Formation; Baker (1978) indicates that there may be others. Each soil has a well developed textural B horizon, overlying a highly calcareous Cca horizon that has a platy structure. A major unconformity separates the Palouse from younger loess, which Baker (1978) correlates to the late Pinedale Stage. The color of the younger loess is paler, and it has less well developed soil, lacking the Cca or K horizons of the older loesses.

#### Late Pleistocene Flood Deposits

Glacial lakes that existed along the southern edges of the Pleistocene ice sheets have been well documented by many workers. Catastrophic failures of ice dams retaining glacial lakes in northern Washington, Idaho, and Montana have occurred since at least the middle Pleistocene. Bretz (1923) first postulated that the scabland morphology was attributable to catastrophic floods coursing across the tract of land between the Columbia and Snake Rivers and flowing in a generally southwest direction toward Wallula Gap.

Subsequent to Bretz' original paper, he insisted against much opposition that the catastrophic flood theory was the only valid one that would explain all the geomorphic forms in what he termed "Channeled Scabland". After many years of skepticism by other workers, Bretz and others (1956) set out to refute every alternative to the catastrophic flood hypothesis. Baker (1978) gives an eloquent history of this controversy, which lasted well over 30 years.

#### The Bonneville Flood Deposits

Bright (1963) and Malde (1968) studied the origins of the Bonneville flood. Bright (1963) showed that the Bear River was diverted by a lava flow about 34,000 y.b.p. that impounded a lake at Thatcher, Idaho. Organic material below the lava flow gave C<sup>14</sup> dates ranging from 23 to 38,000



y.b.p. Continued lava flows formed a barrier higher than the southern rim of Lake Thatcher. The impounded water eventually spilled into Lake Bonneville. The resulting rise of Lake Bonneville caused it to spill over at Red Rock Pass, approximately 18,000 years b.p., according to Bright (1963). Malde (1968), however, believes that the rise in level of Lake Bonneville was brought about by the capture of the Bear River, and possibly by other factors such as climatic changes. He gives a minimum age for the Bonneville flood at  $29.7 \pm 1,000$  years b.p., on the basis of a  $C^{14}$  date obtained from molluscs in alluvial deposits younger than the maximum flood. Recent work by Scott (1978; 1979a, b; 1980a, b; 1981), however, indicates that Lake Bonneville did not start to rise to its maximum level of about 5,184 feet until about 19,000 years b.p. Sudden lowering of the lake took place at about 14,000 y.b.p. during the Bonneville flood, when the level dropped from its Bonneville shoreline to its Provo shoreline at an elevation of 4,790 feet.

The flood coursed down the Snake River from Red Rock Pass and discharged an estimated 1580 kilometers<sup>3</sup> of water at a maximum rate of 1.2 kilometers<sup>3</sup>/h (Malde, 1968). The minimum duration of the flood was calculated to have been 47.5 days, although Malde (1968) postulates that it may have lasted as long as a year. The following, however, are examples of historic floods that ended in a very short period of time (Malde, 1968):

Indus, India (1894):  $1.13 \times 10^9$  m<sup>3</sup> of water discharged in some 24 hours, emptying a 305-m-deep lake and producing a 30-m-high tidal wave.

Vaiont, Italy (1963):  $1.2 \times 10^8$  m<sup>3</sup> of water overtopped and destroyed the Vaiont dam in 15 minutes.

Gohna, India (1968):  $2.83 \times 10^8$  m<sup>3</sup> of water discharged in 4-1/2 hours and lowered a 245-m-deep lake by 394 feet.

These were, however, small floods compared with the 1580 kilometers<sup>3</sup> of the Bonneville flood. In the upper reaches of the Snake River in southeastern Idaho, Malde and Powers (1962) (in Malde, 1968), describe the Melon gravel deposit of boulders and sand left by the Bonneville flood. Boulders up to 3 feet in diameter partly fill the canyon to depth of 328 feet in huge bars, which Malde (1968) compares to those described by Bretz and others (1956) in the Columbia Basin.

Baker (1978) indicates that, since the Bonneville flood was confined to the Snake River Canyon, it skirted to the south of the Channeled Scabland.



Foley (1976) describes two slackwater deposits in Alpowa Creek, a tributary of the Snake River, near the border between Washington and Idaho. The older of the two contains a tephra unit that Foley thinks belongs to the "unnamed" Mount St. Helens unit dating from 18 to 37,600 year b.p.

Lindberg and Brown (1981) state that the Pasco Basin has generally been an area of deposition because it contains the record of many previously undifferentiated large floods of Pleistocene age. They indicate that recently drilled wells in the lower Pasco Basin provide new data concerning these floods in the form of gravel, sand, and silt deposits. Further, they contend that floods that came down the Snake River have dominated the southern portion of the Pasco Basin and Badger Coulee. This idea is supported by paleocurrent directions within the sands and gravels in the area between Kennewick and West Richland. Several large delta or alluvial fans were deposited by the Snake River across the course of the Columbia River. The existence of these flood deposits decreased the Columbia's erosive power and promoted upstream deposition by temporarily ponding the Columbia River.

The confluence of the Snake and Columbia Rivers is about 18 kilometers upstream of Wallula Gap. It lies in the path of any flood coming down the Columbia River, which suggests that a deposit of a Snake River flood occurring prior to the Missoula floods would have been either removed, reworked, or buried by subsequent flood deposits. This may explain why no deposits have definitely been attributed to the Bonneville or any other Snake River flood. Lindberg and Brown (1981) are attempting to trace individual floods across the Pasco Basin and to determine the chronology and stratigraphy of the deposits.

#### The Missoula Flood Deposits

The largest of the late Pleistocene floods was produced by the sudden emptying of flacial Lake Missoula. This flood extensively modified the drainage in central and eastern Washington. It plucked out large blocks of basalt; created hanging valleys and waterfalls; deposited huge gravel bars and ripple marks; and reworked and redeposited vast quantities of gravel, sand, and silt. An area of some 7200 kilometers<sup>2</sup> was stripped to bedrock, while about 2300 kilometers<sup>2</sup> was buried by flood deposits (Bretz, 1928).

Hydraulic damming of Wallula Gap and perhaps the Columbia River Gorge southwest of the Umatilla Basin, and the subsequent surging of floodwater back upstream produced a





marked separation of the sediment load into a coarse-grained facies and a fine-grained slackwater facies. These two principal facies of flood deposits are recognized throughout the Pasco, Walla Walla, Yakima, and Umatilla basins. The coarse grained facies consist of gravel, sand, and minor silt deposits, which are known as the Pasco Gravel (Brown, 1975). The siltly, fine sand facies is known either as the Touchet beds (Flint, 1938) or as slackwater deposits. Minor amounts of ice-rafted debris occur within these deposits, particularly around the edges of the Pasco and Walla Walla Valleys.

#### The Touchet Beds

The central, low parts of smaller basins, such as Walla Walla and Yakima, contain the best preserved slackwater deposits, which exhibit the most complete suite of sedimentary features and structures. At elevations much above 180 m, the rhythmically bedded slackwater deposits give way to more massive deposits. Slackwater deposits have been reported up to elevations of 1,148 feet. The silty facies of flood deposits have been described by many workers since they were first recognized by Bretz (1929) as being flood related. (Flint (1938), in his denouncement of Bretz' flood hypothesis, coined the phrase Touchet beds to describe the series of rhythmically deposited sands and silts that occur in the Walla Walla Valley. Similar deposits have been recognized in the Yakima Valley and Umatilla Basin. Allison (1933) also identified similar rhythmically deposited sands and silts in the Willamette Valley in Oregon, a side valley of the Columbia River downstream of the Pasco Basin.

The principal characteristics of the Touchet beds, at their type locality, is that the sands and silts were deposited in a series of turbidites (Baker, 1973) or rhythmites (Carson and others, 1978). Baker (1973) describes a series of measured stratigraphic sections along the Tucannon River, a tributary of the Snake River. These sections, which show a gradual fining upvalley, are composed of a sequence of rhythmically bedded sand and silt. Each rhythmite typically consists of the following sequence:

1. A basal layer of structureless coarse sand and granules.
2. Horizontally stratified medium and fine sand.
3. Current-ripple bedding in fine sands and coarse silts.

#### 4. Parallel lamination in medium and fine silts.

This sequence corresponds to most of Bouma's (1962) turbidite sequence, which contains five elements (a to e) in a complete unit. Baker (1973) regards the sequence to be precisely what Kuenen (1967) considers to be diagnostic for a turbidite.

Bjornstad (1980), in a study of various localities within the Walla Walla Valley (e.g., Gardena Cliff, Burlingame Ditch, Cumming's Bridge), compares the assemblage of structures to Bouma's (1962) turbidite deposits. Bjornstad (1980) notes that the sections he measured typically contain Bouma's sequence of units "b", "c", and "d", and basal unit "a". The upper pelitic unit "e" is absent. Bouma (1962) ascribes the absence of basal units in the sequence to distance from the source; the absence of upper units could be due to erosion by succeeding turbidites.

Bjornstad (1980) argues that the sections observed in the Walla Walla Valley and Bouma's (1962) definition of a turbidite sequence are comparable. He further argues that the general lack of major erosional features between adjacent rhythmites and the lack of regularly distributed basal gravels, which would be expected to occur between separate floods, indicate that the entire sequence of rhythmites must have been deposited as pulses into a lake produced by a single flood. Bjornstad (1980) has identified 58 rhythmites at the Gardena Cliff exposure and 45 at Burlingame Ditch. A major erosional unconformity that separates two sequences of rhythmites, exposed at the Cummings Bridge locality, indicates there were two separate floods.

Waitt (1980) also compares the rhythmites at Burlingame Ditch with Bouma's (1962) turbidite deposits and considers them analogous. He notes that the basal sand of many rhythmites contain foreset beds that dip up-valley. Waitt notes that at the type locality near Touchet, the coarse base of each rhythmite is conspicuously channeled into the preceding rhythmite. Waitt (1980) proposes that each rhythmite represents a single flood on the basis of: 1) erosion between adjacent rhythmites; 2) the presence of rodent burrows throughout the Burlingame Ditch exposure, which were not observed during this study; 3) the widespread remains of vertebrate fossils; 4) the preservation of unbroken delicate shells, such as charophytes (Charm Sp.), that normally live in water depths of less than 10 m; and 5) the cleanliness of tephra units within the Touchet beds. He suggests that each rhythmite records an up-valley surge of



rapidly deepening water crossing dry land, then retreating again. Waitt (1980) proposes that at least 40 floods (jokulhlaups) have occurred in southern Washington in late Pleistocene time.

There are several factors that can be used to argue either for or against the many-floods hypothesis of Waitt (1980). He notes that the ice sheet that could have produced the ice dam retaining glacial Lake Missoula has been bracketed by  $^{14}\text{C}$  dates to  $19,100 \pm 2,400$  and  $11,000 \pm 1,800$  year b.p. If the Pend Oreille Ice lobe dammed Lake Missoula for perhaps 7000 years, then the mean interval between the 40 floods would be about 175 years. The present rate of flow in the Clark Fork River is about  $7460 \text{ ft}^3/\text{s}$ ; this would fill the 500 miles<sup>3</sup> lake in some 320 years. If the rate of flow or the volume of the lake were varied by a factor of 2, then the lake could completely fill in 160 years or half fill in 80 years. This revised rate would adequately accommodate Waitt's 40 floods.

Bjornstad (1980), however, notes that up to 62 rhythmites exist. This implies that Waitt's model would have to accommodate 62 floods, which would reduce the average interval between floods to less than 115 years.

The presence of undamaged delicate shells and of clean tephra units that occur inter-rhythmite instead of intra-rhythmite, is difficult to explain unless many floods are postulated.

A major drawback to the many-floods hypothesis concerns erosion of the Touchet beds and the deposition of loess. After the first of the postulated 40 floods, the land would be stripped bare and backflooded areas, such as the Walla Walla Valley, would look something like a mud flat after the tide has gone out. Winds, which are common on the meltwater side of an ice sheet, would have blown the recently deposited fine sand and silt into dunes. Gully erosion would rapidly remodel the dune surfaces.

The second of the "40 floods" 80 to 320 years later would have been, therefore, deposited on a significant erosion surface. This sequence would have repeated itself 40 times (according to Waitt, 1980) and a section, such as Burlingame Ditch or Gardena Cliffs, would surely show considerable evidence of the channeling and dune formation. But, in the Burlingame Ditch exposure, the depth of any channeling rarely exceeds the thickness of a single rhythmite, which ranges from about 5 feet near the base to about 2 feet near the top of the section.



The exposure that does most to refute the 40-flood hypothesis is known as Cummings Bridge (Bretz, 1929; Bjornsted, 1980). It is located on the Walla Walla River south of Reese in SE 1/4, Section 35, T7N R32E, and in NE 1/4, Section 2, T6N R32E. The base of the cliff lies on what may be pre-Palouse loess. This loess is overlain by approximately 26 feet of flood gravels, which in turn are overlain by at least 20 brownish rhythmites of the Touchet beds. These rhythmites are collectively about 49-59 feet thick. Lapping onto these brownish rhythmites, both to the south and to the north, and separated by a major erosional unconformity, there is a sequence of younger greyish rhythmites. The older rhythmites are apparently flat lying, while the younger greyish rhythmites have a pronounced dip to the northwest. This exposure clearly records two sequences of rhythmite development that must be the result of two floods. This suggests that the rate of deposition of a rhythmite sequence may be very rapid--measurable in feet per day. Any extended period of nondeposition would have produced erosional features. Significant erosion between adjacent rhythmites is not seen at Cummings Bridge. It is, however, seen between the two distinctly separate sets of rhythmites.

Hammatt and others (1976) and Baker (1978) mention two flood phases, evidence for which consists to two flood slackwater deposits. Baker (1978) notes that the St. Helnes set "S" volcanic ash is preserved in the younger of these two units. Bjornstadd (1980) provides confirmation of two floods which is corroborated by this study.

The analogy between Flint's (1938) Touchet beds and Bouma's (1962) turbidites is clear. Ginsburg (1973) estimated the velocity of a turbidite to be between 30 and 55 kilometers/h (8.3 to 15.3 m/s). The term slackwater deposits, possibly originally coined by Allison (1933), hardly seems appropriate under these circumstances.

Clastic dikes that range from a few tens of an inch to several feet in width are common in most exposures to the Touchet deposits. The nature and origin of these dikes are discussed in detail in Section 5.

#### The Pasco Gravels

Brown (1975) referred to Bretz' flood gravels in the Pasco Basin as the Pasco Gravels. This facies of the late Pleistocene flood deposits mainly consists of poorly sorted sub-rounded to sub-angular gravel, cobble and boulder-sized fragments, and minor amounts of sand. Basalt is the

dominant lithology present, but others, such as granite, conglomerate, diorite, porphyry, gneiss, and schist, also occur. A Columbia Basin provenance for these lithologic types is inferred particularly from the basalts, but the chert pebble conglomerate, which also occurs, has been determined to originate from the Virginian Ridge Formation in the Methow River drainage of the North Cascade Mountains (Bunker, 1980).

The Pasco Gravels are generally found at elevations lower than about 689 feet in the central part of the Pasco Basin, but they occur locally at higher elevations. The dragline trench on the north side of Gable Mountain contains a gravel unit over 16 feet thick. Near the top of the gravel a volcanic ash belonging to the Mount St. Helens set "S" was observed. This ash was ejected 13,000 y.b.p. (Mullineaux and other, 1978). The elevation of the trench is approximately 804 feet. Pasco Gravels occur within the channeled scabland coulees. They also form the basal units of the glaciofluvial deposits in some of the smaller valleys adjacent to the Pasco Basin, such as the Walla Walla and Yakima valleys.

Ann Tallmann (personal communication, 1981) stated that the Mount St. Helens set "S" ash has also been identified in flood gravels in the Yakima Valley. These gravels may, therefore, be correlated with those found in the dragline trench on Gable Mountain and may be assigned to the Pasco Gravel.

The thickest Pasco Gravel deposits occur in the central part of the Pasco Basin, west of the Columbia River. Tallman and others (1979) report that Pasco Gravels underlying the Separation Areas (Section 36, T13N, R25E; Sections 1 to 12, T12N, R25E; Sections 31 to 35, T13N, R26E; Sections 2 to 11, T12N, R26E) range in thickness from 82-344 feet.

#### Clastic Dikes of the Pasco Basin

Jenkins (1925) believed that the clastic dikes of eastern Washington were produced when cracks resulting from earthquake disturbances were filled with sediment injected under pressure in an aqueous environment. He felt that the dikes could be filled from the top and that they would die out at depth.

Lupher (1944) presented a thorough investigation of the occurrence and mode of formation of clastic dikes particularly associated with proglacial deposits in Washington and Idaho. He recognized that the dikes were



being produced concurrently with the deposition of the host units into which they were emplaced. At least four processes were involved in the filling of the dikes, any or all of which may have been involved in the formation of any individual dike. All of the processes involved filling from above, or movement of sediment through groundwater.

Lupher (1944) noted that the open fissures into which clastic dikes were formed could be created in a number of ways. One of Lupher's principal conclusions was that the clastic dikes found in this area must be related to frozen ground or ice and are therefore Pleistocene in age. Three of Lupher's five proposed mechanisms for the creation of the fissures involved ice indirectly: (1) uneven settling of and ultimately cracking of blocks of sediment overlying layers of melting buried ice; (2) gravity sliding and faulting on inclined zones of subsurface melting; (3) formation of cavities where ice blocks and layers melted. The other two postulated mechanisms involved erosion by underground streams and faulting and fissuring by landslides in the Columbia River basalts.

The possibility that clastic dike were formed sub-aerially was examined but discarded as a general method of formation, because many dikes contain medium and even coarse sands that could not be transported aerially. Lupher (1944) likewise discounted injection from below because he could find no evidence of plastic or water-charged sediment being injected from below. He also noted that many dikes were traceable to overlying current-bedded sand.

The idea that clastic dikes might have formed cataclysmically at the time of deposition of the Touchet beds was rejected by Lupher, an antediluvianist. A geologically instantaneous flood would not have provided enough time for the formation and subsequent melting of ice layers, which Lupher regarded as prerequisite for the creation of the fissures into which clastic dikes were emplaced. Also, Lupher could not believe that clastic dikes containing up to a maximum of 80 dikelets could be related, other than marginally, to earthquake activity in the Pasco area.

Newcomb (1962) investigated the dikes described by Lupher (1944) and added a number of observations pertaining to their mode of origin:

1. Some dikes occur in polygonal networks that have cell diameters ranging from 49 to 394 feet.

2. The dikes are most profuse within the altitude range of 394 to 787 feet and are scarce above 984 feet.
3. Dikes are most numerous where the Touchet beds overlie highly permeable materials.
4. Dikes typically have "roots", a "trunk", and "branches" near the top.
5. The dikes cuts all but the uppermost 10-20 feet of the thickest sections of the Touchet beds.
6. The silt laminae on the walls, the "wall seams" of Lupper (1944) or "clay skins" of Black (1979), are filter cake, which attest to outward filtration of sediment-carrying fluids from each successive dike lamina.

Newcomb (1962) concluded that the above features indicate that the clastic dikes were formed by the upward injection of groundwater. Each "dikelet" was probably caused by bank storage when a pressure difference was produced by large drawdowns of Lake Lewis, the large body of water ponded upstream of Wallula Gap during the Missoula flood. Lowerings subsequent to the first one caused injection along preferential planes of weakness. Thus, the clastic dikes formed during the first lowering of Lake Lewis.

Alwin and Scott (1970) noted that clastic dikes in the Touchet beds penetrate downwards from a few inches to over 98 feet with near vertical dips. They identified features of clastic dikes, such as composite nature, clay wall linings, cross-stratification, graded beds, and oriented grains. Alwin and Scott concluded that these features indicated a downward infilling of the dikes by silt and sand. They felt that the dikes represent infillings of permafrost-related crevices.

Black (1979) made a detailed study of clastic dikes in the Pasco Basin for Rockwell-Hanford Operations. He visited ten different sites and concluded that the dikes are multi-genetic. He considered that previously suggested mechanisms, such as earthquakes, dessication, deep frost cracking, thermal contraction of permafrost, and upward injection of groundwater are not the primary modes of formation of most cracks. Neither did he discount the possibility that some or all of these mechanisms could have been used to produce some of the cracks. Black observed that the bulk of material filling most observed dikes came



from above during aperiodic and repeated widening and concurrent filling of cracks in an aqueous environment. In seven of the ten observed localities, all of the dikes were composite (Hayashi, 1966) and were filled from above in a stress environment that indicated tension, not compression.

Black (1979) hypothesized that hydraulically dammed late Pleistocene floodwater, which repeatedly covered the area, was responsible for the formation of the fractures - for the aperiodic widening of these cracks - and was the primary source of material that filled the cracks. Sudden loading by floodwater on a ground surface whose ground-water level was not close to the surface produced stresses that were irregularly distributed. These stresses induced cracking of the ground, which would have allowed turbid water to enter. Sediment in the water would at first have been filter pressed against the walls of the crack, creating the "clay skins." Fractures could have been widened as the load increased or as shear resistance decreased with increasing pore pressure. Continued widening of the crack would have permitted coarser sediment to enter. The flow of sediment-laden water along the length of a crack would have produced the foreset-bedding structures frequently seen.

Of the remaining three localities studied by Black (1979), one (site 3: on the Old Inland Empire Highway in Section 9, T9N, R25E) had indications of a tectonic origin for the fractures; another (site 6: near Richland City landfill, SE 1/4 Section 20, T20N, R28E), having a polygonal dike arrangement, was not similar to any other, and no origin was proposed for the fractures; and the last (site 9: SE 1/4 SE 1/4 Section 19, T9N, R27E, a borrowpit near Kiona) was deemed to contain dikes that were not considered to be typical clastic dikes--simply collapse of material into a fracture generated by slope failure. Using Hayashi's classification, the majority of Black's dikes would be composite, injection or composite, infilling clastic dikes.

#### Summary - Previous Work

All previous workers recognize the close relationship between the deposition of the Touchet beds and emplacement of the clastic dikes. Most invoke mechanisms for the formation of the dikes that have characteristics peculiar to both the Pleistocene (ice) and/or the catastrophic floods (water). Only Jenkins (1925) proposes an earthquake source for the original cracks. Black (1979) does not discount earthquakes as a possible source, but notes that the almost ubiquitous presence of clastic dikes in the Touchet beds



would have required a far greater level and a more widespread distribution of seismic activity than has been recognized to far.

#### Recent Work

Clastic dikes were observed all over the Pasco Basin during an investigation by Woodward-Clyde Consultants (1981b). In most cases the dikes were in Touchet beds. No clastic dikes have been observed in the Ringold Formation, although Grolier and Bingham (1978) report one such occurrence. In the non-Touchet cases, clastic dikes were observed in basalt and pre-Palouse loess. The Touchet dikes seen fit almost exclusively into Hayashi's composite category: both injection and infilling types. The dikes seen in basalt were simple. In one case the clastic dikes were intensely weathered and probably predate the late Pleistocene floods. The other clastic dikes in basalt were probably late Pleistocene.

The principal observations made by Woodward-Clyde regarding the formation of clastic dikes in the Pasco Basin and associated valleys are that:

1. No clastic dikes penetrate unequivocally eolian deposits of Holocene age. (This suggests a sub-aqueous development of most of the clastic dikes.)
2. The vast majority of clastic dikes occurring in the Pasco Basin and vicinity occur within the slackwater Touchet beds. However, "Touchet" dikes have been seen in basalts and pre-Palouse soils whose ages are far older than the 13,000 years of the Touchet beds. Dikes have also been reported in the upper Ringold Formation. In all cases the dikes occur below the maximum level of the floodwaters, approximately 1,148 feet.
3. The composite "Touchet" clastic dikes were formed during the deposition of the Touchet beds. The many examples of truncated dikes overlain by more Touchet sediments confirms this idea. Bedding-plane slippage occurred within the Touchet beds coincidentally with the development of some of the clastic dikes.
4. Evidence has been found at the Cummings Bridge exposure for at least two major floods of late Pleistocene age. The rhythmites contained in the

Touchet beds deposited by these two major floods do not represent numerous individual floods of sufficient size to have filled a lake the size of Lake Lewis. Instead they represent pulses into an existing lake. If Baker's (1973) conclusion about the duration of the last late Pleistocene flood is correct, then deposition of the Touchet beds and the formation of the enclosed clastic dikes must have occurred in a matter of weeks.

5. The time required for the deposition of the entire flood deposits was so short that freeze-thaw wedging of fissures or sub-aerial dessication could not have produced the numerous composite dikes. The ice-related clastic dike in tidal flats in northern Canada (Dionne and Shilts, 1974; Dionne, 1976) are features measurable in decimeters, not decameters, as in the Pasco Basin.
6. Most of the clastic dikes in the Pasco Basin taper downwards and were filled from the top. Instances of filling from below have been cited by Newcomb (1962), Black (1979), and in Appendix B, but there are few of these cases.
7. About 5 cm of slip along a fault occurred during the time of the late Pleistocene floods, as evidenced by slickensided clastic dikes and displaced basal flood deposits at Gable Mountain (Golder Associates, 1981a). Muir and Fritsche (1981) described earthquake-related features formed in sediments in California during the 1979 Imperial Valley earthquake. In saturated zones complex dikes were formed, while in unsaturated zones simple dikes were formed. This suggests that some clastic dikes in the Pasco Basin may be earthquake related.

If Baker's (1973) hydraulic model is valid, Lake Lewis both formed and largely disappeared within a period of two weeks. It is conceivable that reservoir induced earthquakes may have been associated with the rapid filling and draining of Lake Lewis.

Shaking resulting from seismic activity induced by the presence of Lake Lewis could provide a mechanism for the sliding of blocks of Touchet sediments and the fissuring of Pasco Gravels, pre-Palouse loess, the Upper Ringold Formation,

and basalt bedrock. However, the abundance and widespread occurrence of clastic dikes in the Pasco Basin, their composite natures, and the relatively short interval during which they formed all indicate that it is unlikely that earthquakes were the primary factor in their formation.

8. The exposure at the gravel pit just northwest of Kennewick shows a flat-lying composite Touchet clastic dike penetrating a thick calcrete developed on an older gravel. The dike is traceable nearly horizontal for over 16 feet. No other such fissures have been seen in calcretes such as this. It is extremely unlikely that a flat-lying fissure would remain open with over 250 m of water above it while the clastic dike gently filled with sediment. (Hydraulic injection of sediment appears to be the most viable mechanism for the formation of this clastic dike. If clastic dikes can penetrate indurated carbonate-cemented conglomerate, then their injection into loose, saturated silts and sands would be easy.)
9. Clastic dikes reportedly created in fissures opened during folding in southern Chile (Winslow, 1977; Bruhn, 1979) are not similar to the composite Touchet dikes of the Pasco Basin. Their modes of origin must, therefore, be dissimilar also.

#### Summary - Recent Work

The lack of clastic dikes in eolian deposits and the predominance of clastic dikes in late Pleistocene flood deposits strongly suggest that they formed at the time of the flooding. This is confirmed by the frequent occurrence of truncated clastic dikes being overlain by younger flood deposits (Touchet beds).

Occasionally clastic dikes penetrate the entire sequence of flood deposits and extend downwards into basalt, Ringold, pre-Palouse loess and 200,000 year cemented gravels.

High pressure injection is considered to be necessary to emplace dikes into the formations beneath the flood deposits, and this mechanism is regarded as the most plausible for the majority of cases, at least in the early phase of a dike's formation. Other processes, such as spreading of blocks of Touchet beds and liquefaction,





presumably were also invoked as Black (1979) suggested, to continue the growth of the number of dikelets in a composite clastic dike.

#### Ash Deposits

The most widespread ash in the Columbia Basin is a thin, but widespread and locally continuous unit in late-glacial lacustrine sediments. It occurs in both the Touchet beds and Pasco gravels throughout the Pasco Basin. Commonly this ash occurs as two subparallel units separated by as much as 2 inches of lacustrine sediment. Studies indicate that this cummingtonite-bearing ash is from Mount St. Helens tephra set "S". The most voluminous layers of tephra set "S" are about 13,000 years old (Mullineaux and others, 1977).

Ash from the Glacier Peak volcano has been positively identified in the Pasco Basin, and in other parts of the Columbia Basin to the north and east of the site. (Powers and Wilcox, 1964; Fryxell, 1965; Woodward-Clyde, 1981b)). Radiocarbon dates indicate that the Glacier Peak ash was erupted about 12,500 years ago (Fryxell, 1965).

Another ash occurs interbedded with Holocene eolian sediments along the margin of the Pasco Basin. This ash layer locally has been correlated with the catastrophic eruption of Mount Mazama in Oregon about 7,000 years ago (Davis, 1978).

#### Latest Pleistocene and Holocene Loess

Much of the Pasco Basin and adjacent areas are covered by a mantle of latest Pleistocene and Holocene loess deposits. The loess is pale brown and has an AC soil horizon. Tallman and others (1979) report that in the Separation areas south and west of Gable Mountain the Holocene loess is up to 16 feet thick in some places.

The loess may be found in contact with any of the older lithologic units. At the southwest end of Burlingame Ditch the loess is over 7 feet thick and overlies the Glacier Peak volcanic ash, dated at about 12,000 y.b.p. The ash overlies the eroded surface of the Touchet beds. At the Badger Road-Keene Road junction (NE 1/4, SE 1/4, Section 11, T8N, R28E, Badger Mountain quadrangle) horizontally bedded Touchet beds that grade northwards into eolian sand or loess contain a volcanic ash from the Mazama eruption dated at about 7,000 y.b.p.



Immediately after the last Pleistocene flood (about 13,000 y.b.p.) hundreds of square kilometers of recently deposited bare Pasco Gravels and Touchet beds would have been exposed to wind erosion. Winds would easily have carried the finer sediments, which had been derived largely from either basalt or from the older loess deposits such as the Palouse.

#### Talus, Slopewash & Landslide Deposits

Talus and slopewash occur along the bases of slopes around and within the Pasco Basin. These are deposits of sand, gravel, and debris developed through processes of creep, rockfall, and slopewash.

Landslides as large as 5 square kilometers in area exist in the Ringold Formation along the White Bluffs, north and east of the project site (Bingham and Grolier, 1966). The major sliding has occurred along interlayered pyroclastic or sedimentary materials of low shear strengths, caused by saturation by subsurface water and oversteepening of slopes. Surficial failures of slope debris occur along the steep flanks of the anticlinal ridges in the region.

#### Alluvium and Terrace Deposits

Holocene alluvium deposited by the Columbia and Yakima Rivers occurs along the present channel courses, but it is often difficult to distinguish from the glaciofluvial deposits. Fan deposits exist along the rim of the Pasco Basin and may be as much as 50 feet thick.

#### 2.5.1.2.3 Columbia Plateau Structural Geology

##### 2.5.1.2.3.1 Badger Mountain, Beezley Hills, Moses Stool Folds

The Badger Mountain-Beezley Hills is a broad, asymmetrical, anticlinal structure in the northwest Columbia Plateau east of Wenatchee. This structure plunges southeastward from the Columbia River at about 100 feet per mile (Figure 2.5-3). The northern limb dips steeply into a broad downwarp known as the Waterville syncline, whereas the southern limb typically dips less than about 5°.

The main development of the Badger Mountain structure was clearly a post-Grande Ronde event, as indicated by deformation of the Vantage Member (Washington Public Power Supply System, 1977e). Although a minimum age for the structure has not been determined with certainty, no



evidence was found to indicate faulting of late Cenozoic sediments which mantle much of the anticline (Washington Public Power Supply System, 1977e; Rigby and Othberg, 1979).

The Moses Stool anticline is an echelon with Badger Mountain and merges with the Beezley Hills east of Moses Coulee. West of Moses Coulee, the Moses Stool anticline merges with Badger Mountain (Swanson and others, 1979a). At the approximate location of the juncture of the Beezley Hills and Moses Stool anticlines, the Beezley Hills curves north and becomes the Coulee monocline, which extends a distance of approximately 48 kilometers to the northeast. The terminus of the monoclinical axis of Beezley Hills coincides with a thrust fault developed in Wanapum Basalt. Southward, a second thrust fault juxtaposes Grande Ronde Basalt above Wanapum Basalt (Swanson and others, 1979a).

#### 2.5.1.2.3.2 Kittitas Valley

The Kittitas Valley (Figures 2.5-11, 2.5-3, and 2.5-12) is a topographic and structural low along the northwestern margin of the Columbia Plateau. It is bounded on the west by the Cascade Mountains, on the north by the Wenatchee Mountains uplift, on the east by the Naneum-Hog Ranch anticline, and on the south by the Manastash-Thrall structure. The geology of the area has been the subject of investigations by Bentley (1977, and in Washington Public Power Supply System, 1977d), Tabor and others (1977), Martin (in Washington Public Power Supply System, 1977j), Waitt (1979b), and Hanson (in Rigby and Othberg, 1979).

Grande Ronde flows and Ellensburg strata, having dips of  $10^{\circ}$  to  $50^{\circ}$ , crop out on the flanks of Kittitas Valley. These same units have dips of about  $5^{\circ}$  near the middle of the valley (Waitt, 1979a). Rocks exposed within the valley also include pre-Tertiary gneiss, early Tertiary volcanics, Thorp Gravel, and glacial drift (Rigby and Othberg, 1979).

Most faults within the Kittitas Valley appear older than the late Cenozoic sediments of the area. However, Martin (in Washington Public Power Supply System, 1977j) and Waitt (1979b) described three east-striking faults in the valley which they interpreted as younger than Thorp Gravel (less than 3.7 m.y.b.p.) and older than Kittitas Drift (120,000 y.b.p.). These faults were later examined by Rigby (Rigby and Othberg, 1979), who concluded that evidence for two of the faults is tenuous (Wilson Creek and Reecer Creek faults), but did confirm a fault in Yakima basalt along Dry Creek. No offsets in the Thorp Gravel or younger units could be found by Rigby along this fault.

### 2.5.1.2.3.3 Frenchman Hills

This east-trending anticlinal fold extends from the eastern edge of Kittitas Valley (Figure 2R G-15 of Washington Public Power Supply System, 1977n) on the west to the Potholes Reservoir on the east. East of the Columbia River the Frenchman Hills anticline is subdued and symmetrical.

### 2.5.1.2.3.4 Manastash Ridge - Hanson Creek

The Manastash Ridge-Hanson Creek anticlines are structures extending from east of the Columbia River near Priest Rapids Dam to the Ellensburg area (Figures, 2.5-12 and 2.5-13). Manastash ridge separates Kittitas Valley to the north from the Squaw Creek syncline to the south.

In the vicinity of Yakima River (Figure 2.5-12 and 2.5-13), the Manastash structure is a broad, low, asymmetrical anticline having steeper dips on the north limb. Two second-order folds, the Thrall syncline and the Thrall anticline, are superimposed on the north flank of the structure. Axes of the Manastash anticline and the Thrall anticline are parallel.

Most faults associated with the Manastash structure are near vertical and located along the steep north limb. The most continuous of these may be part of a longer fault system, termed the Manastash-Hanson Creek fault system (Bentley, 1977). One north-south cross fault displaces the structure at Badger Gap (Shannon and Wilson, 1978; Swanson and others, 1979a). On the basis of remote sensing imagery, this feature cannot be traced westward into Kittitas Valley or eastward across Manastash Ridge (Rockwell, 1979). Bentley (1977) concluded that most deformation on Manastash Ridge occurred after sediments interpreted as Thorp Gravel were deposited, and before development of the Thrall pediment surface (1.0 m.y.b.p.).

### 2.5.1.2.3.5 Yakima Ridge

Yakima Ridge extends from west of the city of Yakima (Figures 2.5-15 and 2.5-16) to the western border of the Hanford Reservation. Yakima Ridge is divided into western, middle, and eastern segments on the basis of topography (Washington Public Power Supply System, 1977k).

The western segment of Yakima Ridge (Figure 2.5-15) extends from Sedge Ridge eastward along Cowiche Mountain to Selah Gap. The ridge in this area is a box-fold with sharp hinge lines along both flanks. The minimum age of deformation on





Yakima Ridge is established by the Tieton andesite which onlaps the eroded north flank of the anticline along Cowiche Creek. K-Ar determinations by J. Dyman (in Washington Public Power Supply System, 1977k) indicate an age of 1.0 and  $\pm 0.1$  m.y.b.p. for the andesite.

The middle segment of Yakima Ridge (Figure 2.5-16) extends eastward from Selah Gap to Cairn Hope Peak. This segment is a box-fold anticline with sharp hinge lines (Waters, 1955; Bentley, 1977). Faults are present locally in the hinge area and core of the anticline.

The eastern segment of the Yakima Ridge structure (Figure 2.5-16) has been studied by Rockwell (1979), Bond and others (1978), and Kienle (in Washington Public Power Supply System, 1977k). The dominant fold within the eastern segment of the Yakima Ridge is the N70-75°W-trending, southeastward plunging Cairn Hope Peak anticline. The shorter and steeper north limb of this anticline dips 30° to 40° north, and its wider southern limb dips 10° to 15° south. The southern limb of the anticline contains two monoclines. The northernmost monocline, the Cairn Hope Peak monocline, trends N60°W and is interpreted (Bond and others, 1978) as merging with the Silver Dollar Fault of Goff and Myers (1978). The southern monocline (unnamed) trends N70°E.

The Silver Dollar fault (Figure 2.5-16) reportedly offsets the Frenchman Springs against Umatilla and Pomona across a fault breccia zone 165 to 230 feet wide (Goff and Myers, 1978). Field reconnaissance by Shannon and Wilson (1980) confirmed this fault west of the Yakima-Benton county line. Based on stratigraphic displacements, Shannon and Wilson (1980) interpreted the fault as a scissor fault having a hinge to the east and increasing displacement westward.

The Yakima Ridge structure is separated from Umtanum Ridge by the Cold Creek syncline which plunges 3° to 5° east-southeastward into the central Pasco Basin.

Based on his geologic mapping of Yakima Ridge, Bentley suggested at least two periods of deformation (Bentley, 1977). The first period involved uplift along a north-trending axis during post-Priest Rapids and pre-Pomona time (12 to 14 m.y.b.p.). The second period involved uplift along N50°-80°W-trending axes in post-Elephant Mountain time (about 10.5 m.y.b.p.). Uplift as indicated by undisturbed Tieton Andesite along Cowiche Creek on the west end of Yakima Ridge ceased by 1 m.y.b.p. (Washington Public Power Supply System, 1977k).



On the basis of remote sensing data, the slopes of Yakima Ridge appear more subdued and symmetrical than the slopes of the anticlines farther south. Landslides appear to cover the flanks.

#### 2.5.1.2.3.6 Ahtanum Ridge

Ahtanum Ridge (Figure 2.5-16), an east-trending anticline, is essentially the western extension of the Rattlesnake Hills. In general, the structure is asymmetrical, having steeply dipping and overturned basalt flows and thrust faults exposed on both flanks (Bentley, in Swanson and others, 1979a).

Late Cenozoic sediments on Ahtanum Ridge were mapped by Campbell (in Rigby and Othberg, 1979). He found no evidence of faulting in recent loess and stream alluvium overlying the surface of the ridge. Faulting of Ellensburg sediments and cemented basalt gravels was observed at two points on the lower slopes of Ahtanum's north flank. The age of deformation of these older sediments post-dates deposition of the Ellensburg strata and pre-dates deposition of the loess and alluvium. The most recent age of deformation on the western end of Ahtanum Ridge appears to be limited by undeformed Tieton Andesite (1 m.y.b.p.) (Shannon & Wilson, 1978).

#### 2.5.1.2.3.7 Toppenish Ridge

Toppenish Ridge is an east-west-trending anticlinal structure located in the western Columbia Plateau, entirely within the Yakima Indian Reservation. At its closest approach Toppenish Ridge is approximately 70 kilometers west of the WNP-2 and WNP-1/4 sites. Linear geomorphic features (scarps) that appear to be related to either Holocene faulting or to recent landsliding were indentified along the north slope of Toppenish Ridge in 1978 (Rigby and Othberg, 1979).

#### Previous Work

Geologic studies of the features of Toppenish Ridge have been conducted previously by a number of investigators but most notably by Newell Campbell of Yakima Valley College and Robert Bentley of Central Washington University, as reported in Rigby and Othberg (1979), Bentley and others (1980), and Cambell and Bentley (1981). Campbell mapped the Quaternary stratigraphy and the scarps on Toppensih Ridge. His mapping was conducted at a scale of 1:12,000 and supplemented with photogeologic interpretation using 1:24,000-scale vertical

aerial photographs. Campbell's work was first published by Rigby and Othberg (1979) and was followed by Bentley and others (1980). This work is currently in press for Campbell and Bentley (1981). Campbell's conclusion in Rigby and Othberg (1979), based on morphologic and stratigraphic relationships, was that the scarps are the result of tectonic faulting during the Holocene.

Bentley mapped the bedrock stratigraphy and structure. His results are reported in Bentley and others (1980) and Campbell and Bentley (1981). Preliminary studies for the Supply System to ascertain the nature and origin of the scarps on Toppenish Ridge have been undertaken by Glass (1979, and 1981, written communication), by Kiel and Davis (1980, unpublished field notes) and by Davis (1981). Based on a remote sensing analysis, using 1:65,000- and 1:130,000-scale aerial photographs Glass (1979) concluded that faults associated with the Toppenish Ridge anticline are probably not active and that the most likely candidates for active faults are the northwest-trending lineaments near the western portion of the ridge. He also noted that if the anticlinal faults are active, the northwest-trending faults are also probably active. Because the small scale of the imagery used for this interpretation could not resolve the scarps reported by Campbell (Rigby and Othberg, 1979), Glass (1981) conducted an aerial reconnaissance of Toppenish Ridge to observe the reported scarps. Based on the length and character of the zone of scarps, he concluded that the scarps are likely tectonic in origin but that a non-tectonic origin cannot be ruled out. In addition, Glass (1981) noted that the scarps on Toppenish Ridge are the youngest of any he has observed on the Columbia Plateau.

Based on aerial reconnaissance and preliminary analysis of the observed geomorphic character of the scarps, Davis (Kiel and Davis, 1980, unpublished field notes and Appendix 2.5N) concluded that gravitationally induced slope failure is a viable alternative to a tectonic origin for the scarps on Toppenish Ridge. Davis (Appendix 2.5-N) states that:

The combination of apparent low-angle thrusting along the northern base of the ridge and normal (extensional) faulting at higher elevations raises the possibility that the two are expressions of gravitationally-induced slope failure (Figure 2.5N-4). Several lines of evidence support the interpretation that the Toppenish structures represent either an aborted phase or the incipient development of massive slope failure along the north flank of Toppenish Ridge. Included among them are the dramatic north flank landslides on the eastern end

of the ridge and around Olney Lake, immediately to the west. These slides demonstrate in spectacular fashion the instability of the northern flank. The close spatial relations between apparent low-angle faults at the base of the ridge and high-angle faults at higher elevations are suggestive of an interrelated landslide toe and headscarp geometry. An active, youthful landslide at the south end of the White Bluffs, on the Columbia River opposite Richland, is characterized by just such prominent headscarps and a subhorizontal plane of movement near the base of the slope. Bentley and others (1980, p. 51) argue that a landslide origin of the Toppenish ground ruptures is "unlikely, because such an interpretation does not explain the abundance of south-side-down faults on the north slope of the ridge." However, such faults can be reasonably interpreted as antithetic faults to the main north-dipping sole fault. The White Bluffs landslide referred to above displays just such an antithetic rupture which defines, with the headscarp fault to the east, the edges of a shallow graben. Until the Toppenish ground ruptures receive further study, it is premature to conclude unequivocally that they represent tectonic activity.

A geologic study of the ridge was initiated in February 1981 by Woodward-Clyde Consultants for Washington Public Power Supply System. Shortly thereafter, permission for access was refused by the Yakima Indian Council and the scope of work was revised to reflect the lack of direct ground access. Based primarily on photogeologic interpretation and aerial reconnaissance, Woodward-Clyde Consultants made the following concluding remarks.

An area of youthful-appearing topographic scarps occurs along the north slope of the central portion of Toppenish ridge in a zone about 24 kilometers long by 2 kilometers wide. Three distinct sets of scarps have been observed. The crestal and midslope set of scarps are quite linear, cut across topography, and are the least continuous. They are high angle, occur in rocks of Miocene to Holocene age, and have scarp heights typically from 3 to 7 feet. The basal set of scarps are the most continuous, are more sinuous, tend to follow the topography, and also occur in rock of Miocene to Holocene age. They typically have scarp heights of from 3 to 10 feet.

Both non-tectonic and tectonic origins have been proposed for the formation of the scarps on Toppenish Ridge. Land-sliding and gravitational ridge spreading appear to be the

most viable non-tectonic processes that could account for the distribution, pattern, and morphology of the observed scarps. However, several lines of evidence tend to preclude these processes as being the primary mechanisms for the formation of the scarps:

1. The long, thin geometry of the zone of scarps (24 kilometers x 2 kilometers) is not easily amenable to a landslide-failure interpretation, given the complexity of the bedrock stratigraphy and structure over the 24 kilometer extent of the zone;
2. given the geometry of the zone (24 kilometers x 2 kilometers) and the incipient nature of failure over the entire zone, a landslide interpretation requiring continuity of failure in space and time over such a distance seems unlikely;
3. the known areas of extensive landsliding in the Columbia Plateau are, overall, morphologically and geologically dissimilar to the zone of scarps on Toppenish Ridge; no examples of known landsliding were found in the literature that could adequately explain the overall pattern, morphology, and character of the scarps in terms of a landslide origin; and
4. the presence of the compressional thrusting (basal set of scarps) at the base of the north slope (not known in areas of gravitational ridge spreading) and the lack of continuous, steeply dipping discontinuities on which gravitational ridge spreading occurs tends to preclude this mechanism as an origin of the scarps.

Overall, the scarp patterns, characteristics, relationships to the known geology and comparisons to historical surface thrust-faulting events best support a tectonic thrust mechanism as the primary origin of the scarps on Toppenish Ridge. The basal set of scarps expresses surface displacement along a primary south-dipping thrust or reverse fault. The crestal and midslope set of scarps represent high-angle secondary (primarily normal) faults resulting from movement along the primary thrust. Several lines of evidence tend to support this tectonic interpretation:

1. The overall extent and geometry of the zone of scarps compares well with known historical surface thrust-faulting events;



2. the pattern of the primary thrust-fault scarps (basal set) in relation to the high-angle secondary fault scarps (crestal and midslope sets) is similar to the patterns of primary and secondary fault scarps observed in known historical thrust-faulting events;
3. the continuity of the basal set of scarps when compared to the crestal and midslope sets suggests that the formation of the basal set is primary;
4. the prominence of secondary normal faulting with numerous antislope scarps is compatible with the pattern observed in known historical thrust-faulting events;
5. the close spatial and apparent geometrical relationship of the basal-set scarps to the mapped trace of the south-dipping Mill Creek thrust fault; and
6. the indication of possible renewed movement of secondary faults suggests renewed movement of the thrust fault. Without well-developed landslide morphology, this condition is more compatible with a tectonic interpretation than a gravitational failure mechanism.

The high-angle secondary faults are interpreted to occur in response to movement along the thrust fault. They may be formed by gravitational adjustments due to extension of the upper plate during thrust or by extension in anticlinal hinge areas that fold during the compressional thrust event. The scarps (thus the faults) are developed in mapped geologic units as old as Miocene Columbia River basalt and as young as Holocene stream alluvium, thus, assuming a tectonic origin, they are considered to be capable.

#### 2.5.1.2.3.8 Horse Heaven Hills

The Horse Heaven Hills is essentially an anticlinal structure extending from east of Wallula Gap to the Cascade Range of northern Oregon, west of the Hood River. The structure is typically asymmetrical with gentle dips on the south limb and a steep northern escarpment. The overall structure can be divided into western, middle, and eastern segments.

The western segment of the ridge contains a northeast-striking fault downthrown to the north (Swanson



and others, 1979a) and appears to be displaced along several northwest-striking cross-faults.

The middle segment is a broad anticlinal arch with associated thrust faults (Anderson in Swanson and others, 1979a). Between Bickleton and Chandler, the middle segment of the structure is dominated by a series of northeast-trending anticlines. Near the crest of the Horse Heaven Hills, dip slopes and gentle folds underlie the intervening flat terrain (Gardner, in Swanson, 1978; Gardner in Swanson and others, 1979a). Thrust faults and high-angle faults associated with these folds cut the youngest (Elephant Mountain) basalt unit present.

Along the middle segment, between Prosser and Bickleton, Campbell (in Rigby and Othberg, 1979) observed a scarp developed in late Cenozoic material. On the southwest, the scarp terminates at a landslide, and it dies out north-eastward in alluvium. Campbell suggested that this scarp represents a dip slope on a resistant unit within ancestral Columbia River gravels.

The eastern segment of the Horse Heaven Hills is a broad northwest-trending anticlinal ridge (Figure 18). Several faults, including the Zintel Canyon fault, are associated with this segment of the Horse Heaven Hills. The Zintel Canyon fault is interpreted as a high-angle, southward-dipping reverse fault (Rockwell, 1979). The fault appears to merge with the anticlinal fold to the east and to decrease in displacement westward.

#### 2.5.1.2.3.9 Columbia Hills

The Columbia Hills anticline (Figure 2.5-3) extends from southwest of The Dalles, Oregon, to the vicinity of McNary Dam. The structure, most of which lies in southernmost Washington, comprises a series of asymmetrical, doubly-plunging anticlines. The amplitude of the structure decreases progressively eastward. The western half of this anticline is intersected by a series of northwest-striking faults, especially along the steep south limb of the structure (Swanson and others, 1979a). Right lateral displacement of the fold hinge along northwest-striking faults is suggested by the en echelon arrangement of small anticlines southeast of Camas Prairie (Swanson and others, 1979a).

Shannon and Wilson (1973d) examined the age of the northwest-trending fault system, and on the basis of K-Ar dating of Simcoe Lavas, concluded that the age of last

movement on the structures was between 3.5 and 4.5 m.y.b.p. However, they also concluded that alignment of volcanic cones (some less than 100,000 years old) along the trend of these structures suggests that the fault system has continued to be a zone of crustal weakness providing conduits for late Cenozoic magmas.

#### 2.5.1.2.4 Pasco Basin Structural Geology

The WNP 1-2-4 site lies within the Pasco Basin (Figure 2.5-4), one of several physiographic basins within the western Columbia Plateau. The Pasco Basin is partly surrounded by large anticlinal ridges. The Saddle Mountains form the northern boundary of the Pasco Basin; Umtanum Ridge and Yakima Ridge form the western boundary; Rattlesnake Hills and Horse Heaven Hills form the southern boundary; and a broad zone of gradually increasing westward dip (Figure 2.5-20) forms the eastern boundary. Umtanum Ridge and Yakima Ridge plunge eastward, decrease in relief, and die out within the basin interior.

Folds within the Pasco Basin trend eastward in the northwestern part of the basin and northwestward in the southeastern part. The anticlines generally correspond to narrow linear ridges, and the synclines to broad alluvium-filled valleys. The folds typically are asymmetrical, with the anticlines steeper to overturned on the north. Faulting is common along the ridges, particularly in areas where folding is most pronounced.

##### 2.5.1.2.4.1 Saddle Mountains

The Saddle Mountains structure marks the northern boundary of the Pasco Basin. It is one of the largest and most prominent anticlinal structures within the Yakima Fold Belt (see Figures 2.5-13, 14, and 17). From its western end, located about 24 kilometers southeast of Ellensburg, Washington, to its eastern end, located about 10 kilometers east of Othello, Washington, it extends nearly 113 kilometers across the western Columbia Plateau. Most of this discussion is from Reidel (1978b) and from Rockwell, 1979.

The Saddle Mountains structure is first-order structure with second-order folds and faults on its flanks. The main structure is the Saddle Mountains anticline which is an asymmetric anticlinal ridge with a steep northern flank. The Saddle Mountains structure changes geometry close along strike from a fold in the northwestern part of the Pasco Basin to an open fold in the northeastern part. Maximum



structural relief, measured on the Wanapum Basalt, is about 2,000 feet in the northwestern Pasco Basin, but diminishes to less than 500 feet in the northeastern basin.

Basalt outcrops in the hinge area of the Saddle Mountains structure have been mapped by Grolier and Bingham (1971), Taylor (1976), Washington Public Power Supply System (1974), and Washington Public Power Supply System (1977h), and most recently by Reidel (1978b). This mapping has revealed that the hinge area can be subdivided into three segments on the basis of fold geometry: (a) a western segment; (b) a central segment; and, (c) an eastern segment (Grolier and Bingham, 1978; Reidel, 1978b). Two major structural trends (east-west and northwest-southeast) and one minor trend (northeast-southwest) are within the segments.

The Saddle Mountains anticline follows a sinuous east-west trend along the Saddle Mountains structure and is principally responsible for topographic relief of the Saddle Mountains. In the western segment of the Saddle Mountains structure near Sentinel Gap, the Saddle Mountains anticline bifurcates into northern and southern axial traces. Recent mapping by Reidel on the west side of Sentinel Gap suggests that the Saddle Mountains anticline there might be overridden by a northwest-trending thrust fault (Section 32, T15N, R23E) in a manner similar to that observed by Farkas (1972) and by Price during work for Rockwell Hanford Operations on Umtanum Ridge (cited in Rockwell, 1979).

Between 120° west longitude and the western edge of Smyrna Bench, the Saddle Mountains anticline is an asymmetric fold. The north limb is nearly vertical where exposed and the south limb is less steeply dipping (Grolier and Bingham, 1978). The south limb is complicated by many parallel-to-subparallel minor folds. The structural low in the Saddle Mountains anticline, the Levering monocline, the convergence of smaller folds, a paleovalley, and a north-south fault, all collectively suggest that this area of the south limb is complex with a long and complicated history.

The boundary between the western segment of the Saddle Mountains structure and the central segment is a complex zone of deformation and marks a change in fold geometry from an open, asymmetrical fold in the western segment to a box fold in the central segment. Near Verified Altitude Bench Mark (VABM) Saddle, the hinge line of the anticline plunges to the southeast. South of Smyrna Bench, the position of the hinge line is south of the topographic crest of the

Saddle Mountains. Eastward from Section 8, T15N, R25E, the trend of the hinge line is almost east-west, overall, but with local variations.

An abrupt change in the trend of the axial trace and change of fold geometry on the east side of Smyrna Bench mark the boundary between the central and eastern segments of the Saddle Mountains structure. Geometry changes from a tight box fold to the west to a more open eastward-plunging fold to the east. The abrupt change in trend was interpreted as a fault by Glass and Slemmons in Washington Public Power Supply System (19771) based on air photo interpretation, but no offset was found by Rockwell geologists. From the east side of Smyrna Bench, the axial trace of the Saddle Mountains anticline swings northeast and then southeast (S65°E) to the Eagle Lake area where an abrupt east-west directional change occurs, and the fold becomes more open and subdued until it is covered by Ringold sediments east of Scooteney Reservoir. This is the easternmost exposure of the Saddle Mountains anticline.

The Smyrna monocline is approximately parallel to the trend of the Saddle Mountains anticline south of Smyrna Bench and forms a northern hinge zone in the central portion of the anticlinal fold. Dips increase along the hinge from 5 to 20° toward the north, south of the hinge, and 60° north to overturned, north of the hinge.

A monocline similar to the Smyrna monocline extends along the north side of the Saddle Mountains from Corfu east approximately to where Washington State Highway 240 crosses the Saddle Mountains. Along the monocline, dips change from 5 to 10° to the north to 20 to 40° to the north. Near Washington State Highway 240, the monocline merges with the Saddle Mountains anticline. This is inferred to be the same monocline on both sides of the landslide block south of Corfu.

North of the Saddle Mountains anticline in the Eagle Lake area (T14N, R29 to 30E) is a series of doubly plunging anticlines and synclines trending from N70°W to N70°E. Most are open folds, but one, in Section 12, T14N, R29E, is a relatively tight fold with a steeply dipping south limb.

The Saddle Mountains fault has been a topic of considerable discussion (Laval, 1956; Grolier, 1965; Grolier and Bingham, 1971, 1978; Jahns 1967; Jones and Deacon, 1966; Taylor, 1976; Washington Public Power Supply System, 1977h). Laval (1956) interpreted this fault to be a thrust fault based on an exposure near Sentinel Gap, but Grolier and Bingham

(1971) interpreted it as a near-vertical fault, noting that "the critical relationships are hidden under talus and sand dunes." Washington Public Power Supply System (1977h) emphasized the change in fault geometry along its strike from a high-angle reverse fault in the Smyrna Bench and Sentinel Gap area to a nearly horizontal thrust fault to the west in the Boylston Mountains.

On the west side of Sentinel Gap, the Saddle Mountains fault is a complex zone with several low-angle fault planes exposed. Neither fault displacements nor attitudes have been measured, but slickensides suggest low-angle, reverse movement. The Sentinel Bluffs sequence is over 900 feet thick on the east side of the river (Taylor, 1976; Long, 1978), but is less than 500 feet thick west of the river, suggesting thinning due to faulting or pinching-out onto a pre-existing structure.

Between Smyrna Bench and Sentinel Gap, the fault could have a maximum stratigraphic displacement of 1,800 feet (Section 1, T15N, R24E), but nowhere is the fault plane exposed. The approximate location of the fault zone is shown on Figure 2.5-13. Only the outcrop east of Sentinel Gap (Sections 33 and 34, T16N, R24E) was found where faulted bedrock might be inferred. The exposures here are poor and relationships are considered tentative at this time. Taylor (1976) interpreted an east-west-trending fault here.

On the east side of Smyrna Bench, Grolier and Bingham (1978) described another exposure of the Saddle Mountains fault (Section 1, T15N, R26E). No significant displacement could be found at that location by Rockwell geologists. This area was discovered to be the westernmost limit of the Huntzinger flow on the north slope of the Saddle Mountains and is interpreted to represent a paleovalley. The overturned Priest Rapids, Huntzinger, and Pomona flows in Section 1, T14N, R26E are thought to be related to a possible northwest-trending cross structure. Exposed in a north-south gully are vertical and locally overturned Grande Ronde Basalt and Frenchman Springs, Roza, Priest Rapids, and Elephant Mountain Members (Laval, 1956; Grolier and Bingham, 1971; Taylor, 1976; Reidel, 1978b).

A short distance to the south (Section 34, T16N, R24E), the Grande Ronde Basalt is folded and sheared from nearly horizontal (to the south) to nearly vertical (in a gully to the north). Individual Grande Ronde Basalt flows could not be mapped through the sheared zone; the two lower flows appear to have been faulted from the vertically standing section. This fault zone is interpreted to be associated

with a northwest-southeast fault zone, the Smyrna fault. Evidence for this fault is based on offset in Section 3, T15N, R25E, a tectonic shear zone in Grande Ronde Basalt described above, and tectonically brecciated Elephant Mountain Member cropping out along the projection of the fault and shear zones (Section 33, T16N, R25E).

A major northwest-southeast anticline, the Smyrna anticline, is located near the west end of the Smyrna Bench (T15N, R25E). Folding along the east-west Saddle Mountains anticline has almost obliterated this structure, but its axis represents the present structural high along the Saddle Mountains anticline. This northwest-southeast structure was recognized primarily on the basis of stratigraphic relationships in the area. Based on flow distribution, an anticlinal ridge several kilometers wide is inferred to have existed from Frenchman Springs time through Pomona time (10 to 14 m.y.b.p.). The anticline apparently reached its greatest topographic relief during Priest Rapids time, when it formed a barrier at least 6 kilometers wide. This structure is now bounded on the west by the Smyrna fault.

On the eastern segment, a third structure is suggested by a change in trend of the Saddle Mountains anticline. Here, the abrupt change in attitude of the beds was interpreted by Glass and Slemmons in Washington Public Power Supply System (19771) as a fault. A northwest-southeast cross structure may cut the Saddle Mountains anticline, but there is no indication of relative displacement.

Northwest-trending folds of lesser amplitude are between Sentinel Gap and Smyrna Bench (Sections 3, 4, and 5, T15N, R24E). These structures are older than the Saddle Mountains fault, but probably are younger than the two northwest-southeast-trending anticlines (Sentinel Mountain and Smyrna). These folds show a relatively long history of deformation. They apparently became active during Priest Rapids time, as indicated by local thickness variations in Priest Rapids flows. Associated synclinal troughs are filled with thick accumulations of Ellensburg sediments and Elephant Mountain basalt which did not overflow the trough. Ellensburg sediments and caliche covering them are deformed, indicating post-Ellensburg deformation along this trend. One syncline has a normal fault bounding its west side.

#### 2.5.1.2.4.2 Umtanum Ridge

The Umtanum Ridge-Gable Mountain structural trend (Figures 2.5-16 and 2.5-17) is a segmented bedrock high extending for a length of 137 kilometers from the western end of Umtanum

Ridge to southeast of Gable Mountain. This structural trend is composed of five segments, which are separated from each other on the basis of changes in style of deformation and the orientations of folds, which form the segments. The five segments are each considered to be first-order folds. Golder Associates, 1981a and 1981b, present more comprehensive descriptions of folding and faulting associated with the eastern segment of Umtanum Ridge and the Gable Butte-Gable Mountain segment of the structural trend. Webster and Crosby (1981) prepared for Golder Associates evidence for deformation associated with the most easterly segment of the structural trend, the Southeast anticline.

Umtanum Ridge consists of three first-order folds which represent three segments of the trend. These three folds show tighter folding and higher structural amplitude than any of the other anticlines along the trend and are separated from one another by differences in vergence (Golder Associates, 1981a).

The next segment to the east, the Gable Butte-Gable Mountain segment (Golder Associates, 1981b), is separated from the Umtanum Ridge segments on the basis of a change in folding style and by a topographic depression in the crest of the structural high south of Vernita Bridge (Figure 2.5-16). East of this area, the first-order fold forming the Gable Butte-Gable Mountain segment is of significantly lesser amplitude than first-order folds to the west. It forms a broad anticlinal warp with a wavelength that is several orders of magnitude greater than the first-order fold forming the eastern segment of Umtanum Ridge. Within the Gable Butte-Gable Mountain segment, three prominent second-order folds (Gable Butte and the east and west anticlines of Gable Mountain) are present on the crest of the first-order fold. These second-order folds form an echelon pattern and trend northwest-southeast at an acute angle to the generally east-west trending first-order fold. Third-order folds of an even smaller scale (approximately one kilometer in length) are superimposed on the second-order folds of the Gable Butte-Gable Mountain segment.

The most easterly segment of the structural trend, the Southeast anticline segment (Figure 2.5-16), is buried beneath Ringold Formation and younger sediments. This segment is separated from the Gable Butte-Gable Mountain segment by a topographic saddle and extends 2 kilometers to the northwest of the eastern end of the Gable Butte-Gable Mountain segment (Weston Geophysical, 1981). In contrast to the Gable Butte-Gable Mountain segment, the Southeast



anticline trends northwest-southeast for most of its length. Near its southeastern end, its trend turns toward the east.

The three first-order anticlinal segments forming Umtanum Ridge extend from the vicinity of Vernita Bridge northwestward to the margin of the Columbia Plateau (Figure 2.5-16). Umtanum Ridge is separated from the Hansen Creek anticline to the north by the Wahluke syncline and separated from the Yakima Ridge anticline to the south by the Cold Creek syncline. The distance from the WNP 1-2-4 site to the nearest surface expression of the Umtanum anticline is about 35 kilometers.

The eastern segment of Umtanum Ridge is an asymmetric first-order fold overturned to the north with a south-dipping fault (Umtanum fault) along its northern margin (Price, 1980; Goff, 1981; and Golder Associates, 1981a). This segment extends 31 kilometers from Vernita Bridge on the east to Hog Ranch Buttes on the west. The central segment of Umtanum Ridge extends 29 kilometers farther west and is overturned to the south in an asymmetric fold structure with a north-dipping reverse fault along its southern margin (Bentley, 1977). Vergence of the fold is again to the north from the Yakima River westward along the 40-kilometers-long western segment, which passes into a series of complex folds and dies out west of Bald Mountain (Figure 2.5-16).

The eastern segment of Umtanum Ridge is a concentric, non-cylindrical anticline in brittle basalt layers (Price, 1981a; Goff, 1981; and Golder Associates, 1981a). This fold is broken along its north limb by three (possibly four) east-west trending reverse faults: the Umtanum fault, the upper reverse fault (Buck thrust), the north reverse fault, and a possible unnamed reverse fault lying between the Umtanum and north reverse faults (Golder Associates, 1981a).

The Umtanum fault (Golder Associates, 1981a) separates overturned, generally south-dipping Grande Ronde and Wanapum Basalt flows in the hanging wall from more gently dipping Grande Ronde and Wanapum basalt flows in a lower imbricate thrust wedge which is bounded on the north by the north reverse fault. The Umtanum fault, which dips  $30^{\circ}$  to  $40^{\circ}$  south based on drilling data, is structurally analogous to a south-dipping ( $20^{\circ}$  to  $40^{\circ}$ ) reverse fault exposed by the Yakima River where it cuts through the western segment of Umtanum Ridge (Washington Public Power Supply System, 1977h; Bentley, 1977; Price, 1981a).

The upper reverse fault (Golder Associates, 1981a) and the Buck thrust (Price, 1980) form a discontinuous zone of thrust faulting which dips gently to the south in the hinge area of the first-order anticlinal fold near Priest Rapids Dam. Basalt flows are steeply north-dipping to overturned in the footwall of this thrust; flows in the hanging wall dip gently south. Price (1981a) described the Buck thrust as a zone of faulting where the gently dipping south limb of the anticline has locally overridden the steeply dipping north limb in the hinge area of the fold.

The existence of the north reverse fault (Golder Associates, 1981a) is indicated by a repeated sequence of Wanapum basalt flows, and the possible fourth unnamed reverse fault is inferred from stratigraphic relationships and structural attitudes at either end of its mapped trace. Both faults are inferred to dip south based on stratigraphic relationships, which indicate overthrusting of units to the north along their concealed traces, and based on their apparent imbricate relationship to the south-dipping Umtanum fault.

A fifth northeast-southwest trending fault (Golder Associates, 1981a), referred to as the Twin fault by Bentley and shown on the Regional Map, Sheet 4 in Rockwell (1979), is inferred along the southeast margin of a large landslide complex east of Filey Road. It is a minor fault formed by differential folding in the hinge area of the first-order fold forming the eastern segment of Umtanum Ridge.

The Umtanum fault and other east-west trending reverse faults are inferred to be products of fold deformation in a north-south compressional stress regime (Golder Associates, 1981a). Horizontal shortening within the eastern segment of the Umtanum Ridge fold appears to have caused low-angle reverse faults to propagate in the direction of overturning from the core of the fold toward the ground surface at the base of the north limb. The Umtanum fault is inferred to have relatively shallow dip of  $30^{\circ}$  to  $40^{\circ}$  south based on: (1) drilling data (Golder Associates, 1981a); (2) geologic mapping, which indicates a subhorizontal to gently north-dipping fault attitude near Sourdough Canyon and, thus, a relatively shallow dip for the fault within the core of the fold (Golder Associates, 1981a); and (3) the structural similarities between the Umtanum fault and the fault observed to dip  $20^{\circ}$  to  $40^{\circ}$  south in the western segment of Umtanum Ridge.

This inferred low dip angle is compatible with the hypothesis that the Umtanum fault grew from the core of the anticline in response to progressively tighter folding and



that faulting is a direct result of folding in this structure. On this basis, maximum fault lengths should be no longer than the lengths of individual segments of Umtanum Ridge. Fault widths (down-slip lengths) should not extend much deeper than the core of the fold and, at a maximum, should be no wider than the width of the fold itself. None of the mapped faults in the eastern segment of Umtanum Ridge appear to displace Quaternary deposits or apparently old geomorphic surfaces (Golder Associates, 1981a).

#### 2.5.1.2.4.3 Gable Mountain

Gable Mountain and Gable Butte are topographically isolated anticlinal ridges of basalt and interbedded sediments that form the only bedrock outcrops in the central Pasco Basin. These ridges are underlain by three prominent second-order folds, two on Gable Mountain and one underlying Gable Butte (Golder Associates, 1981b). These second-order folds are superimposed on the first-order fold forming the Gable Butte-Gable Mountain segment of the Umtanum Ridge-Gable Mountain structural trend (Golder Associates, 1981b). This segment of the structural trend is flanked by the Wahluke syncline to the north and Cold Creek syncline to the south. Minor third-order folds have been mapped on the flanks of the second-order folds where basalt crops out on Gable Mountain and Gable Butte.

Portions of Gable Mountain and Gable Butte have been mapped by Newcomb and others (1972), Bingham and others (1970), Washington Public Power Supply System (1974), Brooks (1974), and Fecht (1978). Three faults (the central, south, and west faults) have been mapped on Gable Mountain, and a fourth (the north-dipping reverse fault) was encountered in drill holes on the south side of the mountain (Golder Associates, 1981b). Two other faults were encountered in drill hole DB-10 2 kilometers south of the mountain. Structural relationships and faulting on and near Gable Mountain are discussed in detail (Golder Associates, 1981b).

#### Central Fault

The central and south faults on Gable Mountain were originally mapped as a single, curvilinear structure (Bingham and others, 1970; Newcomb and others, 1972; Fecht, 1978), which separated the oppositely verging east and west anticlines. However, more recent work has shown the south fault to be a separate structure and not connected to the central fault.

The central fault (Golder Associates, 1981b) on Gable Mountain is a northeast-trending, south-dipping reverse fault which dies out into the east Gable Mountain anticline at its northeastern end. It varies in strike from N55°E near its northern end to N45°E along the central section of the fault. The dip increases from 26° south to approximately 50° south along this same portion of the fault. Farther south, drilling data indicate that displacement on the central fault also decreases to the southwest and that its strike becomes more westerly (N71°E) near its intersection with the west anticline. Movement is assessed to be primarily dip-slip on the basis of striae orientations observed in fault gouge and clastic dikes and the absence of any features indicating lateral offset. Cumulative dip-slip displacement was measured to be approximately 200 feet near the central portion of this fault, and long-term displacement rates calculated for the central fault are very low ( $2 \times 10^{-4}$  inches/year).

The change in trend and the decrease in displacement at both ends of the central fault indicate that it displays similar structural characteristics at opposite ends (Golder Associates, 1981b). North-south to northeast-southwest compression produced the second-order east and west anticlines with which the fault is associated, and thrusting of hanging-wall rocks to the north-northwest on the central fault plane is compatible with this general sense of north-south crustal shortening. The central fault is inferred to be a tear fault which developed to accommodate differential movement resulting from interference between growth of the east anticline to the northwest and growth of the west anticline to the southeast. The overall length of the central fault is inferred to be 3 kilometers or less (measured from where it is inferred to die out to the southwest in the axis of the west anticline to its termination in the hinge area of the east anticline).

The central fault displaces glaciofluvial deposits and clastic dikes derived from these deposits along an 1100-foot interval of the fault trace at its northern end (Golder Associates, 1981b). These displacements are small (0.2 foot) reverse offsets at the base of the glaciofluvial deposits which do not extend into the upper part of the sequence. However, minor shears and fractures subparallel to the central fault plane extend into the glaciofluvial deposits where the displacements occur. Associated, minor normal displacements (0.3 foot) also occur in the hanging wall at one location. Clastic dikes parallel to the fault



September 1981

plane are internally slickensided with striae plunging down the dip of the fault plane. However, no measurable displacement of the clastic dikes was detected.

Glaciofluvial deposits overlying the central fault (and the south fault) and clastic dikes derived from these deposits are assessed to be at least 13,000 years old based on the presence of Mount St. Helens "S" ash near the top of the flood deposit sequence, but no older than 13,000 to 19,000 years on the basis of their probable correlation with similar glaciofluvial deposits elsewhere in the Pasco Basin (Golder Associates, 1981c). Thus, the displacement at the base of these deposits over the central fault is assessed to be no more than 19,000 years old.

#### South Fault

The south fault (Golder Associates, 1981b) is a reverse fault which strikes nearly east-west and dips southward  $25^{\circ}$  to  $54^{\circ}$  (Golder Associates, 1981b). This fault dies out to the east along strike, and stratigraphic throw has been less than 40 feet where the south fault is exposed in trenches. Drilling data show the south fault confined to the hanging wall of the north-dipping reverse fault. The south fault is inferred to be present in the subsurface for a distance of at least 1700 feet to the west of where it dies out at its eastern end (Golder Associates, 1981b). However, based on its apparent confinement to the hanging wall of the north-dipping reverse fault, the south fault (like the north-dipping reverse fault discussed below) can be no longer than 6 kilometers, the approximate length of the west anticline.

Recent trenching (Golder Associates, 1981b) exposed unfaulted glaciofluvial deposits overlying the south fault, and Bingham and others (1970) also reported glaciofluvial deposits to be undisplaced in earlier trench investigations of the south fault. However, some trenches across this fault exposed slickensides and striations on some clastic dikes present along the fault plane. Striations on polished surfaces within the dike material plunge parallel to the dip of the fault. This dike material is believed to be derived from overlying glaciofluvial sediments. These sediments were interpreted to be 40,000 years old (Bingham and others, 1970) on the basis of radiocarbon dating of wood fragments taken from the sediments. However, comparison of these sediments with other glaciofluvial sediments in the Pasco Basin suggests that they are correlative with Missoula flood deposits and are, therefore, probably 13,000 to 19,000 years

in age. The presence of these slickensides within the clastic dikes suggests very minor dip-slip displacement on the south fault since dike emplacement.

#### North-Dipping Reverse Fault

The north-dipping reverse fault (Golder Associates, 1981b) has been traced in drill holes for approximately 2000 feet along the southern flank of the west Gable Mountain anticline (Golder Associates, 1981b). This fault strikes N63°W and dips 13° north at the eastern limit of its mapped trace. Minimum stratigraphic throw on the fault is 140 feet in this same area. Farther west, stratigraphic throw on this fault has been approximately 320 feet, and it strikes N72°E and dips 19° north. Both the north-dipping reverse fault and the south fault are compatible with north-south crustal shortening and folding of the Gable Mountain structure. The apparent structural position of the north-dipping reverse fault in the west anticline is compatible with the generation of thrust faulting from the core of a fold in brittle rock layers where movement of the hanging wall is in the direction of fold vergence (to the south). This interpretation is similar to the interpretation of the relationship between faulting and folding along the eastern segment of Umtanum Ridge (Price, 1981a; Golder Associates, 1981b). The south fault is inferred to be a minor structure in the hanging wall of the north-dipping reverse fault near the eastern end of the west anticline. The approximate length of the west anticline is 6 kilometers, and thus, both the north-dipping reverse fault and south fault are inferred to be no longer than 6 kilometers.

#### West Fault

The west fault (Golder Associates, 1981b) is a minor tear fault in the hinge area of the west anticline on Gable Mountain caused by differential folding along the anticlinal axis. Rocks to the west of the fault have been more sharply folded than rocks to the east, thus producing the normal displacement observed in trenches. It is a normal fault, which strikes N34°E and dips steeply west (55° or more) with less than 15 feet of stratigraphic throw. Maximum displacement is toward the hinge area of the fold, which in this case has been removed by erosion along the southwest flank of Gable Mountain. Within a distance of 200 feet of its exposure near the crest of the west anticline, faulting dies out rapidly to the northeast along the strike in the gently-dipping northern limb of the anticline. Total length



of the fault is 1 kilometer (measured from the approximate location of the hinge area to where the fault dies out to the northeast along the strike).

#### Upper DB-10 Fault

Core hole DB-10 (Rockwell, 1979) penetrated two faults approximately 2 kilometer south of Gable Mountain. Investigations have shown that the upper of these two faults is confined to the width of a buried second-order anticline and not structurally connected to other faults in the Gable Mountain area. This conclusion is based on geophysical data (Weston Geophysical, 1981) and fault attitudes determined from drill hole data (Golder Associates, 1981b). The upper DB-10 fault strikes almost due north-south and dips  $25^{\circ}$  to  $45^{\circ}$  west. The length of the upper DB-10 fault is estimated to be a kilometer based on seismic refraction data (Weston Geophysical, 1981). The upper DB-10 fault appears to be a minor fault in the hinge area of a second-order anticline on the basis of its limited length (1 kilometer) and stratigraphic throw (approximately 165 feet).

#### 2.5.1.2.4.4 Rattlesnake-Wallula Alignment

The Rattlesnake-Wallula alignment is part of a topographic and structural alignment that trends northwest from near Milton-Freewater, Oregon, to the northwest end of the Rattlesnake Mountain (Figure 2.5-18). This feature is expressed by an alignment of topographically defined anticlines between Wallula Gap and Horsethief Point (Rattlesnake-Wallula alignment) and by the alignment of parallel and subparallel linear structural features from Wallula Gap south-eastward. The axis of this alignment approaches to within 20 kilometers southwest of the WNP 1-2-4 site.

The Rattlesnake-Wallula alignment between the Yakima River and Wallula Gap is defined by a series of ten elongate (northwest-southeast) hills. These hills appear as distinct, subparallel, doubly-plunging anticlines generally aligned along a  $N50-60^{\circ}W$  trend. The folds are commonly overlain by loess above elevations of 1000 feet, and by undifferentiated loess and Touchet beds below this elevation. Basalt bedrock crops out generally near the crest of the hills. The flanks are mantled by colluvium and silt.

The part of the Rattlesnake-Wallula alignment that is mapped from Badger Coulee northwestward to the Yakima River (Figure 2.5-18) contains four discontinuous, sub-parallel, doubly-

plunging anticlines generally aligned along a N50°W trend. From southeast to northwest the structures include O-Hill, southeast of Badger Mountain, Badger Mountain, an unnamed mountain northwest of Badger Mountain, and Red Mountain.

These anticlines are structurally similar. The northeast limbs generally dip slightly more steeply than the topographic slope and somewhat less steeply than the southwest limbs. The axes of the individual folds generally parallel the overall Rattlesnake-Wallula alignment. The Umatilla, Priest Rapids and Roza basalts are locally exposed in the core of the folds, while the Pomona, Elephant Mountain-Ward Gap, and Ice Harbor flows are widespread.

The structure continues from the Yakima River gap northwestward to the north end of Rattlesnake Mountain (Figure 2.5-18), where it adjoins the east trending section of Rattlesnake Hills. Rattlesnake Mountain is a box-shaped anticline with an over-steepened north limb along much of its length. A thrust fault or high angle, reverse fault has been interpreted to exist along the steep, northern limb (Rockwell, 1979).

On the basis of remote sensing analysis, recent faulting does not appear to have occurred along the Rattlesnake segment of the alignment as indicated by a lack of scarps across the abandoned Yakima River channel at Vista. The Rattlesnake anticline cannot be traced as a single continuous structure beyond Snively Ranch.

The following sections include discussions of the Rattlesnake-Wallula alignment, by geographic or structural section, commencing with the Rattlesnake Mountain area at the northwestern extent of the alignment.

#### 2.5.1.2.4.4.1 Rattlesnake Hills and Rattlesnake Mountain Anticlines

In the area of Rattlesnake Mountain, the east-west Rattlesnake Hills anticline changes direction and merges with the northwest trending section of the Rattlesnake-Wallula alignment (Figures 2.5-18 and 2.5-19). The Rattlesnake Hills Anticline (Figure 2.5-18) extends from the north end of Rattlesnake Mountain westward to Horsethief Point (Section 11, T12N, R23E). The Rattlesnake Hills alignment in this area is defined by the sinuous, east-west trending anticline. The anticline is asymmetrical with dips of 2 to 10° on the south flank and dips of 10 to 25° on the north flank.

The structure of this segment from the Yakima River to the northwest end of Rattlesnake Mountain is described primarily as a box-shaped anticline with an oversteepened north limb along most of its length (Rockwell, 1979). The central part of the anticline is breached and is estimated to have 3000 feet of structural relief. About 2 kilometers northwest of the Yakima River, the anticline plunges gently to the southeast and dies out on the flank of a northeast trending, southeast dipping monocline.

Known faulting in this area is confined to the western portion of the Rattlesnake Hills anticline. The 3926 fault is a 4 kilometer long, north-south striking, vertical scissor fault located in Sec. 8, T11N, R24E, (Rockwell, 1979). The western side of the fault is up and juxtaposes Pomona against Priest Rapids flows with an estimated 300 feet of vertical displacement. The Maiden Spring fault occurs about 2 kilometers south of the axis of the Rattlesnake Hills anticline, is parallel to it for about 2 kilometers in Sec. 18, T11N, R24E, and appears to connect with the southern end of the 3926 fault (Figure 2.5-18). It is a high angle, north dipping, reverse fault that juxtaposes Elephant Mountain and Umatilla flows; with up to 200 feet of displacement. The Rattlesnake Hills anticline at the west end (Horsethief Point), is a structurally complex area that includes several folds and an unnamed high angle fault that juxtaposes Elephant Mountain and Umatilla flows. Much of the structure of the eastern portion in the Horsethief Point area is hidden by landslide debris of the Snively Basin and by extensive loess cover.

Faulting along Rattlesnake Mountain apparently occurs along the northeastern limb of the anticline (Figure 2.5-18). This steeply dipping fault is interpreted as a reverse fault (Washington Public Power Supply System, 1977k; Rockwell, 1979). Displacement is estimated to be 1,300 feet (Rockwell, 1979). The fault is inferred to be about 7 kilometers in length. Two kilometers to the northwest and on the projection of the Rattlesnake Mountain fault, a south dipping thrust fault has been inferred by Rockwell (1979). Neither the Rattlesnake Mountain fault nor the thrust fault appear to displace mapped Quaternary units.

#### 2.5.1.2.4.4.2 Red Mountain

Red Mountain is a doubly plunging anticline about 6 kilometers in length located southeast of the Rattlesnake Mountain anticline and on a line with the Rattlesnake-Wallula structural trend. Its northeastern limb dips more steeply than its southwestern limb. Pomona basalt is

exposed in its core. A fault has been mapped near the axis of the fold in Section 4. The fault strikes approximately N55°W; the dip is unknown. The fault juxtaposes Pomona to the southwest against Ice Harbor and Elephant Mountain to the northeast. Detailed mapping shows the axis of the Red Mountain anticline trends between N50°W and N60°W. The Rattlesnake-Wallula trend in the vicinity of Red Mountain is approximately N50°W. Several warped, abandoned stream channels and terraces suggest that to the north of Red Mountain the only Quaternary deformation has been a gentle warping.

#### 2.5.1.2.4.4.3 Badger Mountain

In the area between the Yakima River and Badger Coulee, there are four structurally similar anticlines. Their southwest limbs generally dip slightly steeper than the topographic slope and somewhat less steep than the northeast limbs. The axes of the individual folds are subparallel to the overall Rattlesnake-Wallula alignment. The Umatilla, Priest Rapids and Roza basalts are locally exposed in the cores of the folds, while the Pomona, Elephant Mountain-Ward Gap, and Ice Harbor flows are widespread.

Badger Mountain is defined as the three doubly plunging anticlines between the mouth of Badger Coulee at Vista and Red Mountain. The southernmost of these folds is called O-Hill, the central is called Middle Badger Mountain, and the north hill is unnamed.

The Badger Mountain fault is a northwest-striking fault that Bond and others (1978) and Rockwell (1979) inferred to extend from O-Hill to the southern end of the unnamed hill northwest of Middle Badger Mountain. Where the existence and location of the fault are constrained, no evidence of Quaternary displacement has been observed.

Mapping of O-Hill (Woodward-Clyde Consultants, 1981c) shows no persuasive evidence for faulting. Mapping of the Middle Badger Mountain (Woodward-Clyde Consultants, 1981c) shows a fault at approximately the position shown by Rockwell (1979). The fault juxtaposes Roza to the southwest against Pomona to the northeast. Exposures are inadequate to confidently assess the total length of the fault, however, existing exposures suggest the fault is confined within the dome.

## 2.5.1.2.4.4.4 N-Hill/M-Hill

N-Hill and M-Hill are tightly folded, doubly plunging anticlines. On N-Hill the Pomona member is brecciated over a horizontal distance of at least 1200 feet. The brecciated Pomona is overlain by Elephant Mountain member and underlain by a thin conglomerate. The conglomerate contains well rounded clasts of basalt and metamorphics that are up to 5 to 6 inches in diameter. These clasts are enclosed in a feldspathic-sandstone matrix. The presence of a conglomerate, which is probably fluvial in origin, beneath the brecciated part of the Pomona suggests the breccia was produced by phreatic effects when the basalt flow entered water (Figure 2.5-21). No faults have been detected on M-Hill.

## 2.5.1.2.4.4.5 L-Hill

L-Hill is topographically the smallest hill of the Rattlesnake-Wallula alignment. Although exposures are not adequate to fully define the structural relationships in the area, L-Hill is probably the southeastern continuation of the plunging nose of M-Hill. Several 2- to 5-inch wide north-dipping normal faults in the Umatilla basalt are exposed in quarries. Down-dip striae are present along these faults (Table 1, Appendix 2.5-N). These minor faults are cross-cut by clastic dikes that are not offset.

## 2.5.1.2.4.4.6 K-Hill

K-Hill, also known as Game Farm Hill, is a doubly-plunging anticline. Jones and Landon (1978) mapped a 1 kilometer long fault (Game Farm Hill fault) along the south flank of the anticline. A second fault is prominently exposed in a quarry at the southeastern end of the hill. Sub-horizontal striae are prominently developed along the fault (Table 1, Appendix 2.5-N). Shear zones in the quarry are cross-cut by clastic dikes that show no fault displacements.

## 2.5.1.2.4.4.7 The Butte

The Butte is a faulted monoclinial structure. The northeast limb dips steeply to the northeast and is separated from nearly horizontal units to the southwest by a northwest-striking fault zone. Locally, units to the southwest of the zone dip gently to the southwest. The fault zone is exposed in Finley Quarry where it consists of three traces that cut Columbia River Basalt and younger alluvial sediments. The northern and middle faults displace older alluvial sediments but do not displace an alluvial unit that is estimated to be

at least 125,000 years old. The southernmost fault juxtaposes Pomona against Umatilla. It is overlain by, and does not displace, Holocene loess and colluvium. The fault striae within the zone vary from horizontal to down-dip in orientation. Mapping by Woodward-Clyde Consultants (1981c) has extended the Finley Quarry Fault for slightly more than 2 kilometers to the southeast. Its southeastern terminus has not been defined. The Finley Quarry fault lies along the projected trend of the Wallula fault zone (Shannon and Wilson, 1979; 1980).

#### 2.5.1.2.4.4.8 Molly Hill

Molly Hill is a northwest trending doubly plunging anticline with a faulted northeast limb. The fault strikes approximately N60W. Offset is interpreted to be less than 100 feet (Jones and Landon, 1978). This fault may be related to the Finley Quarry fault (Jones and Landon, 1978), and it is implied to be the northwest extension of the Wallula fault zone (Shannon and Wilson, 1979a; Washington Public Power Supply System, 1977m) described below.

#### 2.5.1.2.4.4.9 Kennewick, Horn Rapids, Cold Creek Lineaments

The Kennewick, Horn Rapids, and Cold Creek lineaments are subparallel to the Rattlesnake-Wallula lineament from the vicinity of Wallula Gap to near the east end of Yakima Ridge (Figures 2.5-18 and 2.5-21). It can be seen on topographic maps, aerial photographs, LANDSAT imagery, and on various geologic maps.

The Kennewick and Cold Creek lineaments were recognized and described by Glass (Washington Public Power Supply System, 1977o) as follows:

The Kennewick lineament parallels the Rattlesnake structure from Wallula Gap to approximately Kennewick. The lineament is characterized by an abrupt vegetation contrast and an east-facing break in slope (Figure 2R K-15 of Washington Public Power Supply System, 1977o). A number of factors have led me to interpret this feature as a terrace. At its northern end the Kennewick lineament turns to the northeast and joins several similar features originating to the west and northwest. At its southern end the lineament gradually (sic) decreases in height and cannot be followed south of Finley. Several older terraces appear upslope to the west of the Kennewick lineament and trend roughly parallel to it. The Cold Creek lineament extends from Columbia Camp to beyond Benson Ranch (Figure 2R K-24,

Sheet 2 of Washington Public Power Supply System, 1977o). The lineament is eminently detectable on LANDSAT imagery and parallels the Rattlesnake structure.

Glass in Washington Public Power Supply System (1977o) describes the lineament as paralleling the Rattlesnake trend, but about 2 kilometers east of it, and as being formed by a 6 to 9 foot-high topographic break combined with a striking contrast in vegetation. He also noted several ponds resembling sag ponds along the lineament's trend and suggested the lineament may extend onto the Hanford Reservation in the vicinity of Cold Creek.

Although the lineament may appear to be a single, continuous feature on high-altitude imagery or on larger-scale topographic maps, detailed analysis shows that it actually consists of three distinct, nonaligned segments, each having its own peculiar geomorphic, geologic, and geographic limits.

The Cold Creek lineament consists of two features. The first is the Cold Creek valley, a topographically low linear area parallel to Rattlesnake Mountain. The second feature is the low scarp, seen along the west side of the valley near the confluence with the Yakima River. This feature was probably produced by the lateral planation of Cold Creek. Both of these features are probably post-Wisconsin in age.

The Horn Rapids lineament consists of a series of six low hills trending about N35°W along the southwest side of the Yakima River to just north of Horn Rapids (Jones and Deacon, 1966; and Washington Public Power Supply System, 1974). The hills consist of shallow dipping flows of the Elephant Mountain and Ice Harbor members of the Saddle Mountains Basalt mantled by glaciofluvial deposits (Figure 2.5-18). This group of low, basaltic hills is interpreted to be a series of low amplitude folds subparallel to the Rattlesnake-Wallula alignment. These hills have been modified by the plucking action of Spokane flood waters and subsequently nearly buried under glaciofluvial deposits.

The Kennewick Lineament is a distinct feature on topographic maps and can be plainly seen as a slope break and vegetative change on aerial photographs (Figures 2R K-12 and 2R K-15 of Washington Public Power Supply System, 1977o) as well as on LANDSAT photos of the area. It is a portion of a broader pattern of terraces (Washington Public Power Supply System, 1977h).

The Kennewick lineament chiefly consists of the break in slope between terrace levels T<sub>3</sub> and T<sub>2</sub>, and was probably

produced as an erosional feature during one of the later episodes of Spokane flooding (Wisconsinan age) (Shannon and Wilson, 1980). The linear nature of the feature, although long and distinct, is not unique among erosional or depositional features produced by Spokane flooding. For example, between Umatilla and Boardman Junction in Oregon, a 400 foot-terrace can be traced as a near-straightline feature for about 18 kilometers, while in the Portland, Oregon area a 200 foot-terrace can be traced for about 10 kilometers. Thus, it appears that the Kennewick lineament may represent a streamlined erosional feature produced by flood waters rushing toward Wallula Gap. The dramatic, vegetational change along the lineament coincides with the proximity of groundwater to the surface. In fact, the ponding of spring water issuing from the gravel near the base of the break in slope between terrace  $T_2$  and  $T_3$  was noted by Glass in Washington Public Power Supply System (1977o), who originally thought they might be sag ponds. Ponding appears to be caused in part by the pervious lining of the irrigation ditch, which parallels the break in slope. The possibility of right-lateral motion along this trend was hypothesized and then discarded by Glass in Washington Public Power Supply System (1977o), Figures 2R K-10 and 2R K-11.

According to Glass' interpretation given above, the Kennewick lineament would have been produced in late Wisconsin time. Alluvial fans produced since that time, by sidestreams debouching onto terrace  $T_2$ , show no features that can be considered part of the alignment. No surficial evidence could be found for either horizontal or vertical movement along the Kennewick-Cold Creek lineament.

#### 2.5.1.2.4.5 Wallula Fault Zone

The Wallula fault zone (Figure 2.5-21) extends southeastward from slightly west of Wallula Gap to the vicinity of Milton-Freewater, Oregon (Shannon and Wilson, 1979a). This zone has clear topographic expression from Wallula Gap southeastward to a point about 3 kilometers east of Warm Springs Canyon. Beyond this point the fault zone is covered by the Touchet Beds of glacial age (approximately 13,000 y.b.p.) and is not clearly defined (Shannon and Wilson, 1979a).

Near Wallula Gap, the Wallula fault zone may consist of two major strands. The northern inferred strand may continue to the doubly-plunging anticlines and domes of the Rattlesnake-Wallula alignment. Bingham and others (1970) first proposed this link between the Wallula fault zone and the



doubly-plunging folds. This link has not been verified because of a lack of bedrock exposures between Molly Hill and the inferred junction of the two strands. Additional discussion of the connection between the Wallula fault zone and the Rattlesnake-Wallula alignment is contained in Appendix 2.5-N.

The southern strand is the Wallula Gap fault (Jones and Deacon, 1966). West of Yellepit the terminus of the fault is in dispute (Farooqui in Washington Public Power Supply System, 1977i; Shannon and Wilson, 1979a; Foundation Sciences, 1980). A trench excavated across the Wallula Gap fault near Yellepit (see Washington Public Power Supply System, 1977i) revealed that the fault does not displace the Kennewick fanglomerate. Uranium-Thorium age dates on caliche deposited on the fanglomerate indicate that the fanglomerate is at least 20,000 years old (personal communication Dr. T. L. Ku to J. Black of Woodward-Clyde Consultants). In the Yellepit trench both vertical and horizontal striations were observed; the former were prominent.

The Wallula Gap fault is not exposed between Wallula Gap and a point immediately west of Vansycle Canyon. Its presence is inferred from zones of tectonic breccia and a series of faceted spurs. Approximately 4 kilometers east of Wallula Gap, the Wallula Gap fault may merge with the inferred northern strand and continue southeastward across Vansycle Canyon to the vicinity of Warm Springs Canyon. Scarp-like features along the fault appear at the mouth of Vansycle Canyon but appear not to displace recent alluvium. Aerial photo analysis of the Wallula Gap fault indicates that it does not appear to be active (Glass, in Washington Public Power Supply System, 1977o). Most striae measured from within tectonic breccias along the trace of the Wallula fault trend approximately perpendicular to the strike of the fault.

Bingham and others (1970), while investigating this segment of the Wallula fault zone, observed a youthful, curved linear feature they interpreted to be the result of recent faulting. Trenching across this linear feature in 1981 by Woodward-Clyde Consultants does not confirm the conclusions of Bingham and others (1970). Although minor displacements associated with clastic dikes in the Touchet deposits were exposed in these trenches, continuous strata (including the Mount St. Helens "S" ash) across the lineament zone indicate the absence of post-Touchet faulting having enough vertical displacement to account for the topographic relief (locally as much as about 3 feet) associated with the lineament.

In the Warm Springs area, mapping, trenching and geophysical studies have defined a complicated zone of faulting that displaces pre-Touchet colluvium of probable Quaternary age. Two prominent fault strands dip steeply to the south and exhibit sub-horizontal fault striae. Discussions of this zone can be found in Shannon and Wilson (1979a) and Woodward-Clyde Consultants (1981c).

Approximately 3 kilometers east of Warm Springs canyon, the Wallula fault zone is concealed by Touchet deposits and cannot be clearly defined to the southeast (Shannon and Wilson, 1979a). Although the topographically-defined trace of the fault zone becomes indistinct, the continued presence of northwest-striking faults in the hills to the south of the fault zone as far east as Milton-Freewater implies an extension of the Wallula fault zone into that region. Because of extensive surficial cover, neither these en echelon fault planes nor their intersections with the Wallula fault are exposed. The geometry of the escarpments produced by these en echelon faults shows that the displacement decreases to the southeast.

In the area of the Walla Walla Basin the location of the Wallula fault zone is uncertain but several occurrences of faulting have been identified. South of Umapine, Oregon, north-dipping ( $30^{\circ}$  to  $60^{\circ}$ ) faults of tectonic or slump origin displace Touchet beds and cross-cutting clastic dikes having maximum offset of 1.5 feet (Shannon and Wilson, 1979b). Faulting 10 kilometers southeast of the Umapine locality is suspected by Shannon and Wilson (1979b) but not demonstrated.

Two other Quaternary fault localities are the Buroker thrust fault east of Walla Walla and the Little Dry Creek fault south of Milton-Freewater. The base of the Pleistocene Palouse Formation is offset approximately three feet along the former fault, a west-dipping ( $26^{\circ}$ ) reverse fault that strikes north-south. Loess deposits (Holocene?) overlying the Palouse appear to be unfaulted (Shannon and Wilson, 1980). Near Little Dry Creek, basalt and Palouse soil are downdropped about 1.5 feet along a steep ( $75^{\circ}$ ) northwest-striking, northeast dipping fault. This fault lies south of the eastward projection of the Wallula fault zone and is not in alignment with it.

The southern extent of the Wallula fault zone could be inferred to extend along the South Fork of the Walla Walla River to the southeast of Milton-Freewater. Raisz (1945) believed that the South Fork of the Walla Walla River formed part of the Olympic-Wallowa lineament which continues



southeasterly across the Blue Mountains to the Wallowa Mountains and which is coincident with the Wallula fault zone northwest of Milton-Freewater. However, mapping by D. Swanson (U.S.G.S., unpublished), by Shannon and Wilson (1979b), and by R. Dale and J. Kendall (Kendall and others, 1981) has demonstrated the continuity of major vertical faults (including the Hite fault) and the west-dipping dikes of Frenchman Springs basalt across the South Fork of the Walla Walla River. Thus, the Wallula fault zone can continue no farther southeastward than the Milton-Freewater, Oregon area.

#### 2.5.1.2.5 Olympic-Wallowa Lineament

The Olympic-Wallowa lineament (OWL), originally postulated by Raisz (1945) as a northwest-trending alignment of topographic features between the Olympic Peninsula, Washington, and the Wallowa Mountains, Oregon, is a cryptic feature of Pacific Northwest geology that may have bearing on the tectonic history of the Columbia Plateau. Raisz believed that the lineament was probably fault-controlled, but he stated (1945, p. 483) "that in most places the lineament is rather a zone than a line, with many parallel ridges and splinters...(p. 484) it appears to be a more complex structural line than a simple fault. It may have started as a transcurrent fault, but the line of weakness thus created probably suffered further dislocation." His reference to transcurrent faulting alludes to his perception from physiographic relations that both the crests of the Cascades and the Blue Mountains have been offset along the lineament for about 10 kilometers -- in a left-lateral sense..

Skehan (1965) suggested that the lineament may mark a fundamental boundary in the continent between former oceanic crust to the south and older continental crust to the north. Davis (in Washington Public Power Supply System, 1977a) proposed that the basement for much of the Columbia Plateau on both sides of the lineament is Mesozoic oceanic crust and associated sedimentary rocks, accreted to the continent prior to the Cenozoic era. His conclusion is generally supported by Hill's 1972 interpretations that the crust beneath the plateau is: 1) thinner than that of the granitic-metamorphic terrane of northern Washington by as much as 12 kilometers, or 2) that it has an average P-wave velocity as much as 0.8 kilometer/sec higher than that terrane, or 3) that some combination of 1) and 2) prevails. In 1980, however, Hill concluded that the crust beneath the Pasco Basin is indeed thin (ca. 24 kilometers minimum), but that it has a low P-wave velocity (ca. 6.1 kilometers/sec.). This low velocity, if valid, is difficult

to reconcile with an accreted basement of oceanic character. As an alternative, Laubscher (Appendix 2.5-O) has proposed that the basement is genuinely continental, but was thinned during early Tertiary regional doming -- expression of the doming and resultant crustal thinning is represented by the Eocene grabens of the northern Cascades and Okanogan terranes. He ascribed thinning of the crust to the combined consequences of east-west stretching, subareal erosion of the crest of the dome, and subcrustal "erosion" by processes unknown. Davis (Appendix 2.5-N) still believes that exposures of ophiolitic rocks and associated marine sediments north (Ingalls' ophiolite of Washington Cascades) and west (Rimrock Lake) of the plateau imply an accreted, oceanic basement beneath central areas of the plateau.

Recent geophysical studies support both Davis' (Washington Public Power Supply System, 1977a) and Laubscher's (Appendix 2.5-O) contentions that the crust below the plateau does not change across OWL. No evidence is seen in a recently compiled total Bouguer gravity anomaly map of the Columbia Plateau (1:500,000; c.i. = 4 mgal) (Figure 2.5-9, see Appendix 2.5L) that a change in basement rocks or crustal character occurs along the lineament. Furthermore, a pronounced gravity gradient separates the Yakima and Pasco Basins and trends north-south across OWL (see Appendix 2.5L). One edge of the causative body extends north-south with a density contrast that is positive with respect to the rocks toward the west. Because the contours are relatively straight, any faults striking between N45°W and S45°W that cross the gradient would have horizontal displacements less than 2-3 kilometers (Appendix 2.5L). This conclusion supports Laubscher's contention (Appendix 2.5-O) that any strike-slip displacement along Raisz's lineament (CLEW) must be less than 2 kilometers. The north-south gravity gradient referred to above is interpreted by Laubscher to delineate the western edge of a master north-south trending graben of Eocene age developed longitudinally along the crest of the regional dome he has postulated and by Weston Geophysical (Appendix 2.5L) to be related to the edge of a relatively dense rock mass which underlies the Columbia Plateau. This rock mass is interpreted to consist of extrusive rocks that filled an elongate subsiding basin.

A recent study (Systems, Science, and Software, 1980) to model the three-dimensional structure of crust and upper mantle beneath the Columbia Plateau utilized joint inversions of regional Bouguer gravity data and P-wave travel-time residuals for teleseismic events recorded at stations in eastern Washington. The joint inversion model

revealed no changes in crustal or mantle structure at depths greater than 10 kilometers coincident with the surface trace of OWL.

It thus seems unlikely that the Olympic-Wallowa lineament is a fundamental or profound crustal break, or that diffuse transcurrent displacement along its inferred plateau segment, if present, has been greater than a few kilometers since extrusion of the Miocene Columbia River basalts.

The northwest-trending northern margin of the Olympic Peninsula, the western end of the Olympic-Wallowa lineament, is controlled by the strike and steep dip of Eocene units on the northern flank of a major Miocene or younger antiform which plunges steeply eastward beneath Puget Sound. The prominent horseshoe-shaped outcrop pattern of the Eocene Crescent Volcanics around the northern, eastern, and southern margins of the Olympic Mountains defines this antiformal structure (Tabor and Cady, 1978b). A recent U.S.G.S. report on the geology of the Olympic Peninsula (Tabor and Cady, 1978b) does not refer to Raisz's speculations about an Olympic-Wallowa lineament, but does show high-angle faults along most of the valleys believed by Raisz to define his lineament. The faults generally parallel steeply inclined bedding within Eocene units and much of their traces are mapped as concealed beneath Quaternary glacial deposits. Although the displacement history of the faults is difficult to evaluate, they appear to be unlikely representatives of a hypothesized 644 kilometer-long fault zone -- a zone postulated in no small measure on their existence. There are no a priori reasons why structures related to the Olympic antiform should extend to the east of Puget Sound, and at present, no evidence that they do so.

Raisz believed that the easternmost segment of the lineament extended up the troughlike valley of the South Fork of the Walla Walla River and across the Blue Mountains to the Wallowa Mountains. However, mapping by D. Swanson, U.S.G.S. (unpublished), by Shannon and Wilson (1979b), and by R. Dale and J. Kendall (Kendall and others, 1981) has demonstrated the continuity of vertical major faults and west-dipping dikes across the South Fork of the Walla Walla River. It is, therefore, clear that this segment of the topographically defined Olympic-Wallowa lineament cannot be related to faulting in rocks of Miocene age.

Davis (in Washington Public Power Supply System, 1977a, p. 2RC-34) states that the Olympic-Wallowa lineament is "as originally defined a fictional structural element of the

Pacific Northwest." In 1981 Davis (Appendix 2.5-N) is still inclined to this view when the entire lineament postulated by Raisz is considered, but the existence of a disturbed plateau structural zone (including the Wallula fault zone) coincident with the central third of Raisz's lineament cannot be questioned. This is the CLEW zone of Laubscher (Appendix 2.5-O).

#### 2.5.1.2.6 Hazards

Actual or potential hazards or problems related to natural geologic features or to man's activities in the region and site vicinity have been assessed. It was determined that there are no potential hazards or problems to the site due to any of these phenomena.

##### 2.5.1.2.6.1 Volcanic Hazards

There are several major volcanoes in the Cascade Range west of the WNP1-2-4 site. The closest is Mount Adams about 164 kilometers distant; the most active is Mount St. Helens approximately 220 kilometers west-southwest of the site. Because most volcanic activity is confined to the immediate area of the volcano, mud flows, avalanches, pyroclastic rock flows, lava flows, and shock waves that may be associated with such activity do not pose a hazard to the site. The only potential hazard to the site is ash fall resulting from a major eruption of one of these volcanoes.

Several ash deposits have been detected in the Columbia Basin but only two are known to be present in the vicinity of the site. Although the ash falls may be widespread in extent, commonly they are not found everywhere owing to the nature of their depositional environment and to subsequent erosion. The oldest ash layer identified in the site vicinity occurs in the upper Touchet Beds. In the past, investigators have considered it to be a Glacier Peak ash with an age of approximately 12,000 y.b.p. (Brown, 1970). However, recent studies by the U.S.G.S. indicate that it may be from a Mount St. Helens eruption that occurred approximately 13,000 y.b.p. (Mullineaux and others, 1975). Glacier Peak ash has been positively identified in the vicinity of the site (Woodward-Clyde Consultants, 1981b), and localities in the Columbia Basin north and east of the site (Fryxell, 1965). The second ash identified in the site vicinity occurs locally interbedded and mixed with post-glacial eolian deposits that are stratigraphically above the Touchet beds. These ash deposits have been correlated with an ashfall from the eruption of Mount Mazama in Oregon that

occurred about 7,000 y.b.p. (Davis, 1978). None of the ash deposits, however, were noted during the geologic examinations of the WNP-2 or the WNP-1 and 4 excavations.

A period of renewed volcanic activity on Mount St. Helens began in late March 1980, climaxed in a major eruption on May 18, 1980, and resulted in about 1 mm of ash fall at the site over a 9-hour period. Lesser eruptions of steam and ash followed on May 25 and June 12, but prevailing winds carried the respective low level and low volume plumes northwestward and southwestward from the mountain.

The potential effects of a hypothetical, "worst-case" ash fall at the WNP 1-2-4 site were evaluated, utilizing relevant data from the Mount St. Helens eruptions and detailed studies made by Shannon & Wilson, (1976) for the Pebble Springs Nuclear Plant Site. The Pebble Springs site is located near Arlington, Oregon, approximately 105 kilometers southwest of the WNP1-2-4 site.

#### Potential Source of Volcanic Ash

There are ten major volcanic peaks of the Cascade Range (Figure 2.5-22). Even before the activity displayed by Mount St. Helens in 1980, several recent investigations, including those of Coombs (1974), Crandell (1973, 1976), Crandell and others (1975), and Crandell and Mullineaux (1976) concluded that essentially all the major Cascade volcanoes have a potential for future activity.

Despite the fact that some of the Cascade volcanoes have been active in the last several thousand years, and hence, all must be considered as having a potential for future activity, all are not equally likely to erupt large amounts of volcanic ash in the WNP-1-2-4 plant lifetimes. Of the volcanoes in the site region, only Mount St. Helens, Glacier Peak, and Mount Mazama have produced large volumes of volcanic ash during late Quaternary time. Based on past behavior, therefore, Mount St. Helens and Glacier Peak are the most likely sources of large ash eruption in the future. Although Mount Hood also could conceivably produce a major tephra eruption, its potential is considered to be much less than the other two. Thus, the nearest source of a major eruption of volcanic ash would be either Mount St. Helens or Mount Hood, both about 220 kilometers from the WNP 1-2-4 site. Although Mount Rainier and Mount Adams are closer to the site, neither are considered to be potential sources of large amounts of ash in the near future (Shannon and Wilson, 1976).



September 1981

### Potential for Ash Reaching Site

The principal factor in the dispersal of ash is the vertical coherency in the direction and velocity of the high altitude winds. If these are steady state during an eruption, the ash is deposited as an semi-elliptical pattern downwind of the volcano. Fairly steady state conditions prevailed during the May 18, 1980 eruption of Mount St. Helens when ash began falling at the site between 2 and 3 hours after the eruption.

Available wind data from Salem, Oregon, and Quillayute, Washington (Crandell and Mullineaux, 1976) indicate that the prevailing high-altitude winds in the site region are from the west. The data from Salem (Figure 2.5-23) indicate that, in terms of wind patterns between 10,000 and 80,000 feet, the site is continuously directed downwind from Mount Hood and Mount St. Helens about 6 to 12 percent of the time for 12-hour periods and would receive less than or center-line ash fall up to 30% of the time with various wind vector-altitude combinations.

### Potential Thickness of Ash Fall

Estimating a potential maximum ash fall is difficult given the limited number of reliable historical data on volcanic events. Thickness-distance relationships based on observed and estimated ash fall from a number of eruptions are plotted in Figure 2.5-24. From this plot, five inches is a conservative estimate of a potential ash fall for the WNP 1-2-4 site.

### Rate and Duration of Ash Fall

Only limited data are available on the rate of volcanic ash fall. From the June 1912 eruption of Mount Katmai, Alaska, and for purposes of evaluating hazards resulting from a hypothetical ash fall, depositional rates of 0.2 in/hr average are assumed. It also is assumed that significant deposition would continue for less than 24 hours.

### Density and Compaction of Ash Fall

Data on the recent Mount St. Helens eruptions suggest that a dry unit weight of 80 p.c.f. and a compacted (wet or dry) unit weight of 110 p.c.f. are conservative, given the distances from the site to potential ash sources (see Figure 2.5-25). The same data show that compaction could be 20-40 percent.

### Sorting and Composition of Ash

The Mount St. Helens eruptions of 1980 provide the most reliable characterization of a potential ash fall. Figure 2.5-26 shows the observed grain-size distribution for the Mount St. Helens ash at a number of sites with the Mount Mazama (6,600 y.b.p.) grain-size distribution superimposed. From these data the following grain-size distribution at the project site is hypothesized; 84 percent less than 75 microns, 50 percent less than 20 microns, 34 percent less than 10 microns, 28 percent less than 7 microns, 20 percent less than 5 microns. The composition of the tephra at distances of approximately 241 kilometers from the mountain included 15-20 percent crystals, 50-80 percent glass, and 5-25 percent pumice fragments and dust. Seventy percent of the crystals were feldspars.

#### 2.5.1.2.6.2 Subsidence

Karst terrains, cavernous conditions, local tectonic depressions, uplifts, or related features have not been identified in the vicinity of the site.

#### 2.5.1.2.6.3 Landslides

The closest landslide occurrence is 5 kilometers or more distant in the White Bluffs adjacent to the Columbia River. Slope stabilities at the site are addressed in 2.5.5.

#### 2.5.1.2.6.4 Regional Warping

Studies by R. E. Brown (1969) and Tillson (1970) suggest that the Pasco Basin is continuing to subside. Brown indicates rates of 1 foot in 5,000 years to 1 foot in 1,000 years. Tillson determined an average rate of 1 mm per year from available leveling data. Although these analyses are not positive indicators of continued basining, they do provide data which precludes regional warping as a problem at the proposed site.

#### 2.5.1.2.6.5 Man's Activities

The extraction and recharge of groundwater in the region and site vicinity is discussed in Sections 2.4.13 and 2.5.1.2.7.6.

The abandoned Rattlesnake Hills gas field is located on the northeast slope of the Rattlesnake Hills, Benton County, Washington, approximately 19 kilometers from the site. This small accumulation of low pressure methane gas is located on



the Rattlesnake Hills anticline. The two producing reservoirs were in vesicular and scoriaceous basalt flows at depths of 700 to 1,260 feet below the ground surface (Glover, 1935).

The gas field was discovered in 1913. Commercial production began in 1929 and the field was abandoned in 1941. The total recorded production is 1,321,145 m.c.f. Additional unrecorded amounts of gas were wasted in the preliminary development of the field (Glover, 1953). The nature of this withdrawal and the distance from the proposed site indicate that it presents no problem to stability of the site.

#### 2.5.1.2.7 Site Geology

The WNP 1-2-4 site lies within the Pasco Basin (Figure 2.5-4), one of several physiographic basins within the western Columbia Plateau. For details of the Pasco Basin, see the previous discussion in section 2.5.1.2.4.

##### 2.5.1.2.7.1 Geologic History

The Geologic history of the WNP 1-2-4 site vicinity has been discussed on a site province basis in section 2.5.1.2.1.

##### 2.5.1.2.7.2 Physiography

The site (Figures 2.5-1 and 2.5-4) lies in the Pasco Basin, a local physiographic depression within the Columbia Plateau. The Pasco Basin encompasses 4,144 square kilometers in south central Washington. Within the basin, the ground surface is a gently undulating, semiarid plain, interrupted by low-lying hills and dunes that are dissected by intermittent streams. The basin is transected by the Columbia River which enters the Pasco Basin from the northwest at Sentinel Gap and exits to the southeast at Wallula Gap.

The Columbia River is joined on the west by the Yakima River south of Richland, Washington, and on the east by the Snake River at Pasco, Washington. The northern and southern boundaries of the Pasco Basin are defined by the Saddle Mountains and the Rattlesnake Hills. The easterly end of Manastash-Hanson Creek, Umtanum and Yakima Ridges mark the western boundary of the basin. To the east the basin merges into a vast expanse of dunes, dissected flatlands, and coulees.

The WNP 1-2-4 site lies in the central eastern part of the Pasco Basin (Figure 2.5-4). The most prominent drainage

feature in this area is the Columbia River, which flows southeasterly several kilometers north of the site until about 8 kilometers northeast of the site where it bends and flows in a southerly direction.

East of the river, opposite the site, steep bluffs known as the White Bluffs rise 400 to 500 feet above the river level. The bluffs were created by erosion of the Ringold Formation by both the Columbia River and glacial floodwaters. To the northeast, where the Columbia River bends southward, two large coulees intersect on the east side of the river. These coulees were formed by the scouring action of glacial floods and are partially filled with glaciofluvial deposits.

The site is located west of the Columbia River in an area composed of a gently undulating, low-profile plain, stretching southwesterly to the Rattlesnake Hills. The topography is largely controlled by Pleistocene glaciofluvial deposits and overlying eolian deposits.

There have been no karst terrains, cavernous conditions, local tectonic depressions or related features identified in the vicinity of the site. However, some regional downwarping may be still going in the Pasco Basin.

Figures 2.5-29 and 2.5-35 show the topography and the geology of the area around the site. The rolling plain topography occurs on glaciofluvial and eolian deposits. At the site, the ground surface varies in elevation from approximately 420 to 470 feet. The average ground surface elevation is about 440 feet with approximately 4 feet of variation from this elevation across the area. A large swarm of active dunes lies to the north of the site area but its migratory direction is northeasterly away from the site.

#### 2.5.1.2.7.3 Stratigraphy and Lithology

The areal geology of the site and vicinity was studied in road cuts, trenches, and outcrops with the aid of aerial photographs. This geology is shown on Figures 2.5-29 and 2.5-35 for the site vicinity and plant site, respectively. The subsurface geology is based on data from 140 boreholes drilled for the site investigations (see Figures 2.5-30, 2.5-31, 2.5-32, 2.5-33, and 2.5-34). Ten of these boreholes provided bedrock information, bottoming in flows of the Yakima Basalt. The logs of these borings are presented in Appendix 2.5-A. Locations of boreholes drilled at the site and in the immediate vicinity are shown on Figures 2.5-61, 2.5-62, and 2.5-63. A trench excavated for this



investigation is located on Figure 2.5-62 and the logs of the trench are shown in Appendix 2.5-F. Results of geologic mapping of excavations during construction of the WNP-2 site are presented in Appendix 2.5-H.

The stratigraphy of the Pasco Basin is presented on Figure 2.5-5. The stratigraphic section at the site is illustrated on Figure 2.5-28. The correlation of the geologic units at the site was made on the basis of stratigraphic position, lithology, and other criteria. The basalt flows were core drilled in order to provide a means of utilizing direct lithologic examination (Appendix 2.5-A) and geochemical analysis (Appendix 2.5B). An evaluation of these and other correlation methods is given by Brown and Ledgerwood (1973). The resulting correlations at the site are shown on Figures 2.5-31, 2.5-33, and 2.5-34.

The plant site is underlain by three geologic units: Pre-Columbia River Basalt Group rocks; Columbia River Basalt Group (includes the Ellensburg Formation); and late Cenozoic sediments (includes the Ringold Formation, Palouse Soil, and Hanford formation [Pasco Gravel]). The succession of materials encountered in the subsurface is shown in the stratigraphic section at the plant site, Figure 2.5-28. This section was developed from ten deep geologic borings (see Appendix 2.5A). Five basalt flows and several associated interbedded sediments were identified beneath the site on the basis of these deep borings. From oldest to youngest, the units are: undifferentiated Saddle Mountain Basalt flows, Selah Member of the Ellensburg Formation, Pomona Basalt, Rattlesnake Ridge Member of the Ellensburg Formation, and the Ward Gap-Elephant Mountain Basalt. These rocks are of late Miocene to early Pliocene age. The Ringold Formation of Pliocene age unconformably overlies the Ward Gap-Elephant Mountain Basalt, which in turn, is mantled locally by glaciofluvial and glaciolacustrine sediments and by Holocene eolian and alluvial deposits. Lithologic descriptions of these stratigraphic units can be found in section 2.5.1.2.2.

#### 2.5.1.2.7.4 Structural Geology

The WNP 1-2-4 site is located in the Pasco Basin between the west-northwest trending Gable Butte-Gable Mountain anticlines on the north and the Rattlesnake Hills-Wallula alignment anticline on the south. The few mapped faults that occur in the Pasco Basin are associated with folds.

Aerial photographic analysis and ground inspection were made of the area 8 kilometers around the site in all directions.





No geologic, geomorphic, or topographic indicators of faulting were identified in material younger than the Ringold formation within 8 kilometers of the site. The closest mapped surface fault is on Gable Mountain about 18 kilometers northeast of the site (Figure 2.5-17).

A continuity survey was made in the upper Ringold Formation exposed in the White Bluffs east of the site across the Columbia River for a distance of approximately 45 kilometers (Figures 2.5-36 and 2.5-37). Results of this survey and subsequent mapping of the area east of Wooded Island (Figure 2.5-36) indicate that beds within the exposed upper Ringold Formation are essentially horizontal. No faulting was observed in these units, but a variety of landslide features are observed along the river.

Figure 2.5-30 illustrates the structural geology of the site vicinity. Data from all available wells and boreholes in the vicinity which penetrated basalt were used to develop the top of basalt contours shown on Figure 2.5-30. The contours represent the contact between the upper Yakima Basalt and Ringold Formation. An erosional unconformity exists between these two units and the contours probably reflect some buried topography on the eroded basalt surface. In the area shown on Figure 2.5-30, the amount of variation from a structural datum appears to be less than the contour interval of the map.

The lowest known elevation of the top of the basalt in the Cold Creek Syncline (Figure 2.5-30) is 163 feet below sea level (Hanford Well 15-15, Blume and Associates, 1971). The elevation of the top of basalt beneath the site is about 85 feet below sea level. The total relief of the cross-section (Figure 2.5-31) is about 630 feet in a distance of 28 kilometers.

Figures 2.5-33 and 2.5-34 present three cross-sections through the site area. The horizontal and vertical scales of the cross-sections are the same so that there is no exaggeration or distortion of the presentation. The elevations relative to sea level of all of the diagnostic contacts indicate there is very little structural relief in the area of the investigations.

A distinct structural high that is about 150 feet above the surrounding gradient was encountered in BH-139A. Seismic refraction profiles (Appendix 2.5D) also identify this high but show nothing other than a local fold structure. A

11

12



comparison of the seismic profile data of this structure with Figure 2.5-32 supports the interpretation of a fold occurring at this locality.

The local gradient on the Pomona Basalt in the site area is about 15 to 20 feet vertical per 1,000 feet horizontal to the southwest. Although the gradient is 3 to 5 times steeper on the high at BH-139A, the gradients on the major anticlinal structures are on the order of 100 to 200 feet vertical per 1,000 feet horizontal.

#### 2.5.1.2.7.5 Engineering Geology

There are no deformational zones, shears, joints, fractures, or folds at this site that would have an influence on structural foundations.

There are no zones of alteration, irregular weathering profiles, or zones of structural weakness at this site that would have an influence on structural foundations.

Because basalt bedrock is at an approximate depth of 525 feet at WNP-2 site, unrelieved residual stresses in bedrock would have no influence on structural foundations and are not a consideration at this site.

The soils beneath the site are derived from predominantly basaltic and silicic rock types that are chemically stable. None of the rocks or soils beneath the site would be unstable because of their mineralogy.

There is no evidence that man might have altered the subgrade mineral condition at the site. The only known commercial value of the mineral substances beneath the site arises from the possible use of the glaciofluvial sand as borrow. These materials abound in the region and have no special foreseeable value that would induce any removals near the plant site.

#### 2.5.1.2.7.6 Groundwater

Groundwater occurs at the site under confined and unconfined conditions. Water existing in an unconfined state in the glaciofluvial deposits and Ringold Formation comprises the regional groundwater system. Locally, water may occur under confined conditions within these sediments. Water in the lower part of the Ringold Formation is confined when it is separated from the overlying unconfined system by relatively impermeable material. Water in the deeper basalt aquifer system is in a confined state.

The water table at the plant site occurs at approximately elevation 380 feet. This elevation is below the foundation of Category I structures. Existing water-level data shows that the elevation of the water table is relatively stable at the plant site. Groundwater conditions of the plant site are discussed in detail in Subsection 2.4.13.



## 2.5.2 VIBRATORY GROUND MOTION

The geology and seismology of the site, as presented in the Preliminary Safety Analysis Report, were reviewed by the AEC Staff and the U.S. Geological Survey (USGS) during the construction permit phase. Washington Public Power Supply System proposed in the PSAR to use a design horizontal peak acceleration value of 0.25 g resulting from the Safe Shutdown Earthquake. The Staff agreed with Washington Public Power Supply System that an acceleration of 0.25 g was adequate to represent the ground motion from the maximum earthquake likely to affect the site (Safety Evaluation of WNP-2 by AEC staff, September 22, 1972, Article 2.4.2). The USGS concurred with the Staff's finding on the basis of all available data, and added that major seismic source structures do not appear to be present in the immediate vicinity of the site (WNP-2 Initial Decision, LBP-73-10, 6 AEC 197 (1973)).

The Safe Shutdown Earthquake can be defined by either a maximum intensity or a magnitude. Magnitude is a measure of earthquake size using instrumental recordings of ground motion. Intensity is a measure of earthquake size using observed damage and felt effects. The potential vibratory ground motions that were used in the design of the WNP-2 and WNP-1/4 plants were based on the maximum historical earthquake intensity that has occurred in the Columbia Plateau. That earthquake was the July 16, 1936 Milton-Freewater earthquake, which had a maximum intensity of (MM) VII and occurred about 84 km southeast of the site. It was assumed that an earthquake of this size could occur on the Rattlesnake-Wallula alignment, which was considered to be the closest tectonic structure of significance to the site. No allowance was made for attenuation between the assumed source and the site, a distance of 20 km. An event of intensity (MM) VII would be associated with a peak acceleration of 0.125 g (Subsection 2.5.2.4.1). For conservatism, the Safe Shutdown Earthquake (SSE) was assumed to be an intensity (MM) VIII earthquake associated with a peak acceleration of 0.25 g. The Operating Basis Earthquake (OBE) was taken as one half of the SSE.

Seismological studies that have been conducted since the construction permit was issued do not change the assessment that the maximum historical earthquake to have occurred in the Columbia Plateau was intensity (MM) VII. However, recent geologic investigations suggest that some of the fault structures associated with folds in the Columbia Plateau may be capable faults as defined by U.S. Nuclear Regulatory Commission criteria (Appendix A, 10 CFR 100). Therefore, potential seismic sources in the site region are analyzed. In response to recommendations from the NRC Staff (reference Question No. 361.13), the data regarding potential seismic sources are treated probabilistically in a seismic exposure analysis (Appendix 2.5K). This approach is utilized in order to account for uncertainties in applying a geologic structure approach to assess the potential vibratory ground motion in the Columbia Plateau. These uncertainties are due to poor geologic exposures in the Plateau. The locations and dimensions of faults are not well known within the Plateau, where the primary mode of crustal deformation appears to be folding rather than faulting. The rate of apparent crustal deformation and the level of historical seismicity are low, and the correlation between seismicity and structure is poor. Also, the late Pleistocene catastrophic floods in the central Columbia Plateau removed most of the older Quaternary deposits that would have been useful for assessing the capability of faults.

The seismic exposure analysis includes estimates of: the geometry and locations of potential seismic sources, the capability of the sources, the maximum earthquake magnitude, earthquake recurrences, and ground motion attenuation. The seismic exposure analysis indicates that the annual probability of exceeding the SSE peak ground acceleration of 0.25 g at the WNP-2 and WNP-1/4 site is  $1.1 \times 10^{-4}$ , and that the annual probability of exceeding the SSE design response spectrum in the period range of about 0.1 to 0.4 seconds varies from 2.9 to  $9.2 \times 10^{-5}$ . Because the major contributions to seismic exposure come from small magnitude earthquakes (magnitude 4 to 5) that are of limited duration

and energy content, this analysis provides a conservative assessment of the probabilities of exceedance of the SSE with respect to ground motion of engineering significance. When compared to other previously licensed plants, the exposure analysis results support the adequacy of the current 0.25 g SSE design basis.

For operating license reviews, the NRC Staff requires the submittal in the Final Safety Analysis Report of all new information gathered since the construction permit review relating to regional and site geology and seismology. This Amendment No. 18 of the FSAR for WNP-2 provides that updated information. The conclusion of the basis of the exhaustive study efforts undertaken since issuance of the construction permit is that a peak acceleration of 0.25 g is adequate and conservative for the ground motion resulting from the maximum earthquake likely to affect the WNP-2 and WNP-1/4 sites.

#### 2.5.2.1 Seismicity

Reviews of historical seismicity for Washington and Oregon have been conducted by Townley and Allen (1939), Coombs (1953), Berg and Baker (1963), Rasmussen (1967), and Couch and Lowell (1971), and Washington Public Power Supply System (1974 and 1977). These reviews rely upon felt reports of earthquakes and, during more recent decades, upon reports based on seismographic recordings of earthquakes.

Historical records available to report earthquake effects in Washington began with the construction of trading posts and military forts on the Spokane and Okanogan Rivers in 1812-1813. Steppe (1972) concluded that observations of intensity (MM) VII or greater are complete for at least the past 80 years for the Pacific Northwest region. However, based on the population growth pattern (Schmid et al., 1955; Androit, 1980), earthquakes of this size would have been felt over a sufficient area to have been reported much earlier. Thus, the detection of earthquakes having epicentral intensity (MM) VII or greater is considered complete for most of the 320 km (200 mi) radius region



surrounding the site since about 1830. Detection of epicentral intensity (MM) VI events is considered complete for the region from about 1890, with a lower-intensity detection level in the most populated portions of the region.

Instrumental recording of earthquakes in eastern Washington began on June 30, 1909, with the installation of a Wiechert seismograph station (SPO) in the Jesuit Seminary at Gonzaga University, near Spokane. The relatively low-magnification and low-frequency response of this instrument made it of limited use in recording local or regional earthquakes. Station SPO was similar to other instruments in Victoria, British Columbia, where a Milne horizontal seismograph was installed in 1899, and Seattle, Washington, where a Bosch-Omori seismograph began operating in 1906. In 1946, the Wiechert instrument at SPO was replaced by a Wood-Anderson seismograph. Station SPO operated intermittently until 1970 as a function of the availability of trained clergy at the seminary; the station did record the 1918 Corfu and the 1936 Milton-Freewater earthquakes (Subsection 2.5.2.1.1.1).



In eastern Washington, modern instruments were installed for short periods by Geotech in 1962 and 1963 at Yakima and Ellensburg and by the US Coast and Geodetic Survey (USCGS) in 1966 at Newport (Poppe, 1979). In March 1969, a network of six vertical seismometers was installed by the U. S. Geological Survey (USGS) in the vicinity of the Atomic Energy Commission's Hanford Reservation. This network was enlarged to 24 stations by October 1971. In 1975, when the operation of the network was taken over by the University of Washington, the network included 29 stations. The University of Washington has since expanded the network to cover much of central Washington and part of northern Oregon, and Rockwell Hanford Operations is presently operating additional stations on the Hanford Reservation. Since 1969, the detection level has been  $M_L 1.5$  for the immediate Hanford vicinity and  $M_L 1.5$  to 2.5 for remaining portions of the Columbia Plateau. Microearthquake detection levels and other aspects of the eastern Washington seismic network are discussed by Woodward-Clyde Consultants (1980a), Appendix 2.5I, and Appendix 2.5J.

The complete historical catalog of earthquakes for the Pacific Northwest region, including the area within 320 km (200 mi) of the site, is listed in Section 8.0 of Table 2.5-5. The list includes all reported earthquakes of magnitude greater than 3 or of modified Mercalli intensity greater than III, a total of more than 2100 events. Sections 1.0 through 7.0 of Table 2.5-5 describe the data presented in the catalog as they were compiled from 23 published and unpublished sources. The period of coverage of the catalog is from about 1830 to 1 March 1981, with the exception that (as noted in Section 1.1 of Table 2.5-5) some University of Washington data that are primarily from western Washington, are not included for the years 1978, 1979, 1980, and 1981. The historical and instrumental seismicity of the region within 320 km (200 mi) of the site is shown on the epicentral location map (Figure 2.5-38) and the tectonic provinces map (Figure 2.5-39), as plotted from Table 2.5-5.

Table 2.5-5 was compiled from published and unpublished earthquake computations, reports, personal interviews, and contacts with authorities on the seismicity of the site region. The information has been merged, cross-checked, and edited to produce the earthquake catalog. When conflicting data were given for individual earthquakes, a reasonable and conservative interpretation was selected. The epicentral coordinates for felt earthquakes have been assigned on the basis of the location of the highest reported intensity. The following information is listed for each earthquake in the catalog: origin date and time; epicenter latitude and longitude; source of data; comments; and maximum intensity, magnitude, and focal depth if they were determined. Additional source parameters for selected earthquakes are discussed in Subsection 2.5.2.1.1.1, Appendix 2.5I,



AMENDMENT No. 18  
September 1981

and in Appendix 2.5J.

For purposes of completeness, Table 2.5-5a supplements Table 2.5-5 and lists earthquakes reported in published and unpublished literature that have no reported intensity and for which data are very limited. These events occurred primarily during the early historical period. It is not known whether they meet the minimum magnitude or intensity criteria for Table 2.5-5.

Compared to coastal California or Alaska, the historical seismicity of the area within 320 km of the site is generally low to moderate in the frequency of occurrence of felt events and in the frequency of earthquakes having magnitudes that exceed 3.0. The most active seismic zones in the area are associated with: 1) earthquakes inferred to occur within a subducted oceanic slab at depths of 40 to 70 km (Crosson, 1980) beneath the Puget Trough (Subsection 2.5.1.1.2.3); and 2) the crustal Puget Trough and Cascade Mountains (Subsections 2.5.1.1.2.3 and 2.5.1.1.2.8), where earthquakes occur in the depth range 0 to 30 km. Historical earthquake activity associated with the Columbia Plateau and adjacent provinces is summarized in Subsection 2.5.2.3. The current tectonic setting of these provinces is summarized by Davis (1981) and in Section 2.5.1.

Within the Columbia Plateau, historical earthquakes have been generally small and scattered, as shown in Figure 2.5-38. Relative concentrations of activity are noted between Wenatchee and Chelan (at a distance of 140 km from the site and discussed in Appendix 2.5I) and trending northeast and southwest from Walla Walla (at a distance of about 90 km from the site and discussed in Woodward-Clyde Consultants, 1980a). The areas of these two concentrations have been seismically active throughout the historical period, with the occasional occurrence of felt earthquakes (Figure 2.5-38 and Table 2.5-5). However, felt events have been reported less frequently from within the Columbia Plateau than in these areas (Figure 2.5-52). Because the historical population distribution has been similar for these areas, the lower frequency of reported felt events within the interior of the Plateau appears real.

The operation of a seismic network at the Hanford Reservation since 1969 greatly increased the number of earthquakes detected in the area (Subsection 2.5.2.1.2.2) but the frequency of occurrence of felt events ( $MM > IV$ ) is generally consistent with the pre-network period (Table 2.5-5). Analyses of the instrumental seismicity for the Columbia Plateau have indicated additional features of earthquake activity for the 11.3-year period that are consistent with the longer-term historical seismicity and geologic record within the Columbia Plateau (see Appendix 2.5J). The deformation style in the Plateau appears to be due to regional north-south compression, and the strain rate

is low compared to other areas of the western United States. However, the initiation of irrigation in 1952 is likely to have triggered an increased occurrence rate of small-magnitude ( $M_L < 3.0$ ) earthquakes within irrigated areas of the Plateau.

#### 2.5.2.1.1 Earthquakes Felt At the Site

There have been few intensity reports from the site itself. Prior to the establishment of the Hanford Reservation in 1943, there were small towns within the site called Wahluke, White Bluffs, and Hanford for which felt reports are available. Intensity estimates at the site are based either on these reports or on isoseismal maps that are based on reports from more distant towns surrounding the site.

Table 2.5-6 lists 13 earthquakes that are postulated to have been felt at or to have possibly affected the site. The largest potential effects at the site were an estimated intensity (MM) V associated with the 14 December 1872 North Cascades earthquake, and an estimated intensity (MM) IV associated with the 16 July 1936 Milton-Freewater earthquake in southeastern Washington. Twelve of the earthquakes listed in Table 2.5-6 occurred within 320 km (200 mi) of the site, and one (Hebgen Lake, Montana, 1959) was farther than 320 km (200 mi). Earthquakes discussed in Subsection 2.5.2.1.1.1 are listed in order of decreasing estimated site intensity.

##### 2.5.2.1.1.1 Earthquakes Within 320 km (200 mi) of the Site

The 14 December 1872 earthquake is one of the largest earthquakes in the recorded history of the Pacific Northwest, having been reported felt throughout an area extending from the Pacific coast eastward to Montana, northward well into British Columbia, and southward into central Oregon. The epicenter for the earthquake is located within a meizoseismal zone that extends from Lake Chelan on the south to southern British Columbia on the north, as defined by Coombs et al. (1976).

Although the exact epicentral location of the 14 December 1872 earthquake has not been established, most investigators who have studied this event conclude that the epicentral area is in the Northern Cascades province, an area that is distinct and different, both geologically and tectonically, from the Columbia Plateau. The basis and data for this location come from the results of an intensive search for historical information, acquisition of geologic and geophysical data, and a critical evaluation of these data by separate consultants and an independent panel of expert geologists and seismologists.

As discussed in Amendment 23 of the WNP-1/4 PSAR (Washington Public Power Supply System, 1977), the main earthquake occurred



AMENDMENT No. 18  
September 1981

at about 10:00 pm on the evening of 14 December 1872. Two to four earthquakes of slightly smaller magnitude were felt over a broad area after the main shock during the night of 14-15 December 1872. The large felt area ascribed to the 14 December 1872 earthquake suggests that the earthquake had a magnitude near ( $M_s$ ) 7 to 7-1/4. The maximum intensity (MM) VIII is based on all felt reports that can be related to vibration damage to structures. If the focal depth of the 14 December 1872, earthquake were shallow (i.e., 5 to 15 km), and if the earthquake had a magnitude near ( $M_s$ ) 7, then the ground surface should have been broken by faulting in the epicentral area. If the 14 December 1872, earthquake occurred in the deeper crust (20 to 30 km) or within the subducted plate in the mantle, surface fault rupture by attendant faulting would not be expected. Surface rupture dating from 1872 and of an extent compatible with an earthquake of magnitude near ( $M_s$ ) 7 has never been found, thus leading to the conclusion that the 1872 event probably occurred at lower crustal or upper mantle depths.

In a report prepared by Weston Geophysical Corporation (1976), the most probable location of the epicenter for the 1872 earthquake is considered to be the original location shown by Milne (1956), but the epicenter could have been as far east as the western border of the Okanogan Highlands. The highest intensity assigned by Weston was a (MM) VII at Wenatchee. Weston estimated the epicentral intensity as (MM) VIII and the felt area as about 1,250,000 km<sup>2</sup> (435,000 mi<sup>2</sup>).

A draft report by Woodward-Clyde Consultants was later modified and expanded to become Appendix 2RB of Amendment 23 of the WNP 1/4 PSAR (Washington Public Power Supply System, 1977p). Appendix 2RB concluded that the center of the maximum intensity zone remained within the area proposed by Milne (1956). The Woodward-Clyde Consultants isoseismal map (Figure 2.5-40) excluded ground failure and water effects for the purpose of defining the meizoseismal area, and estimated the earthquake felt area for (MM) IV and greater to be 1,140,000 km<sup>2</sup>. Despite the very large felt area, the structural damage was minimal, consisting of a chimney shaken down at Osoyoos, British Columbia; two upper logs and the roof displaced on a log cabin in Wenatchee, Washington Territory (now in Washington state); a tower and dwelling badly cracked in New Dungeness, Washington Territory; and the front wall of a brick building cracked in Victoria, British Columbia. This damage and other felt effects reported from the region were used to identify the epicentral region and are the basis for considering the maximum intensity to be (MM) VIII for purposes of evaluating structural response. Widely scattered ground effects, including landslides, ground cracks, and water ejection, occurred in the intensity (MM) IV to VII areas defined above. Strong ground roll, "displaced" fencing, and sloshing of the Fraser River over its banks at



Chilliwack, British Columbia in the epicentral region are the basis for the (MM) IX intensity shown in Table 2.5-5. The intensity at the site is estimated to have been (MM) V from the isoseismal map described above.

Comparison of the 1872 earthquake with modern data suggests that the 1872 isoseismals correspond to an event in the magnitude range from ( $M_s$ ) 6.8 to 7.2. The comparable intensity (MM) IV felt area is slightly smaller than the intensity (MM) IV felt area of the 1959 Hebgen Lake, Montana earthquake (Subsection 2.5.2.1.1.1), which had a magnitude of ( $M_s$ ) 7.1. Generalized intensity versus felt area relationships by Algermissen (1969) and Howell and Schultz (1975) suggest an epicentral intensity of (MM) IX and a magnitude of ( $M_s$ ) 7.0, while Brazee (1980) indicates an epicentral intensity of (MM) X. Shebalin (1968) presents intensity-magnitude-depth relationships that indicate a magnitude in the range ( $M_s$ ) 7.0 to 7.2, with the focal depth inversely proportional to the epicentral intensity  $I_0$  (about 40 km if  $I_0$  = (MM) VIII; about 20 km if  $I_0$  = (MM) IX; and about 10 km if  $I_0$  = (MM) X). The 1872 isoseismal data fit Shebalin's relationships best at depths of 20 km or less. Gutenberg and Richter (1956) also present a magnitude-intensity-depth relationship yielding the same intensity and focal depth results as Shebalin but suggest a magnitude of ( $M_s$ ) 6.8. These results are reported in the WNP-1/4 PSAR, Amendment 23, Appendix 2R-B. (Note: An error in Appendix 2R-B indicates the magnitude is also a function of the focal depth). The suggestion of a crustal focal depth is also supported by the numerous aftershocks reported from the epicentral area in 1873, because large earthquakes having magnitudes of ( $M_s$ ) 6.9 to 7.1 that have occurred at focal depths of 60 to 70 km in the Pacific Northwest have been devoid of significant aftershock activity.

Using the 1872 earthquake intensity data reported by the other workers (Washington Public Power Supply System, 1977p), Malone and Bor (1979) analyzed the location and size of the 1872 earthquake in terms of an attenuation model that accounts for local corrections to regional intensity attenuation. They tested several location assumptions; a location near Ross Lake was favored, but the data also fit the Milne (1956) location to the northeast. A location near Lake Chelan was definitely ruled out. Malone and Bor (1979) felt that the depth of focus could be 40 to 60 km, based on the known depths of other large earthquakes in the area, but the intensity data also allow a much shallower focal depth.

In summary, the comparison of the data from the 1872 event to modern data suggests that the 1872 earthquake had a magnitude of ( $M_s$ ) 7 to 7-1/4 and probably occurred at a focal depth of about 20 km with an epicentral intensity (MM) VIII for structural response.

AMENDMENT No. 18  
September 1981

On 16 July 1936, the Milton-Freewater earthquake ( $M_s$  5-3/4 reported by Gutenberg and Richter, 1965;  $M_L$  6.1 reported by Woodward-Clyde Consultants, 1980a) occurred 85 km southeast of the site. This earthquake, which was felt over an area of approximately 270,000 km<sup>2</sup>, is the closest earthquake of maximum intensity (MM) VII or greater to have affected the site region. The isoseismal map for the earthquake is shown on Figure 2.5-41 and indicates an intensity (MM) IV level of shaking in the vicinity of the site. Estimates by observers for the duration of rapid ground motion in the epicentral region ranged from 10 to 30 seconds. The intensity effects of this earthquake have been described in detail by Brown (1937), USCGS, and Neumann (1938) and are discussed in Washington Public Power Supply System (1974).

Considerable property damage occurred but no serious injuries were noted in the area of highest intensity, particularly at Milton-Freewater, State Line, and Umapine in northern Oregon. Brown (1937) reported that, in the Milton-Freewater area, many chimneys were broken or shifted, plaster and windows were broken, several houses were moved off their foundations, a two-story concrete house lost part of the top of its second story, the ornamental railing on top of a cement block office building in Milton-Freewater was greatly damaged, and many capstones in cemeteries were rotated. He also reported numerous changes in springs and water wells and some local ground cracking.

In the Pasco area, the shock was reported to have lasted for 30 seconds, causing dishes to rattle and pictures on walls to sway, but producing minimal property damage.

As discussed by Woodward-Clyde Consultants (1980b), the instrumental location for the Milton-Freewater earthquake was computed to be latitude 46°12.5' north, longitude 118°14.0' west, with an uncertainty of about 20 km. This epicenter is likely to be the point of initiation of rupture, and the aftershock reports and other intensity data suggest that the earthquake occurred on a buried fault surface that ruptured from the instrumental epicenter to the southwest, toward the area of highest intensity. This trend is parallel to the structural trend of the Blue Mountains anticline and to the trend of the Hite fault (Figure 2.5-38 and Shannon and Wilson, 1979b). The felt reports indicate that the zones of maximum structural damage during the main shock were also generally aligned along a northeast-southwest trend. Also, soil fissuring occurred at two locations in the maximum intensity region of the main shock. At the first location, the fissuring was aligned in an east-west direction along a highway cut; at the other, a railway cut, it occurred in an east-southeast direction. These cuts appear to have controlled the orientation and nature of the soils failures. Surface fault

AMENDMENT No. 18  
September 1981

ruptures were not observed.

On 29 April 1965 a magnitude ( $M_b$ ) 6-1/2 earthquake having an epicentral intensity of (MM) VII-VIII occurred near Seattle, 255 km west-northwest of the site. The earthquake was felt over an area of 335,000 km<sup>2</sup> as shown on the isoseismal map, Figure 2.5-42. The site, located on the higher side of the I-VI intensity (MM) zone, has been assigned an intensity (MM) IV.

In the Seattle-Tacoma region, damage effects of intensity (MM) VII and VIII are closely related to poor foundation conditions in the epicentral region (unconsolidated deposits characteristic of parts of the Puget Sound area). The effects at the Hanford Reservation are summarized in the following excerpt:

Richland (Hanford Project). Motion rapid, lasted 45 seconds to 2 minutes. Felt by many in community. Hanging objects swung north-northeast. (USCGS)

The 1 November 1918 Corfu earthquake had an epicentral intensity of (MM) V-VI, based on intensity reports from the town of Corfu, Washington, and on reported landslides in the vicinity of Corfu. Based on the seismograph record at the Gonzaga University station (SPO) in Spokane, Washington, it is estimated that this earthquake had a magnitude ( $M_s$ ) of approximately 4.4.

The Corfu earthquake and aftershock sequence was reported in the Bulletin of the Seismological Society of America (1918):

The first shock was on November 1st, between 9:15 and 9:30 a.m. This was the most severe and lasted several seconds; it shook goods from the shelves and caused landslides for several miles along the hills. We have had on an average about three shocks every twenty-four hours since, but lighter. The intensity is estimated at IV of the RF Scale.

Bingham et al. (1970) refer to a landslide east of Smyrna Bench, which they attribute to the Corfu earthquake, but it was not investigated in detail in their field studies.

Fifer (1966) gathered reports that suggest a maximum intensity (MM) IV at White Bluffs which is located 26 km northwest of the present plant site and 16 km south of Corfu. The White Bluffs felt reports indicate that the epicenter was probably close to the town of Corfu. This further suggests that the site intensity was likely to be less than (MM) IV.

The intensity data are shown in Figure 2.5-43 along with an arc



AMENDMENT No. 18  
September 1981

D corresponding to the S-P time of 21.7 seconds measured from the SPO record of the event. An uncertainty of approximately 1 second or 8 km is noted for the S-P time. Based on these data, the most likely location for the 1918 event is considered to be slightly east of Corfu, within the central portion of the epicentral region shown in Figure 2.5-43. The coordinates for this point are listed in Table 2.5-5. The 1918 Corfu earthquake is similar in location to the 20 December 1973,  $M_c$  4.4 Royal Slope event, as discussed in Appendix 2.5J. The Royal Slope event had a focal depth of 2.1 km (Malone, 1979), a maximum intensity of (MM) V, and was felt to a distance of 30 km (Appendix 2.5I).

On 13 April 1949 the largest earthquake recorded instrumentally within 320 km (200 mi) of the site occurred in the Puget Sound region of Washington. This magnitude ( $M_s$ ) 7.1 earthquake, with a maximum epicentral intensity of (MM) VIII, was felt over a 390,000 km<sup>2</sup> (150,000 mi<sup>2</sup>) area centered near southern Puget Sound, 250 km west-northwest of the site. The site is located near the middle of the (MM) I-IV intensity zone on the isoseismal map for this earthquake (Figure 2.5-44).

On 29 April 1945, a magnitude ( $M_s$ ) 5-1/2 maximum intensity (MM) VII earthquake occurred near North Bend, Washington, 210 km northwest of the site. This earthquake had a 130,000 km<sup>2</sup> (50,000 mi<sup>2</sup>) felt area and a possible site intensity of (MM) I-IV, as shown on the isoseismal map on Figure 2.5-45 (USCGS).

On 15 February 1946 a magnitude 5-3/4  $M_s$ , maximum intensity (MM) VII earthquake occurred in the Puget Sound area 285 km from the site. The isoseismal map for this earthquake, Figure 2.5-46, indicates a possible site intensity of (MM) I-IV; however, this earthquake was not felt in Richland, Kennewick, or Mesa in the site region (USCGS).

On 13 November 1939 a magnitude ( $M_s$ ) 5-3/4, maximum intensity (MM) VII earthquake occurred at Olympia, 290 km west-northwest of the site. The isoseismal map for this earthquake, Figure 2.5-47, gives an estimated intensity (MM) I-IV at the site. The earthquake was felt at Moxee City, west of the site, but not felt at the town of Hanford (USCGS).

On 24 April 1943 a magnitude ( $M_L$ ) 4.3, maximum intensity (MM) VI earthquake occurred at Leavenworth, 130 km northwest of the site, having a felt area of 26,000 km<sup>2</sup> (10,000 mi<sup>2</sup>). The isoseismal map, Figure 2.5-48 indicates a possible site intensity of (MM) I-IV. The earthquake was felt at Sunnyside (III), and Connell (III), but was not felt at Othello or Pasco (USCGS).

On 6 August 1959 a magnitude ( $M_L$ ) 4.4, maximum intensity (MM) VI earthquake occurred at Chelan, 158 km northwest of the site. This earthquake was felt over a 65,000 km<sup>2</sup> (25,000 mi<sup>2</sup>) area of

central Washington, as shown in Figure 2.5-49. The site is located near the outer boundary of the (MM) I-IV intensity zone. It was not felt in Richland or Sunnyside, Washington (USCGS).

On 30 December 1926 an intensity (MM) V earthquake occurred north of Wenatchee, 150 km from the site. This earthquake was felt over a 40,000 km<sup>2</sup> (15,000 mi<sup>2</sup>) area. Based on felt reports, the site intensity is estimated to be in the (MM) I-III intensity range. The epicenter is probably near Wenatchee, which experienced intensity (MM) V effects; (i.e., felt by many, furniture moved, rocks rolled onto the road). At Quincy, about 40 km from Wenatchee, buildings swayed and dishes fell from shelves, indicating an intensity of (MM) IV-V. At Yakima, about 100 km from Wenatchee, the shock was reported felt; it was also felt in Spokane and at Davenport (Townley and Allen, 1939).

On 16 September 1961, a magnitude ( $M_L$ ) 4.3, maximum intensity (MM) VI earthquake occurred near Cougar, Washington, 225 km west of the site. Although the site is well outside the felt area indicated on the isoseismal map, Figure 2.5-50, the USCGS reports the following observation from the Hanford Reservation:

Three in building felt building movement but did not realize it was caused by an earthquake at the time.

No exact location was given for the felt report. The site intensity is listed as (MM) II in Table 2.5-6.

#### 2.5.2.1.1.2 Earthquakes Farther Than 320 km (200 Mi) From the Site

Figure 2.5-51 is the isoseismal map of the Hebgen Lake, Montana, earthquake, that occurred on 17 August 1959. This magnitude ( $M_s$ ) 7.1 earthquake had an epicentral intensity of (MM) X, 670 km southeast of the site. The isoseismal map shows that the site is just at the limit of the felt area of this earthquake (USCGS).

No other earthquakes outside the 320-km (200-mi) radius about the site are known to have affected the site area.

#### 2.5.2.1.2 Seismicity Within the Columbia Plateau

##### 2.5.2.1.2.1 Historical Earthquakes

A seismicity map for the area within 80 km (50 mi) of the site is shown on Figure 2.5-52, based on data tabulated in Table 2.5-5. As noted in Subsection 2.5.2.1 this listing includes historical earthquakes of intensity (MM) III or greater, and instrumental

earthquakes of magnitude 3 or greater. The 25 October 1971 magnitude ( $M_c$ ) 3.8 earthquake and the 2 October 1970 magnitude  $M_c$  3.3 earthquake are the only earthquakes reported within approximately 32 km (20 mi) of the site. Neither was felt at the site. The Corfu earthquake (Subsection 2.5.2.1.1.1) is the only earthquake within 80 km of the site that is postulated to have been felt at the site.

The only other earthquake larger than intensity (MM) V within 80 km of the site was the 5 March 1893 shock that occurred near Umatilla, Oregon, about 62 km south of the site. Townley and Allen (1939) reported the earthquake as follows:

1893 March 6 (sic) Umatilla. A succession of shocks were felt here to-night. One of the walls of a large stone building was thrown down by the force of the shock (VII? VIII?).

A VII? to VIII? Rossi-Forel (RF) intensity would correspond to a (MM) VII? intensity.

The East Oregonian, (1893), Pendleton, newspaper of Monday, March 6, 1893, had the following headline and article:

Earthquake at Umatilla - the little city in the sand badly shaken up.

Umatilla, Oregon March 6 - At three minutes past 5 o'clock yesterday afternoon an earthquake shock lasting several seconds passed over this section of the country. One side of a large stone warehouse tumbled down, and the building was so badly cracked on all sides that it will have to be torn down. D. Harris, agent for the Union Pacific, who was possessing the building at the time, barely escaped being buried in the debris.

This appears to have been an earthquake of very limited extent, because no felt reports from Pendleton itself nor any towns in the surrounding area were found in the search of newspapers in Pendleton and Milton-Freewater, Oregon, and Yakima, Walla Walla, and Spokane, Washington.

The largest circular area about Umatilla that excludes Pendleton and Yakima has an area of 7,800 km<sup>2</sup>. The intensity-felt-area plot, Figure 2.5-53, is based on data from Table 2.5-6 and shows that a 7,800-km<sup>2</sup> area is compatible with an intensity (MM) V-VI but is an order of magnitude less than the felt areas associated with intensity (MM) VII earthquakes. Consequently, the intensity rating of this earthquake has been reduced to (MM) VI in Table 2.5-5.

#### 2.5.2.1.2.2 Microearthquakes Within the Columbia Plateau

As discussed in Subsection 2.5.2.1, microearthquake recording (events of magnitude  $M_L$  3.0 or less) has been conducted in the vicinity of the Hanford Reservation for more than 12 years (since March, 1969). The eastern Washington network was operated initially by the USGS and subsequently by the University of Washington. Malone (1979) reprocessed all of the earthquake data recorded since 1969 using uniform computational procedures, revised regional velocity models, individual station corrections, and a coda-length magnitude formula that has been calibrated for the region. Thus, the earthquake data set is homogeneous for the period 1969 through 1980. This data set has been used (Appendix 2.5J) to study the seismicity of the Columbia Plateau. In that document the differences between the very shallow earthquakes that are characteristic of the region and deeper earthquakes are discussed. The shallow earthquakes (focal depth less than about 3 km) appear to occur within the Columbia River basalt flows. Deeper earthquakes occur within the older volcanic and sedimentary (?) rocks that underlie the shallow basalts and also within the basement.

##### Shallow Seismicity

Approximately 80 percent of the seismicity that has been instrumentally recorded in the Columbia Plateau has occurred within the uppermost 3 km of the crust, which is considered to be composed of multiple layers of Columbia River flood basalts. This shallow seismicity is dominated by occurrences of micro-earthquake swarms that are confined within small (approximately 1 to 10 km<sup>3</sup>) source volumes and that have durations of a few days to several months. Focal mechanisms for shallow earthquakes vary but generally indicate a horizontal stress field oriented north-south. Available data suggest that the shallow seismicity is associated with tectonic deformation occurring at a low rate, and that the shallow earthquakes are likely to occur on faults, fractures, and joints in the basalt flows. Shallow seismicity has been concentrated outside the boundaries of the Hanford Reservation in areas where major irrigation and associated changes in the elevation of the ground-water table have taken place. This suggests a causative relationship between shallow seismicity and ground-water level changes.

##### Deeper Crustal Seismicity

Earthquakes that have occurred in the depth range of 9 to 25 km, within the basement defined by time-term studies, have been discussed by Woodward-Clyde Consultants (1980b). That study and a recent investigation (Appendix 2.5J), indicate that these deeper earthquakes are associated with deformation of the



basement over a broad region centered on the central Columbia Plateau in response to regional horizontal north-south compression. The scatter of deeper earthquakes suggests regionally coherent low-level deformation. No linear or planar trends of earthquake hypocenters are evident. The regional stress field favors thrusting on east-west oriented planes, as indicated by focal mechanisms. The depth zone from 3 to 8 km beneath the central Columbia Plateau, which is between the shallow basalt flows and the basement, exhibits a higher concentration of earthquakes than the basement. However, the level of microseismicity within this zone has been much lower than that within the uppermost 3 km of the crust, and the microseismicity does not exhibit predominant earthquake swarm behavior.

#### 2.5.2.2 GEOLOGIC STRUCTURES AND TECTONIC ACTIVITY

The regional geologic structures and tectonic activity pertinent to an evaluation of the potential vibratory ground motions at the site are discussed in the various Subsections of 2.5.1.1 and are shown on Figure 2.5-2. The site is located in the Pasco Basin, one of several physiographic depressions occupying the Columbia Plateau. The geologic and tectonic setting of the Pasco Basin relative to other parts of the Columbia Plateau is shown on Figure 2.5-4. The geology and structure of the Pasco Basin and of the plant site and vicinity are described in Subsections 2.5.1.1.1, 2.5.1.2.1, and 2.5.1.2.4.

##### 2.5.2.2.1 Tectonic Provinces

In a general way, the physiographic provinces in the Pacific Northwest reflect tectonic provinces. However, it is not possible to determine exact locations of tectonic province boundaries because of the onlapping of the Columbia River basalts onto the adjacent provinces and the uncertainties regarding the geology beneath the basalts. The site is located within the Columbia Plateau, a major physiographic province bounded by the Blue Mountains and High Lava Plains provinces on the south, the Northern Rocky Mountains and Idaho Batholith provinces on the east, the Okanogan Highlands province on the north, and the Cascade Mountains provinces on the west. These provinces are described in Subsection 2.5.1.1.2. Because geologic structures in the Columbia Plateau are considered to be potential sources of the SSE, the earthquake potential of these more distant provinces is not a significant factor in assessing the potential vibratory ground motions at the site.

##### 2.5.2.2.2 Geologic Structures of the Columbia Plateau

The major structural trends within the Columbia Plateau are the generally east-west asymmetric Yakima folds that are associated



along parts of their lengths with mapped and inferred reverse faults, and the northwest-trending alignment of folds, domes, and faults that defines the Cle Elum-Wallula lineament (CLEW). In the Columbia Plateau, there is uncertainty regarding structural relationships at depth. Therefore, constraints on fault geometry have to be based largely on tectonic models that are inferred from the style of deformation observed at the surface. Descriptions of the tectonic history of the Columbia Plateau and of the timing and style of deformation have been given by Bentley (1977), Laubscher (in Appendix 2.5-O), Davis (in Appendix 2.5N), Price (1980; written communication, 1981b), and Bruhn (1981). Their models provide a basis for alternative interpretations regarding the origin, deformational history, capability, and dimensions of potential earthquake sources. Implications of the alternative tectonic models to the assessment of the earthquake potential at the site are described by Woodward-Clyde Consultants (Appendix 2.5K) and are summarized below.

#### 2.5.2.2.2.1 Yakima Folds and Associated Reverse Faults

The Yakima folds are described in Subsection 2.5.1.1 and shown in Figure 2.5-3. Proposed models of Columbia Plateau deformation suggest that the folds, which are asymmetric kink-type folds, developed either as: a) primary folds with localized secondary reverse faults, or b) secondary folds related to primary crustal reverse faults.

##### 2.5.2.2.2.1.1 Primary Folding With Secondary Reverse Faulting

This model of plateau deformation is supported by Price (1980; written communication, 1981b), Davis (in Appendix 2.5N), and Golder Associates (1981a, 1981b) who conclude that the folds developed as the primary response of the Columbia River basalts to general north-south compression. The folding may have been facilitated by localized or shallow detachment. North- and south-dipping reverse faults that flank some of the folds formed during the late stages of fold development and are secondary to the fold structures.

##### 2.5.2.2.2.1.2 Primary Reverse Faulting and Secondary Folding

The spatial distribution and geometry of the Yakima folds can also be used to infer the presence of thorough-going crustal reverse faults that are the controlling structures in fold development. However, there are no data that demonstrate that these faults actually exist. Bentley (1977) proposed that the Yakima folds developed above zones of high-angle faults that extend from the basement. Laubscher (in Appendix 2.5-O) suggests that the Yakima folds are narrow structures developed on broader warps and he infers the presence of multiple décollements in the

AMENDMENT No. 18  
September 1981

Columbia Plateau. He suggests that the broad warps were localized by thrust ramps rising from a deep (approximately 20 km) regional decollement and that the narrow folds (the Yakima folds) formed above a shallow (1- to 3-km deep) decollement. A geometric analysis of some of the Yakima folds, based on a fault ramp-flexure model (Bruhn, 1981), suggests the presence of fault ramps below the folds that extend to decollements at preferred depths of 3 to 5 km. Bruhn (1981) notes that these fault ramps could consist of loci of interconnected faults and kink-bands rather than large, discrete fault planes.

#### 2.5.2.2.2.2 Cle Elum-Wallula Lineament (CLEW)

The Cle Elum-Wallula Lineament (CLEW) is described in Subsection 2.5.1.1, and its location is shown in Figure 2.5-4. The present field data base does not provide adequate constraints for a unique tectonic model to explain the northwest-trending alignment of structural features that defines CLEW.

Laubscher (in Appendix 2.5-0) defines CLEW as a northwest-trending zone of en echelon anticlines that represents the upper crustal expression of a deep-seated (15- to 20-km) right-lateral crustal shear. Davis (Appendix 2.5N) interprets CLEW as a zone of right-lateral shear in the crust of the Columbia Plateau that developed synchronously with, and interacted with, the Yakima folds. He defines three structural domains and concludes that the zone of right-lateral shear is narrow and occurs at the surface in the southern domain (along the Wallula fault) and becomes progressively deeper and/or broader to the northwest. By contrast, Price (written communication, 1981b) suggests that the northwest-striking folds that occur along the Rattlesnake-Wallula (RAW) portion of CLEW can be interpreted as asymmetric folds that developed as the Columbia River basalts were folded across a northwest-trending irregularity in the plateau basement. In this model, right-lateral strike-slip faulting is not required; rather, the basement behaves passively, and deformation along the RAW trend occurs primarily as folding with secondary reverse or reverse-oblique-slip faulting. Investigations by Woodward-Clyde Consultants along the Rattlesnake-Wallula alignment (Subsection 2.5.1.2.4.4) also suggest that shortening normal to the alignment has been important in the development of the observed structures.

#### 2.5.2.2.3 Potential Earthquake Sources

The only fault in the vicinity of the site that is capable according to US Nuclear Regulatory Commission criteria (Appendix A, 10 CFR 100) is the Central fault on Gable Mountain. The fault, which is located 18 km northwest of the site, displaces 13,000- to 19,000-year old glaciofluvial deposits (Golder Associates, 1981a). They conclude that the available data are insufficient to demonstrate a non-tectonic mechanism for the

origin of the observed displacement along the Central fault. The maximum earthquake magnitude assessment for the Central fault is presented in Subsection 2.5.2.4.2.2.

Investigations along the Rattlesnake-Wallula alignment at Finley Quarry (Subsection 2.5.1.2.4.4) and Warm Springs (Woodward-Clyde Consultants 1981c, in preparation), and at Toppenish Ridge (Woodward-Clyde Consultants, 1981a), suggest that there may be capable faults at these locations. The alternative tectonic models also allow the possibility that other faults, either observed or inferred, associated with the Yakima folds and CLEW may be capable. Because of the uncertainty in both the existence and capability of these faults, structures that could be significant if they are capable sources have been evaluated in a seismic exposure analysis (Appendix 2.5K). These potential sources are the Umtanum Ridge-Gable Mountain structural trend, Rattlesnake Wallula alignment (RAW), Saddle Mountains, Rattlesnake Hills, Yakima Ridge, and Horse Heaven Hills. Distances to the site and maximum earthquake magnitude distributions for each potential source are given in Subsections 2.5.2.4.2.1 and 2.5.2.4.2.3, respectively.

#### 2.5.2.2.4      Implications of Alternative Tectonic Models to Fault Parameters

The alternative tectonic models result in significantly different fault parameters (such as length, down-dip width, sense of displacement, and segmentation) and, therefore, different potential maximum magnitude earthquakes for individual structures. It is unlikely that one model can be applied to all Columbia Plateau structures. Studies at Umtanum Ridge (Price, 1980; Golder Associates, 1981b) and Gable Mountain (Golder Associates, 1981a) indicate that observed reverse faults are narrow and are secondary to the folds. However, the presence of scarps along the base of Toppenish Ridge suggests the possibility of Holocene surface faulting and, therefore, the existence of a fault plane having significant area (Woodward Clyde Consultants, 1981a). These observations indicate that there may be a range of fault geometries associated with the plateau folds and emphasize the need to evaluate the earthquake potential of each structure separately (Appendix 2.5K).

If a reverse fault is secondary to a fold, its maximum length will be limited to the length of the fold, and its down-dip width will probably be no greater than the width of the fold. Faults developed in this manner will generally have small surface areas and, if they are seismogenic, have the potential to produce only small- to moderate-magnitude earthquakes (Appendix 2.5K).

If the Yakima folds are related to deeper reverse faults, then



fault length may be constrained by the length of major folds or fold segments, and down-dip fault width may vary from approximately 5 to 23 km. These faults, if they are seismogenic, have the potential to produce moderate- to large-magnitude earthquakes (Appendix 2.5K).

If CLEW is modeled as a vertical strike-slip fault zone, the available data indicate probable depths of faulting of between 7-1/2 km. to 20 km and the potential for moderate- to large-magnitude earthquakes (Appendix 2.5K). If structures along the CLEW trend represent primary folds with secondary reverse faults or primary reverse faults, then fault parameters and earthquake magnitudes derived above for the Yakima folds are applicable.

### 2.5.2.3 CORRELATION OF EARTHQUAKE ACTIVITY WITH GEOLOGIC STRUCTURES OR TECTONIC PROVINCES

No well-defined correlation exists between the earthquake activity (shown in Figure 2.5-38) in the 320-km (200-mi) radius region surrounding the site and individual mapped geologic structures, such as faults, graben, or anticlines (shown in Figure 2.5-39 and discussed in Section 2.5.1). Earthquake activity associated with, and occurring within, the Columbia Plateau and adjacent provinces is discussed in the following subsections. The provinces are described in Subsection 2.5.1.1.2.

#### 2.5.2.3.1 Puget-Willamette Trough

The larger-magnitude, deeper-focus earthquakes in the Pacific Northwest occur west of the volcanic chain of the Cascade Mountains where there is a general zone of seismic activity in the crustal and sub-crustal portions of the Puget-Willamette Trough (Subsections 2.5.1.1.2.3 and 2.5.2.1, and Figure 2.5-39). The earthquakes that are specifically discussed in Subsection 2.5.2.1.1.1 and that occurred in this province or in the Juan de Fuca Plate are the events of 13 November 1939, 29 April 1945, 14 February 1946, 13 April 1949, and 29 April 1965. At its closest approach, either within the crust or within the subducted Juan de Fuca Plate, this province is at least 200 km from the site (Figure 2.5-39), and none of the earthquakes that have occurred in the province has significantly affected the site.

#### 2.5.2.3.2 North Cascades

As discussed in Subsection 2.5.2.1.1.1, the 14 December 1872 earthquake is related either to faulting in the North Cascades province or to faulting in the subducted Juan de Fuca Plate. The occurrence of the 1872 earthquake outside of the Columbia Plateau is also discussed by Coombs et al. (1976). A clustering of epicenters occurs in the Wenatchee-Chelan area in the vicinity of

the junction of the North Cascades, Okanogan Highlands, and Columbia Plateau provinces. Events discussed in Subsection 2.5.2.1.1.1 that occur in the vicinity of this cluster are the 30 December 1926, 24 April 1943, and 6 August 1959 earthquakes. No well-defined correlation exists between this cluster and known geologic structures (Appendix 2.5I).

Because of the distance of this province from the site, in excess of 110 km (Figure 2.5-39), its earthquake potential is not considered further (Subsection 2.5.2.2.1).

#### 2.5.2.3.3. Blue Mountains

A grouping of epicenters occurs in the Walla Walla basin area, along the boundary of the Columbia Plateau and the Blue Mountains provinces. The 16 July 1936 Milton-Freewater earthquake is the largest historic event in this area and appears to have occurred in the crust beneath the Columbia River basalt flows (Subsection 2.5.2.1.1.1). Although the northeast trends of felt effects and aftershocks are generally compatible with mapped fault trends in the vicinity of Walla Walla, such as the Hite fault, no specific association has been made between the source of the 1936 earthquake or other events in the area and a mapped geologic structure or fault (Subsection 2.5.2.1.1.1; Woodward-Clyde Consultants, 1980a). Additional small and generally scattered earthquakes occur within the province (Figure 2.5-39) with no apparent correlation to known geologic structures.

#### 2.5.2.3.4 Other Provinces Adjacent to the Columbia Plateau

The Middle Cascade Mountains province, which is more than 110 km from the site, has generated scattered, small to moderate magnitude earthquakes, such as the 16 September 1961 event (Subsection 2.5.2.1.1.1) near Mount St. Helens. The Northern Rocky Mountains province, which is more than 160 km from the site, generated the 17 August 1959 Hebgen Lake earthquake (Subsection 2.5.2.1.1.1). Because of the distance of each of these provinces from the site, their earthquake potential is not considered further.

#### 2.5.2.3.5 Columbia Plateau

The Columbia Plateau is characterized by small, scattered, infrequent earthquakes (Figures 2.5-38 and -52). Two concentrations of seismicity occur along the northwest boundary with the North Cascades (Chelan-Wenatchee area) and along the southeast boundary with the Blue Mountains (Walla Walla area) and are discussed in Subsection 2.5.2.3.3. Within 80 km (50 mi) of the site in the central Columbia Plateau, a minor concentration of earthquakes is located between Frenchman Hills and Saddle Mountains, and three additional events are located between Saddle



Mountains and Gable Mountain (Figure 2.5-52). The 20 December 1973 Royal Slope and the 1 November 1918 Corfu earthquakes have been located between Saddle Mountains and Frenchman Hills (Figure 2.5-52). There is no well-defined correlation of this earthquake activity with the Frenchman Hills, Saddle Mountains, or Gable Mountain structures. However, because of the uncertainties in the epicentral location of the 1918 event (Subsection 2.5.2.1.1.1 and Appendix 2.5J) it is possible that this earthquake occurred on a fault associated with the Saddle Mountains anticline.

Analysis of microearthquake activity ( $M_L$  less than 3.0) for the data collected from 1969 through 1980 within the Columbia Plateau is discussed in Appendix 2.5I, Appendix 2.5J, and Woodward-Clyde Consultants (1980b), and is summarized in Subsection 2.5.2.1.2.2. The shallow, swarm-dominated microearthquake activity does exhibit some broad spatial trends, such as the northwest-southeast pattern lying between Frenchman Hills and Saddle Mountains. The shallow activity appears to be associated with low-level deformation within the upper Columbia River basalts and to be triggered by the presence of high ground-water levels resulting from irrigation. However, no correlations between specific faults or fold structures and microearthquakes have been identified (as discussed in Appendix 2.5J). The microseismicity occurring beneath the flood basalt flows at depths from about 3 to 25 km appears to be distinct from the shallow activity (Woodward-Clyde Consultants 1980b; Appendix 2.5J). The deeper seismicity does not define any linear or planar patterns, nor is there any apparent association with the folds on other surface geologic structures of the Columbia Plateau.

#### 2.5.2.4 MAXIMUM EARTHQUAKE POTENTIAL

The maximum earthquake potential at the site was assessed based on the maximum historical intensity (Subsection 2.5.2.4.1). Recent investigations have indicated that the Central fault on Gable Mountain is capable according to US Nuclear Regulatory Commission criteria (Appendix A, 10 CFR 100), and other studies have suggested that some of the fold structures of the Columbia Plateau may be associated with capable faults (Subsection 2.5.2.2.2.3). Uncertainties exist regarding the association of faults with known folds, fault capability, source geometry, and tectonic framework (Subsection 2.5.2.2). To account formally for these uncertainties, maximum earthquake magnitudes for potential fault sources were assessed probabilistically. The results of the maximum magnitude assessment are incorporated into a seismic exposure analysis (Appendix 2.5K) to evaluate the probability of exceeding the SSE design basis ground motion (0.25g) that was based on the maximum historical intensity in the Columbia Plateau.



#### 2.5.2.4.1 Maximum Historical Intensity

The potential vibratory ground motions that were used in the design of the WNP-2 plant were based on the maximum historical earthquake intensity that has occurred in the Columbia Plateau (Washington Public Power Supply System, 1974), which is the 16 July 1936 Milton-Freewater earthquake. It had a maximum intensity of (MM) VII and occurred about 84 km southeast of the site. The 14 December 1872 earthquake had a maximum intensity of (MM) VIII and is thought to have occurred in the North Cascades province approximately 250 to 300 km from the site. The largest historical earthquake effects at the site are conservatively estimated to have been an intensity (MM) IV-V from the 1872 Northern Cascades earthquake, and an intensity (MM) IV from the 16 July 1936 Milton-Freewater earthquake (Subsection 2.5.2.1.1). The closer (1936) earthquake probably produced a higher acceleration level at the site because of attenuation of the higher frequency wave components from the more distant event.

The 1936 Milton-Freewater earthquake epicentral region is near the intersection of the southeast extension of the Rattlesnake-Wallula alignment and the northeast-striking structures parallel to the Hite fault zone (Figure 2.5-52). There is no apparent correlation of seismicity with the Rattlesnake-Wallula alignment (Subsection 2.5.2.3). Nevertheless, for conservatism, it was postulated that an earthquake of intensity (MM) VII, similar to the 1936 Milton-Freewater event, could occur on the Rattlesnake-Wallula alignment, approximately 20-km from the site. If no attenuation is considered over the 20-km distance between the alignment and the site, such an earthquake would result in an acceleration of 0.125 g (Figure 2.5-54) at the site.

The maximum earthquake potential from any other tectonic province within the site region was not considered high enough to be capable of exceeding the 0.125-g level of shaking at the site resulting from earthquakes originating in the site province.

#### 2.5.2.4.2 Geologic Structure Approach

A geologic structure approach for assessing maximum earthquake magnitudes and the potential vibratory ground motions is appropriate for sites in the vicinity of capable faults. The 3-km-long Central fault on Gable Mountain is the only fault in the site vicinity that has been shown to be capable according to US Nuclear Regulatory Commission criteria. Tectonic models proposed for the Columbia Plateau postulate the presence of faults, both primary and secondary, associated with the major folds (Subsection 2.5.2.2). Although the capability of these mapped or inferred faults is uncertain, estimates of maximum earthquake potential can be made assuming that there is some likelihood both that the faults exist and that they are capable. Alternative

tectonic models and the associated geometry of the faults are considered in a probabilistic assessment of maximum earthquake magnitudes for each source.

Maximum earthquake magnitude on a fault is related to source geometry (rupture length, rupture area) and fault behavior (maximum and average displacement per event, slip rate, and sense of displacement). Based on these fault parameters, empirical and analytical relationships can be used to estimate maximum magnitudes. The use of a number of magnitude estimation techniques can result in more reliable estimates of maximum magnitude than the application of any single technique.

Alternative tectonic models have been proposed to account for the known and inferred structural elements of the Columbia Plateau; each model has implications to magnitude-related fault parameters (Subsection 2.5.2.2). Because more than one of these models may be compatible with the available data, the fault parameters associated with all possible models must be considered in the maximum magnitude assessment. As part of the probabilistic assessment of maximum magnitudes, the full range of possible fault parameters are considered. Degrees of confidence in the various tectonic models and parameters are assigned based on available data. In addition, the applicability of various techniques for estimating maximum magnitude is assessed for each tectonic model.

A discussion of the probabilistic methodology and the justification for decisions regarding tectonic models, fault parameters, and maximum magnitude assessment techniques are given in (Appendix 2.5K).

#### 2.5.2.4.2.1 Potential Seismic Sources Significant to the Site

The geologic structures that may be potential sources significant to assessing the probability of exceeding the SSE vibratory ground motions at the site are listed below and are shown in Figure 2.5-55.

<u>Potential Seismic Sources</u>	<u>Closest Surface Distance to Site (km)</u>
Umtanum Ridge-Gable Mountain Structural Trend	
Central fault	18
Gable Mountain-Southeast anticline segment	7
Umtanum Ridge eastern segment	38
Umtanum Ridge central segment	63
Umtanum Ridge western segment	92
Rattlesnake-Wallula Alignment (RAW)	
Rattlesnake Mountain segment	20
Rattlesnake-Wallula segment	20
Wallula segment	53

Saddle Mountains	31
Rattlesnake Hills	27
Yakima Ridge	32
Horse Heaven Hills	30

All of the potential sources, except the Central fault, are structural folds. Observed or inferred faults of uncertain capability are associated with these fold structures. On the basis of the geologic and geomorphic data discussed by Woodward-Clyde Consultants in Appendix 2.5K, potential sources were segmented and, in some cases, parts of structural trends were assumed to be separate potential sources.

#### 2.5.2.4.2.2 Maximum Magnitude Assessment of the Central Fault on Gable Mountain

The Central fault on Gable Mountain is capable according to US Nuclear Regulatory Commission criteria, and the maximum magnitude for the Central fault is assessed deterministically. Although some evidence supports nontectonic hypotheses for the origin of the displacement along the Central fault, data gathered to date are insufficient to demonstrate a nontectonic mechanism for the origin of the observed displacement. The magnitude assessment presented in this section is applicable only to the Central fault; magnitude estimates for the Gable Mountain-Southeast anticline segment of the Umtanum Ridge-Gable Mountain structural trend are made probabilistically and are summarized in Appendix 2.5K.

Magnitude-related data on the Central fault are presented by Golder Associates (1981a) and are summarized in this section. The Central fault is a northeast-striking reverse fault that dips to the southeast. The fault is interpreted to be the result of the interference of two en echelon folds, the east and west Gable Mountain anticlines. The maximum inferred length of the Central fault is about 3 km (2 mi). The fault displaces glaciofluvial deposits correlative with late-Pleistocene Missoula flood deposits that are between 13,000 and 19,000 years old. The glaciofluvial deposits are displaced up to 6 cm (0.2 ft).

Inferences based on the available data regarding the geometry and behavior of faulting on the Central fault can be made to estimate magnitudes. The east and west Gable Mountain anticlines are second-order folds that have wavelengths of less than 1 km; the folds may extend as deep as one wavelength but probably no deeper than three wavelengths. Because the Central fault is secondary to folding, the down-dip width of the fault surface is probably no greater than the depth of the en echelon folds. Therefore, the maximum width of the Central fault is estimated to be 3 km. The 6-cm (0.2-ft) displacement of the glaciofluvial deposits is the largest displacement that can reasonably be assumed to have



occurred as a single event. In addition, the seismic moment can be estimated if the 6-cm (0.2-ft) displacement is assumed to be an average displacement over the fault surface.

The limited dimensions of the Central fault on Gable Mountain raise questions regarding its ability to generate significant earthquakes. However, assuming the Central fault is seismogenic, the following magnitudes are derived using the magnitude relationships presented in Appendix 2.5K:

<u>Magnitude Relationship</u>	<u>Estimated Magnitude</u>
Area vs M (A = 9 km <sup>2</sup> )	5.1
Displacement vs. M (D = 6 cm)	4.4
Moment Magnitude (A = 9 km <sup>2</sup> , = 3 x 10 <sup>11</sup> dyn/cm <sup>2</sup> , D = 6 cm)	4.8
Length vs. M (L = 3 km)	6.6

All of the magnitude estimates are subject to much uncertainty, primarily because the values of the parameters for the Central fault are smaller than those in the empirical data sets for the various magnitude relationships. The length-magnitude relationship is especially unreliable for short faults, such as the Central fault, that have limited down-dip widths. The area-magnitude relationship accounts for the limited total size of the rupture surface available for energy release on narrow faults. On the basis of these assessments, the maximum earthquake magnitude for the Central fault is estimated to be magnitude 5. The ground motions that would be produced at the site by this earthquake would be less than 0.1 g, as discussed in Subsection 2.5.2.6.1.

#### 2.5.2.4.2.3 Maximum Earthquake Magnitude Distributions for Potential Seismic Sources

As part of the seismic exposure analysis, maximum magnitudes are estimated for potential sources. For the magnitude analysis, it is assumed that the structures are capable seismogenic sources. The actual assessment of the capability of the potential sources is considered probabilistically in the seismic exposure analysis Appendix 2.5K).

As noted in Subsection 2.5.2.3, the shallow-focus microearthquakes that occur within the Columbia River basalts do not correlate with specific geologic structures. Based on the historical earthquake record and on associated detailed analyses

of potential source characteristics within the Columbia River basalts, the maximum magnitude for the shallow focus earthquakes in the vicinity of the site is unlikely to be larger than  $M_L$  4.0 Appendix 2.5J. Earthquakes of magnitude 4 or less are considered not to be of engineering significance to the plant because of the very short duration of vibratory motion associated with such earthquakes.

#### 2.5.2.5 SEISMIC WAVE TRANSMISSION CHARACTERISTICS OF THE SITE

At the site, about 14 m (to elevation 120 m) of glaciofluvial sand overlies the middle and lower members of the Ringold Formation. The middle member extends to a depth of about 76 m (elevation 58 m) and consists of dense gravel that contains relatively thin silt and sand zones at various depths. The lower member is predominantly a compact interbedded gravel, sand, and silt that extends to a depth of about 160 m (elevation -26 m) where it is underlain by basalt bedrock.

Compressional and shear wave velocities are based on geophysical surveys that are described in Appendix 2.5D. In the glaciofluvial sand, compressional velocities average 410 m/s and shear velocities average 200 m/s. In the upper part of the middle member of the Ringold Formation, compressional velocities range from 1,040 to 1,370 m/s and shear velocities from 520 to 580 m/s. A marked increase in compressional velocities (2,700 to 3,200 m/s) and shear velocities (1,280 to 1,370 m/s) was encountered at a depth of about 24 m (elevation 110 m), which is interpreted to indicate more compact material below this depth in the middle member of the Ringold. In the lower member of the Ringold, below 76 m depth (elevation 58 m), shear velocities range from 580 to 1370 m/s. The seismic wave velocities at the site are summarized in Table 2.5-8. The dynamic properties of the materials are also described in Subsection 2.5.4.2.

Compressional and shear-wave velocities of the soils above basalt bedrock have also been measured at WNP-1/4 (Appendix 2L of the WNP-1/4 PSAR). The changes in the wave velocities with depth at WNP-1/4 have a similar trend to those described above for WNP-2.

Because of the presence of relatively thick layers of soils above basalt bedrock, attenuation relationships applicable to soils rather than rock have been selected for use in the seismic exposure analysis. Attenuation relationships are described in Appendix 2.5K.

Available data describing material properties of the basalt flows, interflow materials, and deeper structures beneath the site have been reviewed for the purpose of evaluating the attenuation characteristics of the crustal structure. The best currently available information for characterizing the basalt-



interflow materials has been obtained from logs of deep wells drilled in the area. The deepest of these is the Rattlesnake Hills No. 1 well, which extends to a depth of 3,230 m. The sonic log from this well indicates that the compressional-wave velocity is highly variable as a function of depth, with relatively high velocities of 5.0 to 5.7 km/s occurring in competent basalt flows and lower velocities of 4.0 to 4.5 km/s being typical of interflow materials. The lower-velocity materials were generally of lower density also. This variation in compressional-wave velocities in the basalt flows and interflow materials is also likely to characterize the shear-wave velocities, although no direct measurements of the shear-wave velocity at depth were made. Theoretical calculations, described in Woodward-Clyde Consultants (1981d), have indicated that this wave-velocity structure may substantially decrease peak strong ground motions at the site for earthquake sources beneath the higher-velocity layers in the basalt, relative to ground motions that would occur in the absence of these strong vertical material heterogeneities. The physical basis of this decrease in ground motions is known as the tunneling phenomenon; it is associated with waves incident from a relatively low to a relatively high velocity layer at angles from the vertical greater than a critical value that depends on the velocity contrast. The tunneling phenomenon has been modeled (Woodward-Clyde Consultants, 1981d) and found to decrease peak motions by 50 percent or more at epicentral distances of 6 to 15 km for source depths beneath the high-velocity layers. This conclusion is dependent on several assumptions regarding kinematic descriptions of the seismic source, the relationship between shear and compressional wave velocities in the basalts, the source depth, and the nature of the crust beneath the basalts. These theoretically predicted attenuation effects have been conservatively neglected in modeling attenuation in the seismic exposure analysis (Appendix 2.5K).

#### 2.5.2.6 SAFE SHUTDOWN EARTHQUAKE

##### 2.5.2.6.1 Vibratory Ground Motion of the SSE

The maximum vibration level at the site from historical earthquakes within the Columbia Plateau is estimated to have been 0.015 g associated with the site intensity (MM) IV from the Milton-Freewater earthquake (See Subsection 2.5.2.4 and Figure 2.5-54).

A peak acceleration of 0.25 g at ground surface in the site area has been assigned for the SSE. This value is consistent with the conservatism previously adopted for design criteria at the Hanford Reservation (Atomic Energy Commission, 1972) and is consistent with the vibratory accelerations associated with an intensity (MM) VIII earthquake (Figure 2.5-54), which is larger

than any known earthquake east of the Cascades in Washington or Oregon. This earthquake was assigned to the Rattlesnake-Wallula alignment, which was considered to be the closest tectonic structure of significance to the site. The Rattlesnake-Wallula alignment is 20 km from the site. No attenuation was taken in the selection of the SSE.

As summarized in Subsection 2.5.2.4, the Central fault on Gable Mountain is capable according to US Nuclear Regulatory Commission criteria. Magnitude 5 is estimated to be the maximum magnitude, and the closest distance from the fault to the site is 18 km. Using the magnitude-distance-acceleration attenuation relationships given in Appendix 2.5K, the estimated peak acceleration at the plant site for this earthquake is less than 0.1 g.

The design response spectra for the SSE corresponding to the maximum vibratory acceleration of 0.25 g are shown on Figures 3.7-1 and 3.7-2.

#### 2.5.2.6.2 Evaluation of the Probability of Exceedance of the Vibratory Ground Motion of the SSE

A seismic exposure analysis has been performed to estimate the probability of exceeding the vibratory ground motions of the SSE. The uncertainties regarding fault segmentation, fault capability, fault geometry, maximum earthquake magnitude, earthquake recurrence, and attenuation have been formally addressed and incorporated in the seismic exposure analysis.

The methodology and inputs for the seismic exposure analysis are described in detail in Appendix 2.5K. The methodology is shown schematically in Figure 2.5-56 and is briefly summarized below.

- o All geologic structures that have the potential to be seismic sources (faults) of significance to the plant site are included in the analysis. These structures are identified in Subsection 2.5.2.4.2.1.
- o Alternative fault segmentation models are defined, and the probabilities of each segmentation model representing the actual conditions are estimated.
- o The conditional probabilities that each fault is a capable seismic source are estimated.
- o Alternative tectonic models, described in Subsection 2.5.2.2, are defined for each fault. The conditional probabilities of each tectonic model representing the actual conditions are estimated.

AMENDMENT No. 18  
September 1981

- o Alternative fault geometries (dips and widths of fault plane) are defined for each tectonic model for each fault. The conditional probabilities of each of these geometries being the actual geometry are estimated.
- o Maximum earthquake magnitudes are estimated using different techniques for the geometries and tectonic models of each fault. The conditional probabilities of each maximum magnitude being the actual maximum magnitude are estimated.
- o The recurrence of earthquakes of various magnitudes in the site region is evaluated based both on historical seismicity and geological evidence. Recurrence is distributed to the various faults in proportion to their lengths. The uncertainty in recurrence relationships is evaluated and included in the exposure analysis.
- o Magnitude-distance-instrumental ground motion attenuation relationships are estimated. The uncertainty in predicted ground motion values associated with these relationships is estimated and included in the exposure analysis. The selected attenuation relationships are judged to be conservative because they neglect the apparent highly attenuating effect of the basalt-interbed layering (Subsection 2.5.2.5).
- o A seismic exposure analysis case is defined by each combination of segmentation, tectonic model, fault geometry, and maximum earthquake magnitude for a given fault. These parameters are then combined with the recurrence and attenuation relationships to calculate the seismic exposure (probability of exceeding a certain ground motion value) for that case. Standard procedures for seismic exposure analysis are used for these calculations.
- o The seismic exposure due to each fault is then calculated by appropriately combining the probabilities for each analysis case for that fault with the probabilities associated with maximum magnitudes, fault geometry, tectonic models, fault capability, and fault segmentation. Then the total exposure for the plant site is obtained by combining the probabilities for all the sources.

From the results of the seismic exposure analysis, the estimated probability of instrumental ground motions exceeding the SSE peak ground acceleration (0.25 g), which is also the SSE design response spectral acceleration in the period range 0 to 0.03 second (Figure 3.7-1), is summarized below. Also summarized are

the estimated probabilities of exceedance of SSE design response spectral acceleration at two other selected periods, 0.125 second and 0.40 second. These periods are selected because they correspond approximately to control points of the design response spectra in the low-period to mid-period range (Figure 3.7-1).

<u>Ground Motion Parameter</u>	<u>Annual Probability of Exceedance</u>
Peak ground acceleration of 0.25 g (zero-period response spectral acceleration)	$1.1 \times 10^{-4}$
Response spectral acceleration at a period of 0.125 second (damping ratio of 0.02)	$9.2 \times 10^{-5}$
Response spectral acceleration at a period of 0.40 second (damping ratio of 0.02)	$2.9 \times 10^{-5}$

The values summarized above are the expected values, or best estimates, of the probabilities of exceedance. Confidence levels on the probabilities of exceedance have also been estimated in the seismic exposure analysis. At the 90-percent confidence level, the estimated probabilities of exceedance exceed the values tabulated above by a factor of about 2.5.

The analysis indicates that for peak ground acceleration and for response spectral acceleration at 0.125 second, approximately 70 percent of the exposure is due to earthquakes in the range of magnitude 4 to 5. For response spectral acceleration at 0.40 second, approximately 50 percent of the exposure is from the same magnitude range. These small-magnitude earthquakes are of less engineering significance than large-magnitude earthquakes due to their shorter duration and lower energy content. Consequently, this analysis is a conservative assessment of the probability of exceedance for ground motions of engineering significance.

#### 2.5.2.7 OPERATING BASIS EARTHQUAKE

A peak acceleration of 0.125 g, or one-half that of the SSE, has been assigned for the Operating Basis Earthquake (OBE). The chosen value for the OBE is consistent with the epicentral intensity of the largest historical earthquake that has occurred in the Columbia Plateau (Subsection 2.5.2.4 and Figure 2.5-54). The design response spectra for the OBE are shown on Figures 3.7-3 and 3.7-4.

The probability of exceeding the OBE ground motions has been evaluated from the seismic exposure analysis described in Subsection 2.5.2.6. The estimated probabilities of exceeding the

AMENDMENT No. 18  
September 1981

OBE peak ground acceleration and selected spectral accelerations of the OBE design response spectrum (Figure 3.7-3) are as follows:

<u>Ground Motion Parameter</u>	<u>Annual Probability of Exceedance</u>
Peak ground acceleration of 0.125 g (zero-period response spectral acceleration)	$4.6 \times 10^{-4}$
Response spectral acceleration at a period of 0.125 second (damping ratio of 0.02)	$4.0 \times 10^{-4}$
Response spectral acceleration at a period of 0.40 second (damping ratio of 0.02)	$1.7 \times 10^{-4}$

At the 90-percent confidence level, the estimated probabilities of exceedance exceed the expected values tabulated above by a factor of about 2.2. Similar to the results for the SSE described in Subsection 2.5.2.6, small-magnitude earthquakes are found to dominate the seismic exposure for the OBE. For peak acceleration and for response spectral acceleration at 0.125 second, approximately 70 percent of the seismic exposure is due to earthquakes in the range of magnitude 4 to 5. For response spectral acceleration at 0.40 second, approximately 60 percent of the exposure is due to earthquakes in the same magnitude range.

REFERENCES

- Abbott, A. T., 1953, Geology of the Northwest Portion of the Mount Aix Quadrangle: Ph.D. Dissertation, University of Washington, Seattle.
- Adams, J. B., 1961, Petrology and Structure of the Stehekin-Twisp Pass Area, Northern Cascades, Washington: Ph.D. Dissertation, University of Washington, Seattle.
- Algermissen, S. T., Stepp, J. C., Rinehart, W. A., and Arnold, E. P., 1969, Studies in Seismicity and Earthquake Damage Statistics, 1969-Appendix B: U.S. Department of Commerce, 68 p.
- Allen, J. E., 1959, Columbia River Gorge: in Guidebook for Geological Society of America Field Trip Excursions, 1958, University of Oregon, Oregon Department of Geology and Mineral Industries Field Trip Guidebook, Bulletin 50.
- Allison, I. S., 1933, New Version of the Spokane Flood: Geological Society of America Bulletin, v. 44, p. 675-722.
- Alwin, J. A., and Scott, W. F., 1970, Clastic Dikes of the Touchet Beds, Southeastern Washington: Northwest Science, v. 44, no. 1, p. 58.
- Anderson, C. A., 1965, Surficial Geology of the Fall City Area, Washington: Master's Thesis, University of Washington, Seattle.
- Anderson, J. L., 1978, Stratigraphy and Structure of the Columbia River Basalt in the Clackamas River Drainage: Master's Thesis, Portland State University, Portland.
- Anderson, J. L., 1980, Deformation and Canyon Cutting in Post-Grande Ronde, pre-Frenchman Springs Time, Grayback Mountain, South-Central Washington: Geological Society of America, Abstracts with Programs, V. 12, No. 3, p. 93.
- Andriot, J. L. Ed., 1980, Population Abstract of the United States: Andriot Associates, McLean, Virginia, p. 864-869.
- ARHCO, 1976, Preliminary Feasibility Study on Storage of Radioactive Waste in Columbia River Basalts: Atlantic Richfield Hanford Company, Report ARH-ST-137, Richland, Washington.



Armstrong, R. L., 1979, Cenozoic Igneous History of the United States Cordillera from latitude 42° to 49° N, in Smith, R. B., and Eaton, G. P., Eds.: Cenozoic Tectonics and Regional Geophysics of the Western Cordillera, Geological Society of America Memoir 152, p. 265-282.

Artim, E. R., and Wunder, J. M., 1976, Preliminary Geologic Map of the LaConner Quadrangle, Skagit County, Washington: Washington Division of Geology and Earth Resources Open-File Map OF-76-1.

Atwater T., 1970, Implications of Plate Tectonic Evolution of Western North America: Geological Society of America Bulletin, v. 81, No. 12, p. 3513-3536.

Baker, V. R., 1973, Paleohydrology and Sedimentology of Lake Missoula Flooding in Eastern Washington: Geological Society of America Special Paper 144, 79 p.

Baker, V. R., 1978, Quaternary Geology of the Channeled Scabland and Adjacent Areas, in Baker, V. R., and Nummedal D., Eds., The Channeled Scabland, A Guide to the Geomorphology of the Columbia Basin, Washington: NASA Comparative Geology Conference, p. 17-35.

Baldwin, E. M., 1969, Geology of Oregon: University of Oregon Book Store, Eugene, Oregon, 136 p.

Baldwin, E. M., Brown, R. D., Jr., Gair, J. E., and Pease, M. H., Jr., 1955, Geology of the Sheridan and McMinnville Quadrangles, Oregon: U.S. Geological Survey Oil and Gas Investigation Map OM-155.

Baldwin, E. M., and Roberts, A. E., 1952, Geology of the Spirit Mountain Quadrangle, Oregon: U.S. Geological Survey Oil and Gas Investigation Map OM-129.

Barksdale, J. D., 1975, Geology of the Methow Valley, Okanogan County, Washington: Washington Division of Mines and Geology Bulletin 68, 72 p.

Beaulieu, J. D., 1973, Environmental Geology of Inland Tillamook and Clatsop Counties, Oregon: Oregon Department of Geology and Mineral Industries Bulletin 79, 65 p.

Beaulieu, J. D., 1974, Geologic Hazards of the Bull Run Watershed, Multnomah and Clackamas Counties, Oregon: Oregon Department of Geology and Mineral Industries Bulletin 82, 77 p.



Beaulieu, J. D., 1977, Geologic Hazards of Parts of Northern Hood River, Wasco, and Sherman Counties, Oregon: Oregon Department of Geology and Mineral Industries Bulletin 91, 95 p.

Beaulieu, J. D., 1980, Geologic Field Trips in Northern Oregon and Southern Washington: Oregon Department of Geology and Mineral Industries Bulletin 77, 206 p.

November 20, 1956.

Becraft, G. E., 1966, Geologic Map of the Wilmont Creek Quadrangle, Ferry and Stevens Counties, Washington: U.S. Geological Survey Geologic Quadrangle Map GQ-538, Scale 1:62,500.

Becraft, G. E., and Weis, P. L., 1963, Geology and Mineral Deposits of the Turtle Lake Quadrangle, Washington: U.S. Geological Survey Bulletin 1131, 73 p.

Beeson, M. H., Benson, G. T., Johnson, A., and others, 1975, Portland Environmental Geology, Fault Identification, Portland: Portland State University Department of Earth Sciences.

Beeson, M. H. and Moran, M. R., 1979, Stratigraphy and Structure of the Columbia River Basalt Group in the Cascade Range, Oregon: U.S. Department of Energy Report RLO-1040-T1, p. 5-77.

Bentley, R. D., 1977, Stratigraphy of the Yakima Basalts and Structural Evolution of the Yakima Ridges in the Western Columbia Plateau: Geology Excursions in the Pacific Northwest, Geological Society of America Annual Meeting, Seattle, Washington, p. 339-389.

Bentley, R. D., Anderson, J. L., Campbell, N. P., and Swanson, D. A., 1980, Stratigraphy and Structure of the Yakima Indian Reservation, with Emphasis on the Columbia River Basalt Group: United States Geological Survey Open-File Report 80-200, 83 p.

Berg, J. W., Jr. and Baker, C. D., 1963, Oregon Earthquakes, 1841 through 1958: Seismological Society of America Bulletin, v. 53, no. 1, p. 95-108.

Bingham, J. W. and Grolier, M. J., 1966, The Yakima Basalt and Ellensburg Formation of South-Central Washington: United States Geological Survey Bulletin 1224-G, 15 p.

Bingham, J. W., Londquist, C. J., and Baltz, E. H., 1970, Geologic Investigation of Faulting in the Hanford Region, Washington: (with a Section on the Occurrence of Microearthquakes by A. M. Pitts): United States Geological Survey Open File Report, 70-27, 104 p.

Birdseye, R. U., 1976, Geologic Map of East-central Jefferson County, Washington: Washington Division of Geology and Earth Resources Open-File Map OF-76-26.

Bjornstad, B. N., 1980, Sedimentary and Depositional Environment of the Touchet Beds, Walla Walla River Basin, Washington: Rockwell Hanford Operations, Richland, Washington, Report RHO-BWI-SA-44.

Black, R. F., 1979, Clastic Dikes of the Pasco Basin, Southeastern Washington: Rockwell Hanford Operations, Richland, Washington, Report RHO-BWI-C-64.

Blume, J. A. and Associates, 1972, Seismic Exposure and Criteria for Seismic Analysis of Grand Coulee Dam, Columbia River, Grand Coulee, Washington: A report prepared for Washington Public Power Supply System, 46 p.

Bond, J. G., 1963, Geology of the Clearwater embayment: Idaho Bureau of Mines and Geology Pamphlet 128, 83 p.

Bond, J. G., 1978, Geologic Map of Idaho: Idaho Department of Lands, Bureau of Mines and Geology.

Bond, J. G., Kauffman, T. D., Miller, D. A., and Barrash, W., Geoscience Research Consultants, 1978, Geology of the Southwest Pasco Basin: RHO-BWI-C-25, Rockwell Hanford Operations, Richland, Washington.

Bostock, H. S., 1963, Geology, Squamish, British Columbia: Geological Survey of Canada Map 42-1963.

Bouma, A. H., 1962, Sedimentology of Some Flysch Deposits, Graphic Approach to Facies Interpretation: Elsevier Publishing Co., Amsterdam, 168 p.

Bradshaw, H. E., 1964, Geology of the Palmer Volcanics: Masters Thesis, University of Oregon, Eugene.

Brazee, R. J., 1980, Reevaluation of Modified Mercalli Intensity Scale, Using Distance as Determinant: U.S. Nuclear Regulatory Commission, NUREG/CR-1804; NOAA Technical Memorandum EDIS NGSDC-4.



Bretz, J. H., 1923, The Channeled Scablands of the Columbia Plateau: Journal of Geology, V. 31, No. 8, p. 617-649.

Bretz, J. H., 1928, The Channeled Scabland of Eastern Washington: American Geological Society, Geology Review, v. 18, no. 3, p. 446-477.

Bretz, J. H., 1929, Valley Deposits Immediately East of the Channeled Scabland of Washington II: Journal of Geology, v. 37, no. 6, p. 505-541.

Bretz, J. H., Smith, H. T. U., and Neff, G. E., 1956, Channeled Scabland of Washington--New Data and Interpretations: Geological Society of America Bulletin, v. 67, No. 8, p. 957-1049.

Bright, R. C., 1963, Pleistocene Lakes Thatcher and Bonneville, Southeastern Idaho: Ph.D. Dissertation, University of Minnesota, Minneapolis.

Brooks, W. E., Jr., 1974, Stratigraphy and Structure of the Columbia River Basalt in the Vicinity of Gable Mountain, Benton County, Washington: Master's Thesis, University of Washington, Seattle Washington.

Brown, B. H., 1937, The State Line Earthquake at Milton and Walla Walla: Seismological Society of America Bulletin, v. 27, no. 3, p. 205-209.

Brown, D. E., McLean, G. D., Priest, G. R., Woller, N. M., and Black, G. L., 1980a, Preliminary Geology and Geothermal Resource Potential of the Belknap-Foley Area, Oregon: Oregon Department of Geology and Mineral Industries Open-File Report 0-80-2, 58 p., 1 plate.

Brown, D. E., McLean, G. D., Woller, N. M., and Black, G. L., 1980b, Preliminary Geology and Geothermal Resource Potential of the Willamette Pass Area, Oregon: Oregon Department of Geology and Mineral Industries Open-File Report 0-80-3, 65 p., 1 plate.

Brown, D. E., McLean, G. D., and Black, G. L., 1980c, Preliminary Geology and Geothermal Resource Potential of the Northern Harney Basin, Oregon: Oregon Department of Geology and Mineral Industries Open-File Report 0-80-6, 52 p., 4 plates.

Brown, D. E., McLean, G. D., and Black, G. L., 1980d, Preliminary Geology and Geothermal Resource Potential of the Southern Harney Basin, Oregon: Oregon Department of Geology and Mineral Industries Open-File Report 0-80-7, 90 p., 8 plates.

Brown, D. J. and Ledgerwood, R. K., 1973, Stratigraphy and Structure of Yakima Basalt in the Pasco Basin, Washington: Geological Society of America Bulletin 77, Cordilleran Section Field Trip No. 6.

Brown, R. E., 1969, Some Suggested Rates of Deformation of the Basalts in the Pasco Basin, and Their Implications: Battelle Northwest Laboratory, Report No. BNWL-SA-2443, 10 p.

Brown, R. E., 1970, Interrelationships of Geologic Formations and Processes Affecting Ecology as Exposed at Rattlesnake Springs, Hanford Project: Battelle Northwest Laboratory, Arid Land Ecology Program, Reprint Series No. 3, BNWL-B-29.

Brown, R. E., 1975, Groundwater and the Basalts in the Pasco Basin: 13th Engineering Geology and Soils Engineering Symposium Proceedings, April 1975, Moscow, Idaho.

Brown, R. E., and McConiga, M. W., 1960, Some Contributions to the Stratigraphy and Indicated Deformation of the Ringold Formation: Northwest Science, v. 34, no. 2, p. 43-54.

Brown, R. E. and Brown, D. J., 1961, The Ringold Formation and its Relationships to Other Formations: Hanford Atomic Projects Operation, Report No. HW-SA-2319, 17 p.

Bruhn, R. L., 1979, Rock Structures Formed During Back-arc Basin Deformation in the Andes of Tierra del Fuego: Geological Society of America Bulletin, part 1, v. 90, p. 998-1012.

Bruhn, R. L., 1981, Preliminary Analysis of Deformation in Part of the Yakima Fold Belt, South-central Washington: Draft report prepared for Washington Public Power Supply System, Richland, Washington, 11 p.

Buckovic, W. A., 1974, The Cenozoic Stratigraphy and Structure of a Portion of the West Mt. Rainier Area, Pierce County, Washington: Master's Thesis, University of Washington, Seattle.

Bunker, R. C., 1980, Catastrophic Flooding in the Badger Coulee Area, South-central Washington: Unpublished Thesis, University of Texas at Austin, 184 p.

Bureau of Reclamation, 1974, Geologic and Seismic Evaluation of Grand Coulee Dam and Forebay: U.S. Department of the Interior, Bureau of Reclamation.

Byerly, G. and Swanson, D., 1978, Invasive Columbia River Basalt Flows along the Northwestern Margin of the Columbia Plateau, North-Central Washington: Geological Society of America Abstracts with Programs, V. 10, No. 3, p. 98.

Camp, V. E., 1976, Petrochemical Stratigraphy and Structure of the Columbia River Basalt, Lewiston Basin Area, Idaho-Washington: Ph.D. Dissertation, Washington State University, Pullman, Washington.

Camp, V. E. and Hooper, P. R., 1980, Tectonic Evolution of the Southeastern Part of the Columbia River Basalt Plateau: Geological Society of America Abstracts with Programs, V. 12, No. 3, p. 100-101.

Camp, V. E., Price, S. M., and Reidel, S. P., 1978, Descriptive Summary of the Grande Ronde Basalt Type Section Columbia River Basalt Group: RHO-BWI-LD-15, Rockwell Hanford Operations, Richland, Washington.

Campbell, A. B., and Raup, O. B., 1964, Preliminary Geologic Map of the Hunters Quadrangle, Stevens and Ferry Counties, Washington: U.S. Geological Survey Field Studies Map MF-176, Scale 1:48,000.

Campbell, N. and Bentley, R. 1980, Late Quaternary Faulting, Toppenish-Ridge-Southcentral Washington, Geological Society of America, Abstracts with Programs, V. 12, No. 3, p. 101.

Campbell, N. P. and Bentley, R. D., 1981, Late Quaternary Deformation of the Toppenish Uplift - a Yakima Fold in Southeastern Washington: unpublished manuscript submitted to Geology.

Canadian Geological Survey, 1973, Preliminary Compilation of the Geology of Parts of British Columbia and Washington, N.T.S. 92, Fraser River: Open-File Map 165, Scale 1:1,000,000.



Canadian Geological Survey, 1978, Preliminary Draft of Compilation of the Geology of Parts of British Columbia and Washington, N.T.S. 82, Kootenai River: Open-File Map 2216, Scale 1:1,000,000.

Cantwell, T. and Orange, A., 1965, Further Deep Resistivity Measurements in the Pacific Northwest: Journal of Geophysical Research, V. 70, No. 16, p. 4068.

Carnahan, G. L., 1962, Geology of Southwestern Part of the Eagle Cap Quadrangle, Wallowa Mountains: Master's Thesis, Oregon State University, Corvallis.

Carson, R. J., 1976, Preliminary Geologic Map of the Brinnon Area, Jefferson County: Washington Division of Geology and Earth Resources Open-File Map OF-76-3.

Carson, R. J., McKhann, C. F., and Pizey, M. H., 1978, The Touchet Beds of the Walla Walla Valley, in Baker, V. R., and Nummedal, D., eds., The Channeled Scabland: A guide to the geomorphology of the Columbia Basin, Washington: NASA Comparative Geology Conference, p. 173-186.

Cashman, S. M., 1974, Geology of the Peshastin Creek Area, Washington: Masters Thesis, University of Washington, Seattle.

Cater, F. W., and Crowder, D. F., 1967, Geologic Map of the Holden Quadrangle, Snohomish and Chelan Counties, Washington: U.S. Geological Survey Geologic Quadrangle Map GQ-646.

Cater, F. W., and Wright, T. L., 1967, Geologic Map of the Lucerne Quadrangle, Chelan County, Washington: U.S. Geological Survey Geologic Quadrangle Map GQ-647.

Christiansen, R. L., and McKee, E. H., 1979, Late Cenozoic Volcanic and Tectonic Evolution of the Great Basin and Columbia Intermontane Regions" in Smith, R. B., and Eaton, G. P., Eds.: Cenozoic Tectonics and Regional Geophysics of the Western Cordillera, Geological Society of America Memoir 152, p. 283-311.

Coates, J. A., 1970, Stratigraphy and Structure of Manning Park Area, Cascade Mountains, British Columbia: Geological Association of Canada Special Paper 6, p. 149-154.

Cockfield, W. E., 1961, Geology and Mineral Deposits of the Nicola Map-area, British Columbia: Canadian Geological Survey Memoir 249, Map 886-A.



Compton, R. R. et al., 1977, Oligocene and Miocene Metamorphism, Folding and Low Angle Faulting in Northwestern Utah: Geological Society of America Bulletin, V. 88, No. 9, p. 1237-1250.

Coney, P. J., 1979, Mesozoic-Cenozoic Cordilleran Plate Tectonics, in Smith, R. B., and Eaton, G. P., Eds., Cenozoic Tectonics and Regional Geophysics of the Western Cordillera, Geological Society of America Memoir 152, p. 33-50.

Conway, R. D., 1971, Geochemistry of the Cypress Island Ultramafic Body, Washington: Ph.D. Dissertation, University of Washington, Seattle, 108 p.

Coombs, H. A., 1941, Hornblende and Magnetite Heavies in the Ellensburg of Central Washington: Journal of Sedimentary Petrology, V. 11, No. 3, p. 142-144.

Coombs, H. A., 1953, A Summary of Washington Earthquakes: Seismological Society of America Bulletin, v. 43, no. 1., p. 1-5.

Coombs, H. A. (Chairman, Ad Hoc Committee on Geologic Hazards), 1974, Meeting the Geologic Hazards Challenge: Report to Washington State Legislature, December.

Coombs, H. A., Milne, W. G., Nuttli, O. W., and Slemmons, D. B., 1976, Report of the Review Panel on the December 14, 1872 Earthquake: Submitted to Washington Public Power Supply System, Richland, Washington.

Couch, R. W., and Lowell, R. P., 1971, Earthquakes and Seismic Energy Release in Oregon: The Ore Bin, v. 33, no. 4, p. 61-84.

Crandell, D. R., 1963, Surficial Geology and Geomorphology of the Lake Tapps Quadrangle, Washington: U.S. Geological Survey Professional Paper 388-A, 84 p.

Crandell, D. R., 1973, Map Showing Potential Hazards from Future Eruptions of Mount Rainier, Washington: United States Geological Survey, Miscellaneous Investigations Map I-836.

Crandell, D. R., 1976, Preliminary Assessment of Potential Hazards from Future Volcanic Eruptions in Washington: United States Geological Survey, Miscellaneous Field Studies Map MF-774.



Crandell, D. R., Mullineaux, D. R. and Rubin, M., 1975, Mount St. Helens Volcano: Recent and Future Behavior: Science, V. 187, No. 4175, p. 438-441.

Crandell, D. R., Mullineaux, D. R., 1976, Potential Hazards from Future Eruptions of Mount St. Helens Volcano, Washington: United States Geological Survey Open File Report 76-491, 25 p.

Crosson, R. J., 1980, Review of Seismicity in the Puget Sound Region from 1970 through 1978 - Brief Summary: Geophysics Program, University of Washington, Seattle, Washington.

Crowder, D. F., Tabor, R. W., and Ford, A. B., 1966, Geologic Map of the Glacier Peak Quadrangle, Snohomish and Chelan Counties, Washington: U.S. Geological Survey Geologic Quadrangle Map GQ-473..

Danes, Z. F., 1969, Gravity Results in the State of Washington: Northwest Science, V. 43, No. 1, p. 34.

Danner, W. R., 1966, Limestone Resources of Western Washington: Washington Division of Mines and Geology Bulletin 52, 474 p.

Davis, J. O., 1978, Quaternary Tephrochronology of the Lake Lahontan Area, Nevada and California: Nevada Geological Survey Archeological Research Paper No. 7.

Dings, M. G., and Whitebread, D. H., 1965, Geology and Ore Deposits of the Metaline Zinc-Lead District, Pend Oreille County, Washington: U.S. Geological Survey Professional Paper 489, 107 p.

Dionne, J. C., 1976, Miniature Mud Volcanoes and Other Injection Features in Tidal Flats, James Bay, Quebec: Canadian Journal of Earth Sciences, v. 13, no. 3, p. 422-428.

Dionne, J. C., and Shilts, W. W., 1974, A Pleistocene Clastic Dike, Upper Chaudiere Valley, Quebec: Canadian Journal of Earth Sciences, v. 11, p. 1594-1605.

Duffell, S., and McTaggart, K. C., 1952, Ashcroft Map-area, British Columbia: Canadian Geological Survey Memoir 262, Map 1010-A.



Dungan, M. A., 1974, The Origin, Emplacement, and Metamorphism of the Sultan Mafic-Ultramafic Complex, Snohomish County, Washington: Ph.D. Dissertation, University of Washington, Seattle.

Easterbrook, D. J., 1968, Pleistocene Stratigraphy of Island County; Part 1: Washington Department of Water Resources Water-Supply Bulletin No. 25.

Easterbrook, D. J., 1976, Geologic Map of Western Whatcom County, Washington: U.S. Geological Survey Miscellaneous Investigation Series Map I-854-B, Scale 1:62,500.

Eddy, P. A., 1971, Investigations - Geology and Ground Water Resources, Vicinity of Toutle River and SR 504, Cowlitz County, Washington: Washington Department of Ecology Technical Report 71-18.

Farkas, S. E., 1972, Structural Relationships of Folds and Faults in Yakima Basalt and Ellensburg Formation, Central Washington: Geological Society of America Abstracts with Programs, V. 4, No. 6, p. 375.

Fecht, K. R., 1978, Geology of Gable Mountain-Gable Butte Area: RHO-BWI-LD-5, Rockwell Hanford Operations, Richland, Washington.

Fifer, N. F., 1966, 1918 Corfu Earthquakes: Douglas United Nuclear, Richland, Washington, Report 1524, 3 p.

Fischer, J. F., 1971, The Geology of the White River-Carbon Ridge Area, Cedar Lake Quadrangle, Cascade Mountains: Ph.D. Dissertation, University of California, Santa Barbara.

Fischer, R. V., 1957, Stratigraphy of the Puget Group and Keechelus Group in the Elbe-Packwood Area of Southwestern Washington: Ph.D. Dissertation, University of Washington, Seattle, 157 p.

Fiske, R. S., Hopson, C. A., and Waters, A. E., 1963, Geology of the Mount Rainier National Park, Washington: U.S. Geological Survey Professional Paper 444.

Flint, R. F., 1938, Origin of the Cheney-Palouse Scabland Tract, Washington: Geological Society of America Bulletin, v. 49, p. 461-523.

Foley, L. L., 1976, Slack Water Sediments in the Alpowa Creek Drainage, Washington: M.A. thesis, Washington State University, Department of Anthropology, Pullman, Washington.



Foundation Sciences, Inc., 1980, Geologic Reconnaissance of Parts of the Walla Walla and Pullman, Washington, and Pendleton, Oregon 1° x 2° AMS Quadrangles: Prepared by Kienle, C. F., 76 p.

Fox, K. F., 1978, Geologic Map of the Mt. Bonaparte Quadrangle, Okanogan County, Washington: U.S. Geological Survey Open File Report 78-732, 1 plate, Scale 1:48,000.

Fox, K. F., Jr., and Rinehart, C. D., 1972, Distribution of Copper and Other Metals in Gully Sediments of Part of Okanogan County, Washington: Washington Division of Mines and Geology Bulletin 65, 38 p.

Fox, K. F., Jr., Rinehart, C. D., and Engels, J. C., 1977, Plutonism and Orogeny in North Central Washington: United States Geological Survey Professional Paper 989, 27 p.

Fruchter, J. S. and Baldwin, S. F., 1975, Correlations Between Dikes of the Monument Swarm, Central Oregon, and Picture Gorge Basalt Flows: Geological Society of America Bulletin, V. 86, No. 4, p. 514.

Fryxell, R., 1965, Mazama and Glacier Peak Volcanic Ash Layers; Relative Ages: Science, V. 147, No. 3663, p. 1288-1290.

Fulton, R. J., 1972, Bedrock Topography of the North Okanogan Valley and Stratigraphy of Unconsolidated Valley Fill: Canadian Geological Survey Paper 72-8, pt. B.

Garling, M. E., Molenaar, D., Bailey, E. G., and others, 1965, Water Resources and Geology of the Kitsap Peninsula and Certain Adjacent Islands: Washington Division of Water Resources Bulletin 18, 309 p.

Gayer, M. J., 1976, Geologic Map of Northeastern Jefferson County, Washington: Washington Division of Geology and Earth Resources Open File Map OF-76-21.

Ginsberg, R. N., 1973, Evolving Concepts in Sedimentology: Johns Hopkins University Press, Baltimore and London.

Glass, C. E., 1979, Interpretation of U-2 and Forest Service photography, Letter to David Tillson, Principal Geologist, Washington Public Power Supply System regarding air photo interpretation of Toppenish Ridge.





Glass, C. E., 1981, Washington Public Power Supply System Hanford Projects Remote Sensing Task C-9, Trip Report 2-21-81: Letter to John Doherty, Project Manager, Weston Geophysical Corporation regarding aerial reconnaissance of Toppenish Ridge.

Glover, S. L., 1935, Preliminary Report on Petroleum and Natural Gas in Washington: Washington Department of Conservation and Development, Report of Investigation No. 4, p. 10-15.

Glover, S. L., 1953, Addenda to Preliminary Report on Petroleum and Natural Gas in Washington: Washington Department of Conservation and Development.

Goff, F. E., 1981, Preliminary Geology of Eastern Umtanum Ridge, South-Central Washington: Rockwell Hanford Operations, Richland, Washington, Report RHO-BWI-C-21, 100 p.

Goff, F. E. and Myers, C. W., 1978, Structural Evolution of East Umtanum and Yakima Ridges, South-Central Washington: Geological Society of America, Abstracts with Programs, V. 10, No. 7, p. 408.

Golder Associates, 1981a, Gable Mountain: Structural Investigations and Analyses: Report prepared for Northwest Energy Services Company, June 1981, 54 p.

Golder Associates, 1981b, Geologic Structure of Umtanum Ridge: Priest Rapids Dam to Sourdough Canyon: Report prepared for Northwest Energy Services Company, 54 p.

Gower, H. D., 1978, Tectonic Map of the Puget Sound Region, Showing Locations of Faults, Principal Folds and Large-Scale Quaternary Deformation: U.S. Geological Survey Open-File Report OF-78-426.

Gower, H. D., and Pease, M.H., Jr., 1965, Geology of the Montesano Quadrangle: Washington: U.S. Geological Survey Geologic Quadrangle Map GQ-374.

Gresens, R. L., 1976, A New Tertiary Formation Near Wenatchee, Washington: Geological Society of America Abstracts with Programs, v. 8, no. 3, p. 376-377.

Griggs, A. B., 1973, Geologic Map of the Spokane Quadrangle, Washington, Idaho, and Montana: U.S. Geological Survey Miscellaneous Investigations Map I-768.



Grolier, M. J., 1965, Geology of Part of the Big Bend Area in the Columbia Plateau, Washington: Ph.D. Dissertation, The Johns Hopkins University, Baltimore, Maryland.

Grolier, M. J., and Bingham, J. W., 1971, Geologic Map and Sections of Parts of Grant, Adams, and Franklin Counties, Washington: United States Geological Survey, Miscellaneous Geologic Investigations Map I-589.

Grolier, M. J., and Bingham, J. W., 1978, Geology of Parts of Grant, Adams, and Franklin Counties, East-Central Washington: Washington Division of Mines and Geology Bulletin 71, Olympia, Washington, 91 p.

Gunning, H. C. and White, W. H., Editions, 1966, Tectonic History and Mineral Deposits of the Western Cordillera: Canadian Institute of Mining and Metallurgy, Special Volume No. 8.

Gustafson, E. P., 1973, The Vertebrate Fauna of the Late Pliocene Ringold Formation, South-Central Washington: Masters's Thesis, Washington State University, Pullman, Washington.

Gustafson, E. P., 1978, The Vertebrate Faunas of the Pliocene Ringold Formation, South-central Washington: Museum of Natural History Bulletin no. 23, University of Oregon, Eugene, Oregon, 62 p.

Gutenberg, B., and Richter, C. F., 1965, Seismicity of the Earth and Associated Phenomena: Hafner Publishing Company, New York, New York, 310 p.

Hamilton, W., 1969, Reconnaissance Geologic Map of the Riggins Quadrangle, West-central Idaho: U.S. Geological Survey Miscellaneous Investigations Map I-579.

Hammatt, H. H., Foley, L. L., and Leonhardy, F. C., 1976, Late Quaternary Stratigraphy in the lower Snake River Canyon: Toward a Chronology of Slackwater Sediments: Geological Society of America Abstracts with Programs, v. 8, no. 3, p. 379.

Hammond, P. E., 1975, Preliminary Geologic Map and Cross Sections With Emphasis on Quaternary Volcanic Rocks, Southern Cascade Mountains, Washington: Washington Division of Geology and Earth Resources Open-File Map OF-75-13.

Hammond, P. E., Pederson, S. A., Hopkins, K. D., Aiken, D., Harle, D. S., Danes, Z. F., Konicek, D. L. and Stricklin, C. R., 1976, Geology and Gravimetry of the Quaternary Basaltic Volcanic Field, Southern Cascade Range, Washington: in Proceedings of the Second United Nations Symposium on the Development and Use of Geothermal Resources, San Francisco, 1975, Vol. 1, p. 397-404.

Hampton, E. R., and Brown, S. G., 1964, Geology and Ground-water Resources of the Upper Grande Ronde River Basin, Union County, Oregon: U.S. Geological Survey Water-Supply Paper 1597, 99 p.

Hanson, K. L., 1976, Geologic Map of the Orcas-Port Ludlow Area, Jefferson County, Washington: Washington Division of Geology and Earth Resources Open-File Map OF-76-20.

Hart, D. H., and Newcomb, R. C., 1967, Geology and Ground-water of the Tualatin Valley, Oregon: U.S. Geological Survey Water-Supply Paper 1697, 172 p.

Hartman, D. A., 1973, Geology and Low-grade Metamorphism of the Greenwater River Area, Central Cascade Range, Washington: Ph.D. Dissertation, University of Washington, Seattle.

Hawkins, J. W., 1968, Regional Metamorphism, Metasomatism and Partial Fusion in the Northwestern Part of the Okanogan Range, Washington: Geological Society of America Bulletin, Vol. 79, No. 12, p. 1785-1820.

Hayashi, Tadaichi, 1966, Clastic Dikes in Japan: Japanese Journal of Geology and Geography, v. 37, no. 1, p. 1-20.

Heath, M. T., 1971, Bedrock Geology of the Monte Cristo Area, Northern Cascades, Washington: Ph.D. Dissertation, University of Washington, Seattle.

Henriksen, D. A., 1956, Eocene Stratigraphy of the Lower Cowlitz River - Eastern Willapa Hills Area, Southwestern Washington: Washington Division of Mines and Geology Bulletin 43, 122 p.

Hibbard, M. J., 1971, Evolution of a Plutonic Complex, Okanogan Range, Washington: Geological Society of America Bulletin, Vol. 82, No. 11, p. 3013-3048.

Hietanen, A., 1963a, Anorthosite and Associated Rocks in the Boehls-Butte Quadrangle and Vicinity, Idaho: U.S. Geological Survey Professional Paper 344-B, 78 p.



Hietanen, A., 1963b, Metamorphism of the Belt Series in the Elk River-Clark Area, Idaho: U.S. Geological Survey Professional Paper 344-C, 49 p.

Hill, D. P., 1972, Crustal and Upper Mantle Structure of the Columbia Plateau from Long Range Seismic-Refraction Measurements: Geological Society of America Bulletin, V. 83, No. 6, p. 1639-1648.

Hill, D. P., 1980, Seismic Evidence for the Structure and Cenozoic Tectonics of the Pacific Coast States, in Smith, R. B., and Eaton, G. P., Eds., Cenozoic Tectonics and Regional Geophysics of the Western Cordillera, Geological Society of America Memoir 152, p. 145-174.

Hogenson, G. M., and Foxworthy, B. L., 1965, Groundwater in the East Portland Area, Oregon: U.S. Geological Survey Water-Supply Paper 1793, 78 p.

Holden, G. S., 1974, Chemical and Petrographic Stratigraphy of the Columbia River Basalt in the Lower Salmon River Canyon, Idaho: Master's Thesis, Washington State University, Pullman, Washington.

Hopson, C. A. and Mattinson, J. M., 1973, Ordovician and Late Jurassic Ophiolitic Assemblages in the Pacific Northwest: Geological Society of America Abstracts with Programs, V. 5, No. 1, p. 57.

Hosterman, J. W., Scheid, V. E., Allen, V. T., and Sohn, I. G., 1960, Investigations of Some Clay Deposits in Washington and Idaho: U.S. Geological Survey Bulletin 1091, 147 p.

Howell, B. F., Jr., and Schultz, T. R., 1975, Attenuation of Modified Mercalli Intensity with Distance from the Epicenter: Seismological Society of America Bulletin, v. 65, no. 3, p. 651-665.

Hunting, M. T., Bennett, W. A., Livingston, V. E., and Moen, W. S., compilers, 1961, Geologic Map of Washington: Washington Department of Conservation, Scale 1:500,000.

Hyndman, D. W., 1968, Petrology and Structure of Nakusp Map-area, British Columbia: Canadian Geological Survey Bulletin 161.

Jahns, R. H., 1967, Geologic Factors Relating to Engineering Seismology in the Hanford Area, Washington: Douglas United Nuclear, Inc., Report DUN-3100, Richland, Washington.

Jenkins, O. P., 1925, Clastic Dikes of Eastern Washington and Their Geologic Significance: American Journal of Science, 5th series, v. 10, p. 234-246.

Jones, A. G., 1959, Vernon Map-area, British Columbia: Canadian Geological Survey Memoir 296, Map 1059A, 186 p.

Jones, F. O., and Deacon, R. J., 1966, Geology and Tectonic History of the Hanford Area and its Relation to the Geology and Tectonic History of the State of Washington and the Active Seismic Zones of Western Washington and Western Montana: Report Prepared for Douglas United Nuclear, Inc., DUN-1410, Richland, Washington.

Jones, M. G., and Landon, R. D., 1978, Geology of the Nine Canyon Map Area: RHO-BWI-LD-6, Rockwell Hanford Operations, Richland, Washington.

Kendall, J. J., and Dale, R. C., and Davis, G. A., 1981, The Structural Relationship of the Olympic-Wallula Lineament, Hite Fault System and LaGrande Fault System, the Blue Mountains of Umatilla County Oregon: Geological Society of America Abstracts with Programs V. 13, No. 2, p. 64.

Kiel, W. and Davis, G., 1980, Unpublished Field Notes - Aerial Reconnaissance of Toppenish Ridge.

King, P. B., 1959, The Evolution of North America: Princeton University Press, Princeton, N. J., 190 p.

King, P. B., 1969, The Tectonics of North America - A Discussion to Accompany the Tectonic Map of North America: United States Geological Survey, Professional Paper 628, 94 p.

Kleck, W. D., 1976, Chemistry, Petrography, and Stratigraphy of the Columbia River Group in the Imnaha River Valley Region, Eastern Oregon and Western Idaho: Ph.D. Dissertation, Washington State University, Pullman, Washington.

Kleinkopf, M. D., Harrison, J. E., and Zartman, R. E., 1972, Aeromagnetic and Geologic Map of Part of Northwestern Montana and Northern Idaho.: U.S. Geological Survey Geophysical Investigations Map GP-830.

Ku, T. L., Personal communication to Woodward-Clyde Consultants.

Kuenen, P. H., 1967, Geosynclinal Sedimentation: Geologische Rundschau, v. 56, no. 1, p. 1-19.

Laravie, J. A., 1976, Geologic Field Studies Along the Eastern Border of the Chiwaukum Graben, Central Washington: Master's Thesis, University of Washington, Seattle.

Laval, W. N., 1956, Stratigraphy and Structural Geology of Portions of South-Central Washington: Ph.D. Dissertation, University of Washington, Seattle.

Lawrence R. D., 1968, The Eightmile Creek Fault, Northeastern Cascade Range, Washington: Ph.D. dissertation, Stanford University.

Lawrence, R. D., 1976, Strike-slip Faulting Terminates the Basin and Range Province in Oregon: Geological Society of America Bulletin, V. 87, No. 6, p. 846-850.

Lentz, R. T., 1977, Petrology and Stratigraphy of the Portland Hills Silt: Master's Thesis, Portland State University, Portland, 144 p.

Lindberg, J. W., and Brown, R. E., 1981, Pleistocene Catastrophic Flood Deposits of the Pasco Basin, Washington, and the Role of the Snake River: Geological Society of America, Abstracts with Programs, v. 13, no. 2, p. 67.

Little, H. W., 1957, Kettle River (east half), Similkameen, Kootenay and Osoyoos Districts, British Columbia: Canadian Geological Survey Map 6-1957, Scale 1:253,440.

Little, H. W., 1960, Nelson Map-area, West Half, British Columbia: Canadian Geological Survey Memoir 308, 205 p.

Little, H. W., 1961, Geology, Kettle River (west half), British Columbia: Canadian Geological Survey Map 15-1961, Scale 1:253,440.

Livingston, V. E., Jr., 1966, Geology and Mineral Resources of the Kelso-Cathlamet Area, Washington: Washington Division of Mines and Geology Bulletin 54.

Livingston, V. E., Jr., 1969, Geologic History and Rocks and Minerals of Washington: Washington Division Mines and Geology, Information Circular 45, 42 p.

Livingston, V. E., Jr., 1971, Geology and Mineral Resources of King County, Washington: Washington Division of Mines of Geology Bulletin 63.



Long, P. E., 1978, Characterization and Recognition of Intraflow Structures, Grande Ronde Basalt: Rockwell Hanford Operations, Richland, Washington, Report RHO-BWI-LD-10.

Loring, A. K., 1976, Distribution in Time and Space of Late Phanerozoic Normal Faulting in Nevada and Utah: Utah Geology, V. 3, No. 2, p. 97-109.

Lovseth, T. P., 1975, The Devils Mountain Fault Zone, Northwestern Washington: Master's Thesis, University of Washington, Seattle, 29 p.

Lowes, B. E., 1971, Metamorphic Petrology and Structural Geology of the Area East of Harrison Lake, British Columbia: Ph.D. Thesis, University of Washington, Seattle.

Lupher, R. L., 1944, Clastic Dikes of the Columbia Basin Region, Washington and Idaho: Geological Society of America Bulletin, V. 55, No. 12, p. 1431-1462.

Mackin, J. H., 1961, A Stratigraphic Section in the Yakima Basalt and the Ellensburg Formation in South-Central Washington: Report of Investigations No. 19, Washington Division of Mines and Geology, Olympia, Washington, 45 p.

MacLeod, N. S., Tiffin, D. L., Snavelly, P. D., Jr., and Currie, R. G., 1977, Geologic Interpretation of Magnetic and Gravity Anomalies in the Strait of Juan de Fuca, U.S.-Canada: Canadian Journal of Earth Science, Vol. 14, No. 2, p. 223-238.

Malde, H. E., 1968, the Catastrophic Late Pleistocene Bonneville Flood in the Snake River Plain, Idaho: U.S. Geological Survey Professional Paper 506, 52 p.

Malde, H. E., and Powers, H. A., 1962, Upper Cenozoic Stratigraphy of Western Snake River Plain, Idaho: Geological Society of America Bulletin, v. 73, no. 10, p. 1197-1219.

Malone, S. D., 1979, Annual Technical Report on Earthquake Monitoring of the Hanford Region, Eastern Washington: Report prepared for the U.S. Department of Energy and Washington Public Power Supply System by the Geophysics Program, University of Washington, Seattle, Washington.

Malone, S. D., and Bor, S. S., 1979, Attenuation Patterns in the Pacific Northwest Based on Intensity Data and the Location of the 1872 North Cascades Earthquake: Seismological Society of America Bulletin, v. 59, no. 2, p. 531-540.

Mattinson, J. M., 1977, Emplacement History of the Tatoosh Volcanic-plutonic Complex, Washington: Ages of Zircons: Geological Society of America Bulletin, Vol. 88, No. 10, p. 1509-1514.

Mayers, I. R., 1971, An Analysis of Continuous Seismic Profiles From the Strait of Juan de Fuca: Master's Thesis, University of Washington, Seattle.

McConiga, M. W., 1955, Deformation of the Ringold Formation: Hanford Atomic Products Operation, Richland, Washington.

McKee, 1972, Cascadia, The Geologic Evolution of the Pacific Northwest: McGraw-Hill Book Company, New York, N.Y., 394 p.

McKee, E. H., Swanson, D. A., and Wright, T. L., 1977, Duration and Volume of Columbia River Basalt Volcanism; Washington, Oregon and Idaho: Geological Society of America Abstracts with Programs, V. 9, no. 4, p. 463.

McLean, Hugh, 1977, Lithofacies of the Blakeley Formation, Kitsap County, Washington, a Submarine Fan Complex: Journal of Sedimentary Petrology, Vol. 47, No. 1, p. 78-88.

Menzer, F. J., Jr., 1964, Geology of the Crystalline Rocks West of Okanogan, Washington: Ph.D. Dissertation, University of Washington, Seattle.

Menzer, F. J. and Swanberg, C., 1969, Reverse Faulting Along the West Border of the Central Okanogan Range, Washington: Geological Society of America Special Paper 121, p. 405.

Merriam, J. C., and Buwalda, J. P., 1917, Age of Strata Referred to the Ellensburg Formation in the White Bluffs of the Columbia River: University of California Publications, Bulletin of Geology, v. 10, no. 15, p. 255-266.

Miller, F. K., 1974a, Preliminary Geologic Map of the Newport Number 1 Quadrangle, Pend Oreille County, Washington and Bonner County, Idaho: Washington Division of Geology and Earth Resources Geologic Map GM-7.

Miller, F. K., 1974b, Preliminary Geologic Map of the Newport Number 2 Quadrangle, Pend Oreille and Stevens Counties, Washington: Washington Division of Geology and Earth Resources Geologic Map GM-8.

Miller, F. K., 1974c, Preliminary Geologic Map of the Newport Number 3 Quadrangle, Pend Oreille, Stevens, and Spokane Counties, Washington: Washington Division of Geology and Earth Resources Geologic Map GM-9.

Miller, F. K., 1974d, Preliminary Geologic Map of the Newport Number 4 Quadrangle, Spokane and Pend Oreille Counties, Washington and Bonner County, Idaho: Washington Division of Geology and Earth Resources Geologic Map GM-10.

Miller, F. K., and Clark, L.D., 1975, Geology of the Chewelah-Loon Lake Area, Stevens and Spokane Counties, Washington: U.S. Geological Survey Professional Paper 806.

Miller, F. K., and Yates, R.G., 1976, Geologic Map of the West Half of the Sandpoint 1°x2° Quadrangle, Washington: U.S. Geological Survey Open-File Report OF-76-327.

Miller, G. M., 1979, Western Extent of the Shuksan and Church Mountain Thrust Plates in Whatcom, Skagit, and Snohomish Counties, Washington: Northwest Science, Vol. 53, No. 4, p. 229-240.

Miller, R. B., 1977a, oral communication to Dr. G. A. Davis.

Miller, R. B., 1977b, Structure and Petrology of the Ingalls Mafic - Ultramafic Complex and Associated Pre-Tertiary Rocks, Central Washington Cascades: Geological Society of America Abstracts with Programs, V. 9, No. 4, p. 468.

Milne, W. G., 1956, Seismic Activity in Canada West of the 113th Meridian, 1841-1951: Canadian Dominion Observatory Publication, v. 18, no. 7, p. 119-146.

Misch, P., 1966, Tectonic Evolution of Northern Cascades of Washington State, a West-Cordilleran Case History: in, Gunning, H. C., Ed., A Symposium on the Tectonic History and Mineral Deposits of the Western Cordillera in British Columbia and Neighboring Parts of the United States: Special Report, Canadian Institute of Mining and Metallurgy, V. 8, p. 101-148.



Misch, 1977a, Bedrock Geology of the North Cascades: in Brown, E. H. and Ellis, R. C. Eds., Geological Excursions in the Pacific Northwest: Geological Society of America 1977 Annual Meeting, Seattle, Washington, p. 1-62.

Misch, P., 1977b, Dextral Displacements at some Major Strike Faults in the North Cascades: Geological Association of Canada Program with Abstracts, p. 37.

Molenaar, D., and Noble, J.B., 1970, Geology and Related Groundwater Occurrence, Southeastern Mason County, Washington: Washington Department of Water Resources Water-Supply Bulletin 29, 145 p.

Monger, J. W. H., 1968, Early Tertiary Stratified Rocks, Greenwood Map-area, (82 E/2) British Columbia: Canadian Geological Survey Paper 67-42, 39 p.

Monger, J. W. H., 1969, Hope (west half), British Columbia: Canadian Geological Survey Paper 69-47, Map 12-1969.

Moore, J. L., 1965, Surficial Geology of the Southwestern Olympic Peninsula: Master's Thesis, University of Washington, Seattle.

Muessig, 1967, Geology of the Republic Quadrangle and a Part of the Aeneas Quadrangle, Ferry County, Washington, U.S. Geological Survey Bulletin 1216, 135 p.

Muir, S. C., and Fritsche, A. E., 1981, Three Dimensional Model of Probable Earthquake-induced Intrusion Structure in Kern Lake Sediment Compared with Sandblow Feature Formed During the 1979 Imperial Valley Earthquake: Geological Society of America Abstracts with Programs, v. 13, no. 2, p. 98.

Mulcahey, M. T., 1975, The Geology of Fidalgo Island and Vicinity, Skagit County, Washington: Master's Thesis, University of Washington, Seattle, 49 p.

Muller, J. E., 1977, Geology of Vancouver Island: Canadian Geological Survey Open-File Report 463.

Mullineaux, D. R., Hyde, J. H. and Rubin, M., 1975, Widespread Late Glacial and Postglacial Tephra Deposits from Mount St. Helens Volcano, Washington: United States Geological Survey, Journal of Research, V. 3, No. 3, p. 329-335.

Mullineaux, D. R., Wilcox, R. E., Ebaugh, W. F., Fryxell, R., and Rubin, M., 1977, Age of the Last Major Scabland Flood of Eastern Washington, as Inferred from Associated Ash Beds of Mount St. Helens Set S: Geological Society of America Abstracts with Programs, V. 9, No. 7, p. 1105.

Mullineaux, D. R., Wilcox, R. E., Ebaugh, W. F., Fryxell, R., and Rubin, M., 1978, Age of the Last Major Scabland Flood of the Columbia Plateau in Eastern Washington: Quaternary Research, v. 10, p. 171-180.

Mundorff, M. J., 1964, Geology and Groundwater Conditions of Clark County, Washington: Washington Division of Water Resources Water-Supply Bulletin 9.

Myers, C. W., 1973, Yakima Basalt Flows near Vantage, and from Core Holes in the Pasco Basin, Washington: Ph.D. Dissertation, University of California at Santa Cruz, Santa Cruz, California.

Myers, D. A., 1970, Availability of Ground Water in Western Cowlitz County, Washington: Washington Department of Ecology Water-Supply Bulletin 35.

Nathan, S. and Fruchter, J. S., 1974, Geochemical and Paleomagnetic Stratigraphy of the Picture Gorge and Yakima Basalts (Columbia River Group) in Central Oregon: Geological Society of America Bulletin, V. 85, No. 1, p. 63 - 76.

Neumann, F., 1938, United States Earthquakes, 1936: U.S. Coast and Geodetic Survey, Serial No. 610, p. 45.

Newcomb, R. C., 1952, Ground-water Resources of Snohomish County, Washington: U.S. Geological Survey Water-Supply Paper 1135.

Newcomb, R. C., 1958, Ringold Formation of Pleistocene Age in Type Locality, the White Bluffs, Washington: American Journal of Science, V. 256, No. 5, p. 328-340.

Newcomb, R. C., 1961, Age of the Palouse Formation in the Walla Walla and Umatilla River Basins, Oregon and Washington: Northwest Science, v. 35, no. 4, p. 122-127.

Newcomb, R. C., 1962, Hydraulic Injection of Clastic Dikes in the Touchet Beds, Washington, Oregon, and Idaho: Geological Society of Oregon Country Geology Newsletter, v. 28, No. 10, p. 70.



Newcomb, R. C., 1965, Geology and Groundwater Resources of the Walla Walla River Basin, Washington-Oregon: Washington Division of Water Resources Water Supply Bulletin 21.

Newcomb, R. C., 1969a, Geology of the Deschutes-Umatilla Plateau: in Mineral and Water Resources of Oregon, Oregon Department of Geology and Mineral Industries Bulletin 64, in cooperation with U.S. Geological Survey, p. 60-66.

Newcomb, R. C., 1969b, Effect of Tectonic Structure on the Occurrence of Groundwater in the Basalt of the Columbia River Group of The Dalles Area, Oregon and Washington: U.S. Geological Survey Professional Paper 383-C.

Newcomb, R. C., 1970, Tectonic Structure of the Main Part of the Columbia River Group, Washington, Oregon, and Idaho: U.S. Geological Survey Miscellaneous Investigations Map I-587.

Newcomb, R. C., Sceva, J. E., and Stromme, O., 1949, Ground-water Resources of Western Whatcom County, Washington: U.S. Geological Survey Open-File Report, 133 p.

Newcomb, R. C., Strand, J. R., and Frank, F. J., 1972, Geology and ground-water characteristics of the Hanford Reservation of the Atomic Energy Commission, Washington; U.S. Geological Survey Professional Paper 717, 78 p.

Newton, V. C., Jr., and Van Atta, R. O., 1976, Geology, Prospective Fold Structures, and Reservoir Characteristics in the Upper Nehalem River Basin, Oregon: Oregon Department of Geology and Mineral Industries Short Paper No. 5, p. 1-25.

Noble, J. B., and Wallace, E. F., 1966, Geology and Ground-water Resources of Thurston County, Washington: Washington Division of Water Resources Water-Supply Bulletin 10, Vol. 2, 141 p.

Nolf, B., 1966, Structure and Stratigraphy of Part of the Northern Wallowa Mountains, Oregon: Ph.D. Dissertation, Princeton University, Princeton, N.J., 193 p.

Norbisrath, H., 1939, Geology of the Mt. Vernon Area: B.S. Thesis, University of Washington, Seattle.

Oles, K. F., 1956, Geology and Petrology of the Crystalline Rocks of the Beckler River-Nason Ridge Area, Washington: Ph.D. Dissertation, University of Washington, Seattle.





Othberg, K., 1978, Reconnaissance Surficial Geologic Map of Eastern Clallam County Washington: Washington Division of Geology and Earth Resources, unpublished map.

Pardee, J. T., 1942, Unusual Currents in Glacial Lake Missoula, Montana: Geological Society of America Bulletin, v. 53, no. 11, p. 1569-1600.

Parker, R. L., and Calkins, J. A., 1964, Geology of the Curlew Quadrangle, Ferry County, Washington: U.S. Geological Survey Bulletin 1169, 95 p., Scale 1:62,500.

Pearson, R. C., 1967, Geologic Map of the Bodie Mountain Quadrangle, Ferry and Okanogan Counties, Washington: U.S. Geological Survey Geologic Quadrangle Map GQ-636.

Pearson, R. C., and Obradovich, J. D., 1977, Eocene Rocks in Northeast Washington - Radiometric Ages and Correlation: U.S. Geological Survey Bulletin 1433.

Pease, M. H., Jr., and Hoover, L. Jr., 1957, Geology of the Doty-Minot Peak Area, Washington: U.S. Geological Survey Oil and Gas Investigations Map OM-188.

Peck, D. L., 1961, Geologic Map of Oregon West of the 121st Meridian: U.S. Geological Survey Miscellaneous Investigations Map I-325, Scale 1:500,000.

Peck, D. L., Griggs, A. B., Schlicker, H. G., and others, 1964, Geology of the Central and Northern Parts of the Western Cascade Range in Oregon: U.S. Geological Survey Professional Paper 449, 56 p.

Pierce, R. L., Obradovich, J. D., and Friedman, I., 1976, Obsidian Hydration Dating and Correlation of Bull Lake and Pinedale Glaciations Near West Yellowstone, Montana: Geological Society of America Bulletin, V. 87, No. 1, p. 61-75.

Piper, A. M., 1942, Ground-water Resources of the Willamette Valley, Oregon: U.S. Geological Survey Water-Supply Paper 890, 194 p.

Plummer, C. C., 1964, Geology of the Mount Index Area of Washington State: Master's Thesis, University of Washington, Seattle.

Pongsapich, W., 1970, A Petrographic Reconnaissance of the Swauk, Chuckanut, and Roslyn Formations, Washington: Master's Thesis, University of Washington, Seattle.



Poppe, B. B., 1979, Historical Survey of U.S. Seismograph Stations: U.S. Geological Survey Professional Paper 1096.

Porter, S. C., 1976, Stratigraphy and Distribution of Tephra from Glacier Peak (of 12,000 Years Ago) in the Northern Cascade Range, Washington, United States Geological Survey Open-File Report 76-186.

Powers, H. A. and Wilcox, R. E., 1964, Volcanic Ash from Mount Mazama (Crater Lake) and from Glacier Peak: Science, V. 144, No. 3624, p. 1334-1336.

Pratt, R. M., 1954, Geology of the Deception Pass Area, Chelan, King, and Kittitas Counties, Washington: Master's Thesis, University of Washington, Seattle.

Pratt, R. M., 1958, Geology of the Mount Stuart Area, Washington: Ph.D. Dissertation, University of Washington, Seattle.

Price, D., 1967a, Geology and Water Resources in the French Prairie Area, Northern Willamette Valley, Oregon: U.S. Geological Survey Water-Supply Paper 1833, 98 p.

Price, D., 1967b, Ground-water in the Eola-Amity Hills Area, Northern Willamette Valley, Oregon: U.S. Geological Survey Water-Supply Paper 1847, 66 p.

Price, E. H., 1980, Strain Distribution and Model for Formation of Eastern Umtanum Ridge Anticline, South-Central Washington: Rockwell Hanford Operations, Richland, Washington, Report RHO-BWI-SA-30.

Price, E. H., 1981a, Structural Geometry, Strain Distribution and Tectonic Evolution of Umtanum Ridge at Priest Rapids and a Comparison with Other Selected Localities within Yakima Fold Structures, South-Central Washington: In press, Rockwell Hanford Operations, Richland, Washington, Report RHO-BWI-FA-138.

Price, E. H., 1981b, Written communication to Woodward-Clyde Consultants.

Price, S. M., 1977, An Evaluation of Dike-Flow Correlations Indicated by Geochemistry, Chief Joseph Swarm, Columbia River Basalt: Ph.D. Dissertation, University of Idaho, Moscow, Idaho.



Puget Power and Light Company, 1974, Skagit Nuclear Power Project, Preliminary Safety Analysis Report: Docket Nos. STN-50-522/523, 9 Volumes.

Ragan, D. M., 1963, Emplacement of the Twin Sisters Dunit, Washington: Washington Division of Mines and Geology Reprint No. 8, p. 549-565.

Raisz, E., 1945, The Olympic-Wallowa Lineament: American Journal of Science, V. 243-A, p. 479-485.

Rasmussen, N., 1967, Washington State Earthquakes, 1940 through 1965: Seismological Society of America Bulletin, v. 57, no. 3, p. 463-476.

Rau, W. W., 1966, Stratigraphy and Foraminifera of the Satsop River Area, Southern Olympic Peninsula, Washington: Washington Division of Mines and Geology Bulletin 53, 66 p.

Rau, W. W., 1967, Geology of the Wynoochee Valley Quadrangle, Grays Harbor County, Washington: Washington Division of Mines and Geology Bulletin 56, 51 p.

Rau, W. W., 1975, Geologic Map of the Destruction Island and Taholah Quadrangles, Washington: Washington Division of Geology and Earth Resources Geologic Map GM-13.

Raymond, J. R. and Tillson, D. D., 1968, Evaluation of a Thick Basalt Sequence in South-Central Washington, Geophysical and Hydrological Exploration of Rattlesnake Hills Deep Stratigraphic Test Well: Battelle Pacific Northwest Laboratory, Report BNWL-776, Richland, Washington.

Read, P. B., 1976, Lardeau Map-area, British Columbia: Canadian Geological Survey Paper 76-1A, p. 95-96.

Reber, S. J., 1977, Chevron Oil, personal communication to Dr. G. A. Davis.

Reesor, J. E., 1957, Lardeau Map-area, East Half, British Columbia: Canadian Geological Survey Map 12-1957.

Reesor, J. E., 1958, Dewar Creek Map-area, British Columbia: Canadian Geological Survey Memoir 292.

Reesor, J. E., 1965, Structural Evolution and Plutonism in Valhalla Gneiss Complex, British Columbia: Canadian Geological Survey Bulletin 129, 128 p.

Reesor, J. E., 1973, Geology of the Lardeau Map-area, East Half: Canadian Geological Survey Memoir 369, Map 1326 A.

Reesor, J. E., and Moore, J. M., Jr., 1971, Petrology and Structure of Thor-Odin Gneiss Dome, Shuswap Metamorphic Complex, British Columbia: Canadian Geological Survey Bulletin 195, 149 p.

Reidel, S. P., 1978a, Stratigraphy and Petrogenesis of the Grande Ronde Basalt in the Lower Salmon and Adjacent Snake River Canyons: RHO-SA-62, Rockwell Hanford Operations, Richland, Washington.

Reidel, S. P., 1978b, Geology of the Saddle Mountains Between Sentinel Gap and 119° 31' Longitude: RHO-BWI-LD-4, Rockwell Hanford Operations, Richland, Washington.

Reidel, S. P., 1980, Oral presentation to Rockwell Hanford Operations.

Reidel, S. P., et al., 1980, Rate of Deformation in the Pasco Basin During the Miocene as Determined by Distribution of Columbia River Basalt Flows: Rockwell International, Rockwell Hanford Operations, report prepared by United States Department of Energy, RHO-BWI-SA-29, 43 p.

Rice, H. M. A., 1941, Nelson Map-area, East Half, British Columbia: Canadian Geological Survey Memoir 228.

Rice, H. M. A., 1947, Geology and Mineral Deposits of the Princeton Map-area, British Columbia: Canadian Geological Survey Memoir 243, Map 888-A, 136 p.

Richmond, G. M., 1965, Glaciation of the Rocky Mountains, in Wright, H. E. and Frey, D. G., eds., The Quaternary of the U.S.: Princeton University Press, Princeton, N.J.

Richmond, G. M., Fryxell, R., Neff, G. E., and Weis, P. L., 1965, The Cordilleran Icesheet of the Northern Rocky Mountains and Related Quaternary History of the Columbia Plateau: In Wright, H. E., and Frey, D. G., eds., The Quaternary of the United States: Princeton University Press, Princeton, New Jersey, p. 231-242.

Riddihough, R. P. and Hyndman, R. D., 1976, Canada's Active Western Margin - the Case for Subduction: Geoscience Canada, V. 3, No. 4, p. 269-278.

Rigby, J. G. and Othberg, K., 1979, Reconnaissance Surficial Geologic Mapping of the Late Cenozoic Sediments of the Columbia Basin, Washington: State of Washington, Department of Natural Resources, Open-File Report 79-3,

Rinehart, C. D., 1976, Reconnaissance Geochemical Survey of Gully Sediments and Geologic Summary in Part of the Okanogan Range, Okanogan County, Washington: U.S. Geological Survey Open-File Report OF-76-680.

Rinehart, C. D., and Fox, K.F., Jr., 1972, Geology and Mineral Deposits of the Loomis Quadrangle, Okanogan County, Washington: Washington Division of Mines and Geology Bulletin 64, 124 p.

Rinehart, C. D., and Fox, K.F., Jr., 1976, Bedrock Geology of the Conconully Quadrangle, Okanogan County, Washington: U.S. Geological Survey Bulletin 1402, Scale 1:62,500.

Robbins, S. L., Burt, R. J., and Gregg, D. D., 1975, Gravity and Aeromagnetic Study of Part of the Yakima River Basin, Washington: U.S. Geological Survey Professional Paper 726-E.

Roberts, A. E., 1958, Geology and Coal Resources of the Toledo-Castle Rock District, Cowlitz and Lewis Counties, Washington: U.S. Geological Survey Bulletin 1062.

Robyn, T. L., 1977, Geology and Petrology of the Strawberry Volcanics, NE Oregon: University of Oregon, Ph.D. dissertation, 197 p.

Robyn, T. L., Hoover, J. D., and Thayer, T. P., 1977, Geology and Geochronology of the Strawberry Volcanics, NE Oregon: Geological Society of America Abstracts with Programs, V. 9, No. 4, p. 488-489.

Rockwell, 1979, Geologic Studies of the Columbia Plateau, a Status Report: Rockwell Hanford Operations, Richland, Washington, Report RHO-BWI-ST-4.

Roddick, J. A., 1965, Vancouver North, Coquitlam, and Pitt Lake Map-areas: Canadian Geological Survey Memoir 335.

Rosenberg, E. A., 1961, Geology and Petrology of the Northern Wenatchee Ridge Area, Northern Cascades, Washington: Master's Thesis, University of Washington, Seattle.





Rosenmeier, F. J., 1968, Stratigraphy and Structure of the Table Mountain - Mission Peak Area in the Wenatchee Mountains, Central Washington: Masters Thesis, University of Washington, Seattle, 44 p.

Ross, C. P., 1938, The Geology of Part of the Wallowa Mountains: Oregon Department of Geology and Mineral Industries Bulletin 3, 74 p.

Ross, C. P., Andrews, D. A., Witkind, I. J., 1955, Geologic Map of Montana: Montana Bureau of Mines and Geology.

Ross, M. E., 1978, Stratigraphy, Structure and Petrology of the Columbia River Basalt in a Portion of the Grande-Ronde-Blue Mountains of Oregon and Washington: RHO-SA-58, Rockwell Hanford Operations, Richland, Washington.

Ross, S. H. and Savage, C. N., 1967, Idaho Earth Science; Geology, Fossils, Climate, Water and Soils: Idaho Bureau of Mines and Geology Earth Science Series No. 1, 271 p.

Routson, R. C., and Fecht, K. R., 1979, Soil (sediment) Properties of Twelve Hanford Wells: Rockwell Hanford Operations, Richland, Washington, Report, RHO-LD-82.

Savage, C. N., 1967, Geology and Mineral Resources of Bonner County: Idaho Bureau of Mines and Geology County Report 6, 131 p.

Sceva, J. E., 1950, Preliminary Report on the Ground-water Resources of Southwestern Skagit County, Washington: U.S. Geological Survey Open-File Report, 40 p.

Schlicker, H. G. and Deacon, R. J., 1967, Engineering Geology of the Tualatin Valley Region, Oregon: Oregon Department of Geology and Mineral Industries Bulletin 60, 103 p.

Schlicker, H. G., and Deacon, R. J., 1971, Engineering Geology of the La Grande Area, Union County, Oregon: Oregon Department of Geology and Mineral Industries.

Schlicker, H. G., Deacon, R. J., Beaulieu, J. D., and Olcott, G. W., 1972, Environmental Geology of the Coastal Region of Tillamook and Clatsop Counties, Oregon: Oregon Department of Geology and Mineral Industries Bulletin 74, 164 p.



Schmid, C. F., Darnbusch, S. M., and Miller, V. P., 1955, Population Growth and Distribution, State of Washington: Washington State Census Board, Seattle, Washington, 1955.

Schmincke, H. U., 1967a, Stratigraphy and Petrography of Four Upper Yakima Basalt Flows in South-Central Washington: Geological Society of America Bulletin, V. 78, No. 11, p. 1385-1422.

Schmincke, H. U., 1967b, Flow Directions in Columbia River Basalt Flows and Paleocurrents of Interbedded Sedimentary Rocks, South-Central Washington: Geologische Rundschau, V. 56, p. 992.

Scott, W. E., 1978, Quaternary Stratigraphy of Wasatch Front: National Earthquake Hazards Reduction Program Summaries of Technical Reports, v. 7, December 1978.

Scott, W. E., 1979a, Quaternary Stratigraphy of Wasatch Front: National Earthquake Hazards Reduction Program Summaries of Technical Reports, v. 8, June 1979.

Scott, W. E., 1979b, Quaternary Stratigraphy of Wasatch Front: National Earthquake Hazards Reduction Program Summaries of Technical Reports, v. 9, December 1979.

Scott, W. E., 1980a, Field Trip #4, Late Quaternary Lacustrine Geology and Geologic Hazards Along the Wasatch Front: Geological Society of America, Rocky Mountain Section Meeting, May 16-17, 1980, Weber State College, Ogden, Utah.

Scott, W. E., 1980b, Quaternary Stratigraphy of Wasatch Front: National Earthquake Hazards Reduction Program Summaries of Technical Reports, v. 10, June 1980.

Scott, W. E., 1981, Quaternary Stratigraphy of Wasatch Front: National Earthquake Hazards Reduction Program Summaries of Technical Reports, v. 11, January 1981.

Seismological Society of America Bulletin, 1918, Seismological Notes: v. 18, no. 4, p. 138.

Shannon & Wilson, Inc., 1972, Geology and Subsurface Investigation - Proposed Mid-Columbia Thermal Power Plant Sites - Morrow, Gilliam and Umatilla Counties, Oregon: Private Report to Portland General Electric Company.

Shannon & Wilson, Inc., 1973a, Preliminary Geological Studies, Subsurface Investigation and Laboratory Testing for Pacific Power and Light Company Proposed Downing Nuclear Power Plant Site, Oregon: Report to Stone & Webster Engineering Company.

Shannon & Wilson, Inc., 1973b, Robison "Fault" Investigation - Boardman Nuclear Project - Morrow County, Oregon: Private Report to Portland General Electric Company.

Shannon & Wilson, Inc., 1973c, Regional Geologic and Seismic Investigations, Boardman Nuclear Project: Private Report to Portland General Electric Company.

Shannon & Wilson, Inc., 1973d, Geologic Studies of Columbia River Basalt Structures and Age Deformation: Report to Portland General Electric Company, Portland, Oregon.

Shannon & Wilson, Inc., 1974a, Geotechnical Investigation for Central Plant Facilities, Pebble Springs Site - Boardman Nuclear Project - Morrow County, Oregon: Private Report to Portland General Electric Company.

Shannon & Wilson, Inc., 1974b, Geotechnical Studies for Preliminary Evaluation of a Proposed Nuclear Power Plant Site at Lebanon, Oregon: Report to Woodward-Envicon, Inc. for Pacific Power & Light Company.

Shannon & Wilson, Inc., 1975, Geologic Map of the Vicinity, Boardman Nuclear Project, Carty West Site: Private Report to Portland General Electric Company, Scale 1:24,000.

Shannon & Wilson, Inc., 1976, Volcanic Hazard Study-Potential for Volcanic Ashfall, Pebble Springs Nuclear Plant Site, Gilliam County, Oregon: Report to Portland General Electric Company, Portland, Oregon.

Shannon & Wilson, Inc., 1977a, see Washington Public Power Supply system, 1977a-p.

Shannon & Wilson, Inc., 1977b, Geologic Studies of the Southern Continuation of the Straight Creek Fault, Snoqualmie Area, Washington: A report prepared for Washington Public Power Supply System.

Shannon & Wilson, Inc., 1977c, Geologic Reconnaissance of the Cle Elum-Wallula Lineament and Related Structures: Report to Washington Public Power Supply System.

Shannon & Wilson, Inc., 1978, Geologic Reconnaissance of the Cle-Elum-Wallula Lineament and Related Structures: A report prepared for Washington Public Power Supply System, 33 p.

Shannon & Wilson, Inc., 1979a, Evaluation of Faulting in the Warm Springs Canyon Area, Southeast Washington: Report prepared for Washington Public Power Supply System, 18 p.

Shannon & Wilson, Inc., 1979b, Geologic Reconnaissance of the Wallula Gap, Washington - Blue Mountains - LaGrande, Oregon Region: Report prepared for Washington Public Power Supply System, 63 p.

Shannon & Wilson, Inc., 1980, Geologic Evaluation of Selected Faults and Lineaments, Pasco and Walla Walla Basins-Washington: Report prepared for Washington Public Power Supply System, 25 p.

Shea, M. C., 1970, Geology and Highway Location Considerations in the Orofino-Kamiah - Nez Perce Area, Idaho: Master's Thesis, University of Idaho, Moscow.

Shebalin, N. V., 1968, Methods of Using Engineering-Seismology Data in the New Seismic-Zoning Map, in Medvedev, S. F., ed., Seismic Zoning of the USSR: Israel Program for Scientific Translations, Jerusalem, 1976, (Translated from Russian) 533 p.

Sheppard, R. A., 1964, Geologic Map of the Husum Quadrangle, Washington: U.S. Geological Survey Field Studies Map MF-280.

Simmons, G. C., Van Noy, R. M., and Zilka, N. T., 1974, Mineral Resources of the Cougar Lakes - Mount Aix Study Area, Yakima and Lewis Counties, Washington: U.S. Geological Survey Open-File Report OF-74-243, 80 p.

Skehan, J. W., 1965, A Continental-Oceanic Crustal Boundary in the Pacific Northwest: Air Force Cambridge Research Laboratories, Report No. AFCRL-65-904, 52 p.

Smith, M., 1975, Preliminary Surficial Geologic Map of the Edmonds East and Edmonds West Quadrangles, Snohomish and King Counties, Washington: Washington Division of Geology and Earth Resources Geologic Map GM-14.

Smith, M., 1976, Preliminary Surficial Geologic map of the Mukilteo and Everett Quadrangles, Snohomish County, Washington: Washington Division of Geology and Earth Resources Geologic Map GM-20.

Smith, W. D., and Allen, J. E., 1941, Geology and Physiography of the Northern Wallowa Mountains, Oregon, with Petrography by L.W. Staples and Glaciation by W.R. Lowell: Oregon Department of Geology and Mineral Industries Bulletin 12, 64 p.

Snively, P. D., Jr., Brown, R. D., Jr., Roberts, A. E., and Rau, W. W., 1958, Geology and Coal Resources of the Centralia-Chehalis District, Washington: U.S. Geological Survey Bulletin 1053, 159 p.

Snyder, W. S., Dickinson, W. R., and Silberman, M. L., 1976, Tectonic Implications of Space-time Patterns of Cenozoic Magnetism in the Western United States: Earth and Planetary Science Letters, V. 32, p. 91-106.

Southwick, D. L., 1974, Geology of the Alpine-type Ultramafic Complex Near Mount Stuart, Washington: Geological Society of America Bulletin, V. 85, No. 3, p. 391-402.

Staatz, M. H., 1964, Geology of the Bald Knob Quadrangle, Ferry and Okanogan Counties, Washington, U.S. Geological Survey Bulletin 1161-F, 78 p.

Staatz, M. H. et al., 1971, Mineral Resources of the Pasayten Wilderness Area, Washington: U.S. Geological Survey Bulletin 1325, 255 p.

Staatz, M.H. Tabor, R.W., Weis, P.L., and others, 1972, Geology and Mineral Resources of the Northern Part of the North Cascades National Park, Washington: U.S. Geological Survey Bulletin 1359, 132 p.

Stepp, J. C., 1972, Analysis of Completeness of the Earthquake Sample in the Puget Sound Area and Its Effect on Statistical Estimates of Earthquake Hazard: Proceedings of the International Conference on Microzonation for Safer Construction, Research and Application, Seattle, Washington.

Strand, J. R. and Hough, J., 1952, Age of the Ringold Formation: Northwest Science, V. 26, p. 152-154.

Strong, C. P., 1967, Geology of the PeEll-Doty Area, Washington: Master's Thesis, University of Washington, Seattle.

System, Science and Software, 1980, Determination of Three-Dimensional Structures of Eastern Washington from the Joint Inversion of Gravity and Earthquake Travel Time Data. Report prepared for Weston Geophysical Corporation, 143 p.

Swanson, D. A., 1967, Yakima Basalt of the Tieton River area, South-Central Washington: Geological Society of America Bulletin, V. 78, No. 9, p. 1077-1110.

Swanson, D. A., 1978, Geologic Map of the Tieton River Area, Yakima County, South-Central Washington: United States Geological Survey Miscellaneous Field Studies Map MF-968, Scale 1:48,000.

Swanson, D. A. and Wright, T. L., 1976, Guide to Field Trip Between Pasco and Pullman, Washington Emphasizing Stratigraphy, Vent Areas, and Intercanyon-Flows of Yakima Basalt: Geological Society of America (Cordilleran Section) 72nd Annual Meeting, Field Guide No. 1.

Swanson, D. A. and Wright, T. L., 1978, Bedrock Geology of the Northern Columbia Plateau and Adjacent Areas: In Baker, V. R. and Nummedal, D., eds., The Channeled Scabland, Washington NASA Planetary Geology Program, A Guide to the Geomorphology of the Columbia Basin, Washington, p. 37-57.

Swanson, D. A. and Wright, T. L., and Helz, R. T., 1975, Linear Vent Systems and Estimated Rates of Magma Production and Eruption for the Yakima Basalt on the Columbia Plateau: American Journal of Science V. 275, p. 877-905.

Swanson, D. A. and Wright, T. L., Camp, V. E., Gardner, J. N., Helz, R. T., Price, S. M., and Ross, M. E., 1977, Reconnaissance Geologic Map of the Columbia River Basalt Group, Pullman and Walla Walla Quadrangles, Southeast Washington and Adjacent Idaho: United States Geological Survey Open-File Report 77-100.

Swanson, D. A., Anderson, J. L., Bentley, R. D., Camp, V. E., Gardner, J. N., and Wright, T. L., 1979a, Reconnaissance Geologic Map of the Columbia River Basalt Group in Eastern Washington and Northern Idaho: United States Geological Survey Open-File Report 79-1363.

Swanson, D. A. and Wright, T. L., Hooper, P. R., and Bentley, R. D., 1979b, Revisions in Stratigraphic Nomenclature of the Columbia River Basalt Group: United States Geological Survey Bulletin 1457-H, 59 p.



Tabor, R. W., 1961, Crystalline Geology of the Area South of Cascade Pass, Northern Cascades: Ph.D. Dissertation, University of Washington, Seattle.

Tabor, R. W., and Cady, W. M., 1978a, Geologic Map of the Olympic Peninsula, Washington: U.S. Geological Survey Miscellaneous Investigations Map I-994.

Tabor, R. W., and Cady, W. M., 1978b, The structure of the Olympic Mountains, Washington--Analysis of a Subduction Zone: U.S. Geological Survey Professional Paper 1033, 38 p.

Tabor, R. W., Engels, J. C., and Staatz, M. H., 1968, Quartz Diorite-Quartz Monzonite and Granitic Plutons of the Pasayten River Area, Washington - Petrology, Age, and Emplacement: U.S. Geological Survey Professional Paper 600C, p. C45-C52.

Tabor, R. W., and Frizzell, V. A., 1979, Tertiary Movement along the Southern Segment of the Straight Creek Fault and its Relation to the Olympic Wallowa Linement in the Central Cascades, Washington Geological Society of America, Abstracts with Programs, V. 11, No. 3, p. 131.

Tabor, R. W., Waitt, R. B., Frizzell, V. A., Jr., Swanson, D. A., and Byerly, G. R., 1977, Preliminary Map of the Wenatchee 1:100,000 Quadrangle, Washington: United States Geological Survey Open-File Report 77-531.

Tallman, A., 1981, Personal communication to Woodward-Clyde Consultants.

Tallman, A. M., Fecht, K. L., Marratt, M. C., and Last, G. V., 1979, Geology of the Separation Areas, Hanford Site, South-Central Washington: Rockwell Hanford Operations, Richland, Washington, Report RHO-ST-23.

Taubeneck, W. H., 1957, Geology of the Elkhorn Mountains, Northeastern Oregon, Bald Mountain Batholith: Geological Society of America Bulletin, Vol. 68, No. 2, p. 181-238.

Taubeneck, W. H., 1964, Cornucopia Stock, Wallowa Mountains, Northeastern Oregon Field Relationships: Geological Society of America Bulletin, Vol. 75, No. 11, p. 1093-1115.

Taubeneck, W. H., 1970, Dikes of Columbia River Basalt in Northeastern Oregon, Western Idaho, and Southeastern Washington: In Proceedings of the Second Columbia River Basalt Symposium, Cheney, Washington, March 1969, Eastern Washington State College Press, Cheney, Washington, p. 73-96.

Taylor, T. L., 1976, The Basalt Stratigraphy and Structure of the Saddle Mountains of South-Central Washington: Master's Thesis, Washington State University, Pullman, Washington.

Thayer, T. P., and Brown, C. E., 1966, Columbia River Group, in Changes in Stratigraphic Nomenclature by the U. S. Geological Survey 1965: U. S. Geological Survey Bulletin 1244-A, p. A23-A25.

Thiruvathukal, J. V., 1970, Regional Gravity of Oregon: Geological Society of America Bulletin, V. 81, No. 3, p. 725-738.

Tillson, D. D., 1970, Analysis of Crustal Changes in the Columbia Plateau Area from Contemporary Triangulation and Leveling Measurements: Battelle Northwest Laboratory, Report No. BNWL-CC-2174.

Townley, S. D. and Allen, M. W., 1939, Descriptive Catalogue of Earthquakes of the Pacific Coast of the United States, 1769-1928: Seismological Society of America Bulletin, v. 29, no. 1, p. 259-271.

Trimble, D. E., 1963, Geology of Portland, Oregon and Adjacent Areas: U.S. Geological Survey Bulletin 1119, 119 p.

United States Atomic Energy Commission, 1972, Safety Evaluation of the Fast Flux Test Facility: Directorate of Licensing.

United States Coast and Geodetic Survey, 1936 thru 1965, Abstracts of Earthquake Reports for the Pacific Coast and Western Mountain Region: MSA 11, MSA 24, MSA 38, MSA 46, MSA 49, MSA 103, MSA 111, MSA 126.

United States Geological Survey, 1964, Mineral and Water Resources of Idaho, Idaho Bureau Mines and Geology, Special Report 1.

United States Geological Survey, 1966, Mineral and Water Resources of Washington: Washington Division of Mines and Geology, Report 9.

United States Geological Survey, 1969, Mineral and Water Resources of Oregon, Oregon Department of Geology and Mineral Industries, Bulletin 64.



United States Nuclear Regulatory Commission, 1978, Regulatory Guide 1.70, Revision 3, Standard Format and Content of Safety Analysis Reports for Nuclear Power Plants: LWR edition, November.

Vallier, T. L., 1967, Geology of Part of the Snake River Canyon and Adjacent Areas in Northeastern Oregon and Western Idaho: Ph.D. Dissertation, Oregon State University, Corvallis, 267 p.

Vallier, T. L., and Hooper, P. R., 1976, Geologic Guide to the Hells Canyon, Snake River: Geological Society of America, Cordilleran Section, 72nd Annual Meeting, Field Guide No. 5.

Vance, J. A., 1977, The Stratigraphy and Structure of Orcas Island, San Juan Islands, in Geological Excursions in the Pacific Northwest (Guidebook), Geological Society of America, Annual Meeting, Seattle, Washington, 1977, Bellingham, Western Washington University Department of Geology, p. 170-203.

Vance, J. A., Whetten, J. T., and Eddy, P. A., 1975, Geologic Map of the San Juan Islands: in Russell, H., ed., Geology and Water Resources of the San Juan Islands, San Juan County, Washington: Washington Department of Ecology, Water-Supply Bulletin 46.

Vance, J. A., et al., 1980, Tectonic Setting and Trace Element Geochemistry of Mesozoic Ophiolitic Rocks in Western Washington: American Journal of Science, V. 280, p. 359-388.

Van Diver, B. B., 1964, Petrology of the Metamorphic Rocks, Wenatchee Ridge Area, Central Northern Cascades, Washington: Ph.D. Dissertation, University of Washington, Seattle.

Vine, J. D., 1969, Geology and Coal Resources of the Cumberland, Hobart, and Maple Valley Quadrangles, King County, Washington: U.S. Geological Survey Professional Paper 624.

Wagner, H. C., 1967a, Preliminary Geologic Map of the South Bend Quadrangle, Pacific County, Washington: U.S. Geological Survey Open-File Report OF-67-265, Scale 1:62,500.

Wagner, H. C., 1967b, Preliminary Geologic Map of the Raymond Quadrangle, Pacific County, Washington: U.S. Geological Survey Open-File Report OF-67-266, Scale 1:62,500.



Wagner, W. R., 1949, The Geology of the South Slope of the St. Joe Mountains, Shoshone County, Idaho: Idaho Bureau of Mines and Geology Pamphlet 82, 48 p.

Waite, R. B., Jr., 1979a, Late Cenozoic Deposits, Landforms, Stratigraphy, and Tectonism in Kittitas Valley, Washington: United States Geological Survey Professional Paper 1127, 18 p.

Waite, R. B., Jr., 1979b, Forty Late-Wisconsin Catastrophic Lake Missoula Backfloodings of Walla Walla and lower Yakima Valleys, Southern Washington, Geological Society of America Abstracts with Programs, V. 11, No. 3, p. 133.

Waite, R. B., Jr., 1980, About Forty Last-Glacial Lake Missoula Jokulhlaups Through Southern Washington: Journal of Geology, v. 88, p. 653-679.

Waldron, H. H., Liesch, B. A., Mullineaux, D. R., and Crandell, D. R., 1962, Preliminary Geologic Map of Seattle and Vicinity, Washington: U.S. Geological Survey Miscellaneous Investigations Map I-354.

Walker, G. W., 1973, Reconnaissance Geologic Map of the Pendleton Quadrangle, Oregon and Washington: U.S. Geological Survey Miscellaneous Investigations Map I-727.

Walker, G. W., 1977, Geologic Map of Oregon East of the 121st Meridian: U.S. Geological Survey Miscellaneous Investigations Map I-902, Scale 1:500,000.

Walker, G. W., 1979, Reconnaissance Geologic Map of the Oregon Part of the Grangeville Quadrangle, Baker, Union, Umatilla, and Wallawa, Oregon: U.S. Geological Survey Miscellaneous Investigations Map I-1116.

Wallace, W. K., 1976, Bedrock Geology of the Ross Lake Fault Zone in the Skymo Creek Area, North Cascades National Park, Washington: Master's Thesis, University of Washington, Seattle.

Walters, K. L., and Glancy, P. A., 1969, Reconnaissance of Geology and of Ground Water Occurrence in Whitman County, Washington: Washington Department of Water Resources Water-Supply Bulletin 26.

Walters, K. L., and Kimmel, G. E., 1968, Ground-water Occurrence and Stratigraphy of Unconsolidated Deposits, Central Pierce County, Washington: Washington Department of Water Resources Water-Supply Bulletin 22.

Warren, W. C., Norbistrath, H., and Grivetti, R. M., 1945, Geology of Northwestern Oregon, West of Willamette River and North of Latitude 45°15': U.S. Geological Survey Oil and Gas Investigations Preliminary Map 42.

Washington Public Power Supply System, 1974, WNP-1/4 Preliminary Safety Analysis Report, Chapter 2.5, Washington Public Power Supply System, Richland, Washington.

Washington Public Power Supply System, 1977a, Tectonic Evolution of the Pacific Northwest - Precambrian to Present: WNP 1/4 Preliminary Safety Analysis Report, Amendment 23, Vol. 2A, Subappendix 2R C.

Washington Public Power Supply System, 1977b, Regional Geology: WNP 1/4 Preliminary Safety Analysis Report, Amendment 23, Vol. 2A, Subappendix 2R D, Chapter 3.0.

Washington Public Power Supply System, 1977c, Fault Studies in the North Cascades: WNP 1/4 Preliminary Safety Analysis Report, Amendment 23, Vol. 2A, Subappendix 2R D, Chapter 5.0.

Washington Public Power Supply System, 1977d, Western Columbia Plateau Margin Studies: WNP 1/4 Preliminary Safety Analysis Report, Amendment 23, Vol. 2A, Subappendix 2R D, Chapter 6.0.

Washington Public Power Supply System, 1977e, Western Columbia Plateau Margin Studies, Wenatchee to Alameda Flat: WNP 1/4 Preliminary Safety Analysis Report, Amendment 23, Vol. 2A, Subappendix 2R D, Chapter 8.0.

Washington Public Power Supply System, 1977f, Regional Geology: WNP 1/4 Preliminary Safety Analysis Report, Amendment 23, Vol. 2B, Subappendix 2R H, Chapter 3.0.

Washington Public Power Supply System, 1977g, Geophysical and Seismological Studies in the 1872 Earthquake Epicentral Region: WNP 1/4 Preliminary Safety Analysis Report, Amendment 23, Vol. 2A, Subappendix 2R E.

Washington Public Power Supply System, 1977h, Geologic Studies of the Saddle Mountains - Manastash Ridge and Umtanum Ridge Structures: WNP 1/4 Preliminary Safety Analysis Report, Amendment 23, Vol. 2B, Subappendix 2R H, Chapter 8.0.





Washington Public Power Supply System, 1977i, Geologic Studies of the Wallula Gap Fault as Exposed in the Trench: WNP 1/4 Preliminary Safety Analysis Report, Amendment 23, Vol. 2B, Subappendix 2R H, Chapter 4.0.

Washington Public Power Supply System, 1977j, Western Columbia Plateau Margin Studies, Yakima River to Wenatchee: WNP 1/4 Preliminary Safety Analysis Report, Amendment 23, Vol. 2A, Subappendix 2R D, Chapter 7.0.

Washington Public Power Supply System, 1977k, Reconnaissance Mapping of the Rattlesnake-Wallula Lineament, Eastern Rattlesnake Hills, and Yakima Ridge: WNP 1/4 Preliminary Safety Analysis Report, Amendment 23, Vol. 2B, Subappendix 2R H, Chapter 7.0.

Washington Public Power Supply System, 1977l, Imagery and Topographic Interpretation of Geologic Structures in Central Washington: WNP 1/4 Preliminary Safety Analysis Report, Amendment 23, Vol. 2B, Subappendix 2R F.

Washington Public Power Supply System, 1977m, Geologic Studies - Wallula Gap to Badger Coulee: WNP 1/4 Preliminary Safety Analysis Report, Amendment 23, Vol. 2B, Subappendix 2R H, Chapter 5.0.

Washington Public Power Supply System, 1977n, Remote Sensing Analysis of the 1872 Earthquake Epicentral Region: WNP 1/4 Preliminary Safety Analysis Report, Amendment 23, Vol. 2B, Subappendix 2R G.

Washington Public Power Supply System, 1977o, Remote Sensing Analysis of the Columbia Plateau: WNP 1/4 Preliminary Safety Analysis Report, Amendment 23, Vol. 2B, Subappendix 2R K.

Washington Public Power Supply System, 1977p, Review of the North Cascade Earthquake of 14 December 1972: WNP 1/4 Preliminary Safety Analysis Report, Amendment 23, Vol. 2A, Subappendix 2R B.

Waters, A. C., 1955, Geomorphology of South-Central Washington, Illustrated by the Yakima East Quadrangle: Geological Society of America Bulletin, V. 66, No. 6, p. 633-684.

Waters, A. C., 1961, Stratigraphic and Lithologic Variations in the Columbia River Basalt: American Journal of Science, V. 159, p. 581-611.

Waters, A. C., 1968, Reconnaissance Geologic Map of the Dufur Quadrangle, Hood River, Sherman and Wasco Counties, Oregon: U.S. Geological Survey Miscellaneous Investigations Map I-556, Scale 1:125,000.

Watkins, N. D. and Baksi, A. K., 1974, Magnetostratigraphy and Oroclinal Folding of the Columbia River, Steens and Owyhee Basalts in Oregon, Washington and Idaho: American Journal of Science, V. 274, p. 148.

Webster, Gary D., and Crosby, James W., III, 1981, Stratigraphic Investigation of the Skagit/Hanford Nuclear Project: Prepared by Washington State University, Geological Engineering Section, for Golder Associates, Kirkland, Washington, 3 volumes.

Weigle, J. M., and Foxworthy, B. L., 1962, Geology and Ground-water Resources of West-central Lewis County, Washington: Washington Division of Water Resources Water-Supply Bulletin 17, 248 p.

Weis, P. L., 1968, Geologic Map of the Greenacres Quadrangle, Washington and Idaho: U.S. Geological Survey Geologic Quadrangle Map GQ-734, Scale 1:62,500.

Weissenborn, A. E., and Weis, P. L., 1976, Geologic Map of the Mount Spokane Quadrangle Spokane County, Washington, and Kootenai and Bonner Counties, Idaho: U.S. Geological Survey Geologic Quadrangle Map GQ-1336.

Weston Geophysical Corporation, 1976, Presentation of Significant Data and Conclusions Concerning the 1872 Earthquake: Report prepared for United Engineers and Constructors, Inc., 4 p. with Appendices.

Weston Geophysical Research, 1981, Compilation and Interpretation of Gravity in Washington, Oregon, and Adjacent Parts of British Columbia and Idaho: Prepared for Washington Public Power Supply System.

Wetherell, C. E., 1960, Geology of Part of the Southeastern Wallowa Mountains, Northeastern Oregon: Master's Thesis, Oregon State University, Corvallis.

Wheeler, J. O., and Read, P. B., 1973, Geology, Lardeau Map-area, West-half: Canadian Geological Survey Open-File Report OF-432.

Whetten, J. T., 1977, Sedimentology and Structure of Part of the Chiwaukum Graben, Washington: Geological Society of America, Abstracts with Programs, V. 9, No. 4, p. 527.

Whetten, J. T. and Laravie, J. A., 1976, Preliminary Geologic Map of the Chiwaukum Graben, Washington: U.S. Geological Survey Miscellaneous Field Studies Map MF-794, scale 1:24,000.

Wilkinson, W. D., Lowry, W. D., and Baldwin, E. M., 1946, Geology of the St. Helens Quadrangle, Oregon: Oregon Department of Geology and Mineral Industries Bulletin 31, 39 p.

Williams, I. A., 1916, The Columbia River Gorge, its Geologic History Interpreted From the Columbia River Highway: Oregon Bureau of Mines and Geology, Vol. 2, No. 3, 130 p.

Williams, R. K., 1952, Geology of Cape Disappointment Quadrangle and a Portion of Fort Columbia Quadrangle, Washington: Master's Thesis, University of Oregon, Eugene, 56 p.

Willis, C. L., 1950a, Geology of the Northeastern Quarter of Chiwaukum Quadrangle, Washington: Ph.D. Dissertation, University of Washington, Seattle.

Willis, C. L., 1950b, The Chiwaukum Graben, a Major Structure of Central Washington: American Journal of Science, V. 251, No. 11, p. 789-797.

Wilcox, R. E. and Fisher, R. V., 1966, Geologic Map of the Monument Quadrangle, Grant County, Oregon: United States Geological Survey Quadrangle Map, 1:62,500.

Winslow, M., 1977, Clastic Dike Swarm Emplacement and Early Phases of Deformation: Structural Studies in the Foreland Fold and Thrust Belt of Southern Chile: Geological Society of America Abstracts with Programs, v. 9, no. 7, p. 1232.

Wise, W. S., 1968, Geology of the Mount Hood Volcano, in Andesite Conference Guidebook: Oregon Department of Geology and Mineral Industries Bulletin 62, p. 81-98.

Wise, W. S., 1969, Geology and Petrology of the Mount Hood Area: A Study of High Cascade Volcanism: Geological Society of America Bulletin, v. 80, No. 6, p. 969-1006.

Wolfe, E. W., and McKee, E. H., 1968, Geology of the Grays River Quadrangle, Wahkiakum and Pacific Counties, Washington: Washington Division of Mines and Geology Map GM-4, Scale 1:62,500.

Woodsworth, G. J., 1977, Geology, Pemberton Map-area: Canadian Geological Survey Open-File Map 482.

Woodward-Clyde Consultants, 1978a, Straight Creek Fault Zone Study, 1872 Earthquake Studies, Washington Public Power Supply System Nuclear Project 1 and 4: Report prepared for United Engineers and Constructors, Inc.

Woodward-Clyde Consultants, 1978b, Paleomagnetic Measurements of the Ringold Formation and Loess Units Near Hanford, Washington and Evaluation of Age Dating Potential of Quaternary Deposits Near Hanford, Washington: Report to Washington Public Power Supply System, Incorporated, Richland, Washington.

Woodward-Clyde Consultants, 1980a, Seismological Review of the July 16, 1936 Milton-Freewater Earthquake Source Region: Report submitted to Washington Public Power Supply System, Richland, Washington.

Woodward-Clyde Consultants, 1980b, Recent Seismicity of the Hanford Region: Report submitted to Washington Public Power Supply System, Richland, Washington, February.

Woodward-Clyde Consultants, 1981a, Toppenish Ridge Study: Prepared for Washington Public Power Supply System, 33 p.

Woodward-Clyde Consultants, 1981b, Quaternary Sediments Study of the Pasco Basin and Adjacent Areas: Prepared for Washington Public Power Supply System.

Woodward-Clyde Consultants, 1981c, Wallula Fault Trenching and Mapping: Draft report prepared for Washington Public Power Supply System, in preparation.

Woodward-Clyde Consultants, 1981d, Wave Propagation and Ground Motion Modeling: Report prepared for Washington Public Power Supply System, Richland, Washington.

Wunder, J. M., 1976, Preliminary Geologic Map of the Utsalady Quadrangle, Skagit and Snohomish Counties, Washington: Washington Division of Geology and Earth Resources Open-File Map OF-76-10.

Yates, R. G., 1964, Geologic Map and Sections of the Deep Creek Area, Stevens and Pend Oreille Counties, Washington: U.S. Geological Survey Miscellaneous Investigations Map I-412, Scale 1:31,680.

Yates, R. G., 1971, Geologic Map of the Northport Quadrangle, Washington: U.S. Geological Survey Miscellaneous Investigations Map I-603.

Yates, R. G., Becraft, G. E., Campbell, A. B., and Pearson, R.C., 1966, Tectonic Framework of Northeastern Washington, Northern Idaho and Northwestern Montana: Canadian Institute of Mining and Metallurgy, Special Volume No. 8, p. 47-59.

Yeats, R. S., Erikson, E. H., Frost, B. R., Hammond, P. E., and Miller, R. B., 1977, Structure, Stratigraphy, Plutonism, and Volcanism of the Central Cascades, Washington: in Geological Excursions in the Pacific Northwest (Guidebook), Geological Society of America, Annual meeting, Seattle, Washington, 1977: Bellingham, Western Washington University, Department of Geology, p. 265-308.

Young, R. E., 1966, Geology and Biostratigraphy of the Knappton Area, Washington: Master's Thesis, University of Washington, Seattle.

Zietz, I., Hearn, B. C., Higgins, M. W., Robinson, G. D., and Swanson, D. A., 1971, Interpretation of an Aeromagnetic Strip Across the Northwestern United States: Geological Society of America Bulletin, V. 82, No. 12, p. 3347-3372.



WNP-2

AMENDMENT NO. 18  
September 1981

TABLE 2.5-5

HISTORICAL EARTHQUAKE CATALOG FOR THE  
PACIFIC NORTHWEST REGION

August 1981





TABLE 2.5-5  
TABLE OF CONTENTS

	<u>Page</u>
1.1 DESCRIPTION OF THE EARTHQUAKE CATALOG	2.5-5-1
2.1 EXPLANATION OF EARTHQUAKE CATALOG COLUMN HEADINGS	2.5-5-2
3.1 SOURCE CODE REFERENCES USED IN "S" COLUMN	2.5-5-4
4.1 MAGNITUDE CODES USED IN "SM" COLUMN	2.5-5-6
5.1 NATIONAL OCEANIC AND ATMOSPHERIC ADMINISTRATION (NOAA) HYPOCENTER DATA FILE FORMAT EXPLANATION	2.5-5-6
5.1.1 REPORTING OF FRACTIONAL EARTHQUAKE MAGNITUDES	2.5-5-6
5.1.2 EXPLANATION OF NOAA CODES USED IN "Q" COLUMN	2.5-5-7
5.1.3 EXPLANATION OF NOAA CODES USED IN "LOCATION AND COMMENTS" COLUMN	2.5-5-7
5.1.4 ISOSEISMAL MAP PUBLISHERS CODES	2.5-5-9
6.1 UNITED STATES GEOLOGICAL SURVEY CENTRAL WASHINGTON DATA FILE CODES EXPLANATION	2.5-5-9
6.1.1 HYPOCENTER SOLUTION QUALITY USED IN "Q" COLUMN	2.5-5-9
6.1.2 EXPLANATION OF ABBREVIATIONS USED IN "LOCATION AND COMMENTS" COLUMN	2.5-5-9
7.1 CANADIAN (EARTH PHYSICS BRANCH) EPICENTER DATA EXPLANATION	2.5-5-10
7.1.1 ORIGINAL DATA SOURCES AND CODES	2.5-5-10
7.1.2 INTENSITY MAGNITUDE CONVERSION	2.5-5-11
8.1 HISTORICAL EARTHQUAKE CATALOG FOR THE PACIFIC NORTHWEST REGION	

### 1.1 DESCRIPTION OF THE EARTHQUAKE CATALOG

The earthquake catalog contained in this table has been produced using Woodward-Clyde Consultants' Earthquake Data Bank. The catalog covers the following region:

Latitudes 42°N to 54°N  
Longitudes 114° to 128°W

The catalog includes located earthquakes of all intensities greater than or equal to intensity III and all magnitudes greater than or equal to magnitude 3.0 that have been reported from the region through December 31, 1980 by the sources cited in the Source Code Reference List on page 2.5-5-4. The earliest earthquake reported by the sources for the region occurred on December 3, 1841. The sources selected are those that provide the most complete data listings for the region, including more obscure sources that provide relatively short lists of small microearthquakes in limited areas. All the data available from the selected sources before March 1, 1981, are included. The main sources used are the National Oceanic and Atmospheric Administration (NOAA); the University of Washington (Western and Eastern Washington Networks); and the Earth Physics Branch of the Canadian Department of Energy, Mines and Resources.

Data from the University of Washington Eastern Washington network for the first half of 1980 are not yet available. Western Washington data for 1978 and 1979 were received after the catalog had been completed.

Many earthquakes appear in two or more of the source listings. Therefore, the catalog was edited by seismologists and duplicate entries were deleted. Although the majority of duplicate entries are almost identical, in cases where the hypocentral solutions differ appreciably, a selection was made based on the amount of data available to each source agency and on geographical considerations. For example, a University of Washington entry for an earthquake that occurred within the coverage of one of their regional networks would be selected rather than Canadian or NOAA entries.

For certain early earthquakes, especially several pre-instrumental events, it is difficult to choose between alternative sources. In these cases a preferred solution

was chosen based on the available data, and only the preferred solution is listed. All the alternative solutions are listed in the previous catalog.\*

Every attempt has been made to accurately reproduce the source material and obvious errors or questionable entries in the source listings have been investigated and, when necessary, corrected. However, the large volume of data obviously precludes exhaustive checking of every source listing, and the possibility of errors in the catalog cannot be completely eliminated. Particular attention was paid to verifying the magnitudes of eastern Washington earthquakes greater than magnitude 3 reported by the University of Washington. The magnitudes of these earthquakes appearing in the catalog were checked against the source listings; in several cases, the University of Washington Geophysics Program staff checked the source listings against original hypocenter solution computer runs. It is important to note that the quality of earthquake locations is not temporarily or spatially consistent from source to source, or even within each source.

## 2.1 EXPLANATION OF EARTHQUAKE CATALOG COLUMN HEADINGS

CAT. NO.	Sequential catalog number assigned to each earthquake.
DATE DAY-MO-YR	Date in Greenwich mean time unless noted otherwise in time column (usually as 'LT' for local time).
TIME (GMT) HR-MIN-SEC	Time in Greenwich mean time unless noted otherwise in time column (usually as 'LT' for local time).
LAT	Latitude, north or south as noted. When original sources have given the latitude or longitude in degrees, minutes, and seconds, or as fractions of a degree, these have been converted to decimal degrees. Although the catalog presents the coordinates in thousandths of a degree, it is important to bear in mind that this does not imply location accuracy to

\*Woodward-Clyde Consultants, 1978, Earthquake catalog of the Northwestern United States and Canada 1841-1977: Report prepared for the Washington Public Power Supply System, Richland, Washington, 427 p.

that precision. In many cases the implicit accuracy is discernible from the coordinate. For example, if a latitude were originally reported as 23 1/4 N, the catalog would list it as 23.250N.

LONG	Longitude, east or west as noted (see note above).
SL	Source of the latitude and longitude if different from the main source (column "S"). Frequently, only a place name is given for an earthquake location in the original data. In many such cases, the coordinates of the place have been assigned to the earthquake by Woodward-Clyde Consultants. The characters 'W', 'W1', or 'W2' are placed in this column to indicate the degree of precision of the place, name, location, as follows:  W    nearest hundredth or thousandth degree; W1   nearest tenth degree; W2   nearest half degree.
INTEN (MM)	Maximum intensity, reported on the modified Mercalli scale of 1931, unless noted otherwise; for example, 'RF' indicates Rossi-Forel intensity scale.
MAG	Earthquake magnitude, usually reported as local Richter, body wave, or surface wave (see "SM" column).
SM	Source of magnitude, if different from the main source (column "S"), or magnitude scale, if known. See Section 4.1 for explanation of magnitude codes.
H (KM)	Hypocenter depth, in kilometers.
DIS (MI) (KM)	Epicentral distance from the site in miles or kilometers, as noted.
Q	Epicenter quality indication as reported in main source. These are not quality judgments assigned by Woodward-Clyde Consultants unless the main source for the event is Woodward-Clyde Consultants. (See also Sections 5.1 and 6.1).



S Main source for earthquake (see Source Code References list). Unless otherwise indicated, the data presented for the earthquake are taken from this source.

### 3.1 SOURCE CODE REFERENCES USED IN 'S' COLUMN

Time periods of coverage as listed are inclusive

<u>Code</u>	<u>Source</u>
BB	Berg, J. W., and Baker, C. D., 1963, Oregon earthquakes, 1841-1958: Seismological Society of America Bulletin, v. 53, no. 1, p. 95-108.
CA	Canadian (Earth Physics Branch) epicenter data file. Period of coverage: 1860-1978.
CR	Crosson, R. S., 1972, Small earthquakes, structure, and tectonics of the Puget Sound region: Seismological Society of America Bulletin, v. 62, no. 5, p. 1133-1172.
C1	Smith, W. E. T., and Milne, W. G., 1969, Canadian earthquakes - 1964: Seismological Series, Dominion Observatory, Canadian Department of Energy, Mines, and Resources, Ottawa.
C2	Smith, W. E. T., and Milne, W. G., 1970, Canadian earthquakes - 1965: Seismological Series, Dominion Observatory, Canadian Department of Energy, Mines, and Resources, Ottawa.
C3	Stevens, A. E., Milne, W. G., Wetmiller, R. J., and Horner, R. B., 1972, Canadian earthquakes - 1966: Seismological Series of the Earth Physics Branch, No. 62, Canadian Department of Energy, Mines and Resources, Ottawa.
C4	Dominion Observatory (Victoria) data file, 1967-1968.
EH	Coffman, J. L., and von Hake, C. A., (eds.), 1973, Earthquake history of the United States: National Oceanic and Atmospheric Administration, Environmental Data Service, Publication 41-1 (revised edition through 1970), 208 p.
GS	U.S. Geological Survey, Central Washington Data File.

- M Milne, W. G., 1956, Seismic activity in Canada west of the 113th meridian, 1841-1951; Canadian Department of Mines and Technical Surveys, Publication of the Dominion Observatory (Ottawa), v. 18, no. 7, p. 119-146.
- N, NO National Oceanic and Atmospheric Administration (NOAA), Hypocenter data file. Period of Coverage: 1638 to September, 1980. Environmental Data Service, Boulder, Colorado.
- NU Neumann, F., 1967, Crustal structure in the Puget Sound area: Extrait Des Publications Du Bureau Central Seismologique International, Series A, Travaux Sientifiques Fascicule 20, p. 153-167.
- R Rasmussen, N., 1967, Washington State earthquakes, 1840-1965: Seismological Society of America Bulletin, v. 57, no. 3, p. 463-476.
- RU Rasmussen, N., 1973, Washington State earthquakes, 1966-1973: (unpublished).
- SD Racine, D., 1979, A seismicity study of the Pacific Northwest region of the United States, November 1961 - August 1965: Report prepared by Teledyne-Geotech for the U.S. Nuclear Regulatory Commission, Washington, D.C., 43 p.
- TA Townley, S. D., and Allen, M. W., 1939, Descriptive catalog of earthquakes of the Pacific Coast of the United States, 1769-1928: Seismological Society of America Bulletin, v. 29, no. 1, p. 1-297.
- TS Tobin, D. G., and Sykes, L. R., 1978, Seismicity and tectonics of the northeast Pacific Ocean: Journal of Geophysical Research, v. 73, no. 12, p. 3821-38.45.
- UE United States Earthquakes; Annual Publication of the U.S. Department of Commerce, 1928-present: by U.S. Coast and Geodetic Survey, Seismological Society of America, NOAA or Earthquake Data Service.
- UN Underwood, R., 1972, Studies of Victorian seismicity: Royal Society of Victoria Proceedings, v. 2, p. 27-47.
- UW University of Washington. Periods of Coverage. Western Washington (west of longitude 122°W),

18 June 1970-1974, 1978; Eastern Washington (east of longitude 122°W); 25 March 1969-1979, 18 June-December, 1980.

- W Woodward-Clyde Consultants, 1978, 1872 earthquake studies, WPPSS nuclear project Nos. 1 and 4: micro-earthquake study; Report prepared for the Washington Public Power Supply System, Richland, Washington, 32 p.
- WG Weston Geophysical Research, Inc. 1973, Hanford, Washington, Preliminary Safety Analysis Report for U.S. Atomic Safety Commission. Weston Geophysical Research, Inc., British Columbia, May-October, 1978.
- V Vance, D. J., 1971, Relocation of some seismic events in the Puget Sound area, 1951-1968: M.S. thesis, University of Washington, Seattle, Washington.

#### 4.1 MAGNITUDE CODES USED IN "SM" COLUMN

<u>Code</u>	<u>Explanation</u>
MB	Body wave magnitude
MC	University of Washington coda-length magnitude
ML	Local Richter magnitude
MN	Nuttli magnitude
MS	Surface wave magnitude
N1	Magnitude reported by NOAA. See "Location and Comments" column for identification of magnitude source and scale.

#### 5.1 NATIONAL OCEANIC AND ATMOSPHERIC ADMINISTRATION (NOAA) HYPOCENTER DATA FILE FORMAT EXPLANATION

##### 5.1.1 REPORTING OF FRACTIONAL EARTHQUAKE MAGNITUDES

Many early magnitudes in the NOAA data file were originally reported as fractions and have been converted to decimal notations. As is the case with coordinate locations, these decimal notations do not imply accuracy to the nearest hundredth of a unit. For example,





<u>Magnitude originally reported as</u>	<u>Appears as</u>
6 - 6 1/4	6.13
6 1/4	6.25
6 1/4 - 6 1/2	6.38
6 1/2	6.50
6 1/2 - 6 3/4	6.63
6 3/4	6.75
6 3/4 - 7	6.88

For any other range, the median value is listed.

#### 5.1.2 EXPLANATION OF NOAA CODES USED IN "Q" COLUMN

<u>Code</u>	<u>Explanation</u>
*	Assigned to solutions for which poor azimuth, depth control, and other factors contribute to a less reliable solution.
A	Parameters of explosion supplied by U.S. Atomic Energy Commission (AEC).
B	Parameters of epicenter supplied by University of California, Berkeley, California.
D	Authority for time and coordinates: Department of Energy, Mines, and Resources, Canada.
E	Some or all parameters of explosion (controlled or accidental) supplied by any group or individual other than AEC.
G	Parameters of epicenter supplied by the U.S. Geological Survey for any area other than Island of Hawaii.
M	Hypocenter based on macroseismic information.
S	An NEIS solution based on use of dense local networks, a local crustal model, or other methods not routinely applied by NEIS (USGS).
W	Parameters of epicenter supplied by University of Washington, Seattle, Washington.
Z	Noninstrumental.

#### 5.1.3 EXPLANATION OF NOAA CODES USED IN "LOCATION AND COMMENTS" COLUMN

<u>Code</u>	<u>Explanation</u>
A	NOAA depth control designation indicating hypocenter depth assigned for shallow focus (not computed).
BCIS	Bureau Central International De Seismologie.
BRK	University of California, Berkeley, California, Seismograph Station (Haviland).
CGS, CGS-B	U.S. Coast and Geodetic Survey: Number following CGS indicates bi-weekly preliminary determination of epicenter sequence number.
CGSPDE	U.S. Coast and Geodetic Survey: Preliminary determination of epicenter.
D	NOAA depth control designation indicating depth based on two or more reported pP's identified as such.
ERL, ERL#	Environmental Research Laboratories: Number following ERL indicates bi-weekly preliminary determination of epicenter sequence number.
G	NOAA depth control designation indicating depth restrained by geophysicist.
GOL	Colorado School of Mines Seismograph Station, Golden, Colorado.
GUTE	Gutenberg and Richter (1954).
LG	Variation of Nuttli magnitude using LG phase.
N	NOAA depth control designation indicating normal depth (33 km) when data are not sufficient to calculate shallow focal depth.
NOS, NOS#	National Ocean Survey: Number following NOS indicates bi-weekly preliminary determination of epicenter sequence number.
NU	Nuttli magnitude.
OSU	Oregon State University.
PAL	Lamont-Doherty Geological Observatory Seismograph Station, Palisades, New York.

PAS, PA California Institute of Technology, Pasadena,  
California, Seismograph Station.

PDE U.S. Coast and Geodetic Survey: Preliminary  
determination of epicenter.

USE United States Earthquakes, Annual Publication  
of the U.S. Department of Commerce,  
1928-present, by the C&GS, BSSA, NOAA, or EDS.

## 5.1.4 ISOSEISMAL MAP PUBLISHER CODES

<u>Code</u>	<u>Explanation</u>
USE	United States Earthquakes
EQN	Earthquake Notes
PDE	Preliminary Determination of Epicenters

6.1 UNITED STATES GEOLOGICAL SURVEY  
CENTRAL WASHINGTON DATA FILE CODES EXPLANATION

## 6.1.1 HYPOCENTER SOLUTION QUALITY USED IN "Q" COLUMN

This measure is intended to indicate the general reliability  
of a hypocentral solution.

<u>Quality</u>	<u>Epicenter</u>	<u>Focal Depth</u>
A	Excellent	Good
B	Good	Fair
C	Fair	Poor
D	Poor	Poor

The quality is based on both the nature of the station  
distribution with respect to the earthquake and the  
statistical measure of the solution.

6.1.2 EXPLANATION OF ABBREVIATIONS USED IN "LOCATION AND  
COMMENTS" COLUMN

<u>Abbreviation</u>	<u>Explanation</u>
DMIN	Epicentral distance in kilometers to the nearest station; rounded to the nearest integer.
GAP	Largest azimuthal separation in degrees between stations.

- HSE Horizontal standard error of the epicenter in Kilometers:  $HSE = \sqrt{(SDX^2) + (SDY^2)}$ , where SDX and SDY are the standard errors in longitude and latitude, respectively, of the epicenter. When NSTN is less than or equal to four, HSE cannot be computed and is left blank.
- NSTN Number of stations used in locating the earthquake.
- R (In 'SM' column) indicates the Richter magnitude calculated from Wood-Anderson seismograph records.
- RMS Root-mean-square error of the time residuals:  $RMS = \sqrt{(R(I)^2 / NSTN)}$ , where R(I) is the observed seismic-wave arrival time minus the computed time at the I-th station.
- ZSE Standard error of the depth in kilometers.
- \* (At end of statistical data line) indicates earthquake was also reported in Bulletin of the Seismograph Stations of the University of California, Berkeley.

#### 7.1 CANADIAN (EARTH PHYSICS BRANCH) EPICENTER DATA EXPLANATION

The Canadian epicenter data denoted by the source code CA comes from the Earth Physics Branch, Division of Seismology and Geothermal Studies of the Department of Energy, Mines and Resources, Ottawa, Canada.

##### 7.1.1 ORIGINAL DATA SOURCES AND CODES

The following are the codes used in the notation ORIGINAL DATA

SOURCE=xxx in the "Location and Comments" column.

<u>Code</u>	<u>Explanation</u>
EPB	Earth Physics Branch of Dept. of Energy, Mines and Resources, Canada. The great bulk of the EPB data has been published in the Seismological Series of the Earth Physics Branch by the Seismological Service of Canada, Dept. of Energy, Mines and Resources, in the Seismological Series of the Dominion Observatories, Dept. of Mines and Technical surveys, or in the Publications of the Dominion Observatory, Dept. of

Mines and Technical Surveys, by various authors. The above are all one series, characterized by orange covers and a history of name changes.

PDE Preliminary Determination of Epicenters, available through National Earthquake Information Service, U.S.A.

UBC University British Columbia, Canada

ISC International Seismological Center

The data represented here, as provided by EPB, attempts to be faithful to the published material. The source "EPB" is given for all events prior to 1968, despite the fact that not all these epicenters or their parameters can be found in Canadian publications. Some are from ISS (International Seismological Summary), USCGS (United States Coast and Geodetic Survey), Gutenberg and Richter, "Seismicity of the Earth and Associated Phenomena" (Princeton University Press, 1954), and from other references.

#### 7.1.2 INTENSITY MAGNITUDE CONVERSION

In the data supplied by EPB, all events before 1899 and some thereafter are assigned magnitudes calculated from their maximum intensities according to the formula

$$M = (2/3) I + 1$$

For the period before 1899, in order to depict the parameters of events as accurately as possible, magnitudes are reconverted back to intensities in the EQDB catalog according to the formula

$$I = (3/2) (M - 1)$$

However, since there is no way to determine whether a given event in 1899 or later was assigned a calculated magnitude by EPB, no reversion is done for 1899 and later; hence some events in this period may have magnitudes assigned to them despite the fact that there was no original report of magnitude. Such magnitudes are always reported as local magnitudes.



TABLE 2.5-5

This table is being printed.

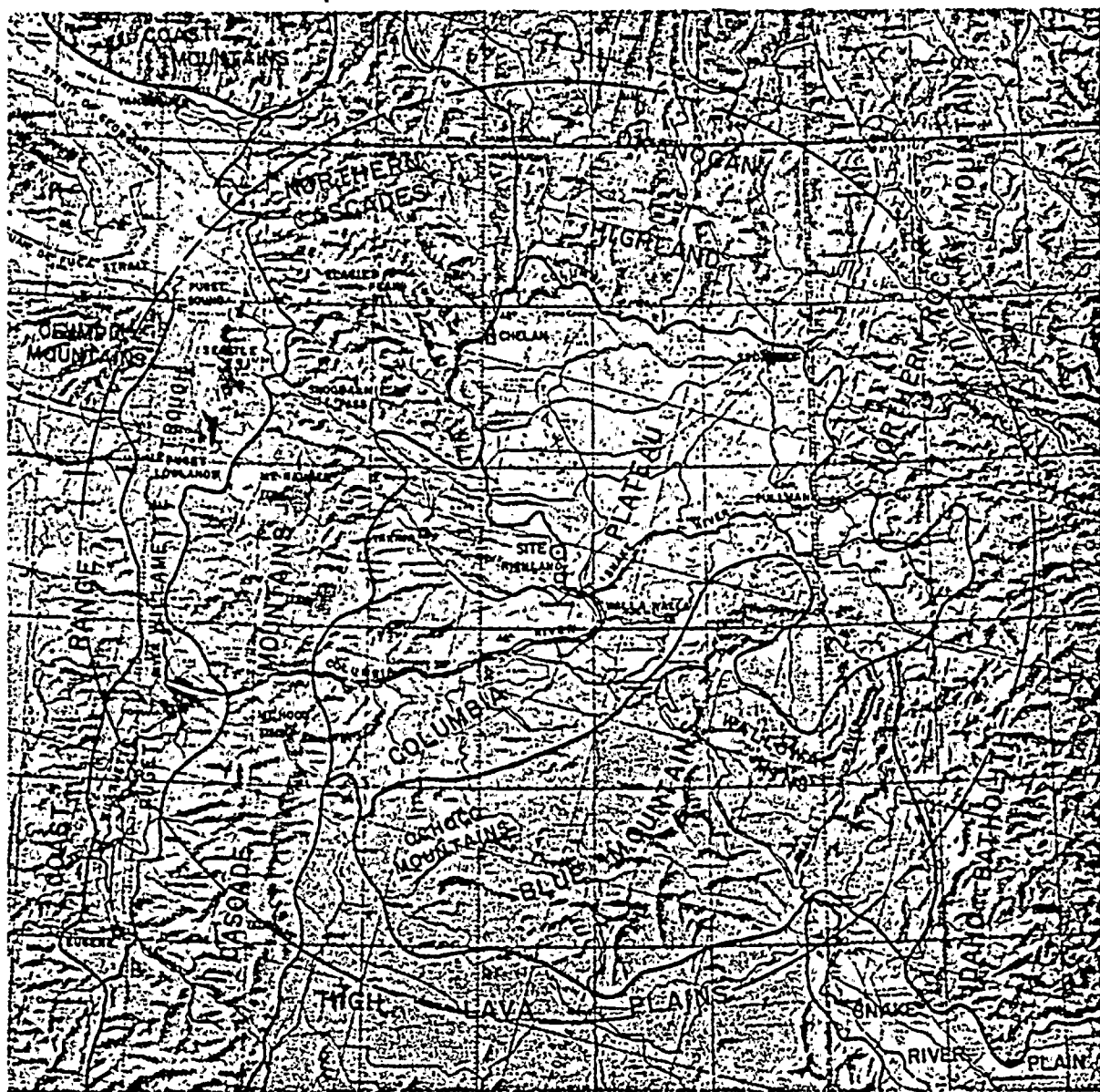




TABLE 6

EARTHQUAKES POTENTIALLY FELT AT THE SITE

<u>Year</u>	<u>Mo.</u>	<u>Day</u>	<u>Location.</u>	<u>Epicentral Intensity (MM)</u>	<u>Estimated Intensity at Site (MM)</u>	<u>Distance from site (km)</u>	<u>Remarks</u>
1872	Dec	14	49.167N., 121.000W.	IX	V	320	North Cascades 1,250,000 km <sup>2</sup> felt area
1936	Jul	16	46.208N., 118.233W.	VII	IV	85	Milton-Freewater, OR M <sub>S</sub> 5-3/4, M <sub>L</sub> 6.1.
1965	Apr	29	47.4N., 122.4W.	VII	IV	255	Seattle, WA, 335,000 km <sup>2</sup> felt area. m <sub>D</sub> 6-1/2.
1918	Nov	1	46.9N., 119.3W.	VI	III-IV	43	Corfu, WA, M <sub>S</sub> 4.4.
1949	Apr	13	47.25N., 122.5W.	VIII	I-IV	250	Puget Sound Region 390,000 km <sup>2</sup> felt area. M <sub>S</sub> 7.0.
1945	Apr	29	47.4N., 121.7W.	VII	I-IV	210	North Bend, WA, 130,000 km <sup>2</sup> felt area. M <sub>S</sub> 5-1/2.
1946	Feb	15	47.3N., 122.9W.	VII	I-IV	285	Puget Sound, WA, 180,000 km <sup>2</sup> felt area. M <sub>S</sub> 5-3/4.
1939	Nov	13	47.2N., 123.0W.	VII	I-IV	290	Olympia, WA, 155,000 km <sup>2</sup> felt area. M <sub>S</sub> 5- 3/4.
1943	Apr	24	47.3N., 120.6W.	VI	I-IV	130	Leavenworth, WA, 26,000 km <sup>2</sup> felt area.
1959	Aug	6	47.8N., 119.9W.	VI	I-IV	158	Chelan, WA, 65,000 km <sup>2</sup> felt area. M <sub>L</sub> 4.4.
1926	Dec	30	47.07N., 120.2W.	VI	I-III	150	Wenatchee, WA, 40,000 km <sup>2</sup> felt area.
1961	Sep	16	46.0N., 122.2W.	VI	II?	225	Cougar Area, WA. 18,000 km <sup>2</sup> area, M <sub>L</sub> 4.3.



0 100 200 MILES  
 Base map: JET NAVIGATION CHART (Series JNC, Sheet 43, Edition 1, Lambert Conformal Conic Projection).

Figure 2.5-1 Regional Physiographic Map.

FIGURES 2.5-2 THROUGH 2.5-21  
ARE CURRENTLY BEING PRINTED.

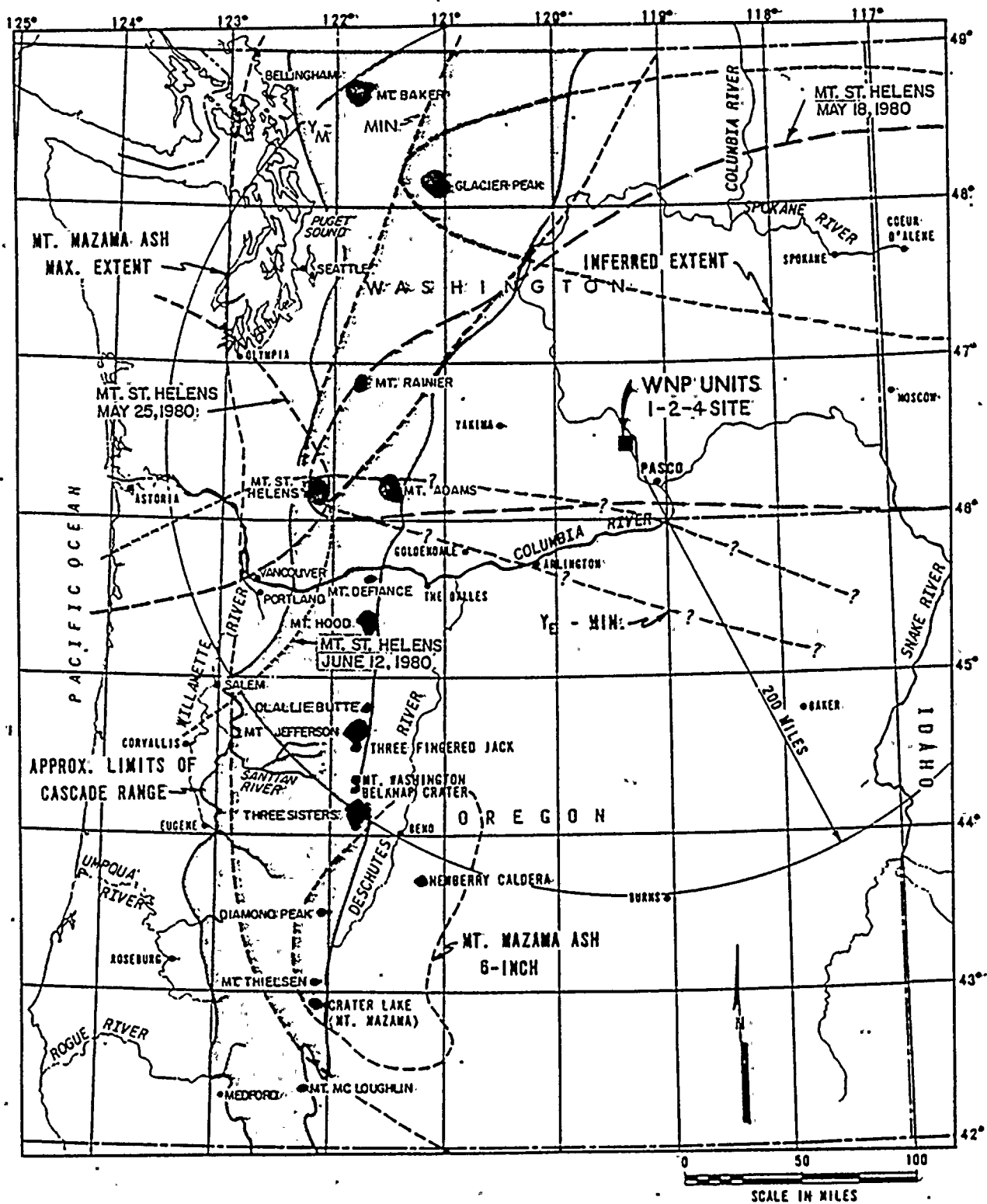
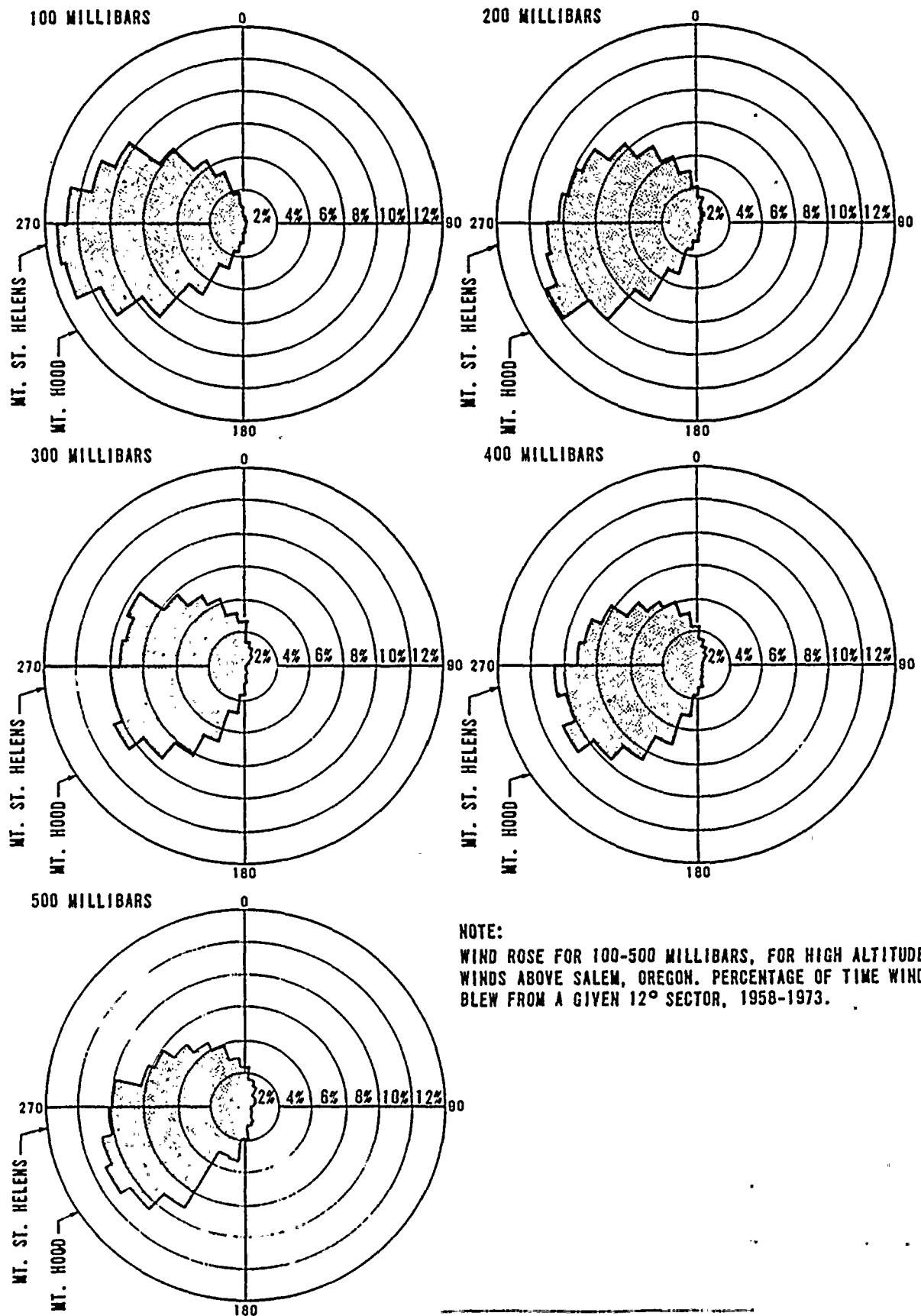


Figure 2.5-22. Major Quaternary Cascade Volcanoes and Ash Falls



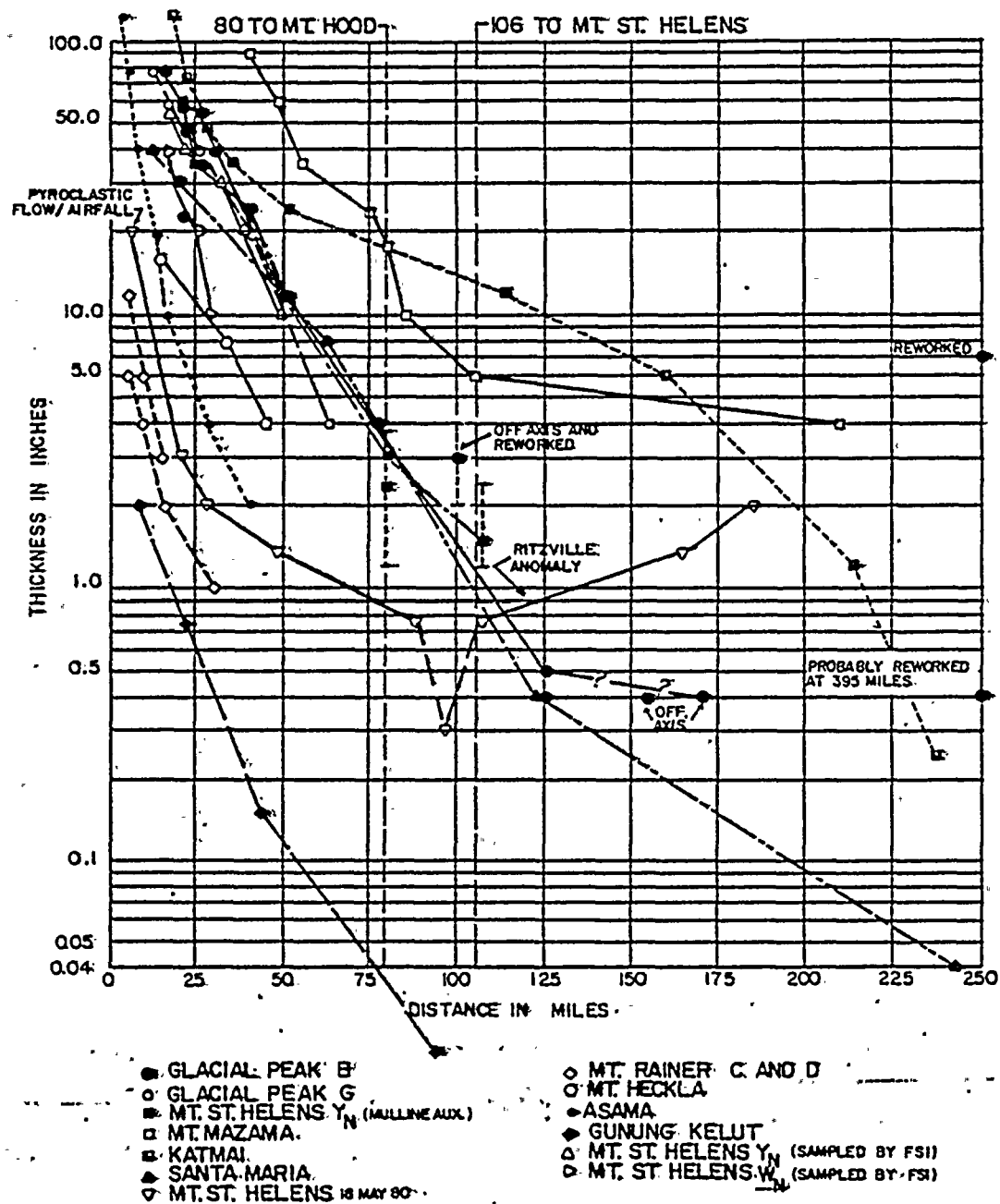


NOTE:  
WIND ROSE FOR 100-500 MILLIBARS, FOR HIGH ALTITUDE  
WINDS ABOVE SALEM, OREGON. PERCENTAGE OF TIME WIND  
BLEW FROM A GIVEN 12° SECTOR, 1958-1973.

Figure 2.5-23 High Altitude Winds Above  
Salem, Oregon

	5/10		Cont. of 2. 10/10/80
REV. No.	DATE	PREPARED BY	COMMENTS

PREPARED BY \_\_\_\_\_  
 DRAFTED BY AS  
 CHECKED BY \_\_\_\_\_

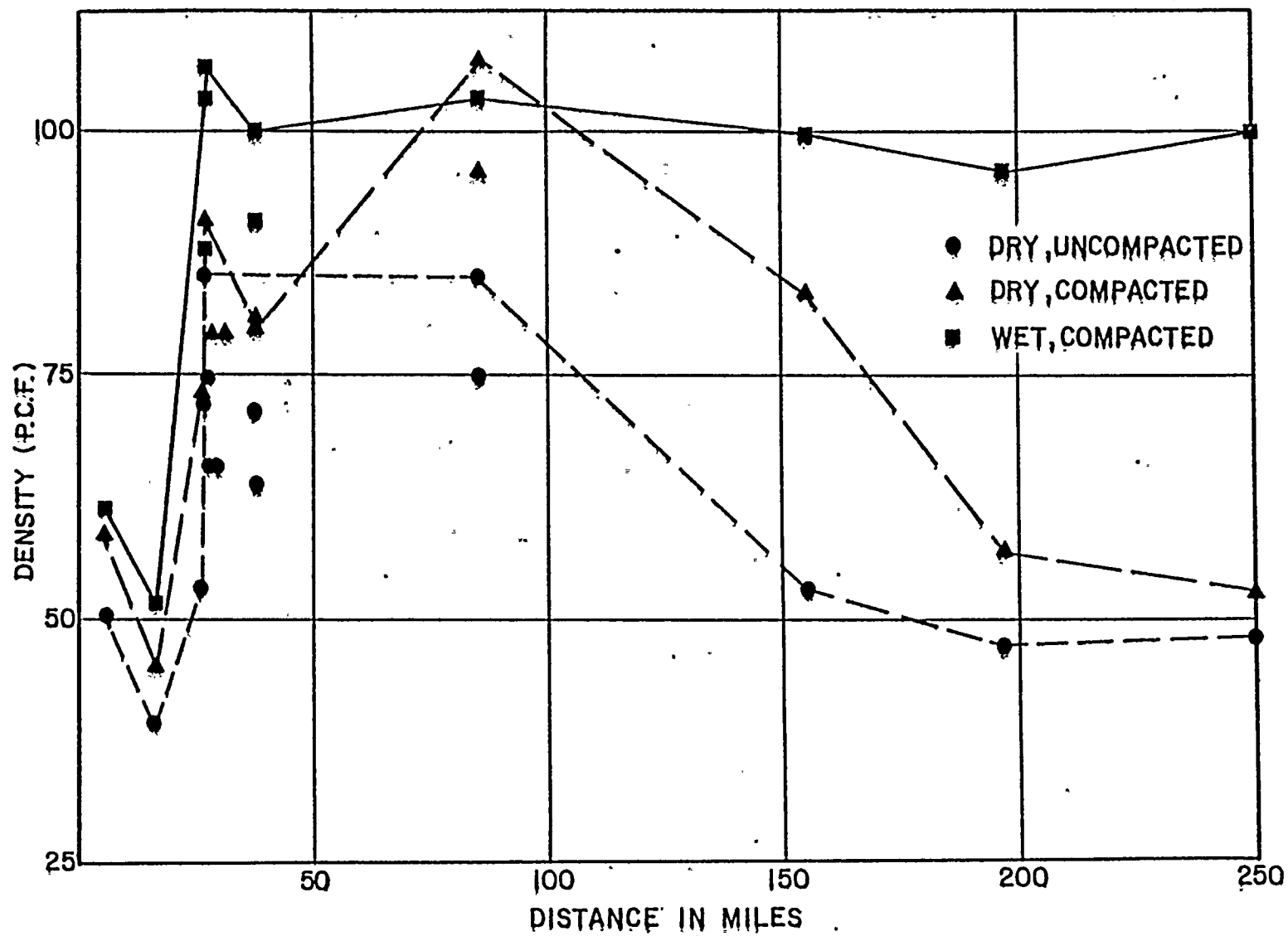


THICKNESS/DISTANCE RELATIONS OF VOLCANIC ASH FALL DEPOSITS

2.5-24



Figure 2.5-25 Distance Versus  
Density - 1980 Mt. St.  
Helens Eruption





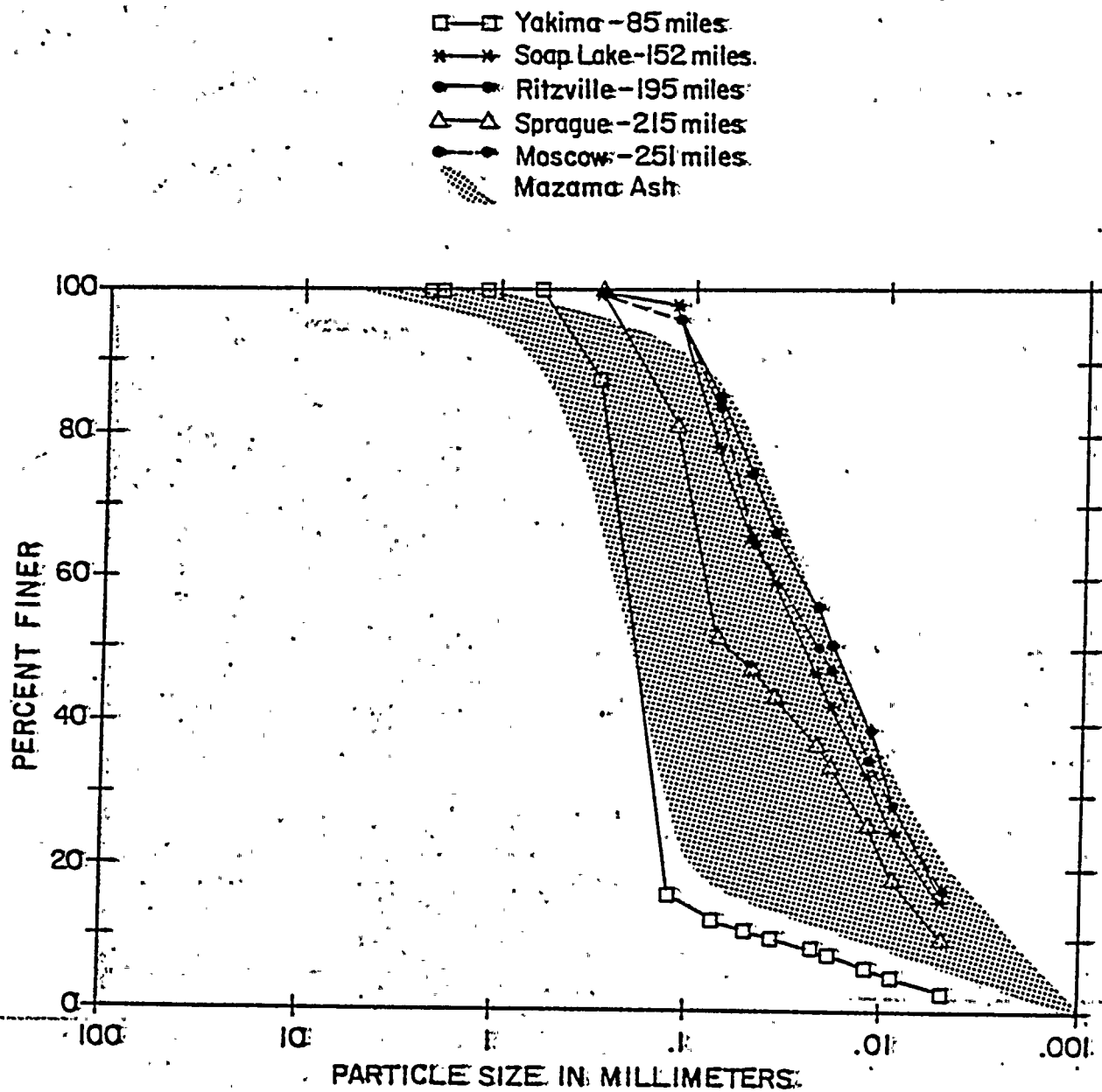
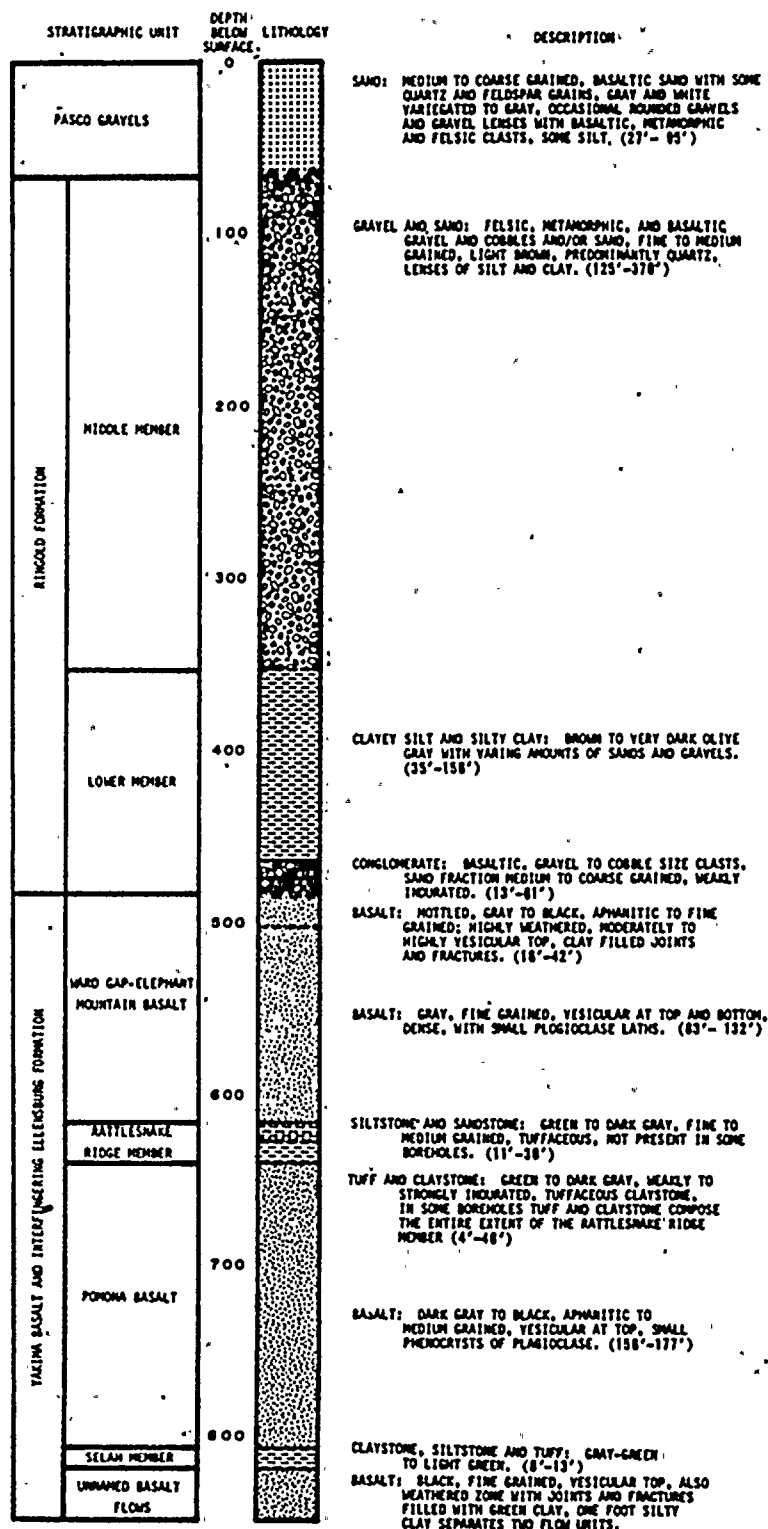


Figure 2.5-26. Grain Size Distribution of Mt. St. Helens and Mt. Mazama



Figure 2.5-27 has been deleted



NOTE:

- 1) GRAPHIC SYMBOLS RELATE TO THOSE USED ON LOGS IN APPENDIX 2.5A.
- 2) THE COLUMNAR SECTION REPRESENTS THE AVERAGE THICKNESS OF INTERVALS ENCOUNTERED, RANGE IN THICKNESS FOUND IN THE BORINGS IS GIVEN IN PARENTHESES

Figure 2.5-28 Stratigraphic Section at the Plant Site



FIGURES 2.5-29 AND 2.5-30  
ARE CURRENTLY BEING PRINTED.





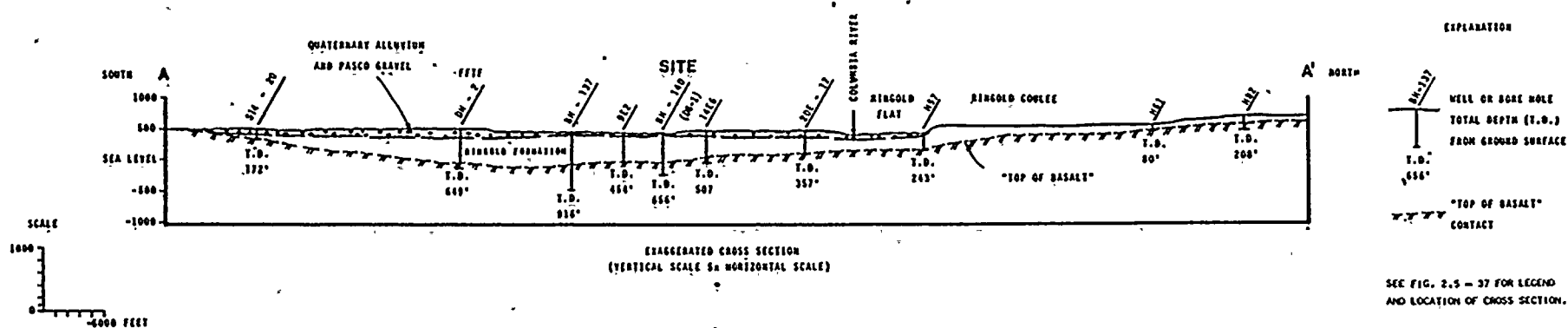
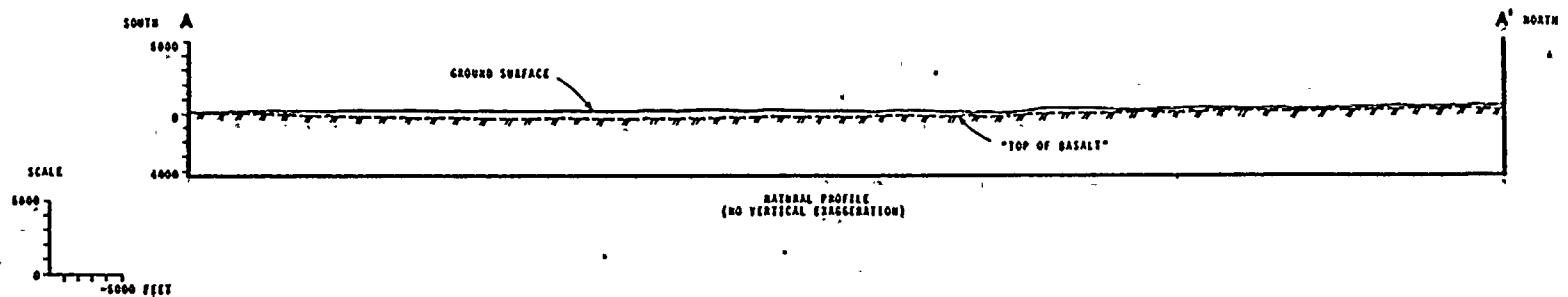


Figure 2.5-31 Geologic Cross Section of the Site Vicinity

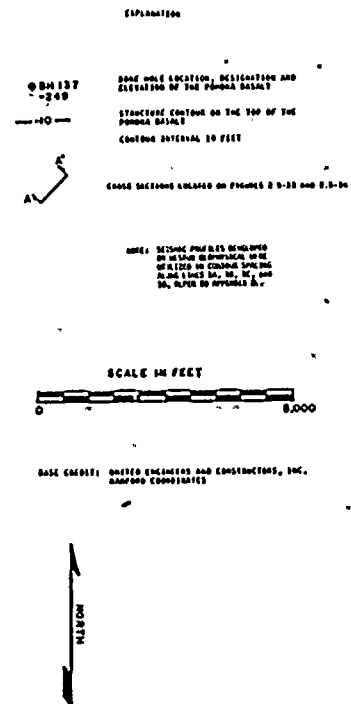
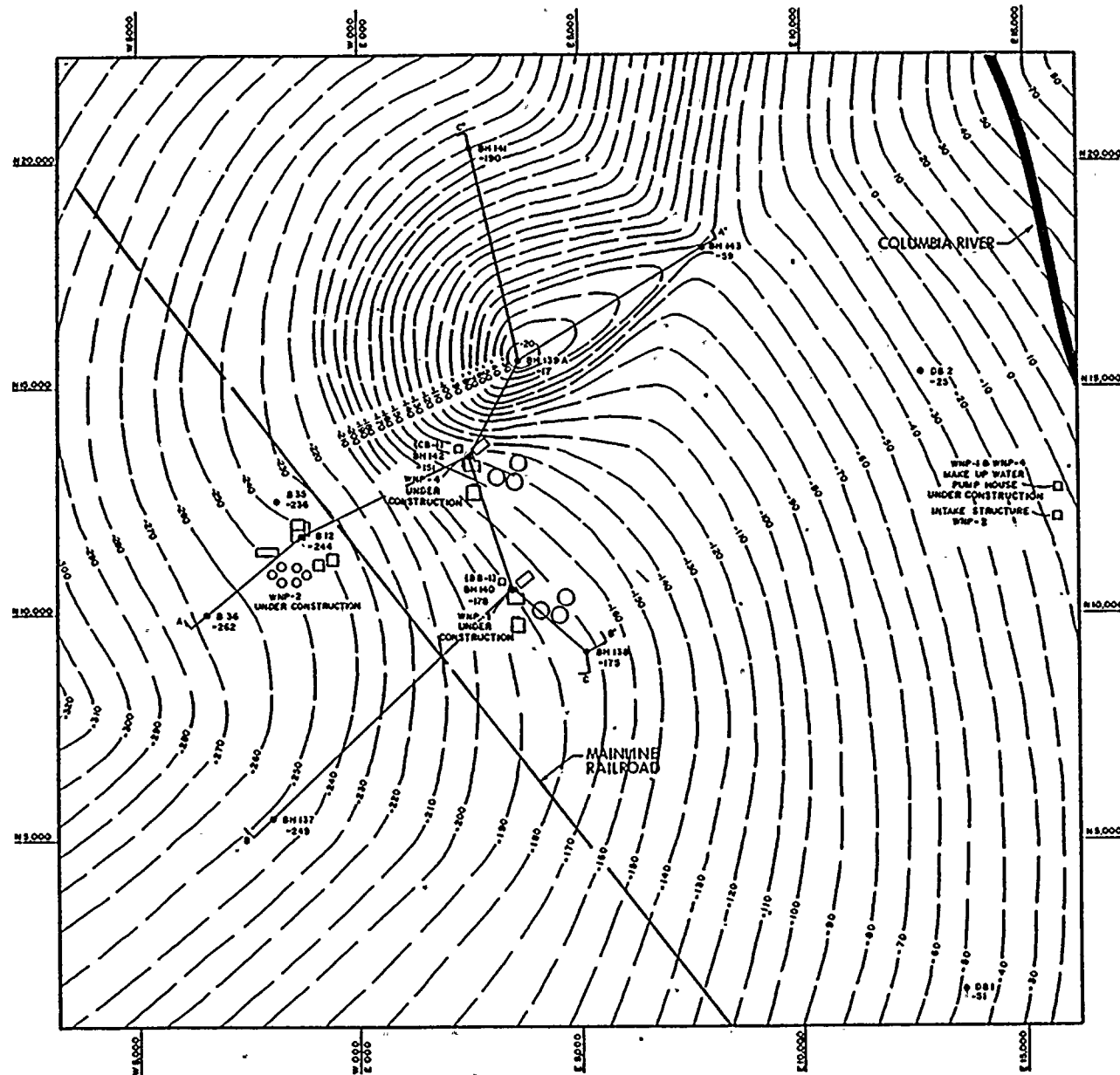


Figure 2.5-32 Structural Contour Map of the Site





FIGURE 2.5-35

IS CURRENTLY BEING PRINTED.

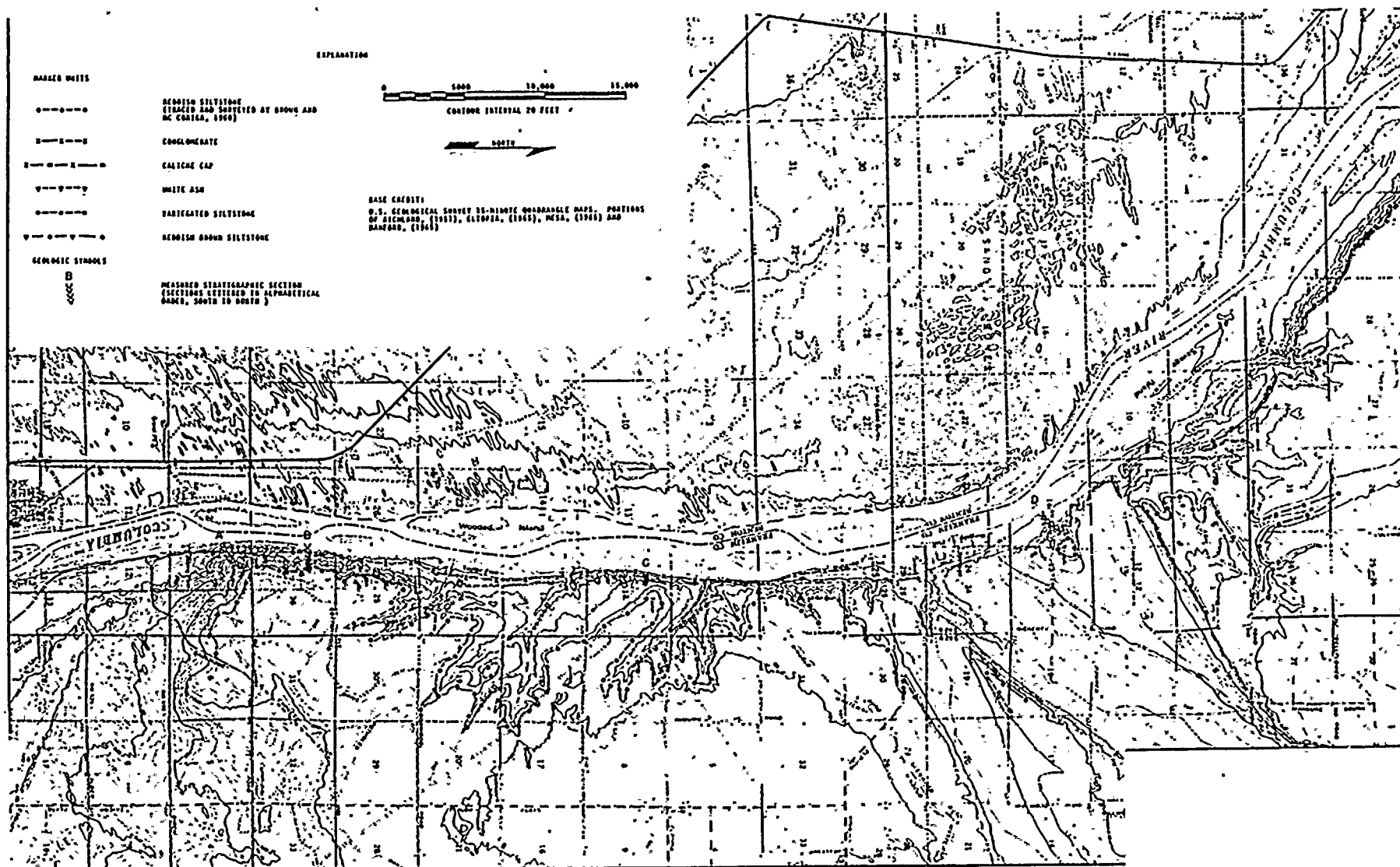


Figure 2.5-36 Continuity Survey of the Ringold Formation - South Portion of White Bluffs

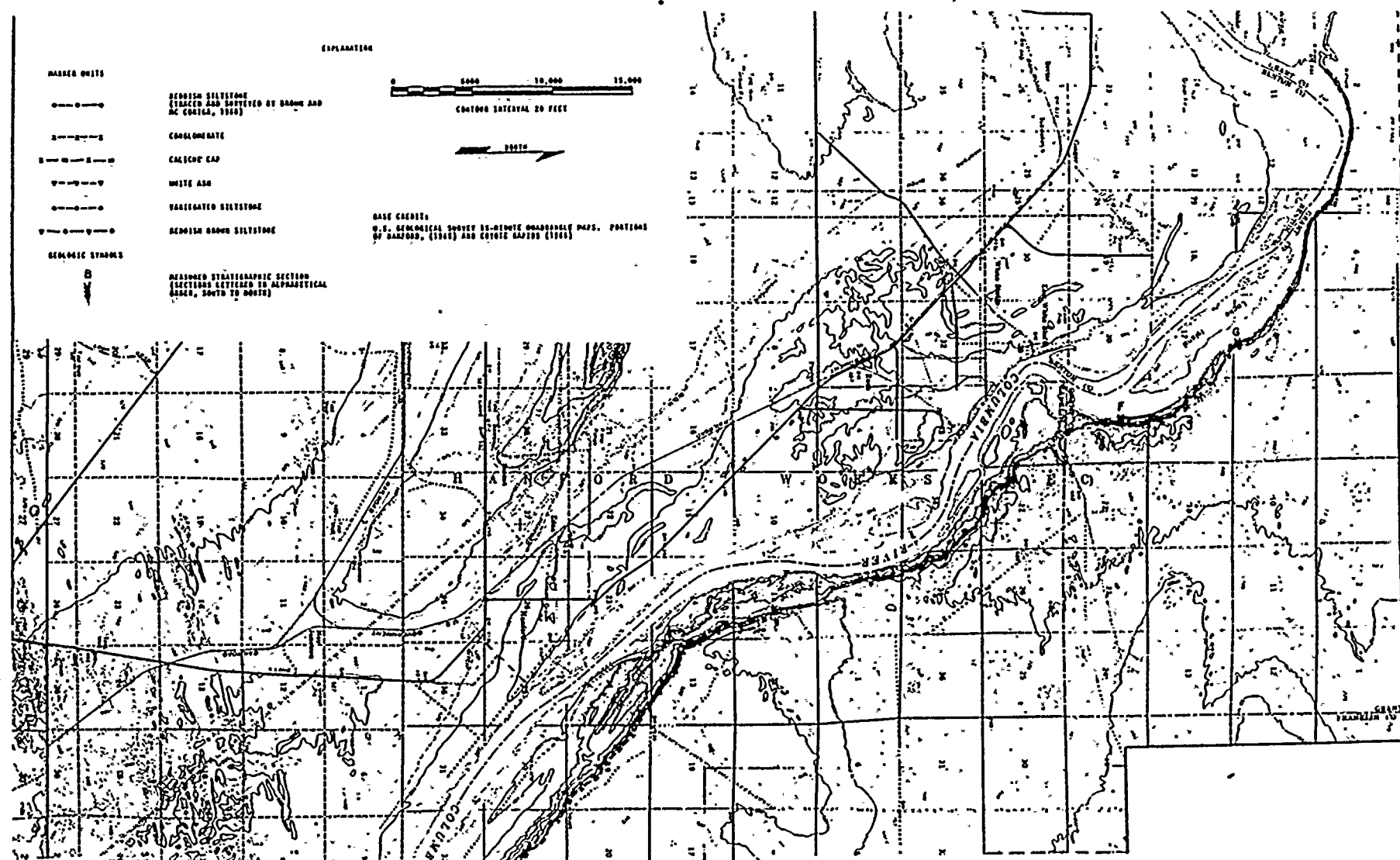
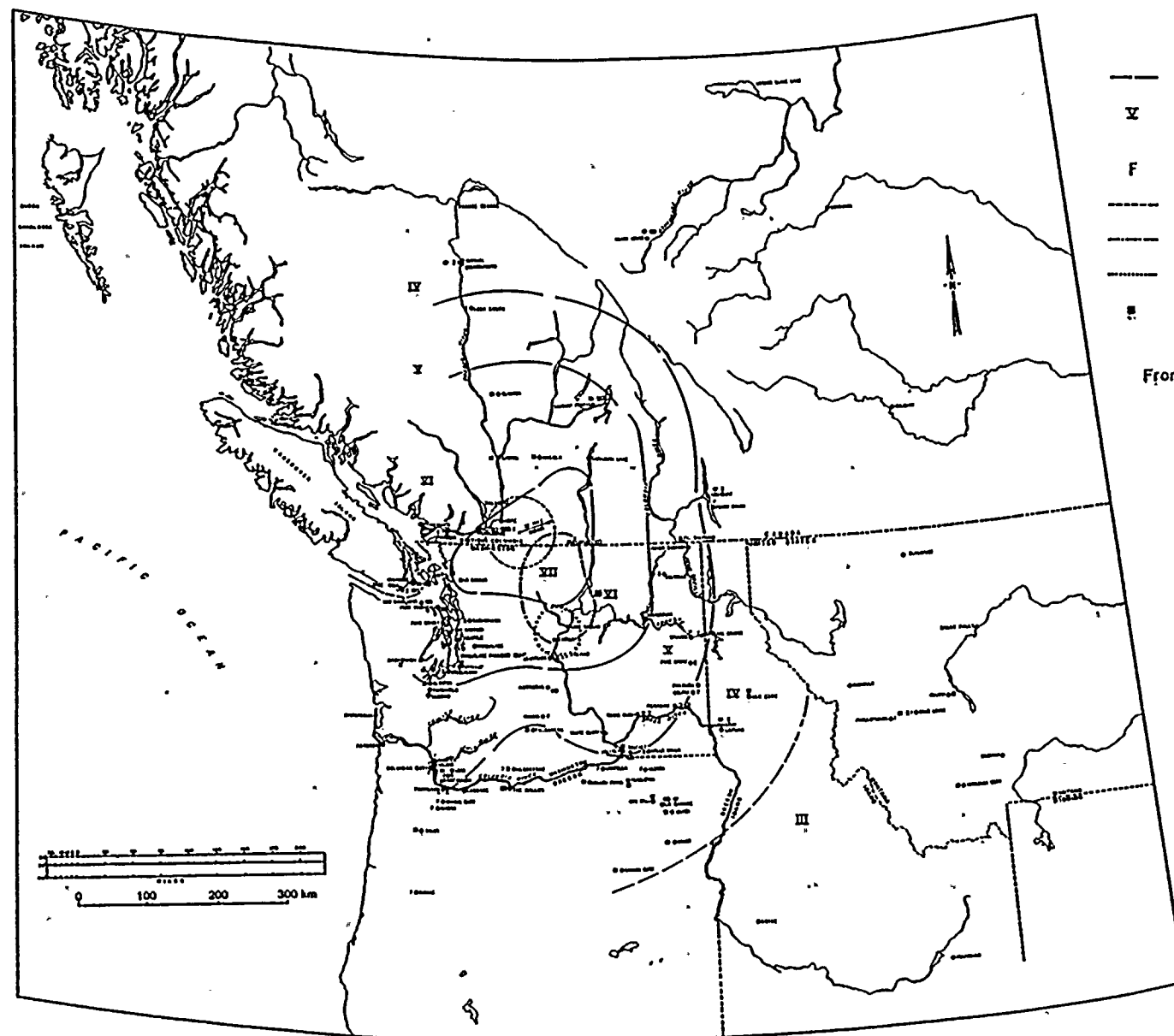


Figure 2.5-37 Continuity Survey of the Ringold Formation - North Portion of White Bluffs



FIGURES 2.5-38 AND 2.5-39  
ARE CURRENTLY BEING PRINTED.

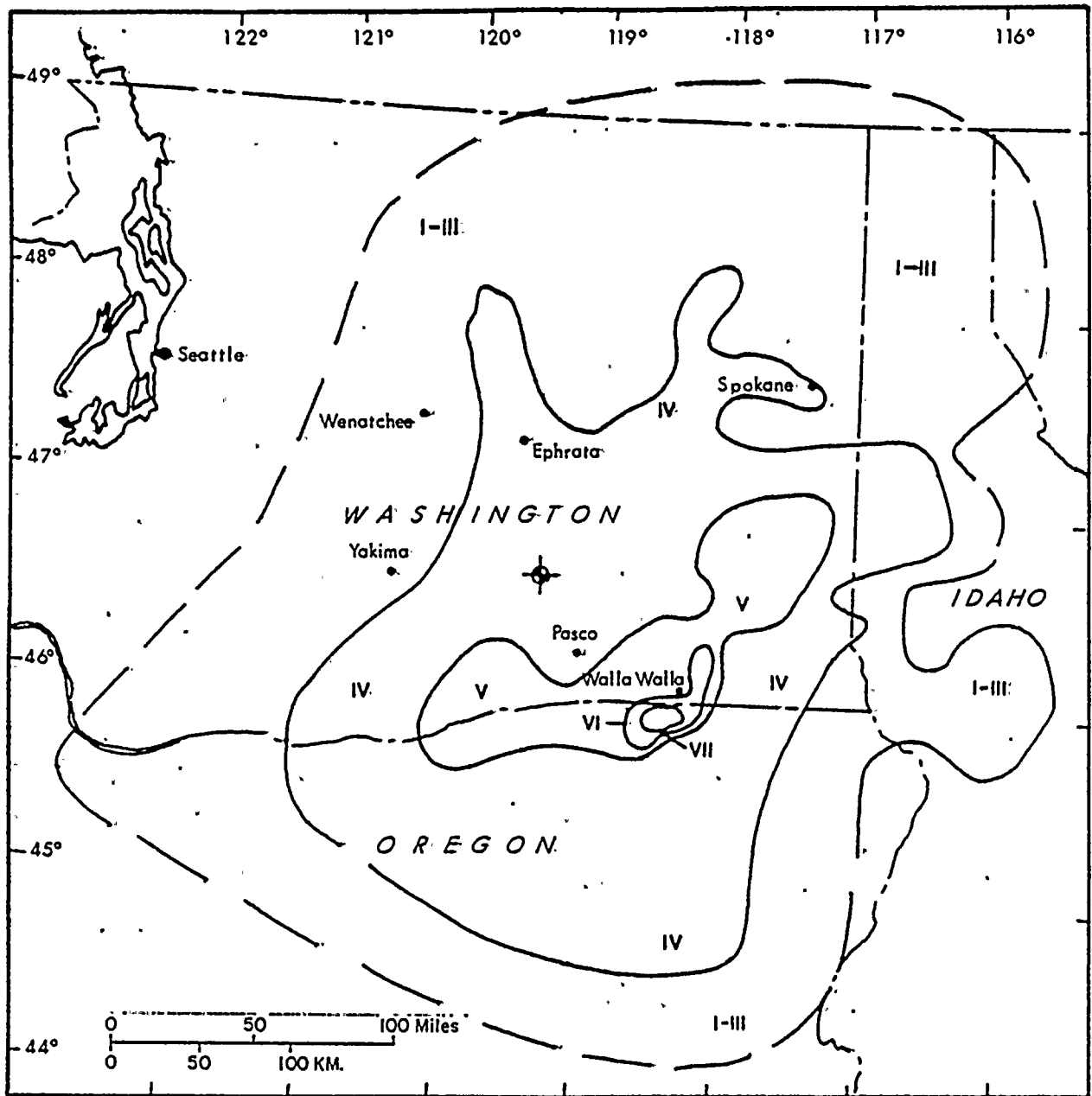


# EXPLANATION

- ISOSEISMAL, DASHED WHERE ASSUMED
- X MODIFIED MERCALLI INTENSITY  
ACCORDING TO WPPSS (1977)
- F FELT
- EPICENTER AREA ACCORDING TO MILNE (1956)
- MEIZOSEISMAL AREA ACCORDING TO COOMBS et al (1976)
- MEIZOSEISMAL AREA ACCORDING TO PSP&L (1977)
- BALANCED ROCK (ONAK LAKE)

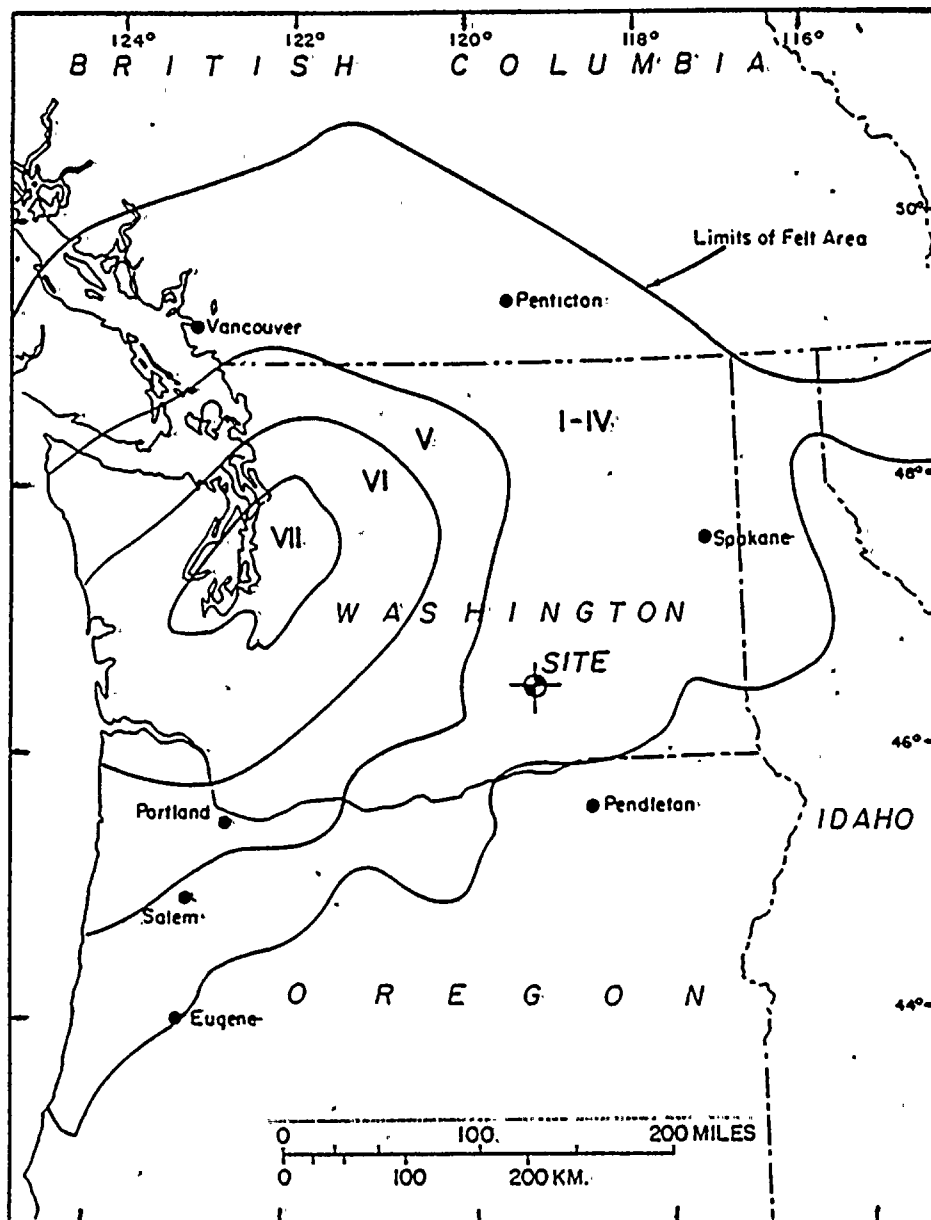
From: Appendix 2RB, Amendment 23, WNP 1/4 PSAR

Figure 2.5-40 Isoseismal Map for  
December 14, 1872

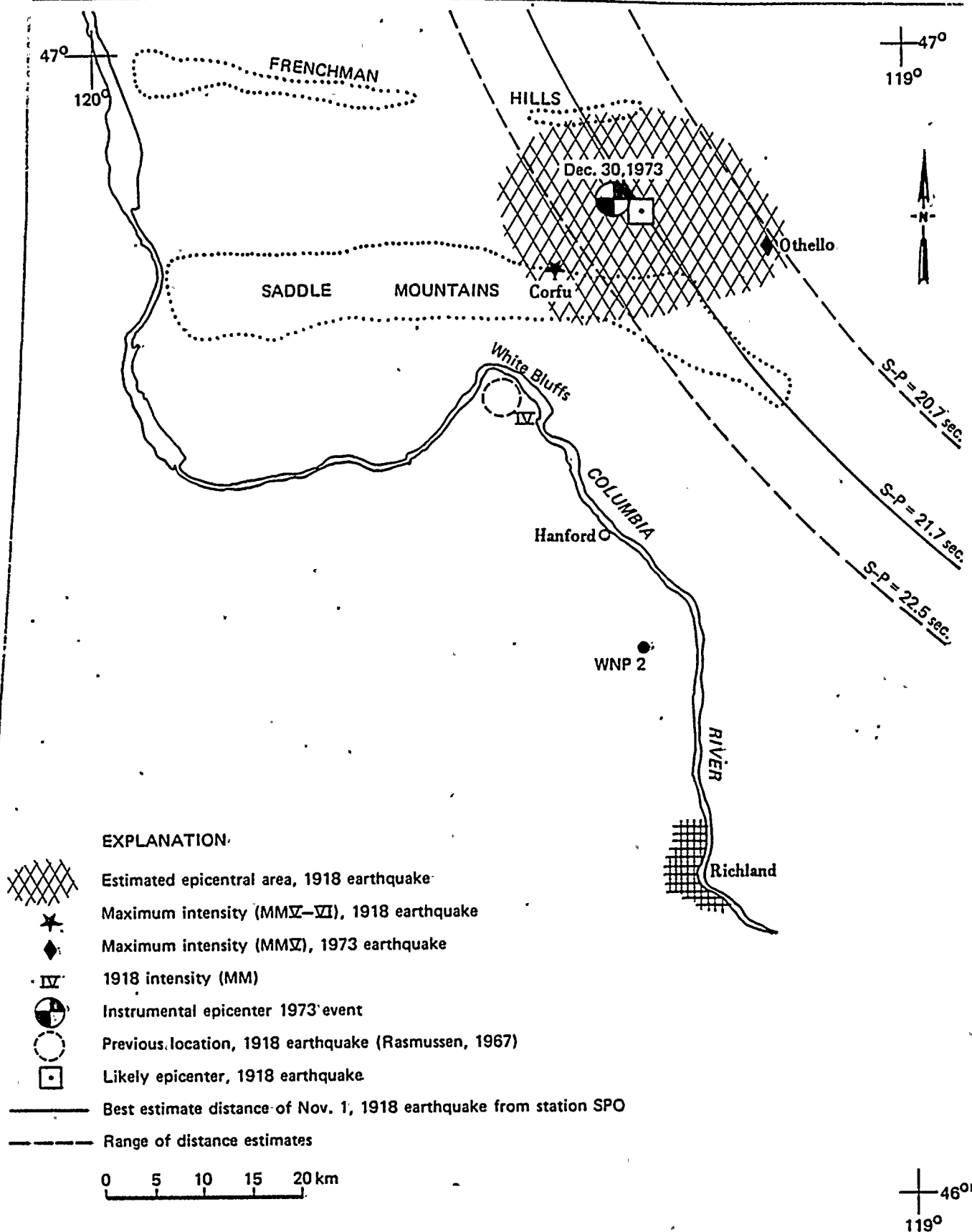


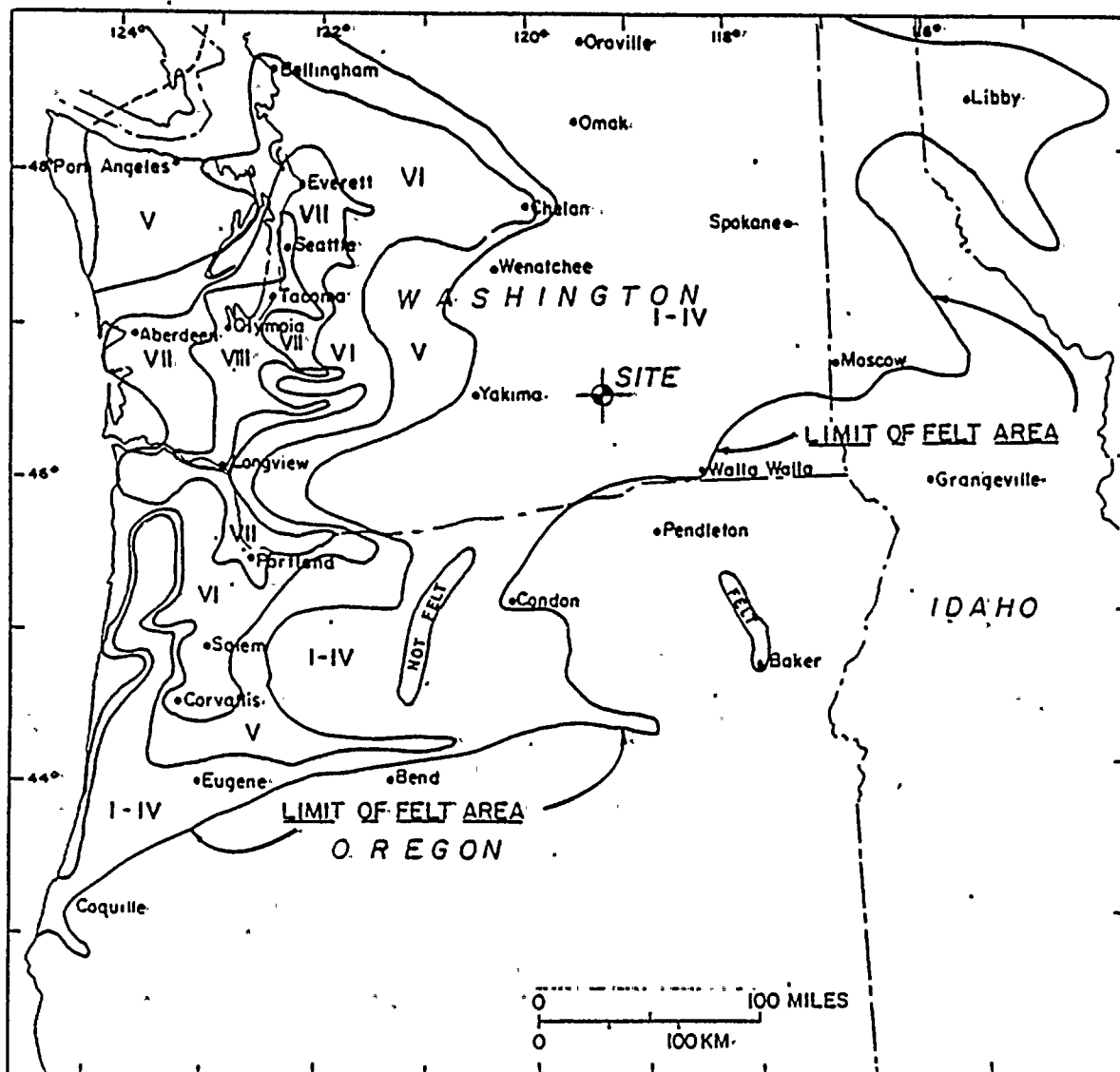
DATA FROM:  
U.S. COAST & GEODETIC SURVEY (NOAA)  
MSA-11

Iseseismal Map for  
July 16, 1936



Isoseismal Map for  
April 29, 1965

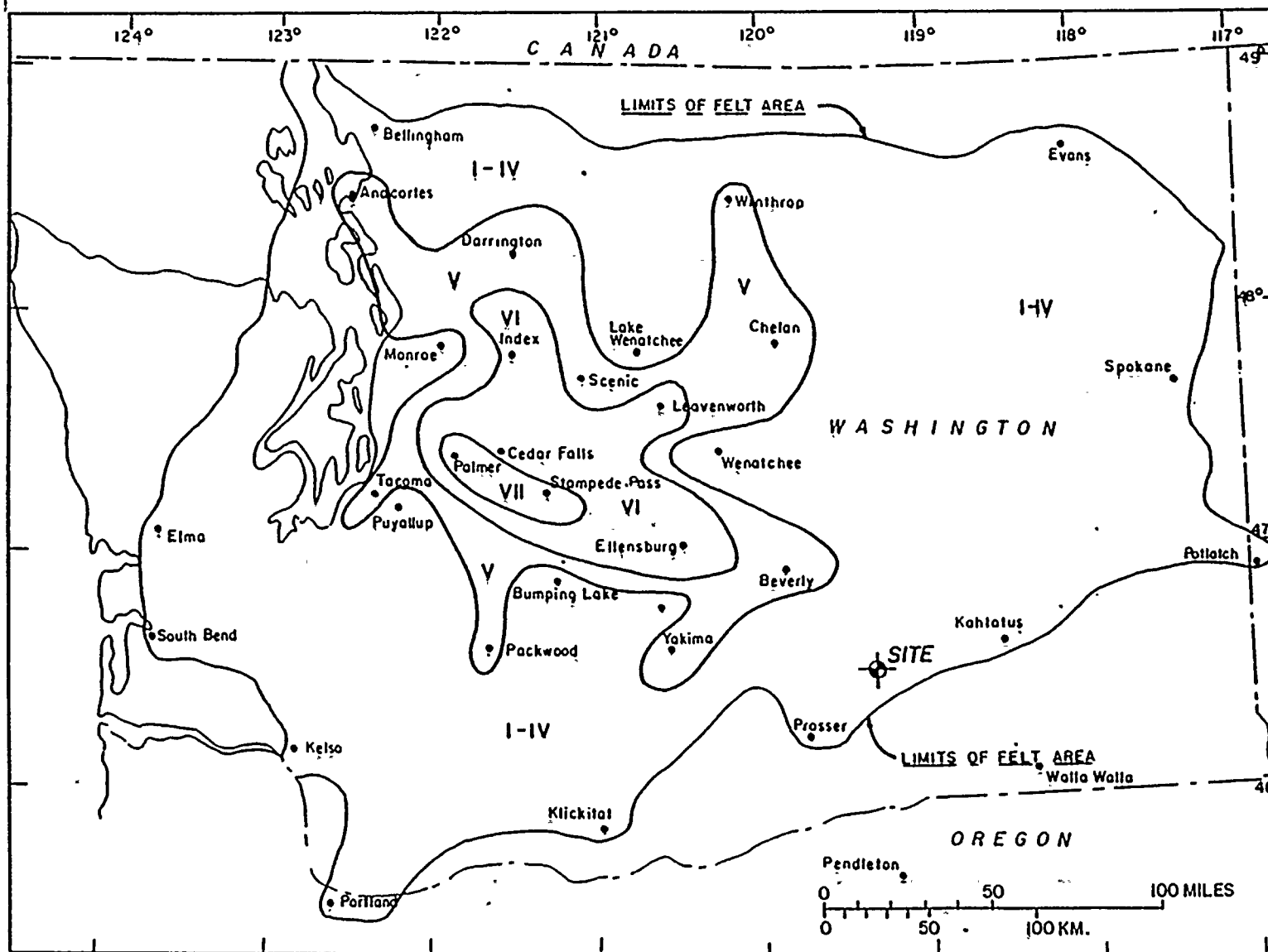




Isoseismal Map for  
April 13, 1949

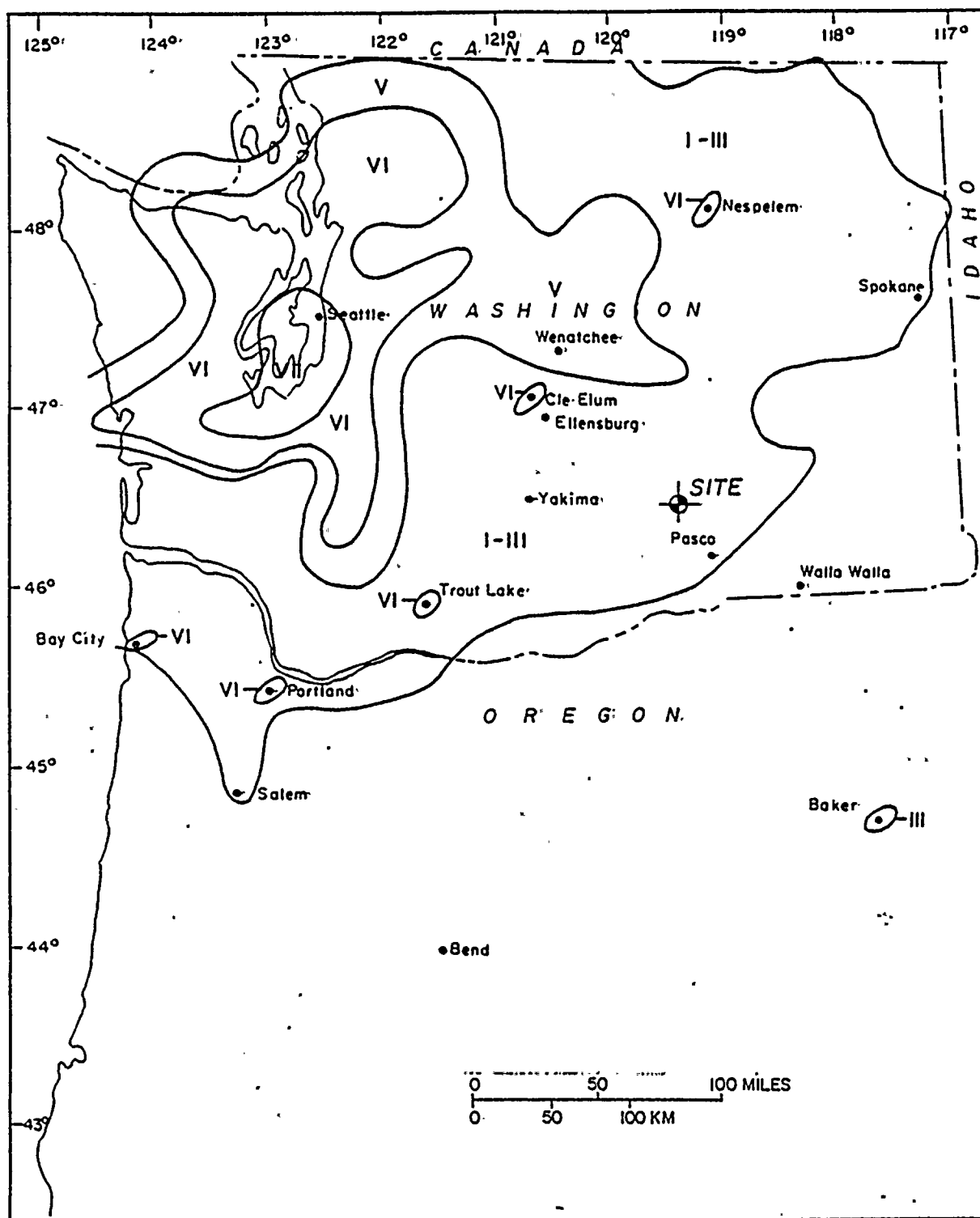


Isosismal Map for  
April 29, 1945

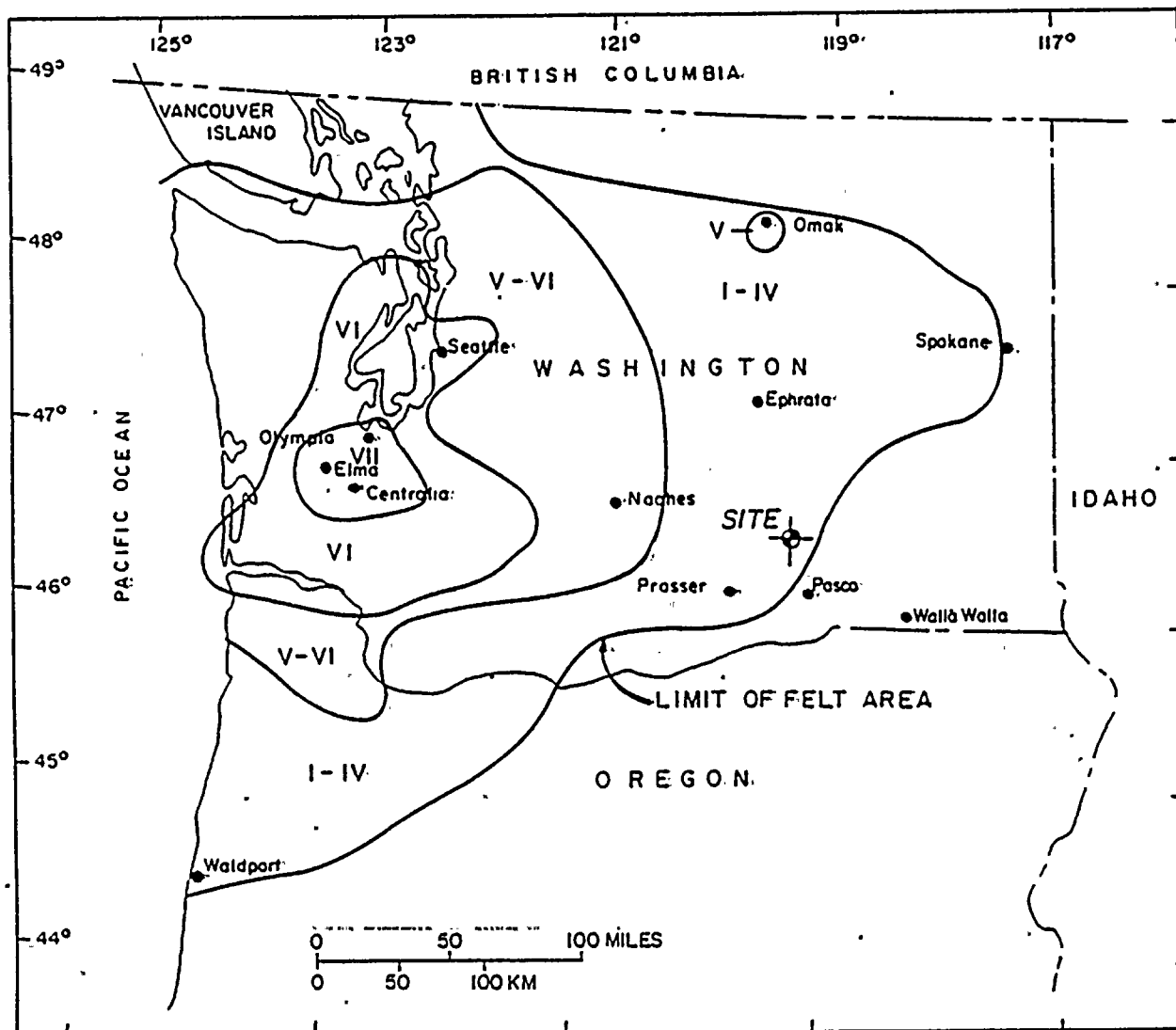


DATA FROM:  
U.S. COAST & GEODETIC SURVEY (NOAA)  
MSA-46





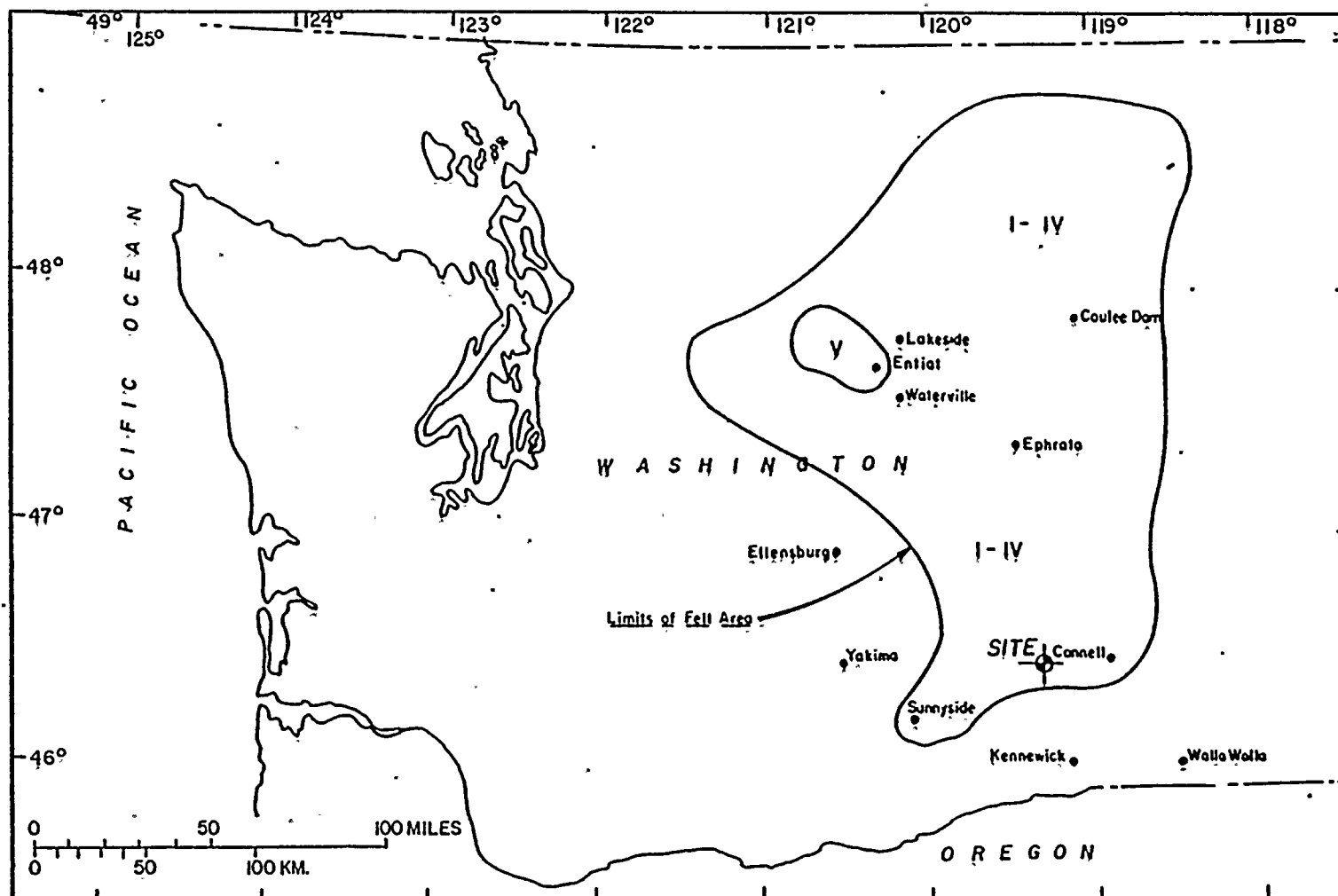




Isoseismal Map for  
November 13, 1939

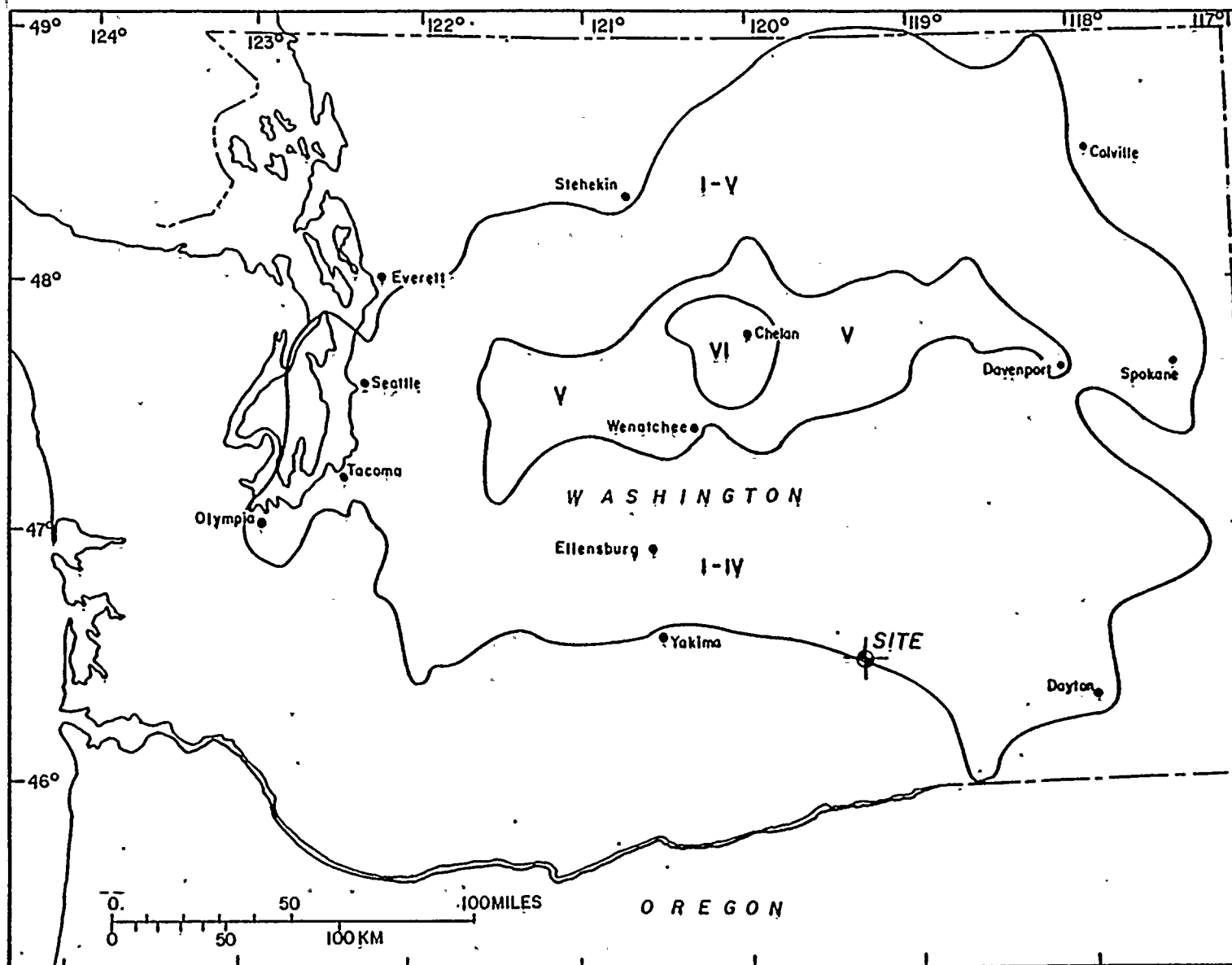


Isosismal Map for  
April 24, 1943



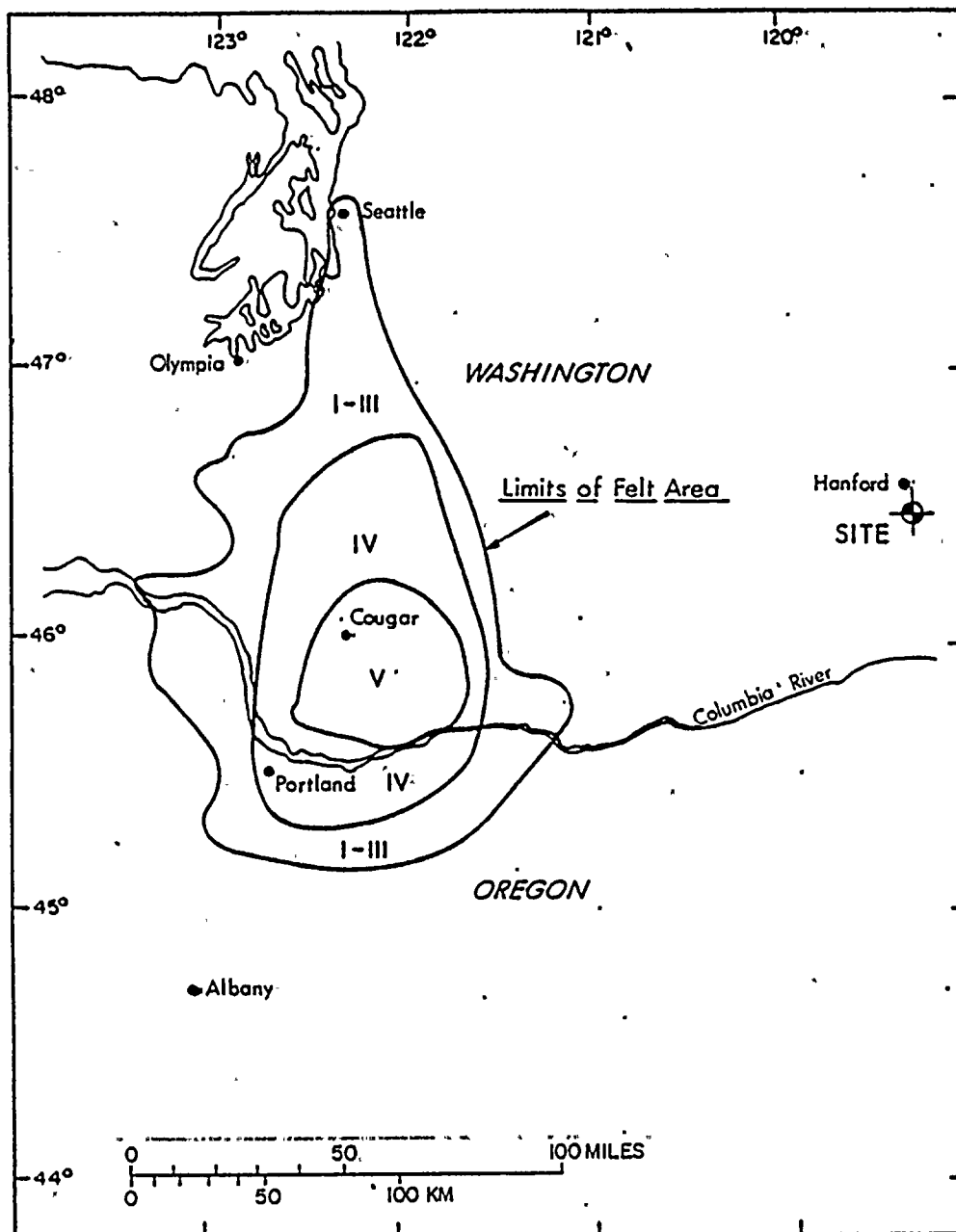
DATA FROM:  
U.S. COAST & GEODETIC SURVEY (NOAA)  
MSA-38

Isoselmal Map for  
August 6, 1959



DATA FROM:  
U.S. COAST & GEODETIC SURVEY (NOAA)

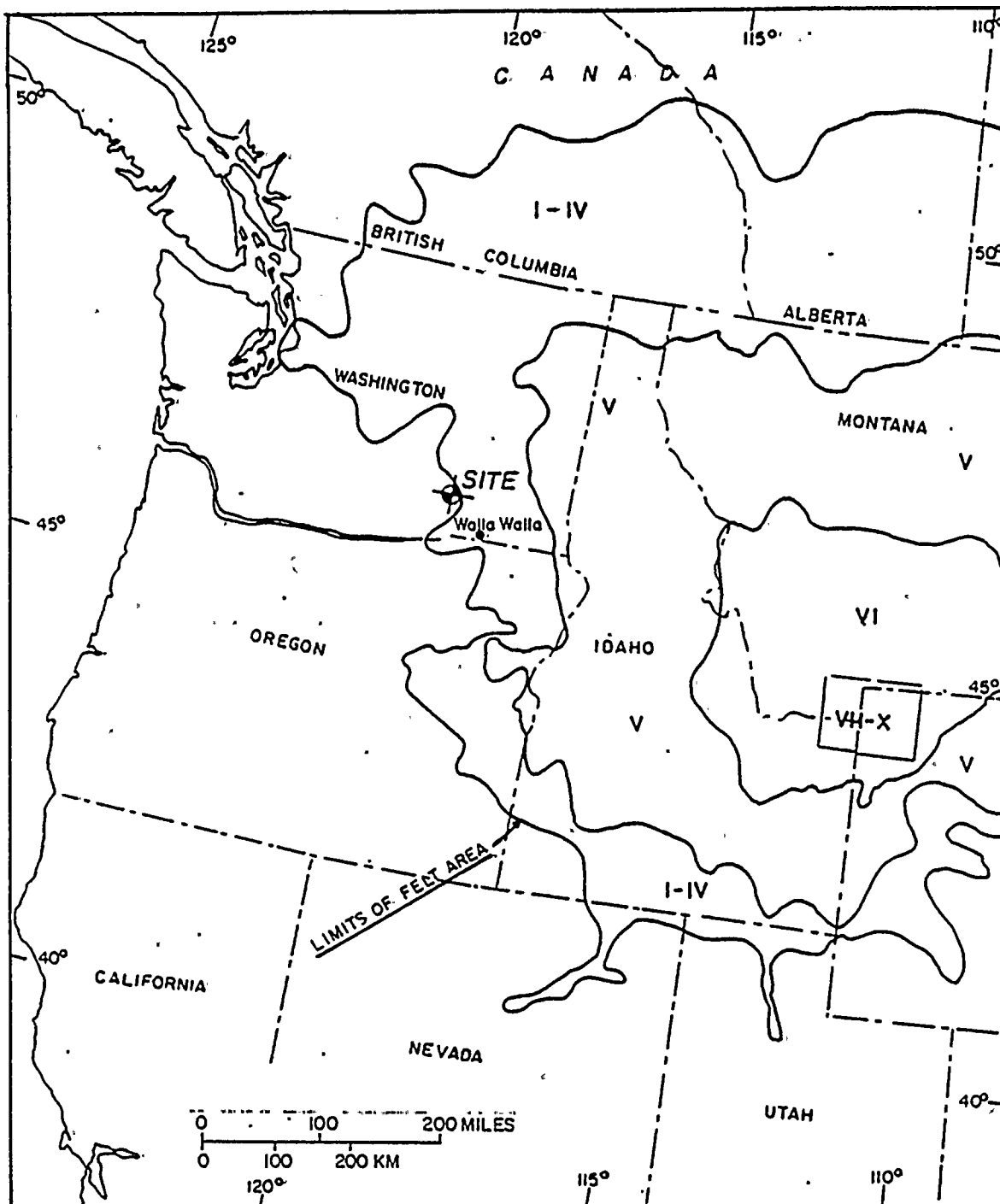




Isoseismal Map for  
September 16, 1961







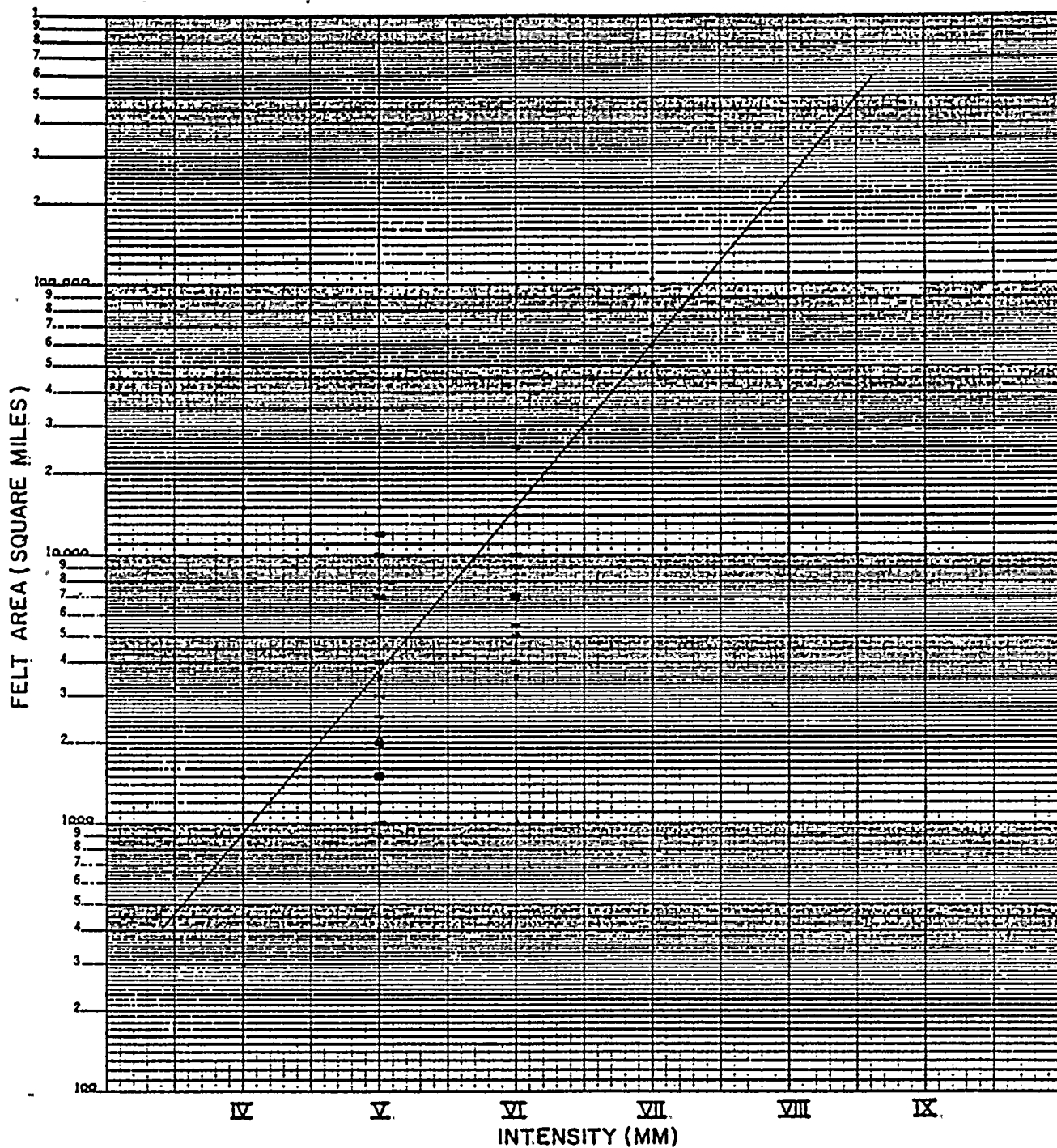
Iseseismal Map for  
August 17, 1959



FIGURE 2.5-52.

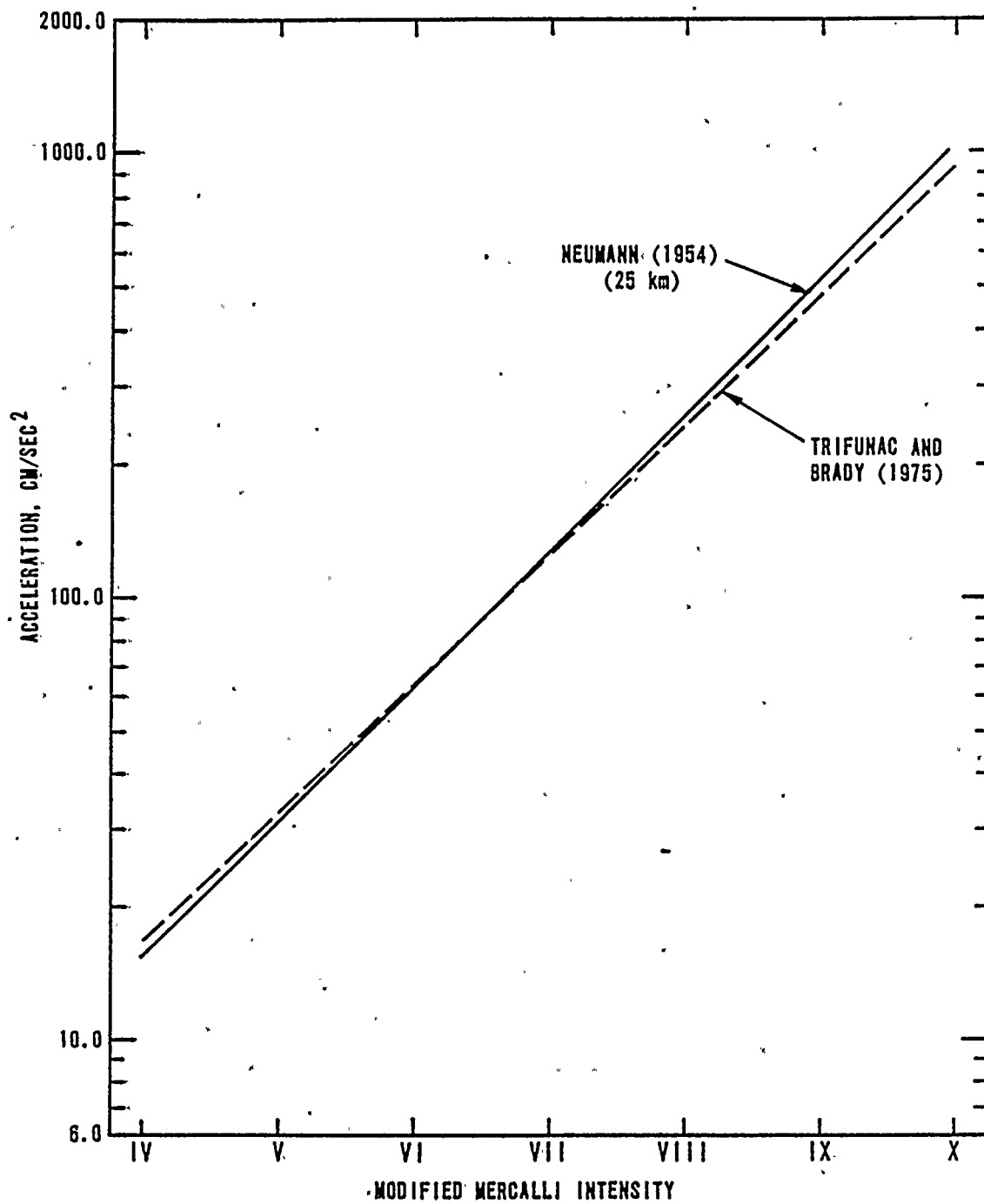
IS CURRENTLY BEING PRINTED.





Intensity Versus Felt  
Area for Earthquakes  
within 200 Miles of  
the Site

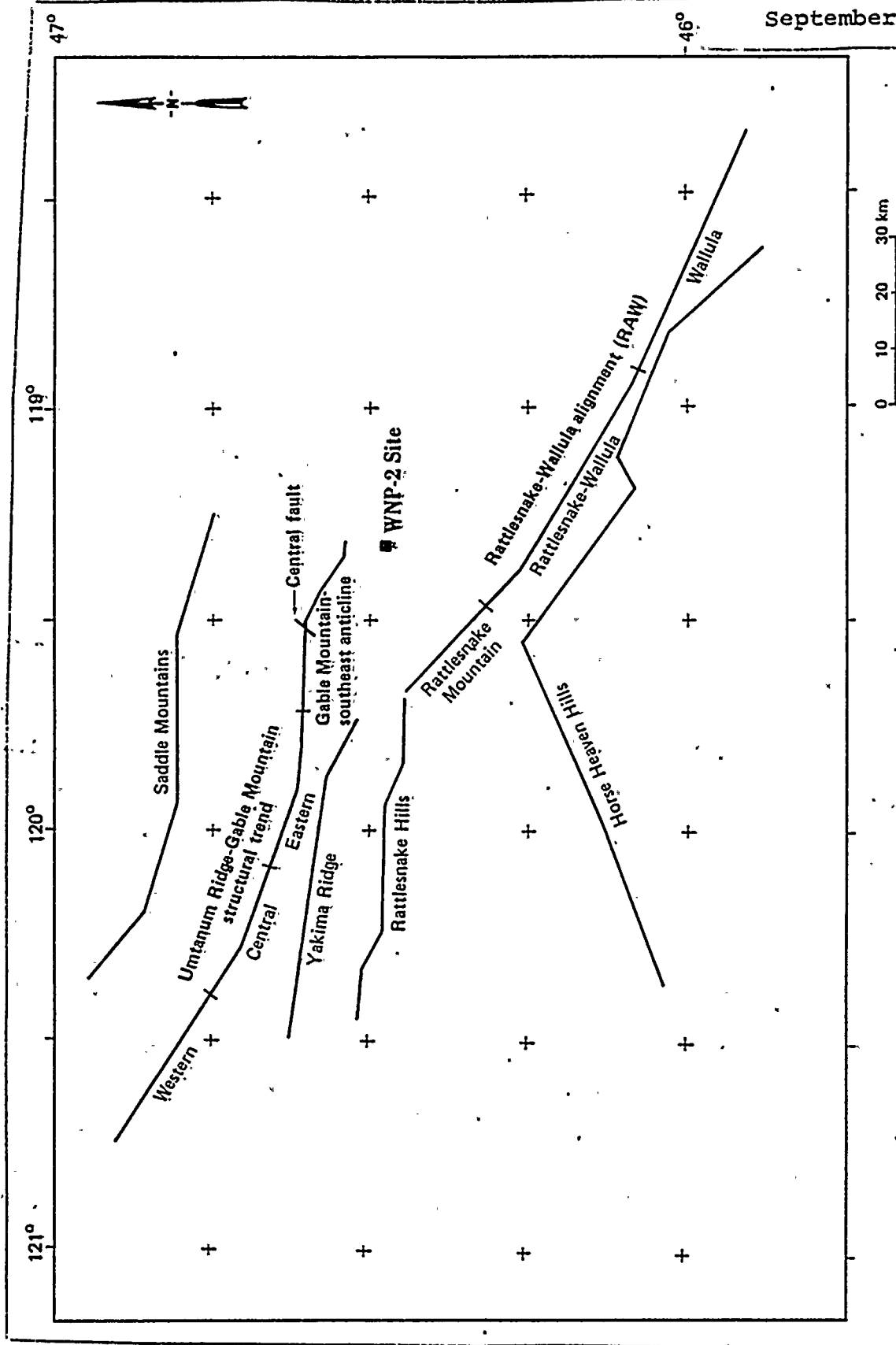




Earthquake Intensity  
Versus Acceleration



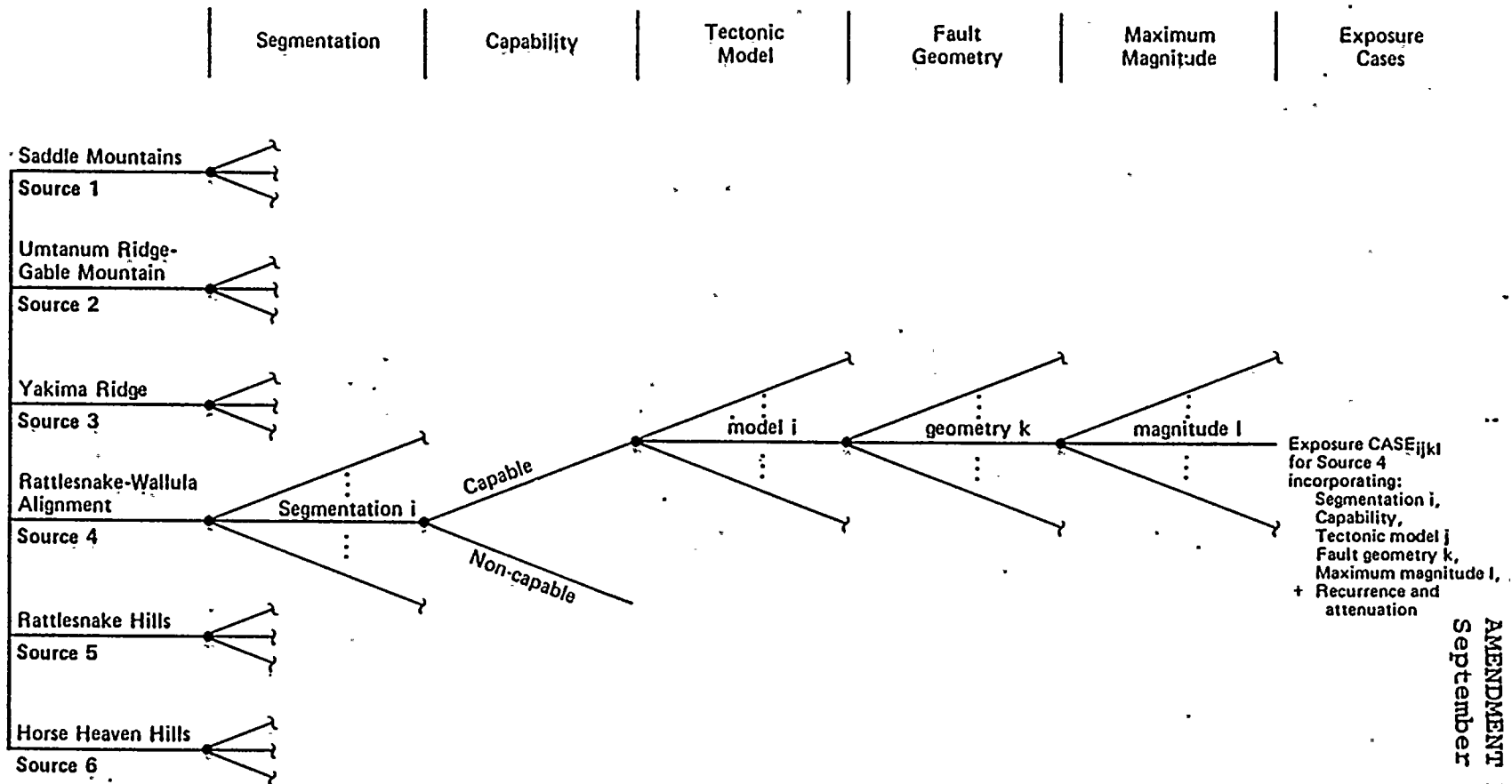




WASHINGTON PUBLIC POWER SUPPLY SYSTEM  
NUCLEAR PROJECT NO. 2

SIMPLIFIED MAP OF POTENTIAL  
SEISMIC SOURCES SIGNIFICANT TO  
THE WNP-2 SITE

FIGURE  
2.5-55



$$P_4 \left\{ \begin{array}{l} \text{exceeding } 0.25g \\ \text{from source 4} \end{array} \right\} = \sum_{\text{all } i} \sum_{\text{all } j} \sum_{\text{all } k} \sum_{\text{all } l} p \left\{ \begin{array}{l} \text{segmentation} \\ i \end{array} \right\} p \left\{ \begin{array}{l} \text{source is} \\ \text{capable} \end{array} \right\} p \left\{ \begin{array}{l} \text{model} \\ j \end{array} \right\} p \left\{ \begin{array}{l} \text{geometry} \\ k \end{array} \right\} p \left\{ \begin{array}{l} \text{magnitude} \\ l \end{array} \right\} p \left\{ \begin{array}{l} \text{exceeding } 0.25g \\ \text{for CASEijkl} \end{array} \right\}$$

$$P \left\{ \begin{array}{l} \text{exceeding } 0.25g \\ \text{from all sources} \end{array} \right\} = 1 - (1 - p_1)(1 - p_2) \cdots (1 - p_6)$$



AMENDMENT NO. 18  
September 1981

DELETED

WASHINGTON PUBLIC POWER SUPPLY SYSTEM  
NUCLEAR PROJECT NO. 2

FIGURE  
2.5-57

AMENDMENT NO. 18  
September 1981

DELETED

WASHINGTON PUBLIC POWER SUPPLY SYSTEM  
NUCLEAR PROJECT NO. 2

FIGURE  
2.5-58

AMENDMENT NO. 18  
September 1981

DELETED

WASHINGTON PUBLIC POWER SUPPLY SYSTEM  
NUCLEAR PROJECT NO. 2

FIGURE  
2.5-59

AMENDMENT NO. 18  
September 1981

DELETED

WASHINGTON PUBLIC POWER SUPPLY SYSTEM  
NUCLEAR PROJECT NO. 2

FIGURE  
2.5-60



TABLE 2.5-7

This table is being printed.

8111250276

$p(TM_k | S_i, C_j)$  = Conditional probability of tectonic model  $k$ , given segmentation  $i$  and capable fault  $j$

$p(FG_1 | S_i, C_j, TM_k)$  = probability of fault geometry  $1$ , given segmentation  $i$ , capable fault  $j$ , and tectonic model  $k$

$p(m_m^u | S_i, C_j, TM_k, FG_1)$  = probability of maximum magnitude  $m^u$ , given segmentation  $i$ , capable fault  $j$ , tectonic model  $k$ , and fault geometry  $1$

$\theta$  = an indicator variable equal to 1.0 if exposure calculated from Equation (2.5K-3) for  $C_j$ ,  $TM_k$ ,  $FG_1$ ,  $m_m$  and  $E[A_n]$  equals  $\nu_n(z)$ ; otherwise equal to 0

- o If the source is segmented into " $j$ " fault segments, the distributions for the individual segments are assumed to be completely correlated; that is, if a particular path through the logic tree is the correct path on one segment, then it is the correct path on all of the other segments in the source. The mean number of events  $\nu_n(z)$  for a particular tectonic model, fault geometry, and maximum magnitude is obtained by summing the contributions from the same branch on each of the faults. The probability of the sum is given by Equation (2.5K-10) for one of the segments.
- o If the source consists of " $j$ " separate sources then it is assumed that the distribution for each source is completely independent. To obtain the total number of events, all possible combinations of " $j$ " capabilities, " $k$ " tectonic models, " $1$ " fault geometries, and " $m$ " maximum magnitudes must be considered.

#### 2.5K.2.2.3 Calculation of Total Seismic Exposure

The probability distribution of the mean number of events exceeding ground motion level  $z$  for source  $s$  is computed using Equations (2.5K-8) through (2.5K-10). The total number of events exceeding  $z$  from all sources is computed by Equation (2.5K-2)

$$\nu(z) = \sum_n \nu_n(z)$$

The expected value of  $\nu(z)$  is computed by summing the expected values from each source



$$E[\nu(z)] = \sum_n E[\nu_n(z)] \quad (2.5K-11)$$

The variance of  $\nu(z)$  is computed using the expression

$$\text{Var}[\nu(z)] = \sum_n \text{Var}[\nu_n(z)] \quad (2.5K-12)$$

Equation (2.5K-12) assumes that each of the sources is acting independently of all other sources.

Confidence intervals for the probability of exceedance can be assessed if the distribution of the mean number of events,  $\nu(z)$ , is known. As  $\nu(z)$  is the sum of independent variables, it can be assumed that the distribution of  $\nu(z)$  is approximately normal. Using the calculated mean and variance of  $\nu(z)$  and the normal cumulative distribution function, various upperbound probability levels can be estimated for  $\nu(z)$  and, consequently, for  $p(Z > z)$ .

The procedure for calculating the probability of exceedance of a specified ground-motion level can be summarized as follows:

- (1) For each segmentation of the source, obtain  $\nu_n[(z)|S_i, E(A_n)]$  from Equation (2.5K-10), including the correlation between segments for multiple fault segmentations.
- (2) Calculate  $p[\nu_n(z)|(E(A))]$  from Equation (2.5K-11) by combining the conditional probability distribution from Step 1 over all possible segmentations of the source.
- (3) Calculate  $p[\nu_n(z)]$  from Equation (2.5K-8) by combining the probability distribution obtained in Step 2 over all possible values of  $A_n$ .
- (4) Calculate the expected value of  $\nu_n(z)$  by summing the expected value of  $\nu_n(z)$  over all sources. The probability of exceedance of  $z$  is then computed using Equation (2.5K-1).
- (5) Calculate confidence levels for the mean number of events using Equation (2.5K-12) and assuming a normal distribution for  $\nu(z)$ .

### 2.5K.3 DEFINITION OF POTENTIAL SEISMIC SOURCES

This section defines the potential seismic sources in terms of location, segmentation, capability, tectonic model, and geometry. Sections 2.5K.3.1 and 2.5K.3.2 discuss the alternative tectonic models and their implications to segmentation, fault width, and capability. In Section 2.5K.3.3, the data on segmentation, capability, tectonic models, and fault width that are used to evaluate both the maximum earthquake and its contribution to seismic exposure of each potential source are summarized; also in this section, the maximum magnitude and exposure logic trees through fault width are developed.

In the Columbia Plateau, there is uncertainty regarding structural relationships at depth; therefore, constraints on fault geometry and other aspects of fault behavior have to be based largely on tectonic models that are inferred from the style of deformation observed at the surface. Descriptions of the tectonic history of the Columbia Plateau and the timing and style of deformation have been given in Bentley (1977), Appendices 2.5N and 2.5-0 (Washington Public Power Supply System, 1981b, 1981c), and Price (1980; written communication, 1981). These descriptions provide a basis for developing alternative tectonic models of Plateau deformation.

All structures that extend within 50 km of the site and that may be associated with faults by consideration of the alternative tectonic models are assumed to be potential seismic sources in the seismic exposure analysis. Based on an assumed maximum earthquake magnitude of 7-1/2 on any potential source, and on the attenuation relationships developed for the site region, the distance from the site beyond which the ground motions from such an earthquake would not contribute to the probability of exceeding the 0.25-g design basis ground motion. The potential seismic sources included in the seismic exposure analysis are: the Umtanum Ridge-Gable Mountain structural trend, the Rattlesnake-Wallula alignment (RAW), Saddle Mountain, Rattlesnake Hills, Yakima Ridge and Horse Heaven Hills (Figure 2.5K-37).

#### 2.5K.3.1 Tectonic Models of Columbia Plateau Deformation

The major structural elements within the Columbia Plateau are the generally east-west asymmetric Yakima folds that are associated with mapped and inferred reverse faults, and the northwest-trending alignment of folds, domes, and faults that define the Cle Elum-Wallula lineament (CLEW). These structural elements are discussed below.

#### 2.5K.3.1.1 Yakima Folds and Associated Reverse Faults

The Yakima folds are shown in Figure 2.5K-38. These folds trend generally east-west, although folds in the northern part of the Plateau trend northwest and those in the south trend northeast. The folds are asymmetric, concentric, kink-type folds. They generally have steeper north-facing limbs, and some have long, gently dipping south limbs that extend for distances of up to several kilometers. The folds vary in structural and geomorphic expression along their strike; variations occur in structural relief, vergence, degree of asymmetry, and development of secondary folds.

Reverse faults, observed and inferred, are associated with many of the folds. These faults commonly occur in close association with the zones of maximum fold flexure. Reverse faults vary in length from hundreds of meters to tens of kilometers. Along the major folds, reverse faults may occur on either side of the fold as the fold changes vergence. Along some folds, parallel reverse faults occur on both sides of the fold and dip toward each other.

Proposed models of Plateau deformation suggest that the Yakima folds developed either as: (1) primary folds with or without secondary reverse faults; or (2) secondary folds related to throughgoing crustal reverse faults.

##### 2.5K.3.1.1.1 Primary Folding with Secondary Reverse Faulting Model

This model of plateau deformation is supported by Price (1980; 1981) and in Appendix 2.5N (Washington Public Power Supply System, 1981b); these conclude that the Yakima folds developed as the primary response of the Columbia River basalts to general north-south compression. The folding may have been facilitated by localized or shallow detachment within the basalts. In this model, north- and south-dipping reverse faults that flank some of the folds were formed during the late stages of fold development and are secondary to the fold structures.

##### 2.5K.3.1.1.2 Primary Reverse Faulting and Secondary Folding Model

The spatial distribution and geometry of the Yakima folds can also be used to infer the presence of major reverse faults that are the controlling structures in fold development. Bentley (1977) proposed that the Yakima folds are faulted monoclines that are localized above zones of high-angle faults that extend from the basement. In Appendix 2.5-0 (Washington Public Power Supply System, 1981c), Laubscher suggests that

the Yakima folds are narrow structures developed on broader warps. From this, he infers the presence of multiple décollements in the Columbia Plateau and suggests that the broad warps were localized by thrust ramps rising from a deep (approximately 20 km) regional décollement and that the narrow folds (the Yakima folds) formed above a shallow (1- to 3-km deep) décollement. A geometric analysis of Umtanum Ridge, Saddle Mountain, and Rattlesnake Hills, based on a fault ramp-flexure model (Bruhn, 1981), suggests the presence of fault ramps below these folds that extend to décollements at preferred depths of 3 to 5 km. Bruhn (1981) notes that these fault ramps could consist of loci of interconnected faults and kink bands rather than large, discrete fault planes.

#### 2.5K.3.1.2 Cle Elum-Wallula Lineament (CLEW) and Rattlesnake-Wallula Alignment (RAW)

The Cle Elum-Wallula lineament (CLEW) and its southern half, the Rattlesnake-Wallula alignment (RAW), are shown in Figure 2.5K-37. The present field data base does not provide adequate constraints for a unique tectonic model to explain the northwest-trending alignment of structural features that define CLEW. Alternative models interpret CLEW as: (1) a generally diffuse zone of right-lateral strain that contains strike-slip faults; or (2) a Yakima fold structure in which deformation along the CLEW trend is primarily folding and reverse faulting.

##### 2.5K.3.1.2.1 Strike-Slip Fault Model

In Appendix 2.5-0 (Washington Public Power Supply System, 1981c), Laubscher defines CLEW as a northwest-trending zone of en echelon anticlines comprising part of the Yakima fold belt; he interprets these to represent the upper crustal expression of a deep-seated (15- to 20-km) right-lateral crustal shear. In Appendix 2.5N (Washington Public Power Supply System, 1981b), based on variation in structural patterns and geomorphology, Davis' interpretation is that CLEW is a zone of right-lateral strain in the crust of the Columbia Plateau and it developed synchronously with, and interacted with, the Yakima folds. Davis defined three structural domains and concluded that the zone is narrow and occurs at the surface in the southern domain (along the Wallula fault) and that it becomes progressively deeper and/or broader to the northwest..

##### 2.5K.3.1.2.2 Yakima Fold Model

Price (written communication, 1981) suggests that the northwest-striking folds that occur along the RAW portion of CLEW can be interpreted as asymmetric folds that developed as the Columbia River basalts were folded across a northwest-





trending rigid buttress in the Plateau basement. In this model, a throughgoing zone of right-lateral strike-slip faulting is not required; the basement behaves passively and deformation along the CLEW trend occurs primarily as folding with secondary reverse or reverse-oblique slip faulting. Investigations by Woodward-Clyde Consultants (1981a) along the RAW alignment also suggest that shortening normal to the alignment has been an important factor in the development of the observed structures.

#### 2.5K.3.2 Implications of Alternative Tectonic Models to Source Definition

The alternative tectonic models proposed for the Columbia Plateau influence the evaluation of the geometry, segmentation, and capability of potential earthquake sources. These are all major factors in assessing the maximum earthquake magnitude of potential earthquake sources and the potential seismic exposure at the site.

##### 2.5K.3.2.1 Segmentation

Segmentation of potential seismic sources is an important factor in the assessment of both maximum magnitude and seismic exposure. Segmentation affects earthquake magnitude estimates by placing constraints on total fault length and fault rupture length. It also affects exposure by defining the number of sources and constraining the location along a source where rupture may occur. Geologic, geomorphic, and seismic data have been used to define fault segments that either represent earthquake rupture segments or portions of a fault that exhibit a uniform behavior through time (Aki, 1979; Bakun, 1980). Because of differences in the mechanics of rupture for dip-slip faults, there appears to be a higher probability that geologically well-defined surface segments represent rupture segments than they do for strike-slip faults.

For the seismic exposure analysis, three models of segmentation are considered for the significant potential sources. These are:

- (1) A single source: in this model, it is assumed that rupture can occur anywhere along the source.
- (2) A segmented source: in this model, the segment length is defined by structural and geomorphic data and constrains the location of rupture and the rupture length.

- (3) Separate sources: in this model, segments behave as individual sources, and fault rupture length is assumed to be a fraction of the source length.

The likelihood that a particular segmentation model is applicable to a source is dependent on the tectonic model. Because the maximum magnitude logic trees for the Umtanum Ridge-Gable Mountain structural trend and the Rattlesnake-Wallula alignment begin by defining the sources by their segmentation (Figures 2.5K-3 through 2.5K-13, the dependence of tectonic models on segmentation must be assessed. This assessment is done by considering the probabilistic interdependence of segmentation and tectonic models. First, the unconditional probabilities of tectonic models and the conditional probabilities of each segmentation model (Figures 2.5K-39 and 2.5K-40) are assessed. Then, through the use of Bayes' theorem, the probabilities of each tectonic model conditional on segmentation are calculated. For example, the probability that the Umtanum Ridge-Gable Mountain structural trend is a primary reverse fault, given that it is a segmented source (Figure 2.5K-39), is:

$$p(\text{primary}|\text{segmented}) = \frac{p(\text{segmented}|\text{primary}) \times p(\text{primary})}{\sum_{\text{all models}} p(\text{segmented}|\text{model}) \times p(\text{model})}$$

$$\text{specifically} = \frac{(0.6)(0.2)}{(0.6 \times 0.2) + (0.2 \times 0.8)} = 0.43$$

#### 2.5K.3.2.2 Capability

The capability of faults, both mapped and inferred, associated with the Yakima folds and CLEW is uncertain. In the seismic exposure analysis, tectonic models and models of segmentation affect the assessment of capability. For example, in the primary faulting model, a source may behave as a single source, a segmented source, or a group of individual sources. If a fault is defined as capable at a point along a single source or along a source segment, then the entire source and all of the segments are also capable because they are structurally associated. However, if a segment defines a separate source, then the capability of each source must be evaluated independently.

#### 2.5K.3.2.3 Fault Width and Length

The alternative tectonic models result in a range of possible down-dip fault widths and fault lengths. If a reverse fault is secondary to a fold, its maximum down-dip width will probably be no greater than the width of the fold, and fault length will be limited to the length of the fold. Faults developed in this manner will generally have small surface

areas and, if they are seismogenic, have the potential to produce only small- to moderate-magnitude earthquakes.

If the Yakima folds are related to deeper reverse faults, then down-dip fault width may vary from approximately 5 to 23 km (Section 2.5K.3.3), and fault length may be constrained by the length of major folds or fold segments. These proposed faults, if they are seismogenic, have the potential to produce moderate-to large-magnitude earthquakes because of their area.

If CLEW is modeled as a vertical strike-slip fault zone, the available data suggest probable depths of faulting between 7.5 and 20 km (Section 2.5K.3.3); fault length may be constrained by structural and geomorphic segments. This fault geometry has the potential to produce moderate-to large-magnitude earthquakes. If CLEW is modeled as a throughgoing reverse fault, then fault parameters will be similar to the primary reverse faulting model proposed for the Yakima folds, and potential earthquake magnitudes could be moderate to large. However, if CLEW is a series of northwest-trending folds with secondary faults, only small- to moderate-magnitude earthquakes would be expected, if the faults are seismogenic.

#### 2.5K.3.3 SEGMENTATION, CAPABILITY, TECTONIC MODELS AND FAULT WIDTH OF SPECIFIC POTENTIAL SOURCES

The alternative tectonic models result in a range of fault parameters. At present, no one model can be applied to all Columbia Plateau structures. Studies at Umtanum Ridge (Price, 1980; Golder Associates, 1981a) and Gable Mountain (Golder Associates, 1981b) indicate that observed reverse faults have narrow widths and are secondary to the folds. In contrast, the presence of scarps along the base of Toppenish Ridge suggests the possibility of a seismogenic reverse fault and, therefore, the existence of a fault plane having significant area (Woodward-Clyde Consultants, 1981b). These observations suggest that a range of styles of deformation and fault geometries may be associated with the Plateau folds. This range may reflect such factors as variations in the thickness of the Columbia River basalts, variations in the mechanical properties of different basalt units, local stress differences, and the influence of basement structures or irregularities on concentrating stress and deformation. Because of these factors, it is necessary to evaluate independently each potential seismic source.

##### 2.5K.3.3.1 Umtanum Ridge-Gable Mountain Structural Trend

For the Umtanum Ridge-Gable Mountain structural trend, the maximum magnitude logic trees are shown in Figures 2.5K-6



through 2.5K-9, and the exposure logic trees are shown in Figures 2.5K-14 through 2.5K-23.

#### 2.5K.3.3.1.1 Segmentation

Figure 2.5K-41 shows the possible variation in fault behavior and segmentation along the Umtanum Ridge-Gable Mountain structural trend. The possible segmentation models are those described in Section 2.5K.3.2.1. Golder Associates (1981a,b) conclude that the Umtanum Ridge-Gable Mountain structural trend is a bedrock high that is composed of five segments. These are: the Umtanum Ridge western segment; the Umtanum Ridge central segment; the Umtanum Ridge eastern segment; the Gable Mountain-Gable Butte segment; and the Southeast anticline segment. The three segments on Umtanum Ridge are based on discontinuities of faulting and changes in fold vergence along the axis of the anticline (Golder Associates, 1981a). Golder Associates (1981b) and Weston Geophysical (1981c) interpret the existence of a Gable Mountain-Gable Butte segment as distinct from the Umtanum Ridge segments on the basis of a change in structural style characterized by the broadening and decrease in structural relief of the first order fold, the development of second and third order folds, and distinctive gravity and magnetic signatures. Weston Geophysical (1981c) defines the Southeast anticline as a subsurface, low amplitude, anticlinal ridge that is separate from, and overlaps, the eastern end of the Gable Mountain-Gable Butte segment. However, for this seismic exposure analysis, the Gable Mountain-Gable Butte and Southeast anticline segments are treated as a single segment because of the similarity in the style of deformation along the structural trend. Data for the Southeast anticline segment are used in the assessment of fault geometry (Section 2.5K-4).

Segmentation of the Umtanum Ridge-Gable Mountain structural trend is dependent on the tectonic model, and the probabilities associated with each model of segmentation are conditional on the tectonic model. This is shown in Figure 2.5K-39. If the tectonic model is a primary reverse fault, then the probability that the fault can be treated as distinct segments defined geologically is greatest (0.6). It is less likely (0.3) that the structure is a single source and there is little chance (0.1) that segments represent separate sources that behave independently. However, if a secondary reverse fault model is applied, the probability that individual faults will behave as separate sources is greatest (0.8). The likelihood that the faults are segments of a larger structure is considerably less (0.2).

## 2.5K.3.3.1.2 Capability

Mapping and trenching studies by Golder Associates (1981b) have shown that the Central fault on Gable Mountain displaces 13,000- to 19,000-year-old glaciofluvial deposits a maximum of 6 cm. Although this fault is capable according to NRC criteria, alternative non-tectonic mechanisms have been proposed for the origin of the displacement of the glaciofluvial deposits (Golder Associates, 1981b). Therefore, a probability of 0.9 is given to the capability assessment.

If the Umtanum Ridge-Gable Mountain structural trend is considered to be a single source, then the probability that the entire source is capable is 0.9. Likewise, the probability that each segment of a segmented source is capable is also 0.9.

If the segments of the Umtanum Ridge-Gable Mountain structural trend are considered as separate sources, the capability of each is evaluated independently. The probability that the Gable Mountain source is capable is 0.9, based on the presence of the Central fault. Detailed work by Golder Associates (1981a) along the eastern segment of Umtanum Ridge suggests that the Umtanum fault, the Buck thrust, and a possible northern splay of the Umtanum fault are not capable; however, a pull-apart structure and a 1.5-km-long, north-facing scarp, both of which are similar in appearance to seismogenically produced fault features, allow the possibility that some Quaternary faulting could have occurred. Based on these observations, the probability that the Umtanum Ridge east segment is capable is 0.3. There are no data that pertain to capability of the Umtanum Ridge central and west segments, and therefore, the probability that they are capable is 0.5.

## 2.5K.3.3.1.3 Tectonic Models

Alternative tectonic models for the Yakima folds are presented in Section 2.5K.3.1.1. The observations that support the model of primary folding with secondary reverse faulting along the Umtanum Ridge-Gable Mountain structural trend are: (1) relationships between fold geometry, strain, and faulting along eastern Umtanum Ridge at Priest Rapids Dam (Price, 1980); (2) the mapped extent of the Umtanum fault and the change in the direction of vergence along the axis of the Umtanum Ridge anticline (Price, 1980; Golder Associates, 1981a); (3) the development of second-order folds and the close spatial relationship between these folds and reverse faults along Gable Mountain-Gable Butte (Golder Associates, 1981b); and (4) the gentle south and north dips of the first-order fold (Fecht, 1978) along the Gable Mountain-southeast anticline segment.



The Central fault on Gable Mountain displaces 13,000- to 19,000-year-old glaciofluvial deposits and appears to have developed between growing folds (Golder Associates, 1981b). In addition scarps and pull-apart features are present on the Umtanum Ridge east segment. Because of these observations, the possibility that a primary fault is associated with the Umtanum Ridge-Gable Mountain structural trend cannot be precluded.

The available data favor the model of primary folding with secondary reverse faulting. Therefore, the relative weight for this tectonic model is 0.8.

#### 2.5K.3.3.1.4 Fault Width

Fault width is independent of segmentation but is dependent on the tectonic model. Data for evaluating fault widths are not well-constrained. Assuming a primary reverse fault, widths of 5, 11, 20, and 23 km are considered. These widths are developed using a range of dips that are reasonable for reverse faults and possible depths of faulting suggested by available geophysical data.

- o The 5-km width is derived using a fault that dips 60 degrees and extends to a depth of 4 km. The 4-km depth is the maximum depth to the base of the Columbia River basalts based on gravity data (Weston Geophysical, 1981a).
- o A width of 11 km is obtained using the average depth to basement of 7.5 km (Eaton, 1976) and a fault dip of 45 degrees.
- o The 20-km width is based on a 30-degree fault dip extending to the maximum depth of the top of basement at 10 km.
- o The 23-km width is obtained using the average maximum depth of seismicity of 20 km, as discussed in Appendix 2.5.J (Washington Public Power Supply System, 1981a) and a fault dipping 60 degrees.

The relative weights of these values, 0.4, 0.4, 0.1, and 0.1, respectively, reflect the greater likelihood that if reverse faults are primary, they are more likely to initiate at mechanical discontinuities; these are most likely defined by the base of the basalt and the top of the basement. These values are the same for all fault segments when a primary reverse fault model is used.



When the model of secondary reverse faulting is considered, values of down-dip fault width will vary for each segment because they are dependent on the width of the associated fold. Widths for the Gable Mountain-southeastern anticline segment are 1 km (average) and 3 km (maximum); widths for the three Umtanum Ridge segments are 2 km and 5 km. In both cases, the average value is given a relative weight of 0.6 because it is more representative.

#### 2.5K.3.3.2 Rattlesnake Wallula (RAW) Portion of the Cle Elum-Wallula Lineament (CLEW)

For RAW, the maximum magnitude logic trees are shown in Figures 2.5K-3 through 2.5K-5, and the exposure logic trees are shown in Figures 2.5K-24 through 31.

##### 2.5K.3.3.2.1 Segmentation

A schematic diagram of segmentation of the Rattlesnake-Wallula alignment (RAW) is shown in Figure 2.5K-42. Three possible segments are considered in the present analysis (Figure 2.5K-37). These are (1) the Wallula fault segment, which is defined by a complex zone of folding and apparent strike-slip faulting; (2) the Rattlesnake-Wallula segment, which is defined by an alignment of structural domes, doubly plunging anticlines, and minor strike-slip or reverse-oblique-slip faults; and (3) the Rattlesnake Mountain segment, which is defined by the continuous northeast flank of a major fold. These segments correspond to the structural domains of CLEW discussed by Davis in Appendix 2.5N (Washington Public Power Supply System, 1981b).

Segmentation of RAW is dependent on the tectonic model (Figure 2.5K-40). For a strike-slip fault model, there is little basis for choosing between the three possible modes of rupture behavior; however, there is a slightly higher probability (0.4) that, given the strike-slip model, rupture could occur anywhere along RAW and extend across structurally defined segment boundaries (Section 2.5K.3.2.1).

If RAW represents a primary reverse fault, there is a higher probability (0.7) that the proposed segments define rupture segments, and a lesser probability (0.2) that rupture would occur anywhere along the trend or that the segments define separate sources (0.1).

If RAW is a major fold with secondary reverse faults, the probability is very high (0.9) that the reverse faults will behave as separate sources, and it is unlikely (0.1) that it will behave as a segmented source.

## 2.5K.3.3.2.2 Capability

Mapping and trenching studies have been conducted by Woodward-Clyde Consultants (1981a) along RAW at Warm Springs Canyon and at Finley Quarry (Figure 2.5K-38). At Warm Springs Canyon, colluvial deposits and loess of uncertain, but probable Quaternary, age are in apparent fault-contact with Frenchman Springs basalt. Although the age of the colluvium and loess, and the contact relationships between these deposits and the basalt, are equivocal, field observations suggest that the deposits have been involved in the displacement. Based on the available evidence, the probability that a capable fault occurs at this location is 0.7.

At Finley Quarry, two faults that displace Quaternary-age gravel are overlain by, and do not displace, a deposit with a caliche soil that is a minimum of 70,000 years old; the deposits may be much older (Section 2.5K.5.1.2). A third fault in this zone is not overlain by these deposits and the age of most recent displacement is not known. Based on these observations, the probability that the faults at Finley Quarry are capable is 0.7.

IF RAW is considered as a single source, then the probability that the entire source is capable is 0.7. The probability that each segment of RAW is capable is also 0.7.

If the segments of RAW are treated as separate sources, the probability of the Wallula and Rattlesnake-Wallula sources are capable is 0.7. The probability that the Rattlesnake Mountain source is capable is 0.5 because no data for assessing capability are available.

## 2.5K.3.3.2.3 Tectonic Models

Tectonic models for CLEW have been discussed in Section 2.5K.3.1.2. There are no extensive geophysical data that provide information on structure below the basalts across RAW, and the available field observations do not strongly support one model over another. Evidence for right-lateral strike-slip faulting is based principally on the presence of generally sub-horizontal striations along the Wallula fault and subparallel structures (Farooqui, 1979), and a very slightly en echelon pattern of domes and doubly plunging anticlines between Rattlesnake Mountain and Wallula Gap (Appendix 2.5N: Washington Public Power Supply System, 1981b). Recent work (Woodward-Clyde Consultants, 1981a) indicates the presence of a major monocline along the Wallula fault zone and, together with the presence of the parallel Horse Heaven Hills anticline immediately to the west, raises questions about the relationship of the Wallula fault to

folding of the basalts and the significance of the zone as a throughgoing crustal strike-slip fault. Also, geometric analysis of individual domes (Woodward-Clyde Consultants, 1981a) shows that their strikes generally vary within 10 degrees in either direction of the RAW trend and not the experimentally determined 30 to 40 degrees that would be expected if they represented a response to right-lateral shear in the basement.

Observations (Woodward-Clyde Consultants, 1981a) that suggest that structures along the RAW alignment represent a fold similar to the other Yakima folds are: (1) folds developed along RAW are parallel to some of the other Yakima folds; (2) folds along RAW show general asymmetry with steeper northeast flanks similar to other Yakima folds; (3) structural relief across the folds in RAW is consistently down to the northeast; and (4) mapped faults along the RAW trend are generally consistent with reverse or reverse oblique-slip faulting.

If the RAW trend represents a Yakima fold, it is uncertain which model of Yakima folding is applicable. Based on evidence from regional reconnaissance and clay modeling studies, Price (written communication, 1981) concludes that the RAW structures are simply folds that were localized and oriented by a northwest-trending rigid buttress in the plateau basement. However, few data demonstrate the presence of a basement contrast or rigid buttress.

In summary, there are no compelling data to make a strong or unequivocal choice of tectonic models. Based on the available data, weights of 0.4 are assigned to both the strike-slip and primary reverse fault models, and 0.2 is assigned to the primary folding model.

#### 2.5K.3.3.2.4 Fault Width

Fault widths for RAW are dependent on the tectonic model. Data on width are not well-constrained. Assuming a vertical throughgoing strike-slip fault, down-dip widths considered in this analysis are 7.5, 12, and 20 km.

- o The 7.5-km width is based on the average depth to basement using the time-term analysis (Eaton, 1976).
- o A 12-km width is derived by extending the fault to the depth above which 95 percent of all microearthquake activity occurs (Woodward-Clyde Consultants, 1981c).

- o A 20-km width is obtained by extending the fault to the average maximum depth of seismicity.

Strike-slip faults capable of producing surface rupture generally extend through the crust and, on a worldwide basis, generally have hypocentral depths of 15 km or less. While little seismicity occurs between 12 and 20 km in the Columbia Plateau, there is some possibility that the brittle crust could extend to this depth. In the Columbia Plateau, it is unlikely that throughgoing strike-slip faults would be restricted to supracrustal material above 7-1/2 km. Therefore, the fault widths are given relative weights of 0.2, 0.5, and 0.3, respectively.

If RAW is interpreted as a Yakima fold structure, segments will have widths of 5, 11, 20, or 23 km if it is a primary reverse fault, and widths of 2 and 5 km if it is a secondary reverse fault. The relative weights and justifications are the same as those described in Section 2.5K.3.3.1.4.

#### 2.5K.3.3.3 Saddle Mountains

For Saddle Mountains, the maximum magnitude logic tree is shown in Figure 2.5K-13, and the exposure logic tree is shown in Figure 2.5K-35.

##### 2.5K.3.3.3.1 Segmentation

The data are insufficient for assessing segmentation of the Saddle Mountains anticline. Therefore, it is treated as a single source.

##### 2.5K.3.3.3.2 Capability

The general spatial relationship between microseismicity and the anticline and the observation that the nearby 1973 Royal Slope earthquake had a thrust mechanism on a plane striking southeast to east and dipping either south or northeast (Woodward-Clyde Consultants, 1981c) suggest that east-trending, south-dipping reverse faults on the north side of the anticline could be capable. Based on these possible correlations, the probability that Saddle Mountains is a capable source is 0.6.

##### 2.5K.3.3.3.3 Tectonic Models

The tectonic models applicable to the Saddle Mountains anticline are folding with secondary reverse faulting and primary reverse faulting. Data on the structure at depth below the anticline are few. The structural style observed along the anticline is characterized by strong asymmetry and the

presence of mapped south-dipping reverse faults along the steep north flank, and is similar to that observed along Umtanum Ridge. However, because of the lack of detailed information on fold-fault relationships, differentiation between models is not well-constrained, and assigned weights are 0.6 for the primary folding model and 0.4 for primary reverse faulting.

#### 2.5K.3.3.3.4 Fault Width

For primary reverse faulting, widths and weights described in Section 2.5K.3.3.1.4 are applicable. For the secondary fault model, widths of 2 and 6 km are used. The 2-km width represents the average width of the Saddle Mountains fold; the 6-km width defines the maximum fold width. The average width is given a slightly higher weight (0.6) because it is more representative.

#### 2.5K.3.3.4 Rattlesnake Hills

For Rattlesnake Hills, the maximum magnitude logic tree is shown in Figure 2.5K-10, and the exposure logic tree is shown in Figure 2.5K-33.

##### 2.5K.3.3.4.1 Segmentation

The data are insufficient for assessing segmentation of Rattlesnake Hills. Therefore, it is treated as a single source.

##### 2.5K.3.3.4.2 Capability

The data are insufficient to evaluate the capability of this potential source. Therefore, the probability that it is capable is 0.5.

##### 2.5K.3.3.4.3 Tectonic Models

The data do not provide a strong basis for weighting alternative tectonic models. Because no mapped faults are associated with the fold, the fold model is given a slightly higher weight of 0.6

##### 2.5K.3.3.4.4 Fault Widths

For primary reverse faulting, widths and weights described in Section 2.5K.3.3.1.4 are applicable. For the secondary fault model, widths of 2 km (average fold width) and 5 km (maximum fold width) are used. A probability of 0.6 is given to the 2-km width because it is more representative.



## 2.5K.3.3.5 Yakima Ridge

For Yakima Ridge, the maximum magnitude logic tree is shown in Figure 2.5K-12, and the exposure logic tree is shown in Figure 2.5K-34.

## 2.5K.3.3.5.1 Segmentation

The data are insufficient for assessing segmentation of Yakima Ridge. Therefore, it is treated as a single source.

## 2.5K.3.3.5.2 Capability

The data are insufficient to evaluate the capability of this potential source. Therefore, the probability that it is capable is 0.5.

## 2.5K.3.3.5.3 Tectonic Models

The data do not provide a strong basis for assigning weights to alternative tectonic models. Because no mapped faults are associated with the fold, the fold model is given a slightly greater weight of 0.6.

## 2.5K.3.3.5.4 Fault Widths

For primary reverse faulting, widths and weights described in Section 2.5K.3.3.1.4 are applicable. For the secondary fault model, widths of 2 km (average fold width) and 4 km (maximum fold width) are used. A probability of 0.6 is given to the 2-km width because it is more representative.

## 2.5K.3.3.6 Horse Heaven Hills

For Horse Heaven Hills, the maximum magnitude logic tree is shown in Figure 2.5K-11, and the exposure logic tree is shown in Figure 2.5K-32.

## 2.5K.3.3.6.1 Segmentation

The data are insufficient for assessing segmentation of Horse Heaven Hills. Therefore, it is treated as a single source.

## 2.5K.3.3.6.2 Capability

The data are insufficient to evaluate the capability of this potential source. Therefore, the probability that it is capable is 0.5.

### 2.5K.3.3.6.3 Tectonic Models

The data do not provide a strong basis for selecting alternative tectonic models. Because no mapped faults are associated with the fold, the fold model is given a higher probability of 0.6.

### 2.5K.3.3.6.4 Fault Widths

For primary reverse faulting, widths and weighting described in Section 2.5K.3.3.1.3 are applicable. For the secondary fault model, widths of 2 km (average fold width) and 5 km (maximum fold width) are used. A probability of 0.6 is given to the 2-km width because it is more representative.

## 2.5K.4 MAXIMUM EARTHQUAKE MAGNITUDES

This section develops the maximum magnitude distributions for the potential sources. Section 2.5K.4.1 discusses the approach to estimating maximum magnitudes. Section 2.5K.4.2 presents the maximum magnitudes for potential sources included in this seismic exposure analysis.

At present, there is no generally accepted method for assigning a maximum earthquake magnitude to a given fault. The various approaches that are used have generally been developed from the empirical relationships between magnitude and a specific fault parameter. These parameters include fault rupture length and surface fault displacement measured in the field following surface faulting earthquakes, and fault length and downdip width assessed from studies of aftershock sequences. Compilations of these data on worldwide historical earthquakes have been used to develop regressions of magnitude on length, magnitude on displacement, and magnitude on area. In addition, seismic moment can be related to static fault parameters and to magnitude. Relationships between magnitude and slip rate have also been proposed.

Geologic and seismologic studies can define physical and behavioral characteristics (fault length, fault width, amount of displacement per event, recurrence interval, and slip rate) for potential earthquake sources. These data, when used in empirical and analytical relationships, can provide an estimate of the most likely earthquake magnitudes for a given parameter. However, each method has some limitations. These include a somewhat limited data set, nonuniformity in the quality of the empirical data, and a inconsistent grouping of data from different tectonic environments. Values for magnitudes derived from these relationships represent expected or average estimates. Assessment of a maximum magnitude is ultimately a judgment based on an understanding of specific



fault characteristics, the regional tectonic environment, similarity of the fault to other faults in the region, and data on regional seismicity.

The combination of several magnitude-estimation techniques can result in more reliable estimates of maximum magnitude than the application of any single technique. In this way, a wide range of fault behavioral information can be included in the analysis, and the resulting magnitude estimates will be those that are best substantiated by the available data. To assess the range of magnitude estimates for a source, uncertainties in fault parameters and in the magnitude relationships must be identified and evaluated. A probabilistic approach to magnitude estimation provides a means for formally accounting for these uncertainties.

#### 2.5K.4.1 Approaches To Estimating Maximum Magnitude

A general discussion of approaches for estimating maximum earthquake magnitudes on faults is presented below. The analysis of maximum magnitudes for specific potential sources that may be significant to the site is presented in Section 2.5K.4.2.

##### 2.5K.4.1.1 Rupture Length Versus Magnitude

The most common approach to estimating maximum magnitude is through a comparison of fault rupture length and earthquake magnitude. Based on historical earthquake data, empirical relationships between rupture length and earthquake magnitude have been established by several authors (Tocher, 1958; Bonilla and Buchanan, 1970; Mark and Bonilla, 1977; Slemmons, 1977; Acharaya, 1979). These relationships allow an average magnitude to be selected for a given rupture length.

In applying this technique to maximum magnitude estimates, a maximum rupture length is assessed for a fault, and a corresponding magnitude is selected based on the regressions of worldwide data. These regressions may have errors resulting from the assessment of the length of surface rupture, as well as in the instrumental magnitude determinations (Bolt, 1978). Also, considerable uncertainty often exists in the selection of the appropriate rupture length to be used in the analysis. Rupture lengths of past surface-rupture events on the fault may provide direct evidence. In the absence of these data, indirect evidence must be used to estimate rupture lengths. Geologic and geomorphic investigations may identify discontinuities in the surface expression of a fault along its length. Individual

segments identified in this way may represent rupture segments whose length can be used in magnitude estimates.

A more indirect method of estimating rupture length is based on the assumption that a fraction of the total fault length will rupture during a given earthquake. The most common practice has been to assume that up to one-half of a fault's total length can rupture during a given earthquake. This assumption, proposed by Wentworth et al. (1969), is based on review of historical surface ruptures in southern California. However, in North America, historical earthquakes have ruptured from 2 percent to more than 75 percent of their total fault length (Wentworth et al., 1969; Slemmons, 1980). In addition, the total length of the fault is often difficult to define. Therefore, the fractional length approach to selecting an appropriate rupture length should only be used in the absence of more direct evidence.

The rupture length versus magnitude relationships used in the maximum magnitude analysis are those of Slemmons (1977):

$$\text{Strike slip:} \quad M_L = 4.651 + 1.351 \log L$$

$$\text{Reverse:} \quad M_L = 6.296 + 0.717 \log L$$

where  $L$  is the rupture length in kilometers, and  $M_L$  is the local magnitude.

#### 2.5K.4.1.2 Fault Area Versus Magnitude

The energy released during an earthquake is related to the size of the earthquake source's rupture surface. Therefore, fault rupture area (the product of the rupture length and the fault width) is more closely related to earthquake magnitude than is fault rupture length. For a given rupture length, different widths of faults may rupture, depending largely on fault type and tectonic environment. To accommodate this variation, empirical relationships have been established between fault rupture area and earthquake magnitude for historical events (Wyss, 1979; Singh et al., 1980). Fault area has a higher correlation with magnitude than does rupture length (Wyss, 1979). Even with errors in areas of up to a factor of two, estimates of magnitude vary only by 0.3 magnitude units (Wyss, 1979).

Estimates of the fault rupture area of earthquakes are usually based on the spatial pattern of aftershocks. The dimensions of a maximum earthquake that can be expected on any particular fault (Bonilla, 1980) is uncertain. However, the maximum depth to which faulting can be expected to occur within a



region can often be estimated, with a fairly high level of confidence, from seismicity data and information on crustal structure. The area versus magnitude relationship used in this analysis is that developed by Wyss (1979) for all fault types:

$$M_S = 4.15 + \log A$$

where A is the rupture area in square kilometers, and  $M_S$  is the surface-wave magnitude or  $M_W$  of Kanamori (1977).

#### 2.5K.4.1.3 Displacement Versus Magnitude

Maximum observed surface displacement can be empirically related to magnitude for historical surface faulting earthquakes (Tocher, 1958; Bonilla and Buchanan, 1970; Slemmons, 1977). As noted by Slemmons (1977), the correlation coefficient for this relationship is higher than for fault rupture length versus magnitude. This relationship may be particularly useful because recent geologic studies (Sieh, 1978; Swan et al., 1980) have shown that displacements from pre-historical earthquakes on a fault can be measured; these displacement values can then be used to estimate magnitudes.

Most of the uncertainty in the displacement versus magnitude relationship is associated with variability in the quality and uniformity of the field measurements of displacement included in the data set. For dip-slip faults, the data base includes measurements of both vertical scarp height and net slip. However, measured scarp height for normal-slip faults may be greater than the net tectonic slip because of modification of the scarp by graben formation and backtilting. For reverse-slip faults, vertical scarp heights may be as much as 50 percent less than the net tectonic slip, depending on the dip of the fault plane. In addition, it is uncertain if maximum displacement, which is usually limited to one location or a short segment of a fault, is a more meaningful physical parameter than average displacement. Average displacement data are not readily available for most historical surface ruptures.

The displacement versus magnitude relationships for strike-slip used in the maximum magnitude analysis are based on Slemmons' (1977) data. The reverse-fault relationship is based on a modification of the combined data sets for reverse and reverse-oblique presented by Slemmons (1977). From a re-examination of the original reports, all slip for reverse and reverse-oblique events has been normalized to net slip in order to increase the uniformity of the data. These relationships are:



AMENDMENT NO. 18  
September 1981

Strike slip:  $M_L = 6.717 + 1.214 \log D$

Reverse:  $M_L = 6.437 + 1.652 \log D$

where  $D$  is the maximum displacement, and  $M_L$  is the local magnitude.

#### 2.5K.4.1.4 Seismic Moment and Moment Magnitude

Because surface-wave magnitude saturates at about  $M_S$  7-1/2, seismic moment ( $M_0$ ) is a more accurate measure of the total energy release during large earthquakes (Kanamori, 1977).  $M_0$  is defined by  $AD\mu$ , where  $\mu$  is the rigidity of the crustal rocks (usually taken as  $3 \times 10^{11}$  dyn/cm<sup>2</sup>),  $D$  is the average displacement on a fault, and  $A$  is the area of the fault surface. Relationships between seismic moment and magnitude have been derived based on worldwide earthquake data. Kanamori (1977) defines a magnitude scale  $M_W$ , which does not saturate at the upper end and is equivalent to surface-wave magnitude in the range 6.0 to 8.0.  $M_W$  can therefore be considered a continuation of the  $M_S$  scale for large earthquakes. For  $M_W$  greater than 7-1/2 and  $M_S$  greater than 5 but less than 7-1/2, Hanks and Kanamori (1979) define a moment magnitude scale  $M$ , which is related to seismic moment ( $M_0$ ) by the relation:

$$M = 2/3 \log M_0 - 10.7 \quad (2.5K-13)$$

$M_0$  can be estimated directly by using long-period seismic waves, and indirectly from measured average surface displacements, rupture lengths, and estimated fault width. Uncertainties involved in the estimation of all of these parameters have been discussed for rupture length and fault area versus magnitude (Sections 2.5K.4.1.1 and 2.5K.4.1.2). Seismic moment can then be calculated, and a moment magnitude can be derived from the Equation (2.5K-13).

An assumption made in the derivation of the moment magnitude relationship is constant stress drop for large-magnitude earthquakes (Kanamori, 1977). Some error may be introduced into moment magnitude calculations because of regional variations in stress drop (Acharya, 1979). In addition, uncertainties in the estimation of displacement, rupture length, and fault width may lead to errors in the estimation of seismic moment.

Table D-1 of Hanks and Kanamori (1979) lists the values of  $M$  and  $M_S$  of 15 large California earthquakes. An analysis of the differences between the two magnitude values shows that, in California,  $M$  is an unbiased estimator of  $M_S$ , with a standard deviation of 0.24. This value implies that an estimate of the

surface-wave magnitude  $M_S$  of an hypothesized earthquake, using the value of  $M$  calculated from its static fault parameters ( $A$ ,  $D$ ,  $\mu$ ) via its moment  $M_0$ , will have a standard deviation of approximately one-quarter of a magnitude unit.

#### 2.5K.4.1.5 Slip Rate Versus Magnitude

The possibility that rate of slip across a fault may be proportional to the maximum earthquake was suggested by Smith (1976). Smith relates total Holocene slip and fault area to total moment on the fault and then uses empirical relationships between moment and magnitude to estimate the corresponding maximum earthquake. Slemmons (1977) relates slip rate and recurrence interval to magnitude, using his regression of displacement and magnitude.

In a comparison of slip rates and maximum historical earthquakes (Woodward-Clyde Consultants, 1979), an upper bound seems to exist for the maximum magnitude earthquake for a given slip rate on strike-slip faults along shear plate boundaries. Thus, slip rate may provide a guide to estimating maximum earthquake magnitude for this tectonic environment. However, preliminary analysis indicates a weak correlation between earthquake magnitude and slip rate for reverse and normal faults.

The relationship used in the maximum magnitude analysis was developed by Woodward-Clyde Consultants (1979) for strike-slip faults:

$$M_S = 7.223 + 1.263 \log S$$

where  $S$  is slip rate in millimeters per year, and  $M_S$  is the surface-wave magnitude.

#### 2.5K.4.1.6 Historical Seismicity

For faults having high rates of activity, such as the San Andreas fault, the maximum historical earthquake generated by the fault may be the maximum earthquake. Uncertainties in this type of evaluation stem from the usual brevity of historical records, uncertainties in measurements of the size of past earthquakes, and uncertainties in the association of historical events with specific faults. Techniques for assessing maximum magnitudes for regions based on historical seismicity have been proposed (Yegulalp and Kuo, 1974; Cosentino et al., 1977; Berrill and Davis, 1980). However, Chinnery (1979) concludes that the existence of a maximum magnitude has not been clearly demonstrated in any instrumental earthquake catalog.





#### 2.5K.4.2 Maximum Magnitudes For Specific Potential Sources

To account for the uncertainties in fault parameters and in the relative applicability of the magnitude estimation technique, maximum magnitudes for potential earthquake sources in the site region are assessed probabilistically. The assessment of maximum magnitude for potential sources is based on an evaluation of tectonic models, segmentation, and fault width (presented in Section 2.5K.3), and on additional magnitude-related parameters (rupture length, maximum and average displacement per event, slip rate, and technique applicability), presented in this section. The discussion of these parameters for each source is followed by a presentation of the unconditional and conditional probability distribution of maximum magnitudes for each potential source.

##### 2.5K.4.2.1 Magnitude-Related Parameters

As shown on the logic trees for each potential source (Figures 2.5K-3 through 2.5K-35), maximum magnitude is related to some of the parameters that also relate to seismic exposure (segmentation, tectonic model, and fault width) and to additional parameters (rupture length, maximum and average displacement per event, and slip rate). Where the data are available, these magnitude-related parameters are assessed, and the justification for the selected values and their relative weights are given in this section. In addition, the various techniques for estimating maximum magnitude are weighted for their relative applicability, given a particular tectonic model for each source.

##### 2.5K.4.2.1.1 Umtanum Ridge-Gable Mountain Structural Trend

The maximum-magnitude logic trees for the Umtanum Ridge-Gable Mountain structural trend are shown in Figures 2.5K-6 through 2.5K-9. Maximum and average displacement per event and technique applicability are independent of segmentation for the Umtanum Ridge-Gable Mountain structural trend and are discussed in Section 2.5K.4.2.1.1.1. Fault rupture lengths, which are dependent on segmentation, are discussed for each segmentation model in Section 2.5K.4.2.1.1.3.

##### 2.5K.4.2.1.1.1 Displacement per Event

Investigations by Golder Associates (1981b) have shown a maximum displacement of 6 cm in glaciofluvial deposits overlying the Central fault on Gable Mountain. The Central fault on Gable Mountain is interpreted to be a secondary fault related to the development of second-order folds on Gable Mountain (Golder Associates, 1981b). Six cm is assumed to be the maximum displacement that could occur on a secondary



reverse fault associated with the Umtanum Ridge-Gable Mountain structural trend when using the displacement versus magnitude relationship. It is assumed to represent the average displacement when using the moment magnitude relationship.

Assessment of the relative applicability of the magnitude estimation techniques is conditional on the tectonic model. For the primary reverse fault model, the rupture length versus magnitude and area versus magnitude relationships are used. As discussed in Section 2.5K.4.1.2, the magnitude of an earthquake is more closely related to the area of the rupture surface than to the rupture length. Therefore, the area versus magnitude relationship is given a slightly higher weight (0.6) than the rupture length versus magnitude relationship (0.4).

#### 2.5K.4.2.1.1.2 Technique Applicability

For the secondary reverse fault model, the maximum magnitudes are estimated from the fault area, maximum displacement prevent, and seismic moment (assuming 6 cm is the average displacement). Rupture length versus magnitude is not considered an applicable technique for this model because the empirical relationship is based on data from surface ruptures along primary reverse faults; the relationship is unreliable for faults having limited downdip widths. The fault area versus magnitude relationship is given the highest weight (0.7) because it accounts for the limited total size of the rupture surface on a secondary fault having small width. The displacement versus magnitude relationship is assigned a relatively low weight (0.2) because the empirical data set upon which the relationship is based does not include displacements less than 40 cm. The moment magnitude approach is the least favored technique (0.1) because, in addition to uncertainties in fault length and width, it is uncertain that the 6-cm displacement is an average displacement over the total fault surface.

#### 2.5K.4.2.1.1.3 Fault Rupture Length

##### Umtanum Ridge-Gable Mountain Structural Trend--Single Source

If the Umtanum Ridge-Gable Mountain structural trend is assumed to be a single source, the primary reverse fault model is the only applicable tectonic model (Figure 2.5K-6). The fault rupture length may be estimated to be one-half of the total length (72 km) or to be the length of the longest segment (the 43-km-long Umtanum Ridge western segment). As noted in Section 2.5K.4.1.1, the assessment of rupture length on the basis of geologic or geomorphic evidence of segmentation is considered more reliable than an assessment



using an arbitrary fractional fault length. For this reason, the 43-km-length is given a relatively higher probability (0.7) than the 72-km-length (0.3).

#### Umtanum Ridge-Gable Mountain Structural Trend-Segmented Source

If the Umtanum Ridge-Gable Mountain structure is a segmented single source, the fault rupture length will be specific to each segment, as discussed below.

Gable Mountain-Southeast Anticline Segment - The maximum rupture length for this segment is dependent on the tectonic model. For a primary reverse fault model, the rupture length could be equal to the total segment length (39 km). A secondary reverse fault may have a rupture length equivalent to the maximum inferred length (3.2 km) of the Central fault, which is the longest mapped fault on Gable Mountain (Golder Associates, 1981b). Geophysical studies and drilling along the Southeast anticline have indicated a fault along the southwest flank of the anticline; this fault has a maximum inferred length of 6.7 km (Golder Associates, 1981, personal communication). If the fault is related to the second-order fold, its maximum length may be as long as the entire Southeast anticline (11 km), and this length is used in the magnitude analysis. Because the 11-km rupture length is largely based on a postulated extension of the mapped fault along the entire length of the Southeast anticline, a rupture of 3-km is given a slightly higher weight (0.6) than the 11-km rupture length (0.4).

Umtanum Ridge Eastern Segment - A south-dipping thrust fault has been mapped along the northern flank of the Umtanum Ridge anticline (Myers and Price, 1979; Gaff, 1981; Price, 1980, 1981; Golder Associates, 1981a). The minimum length of the fault is 13 km. If the Umtanum Ridge eastern segment is related to a primary reverse fault, the length of rupture associated with the maximum earthquake may be the total length of the segment (32 km). If the structure is associated with secondary reverse faults, the rupture length may be the length of the Buck thrust (2 km), mapped by Price (1980, 1981) or the upper reverse fault (2 km) mapped by Myers and Price (1979). The Buck thrust is interpreted to be a secondary fault related to deformation in the hinge area of the Umtanum Ridge anticline (Price, 1981), and the upper reverse fault is considered to have a similar structural setting (Golder Associates, 1981a). Another postulated rupture length for a secondary fault model is one-half of the total segment length (16 km). Because rupture length assessments based on geologic evidence are considered more reliable than estimates based on an

arbitrary fractional fault length, a rupture length of 2 km is given a slightly higher weight (0.6) than the 16 km rupture length (0.4).

Umtanum Ridge Central Segment - Detailed geologic mapping has not been done on this segment to identify faults. The postulated rupture length for a primary reverse fault model is 30 km, which is the total length of the segment. However, rupture lengths for secondary faults may equal half of the segment length (15 km) or may equal the maximum mapped length of the secondary Central fault on the Gable Mountain-Southeast anticline segment (3 km). The data do not provide a basis for relatively weighting these values; therefore, both are assigned a probability of 0.5.

Umtanum Ridge Western Segment - The basis for the selection of rupture lengths and relative weights for this segment is the same as for the Umtanum Ridge Central segment. The potential rupture length for a primary reverse fault model is 43 km. The rupture lengths, assuming a secondary fault model, are 3 km and 21 km; probabilities for both are 0.5.

Umtanum Ridge-Gable Mountain Structural Trend--Separate Sources

If the Umtanum Ridge-Gable Mountain structural trend comprises four separate sources, then the fault rupture lengths will be specific to each source and are discussed below.

Gable Mountain-Southeast Anticline Source - If it is assumed that this source is a primary reverse fault, the fault rupture length may be 19 km, which is one-half of the 39-km total source length. If the anticline is associated with secondary reverse faults, the postulated rupture lengths and associated probabilities are the same as for the Gable Mountain-Southeast anticline segment. These are 3 km (0.6) and 11 km (0.4).

Umtanum Ridge Eastern Source - If the Umtanum Ridge eastern source is a primary reverse fault, the rupture length may be 16 km, which is one-half of the total source length. Assuming a secondary reverse fault model, the postulated rupture lengths and associated probabilities are the same as for the Umtanum Ridge eastern segment. These are 3 km (0.6) and 16 km (0.4).

Umtanum Ridge Central Source - If the Umtanum Ridge central source is a primary reverse fault, the rupture length may be 15 km, one-half of the total source length. Assuming a secondary reverse fault model, the postulated rupture lengths

and associated probabilities are the same as for the Umtanum Ridge central segment. These are 3 km (0.5) and 15 km (0.5).

Umtanum Ridge Western Source - If the Umtanum Ridge western source is a primary reverse fault, the rupture length may be 21 km, which is one-half of the total source length. Assuming a secondary reverse fault model, the postulated rupture lengths and associated probabilities are the same as for the Umtanum Ridge western segment. These are 3 km (0.5) and 21 km (0.5).

#### 2.5K.4.2.1.2 Rattlesnake-Wallula Alignment (RAW)

The maximum magnitude logic trees for RAW are shown in Figures 2.5K-3 through 2.5K-5. Slip rate and technique applicability, which are independent of segmentation for RAW, are discussed in Section 2.5K.4.2.1.2. Fault rupture lengths are dependent on segmentation and are presented in Section 2.5K.4.2.1.2.3.

##### 2.5K.4.2.1.2.1 Slip Rate

Slip rates estimated for RAW assume a strike-slip fault model and are based on indirect evidence. Bentley (1980) presents data on amounts of crustal shortening across the east-west folds of the Yakima fold belt along various meridians. If it is assumed that the amount of north-south shortening across the Yakima folds occurs along the northwest-striking RAW as strike-slip faulting, then the cumulative strike-slip displacement can be estimated. At longitude 120 degrees, the displacement is about 9 km, based on Bentley's (1980) data. If this displacement is assumed to have initiated at the time of the initial deposition of the Columbia River basalts about 14 m.y. ago, the rate of slip is 0.6 mm/yr. Structural analysis of the Columbia Plateau folds, by Laubscher (Appendix 2.5-0, Washington Public Power Supply System, 1981c), suggests that the maximum dextral shear across CLEW is 3 km. In addition, Weston Geophysical (1981a) has identified a prominent north-south gravity anomaly that crosses the CLEW trend at about longitude 120°W. Weston Geophysical (1981a) estimates that the cumulative strike-slip offset of the anomaly can be no more than 3 km. A 3-km displacement during a 14-m.y. period gives an average slip rate of 0.2 mm/yr.

Some studies suggest that the rate of deformation of the Columbia Plateau has been declining during the Quaternary period (Myers and Price, 1979; Bentley et al., 1980), and geodetic data suggest deformation has either stopped or is continuing at a low rate (Savage et al., 1981). Therefore, the present-day slip rate may be considerably less than the 0.2 to 0.6 mm/yr rates, based on the deformation that has occurred during the past 14 m.y. The relative weights for the

slip rates reflect the lack of a strong basis for establishing a preference between the values. A slightly higher weight (0.6) is given to 0.2 mm/yr because it is based on both geophysical and structural geologic constraints.

#### 2.5K.4.2.1.2.2 Technique Applicability

The relative applicability of the magnitude estimation techniques is dependent on tectonic models. For a strike-slip fault model, the area versus magnitude relationship is given slightly higher weight (0.6) than the rupture length versus magnitude relationship (0.4) because the magnitude of an earthquake is more closely related to the area of the rupture surface than to the rupture length (Section 2.5K.4.1.2). The slip rate versus magnitude technique is given a low weight because most of the data points used the relationship are based on plate-boundary strike-slip faults that have considerably higher slip rates than those postulated for RAW. For a primary reverse fault model, the relative weights of 0.6 for the area versus magnitude and of 0.4 for rupture length versus magnitude relationships are assigned, based on the arguments presented in Section 2.5K.4.1.2. For the secondary reverse fault model, rupture length versus magnitude is not considered an applicable technique because the empirical relationship is based on data from surface ruptures along primary reverse faults; the relationship is unreliable for small faults having limited downdip widths. The area versus magnitude relationship accounts for the limited total size of the rupture surface of a secondary fault having small width and, therefore, is used in the magnitude assessment.

#### 2.5K.4.2.1.2.3 Fault Rupture Length

##### Rattlesnake-Wallula Alignment--Single Source

If RAW is assumed to be a single source, then the strike-slip and primary reverse fault models are the only applicable tectonic models. The fault rupture length is estimated to be 58 km, which is one-half of the total length or equal to the length of the longest segment (the 50-km-long Rattlesnake-Wallula segment). As discussed in Section 2.5K.4.1.1, the assessment of rupture length on the basis of geologic or geomorphic evidence of segmentation is more reliable than assessment on the basis of an arbitrary fractional fault length. For this reason, the 50-km length is given a relatively higher weight (0.7) than the 58-km length (0.3).





Rattlesnake-Wallula Alignment--Segmented Source

If the Rattlesnake-Wallula alignment is a segmented single source, the fault rupture length will be specific to each segment, as discussed below.

Rattlesnake Mountain Segment - Assuming a strike-slip or primary reverse fault model, the maximum rupture length for this segment may equal the total length of the segment (20 km). If the segment is associated with secondary reverse faults, the rupture length may be 10 km, which is one-half of the segment length or may equal the length of the Rattlesnake Hills fault (7 km) as mapped along the northeastern flank of Rattlesnake Mountain (Myers and Price, 1979). Because the 7-km rupture length is based on geologic data, it is given a higher weight (0.6) than the 10-km estimate based on an arbitrary fractional fault length.

Rattlesnake-Wallula Segment - The length of rupture associated with the maximum earthquake on this segment may be the total length of the segment (50 km) if the structure is related to a strike-slip or primary reverse fault. If the structure is associated with secondary reverse faults, the rupture length may equal the length of the longest doubly plunging anticline along this segment (6 km) or equal 25 km, which is one-half of the segment length. Because secondary faults are related to the folding process, it is considered unlikely that faults would extend well beyond individual fold structures. In addition, the assessment of rupture length on the basis of geologic data is preferable to arbitrary fractional fault lengths. For these reasons, the 6-km estimate is given higher weight (0.7) than the 25-km estimate (0.3).

Wallula Segment - Assuming a strike-slip or primary reverse fault model, the rupture length for this segment may equal the total segment length (45 km). Assuming a secondary fault model, rupture lengths may be 6 km by analogy to the adjacent Rattlesnake-Wallula segment or may equal 23 km, which is one-half of the segment length. The data do not provide a basis for relatively weighting these values; therefore, both are assigned a probability of 0.5.

Rattlesnake-Wallula Alignment - Separate Sources

If RAW comprises three separate sources, then the fault rupture lengths will be specific to each source, as discussed below.

Rattlesnake Mountain Source - If the Rattlesnake Mountain source is a strike-slip fault or primary reverse fault, the rupture length may equal 10 km, which is one-half of the total source length. Assuming a secondary reverse fault model, the assessment of rupture lengths is the same as for the Rattlesnake Mountain segment. These are 7 km (0.6) and 10 km (0.4).

Rattlesnake-Wallula Source - If the Rattlesnake-Wallula source is a primary reverse fault, the rupture length may equal 25 km, which is one-half of the total source length. Assuming a secondary reverse fault model, the postulated rupture lengths and associated probabilities are the same as for the Rattlesnake-Wallula segment. These are 6 km (0.7) and 25 km (0.3).

Wallula Fault Source - If the Wallula fault source is a strike-slip or a primary reverse fault, the rupture length may equal 23 km, which is one-half of the total source length. Assuming a secondary reverse fault model, the postulated rupture lengths and associated probabilities are the same as for the Wallula fault segment. These are 6 km (0.5) and 23 km (0.5).

#### 2.5K.4.2.1.3 Saddle Mountains

Both rupture length and technique applicability are related to tectonic models. Assuming a primary reverse fault model, potential rupture lengths are 12, 20, 30, and 40 km. Smyrna Bench is 12 km long; two of four of the aeromagnetic segments defined by Weston Geophysical (1981b) are about 20 km long; the longest aeromagnetic segment is 30 km long. One-half of the total length of the Saddle Mountains structure is about 40 km. The highest weight (0.4) is given to 30 km because it is the longest aeromagnetic segment and may be most valid in defining the maximum rupture for a primary reverse fault. The two 20-km aeromagnetic segments are given slightly less weight because they are not the maximum lengths. A lesser weight (0.2) is given to the 12-km length because it is uncertain whether the features on Smyrna Bench are an expression of a primary fault or whether they are related to secondary deformation associated with secondary faulting, folding, and/or landsliding. Finally, the 40-km length is given lowest weight (0.1) because it is not based on physical evidence for segmentation but on a fractional fault length.

Rupture lengths for a secondary fault model are 10, 12, and 15 km. One-half of the length of two of the four aeromagnetic segments is 10 km; 12 km is the length of Smyrna Bench, and 15 km is one-half of the length of the longest aeromagnetic segment. The data do not provide a strong basis for relative

weighting of these values; however, 12 km is given a slightly higher weight (0.4) because it is based on geomorphic evidence for segmentation rather than on arbitrary fractional fault length.

For a primary reverse fault model, the area versus magnitude relationship is given slightly higher weight (0.6) than the rupture length versus magnitude relationship (0.4) because, as discussed in Section 2.5K.4.1.2, the magnitude of an earthquake is more closely related to the area of the rupture surface than to the rupture length. For a secondary reverse fault model, rupture length versus magnitude is not considered an applicable technique because the empirical relationship is based on surface ruptures along primary reverse faults. The area versus magnitude relationship accounts for the limited total size of the rupture surface of a secondary fault with small width.

#### 2.5K.4.2.1.4 Rattlesnake Hills

Assuming a primary reverse fault model, the rupture lengths are estimated to equal 30 km, which is one-half of the total fault length or the length of the longest aeromagnetic segment (36 km) defined by Weston Geophysical (1981b). The data do not provide a basis for relative weighting of these postulated rupture lengths. For a secondary reverse fault model, the rupture length is assumed to equal 18 km, which is one-half of the longest aeromagnetic segment.

The evaluation of technique applicability is the same for Rattlesnake Hills as for Saddle Mountains (Section 2.5K.4.2.1.3). For a primary fault model, area versus magnitude is assigned a probability of 0.6, and rupture length versus magnitude is assigned a probability of 0.4. For the secondary fault model, the area versus magnitude relationship is the only applicable technique.

#### 2.5K.4.2.1.5 Yakima Ridge

Fault rupture lengths on Yakima Ridge, assuming a primary reverse fault tectonic model, are estimated to equal either one-half of the total fault length (50 km), or the length of the longest aeromagnetic segment (36 km). The data do not provide a basis for relatively weighting these postulated rupture lengths; therefore, they are both assigned a probability of 0.5. For a secondary reverse fault model, rupture lengths may be equal to one-half of the length of one of the aeromagnetic segments (15 km) or one-half of the length of the longest aeromagnetic segment (18 km). The data are not sufficient to relatively weight these postulated rupture

lengths; therefore, they are both assigned a probability of 0.5.

The evaluation of technique applicability is the same for Yakima Ridge as for Saddle Mountains (see Section 2.5K.4.2.1.3). For a primary fault model, area versus magnitude is assigned a probability of 0.6, and rupture length versus magnitude is assigned a probability of 0.4. For the secondary fault model, the area versus magnitude relationship is the only applicable technique.

#### 2.5K.4.2.1.6 Horse Heaven Hills

Assuming a primary reverse fault model, the postulated rupture lengths are equal to the lengths of two northwest-striking aeromagnetic segments (24 km) or to one-half the length of the northeast-striking portion of Horse Heaven Hills (32 km). The 24-km estimate is given greater weight (0.7) because the aeromagnetic data provide geophysical constraints on two segments of the structure, which have comparable lengths. For a secondary reverse fault model, rupture lengths are postulated to be 12 km, which is one-half of the length of the two aeromagnetic segments or 16 km, which is one-half of the length of the single northeast-striking aeromagnetic segment. The data are not sufficient to relatively weight these two values; therefore, they are both assigned a probability of 0.5.

The evaluation of technique applicability is the same for Yakima Ridge as for Saddle Mountains (Section 2.5K.4.2.1.3). For the primary reverse fault model, area versus magnitude is assigned a probability of 0.6, and rupture length versus magnitude is assigned a probability of 0.4. For the secondary fault model, the area versus magnitude relationship is the only applicable technique.

#### 2.5K.4.2.2 Unconditional Magnitude Probability Distributions

The unconditional magnitude probability distributions for each potential source are presented in Table 2.5K-2. The magnitude distributions are presented as cumulative distribution functions (CDF). In each distribution, the range of magnitude values reflects the variation in fault parameters; the probabilities for each magnitude reflect the relative confidence in the parameter values based on the available data. The probability at any given magnitude expresses the likelihood that the actual maximum magnitude for that source is less than or equal to the given magnitude. The probabilities do not represent the likelihood of occurrence of a particular magnitude earthquake.



## 2.5K.4.2.3 Conditional Magnitude Distributions for Seismic Exposure Model

Because both the maximum magnitudes and seismic exposure are dependent on segmentation, tectonic model, and fault width, the maximum magnitude probability distributions for each source must be made conditional on these parameters in order to be included in the seismic exposure analysis. The procedure for assigning the maximum magnitude conditional probabilities for their incorporation into the seismic exposure analysis is illustrated in Figure 2.5K-43. Part of a maximum magnitude logic tree shown in Figure 2.5K-43 is for a particular segmentation, tectonic model, and fault width. For each of the end branches, a maximum magnitude is computed. The conditional probability for each maximum magnitude is:

$$p(m^u) = p(FRL_p) \cdot p(SR_q) \cdot p(TA_r) \quad (2.5K-14)$$

where:

- $m^u$  = maximum magnitude computed for fault width  $l$ , using fault rupture length  $p$ , slip rate  $q$ , and technique  $r$
- $p(m^u)$  = conditional probability of maximum magnitude  $m^u$  given segmentation  $i$ , capable fault  $j$ , tectonic model  $k$ , and fault width  $l$
- $p(FRL_p)$  = conditional probability of fault rupture length  $p$ , given segmented source  $i$ , capable fault  $j$ , and tectonic model  $k$
- $p(SR_q)$  = conditional probability of slip rate  $q$ , given tectonic model  $k$
- $p(TA_r)$  = conditional probability of technique applicability  $r$ , given tectonic model  $k$ .

The branches define a discrete probability mass function for  $m^u$  computed in 0.1 magnitude increments, as shown in Figure 2.5K-43.

For the exposure model, the conditional distribution is rediscritized in increments of 1/4 magnitude. Each point in the aggregated distribution defines a maximum magnitude branch on the exposure model logic tree, as shown at the bottom of Figure 2.5K-43. The conditional probability assigned to each branch is set equal to the probability mass





in the aggregated distribution. The above procedure was repeated for each fault width. The maximum magnitudes and conditional probabilities assigned to each fault width are shown in Figures 2.5K-14 through 2.5K-35.

#### 2.5K.5 EARTHQUAKE RECURRENCE

The earthquake recurrence on potentially capable faults is an important factor in the seismic exposure analysis. The more frequent the earthquakes, the greater is the seismic exposure. The approach used to calculate the seismic exposure requires fault-specific relationships between earthquake magnitude and recurrence.

The low level of seismicity in the Columbia Plateau and the general lack of geomorphic or other geologic evidence for Holocene faulting, indicate that faults in the site region are either: (1) not capable; (2) cannot produce large-magnitude events associated with surface faulting; or (3) have long recurrence intervals. Because of the low level of seismicity in the Columbia Plateau, as discussed in Appendix 2.5J (Washington Public Power Supply System, 1981a) and the catastrophic late-Pleistocene floods (Woodward-Clyde Consultants, 1981d), the evidence regarding the capability of faults in the site region is equivocal. The available data suggest that capable faults may be associated with at least some of the Yakima folds and with the Rattlesnake-Wallula alignment (Section 2.5K.3.4.2). Similarly, the maximum earthquake magnitudes associated with these structures are not well known, but some of the proposed tectonic models suggest that faults that may be associated with these structures can produce moderate- to large-magnitude events (Section 2.5K.4.2.2). If the significant potential sources in the site region are capable of producing large-magnitude surface-faulting events, the recurrence for such events, on any one fault must be significantly longer than the Holocene record (approximately 10,000 years).

Because of the paucity of data on the known and inferred faults in the site region, earthquake recurrence intervals cannot be determined for each structure. Therefore, a fault-specific recurrence relationship is estimated based on: (1) the combined geologic evidence for past surface-faulting events for faults in the site region; (2) an estimated b-value (slope of the frequency-magnitude recurrence relationship); and (3) the overall length of the inferred fault. The geologic evidence for past surface faulting in the site region, discussed in Section 2.5K.5.1, is used to estimate the recurrence of large-magnitude events. The seismologic basis for estimating the b-value used in this recurrence relationship is discussed in Section 2.5K.5.3.2. Using these

estimates, a mean recurrence rate is developed for the number of earthquakes of magnitude greater than 4.0 per year, per kilometer of fault length. This value is then used to compute the mean recurrence rate for each of the potential geologic sources.

The frequency of smaller-magnitude earthquakes that is predicted based on this recurrence relationship is compared to the historical seismicity data (Section 2.5K.5.3.4). The predicted values are generally consistent with the historical data.

#### 2.5K.5.1 Geologic Evidence For Quaternary Surface Faulting

The only fault in the site vicinity that is known to be capable according to the NRC criteria is the Central fault on Gable Mountain. Evidence suggestive of Quaternary surface faulting has been found at two other localities along structures that are included in the seismic exposure analysis for the site. These are: (1) Finley Quarry along the Rattlesnake-Wallula segment of RAW; and (2) the Warm Springs trench locality on the Wallula segment of RAW (Figure 2.5K-38). In addition, evidence suggests that Quaternary faulting has occurred at Toppenish Ridge (Rigby and Othberg, 1979; Campbell and Bentley, 1981; and Woodward-Clyde Consultants, 1981b) and at the eastern end of Ahtanum Ridge near Union Gap (Campbell, 1980). Toppenish Ridge and Ahtanum Ridge are not included in the seismic exposure analysis because they are too far from the site to make a significant contribution to the seismic exposure of the site (Section 2.5K.3). They are discussed here only because the data from these locations provide information regarding the recurrence of surface faulting on faults associated with the Yakima folds.

##### 2.5K.5.1.1 Central Fault on Gable Mountain

Detailed investigations of the Central fault on Gable Mountain have been conducted by Golder Associates (1981b). The Central fault displaces Late Quaternary flood deposits a maximum of 6 cm. The small amount of displacement and the simple nature of the shear surface suggests that this displacement was produced by a single event.

Two gravel deposits are exposed in the trenches on Gable Mountain. The exact age of the displaced gravels is uncertain. However, they are no younger than 13,000 years, which is the approximate age of the St. Helen's "S" ash contained in the youngest late Pleistocene flood deposits. The late Pleistocene and Holocene eolian and slope wash deposits that overlie the Central fault are not displaced.

The maximum earthquake that can occur on this fault is estimated to be magnitude 5 (WNP-2 FSAR, Subsection 2.5.2.4.2.2). If the displacement of the Quaternary deposits represents a seismogenic event, the earthquake was probably less than or equal to magnitude 5.

Based on the elapsed time since the most recent surface faulting event, the available evidence suggests a minimum recurrence interval of at least 10,000 years for magnitude 5 earthquakes associated with surface faulting along the Central fault.

#### 2.5K.5.1.2 Finley Quarry

Woodward-Clyde Consultants (1981e) has made detailed logs of faults exposed in trenches and in the wall of Finley Quarry. The exposed faults are at the northwest end of the Butte, which is a faulted northeastward-dipping monocline located along the Rattlesnake-Wallula alignment. A 13-m-wide zone containing three fault traces was exposed. The northern and central fault traces displace and die out within a sequence of sedimentary deposits that could be as old as the Ringold Formation (Miocene-Pliocene), but are probably Pleistocene in age. The southern trace occurs entirely within Tertiary volcanic deposits, and it is not possible to determine the age of the most recent displacement on this trace.

The northern and central fault traces displace two unconsolidated gravelly sand units. The older gravel unit has thick (up to 15 mm) weathering rinds on the basalt clasts. The younger unit lacks well-developed weathering rinds. These two units are overlain by unfaulted sand and sandy gravel. At the northern end of the exposure, this unfaulted unit is overlain by two thick caliche soil horizons. Uranium-thorium dates on caliche rinds indicate that the upper caliche soil horizon is at least 70,000 years old (Woodward-Clyde Consultants, 1981e). Presumably the lower caliche, which is much thicker, is much older; conceivably, it is equivalent in age to pre-Quaternary soils developed on fanglomerates that grade to the Ringold Formation in the Pasco Basin.

The southern fault trace is only overlain by Holocene eolian and slope wash deposits, and the age of the most recent faulting on this trace cannot be determined. By inference, the southern trace may be equivalent in age to the northern and central fault traces. If so, the available evidence from Finley Quarry is compatible with an earthquake recurrence interval (based on the elapsed time since the most recent event) for earthquakes associated with surface faulting of at least several tens of thousands of years. The actual

recurrence interval could be on the order of hundreds of thousands of years.

#### 2.5K.5.1.3 Wallula Fault Zone

Near Wallula Gap, the Wallula fault zone consists of two major strands, the Wallula Gap fault and the Wallula fault (WNP-2 FSAR, Subsection 2.5.1.2.4.5). Trenches have been excavated across both faults to assess the age of the most recent displacement. The trench across the Wallula Gap fault west of Yellepit Station is described by Farooqui (1977). Trenches across the Wallula fault near Warm Springs are described by Woodward-Clyde Consultants (1981a).

The age of the most recent displacement on the Wallula Gap fault is not known. The fault has not had any displacement since the deposition of the Kennewick Fanglomerate, which unconformably overlies the fault (Farooqui, 1977). Uranium-thorium dates on caliche that has formed on the fanglomerate indicate the caliche is at least 20,000 years old (Woodward-Clyde Consultants, 1978, 1981a); the fanglomerate deposits may be much older. The Wallula Gap fault is either inactive, or it has a recurrence interval of at least a few tens of thousands of years.

The Wallula fault displaces eolian and colluvial silt and fine sand deposits that are probably Quaternary in age (Woodward-Clyde Consultants, 1981a). These sediments have a well-developed pedogenic carbonate soil (caliche), which suggests the deposits are Sangamon (128,000 to 75,000 years BP) or older. Based on the degree of soil development, the deposits are no younger than the Palouse loess, which Baker (1978) considers to be lower to middle Pinedale in age (approximately 75,000 to 35,000 years BP). The Wallula fault is unconformably overlain by, and does not displace, slackwater sediments deposited by the Missoula flood (about 13,000 years BP). Based on the elapsed time since the most recent surface-faulting event, these data suggest that the recurrence interval of surface-faulting earthquake along Wallula fault is at least 10,000 years and may be much longer.

#### 2.5K.5.1.4 Toppenish Ridge

Investigations of the scarps that occur on the north flank of Toppenish Ridge are summarized by Woodward-Clyde Consultants (1981b). The available data on the scarps along Toppenish Ridge are based primarily on photo-geologic interpretations and reconnaissance geologic mapping.

The presence of scarps that have a young, fresh-looking appearance and scarps that have an older, more subdued-looking

AMENDMENT NO. 18  
September 1981

appearance suggest that there may have been at least two Late Quaternary surface-faulting events. Although the ages of the deposits that are displaced are not well documented, the most recent surface-faulting event was probably Holocene.

If the scarps along Toppenish Ridge represent tectonic surface-faulting events, they indicate that the recurrence interval for earthquakes associated with surface faulting could be on the order of thousands of years to a few tens of thousands of years.

If the recurrence interval is only a few thousand years, the surface faulting along Toppenish Ridge may be characterized by a shorter recurrence interval than the other Columbia Plateau structures; where similar fault scarps are not observed. Alternatively, the other Plateau structures may not be associated with capable faults, or the Plateau faulting may be characterized by episodes of faulting separated by long periods of quiescence.

#### 2.5K.5.1.5 Union Gap Fault

A late Cenozoic fault was exposed in a road cut near Union Gap the eastern end of Ahtanum Ridge (Figure 2.5K-38). The exposure was described by Campbell (1980) before it was covered by a retaining wall.

The fault strikes N80°W and dips 43 degrees to the north. Yakima River terrace gravels are displaced at least 7 m vertically, south-side down (apparent reverse slip). The apparent sense of displacement is the opposite of the topographic relief. Late Pleistocene slackwater deposits containing the St. Helens "S" (?) ash (13,000 years BP), and Holocene loess deposits overlie the fault and are not displaced.

The age of the faulted terrace gravel is not known. Campbell (1980) describes the basalt clasts in the terrace gravel as "relatively fresh" and the caliche at the top of the gravel as "poorly developed." The gravel, which is 10 m above the present flood plain of the Yakima River, is probably Pleistocene in age.

The cumulative displacement of the terrace gravel was probably produced by multiple faulting events and, therefore, suggests there have been repeated Pleistocene surface faulting events. The elapsed time since the most recent event has been at least 13,000 years and may have been significantly longer. This suggests that the recurrence interval for earthquakes associated with surface faulting is on the order of at least tens of thousands of years.

### 2.5K.5.2 Absence of Post-Missoula Flood Surface-Faulting Events

The catastrophic floods that flowed through the Pasco Basin during the late Pleistocene present a major problem in the assessment of the history of Quaternary faulting in the site vicinity (Woodward-Clyde Consultants, 1981d). The faults may have eroded fault scarps that might have existed previously, and/or the flood deposits and associated eolian deposits may have buried scarps and other fault-related features. Erosion of the edges of the basalt flows along pre-existing fractures and faults has also formed faceted spurs and hanging valleys that mimic youthful fault features. In addition, the floods stripped the area of the older Pleistocene deposits that are essential for assessing fault capability and deformation rates.

Deposits from the most recent flood in the Pasco Basin contain St. Helen's "S" and Glacier Peak ash deposits, which are approximately 13,000 and 12,500 years old, respectively. There have been no catastrophic floods similar to the Missoula flood during the Holocene, or approximately the past 10,000 years. Except for local reworking of loess deposits on the upland areas and active fluvial processes along major channels and flood plains, the Holocene landscape has been relatively stable. Therefore, if any major earthquakes have been associated with surface faulting during the Holocene, evidence of these events should be relatively well preserved.

The six potential seismic sources considered in this seismic exposure analysis include all the major structures that are potentially significant to the seismic exposure of the site (Section 2.5K.3). No large surface-faulting events are known to have occurred along any of these structures during the Holocene. Although small displacements (such as those observed on the Central fault on Gable Mountain) might not be detected, it is unlikely that large scarp-producing displacements (2 m or more), which would be associated with magnitude 7 or larger earthquakes, would not be detected. This suggests that the average recurrence interval for large earthquakes (magnitude 7 or larger) is significantly longer than 10,000 years, if there are capable faults associated with these structures; it is unlikely that the recurrence interval at a given location along any of the postulated seismic sources is shorter than 30,000 years. The average recurrence interval for such an event is assessed probabilistically in Section 2.5K.5.3.

2.5K.5.3 Estimated Earthquake Recurrence Rates For Geologic Sources

## 2.5K.5.3.1 Large-Magnitude Recurrence Rate

The geologic evidence discussed in Section 2.5K.5.2 indicates that no evidence of the occurrence of events of magnitude greater than or equal to 7.0 in the past 10,000 years has been observed on any of the six geologic structures identified as potential earthquake sources. Based on this observation, the average recurrence rate large-magnitude surface-faulting earthquakes (magnitudes greater than 7.0) is estimated probabilistically.

The data on magnitude versus rupture length presented by Slemmons (1977) for the data set that includes both strike-slip and reverse faults indicate that the mean rupture length for a magnitude 7.0 earthquake is approximately 45 km. Assuming the recurrence of earthquakes is a Poisson process (Section 2.5K.2.2.1), the probability of an earthquake of magnitude greater than 7.0 on any 45-km section of fault in the time period  $t$  is given by:

$$p = 1 - e^{-\lambda t} \quad (2.5K-15)$$

where  $\lambda$  is the mean recurrence rate for magnitudes greater than 7.0.  $\lambda$  can be expressed as  $\frac{1}{T}$ , where  $T$  is the mean time between events of magnitude greater than 7.0.

Because the total length of the postulated geologic structures is several times longer than 45 km, there are several opportunities for observing surface rupturing events. Assuming that each 45-km-long section of fault offers an independent chance of observing earthquake displacements, the number of events occurring in a specified number of trials is binomially distributed. The probability of seeing  $x$  events in  $n$  trials is given by:

$$p(x) = \frac{n!}{x! (n-x)!} p^x (1-p)^{n-x} \quad (2.5K-16)$$

where  $p$  is the probability of success in any one trial given by Equation (2.5K-15). The probability of seeing  $x$  or fewer events is given by the cumulative binomial distribution function:

$$p(X \leq x) = \sum_{y=0}^x \frac{n!}{y! (n-y)!} p^y (1-p)^{n-y} \quad (2.5K-17)$$

The estimate of the number of trials is based on the total length of faulting in the source region. The total length of the six geologic structures considered as potential sources is 624 km. However, none of the structures are known with certainty to be capable faults, although each has some probability of being able to generate an earthquake of magnitude greater than 7.0. The combined weighted average of fault capability for all of the structures is 0.59. Multiplying 624 km by 0.59 gives 369 km of assumed capable fault within the source region.

Dividing 369 km by an average rupture length of 45 km gives a minimum number of 8 trials, assuming no overlap of rupture. Using  $n = 8$ ,  $t = 10,000$  years, and Equation (2.5K-17), the probability of having seen  $x$  or fewer events is tabulated in Table 2.5K-3 for various mean recurrence intervals  $T$ , and number of events  $x$ .

The recurrence interval for an event greater than magnitude 7.0 on a 45-km length of fault was selected as the value of  $T$  for which there is a 50-percent chance of having seen no events in the past 10,000 years. The 50-percent level was judged to mean that over an extended sequence of 10,000-year intervals; in one-half of the intervals, no earthquake would be observed. The corresponding recurrence interval for one event having a magnitude greater than 7.0 is 115,000 years on each 45-km fault length (Table 2.5K-3). This suggests that, on the average, there could be an earthquake of magnitude greater than 7.0 somewhere on the six potential sources every 14,400 years.

Based on geologic evidence (Section 2.5K.5.2), 30,000 is judged to be a lower bound for the recurrence interval of a magnitude greater than 7.0 event on a 45-km fault section. For this recurrence interval, there is only a 7-percent chance of having observed no events in the last 10,000 years (Table 2.5K-3).

#### 2.5K.5.3.2 Relative Frequency of Various Magnitudes

As discussed in Section 2.5K.2.2.2, the relative frequency of various magnitude events is controlled by the parameter  $b$  in the Gutenberg-Richter equation. Analysis of recorded data in the Columbia Plateau indicates that a " $b$ " value of 0.85 best represents the relative frequency of occurrence of earthquakes occurring at all depths, as discussed in Appendix 2.5J (Washington Public Power Supply System, 1981a). This " $b$ " value is based on recordings of events of magnitude  $M_L$  2.0 to 4.0 over a 10.5-year period.



The Gutenberg-Richter relationship [Equation (2.5K-4)] is based on many worldwide observations of numbers of earthquakes as a function of magnitude. These observations supporting a log-linear relationship (constant slope as a function of magnitude) apply to regions that include numerous earthquake sources. The application of this relationship to single faults is not well-established by observations; however, when a number of faults are to be modeled, the regional observations support the use of a linear recurrence model as an appropriate model for average fault behavior.

#### 2.5K.5.3.3 Distribution for Recurrence

Using the Gutenberg-Richter equation,  $T = 115,000$  years and  $b = 0.85$ , the mean number of events of magnitude greater than 4.0 per year, per kilometer of fault, is  $6.86 \times 10^{-5}$ . This value was assumed to be the mean or expected value of parameter A (Equation 2.5K-5). The expected value of  $A_n$  for each source segment, assuming the source is capable, was obtained by multiplying  $6.86 \times 10^{-5}$  by the source segment length. Table 2.5K-4 lists the lengths and expected values of  $A_n$  for each of the potential sources and their segments.

The dispersion in recurrence was modeled by specifying a distribution for parameter "A." Because the uncertainty in parameter "b" is much smaller than the uncertainty in A, b was assumed to be known. The distribution for parameter A was assumed to be lognormal. This assumption is reasonable because: (1) parameter A should always be positive, which is satisfied by the lognormal assumption; (2) the Gutenberg-Richter equation was derived in terms of the log of the number of events, and the dispersion about the log was judged symmetric on a log scale. The variance of A was estimated by assuming that the return period of 30,000 years for an event of magnitude greater than 7.0 constituted a mean plus two standard deviation level for  $\ln N$ , where N is the number of events of magnitude greater than 7.0. This gives a standard error of  $\ln A$  of 0.85.

#### 2.5K.5.3.4 Comparison with Historical Seismicity

Within the past 60 years, three events of magnitude greater than 4 have been recorded in the Hanford region. These events were recorded in 1918, 1973, and 1979, within a  $25,000\text{-km}^2$  area, which is approximately 50 percent larger than the area encompassing the six geologic structures. Normalizing to an area equal to the source region the historical data indicate a recurrence rate of 0.033 events of magnitude greater than 4.0 per year.

The recurrence relationship derived in Section 2.5K.5.3.3 can be used to estimate a recurrence rate for the source region. Multiplying the mean recurrence rate per kilometer of fault by 369 km of capable fault yields an estimated mean recurrence rate of 0.025 events of magnitude greater than 4.0 per year. Using the dispersion in parameter A, the 84-percent recurrence rate is 0.041 events per year. The very limited historical data falls within the range of recurrence rates used in the analysis.

#### 2.5K.5.3.5 Recurrence Relationship for Exposure Analysis

The recurrence relationship used in an exposure analysis is given by Equation (2.5K-5). For each source, the total number of earthquakes per year with magnitudes greater than 4.0 remains constant. The relative frequency of individual magnitudes is dependent on the b value and the maximum magnitude,  $m^u$ . Figure 2.5K-44 shows the recurrence relationships per kilometer of fault length for various maximum magnitudes. Similar curves are input for each exposure analysis, depending on the value of  $A_n$  and  $m^u$  for that analysis case.

#### 2.5K.6 MAGNITUDE/RUPTURE-LENGTH CRITERIA

##### 2.5K.6.1 Approach

The development of the probability function for the closest distance to the fault rupture requires specification of the rupture-length for each magnitude. The magnitude/rupture-length criteria used in the exposure analyses are developed from a relationship between rupture area and magnitude. As discussed in Section 2.5K.4.1.2, rupture area has a higher correlation with magnitude than does rupture length. Wyss (1979) presents rupture area and magnitude data for 83 earthquakes in the magnitude ( $M_S$ ,  $M_W$ ) range 5.6 to 9.6. He develops a relationship for magnitude as a function of area, A:

$$m = \log_{10} A + 4.15 \quad (2.5K-18)$$

Since the exposure analysis requires area as a function of magnitude, a regression analysis of area on magnitude was performed using Wyss' (1979) data. The resulting relationship is:

$$\ln A = 2.146 m - 8.384 \quad (2.5K-19)$$

A magnitude-rupture length criterion is derived as follows.

It is assumed that for small magnitudes, the rupture surface is a square. The rupture length for each magnitude is computed by taking the square root of the area computed using Equation (2.5K-19). The resulting relationship is

$$\ln L = 1.073m - 4.192 \quad (2.5K-20)$$

For magnitudes whose rupture area exceeds the square of the fault width, a second relationship is used. The rupture width is assumed to be equal to the fault width, and the length is computed by dividing the rupture area by the fault width. The resulting relationship is:

$$\ln L = 2.146m - 8.384 - \ln (\text{fault width}) \quad (2.5K-21)$$

The magnitude whose rupture area equals the square of the fault width is defined as  $m_j$  and is given by the relationship:

$$m_j = \frac{\ln (\text{fault width}) + 4.192}{1.073} \quad (2.5K-22)$$

Equation (2.5K-21) was applied for magnitudes greater than  $m_j$ .

## 2.5K.7. ATTENUATION RELATIONSHIPS

Attenuation relationships, which describe the variations of horizontal peak ground acceleration and response spectral values with earthquake magnitude and distance, have been selected for use in the seismic exposure analysis. These attenuation relationships describe ground motions that would be recorded by an accelerograph at the ground surface in the free field. The basis for the attenuation relationships is given in Attachment A. A summary of the basis and the relationships used are presented in this section.

### 2.5K.7.1 Basis for Selection

The attenuation relationships have been selected on the basis of examination and statistical analysis of empirical data consisting of strong-motion recordings from historical earthquakes. In selecting an empirical data base and developing attenuation relationships, various site-specific factors may be considered, including: the predominant sense of displacement (type of faulting) for postulated earthquakes in the site region; the subsoil conditions at the plant site; and the deeper crustal structure between potential earthquake sources and the plant site. The way in which these factors have been considered in selecting attenuation relationships is summarized below.



### 2.5K.7.1.1 Type of Faulting

As discussed in Section 2.5K.3, reverse faulting is the expected predominant type of faulting for potential significant earthquake sources. To account for possible effects of the type of faulting on strong ground motions, recorded data from the 1971 San Fernando earthquake, a reverse faulting event, are used as a primary basis for selecting attenuation relationships for higher-magnitude earthquakes. Comparisons that are presented in Attachment A show that attenuation relationships developed for the San Fernando earthquake data base lead to higher accelerations than a data base incorporating records from strike-slip earthquakes of comparable magnitude.

### 2.5K.7.1.2 Subsoil Conditions

As described in Subsection 2.5.2.5 of the FSAR, the plant site is underlain by approximately 160 m of sediments of varying stiffness above the basalt bedrock. Because of the presence of relatively thick soil layers above the bedrock, the attenuation relationships are developed using a data base of recordings from soil sites rather than rock sites.

### 2.5K.7.1.3 Crustal Structure

The basalt flows and interflows that underlie the Columbia Plateau are characterized by wave velocities that are highly variable with depth (Subsection 2.5.2.5 of FSAR and Woodward-Clyde Consultants, 1981c). These strong vertical material heterogeneities do not exist at locations in California where the great majority of strong-motion data for the United States have been recorded.

To evaluate the attenuation characteristics of the Columbia Plateau crustal structure, a wave propagation and modeling study has been conducted. The results of this study, which are summarized in Subsection 2.5.2.5 of the FSAR and presented in detail in Woodward-Clyde Consultants (1981c), indicate that the basalt structure may substantially increase attenuation (i.e., substantially decrease strong ground motion at the plant site) due to earthquake sources beneath the higher velocity layers in the basalt, relative to ground motions that would occur in the absence of this layered structure. This conclusion is dependent on several assumptions regarding kinematic descriptions of the seismic sources, the relationship between shear and compressional wave velocities in the basalts, the source depth, and the nature of the crust beneath the basalts. These theoretically predicted attenuation effects have been conservatively neglected in selecting the attenuation relationship for the seismic exposure analysis.

### 2.5K.7.2 Selected Relationships

The selected attenuation relationships for peak horizontal ground acceleration for the magnitude ( $M_S$ ) range of 4 to 7.5 are presented in Figure 2.5K-45.

Seismic exposure analyses have also been made for horizontal response spectral accelerations (2-percent damping) for two selected periods, 0.125 and 0.40 seconds. The period of 0.125 second is selected to be close to the low-period control point (0.11 second) of the NRC Regulatory Guide 1.60 spectrum that was used to define the design response spectra for the plant (Section 3.7 of the FSAR). The period of 0.40 second is selected to be equal to the mid-period control point of the design response spectra. The selected attenuation relationships for response spectral accelerations for periods of 0.125 second and 0.40 second are shown in Figure 2.5K-46 and Figure 2.5K-47, respectively.

Uncertainty in the ground motions predicted by the attenuation relationships is incorporated in the analysis by using a log-normal distribution and allowing ground motions to vary within a three-standard-deviation range. The reasonableness of the assumption of a log-normal distribution is substantiated in a number of studies (e.g., Esteva, 1969; Donovan, 1973; McGuire, 1974). A three-standard-deviation range incorporates virtually all the dispersion in measured ground-motion values. The values of the standard deviation,  $S$ , are selected as a function of magnitude; higher values of  $S$  are selected for lower magnitudes that reflect the greater scatter in recorded strong-motion data for lower-magnitude earthquakes. The values of  $S$  used in the analysis are summarized in Attachment A.

### 2.5K.8 RESULTS

#### 2.5K.8.1 Exposure for Peak Acceleration

The procedure followed in evaluating the seismic exposure of the site is described in Section 2.5K.2 and is summarized as follows:

- o The variations in source segmentation, source capability, tectonic models, fault geometry, and maximum magnitude are addressed by constructing logic trees for each possible source of significance to the exposure. These exposure logic trees are shown in Figures 2.5K-48 through 2.5K-67.
- o Seismic exposure analyses are conducted for each of the cases defined by the end branches on the logic trees using the mean recurrence rate for the source. The annual mean

number of events that exceed a specified peak acceleration are computed for acceleration levels between 0.05 g and 1.0 g. The annual mean number of events exceeding 0.25 g for each of the analysis cases are shown on the right hand column of Figures 2.5K-48 through 2.5K-67. It should be noted that, for the mean number of events less than  $10^{-2}$ , the probability of exceedance is essentially equal to the mean number of events  $[p(Z > z) \approx \nu(z)]$ .

- o The probability distribution for the annual mean number of events from each source is determined by incorporating the conditional distributions defined by the logic tree and the variation in recurrence rate.
- o Finally, the results from each of the possible sources are combined to calculate total exposure for the site.

#### 2.5K.8.1.1 Expected Value of Probability of Exceedance

Using the formulations developed in Section 2.5K.2.3, the expected annual mean number of events exceeding a specific ground acceleration level was computed. Figure 2.5K-68 shows the relationship between the expected number of events and peak acceleration level for the six geologic sources. It also shows the combined total exposure. The annual probabilities of exceeding 0.125 g (for the OBE) and 0.25 g (for the SSE) are tabulated below:

<u>ANNUAL PROBABILITY OF EXCEEDANCE (<math>10^{-4}</math>)</u>		
<u>Potential Source</u>	<u>OBE - 0.125g</u>	<u>SSE - 0.25 g</u>
Umtanum Ridge-Gable Mountain	3.5	1.0
Rattlesnake Wallula Alignment	0.75	0.06
Horse Heaven Hills	0.09	0.004
Rattlesnake Hills	0.05	0.003
Yakima Ridge	0.03	0.003
Saddle Mountain	0.15	0.01
Total	4.6	1.1

As can be seen for the SSE peak acceleration, 93 percent of the exposure comes from the Umtanum Ridge-Gable Mountain source. For the OBE peak acceleration, 84 percent comes from the Umtanum Ridge-Gable Mountain source. Examination of the exposure results for individual segments of Umtanum Ridge-Gable Mountain structural trend (Figures 2.5K-48 through 2.5K-

56) indicate that the exposure comes primarily from the Gable Mountain Southeast anticline segment.

#### 2.5K.8.1.2 Confidence Levels for Probability of Exceedance

As discussed in Section 2.5K.2.2.3, confidence levels on the annual mean number of events can be estimated using the computed variance for the distribution of  $\nu(z)$ . Assuming a normal distribution for the total exposure, a 90-percent confidence level occurs at the mean plus 1.3 standard deviations. (The 90-percent confidence level is the 90-percent level of the cumulative distribution) The 90-percent confidence levels for the OBE and SSE peak accelerations are given below:

<u>Peak Acceleration</u>	<u>Expected Annual Probability of Exceedance (<math>10^{-4}</math>)</u>	<u>90-Percent Confidence Level of Annual Probability of Exceedance (<math>10^{-4}</math>)</u>
0.125 g	4.6	9.8
0.25 g	1.1	2.7

#### 2.5K.8.2 Exposure for Spectral Acceleration

The probability of exceedance of spectral acceleration was evaluated for two periods, 0.125 and 0.40 second for 2-percent spectral damping. Figure 2.5K-69 shows the variation in probability of exceedance with spectral acceleration for the two selected periods. The results are summarized below:

<u>Spectral Period (seconds)</u>	<u>Spectral Acceleration Level</u>	<u>Expected Annual Probability of Exceedance (<math>10^{-4}</math>)</u>	<u>90-Percent Confidence Level of Annual Probability of Exceedance (<math>10^{-4}</math>)</u>
0.125	OBE-0.45 g	4.0	8.9
	SSE-0.90 g	0.92	2.3
0.40	OBE-0.53 g	1.7	3.5
	SSE-1.06 g	0.29	0.77



The Umtanum Ridge-Gable Mountain structural trend dominates the contribution to the probabilities of exceedance of spectral accelerations, as it does for peak acceleration. For spectral accelerations at 0.125 seconds, the Umtanum Ridge-Gable Mountain structural trend contributes 84 percent of the seismic exposure for the OBE and 93 percent for the SSE. For spectral accelerations at 0.40 second, this source contributes 74 percent of the exposure for the OBE and 86 percent for the SSE.

### 2.5K.8.3 Discussion of Results and Sensitivity

Because probabilistic distributions are incorporated for all the key input parameters to this seismic exposure analysis, the sensitivity results to variations in parameter values is basically self-contained within the analysis. The sensitivity of the results to variations in source definition (segmentation, capability, tectonic model, fault geometry, and maximum magnitude) can be evaluated by the distribution defined by the logic tree. The sensitivity to variations in recurrence can be evaluated by the distribution for recurrence. Summarized below are the standard deviations in the probabilities of exceeding 0.25 g due to (1) variations in source definition, and (2) variations in both source definition and recurrence:

<u>Potential Source</u>	<u>Expected Annual Probabilities of Exceeding 0.25 g (<math>10^{-4}</math>)</u>	<u>Standard Deviation of Annual Probability of Exceeding 0.25g (<math>10^{-4}</math>)</u>	
		<u>Due to Variations in Source Definition</u>	<u>Due to Variations in Source Definition and Recurrence</u>
Umtanum Ridge-Gable Mountain	1.0	0.5	1.2
Rattlesnake-Wallula Alignment	0.06	0.07	0.11
Horse Heaven Hills	0.004	0.01	0.02
Rattlesnake Hills	0.003	0.01	0.02
Yakima Ridge	0.002	0.006	0.008
Saddle Mountains	<u>0.01</u>	<u>0.02</u>	<u>0.03</u>
Total Exposure	1.1	0.51	1.2



The tabulated values indicate that, except for the Umtanum Ridge-Gable Mountain structural trend, the variations in source definition have the predominant impact on the dispersion in the computed probability of exceeding 0.25 g. For the Umtanum Ridge-Gable Mountain structural trend, variations in source definition have a relatively smaller impact on the computed exposure values; the primary source of dispersion in exposure for this source is variation in the recurrence rate. As the Umtanum Ridge-Gable Mountain source contributes most to the total site exposure, the total exposure is not as sensitive to variations in source definition as to variations in recurrence.

The reason for the relatively small impact of source definition on exposure is illustrated by examining the contributions to the computed probability of exceedance from various magnitude bands. These are summarized below:

Magnitude Range	<u>Percentage of Contribution to Annual Exposure</u>			
	Peak Acceleration and Spectral Acceleration at T = 0.125 second		Spectral Acceleration at T = 0.4 second	
	<u>OBE</u>	<u>SSE</u>	<u>OBE</u>	<u>SSE</u>
>4-5	68	70	58	51
>5-6	22	20	30	30
>6-7	9	9	12	18
>7	1	1	<1	1

As can be seen, 70 percent of the exposure for peak acceleration results from the occurrence of events of magnitude greater than 4 to 5. For spectral accelerations at a period of 0.40 second, 50 to 60 percent of the exposure results from the occurrence of magnitude 4 to 5 events. This is due to the short distance between the site and the Gable Mountain-Southeast anticline segment (approximately 7 km). As the smaller-magnitude events contribute most of the exposure, there is only a small sensitivity of the total results to the choice of maximum magnitude on the Gable Mountain-Southeast anticline segment. Although the choice of maximum magnitude has a larger impact on the exposure from the other five sources, they contribute little to the total exposure.



In this seismic exposure analysis, equal weight has been given to the contribution of small-magnitude and large-magnitude earthquakes in calculating the probabilities of exceedance. However, small-magnitude earthquakes, especially in the range of magnitude 4 to 5, have less engineering significance than large-magnitude earthquakes because of their short duration and low-energy content. Analyses that give less weight to the small-magnitude earthquakes because of their lesser potential effects would substantially decrease the contributions of these earthquakes and reduce the total seismic exposure. Consequently, the present analysis is a conservative assessment of the probabilities of exceedance for ground motions of engineering significance.

The seismic exposure analysis described herein was conducted for the WNP-2 plant site. The WNP-1/4 plants are located approximately 1 km. to the east of the WNP-2 plant. The distances of the potential earthquake sources from the WNP-1/4 plants are not significantly different than the distances from the WNP-2 plant. Therefore, the seismic exposure is essentially the same at all three plants.

## 2.5K.9 REFERENCES

- Acharaya, H.K., 1979, Regional Variations in the Rupture-Length Magnitude Relationships and Their Dynamical Significance: Bulletin of the Seismological Society of America, v. 69, no. 6, p. 2063-2084.
- Aki, K., 1979, Characterization of Barriers on an Earthquake Fault: Journal of Geophysical Research, v. 84, no. B11, p. 6140-6148.
- Baker, V.R., 1978, Quaternary Geology of the Channeled Scabland and adjacent areas, in Baker, V.R., and Nummedal D. (eds): The Channeled Scabland, A Guide to the Geomorphology of the Columbia Basin, Washington: NASA Comparative Geology Conference, p. 17-35.
- Bakun, W.H., Stewart, R.M., Bufe, C.G., and Marks, S.M., 1980, Implication of Seismicity for Failure of a Section of the San Andreas Fault: Bulletin of the Seismological Society of America, v. 70, p. 185-201.
- Bentley, R.D., 1977, Stratigraphy of the Yakima Basalts and Structural Evolution of the Yakima Ridges in the Western Columbia Plateau: Geological Excursions of the Pacific Northwest, Department of Geology, Washington State University, Bellingham, WA, p. 339-389.
- Bentley, R.D., 1980, Magnitude of Neogene Horizontal Shortening in the Western Columbia Plateau, Washington-Oregon, (abstract): American Geophysical Union Transactions, v. 62, no. 6, p. 60.
- Bentley, R.D., Anderson, J.L., Campbell, N.P., and Swanson, D.A., 1980, Stratigraphy and Structure of the Yakima Indian Reservation, with Emphasis on the Columbia River Basalt Group: U.S. Geological Survey, Open-File Report 80-200, 83 p.
- Berrill, J.B., and Davis, R.O., 1980, Maximum Entropy and the Magnitude Distribution: Bulletin of the Seismological Society of America, v. 70, p. 1823-1831.
- Bolt, B.A., 1978, Incomplete Formulations of the Regression of Earthquake Magnitude with Surface Fault Rupture Length: Geology, v. 6, p. 233-234.
- Bonilla, M.G., 1980, Comment and Reply on "Estimating Maximum Expectable Magnitudes of Earthquakes from Fault Dimensions": Geology, v. 8, p. 162-164.

- Bonilla, M.G., and Buchanan, J.M., 1970, Interim Report on Worldwide Historic Surface Faulting: U.S. Geological Survey, Open-File Report, 32 p.
- Bruhn, R., 1981, Preliminary Analysis of Deformation in Part of the Yakima Fold Belt, South-central Washington: Draft report prepared for Washington Public Power Supply System, Richland, WA, 11 p.
- Campbell, N., 1980, Union Gap Fault: unpublished draft manuscript, June.
- Campbell, N.P., and Bentley, R.D., 1981, Late Quaternary Deformation of the Toppenish Uplift - A Yakima Fold in Southeastern Washington: unpublished manuscript submitted to Geology.
- Chinnery, M.A., 1979, Investigations of the Seismological Input to the Safety Design of Nuclear Power Reactors in New England: U.S. Nuclear Regulatory Commission, NUREG/CR-0563.
- Cornell, C.A., 1968, Engineering Seismic Risk Analysis, Bulletin of the Seismological Society of America, v. 58, no. 5, p. 1583-1606
- Cosentino, P., Ficara, V., and Luzio, D., 1977, Truncated Exponential Frequency-magnitude Relationship in Earthquake Statistics: Bulletin of the Seismological Society of America, v. 67, no. 6, p. 1615-1623.
- de Finetti, B., 1964, Foresight; its Logical Laws, its Subjective Sources: in Kyburg, H.E., Jr., and Smokler, H.E. (eds), Studies in Subjective Probability: John Wiley, New York, NY.
- Donovan, N.C., and Bornstein, A.E., 1978, Uncertainties in Seismic Risk Procedures: Journal of the Geotechnical Engineering Division, American Society of Civil Engineers, v. 104, no. GT7, July.
- Donovan, N.C., 1973, A Statistical Evaluation of Strong Motion Data, Including the February 9, 1971 San Fernando Earthquake: Proceedings of the Fifth World Conference on Earthquake Engineering, Rome, 25-29 June 1973, v. 1., p. 1252-1261.
- Eaton, J.P., 1976, Notes on the Distribution of Earthquakes within and near the Hanford Seismic Network, 1969-1974, and Preliminary Results on Crustal Structure of the Region Obtained from an Analysis (by the Time-Term Method) of

Industrial Explosions Recorded by the Network, Informal Notes: United States Geological Survey, Menlo Park, California, 22 p.

Esteva, L., 1969, Seismicity Prediction: A Bayesian Approach: Proceedings of the Fourth World Conference on Earthquake Engineering, Santiago, Chile, January 13-18, 1969, v. 1, p. A1 172-184

Farooqui, S.M., 1977, Geologic Studies of the Wallula Gap Fault as Exposed in the Trench: Subappendix 2RH Chapter 4.0, in WNP-1/4 PSAR, Amendment 23.

Farooqui, S.M., 1979, Evaluation of Faulting in the Warm Springs Canyon Area, Southeast Washington: Report prepared by Shannon and Wilson, Inc. for Washington Public Power Supply System, December.

Fecht, K.R., 1978, Geology of Gable Mountain-Gable Butte Area: Rockwell Hanford Operations, RHO-BWI-LD-5, Richland, WA 57 p.

Goff, F.E., 1981, Preliminary Geology of Eastern Umtanum Ridge, South-Central Washington: RHO-BWI-C-21, Rockwell Hanford Operations, Richland, WA, 100 p.

Golder Associates, 1981a, Geologic Structure of Umtanum Ridge -- Priest Rapids Dam to Sourdough Canyon: Draft report prepared for Northwest Energy Services Company, Kirkland, WA, 54 p.

Golder Associates, 1981b, Gable Mountain: Structural Investigations and Analyses: Draft report prepared for Northwest Energy Services Company, Kirkland, WA, 54 p.

Hadley D.M., Helmberger, D. V., and Orcutt, J. A., 1979, Peak Acceleration Scaling Studies: Earthquake Notes, Eastern Section, Seismological Society of America, v. 50, no. 4, Seattle, October - December.

Hanks, T.C., and Kanamori, H., 1979, A Moment Magnitude Scale: Journal of Geophysical Research, v. 84, no. 20, p. 2981-2987.

Idriss I.M., Sadigh, K., and Power, M.S., 1981, Variations of Peak Accelerations and Velocities with Magnitudes at Close Distances to the Source: Paper Prepared for submission to the Seismological Society of America for possible publication.



- Joyner, W.B., Boore, D.M., and Porcella, R.L., 1981, Peak Horizontal Acceleration and Velocity From Strong Motion Records Including Records from the 1979 Imperial Valley, California Earthquake: U.S. Geological Survey, Open-File Report 81-365, 45 p.
- Kanamori, H., 1977, The Energy Release in Great Earthquakes: Journal of Geophysical Research, v. 82, no. 20, p. 2981-2987.
- Kiureghian, A. and Ang, A.H., 1977, A Fault-Rupture Model for Seismic Risk Analysis, Bulletin of the Seismological Society of America, v. 67, no. 4, p. 1173-1194.
- Kulkarni, R.B., Sadign, K. and Idriss, I.M., 1979, Probabilistic Evaluation of Seismic Exposure: Proceedings of the Second U.S. National Conference on Earthquake Engineering, Stanford, California, August 22-24, 1979, p. 90-99.
- Lomnitz, C., 1966, Statistical Prediction of Earthquakes, Reviews of Geophysics, v. 4, no. 3, p. 377-393.
- McGuire, R.K., 1974, Seismic Structural Response Risk Analysis, Incorporating Peak Response Regressions On Earthquake Magnitude and Distance, Massachusetts Institute of Technology, Department of Civil Engineering, Research Report R74-51, August.
- McGuire, R.K., 1978, FRISK: Computer Program For Seismic Risk Analysis Using Faults as Earthquake Sources: U.S. Geological Survey, Open-File Report 78-1007.
- Mark, R.K., and Bonilla, M.G., 1977, Regression Analysis of Earthquake Magnitude and Surface Fault Length Using the 1970 data of Bonilla and Buchanan: U.S. Geological Survey, Open-File Report, 10 p.
- Myers, C.W., and Price, S.M., 1979, Geologic Studies of the Columbia Plateau: A Status Report (draft): Rockwell-Hanford Operations, Richland, WA, RHO-BWI-ST-4.
- Nair, K., and Cluff, L.S., 1977, An Approach to Establishing Design Surface Displacements for Active Faults: Proceedings, of the Sixth World Conference on Earthquake Engineering, New Delhi, India.
- Price, E.H., 1980, Strain Distribution and Model for Formation of Eastern Umatum Ridge Anticline, South-Central Washington: Rockwell Hanford Operations, Report prepared for U.S. Department of Energy, RHO-BWI-SA-30, 27 p.

- Price, E.H., 1981, Written communication to Woodward-Clyde Consultants, San Francisco, CA.
- Price, E.H., 1981, Structural Geometry, Strain Distribution and Tectonic Evolution of Umtanum Ridge at Priest Rapids and a Comparison with Other Selected Localities within Yakima Fold Structures, South-Central Washington: Rockwell Hanford Operations, Richland, WA, RHO-BWI-FA-138 in press.
- Richter, C.F., 1958, Elementary Seismology: W.H. Freeman, San Francisco, CA.
- Rigby, J.G., and Othberg, K., 1979, Reconnaissance Surficial Geologic Mapping of the Late Cenozoic Sediments of the Columbia Basin, Washington: State of Washington, Department of Natural Resources, Open-File Report 79-3.
- Savage, J.C., Lisowski, M., and Prescott, W.H., 1981, Geodetic Strain Measurements in Washington: Journal of Geophysical Research, v. 86, no. B6, p. 4929-4940.
- Savage, L.J., 1954, The Foundations of Statistics: John Wiley, New York, NY.
- Schnabel, P.B., and Seed, H.B., 1973, Accelerations in Rock for Earthquakes in the Western United States: Bulletin of the Seismological Society of America, v. 63, no. 2, p. 501-516.
- Selvidge, J., 1972, Assigning Probabilities to Rare Events: Ph.D. Thesis, Graduate School of Business Administration, Harvard University, Cambridge, MA.
- Sien, K.E., 1978, Prehistoric Large Earthquakes Produced by Slip on the San Andreas fault at Pallett Creek, California: Journal of Geophysical Research, v. 83, no. B8, p. 3907-3939.
- Singh, S.K., Bazan, E., and Esteva, L., 1980, Expected Earthquake Magnitude from a Fault: Bulletin of the Seismological Society of America, v. 70, p. 903-914.
- Slemmons, D.B., 1977, State-of-the-art for Assessing Earthquake Hazards in the United States, Report 6: Faults and Earthquake Magnitude: U.S. Army Corps of Engineers, Waterways Experiment Station, Soils and Pavements Laboratory, Vicksburg, MS, Miscellaneous Paper S-73-1, 129 p.
- Slemmons, D.B., 1980, Appendix E to Safety Evaluation Report Related to the Operation of San Onofre Nuclear Generating

Station Units 2 and 3: U.S. Nuclear Regulatory Commission, NUREG-0712, Docket Nos. 50-361 and 50-362, 28 p.

Smith, S.W., 1976, Determination of Maximum Earthquake Magnitude: Geophysical Research Letters, v. 3, no. 6, p. 351-354.

Stael von Holstein, C.A., 1970, Assessment and Evaluation of Subjective Probability Distributions: The Economic Research Institute, Stockholm School of Economics, Sweden.

Swan, F.H., III, Schwartz, D.P., and Cluff, L.S., 1980, Recurrence of Moderate to Large Magnitude Earthquakes Produced by Surface Faulting on the Wasatch Fault Zone, Utah: Bulletin of the Seismological Society of America, v. 70, p. 1431-1462.

Tocher, D., 1958, Earthquake Energy and Ground Breakage: Bulletin of the Seismological Society of America, v. 48, no. 2, p. 147-153.

U.S. Nuclear Regulatory Commission, 1978, Development of Criteria for Seismic Review of Selected Nuclear Power Plants: by N.M. Newmark and W.J. Hall.

Washington Public Power Supply System, (undated), WPPSS Nuclear Project No. 2 Final Safety Analysis Report.

Washington Public Power Supply System, 1981a, Appendix 2.5J: Analysis of the Seismicity of the Columbia Plateau: prepared by Woodward-Clyde Consultants, San Francisco, CA.

Washington Public Power Supply, 1981b, Appendix 2.5N: Late Cenozoic Tectonics of the Pacific Northwest with Special Reference to the Columbia Plateau, prepared by G.A. Davis, 47 p.

Washington Public Power Supply System, 1981c, Appendix 2.5 O: Models of the Development of Yakima Deformation: prepared by H.P. Laubscher, 69 p.

Wentworth, C.M., Bonilla, M.G., and Buchanan, J.M., 1969, Seismic Environment of the Sodium Pump Test Facility at Burro Flats, Ventura County, California: U.S. Geological Survey, Open-File Report.

Weston Geophysical Corporation, 1981a, Compilation and Interpretation of Gravity in Washington, Oregon, and Adjacent Parts of British Columbia and Idaho: Report prepared for Washington Public Power Supply System, WNP-2 FSAR, Appendix 2.5L, 28 p.



- Weston Geophysical Corporation, 1981b, Geologic Interpretation of an Aeromagnetic Survey of the Central Columbia Plateau, Washington and Oregon: Report prepared for Washington Public Power Supply System, Richland, WA, 57 p.
- Weston Geophysical Corporation, 1981c, Geophysical Investigations, Umtanum Ridge to Southeast Anticline, Hanford Reservation, WA: Prepared for Northwest Energy Services Company, Kirland, WA.
- Winkler, R.L., 1967, The Quantification of Judgment; Some Methodological Suggestions: Journal of the American Statistical Association, v. 62, no. 320, p. 1105-1120.
- Winkler, R.L., and Murphy, A.H., 1968, Evaluation of Subjective Precipitation Probability Forecasts: Proceedings, American Meteorological Society, First National Conference on Statistical Meteorology, Boston, MA.
- Woodward-Clyde Consultants, 1978, 1372 Earthquake Studies for Washington Public Power Supply System Units WNP 1 and 4, Paleomagnetic Measurements of the Ringold Formation and Loess Units near Hanford, Washington: Report prepared for Washington Public Power Supply System, Richland, WA.
- Woodward-Clyde Consultants, 1979, Report of the Evaluation of Maximum Earthquake and Site Ground Motion Parameters Associated with the Offshore Zone of Deformation, San Onofre Nuclear Generating Station: Unpublished report submitted to Southern California Edison Company, 241 p.
- Woodward-Clyde Consultants, 1981a, Wallula Fault Trenching and Mapping: Draft report prepared for Washington Public Power Supply System, Richland, WA.
- Woodward-Clyde Consultants, 1981b, Toppenish Ridge Study: Report prepared for Washington Public Power Supply System, Richland, WA.
- Woodward-Clyde Consultants, 1981c, Wave Propagation and Ground Motion Modeling: Report prepared for Washington Public Power Supply System, Richland, WA.
- Woodward-Clyde Consultants, 1981d, Quaternary Sediments Study of the Pasco Basin and Adjacent Areas: Report prepared for Washington Public Power Supply System, Richland, WA.
- Woodward-Clyde Consultants, 1981e, Logs of Trenches at Finley Quarry: Field logs prepared for Washington Public Power Supply System, Richland, WA.

AMENDMENT NO. 18  
September 1981

Wyss, M., 1979, Estimating Maximum Expectable Magnitude of Earthquakes from Fault Dimensions: Geology, v. 7, no. 7, p. 336-340.

Yegulalp, T.M., and Kuo, J.T., 1974, Statistical Prediction of the Occurrence of Maximum Magnitude Earthquakes: Bulletin of the Seismological Society of America, v. 64, no. 2.



TABLE 2.5K-1

PARTICIPANTS IN ASSESSMENT OF SUBJECTIVE PROBABILITIESWashington Public Power Supply System

W. Kiel

Geology Advisory BoardH. Coombs  
G. Davis  
R. Smith  
D. TillsonNorthwest Energy Services CompanyJ. Kearnes  
D. Caldwell - Golder Associates  
G. Antonnen - Golder AssociatesConsultants to WPPSS

R. Bruhn

Woodward-Clyde ConsultantsJ. Black  
L. Cluff  
K. Coppersmith  
W. Foxall  
D. Gross  
D. Hitchcock  
W. Savage  
D. Schwartz  
F. Swan  
R. Wagner  
D. WestOthers

E. Price



TABLE 2.5K-2

MAXIMUM EARTHQUAKE MAGNITUDE DISTRIBUTIONS  
FOR POTENTIAL SEISMIC SOURCES

Potential Source	Magnitude													
	4.25	4.5	4.75	5.0	5.25	5.5	5.75	6.0	6.25	6.5	6.75	7.0	7.25	7.5
Gable Mtn.-South-East Anticline	0.15	0.36	0.40	0.54	0.66	0.66	0.75	0.76	0.77	0.83	0.87	0.91	0.98	1.0
Umtanum Ridge Eastern	0.15	0.17	0.17	0.37	0.47	0.49	0.64	0.76	0.76	0.82	0.87	0.90	0.98	1.0
Umtanum Ridge Central	0.15	0.17	0.17	0.37	0.49	0.64	0.64	0.76	0.79	0.83	0.87	0.93	0.93	1.0
Umtanum Ridge Western	0.15	0.17	0.17	0.34	0.47	0.49	0.49	0.64	0.76	0.82	0.86	0.90	0.93	1.0
RAW-Rattlesnake Mountain						0.12	0.21	0.35	0.41	0.61	0.76	0.85	0.97	1.0
RAW-Rattlesnake Wallula					0.09	0.16	0.18	0.19	0.23	0.43	0.56	0.83	0.86	1.0
RAW-Wallula				0.04	0.04	0.12	0.18	0.21	0.23	0.43	0.62	0.83	0.86	1.0
Saddle Mountains						0.24	0.24	0.47	0.56	0.63	0.72	0.81	0.88	1.0
Rattlesnake Hills							0.36	0.60	0.65	0.70	0.79	0.84	0.84	1.0
Yakima Ridge						0.18	0.36	0.60	0.65	0.70	0.79	0.84	0.84	1.0
Horse Heaven Hills						0.18	0.36	0.60	0.67	0.76	0.83	0.84	0.95	1.0

Note: The value for the cumulative distribution function (CDF) is given for each magnitude. The CDF value at any given magnitude expresses the probability that the maximum magnitude is less than or equal to the given magnitude. The median of the CDF is the 0.5 probability level.



TABLE 2.5K-3

PROBABILITY OF OBSERVING LARGE-MAGNITUDE EVENTS

Recurrence Interval for Magnitude >7.0 T (years)	Probability of Observing x or Fewer Events in 8 trials, in 10,000 Years							
	x =	0	1	2	3	4	5	6
10,000		0.0003	0.005	0.033	0.13	0.33	0.61	0.86
30,000		0.069	0.29	0.59	0.83	0.95	0.99	1.0
115,000		0.50	0.86	0.98	1.0	-	-	-
300,000		0.77	0.97	1.0	-	-	-	-



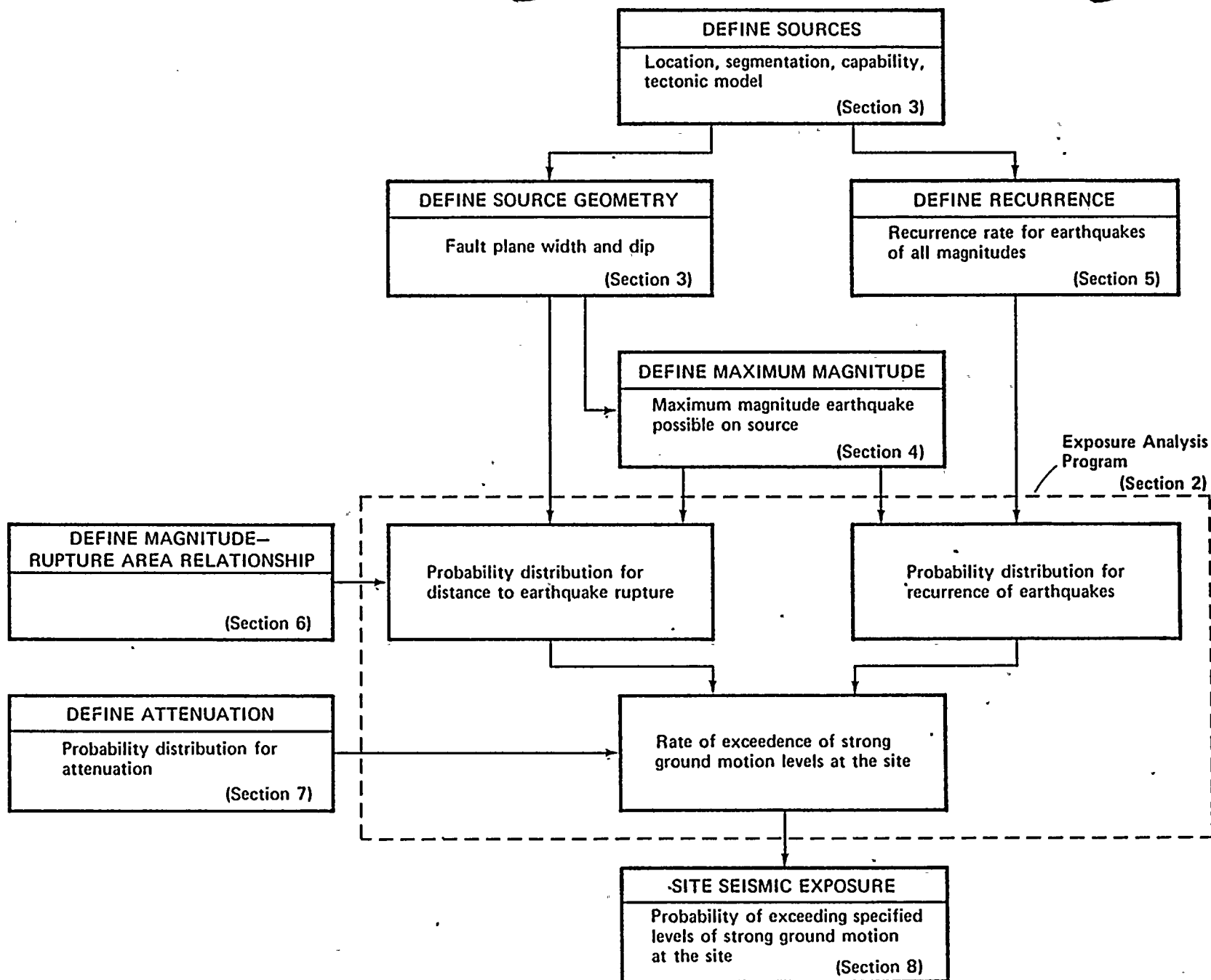
TABLE 2.5K-4

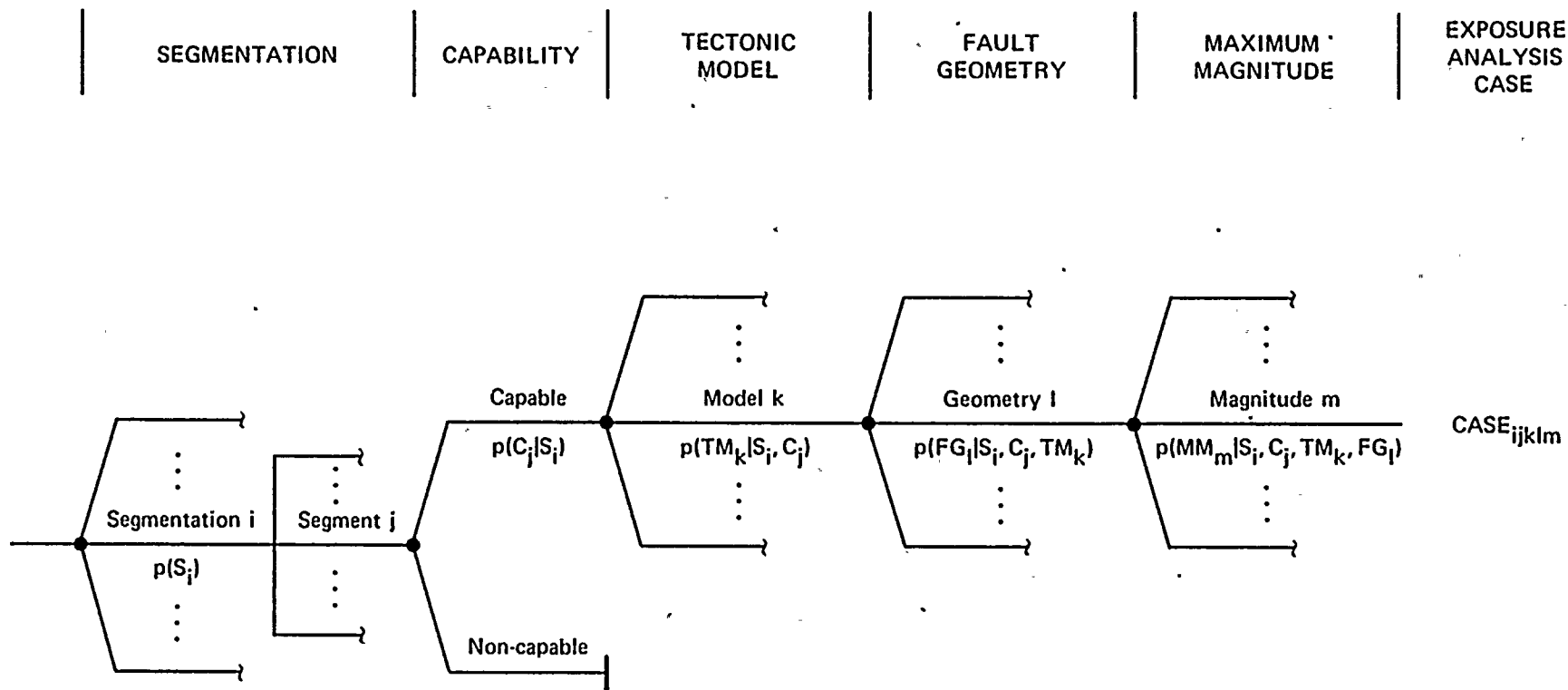
MEAN NUMBER OF EVENTS OF MAGNITUDE GREATER THAN 4.0  
ON PROPOSED SOURCES

<u>Source/Source Segment</u>	<u>Length (km)</u>	<u>Parameter A<sub>n</sub> No. of Events Magnitude &gt;4.0 Per Year (x 10<sup>-3</sup>)</u>
Umtanum Ridge-Gable Mountain Structural Trend	144	9.9
Gable Mountain Segment*	39	2.7
Umtanum Ridge, East Segment*	32	2.2
Umtanum Ridge, Central Segment*	30	2.1
Umtanum Ridge, West Segment*	43	3.0
Rattlesnake-Wallula Alignment	115	7.9
Rattlesnake Mountain Segment*	20	1.4
Rattlesnake-Wallula Segment*	50	3.4
Wallula Segment*	45	3.1
Horse Heaven Hills	155	10.6
Rattlesnake Hills	60	4.1
Yakima Ridge	60	4.1
Saddle Mountains	90	6.2

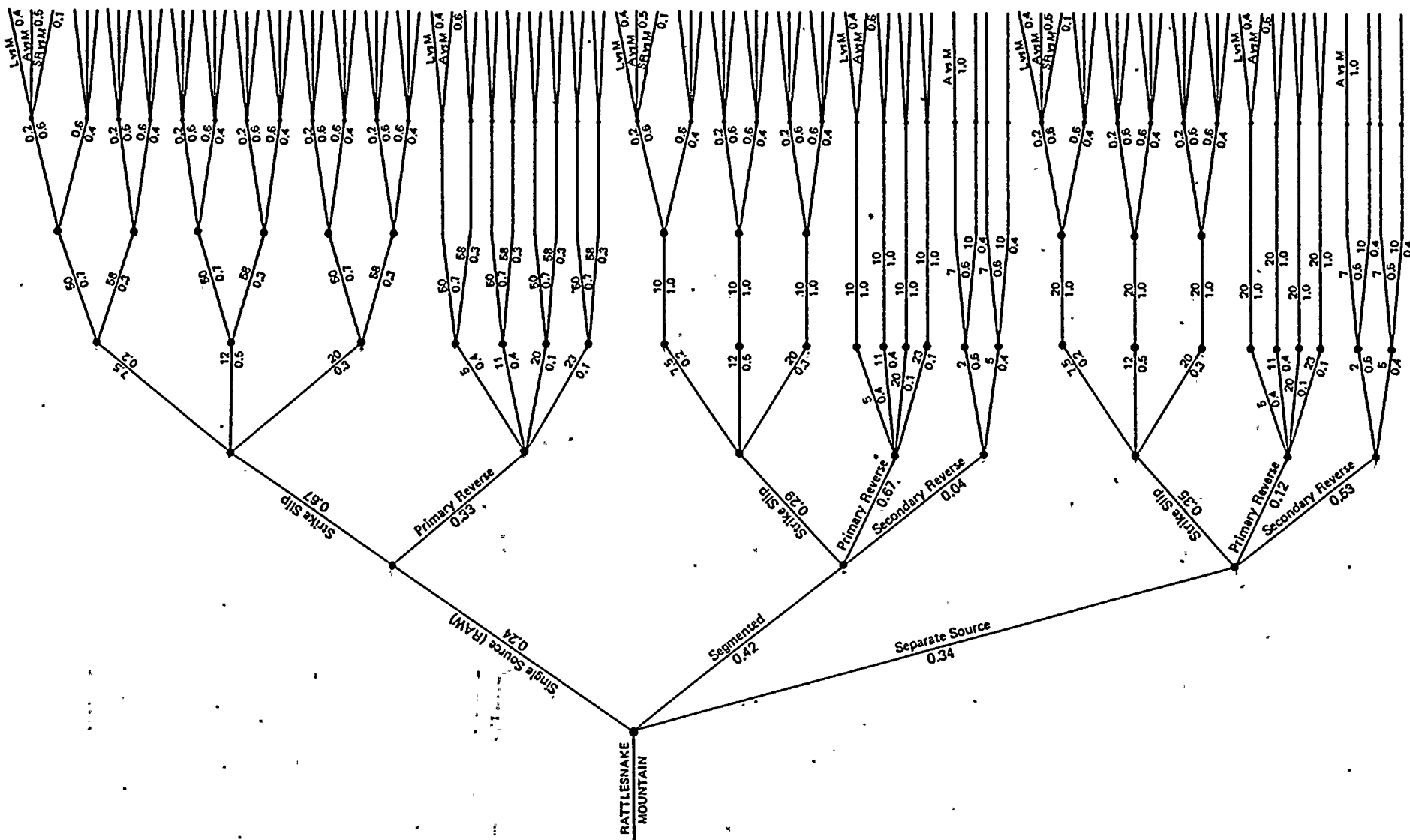
---

\* Segment of Larger Source





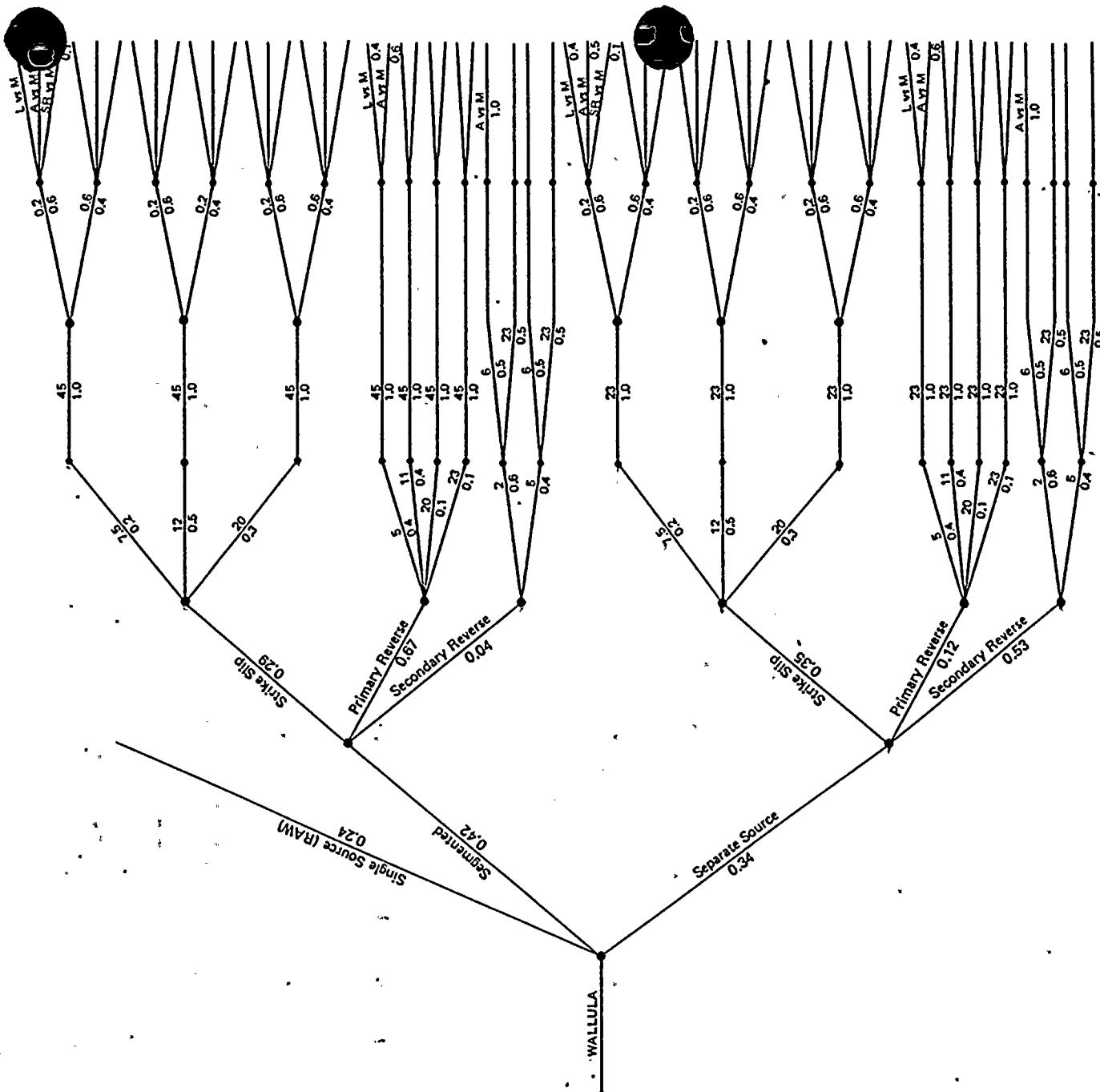
$$\text{Probability of CASE}_{ijklm} = p(S_i) \cdot p(C_j|S_i) \cdot p(TM_k|S_i, C_j) \cdot p(FG_l|S_i, C_j, TM_k) \cdot p(MM_m|S_i, C_j, TM_k, FG_l)$$



Project No. 14940	Hanford FSAR	MAXIMUM MAGNITUDE LOGIC TREE FOR RATTLESNAKE MOUNTAIN SEGMENT OF RAW	Figure 2.5K-3
Woodward-Clyde Consultants			



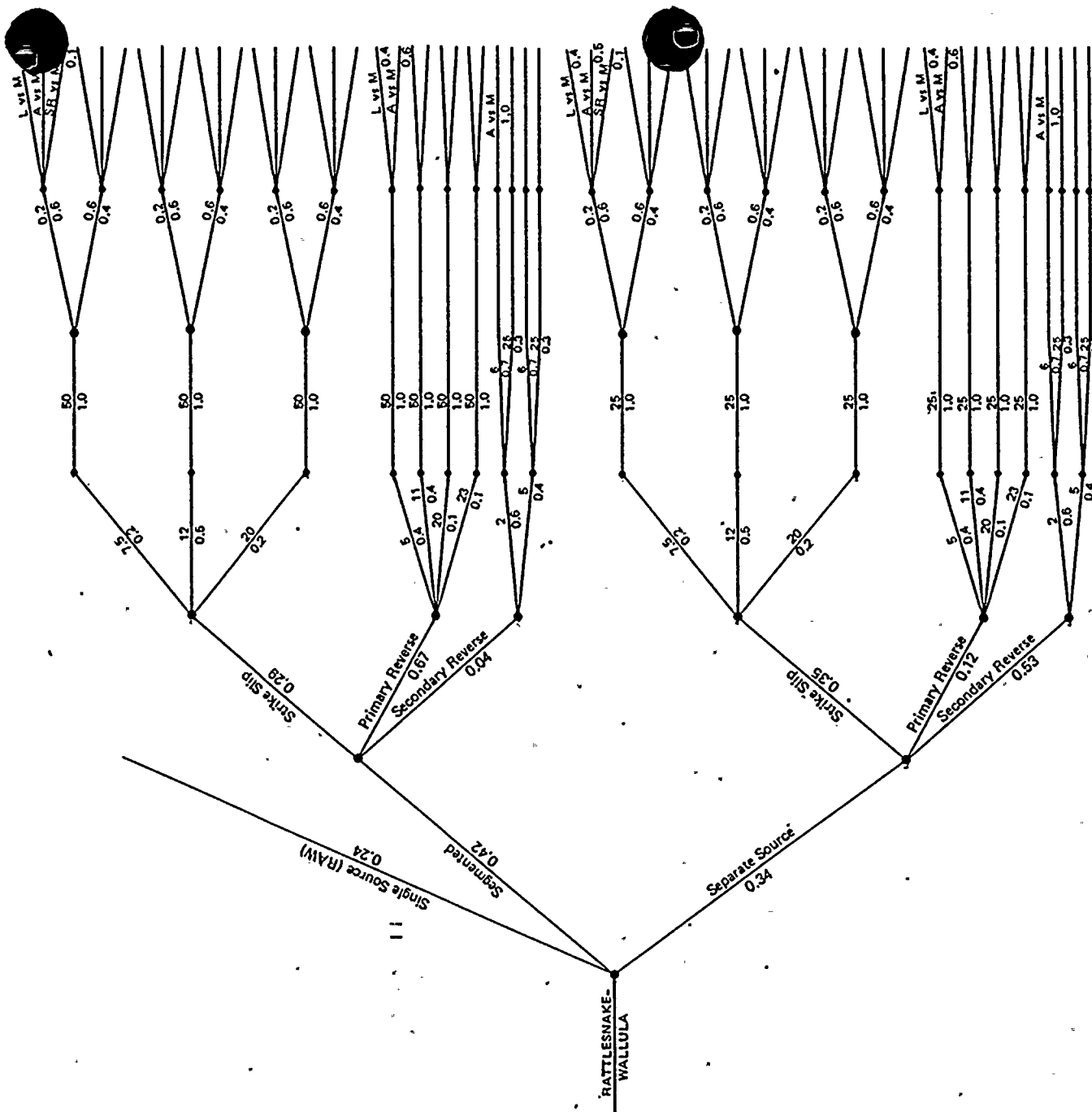
Source	Segmentation	Tectonic Model	Fault Width (km)	Fault Rupture Length (km)	Slip Rate (mm/yr)	Technique Applicability
--------	--------------	----------------	------------------	---------------------------	-------------------	-------------------------



Project No. 14940	Hanford FSAR	MAXIMUM MAGNITUDE LOGIC TREE FOR WALLULA SEGMENT OF RAW	Figure 2.5K-4
Woodward-Clyde Consultants			

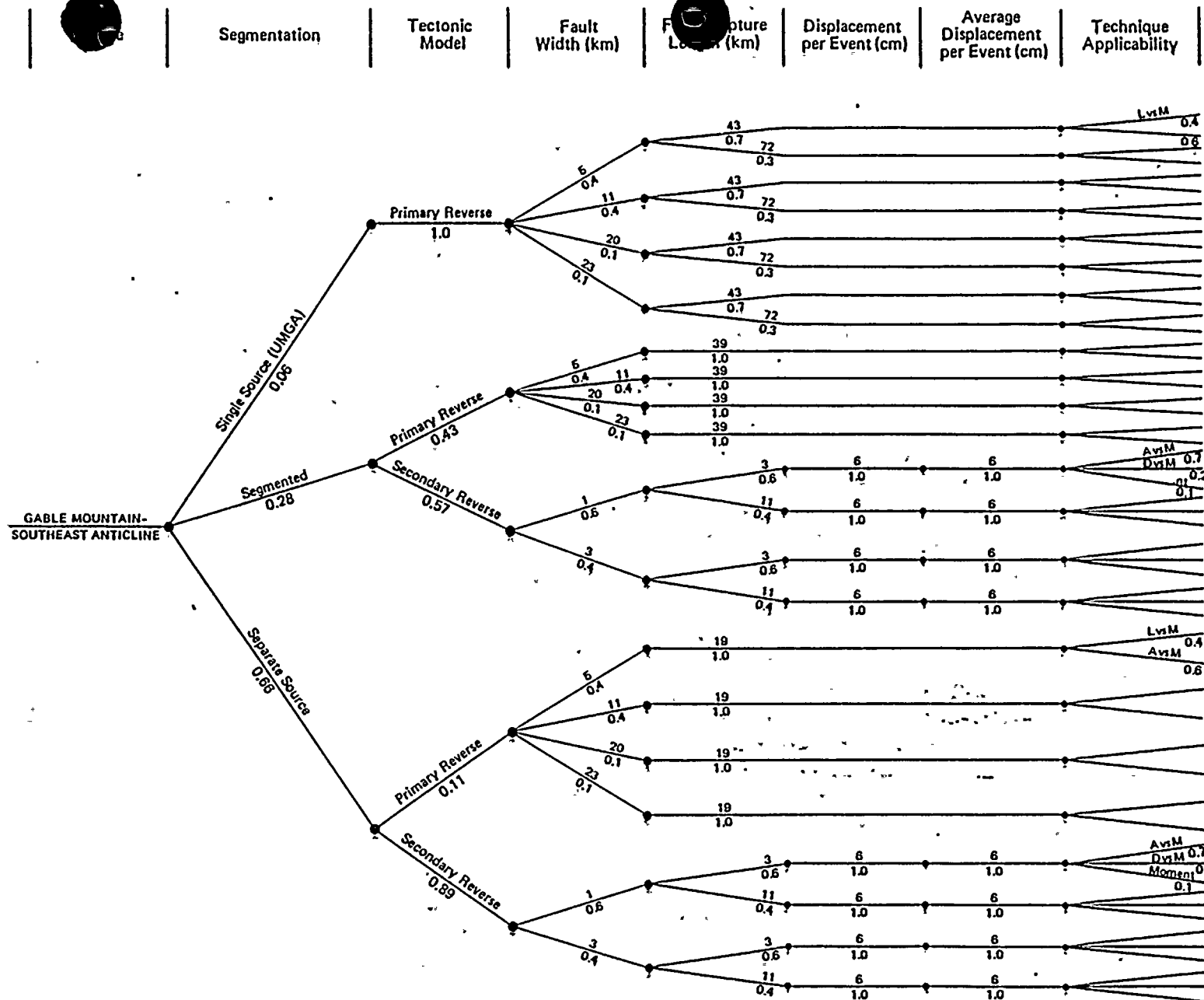


Source	Segmentation	Tectonic Model	Fault Width (km)	Fault Rupture Length (km)	Slip Rate (mm/yr)	Technique Applicability
--------	--------------	----------------	------------------	---------------------------	-------------------	-------------------------



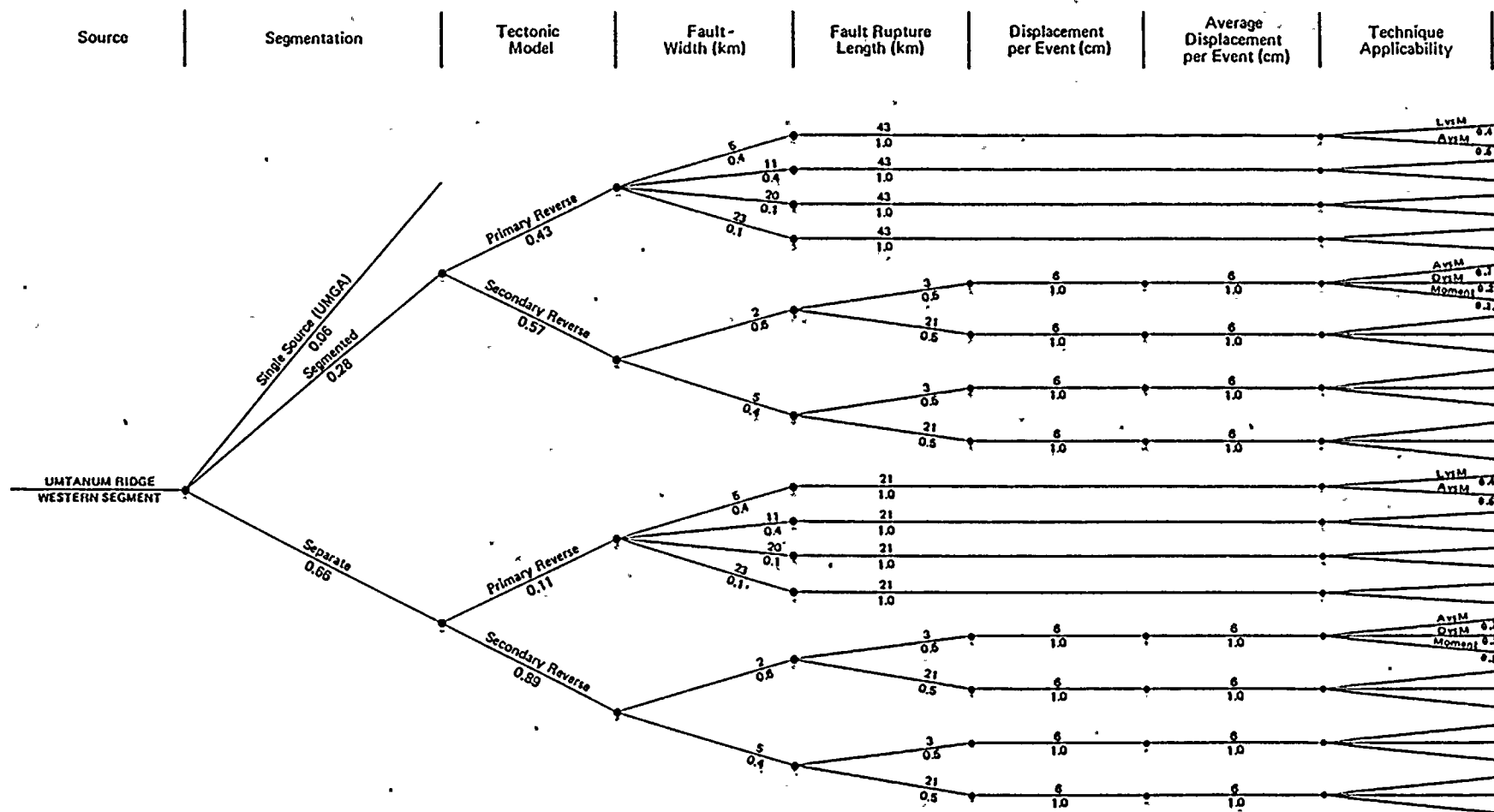
Project No. 14940	Hanford FSAR	MAXIMUM MAGNITUDE LOGIC TREE FOR RATTLESNAKE-WALLULA SEGMENT OF RAW	Figure 2.5K-5
Woodward-Clyde Consultants			

WNP-2 Amendment No. 18  
September 1981



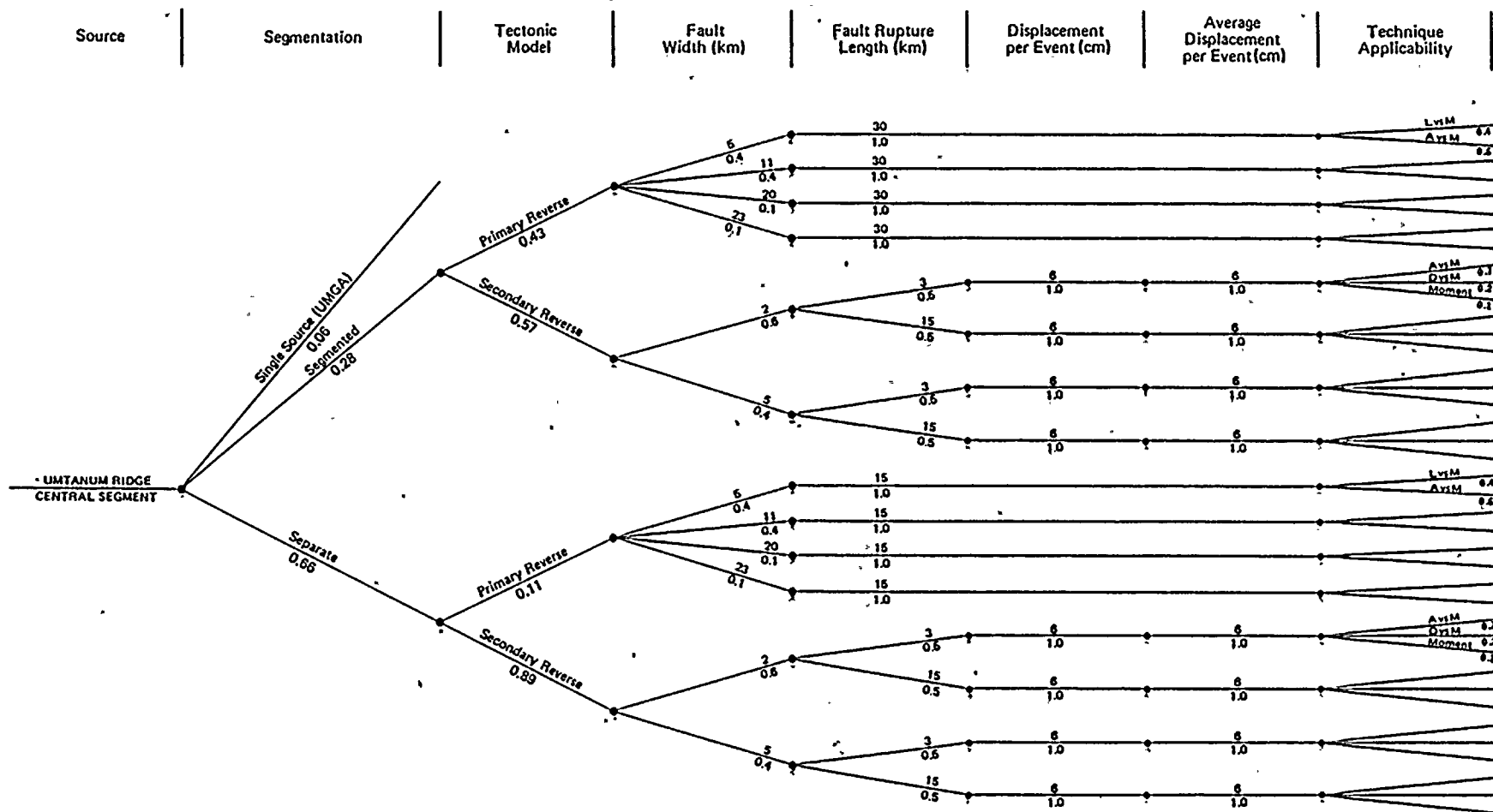
Project No. 14940	Hanford FSAR	MAXIMUM MAGNITUDE LOGIC TREE FOR GABLE MOUNTAIN-SOUTHEAST ANTICLINE SEGMENT OF THE UMTANUM RIDGE-GABLE MOUNTAIN STRUCTURAL TREND	Figure 2.5K-6
Woodward-Clyde Consultants			





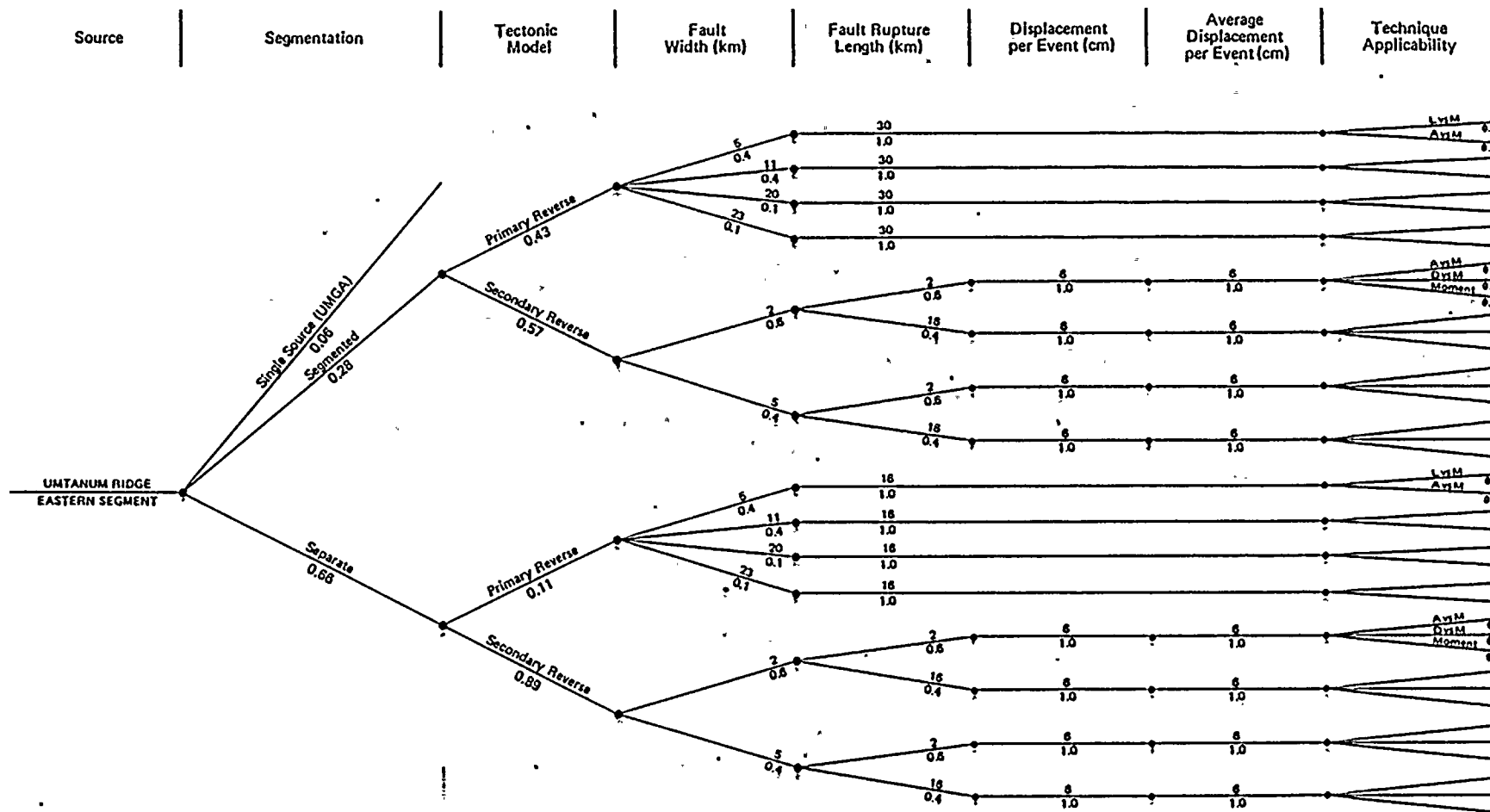
Project No. 14940	Hanford FSAR	MAXIMUM MAGNITUDE LOGIC TREE FOR UMTANUM RIDGE WESTERN SEGMENT OF THE UMTANUM RIDGE-GABLE MOUNTAIN STRUCTURAL TREND	Figure 2.5K-7
Woodward-Clyde Consultants			

WNP-2 Amendment No. 18  
September 1981



Project No. 14940	Hanford FSAR	MAXIMUM MAGNITUDE LOGIC TREE FOR UMTANUM RIDGE CENTRAL SEGMENT OF THE UMTANUM RIDGE-GABLE MOUNTAIN STRUCTURAL TREND	Figure 2.5K-8
Woodward-Clyde Consultants			

WNP-2 Amendment No. 18  
September 1981



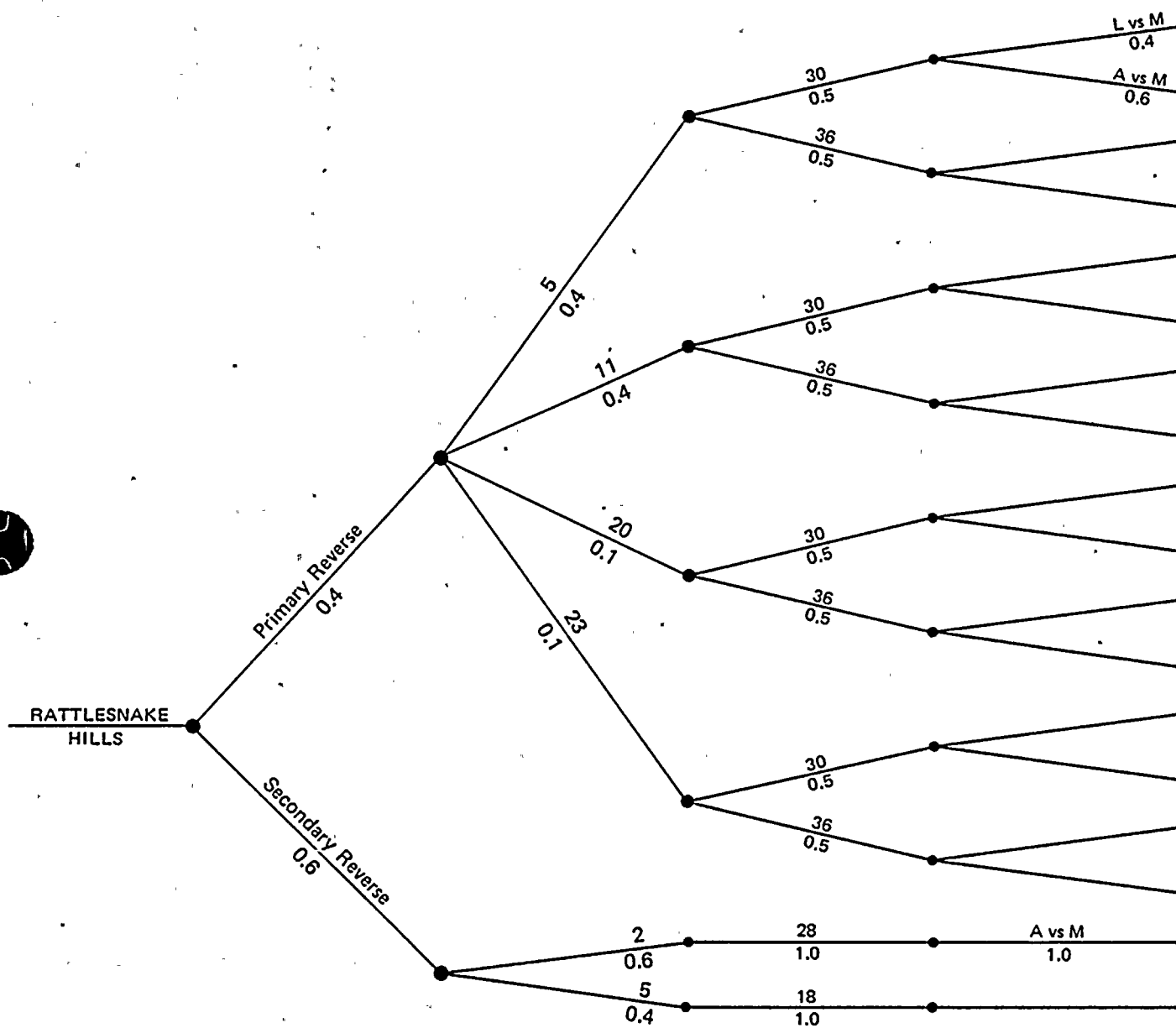
Project No. 14940	Hanford FSAR	MAXIMUM MAGNITUDE LOGIC TREE FOR UMTANUM RIDGE EASTERN SEGMENT OF THE UMTANUM RIDGE-GABLE MOUNTAIN STRUCTURAL TREND	Figure 2.5K-9
Woodward-Clyde Consultants			

WNP-2 Amendment No. 18  
September 1981





Source

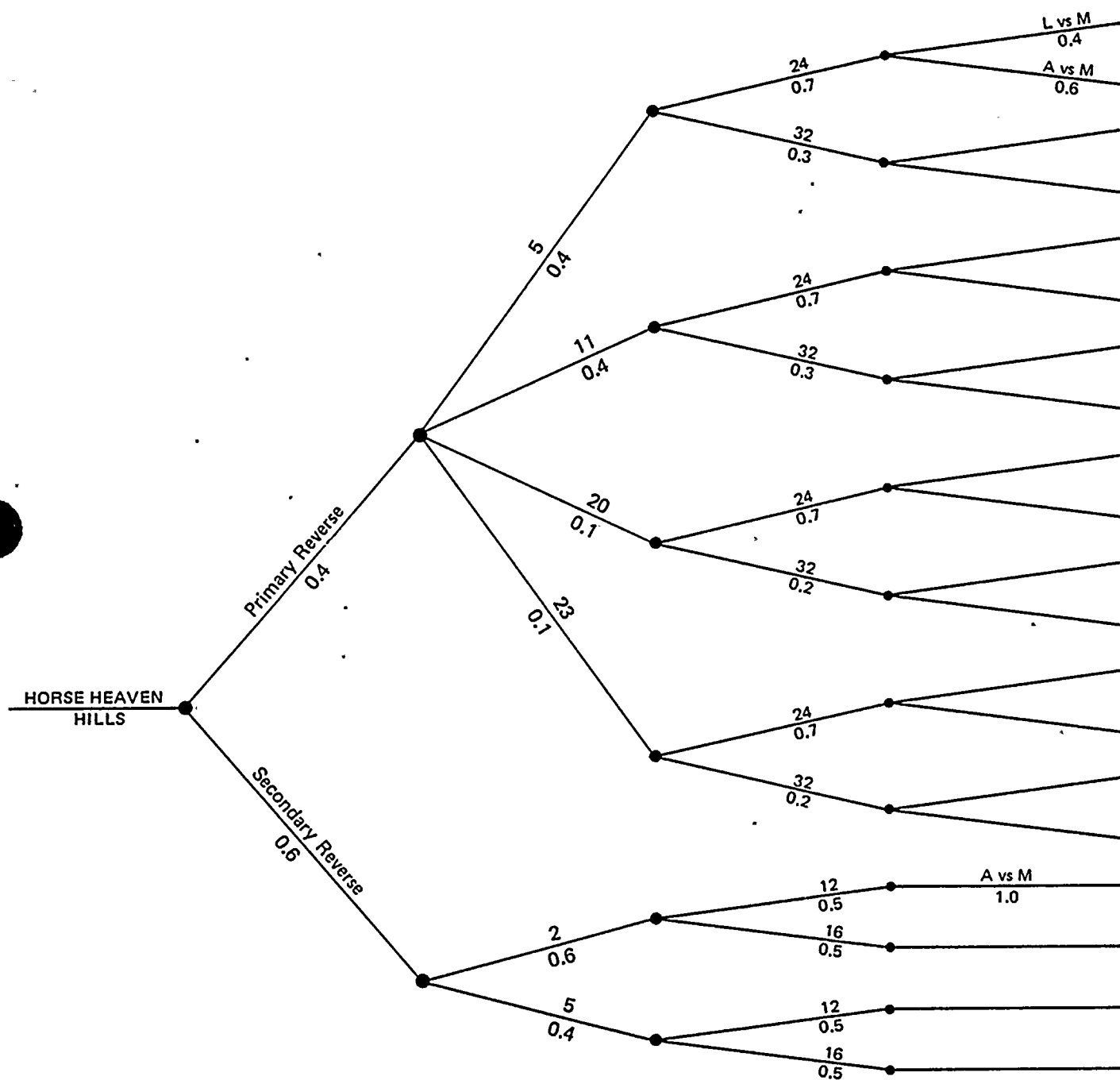
Tectonic  
ModelFault  
Width (km)Fault Rupture  
Length (km)Technique  
ApplicabilityProject No.  
14940

Hanford FSAR

Woodward-Clyde Consultants.

MAXIMUM MAGNITUDE LOGIC TREE  
FOR RATTLESNAKE HILLSFigure  
2.5K-10

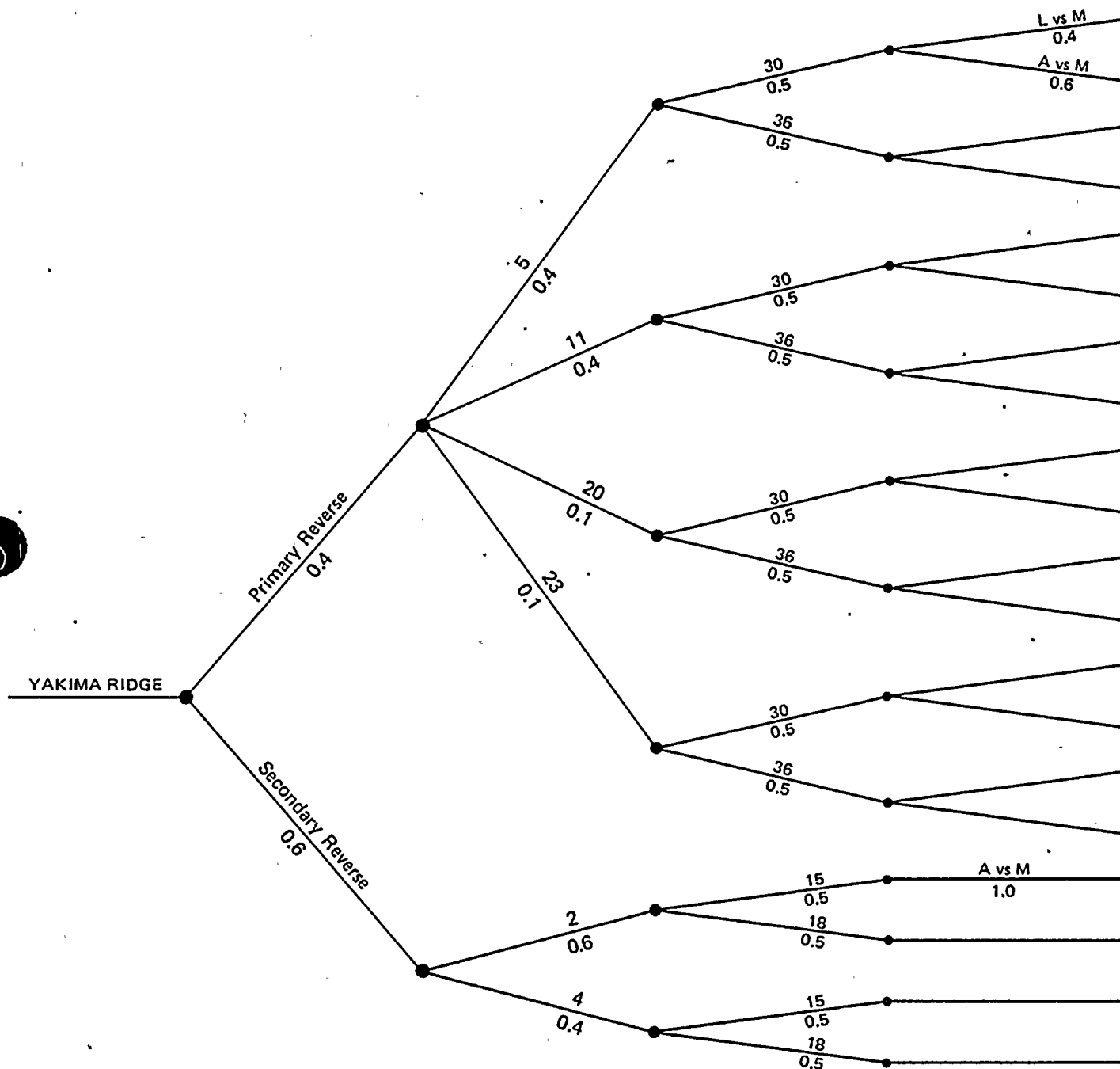
Source

Tectonic  
ModelFault  
Width (km)Fault Rupture  
Length (km)Technique  
ApplicabilityProject No.  
14940

Hanford FSAR

**Woodward-Clyde Consultants****MAXIMUM MAGNITUDE LOGIC TREE  
FOR HORSE HEAVEN HILLS****Figure  
2.5K-11**

Source

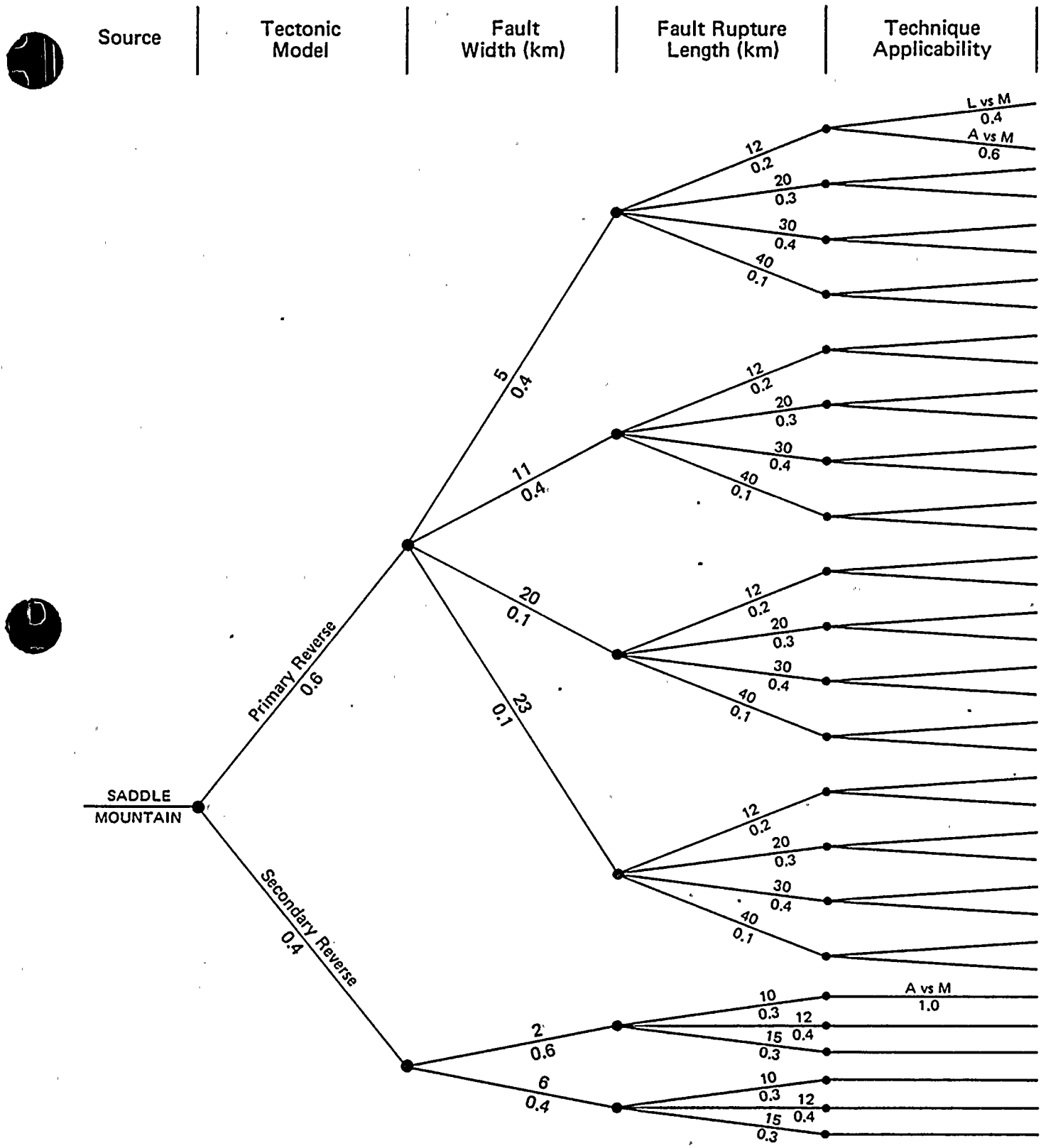
Tectonic  
ModelFault  
Width (km)Fault Rupture  
Length (km)Technique  
ApplicabilityProject No.  
14940

Hanford FSAR

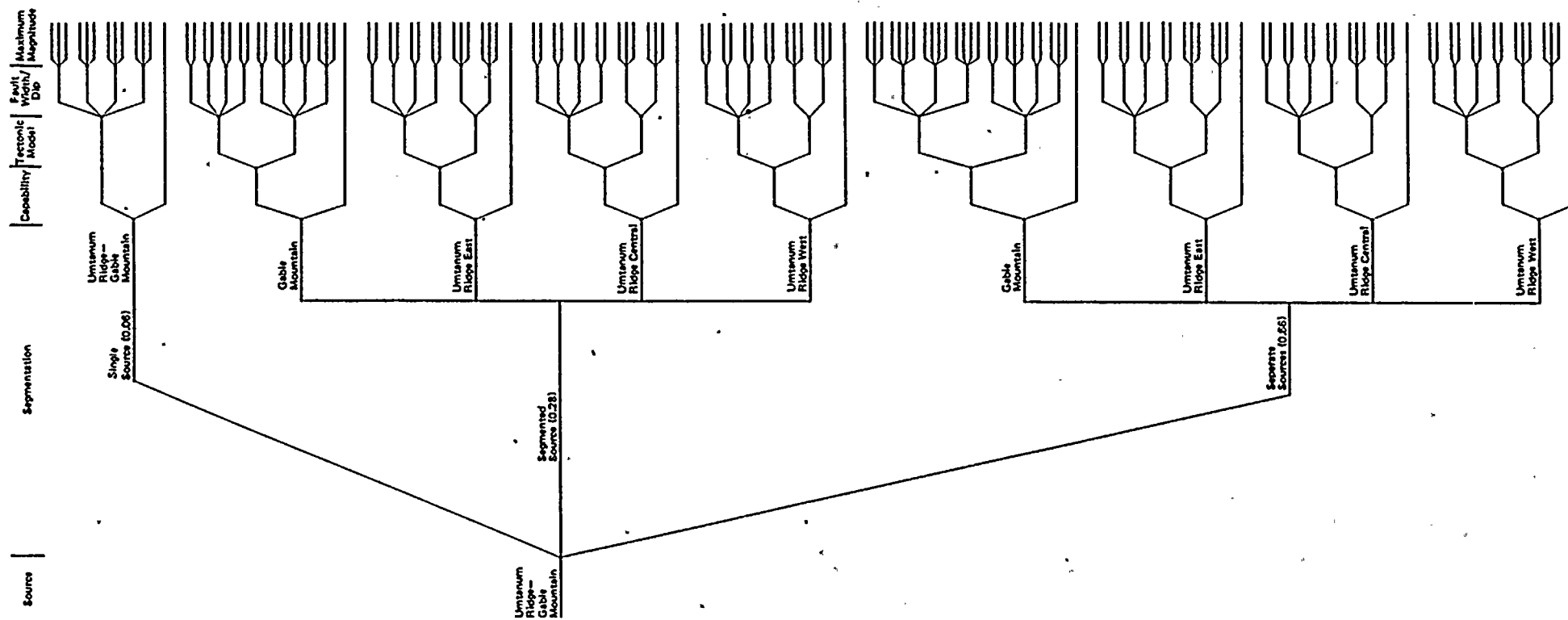
Woodward-Clyde Consultants

MAXIMUM MAGNITUDE LOGIC TREE  
FOR YAKIMA RIDGEFigure  
2.5K-12WNP-2 Amendment No. 18  
September 1981





Project No. 14940	Hanford FSAR	MAXIMUM MAGNITUDE LOGIC TREE FOR SADDLE MOUNTAIN	Figure 2.5K-13
Woodward-Clyde Consultants			

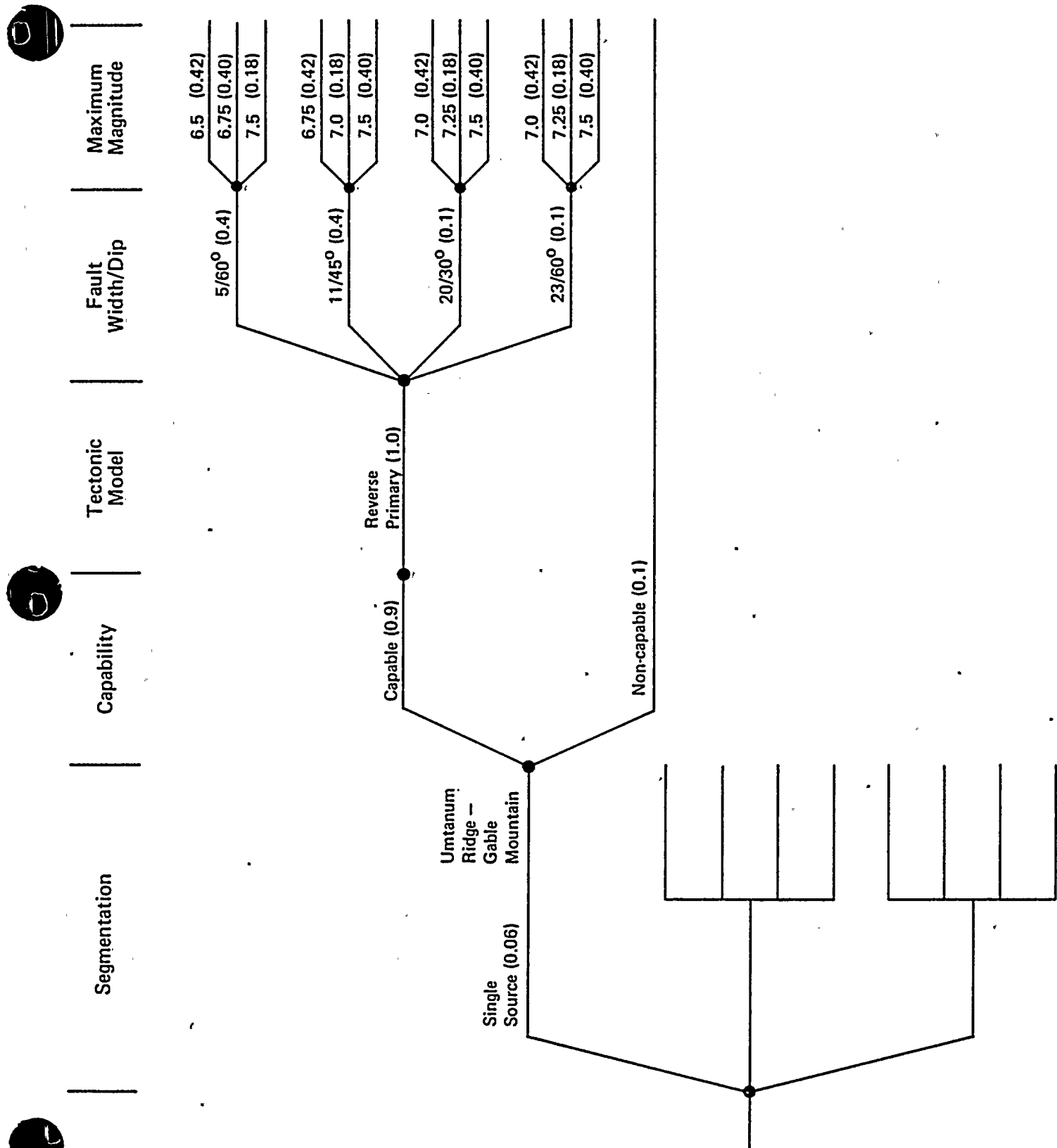


Project No. 14940	Hanford FSAR	EXPOSURE LOGIC TREE FOR UMTANUM RIDGE - GABLE MOUNTAIN STRUCTURAL TREND	Figure 2.5K-14
Woodward-Clyde Consultants			

WNP-2 Amendment No. 18  
September 1981

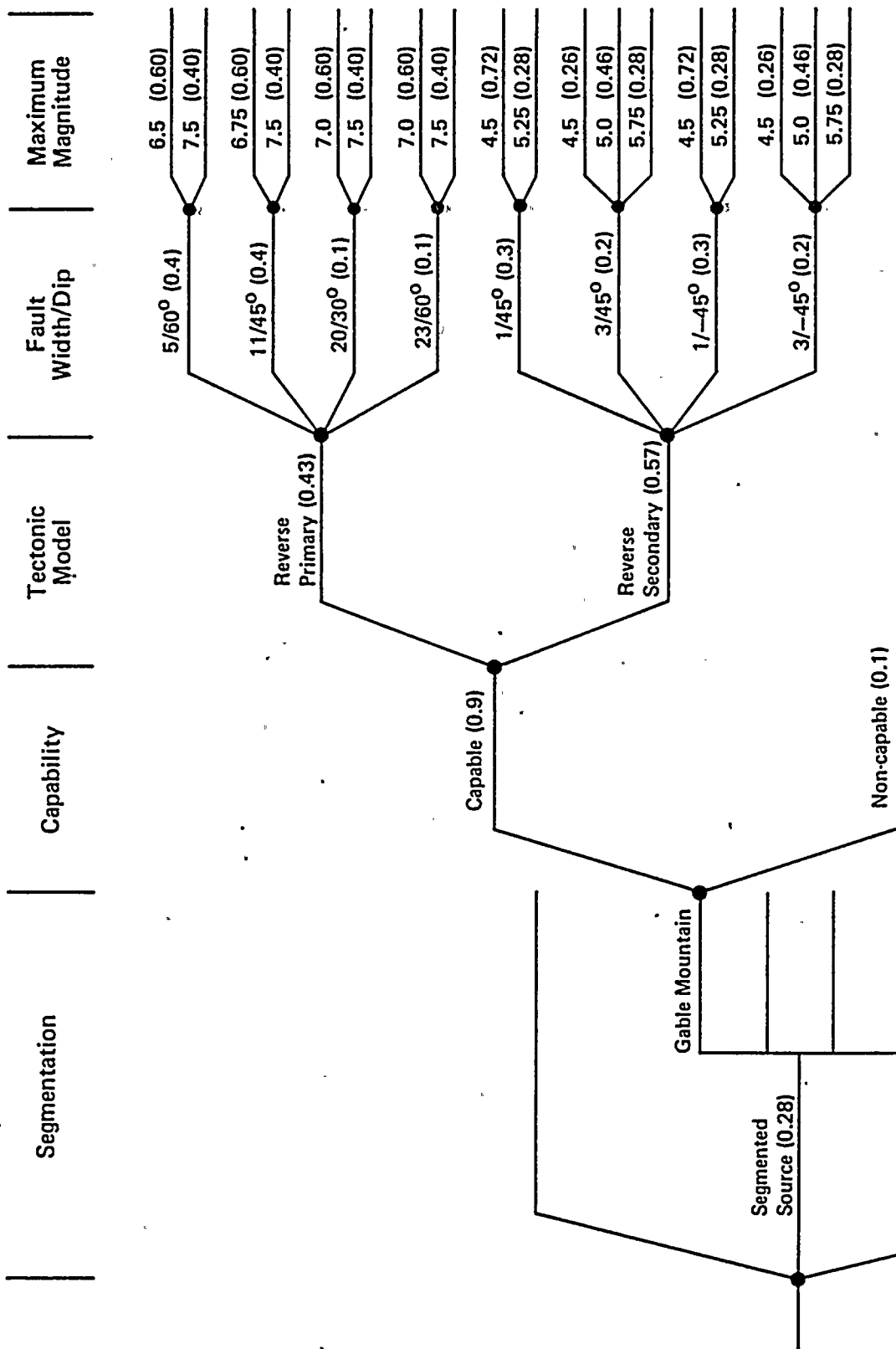






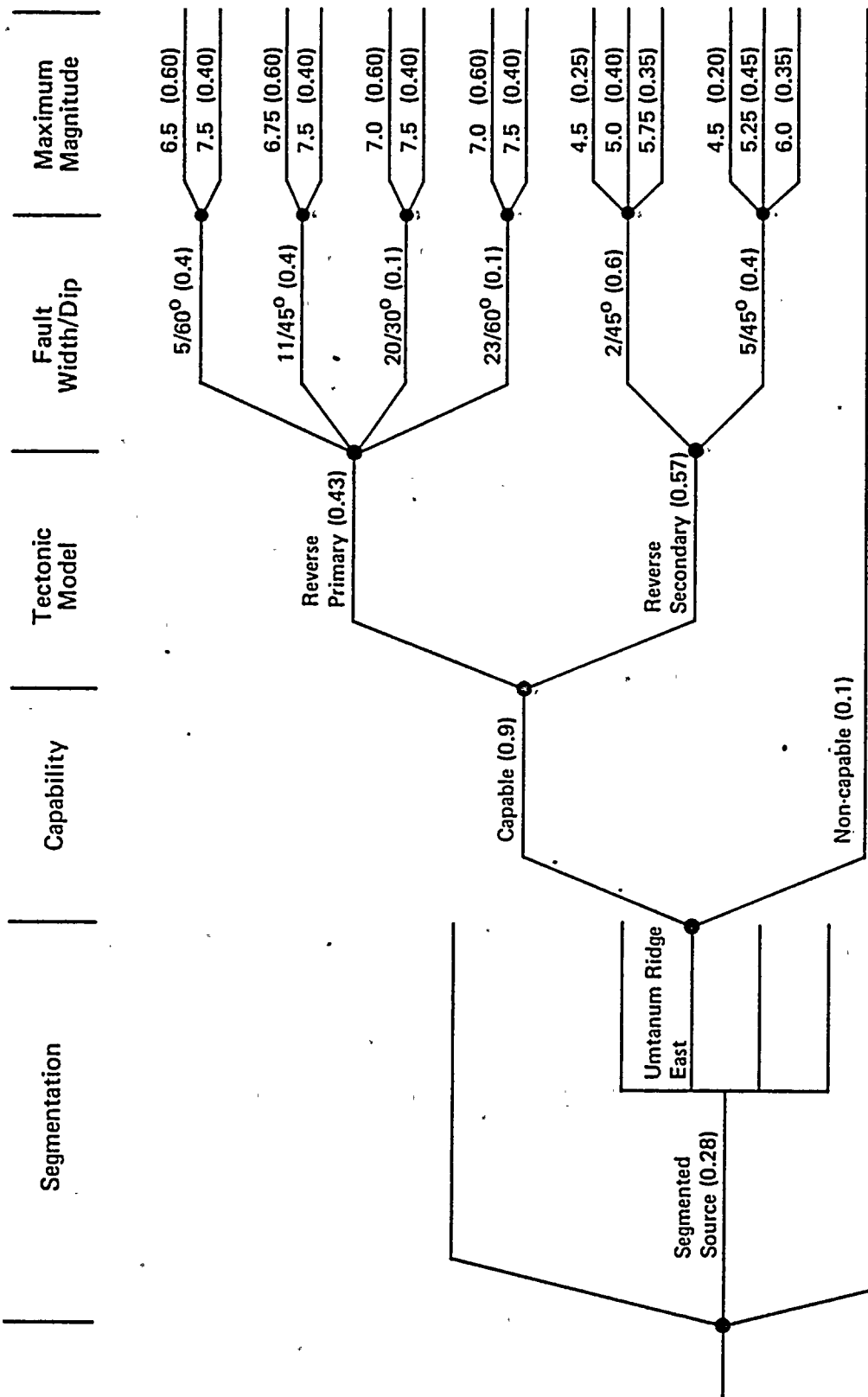
Project No. 14940	Hanford FSAR	EXPOSURE LOGIC TREE FOR UMTANUM RIDGE—GABLE MOUNTAIN STRUCTURAL TREND: SINGLE SOURCE	Figure 2.5K—15
Woodward-Clyde Consultants			



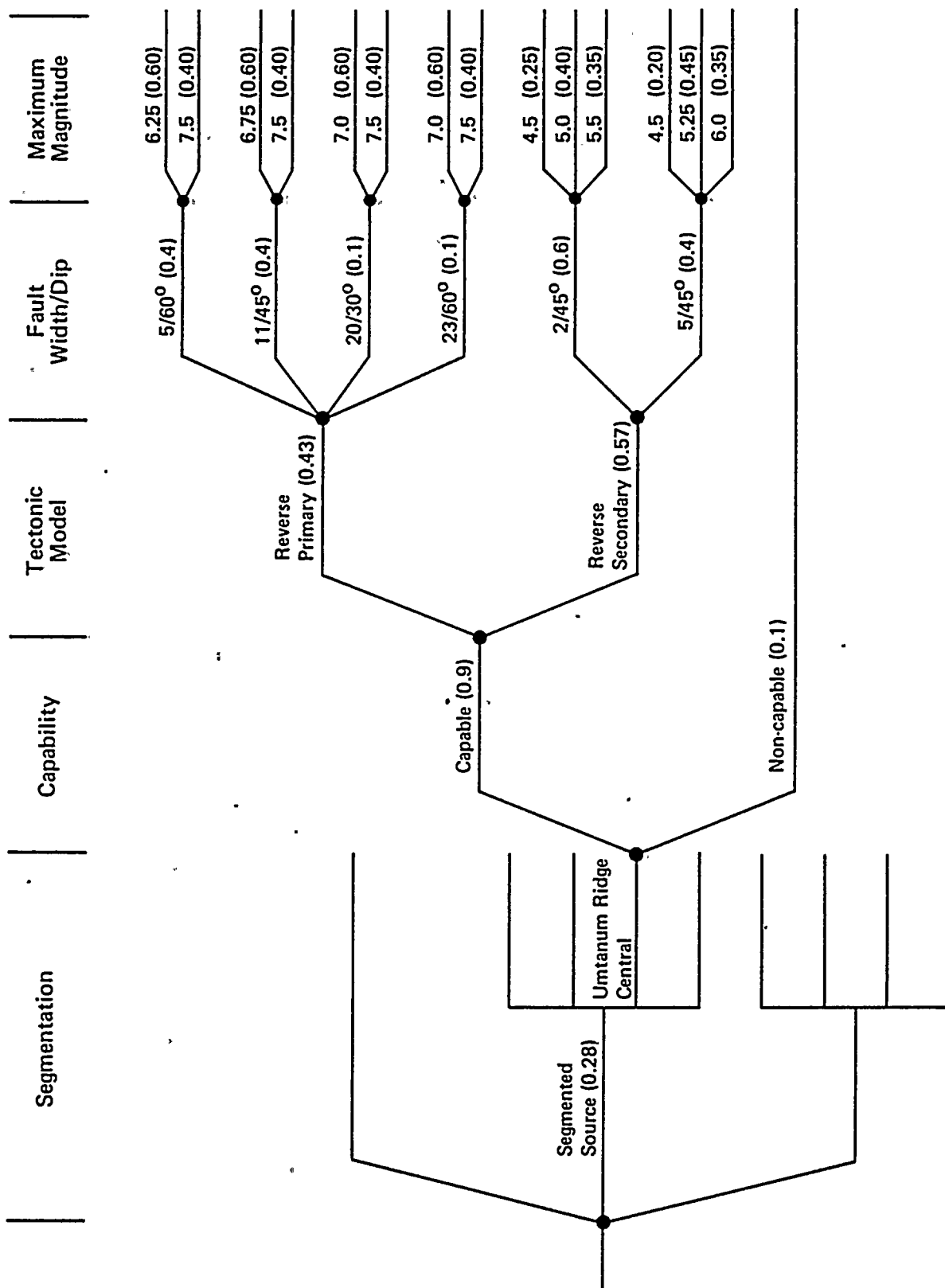


Project No. 14940	Hanford FSAR	EXPOSURE LOGIC TREE FOR GABLE MOUNTAIN: SEGMENTED SOURCE	Figure 2.5K-16
Woodward-Clyde Consultants			



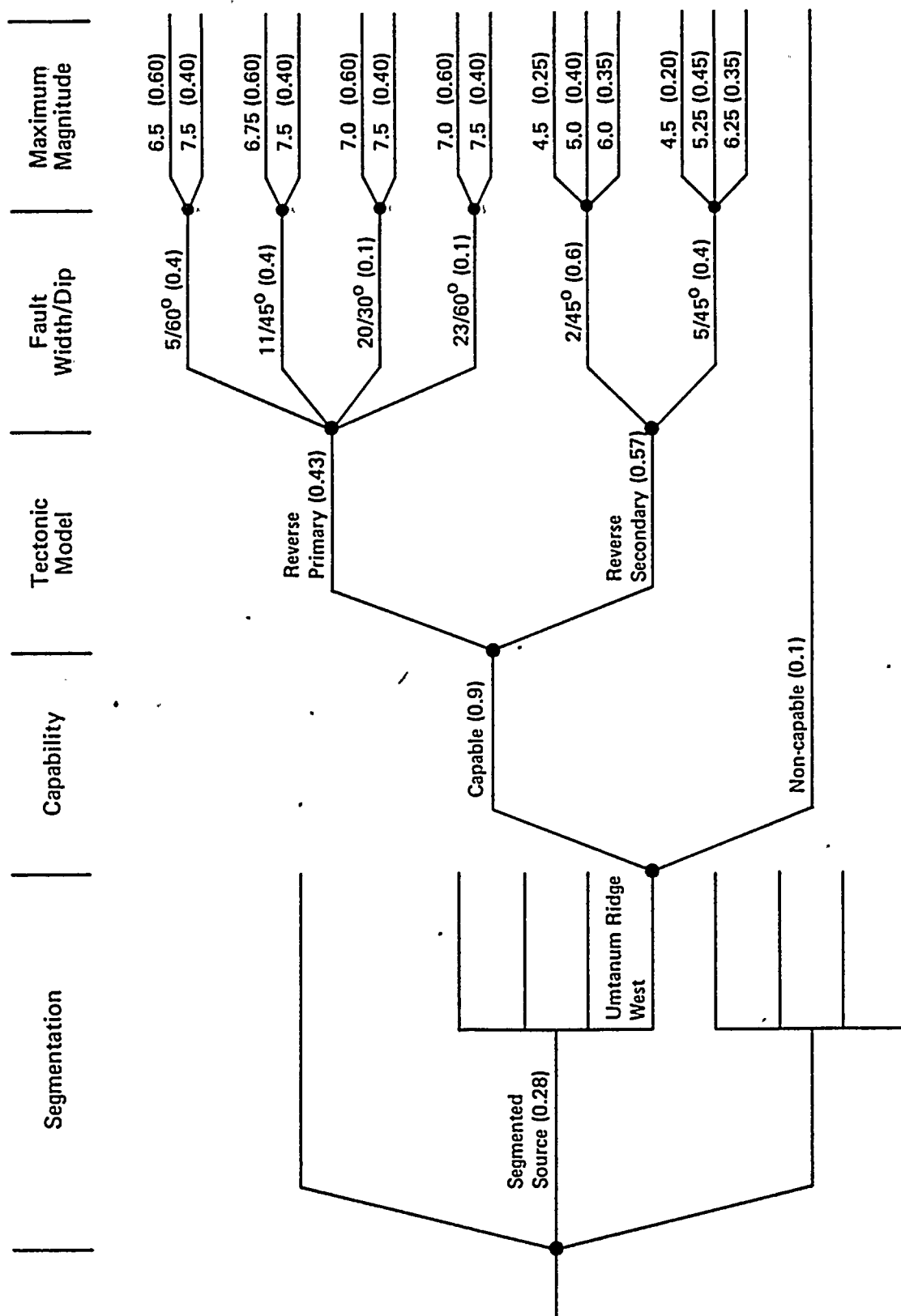


Project No. 14940	Hanford FSAR	EXPOSURE LOGIC TREE FOR UMTANUM RIDGE EAST: SEGMENTED SOURCE	Figure 2.5K-17
Woodward-Clyde Consultants			



Project No. 14940	Hanford FSAR	EXPOSURE LOGIC TREE FOR UMTANUM RIDGE CENTRAL: SEGMENTED SOURCE	Figure 2.5K-18
Woodward-Clyde Consultants			

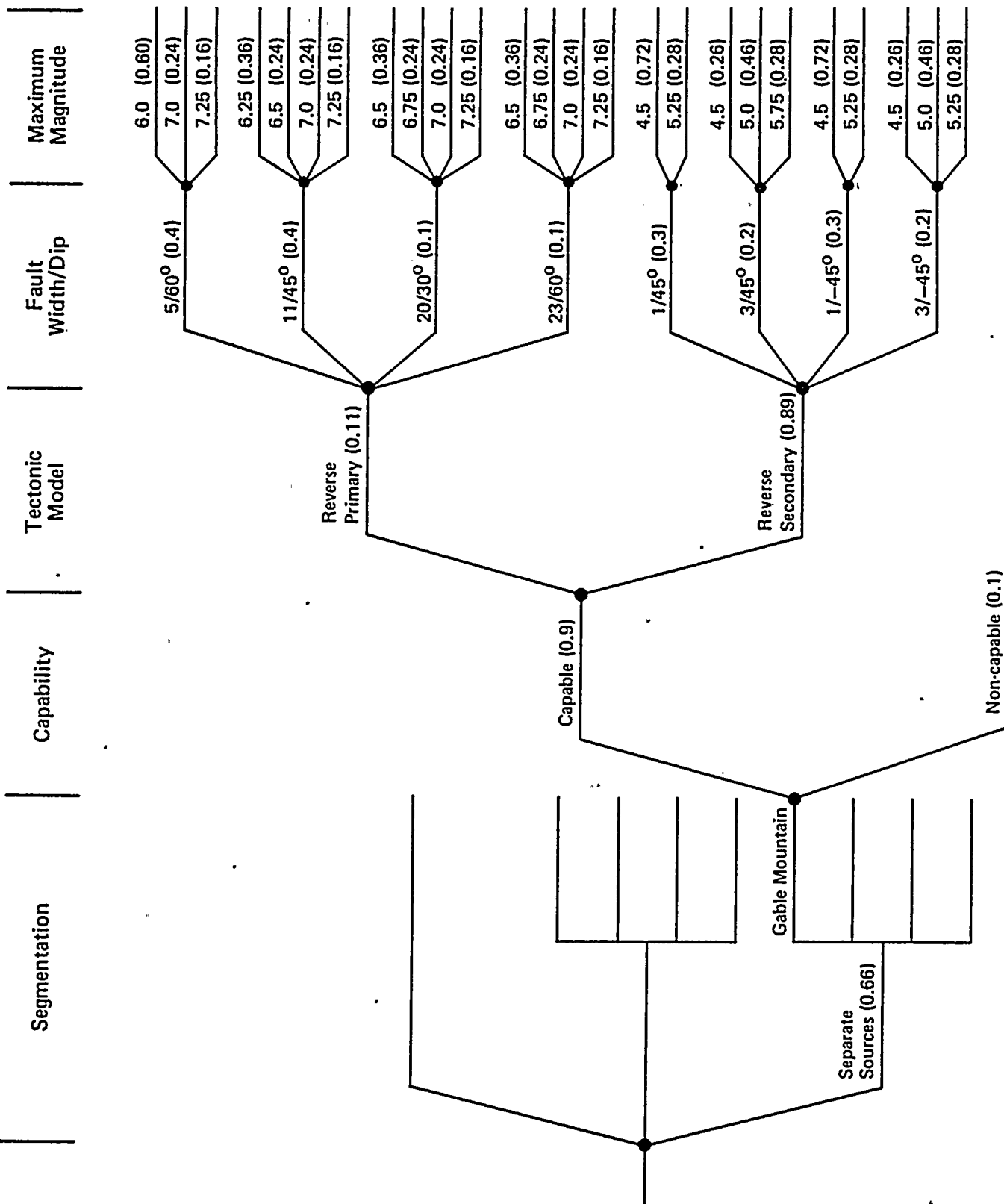




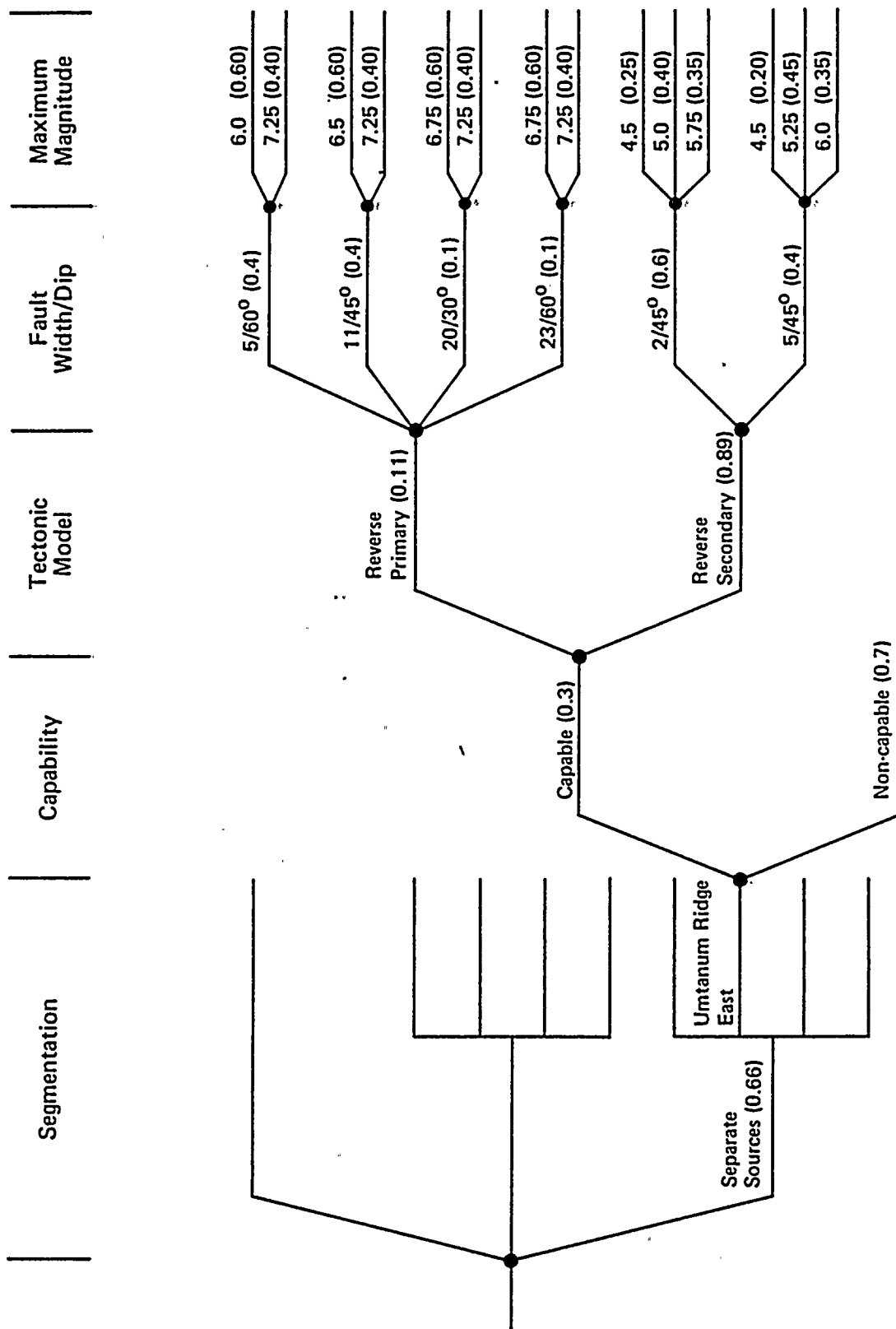
Project No. 14940	Hanford FSAR	EXPOSURE LOGIC TREE FOR UMTANUM RIDGE WEST: SEGMENTED SOURCE	Figure 2.5K-19
Woodward-Clyde Consultants			



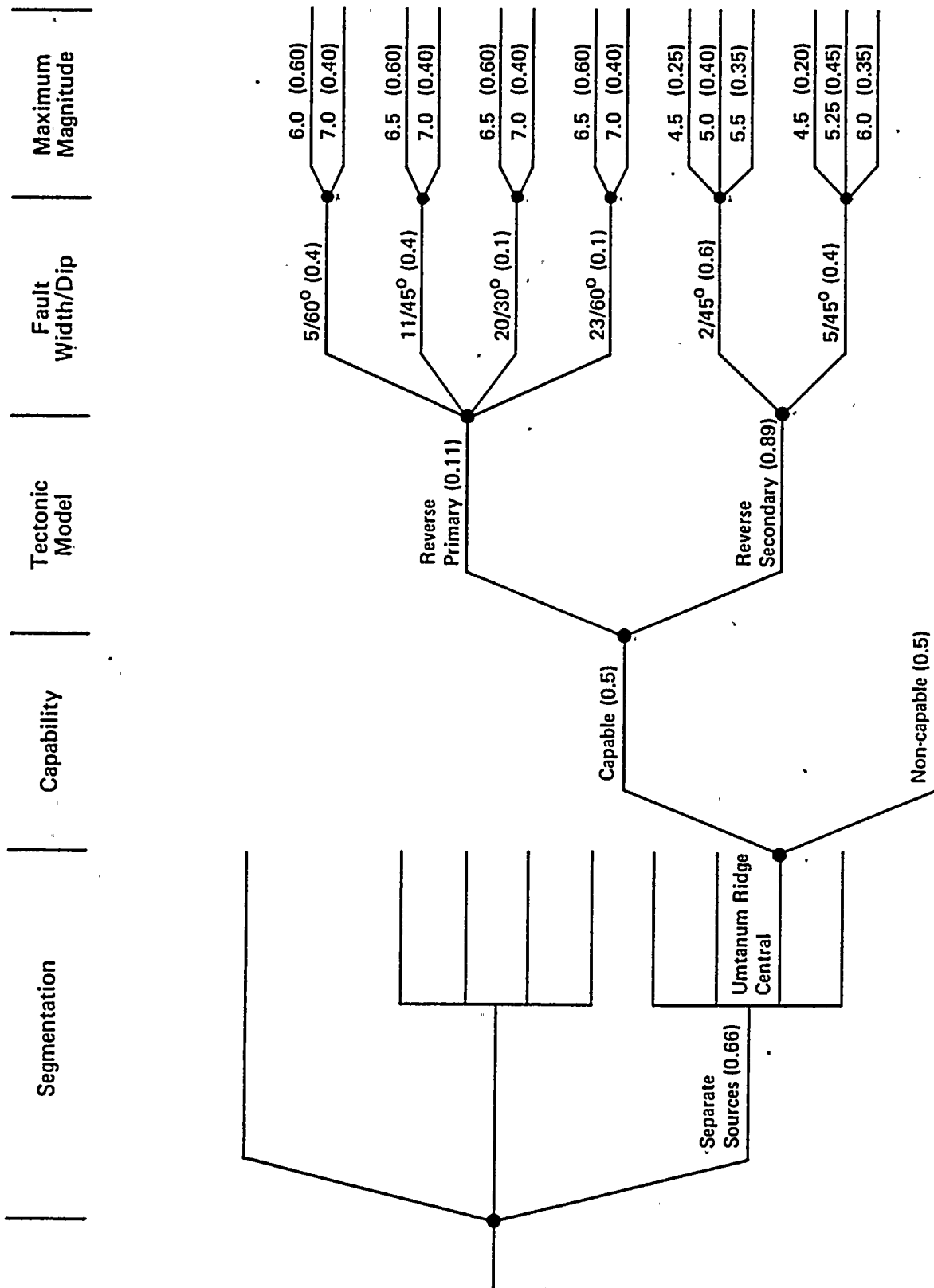




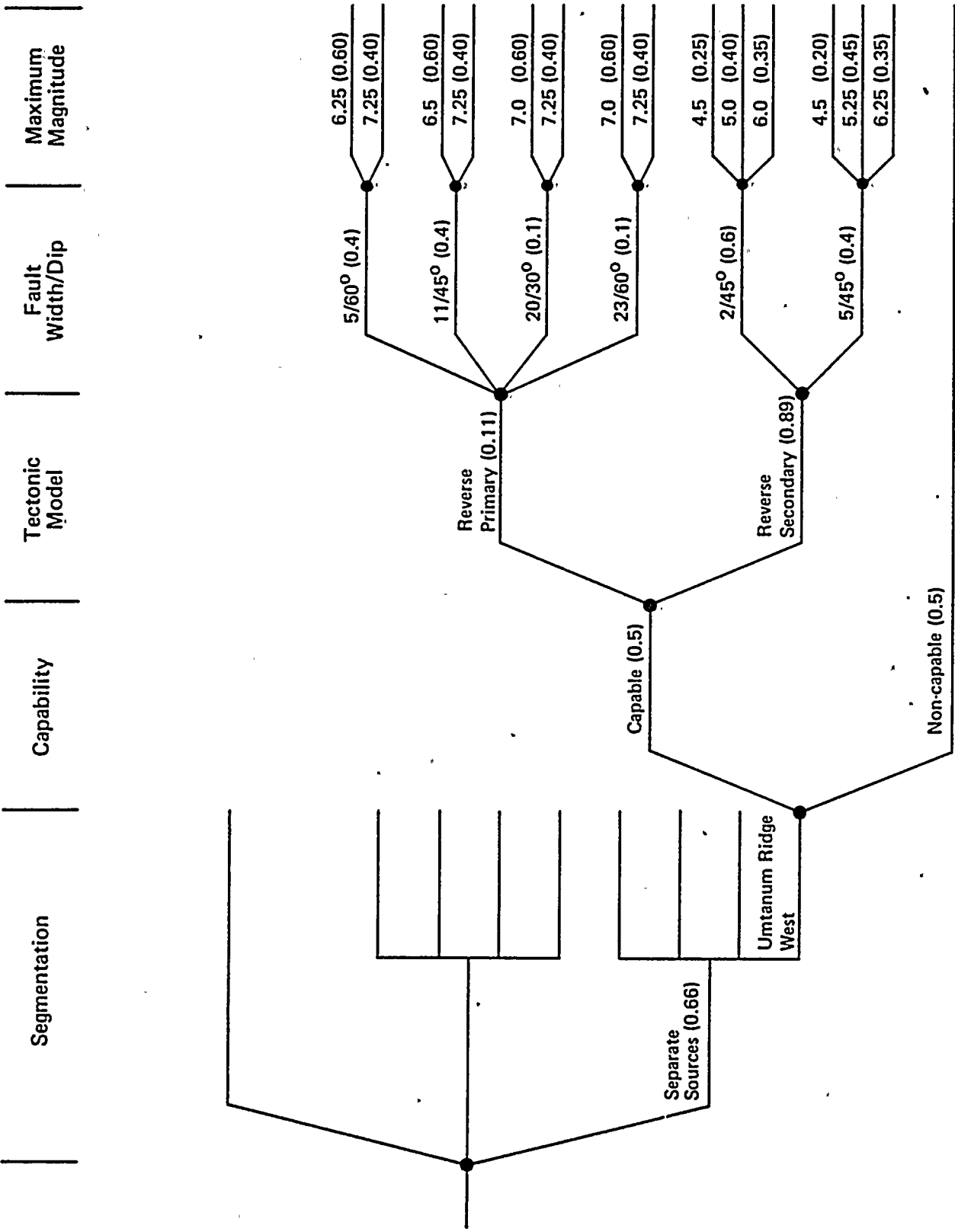
Project No. 14940	Hanford FSAR	EXPOSURE LOGIC TREE FOR GABLE MOUNTAIN: SEPARATE SOURCE	Figure 2.5K-20
Woodward-Clyde Consultants			



Project No. 14940	Hanford FSAR	EXPOSURE LOGIC TREE FOR UMTANUM RIDGE EAST: SEPARATE SOURCE	Figure 2.5K-21
Woodward-Clyde Consultants			



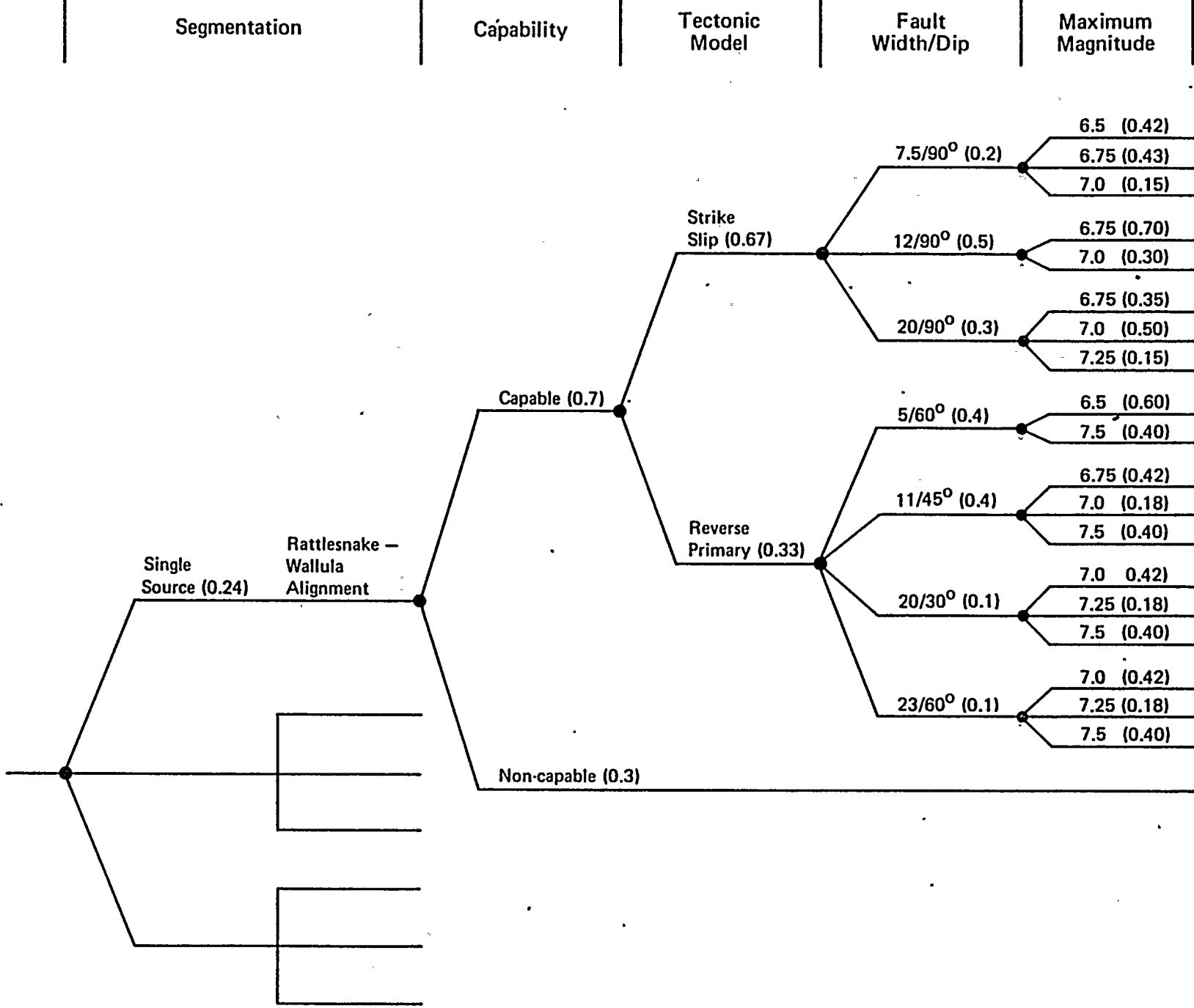
Project No. 14940	Hanford FSAR	EXPOSURE LOGIC TREE FOR UMTANUM RIDGE CENTRAL: SEPARATE SOURCE	Figure 2.5K-22
Woodward-Clyde Consultants			



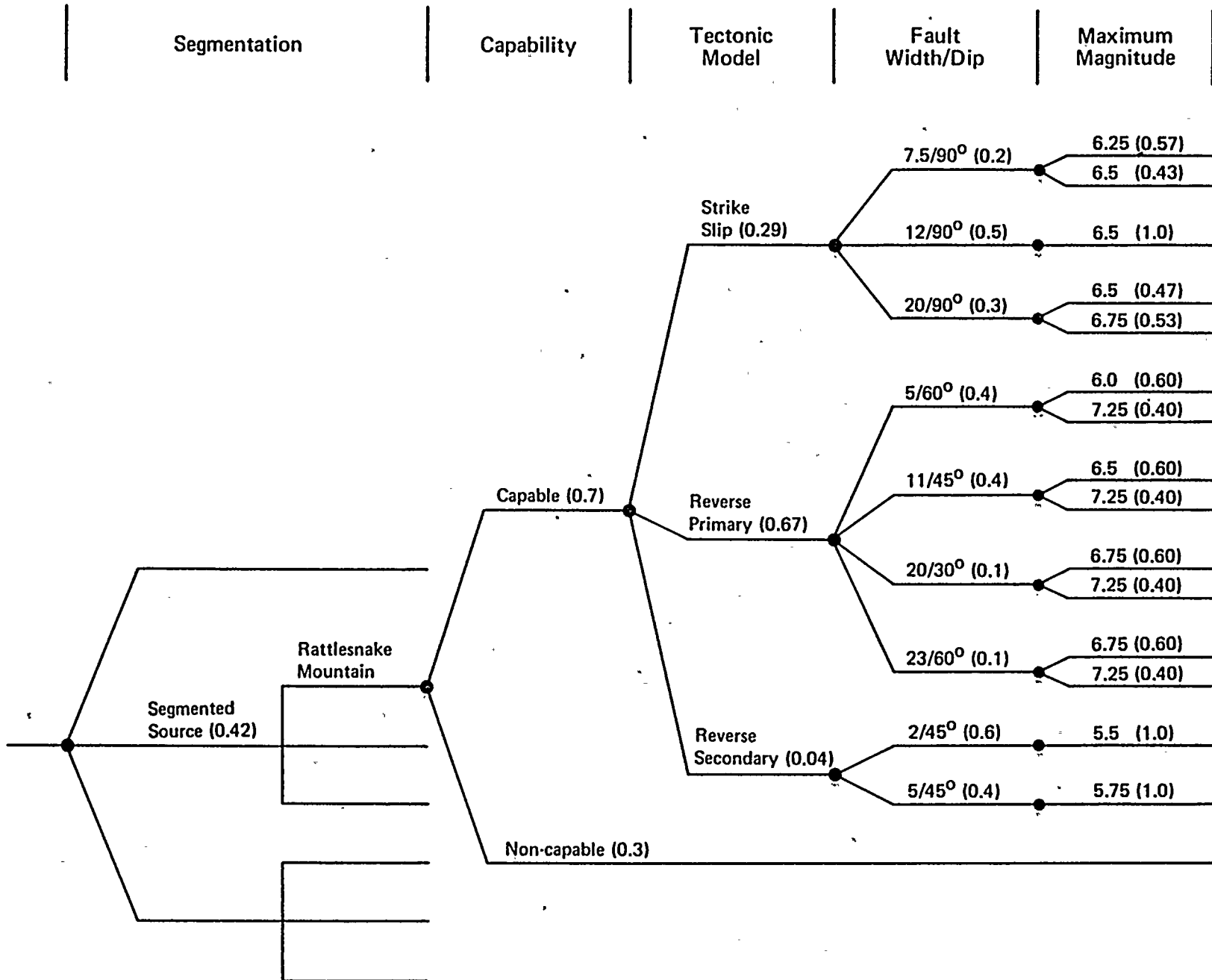
Project No. 14940	Hanford FSAR	EXPOSURE LOGIC TREE FOR UMTANUM RIDGE WEST: SEPARATE SOURCE	Figure 2.5K-23
Woodward-Clyde Consultants			











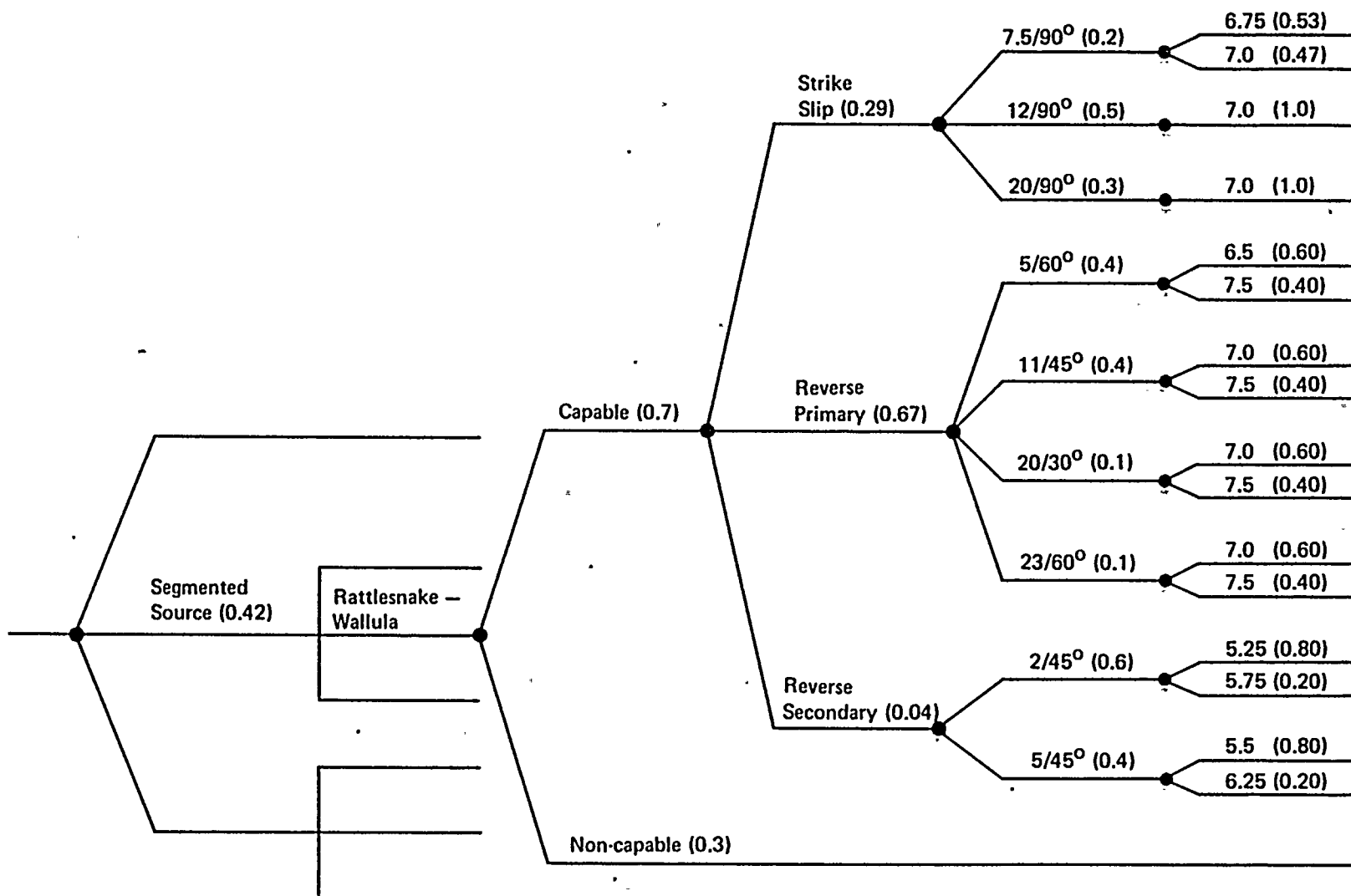
Segmentation

Capability

Tectonic  
Model

Fault  
Width/Dip

Maximum  
Magnitude



Project No.  
14940

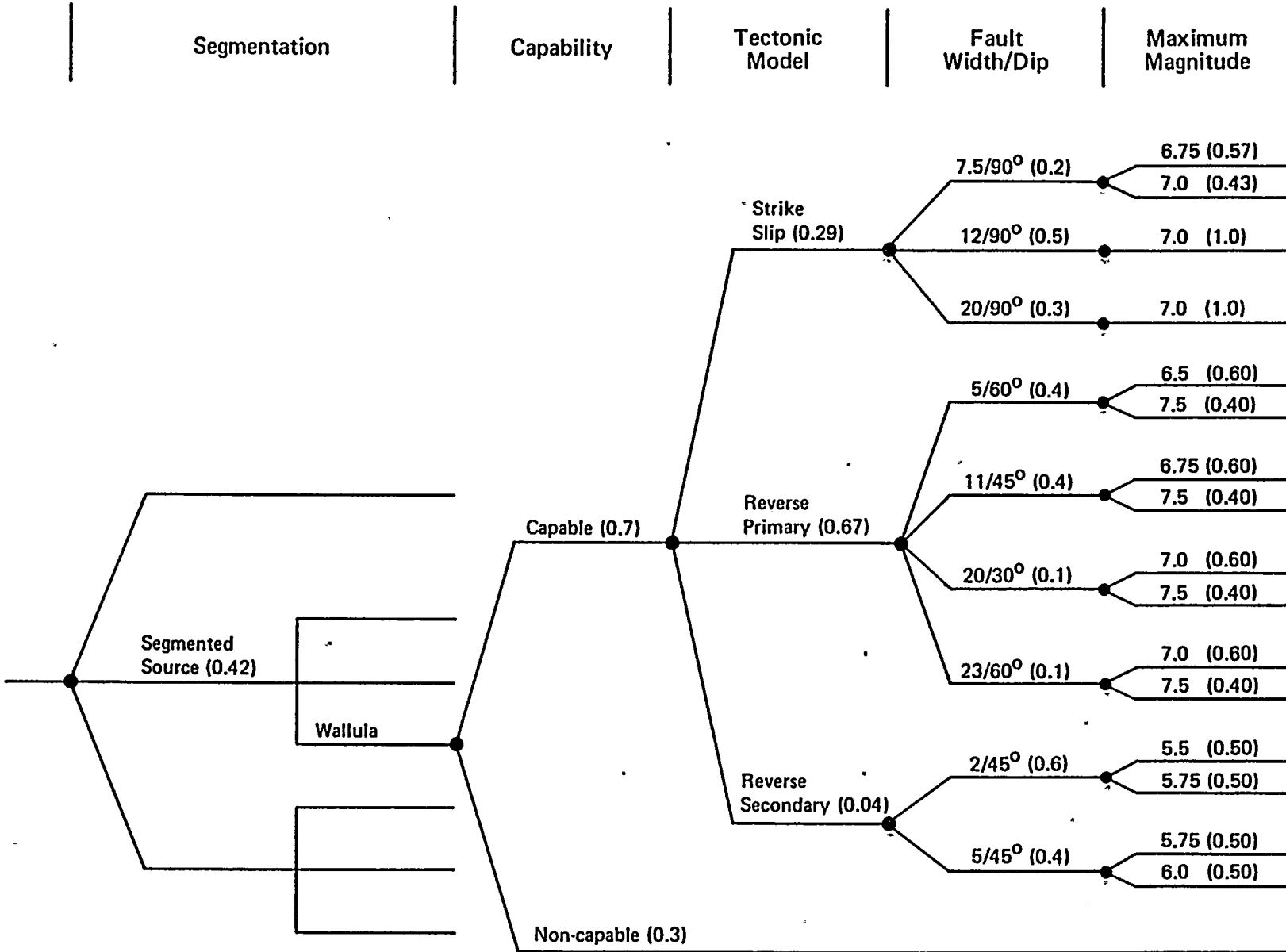
Woodward-Clyde Consultants

Hanford FSAR

EXPOSURE LOGIC TREE FOR RATTLESNAKE -  
WALLULA: SEGMENTED SOURCE

Figure  
2.5K-27





Project No.  
14940

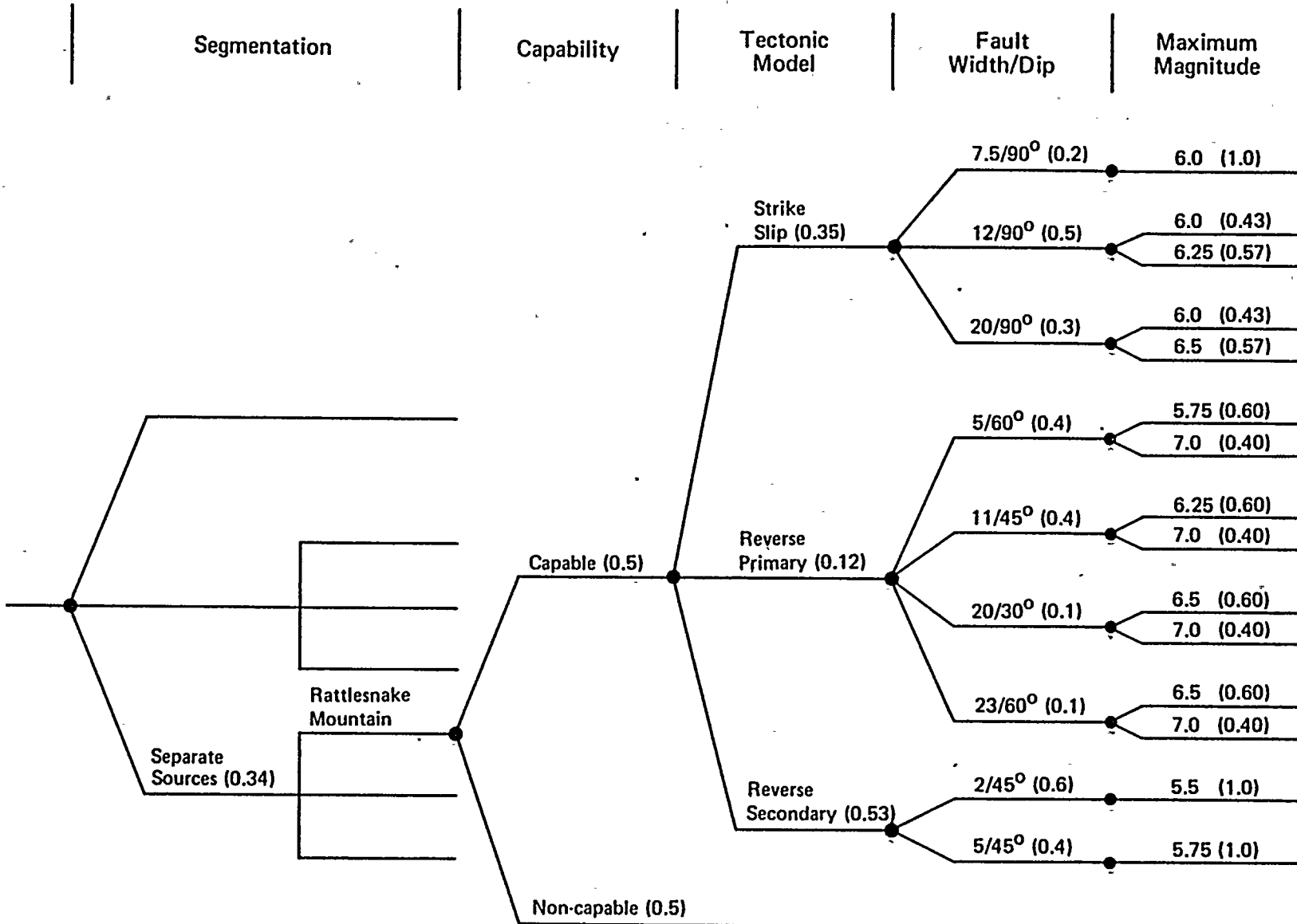
Hanford FSAR

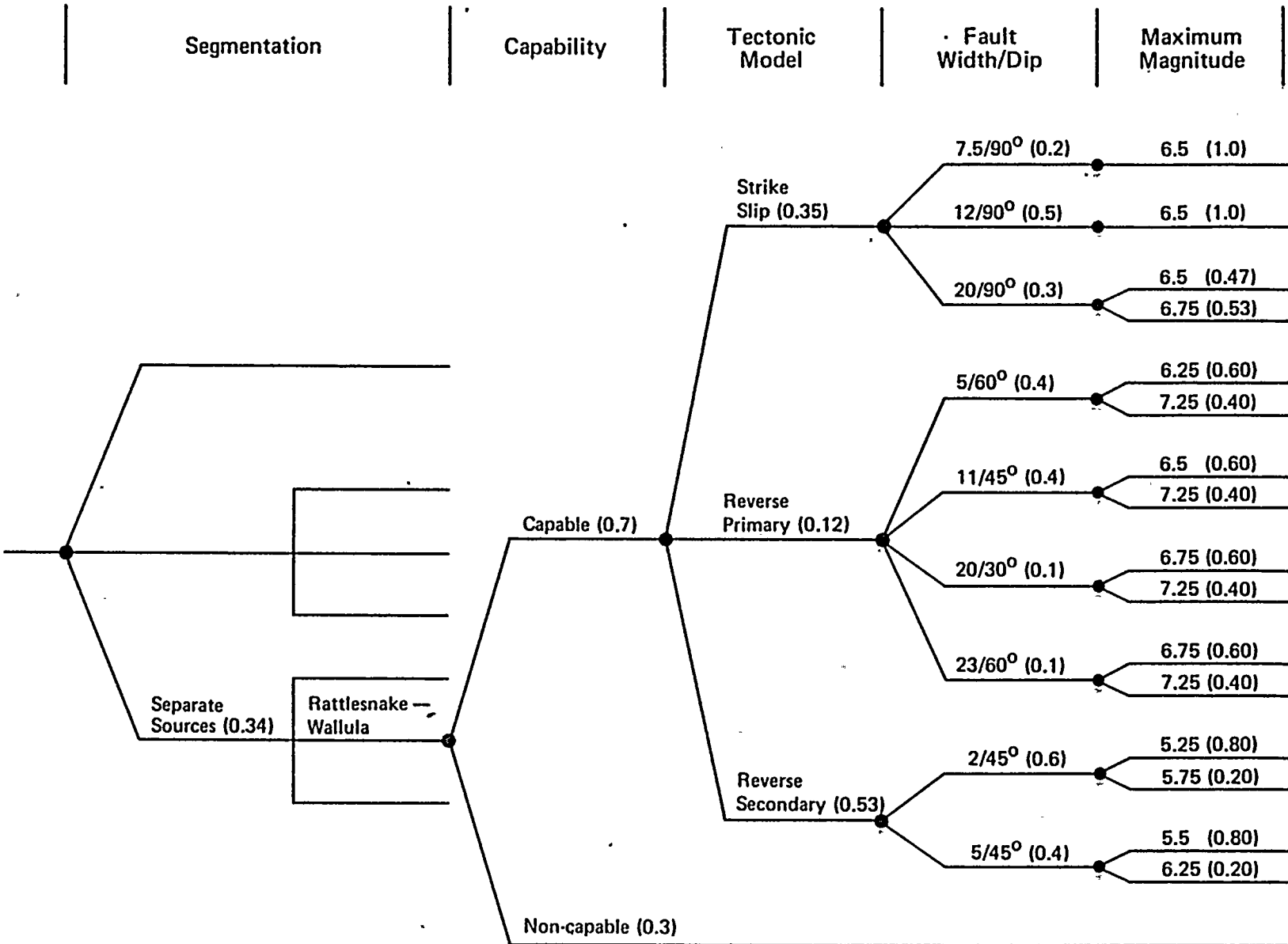
Woodward-Clyde Consultants

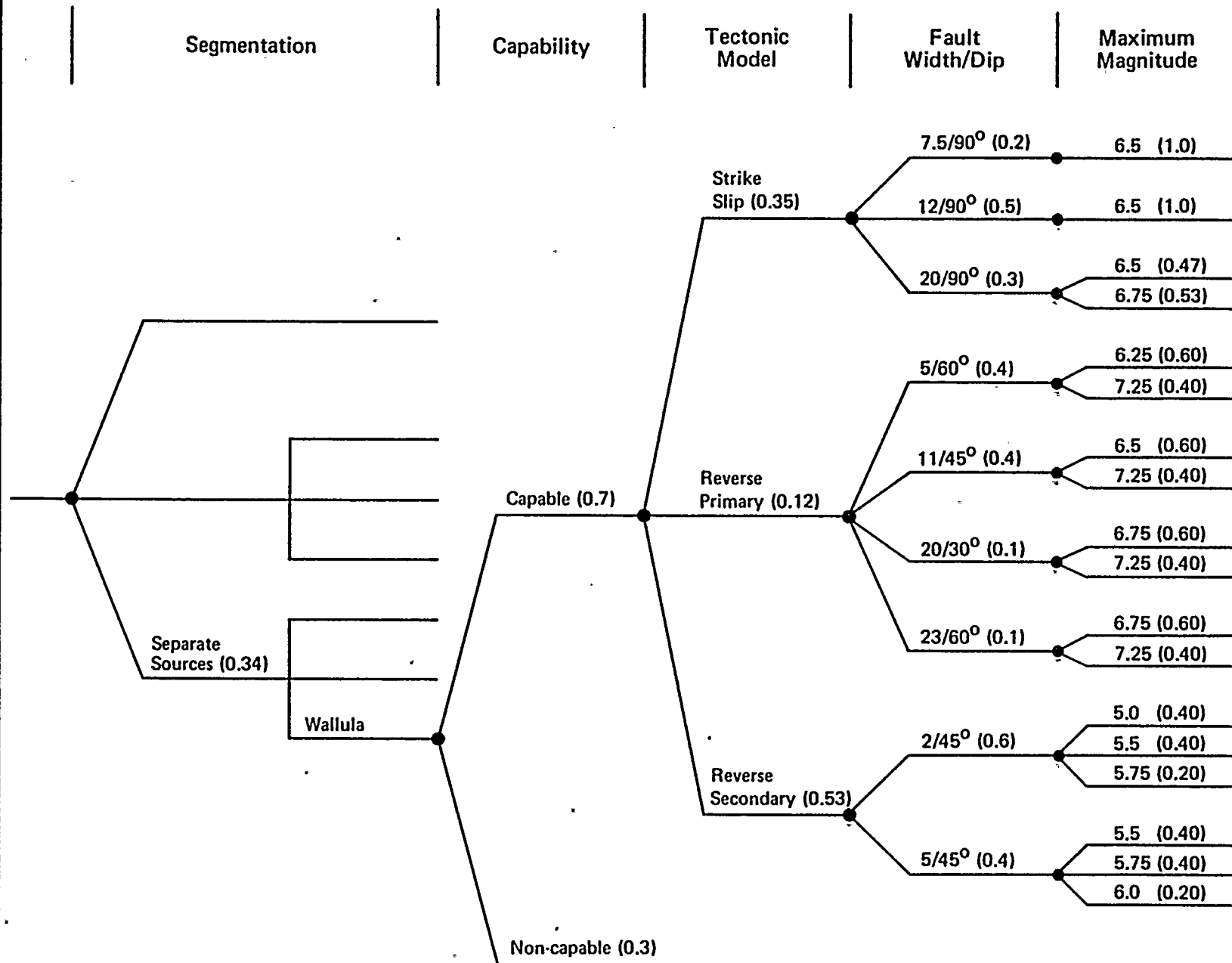
EXPOSURE LOGIC TREE FOR  
WALLULA: SEGMENTED SOURCE

Figure  
2.5K-28





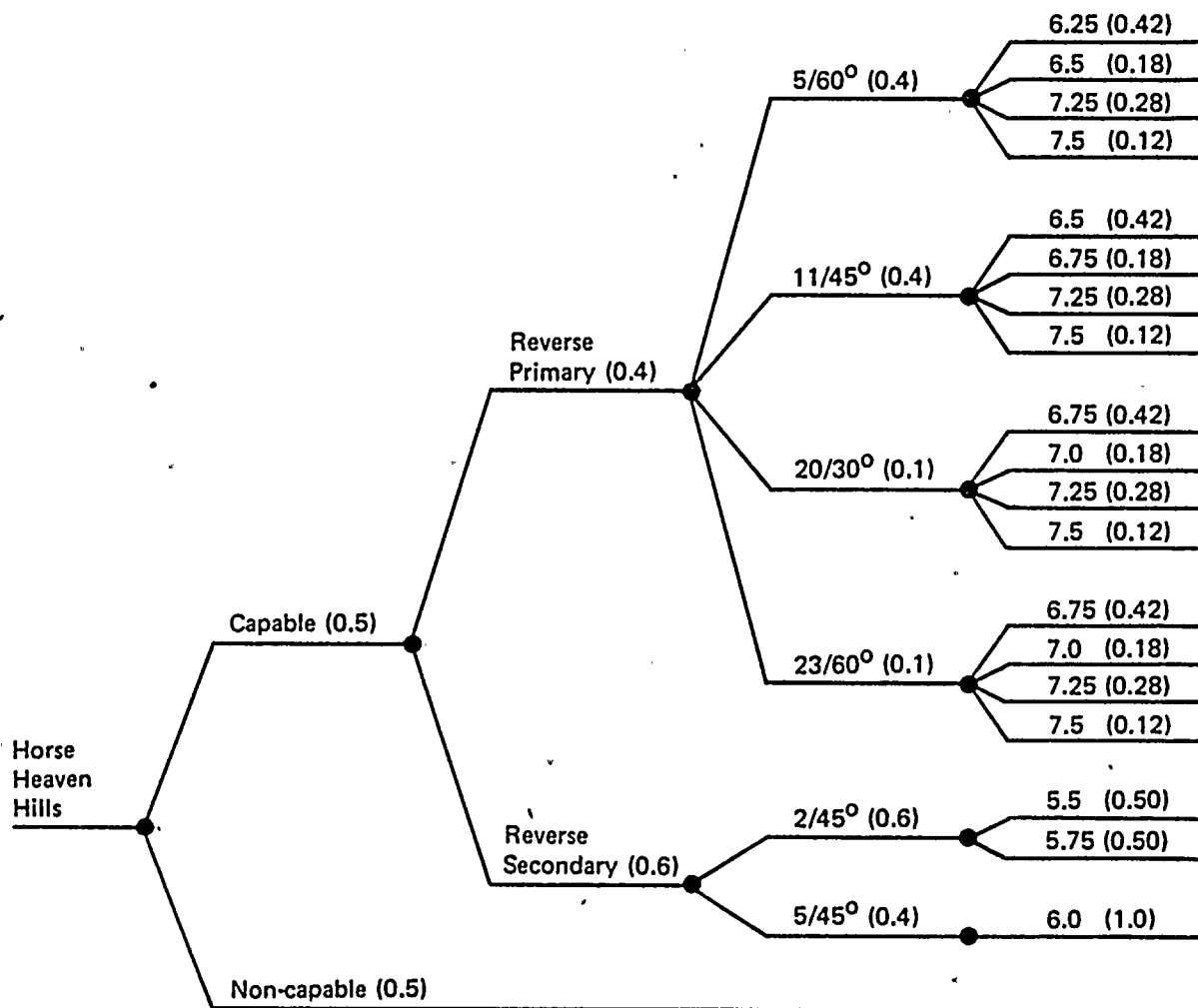






Source

Capability

Tectonic  
ModelFault  
Width/DipMaximum  
MagnitudeProject No.  
14940

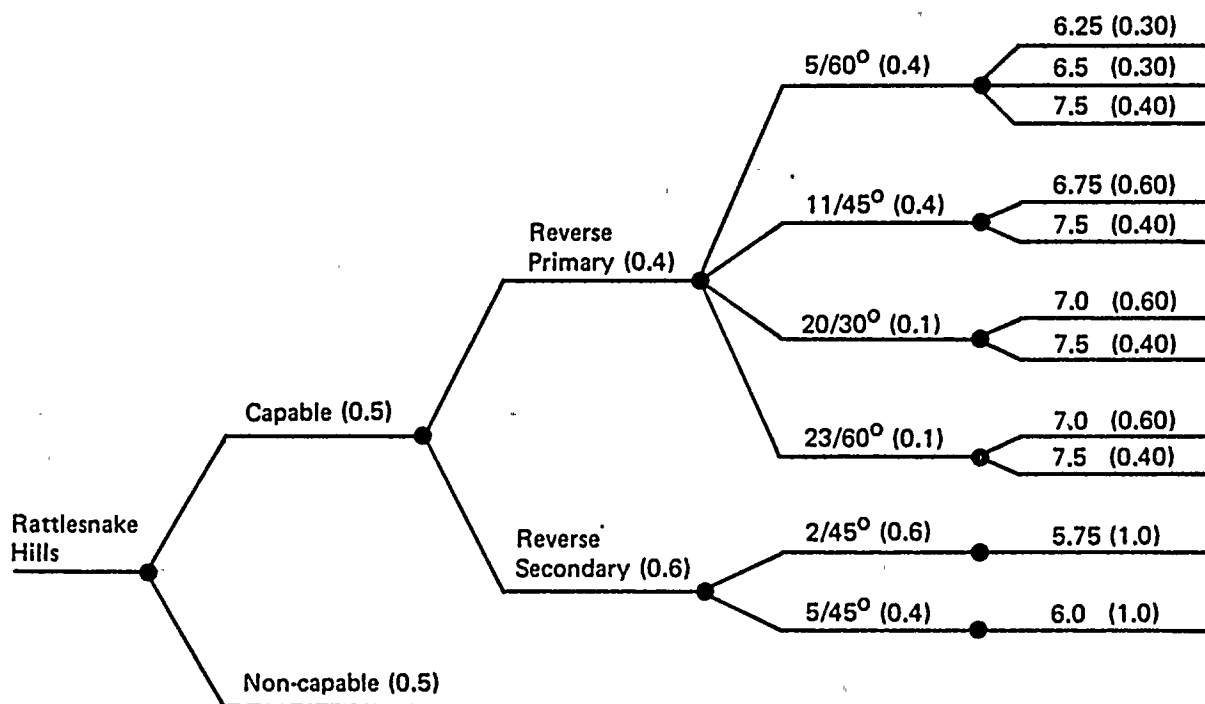
Hanford FSAR

**Woodward-Clyde Consultants****EXPOSURE LOGIC TREE FOR  
HORSE HEAVEN HILLS SOURCE****Figure  
2.5K-32**



Source

Capability

Tectonic  
ModelFault  
Width/DipMaximum  
MagnitudeProject No.  
14940

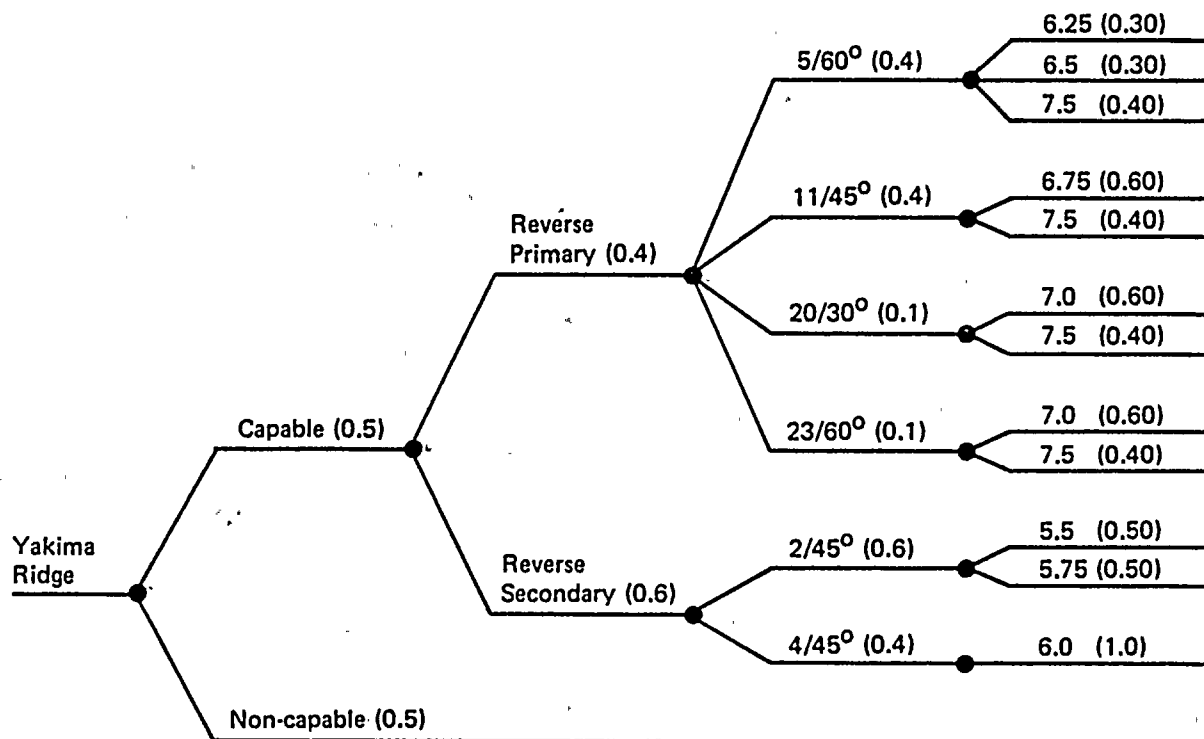
Hanford FSAR

Woodward-Clyde Consultants

EXPOSURE LOGIC TREE FOR  
RATTLESNAKE HILLS SOURCEFigure  
2.5K-33WNP-2 Amendment No. 18  
September 1981

Source

Capability

Tectonic  
ModelFault  
Width/DipMaximum  
MagnitudeProject No.  
14940

Hanford FSAR

EXPOSURE LOGIC TREE FOR  
YAKIMA RIDGE SOURCEFigure  
2.5K-34

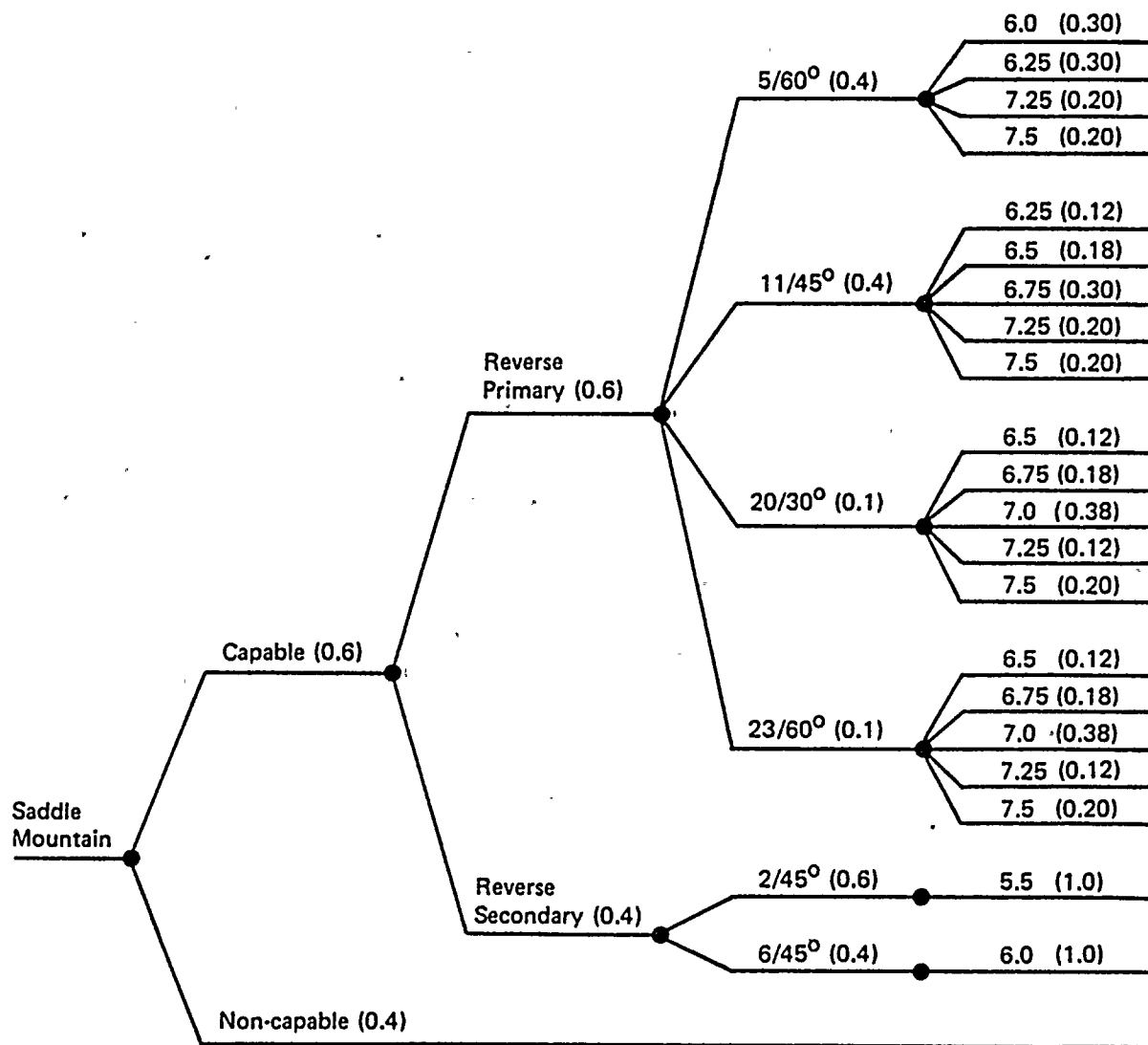
Woodward-Clyde Consultants

WNP-2 Amendment No. 18  
September 1981



Source

Capability

Tectonic  
ModelFault  
Width/DipMaximum  
MagnitudeProject No.  
14940

Hanford FSAR

**Woodward-Clyde Consultants****EXPOSURE LOGIC TREE FOR  
SADDLE MOUNTAIN SOURCE****Figure  
2.5K-35**WNP-2 Amendment No. 18  
September 1981

for  $r < r_1$

$$= \frac{\sqrt{r^2 - r_p^2 - L_o}}{L - L_{m_i}} \quad \text{for } r_1 < r < r_2$$

$$= 1 \quad \text{for } r < r_2$$

$$\text{for } r < r_p$$

$$\begin{aligned} &= \frac{L_{m_i}}{L_1 + L_2 - L_{m_i}} \quad \text{for } r = r_p \\ &= \frac{L_{m_i} + 2\sqrt{r^2 - r_p^2}}{L_1 + L_2 - L_{m_i}} \quad \text{for } r_p < r < r_1 \\ &= \frac{L_1 + \sqrt{r^2 - r_p^2}}{L_1 + L_2 - L_{m_i}} \quad \text{for } r_1 < r < r_2 \end{aligned}$$

$$= 1 \quad \text{for } r < r_2$$

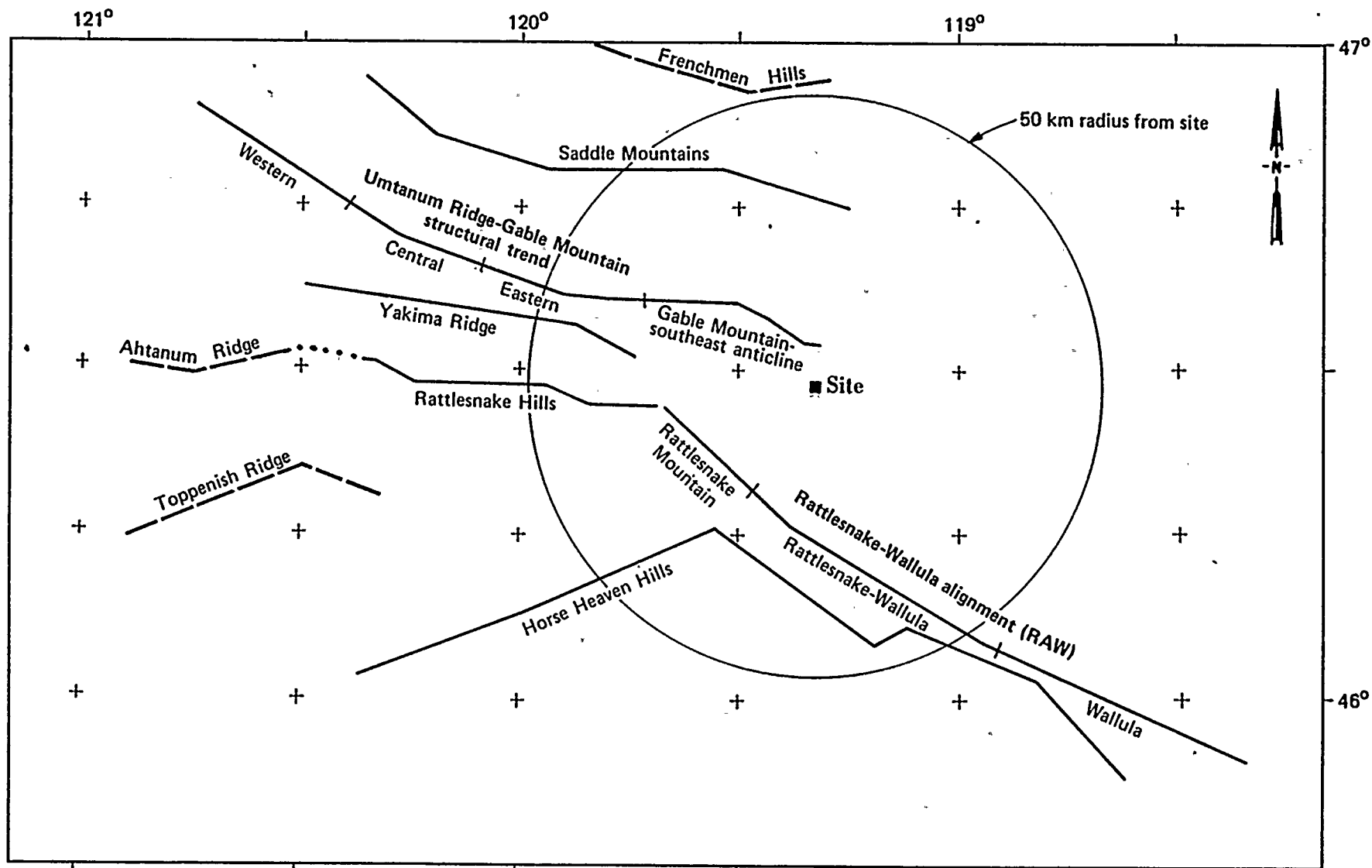
Note:  $L_{m_i}$  = fault rupture length for magnitude  $m_i$

Project No. 14940	Hanford FSAR	CUMULATIVE PROBABILITY FUNCTION FOR CLOSEST DISTANCE TO FAULT RUPTURE	Figure 2.5K-36
Woodward-Clyde Consultants			

**WNP-2 Amendment No. 18**  
**September 1981**







- +— Potential source considered in seismic analysis; ticks indicate segment boundaries described in text  
 - - - Anticlinal ridge beyond 50-km radius

0 10 20 30 km

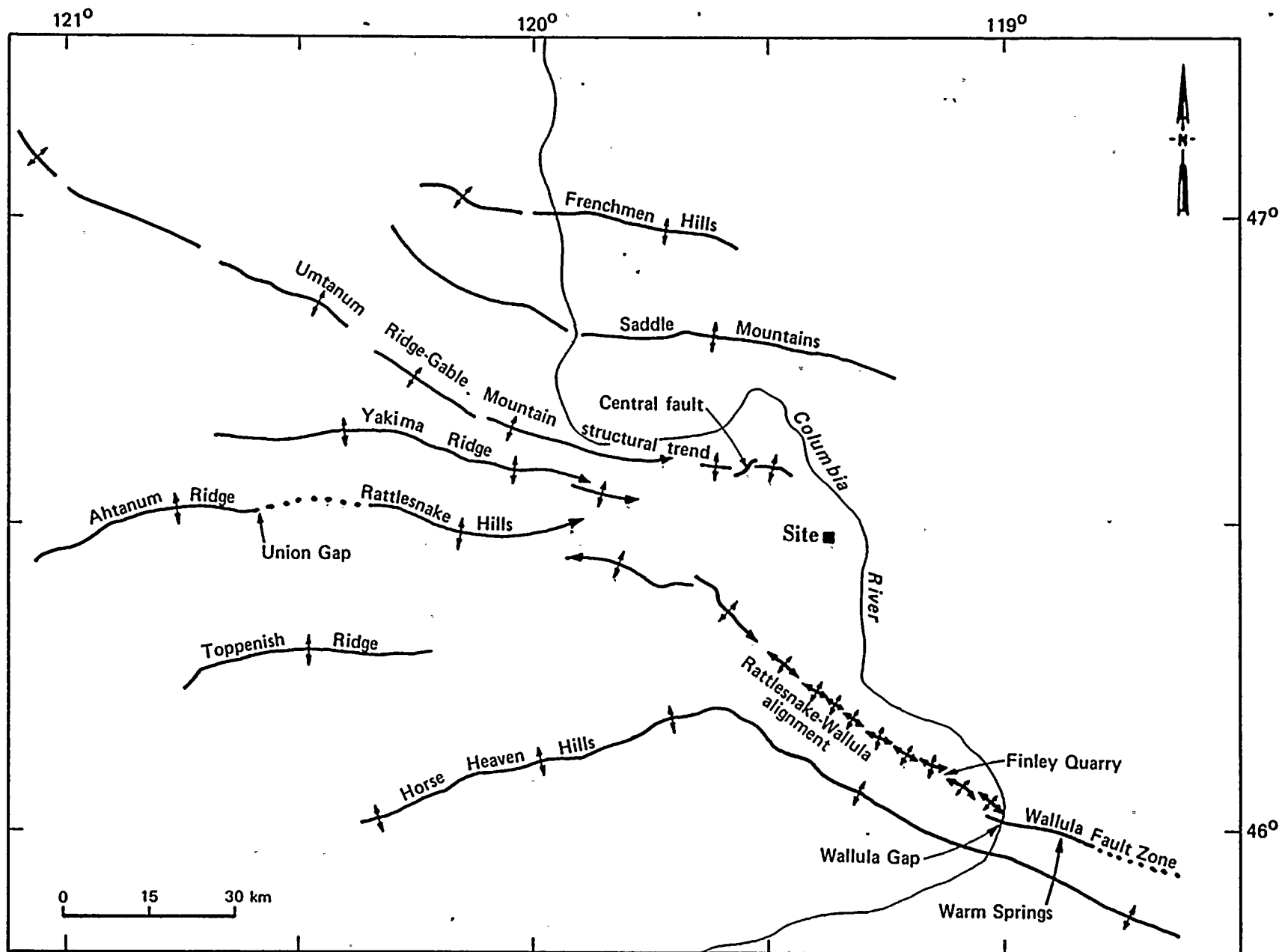
Project No.  
14940

Hanford FSAR

Woodward-Clyde Consultants

SIMPLIFIED MAP OF POTENTIAL SEISMIC  
SOURCES SIGNIFICANT TO THE SITE

Figure  
2.5K-37



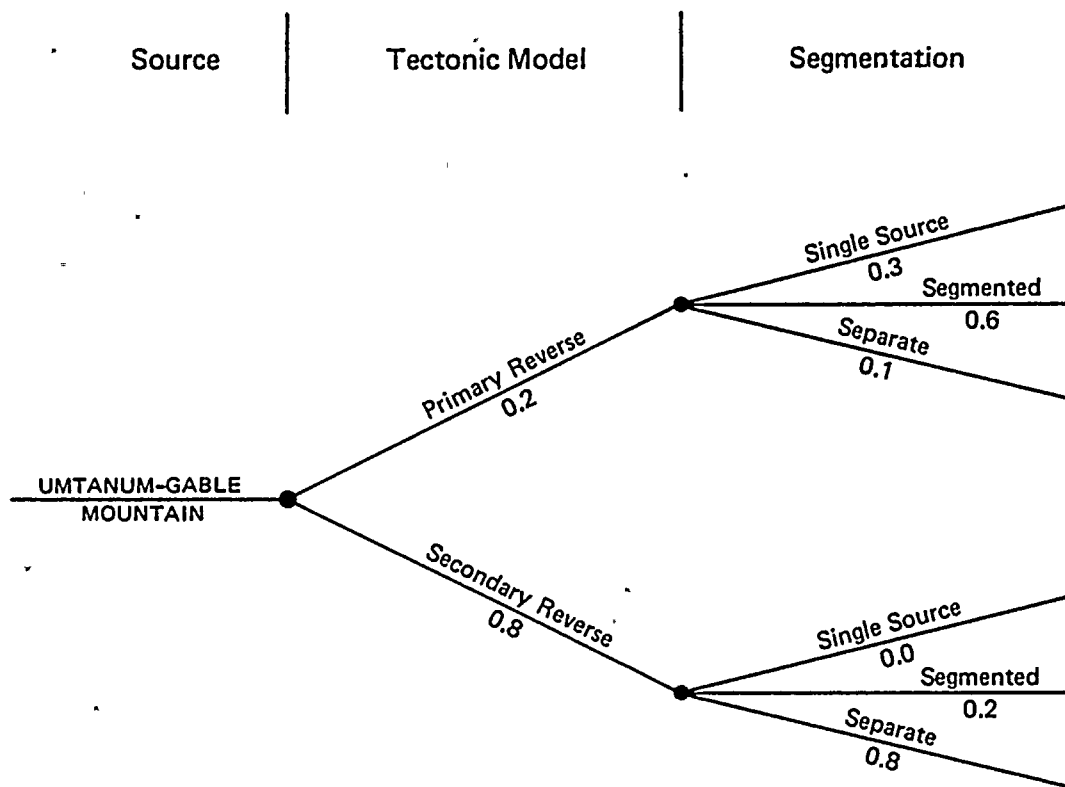
Project No.  
14940

Hanford FSAR

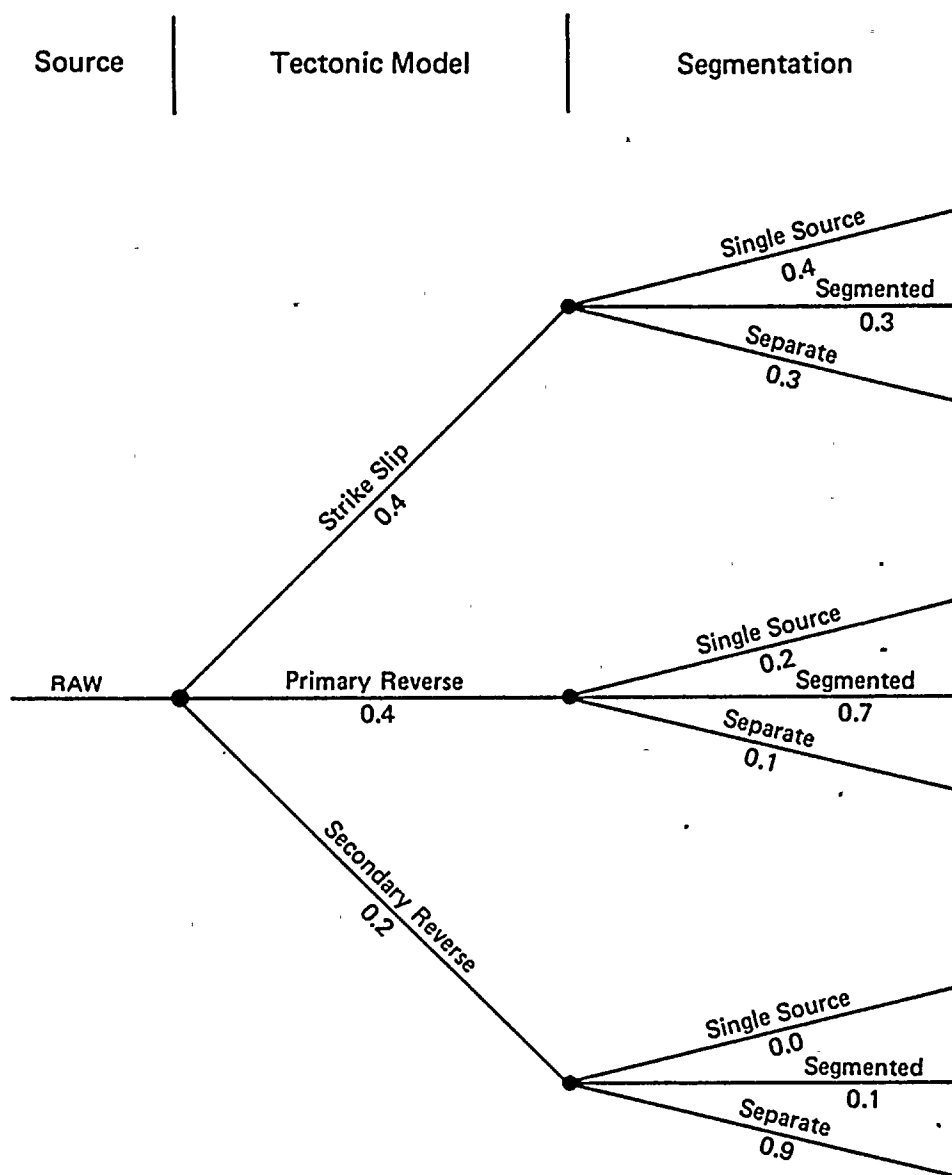
Woodward-Clyde Consultants

SIMPLIFIED MAP OF LOCALITIES AND  
MAJOR STRUCTURAL ELEMENTS

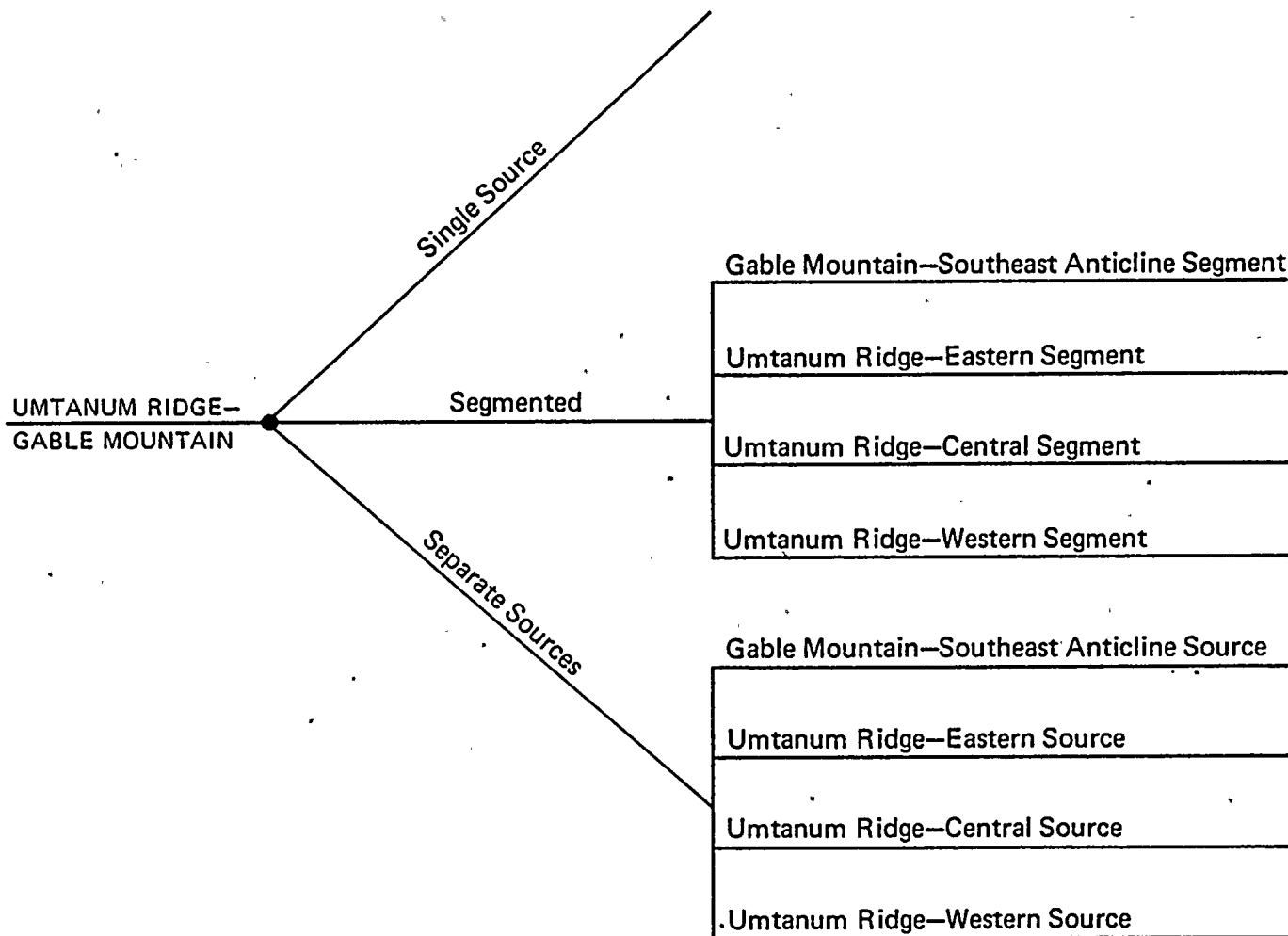
Figure  
2.5K-38



Project No. 14940	Hanford FSAR	LOGIC TREE SHOWING DEPENDENCE OF SEG- MENTATION TECTONIC MODEL FOR UMTANUM RIDGE-GABLE MOUNTAIN STRUCTURAL TREND	Figure 2.5K-39
Woodward-Clyde Consultants			

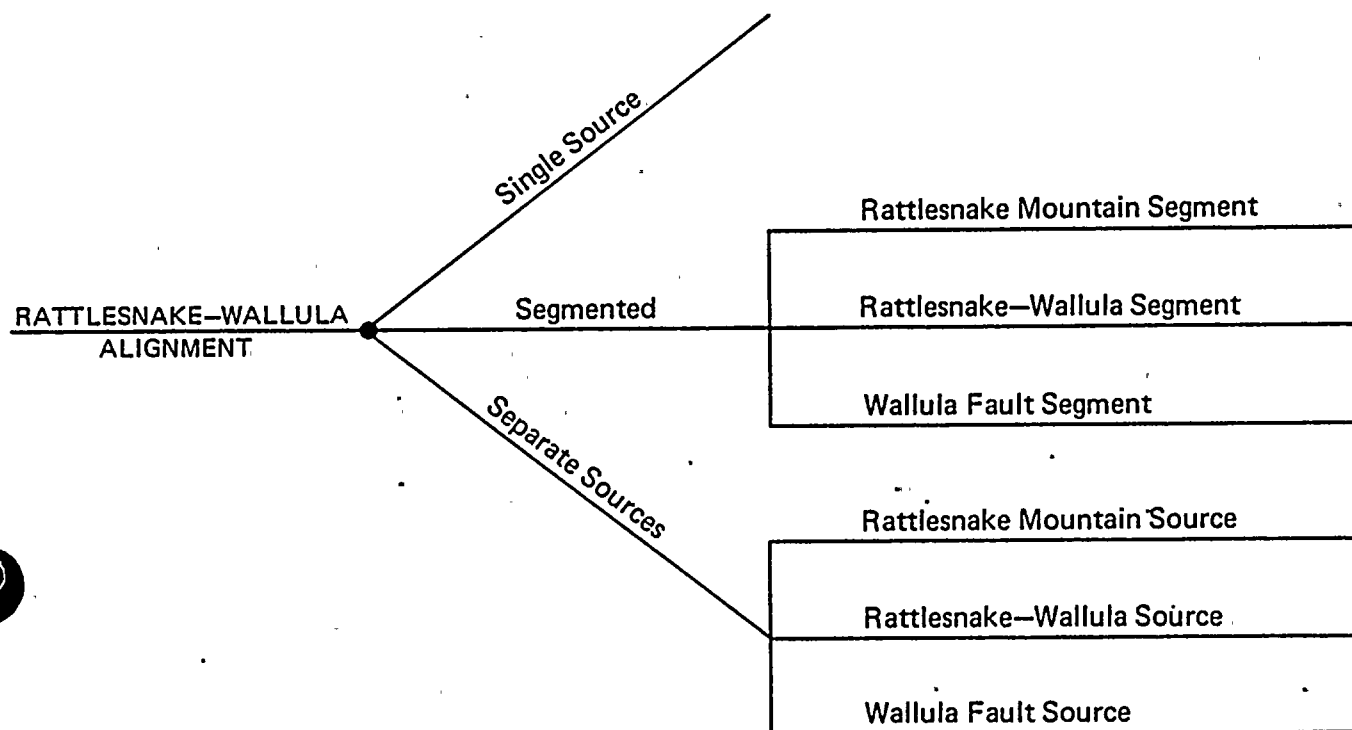


Project No. 14940	Hanford FSAR	LOGIC TREE SHOWING DEPENDENCE OF SEGMENTATION TECTONIC MODEL FOR THE RATTLESNAKE-WALLULA ALIGNMENT (RAW)	Figure 2.5K-40
Woodward-Clyde Consultants			



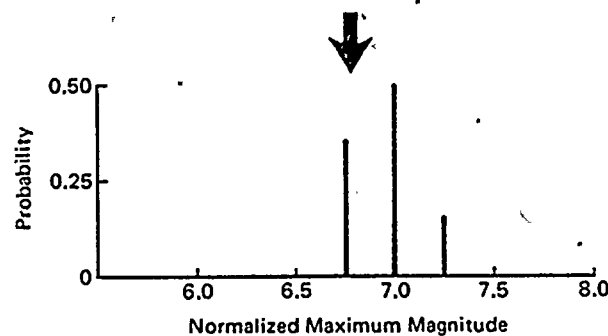
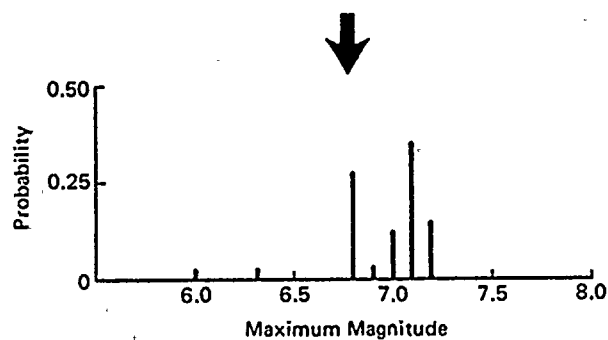
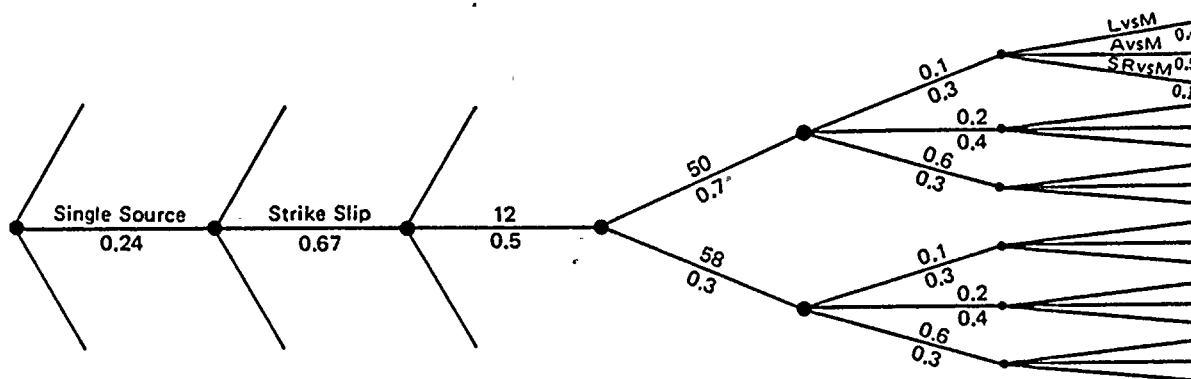
Project No. 14940	Hanford FSAR	SCHEMATIC DIAGRAM OF SEGMENTATION OF UMTANUM RIDGE-GABLE MOUNTAIN STRUCTURAL TREND	Figure 2.5K-41
Woodward-Clyde Consultants			



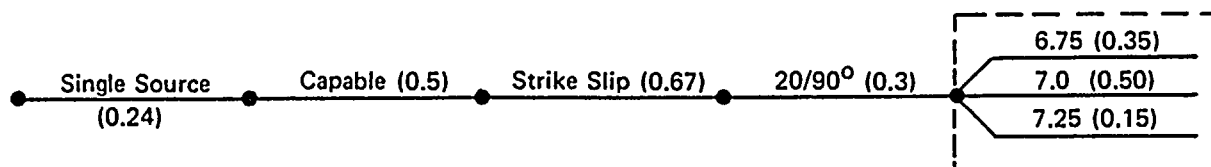


Project No. 14940	Hanford FSAR	SCHEMATIC DIAGRAM OF SEGMENTATION OF THE RATTLESNAKE-WALLULA ALIGNMENT (RAW)	Figure 2.5K-42
Woodward-Clyde Consultants			

Segmentation	Tectonic Model	Fault Width (km)	Fault Rupture Length (km)	Slip Rate (mm/yr)	Technique Applicability
--------------	----------------	------------------	---------------------------	-------------------	-------------------------

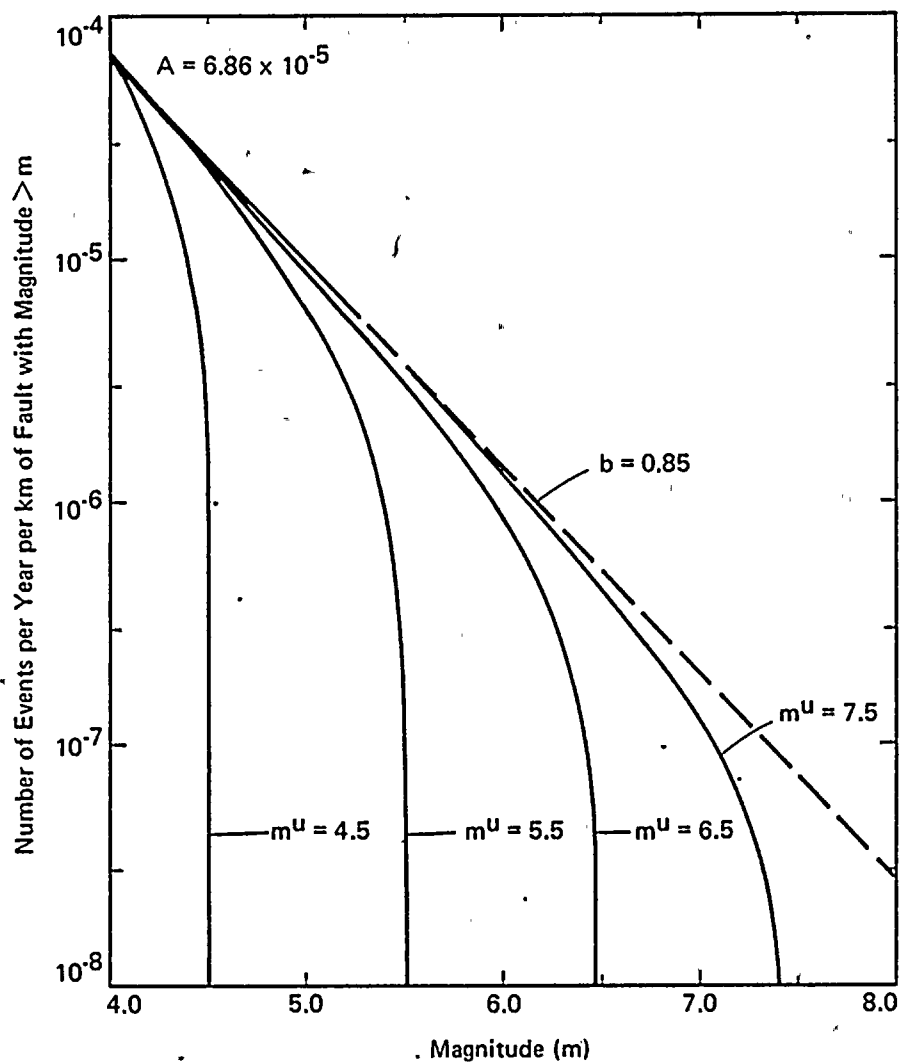


Segmentation	Capability	Tectonic Model	Fault Width/Dip	Maximum Magnitude
--------------	------------	----------------	-----------------	-------------------



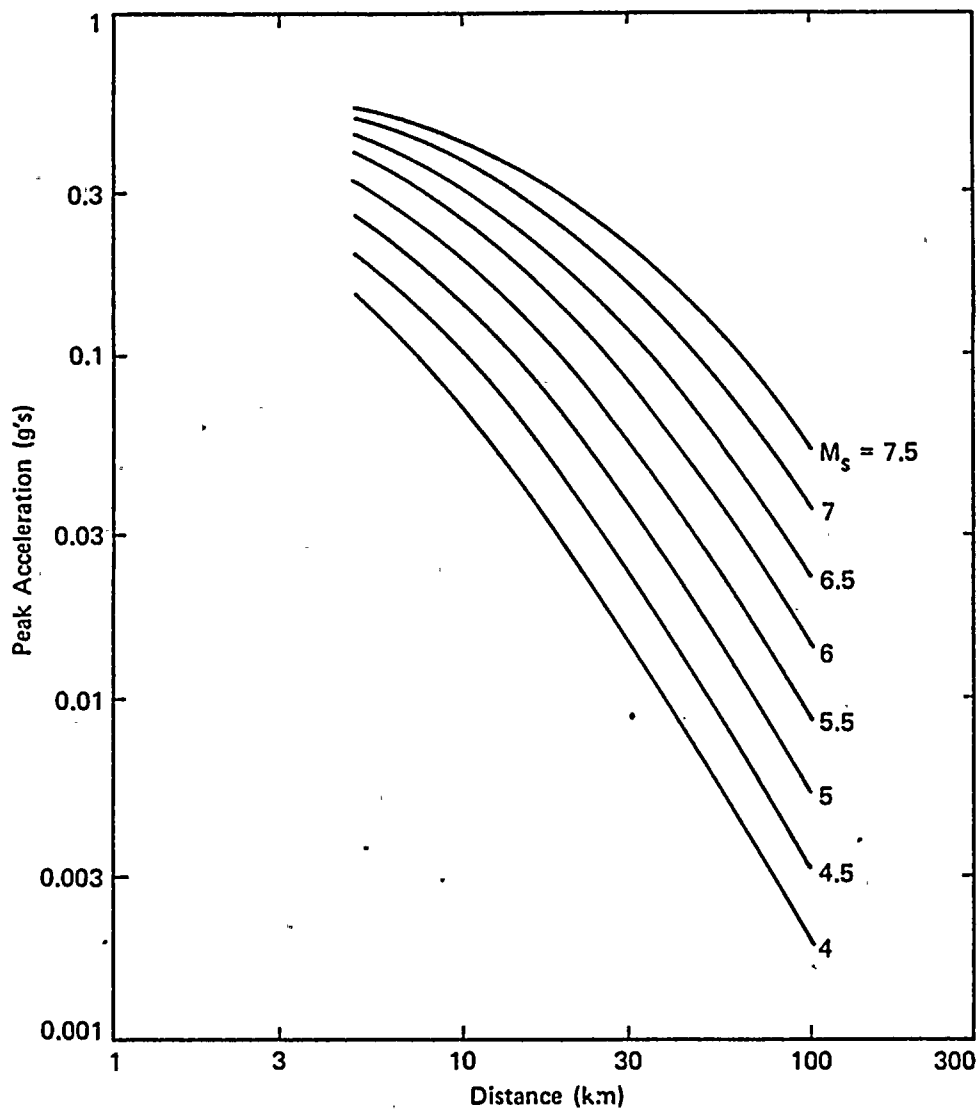
Project No. 14940	Hanford FSAR	SCHEMATIC FOR DETERMINATION OF MAXIMUM MAGNITUDE CONDITIONAL PROBABILITY	Figure 2.5K-43
Woodward-Clyde Consultants			





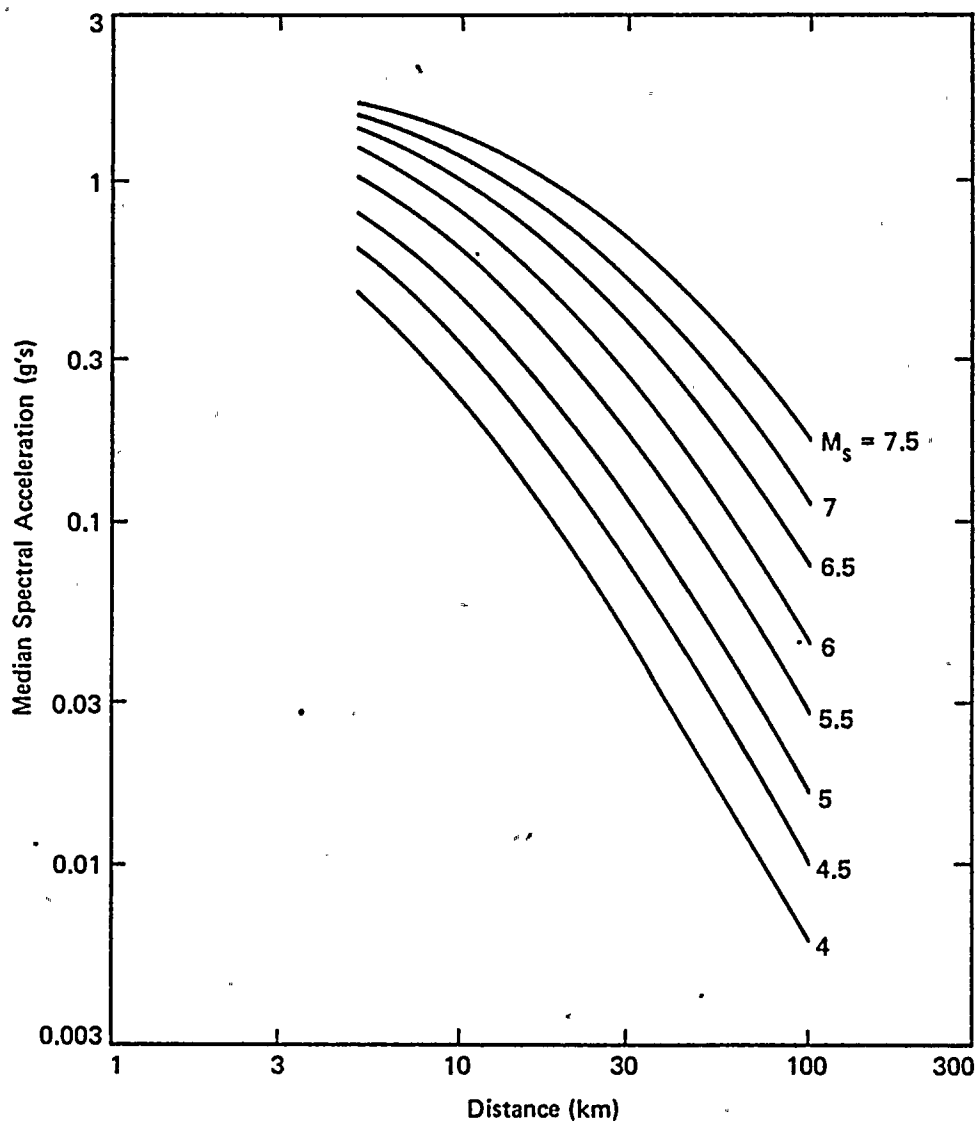
$m^u$  = maximum magnitude

Project No. 14940	Hanford FSAR	RECURRENCE RELATIONSHIPS AS A FUNCTION OF MAXIMUM MAGNITUDE	Figure 2.5K-44
Woodward-Clyde Consultants			



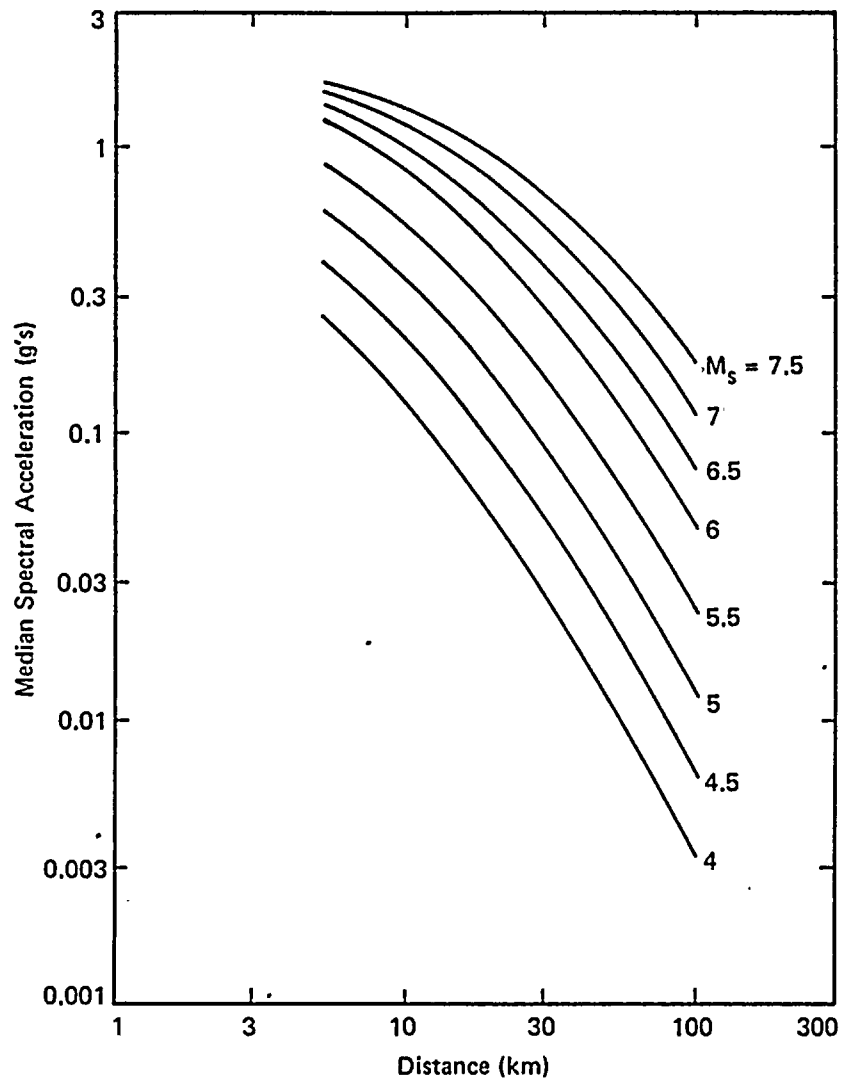
Project No. 14940	Hanford FSAR	SELECTED ATTENUATION RELATIONSHIPS FOR PEAK ACCELERATION	Figure 2.5K—45
Woodward-Clyde Consultants			





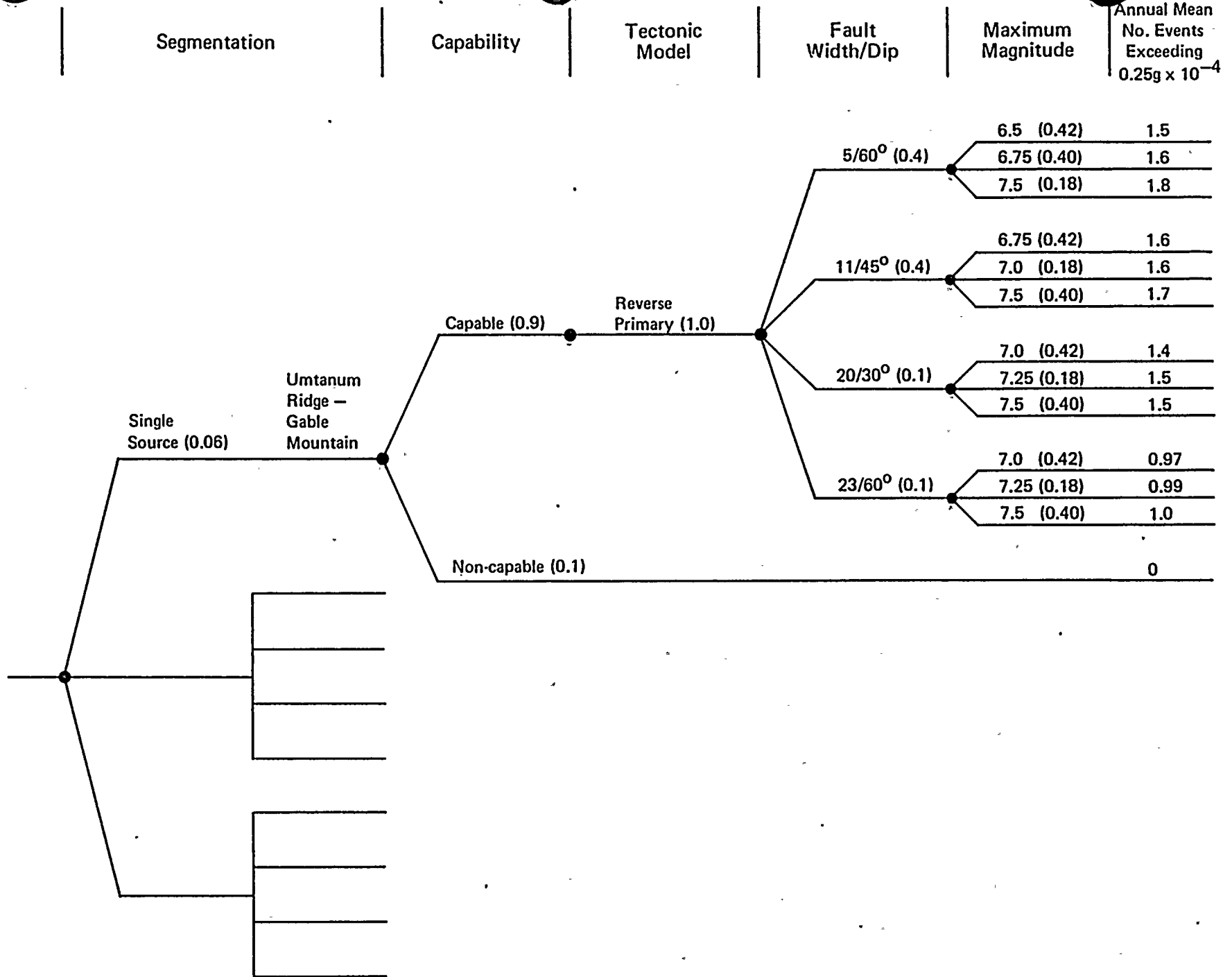
Project No. 14940	Hanford FSAR	SELECTED ATTENUATION RELATIONSHIPS FOR RESPONSE SPECTRAL ACCELERATION (2% damping) at Period = 0.125 sec.	Figure 2.5K-46
Woodward-Clyde Consultants			





Project No. 14940	Hanford FSAR	SELECTED ATTENUATION RELATIONSHIPS FOR RESPONSE SPECTRAL ACCELERATION (2% damping) at Period = 0.40 sec.	Figure 2.5K-47
Woodward-Clyde Consultants			





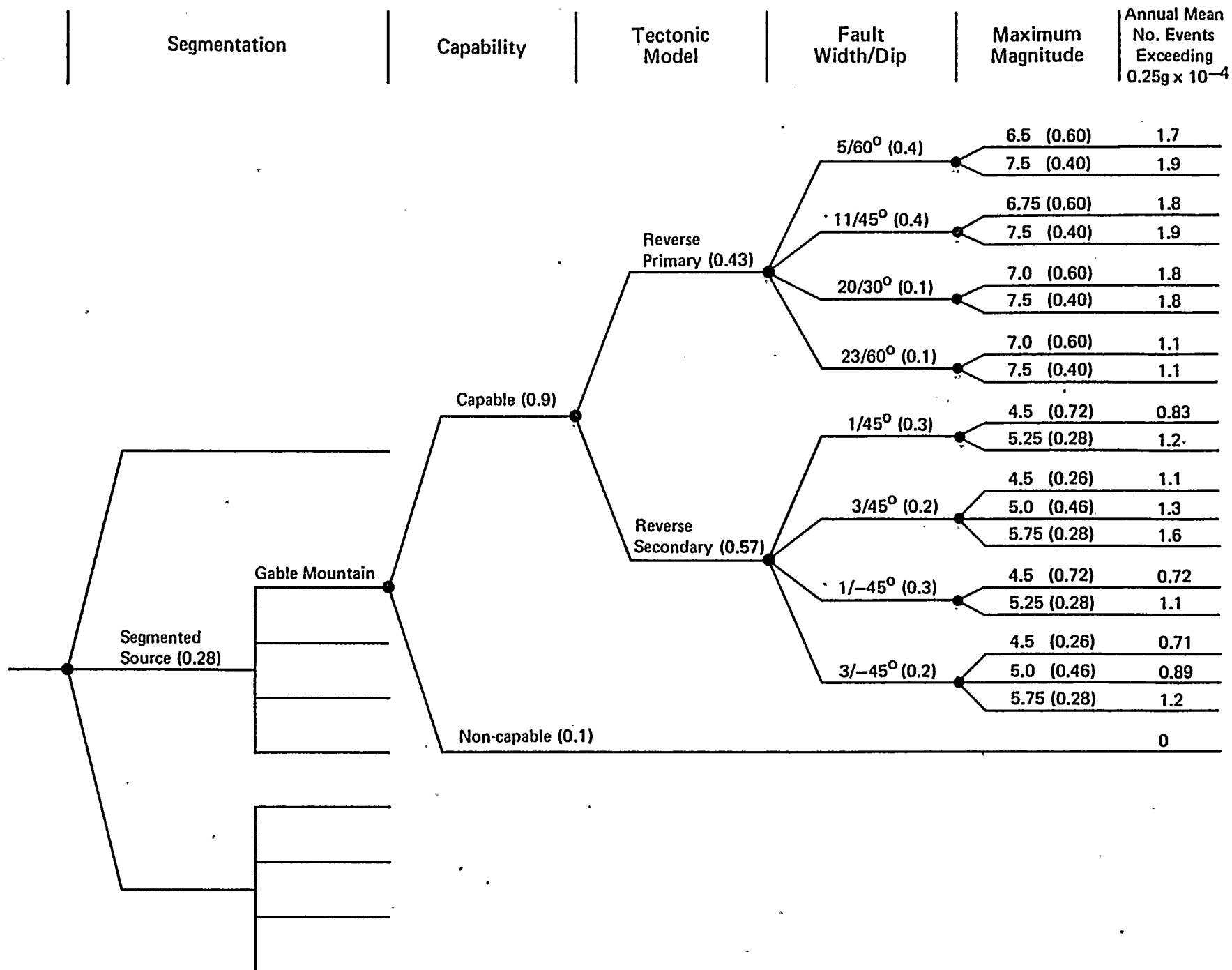
Project No.  
14940

Hanford FSAR

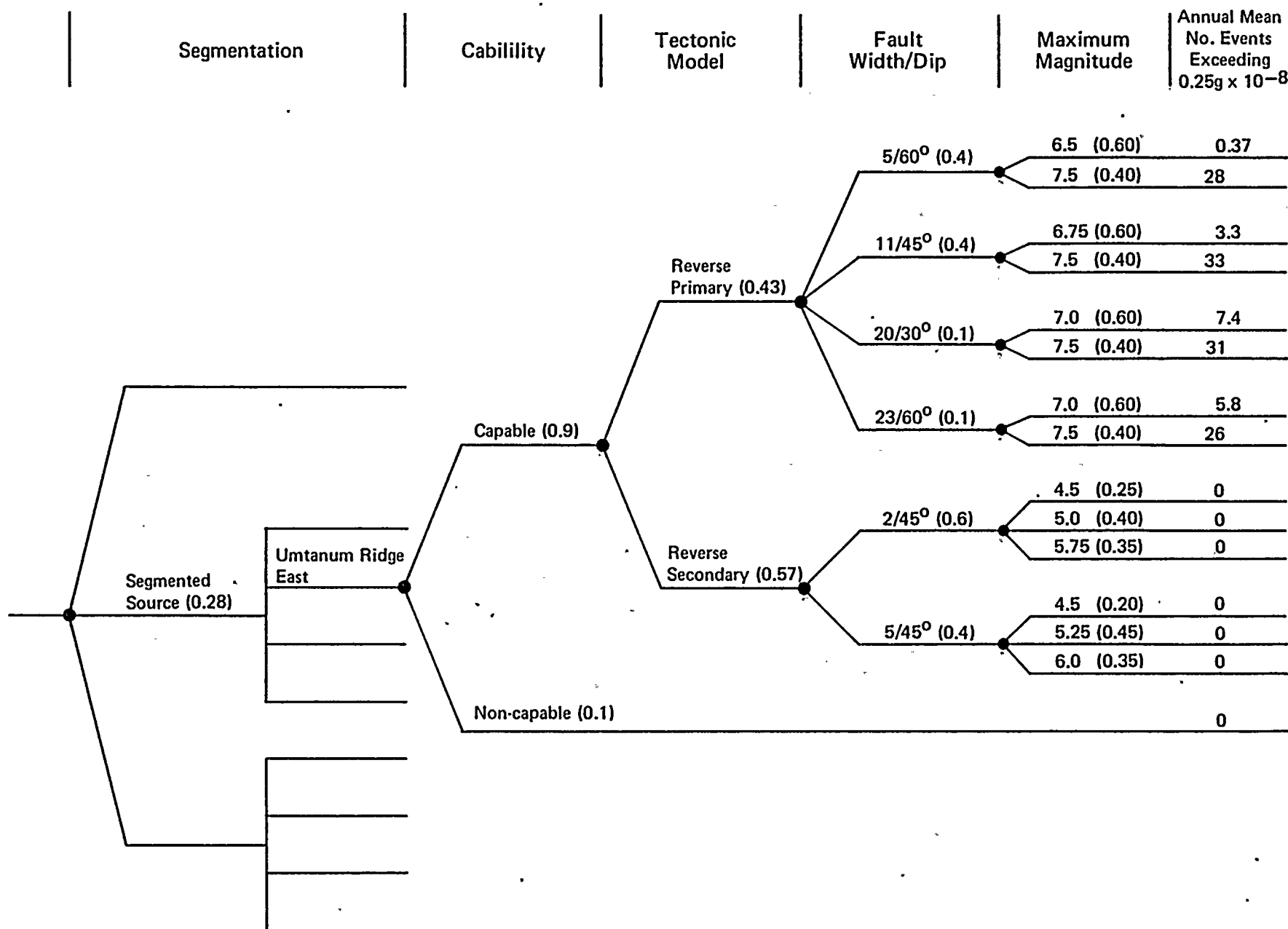
EXPOSURE ANALYSIS RESULTS FOR  
UMTANUM RIDGE - GABLE MOUNTAIN  
STRUCTURAL TREND: SINGLE SOURCE

Figure  
2.5K-48

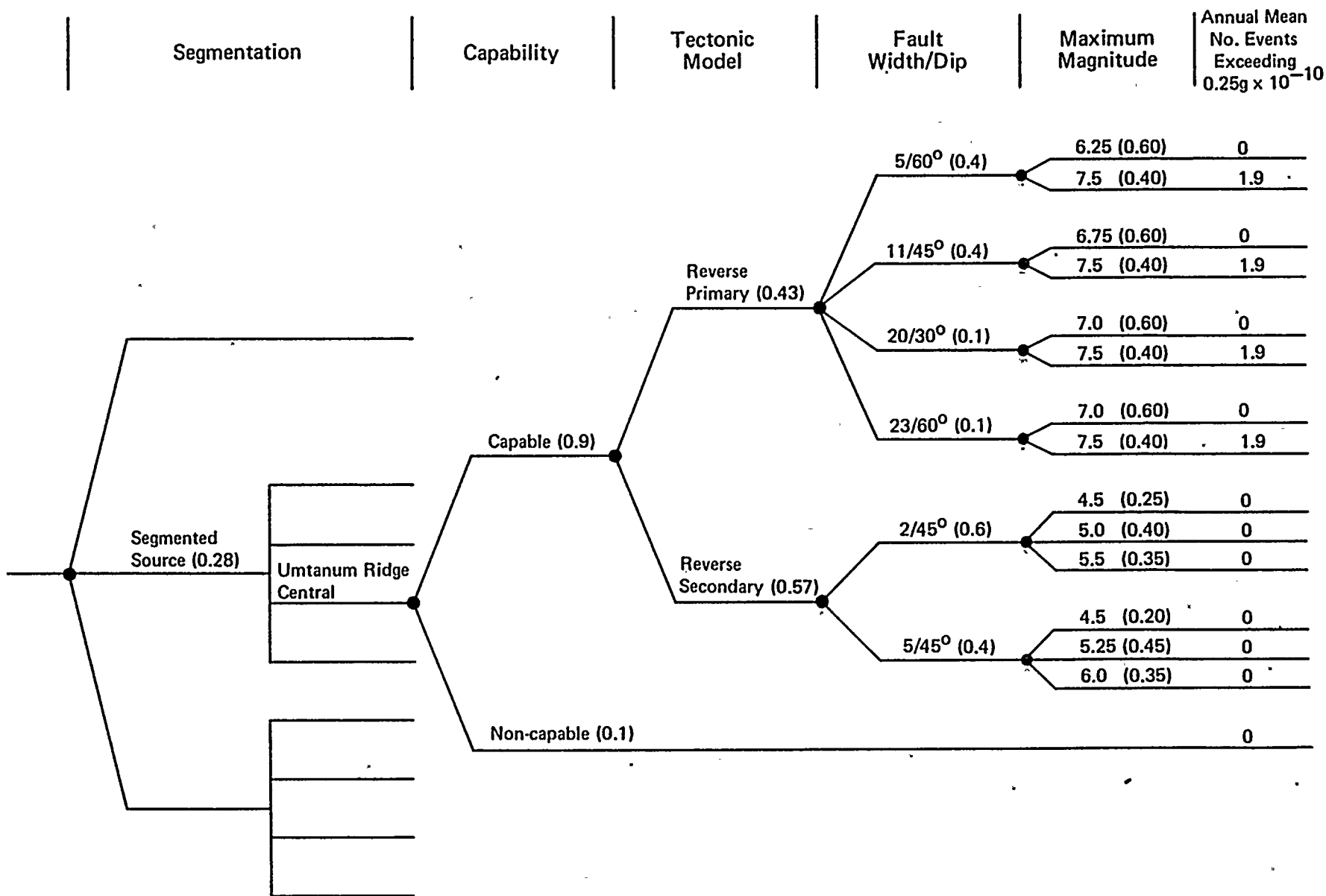


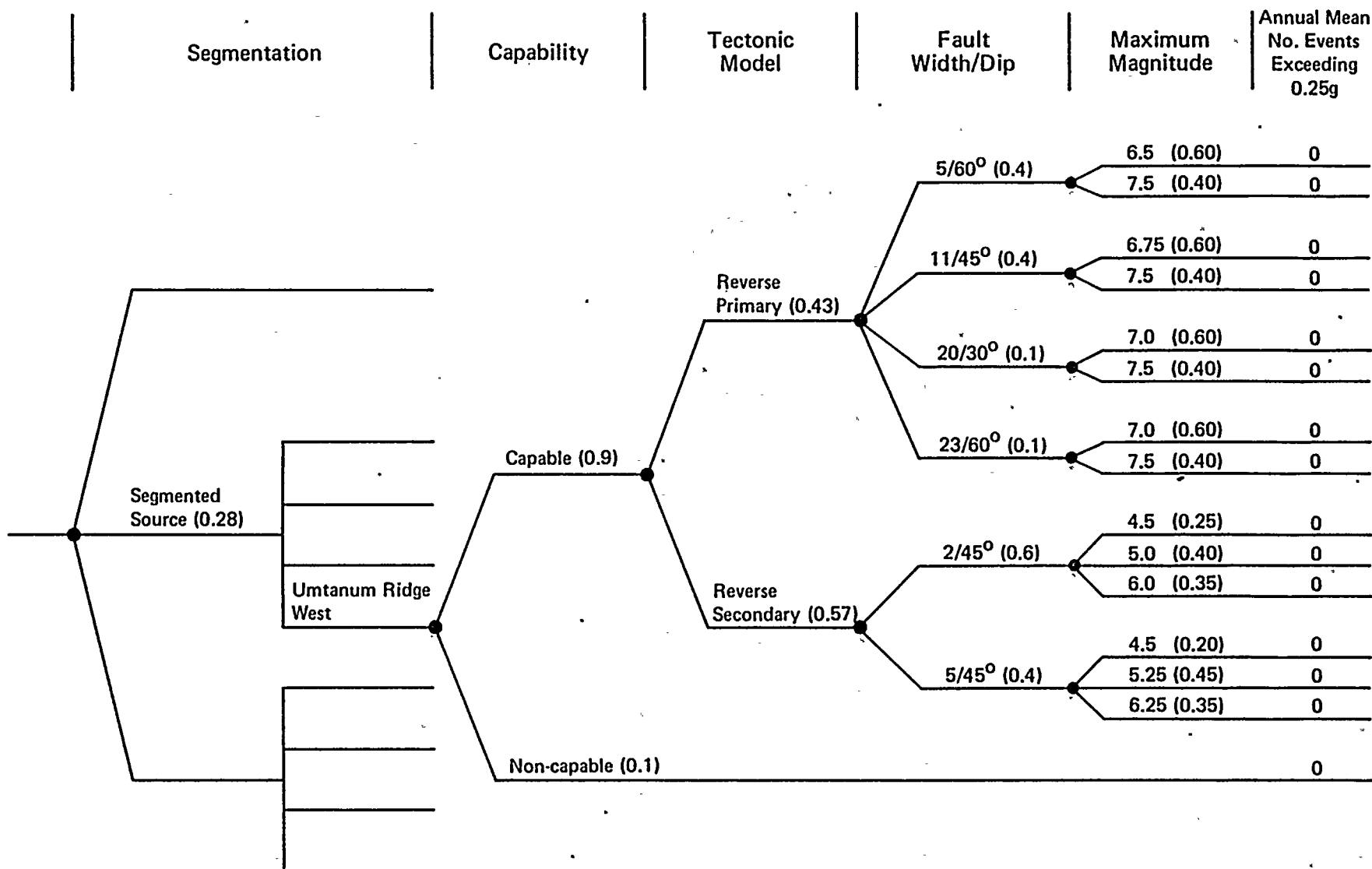


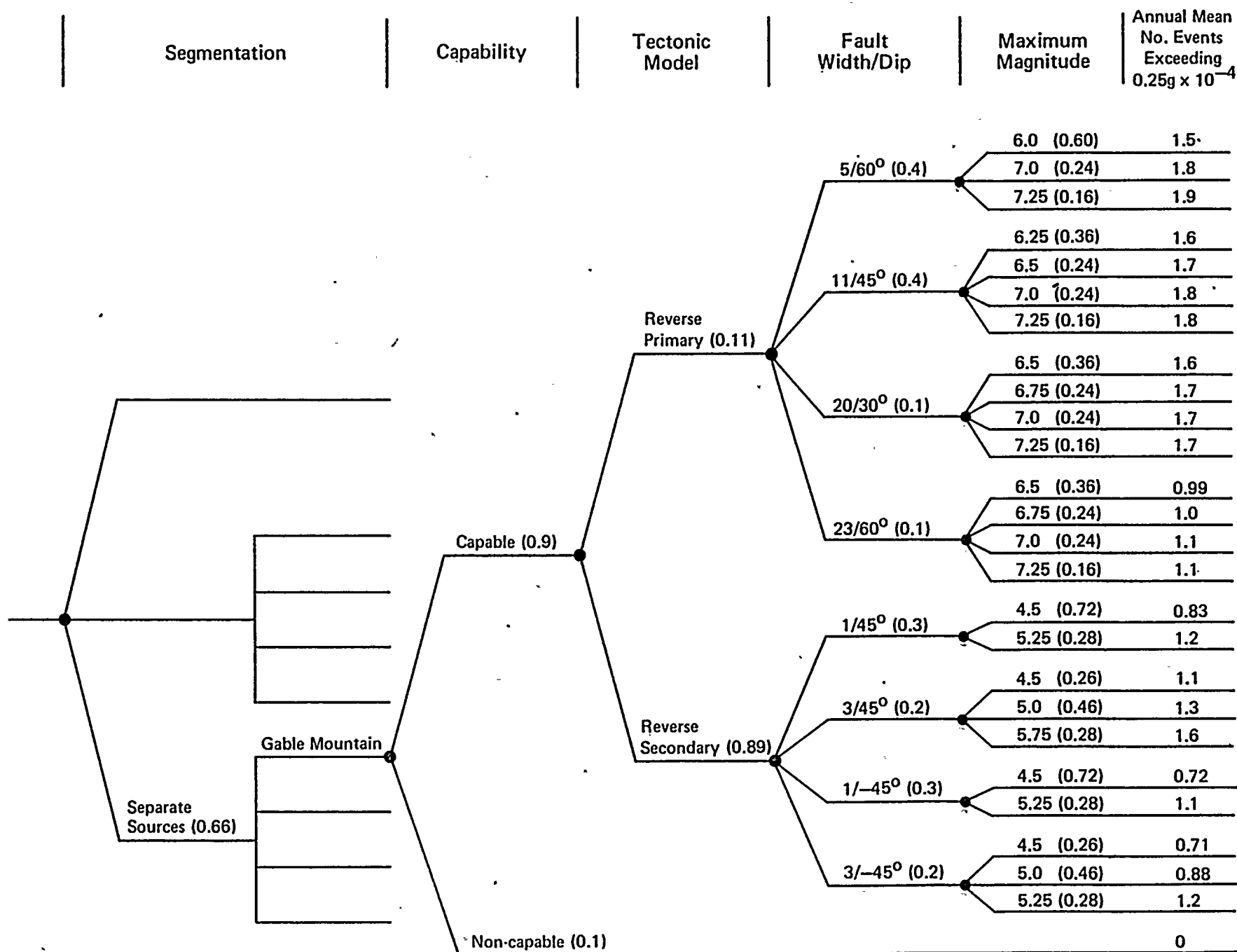


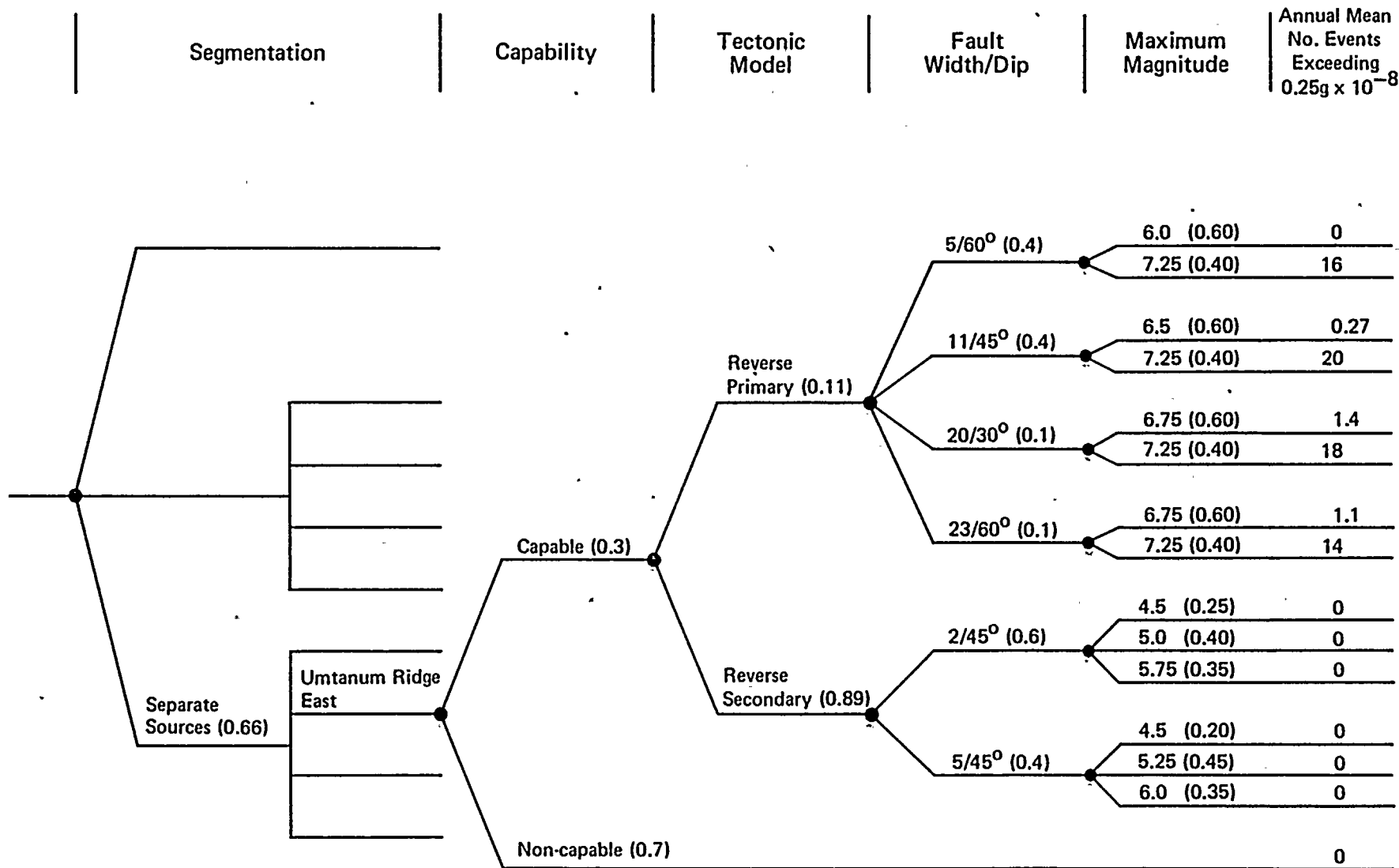






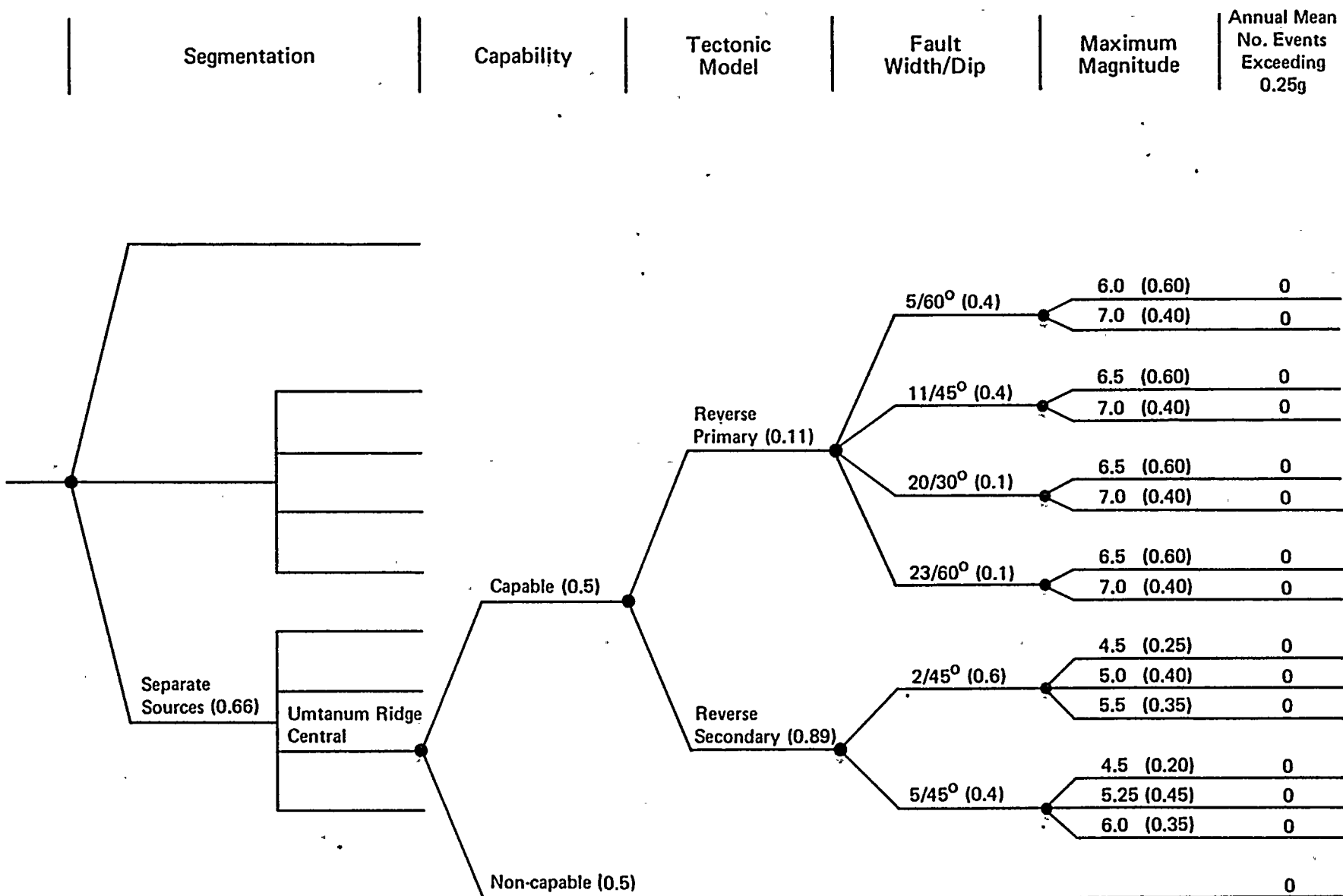


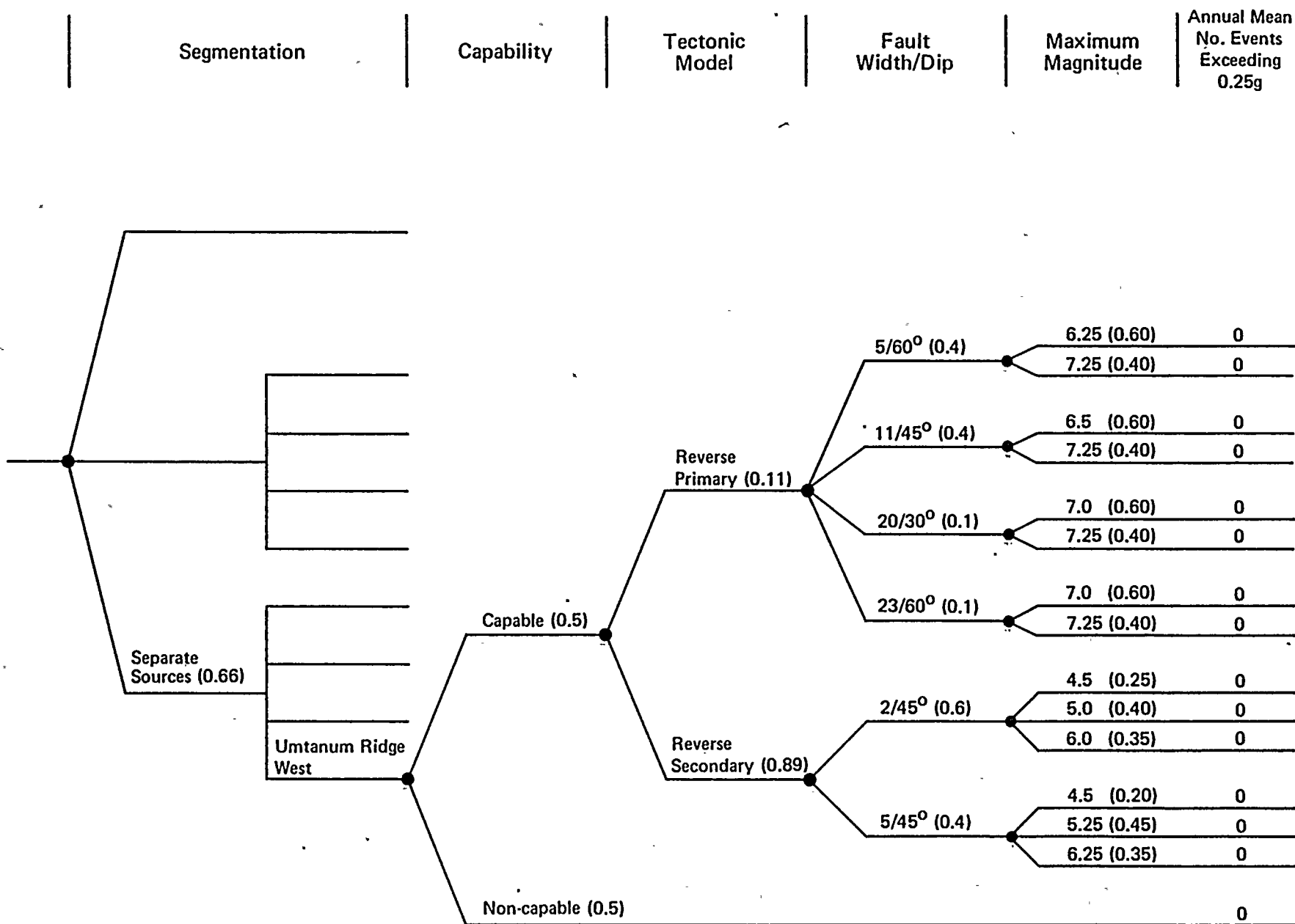




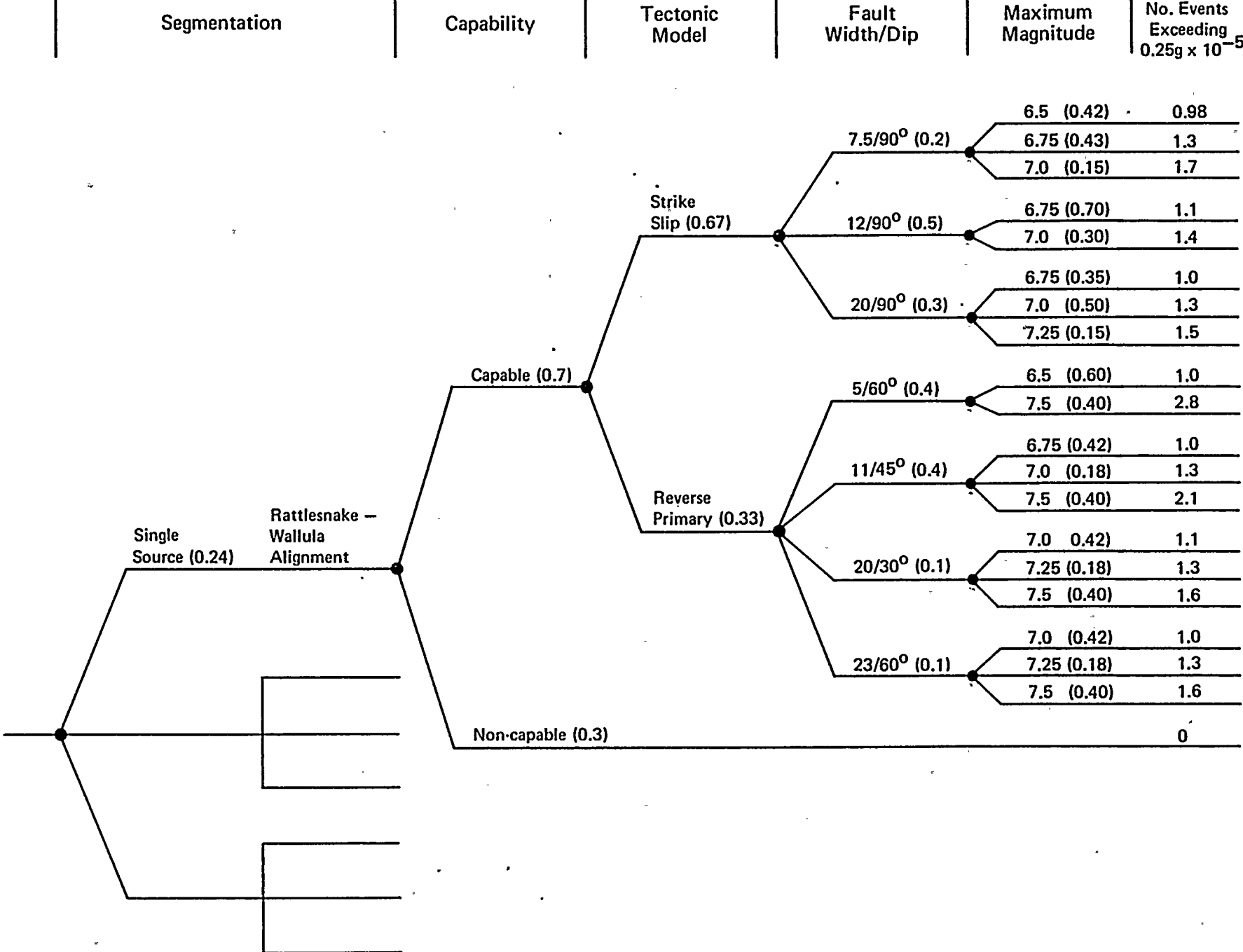


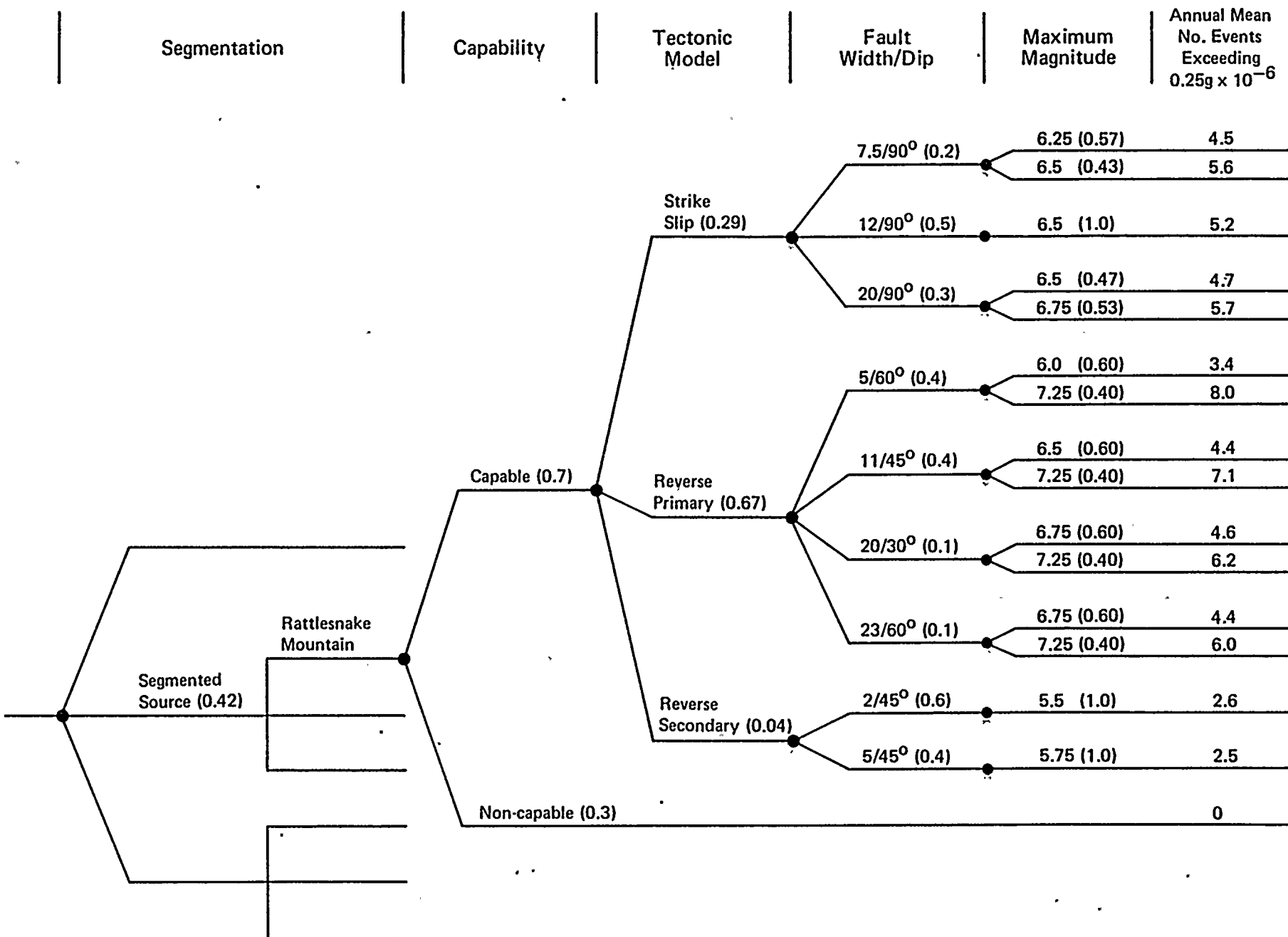


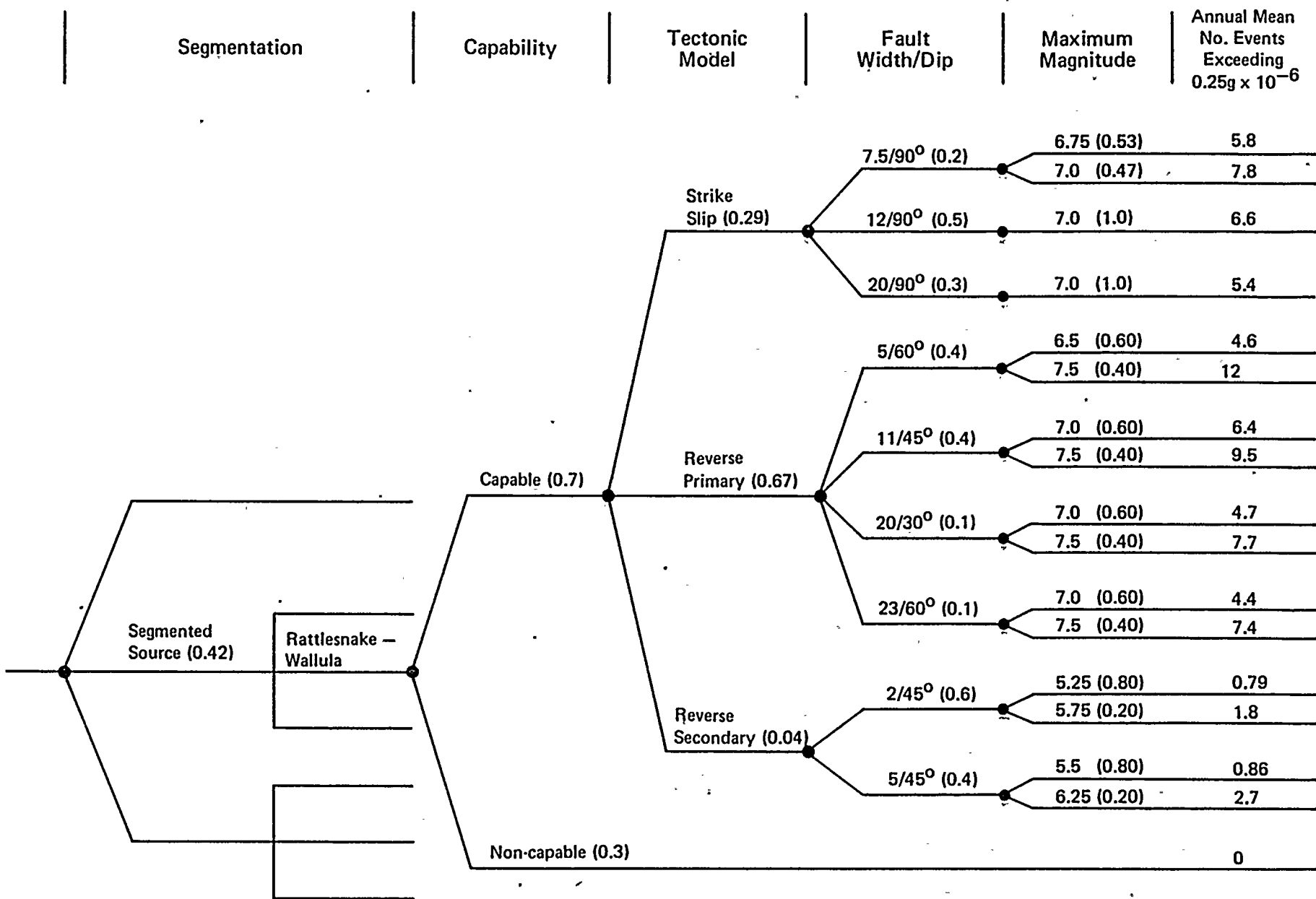


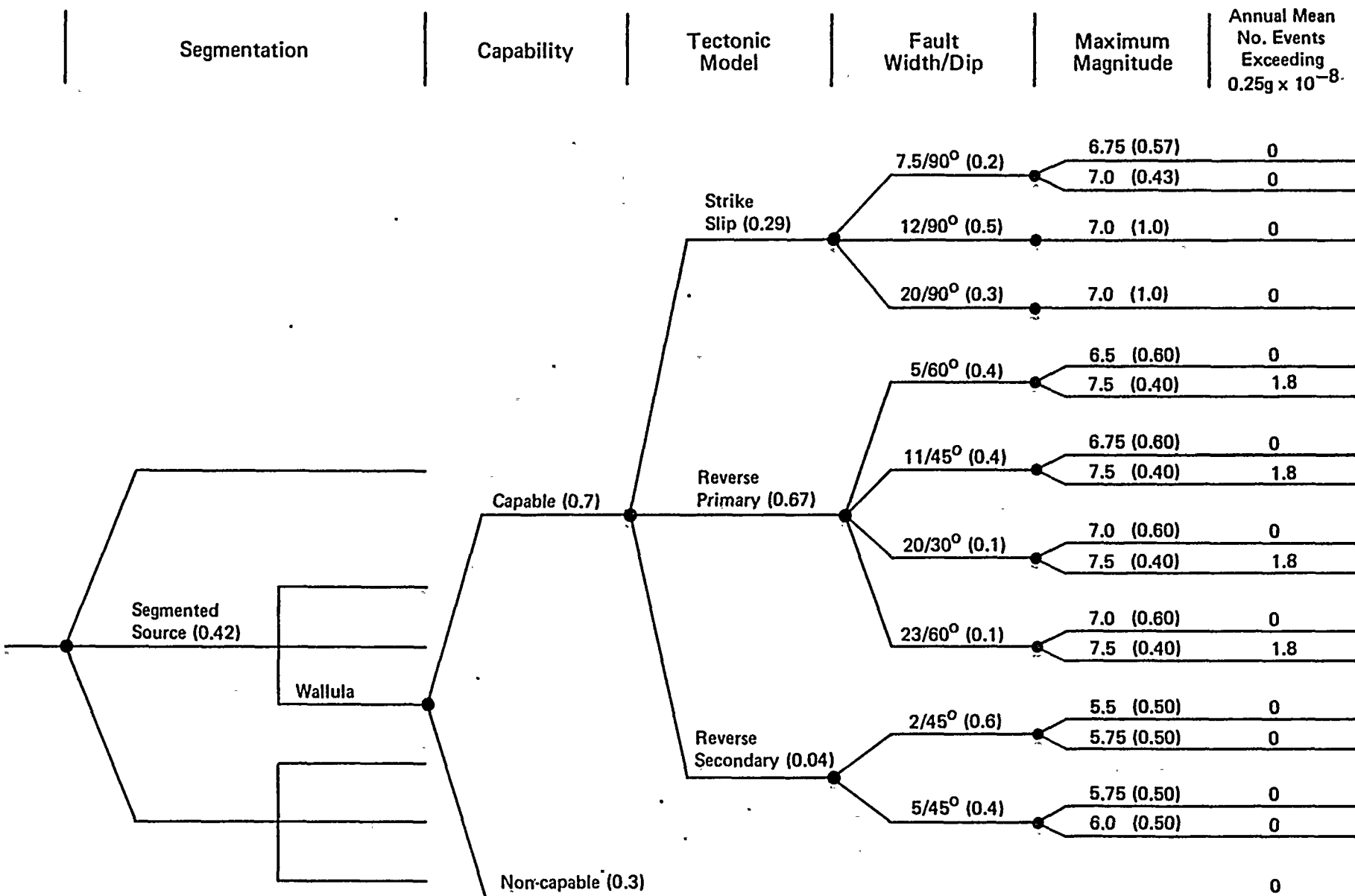




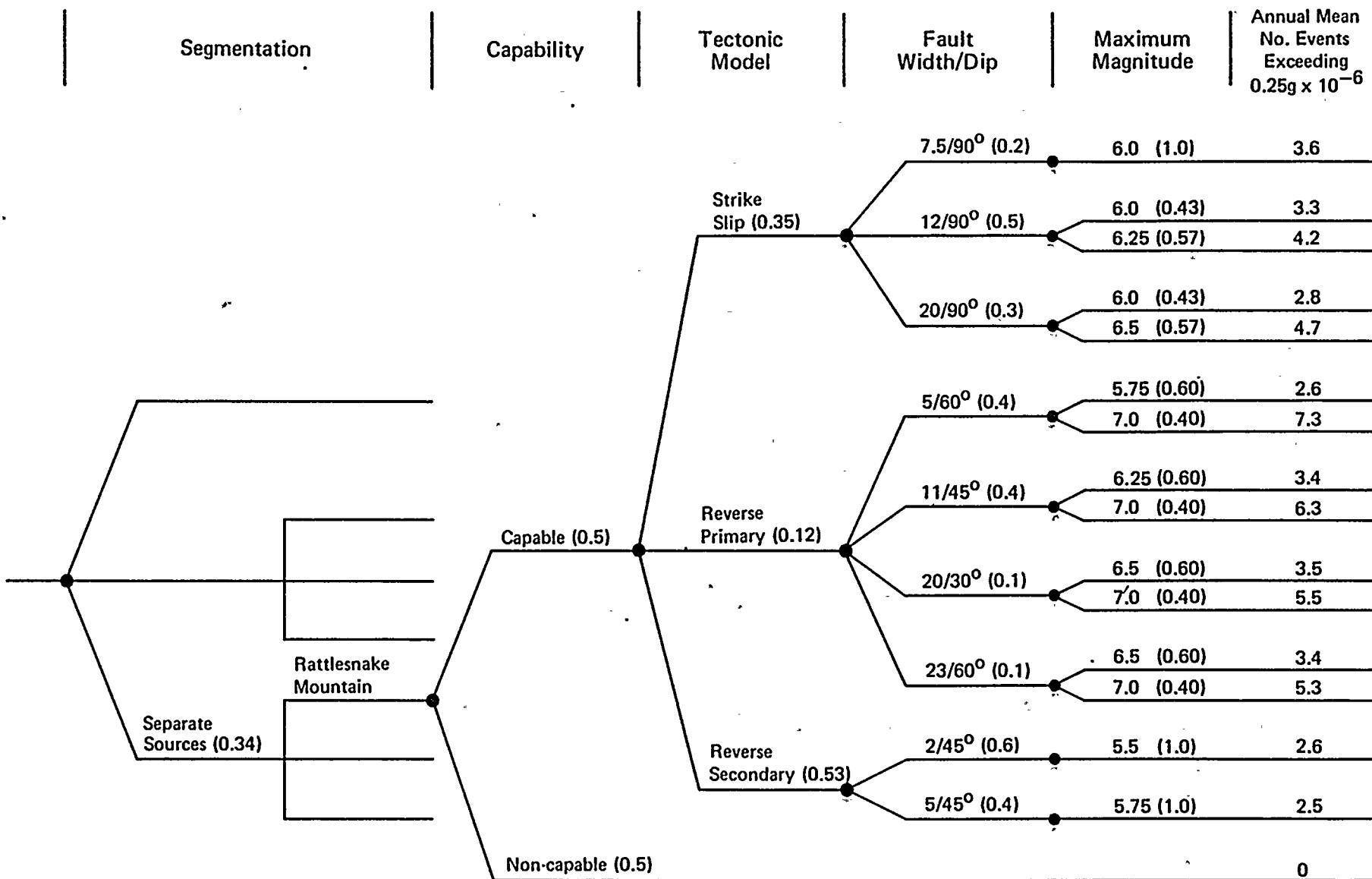


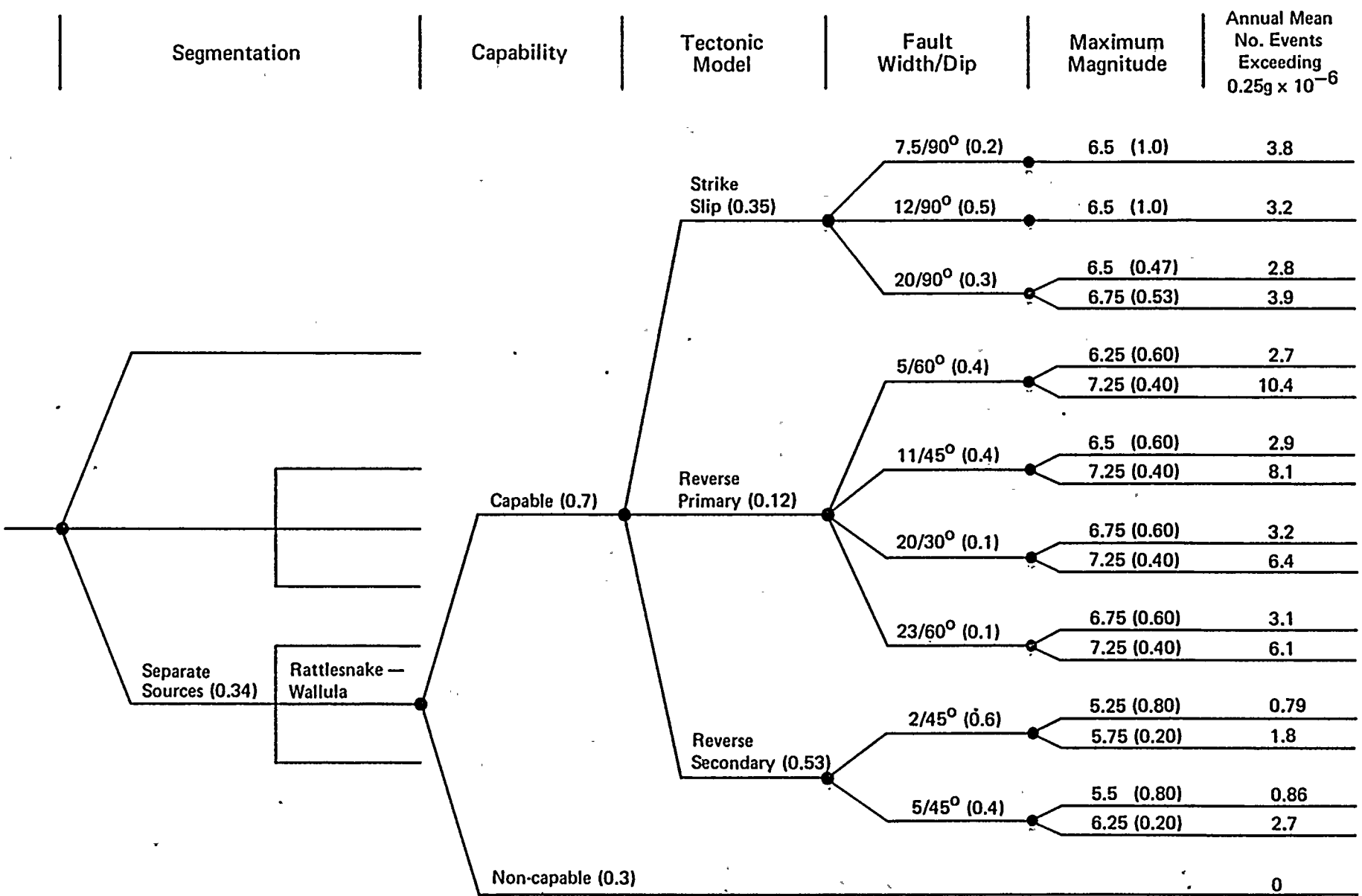


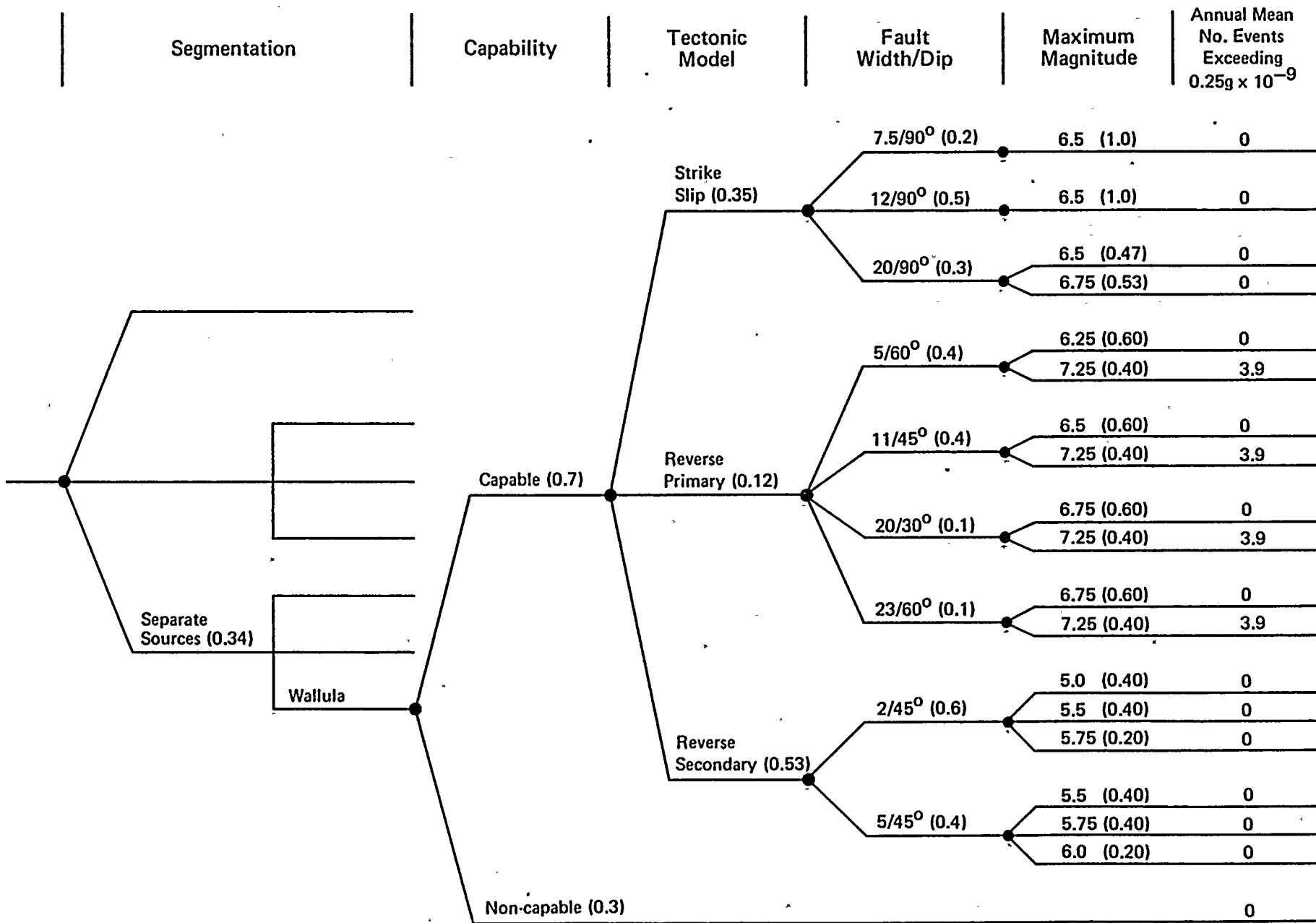


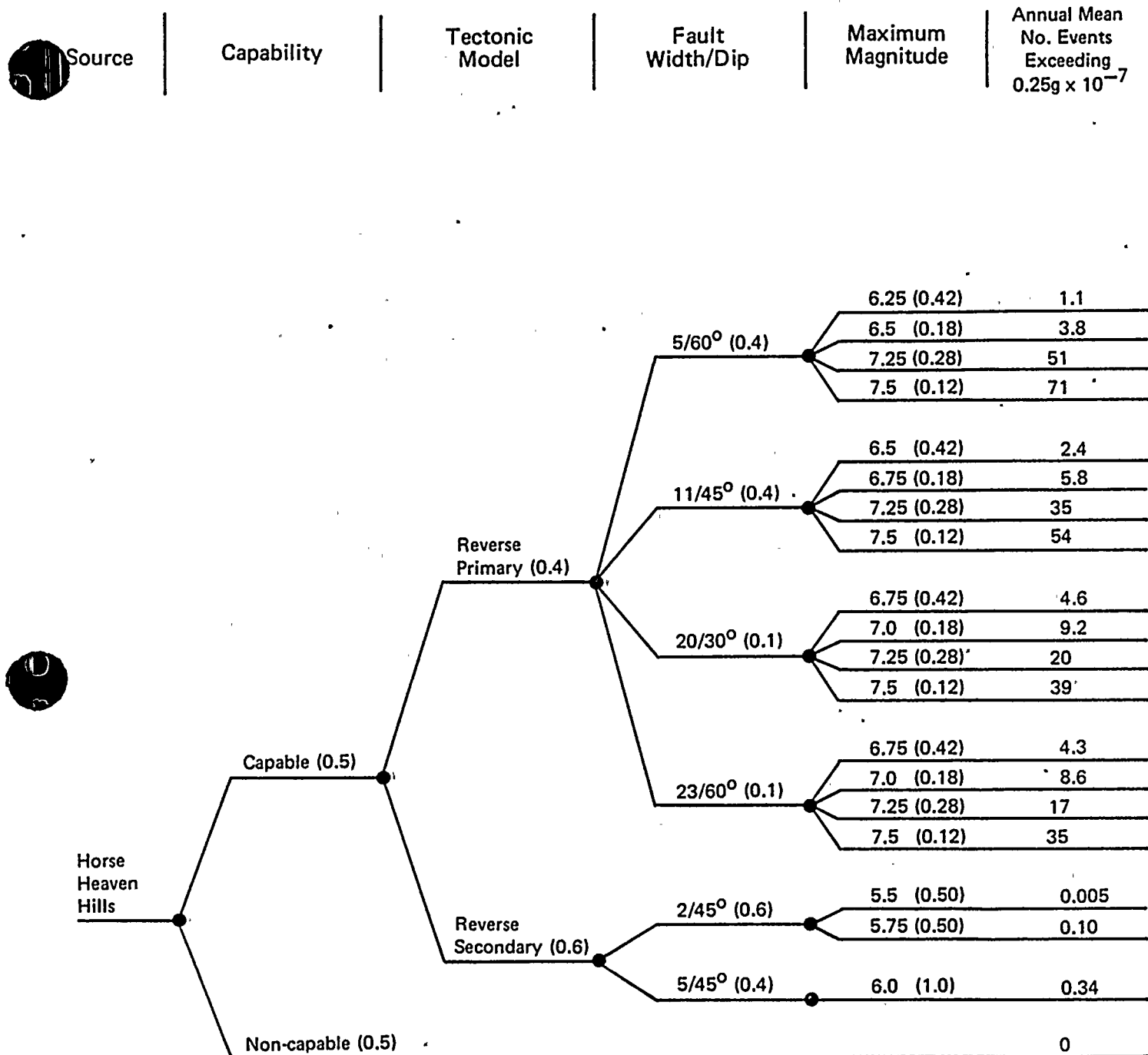








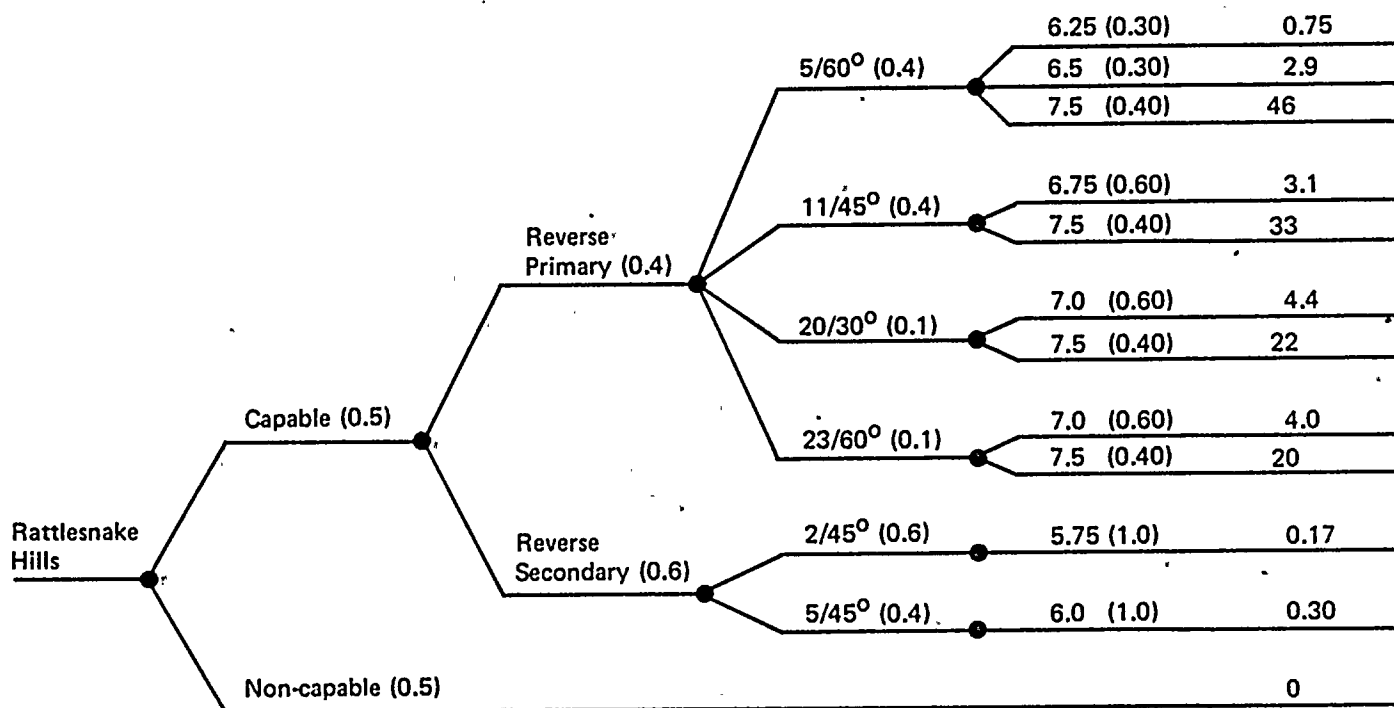




Project No. 14940	Hanford FSAR	EXPOSURE ANALYSIS RESULTS FOR HORSE HEAVEN HILLS SOURCE	Figure 2.5K-64
Woodward-Clyde Consultants			

Source

Capability

Tectonic  
ModelFault  
Width/DipMaximum  
MagnitudeAnnual Mean  
No. Events  
Exceeding  
 $0.25g \times 10^{-7}$ Project No.  
14940

Hanford FSAR

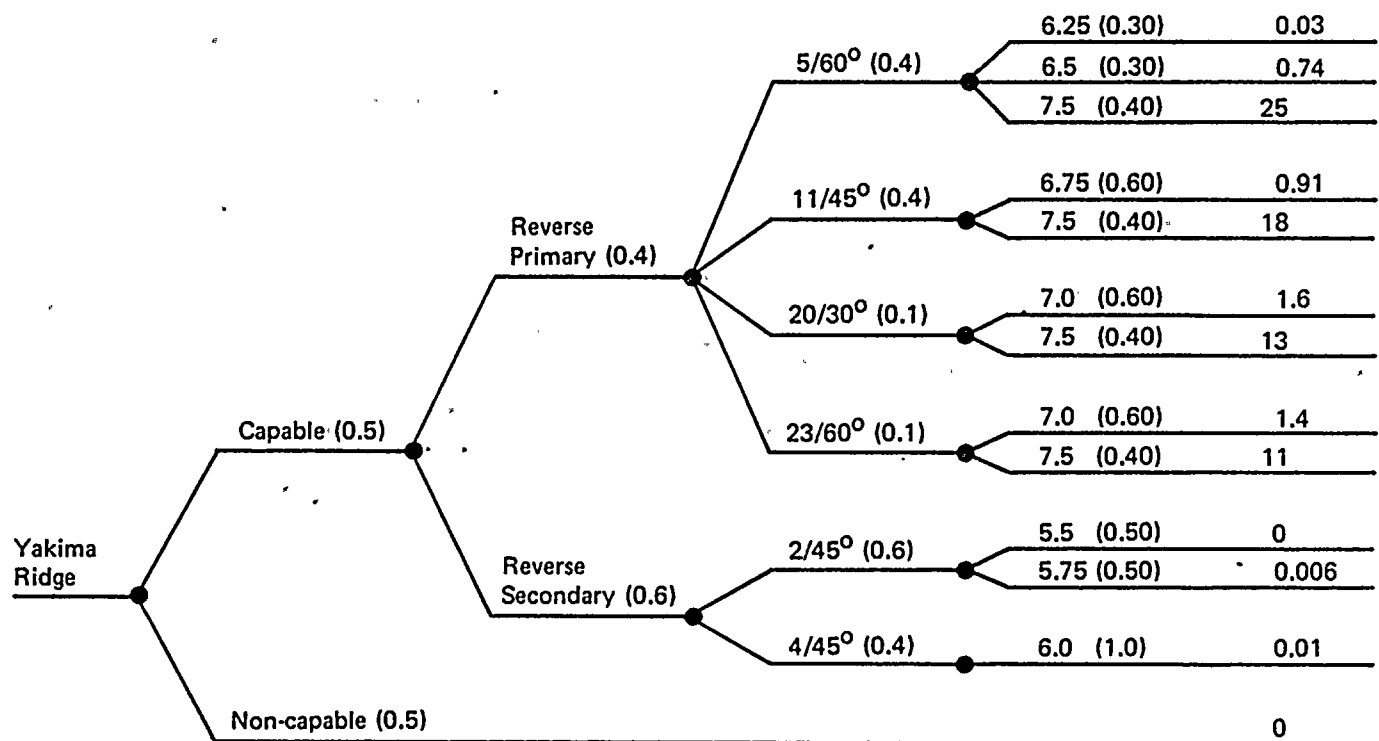
EXPOSURE ANALYSIS RESULTS FOR  
RATTLESNAKE HILLS SOURCEFigure  
2.5K-65

Woodward-Clyde Consultants

WNP-2 Amendment No. 18  
September 1981

Source

Capability

Tectonic  
ModelFault  
Width/DipMaximum  
MagnitudeAnnual Mean  
No. Events  
Exceeding  
 $0.25g \times 10^{-7}$ Project No.  
14940

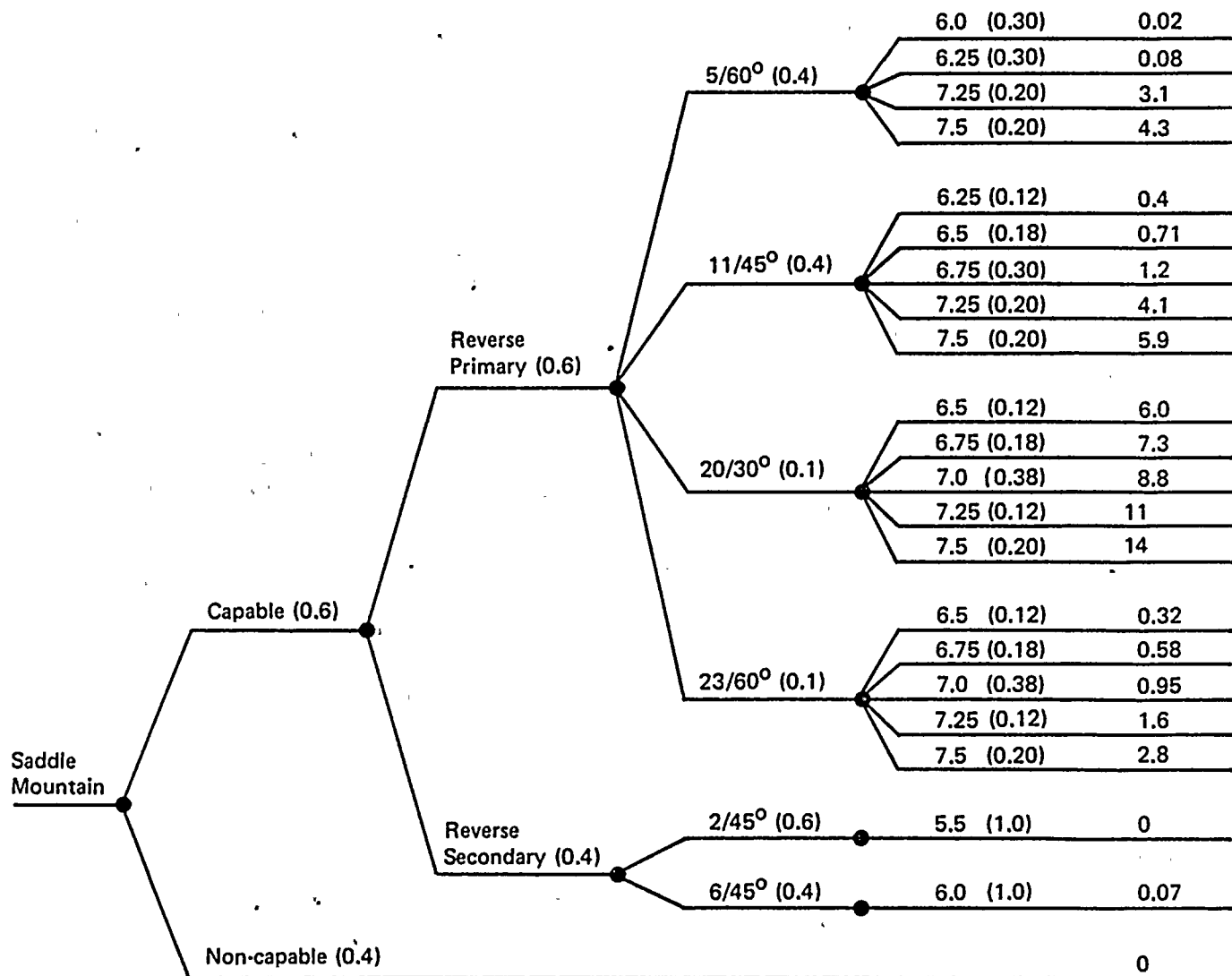
Hanford FSAR

EXPOSURE ANALYSIS RESULTS FOR  
YAKIMA RIDGE SOURCEFigure  
2.5K-66

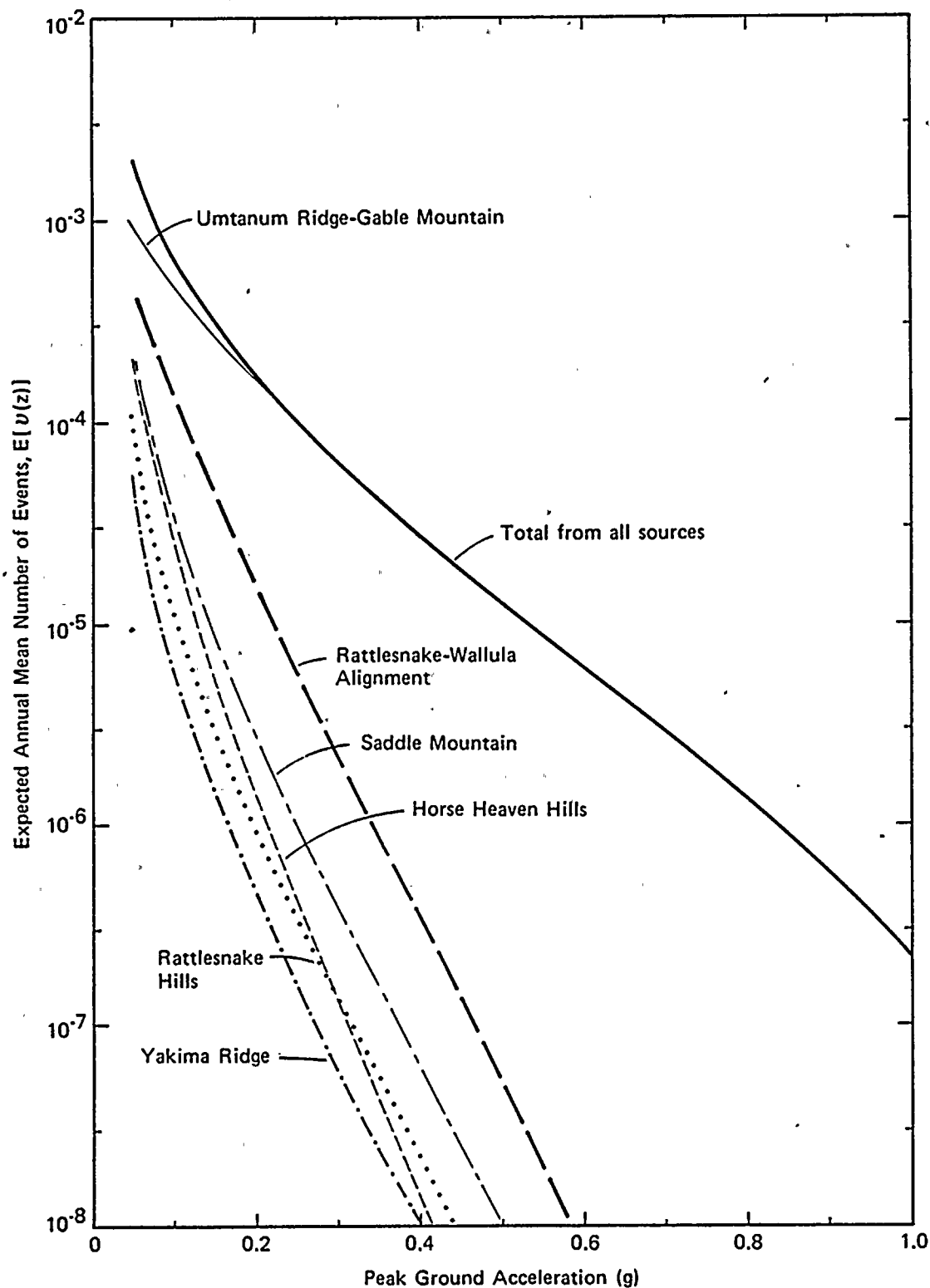
Woodward-Clyde Consultants

WNP-2 Amendment No. 18  
September 1981

Source	Capability	Tectonic Model	Fault Width/Dip	Maximum Magnitude	Annual Mean No. Events Exceeding $0.25g \times 10^{-6}$
--------	------------	----------------	-----------------	-------------------	---



Project No. 14940	Hanford FSAR	EXPOSURE ANALYSIS RESULTS FOR SADDLE MOUNTAIN SOURCE	Figure 2.5K-67
Woodward-Clyde Consultants			



Project No.  
14940

Hanford FSAR

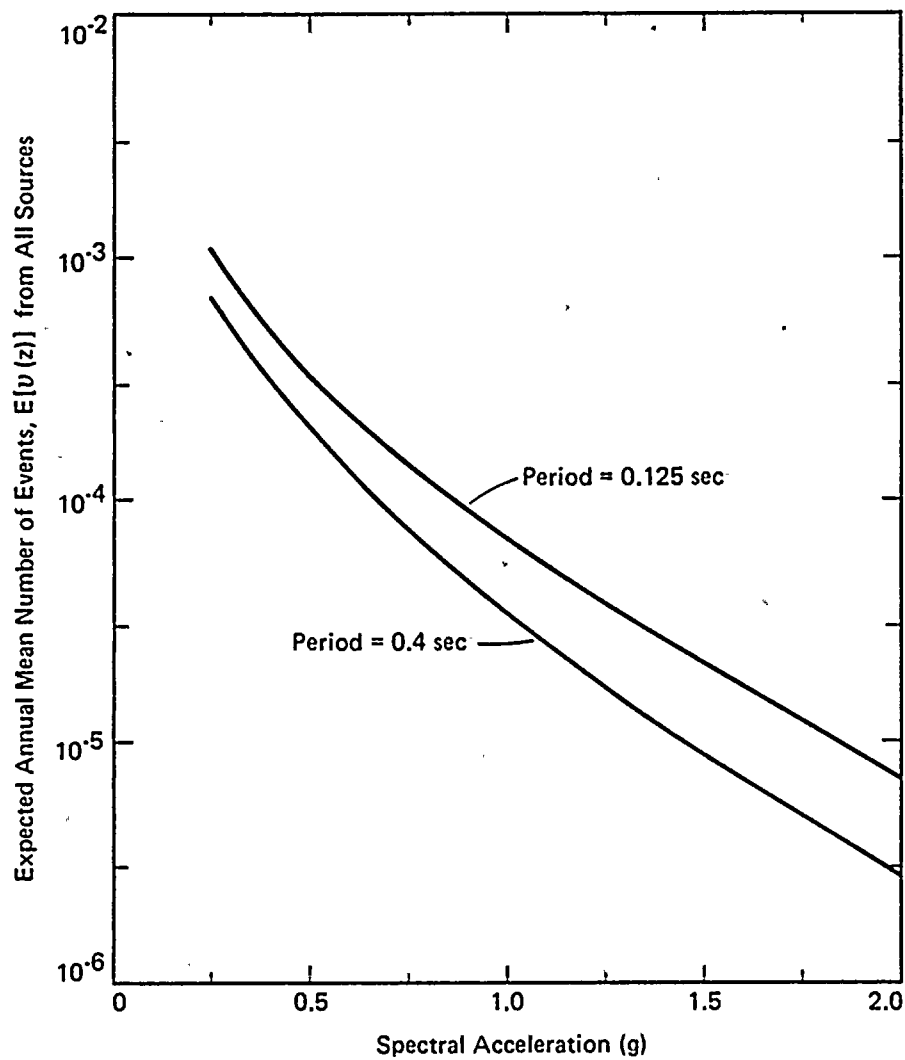
**Woodward-Clyde Consultants**

VARIATION OF EXPOSURE WITH  
PEAK ACCELERATION

Figure  
2.5K-68

WNP-2 Amendment No. 18  
September 1981





Project No. 14940	Hanford FSAR	VARIATION OF EXPOSURE WITH SPECTRAL ACCELERATION	Figure 2.5K-69
Woodward-Clyde Consultants			



APPENDIX 2.5K - ATTACHMENT A

## ATTENUATION RELATIONSHIPS

## 2.5K.A1 INTRODUCTION

The objective of the studies described herein is to select free-field ground motion attenuation relationships for use in the seismic exposure analysis. Attenuation relationships describe the variation of a ground motion parameter with distance from the earthquake source and earthquake magnitude. In the seismic exposure analysis, maximum earthquake magnitudes as large as 7.5 are permitted in some of the scenarios. The lowest earthquake magnitude considered in the analysis is magnitude 4, which is considered to be the smallest earthquake of potential engineering significance to the plant. Therefore, the attenuation relationships cover the magnitude range of 4 to 7.5. (Magnitude is defined herein as surface-wave magnitude ( $M_S$ ), because the correlations used to estimate maximum magnitudes on sources considered in the seismic exposure analysis are primarily based on  $M_S$  magnitudes.) The sources considered in the exposure analysis vary in distance from the site from about 5 to 100 km. Therefore, the attenuation relationships are applicable for that distance range. (Distance, as utilized herein, is defined as the closest distance from the ruptured fault to the site).

Attenuation relationships are selected for peak ground acceleration (zero-period acceleration of a response spectrum). Attenuation relationships are also selected for response spectral accelerations for 2-percent damping for periods equal to 0.125 second and 0.40 second.

## 2.5K.A2 APPROACH

The attenuation relationships are selected on the basis of examination and statistical analysis of empirical data consisting of strong motion data recorded during historical earthquakes. In developing a data base and selecting attenuation relationships, consideration is given to the predominant sense of displacement (type of faulting) associated with tectonic models of the Columbia Plateau and to the subsurface conditions at the plant site. The predominant type of faulting is reverse faulting; data from reverse faulting events are utilized to constrain attenuation relationships for  $M_S$  approximately equal to 6.5, for which abundant strong motion data for a reverse faulting event exist. The subsurface conditions at the plant site consist of approximately 160 m of sediments of varying stiffness above



basalt bedrock. The presence of relatively thick soil layers at the plant site is considered by using a data base of recordings from soil sites rather than rock sites.

As described in Section 2.5K.7 of this appendix, a theoretical wave propagation and modeling study has been conducted to supplement the empirical data analysis by analyzing the attenuation characteristics of the crustal structure in the site vicinity. This study indicates that the basalt layering in the Columbia Plateau may have the effect of significantly reducing site ground motions in comparison to locations in California where the great majority of empirical data have been recorded. However, for the present analysis, these theoretically predicted attenuation effects of the Columbia Plateau crustal structure have been conservatively neglected.

Details of the methodology and the results are contained in subsequent sections of this attachment.

#### 2.5K.A3 PEAK GROUND ACCELERATION

The general approach to selecting attenuation relationships for peak ground acceleration consists of (1) detailed analysis of data and development of an attenuation relationship for  $M_S$  approximately equal to 6.5; and (2) extension of the results to larger and smaller magnitudes by examination of data, previous studies, and judgment.

##### 2.5K.A3.1 Relationship for $M_S$ Approximately Equal to 6.5

The strong motion data base that is apparently most applicable to the predominant type of faulting postulated for the Columbia Plateau is that from the 1971 San Fernando earthquake ( $M_L$  6.4,  $M_S$  6.6), a reverse faulting event. Records from this earthquake that were obtained from the ground floor level of buildings or instrument shelters situated on soil deposits and located within 100 km from the ruptured fault are utilized as a primary data set. This data set is identified in Table 2.5K-A1, and horizontal acceleration values are plotted versus distance in Figure 2.5K-A1. Regression analyses of the data are made using an equation of the form:

$$\ln a = A_1 + B \ln (R + C), \text{ or,} \quad (2.5K-A1)$$

$$a = A'_1 (R + C)^B$$

where  $a$  is a peak horizontal acceleration,  $R$  is closest distance; and  $A_1$ ,  $A'_1$  and  $B$  are regression coefficients; and  $C$  is a constant.

A value for the parameter  $C$  that is greater than zero provides

a curvilinear relationship between  $a$  and  $R$ , with the result that  $a$  tends to level off at small values of  $R$ . Although a curvilinear relationship is well founded in many published attenuation relationships (e.g., Joyner et al., 1981; Schnabel and Seed, 1973; Donovan and Bornstein, 1978), the choice for the value of the parameter  $C$  cannot be uniquely determined by regression analysis of the data in Figure 2.5K-A1. A value of  $C = 20$  is selected on the following basis: the standard deviation from the regression analysis shows a continuous slight decrease as  $C$  increases from zero to values as large as 35, and the predicted accelerations using  $C = 20$  are conservative in comparison to using higher values of  $C$ ; accelerogram simulation studies (Hadley et al., 1979) suggest that a value of  $C$  approximately equal to 20 is reasonable for magnitude 6.5. Using  $C = 20$ , the following equation is obtained for the median value of  $a$ :

$$a_{\text{med}} = 182 (R + 20)^{-1.87} \quad (2.5K-A2)$$

The standard deviation,  $S$ , of  $\ln a$  from the regression analysis is equal to 0.35. For the assumed log-normal distribution of  $a$ , the median (50th percentile), mean, and the 84th percentile values of  $a$  are related as follows:

$$a_{\text{mean}} = a_{\text{med}} e^{S^2/2} \quad (2.5K-A3)$$

$$a_{84\text{th}} = a_{\text{med}} e^S \quad (2.5K-A4)$$

Figure 2.5K-A1 shows the median and the 84th percentile curves obtained from the regression analysis, superimposed on the data.

As noted previously, the data base used for the above analysis consists of recordings from the ground floor of buildings or instrument shelters. This selection criterion excludes recordings from basements. To test the sensitivity of excluding the records from basements, an analysis was made in which the records from basements were included. Thus, this data set included all data recorded on soil sites during the San Fernando earthquake within 100 km of the earthquake source. This data set is summarized in Table 2.5K-A2 and is plotted in Figure 2.5K-A2. The results of a regression analysis of the data set are shown in Figure 2.5K-A2. The median and 84th percentile curves are compared with those obtained from regression analysis of the primary data set in Figure 2.5K-A3. The results in Figure 2.5K-A3 indicate that the basement recordings may provide a downward bias on peak acceleration values and that it was conservative to exclude these records in developing the attenuation relationship given in Equation (2.5K-A2).



A sensitivity analysis was also made in which data from other earthquakes of  $M_S$  approximately equal to 6.5 were included. Consistent with the primary data set, data for this analysis consisted only of records from the ground level of buildings and instrument shelters situated on soils sites located within 100 km of the earthquake source. The resulting data set essentially consists of the San Fernando earthquake primary data base plus records from the 1979 Imperial Valley earthquake ( $M_L$  6.6,  $M_S$  6.9). A single record from the 1954 Eureka earthquake ( $M_L$  6.5,  $M_S$  6.6) also fit the selection criteria and was included in this data set. The type of faulting for the 1979 Imperial Valley earthquake and for the 1954 Eureka earthquake is predominantly strike-slip in comparison to reverse faulting for the San Fernando earthquake. Inclusion of the Imperial Valley earthquake data in this analysis for  $M_S$  approximately equal to 6.5 is conservative since the  $M_S$  of that earthquake is 6.9.

The data from the Imperial Valley and Eureka earthquakes are shown in Table 2.5K-A3 and are plotted along with the primary data set from the San Fernando earthquake in Figure 2.5K-A4. The results of a regression analysis of this combined data set are shown in Figure 2.5K-A4 as median and 84th percentile curves. In Figure 2.5K-A5, the results of this regression analysis are compared with those shown in Figure 2.5K-A1 for the primary San Fernando earthquake data set. The comparisons in Figure 2.5K-A5 indicate that it was conservative to exclude the data from the strike-slip events in developing the attenuation relationships for  $M_S = 6.5$ .

#### 2.5K.A3.2 Generalized Relationships for All Magnitudes

An attenuation relationship of the following form is utilized to describe the variation of peak ground acceleration with both magnitude and distance

$$\ln a = A_2 + D M_S + B \ln (R + C), \text{ or,}$$

$$a = A'_2 e^{D M_S} (R + C)^B \quad (2.5K-A5)$$

where  $C = c_1 e^{c_2 M_S}$  ( $c_1$  and  $c_2$  are constants),  $A_2$ ,  $A'_2$  and  $D$  are constants, and other parameters are as defined previously.

By using the previous results for  $M_S = 6.5$  (Equation 2.5K-A2) and by examining the data for other magnitude earthquakes in the approximate range  $4 \leq M_S \leq 7.5$ , the following relationships have been selected for the median value of  $a$ :

for  $M_S \geq 6$ :





$$a_{med} = 0.154 e^{1.1 M_S} (R + C)^{-1.89} \quad (2.5K-A6)$$

$$\text{where } C = 0.455 e^{0.582 M_S}$$

and for  $M_S < 6$ :

$$a_{med} = 0.154 e^{1.1 M_S} (R + C)^{-1.89} \quad (2.5K-A7)$$

$$\text{where } C = 0.714 e^{0.507 M_S}$$

Note that for  $M_S = 6.5$ , Equation (2.5K-A6) results in accelerations that are essentially equal to (slightly higher than) accelerations from Equation (2.5K-A2), which was the direct result of the regression analysis of the  $M_S = 6.5$  primary data set. Equations (2.5K-A6) and (2.5K-A7) are used in the seismic exposure analysis. The selected attenuation relationships of Equations (2.5K-A6) and (2.5K-A7) are plotted for one-half magnitude bands, from  $M_S = 4$  to 7.5, in Figure 2.5K-A6.

The following relationships have been adopted between the standard deviation,  $S$ , and  $M_S$  for the seismic exposure analysis:

For  $M_S \geq 6$ ,

$$S(\ln a) = 0.70 - 0.05 M_S \quad (2.5K-A8)$$

and for  $M_S < 6$ ,

$$S(\ln a) = 1.402 - 0.167 M_S \quad (2.5K-A9)$$

For  $M_S = 6.5$ , Equation (2.5K-A8) results in a standard deviation that is slightly higher than that obtained from the previously described regression analysis for  $M_S = 6.5$ . The relationships of Equations (2.5K-A8) and (2.5K-A9) reflect the trend for increased scatter of peak acceleration values with decreasing earthquake magnitude.

#### 2.5K.A4 RESPONSE SPECTRAL VALUES

The approach used in selecting attenuation relationships for response spectral values is similar to that used for peak accelerations. First, relationships are developed for  $M_S$  approximately equal to 6.5; the relationships are then extended to cover all magnitudes.

2.5K.A4.1 Relationships for  $M_S$  Approximately Equal to 6.5.

It can be seen in Figure 2.5K-A1 and Table 2.5K-A1 that many accelerograms of the primary data set from the 1971 San Fernando earthquake are in a narrow distance range (24 to 27 km). Statistical analyses are made of the response spectra (2-percent damping) of these accelerograms to develop a median spectral shape. The results of the statistical analyses are presented in Figure 2.5K-A7. The adopted smooth spectrum shape for  $M_S = 6.5$  is shown in Figure 2.5K-A7 for comparison with the statistical results. The adopted shape is conservative. The conservatism for low periods (less than about 0.1 second) is to account for limitations in the strong-motion data processing procedures, which tend to filter out some of the lower-period motions, and to account for the possibility of greater low-period spectral amplifications at distances closer to the earthquake source than the distances for the data set used in the statistical analyses. It is noted that the acceleration amplification of the adopted shape (in the period range 0.125 to 0.46 second) is equal to 3.2, in comparison to the acceleration amplification of 2.74 presented for soil sites in NUREG 0098 (U.S. Nuclear Regulatory Commission, 1978).

The seismic exposure analysis has been made for response spectral accelerations at periods equal to 0.125 second and 0.40 second. Spectral acceleration attenuation relationships for these periods are obtained by combining the amplifications of the smooth spectrum shape shown in Figure 2.5K-A7, with the peak acceleration attenuation relationship given by Equation (2.5K-A6) for  $M_S = 6.5$ . The resulting attenuation relationship (applicable to both periods) is:

$$SA_{med} = 628 (R + 20)^{-1.89} \quad (2.5K-A10)$$

where SA is spectral acceleration (in g's) at periods, T, equal to 0.125 and 0.40 second.

From examination of the statistical results, the standard deviation of the prediction of  $\ln SA$  is estimated to equal 0.4 for  $T = 0.125$  second and 0.45 for  $T$  equal to 0.40 second.

To test the adopted attenuation relationship given in Equation (2.5K-A10), regression analyses (similar to those made for peak acceleration) were made for response spectral acceleration at periods of 0.125 second and 0.40 second for the data in the primary data set (Table 2.5K-A1). The results of these analyses indicate that Equation (2.5K-A10) provides a conservative prediction of SA in comparison to the regression results.

2.5K.A4.2 Generalized Relationships for All Magnitudes

The attenuation relationships for response spectral ordinates developed for  $M_S = 6.5$  are extended to larger and smaller magnitudes based on the general approach and the guidelines described below. The extension of response spectra from  $M_S = 6.5$  to other magnitudes required the following:

- (1) Relationships between peak acceleration for magnitude  $M_S$  and magnitude 6.5 [i.e.,  $a(M_S)/a(6.5)$ ] as a function of distance.
- (2) Relationships between response spectral shapes for magnitude  $M_S$  and magnitude 6.5 [i.e.,  $(SA/a)_{M_S}/(SA/a)_{6.5}$ ] as a function of period.

Given the above relationships, the response spectra for  $M_S 6.5$  can be readily extended to any other magnitude  $M_S$  using the following relationship:

$$SA(M_S) = SA(6.5) \times [(SA/a)_{M_S}/(SA/a)_{6.5}] \times [a(M_S)/a(6.5)]$$

With regard to item 1 above, the ratio  $a(M_S)/a(6.5)$  at any desired distance is based on the relationships given by Equations (2.5K-A6) and (2.5K-A7).

With regard to item 2 above (i.e., the effect of magnitude on response spectral shape), based on the examination of available data and judgment, the following guidelines were developed:

- (1) For earthquakes with  $M_S$  less than 6.5, in the period range zero to 0.2 second, the normalized response spectral ratios,  $(SA/a)_{M_S}/(SA/a)_{6.5}$ , are constant and equal to unity. Therefore, the response spectral accelerations,  $SA(M_S)$ , are proportional to the peak ground acceleration,  $a(M_S)$ .
- (2) For earthquakes with  $M_S$  less than 6.5, the normalized response spectral ratios,  $(SA/a)_{M_S}/(SA/a)_{6.5}$ , are less than unity for periods greater than 0.2 second, the ratio decreasing with increasing period.
- (3) For earthquakes with  $M_S$  greater than 6.5, the normalized response spectral ratios,  $(SA/a)_{M_S}/(SA/a)_{6.5}$ , are constant and equal to unity for periods up to 0.4 second. Therefore, the response spectral accelerations,  $SA(M_S)$ , are proportional to the peak ground acceleration,  $a(M_S)$ .

By using the previous results for  $M_S 6.5$  (Equation 2.5K-A10),

guidelines 1 and 3 above, and guideline 2 above (with appropriate reduction factors for periods greater than 0.2 second, the following relationships are obtained for the median values of SA:

for  $M_S \geq 6$ ; and for periods 0.125 and 0.40 second:

$$(SA)_{med} = 0.493 e^{1.1 M_S} (R + C)^{-1.89} \quad (2.5K-A11)$$

$$\text{where } C = 0.455 e^{0.582 M_S}$$

for  $M_S < 6$ ; and for period 0.125 second:

$$(SA)_{med} = 0.493 e^{1.1 M_S} (R + C)^{-1.89} \quad (2.5K-A12)$$

$$\text{where } C = 0.7135 e^{0.507 M_S}$$

for  $M_S < 6$ ; and for period 0.40 second:

$$(SA)_{med} = 0.0838 e^{1.395 M_S} (R + C)^{-1.89} \quad (2.5K-A13)$$

$$\text{where } C = 0.7135 e^{0.507 M_S}$$

Note that for  $M_S = 6.5$ , Equation (2.5K-A11) reduces to

$$(SA)_{med} = 628 (R + 20)^{-1.89}$$

which is identical to Equation (2.5K-A10).

The spectral acceleration attenuation relationships given by Equations (2.5K-A11) through (2.5K-A13) are plotted in Figures 2.5K-A8 and 2.5K-A9 for periods of 0.125 second and 0.40 second, respectively.

For the reasons described previously, Equation (2.5K-A10) provides a conservative prediction of SA for the periods 0.125 and 0.40 second. Therefore, the relationships derived by extending Equation (2.5K-A10) to other magnitudes also contains the conservatism inherent in Equation (2.5K-A10). The appropriateness and conservatism of the selected relationships have been substantiated by comparing the spectral values predicted by Equations (2.5K-A12) and (2.5K-A13) at periods 0.125 and 0.40 second, respectively, for magnitudes in the range 4 to 6, to the available data for recordings from earthquakes in this magnitude range, in particular the 1975 Oroville earthquake aftershocks, and the 1979 Coyote Lake earthquake.

The standard deviation,  $S$ , of  $\ln SA$  is described by equations similar in form to Equations (2.5K-A8) and (2.5K-A9) for peak acceleration. The following relationships between  $S$  for

spectral acceleration and  $M_S$  are adopted for the seismic exposure analysis:

For  $T = 0.125$  second,

$$M_S \geq 6,$$

$$S(\ln SA) = 0.75 - 0.05 M_S \quad (2.5K-A14)$$

$$M_S < 6,$$

$$S(\ln SA) = 1.452 - 0.167 M_S \quad (2.5K-A15)$$

For  $T = 0.40$  second,

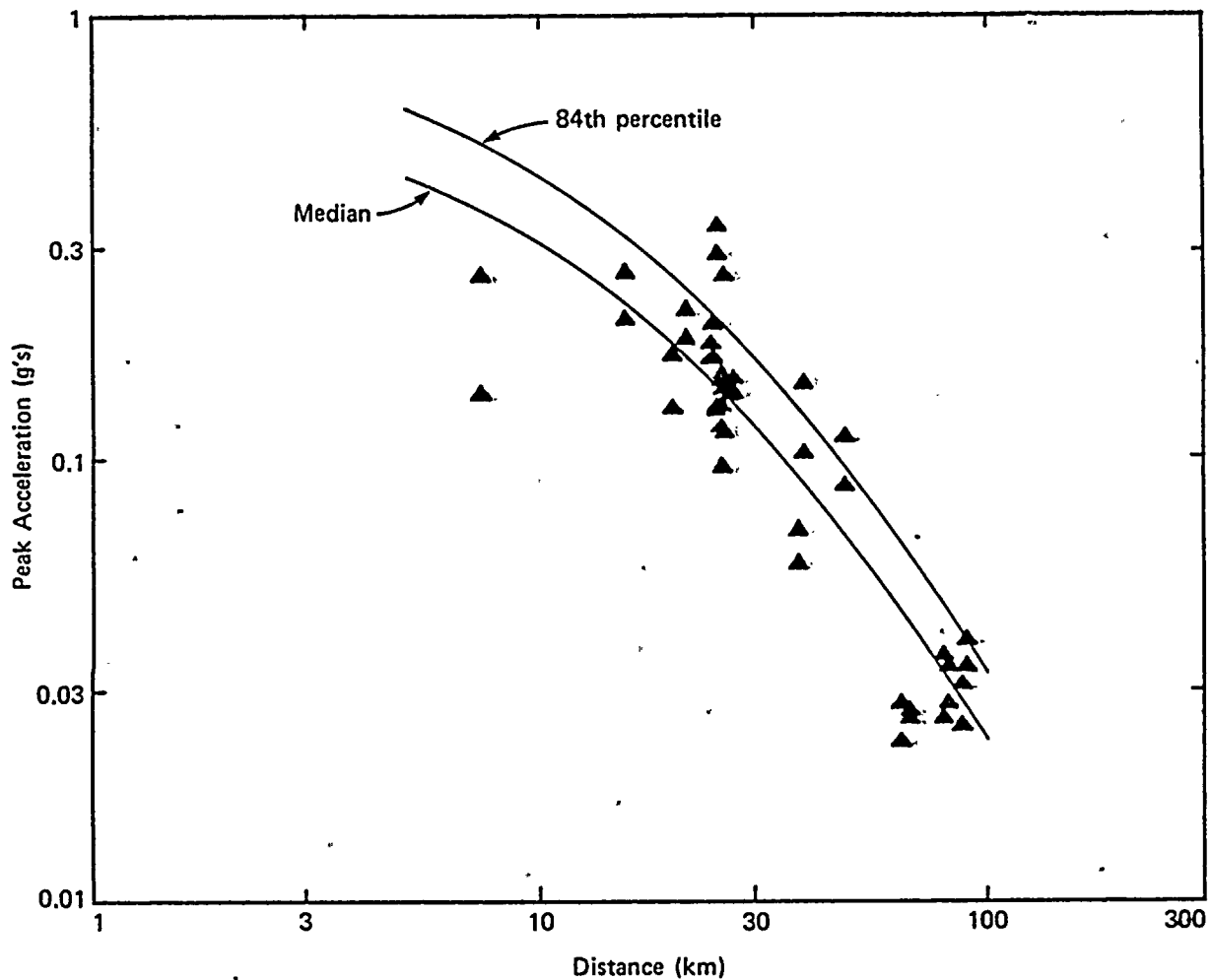
$$M_S \geq 6,$$

$$S(\ln SA) = 0.80 - 0.05 M_S \quad (2.5K-A16)$$

$$M_S < 6,$$

$$S(\ln SA) = 1.502 - 0.167 M_S \quad (2.5K-A17).$$

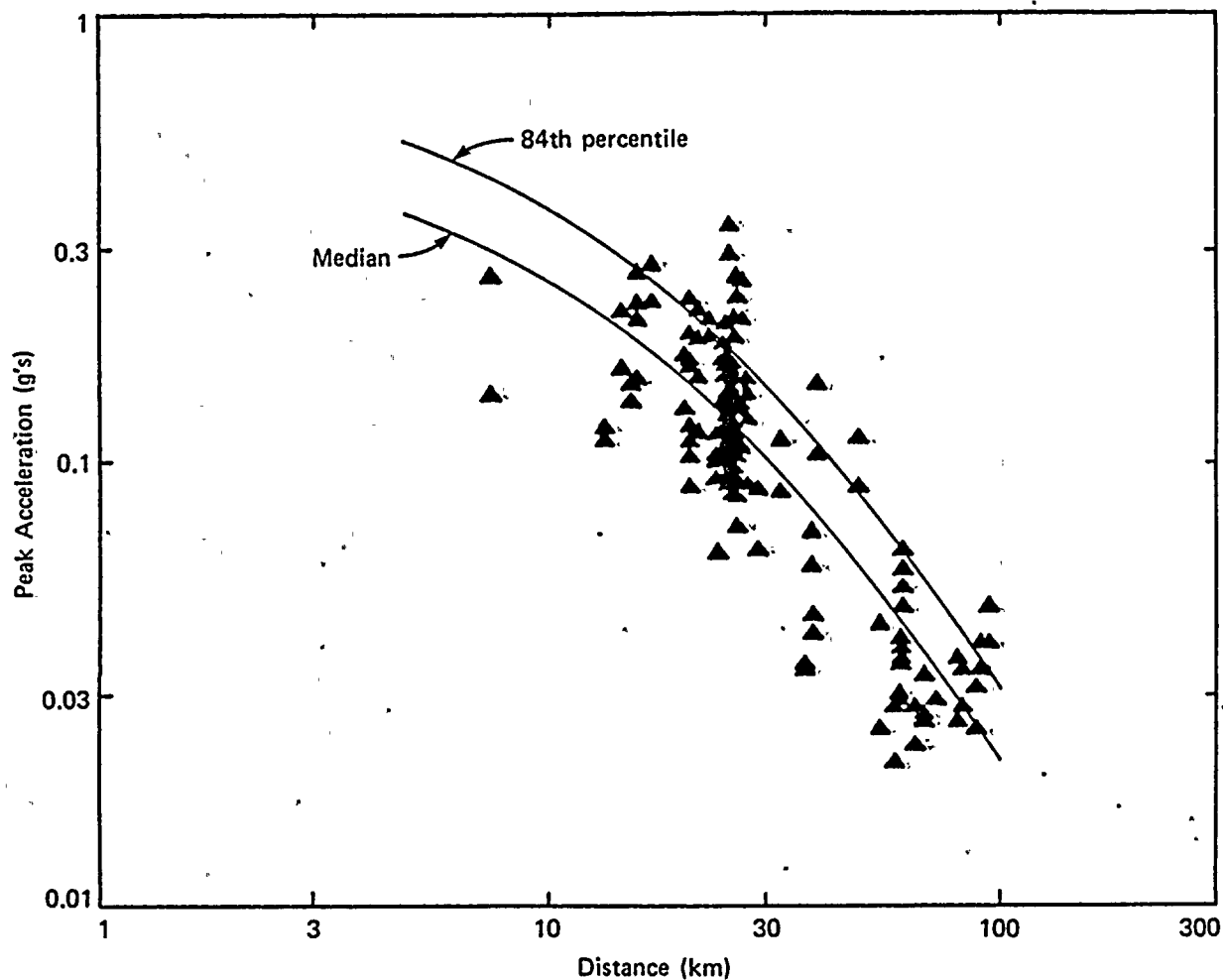
Equations (2.5K-A14) through (2.5K-A16) describe somewhat higher standard deviations than the standard deviations for peak acceleration [Equations (2.5K-A8) and (2.5K-A9)]. The higher standard deviations for response spectral values relative to those for peak acceleration have been estimated based on the statistical analyses of data for  $M_S = 6.5$ .



Project No. 14940	Hanford FSAR	REGRESSION ANALYSIS RESULTS FOR SAN FERNANDO EARTHQUAKE PRIMARY DATA SET	Figure 2.5K-A1
Woodward-Clyde Consultants			







Project No.  
14940

Hanford FSAR

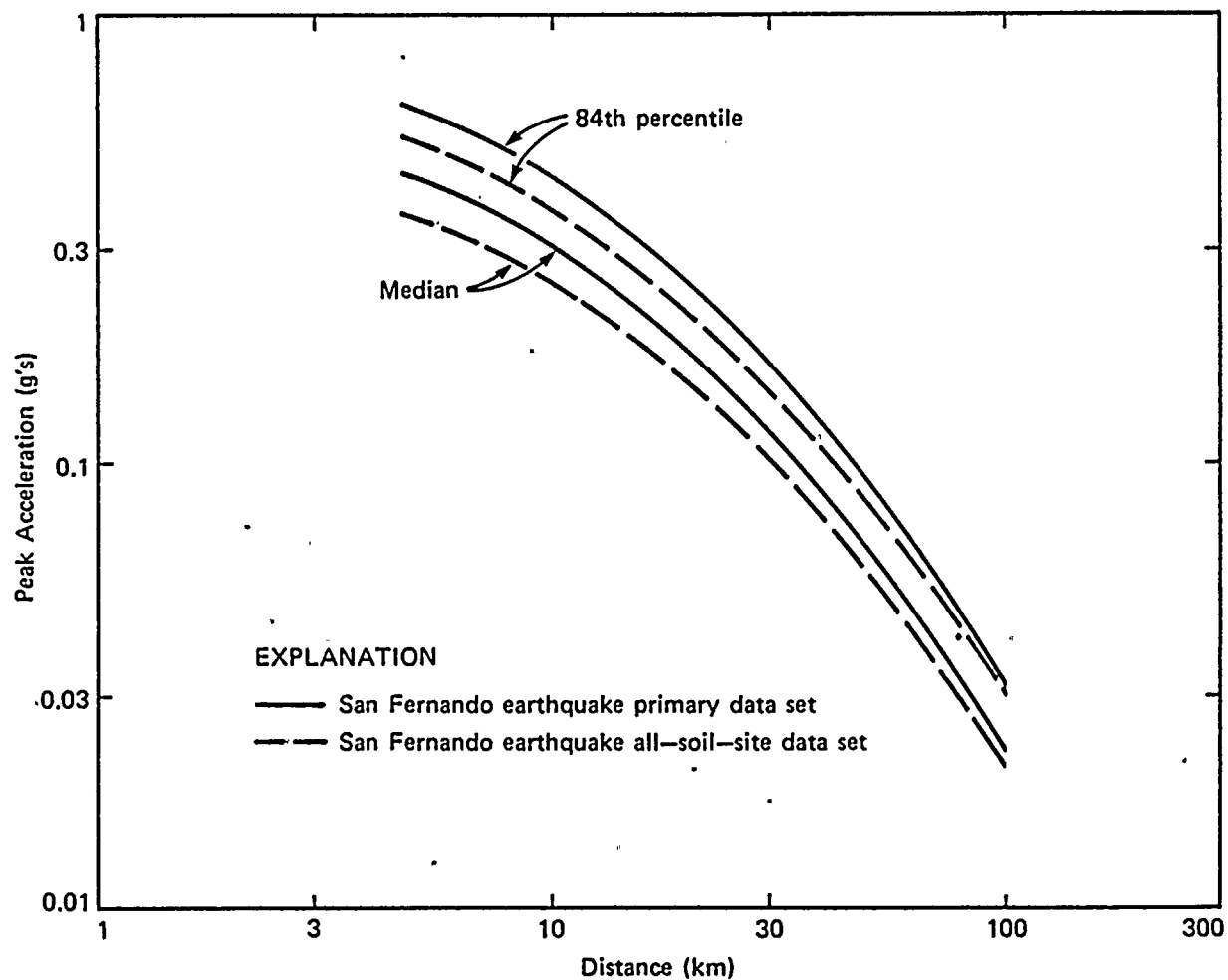
REGRESSION ANALYSIS RESULTS FOR  
SAN FERNANDO EARTHQUAKE  
ALL-SOIL-SITE DATA SET

Figure  
2.5K-A2

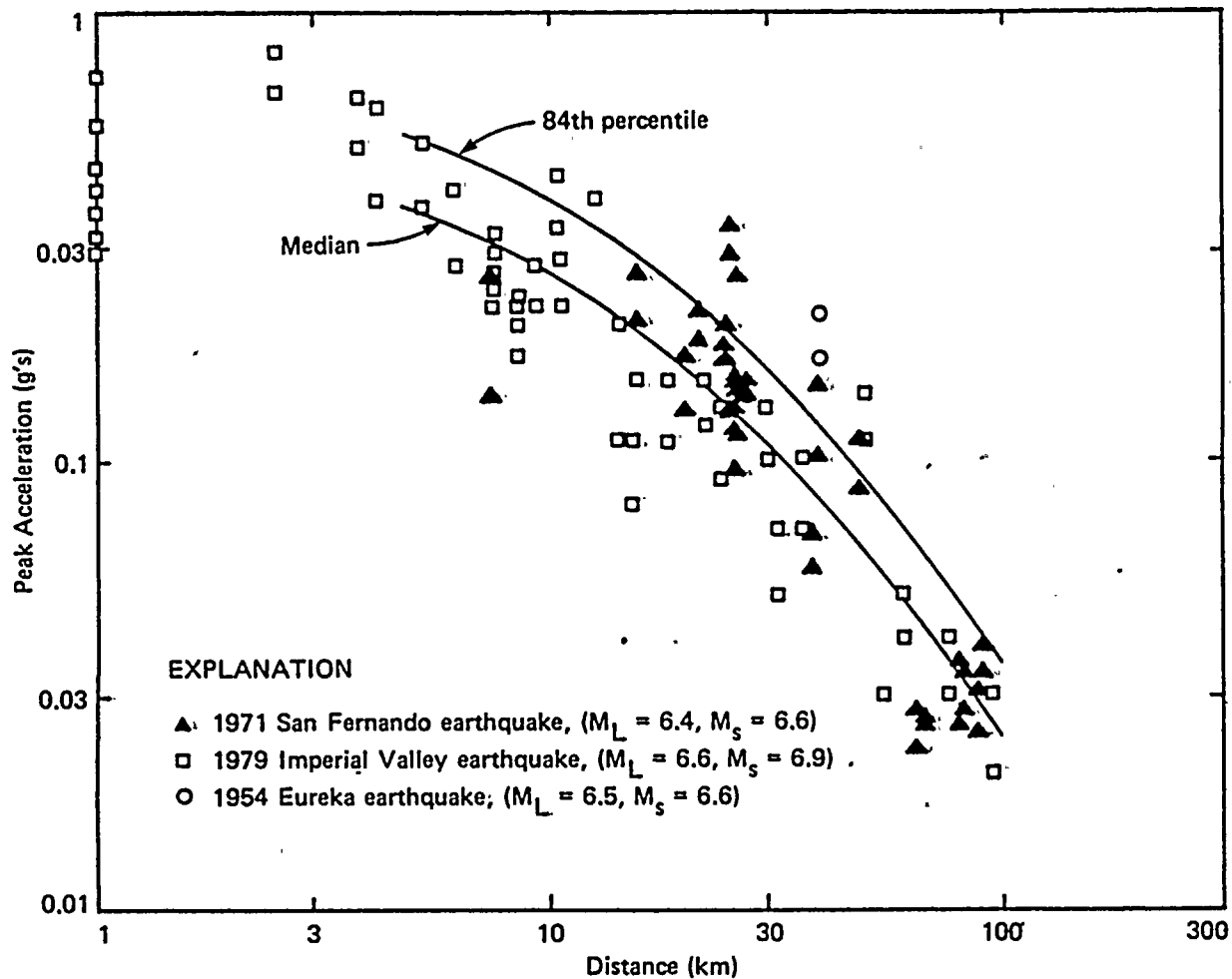
**Woodward-Clyde Consultants**

WNP-2 Amendment No. 18  
September 1981

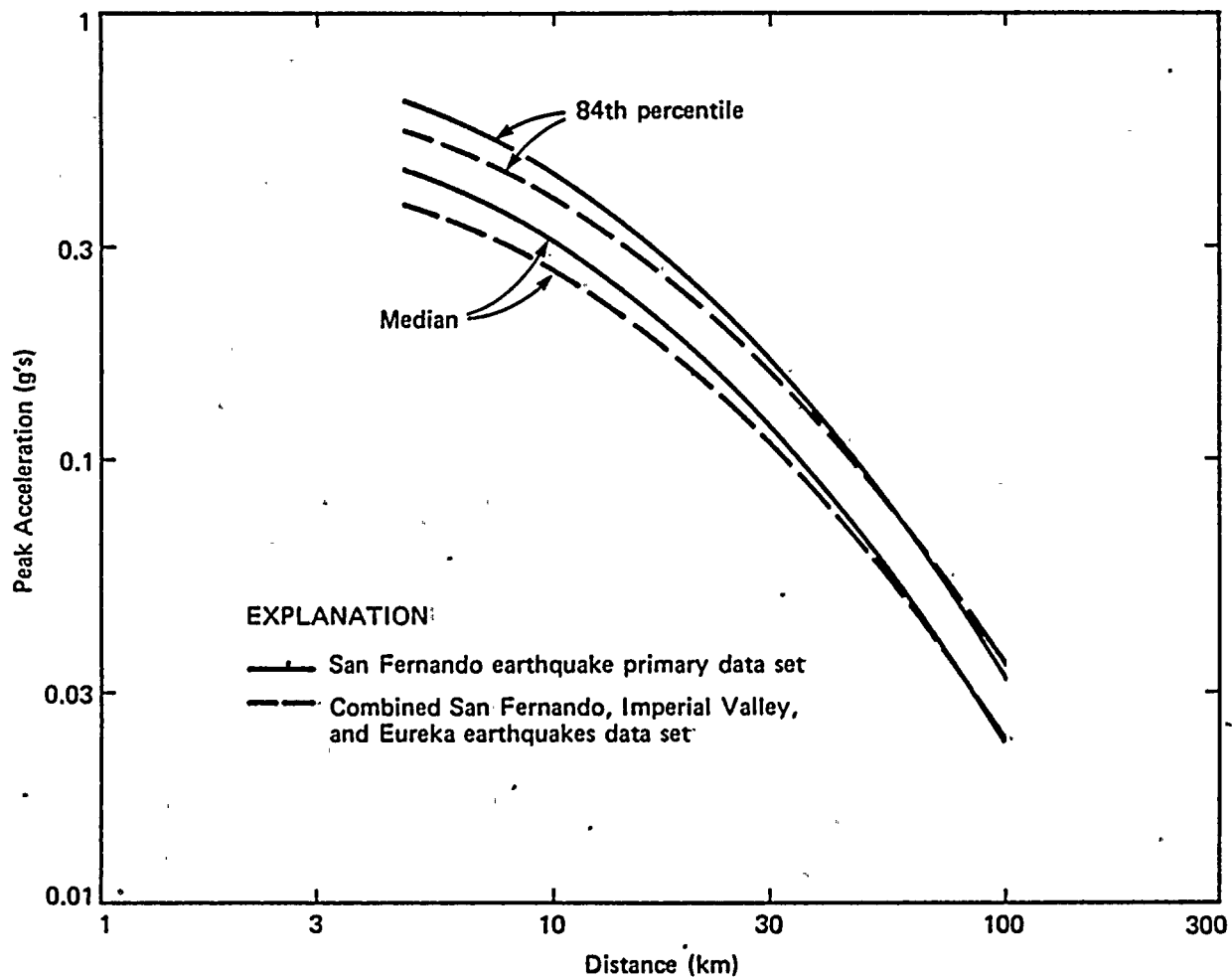




Project No. 14940	Hanford FSAR	COMPARISON OF REGRESSION RESULTS FOR TWO DATA SETS FROM THE SAN FERNANDO EARTHQUAKE	Figure 2.5K-A3
Woodward-Clyde Consultants			



Project No. 14940	Hanford FSAR	REGRESSION ANALYSIS RESULTS FOR DATA SET FROM SAN FERNANDO, IMPERIAL VALLEY, AND EUREKA EARTHQUAKES	Figure 2.5K-A4
Woodward-Clyde Consultants			



Project No.  
14940

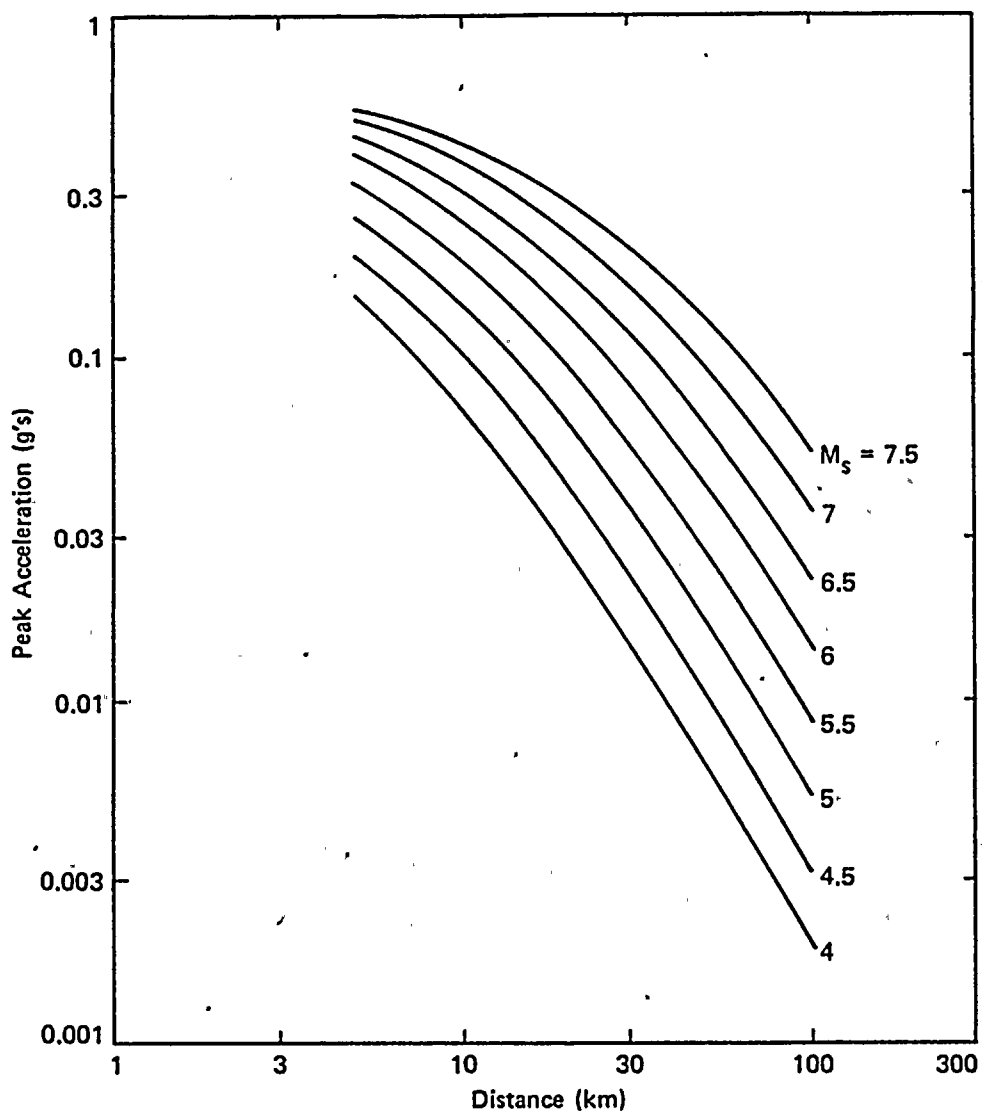
Hanford FSAR

**Woodward-Clyde Consultants.**

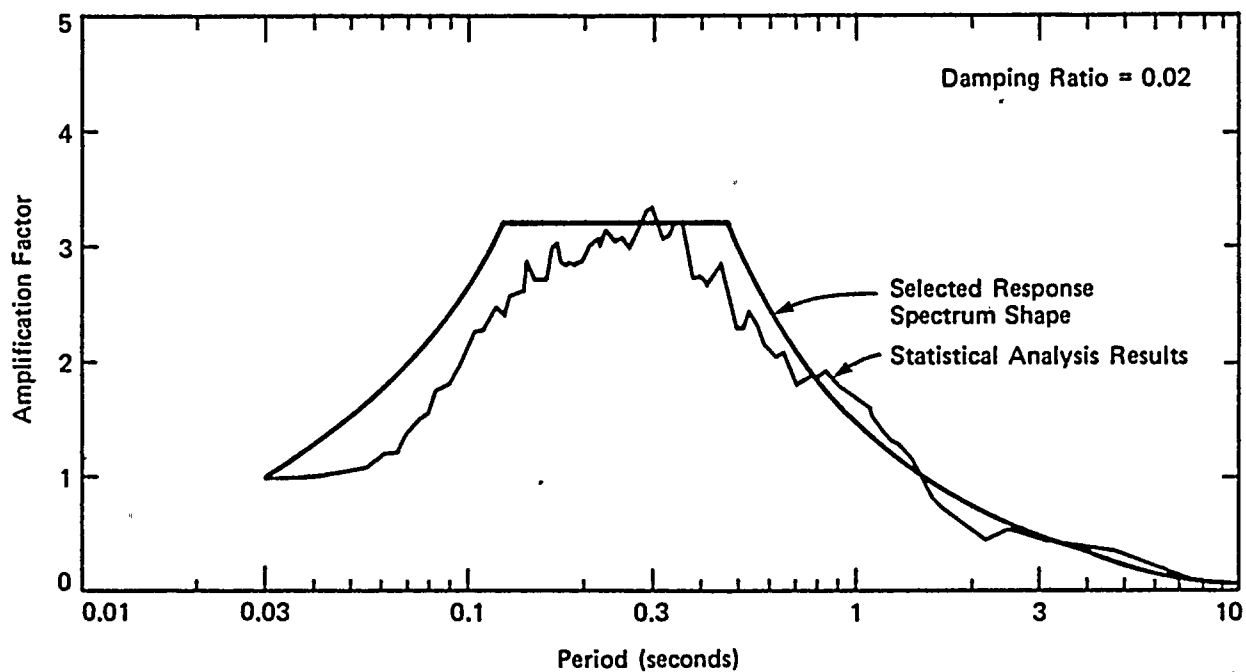
COMPARISON OF REGRESSION RESULTS FOR  
TWO DATA SETS FROM SAN FERNANDO,  
IMPERIAL VALLEY, EUREKA EARTHQUAKES

Figure  
2.5K-A5

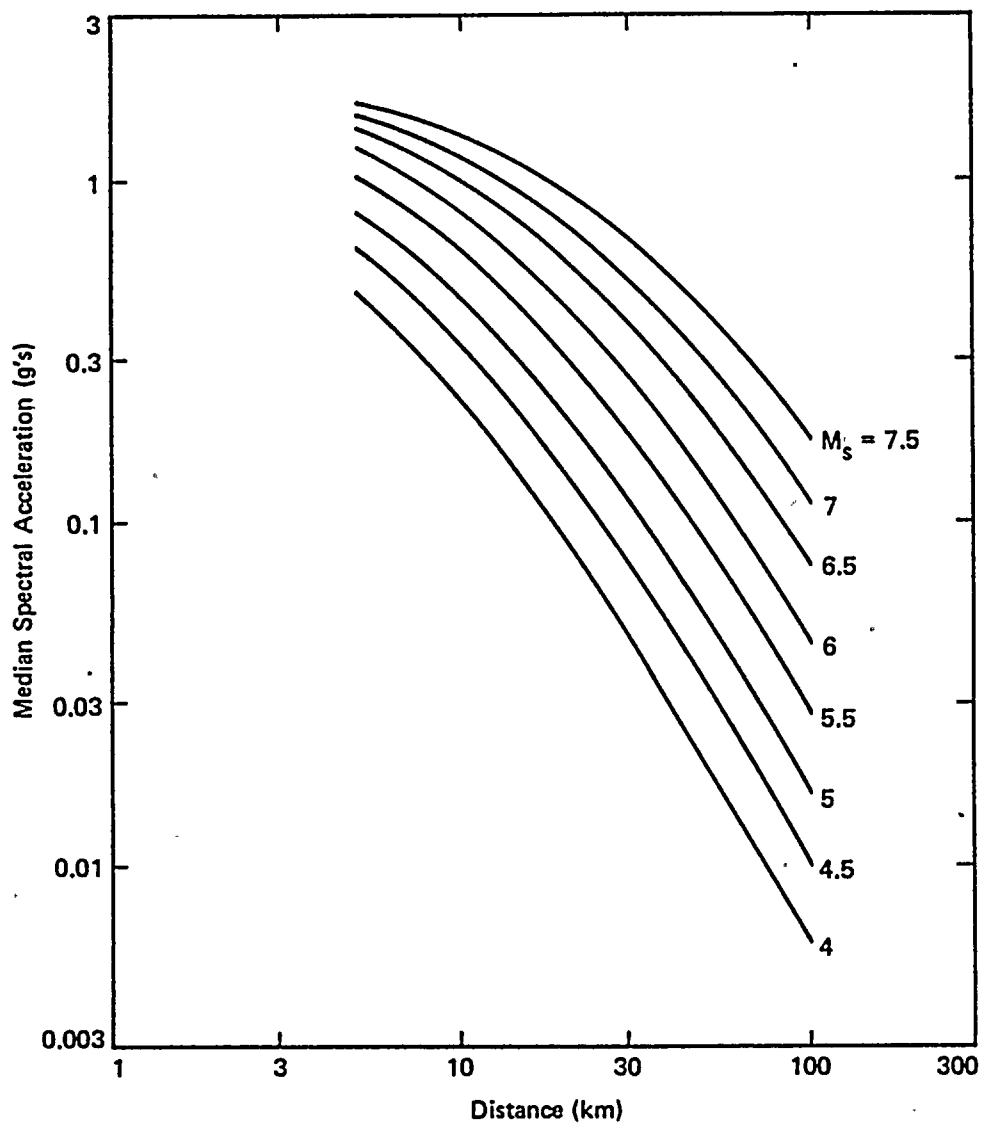
WNP-2 Amendment No. 18  
September 1981



Project No. 14940	Hanford FSAR	SELECTED ATTENUATION RELATIONSHIPS FOR PEAK ACCELERATION	Figure 2.5K-A6
Woodward-Clyde Consultants			



Project No. 14940	Hanford FSAR	COMPARISON OF STATISTICAL ANALYSIS RESULTS WITH SELECTED RESPONSE SPECTRUM SHAPE FOR $M_s = 6.5$	Figure 2.5K-A7
Woodward-Clyde Consultants			

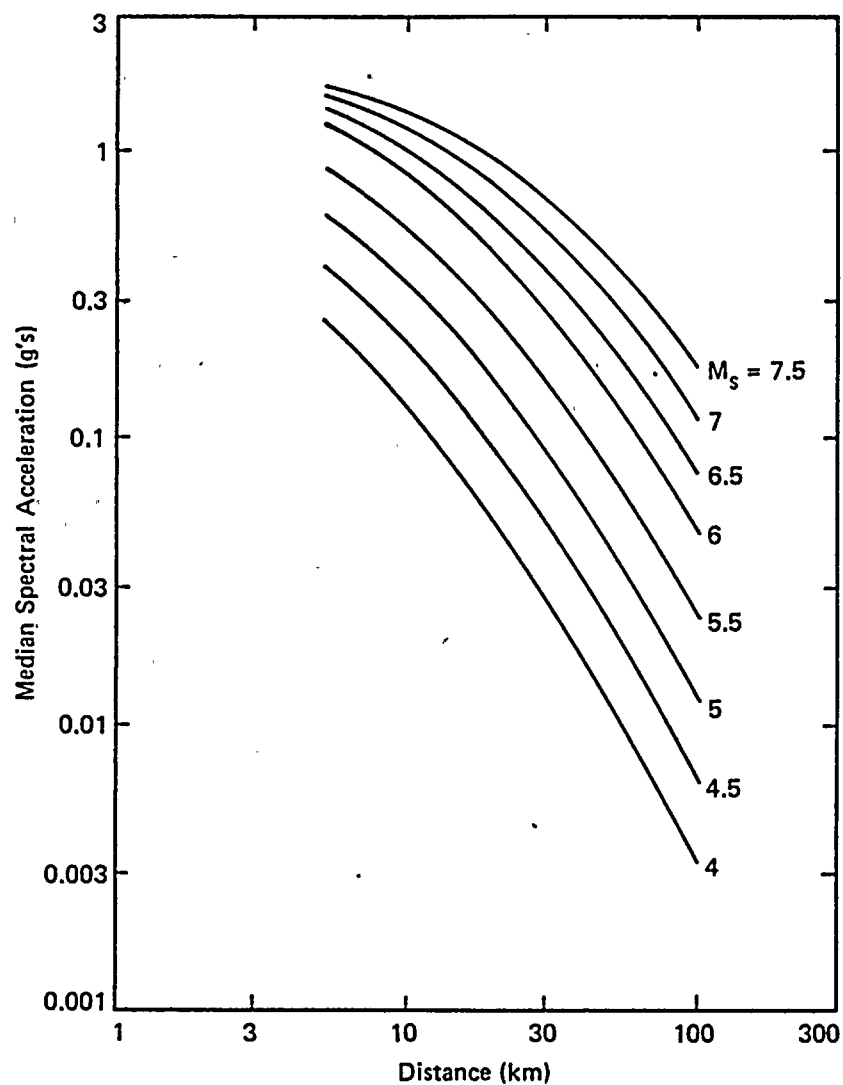


Project No. 14940	Hanford FSAR	SELECTED ATTENUATION RELATIONSHIPS FOR RESPONSE SPECTRAL ACCELERATION (2% damping) at Period = 0.125 sec.	Figure 2.5K-A8
Woodward-Clyde Consultants			

WNP-2 Amendment No. 18  
September 1981







Project No. 14940	Hanford FSAR	SELECTED ATTENUATION RELATIONSHIPS FOR RESPONSE SPECTRAL ACCELERATION (2% damping) at Period = 0.40 sec.	Figure 2.5K-A9
Woodward-Clyde Consultants			



APPENDIX 2.5L

COMPILATION AND INTERPRETATION OF GRAVITY IN WASHINGTON,  
OREGON, IDAHO AND ADJACENT PARTS OF BRITISH COLUMBIA

Prepared by  
WESTON GEOPHYSICAL CORPORATION  
September 1981

APPENDIX 2.5LTABLE OF CONTENTS

	<u>Page</u>
1.1 INTRODUCTION	2.5L-1
2.1 SUMMARY AND CONCLUSIONS	2.5L-1
2.1.1 GENERAL	2.5L-1
2.1.2 HANFORD 1° AREA	2.5L-2
2.1.3 PASCO-WALLA WALLA AREA	2.5L-2
2.1.4 Pacific Northwest Area	2.5L-4
2.1.5 COMPARISON OF GRAVITY WITH SEISMICITY AND AEROMAGNETIC ANOMALIES	2.5L-5
3.1 DATA BASE	2.5L-5
4.1 DATA REDUCTION	2.5L-7
5.1 OTHER DATA	2.5L-8
6.1 INTERPRETATION OF GRAVITY MAPS	2.5L-8
6.1.1 HANFORD 1° AREA	2.5L-8
6.1.1.1 Introduction	2.5L-8
6.1.1.2 Interpretation of Total Bouguer in the Hanford 1° Map Area Anomaly	2.5L-9
6.1.1.3 Interpretation of Regional Bouguer Anomaly in the Hanford 1° Map Area	2.5L-9
6.1.1.4 Interpretation of Residual Bouguer Gravity Anomalies in the Hanford 1° Map Area	2.5L-9
6.1.2 PASCO-WALLA WALLA AREA	2.5L-11
6.1.2.1 General-Pasco-Walla Walla Area	2.5L-11
6.1.2.2 Interpretation of the Total Bouguer Gravity Anomaly Map in the Pasco-Walla Walla Area	2.5L-11

TABLE OF CONTENTS (Continued)	<u>Page</u>
6.1.2.3 Interpretation of the Regional Bouguer Gravity Anomaly Map in the Pasco-Walla Walla Area	2.5L-12
6.1.2.4 Interpretation of the Residual Gravity Anomalies in the Pasco-Walla Walla Area	2.5L-12
6.1.2.4.1 Wallowa Mountains	2.5L-12
6.1.2.4.2 Blue Mountains Anticline	2.5L-13
6.1.2.4.3 Grande Ronde Valley	2.5L-13
6.1.2.4.4 A Major Buried Rock Mass in Central Columbia Plateau	2.5L-14
6.1.2.4.5 Yakima Basin	2.5L-16
6.1.2.4.6 Pasco and Quincy Basins	2.5L-16
6.1.2.4.7 Chiwaukum Graben	2.5L-16
6.1.2.4.8 Olympic-Wallowa-Lineament	2.5L-16
6.1.2.5 Comparison of Gravity Maps with Aeromagnetic and Seismicity Maps of Pasco-Walla Walla Area	2.5L-17
6.1.3 PACIFIC NORTHWEST MAPS	2.5L-18
6.1.3.1 General - Pacific Northwest Maps	2.5L-18
6.1.3.2 Interpretation of the Total Bouguer Anomaly Map for the Pacific Northwest Map Area	2.5L-18
6.1.3.3 Interpretation of the Regional Bouguer Anomaly Map for the Pacific Northwest Map Area	2.5L-19
6.1.3.4 Interpretation of Residual Gravity Anomalies for the Pacific Northwest Map Area	2.5L-19
7.1 REFERENCES	2.5L-21

TABLE OF CONTENTS (Continued)		<u>Page</u>
TABLE 1	GRAVITY MAP	2.5L-22
TABLE 2	SOURCE OF GRAVITY DATA	2.5L-23
ATTACHMENT I	GEOLOGIC MODELS IN THE COLUMBIA PLATEAU CONSTRAINED BY GRAVITY DATA	2.5L-34

APPENDIX 2.5LLIST OF FIGURES

<u>Number</u>	<u>Title</u>
2.5L-1	Hanford 10 Area. Index Map. Station location map.
2.5L-2	Hanford 10 Area. Total Bouguer gravity anomaly map.
2.5L-3	Hanford 10 Area. Overlay for gravity maps.
2.5L-4	Hanford 10 Area. Regional Bouguer gravity anomaly map.
2.5L-5	Hanford 10 Area. Residual Bouguer gravity anomaly map.
2.5L-6	Effect of density on total Bouguer gravity anomaly.
2.5L-7	Bedrock topography for Hanford Reservation.
2.5L-8	Pasco-Walla Walla Area. Station location map.
2.5L-9	Pasco-Walla Walla Area. Total Bouguer gravity anomaly.
2.5L-10	Pasco-Walla Walla Area. Regional Bouguer anomaly map.
2.5L-11	Pasco-Walla Walla Area. Residual Bouguer gravity anomaly map.
2.5L-12	Pasco-Walla Walla Area. Interpretation overlay for gravity maps.
2.5L-13	Dayton-Weller Butte Area, Washington. Total Bouguer gravity map.
2.5L-14	Dayton-Weller Butte Area, Washington. Station location map.
2.5L-15	Dayton-Weller Butte Area, Washington. Overlay for gravity map.
2.5L-16	Gravity Profile AA', Dayton-Weller Butte Area, Washington.



APPENDIX 2.5LLIST OF FIGURES (Continued)

<u>Number</u>	<u>Title</u>
2.5L-17	Grande Ronde Area, Washington. Total Bouguer gravity anomaly map.
2.5L-18	Grande Ronde Area, Washington. Station location map.
2.5L-19	Model Strike-Slip Faults.
2.5L-20	Model for strike-slip fault computations.
2.5L-21	Pacific Northwest. Station location map.
2.5L-22	Pacific Northwest. Total Bouguer gravity anomaly map.
2.5L-23	Pacific Northwest. Regional Bouguer gravity anomaly map.
2.5L-24	Pacific Northwest. Residual Bouguer gravity anomaly map.
2.5L-25	Aeromagnetic Map for Pasco-Walla Walla Area.
2.5L-26	Earthquake epicenters for Pasco-Walla Walla Area.

## 1.1 INTRODUCTION

Spatial variations in the earth's gravity field can be used to constrain models of the distribution of density inside the earth. Therefore, gravity maps provide information on (1) rock types that exist below the surface of the earth, (2) their size, and (3) their three-dimensional shape even though completely hidden. Not only can the presence of certain faults be detected, but their displacements within limitations can be measured. In favorable circumstances, even the nonexistence of faults can be demonstrated unequivocally (also within the limits of resolution posed by station spacing and various sources of noise).

The value of gravity, after removing the known effects of elevation and latitude, is termed Bouguer gravity anomaly. The geologic interpretation of gravity is facilitated by separating this Bouguer anomaly into two parts. One part, termed the residual gravity anomaly, contains relatively large gradients and is due solely to relatively shallow masses. The second part, regional anomaly, is caused primarily by the relatively deeper masses.

## 2.1 SUMMARY AND CONCLUSIONS

### 2.1.1 GENERAL

Gravity data for about 85,000 stations in Washington, Oregon, and parts of adjacent Idaho and British Columbia were compiled and adjusted to a common datum. Within the areas of the Hanford 1° and Pasco-Walla Walla maps, the following new gravity stations were established: 2,000 for the Supply System; 10,000 for Northwest Energy Services Company.

Three sets of maps were prepared with different contour intervals and different scales. Each set consists of a total, a residual and a regional Bouguer anomaly map. The data for each map are given in Table 1.

Gravity anomalies correlate well in many areas with geographic features, mapped geologic rock types and structures, aeromagnetic anomalies, and epicentral distribution of earthquakes. However, not every feature in each field has an expression in the gravity map nor does every feature in the gravity map correspond to some feature in each of the other maps.

### 2.1.2 HANFORD 10 AREA (FIGURES 1 THROUGH 5)

The Hanford 10 maps (Figures 1 - 5) extend from 119°00' to 120°07 1/2' west longitude and from 46°07 1/2' to 46°48' north latitude. Pasco is situated in the southeast corner, Ginko State Park in the northwest corner. The maps (Figures 2, 4, and 5) show the gravity anomalies for the Hanford Reservation and environs at 1 or 2 mgal contour intervals.

Contours on a relatively steep gravity gradient trend parallel to the Columbia River from Taylor Flats to White Bluffs, a distance of approximately 16 kilometers (Figures 2 and 3). This feature is due primarily to the use of 2.67 gm/cm<sup>3</sup> for the density in preparation of the Bouguer gravity maps when the density of the material east of the river above the basalt is less. It is an artifact and does not indicate geologic structure.

In the region 0.6 kilometer south of Gable Butte/Gable Mountains, a known bedrock high produces a small positive residual gravity anomaly.

The gravity anomaly associated with the Rattlesnake Hills anticline can be used to constrain estimates of the maximum vertical displacement of the small faults which have been mapped geologically at the surface. Although no feature in the gravity data indicates the presence of a fault at the base of the basalt, the minimum recognizable vertical displacement is approximately 100 meters. The minimum recognizable horizontal displacement (discussed in section Pasco-Walla Walla area) is 2-3 kilometers. Both estimates are limited by the resolution of the gravity method. The actual values of displacement could be zero.

### 2.1.3 PASCO-WALLA WALLA AREA (FIGURES 8 THROUGH 18)

This area is bounded by 117° and 121° west longitude and by 45° and 47°30' north latitude and includes the Hanford 10 area.

A strong gravity anomaly is associated with the Wallowa Mountains. The rocks of the Wallowa Mountains probably extend westward in the subsurface below the Columbia basalts to the eastern edge of the Grande Ronde Valley.

The Grande Ronde Valley is coincident with a gravity low. The gravity low in Grande Ronde Valley is interrupted in many localities by small residual gravity anomalies of small areal extent.

The Blue Mountains Anticline is marked by prominent gravity anomalies - a gravity low north of Grande Ronde and a gravity high near Ukiah, Oregon. The rock that forms the core of this anticline therefore changes type along the axis of the anticline.

The prominent gravity gradient that is apparent in the total Bouguer anomaly map and extends northeasterly across the area from Fossil, Oregon, to Tekoa, Washington, is most likely not reflective of structure. The residual gravity anomaly map supports the opinion that this apparent feature is due to the locations of several different anomalous masses.

Neither the Pasco Basin nor the Quincy Basin correlates with any obvious residual gravity anomaly. Either the density contrasts of the material filling the basins do not differ significantly from the surrounding basalt or the material is quite thin. The eastern and western margins of both basins and the northern boundary of the Quincy Basin coincide approximately with the edge of a buried rock mass, termed Layer 2 and discussed below.

The gravity maps (Figures 9 and 11) show that a relatively dense rock mass underlies the Columbia Plateau basalt (Figure 12). The surface layer, termed Layer 1, is relatively thin (0 to 2 km), extends over a larger geographic area, and apparently completely covers the lower body termed Layer 2. The presence of several geologic structures (such as the Chiwaukum and Republic grabens), below the upper layer and outside Layer 2 can be recognized from the gravity maps. Layer 2 is much thicker than the upper Layer 1, is roughly tabular (NS dimension, 93 kilometers, and EW dimension, 47 kilometers) and has two subsurface lobes on its southern end. One lobe extends SW for approximately 31 kilometers. The other lobe extends from Wallula to Walla Walla, a distance of about 31 kilometers also. The gravity expression for Layer 2 appears to be quite uniform and the edge appears to have been unbroken by any significant strike-slip faulting or other geologic structures since the layer was formed. Layer 2 is inferred to consist of extrusive rocks that filled an elongate subsiding basin.

The western edge of Layer 2 is the source of a prominent gravity gradient that trends almost north-south for 50 kilometers, extends from south of Toppenish Ridge to north of Quincy (WA). The anomaly passes about 9 kilometers east of Yakima and is extraordinarily straight. Models have been used to obtain an upper bound on the horizontal



displacements of any potential faults that may have occurred since the time of emplacement of Layer 2 (Figures 19 and 20). With the present station spacing, the maximum horizontal displacement that could have occurred on any fault, or could have been distributed over any fault zone crossing the feature, is 2-3 kilometers. This conclusion is independent of the origin of the anomalies, the age of the rocks that occur in the area, and specific models of the distribution of density. Models also yield additional constraints on the timing of any horizontal displacement. The minimum time span would be 17 m.y. (the age of the oldest basalt of the area) and the maximum time span could be as old as the age of basement rocks.

The Olympic-Wallowa lineament (OWL) proposed by Skehan and others (1965) previously as a major crustal (and possibly mantle) structure is at most a very minor feature if it exists at all. Neither residual gravity anomaly nor gravity linear is associated with it. It would cross necessarily the western edge of the lower Layer 2, but does not produce any obvious disruption of that body. The maximum vertical displacement that can be discerned by this data set is 300 feet and is located in the vicinity of Pasco. Maximum horizontal displacement during the past 17 m.y. (and possibly much longer) that can be discerned with this data set is 2-3 kilometers.

Known geologic structures that correlate with gravity anomalies include the Yakima Basin, Badger Mountains Anticline, and a structure north of Crab Creek (Frenchman Hills). A few prominent features in the gravity map do not appear to correlate with any known geologic features.

#### 2.1.4 PACIFIC NORTHWEST AREA (FIGURES 22 THROUGH 25)

This large geographic area extends from 117° west longitude to the Pacific coast and from 42° to 52° north latitude. It includes Oregon, Washington, and parts of British Columbia and Idaho. In this area, most gravity anomalies and many gravity linears appear to correlate well with mapped rock masses and geologic structures.

A strong fabric is present in the gravity maps and is attributed to the present geologic fabric of the area. The trend of the fabric, as well as the pattern, differ significantly east and west of a north-south line that coincides approximately with the Straight Creek Fault and its extensions. It is a distinct possibility that the Straight Creek Fault may be the surface expression of a fundamental crustal (and possibly upper mantle) structure.

### 2.1.5 COMPARISON OF GRAVITY WITH SEISMICITY AND AEROMAGNETIC ANOMALIES

Earthquake epicenter maps and aeromagnetic anomaly maps have been compared with the gravity maps for Hanford 1° and Pasco-Walla Walla areas.

Examples of the more prominent features present on both the gravity and aeromagnetic maps are the following: (1) the Wallula-Walla Walla gravity linear (due to the postulated Walla Walla lobe of the lower basalt body) and a significant change in the character of the magnetic field; (2) a north northwesterly trending, broad gravity (gradient) linear that passes near Ice Harbor Dam and prominent magnetic linears (which have been attributed to dikes) (Swanson et al, 1978); and (3) gravity and magnetic anomalies at Horse Lake Mountain (ca. 10 kilometers west of Wenatchee).

The Saddle Mountains are marked by seismicity and magnetic anomalies but have no significant gravity expression on east and central sections. The magnetic anomaly can be traced continuously to anomalies east of Pasco that do not correlate with a linear-trending gravity anomaly. Our interpretation of the relationships indicates that the seismic activity along the Saddle Mountains should be confined to that structure.

Examples of aseismic features that have gravity expressions are the Blue Mountains Anticline and a prominent gravity gradient that extends from Fossil, Ore, to Tekoa Ore.

Some gravity anomalies appear to be associated with seismicity. For example, a dozen epicenters have been located near the boundary of the causative body of the gravity anomaly centered on Little Goose Lock and Dam.

### 3.1 DATA BASE

The approximate number of stations and the number of individual surveys for each set of maps are given in Table 1.

A complete listing of the sources of all gravity data is given in Table 2. The data compilations from secondary sources (National Oceanographic and Atmospheric Administration; Earth Physics Branch of the Dominion Observatory; Oregon State University; and Dr. Frank Danes, University of Puget Sound) were supplemented with data obtained from additional primary sources. About 2,000 new stations have been occupied by Weston Geophysical (1979a)





for the Supply System. An additional 8,000 stations occupied by Weston Geophysical for Northwest Energy Services Company have been included.

Because different surveys established at different periods of time and with instruments of differing characteristics may vary significantly, adjustments have been made in the levels of the individual surveys to bring them into general coincidence. These adjustments involved changing the observed gravity for all stations in a single survey by an amount that did not exceed a few milligals. No other corrections were applied to individual stations except for sign changes, that were obvious. For example, a station with a value of +60 mgals in the midst of two dozen stations with values in the neighborhood of -60 mgals would be changed to -60.

A few stations were deleted. However, the criteria for deletion differed for the three sets of maps. For the Hanford 10 map, stations whose elevations differed by more than 100 feet from the elevation shown on the most recent available topographic map (15 feet or 7 1/2 feet) were deleted. Approximately 200 stations established by Peterson (1965) were not used because of uncertainty in locations that exceeded 1,000 feet. Several stations that were suspected of having incorrect values were reoccupied and new values established.

The locations and elevations of the gravity stations established for Northwest Energy Services Company (NESCO) were surveyed and are believed to be accurate to at least 0.1 feet. Because elevation and latitude are the chief sources of uncertainty in Bouguer gravity anomalies, the NESCO stations are considerably more precise than the other stations. In addition, the spacing between NESCO stations is rather small. Therefore, all other stations within the areas studied gravitationally for NESCO were deleted from the data base used for the present study.

For the Pasco-Walla Walla map, those stations whose elevations differed by more than 1,000 feet from the values given on the most recent topographic maps and those stations whose Bouguer gravity values differed by five mgals or more from the value expected on the basis of adjacent stations were not utilized. If such stations had been retained in the data base without modification, they would have probably resulted in single-point gravity anomalies that exceeded five mgals (in the residual gravity anomaly). Although such anomalies may be real, they appear to be unlikely and were



eliminated from the present gravity maps. A few stations whose values were suspected of being incorrect were reoccupied and new values established.

For the Pacific Northwest map, only those specific stations whose values differed by more than 20 mgals from the value expected on the basis of adjacent stations were deleted.

The quality and spacing of the data are therefore adequate for the most part to contour maps of the earth's gravity field at intervals of one, two, and four mgals for the Hanford 10, Pasco-Walla Walla, and the Pacific Northwest maps, respectively. In the northeast corner of the Pacific Northwest map area, the data are inadequate for four mgal contours and the contours have been omitted in that region.

#### 4.1 DATA REDUCTION

The Bouguer gravity anomaly at a given gravity station was calculated from the following equation:

$$g_{BA} = g_{OBS} - g_{theor} - Ah + 2\pi G\rho h + TC$$

where  $g_{BA}$  = Bouguer anomaly,  
 $g_{OBS}$  = observed gravity,  
 $g_{theor}$  = theoretical gravity,  
 $A$  = rate of change of gravity with elevation,  
 $G$  = universal gravitational constant,  
 $\rho$  = density,  $2.67 \text{ g/m}^3$ ,  
 $h$  = elevation of the observation in meters,  
 $TC$  = terrain correction.

The theoretical gravity is obtained from the equation

$$g_{theor} = 978,031.85 (1 + .005278895 \sin^2 \theta + .000023462 \cdot \sin^4 \theta) \text{ where } \theta = \text{latitude.}$$

The Bouguer anomalies were corrected for terrain effects if the original survey contained the numerical values of the terrain effects.

The Bouguer gravity field was separated into two parts - residual gravity and regional gravity anomaly. The regional gravity anomaly at a point was calculated to be the average of the Bouguer gravity anomaly over a circular region of 80 kilometers diameter centered on the point. The residual gravity anomaly was calculated as the numerical difference between the Bouguer gravity value at the point and the regional gravity anomaly at the point. The effect of this separation is to place the portion of the gravity anomaly in the residual gravity anomaly map that corresponds to the

effects of masses relatively near the earth's surface and to place that portion of the gravity anomaly in the regional Bouguer gravity anomaly map that corresponds to masses that may be located at a greater depth in the earth.

## 5.1 OTHER DATA

The interpretation of gravity maps in terms of geologic models was improved significantly by comparing the gravity anomaly maps with maps of other types of data. More specifically, the seismicity map contained in the WNP 1/4 PSAR, Amendment 23 (Washington Public Power Supply System, 1977), the aeromagnetic maps and various geologic maps (Washington Public Power Supply System, 1977, and Swanson et al, 1977) were used.

## 6.1 INTERPRETATION OF GRAVITY MAPS

### 6.1.1 HANFORD 10 AREA

#### 6.1.1.1 Introduction

Approximately 10,000 stations from 31 different surveys were used. The average station spacing was 2 1/2 kilometers with variations from about 0.1 kilometer per station in several high density areas to as much as 10 kilometers between a few widely scattered stations. A significant fraction of the DOE Hanford Reservation part of the area is now covered with stations located on grids with spacing of 0.6 kilometer or less. Station locations are shown in Figure 1.

Several new stations in the area were established in 1979 by the Supply System. Three-fourths of the stations originally established by Peterson (1965) were used in the present compilation. However, the exact locations of about 200 of Peterson's stations could not be determined from his field notes with a precision of better than 1,000 feet and, were therefore not used.

Approximately 8,000 new stations were established by Weston Geophysical for the Northwest Energy Services Company (NESCO) in 1980 and 1981. Most of those stations were located on the Hanford Reservation; a few of them were east of the Columbia River and outside the Reservation. Locations and elevations were surveyed.

The precision of the Bouguer gravity anomaly at individual stations depends upon the survey and is divided into three groups. In the first group are the NESCO stations with a precision of about 0.1 mgal, a value determined by

re-occupation of stations that are common to two different gravity profiles. No station within the area of the NESCO stations on the Reservation established in other surveys was used in this study. In the second group are the Peterson (1965) stations. They were located at benchmarks and their precision is judged to be at least 0.25 mgals. In the third group are all other surveys. The average precision of the stations along high-density profiles is believed to be at least as good as 1/2 mgal. In general, those profiles were measured by a single field crew with a single gravimeter. More widely scattered stations were established by various individuals with different gravimeters, different base stations, and probably different values for the base stations. The precision of the stations that were not established along high-density profiles is believed to be no better than 1 mgal.

#### 6.1.1.2 Interpretation of Total Bouguer Anomaly in the Hanford 1<sup>0</sup> Map Area

The Hanford 1<sup>0</sup> total Bouguer gravity anomaly map (shown in Figure 2) has several prominent features in the gravity field; they are shown on Figure 3. These features are discussed in detail in the section on residual gravity anomaly for the Hanford 1<sup>0</sup> map area.

#### 6.1.1.3 Interpretation Regional Bouguer Anomaly in the Hanford 1<sup>0</sup> Map Area

The regional Bouguer gravity anomaly map, shown in Figure 4, most likely corresponds to density contrasts at a depth of 20 kilometers or more. For the preparation of this map, gravity data in an area much larger than the map shown on Figure 4 were used. The total area (approximately 200 kilometers by 200 kilometers) was centered on the area shown in Figure 4. Gentle warping of a crustal discontinuity, at a depth of 20 kilometers or more, was considered sufficient to produce the gravity anomalies present in the regional anomaly field. The regional gravity anomaly shown in Figure 4 is consistent with the regional gravity anomaly calculated previously (WPPSS, 1977) and therefore no additional interpretation or modeling was done.

#### 6.1.1.4 Interpretation of Residual Bouguer Gravity Anomalies in the Hanford 1<sup>0</sup> Map Area

The interpretation of the residual gravity anomalies was made from the residual gravity map, shown in Figure 5 and from the total Bouguer gravity map shown in Figure 2. In Area A (Figures 2 and 5) contours on a steep gradient trend



appear generally to parallel the Columbia River from the southern end of Taylor Flats to the northern end of White Bluffs, a distance of approximately 16 kilometers. This feature is most likely an artifact of the normal preparation of a Bouguer gravity anomaly map using a standard density of  $2.67 \text{ gm/cm}^3$ . The topographic surface of the land east of the river is 500 to 600 feet above the topographic surface of the land west of the river. The known surface geologic section, east of the Columbia River, consists primarily of silts, sands, and gravels of the Ringold Formation; some Pasco gravels; and possibly the Touchet Formation. The density of drained samples of this material is estimated to be 2.0 to  $2.3 \text{ gm/cm}^3$ . Thus, the four to five mgal residual gravity anomaly with a steep gradient along the Columbia River from Taylor Flats to White Bluffs is most likely due chiefly to the difference between the value of density used for the preparation of the Bouguer gravity anomaly maps and the actual density of the material in-situ. An elevation difference of 534 feet and density of  $2.0 \text{ gm/cm}^3$  would produce a gravity low of five mgals on a Bouguer anomaly map prepared with a density of  $2.67 \text{ gm/cm}^3$ .

In order to verify the foregoing hypothesis that the feature seen in Area A is in fact due to an artifact of the preparation of the gravity maps and not due to buried structure on, or in, the basalts, the effects of various "true densities" were calculated along a profile in the vicinity of Taylor Flats. They are shown in Figure 6. For densities of the sediments and sedimentary rocks that are present on the east side of the Columbia River and occur between the highest elevation within a few kilometers east of the river and the lowest elevation within a few kilometers west of the river of  $2.00$  to  $2.24 \text{ gm/cm}^3$  the maximum effect ranges from 4.0 to 1.5 mgals. Most of the residual anomaly is therefore attributable to the low density of the sediments and sedimentary rocks. In addition, on the basis of drilling done for NESCO by Golder Associates, Inc. and of interpretation of detailed gravity maps (scale of 1:12,000) done for NESCO by Weston Geophysical, the gentle dip accounts for 1-2 mgals of the residual gravity anomaly. We conclude that the residual gravity anomaly of Area A is not caused by structure.

Area B (Figure 3) shows a small anomaly of about five mgals. The number of stations in the area is very high and considered to be adequate to insure that the positive residual gravity anomaly that covers most of Area B is real. Comparison of the gravity map with the contoured top of bedrock map (shown in Figure 7), indicates general correspondence between this positive residual gravity

anomaly and a bedrock high. Portions of the bedrock high have been examined in detail by drilling by the Northwest Energy Services Company. The cause of this gravity anomaly is a combination of the variation in the elevation of the surface of the basalt and the density contrast between the basalt ( $2.6-2.8 \text{ gm/cm}^3$ ) and the overlying sediments and poorly consolidated sedimentary rock ( $2.0-2.4 \text{ gm/cm}^3$ ).

Contours in Area C (Figure 3) were omitted from the maps of Figures 2 and 5 because station coverage was considered inadequate for the preparation of a one mgal contour interval map.

Comparison of the gravity maps with Figure 7 (bedrock topography), shows rather good correspondence. The large bedrock high south of Gable Butte and Gable Mtn., the Southeast Anticline, Cold Creek Syncline, and associated anticline on the northeast side, the gentle slope in the vicinity of May Junction, and numerous small features all have corresponding expressions in the Bouguer gravity anomaly maps.

The gentle gravity gradient with contours that trend northwest in Area D is caused by a rock mass of relatively high density (probably mafic igneous rocks) that do not crop out but are buried a few kilometers everywhere. This rock mass is discussed further in Section 6.1.2.

Area E (Figure 3) includes a major anomaly with strong east-west gradient and contour lines that extend in a general north-south direction. The gravity field in this area places significant constraints on any geologic models of structures that have been proposed to cross the region. The interpretation of this area is discussed in Section 6.2.

#### 6.1.2 PASCO-WALLA WALLA AREA

##### 6.1.2.1 General - Pasco-Walla Walla Area

Approximately 16,000 stations from 31 different surveys were used for the Pasco-Walla Walla area. The average station spacing is 1.4 kilometers with variations from about 0.03 kilometer per station to as much as 15 kilometers between a few widely scattered stations. Station locations are shown in Figure 8.

##### 6.1.2.2 Interpretation of the Total Bouguer Gravity Anomaly Map in the Pasco-Walla Walla Area

The total Bouguer gravity anomaly map of the Pasco-Walla Walla area, shown in Figure 9, includes the effects of



density contrasts at all depths. This map has been interpreted together with the residual gravity anomaly map shown in Figure 11 (see Section 6.2.4).

#### 6.1.2.3 Interpretation of the Regional Bouguer Gravity Anomaly Map in the Pasco-Walla Walla Area

The regional Bouguer gravity anomaly map of the Pasco-Walla Walla area, shown in Figure 10, most likely corresponds to density contrasts at a depth of 20 kilometers or more. Gentle warping of a crustal discontinuity at that depth would be sufficient to produce the gravity anomalies present in the regional gravity field. The regional gravity anomaly shown in Figure 10 is consistent with the regional gravity anomaly previously calculated (WPPSS, 1977) and no additional modeling or interpretation was done.

#### 6.1.2.4 Interpretation of the Residual Gravity Anomalies in the Pasco-Walla Walla Area

The interpretation of the residual gravity anomalies was made from both the residual Bouguer gravity map and from the total Bouguer gravity map.

The residual gravity anomaly map, (Figure 11), appears to correlate well with known geology in many areas. The residual gravity therefore extends to the subsurface much of the geologic information that has been obtained from surface exposures and provides new insights into the distribution of rock masses in several areas that are entirely concealed by the Columbia River Basalts. The interpretation shown in Figure 12, can be used with both the total and residual gravity maps. The interpretation of several features that are present in both the total and residual gravity maps are discussed in the following paragraphs.

##### 6.1.2.4.1 Wallowa Mountains

The Wallowa Mountains appear to correlate well with a relatively strong gravity anomaly. Because this gravity anomaly, does not appear to be confined to the present known surface exposure of these rocks, the areal distribution of the rock type is shown in the overlay, Figure 12. The distribution is extended toward the northwest to the eastern edge of the Grande Ronde Valley, a distance of 10 kilometers from the nearest mapped surface exposure.



#### 6.1.2.4.2 Blue Mountains Anticline

The Blue Mountains Anticline appears to correlate well with residual gravity anomalies. However, along one portion (north of the Grande Ronde Valley), the residual gravity anomaly is negative, and along another portion (near Ukiah, Oregon), the residual anomaly is positive. Therefore, the predominant rock types that occur in the core of the Blue Mountains Anticline are most likely different in these two regions. The continuity of the Blue Mountains Anticline in the vicinity of Meacham, northwest of LaGrande, appears to be interrupted. The nature of the cross structure is unclear.

The northeastern end of the Blue Mountains Gravity Low was processed at a grid spacing of 0.6 kilometer and a contour interval of one mgal in order to facilitate investigation of features that did not show well in the two mgal Pasco-Walla Walla map. This area is designated Dayton-Weller Butte. The total Bouguer gravity map, station location map, and an interpretation overlay are shown in Figures 13, 14, and 15, respectively. The Hite fault (Shannon & Wilson, 1979) does not appear to have a significant gravity signature. Two small earthquakes thought to have occurred in the region have rather large uncertainties in their location and could be spatially correlated with either a mafic body identified from the gravity high in the northwest corner of the map or the Hite Fault. An anomalous gravity gradient appears to be present in the south-central region of the map. The gravity along profile AA' is shown in Figure 16. Possible interpretations of the very sharp gradient include a fault and a dike crossed by the profile.

#### 6.1.2.4.3 Grande Ronde Valley

The Grande Ronde Valley roughly coincides with a residual gravity low of 20 to 30 mgals and contains several very local anomalies of a few mgals amplitude and 1-2 kilometers width. The total Bouguer gravity map processed with 0.6 kilometer grid is shown in Figure 17. A station location map is shown in Figure 18. The small anomalies may be real even though they are based on single gravity stations. The valley is known from drilling data to contain sediments and unconsolidated sedimentary rocks. A thickness of 300-400 meters of material with a density contrast of  $1.0 \text{ gm/cm}^3$  appears to be consistent with the main residual gravity anomaly.



#### 6.1.2.4.4 A Major Buried Rock Mass in Central Columbia Plateau

The basalt of the Columbia Plateau is known to consist of a thick sequence of flows that extend in time backward to about 16-18 m.y. (Swanson et al, 1977). On the basis of the gravity maps for the Pasco-Walla Walla and the Hanford 10 areas, the Columbia Plateau basalts appear to cover an older rock mass of relatively high density (with respect to the adjacent rocks). The approximate outline of the body is shown in Figure 12. This rock mass is termed Layer 2. The gravity maps for this area show several notable features. First, the mapped edge of the basalts in many areas has a relatively small residual anomaly (zero-five mgals) associated with it. The basalt in those areas is most likely thin (80 meters/mgal plus the elevation of the surface for a density contrast of  $0.3 \text{ gm/cm}^3$ ). Second, inspection of the gravity maps reveals a prominent positive anomaly of 12 to 15 mgals amplitude that occurs entirely within the region of mapped basalt and extends north-south from approximately the Oregon-Washington state line to the Potholes Reservoir and east-west from Sunnyside to a few kilometers east of Richland. On the basis of this anomaly, we infer the presence of a relatively dense mass of rock (Layer 2) beneath the Columbia River basalts. There is no indication from the gravity data that this body would outcrop anywhere. Third, the relatively steep gravity gradient that trends east-west and extends from Wallula to a few kilometers south of Walla Walla is attributed to an eastward extension of Layer 2. Fourth, the broad gravity high centered roughly on Prosser and approximately outlined by the -56 mgal contour is attributed to a thickened section of Layer 2. Fifth, a lobe of the gravity anomaly that outlines Layer 2 extends southwest along the Columbia River to about 4 kilometers east of Goodnoe Hill and is attributed to a southwestern extension of the body.

Layer 2 is a large mass of rock of relatively high density. Its top is approximately 2 to 4 kilometers deep in the southern part and the unit is likely several kilometers thick. The product of thickness and density contrast is known unequivocally from the amplitude of the gravity anomaly. In addition, the maximum depth of the bottom of the unit is constrained by the width of the gravity anomaly associated with the edges of the body. The total anomalous mass of Layer 2 is  $7 \times 10^{18} \text{ gm}$ , a value that is independent of models and requires no assumption about density. If the density contrast is  $0.187 \text{ gm/cm}^3$ , a value determined from the "better fitting" models discussed in Section 6.1.2.4.6, then the volume occupied by Layer 2 is



37,000 kilometers<sup>3</sup>. However, the volume is sensitive to the density contrast. We have used a density contrast of +0.187. Values as small as 0.15 are marginally acceptable within the constraint of the width of the gravity anomaly along the western edge of Layer 2 where the anomaly is known best (because of the high density of stations). The upper limit is constrained only by 'geologic reasonableness' of the densities of large rock masses. For example, a density contrast of 2.0 gm/cm<sup>3</sup> would require the presence of rock types that are unknown on the earth in single bodies with volumes of order of 1000 and 10,000 cubic kilometers. A range of values from 0.15 to 0.30 gm/cm<sup>3</sup> is 'geologically reasonable', consistent with the rock types known to occur at the surface within a few tens of kilometers west of the inferred western edge of Layer 2, and within the constraints of the width of the anomaly at the western edge. For this range of density contrasts, the estimated volume ranges from 46,000 kilometers<sup>3</sup> to 23,000 kilometers<sup>3</sup>.

Several two dimensional models across the edges of Layer 2 are described in Appendix 2:5L-1. They are located near Vantage, Potholes Reservoir, Moses Lake, and Wallula Gap. They are consistent with edges of the unit that dip a few degrees toward the interior of the body. We infer that the body is a relatively thick pile of extrusive rocks, say andesite or basalt, that accumulated in a subsiding basin that is elongated in a north-south direction.

The body is thicker towards the south. For example, it thickens appreciably south of the Rattlesnake Hills alignment. It attains a thickness of 8 to 10 kilometers in the vicinity of Lenzie Ranch, 25 kilometers southwest of Richland.

The two lobes on the southern end of Layer 2 are possible indications of the locations of vents through which the rock was extruded. We suggest two possible interpretations but prefer the first interpretation: (1) The uppermost and geographically more extensive portion of Layer 2 was extruded through a vent in the vicinity of Walla Walla and flowed through the region now filled with the Walla Walla lobe. The lowermost portion of Layer 2 which is also geographically restricted to the region south of the Rattlesnake Hills alignment flowed through the southwest lobe from a vent located near Blalock Canyon, Oregon, (2) Both vents were active throughout the time during which Layer 2 was extruded. Our preference for the first hypothesis is based on the correlation of the gravity anomaly for the southwest lobe with the lower portion of Layer 2.

Layer 2 appears to vary in thickness north of the Gable Mtn.-Gable Butte-Umtanum Ridge area. Figures 9 and 11 show a gravity anomaly of 4 to 6 mgals that extends northward from Gable Mtn. to a point north of Potholes Reservoir, a distance of about 28 kilometers, and is 9 to 12 kilometers wide.

#### 6.1.2.4.5 Yakima Basin

The Yakima Basin appears to correlate with a small residual gravity anomaly and therefore probably has a shallow depth. (Robbins et al, 1975) The basin extends east of Yakima approximately 20 kilometers. The Yakima gravity low is similar in amplitude and size to several other residual gravity anomalies that occur along the western side of the Columbia Plateau such as the Cleveland, Satus Creek, and Ellensburg gravity anomalies. The cause of these other anomalies may be similar to the origin of the Yakima anomaly.

#### 6.1.2.4.6 Pasco and Quincy Basins

Neither the Pasco nor Quincy Basin correlates directly with a residual gravity anomaly. However, comparison of Figures 9, 11, and 12 with a geologic map of the area (Plate 1, WNP-1/4, Amendment 23) shows that the edges of these basins for a total distance of 150 miles coincide with the gravity anomaly attributed to Layer 2. Within the limitations of the present set of data, it appears that the spatial coincidence is probably continuous along these sections: (1) for the Pasco Basin, most of the eastern boundary and the western boundary north of Priest Rapids and (2) for the Quincy Basin, the eastern, northern, and western boundaries. Thus, there appears to be a strong spatial correlation between the edges of these basins and Layer 2. Such a strong correlation may imply a causal relationship.

#### 6.1.2.4.7 Chiwaukum Graben

A residual gravity low correlates with the Chiwaukum graben and its bounding faults. The gravity expression for this feature does not appear to extend east of the Columbia River. Therefore, the Chiwaukum graben and its bounding faults most likely do not extend beneath Layer 2, the lower basalt unit.

#### 6.1.2.4.8 Olympic-Wallowa-Lineament

The strong gravity gradient that trends north-south for approximately 50 kilometers and passes about 9 kilometers east of Yakima, attributed to the western edge of Layer 2,





is significant to understanding the origin of the Olympic-Wallowa lineament (OWL) and other geologic structures related to the Hanford region. This gradient has been used to constrain estimates of the maximum horizontal displacement of any fault that could cross the feature. One edge of the causative body extends north-south with a density contrast that is positive with respect to the rocks toward the west. Because the contours are relatively straight, any faults striking between about N45°W and S45°W that cross the gradient would have horizontal displacements less than 2-3 kilometers. The exact value would depend on the location and strike of the fault, the density of stations in the vicinity of the crossing, and the noise in the gravity data. For comparison with the gravity map, the results of several strike-slip fault models are shown as contour maps in Figure 19.

#### 6.1.2.5 Comparison of Gravity Maps with Aeromagnetic and Seismicity Maps of Pasco-Walla Walla Area

Aeromagnetic maps (Weston Geophysical, 1978) and seismicity maps were compared with the gravity maps for the Pasco-Walla Walla area. The work was done at map scales of both 1/62,000 and 1/250,000. Aeromagnetic and seismicity data at map scale 1:250,000 are shown in Figures 25 and 26, respectively. Many gravity anomalies do not appear to correlate spatially with regions that contain earthquake epicenters. For example, the Blue Mountains Anticline appears to be aseismic. In the Grande Ronde area, only one earthquake is known and its intensity is less than MM IV is known. The epicenter is located on the northwest-trending gravity gradient north of Summerville.

The Saddle Mountains show no obvious correlation with gravity. They do however, correlate with a prominent magnetic anomaly that can be traced continuously from Sentinel Gap eastward for 60 kilometers almost to Scootney Lake and then southeastward for 100 kilometers to the Washington-Oregon state line where it terminates. The southeastward-trending portion of the magnetic anomaly has been attributed by Swanson et al (1979) to dikes. It is our interpretation that the anomaly may be due to the edge of basalt flows that dip gently to the west. The east-west fault observed on the north flank of the Saddle Mountains must be primarily a surface feature that is restricted in both depth and lateral extent toward the southeast or a low angle thrust fault. The fault probably does not reach the base of the basalt column in the vicinity of Saddle Mountains, because no expression is present in the gravity field. The displacement probably dies out toward the east

where the aeromagnetic anomaly goes to zero. No fault has been identified along the linear magnetic anomaly that trends NW-SE. The seismic activity observed in the vicinity of Saddle Mountains is not expected to extend southeasterly from the Adams-Franklin county line.

Some features in the gravity field do not appear to correlate with known geology but do appear to correlate with seismicity. For example, a prominent circular gravity low centered on the Little Goose Lock and Dam has a dozen epicenters located around the inferred periphery of the causative body.

Several linear zones that contain relatively steep gravity gradients also contain earthquake epicenters. For example, the northeast-trending zone that lies along the northwest side of the Blue Mountains Anticline and the zone along the western edge of the inferred lower basalt body of the Columbia Plateau contain several small earthquake epicenters.

### 6.1.3 PACIFIC NORTHWEST MAPS

#### 6.1.3.1 General - Pacific Northwest Maps

Approximately 85,000 stations from 51 different surveys were used. The average station spacing was 5 kilometers with spacing variations from less than 0.1 kilometer per station along several profiles to as much as 50 kilometers between a few widely scattered stations. Station locations are shown in Figure 22.

The precision of the station values in the larger map varies between 0.5 mgals for station values obtained along high-density profiles to 2-10 mgals for station values that were not established along high-density profiles. The precision of the stations in the Pacific Northwest area is considered sufficient in most areas to construct maps with a contour interval of four mgals.

No detailed interpretation of the gravity data for the Pacific Northwest was attempted. The interpretation was limited to the major features that would have implications for the Columbia Plateau.

#### 6.1.3.2 Interpretation of the Total Bouguer Anomaly Map for the Pacific Northwest Map Area

The Pacific Northwest total Bouguer anomaly map is shown in Figure 22. Prominent features in the gravity map of



particular significance for the WNP 1-2-4 sites will be discussed below in the section on residual gravity anomalies for the Pacific Northwest area.

#### 6.1.3.3 Interpretation of the Regional Bouguer Anomaly Map for the Pacific Northwest Map Area

The Pacific Northwest Regional Bouguer gravity anomaly map, shown in Figure 23, most likely corresponds to density contrasts at a depth of 20 kilometers or more. In preparing this map, gravity data in an area approximately 200 kilometers by 200 kilometers and centered in the middle of the area shown in Figure 23 was used. Gentle warping of any crustal discontinuity, at a depth of 20 kilometers or more would be sufficient to produce gravity anomalies present in the regional anomaly field. The regional gravity anomaly shown in Figure 23 is consistent with the regional gravity anomaly calculated previously (Washington Public Power Supply System, 1977) and no additional modeling has been done.

#### 6.1.3.4 Interpretation of Residual Gravity Anomalies for the Pacific Northwest Map Area

Residual gravity anomalies were interpreted from the residual gravity map (Figure 24) and the total Bouguer gravity map (Figure 22).

Comparison of the gravity maps with the appropriate geologic and tectonic maps shows a good correlation between gravity anomalies and known geology in several geographic areas. Examples are (a) the Chiwaukum graben, (b) the Entiat Fault, (c) the Republic graben with its boundary faults, (d) the Chewack-Pasayten fault, (e) the Straight Creek fault and its northward continuation, the Hope-Frasier River Fault system, and (f) the Chilliwack batholith.

The Methow and Republic graben, and their bounding faults appear to be traceable beneath the younger (uppermost) basalt, of the Columbia Plateau but only outside the region underlain by Layer 2. No such feature appears to be present within or below Layer 2.

One of the more striking features of the total Bouguer gravity anomaly and the residual gravity anomaly maps is the fabric which is apparently reflecting the principal underlying regional geologic features. In the area north of Olympia, Washington, and west of the Straight Creek Fault, the fabric trends N40°-50°W. The trend and character of the pattern changes significantly at the Straight Creek

Fault (and its extensions north and south). This relationship is suggestive that the Straight Creek Fault may be the surface expression of a portion of a major crustal, and possibly upper mantle, structure that extends from at least Boston Bar, B.C., to the southern Oregon state line. There is no similar strong fabric extending into the Columbia Plateau.

## 7.1 REFERENCES

Peterson, D. E., 1965, Field notebook - Hanford gravity survey, September and October.

Raisz, E., 1945, The Olympic-Wallowa Lineament, American Journal of Science, v. 243-A, p. 479-485.

Raymond, J. R. and Tillson, D. D., 1968, Evaluation of a thick basalt sequence in south central Washington - Geophysical and hydrological exploration of the Rattlesnake Hills deep stratigraphic test well: Report BNWL-776, submitted to Atomic Energy Commission, 126 p.

Robbins, S. L., Burth, R. J., and Gregg, D. O., 1975, Gravity and aeromagnetic study of part of Yakima River Basin, Washington: Geological Survey Professional Paper 726-E.

Shannon & Wilson, 1979, Geologic Reconnaissance of the Wallula Gap, Washington-Blue Mountains-LaGrande, Oregon Region: Prepared for Washington Public Power Supply System under the direction of United Engineers and Constructors, 58 p.

Skehan, J. W., 1965, A continental-oceanic crustal boundary in the Pacific Northwest: Report AFCRL-65-904, submitted to Air Force Cambridge Research Laboratories, 52 p.

Swanson, D. A., et al., 1977, Reconnaissance geologic map of the Columbia River Basalt Group, Pullman and Walla Walla Quadrangles, Washington and Idaho: Geological Survey Open-File Report 77-100, 11 p., 2 maps.

Swanson, D. S., Wright, T. L., and Zietz, I., Isidore, 1979, Aeromagnetic map and geologic interpretation of the west-central Columbia Plateau, Washington and adjacent Oregon: Geological Survey Geophysical Investigations Maps GP-917.

Talwani, Manik, Ewing, and Maurice, 1960, Rapid computation of gravitational attraction of three-dimensional bodies of arbitrary shape: Geophysics, v. 25, p. 203-225.

Weston Geophysical Research, Inc., 1978a, Qualitative aeromagnetic evaluation of structures in the Columbia Plateau and adjacent Cascade Mountains: Prepared for Washington Public Power Supply System under the direction of United Engineers & Constructors, Inc.

TABLE 1  
GRAVITY MAPS

Name	Area	Location	Contour Interval (mgals)	Number Stations	Number of Surveys
Hanford 1°	1°x1°		1.0	10,000	31
Pasco-Walla Walla	2 1/2°x4°		2.0	16,000	31
Pacific Northwest	10°x10°		4.0	75,000	30

2.5L-22

WNP-2

AMENDMENT NO. 18  
September 1981





TABLE 2  
SOURCE OF GRAVITY DATASecondary Source  
(if used)Primary Source  
(if known)

## Canadian

Danes, Z. F., 1979 personal communication.

Weston Geophysical, 1977, this report.

Northwest Energy Service Company, 1980 and 1981; data obtained by Weston Geophysical Corporation.

No known primary.

Weston Geophysical, 1979, 1980, this report.

Carlson, R. L., A gravity study of the Cypress Island Peridotite, Washington, M.S. thesis, University of Washington, 1972.

Harding and Lawson

Travis, P. L., Jr., Geology of the area near the north End of Summer Lake, Lake County, Oregon, M.S. thesis, University of Oregon, 1977.

Johnson

Seymour, F. F., Gravity of the Area surrounding the Blue Mountains Seismological Observatory, M.S. thesis, Southern Methodist University, 1965.

TABLE 2 (Cont'd)

## SOURCE OF GRAVITY DATA

Secondary Source  
(if used)Primary Source  
(if known)

Griscom, A. and A. Conradi, Jr., Principal facts and preliminary interpretation for gravity profiles and magnetometer profiles in the Alvord Valley, Oregon, U.S.G.S. Open File Report 75-293, 1975.

Peterson, D. E., Field Notebook Hanford Gravity Survey, September and October 1965.

Couch, R. and B. Baker, Geophysical investigations in the Cascade Range in Central Oregon, Technical Report #2 to U.S.G.S. grant no. 14-08-0001-G-231, 1977.

NOAA

Bonini, W. E., Gravity Anomalies in Idaho, Wyoming, Montana, Washington, and Oregon, Idaho Bureau of Mines and Geology, 1963, ID, 5465 pts.

NOAA

Colcord, J. E., Geodetic implications of a local gravity survey presented at the AGU 44th Annual Meeting, University of Washington, Department of Civil Engineering, Apr. 1963, DC, 292 pts.

NOAA

Coast and Geodetic Survey, U.S. (NOAA) National Gravimeter Base Network USC and GS, 3836 pts.

NOAA

Berg, J. W. and J. V. Thiruvathukal, Gravity Base Station Network, Oregon Department of Oceanography, Oregon State University, 28 pts.



TABLE 2 (Cont'd)

## SOURCE OF GRAVITY DATA

Secondary Source (if used)	Primary Source (if known)
NOAA	Woollard, G. P., Trip SS, Rockies Authority Unknown, 1029 pts., Geological Survey, U.S. Gravity Reduction, Snake River Plain, Idaho USGS, ID, 2551 pts.
NOAA	Geological Survey, U.S. Gravity Reductions, Nevada Basin and Range Project. Group 1 USGS, NV, 3095 pts.
NOAA	Stuart, D. J., Gravity data and Bouguer gravity map of western Washington.
NOAA	Oregon State University, Gravity data in Oregon, Authority Unknown, 9163, 1322 pts.
NOAA	Naval Oceanographic Office . Gravity Data, Channel Islands, California Navoceano, 1963, 753 pts.
NOAA	Army Map Service (USATOPCOM) Washington State Gravity Survey USGS, UT, 344 pts.
NOAA	Oregon State University, Oregon State Gravity Data, Oregon State University, 3945 pts.
NOAA	Army Map Service (USATOPCOM) Washington State Gravity Base Network, Project AMS, May, 1965, 28 pts.
NOAA	Chapman, R. H., California Gravity Base Station Network, CA Division of Mines and Geology, 357 pts.



TABLE 2 (Cont'd)

## SOURCE OF GRAVITY DATA

Secondary Source (if used)	Primary Source (if known)
NOAA	Lafehr, T. R., Gravity Survey in Southern Cascade Range, California USGS, 2965, 1117 pts.
NOAA	Geological Survey, U.S. Gravity Survey, Northern California Outside Sierra USGS, 1965, 453 pts.
NOAA	Geodetic Survey Squadron, 1st National Gravity Base Net and Excenters 1st GSS, 1967, 252 pts.
NOAA	Geological Survey, U.S. Gravity Data in Alturas, California Area USGS, 1967, 424 pts.
NOAA	Davis, W. E. and Kinoshita, W. Principal Facts for Gravity Stations in Northeastern Washington, USGS, 1962, 402 pts.
NOAA	Kim, C. K., Gravity Data in the Weed AMS Sheet, California, University of Oregon, 1969, 1035 pts.
NOAA	California Division of Mines and Geology, Gravity Data for Alturas AMS Sheet in California, California Division of Mines and Geology, California, 1970, 101 pts.
NOAA	Peterson, D. L., Gravity Data, Rathdrum Prairie, Idaho, U.S. Geological Survey, 1970, 355 pts.

TABLE 2 (Cont'd)

## SOURCE OF GRAVITY DATA

Secondary Source (if used)	Primary Source (if known)
NOAA	United States Army Topographic Command, Washington Regional Gravity Report Topocom, Report Number 27, Feb. 1972, 537 pts.
NOAA	University of Puget Sound University of Puget Sound, 1966 Regional Gravity Report USATOPCOM, 1971, 279 pts.
NOAA	Pemberton, Trip AD, Series PI University of Wisconsin, 1954, 820 pts.
NOAA	Mack, J. and Iverson, R. M., Trip AI, Series M, University of Wisconsin, 1955, 435 pts.
NOAA	Behrendt, J. C., Trip BN, Series BE, University of Wisconsin, 1959, 76 pts.
NOAA	Jones, J. W., Trip OR, Series AD, University of Wisconsin, 238 pts.
NOAA	Rose, J. C., Trip TT, Series F, University of Wisconsin, 1949, 913 pts.
NOAA	Black, W. E., Trip TW, Series F, University of Wisconsin, 1950, 756 pts.
NOAA	Ostenso, N. A., Trip ZZ, Series NI, University of Wisconsin, 1953, 1082 pts.
NOAA	United States Army Topographic Command Oregon State Gravity Base Network USATOPCOM, June - August 1971, 26 pts.



TABLE 2 (Cont'd)

## SOURCE OF GRAVITY DATA

Secondary Source (if used)	Primary Source (if known)
NOAA	University of Puget Sound Washington Regional Gravity Survey, USATOPCOM, Reports 69, 69A, 69B, March 1972, 557 pts.
NOAA	Rogers, W., A Geological and Geophysical Study of the Central Puget Sound Lowland, University of Washington, 1970, WA, 815 pts.
NOAA	Defense Mapping Agency Topographic Center, Oregon Regional Gravity Survey, DMATC, July 1972, OR, 91 pts.
NOAA	Defense Mapping Agency Topographic Center, Oregon State Regional Gravity Anomaly Survey, Report 56C, DMATC. October 1972, OR, 36 pts.
NOAA	Defense Mapping Agency Topographic Center, Oregon State Regional Gravity Anomaly Survey.
NOAA	Defense Mapping Agency Topographic Center, Washington Regional Gravity Survey, Report 96-A, DMATC 1973, WA, 122 pts.
NOAA	Defense Mapping Agency Topographic Center, Oregon Regional Gravity Survey, DMATC, Report 56-E, March 1973, OR, 51 pts.



TABLE 2 (Cont'd)

## SOURCE OF GRAVITY DATA

Secondary Source (if used)	Primary Source (if known)
NOAA	Defense Mapping Agency Topographic Center, Oregon Regional Gravity Survey, DMATC, Report 56-F, March 1973, OR, 51 pts.
NOAA	Defense Mapping Agency Topographic Center, Idaho Regional Gravity Survey, DMATC, Report 94-A, March 1973, ID, 17 pts.
NOAA	Defense Mapping Agency Topographic Center, Idaho Regional Gravity Survey, DMATC, Report 94-B, March 1973, ID, 82 pts.
NOAA	Woollard, G. P., Trip BU, Series JB, University of Oregon, 2335 pts.
NOAA	Chapman, R. and Bishop, C., Source of Data for Bouguer Anomaly Map of California, Calif. Div. of Mines and Geology, 1967, 171 pts.
NOAA	Army Map Service (USATOPCOM), Gravity Data in the United States, North-South Profiles, Hawaii Inst. of Geophysics, 1967, 1651 pts.
NOAA	Danes, Z. F., Washington Gravity Survey, Princeton University, Undated, WA, 206 pts.

TABLE 2 (Cont'd)

## SOURCE OF GRAVITY DATA

Secondary Source (if used)	Primary Source (if known)
NOAA	Bonini, W. E., K Series - Washington State Gravity Data, Princeton University, Undated, WA, 185 pts.
NOAA	Swanberg, C. A., Gravity Survey over the Central Part of the Okanogan Range, Washington Southern Methodist University, 1968, US, WA, 442 pts.
NOAA	Geological Survey, U.S., Yakima Basin, Washington Gravity Data USGS, 1974, US, WA, 462 pts.
NOAA	Danes, Z. F., Gravity Survey, State of Washington, University of Puget Sound, 1973, US, WA, 5800 pts.
NOAA	Meyer, R. F. and Wilson, D. M. Principal Facts for Gravity Stations in the Spokane Area, Washington, USGS, Open-File Report 75-503, August-September 1974, US, WA, 265 pts.
NOAA	Chapman, R. H. Gravity Data, Alturas Area of California, California Division of Mines and Geology (Revised with Terrain Corrections), Date Unknown, US, CA, 50 pts.
NOAA	Geological Survey U.S., Principal Facts for Gravity Observations in the Charles Sheldon Antelope Range, Nevada and Oregon, USGS Open-File Report 76-601, 1976, US, NV, OR, 269 pts.

TABLE 2 (Cont'd)

## SOURCE OF GRAVITY DATA

Secondary Source (if used)	Primary Source (if known)
NOAA	Geological Survey U.S., Principal Facts for Gravity Observations Near McDermitt, Nevada, USGS Open-File 76-599, 1976, US, NV, 245 pts.
NOAA	Defense Mapping Agency Topographic Center, WCGP Washington, DMATC, November 1975, WA, 38 pts.
NOAA	Yost, C., Gravity Survey of the Cheney Quadrangle, Washington, Eastern Washington State College, 1976, US, WA, 250 pts.
NOAA	Couch, R. and Baker, B., Geophysical Investigations of the Cascade Range and Vale-Owyhee Region in Oregon, Oregon State University, 1976, US, OR, 2797 pts.
NOAA	Meyer, R. F., Principal Facts for Gravity Stations in the Spokane Area, Washington, USGS, 1976, US, WA, 265 pts.
NOAA	Jackson, D. B., and others, Principal Facts for Gravity Stations in the Pullman, Washington to Moscow, Idaho Area USGS, 1976, US, ID, WA, 245 pts.
NOAA	Cady, J. W., and Meyer, R. F., Principal Facts for Gravity Stations in the Okanogan Sandpoint, Ritzville and Spokane Quadrangles USGS, 1976, US, ID, WA, 2077 pts.

TABLE 2 (Cont'd)

## SOURCE OF GRAVITY DATA

Secondary Source (if used)	Primary Source (if known)
NOAA	Peterson, D. L. and Meyer R. F., Principal Facts for a Gravity Survey of Summer Lake Known Geothermal Resource Area, Oregon USGS, 1976, US, OR, 85 pts.
NOAA	Plouff, D., Gravity Data in Crump Geyser Area, Oregon, USGS, 1975, US, OR 353 pts.
NOAA	Hassemer, J. H. and Peterson, D. L., Principal Facts for a Gravity Survey of Breitenbush Known Geothermal Resources Area, Oregon
NOAA	Cogbill, A. H., Regional Gravity Survey of Western Nevada, Northeastern University, Nov. 1976, US, NV, 879 pts.
NOAA	Geodetic Survey Squadron, 1st Gravity Data, Nevada, 1968, 1st GSS, WY, 593 pts.
NOAA	Geodetic Survey Squadron, 1st Gravity Data for the State of Idaho, 1st GSS, 1970, 196 pts.
NOAA	Geodetic Survey Squadron, 1st Gravity Data for the State of Nevada, 1st GSS, 1971, 1370 pts.
NOAA	Geodetic Survey Squadron, 1st Gravity Data for the State of Idaho, 1st GSS, 1970, 171 pts.
NOAA	Geodetic Survey Squadron, 1st Nevada Regional Gravity Survey 1st GSS, 1972, 81 pts.



TABLE 2 (Cont'd)

## SOURCE OF GRAVITY DATA

Secondary Source  
(if used)Primary Source  
(if known)

NOAA

Geodetic Survey Squadron, 1st  
Idaho Regional Gravity Survey,  
1st GSS, 1972, 295 pts.

NOAA

DMAAC Geodetic Survey Squadron,  
Idaho Regional Gravity Survey,  
DMAAC/GSSQ, 1972, ID, 797 pts.

NOAA

Defense Mapping Agency  
Aerospace Center Geodetic  
Survey Squadron, Oregon  
Regional Gravity Survey,  
DMAAC/GSSQ, 1975, US, OR, 8 pts.

NOAA

Defense Mapping Agency  
Aerospace Center Geodetic  
Survey Squadron, Washington  
Regional Gravity Survey,  
DMAAC/GSSQ, 1975, US, WA, 70  
pts.

NOAA

Defense Mapping Agency  
Aerospace Center Geodetic  
Survey Squadron, California  
Regional Gravity Survey,  
DMAAC/GSSQ, 1975, US, CA, 102  
pts.





FIGURE 2.5L-1

IS CURRENTLY BEING PRINTED.

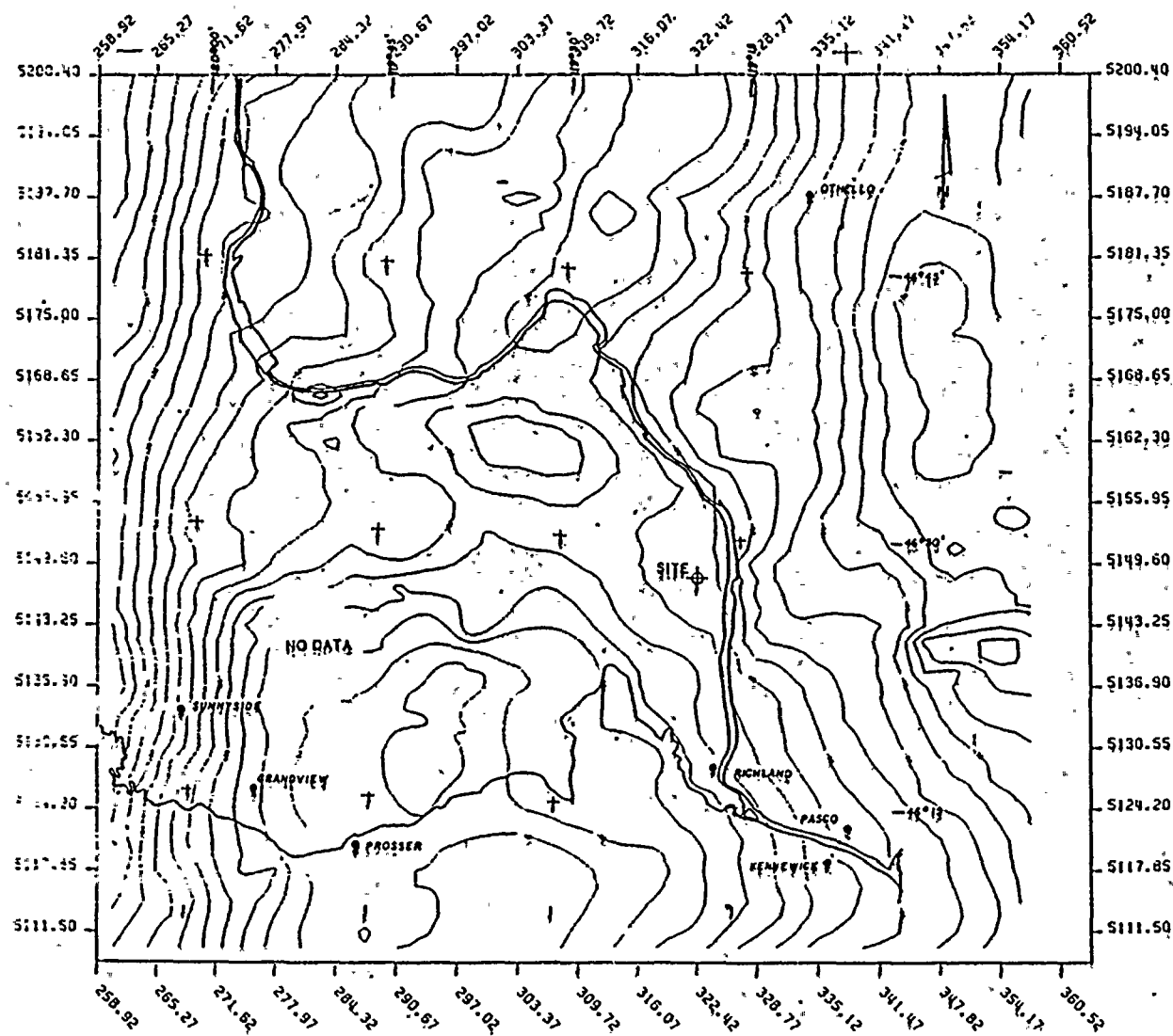


Figure 2.5L-2  
Hanford 1° Area.  
Total Bouguer gravity anomaly map.

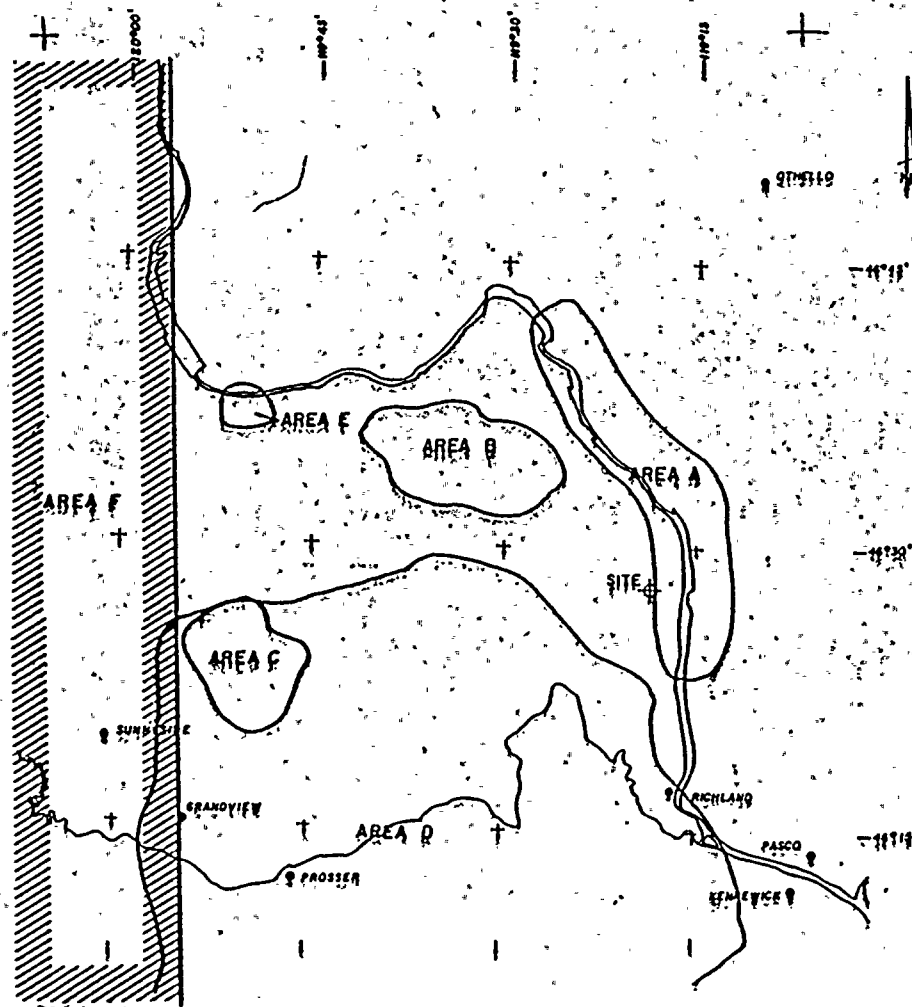


Figure 2.SL-3  
 Hanford 1st Area.  
 Overlay for gravity maps.

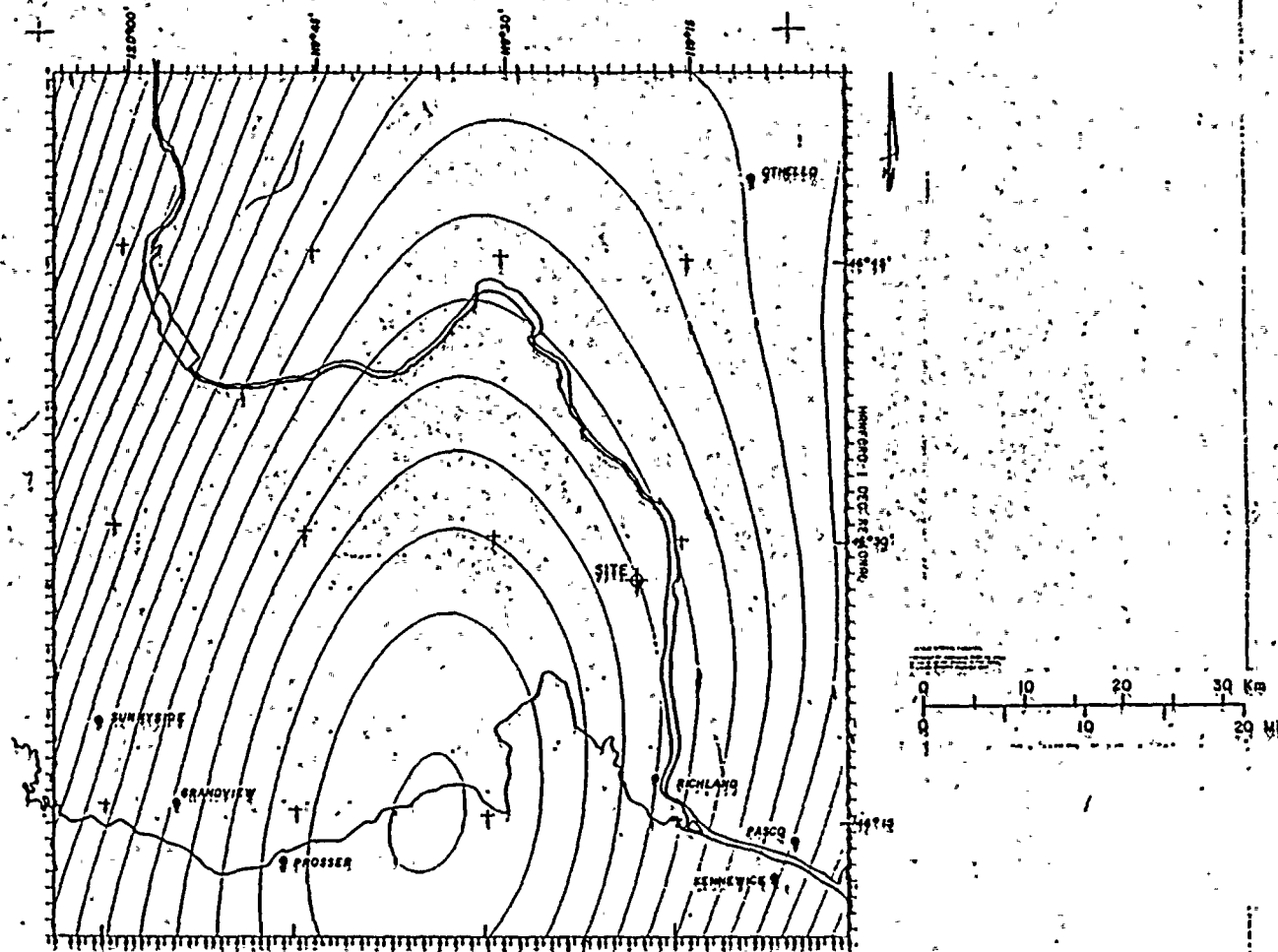
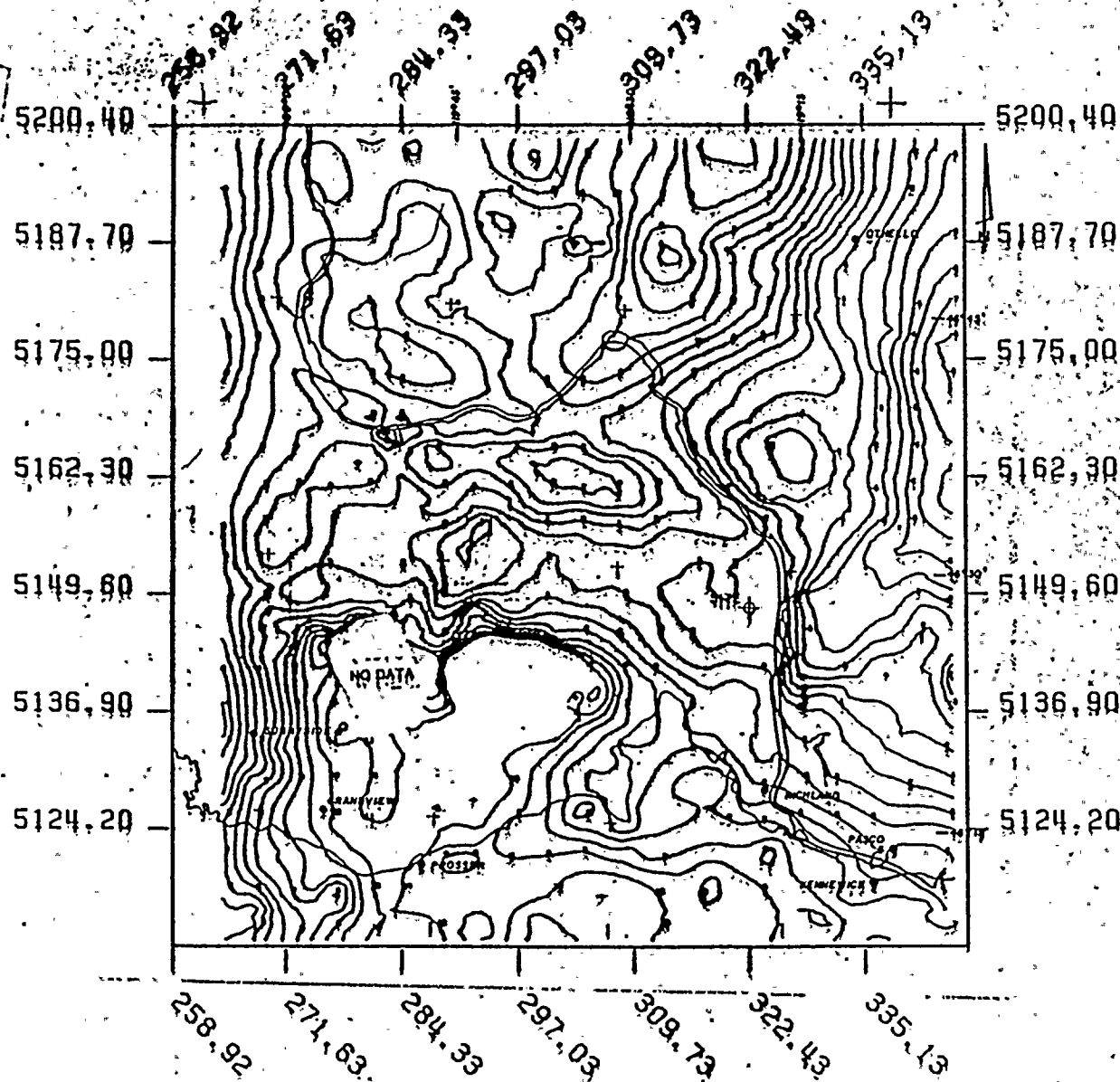


Figure 2.5L-4  
Hanford 1° Area.  
Regional Bouguer gravity anomaly map.



SCALE RATIO: 1/ 500000.00  
 MAP TYPE: 79.37 KM RESIDUAL  
 CONTOUR INTERVAL: 1.00 MGAL  
 GRID SPACING: 1.59 KM  
 RD: 20.00KM  
 RM: 8.26KM  
 RMV: 23.72KM

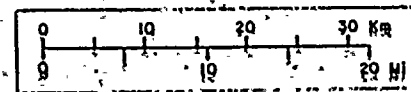


Figure 2.5L-5  
 Hanford 1° Area.  
 Residual Bouguer gravity anomaly map.



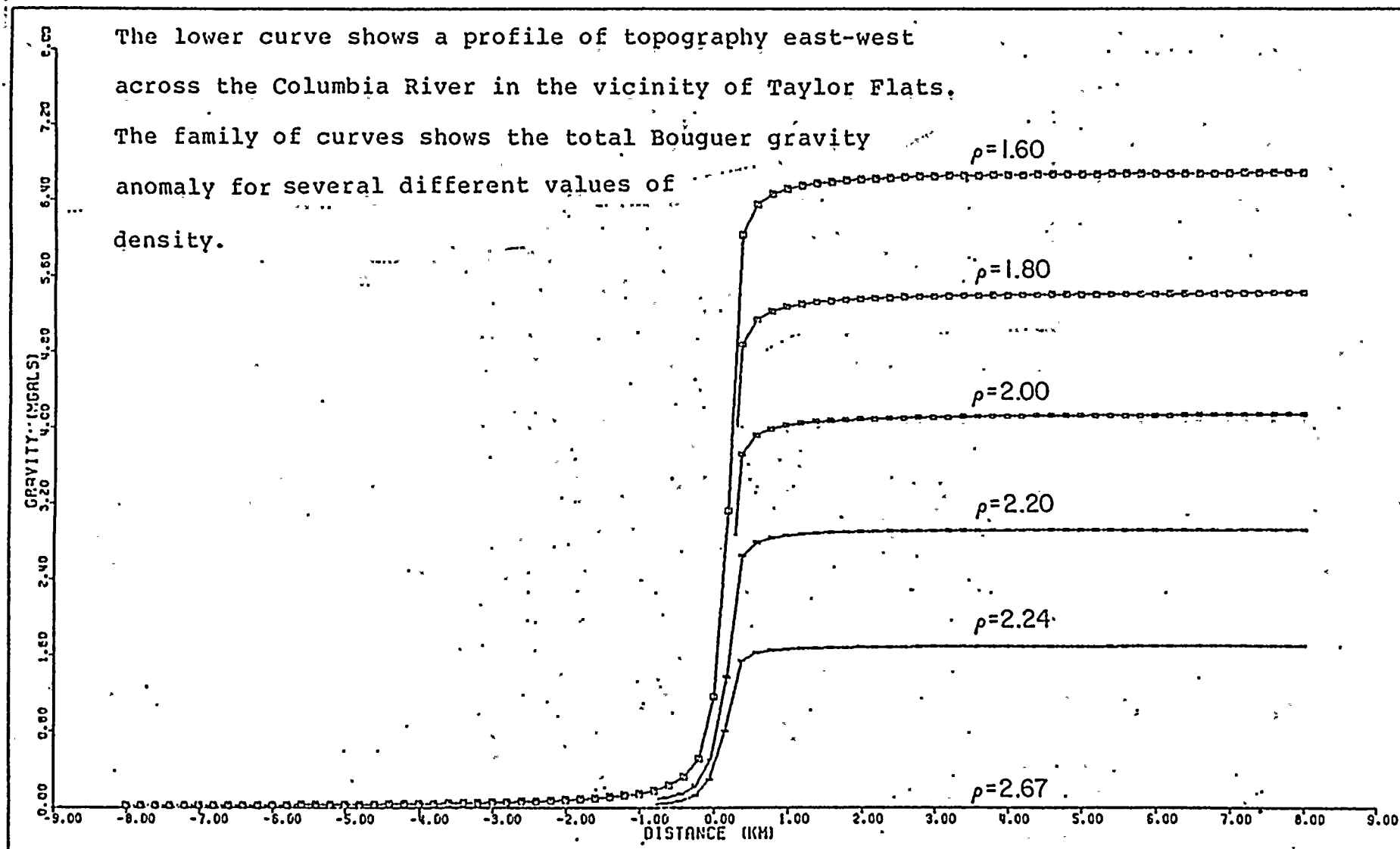


Figure 2.5L-6  
Effect of density on  
total Bouguer gravity anomaly.



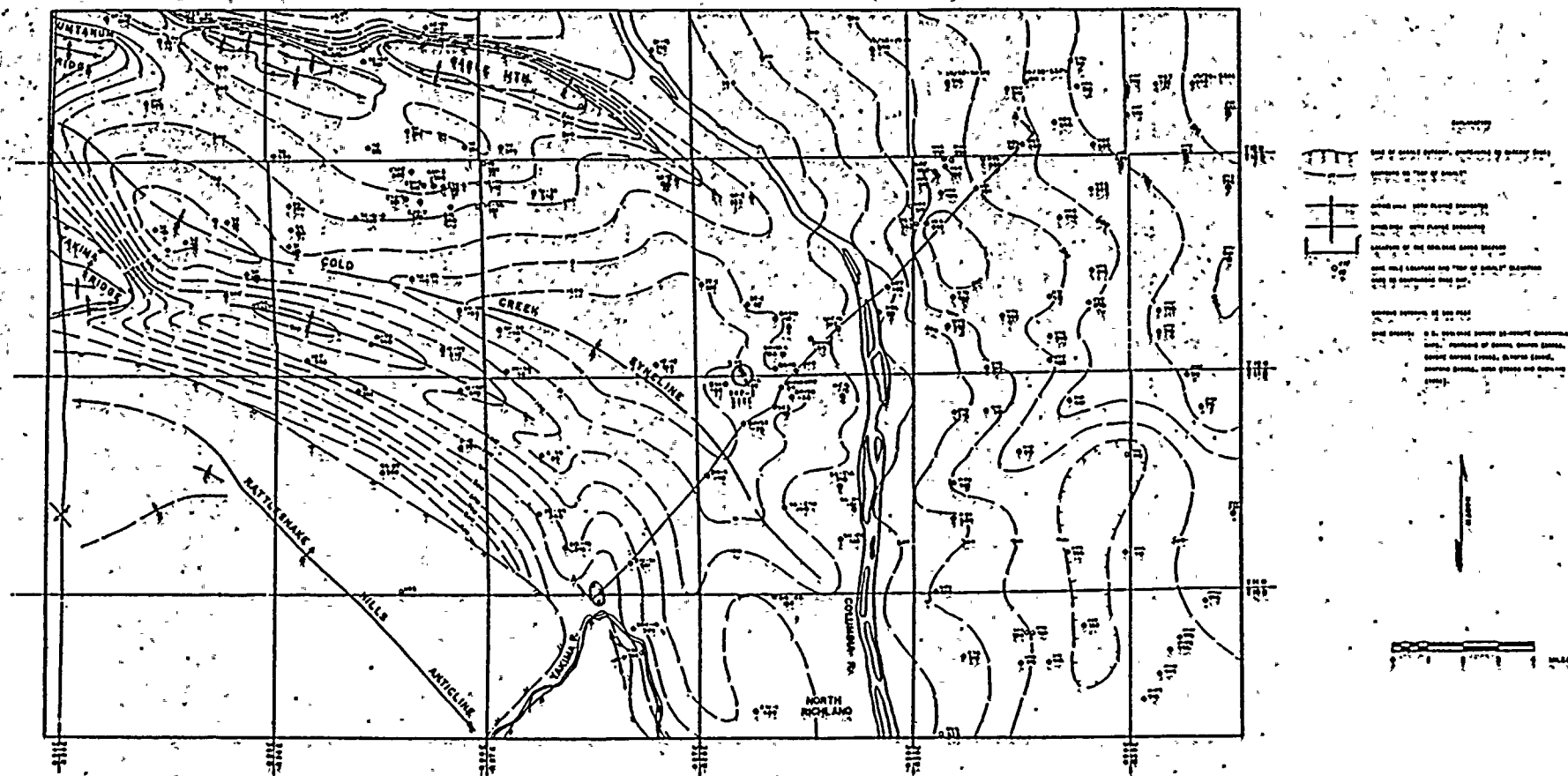
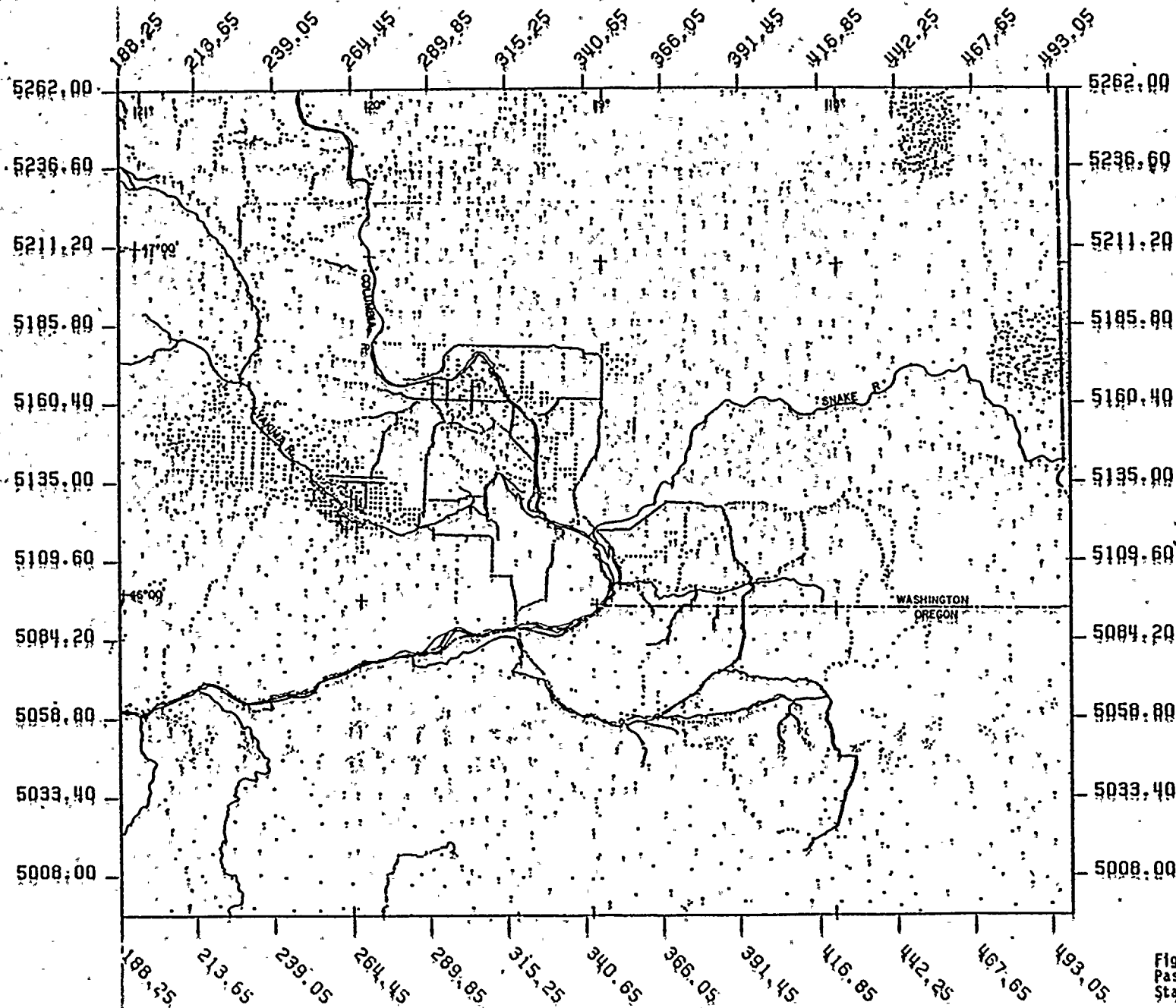


Figure 2.5L-7  
Bedrock topography for  
Hanford Reservation.



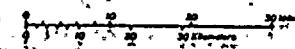
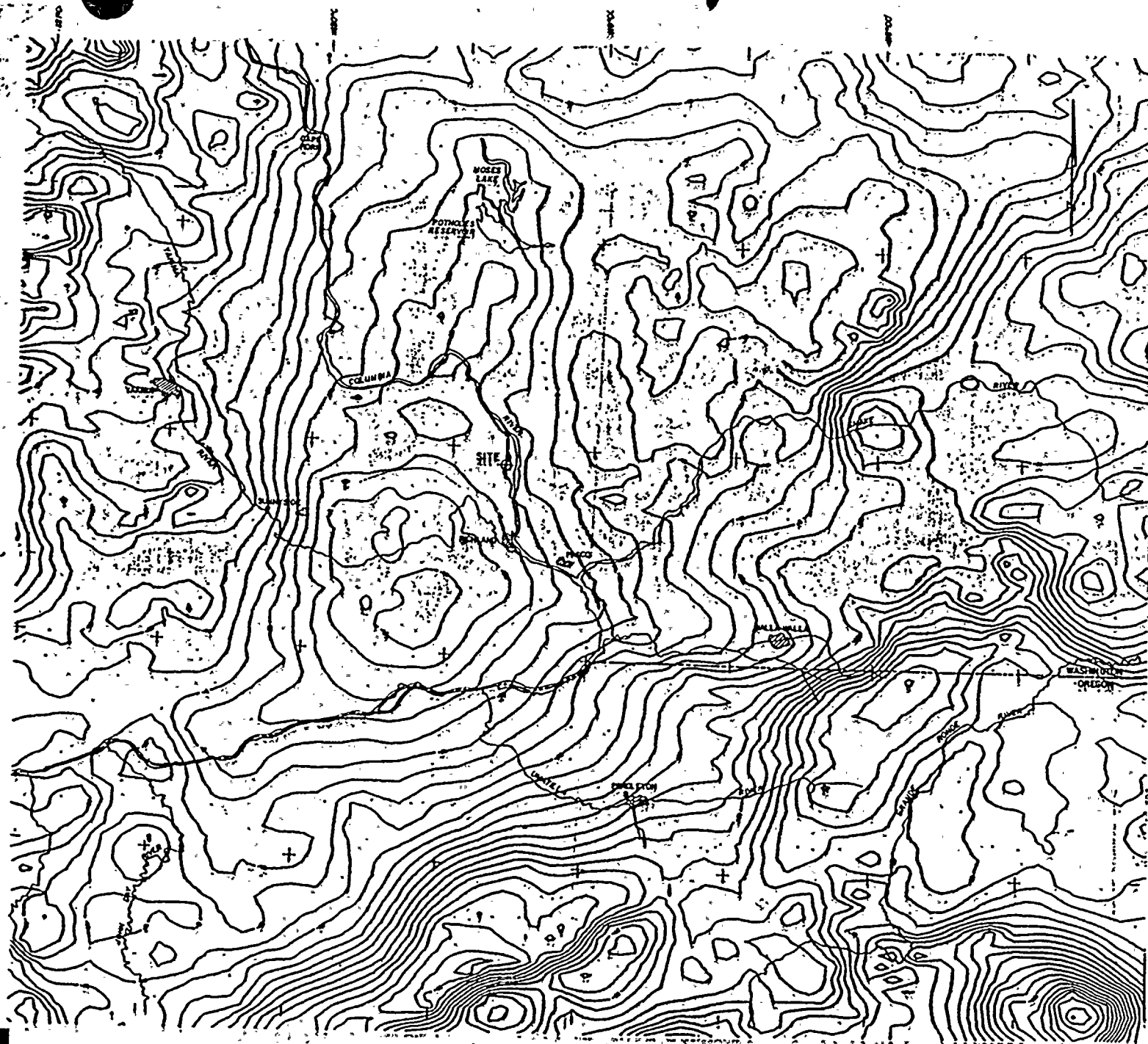
SCALE

25.40 KM  
15.78 MILES

% OF STATIONS ON MAP

Figure 2.5L-8

Pasco-Walla Walla Area.  
Station location map.



CONTOUR INTERVAL 4.00 MGAL  
 GRID SPACING 6.35 KM  
 RQ 20.00KM  
 RMH 10.00KM  
 RMV 30.00KM

Figure 2.5L-9  
 Pasco-Walla Walla Area.  
 Total Bouguer gravity anomaly.

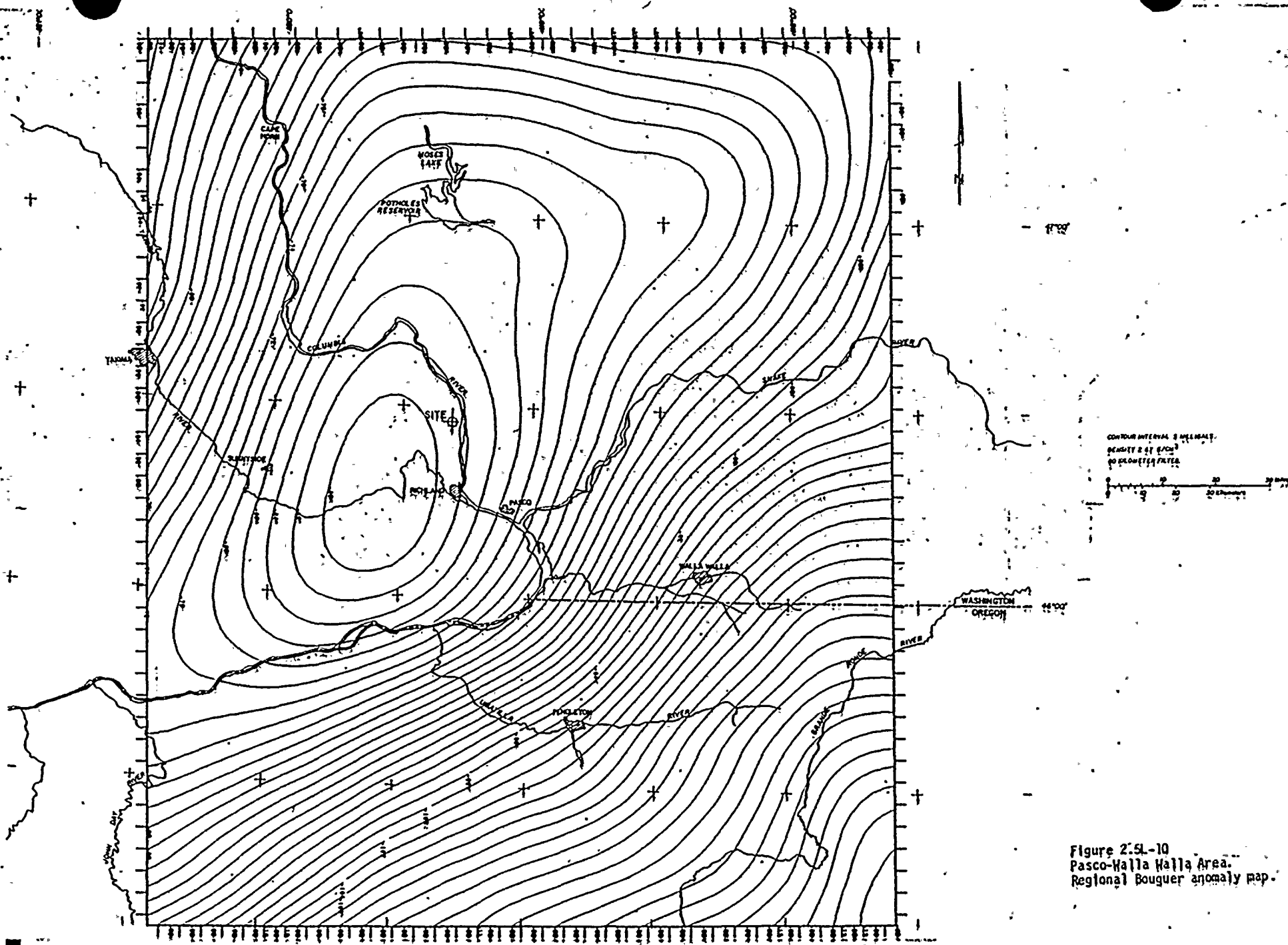


Figure 2.5L-10  
 Pasco-Walla Walla Area.  
 Regional Bouguer anomaly map.

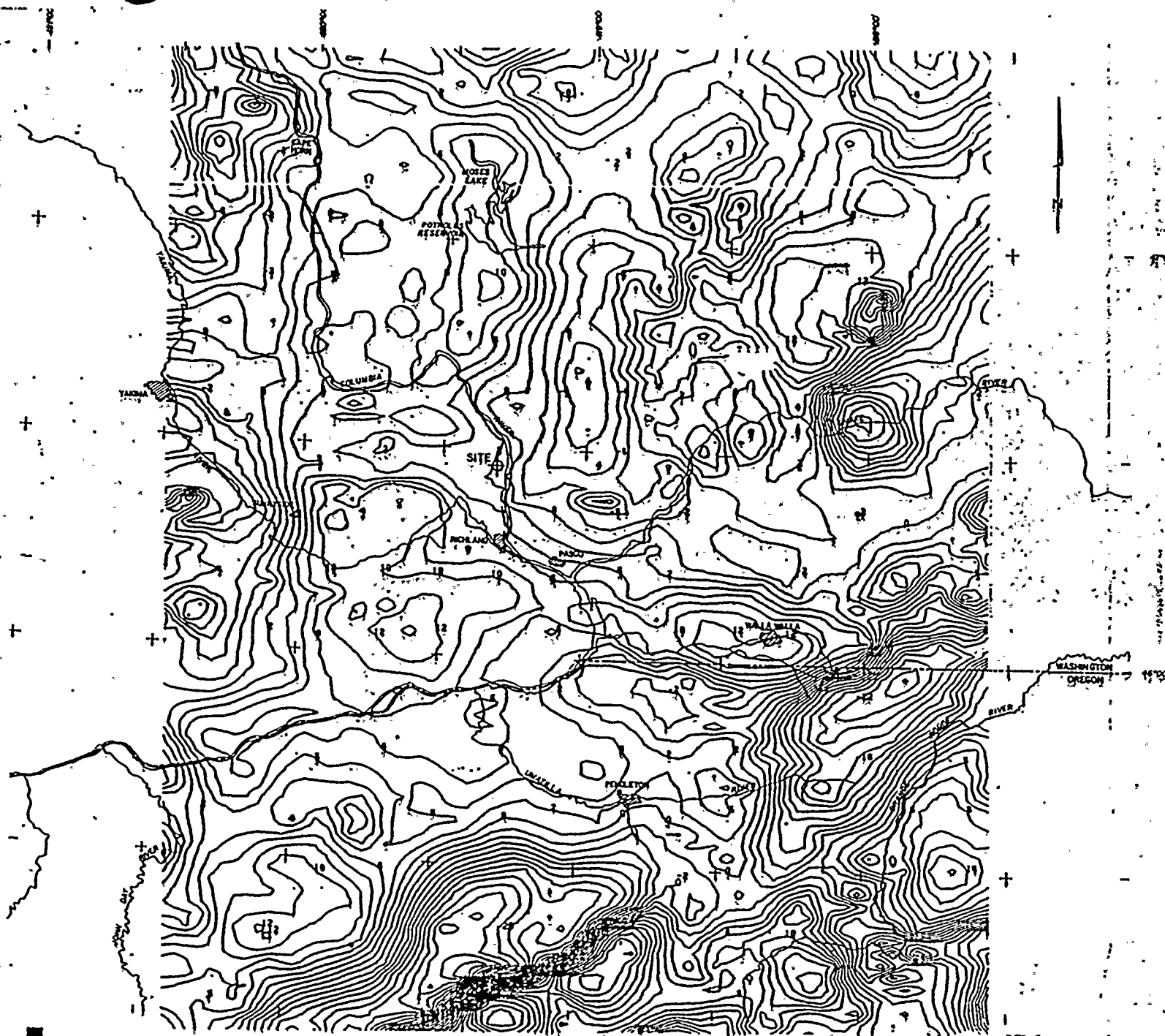


Figure 2.5L-11  
Pasco-Walla Walla Area.  
Residual Bouguer gravity anomaly map.



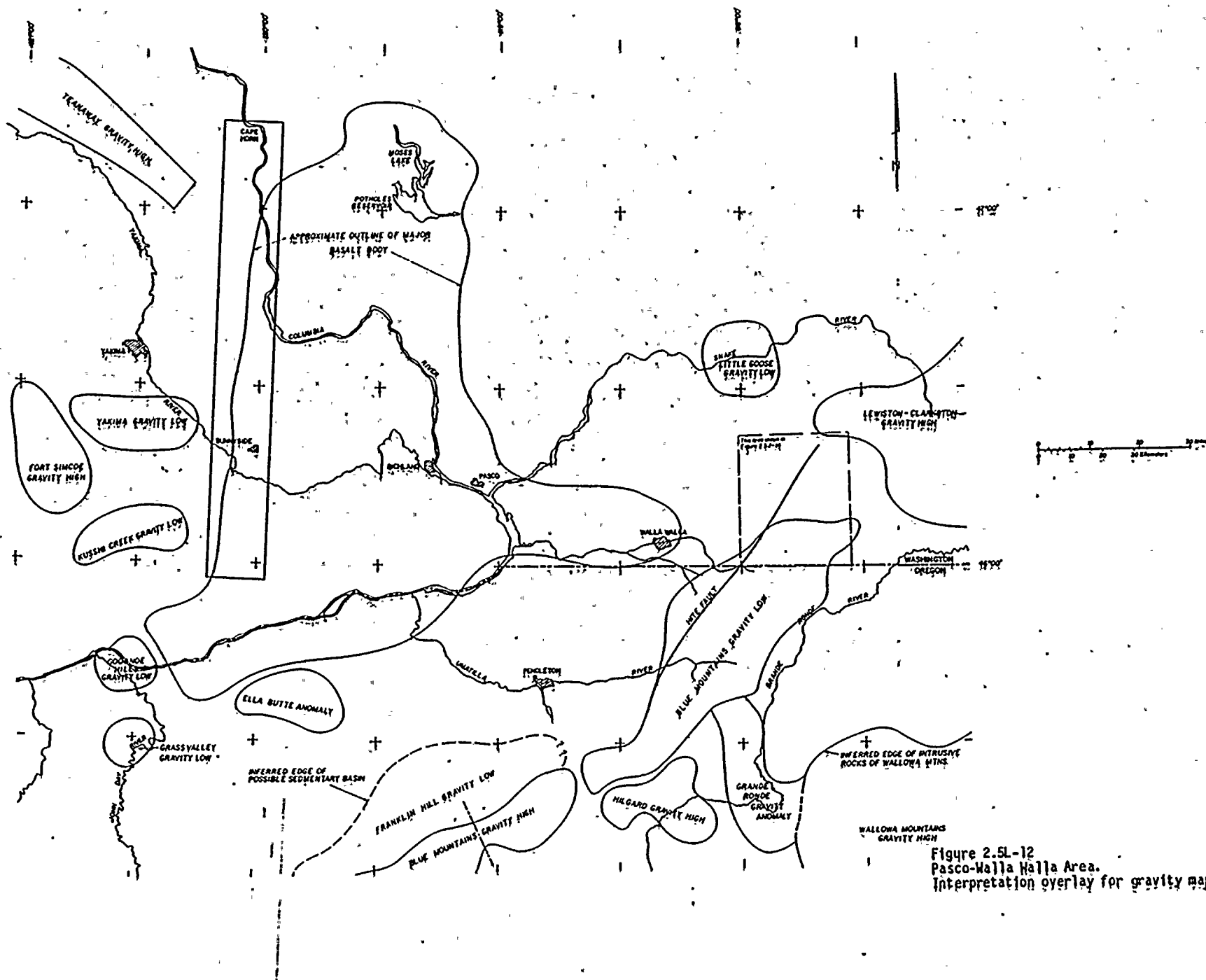
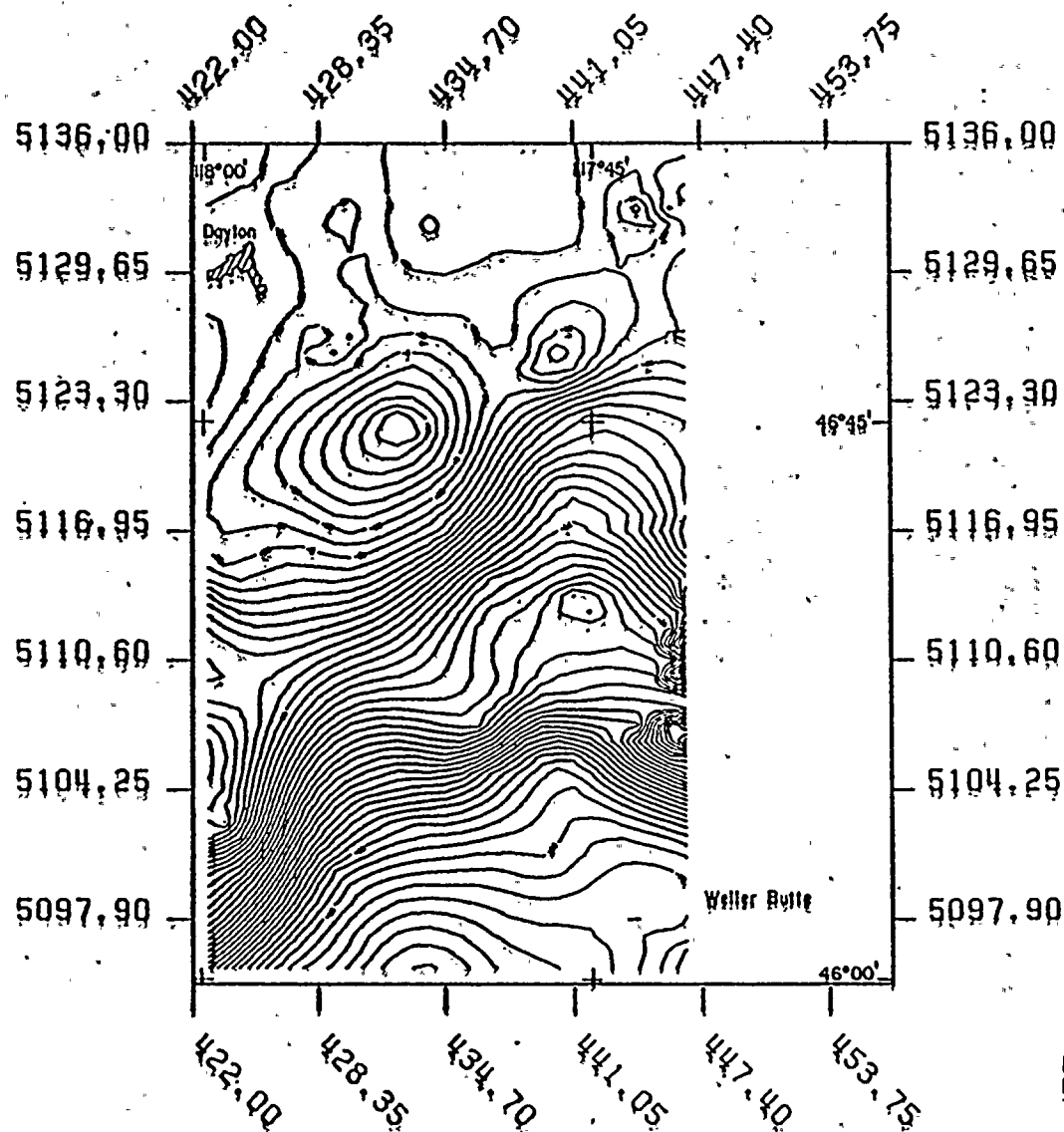


Figure 2.5L-12  
Pasco-Walla Walla Area.  
Interpretation overlay for gravity maps.



SCALE RATIO: 1/250000.00  
 MAP TYPE: TOTAL BOUGUER  
 CONTOUR INTERVAL: 1.00 MGAL  
 GRID SPACING: 1.50 KM  
 AD: 30 KM  
 MIN: 30 KM  
 MAX: 30 KM

SCALE



6.35

KM

3.95

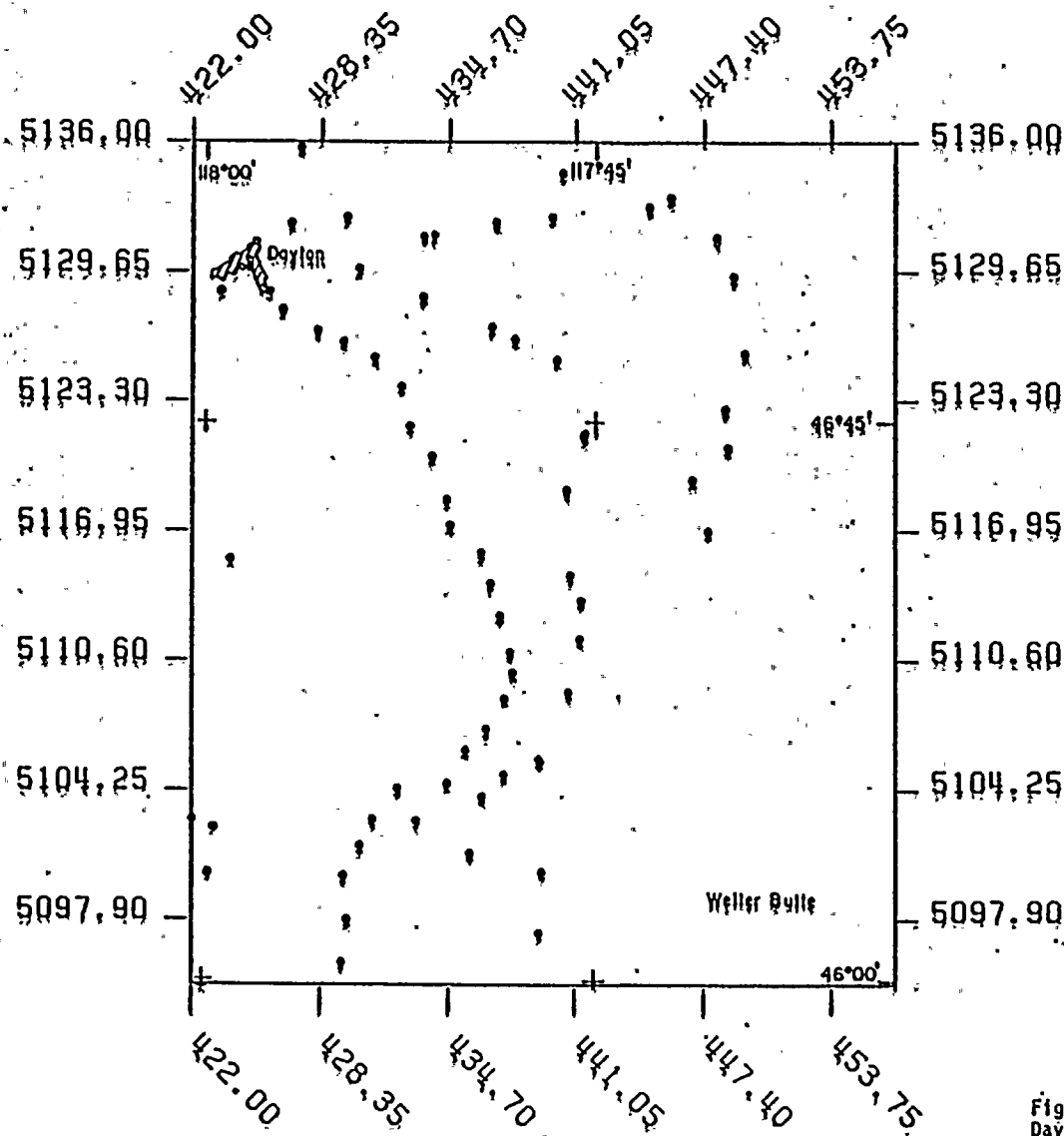
MILES

Figure 2.5L-13  
 Dayton-Heller Butte Area, Washington.  
 Total Bouguer gravity map,

Density  $2.67 \text{ gm/cm}^3$ .

Contour interval 1 mgal.





SCALE

0.35 KM  
3.95 MILES

OF STATIONS ON MAP - 74

3110 11

Figure 2.5L-14  
Dayton-Heller Butte Area, Washington.  
Station location map.



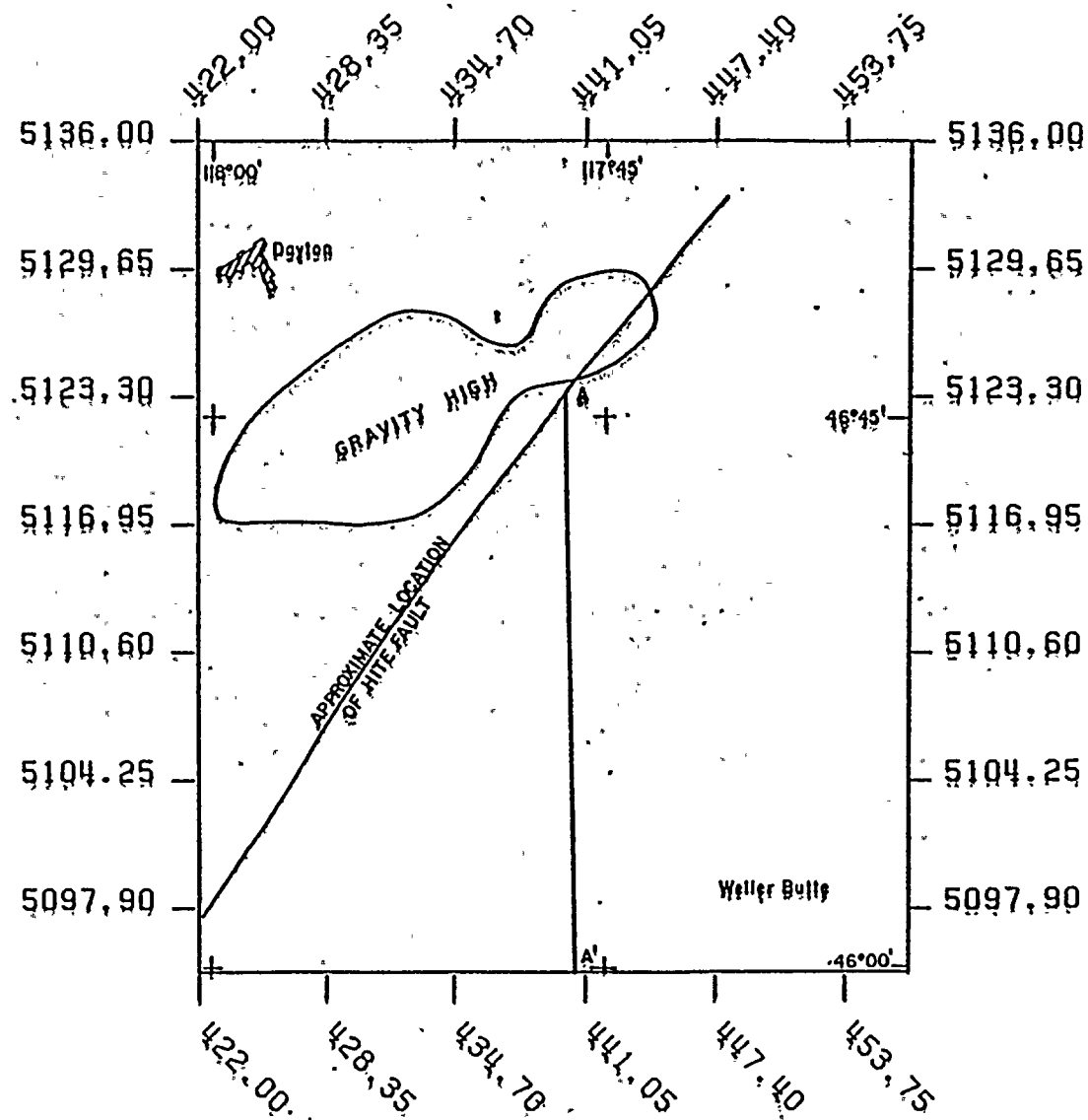


Figure 2.5L-15  
Dayton-Heller Butte Area, Washington.  
Overlay for gravity map.

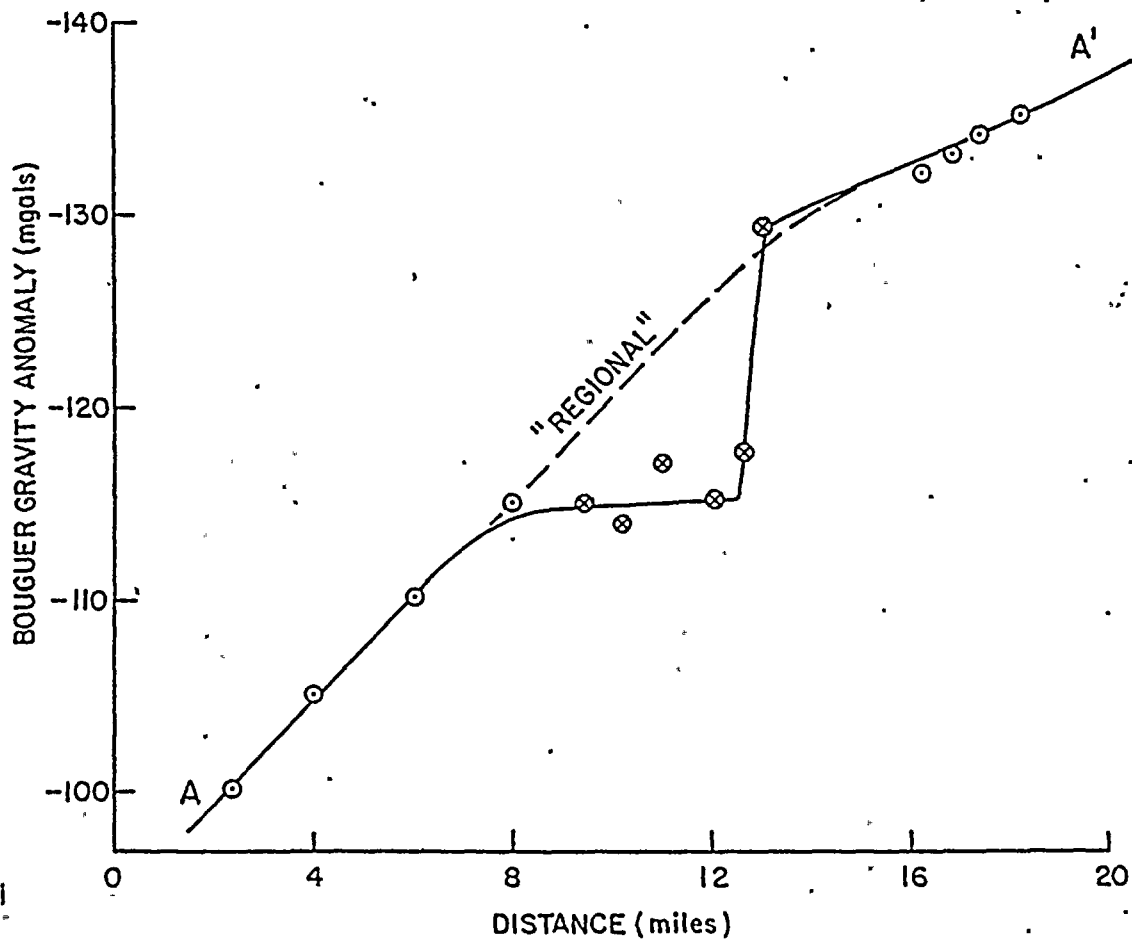
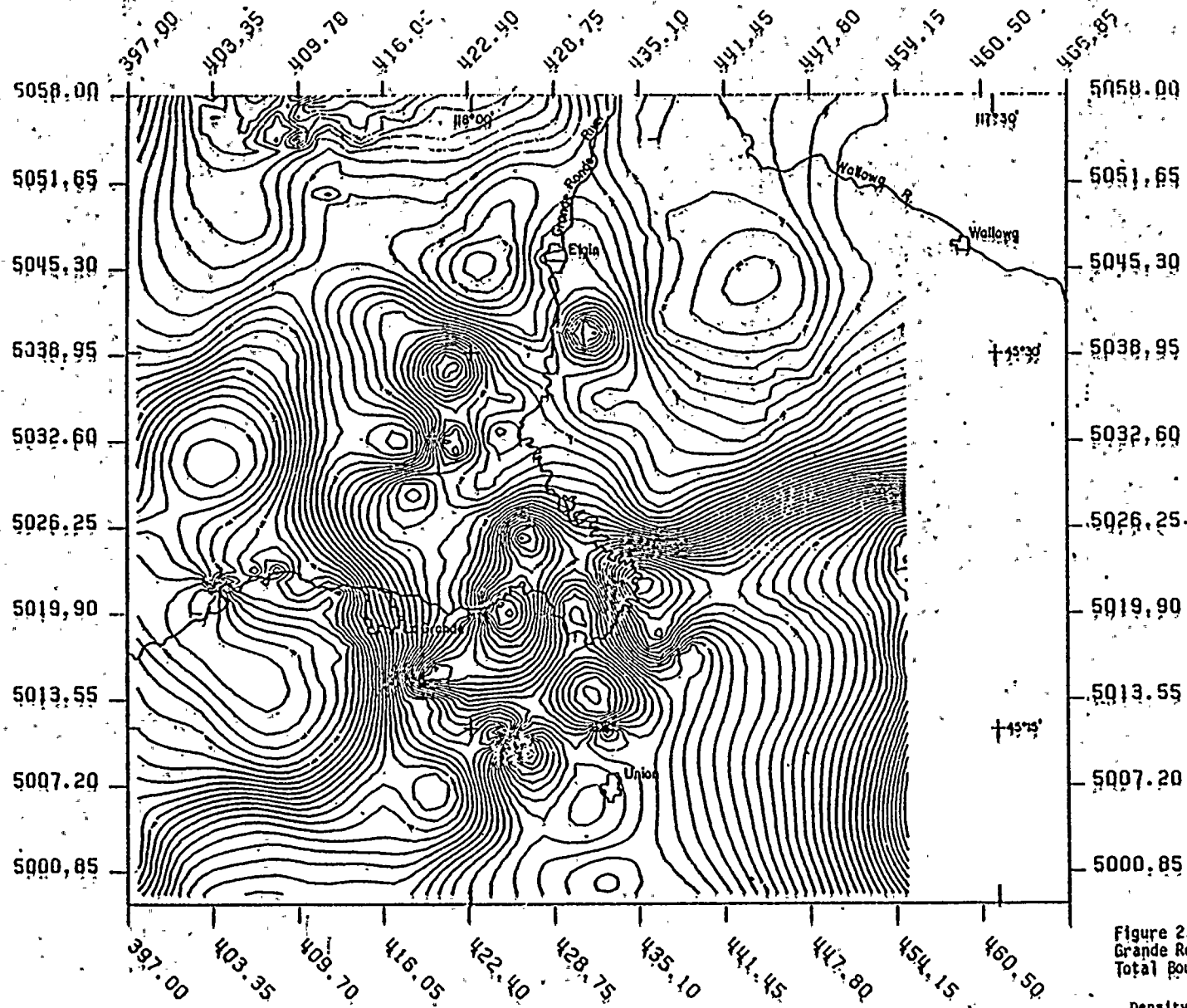


Figure 2.5L-16  
Gravity Profile AA',  
Dayton-Weller Butte Area, Washington.





S.P. 84-10, 17 250000.00  
 MAP TYPE: TOTAL BOUGUER  
 CONTOUR INTERVAL: 1.00 MGAL  
 GRID SPACING: 3.50 KM  
 BOX: 20 KM  
 EASE: 10 KM

SCALE  
 6.35 KM  
 3.95 MILES

Figure 2.5L-17  
 Grande Ronde Area, Washington.  
 Total Bouguer gravity anomaly map.

Density  $2.67 \text{ gm/cm}^3$ .

Contour interval 2 mgals.

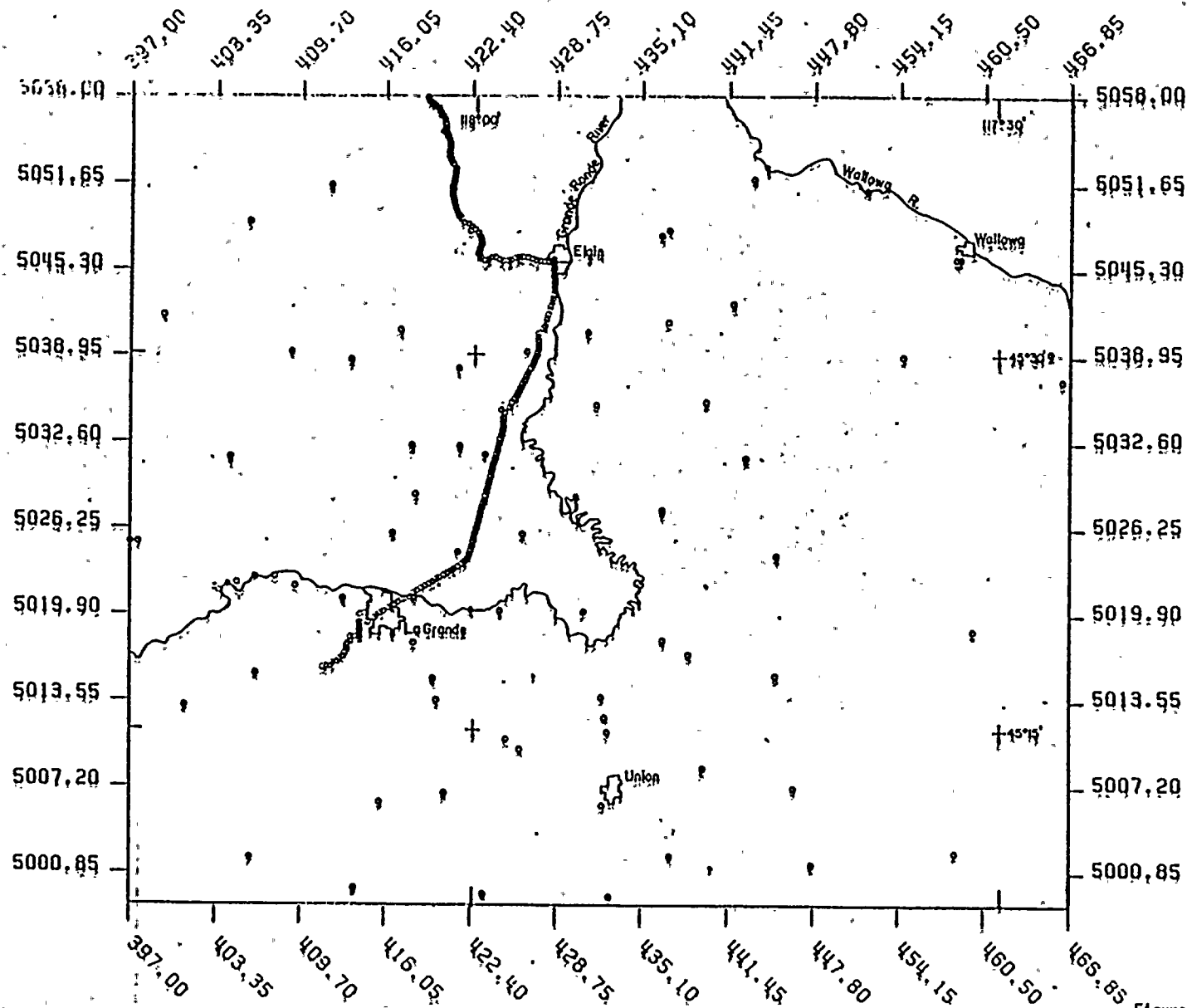


Figure 2.5L-18  
Grande Ronde Area, Washington.  
Station location map.

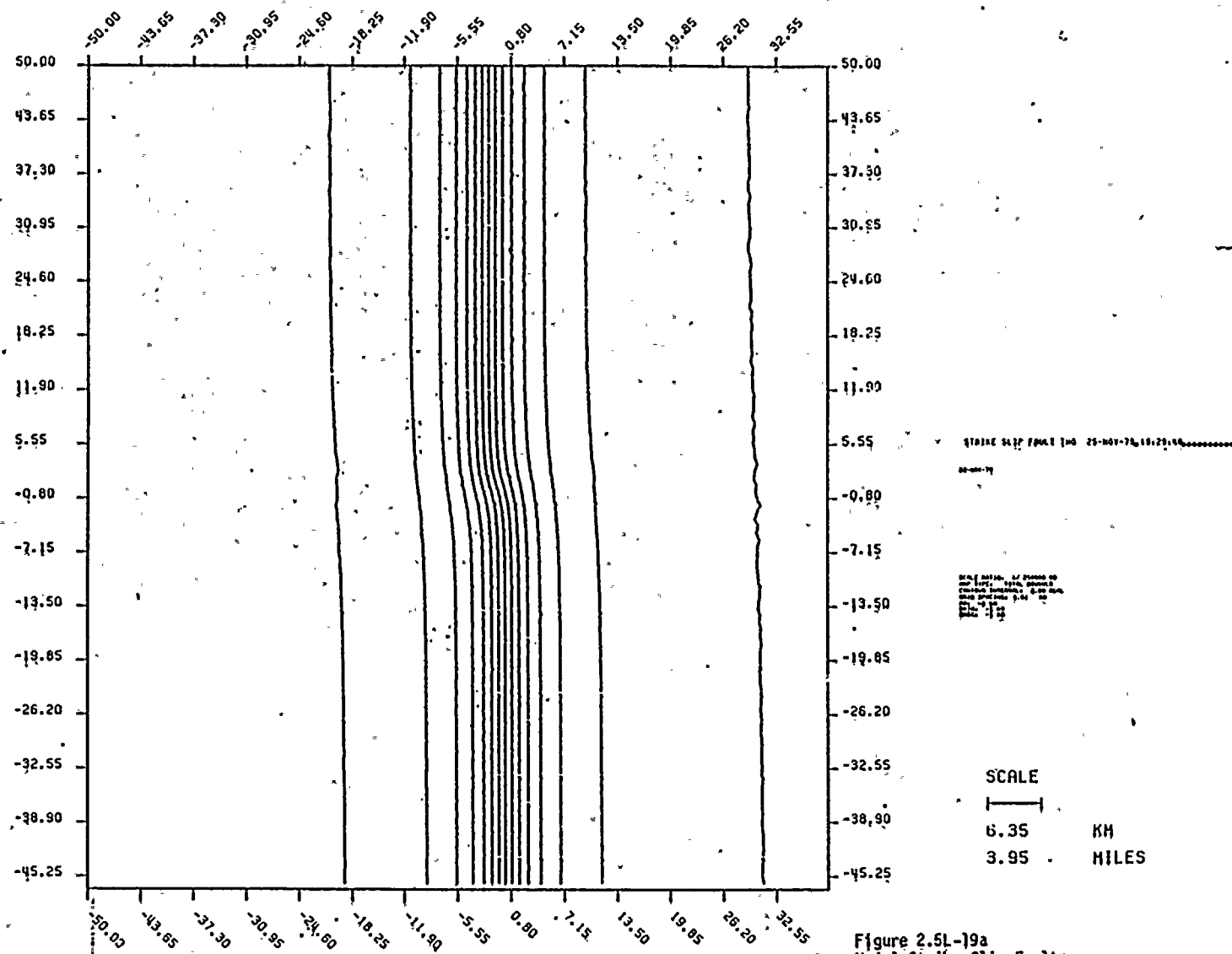


Figure 2.5L-19a  
Model Strike-Slip Faults.  
Model shown in Figure 2.5L-20  
d = 2 km scale: 1/250,000 strike: N90°W.



FIGURE 2.5L-19b  
IS CURRENTLY BEING PRINTED.

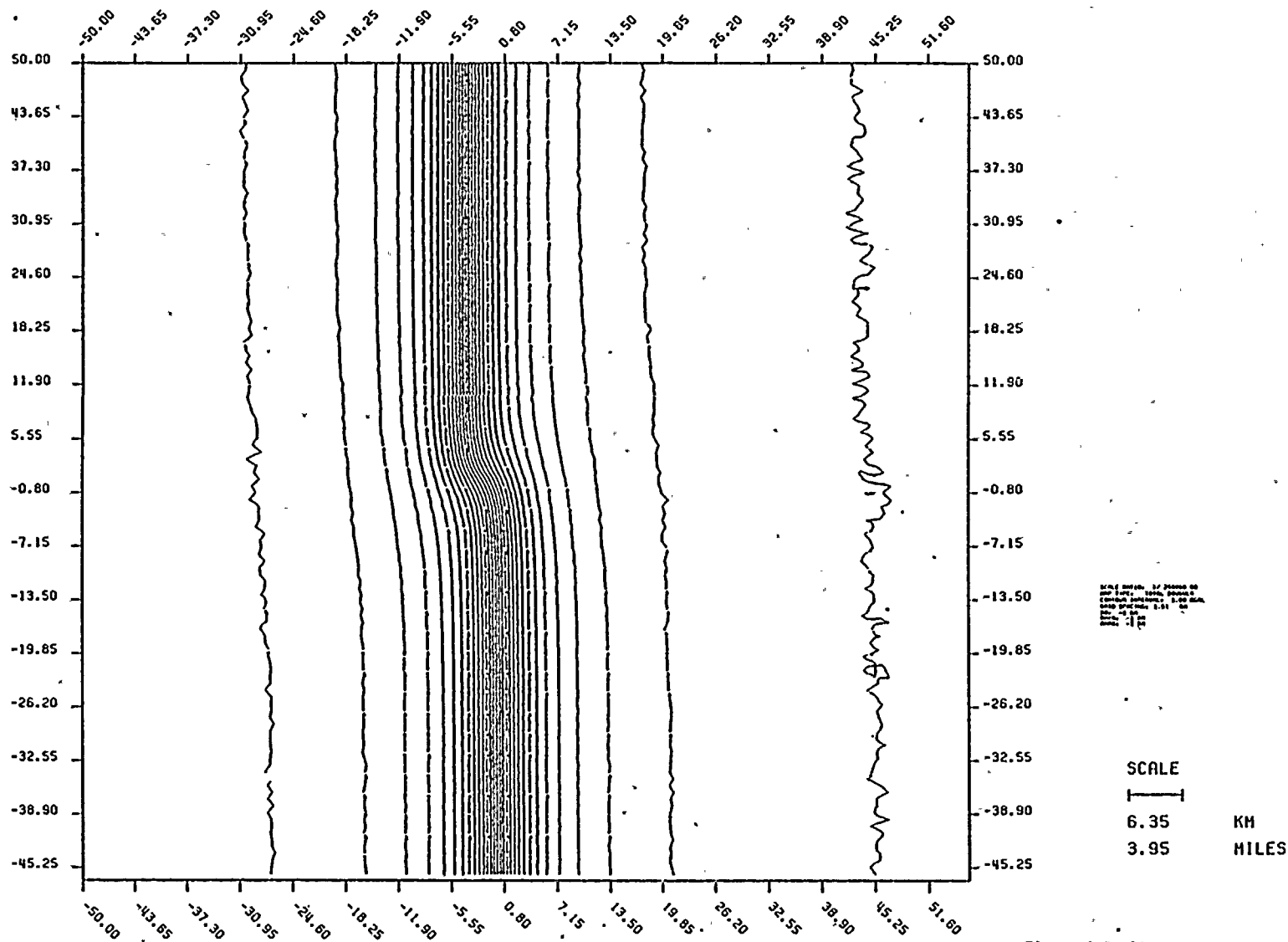
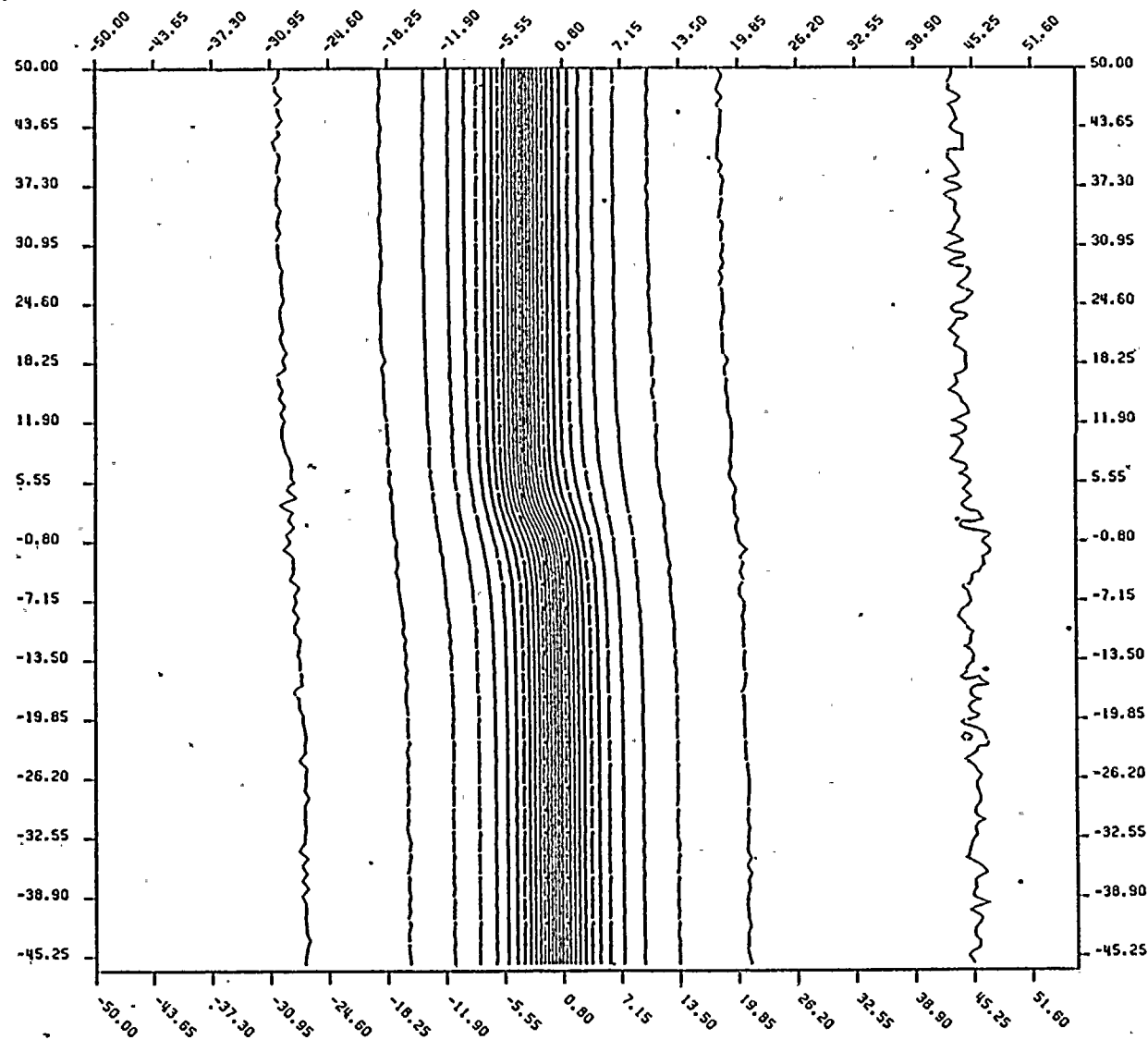


Figure 2.5L-19c  
Model Strike-Slip Faults.  
Model shown in Figure 2.5L-20  
d = 4 km scale: 1/250,000 strike: N75°W.





5573 0  
00-200-00  
00-200-00

Scale 1:250,000  
and 1:100,000  
Scale 1:250,000  
Scale 1:100,000  
Scale 1:50,000  
Scale 1:25,000

SCALE  
6.35 KM  
3.95 MILES

Figure 2.5L-19d  
Model Strike-Slip Faults.  
Model shown in Figure 2.5L-20  
d = 4 km scale: 1/250,000 strike: N60°W.



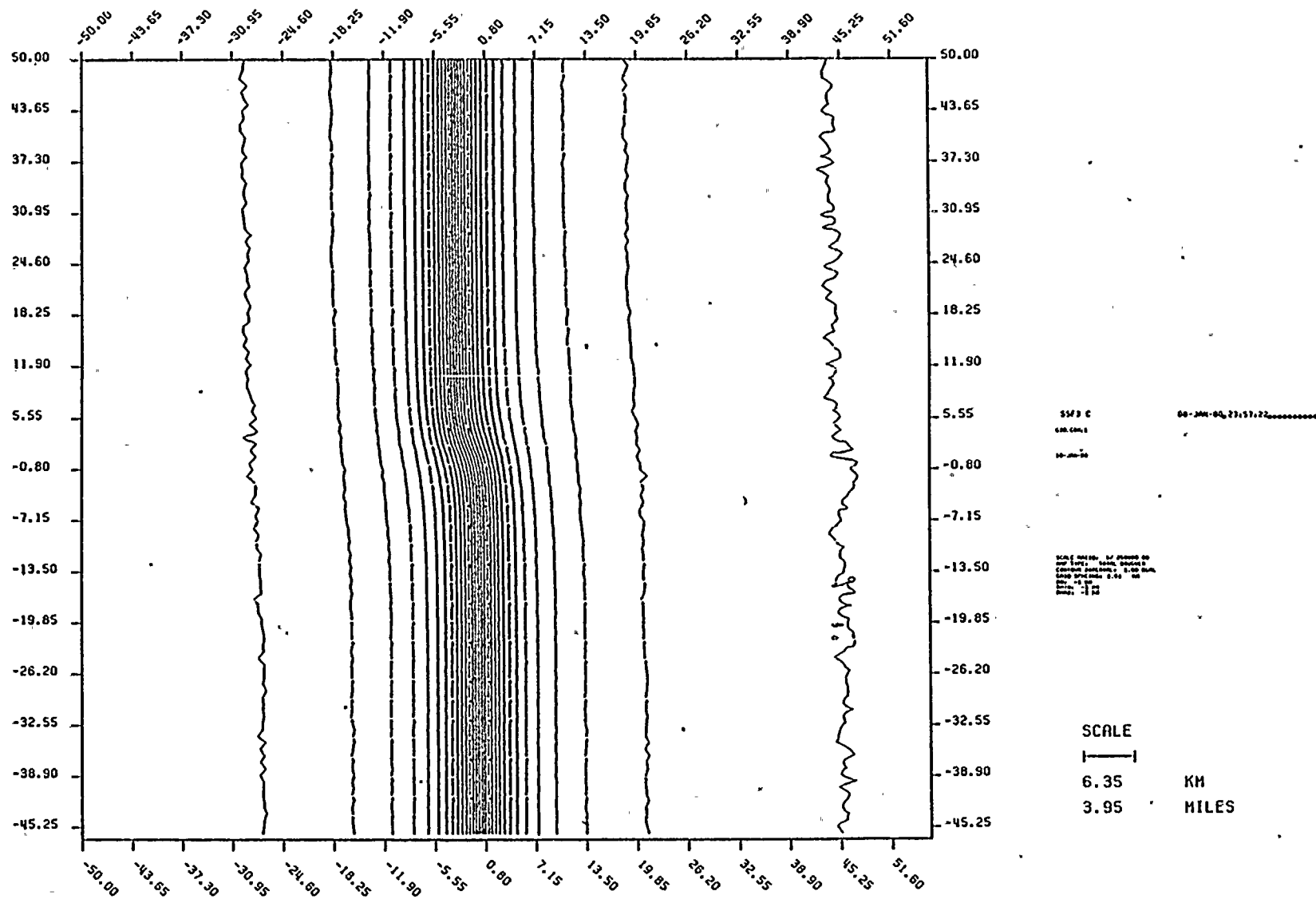


Figure 2.5L-19e  
Model Strike-Slip Faults.  
Model shown in Figure 2.5L-20  
d = 4 km scale: 1/250,000 strike: N45°W.



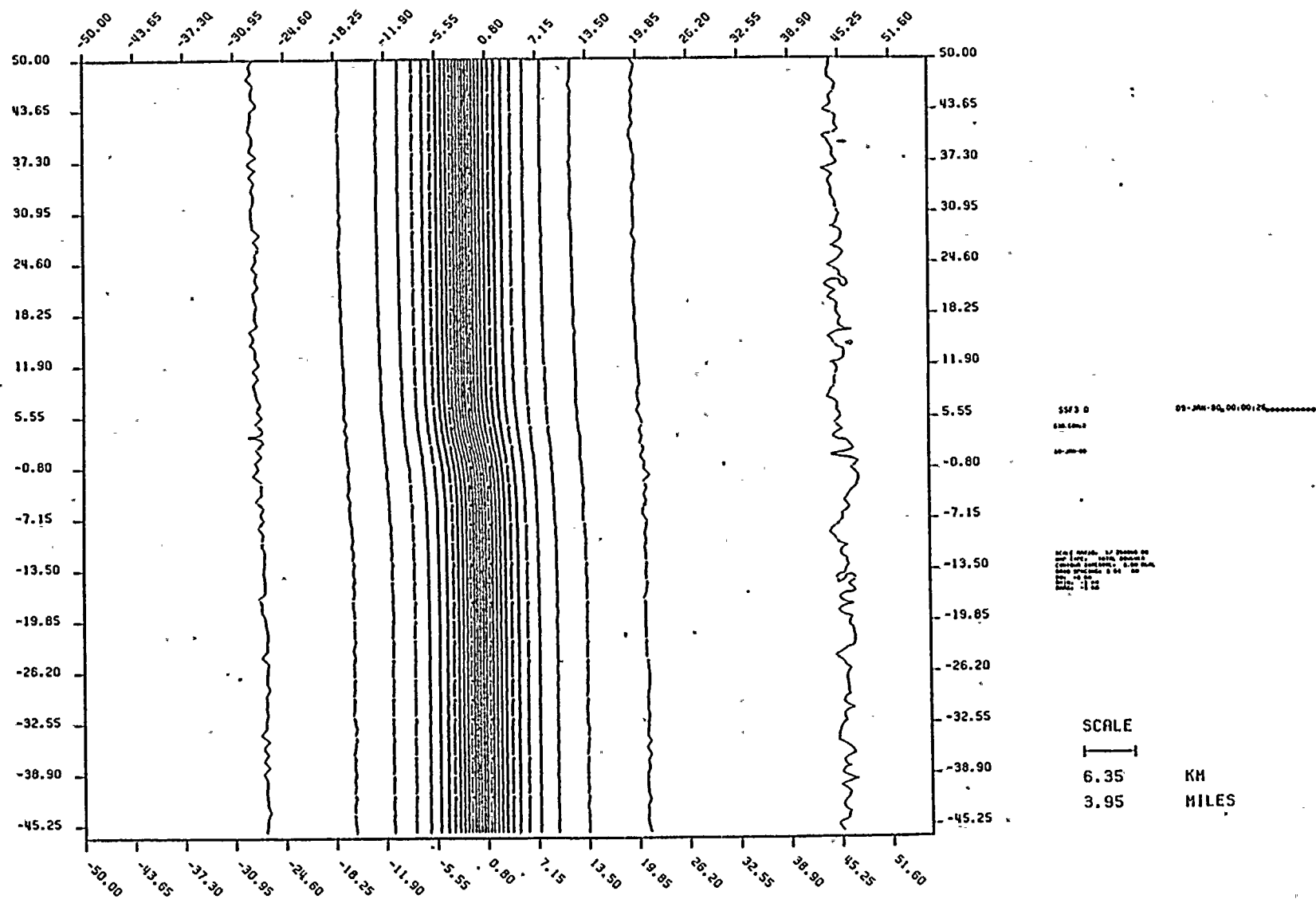


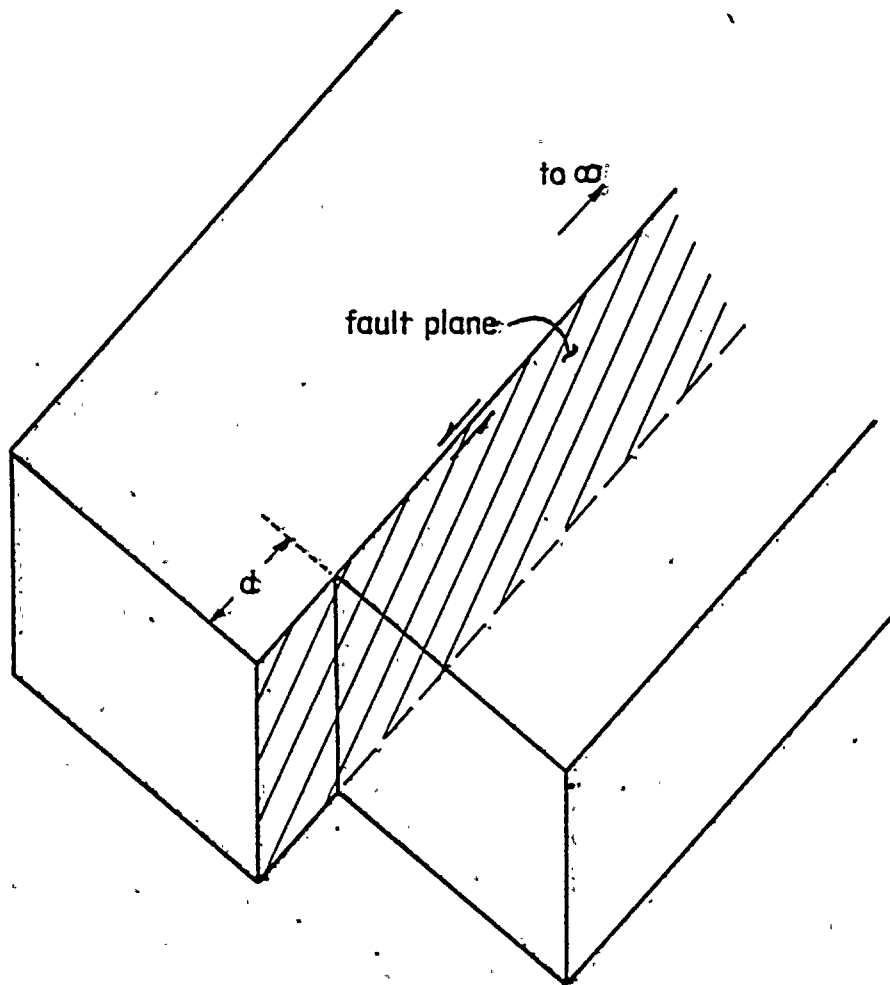
Figure 2.5L-19f  
Model Strike-Slip Faults.  
Model shown in Figure 2.5L-20  
d = 4 km scale: 1/250,000 strike: N30°W.











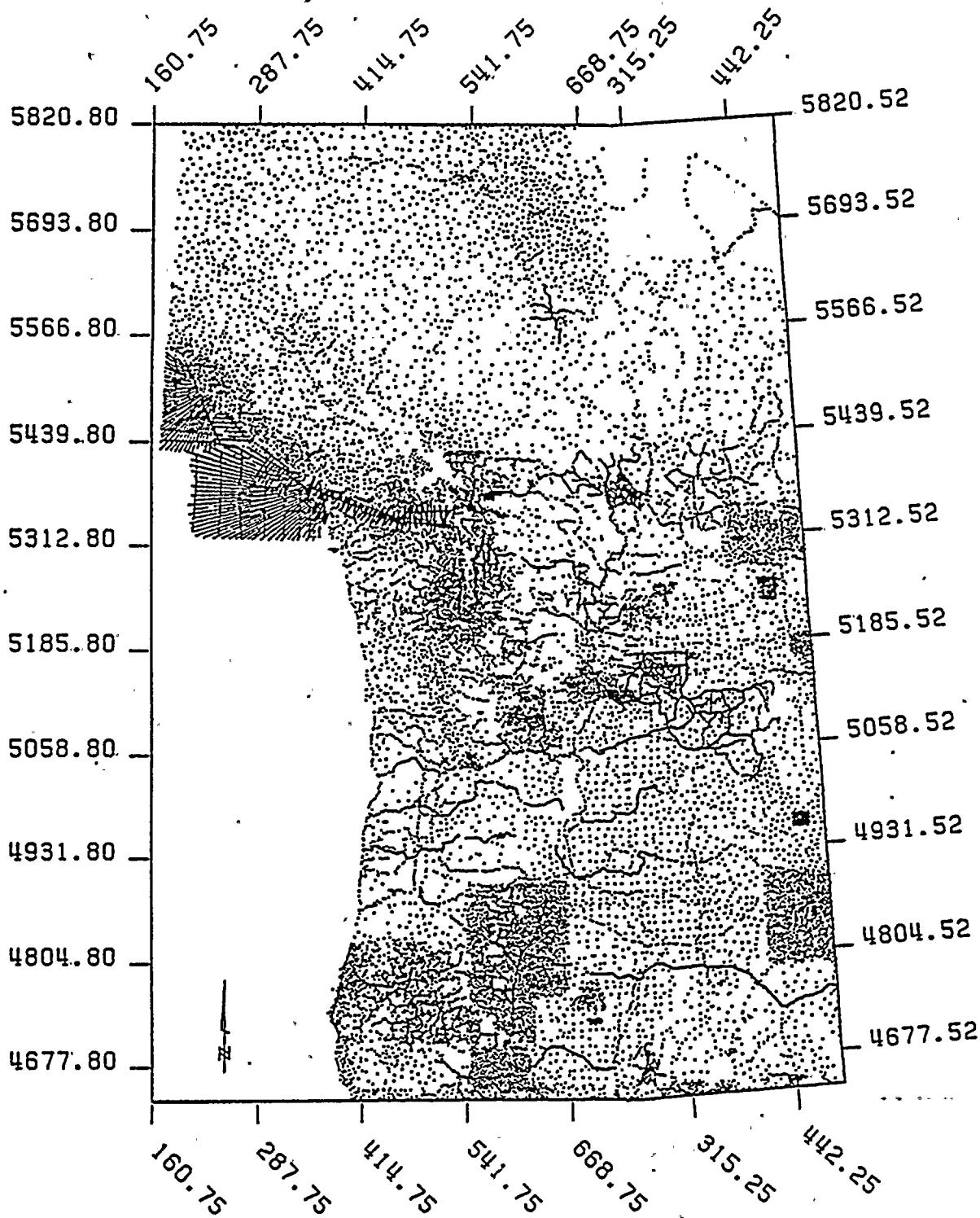


Figure 2-SL-21  
Pacific Northwest.  
Station location map.

SCALE

127.00KM  
78.91 MILES

No. OF STATIONS ON MAP 44038



FIGURES 2.5L-22 THROUGH 2.5L-25

ARE CURRENTLY BEING PRINTED.





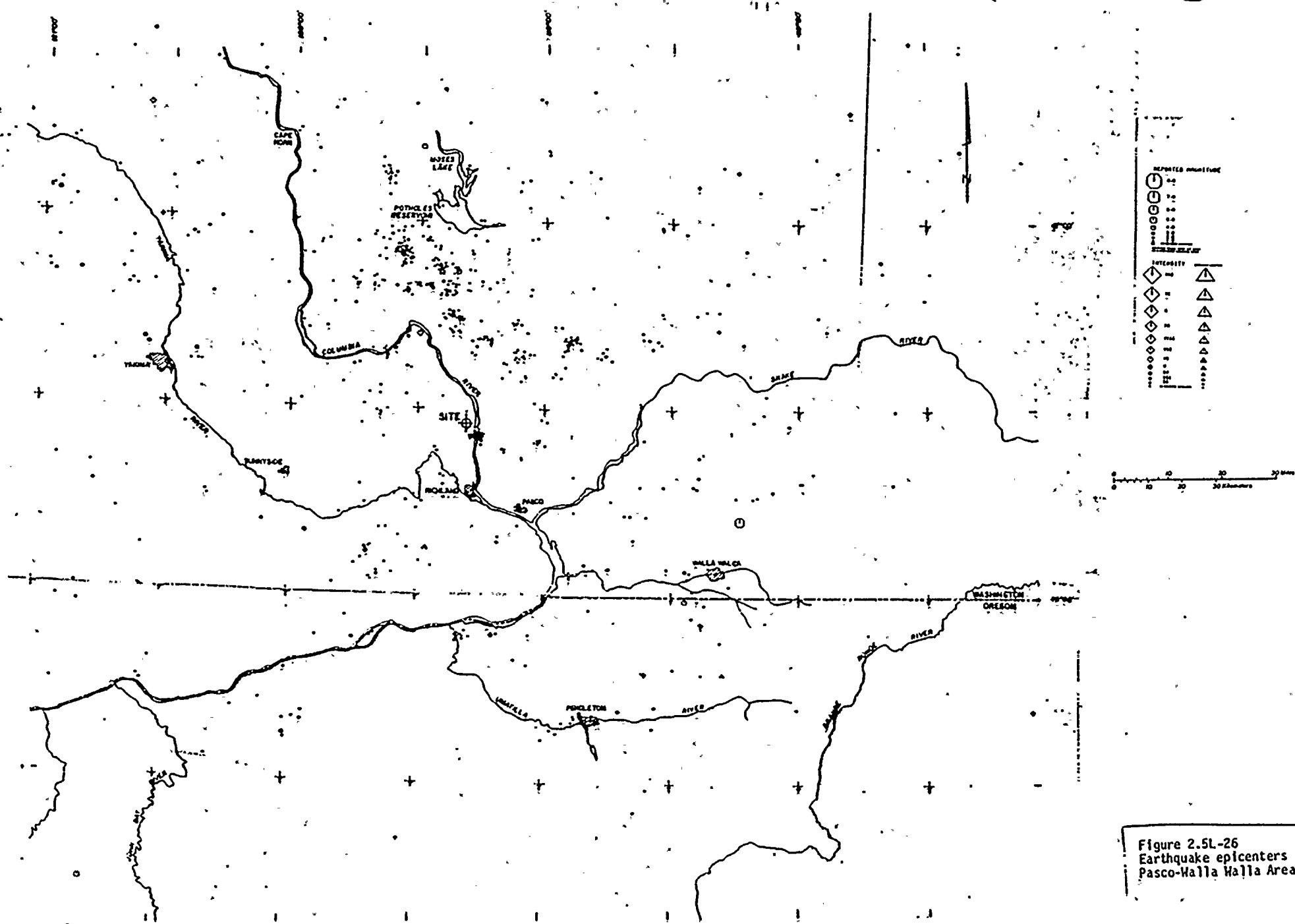


Figure 2.5L-26  
Earthquake epicenters for  
Pasco-Walla Walla Area.

ATTACHMENT I

GEOLOGIC MODELS IN THE COLUMBIA PLATEAU  
CONSTRAINED BY GRAVITY DATA

Prepared by  
WESTON GEOPHYSICAL CORPORATION

August 1981

ATTACHMENT ITABLE OF CONTENTS

	<u>Page</u>
1.1 INTRODUCTION	2.5L-37
2.1 SUMMARY AND CONCLUSIONS	2.5L-38
3.1 PROCEDURES	2.5L-39
4.1 MODELS	2.5L-40
4.1.1 RICHLAND PROFILE	2.5L-40
4.1.2 WALLULA PROFILE	2.5L-40
4.1.3 VANTAGE PROFILE	2.5L-42
4.1.4 POTHOLES PROFILE	2.5L-42
4.1.5 MOSES LAKE PROFILE	2.5L-42
4.1.6 YAKIMA AREA	2.5L-43
4.1.7 SUNNYSIDE REGION	2.5L-43
5.1 INTERPRETATION OF LAYER 2	2.5L-44
6.1 REFERENCES	2.5L-46

ATTACHMENT ILIST OF FIGURES

<u>Number</u>	<u>Title</u>
Figure 1	Pasco-Walla Walla Area. Total Bouguer Gravity Anomaly Map.
Figure 2	Pasco-Walla Walla Area. Regional Bouguer Gravity Anomaly Map.
Figure 3	Pasco-Walla Walla Area. Residual Bouguer Gravity Anomaly Map.
Figure 4	Geologic Map of Pasco-Walla Walla Area.
Figure 5	Location Map of Gravity Model Profiles.
Figure 6	Gravity Model - Richland Profile (C-C').
Figure 7	Gravity Model - Wallula Profile (I-I').
Figure 8	Gravity Model - Vantage Profile (H-H').
Figure 9	Gravity Model - Potholes Profile (E-E').
Figure 10	Gravity Model - Moses Lake Profile (G-G').

## 1.1 INTRODUCTION

Gravity maps for the central Columbia Plateau, prepared previously for the Supply System and discussed in Appendix 2.5L, are shown in figures 1, 2, and 3. The data contained in those maps constrain models of the three-dimensional spatial variation of density. In regions where different lithologic units have different densities, the constraints on density are also strong constraints on geologic structures. In the Columbia Plateau, the densities of basalt differ significantly from the densities of other rock types found there. Hence, the observed gravity anomalies of figures 1, 2, and 3 provide constraints on models of geologic structures in the Columbia Plateau. They also provide very strong constraints on models of the topography of basalt surfaces that are buried beneath unconsolidated sediments. Dr. Gene Simmons was Weston's consultant for this study.

We have explored the constraints posed by the gravity data on permissible geologic models for several areas in the central Columbia Plateau. The models described in this report are consistent with the gravity data of figures 1-3 and with the geologic observations summarized on the geologic map, figure 4, and in various reports (Washington Public Power Supply System, 1977; Shannon and Wilson, 1979a, b; Rockwell, 1979).

Inspection of the gravity maps reveals a prominent anomaly of 12 to 15 mgals amplitude that extends north-south from approximately the Oregon-Washington state line to the Potholes Reservoir and east-west from Sunnyside to a few kilometers east of Richland. On the basis of this anomaly, we inferred (Appendix 2.5L) the presence of a relatively dense mass of rock (termed Layer 2) beneath the Columbia River basalts. The top of Layer 2 is approximately 2 to 4 kilometers deep in the southern part and the unit is likely several kilometers thick. The product of thickness and density contrast is known unequivocally from the amplitude of the gravity anomaly. In addition, the maximum depth of the bottom of the unit is constrained by the width of the gravity anomaly associated with the edges of the body. In Appendix 2.5L, we used a density contrast of +0.187. This value has been retained in the models given in this report. Values as small as 0.15 are marginally acceptable within the constraint of the width of the gravity anomaly along the western edge of Layer 2 where the anomaly is known best (because of the high density of stations). The upper limit is constrained only by 'geologic reasonableness' of the densities of large rock masses. For



example, a density contrast of  $2.0 \text{ gm/cm}^3$  would require the presence of rock types that are unknown on the earth in single bodies with volumes of order of 1,000 and 10,000 cubic kilometers. A range of values from 0.15 to  $0.30 \text{ gm/cm}^3$  is 'geologically reasonable', consistent with the rock types known to occur at the surface within a few tens of kilometers west of the inferred western edge of Layer 2, and within the constraints of the width of the anomaly at the western edge. There is no practical effect on our results from using  $0.187 \text{ gm/cm}^3$  rather than any other value within the range  $0.15\text{--}0.30 \text{ gm/cm}^3$ . Models with a different value of the density contrast ( $\Delta\rho$ ) would have the same shape but a thickness,  $t$ , given by  $t = .187T$  where  $T$  is the thickness determined with a density contrast of  $0.187 \text{ gm/cm}^3$ . Dr. Gene Simmons was Weston's consultant for this study.

## 2.1 SUMMARY AND CONCLUSIONS

In the central Columbia Plateau, the dominant feature in the Bouguer gravity anomaly map (Figure 1) is a relatively large gravity anomaly that extends north-south for approximately 93 kilometers, east-west for 47 kilometers, and has two lobes on its southern end. That anomaly has been interpreted previously (Appendix 2.5L) to indicate the presence of a subsurface unit, termed Layer 2. It is roughly tabular, several kilometers thick south of the Rattlesnake Hills alignment, 2-4 kilometers thick in the vicinity of Vantage, and thins appreciably towards the northern end. It has two lobes on the southern end. All profiles for the present study cross edges or lobes of the inferred body.

The Wallula profile, which extends northeast-southwest, passes through Wallula Gap and crosses an unnamed sediment-filled basin north of Touchet, for a distance of approximately 90 kilometers. This profile crosses the Walla Walla lobe of Layer 2. The gravity data are matched very well with a model in which the Walla Walla lobe is approximately 1 to 2 kilometers thick (density contrast 0.187) and the basin contains low density sediments or sedimentary rocks with a maximum thickness of approximately 150 meters (density contrast  $-0.67 \text{ gm/cm}^3$ ).

Models were investigated for profiles that cross the boundary of Layer 2 in the vicinity of Vantage, Potholes Reservoir, Moses Lake, and Richland. The gravity constraints are consistent with a thickness of the layer of 2-4 kilometers and a density contrast of  $+0.187 \text{ gm/cm}^3$  along these profiles. The outer edges of this unit dip

inward toward the center of the body at angles of 5 to 10°. A plausible geological interpretation of this model is a basin that has subsided with time and has been filled with extrusive igneous rocks. The rock now forming the lower part of Layer 2 south of Rattlesnake Hills alignment flowed through a vent probably located near Blalock Canyon, Oregon. The upper part of Layer 2, which is geographically more extensive, was extruded through a vent probably located near Walla Walla. Another permissive interpretation would allow extrusion through both vents.

The gravity data were examined in the vicinity of several large anticlinal folds and their projections into adjacent regions where the folds were not exposed at the surface: the Rattlesnake structure, the extension of the Toppenish Ridge to the east, and Manastash Ridge in the vicinity of Yakima. No evidence of displacement in the lower basalt interface beneath the Rattlesnake structure in the Yakima area was found. The residual gravity anomalies associated with the extensions of Toppenish and Manastash Ridges are zero. The interpretation of the gravity data along such profiles indicates that no displacement greater than 100 meters has occurred at the lower basalt interface and that topographic relief on the buried upper basalt surface must be less than 100 meters (a value required by the precision of the present set of gravity data).

### 3.1 PROCEDURES

Each region included in this study was selected because it contained a significant geologic structure with little data on its vertical extent. We expected the gravity data to allow us to improve models of the structure at depth. Within each region, the exact location and azimuth of the profile were chosen on the basis of the nature and orientation of the gravity anomalies. We prefer to work with a single gravity anomaly (rather than composite anomalies that must be separated). Furthermore, the length of an individual anomaly should be at least three times its width for two-dimensional models to be suitable.

The gravity anomalies for each model were calculated with the two-dimensional algorithm described by Talwani and others (1959). They were compared with the observed gravity anomaly. If the two anomalies differed by more than a 1/2 mgal, the model of density was modified and a new anomaly for the model was calculated. This iterative procedure was continued until a satisfactory match was obtained. Normally, 10 to 30 different models were explored for each profile.



All models were examined by two different experienced analysts, Gene Simmons and Jeffrey Mann. In every instance, the final model was reached independently by each of them. Such convergence lends a higher degree of confidence in the validity of the model, as judged geologically, than a procedure in which a single individual examines several models.

#### 4.1 MODELS

The locations of the individual profiles are shown in figure 5. The locations were selected to provide data in critical areas and to provide data that could be modelled satisfactorily with a two-dimensional algorithm.

##### 4.1.1 RICHLAND PROFILE

The observed gravity, topography, and model for the Richland profile are shown in figure 6. The match between observed gravity and calculated gravity is sufficient to conclude that the model shown in figure 6 fits the data. The major contribution to calculated gravity is the gravitational attraction of Layer 2. Because the surface elevation varies considerably along the profile, a portion of the observed gravity anomaly is due to an artifact. If the density of the rock between the surface of the earth and sea level differs from the density used for the Bouguer reduction, then the Bouguer reduction produces an 'extra' anomaly of  $2\pi G(\rho_{\text{true}} - \rho_{\text{Bouguer}})h$ , where  $G$  is the universal gravitational constant,  $\rho_{\text{true}}$  is the actual density of the rock,  $\rho_{\text{Bouguer}}$  is the value of density used in the Bouguer reduction, and  $h$  is the elevation. After accounting for the contributions from these two sources, the remaining gravity anomaly is quite small. There is no indication in the gravity data of a significant vertical component of displacement at the bottom of Layer 2.

##### 4.1.2 WALLULA PROFILE

The location of the Wallula profile is shown in figure 5. It crosses the Rattlesnake Hills structure, the Olympic-Wallula Lineament, and several smaller mapped faults in the vicinity of Wallula.

Inspection of the total Bouguer gravity anomaly map (figure 1) reveals that three separate gravity anomalies are present in the vicinity of Wallula. At different locations within the region the separate anomalies interfere with each other. One anomaly can be traced reliably into the Wallula region from the nearby edges of Layer 2; it is attributed to

the presence in the subsurface of a lobe of Layer 2 that extends east from Wallula to the vicinity of Walla Walla. A second anomaly correlates with the unnamed basin north of the highway between Wallula and Walla Walla. It is attributed to low density sediments that fill the basin. A third anomaly, distinct from the other anomalies, can be traced reliably into the Wallula region from the vicinity of Service Buttes (OR), a distance of 80 kilometers. This anomaly trends parallel to the axis of the Blue Mountain anticline. All three of these anomalies are recognized in regions away from the profile. The location of the profile was chosen to minimize the interference effects of three anomalies along the profile. )

The topography, observed gravity anomaly, calculated gravity anomaly, and model are shown in figure 7. The observed gravity is matched sufficiently well by the calculated gravity anomaly that we conclude the model is valid. (The 1 1/2 mgal difference near 25 kilometers distance is ignored; it is an artifact caused by the contouring algorithm in a region of few stations.) The gravity variations observed along the profile are attributed to two anomalous masses; namely, the Walla Walla lobe of Layer 2 and the sediments that fill the unnamed basin north of Wallula-Walla Walla highway.

In the vicinity of Wallula, the Walla Walla lobe of Layer 2 is 1-2 kilometers thick. Although the exact thickness depends on the density contrast of the rocks, the more likely values of thickness are in the range of 1 to 2 kilometers..

The gravity anomaly that extends from approximately 40 to 70 kilometers along the profile, attributed to the presence of low density sediments in the basin, is matched by the anomaly calculated with a density of 2.0 (contrast -0.67) gm/cm<sup>3</sup> and thickness of 140 meters for the sediments. If the density contrast is lower, then the thickness is proportionally larger.

Inspection of the gravity maps shows rather steep gradients to be present southeast of Wallula. The zone of increased gradients extends east through College Place and Umapine to the vicinity of Walla Walla. Both the increase of gradient and the gravity lineament is produced by the interference of two gravity anomalies: One anomaly is due to the Walla Walla lobe of Layer 2 and the other anomaly can be traced over the region between Little Goose Lock and Dam to the Umatilla River.

Although faulting has been observed at the surface (see, e.g., Newcomb, 1965; Shannon & Wilson, 1979) in the vicinity of the southern edge of the Walla Walla lobe of Layer 2 in the vicinity of Wallula, there is no indication in the gravity field that it extends to depth. Neither is the increase of gravity gradient due to the fault.

#### 4.1.3 VANTAGE PROFILE

The Vantage profile is one of several profiles across the edge of Layer 2. Its location is shown in figure 5. It crosses Layer 2 a few kilometers south of Vantage, Washington.

The topography, observed and calculated gravity anomalies, and model for the profile are shown in figure 8. The gravity anomaly is consistent with a thickness of 5 kilometers, and density contrast of  $+0.187 \text{ gm/cm}^3$ , respectively, for Layer 2. Our interpretation of this profile is that the anomaly is due chiefly to the density contrast provided by Layer 2 with respect to the surrounding rocks. The base of the unit dips inward along this profile at approximately  $70^\circ$ . The implications of this profile on the origin of Layer 2 are discussed in section 5.0.

#### 4.1.4 POTHOLE PROFILES

The Potholes profile is one of several profiles across the edge of Layer 2. It is located at the north end of Layer 2 and crosses the edge in a north-south direction.

The topography, observed and calculated gravity anomalies, and model are shown in figure 9. Along this profile, Layer 2 varies in thickness from 0 to 3 kilometers for a density contrast of  $+0.187 \text{ g./cm}^3$ . This profile, the model, and the interpretation of gravity were consistent with the other models and interpretations for the other profiles that cross Layer 2. The implication of this profile on the origin of Layer 2 are discussed in section 5.0.

#### 4.1.5 MOSES LAKE PROFILE

The Moses Lake profile is one of several profiles that cross the edge of Layer 2. Its location, on the west side of Layer 2, is shown in figure 5. The topography, calculated and observed gravity anomalies, and model are shown in figure 10. Maximum thickness of Layer 2 along this profile is approximately 2 kilometers for a density contrast of  $0.187 \text{ gm/cm}^3$ . The bottom of the unit slopes toward the center of the mass at an angle of approximately  $8-10^\circ$ .

This model and its interpretation are consistent with the other models and interpretations of profiles that cross Layer 2. The implications of this profile for the origin of Layer 2 are discussed in section 5.0.

#### 4.1.6 YAKIMA AREA

The region around Yakima was examined for possible gravity anomalies that might be associated with the Yakima ridges. It was hoped that such anomalies, if present, would provide strong constraints on the distribution of density of subsurface rock masses. The same gravity data for the region used originally for the preparation of the Pasco-Walla Walla map were recontoured at a smaller contour interval. No gravity anomaly is associated with the ridges or with their extensions. Therefore, no profile was constructed and no model was examined.

The absence of a gravity anomaly on the extensions of the ridges, together with the large density contrast between basalt and the sediments that fill the basins (at least  $0.5 \text{ gm/cm}^3$ ), constrain models of the basalt surface beneath the sediment. Topographic relief of 300 feet, whether due to erosion, folding, faulting, or a combination of the processes, would have produced a gravity anomaly of about 2 mgals. Such an anomaly, which should have been recognized with the present set of data, is not present. The interpretation of the gravity data along this profile indicates that no displacement greater than 100 meters has occurred at the lower basalt interface and that topographic relief on the buried upper basalt surface must be less than 100 meters (a value required by the precision of the present set of gravity data).

#### 4.1.7 SUNNYSIDE REGION

The Toppenish Ridge appears to terminate a few kilometers west of Sunnyside. About 300 gravity stations at a spacing of 0.6 kilometer had been established in this region in 1979 and 1980. The data were used to construct the Pasco-Walla Walla map. The same data were recontoured in the present study at a smaller contour interval for the purpose of determining whether residual anomalies might exist along the continuation of Toppenish Ridge toward the east. No gravity anomaly that might be associated with the eastward subsurface continuation of Toppenish Ridge was found. Therefore, no gravity model was constructed.

The absence of a gravity anomaly on the extension of Toppenish Ridge constrains models of the basalt surface.



The density contrast between basalt and the sediments that fill the basin is at least  $0.5 \text{ gm/cm}^3$ . Relief on the basalt surface of 100 meters would produce an anomaly of 2 mgal. The present data set is adequate for the detection of an anomaly of 2 mgal but none was detected. The interpretation of the gravity data along this profile indicates that no displacement greater than 100 meters has occurred at the lower basalt interface and that topographic relief on the buried upper basalt surface must be less than 100 meters (a value required by the precision of the present set of gravity data).

### 5.1 INTERPRETATION OF LAYER 2

Layer 2 is a large mass of rock relatively high density that occurs in the central Columbia Plateau. Its total anomalous mass is  $7 \times 10^{18} \text{ gm}$ , a value that is independent of models and requires no assumption about density. If the density contrast is  $0.187 \text{ gm/cm}^3$ , a value justified in Appendix 2.5L and discussed earlier in this report, then the volume occupied by Layer 2 is  $37,000 \text{ kilometers}^3$ . For the range of density contrasts  $0.15\text{--}0.30 \text{ gm/cm}^3$ , the estimated volume ranges from  $46,000 \text{ kilometers}^3$  to  $23,000 \text{ kilometers}^3$ .

The profiles across the edges of Layer 2 (Vantage, Potholes Reservoir, and Moses Lake) are consistent with edges of the unit that dip a few degrees toward the interior of the body. We infer that the body is a relatively thick pile of extrusive rocks, say andesite or basalt, that accumulated in a subsiding basin that is elongated in a north-south direction.

The body appears to be thicker towards the south. It thickens appreciably south of the Rattlesnake Hills alignment and attains a thickness of 8 to 10 kilometers in the vicinity of Lenzie Ranch, 25 kilometers southwest of Richland.

The two lobes on the southern end of Layer 2 are possible indications of the locations of the vents through which the rock was extruded. We suggest that the uppermost and geographically more extensive portion of Layer 2 was extruded through a vent in the vicinity of Walla Walla and flowed through the region now filled with the Walla Walla lobe. We suggest that the lowermost portion of Layer 2 which is also geographically restricted to the region south of the Rattlesnake Hills alignment flowed through the



southwest lobe from a vent located near Blalock Canyon, Oregon. An alternate model would have extrusion through both vents.

After the emplacement of Layer 2, the Columbia River basalts covered Layer 2. The age of Layer 2 is unknown but must be greater than the age of the oldest Columbia River basalt.



## 6.1 REFERENCES

Newcomb, R. C., 1965, Geology and Ground Water Resources of the Walla Walla River Basin, Washington-Oregon: Washington Division of Water Resources, Water Supply Bulletin No. 21, 151 p.

Rockwell, 1979, Geologic Studies of the Columbia Plateau, a Status Report: Rockwell Hanford Operations, Richland, Washington, Report RH0-BWI-ST-4.

Shannon & Wilson, Inc., 1979a, Evaluation of Faulting in the Warm Springs Canyon Area, Southeast Washington: Report prepared for Washington Public Power Supply System, 18 p.

Shannon & Wilson, Inc., 1979b, Geologic Reconnaissance of the Wallula Gap, Washington-Blue Mountains-LaGrande, Oregon Region: Report prepared for Washington Public Power Supply System, 63 p.

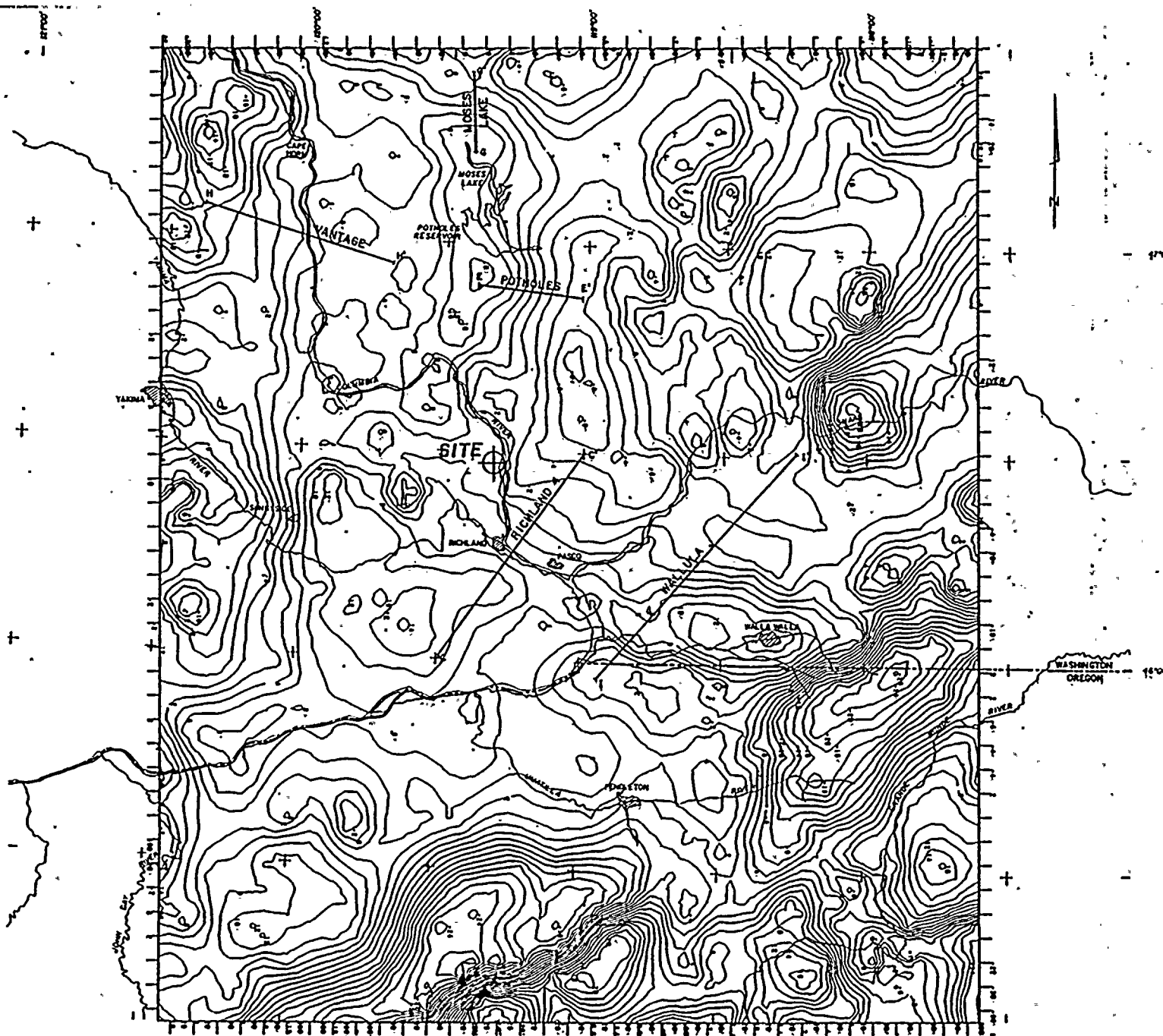
Talwani, M., Worzel, J. L. and Landisman, M., 1959, Rapid Gravity Computations for Two-Dimensional Bodies with Application to the Mendocino Submarine Fracture Zone: Journal of Geophysical Research, V. 64, No. 1, p. 49-59.

Washington Public Power Supply System, 1977, WNP 1/4 Preliminary Safety Analysis Report, Amendment 23.

Weston Geophysical Corporation, 1981, Compilation and Interpretation of Gravity in Washington, Oregon, and Adjacent Parts of British Columbia and Idaho, Draft of Appendix 2.5L to the WNP 2 FSAR, prepared for Washington Public Power Supply System under the direction of United Engineers and Constructors, 28 p.

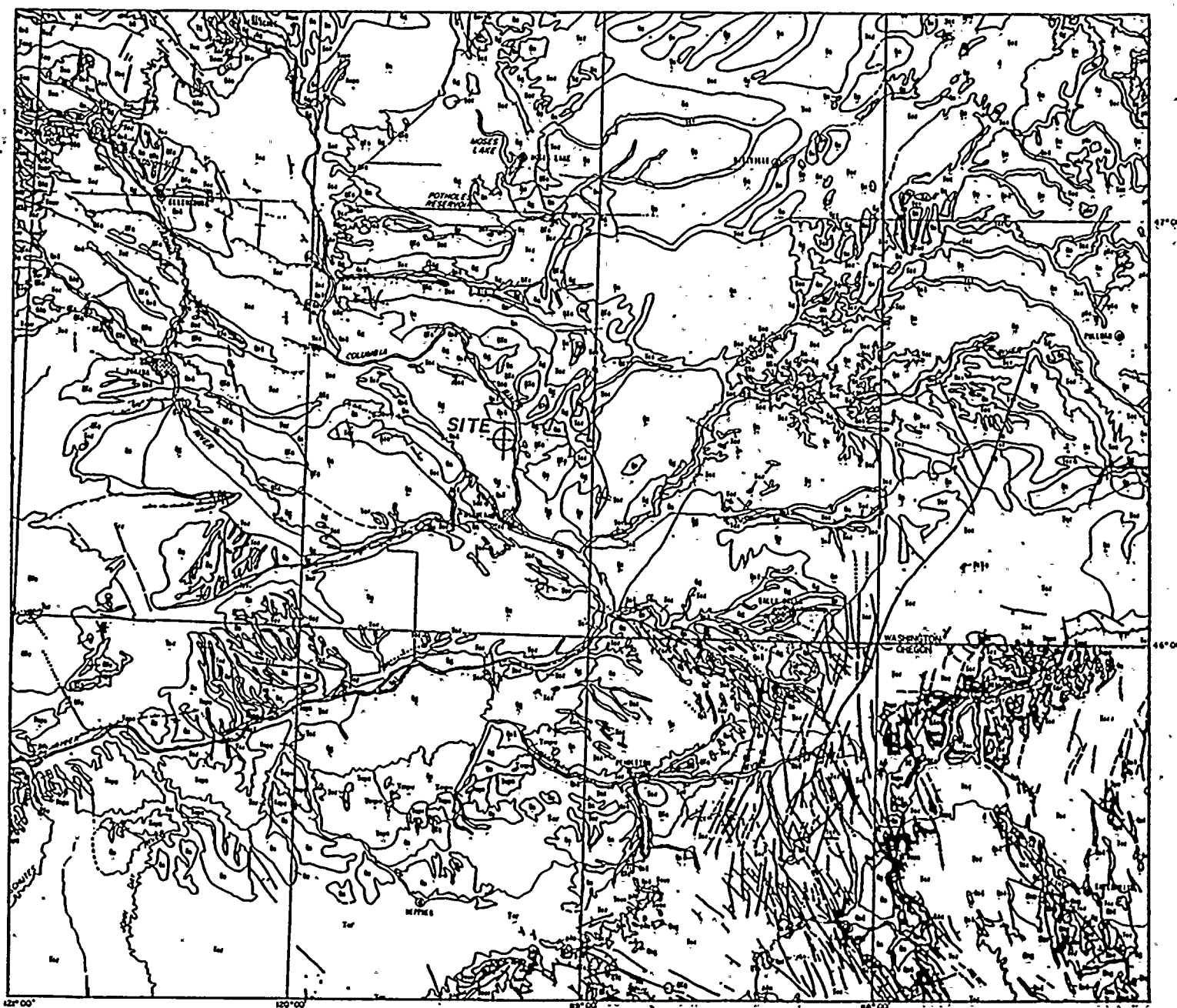






CONTOUR INTERVAL 20 FEET  
 DENSITY 0.01 g/cm<sup>3</sup>

ATTACHMENT 1  
 FIGURE 3  
 PASCO-WALLA WALLA AREA  
 RESIDUAL BOUGUER GRAVITY ANOMALY



#### GEOLOGIC UNITS

Qa	ALLUVIUM
Qd	LANDSLIDE DEPOSITS
Qp	GLACIAL DRIFT UNDIFFERENTIATED
Qs	PROGLACIAL DEPOSITS
Qt1	PLIOCENE-PLISTOCENE NONMARINE SEDIMENTARY ROCKS
Qt2	PLIOCENE-PLISTOCENE VOLCANIC ROCKS
Tm1	MIocene-PLIOCENE NONMARINE SEDIMENTARY ROCKS
Tm2	MIocene-PLIOCENE VOLCANIC ROCKS
Tc	COLUMBIA RIVER BASALT GROUP
Tm3	OLIGOCENE-MIOCENE VOLCANIC ROCKS
Tm4	EOCENE-OLIGOCENE NONMARINE SEDIMENTARY ROCKS
Tm5	EOCENE-OLIGOCENE VOLCANIC ROCKS
Tm6	EOCENE-OLIGOCENE GRANITE ROCKS
Tm7	EOCENE-NONMARINE SEDIMENTARY ROCKS
Tm8	EOCENE NONMARINE VOLCANIC ROCKS
Am	PRE-AMALGAM METAMORPHIC ROCKS
M	PALEOZOIC TO TERTIARY MAFIC INTRUSIVE ROCKS

#### GEOLOGIC MAP SYMBOLS

##### CONTACT

Dashed where of doubtful or inferred.  
Indicates the same unit occurs across other map symbols.

##### FAULTS

Solid where approximately located.  
Dashed where uncertain; dotted where concealed.

##### NORMAL FAULT

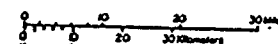
Bar and half on downthrown side.

##### STRIKE-SLIP FAULT

Showing relative horizontal movement.

##### THRUST FAULT

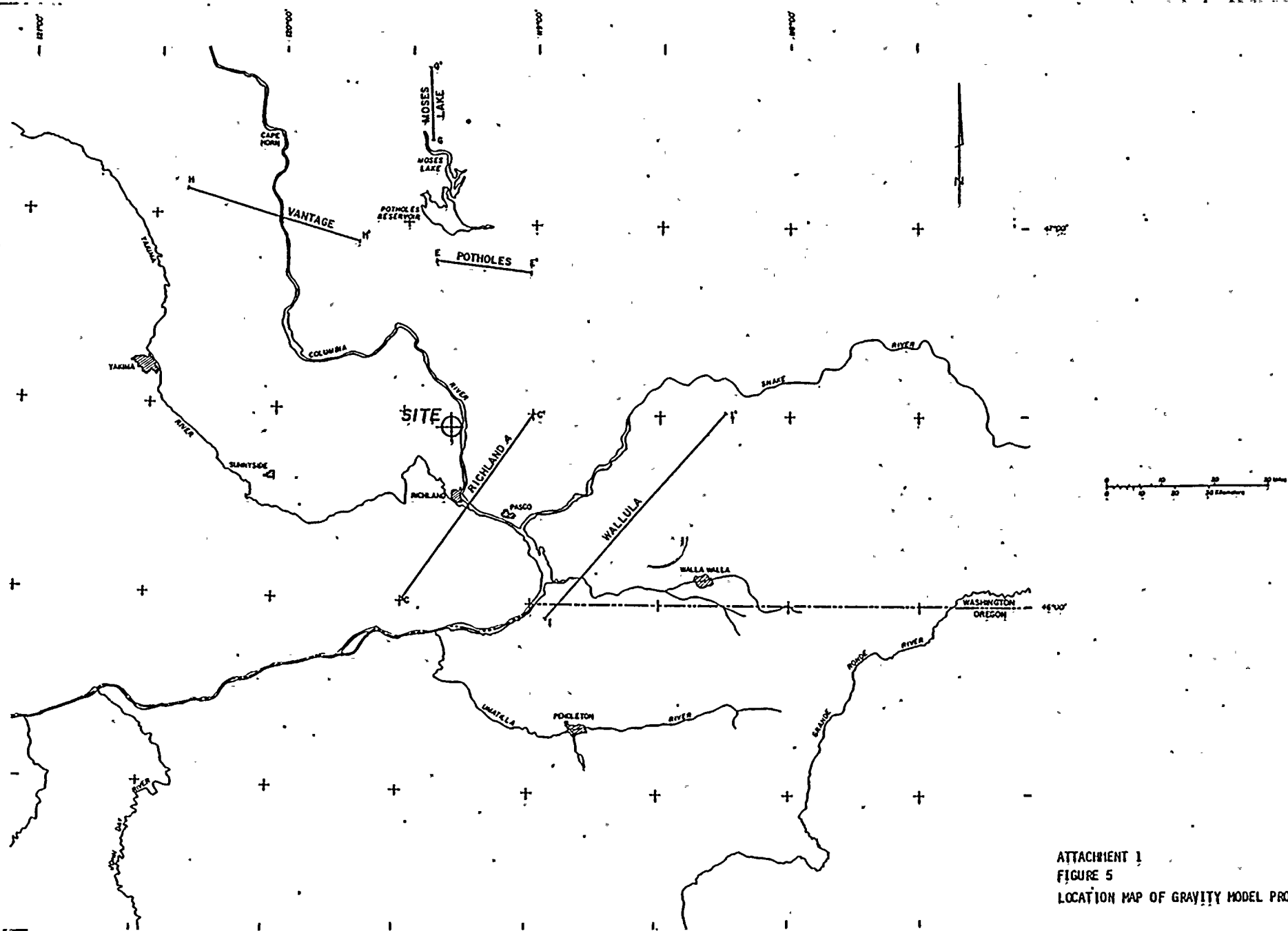
Bar on upper plate.



ATTACHMENT 1  
FIGURE 4

GEOLOGIC MAP OF PASCO-HALLA HALLA AREA

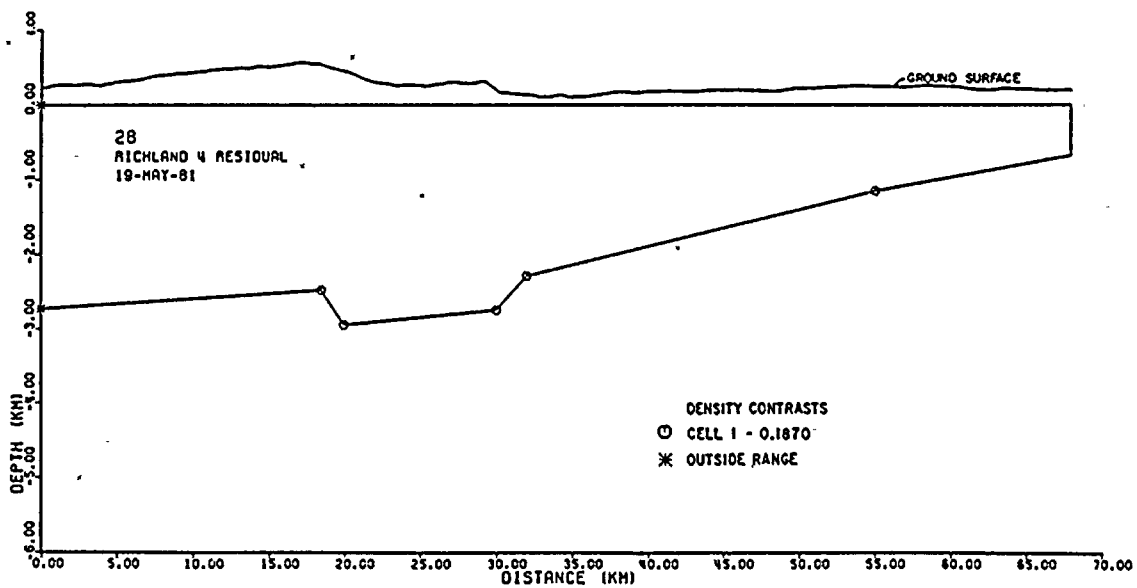
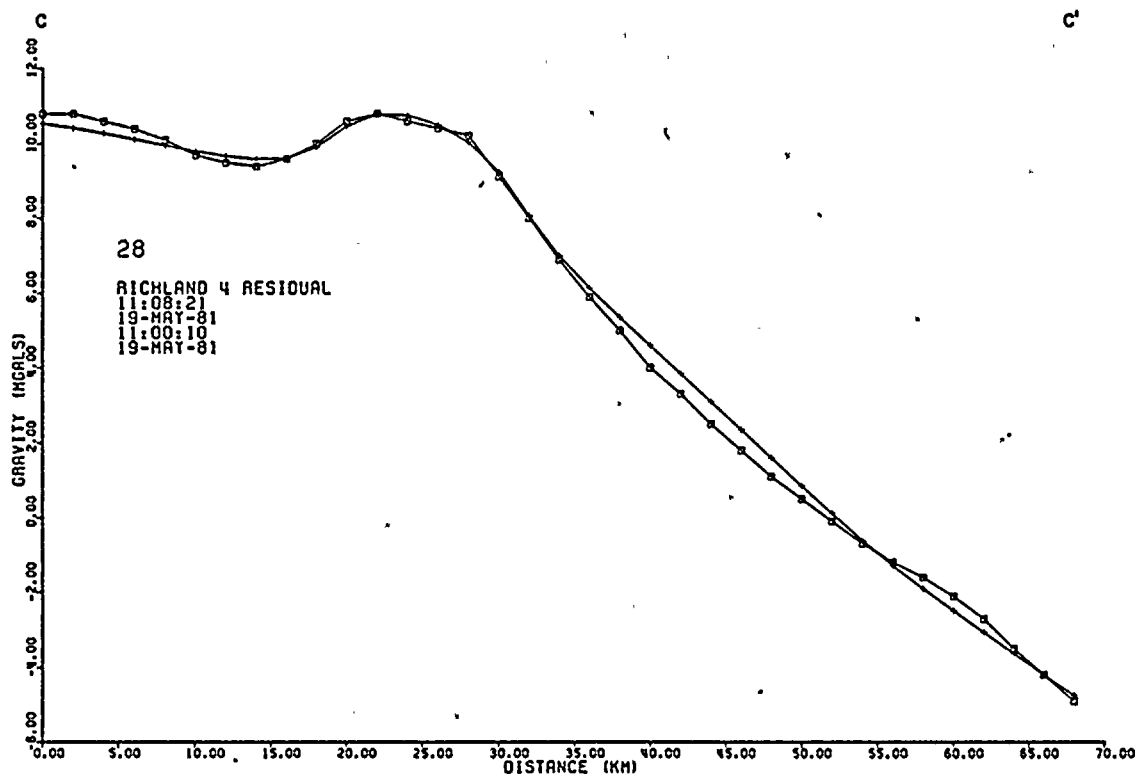




ATTACHMENT 1  
FIGURE 5  
LOCATION MAP OF GRAVITY MODEL PROFILES





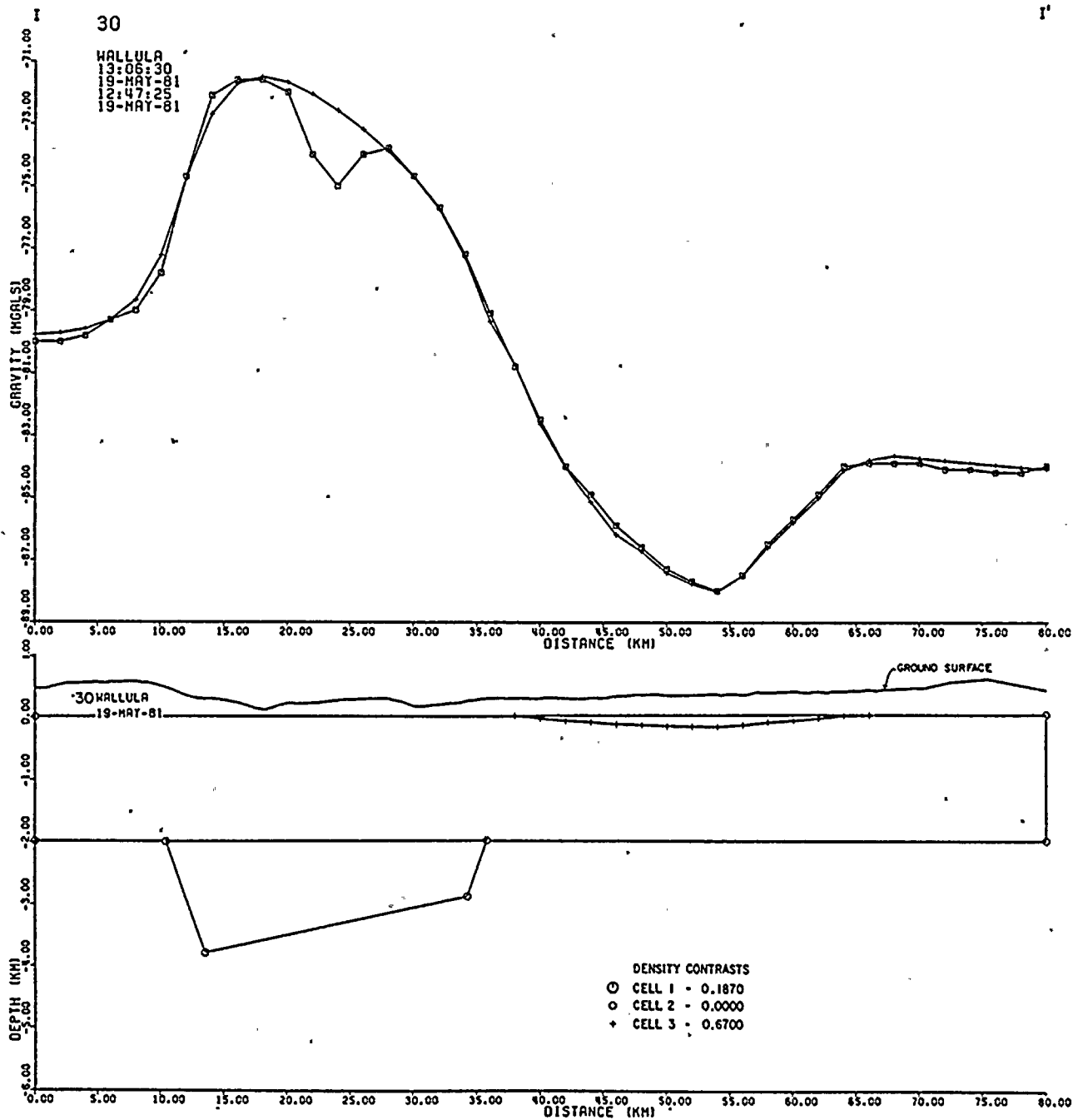


ATTACHMENT 1

FIGURE 6

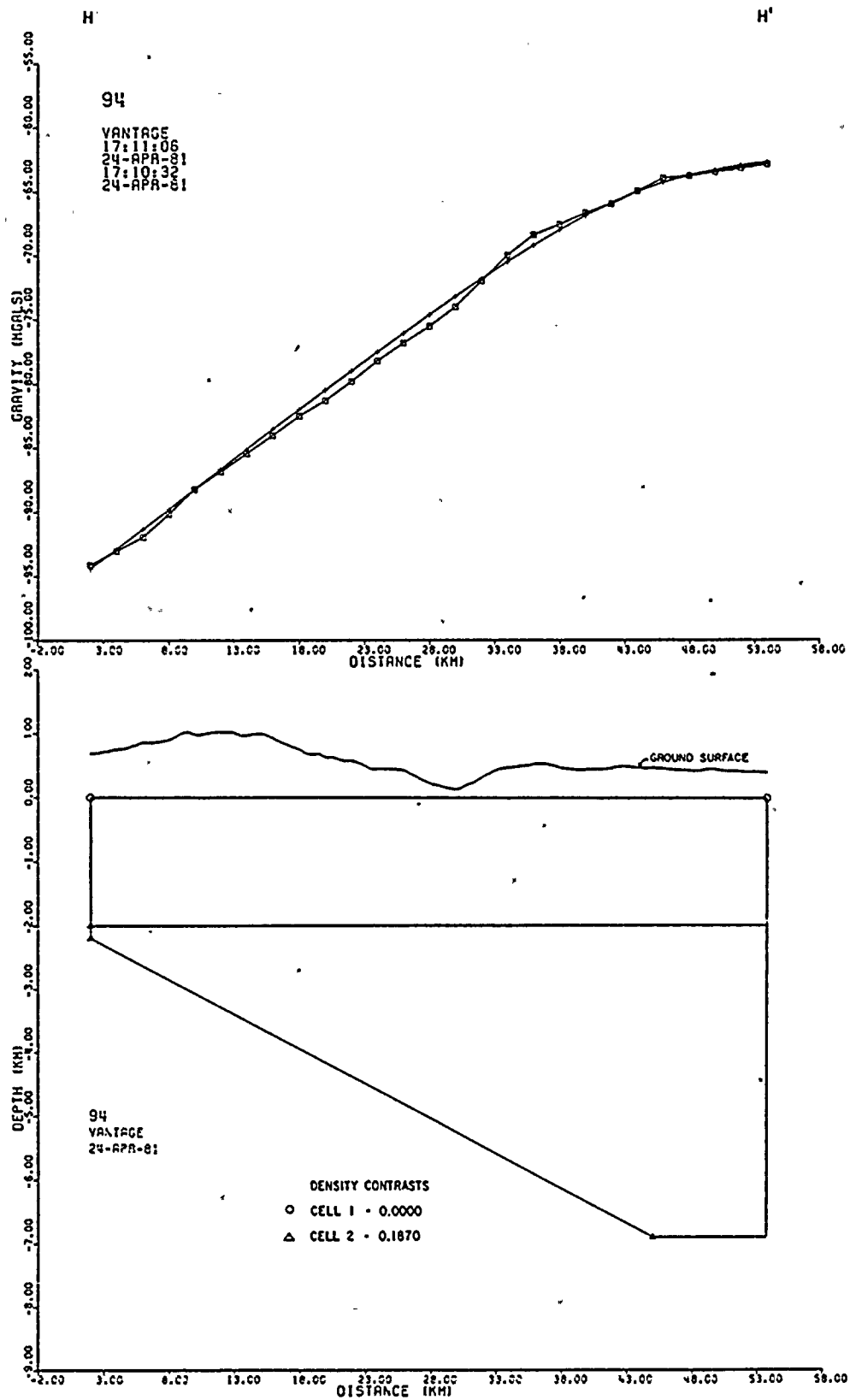
GRAVITY MODEL - RICHLAND PROFILE (C-C')





ATTACHMENT 1 . . .  
 FIGURE 7'  
 GRAVITY MODEL - WALLULA PROFILE (I-I')



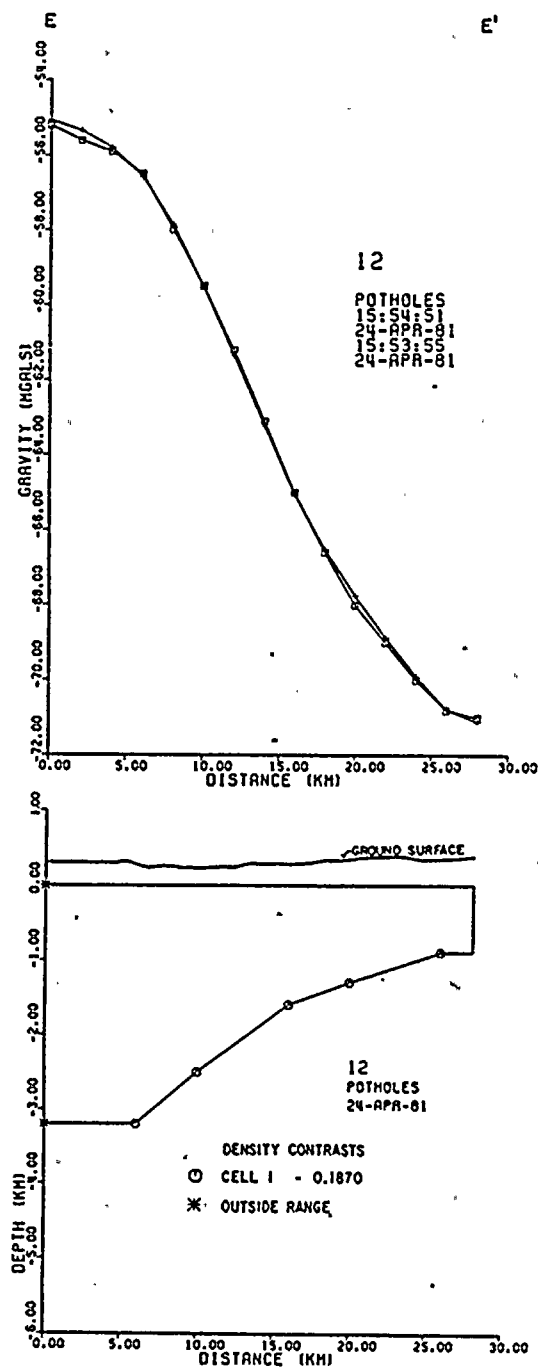


ATTACHMENT 1

FIGURE 8

GRAVITY MODEL - VANTAGE PROFILE (H-H')

(1)



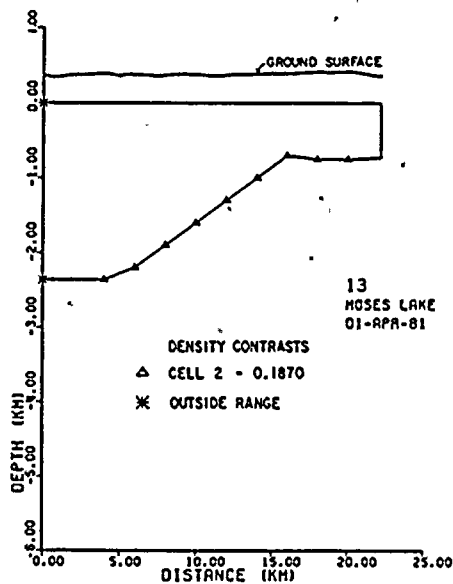
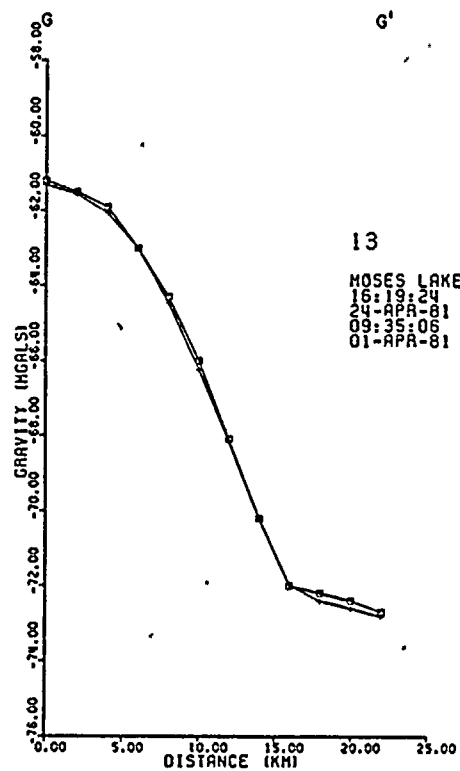
ATTACHMENT 1

FIGURE 9

GRAVITY MODEL - POTHOLES PROFILE (E-E')







ATTACHMENT 1

FIGURE 10

GRAVITY MODEL - MOSES LAKE PROFILE (G-G')

21 2



APPENDIX 2.5N

LATE CENOZOIC TECTONICS OF THE PACIFIC  
NORTHWEST WITH SPECIAL REFERENCE  
TO THE  
COLUMBIA PLATEAU

by  
Dr. G. A. Davis

August 1981



APPENDIX 2.5N

<u>TABLE OF CONTENTS</u>	<u>Page</u>
1.1 INTRODUCTION	2.5N-1
2.1 PLATE TECTONIC SETTING OF THE PACIFIC NORTHWEST	2.5N-1
3.1 KINEMATIC INTERRELATIONS BETWEEN THE GREAT BASIN AND THE BLUE MOUNTAINS AND COLUMBIA PLATEAU	2.5N-4
3.1.1 INTRODUCTION	2.5N-4
3.1.2 OLIGOCENE TO EARLY MIOCENE EVENTS	2.5N-4
3.1.3 POSSIBLE KINEMATIC LINKAGE BETWEEN GREAT BASIN AND THE PACIFIC NORTHWEST	2.5N-6
3.1.4 NORTHERN MARGIN OF BASIN AND RANGE PROVINCE IN CENTRAL OREGON	2.5N-7
4.1 TEMPORAL AND SPATIAL RELATIONS BETWEEN EXTRUSION AND DEFORMATION OF COLUMBIA PLATEAU RIVER BASALTS	2.5N-9
5.1 TIMING OF PLATEAU FOLDING AND ASSOCIATED FAULTING	2.5N-10
5.1.1 MIOCENE DEFORMATION	2.5N-10
5.1.2 PLIOCENE DEFORMATION	2.5N-13
5.1.3 PLEISTOCENE DEFORMATION	2.5N-15
6.1 HOLOCENE AND CONTEMPORARY TECTONICS	2.5N-16
6.1.1 INTRODUCTION	2.5N-16
6.1.2 DATA FROM SEISMOLOGY	2.5N-16
6.1.3 LATE QUATERNARY FAULTING	2.5N-18
6.1.3.1 Toppenish Ridge	2.5N-18
6.1.3.2 Wallula Gap and Milton-Freewater Areas	2.5N-20
6.1.3.3 Gable Mountain	2.5N-21
7.1 OLYMPIC-WALLOWA LINEAMENT	2.5N-22



TABLE OF CONTENTS (Continued)	<u>Page</u>
8.1 ORIGIN OF COLUMBIA PLATEAU STRUCTURES	2.5N-25
8.1.1 INTRODUCTION	2.5N-25
8.1.2 STRUCTURAL ANALYSES OF LAUBSCHER	2.5N-26
8.1.3 GEOMETRY AND KINEMATICS OF CLEW	2.5N-29
8.1.4 ORIGIN OF CLEW	2.5N-33
8.1.5 NATURE OF THE BASEMENT CONTROL OF CLEW	2.5N-34
8.1.6 AGE OF CLEW AND THE QUESTION OF ITS CAPABILITY	2.5N-36
9.1 REFERENCES	2.5N-39
TABLE 1 SPECIFICATIONS OF FAULTS EXPOSED WITHIN THE RED MOUNTAIN-WALLULA GAP STRUCTURAL DOMAIN	2.5N-48





APPENDIX 2.5NLIST OF FIGURES

<u>Number</u>	<u>Title</u>
2.5N-1	Major topographic linear features within Brothers fault zone, central Oregon.
2.5N-2	Generalized distribution of feeder dikes for Columbia River Basalts.
2.5N-3	Major structural elements of the south-central Columbia Plateau, Washington (from Kienle and others, 1978).
2.5N-4	Alternative structural interpretations for surface ground ruptures along Toppenish Ridge.
2.5N-5	Tectonic map of Wallula fault zone and vicinity (from Kienle and others, 1979).
2.5N-6	"Thick-skinned" tectonic interpretation for Columbia Plateau folding and faulting from Bentley (1977).
2.5N-7	"Thin-skinned" crustal decollement interpretation for Columbia Plateau deformation from Laubscher (1981; 1980ms).
2.5N-8	Hypothetical stages in the kinematic development of doubly-vergent anticlinal structures on the Columbia Plateau (e.g. Umtanum, Gable Mountain).
2.5N-9	Diagrammatic kinematic interpretation of the Wallula fault zone.
2.5N-10	Generalized tectonic map of Newport-Inglewood fault zone, Los Angeles Basin, California (after Harding, 1973; Yeats, 1973).
2.5N-11	Kinematic interpretations of differential response of plateau stratigraphic units (A) and deeper "basement" rocks (B) to north-south compression in the Columbia Plateau.

## LATE CENOZOIC TECTONICS OF THE PACIFIC NORTHWEST WITH SPECIAL REFERENCE TO THE COLUMBIA PLATEAU

### 1.1 INTRODUCTION

This discussion of the late Cenozoic tectonics of the Pacific Northwest is primarily concerned with Miocene and younger events in the Columbia Plateau and adjacent geologic provinces, unlike an earlier review (Washington Public Power Supply System, 1977a) which treated evolution of the entire Pacific Northwest from Precambrian time to the present. The paper relies heavily on data and concepts developed by earth scientists since 1977, particularly on the structural analyses of Columbia Plateau deformation by Laubscher (1977; 1981). Specific topics to be treated include: (1) late Cenozoic kinematic relationships between the Great Basin and the Pacific Northwest; (2) the timing of plateau deformation; (3) the nature of the Olympic-Wallowa lineament; and (4) a tectonic model for plateau deformation.

### 2.1 PLATE TECTONIC SETTING OF THE PACIFIC NORTHWEST

The Miocene and younger tectonics of the Pacific Northwest are the consequences of incompletely understood interactions between the Pacific, North American, and Juan de Fuca plates. The latter, a vestigial remnant of the once extensive Farallon plate, lies offshore of Oregon, Washington, and Vancouver Island. It is separated from the Pacific Plate to the north, west and south by the Gorda, Juan de Fuca, and Explorer ridges (from south to north) and the transform faults (fracture zones) which bound them. To the east, the Juan de Fuca-North American plate boundary is one of past convergence and, in the opinion of most recent workers, one along which subduction still continues at rates of several centimeters per year.

Washington Public Power Supply System (1977a), in agreement with Riddiough and Hyndman (1976) and Carlson (1976), concluded that despite the lack of an inclined seismic (Benioff) zone beneath western Washington and Oregon, eastward subduction of the Juan de Fuca plate beneath North America is probably an ongoing process. More recently, Crosson (1980) has presented seismic focal data that indicates that a shallow east-dipping Benioff zone does exist beneath western and central parts of the Puget Trough at the latitude of the Olympic Peninsula. Other features supportive of Quaternary subduction beneath the continent include the compressive deformation of late Pleistocene sediments along the base of the Oregon-Washington

continental slope, the linear array of Quaternary volcanoes of the High Cascades, the present gravity field of the continental margin (see below), and the nature of the deep (60-70km) Puget Sound-Gulf Islands earthquakes. Based on focal mechanism solutions, the deep earthquakes of 1965 (April 29, Puget Sound) and 1976 (May 16, Gulf Islands) were produced by normal faults with north-south strikes, a type of faulting attributed by Washington Public Power Supply System (1977a) to extensional strain in the outer (upper) part of the subducting oceanic plate where it abruptly bends to steepen eastward. That plate, therefore, must dip only  $10^{\circ}$  to  $15^{\circ}$  eastward from the base of the offshore continental slope to a 60 km depth below Puget Sound. It must then steepen to  $30^{\circ}$  to  $50^{\circ}$ , however, if the Quaternary Cascade volcanoes east of the Puget Trough lie 100 km to 120 km above the subducting plate as many petrologists believe (cf. Washington Public Power Supply System, 1977a, Figure 2R C-7). McKenzie and Julian (1971) had earlier concluded from a study of travel-time residuals of the 1965 Seattle earthquake that a slab of high-velocity material, interpreted by them as subducted oceanic crust, dips eastward ( $50^{\circ} \pm 10^{\circ}$ ) beneath the Cascades. The results of their studies have recently been confirmed by A. Rohay (oral communication, Cascadia Conference, May 1980).

On the basis of a recent analysis of the regional gravity field in western Oregon, Washington, and southwestern British Columbia, Riddihough (1979, p. 351) concludes that the field, which shows an outer "low" and an inner "high", is "similar to that over other subduction zones." A crustal section drawn by Riddihough (his Figure 5, Profile 3) through the Olympic Peninsula, Puget Sound, and Mount Baker, has a structural interpretation from a gravity profile closely approximating the interpretation drawn by Washington Public Power Supply System (1977a) from other evidence. The descending Juan de Fuca plate is shown to dip  $5^{\circ}$  eastward to a position beneath Puget Sound, then to dip steeply and abruptly to  $40^{\circ}$ .

Ando and Balazs (1979) have used geodetic data to conclude that the Juan de Fuca plate is aseismically underthrusting the North American plate at the present time. Leveling surveys across western Washington over the past 70 years indicate a regional down-to-the-east crustal tilting, which Ando and Balazs relate to continuous creep on the interface between the two converging plates. They state that pre-seismic deformation along active subduction boundaries characterized by thrust-type earthquakes (for which there is no evidence in the Pacific Northwest) should be characterized in western Washington by tilting of the coastal area toward the offshore trench (i.e., to the west).



The relative direction of convergence between the North American and Juan de Fuca plates, assuming that such convergence continues today, is imperfectly known. Recent estimates for the vector of convergence between North America and that segment of oceanic crust generated along the Juan de Fuca Ridge range from N 39° E to N 57° E, all at about 4 cm per year (Washington Public Power Supply System, 1977a); the most recent estimate, by Riddihough (1979), is approximately N 55° E. A northeastward direction of convergence is at a high angle to the Washington segment of the plate boundary, but oblique enough to conceivably impose a dextral component of strain in the upper, North American plate.

Rogers (1979) suggests that the north-south compressive stress responsible for earthquakes in the Vancouver Island region may be the direct consequence of north-south convergence between the small northerly Explorer plate and North America. This possibility cannot be discounted, but the southerly continuation of that stress field into areas east of the Juan de Fuca-North American plate boundary (with its different vector of convergence) and into northern and western California (astridge the Pacific-North American transform plate boundary) favors a more regional pattern of plate interaction as its cause. Specifically, the stress field may be the combined consequence of well-documented dextral transform motion between the Pacific and American plates and oblique, northeast-southwest convergence between the Juan de Fuca and American plates. The two major segments of the Pacific-American plate boundary, extending northward from the mouth of the Gulf of California to the Mendocino fracture zone (San Andreas fault), and from offshore Vancouver Island to the Gulf of Alaska (Queen Charlotte Islands fault), are sharply defined, but strain effects related to the boundary appear to extend far inland, particularly in areas adjacent to the San Andreas segment (e.g., the western Great Basin).

The idea that the late Cenozoic tectonics of the western United States are related to a broad zone of dextral shear along the western continental margin was popularized by Atwater (1970). Her concept of a broad "transform zone" of plate interaction was essentially inherited from similar, pre-plate tectonics hypotheses of Carey (1958), Eardley (1962), Wise (1963), and Hamilton and Myers (1966). More recently it has been variably developed by Smith (1977, 1979), Eaton (1979), and Christiansen and McKee (1979), all of whom emphasize the extensional phenomena of the Basin and Range province as the critical aspect of late Cenozoic plate margin deformation.



### 3.1 KINEMATIC INTERRELATIONS BETWEEN THE GREAT BASIN AND THE BLUE MOUNTAINS AND COLUMBIA PLATEAU

#### 3.1.1 INTRODUCTION

A number of recent workers (e.g. Washington Public Power Supply System, 1977a, 1980; Zoback and Thompson, 1978; Eaton, 1979) have called attention to the fact that essentially synchronous ENE-WSW crustal extension occurred in the Great Basin (by normal faults and igneous dikes) and in the central and eastern Blue Mountains and Columbia Plateau (basaltic dikes) beginning about 17 m.y. ago--although the amount of extension greatly diminished northwards into the latter areas. Because plateau basalts continued to be erupted from northerly striking dikes until at least 8.5 m.y. ago (Ice Harbor dikes near Pasco, with strikes of N 20° - 30° W; Swanson and others, 1979), the view has been widely held (e.g. Washington Public Power Supply System, 1977a; Eaton, 1979; Laubscher, 1981) that the eastern Columbia Plateau and the Great Basin shared a common extensional strain history until then (recognizing that plateau extension was much less than that of the Great Basin). That view, in light of new information about the structural evolution of the Columbia Plateau (see below) must now be regarded as overly simplistic, and probably misleading to those who build tectonic syntheses upon it.

#### 3.1.2 OLIGOCENE AND EARLY MIOCENE EVENTS

As a prelude to further discussion of the point just made, a comparison of the Oligocene and Early Miocene histories of the Great Basin, Blue Mountains, and Columbia Plateau prior to the inception of extensional deformation 17 m.y. ago is in order. Between 40 and 20 million years ago volcanic arc activity related to eastward subduction of oceanic lithosphere beneath western North America was widespread. Such activity affected the central longitudinal third of Washington, most of Oregon with the exception of coastal and northeasternmost areas, and all of what is now the Great Basin (Snyder and others, 1976; Armstrong, 1979). Coney (1979) describes this time period, particularly in the Great Basin area, as one of (1) great ash-flow or ignimbrite eruptions from caldera centers, and (2) the development of amphibolite-grade metamorphic-mylonitic complexes at relatively shallow crustal levels (i.e. into Paleozoic and Mesozoic strata; cf. Compton and others, 1977; some of these complexes are now dated as Mesozoic in age, e.g., the Whipple Mountains of southeastern California; this author, unpublished studies). Loring (1976) has documented widespread examples of Oligocene normal faulting of variable





trend (north-south to east-west) within Utah and Nevada, but two lines of evidence suggest that topography and, by inference, tectonic activity were generally subdued. A paucity of Oligocene and Early Miocene sedimentary rocks in the Great Basin suggests that there were few major basins for sediment entrapment (Christiansen and McKee, 1979), and sheetlike Late Oligocene-Early Miocene ignimbrites mantled a topography of low relief over regionally extensive areas 25 to 20 million years ago.

The Oligocene to Early Miocene history of the Columbia Plateau is obscured by its cover of Columbia River basalts and younger units, but the history of the Blue Mountains during this time period is at least partly recoverable. The province was deformed at some time after Eocene arc volcanism (Clarno Fm.), but prior to Columbia River basaltic volcanism. Clarno strata were folded locally as steeply as 60° before deposition overlying Picture Gorge basalts (Thayer and Brown, 1966) on the northern limb of the major east-west Aldrich Mountain anticline, the structural axis of the western Blue Mountains. Robyn (1977) suggests that this deformation occurred between 25 and 20 m.y. ago, but his older age limit is not well-constrained. If folding was earlier, deposition of the Oligocene (less than 43 m.y. ago) to Early Miocene John Day Formation may have been limited to the south by the high-standing Blue Mountains block (Thayer and Brown, 1966), and partly controlled by synchronous folding in the basin of deposition. According to McKee (1972, p. 236-237), "The John Day Formation appears to be thickest near the centers of northwest-trending synclines. The folds are, in part, younger than the Columbia River Basalt, as that unit has been warped by the fold. The thickness data from the John Day strata suggest that the same folds existed in the Oligocene and that deformation along northwest-trending lines has been going on for at least 30 million years." Supporting evidence for early folding (pre-Columbia River Basalt) comes from the Blue Mountains anticline along the northern edge of the John Day basin. This major fold constituted a topographic barrier in Middle Miocene time that separated, except locally, flows of the Lower Yakima and Picture Gorge Basalts (Nathan and Fruchter, 1974). McKee's suggestion, that folding with trends and geometries characteristic of the Columbia Plateau began in Oligocene time, is an extremely important one when the genesis of the younger folds that deform the Columbia River basalts is considered.

### 3.1.3 POSSIBLE KINEMATIC LINKAGE BETWEEN GREAT BASIN AND THE PACIFIC NORTHWEST

As reviewed below, compressional deformation in the Blue Mountains and Columbia Plateau may have peaked in Late Miocene and Pliocene time, roughly between 10.5 and 3 to 4 m.y. ago. This time period was significant for the Great Basin area as well, since it includes the kinematic transition between east-west extension within the northern and western Great Basin to a west-northwest to northwest direction of extension. According to Eaton (1979) this change in "spreading" direction occurred between 7 and 4 m.y. ago and accompanied the progressive northward development in California of the transform boundary between Pacific and North American plates.

The general coincidence in timing between (1) the onset of west-northwest to northwest extension in the western Great Basin and (2) an acceleration in similarly oriented (although not necessarily aligned) compression in the provinces to the north, may be interpreted to indicate that a kinematic linkage exists between them. Laubscher (1977), for example, referred in general terms to the Columbia Plateau as a compressional "sink" for extensional strain in the Great Basin to the south (the "source"). He does not believe, however, that the large amounts of extension in the southern region are equally compensated by compression in northern areas. Such a direct kinematic linkage is geologically unrealistic, considering the relatively small compressional strain of the Columbia Plateau and Blue Mountains areas.

As outlined above, folding in north-central Oregon along northeast trends began before Columbia River basalt volcanism and the initiation of east-northeast-west-southwest extension in the Great Basin area. Plateau folding continued from 14 to 7 million years ago--within which time interval, according to Eaton (1979) the direction of extension in the Great Basin changed to east-west. Thus to this writer, an explanation for subsequent, but similar plateau deformation that is tied to a radical reorientation of Great Basin extension from east-west to a northwest-southeast direction (ca. 7 m.y. ago) seems forced. Nevertheless, the entire question of kinematic linkage between extension in the Great Basin and the tectonics of the Pacific Northwest has become enormously complicated by the just-published paper of Magill and Cox (1981). These writers conclude that the entire Cascade Range south of southern Washington has rotated about 270° in a clockwise sense since 25 m.y. ago. They attribute this

impressive rotation, which may have affected the Klamath and Sierra Nevada provinces as well, to post-early Miocene extension in the Basin and Range province. The implications of their paper are beyond the scope of this report but may be profound.

#### 3.1.4 NORTHERN MARGIN OF BASIN AND RANGE PROVINCE IN CENTRAL OREGON

A correct understanding of the kinematic interrelationships between the Basin and Range province and the Blue-Mountains/Columbia Plateau must focus on the tectonic boundary between them in central Oregon. There is, however, no unanimity of opinion on exactly how this intraplate provincial boundary is defined. Some writers (e.g. Smith, 1979; Christiansen and McKee, 1979) speak of the High Lava Plains of central and eastern Oregon, with its youthful volcanism and high heat flow, as a geologic transitional zone between the two provinces. Others (e.g. Lawrence, 1976; Eaton, 1979) emphasize structural elements, most importantly the northwest-striking Brothers fault zone, as defining the boundary. Laubscher (1981), most recently has considered the Brothers fault zone as a portion of the southern margin of a broad zone of dextral transform strain extending from western Idaho to the Olympic Mountains (IDOL). However defined, the boundary has generally been accepted as one characterized by dextral transform motion since the interesting paper by Lawrence (1976).

Reasons for postulating dextral slip along a tectonic boundary between the Basin and Range and Blue Mountains provinces include the following: (1) an en echelon pattern of fractures within the Brothers fault zone, reported by Lawrence (1976) and interpreted by him as Riedel shears in a youthful zone of limited dextral shear; (2) eastward termination of the Brothers zone at the throughgoing, north-south Steens normal fault, a geometry necessitating a westward dilation of the normal faulted terrain south of the Brothers zone with respect to the northern, more stable block (Lawrence, 1976); (3) Lawrence's contention that the northwestern end of the Brothers zone merges with a more northerly striking system of normal faults along the eastern edge of the High Cascades; and (4) the northwesterly trend of the Brothers zone--an orientation within the dextrally strained margin of the North American plate that should be characterized by components of right-slip (cf. Atwater, 1970).

Lawrence (1976, p. 849) states that "relatively little displacement has taken place along the Brothers fault zone",



a conclusion compatible with the absence within the zone of a single, throughgoing strike-slip fault. However, his interpretation of right-slip along the Brothers zone--based on an inferred en echelon pattern of fractures within it--deserves scrutiny. Lawrence claims that the N 60° W trend of the zone contrasts significantly with a N. 40° W strike of discontinuous, en echelon fractures within it, and that the acute angle between these structural elements indicates right-lateral displacement along the zone.

The most strongly en echelon structural elements of the Brothers zone are a series of northwest (N 50° W  $\pm$  10°)-trending ridges that lie north of Oregon State Highway 20 between Brothers and Horse Ridge Summit west of Millikan, and continue south and west of the summit as components of Horse Ridge (Figure 1). Lawrence interpreted these ridges as "fractures" on the basis of his analysis of Landsat imagery (they are plotted within the zone in his Figure 2). However, at least two of the westernmost component ridges of Horse Ridge appear to be elongated, doubly plunging anticlines based on the configuration of lava flows within them. The morphology of the easternmost two ridges of Horse Ridge and those ridges farther east (north of Highway 20) is also indicative of folding. The ridges rise as much as 700 feet above the surrounding lava plains and lose elevation both northwestward and southeastward along their axes. Most are asymmetric, with steeper southwestern flanks. Their grand isolation above the largely unfaulted lava plains would seem to rule out an origin for them by block faulting of Basin-and-Range type (i.e. normal faulting). Scarplike slopes on the southwestern margin of most of the ridges appear to be fault controlled, possibly with reverse or thrust components of slip in light of their association with probable anticlinal folds. This writer's tentative interpretation of the ridges as compressional features (made in the summer of 1979) has subsequently received independent support from an unpublished photogeologic study of the region made by a major oil company in the mid-1950's. In that study, the ridge directly east of Horse Ridge Summit was mapped as a northerly-plunging anticline. If the dozen or so ridges in question are indeed anticlinal, their pronounced en echelon orientation (Figure 1) suggests strongly that they are brachyanticlines formed within, or bordering on the north, a zone of sinistral (left-lateral) shear with a strike in this area of approximately east-west. En echelon ridges of similar trend and morphology are also present south of Highway 20 in the same general area (e.g. Pine Ridge), and because they too rise abruptly above the level of the surrounding lava plains, they are also favored as compressional features. The ridges



of the Millikan-Brothers area thus appear to complicate Lawrence's interpretation of dextral slip within the Brothers fault zone, based on his erroneous assumption that the ridges are expressions of Riedel shears with transcurrent displacement.

Another aspect of Lawrence's tectonic analysis also needs reconsideration. He (1976, p. 850) believes that the northwest-trending Brothers zone separates the Basin and Range province from the Blue Mountains of central Oregon. "Extension virtually ceases at the northern end of the province along the Vale and Brothers fault zones." However, the Brothers zone as he has defined it from Landsat imagery (his Figure 2) appears much too selective when compared with patterns of faulting mapped by Green and others (1972) in the Burns 20 map sheet (see also Walker, 1977). Lawrence shows the Brothers zone as a linear zone that extends southeastwards from Bend and passes south of Harney Lake. Yet Greene and others map scores of minor normal faults north of Lawrence's zone between Hampton (on Highway 20) and Harney Lake that are identical in field appearance and trend to those of the zone as Lawrence defines it. In other words, the eastern linearity and location of Lawrence's zone can be questioned. Certainly, the northern limit of northwest-striking normal faults of the Basin and Range province does not lie along the Brothers zone in this region, but in a more northerly position--roughly along an irregular east-west line connecting Hampton and Burns. Inspection of the Burns map sheet (Greene and others, 1972) suggests that the deformation of the High Lava Plains west and southwest of Burns is more one of crustal extension in a northeast-southwest direction across scores of normal faults than dextral slip across northwest-striking Riedel shears. The northwest orientation of the normal faults is, of course, compatible with right-lateral displacement of the High Lava Plains relative to the northern, Blue Mountains block if the faults are extensional fractures in a zone of distributed dextral strain.

#### 4.1 TEMPORAL AND SPATIAL RELATIONS BETWEEN EXTRUSION AND DEFORMATION OF COLUMBIA RIVER BASALTS

Tectonic models for the origin of Columbia Plateau structures must be cognizant of the relations in space and time of the two major geologic events of the plateau: (1) the extrusion of basaltic lavas from north-northwest trending dikes; and (2) the deformation of these lavas and coeval and younger sedimentary rocks along northeast, east, and northwest trends. The former is known to have occurred from approximately 16.5 to 6 m.y. ago, although Swanson and

Wright (1978) estimate that 99% of the lavas were extruded between 16 and 14 m.y. ago. As amplified below, deformation of the basalts began about 14 m.y. ago and continues to the present.

Figure 2 draws attention to an important spatial relationship between the two plateau phenomena. That is, that with the exception of basalts among the oldest (Picture Gorge) and youngest (Ice Harbor), the feeder dikes for the Columbia River flows were in eastern plateau areas unaffected by plateau folding. To state this relation differently, the Columbia Plateau can be divided into two areas with differing late Cenozoic strain histories--an eastern area, the Palouse subprovince of Rockwell (1979), characterized by east-northeast extension totalling more than 1 km (Taubeneck, 1970), and a western area, the Yakima fold belt subprovince, characterized by north-south compression. Bentley (1980) has recently estimated that north-south shortening across the subprovince decreases from a value of 15 km, west of 120° W longitude, to 4 km, east of 120° W. Although maximum development of structures within the two strain fields did not overlap (dikes, 16 to 14 m.y. ago; folds, 10.5 to 3 or 4 m.y. ago), the fields did coexist for approximately 8 million years (14 to 6 m.y. ago).

Because total strains within each field are small, the structural boundary between them is not clearly expressed. Laubscher (1977, 1981) refers to the eastern, north-south trending boundary of the Yakima subprovince as the Wallula Gap-Moses Lake Belt. It connects the eastern topographically-expressed terminations of the Saddle Mountain and Frenchman Hills structures. He believes the diffuse belt is characterized by dextral transcurrent strain since it separates a north-south-shortened block to the west (Yakima) from the more stable Palouse block to the east.

## 5.1 TIMING OF PLATEAU FOLDING AND ASSOCIATED FAULTING

### 5.1.1 MIOCENE DEFORMATION

It has become clear in the last several years that plateau folds and parallel faults, usually with thrust or reverse fault geometries, were developing during the extrusion of some Miocene Columbia River basalts from fissures farther east. The best evidence for the earliest recognized deformation, that of late Grande Ronde time after nearly 85% of the basalts had been extruded, comes from the recent work of Beeson and Moran (1979) in the northern Cascades of Oregon. They report that folds trending N 40° - 65° E began to develop during youngest Grande Ronde time. At some



localities pillow lavas and sedimentary interbeds of this age are restricted to synclinal troughs and anticlinal volcanic sections are abbreviated. Similarly at the northern edge of the Columbia Plateau, in the Wenatchee Mountains of Washington, the Vantage Member of the Ellensburg Formation (post-Grande Ronde Basalt, pre-Frenchman Spring Member of Wanapum Basalt) thins toward the crest of Taneum Ridge anticline (Meyers and Price, 1979, p. 1V-16).

Evidence for deformation during Wanapum time, approximately 14.5 to 13.6 m.y. ago, is geographically more widespread. Again, in the northern Oregon Cascades, Beeson and Moran (1979) found evidence for uplift, northeast-southwest faulting, and erosion of the Frenchman Springs member of the Wanapum Basalt prior to deposition of Priest Rapids flows (also Wanapum Basalt). In the Pasco Basin area, stratigraphic and geochemical studies by geologists of the Rockwell Hanford group (Reidel and others, 1980; Rockwell, 1979) indicate that the Saddle Mountains structures (Figure 3) began to form in post-Grande Ronde time, ca. 14.5 m.y. ago. Thinning of Frenchman Springs flows has been noted across the northwest-trending Smyrna anticline on Saddle Mountain. The distribution of overlying flows of the Roza Member of the Wanapum Basalt on Saddle Mountain suggests east-west folding or arching during their deposition.

Evidence for post-Wanapum deformation is still more widespread. Bentley and others (1980, p. 59) state that "broad, structurally controlled basins had become noticeable at the onset of Saddle Mountain time, about 13 - 13.5 million years ago." They report that anticlinal ridges were locally high enough to confine flows of the oldest member of the Saddle Mountain Basalt, the Umatilla Member. These flows thin over the present site of the Rattlesnake Hills, suggesting that this fold structure began to form at the close of Wanapum time (Rockwell, 1979). The thinning of flow units across Saddle Mountain noted above continued to occur until Elephant Mountain time (ca. 10.5 m.y. ago), enabling Reidel and others (1980; oral presentation, 1980) to conclude that the rate of uplift of this structure between 14.5 and 10.5 m.y. ago was approximately 39 meters/million years.

Some of the clearest evidence for intra-plate Miocene deformation on the Columbia Plateau comes from the Yakima and Umtanum anticlinal structures (Figure 3). Bentley (1977, p. 339) describes "locally substantial deformation...14 to 12 m.y. ago" near Priest Rapids (Umtanum Ridge) and Yakima (Yakima Ridge). In the latter area, just



east of the Yakima River, steeply-dipping Wanapum basalts (as young as the Priest Rapids Member) are overlain with angular unconformity by flat-lying Selah conglomerates of the Saddle Mountains Basalt (Bentley, 1977, p. 364); the conglomerates are older than the 12 m.y. old Pomona Member of the Saddle Mountains Basalt.

Somewhat similar relations are reported by Bentley (1977, p. 377 and summarized in Rockwell, 1979, p. III-166) from the Filey Road area of eastern Umtanum Ridge. Here, 3 km west of Priest Rapids Dam, Grande Ronde and Wanapum basalts, including the Priest Rapids Member of the latter, were tightly folded, overturned, reverse faulted, and eroded prior to the deposition of conglomerates across them. The conglomerates intertongue northward with fluvial sediments of Selah age that underlie the Pomona Member. The Pomona basalt in this area is described as relatively undeformed" (Rockwell, 1979, p. III-166; see also their Figure III-73).

Farther east, Goff and Myers (1978) also conclude that most deformation of Umtanum Ridge occurred prior to Saddle Mountain time, but the distribution of the 10.5 m.y. old Elephant Mountain basalts around the eastern end of the structure suggests to them that some folding continued through Elephant Mountains time. Bentley (1977, p. 374) states that more than 400 m of structural relief has developed at the eastern end of Umtanum Ridge since the extrusion of Elephant Mountain lavas.

Despite evidence for geographically widespread deformation of the Columbia Plateau prior to extrusion of the 12 m.y. old Pomona lavas, most deformation affecting the Columbia Plateau and the adjacent Blue Mountains province is post-Pomona in age. In the Blue Mountains, strong north-south compressional deformation postdated the extrusion of Columbia River basalts, but preceded eruption 6.6 m.y. ago of the widespread tuff member of the Rattlesnake Volcanics (Thayer and Brown, 1966; Robyn and others, 1977; Robyn, 1977). Robyn (1977) dates this compressional event as occurring between 10 and 7 m.y. ago. Deformation was expressed by renewed folding and rupturing of the north flank of the Aldrich Mountain anticline to form the east-west John Day reverse fault. Northeast and northwest-striking fractures and strike-slip faults formed contemporaneously in the northern footwall of the fault as a conjugate response to north-south shortening. Only minor compression and igneous activity (silicic intrusions and basaltic volcanism) have occurred in the eastern Blue Mountains since 6.6 m.y. ago (Robyn, 1977).



In Washington, the widespread folding of the Elephant Mountain Member of the Saddle Mountains Basalt in the Pasco Basin area demonstrates major plateau deformation younger than the 10.5 m.y. age of the member. Rockwell (1979, p. 1V-17, 20-21) conclude that most deformation in the Pasco Basin area occurred between 10.5 and approximately 5. m.y. ago, although the younger age limit is not well-controlled (as discussed below).

#### 5.1.2 PLIOCENE DEFORMATION

A problem in establishing an upper (younger) limit for most plateau folding and associated faulting is the incomplete Pliocene and Quaternary stratigraphic record of the plateau area. In many areas, late Quaternary deposits rest directly on deformed Miocene basalts, with a resultant hiatus in the geologic record of the region of up to 16 million years.

Pliocene stratigraphic units (ca. 5 to 3 m.y. old) are preserved in the northern and central Pasco Basin area (Ringold Formation), the Yakima-Ellensburg area (upper Ellensburg Formation), and in southwestern portions of the Washington plateau (Simcoe-Volcanics). Unfortunately, plateau workers have differed on the extent of plateau deformation affecting these units, largely because of the lack of precise age controls on them. For example, in the northern Pasco Basin dips of beds in the upper part of the Pliocene Ringold Formation (5.1 - 3.3 m.y. ago, Rockwell, 1979) are very gentle. This relation may indicate waning deformation (Rockwell, 1979, 1V-21) since lower Ringold strata on the flanks of Saddle Mountain to the north dip as steeply as 40° (Washington Public Power Supply System, 1977d, p. 2RH 8-6). However, since basalts beneath the gently dipping Ringold sediments also dip gently, the areal differences in Ringold dips may reflect spatial rather than temporal factors.

Unpublished subsurface studies by Golder and Associates (D. Caldwell, personal communication, 1981) of Ringold sediments that lie across the buried southeastern end of the Gable Mountain anticline (Figure 3) indicate that older Ringold sediments on the flanks of the structure dip more steeply than younger. Golder's data suggest that broad arching of Ringold sediments continued through the Pliocene.

Pliocene fanglomeratic deposits in areas between Yakima and the Kittitas Valley, e.g. the Thorp Gravel, have recently been assigned to the upper Ellensburg "Formation" (Washington Public Power Supply System, 1977d) or "group" (Bentley, 1977). Statements made in the two 1977 papers



about the significance of these deposits to the dating of plateau deformation are, however, somewhat at variance. Bentley states (1977, p. 355) that "major deformation" occurred along Manastash Ridge "after some coarse basaltic fanglomerates of the Thorp (?) Gravel were deposited", despite a reference elsewhere (p. 352) that Thorp (?) conglomerates on the north flank of the Manastash structure dip only 3 - 5°. The inclined conglomerates are truncated by an early (?) Pleistocene pediment surface capped by gravels. The age of the Thorp (?) unit is not known, although tephra layers in upper Thorp Gravels in Kittitas Valley have yielded fission trace and K-Ar ages of 3.7 to 4.8 m.y. ago (Rigby and Othberg, 1979, p. 18). From such relations, Bentley (op. cit., p. 339) derives the tenuous conclusion that "the majority of the 'ridges' rose in Pliocene-Pleistocene times" (6 to 1.5 m.y. ago).

Washington Public Power Supply System (1977d, p. 2RH 8-3), however, although favoring local deposition of upper Ellensburg deposits "during or after" ridge uplift take a more conservative view of the significance of these deposits: "The regional significance and age of these deposits is poorly understood. Most deposits are undeformed; only on west end of Smyrna Bench (Saddle Mountain) and in the Kittitas Valley do small dip slip faults cut these deposits" (*italics by this writer*). Elsewhere, (p. 2RH 8-12) Washington Public Power Supply System concludes that the

"age of deformation in the area of investigation is dominantly post-Elephant Mountain and pre-Thorp Gravel. Some deformation along the cores of the anticlines may be slightly older and minor tilting of pediment surfaces may be younger, but the majority of the deformation (faulting and folding) must have occurred between these two dates."

Their conclusion is, in turn, challenged by Rigby and Othberg, (1979) who report that Ellensburg sedimentary rocks younger than Columbia River basalts (their "supra-basalt Ellensburg Formation") are deformed widely in the Yakima area:

"The deformation exhibited by the supra-basalt Ellensburg Formation indicates that the large-scale uplift and deformation of the basalt ridges in the western Columbia Basin occurred after most, if not all, of these sediments had been deposited, or late Miocene to early (?) Pliocene in age."





Basalt terrace gravels preserved in valleys in the Yakima area are interlayered with and overlie supra-basalt Ellensburg sediments. The gravels, which according to the Rigby and Othberg resemble the Thorp Gravels of the Kittitas Valley, exhibit near vertical to overturned dips at localities along Ahtanum Ridge, in the foothills of Cowiche Mountain, and in Yakima. Unfortunately, the age of these gravels is not known, although Rigby and Othberg (1979) suspect they may be broadly coeval with the Thorp gravels. They believe (p. 23) that some of the terrace gravels "were deposited before deformation began, while others were deposited for some time after deposition occurred. Deformation of this part of the Columbia Basin, at least, apparently came to an end sometime during deposition of this gravel unit."

Pliocene and Pleistocene lavas are widespread in the southwestern corner of the Washington portion of the Columbia Plateau. The relations of these lavas, the Simcoe volcanics, to plateau fold and fault structures are instructive. According to Bentley and others (1980, p. 60):

"Eruptions of basalt and related lava began in the Simcoe volcanic field probably during early Pliocene, about 4-5 million years ago. Much of the deformation of the area had been completed before these eruptions, although some flows appear to have been tilted by later folding. The eruptions, which may have taken place over a 2-4 million year period, produced a broad continuous basalt field dotted with cinder cones".

Disagreement exists in the literature concerning the relative age of east-to-northeast-trending anticlines and northwest-striking, high angle faults in this part of the plateau. One such fault appears to cut a 4.5 m.y. old Simcoe flow, but is overlapped by a flow dated at 3.5 m.y. (Shannon and Wilson, 1973). Shannon and Wilson (1973) interpret the 4.5 to 3.5 m.y. old fault as being synkinematic with formation of the Columbia Hills and Horse Heaven anticlines, but studies by Anderson (1980) and Bentley and others (1980) indicate that the northwest-striking cross faults are younger than the folds (see also Rockwell, 1979, p. II-84, 85).

### 5.1.3 PLEISTOCENE DEFORMATION

Although upper units in the Simcoe Volcanics and the Ringold and Ellensburg Formations may be of Pleistocene age, the Pleistocene stratigraphic record on the plateau is generally represented by poorly dated glacial deposits, flood gravels



and associated sediments, and loess (Rigby and Othberg, 1979). The extent of involvement of these units in plateau folding is uncertain, in part because they tend to be best preserved in basins between major folds, and in part because of their youthfulness and the likelihood of low plateau strain rates.

All workers appear to agree that the uplift of Yakima Ridge ended prior to one million years ago, since the undeformed Tieton Andesite (K/AR age of  $1.0 \pm 0.1$  m.y.) lies in an erosional reentrant across the truncated northern flank of the anticline (Rockwell, 1979, p. 11-77). Bentley (1977, p. 354) concluded that most of the deformation along nearby Manastash Ridge occurred prior to the development of the one m.y. old Thrall pediment surface on its north flank.

## 6.1 HOLOCENE AND CONTEMPORARY TECTONICS

### 6.1.1 INTRODUCTION

Information on the geometry and kinematics of active structural elements in the Pacific Northwest comes primarily from two sources -- field recognition and study of such structures, and fault plane solutions from single or composited seismic events. From a practical standpoint, relatively little is known about Quaternary tectonics in Washington from the direct study of active structural elements. None of the seven states west of the Rocky Mountains have fewer known or inferred examples of active faults than the state of Washington (Howard and others, 1978). This situation may reflect a genuine diminishment of youthful faulting in areas of the United States north and west of the Basin-and-Range province or a lack of bedrock exposures in the western, more seismically active half of the state -- or both.

### 6.1.2 DATA FROM SEISMOLOGY

Washington Public Power Supply System (1977a) summarized evidence, largely from earthquake focal mechanism studies, that the upper lithosphere (less than 25 km depth) of Washington and the northern half and western third of Oregon presently lies within a regional strain field characterized by north-south shortening. Individual and composite focal mechanisms for seismic events within this region typically yield orientations for P, the compressional axis, that have shallow plunges and trends that vary from NNW to NNE. T, the axis of maximum extensional strain, has a more variable orientation, ranging from vertical to east-west and horizontal. The two principal combinations of P and T that



result from these orientations lead to two characteristic types of fault plane solutions for Pacific Northwest earthquakes: 1) east-west striking thrusts or reverse faults (north-south P, vertical to subvertical T); and 2) either steep northwest-striking faults with dextral slip or northeast-striking faults with sinistral slip (north-south P, horizontal to subhorizontal and east-west T). Rogers (1979) has recently documented that the field of north-south shortening extends into the Vancouver Island region of southwestern Canada, where solutions for both strike-slip faulting (predominant) and thrust faulting (subordinate) are also obtained.

However, results of recent seismic studies from the Columbia Plateau indicate that the orientation of P there is considerably more variable than the simple picture of north-south orientation that was presented in WPPSS PSAR Amendment 23 by Washington Public Power Supply System (1977a), Washington Public Power Supply System (1977e), and Washington Public Power Supply System (1977f). In a draft report (Woodward-Clyde Consultants, 1980a) to the Washington Public Power Supply System, orientations of P have been found to vary markedly in different parts of the southeastern Plateau region. For example, composite focal mechanism solutions from microearthquakes with depths of 9 to 24 km yield N-S orientations of P for a more-or-less longitudinal belt (ca. 119°30'W to 119°45'W) that extends southward from east of Priest Rapids Dam to within 15 km of the Columbia River west of McNary Dam. All composite solutions show predominant reverse, dip-slip displacements.

In contrast, composite focal mechanism solutions for areas both east (near Mesa, Washington) and west (near Sunnyside) of the longitudinal belt yield P orientations that are regionally anomalous (N 67° W, 43° and N 74° W, 60°, respectively, for the two areas). Orientations of T for the two areas are not as consistent as those for P, being N 32° E, 9° and N 106° E, 30°, for eastern and western areas respectively. These solutions suggest pure dip-slip normal displacement along north-striking normal faults in the latter case, and faults with oblique-slip (both strike-slip and normal dip-slip components) in the former. The solution for normal faulting is regarded by Woodward-Clyde as inconclusive, although that for oblique faulting is described as "fairly well constrained." Similarly, two of the largest historic earthquakes of the southeastern Plateau region, those of July 16, 1936 ("Milton-Freewater", M = 6.1, Woodward-Clyde Consultants, 1980b), and April 8, 1979 (College Place, M = 4.1, *ibid.*), have also yielded fault plane solutions with marked



departures of P from a regional N-S orientation, i.e. N 56° E, 22° and N 91° W, 10°, respectively. The solution for the 1936 event is poorly constrained, but that for the 1979 event appears quite reliable.

Reasons for the characteristic north-south orientation of P in the Pacific Northwest are unresolved, as are reasons for the local or areally restricted departures from that orientation in southeastern Washington. The general consistency of focal mechanism solutions for Washington, northern and western Oregon, and southeastern British Columbia (Washington Public Power Supply System, 1977a; Rogers, 1979) is, nevertheless, important in documenting the regionality of north-south crustal shortening (shallower than 25km) in these areas. Nowhere in the Pacific Northwest are mappable structural features related to north-south shortening better developed than in the Columbia Plateau, although the geologic record of this area (reviewed above) indicates that most of its east-trending folds and parallel thrust and reverse faults are pre-Quaternary in age.

#### 6.1.3 LATE QUATERNARY FAULTING

The low-level seismicity of portions of the Columbia Plateau attests to ongoing deformation of the region, despite the fact that in most areas, seismicity is not associated with surface manifestations of faulting. Surface ruptures of Quaternary age, essentially unknown in 1977 at the time of submittal of PSAR Amendment 23, have since been recognized in three areas of the Plateau: 1) Toppenish Ridge, approximately 80 km west of Richland (Campbell and Bentley, 1980); 2) about 25 km southeast of Richland, from the vicinity of Wallula Gap on the Columbia River southeastward to the Walla Walla/Milton-Freewater area (Shannon & Wilson, 1980); and approximately 40 km north of Richland on the eastern end of Gable Mountain.

##### 6.1.3.1 Toppenish Ridge

Campbell and Bentley (1980) report that the summit, north flank, and alluvial fans at the base of the north flank of Toppenish Ridge (Figure 3) are broken by nearly 95 surface ruptures up to 9 km in length. Most of the ruptures are less than 1 km long and only six have lengths in excess of 3 km. The faulted zone varies in width from 0.5 to 2.2 km and has a length, more-or-less parallel to the ridge, of 32 km. Most flank and summit ruptures are sub-vertical faults for which no strike-slip displacement is evident. Faults at the base of the north flank are generally lobate in form and are interpreted as comprising a thrust zone coincident with the





older south-dipping Toppenish fault. Some cut glaciofluvial slackwater deposits of Touchet type and others displace post- "Touchet" alluvial fans. Mount St. Helens ash (12,800 y.b.p.) is present in some of the slackwater deposits, but has not yet been shown to be faulted. Campbell and Bentley (1980) attribute the Toppenish faults to north-south compression, with thrusting at the northern base of the anticlinal structure and extension across its hinge (Figure 4). Bentley (1980, personal communication) believes that the 30 km-long faulted segment of Toppenish Ridge may be terminated at its western and eastern ends by northwest-striking strike-slip faults, which may be responsible in some way for localizing Quaternary rupture along the anticline.

Although the surface ruptures on and adjacent to Toppenish Ridge may represent Quaternary tectonic activity, an alternative explanation appears viable at this time. Specifically, the combination of apparent low-angle thrusting along the northern base of the ridge and normal (extensional) faulting at higher elevations raises the possibility that the two are expressions of gravitationally-induced slope failure (Figure 4). Several lines of evidence support the interpretation that the Toppenish structures represent either an aborted phase or the incipient development of massive slope failure along the north flank of Toppenish Ridge. Included among them are the dramatic north flank landslides on the eastern end of the ridge and around Ortney Lake, immediately to the west. These slides demonstrate in spectacular fashion the instability of the northern flank. The close spatial relations between apparent low-angle faults at the base of the ridge and high-angle faults at higher elevations are suggestive of an interrelated landslide toe and headscarp geometry. An active youthful landslide at the south end of the White Bluffs, on the Columbia River opposite Richland, is characterized by just such prominent headscarps and a subhorizontal plane of movement near the base of the slope (Kiel, personal communication, 1980). Bentley and others (1980, p. 51) argue that a landslide origin of the Toppenish ground ruptures is "unlikely, because such an interpretation does not explain the abundance of south-side-down faults on the north slope of the ridge." However, such faults can be reasonably interpreted as antithetic faults to the main north-dipping sole fault. The White Bluffs landslide referred to above displays just such an antithetic rupture which defines, with the headscarp fault to the east, the edges of a shallow graben. Until the Toppenish ground ruptures receive further study, it is premature to conclude unequivocally that they represent tectonic activity.

## 6.1.3.2 Wallula Gap and Milton-Freewater Areas

Youthful faulting in the vicinity of Wallula Gap is apparently related to a zone of dextral transcurrent faulting (Shannon & Wilson, 1979a) that includes the topographically prominent Wallula fault zone (Figure 3). Bingham and others (1970) first noted features within the zone that suggested to them the possibility of Quaternary displacement. Recent studies (Shannon & Wilson, 1979a; Shannon & Wilson, 1979b; Shannon & Wilson, 1980) have documented or indicated the involvement in faulting of Quaternary units (including undated colluvium, Palouse Formation, Touchet Formation, and younger loess) at seven separate localities, the most western of which is at Finley Quarry on the northern end of the Butte (west of Wallula Gap). The three westernmost localities (Figure 5) lie within a 20 km-long segment of the Wallula fault zone. Colluvium of probable Quaternary age is faulted at two localities (Finley Quarry and east of Warm Springs Canyon, Shannon & Wilson, 1979a, loc. C), and horizontal fault striae have been observed within a clastic dike of Touchet (?) silt and clay in basalts near Wallula Gap (Shannon & Wilson, 1979a, loc. A).

Bingham and others (1970, p. 77) believed that Touchet beds in an area east of Vansycle Canyon (east of Wallula Gap and between Shannon & Wilson's localities A and C) had apparently "been ruptured by relatively recent, minor fault movement." A curved linear topographic feature (referred to as "Bingham's linear" in subsequent reports) with a trend at nearly right angles to the drainage of the area was the basis for the conclusion that 12,000 year-old Touchet beds had been displaced by faulting. Preliminary results of trenching across "Bingham's linear" by Woodward-Clyde Consultants in early 1981, do not confirm the existence of a throughgoing fault across Touchet beds exposed in two trenches (D. Hitchcock, personal communication, 1981) although trench logging continues at the time of this writing.

Farther east, two possible fault localities in the Milton-Freewater area are in general alignment with the Wallula zone to the west (Figure 5). South of Umapine, north-dipping ( $30^{\circ}$  to  $60^{\circ}$ ) gravity slump surfaces or normal faults cut Touchet beds and cross-cutting clastic dikes with a maximum offset of 0.5 meters (Shannon & Wilson, 1979b). Youthful faulting 10 km farther to the southeast of the Umapine locality is suspected by Shannon & Wilson, but not demonstrated. Shannon & Wilson (1979b) found angular basaltic debris in loess along the trace of an inferred

bedrock fault. They suggest that the basalt fragments may have been derived from a fault scarp and were subsequently mixed with surficial loess deposits.

The other two eastern fault localities are the Buroker thrust fault east of Walla Walla, and the Little Dry Creek fault south of Milton-Freewater (Figure 5). The base of the Pleistocene Palouse Formation is offset approximately one meter along the former fault, a west-dipping ( $26^{\circ}$ ) reverse fault that strikes north-south. Higher loess deposits (Holocene?) appear to be unfaulted (Shannon & Wilson, 1980, p. 17) near Little Dry Creek, basalt and Palouse beds are downdropped along a steep ( $75^{\circ}$ ) north-east dipping fault about 0.5 meters. This fault lies south of an east-projected trace of the Wallula fault zone, and is not in alignment with it.

#### 6.1.3.3 Gable Mountain

Faulting on the eastern end of Gable Mountain, 40 km north of Richland was studied by Bingham and others in 1970. They concluded 1) that south-dipping low-angle thrust faults on the northern and southern flanks of the structure were connected beneath an intervening cover of glacial flood deposits, and 2) that glaciofluvial deposits exposed in trenches above the faults had not been disturbed by faulting. Both conclusions have been shown to be in error on the basis of detailed trenching and borehole studies conducted since the summer of 1980 by Golder and Associates (D. Caldwell, personal communication, 1981). The two south-dipping thrust faults are separate faults, although the possibility that they merge into a single fault in areas to the southwest is still open. Flood gravels believed by Golder to be of Missoula age (latest Pleistocene - earliest Holocene) can be seen to have been thrust faulted in several trenches across the northern fault. Furthermore, clastic dikes which cut these glaciofluvial deposits and Miocene bedrock units, and which have been injected along both the northern and southern thrust faults, are sheared and striated at a number of localities. In partial support of the conclusions of Bingham and others (1970), glaciofluvial deposits which lie across southwestern portions of the northern fault and the eastern portion of the southern fault have not been disturbed by faulting. Golder's studies of the two faults are currently in progress. It is this writers opinion that both faults have experienced Quarternary displacement of tectonic origin.

## 7.1 OLYMPIC-WALLOWA LINEAMENT

The Olympic-Wallowa lineament (OWL), originally postulated by Raisz (1945) as a northwest-trending alignment of topographic features between the Olympic Peninsula, Washington, and the Wallowa Mountains, Oregon, is a cryptic feature of Pacific Northwest geology that may have bearing on the tectonic history of the Columbia Plateau. Raisz believed that the lineament was probably fault-controlled, but he stated (1945, p. 483) "that in most places the lineament is rather a zone than a line, with many parallel ridges and splinters..." (p. 484) it appears to be a more complex structural line than a simple fault. It may have started as a transcurrent fault, but the line of weakness thus created probably suffered further dislocation." His reference to transcurrent faulting alludes to his perception from physiographic relations that both the crests of the Cascades and the Blue Mountains have been offset along the lineament for about six miles -- in a left-lateral sense.

Skehan (1965) suggested that the lineament may mark a fundamental boundary in the continent between former oceanic crust to the south and older continental crust to the north. Washington Public Power Supply System (1977a) proposed on geologic grounds that the basement for much of the Columbia Plateau on both sides of the lineament is Mesozoic oceanic crust, and associated sedimentary rocks, accreted to the continent prior to the Cenozoic era. His conclusion is generally supported by Hill's 1972 interpretations that the crust beneath the Plateau is 1) thinner than that of the granitic-metamorphic terrane of northern Washington by as much as 12 km, or 2) that it has an average P-wave velocity as much as 0.8 km/sec. higher than that terrane, or 3) that some combination of 1) and 2) prevails. In 1979, however, Hill concluded that the crust beneath the Pasco Basin is indeed thin (ca. 25 km minimum), but that it has a low P-wave velocity (ca. 6.1 km/sec.). This low velocity, if valid, is difficult to reconcile with an accreted basement of oceanic character. As an alternative, Laubscher (1981) has proposed that the basement is genuinely continental, but was thinned during early Tertiary regional doming -- evidence for which are the Eocene grabens of the northern Cascades and Okanogan terranes. He ascribed thinning of the crust to the combined consequences of east-west stretching, subareal erosion of the crest of the dome, and subcrustal "erosion" by processes unknown. This writer still believes that exposures of ophiolite rocks and associated marine sediments north (Ingalls ophiolite of Washington Cascades) and west of the plateau (Rimrock Lake) argue for an accreted oceanic basement beneath central areas of the plateau.



Whatever kind of crust underlies the Pasco Basin, recent geophysical studies support both Washington Public Power Supply System's (1977a) and Laubscher's (1981) contentions that this crust does not change across OWL. No evidence is seen in a recently compiled total Bouguer gravity anomaly map of the Columbia Plateau (1"500,000; c.i. = 4 mgal) that a change in basement rocks or crustal character occurs along the lineament (Weston Geophysical Research, 1981). Furthermore, a strong gravity gradient that separates the Yakima and Pasco Basins trends north-south across OWL. The gradient is so linear that the Weston report states (p. 23). "One edge of the causative body extends north-south with a density contrast that is positive with respect to the rocks toward the west. Because the contours are relatively straight, any faults striking between N 45° W and S 45° W that cross the gradient would have horizontal displacements less than two-three km." This conclusion supports Laubscher's contention (1977, 1981) that any strike-slip displacement along Raisz's lineament (and Laubscher's Cle Elum-Wallula lineament, see below) must be less than 2 km. Incidentally, the north-south gravity gradient referred to above, is interpreted by Laubscher as delineating the western edge of a master north-south trending graben of Eocene age that developed longitudinally along the crest of the regional dome he has postulated.

A recent study (Rodi and others, 1980) to model the three-dimensional structure of crust and upper mantle beneath the Columbia Plateau utilized joint inversions of regional Bouguer gravity data and P-wave travel-time residuals for teleseismic events recorded at stations in eastern Washington. The joint inversion model resulting from the study revealed no changes in crustal or mantle structure at depths greater than 10 km coincident with the surface trace of OWL.

It thus seems unlikely that the Olympic-Wallowa lineament is a fundamental or profound crustal break, or that diffuse transcurrent displacement along its inferred Plateau segment has been greater than a few kilometers since extrusion of the Miocene Columbia River basalts. Is it a throughgoing feature from the Cape Flattery area of the Olympic Peninsula to the linear northeastern margin of the Wallowa Mountains, Oregon (near Enterprise and Wallowa Lake)? Almost certainly not, for the reasons discussed below.

The northwest-trending, northern margin of the Olympic Peninsula, the western end of the Olympic-Wallowa lineament, is controlled by the strike and steep dip of Eocene units on the northern flank of a major, Miocene or younger antiform



which plunges steeply eastward beneath Puget Sound. The Eocene Crescent Volcanics define this antiformal structure, with their prominent horseshoe-shaped outcrop pattern around the northern, eastern, and southern margins of the Olympic Mountains (Tabor and Cady, 1978). A recent U.S.G.S. report on the geology of the Olympic Peninsula (Tabor and Cady, 1978) does not refer to Raisz's speculations about an Olympic-Wallowa lineament, but does show high-angle faults along most of the valleys believed by Raisz to define his lineament. The faults generally parallel steeply inclined bedding within Eocene units and much of their traces are mapped as concealed beneath Quaternary glacial deposits. Although they are thus difficult to evaluate in terms of their displacement history, they appear to this writer to be unlikely representatives of a hypothesized 650 km-long fault zone - a zone postulated in no small measure on their existence. There are no a priori reasons why structures related to the Olympic antiform should extend to the east of Puget Sound, and at present, no evidence that they do so.

Raisz believed that the easternmost segment of the lineament extended up the troughlike valley of the South Fork of the Walla Walla River and across the Blue Mountains to the Wallowa Mountains. Evidence has since accumulated to the contrary. Mapping by D. Swanson, USGS (unpublished), by Shannon & Wilson (1979b), and by R. Dale and J. Kendall (Kendall and others, 1981) have all demonstrated the continuity across the South Fork of the Walla Walla River of vertical major faults (including the Hite fault) and west-dipping dikes of Frenchman Springs basalts. It is, therefore, clear that this segment of the topographically defined Olympic-Wallowa lineament cannot be related to faulting in rocks of Miocene age.

In an earlier report (Washington Public Power Supply System, 1977a, p. 2RC-34) this writer stated that the Olympic-Wallowa lineament is "as originally defined a fictional structural element of the Pacific Northwest." I am still inclined to that view when the entire lineament postulated by Raisz is considered, but the existence of a disturbed plateau structural zone (including the Wallula fault zone) coincident with the central third of Raisz's lineament cannot be questioned. The nature and tectonic significance of this disturbed structural zone ("CLEW" of Laubscher, 1977) is discussed below.





## 8.1 ORIGIN OF COLUMBIA PLATEAU STRUCTURES

### 8.1.1 INTRODUCTION

Much has been written about the origin of the faulted fold structures of the Columbia Plateau with their enigmatic, more-or-less east-west orientations. The plateau folds have long attracted the attention of geologists because of their dramatic topographic rise above a generally subdued topography and because their trends are so atypical of the Cordillera as a whole.

The relationship of plateau fold (and fault) structures to deformation in underlying basement rocks has been a matter of particular contention among geologists since at least the writing of Laval (1956). He proposed that plateau folds could be caused by either 1) draping of basalt strata over reactivated basement faults ("thick-skinned" deformation), or 2) by folding of strata independent of the basement above a shallow-dipping surface of detachment ("thin-skinned" deformation).

Perhaps the most recent proponent of "thick-skinned" deformation is Bentley (1977, p. 343 and Figs. 14 and 20), who contended that the anticlinal folds of the plateau are localized above "basement weakness zones" (Figure 6). Such zones, according to Bentley (p. 343), have "localized the horizontal stresses and 'caused' the vertical uplift of the ridges at successive times. In gross character, the anticlines are 'drape' folds caused by vertical breakup of basement blocks..."<sup>1</sup>

---

<sup>1/</sup> A similar model has recently been proposed by G. H. Davis (1978, not this author) for the widely spaced monoclines and folds of the Colorado Plateau. Davis concludes that the Colorado Plateau structures formed above steep, inactive basement fracture zones or faults that became reactivated in Laramide time when the plateau was subjected to regional compression. As with the Columbia Plateau folds, the impressive uplifts of the Colorado Plateau represent very little lateral shortening of the crust (1% or less according to G. H. Davis as compared with an analysis of Laubscher, 1977, of roughly 2% for the Columbia Plateau between the Columbia River and Kittitas Valley Washington; Bentley's more recent analysis, 1980, concludes approximately 7% shortening in western plateau areas and 2% in eastern).

### 8.1.2 STRUCTURAL ANALYSES OF LAUBSCHER

In the opinion of the writer, the most innovative analyses of plateau structure in the past several years have been those of Laubscher (1977, 1981). Laubscher (1981) relates internal deformation of the Columbia Plateau to its position within a broad belt of late Cenozoic regional dextral shear that separates the distending Basin and Range province from stable North America to the north. This inferred belt is several hundred kilometers wide and extends northwestward from Idaho to the Olympic Peninsula, hence the acronym IDOL given to it by Laubscher. IDOL is viewed as a complex mosaic of nearly two dozen tectonic blocks of variable extent. The most important from the standpoint of Columbia Plateau structure is the Yakima block, that IDOL component that contains all of the plateau folds south of a Cle Elum-Wallula lineament (CLEW) recognized earlier by Laubscher (1977).

A difficulty in testing the IDOL concept is the relatively small translational and rotational strains proposed by Laubscher to have occurred within IDOL. For example, he postulates only about 7 km of dextral shear across the entire 200 to 400 km-wide belt, and no more than 2 km of shear across CLEW itself (1981). Small strains have produced impressive structures in the Columbia Plateau because of the general horizontality of strata and flatness of topography there before latest Cenozoic deformation. Elsewhere, in geologically complex or topographically varied areas, comparable strains might produce structural features so diffuse that they would be difficult or impossible to recognize.

Laubscher's CLEW (1977), which forms a portion of the northern boundary of IDOL and is coincident with the central third of the Olympic-Wallowa lineament as defined by Raisz (1945), is a northwest-trending zone of structural disturbance that extends between Cle Elum to the northwest and Wallula Gap to the southeast (Figure 3). It is now recognized by most plateau workers as a fundamental structural component of the Washington portion of the Columbia Plateau. The zone is characterized by a "system of mostly faulted east-southeast-trending folds, or fold segments deflected in that direction where the long east to east-northeast-trending folds enter CLEW. This pattern is that of a right-lateral en echelon belt" (Laubscher, 1977, p. 11).

In a refinement of his 1977 draft report, Laubscher (1981) has concluded that CLEW developed prior to the plateau

folds, since they either terminate against it or are deflected or otherwise influenced by it. He interprets CLEW as the upper crustal consequence of deep-seated (15 to 20 km) right-lateral shear along a break in the lithosphere of the Columbia Plateau.

Folding within the Yakima Block is attributed by Laubscher to compressive stresses directed from the south as a result of block interactions with IDOL. These stresses are deemed responsible for a northward-migrating detachment (decollement) of the 20 km thick plateau crust from its serpentinitized (?) peridotite mantle. The detachment is believed to root southward in or at the base of the thicker Blue Mountains crust. Broad fold structures spaced at roughly 25 to 30 km intervals lie above south-dipping reverse or thrust faults that progressively left the decollement at depth to ramp upwards (Figure 7). The periodicity of these folds is related by Laubscher to the initial periodic spacing of an echelon anticlinal folds (his "brachyanticlines") in CLEW, possible as the consequence of some kind of interference phenomenon between CLEW and the subcrustal detachment. "It is, therefore, proposed that as decollement instability at the base of the crust spread to the north, the pre-existing regularly-spaced brachyanticlines on CLEW, or rather the corresponding deep faults, were stress concentrators on the decollement surface from which thrusting spread sideways" (Laubscher, 1981). Laubscher believes that the sharply-defined ridges of the Columbia Plateau, which sit atop the much broader fold structures referred to above, are similar to kink bands and are due to "localized decollement at depth of 1-3 km, probably at the base of the Yakima sequence which is a mechanical discontinuity" (1981).

Several features do suggest regional northward translation of the Columbia Plateau and, hence, support some variety of detachment model for the origin of the compressional structures within it. Among these features are the generally asymmetric geometry of the plateau folds (steepest or over-turned flanks to the north -- with some prominent exceptions), and a southwestward deflection of the western ends of several major folds (Columbia Hills, Horse Heaven-Simcoe, Toppenish, Ahtanum?) as they enter the foothills of the Washington Cascades from the east. Laubscher defined the western edge of the Yakima block of the plateau on this basis, and he considered this rather diffuse boundary a zone of sinistral strain (HOOK, Laubscher, 1981). Similarly, the eastern ends of the Saddle Mountains and Umtanum-Gable Mountain structural trends may be deflected southeastward in a dextral sense. If so, and

this latter geometric relationship has not yet been adequately confirmed, then Laubscher's concept of the plateau folded region as a block or slab which has indented more northerly areas gains credence.

A major modification of Laubscher's crustal detachment model seems necessary to this writer, however, because of two important geometric aspects of the plateau folds: 1) north-south shortening across individual fold structures is small (0.5 to 2.5 km according to Bentley, 1980); and 2) the direction of fold vergence is southward in some structures (e.g. Cleman Mountain anticline) and alternatively both southward and northward along trend in others (Manastash, Umtanum, Gable Mountain, Toppenish?).

Both characteristics are compatible with local detachment of strata in the vicinities of the fold structures, much as Laubscher envisioned, but without the associated north-vergent, regional thrust faults which Laubscher postulates as extending to depth for 40 to 50 km across the entire crust (Figure 7). The alternating northward/southward vergence along trend of the Umtanum and Gable Mountain anticlines, with requisite tear faults separating the divergent fold structures is indicative of a history of localized folding, followed by later development of associated faults. Hypothetical stages in the generalized kinematic development of such doubly-vergent structures are presented in Figure 8. As illustrated, variable directions of overturning along the axial trace of the anticlinal fold -- possibly the consequence of pre-existing structural or stratigraphic anisotropies in the rocks being folded -- lead to the development of secondary cross-structure tear faults and, if deformation continues, to still younger flanking thrust (or reverse) faults. Price (1980), in a detailed structural analysis of the Umtanum Ridge anticline near Priest Rapids Dam, has concluded that concentric folding with a kink-like geometry occurred during north-south compression (a geometry similar to that envisioned by Laubscher, 1981). "When shortening reached its maximum amount achievable by folding, it continued by overthrusting along thrust faults" (Price, 1980, p. 21). In other words, folding was not the consequence of the thrusts which now flank the structure.

Theoretical modeling of the plateau folds has yet to be undertaken, but to this writer the existence of a single, regional detachment surface beneath the Yakima fold province seems unlikely in the light of the small compressive strains (2 to 7%, Bentley, 1980), within the province. The distances between individual fold structures and the broad



uplifts they surmount are more likely, in my opinion, to be related to a buckling geometry for the plateau crust than to thrust fault risers ascending from a deep-seated plane of detachment at the base of the crust. Thrust-fault displacements of a kilometer or less for individual fold structures would, in all likelihood, be dissipated within the stratigraphic section well before the next fold-thrust structure some tens of kilometers distant is encountered.

Finally, Laubscher's hypothesis of northward-migrating subcrustal decollement as an explanation for plateau folding appears to be contradicted, as reviewed above, by the irregular development in both time and space of the plateau folds and their associated thrust faults. There is clearly no simple geographic progression of fold development discernible from the geologic record. Stratigraphic studies in the Pasco Basin area, for example, indicate that one of the most northerly fold structures, the Saddle Mountains anticline, began to form prior to some major folds now located to the south. In Laubscher's defense, much of the data bearing on the chronology of plateau fold development was unavailable to him at the time of his most recent writing.

This writer believes that one of Laubscher's principal contributions is his recognition that plateau structures fall into two major categories: (1) the prominent east-trending folds and their associated faults; and (2) CLEW, the zone of dextral strain that traverses the fold belt from northwest to southeast. The concept of CLEW as a structurally disturbed zone impressed upon the more regional plateau fold structures has its origins in Raisz's Olympic-Wallows lineament (1945), but Laubscher appears to have been the first to recognize the kinematic significance of the zone and its characteristics of dextral transcurrent strain.

The origin of CLEW and the timing of its development with respect to the plateau folds are critical aspects of any tectonic model for plateau deformation. In the following section this writer discusses these topics in a context somewhat different than that proposed by Laubscher (1977, 1981). Nevertheless, my indebtedness to his structural analyses will be obvious and is strongly acknowledged here.

#### 8.1.3 GEOMETRY AND KINEMATICS OF CLEW

The plateau disturbed zone named CLEW by Laubscher (1977) can be conveniently divided from northwest to southeast into three structural domains (Figure 3), all of which contain

features characteristic of dextral-transcurrent strain: (I) a broad zone of deflected or anomalous fold and fault trends (south from Cle Elum to Rattlesnake Mountain); (II) a narrower aligned belt of topographically expressed domes and doubly-plunging anticlines (Red Mountain to Wallula Gap) and, to the southwest, the northwest-trending eastern end of the Horse Heaven anticline; and (III) the Wallula fault zone (Wallula Gap to vicinity of Milton-Freewater, Oregon). As illustrated in Figure 3, CLEW narrows southeastward. East of Wallula Gap it is primarily represented by the transcurrent Wallula fault zone.

The Wallula fault zone was studied by Bingham and others (1970) in reconnaissance and by Shannon & Wilson (1979a) in greater detail. Strike-slip displacement within the zone is evidenced by the occurrence of subhorizontal striae at fault localities near Wallula Gap (loc. A, Shannon & Wilson, 1979a) and east of Warm Springs Canyon (loc. C, Shannon & Wilson, 1979a). Dextral (right-lateral) slip is suggested by the en echelon pattern of presumably normal faults directly south of the Wallula fault zone (Figure 5), by possible right-lateral stream deflections along the fault-line scarp east of Wallula Junction, and by the very slight en echelon alignment of the long axes of the domes and doubly-plunging anticlines west of Wallula Gap.

Field studies by Shannon & Wilson (1979b) and J. Kendall and R. Dale (in progress, University of Southern California) lead this writer to the conclusion that the Wallula fault terminates southeastward in the vicinity of Milton-Freewater. It is proposed here that dextral displacements along the Wallula fault can be geometrically explained as the consequence of differential crustal extension in the northern and southern walls of the zone. Horizontal (extensional) components of slip across normal faults south of the Wallula zone between Wallula Gap and Milton-Freewater would produce a northwestward displacement of the southern wall with respect to the northern. As illustrated in Figure 9, this displacement increases northwestward across each successive normal fault. A similar geometry of normal faulting is seen in the southwestern wall of the dextral Furnace Creek fault zone in Death Valley near its area of termination (Wright and Troxel, 1973).

Near Wallula Gap, the dextral strain which is largely concentrated along the Wallula fault to the east, becomes more diffuse. It does so in part by a westward splaying of the fault into two major branches. The southern branch (Wallula Gap fault of Jones and Deacon, 1966) dies out 4 to



6 km west-northwest of Yellepit according to Shannon & Wilson (1979a), although Foundation Sciences (1980) infers that it extends several tens of kilometers farther west. The northern, presumably main branch of the zone is inferred to underlie the next structural domain (II) of CLEW, the slightly en echelon doubly-plunging anticlines and domes that lie between Wallula Gap and Rattlesnake Mountain; this structural alignment has been called the Rattlesnake Hills-Wallula lineament by some previous workers. Here, dextral strain is apparently manifested not by a single throughgoing fault, i.e. the Wallula fault, but by the discontinuous fold and fault structures of the domain (see additional discussion of this point below) and by a southeastward deflection of the eastern end of the Horse Heaven anticline (Figure 3).

Northwest of Red Mountain and the Yakima River, the zone of CLEW (III) in which dextral strain effects can be observed becomes still broader and, presumably, still more diffuse. Laubscher contends on the basis of his geometric analyses (1977, 1981) that cumulative dextral strain across CLEW is less than 2 km, an estimate supported by Weston Geophysical's interpretation (1981) of the linear pattern of north-south-trending gravity anomalies along the western edge of the Pasco Basin. If right-slip within CLEW is geometrically related to crustal extension by limited normal faulting south of the Wallula fault, then estimates of total right-slip (or strain) of less than several kilometers appear reasonable.

The isolated fold structures of the Red Mountain-Wallula Gap domain of CLEW themselves attest to limited strike-slip displacement within the domain. Tchalenko (1970) and Wilcox and others (1973) have demonstrated from field and clay model studies that isolated fold structures such as those of the Red Mountain-Wallula Gap domain are the consequence of limited displacement across diffuse zones of transcurrent strain. As stated by the latter authors:

"...en echelon folds in wrench zones form early. As the amount of displacement on the wrench zone increases, the initial folds are broken first by fractures and then by faults (p. 77). The development of the main, throughgoing wrench fault is the last state in the early phase of wrench-zone deformation (p. 82). After a short interval of concurrent folding and conjugate faulting, the rocks (or clay) fracture in a relatively narrow zone within the overall deformational swath, and the master wrench fault is created (p. 87)."

Because the bedrock-cored folds of the Red Mountain-Wallula Gap structural domain are separated by low-lying areas of Holocene deposits, the existence of a throughgoing wrench fault between them is difficult to establish. Bingham and others (1970) concluded that such linkage does exist in the form of a zone of shearing, the Rattlesnake-Wallula fault, which they interpreted as joining 15 widely spaced outcrops of breccia along the Rattlesnake Hills-Wallula structural trend. Continuity of the fault-breccia zone, according to Bingham and others (1970, p. 74) "can usually be inferred by the presence of subdued topographic features, such as straight scarps, saddles, and gully alignments (sic), along which the breccia is usually concealed by loess." They regarded the hypothesized fault zone as younger than the domal uplifts, but parallel to and almost congruent with the aligned fold structures.

Washington Public Power Supply System (1977b, p. 2R F-17) describes a Wallula Gap-Rattlesnake Hills topographic lineament as being "very gently curved" and appearing as a "northeast-facing break in slope." Washington Public Power Supply System (1977c, p. 2R H.5-8) supports the existence of a throughgoing topographic lineament ("the Rattlesnake Hills-Wallula lineament is formed by a slight en-echelon alignment of discontinuous, tightly-folded, plunging anticlines separated by interfold segments with a north homoclinal dip off of the Horse Heaven anticline"), but he concluded (p. 2R H. 509) that "there is no field evidence that this lineament is fault caused, either continuously or en echelon."

Two other lines of data bear on the question of continuity of fault structure within the Red Mountain-Wallula Gap structural domain. J. Doherty of Weston Geophysical (personal communication, 1980) reports that several aeromagnetic profiles that transect the domain at high angles--across both anticlinal folds and the topographic lows between them--have anomalies at the Rattlesnake Hills-Wallula lineament that consistently model as a steep fault, north side down. However, if a throughgoing fault does exist, it does not appear to lie within the bedrock exposures of the various anticlinal folds. For example, faults exposed in the Butte, south of Finley, and in the next two hills to the northwest are not parallel and have slickenside striae that set each apart from the others in a kinematic sense (Table 1).

The question of fault continuity between the isolated anticlines and domes of CLEW's Red Mountain-Wallula Gap domain has not yet been satisfactorily resolved. A strong

case, based on geometric analogies with wrench fault zones elsewhere, can be made for the existence of a throughgoing transcurrent zone of movement at some depth beneath the fold alignment, but the upward extent of that zone has yet to be defined. Accordingly, additional geological and geophysical studies are planned along the structural trend in early 1981.

The tectonic model proposed here for the geometric and kinematic interrelationships between the three domains of CLEW draws support from geometrically analogous relations along the Newport-Inglewood fault zone in the western Los Angeles Basin. Recent studies of that zone (Harding, 1973; Yeats, 1973; Barrows, 1974) describe it as a wrench fault-controlled zone, consisting of a series of rather evenly spaced and complexly faulted anticlines with an en echelon pattern that requires dextral wrenching. The folds are topographically expressed (Figure 10) along a northwest-southeast trend approximately 65 km in length. Individual folds are cut obliquely by synthetic, right-lateral strike slip faults. Offsets increase southeastward where the disturbed zone is characterized by longer, more throughgoing faults (Figure 10), but total dextral displacement for the zone is no more than 3 km (Yeats, 1973). Despite geometric similarities between the two zones, they differ pronouncedly in present seismicity and regional tectonic setting. No historic earthquakes have conclusively been tied to the Rattlesnake Hills-Wallula structural alignment (see concluding section of this report), but the Newport-Inglewood zone has experienced scores of significant events since 1920 (Barrows, 1974), including earthquakes of magnitude 6.3 (March, 1933, with 78 aftershocks between 3.9 and 5.2), 5.4 (October, 1933), 4.9 (1941), "near" 4.9 (1920), and 4.5 to 4.6 (1939, 1944, 1961, 1969). Unlike CLEW, which lies within an intraplate region of low strain, the Newport-Inglewood zone lies within the San Andreas fault system, the active boundary between the Pacific and North American plates in California. Furthermore, geologic studies summarized elsewhere indicate that most of the development of southern portions of CLEW occurred prior to Pleistocene time, unlike the pronounced contemporary strain along the Newport-Inglewood zone.

#### 8.1.4 ORIGIN OF CLEW

Laubscher (1981) proposes that CLEW initially developed across the Columbia Plateau lithosphere as a zone of "broad and gentle dextral en echelon brachyanticlines" above a deeper wrench fault of very small displacement (much less than 2 km). The early brachyanticlines of CLEW, or the deep fault(s) inferred to lie below them, are viewed by Laubscher

as acting as stress concentrators and nucleating in some way the Yakima-type plateau folds during slightly younger, crustal decollement (detachment).

This writer's view differs somewhat from Laubscher's in terms of the timing of the development of CLEW. The components of CLEW are viewed here as development synchronously with plateau fold and fault structures of more easterly trend. According to this view, north-south shortening of the Columbia Plateau has produced the two major plateau structural elements-- (1) the east-trending fold-fault structures of higher plateau strata by buckling and local detachment ("thin-skinned") mechanisms, and (2) CLEW, by dextral movement along a deeper fault or zone of anisotropy, with the synchronous distortion of developing fold structures at stratigraphic and structural levels directly above the deeper structure (Figure 11). Changes in trend of folds (e.g. Horse Heaven Hills anticline) as they enter CLEW are not interpreted as rotations (drag) of older structures, but rather as expressions of the complex local stress field within CLEW that resulted from interaction of the two levels of differing deformational behavior. The zone of structural interference is very broad in northern parts of CLEW, but narrows progressively southeastward to become the Wallula fault zone east of Wallula Gap. It is not clear whether the end of the Wallula fault near Milton-Freewater coincides with the terminus of the deeper strike-slip structure, or merely represents the south-eastward limit of Miocene and younger reactivation along a pre-existing structure.

#### 8.1.5 NATURE OF THE BASEMENT CONTROL OF CLEW

An important question is whether the location of CLEW was predetermined by a pre-existing fault or structural flaw in the crust of the plateau, and reactivated in Miocene time, or whether it is a pristine zone formed during late Miocene deformation. Laubscher (1981) adopts the latter view, pointing out that neither regional gravity patterns nor isopachs of crustal thickness change across CLEW (in this writer's opinion, his isopach observation is inadequately controlled by data). Alternatively, Shannon & Wilson (1978, p. 23), in an evaluation of CLEW based on Laubscher's 1977 manuscript, favored pre-existing controls on the location of CLEW and the nature of deformation within it: "In our opinion, most individual structures in the CLEW are consistent with a tectonic model of local compression that occurred along trends controlled by regional zones of inherited weakness in a stress system oriented north-south or north-northeast south-southwest." Shannon & Wilson

(1978) did not, however, accept the regional wrench tectonics model proposed by Laubscher for CLEW and endorsed here.

Evidence for the existence along CLEW of an older fault below the Miocene plateau basalts comes from northwestern areas in the Washington Cascades. Both Tabor and Frizzell (1979) and Vance and Miller (1981) report that early Eocene structures of the Straight Creek fault zone turn southeastward, south of Kachess Lake and the Yakima River, into a position coincident with the Olympic-Wallowa lineament (and, therefore, CLEW). According to Vance and Miller the Goat Peak segment of the north-south Straight Creek fault becomes the northwest-striking Taneum Lake fault 15 km south of the Yakima River (Figure 3). They view the Taneum Lake fault as a late dip-slip splay of the Straight Creek fault, -- not the main transcurrent structure. Because the Taneum Lake reverse fault cuts only pre-Miocene units (Bentley, 1977), its age relationship to Miocene plateau basalts is unclear. However, Tabor and Frizzell (1977) conclude that Miocene or younger movement along either the southern Straight Creek fault or the Olympic-Wallowa lineament "must be minimal or absent because the Miocene Snoqualmie batholith and its satellite stocks cut faults in the Straight Creek zone and are unmarked by structures paralleling and on strike with the lineament." The Snoqualmie batholith, dated at 17-18 m.y., is essentially coeval with the earliest Columbia River basalts. Other intrusive and stratigraphic relationships discussed by Vance and Miller (1981) and Tabor and Frizzell (1977) support the conclusion that both strike-slip and dip-slip displacements along southern parts of the Straight Creek fault zone had terminated by mid-Oligocene time, ca. 33 m.y. ago.

Hammond (1977) has described a broad northwest-striking zone of faulting, coincident with OWL, that is exposed along the South Fork of the Snoqualmie River on the west flank of the Cascade Range. This fault zone is presumably intruded by the Snoqualmie batholith (Tabor and Frizzell, 1979), but it too projects towards CLEW. Its geometric and kinematic relationships to the Taneum Lake fault are not known. Collectively, the fault relations described above strongly imply that faulting parallel to CLEW and of an age older than the Columbia River basalts was present in at least northern portions of what was to become CLEW in late Miocene time. Whether such faulting contributed to CLEW's development is not known.



The interpretation of CLEW as a diffuse zone of wrench-fault deformation presupposes the existence at depth of a narrower zone of horizontal strain. In Laubscher's words (1981) CLEW is the consequence of "deep-seated right-lateral shear that drives a deformable sequence of partially decoupled more superficial layers." Drawing upon the studies of Emmons (1969) and Harding and Lowell (1979), Laubscher concludes that the depth to the driving structure is about half the width of the deformed belt that develops above it. Accordingly, he estimates that a throughgoing zone of shear would lie at a 15-20 km depth below what has been called domain I of CLEW in this paper (Figure 3), but less than 2 km below the narrower brachyanticlinal domain II. The zone presumably extends to surface levels in domain III (the Wallula fault zone). Another way of stating relations as perceived by Laubscher is that the depth to the controlling transcurrent (wrench) structure responsible for CLEW increases northwestward from domain III to I. If Laubscher's analysis is correct, the driving structure beneath domain I (Rattlesnake Mountain to Cle Elum), which makes up most of CLEW, lies within the lower plateau crust and/or upper mantle. An alternative explanation for the greater width of CLEW in domain I is not that the controlling wrench structure is deeper there, but that the zone of "basement" wrenching simply becomes broader and more diffuse to the northwest.

#### 8.1.6 AGE OF CLEW AND THE QUESTION OF ITS CAPABILITY

The Wallula fault zone within domain III of CLEW can be inferred to extend from the vicinity of Wallula Gap to near Milton-Freewater. Although the topographically-defined trace of the fault zone becomes indistinct several kilometers east of Warm Springs Canyon, the continued presence of northwest-striking normal (?) faults in the hills to the south as far east as Milton-Freewater argues for an extension of the Wallula zone into that region (Figure 3). Shannon & Wilson (1979a) has concluded that the 45-50 km-long Wallula fault zone thus defined is a "capable fault" from the standpoint of nuclear power plant siting criteria.

In light of preliminary findings from the Woodward-Clyde trenches across "Bingham's linear" that Touchet beds are not offset along this part of the Wallula zone, the evidence for capability of the Wallula structure is diminished. The age of colluvial deposits cut by faulting, both at Finley Quarry and west of Warm Springs, is not known. Fanglomerates dated as 50,000 years old (Woodward-Clyde Consultants, 1978, as referenced in Shannon & Wilson, 1979a) lie unbroken across

the Wallula Gap strand of the fault zone near Yellepit. This relation casts some doubt on a Touchet age (ca. 13,000 y.b.p.) for the sheared clastic dike described by Shannon & Wilson (1979) in the Wallula Gap fault zone 3 km east of Yellepit. Unsheared clastic dikes of probable Touchet origin lie within and across fault zones exposed at Finley Quarry and in quarries on "K" and "L" hills to the northwest (all three localities in CLEW domain II). Touchet beds and associated clastic dikes are definitely offset along north-dipping surfaces in a road cut south of Umapine near Milton-Freewater, but the convex-upwards geometry of the surfaces may indicate an origin for them by gravity slumping rather than by tectonic activity. Even if a tectonic origin for these surfaces is assumed, their normal fault geometry is not obviously compatible with their being part of the strike-slip Wallula zone.

In short, although capability of the Wallula fault zone cannot at present be refuted, its unequivocal designation as "capable" (Shannon & Wilson, 1979a) now appears unwarranted in light of recent trenching along "Bingham's linear." In this regard, the 1979 College Place earthquake ( $M = 4.1$ ) which occurred along the Oregon-Washington state line just north of Umapine is of interest. Slemmons and O'Malley (1980, p. 34) state that historic tectonic activity on CLEWW (a southeast-extended version of CLEW) is "recorded by the College Place earthquake." That conclusion is suspect. Although near the southeast-projected trace of the Wallula fault zone in the Milton-Freewater area, the focal mechanism solution for this significant plateau seismic event is grossly incompatible with right slip along a fault parallel to the Wallula zone ( $P$  in the solution is east-west in orientation; and the  $N 40^\circ W$  - striking fault plane of the solution is characterized by left slip; Woodward-Clyde Consultants, 1980a). The earthquake may indicate that the north-south compressive stress field responsible for the development of CLEW is no longer extant in the Milton-Freewater area, having been replaced by east-west shortening. The "Milton-Freewater earthquake of 1936 ( $M = 6.1$ ) has an instrumentally located epicenter near Waitsburg, Washington, approximately 30 km north-northeast of Milton-Freewater." This conclusion is based on a recent evaluation of historic seismographic records by Woodward-Clyde Consultants (1980b) and is in agreement with the original epicentral determination reported shortly after the event. Reports of an epicenter near Milton-Freewater were based on "felt" reports and intensity data. Thus, this earthquake also did not occur within the Wallula fault zone. It's focal mechanism solutions, although poorly constrained, are not compatible with dextral slip on a fault plane parallel to the Wallula zone.





Evidence is good that the Wallula fault zone terminates southeastward in the vicinity of Milton-Freewater. Its northwestern extent is more problematical. Laubscher (1977, 1981), Shannon & Wilson (1979a), and this writer have suggested that the isolated anticlines of CLEW domain II, which extend like beads in a string northwestward from Wallula Gap, lie above a continuation at depth of the Wallula zone. Although the existence of a throughgoing surficial fault hidden beneath Quaternary deposits and lying directly north of the anticlines cannot be discounted, the geometry of the slightly en echelon folds supports the premise that they lie above a shallow buried zone of limited lateral displacement (cf. Tchaleni, 1970, and Wilcox and others, 1973). As proposed by Laubscher (1981) the greatly increased width of CLEW domain I to the northwest argues for a much deeper position of the controlling wrench fault structure there, or (as proposed here) an increasingly broad zone of transcurrent shear at depth, or both. It is the diffuseness of strain within CLEW domains I and II, coupled with evidence that total dextral strain across CLEW is less than 2 or 3 km, that complicates the question of capability of this zone of wrench tectonics. It is important to point out, however, that no Quaternary fault displacements have been documented northwest of Finley Quarry. If, as discussed above, the structures of CLEW, particularly those of domains I and II, represent the interaction of developing thin-skinned plateau folds above an active deeper wrench system, then the age of the folds gives us the age for the formation of CLEW. For reasons discussed at length elsewhere in this report, most plateau folding appears to be of Pliocene and older age (Washington Public Power Supply System, 1977d; Bentley and others, 1980; Rockwell, 1979) although the possibility of major folding in the Yakima area until one or one and one-half m.y. ago cannot be discounted (Bentley, 1977; Rigby and Othberg, 1979).

Tectonic models for CLEW which link it to synchronous plateau folding, thus lead to the conclusion that strain along CLEW has waned significantly within the past 1 1/2 to 3 or 4 m.y. Unlike the San Andreas fault, a dextral plate boundary with sharp definition and large fault displacements (ca. 300 km) in the past 4 to 6 m.y., CLEW is an intraplate zone of small dextral strain (less than a few kilometers) that is characterized by its diffusiveness and its waning nature in the past several million years. These characteristics must be considered when fault-related design criteria are approved for the Hanford plants.

9.1 REFERENCES

- Anderson, J. L., 1980, Deformation and Canyon Cutting in Post-Grande Ronde, pre-Frenchman Springs Time, Grayback Mountain, South-central Washington: Geological Society of America, Abstracts with Programs, V. 12, No. 3, p. 93.
- Ando, M., and Balazs, E. I., 1979, Geodetic Evidence for Aseismic Subduction of the Juan de Fuca Plate: Journal of Geophysical Research, V. 84, No. B6, p. 3023-3028.
- Armstrong, R. L., 1979, Cenozoic Igneous History of the United States Cordillera from Latitude 42° to 49° N, in Smith, R. B., and Eaton, G. P., Eds., Cenozoic Tectonics and Regional Geophysics of the Western Cordillera, Geological Society of America Memoir 152, p. 265-282.
- Atwater, Tanya, 1970, Implications of Plate Tectonics for the Cenozoic Tectonic Evolution of Western North America: Geological Society of America Bulletin, V. 81, No. 12, p. 3513-3536.
- Barrows, A. G., 1974, A Review of the Geology and Earthquake History of the Newport-Inglewood Structural Zone, Southern California: California Division of Mines and Geology Special Report 114, 115 p.
- Beeson, M. H. and Moran, M. R., 1979, Stratigraphy and Structure of the Columbia River Basalt Group in the Cascade Range, Oregon: U.S. Department of Energy Report RL0-1040-T1, p. 5-77.
- Bentley, R. D., 1977, Stratigraphy of the Yakima Basalts and Structural Evolution of the Yakima Basalts and Structural Evolution of the Yakima Ridges in the Western Columbia Plateau, in Geological Excursions in the Pacific Northwest, Department of Geology, Western Washington State University, p. 339-389.
- Bentley, R. D., 1980, Magnitude of Neogene Horizontal Shortening in the Western Columbia Plateau, Washington-Oregon: American Geophysical Union Transactions, V. 62, No. 6, p. 60.
- Bentley, R. D., Anderson, J. L., Campbell, N. P., and Swanson, D. A., 1980, Stratigraphy and Structure of the Yakima Indian Reservation, with Emphasis on the Columbia River Basalt Group: United States Geological Survey Open-File Report 80-200, 83 p.

Bingham, J. W., Londquist, E. T., and Baltz, E. H., 1970, Geologic Investigation of Faulting in the Hanford Region, Washington (with a Section on the Occurrence of Micro-earthquakes, by A. M. Pitts); United States Geological Survey Open-File Report 70-27, 104 p.

Campbell, N. and Bentley, R. 1980, Late Quaternary Faulting, Toppenish Ridge-Southcentral Washington, Geological Society of America, Abstracts with Programs, V. 12, No. 3, p. 101.

Carey, S. W., 1958, The Tectonic Approach to Continental Drifting, in Continental Drift, a Symposium: Geology Department, University of Tasmania, Hobart, p. 177-355.

Carlson, R. L., 1976, Cenozoic Plate Convergence in the Vicinity of the Pacific Northwest: A Synthesis and Assessment of Plate Tectonics in the Northeastern Pacific: University of Washington, Ph.D. dissertation., 129 p.

Christiansen, R. L., and McKee, E. H., 1979, Late Cenozoic Volcanic and Tectonic Evolution of the Great Basin and Columbia Intermontane Regions: in Smith, R. B., and Eaton, G. P., Eds. in Cenozoic Tectonics and Regional Geophysics of the Western Cordillera, Geological Society of America Memoir p. 283-322.

Coney, P. J., 1979, Mesozoic-Cenozoic Cordilleran Plate Tectonics, in Smith, R. B., and Eaton, G. P., Eds., Cenozoic Tectonics and Regional Geophysics of the Western Cordillera, Geological Society of America Memoir 152, p. 33-50.

Crosson, R., 1980, Seismicity and Tectonics of the Puget Sound Region: Results from the Regional Seismograph Network: Seismological Society of America Annual Meeting, Seattle, Washington, Earthquake Notes, V. 50, No. 4, p. 58-59.

Davis, G. A., 1980, Problems of Intraplate Extensional Tectonics, Western United States, in Continental Tectonics: National Academy of Sciences, Washington, D.C., p. 84-95.

Davis, G. A., 1978, Monocline Fold Pattern of the Colorado Plateau, in Vincent Matthews, III, Ed., Laramide Folding Associated with Basement Block Faulting in the Western United States, Geological Society of America Memoir 151, p. 215-234.

Eardley, A. J., 1962, Structural Geology of North America (2nd ed.): Harper and Row Publishers., New York, N. Y., 743 p.

Eaton, G. P., 1979, A Plate-Tectonic Model for Late Cenozoic Crustal Spreading in the Western United States, in Riecker, R. E. Ed., Rio Grande Rift: Tectonics and Magmatism, American Geophysical Union, Washington, D. C., p. 7-32.

Emmons, R. C. 1969, Strike-Slip Rupture Patterns in Sand Models: Tectonophysics, V. 7, p. 71-87.

Foundation Sciences, Inc., 1980, Geologic Reconnaissance of Parts of the Walla Walla and Pullman, Washington, and Pendleton, Oregon 10 x 20 AMS Quadrangles: Prepared by Kienle, C. F., 76 p.

Goff, F. E., and Myers, C. W., 1978, Structural Evolution of East Umtanum and Yakima Ridges, South-Central Washington: Geological Society of America, Abstracts with Programs, V. 10, No. 7, p. 408

Green, R. C., Walker, G. W., and Corcoran, R. E., 1972, Geologic Map of the Burns Quadrangle, Oregon: United States Geological Survey Miscellaneous Investigation Map I-680, 1:250,000.

Hamilton, W., and Myers, W. B., 1966, Cenozoic Tectonics of the Western United States: Review of Geophysics and Space Physics, V. 5, p. 509-549.

Hammond, P. E., 1977, Stratigraphy, Structure, and Plutonism along the Upper Yakima and South Fork Snoqualmie River Valleys, Central Cascade Range, Washington, in Geological Excursions in the Pacific Northwest: Department of Geology, Western Washington State University, p. 292-308.

Harding, T. P., 1973, Newport-Inglewood Trend, California - An Example of Wrenching Style of Deformation: American Association of Petroleum Geologists Bulletin, V. 57, No., 1 p. 97-116.

Harding, T. P., and Cowell, J. D., 1979, Structural Styles, Their Plate-Tectonic Habitats, and Hydrocarbon Traps in Petroleum Provinces: American Association of Petroleum Geologists Bulletin, V. 63, No. 1, p.1016-1058.

Harding, T. P. and Lowell, J. D., 1979, Structural Styles, their Plate-Tectonic Habitats, and Hydrocarbon Traps in Petroleum Provinces, American Association of Petroleum Geologists Bulletin, V. 63, No. 7, p. 1016-1058.

Hill, D. P., 1972, Crustal and Upper Mantle Structure of the Columbia Plateau from Long Range Seismic-Refraction Measurements: Geological Society of America Bulletin, V. 83, No. 6, p. 1639-1648.

Hill, D. P., 1980, Seismic Evidence for the Structure and Cenozoic Tectonics of the Pacific Coast States, in Smith, R. B., and Eaton, G. P., Eds., Cenozoic Tectonics and Regional Geophysics of the Western Cordillera, Geological Society of America Memoir 152, p. 145-174.

Howard, K. A., et. al., 1978, Preliminary Map of Young Faults in the United States as a Guide to Possible Fault Activity: United States Geological Survey Miscellaneous Field Studies Map MF-916, 1:5,000,000.

Jones, F. O., and Deacon, R. J., 1966, Geology and Tectonic History of the Hanford Area and its Relation to the Geology and Tectonic History of the State of Washington and the Active Seismic Zones of Western Washington and Western Montana: Report prepared for Douglas United Nuclear, Inc., DUN-1410, Richland, Washington.

Kendall, J. J., Dale, R. C., and Davis, G. A., 1981, The Structural Relationship of the Olympic-Wallula Lineament, Hite Fault System, and LaGrande Fault System, the Blue Mountains of Umatilla County Oregon: Geological Society of America Abstracts with Programs V. 13 No. 2, p. 64.

Laubscher, H. P., 1977, Structural Analysis of Post-Yakima Deformation, Columbia Plateau, Washington: Draft report prepared for United Engineers and Constructors, Inc.

Laubscher, H. P., 1981, Models of the Development of Yakima Deformation: Prepared for United Engineers and Constructors, Inc.

Laval, W. N., 1956, Stratigraphy and Structural Geology of Portions of South-Central Washington: University of Washington, Ph.D. dissertation.

Lawrence, R. D., 1976, Strike-slip Faulting Terminates the Basin and Range Province in Oregon: Geological Society of America Bulletin V. 87, No. 6, p. 846-850.

Loring, A. K., 1976, Distribution in Time and Space of Late Phanerozoic Normal Faulting in Nevada and Utah: Utah Geology, V. 3, No. 2, p. 97-109.

Magill, J., and Cox, A., 1981, Post-Oligocene Tectonic Rotation of the Oregon Western Cascade Range and the Klamath Mountains: *Geology*, V. 9, No. 3, p. 127-131.

McKee, B., 1972, *Cascadia, the Geologic Evolution of the Pacific Northwest*: McGraw-Hill Book Co., New York, N. Y., 394 p.

McKenzie, D., and Julian, B., 1971, Puget Sound, Washington, Earthquake and the Mantle Structure beneath the Northwestern United States: *Geological Society of America Bulletin* V. 82, No. 12, p. 3519-3524.

Nathan, S. and Fruchter, J. S., 1974, Geochemical and Paleomagnetic Stratigraphy of the Picture Gorge and Yakima Basalts (Columbia River Group) in Central Oregon: *Geological Society of America, Bulletin* V. 85, No. 1, p. 63-76.

Price, E. H., 1980, Strain Distribution and Model for Formation of Eastern Umtanum Ridge Anticline, South-Central Washington: Rockwell Hanford Operations, report prepared for U. S. Department of Energy, RH0-BWI-SA-30, 27 p.

Raisz, E., 1945, The Olympic-Wallowa Lineament: *American Journal of Science*, V. 243-A, p. 479-485.

Reidel, S. P., et. al., 1980, Rate of Deformation in the Pasco Basin during the Miocene as Determined by Distribution of Columbia River Basalt Flows: Rockwell Hanford Operations, report prepared by U. S. Department of Energy, RH0-BWI-SA-29, 43 p.

Riddihough, R. P., 1979, Gravity and Structure of an Active Margin -- British Columbia and Washington: *Canadian Journal of Earth Sciences*, V. 16, No. 2, P. 350-363.

Riddihough, R. P., and Hyndman, R. D., 1976, Canada's Active Western Margin--The Case for Subduction: *Geoscience Canada*, V. 3, No. 4, p. 269-278.

Rigby, J. G., and Othberg, K., 1979, Reconnaissance Surficial Geologic Mapping of the Late Cenozoic Sediments of the Columbia Basin, Washington: State of Washington, Department of Natural Resources, Open File Report 79-3.

Robyn, T. L., 1977, *Geology and Petrology of the Strawberry Volcanics, NE Oregon*: University of Oregon, Ph.D. dissertation, 197 p.





Robyn, T. L., Hoover, J. D., and Thayer, T. P., 1977, Geology and Geochronology of the Strawberry Volcanics, NE Oregon: Geological Society of America Abstracts with Programs, V. 9, No. 4. p. 488-489.

Rockwell, 1979, Geologic Studies of the Columbia Plateau, a Status Report: Rockwell Hanford Operations, Richland, Washington, Report RH0-BWI-ST-4.

Rogers, G. C., 1979, Earthquake Fault Plane Solutions near Vancouver Island: Canadian Journal of Earth Sciences, V. 16, No. 3, p. 523-531.

Shannon & Wilson, 1973, Geologic Studies of Columbia River Basalt Structures and Age of Deformation, the Dalles-Umatilla Region, Washington and Oregon: Boardman Nuclear Project: Report to General Electric Co., 52 p.

Shannon & Wilson, Inc., 1978, Geologic Reconnaissance of the Cle-Elum-Wallula Lineament and Related Structures: A report prepared for Washington Public Power Supply System, 33 p.

Shannon & Wilson, Inc., 1979a, Evaluation of Faulting in the Warm Springs Canyon Area, Southeast Washington: Report prepared for Washington Public Power Supply System, 18 p.

Shannon & Wilson, Inc., 1979b, Geologic Reconnaissance of the Wallula Gap, Washington - Blue Mountains - LaGrande, Oregon Region: Report prepared for Washington Public Power Supply System, 63 p.

Shannon & Wilson, Inc., 1980, Geologic Evaluation of Selected Faults and Lineaments, Pasco and Walla Walla Basins-Washington: Report prepared for Washington Public Power Supply System, 25 p.

Skehan, J. W., 1965, A Continental-Oceanic Crustal Boundary in the Pacific Northwest: United States Air Force Cambridge Research Laboratory Report No. AFCRL 65-904, 56 p.

Slemmons, D. B., and O'Malley, P., 1980, Fault and Earthquake Hazard Evaluation of Five United States Corps of Engineers Dams in Southeastern Washington: Prepared for United States Corps of Engineers, 60 p.

Smith, R. B., 1977, Intraplate Tectonics of the Western North American Plate: Tectonophysics, V. 37, p. 323-336.



Smith, R. B., 1979, Seismicity, Crustal Structure, and Intraplate Tectonics of the Interior of the Western Cordillera, in Smith, R. B. and Eaton, G. P., EDS., Cenozoic Tectonics and Regional Geophysics of the Western Cordillera, Geological Society of America Memoir 152, p. 111-144.

Snyder, W. S., Dickinson, W. R., and Silberman, M. L., 1976, Tectonic Implications of Space-time Patterns of Cenozoic Magnetism in the Western United States: Earth and Planetary Science Letters, V. 32, p. 91-106.

Swanson, D. A. and Wright, T. L., 1978, Bedrock Geology of the Northern Columbia Plateau and Adjacent Areas: In Baker, V. R. and Nummedal, D., eds., The Channeled Scabland, Washington NASA Planetary Geology Program, A Guide to the Geomorphology of the Columbia Basin, Washington, p. 37-57.

Swanson, D. A., et. al., 1979, Preliminary Reconnaissance Geologic Maps of the Columbia River Basalt Group in Parts of Eastern Washington and Northern Idaho: United States Geological Survey Open-File Report 79-534, 1:250,000.

System, Science, and Software, Determination of Three-Dimensional Structures of Eastern Washington from the Joint Inversion of Gravity and Earthquake Travel Time Data: report prepared for Weston Geophysical Corporation by Rodi, W. L. et al., 143 p.

Tabor, R. W., and Cady, W. M., 1978, Geologic Map of the Olympic Peninsula: United States Geological Survey Miscellaneous Investigation. Map I-994, 1:125,000.

Tabor, R. W., and Frizell, V. A., 1979, Tertiary Movement Along the Southern Segment of the Straight Creek Fault and its Relation to the Olympic Wallowa Lineament in the Central Cascades, Washington: Geological Society of America, Abstracts with Programs, V 11, No. 3, p. 131.

Taubeneck, W. H., 1970, Dikes of Columbia River Basalt in Northeastern Oregon, Western Idaho and Southeastern Washington: in Proceedings of the Second Columbia River Basalt Symposium, Eastern Washington State College Press, Cheney, Washington, p. 73-96.

Thayer, T. P., and Brown, C. E., 1966, Geologic Map of the Aldrich Mountain Quadrangle, Grant County, Oregon: United States Geological Survey Map GQ-438, 1:62,500.

Vance, J. A., and Miller, R. B., 1981, The Movement History of the Straight Creek Fault in Washington State: Unpublished manuscript, 5 p.

Walker, G. W., 1977, Geologic Map of Oregon East of the 121st Meridian: United States Geological Survey Miscellaneous Investigation Map I-902, 1:500,000.

Washington Public Power Supply System, 1977a, Tectonic Evolution of the Pacific Northwest - Precambrian to Present: WNP 1/4 Preliminary Safety Analysis Report, Amendment 23, Vol. 2A, Subappendix 2R C.

Washington Public Power Supply System, 1977b, Imagery and Topographic Interpretation of Geologic Structures in Central Washington: WNP 1/4 Preliminary Safety Analysis Report, Amendment 23, Vol. 2B, Subappendix 2R F.

Washington Public Power Supply System, 1977c, Geologic Studies - Wallula Gap to Badger Coulee: WNP 1/4 Preliminary Safety Analysis Report, Amendment 23, Vol. 2B, Subappendix 2R H, Chapter 5.0.

Washington Public Power Supply System, 1977d, Geologic Studies of the Saddle Mountains - Manastash Ridge and Umtanum Ridge Structures: WNP 1/4 Preliminary Safety Analysis Report, Amendment 23, Vol. 2B, Subappendix 2R H, Chapter 8.0.

Washington Public Power Supply System, 1977e, Evaluation of Microearthquake Activity in Eastern Washington: WNP 1/4 Preliminary Safety Analysis Report, Amendment 23, Vol. 2B, Subappendix 2R J.

Washington Public Power Supply System, 1977f, Microearthquake Survey and Evaluation of Stress Orientation in Central Washington: WNP 1/4 Preliminary Safety Analysis Report, Amendment 23, Vol. 2B, Subappendix 2R L.

Weston Geophysical Research, Inc., 1980, personal communication.

Weston Geophysical Research, Inc. 1981, Compilation and Interpretation of Gravity in Washington, Oregon, and Adjacent Parts of British Columbia and Idaho: Prepared for Washington Public Power Supply System, WNP-2 FSAR, Appendix 2.5L, 28 p.

Wilcox, R. E., Harding, T. P., and Seely, D. R., 1973, Basic Wrench Tectonics: American Association of Petroleum Geologists Bulletin V. 57, No. 1, p. 74-96.

Wise, D. U., 1963, An Outrageous Hypothesis for the Tectonic Pattern of the North American Cordillera: Geological Society of America Bulletin V. 74, No. 3, p. 357-362.

Woodward-Clyde Consultants, 1978, Paleomagnetic Measurements of the Ringold Formation and Loess Units near Hanford, Washington and Evaluation of Age Dating Potential of Quaternary Deposits near Hanford, Washington: Report prepared for Washington Public Power Supply System under the Direction of United Engineers and Constructors Inc., Philadelphia, Pennsylvania.

Woodward-Clyde Consultants, 1980a, Recent Seismicity of the Hanford Region (Draft Report, January): Prepared for United Engineers and Constructors, 28 p.

Woodward-Clyde Consultants, 1980b, Seismological Review of the July 16, 1936 Milton-Freewater Earthquake Source Region: Prepared for Washington Public Power Supply System, 44 p.

Wright, L. A., and Troxel, B. W., 1973, Shallow-fault Interpretation of Basin and Range Structure, Southwestern Great Basin, in DeJong, K. A., and Scholter, Robert, Eds., Gravity and Tectonics, John Wiley & Sons, New York, N. Y., p. 397-408.

Yeats, R. S., 1973, Newport-Inglewood Fault Zone, Los Angeles Basin, California: American Association of Petroleum Geologists Bulletin V. 57, No. 1, p. 117-135.

Zoback, M. L., and Thompson, G. A., 1978, Basin and Range Rifting in Northern Nevada: Clues from a Mid-Miocene Rift and its Subsequent Offsets: Geology, V. 6, No. 2, p. 111-116.

TABLE 1

SPECIFICATIONS OF FAULTS EXPOSED WITHIN  
THE RED MOUNTAIN-WALLULA GAP STRUCTURAL DOMAIN\*

<u>Fault Locality</u>	<u>Fault Attitude</u> <sup>#</sup>	<u>Orientation of Striae</u>	<u>Type of Fault</u>
Finley Quarry, The Butte	N 85 E, 65 SE (N) N 63 W, 84 SW (S)	S 14 W, 15; S 2 W, 30** S 62 E, 56; S 70 E, 51**	Reverse, with right-slip component
Quarry, SE end of "K" Hill	N 18 W, 70 NE	S 18 E, 15; N 18 W, 0; S 15 E, 7	Strike-slip
Quarry top of "L" Hill	N 17 W, 52 NE N 48 W, 47 NE  N 65 W, 43 to 20 NE	S 73 E, 46 Down dip	Dip-slip, presumably normal

\* Measurements by W. Kiel and G. Davis, 7/80

# For comparison purposes, the trend of the Rattlesnake Hills-Wallula lineament is N 60 W

\*\* Striae found within shear zone adjacent to fault, not along fault surface measured

2.5N-48

WNP-2

AMENDMENT NO. 18  
September 1981

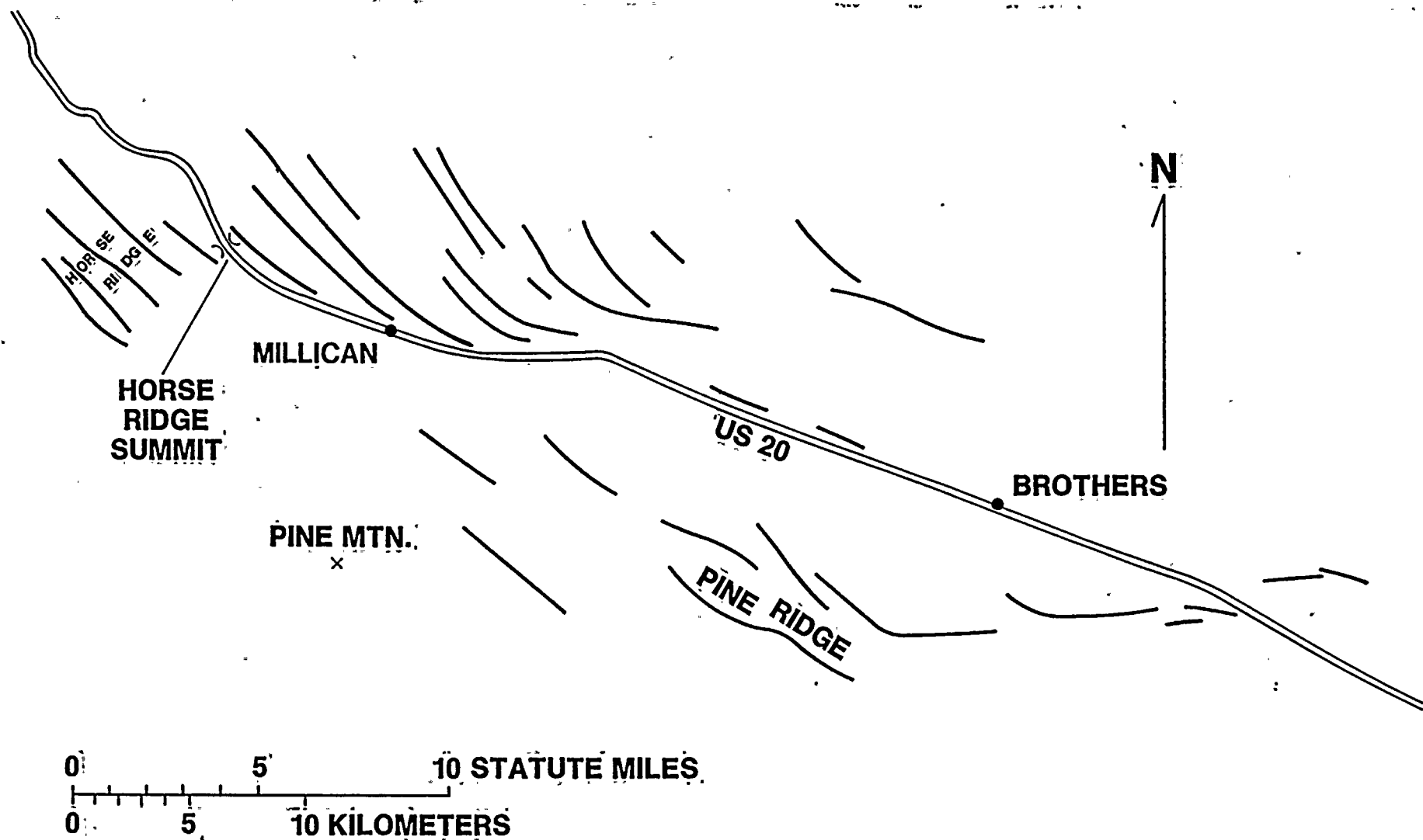
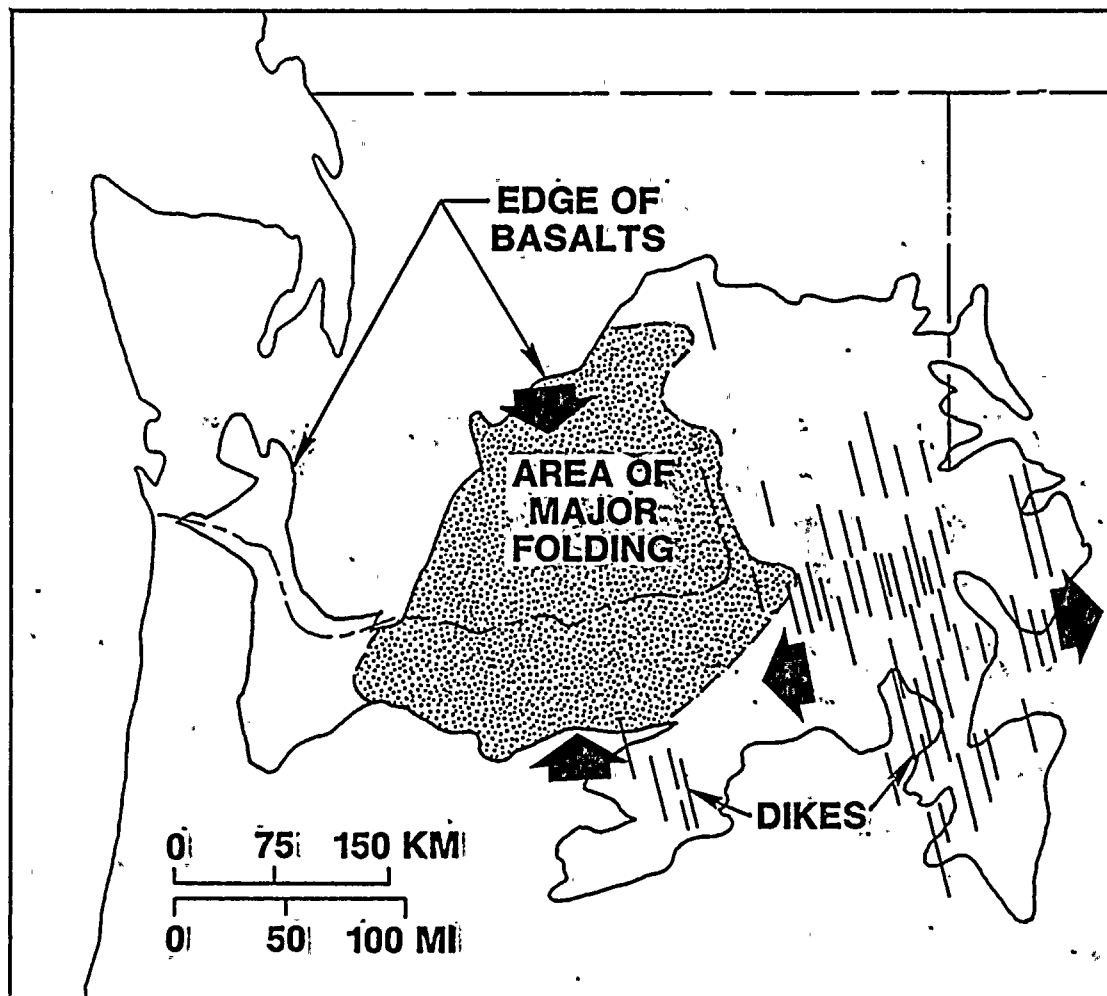


Figure 2.5N-1 Major topographic linear features within Brothers fault zone, central Oregon: Most features between Horse Ridge Summit and Brothers are scarp-like slopes on the south-western margin of elongate ridges. See text for discussion.







**Figure 2.5N-2** Generalized distribution of feeder dikes for Columbia River Basalts. The edge of the basalt field and the area (stippled) of major folding within the basalts are also shown. Dike distribution from Swanson and Wright (1978).

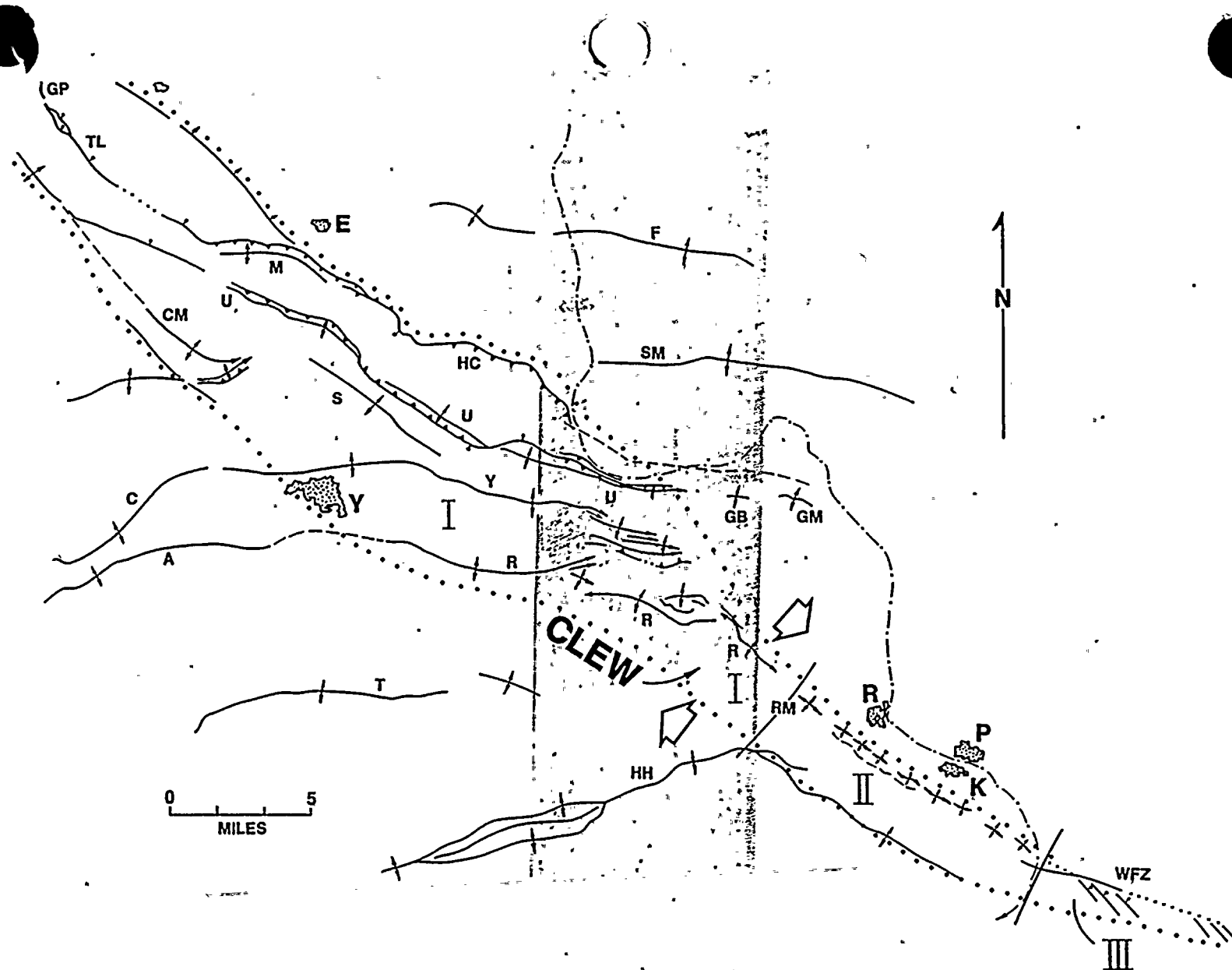
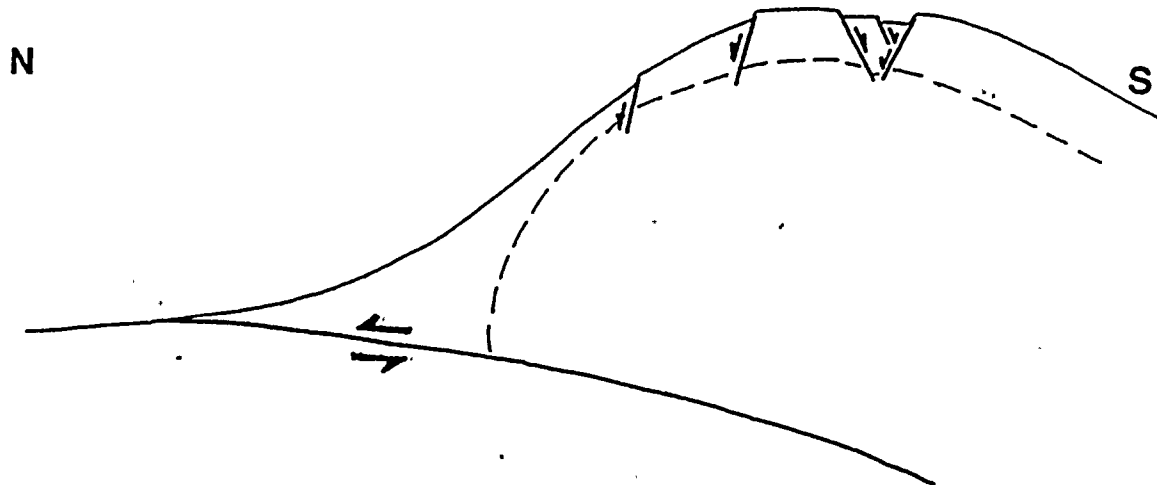


Figure 2.5N-3

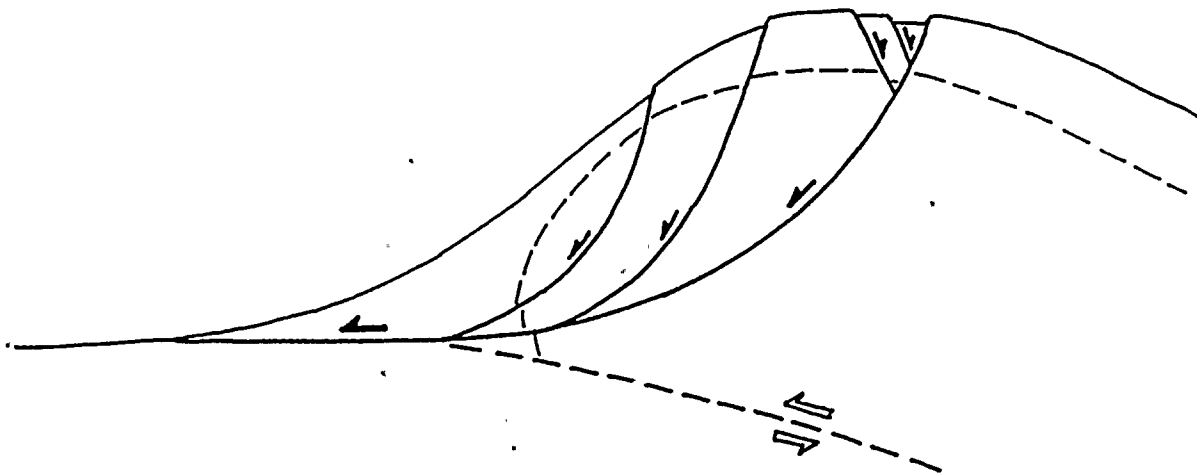
Major structural elements of the south-central Columbia Plateau, Washington (from Kienle and others, 1978). The approximate boundaries of Laubscher's Cle Elum-Wallula lineament (CLEW) are designated by heavy dots. I, II, and III are structural domains within CLEW that are discussed in the text. Stippled areas are cities of Ellensburg (E), Yakima (Y), Richland (R), Pasco (P), and Kennewick (K).



# TOPPENISH RIDGE



## THRUST FAULT MODEL



## LANDSLIDE MODEL

Figure 2.5N-4 *Alternative structural interpretations for surface ground ruptures along Toppenish Ridge.*

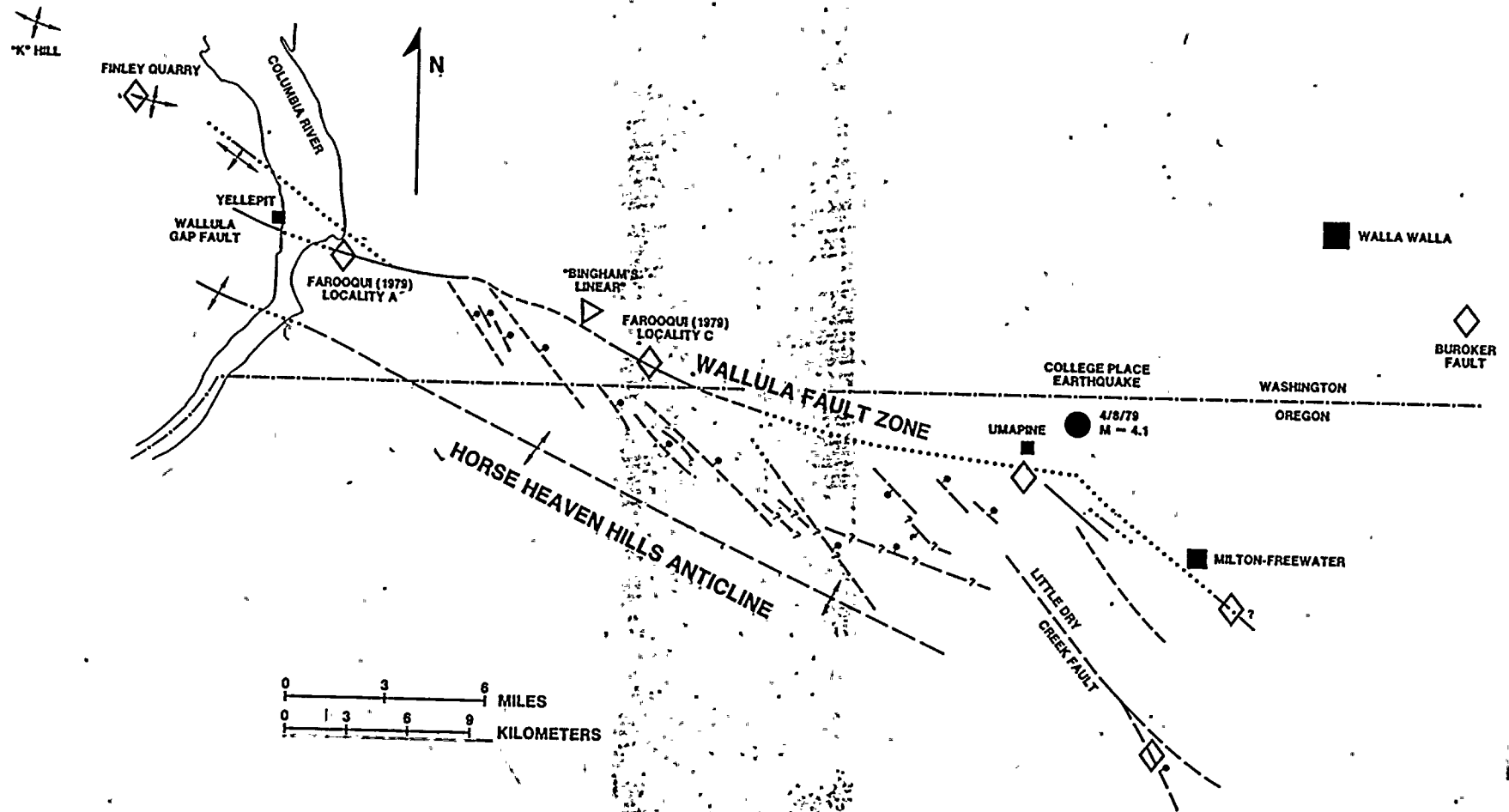


Figure 2.5N-5

*Tectonic map of Wallula fault zone and vicinity (from Kienle and others, 1979) showing localities (diamonds) where Quaternary faulting is confirmed or suspected. Also illustrated are the locations of "Bingham's linear" (triangle) and the epicenter of the 1979 College Place earthquake (black circle).*



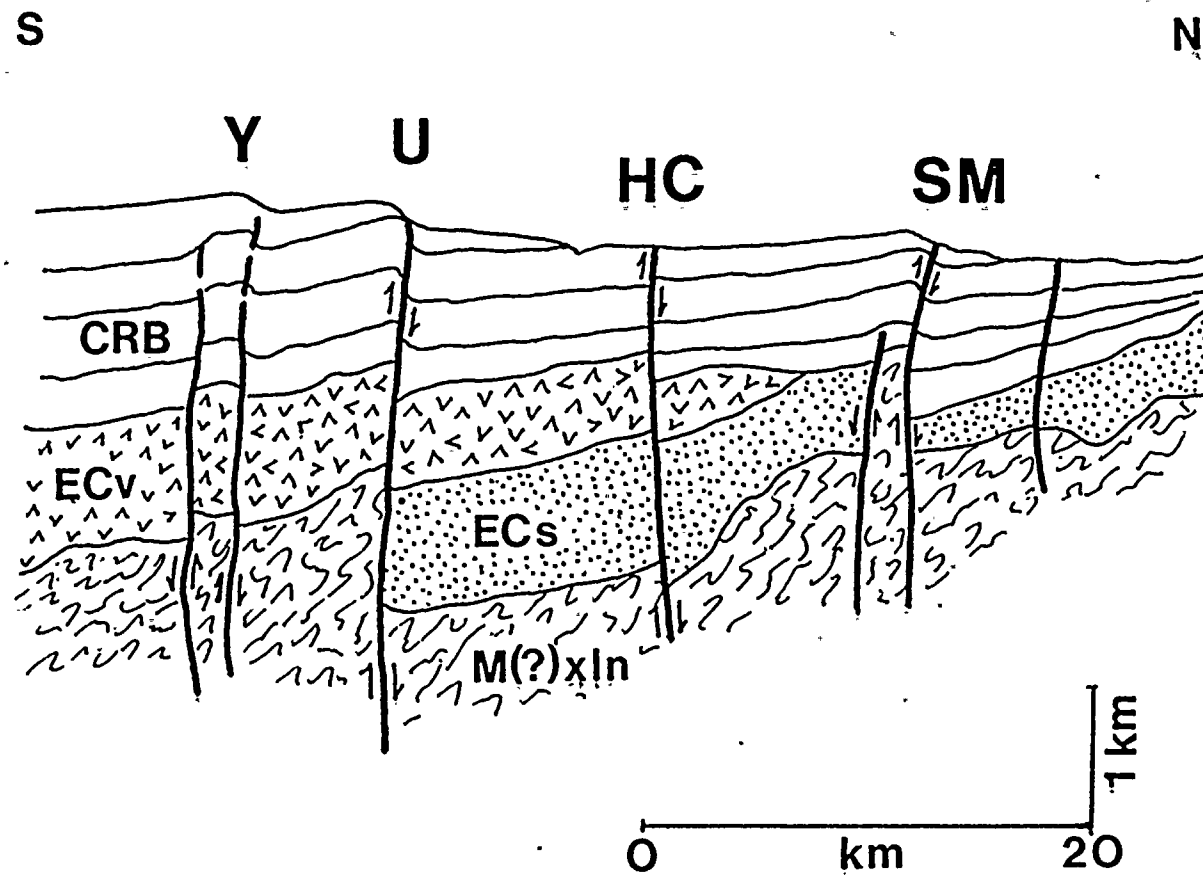


Figure 2.5N-6

"Thick-skinned" tectonic interpretation for Columbia Plateau folding and faulting from Bentley (1977). Note vertical exaggeration.





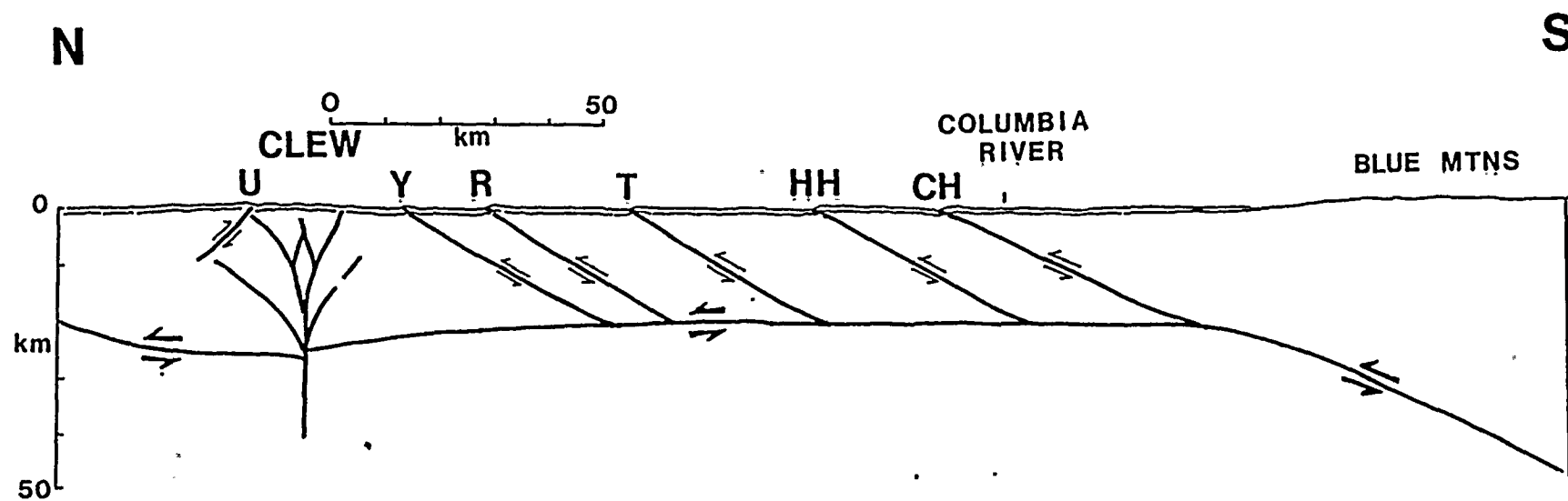


Figure 2.5N-7 "Thin-skinned" crustal decollement interpretation for Columbia Plateau deformation from Laubscher (1981; 1980 ms).



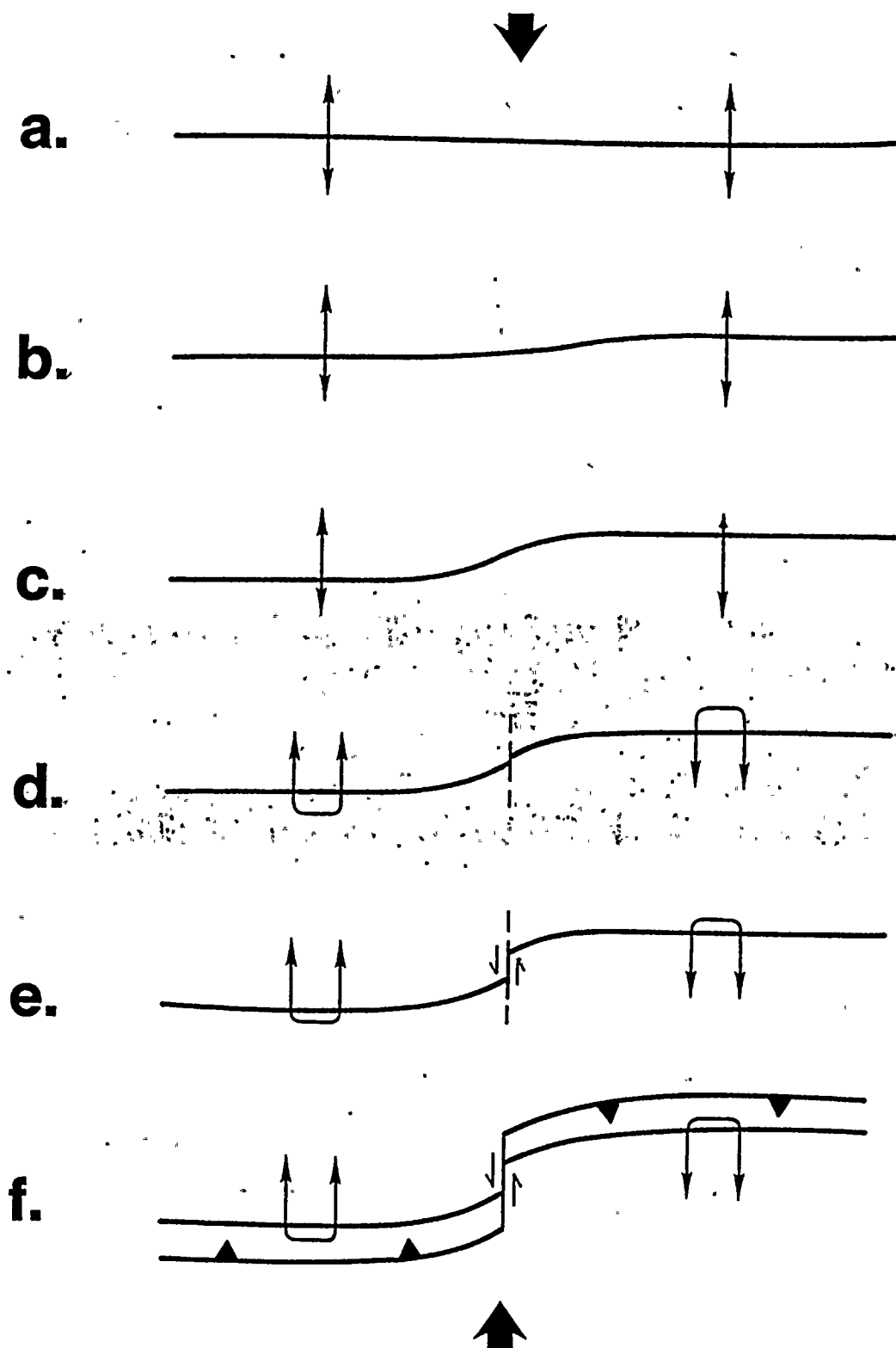


Figure 2.5N-8

*Hypothetical stages in the kinematic development of doubly-vergent anticlinal structures on the Columbia Plateau (e.g. Umtanum, Gable Mountain). Large arrows represent direction of north-south shortening responsible for folding and secondary faulting. Length of arrows on fold axial traces indicates relative dip of fold flanks (the shorter the arrow, the steeper the dip).*

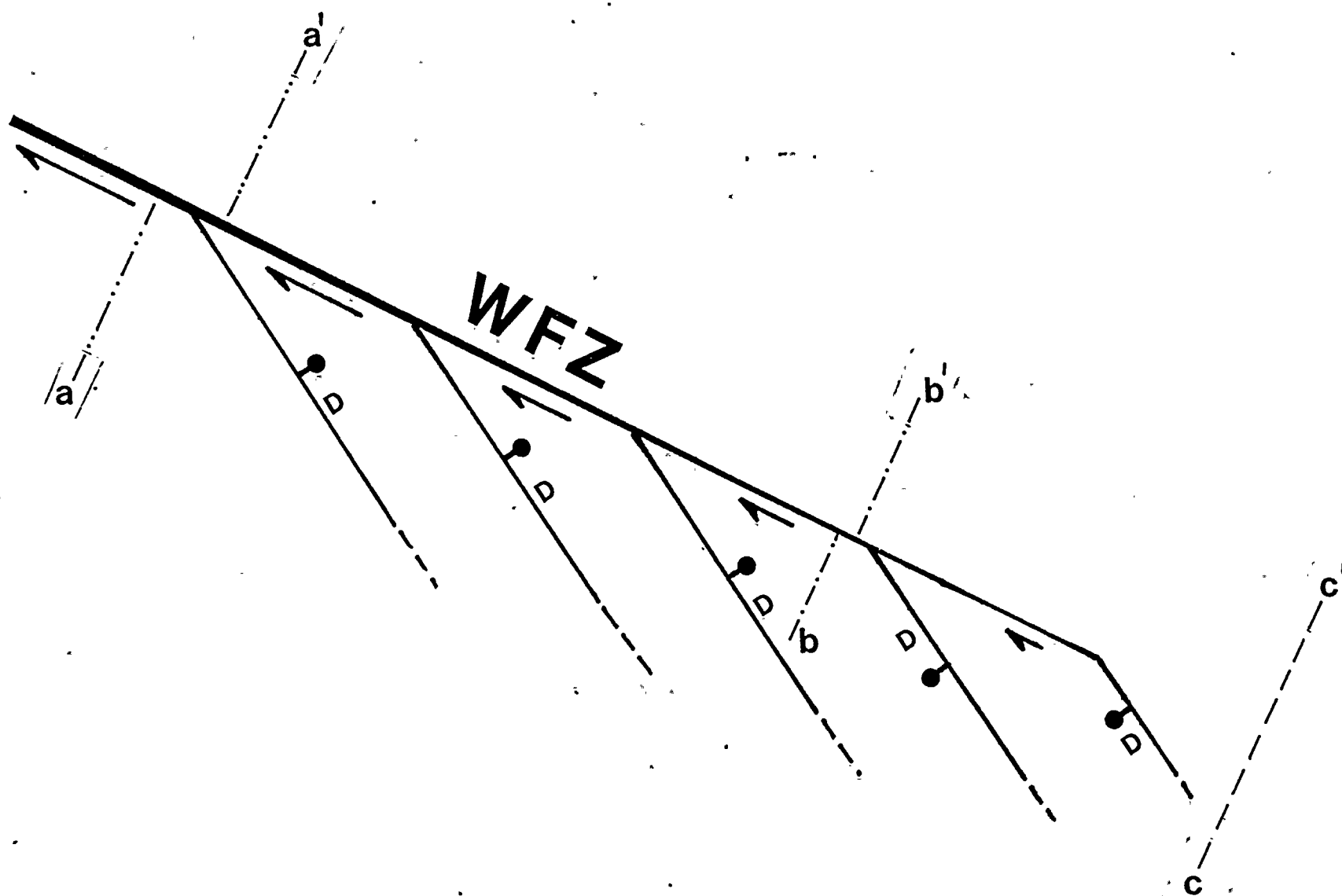


Figure 2.5N-9

Diagrammatic kinematic interpretation of the Wallula fault zone (compare with Figure 5). Dextral displacement along the Wallula zone is accounted for by differential extension of the southern wall of the zone across en echelon normal faults. AA', BB', CC' illustrate hypothetical linear features with progressively greater offsets to the northwest.



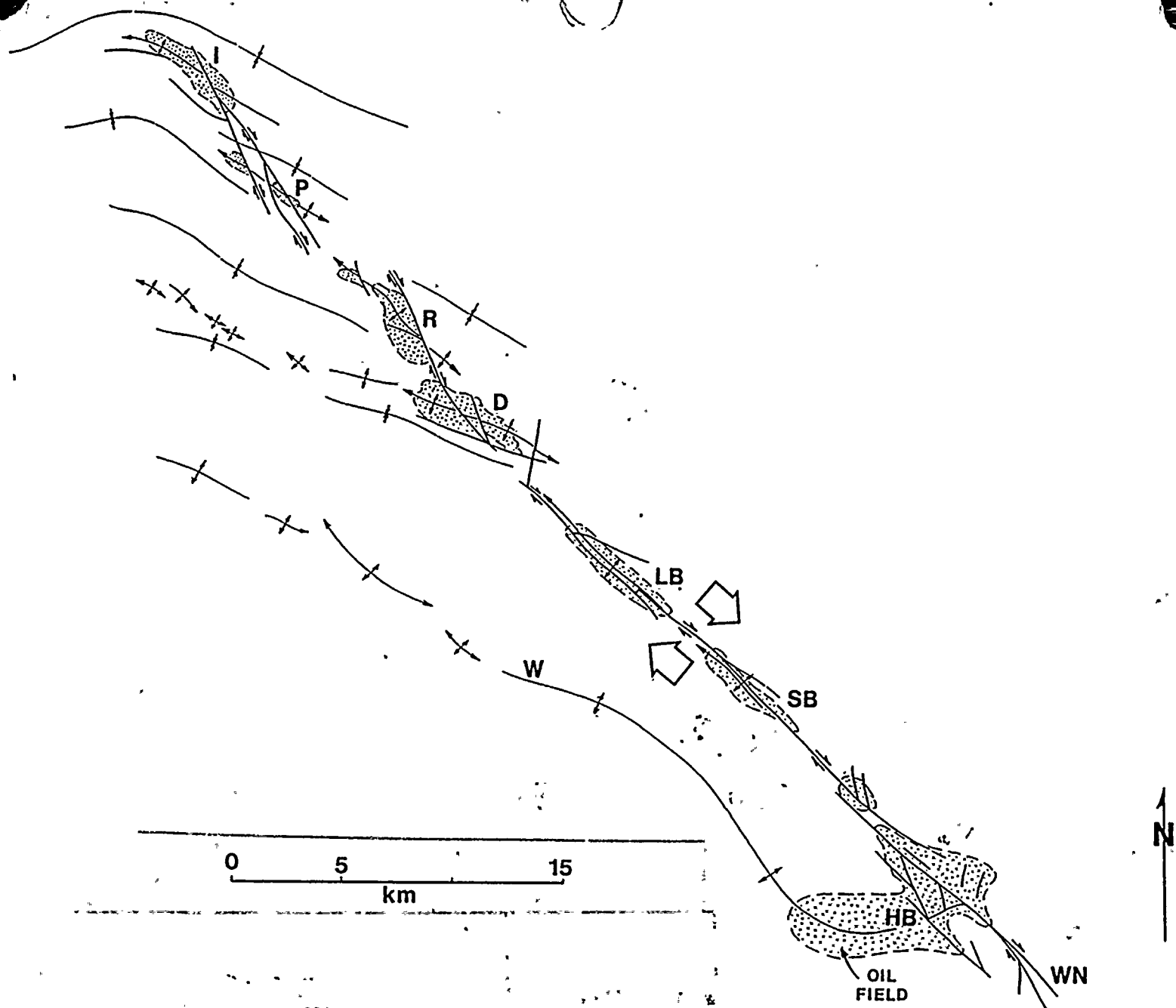
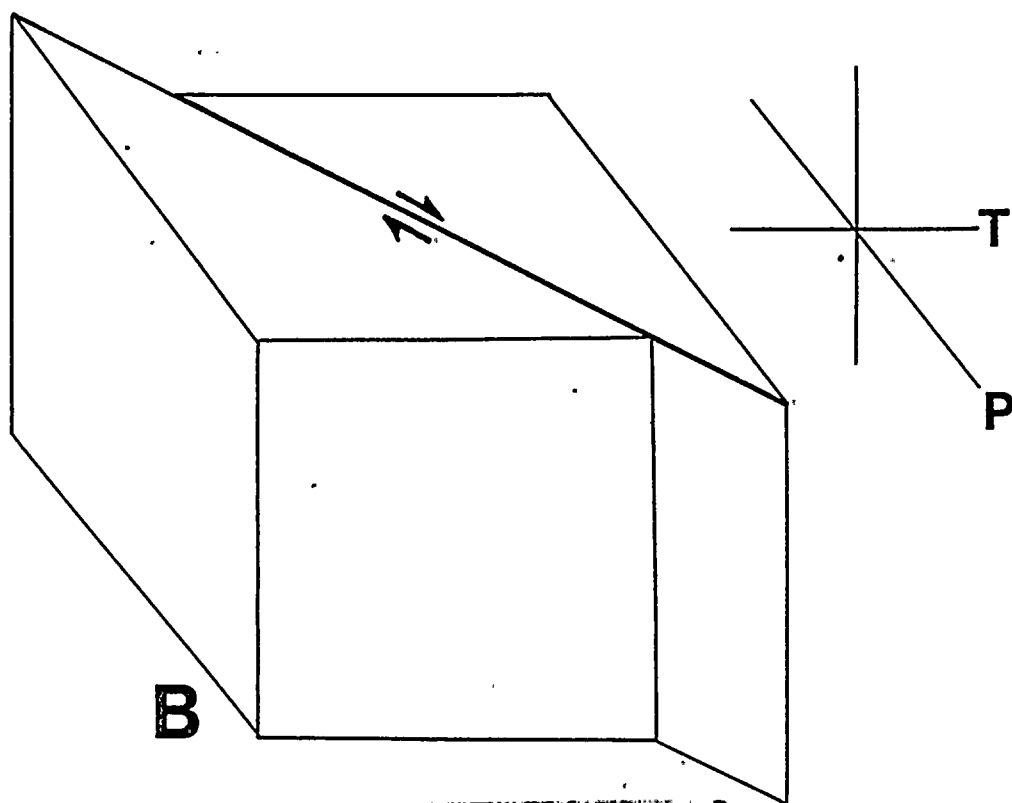
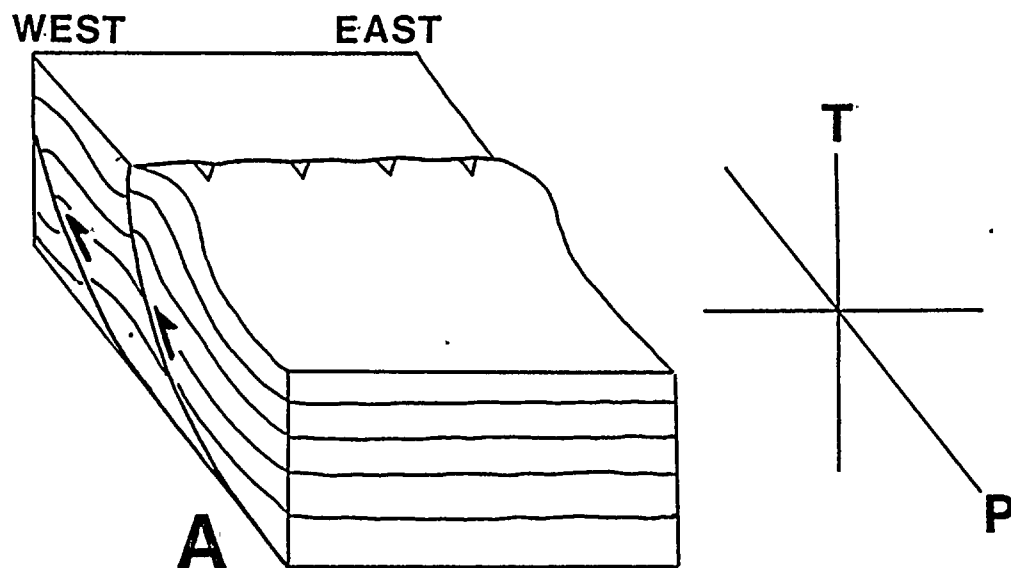


Figure 2.5N-10 Generalized tectonic map of Newport-Inglewood fault zone, Los Angeles Basin, California (after Harding, 1973; Yeats, 1973).



$$\text{CLEW} = \text{A} + \text{B}$$

**Figure 2.5N-11** *Kinematic interpretations of differential response of plateau stratigraphic units (A) and deeper "basement" rocks (B) to north-south compression in the Columbia Plateau. Although a simple transcurrent fault is shown offsetting basement rocks, such faulting may be considerably more diffuse and the width of the zone of shearing may increase northwestwards from CLEW structural domain II to domain I (see Figure 3). The structural elements which define CLEW (Laubscher, 1977, 1981) are interpreted as interference phenomena between the two styles of deformation. Faulting characteristic of B appears to extend to surficial levels within CLEW domain III, the Wallula fault zone.*





APPENDIX 2.5-0

MODELS OF THE DEVELOPMENT OF YAKIMA DEFORMATION

by Dr. H. P. Laubscher .

August 1981

APPENDIX 2:50TABLE OF CONTENTS

	<u>Page</u>
1.1 INTRODUCTION	2.5-0-1
2.1 THE REGIONAL FRAME	2.5-0-1
3.1 KINEMATIC MODELING: THE GENERAL PROBLEM	2.5-0-2
3.1.1 MATERIAL BALANCE	2.5-0-4
3.1.2 STRESS FIELD AND TRANSPORT FIELD	2.5-0-5
3.1.3 RELATIONSHIP OF VARIOUS PARTS OF A TRANSPORT FIELD	2.5-0-5
4.1 MODELING EN ECHELON FOLD BELTS	2.5-0-7
5.1 LOCAL OBSERVATIONS	2.5-0-9
5.1.1 DEFORMATION STYLE AND REHOLOGY	2.5-0-9
5.1.2 THE TIME OF DEFORMATION	2.5-0-11
6.1 A QUALITATIVE ASSESSMENT OF CP KINEMATICS BY INSPECTION	2.5-0-12
7.1 A TENTATIVE QUANTIFICATION OF THE KINEMATIC MODEL	2.5-0-15
7.1.1 THE COMPRESSION OF INDIVIDUAL FOLDS (FIGURE 10)	2.5-0-15
8.1 THE IDOL BLOCK BELT	2.5-0-20
8.1.1 THE IDOL BLOCK BELT (FIGURES 13, 14)	2.5-0-21
9.1 THE KINEMATICS OF THE IDOL MOSAIC	2.5-0-30
10.1 DYNAMICS OF A BLOCK MOSAIC	2.5-0-32
11.1 MAPS OF KINEMATIC DEVELOPMENT IN 8 STAGES	2.5-0-32
11.1.1 INITIAL MOVEMENTS AT THE BOUNDARIES OF YAKIMA BLOCK YA-8	2.5-0-33
11.1.2 INTERNAL DEFORMATION OF THE YAKIMA BLOCK YA-8	2.5-0-34

<u>TABLE OF CONTENTS (Continued)</u>	<u>Page</u>
11.1.3 SUMMARY OF IMPORTANT POINTS IN THE MAP-VIEW KINEMATICS OF THE COLUMBIA PLATEAU	2.5-0-41
12.1 DEVELOPMENT OF THE YAKIMA FOLD SYSTEM, CROSS SECTIONS	2.5-0-42
13.1 THE DEVELOPMENT OF CRUSTAL STRUCTURE IN THE CP AND ITS INFLUENCE ON THE DYNAMICS OF YAKIMA DEFORMATION AT DEEP LEVELS	2.5-0-45
13.1.1 A COMPLETE DEFORMATIONAL SYSTEM CAN BE MODELED, EVEN SCHEMATICALLY, ONLY IF VARIATION WITH DEPTH IS INCLUDED	2.5-0-45
13.1.2 PRESENT-DAY CRUSTAL STRUCTURE IMPLIED BY THE GEOPHYSICAL DATA (COMPARE FIGURES 13, 17)	2.5-0-46
14.1 A COMPARISON OF SUSPECTED EOCENE CP GRABENS WITH SIMILAR STRUCTURES ELSEWHERE	2.5-0-51
15.1 DEEP STRUCTURE OF YAKIMA DEFORMATION: A COMPARISON OF CLEW WITH THE ANDES OF VENEZUELA	2.5-0-54
16.1 CONCLUSIONS	2.5-0-55
17.1 REFERENCES	2.5-0-57

LIST OF FIGURES

<u>Number</u>	<u>Title</u>
2.50-1	The Cenozoic kinematics of the Pacific NW, from Eaton (1979). Elements of Columbia Plateau deformation added.
2.50-2	Experimental extensional block mosaic, from McGill and Stromquist (1979).
2.50-3	Elements of rigid block motion, from Laubscher (1965), map view.
2.50-4	Elements of decollement kinematics, cross section, from Laubscher (1965).
2.50-5	"Flower-structure" in a wrench fault zone, from Harding and Lowell (1979).
2.50-6	Small-scale structures in the Columbia Plateau folds.
2.50-7	Plastic relief map of the western Columbia Plateau and the adjacent highlands.
2.50-8	Decollement, ramps, blind thrusts and kink folds in the Jura, from Laubscher (1977), and possible interpretations of the deep structure of Yakima folds (Figure 8a).
2.50-9	Kinematics of the Columbia Plateau and its surroundings, tentative concepts.
2.50-10	Estimates of compression in Umtanum Ridge, after Bentley (1977).
2.50-11	Axial plunge of Rattlesnake Hills.
2.50-12	A cut-paper kinematic model of rigid-body Yakima tectonics.
2.50-13	The IDOL block belt.
2.50-14	Kinematics of the IDOL block belt.
2.50-15	Map view of kinematic development in the western Columbia Plateau (Yakima folds).

LIST OF FIGURES (Continued)

- 2.50-16 Cross. section of the kinematic sequence of Yakima folds.
- 2.50-17 Crustal isopachs of the Columbia Plateau.
- 2.50-18 The Eocene Pasco graben system. .
- 2.50-19 Domes and grabens, after Cloos (1939).
- 2.50-20 Crustal thinning in graben areas (after Illies, 1975; Ziegler, 1977; Hill, 1978) and early doming followed by later subsidence (Ziegler, 1977).
- 2.50-21 A deep crustal section through the Venezuelan Andes, after Wittke (1977).
- 2.50-22 CLEW, simplified as a small-amplitude crustal fold.
- 2.50-23 A superposition of Figures 21 and 22.
- 2.50-24 CLEW crustal upfold and flanking downfolds.



## 1.1 INTRODUCTION

This report is an attempt at modeling deformations in the Columbia Plateau (CP), primarily their kinematics, but also with some considerations of their dynamics. Detailed information available on the Columbia Plateau itself, especially information contained in WPPSS PSAR Amendment 23 (1977) is presented first. However, in the course of analysis it soon became evident that the interpretation must be enlarged to involve the behavior of the surrounding tectonic units and their relation to the plate boundaries. The scope of the analysis had to be widened in both space and time. The central theme remains Columbia Plateau deformation, and it is modeled in more detail and sophistication than the regional frame.

A particular problem is the deep structures associated with observed surface deformation. For an educated guess - and this is all that is possible at present - geological and geophysical information must be combined and viewed in combination with what is known about similar situations in other parts of the world. These deep structures are important, of course, for earthquake generation, and deserve considerable interpretational effort.

## 2.1 THE REGIONAL FRAME

An up-to-date review of the geological development of the Pacific NW in the light of plate tectonics concepts is given by Davis (1977), and is accompanied by an extensive bibliography.

Eaton (1979) has attempted to fit late Cenozoic structural events, and particularly spreading, in the western United States into a plate tectonics framework. The time of initiation of spreading in the southern Basin and Range province is not well fixed though extensional block faulting seems to have begun about 17 my ago. It began to wane 10 my ago. Extension in the northern Basin and Range (BR) province, including the Columbia Plateau (CP), also began about 17 my ago, while the Mendocino triple junction lay far to the south. Spreading in large parts of the western US continues today, but with a spreading direction different from that active at earlier times (Eaton, 1979, Figure 7).

The relations between the North American, Farallon and Pacific plates underwent various, sometimes drastic changes in the course of events. As a consequence, the various regions of late Cenozoic extension today differ greatly in their topography, structure, and geophysical properties.

This is particularly true for the Columbia Plateau. Between 17 and 14 my ago it was extended in a WSW direction as evidenced by the dyke swarms associated with the Columbia River (CR) basalts. This extension direction agrees with the general direction of extension in the western US at that time (Eaton, 1979, Figures 2a, 3b, 7b). The subsequent deformation of the CR basalts, which is the main concern of this report, is of an entirely different nature, and yet is evidently related to the other plate boundary deformations in the western US. In Eaton's perspective (1979, Figure 7d)), dextral shearing along the Pacific-North America plate boundary now drags along and rotates dextrally a number of splinters of the North American Plate around a pivot somewhere in Manitoba. This regional picture agrees in important ways with the inferences based on the local analysis of CP deformation. In the south, lithospheric rock masses were moved away from the great centers of rifting and crustal stretching such as the Rio Grande rift and the Battle Mountain thermal high-Snake River plain, and were piled up in the north against the highlands of northern Washington and British Columbia. The result is a NNW directed compression in the Columbia Plateau, in agreement with the predominant ENE trend of its folds and also with inferred dextral and sinistral movements along NW and NE trending lineaments, respectively. The Neogene kinematics of the Pacific NW in this view is dominated by adjustments within a mosaic of blocks subjected to NNW compression. Release of this compression to some extent followed pre-existing structures (zones of low strength) though it was dominated by the regional stress field. The structures reflect the stress trajectories and boundary constraints, which, in turn are governed by inherited structures, though often in a complex and unexpected way.

### 3.1 KINEMATIC MODELING: THE GENERAL PROBLEM

Geologic deformation is characterized by belts of concentrated deformation, separating slightly deformed, virtually rigid domains. Globally, this principle is a central tenet of plate tectonics, but similar observations are valid on a smaller scale. Plates and plate boundary zones may be sub-divided into sub-plates and blocks and sub-blocks. These in turn may be recognized to consist of even smaller sub-units with their own comparatively mobile boundary zones etc.

In modeling the kinematics of a region in terms of a block mosaic the first choice concerns the degree of refinement that is desirable for a specific purpose. In this report the Columbia Plateau will first be treated in a



semi-detailed way, then it will be embedded in a more crudely defined belt of blocks that connects the B & R with the Pacific plate boundary. In addition, there will be some considerations which transcend these levels of refinement both towards an even higher regionality on the one hand, and towards local details on the other.

Rigid-block kinematics consist of translations and rotations which, except for trivial cases, are geometrically not quite compatible among the various blocks of the system. It is these incompatibilities of rigid motions that must be adjusted for in the deformation zones. Large-scale incompatibilities in the brittle domain are accommodated along block boundaries of decreasing grain size down to fault gouge. As modeling requires discretization (dissection of the continuum into rigid blocks) of limited resolution, incompatibilities cannot be completely eliminated but will be shown and discussed (compare Hildebrand-Mittlefehldt, 1979).

The type of difficulty that arises is well illustrated by McGill and Stromquist (1979), e.g. Figure 7b, which depicts an experiment. In that figure (redrawn as Figure 2 of this report), the mass that has moved to the left with respect to its surroundings may as a first approximation be considered as one block, bounded on the right by an extensional fault, and near the upper and lower margins of the figure by dextral and sinistral strike-slip ("transform") faults respectively. On the left, the mass moves into free space; in nature this would be a thrust fault if the free space is occupied by some competent material, or it may be an island arc that is largely decoupled from a receding subduction zone (e.g. Cascades; compare Figure 1e) and overrides the subducted slab with little frictional resistance, leaving in its wake an extended back-arc domain; or it may be space offered by a plate moving away from a ridge (e.g., Juan de Fuca Ridge).

This first-approximation block is subdivided by a network of faults into ever finer sub-units, and its boundaries are broad zones of distributed deformation rather than single clear-cut faults. This is particularly true for the lateral strike-slip boundaries which are a clear kinematic necessity though hard to define in the experiment and would not be directly mappable in nature; here they must be inferred from the general distribution of mapped faults and folds.

Poorly defined boundaries of this type are the "postulated distributed transform structures" of Eaton (1979, Figure 1 and Table 1) and also the block boundaries of the CP and



its surroundings are of this nature. Such boundaries cannot be simply mapped but clearly exist and play a key role in the kinematic development.

In choosing boundaries of blocks and subblocks there may be a degree of arbitrariness as one lineup of apparently (on the mapping scale) unconnected structures is preferred to another. This difficulty arises in block modeling generally and in the blocks surrounding the CP in particular. The reasons for choosing such boundaries will be given, but there is doubtlessly much room for improvement. However, the aim of the exercise is to sketch the general relationship of deformation in the CP with the plate boundary, and this is not sensitive to a large variation in the block boundaries.

While none of the block mosaics occurring in nature consists of discrete, rigid bodies, it is nevertheless necessary to begin considerations with simple rigid bodies and relax this condition of rigidity as the necessity arises. The more important topics to be discussed are:

1. Material balance.
2. Stress field and transport field (deformation permitted at block boundaries).
3. Relationship of various parts of a transport field.

### 3.1.1 MATERIAL BALANCE

Matter is conserved during deformation. For shallow deformation down to a depth of about 10 km this implies conservation of volume or, on a cross section, of area, within the limits of observational errors. Particular applications are:

- a) Matter accumulated in compressional features (which are sinks in a transport field) must be taken away from extensional areas (the sources of the field). Sources and sinks in a closed system are of equal magnitude. If the system is not closed, movement of matter across its boundaries may be estimated. (Figures 3, 4.)
- b) Compression (shortening) may be estimated on cross sections (Figure 4.):
  - 1) Curvimentrically, by restoring the undeformed continuation of beds and measuring the

difference in distance across the deformed feature before and after deformation ( $D_s$ ).

- 2) Volumetrically (actually areally on cross sections), by measuring the volume of matter squeezed out above the undeformed horizon ( $D_v$ ).

$D_v/D_s$  gives a figure for the thickness ( $z$ ) of section involved in the deformation. This is particularly important for the question of how much decollement on the base of the Yakima basalts is involved in CP folding. This is one of the rules for the construction of "balanced sections."

### 3.1.2 STRESS FIELD AND TRANSPORT FIELD

Principal stress trajectories and the geometry of the stress field: the geometry of deformational features in a general way defines the stress field in which deformation has taken place. Although all structures with finite displacement grow in a stress field that varies with time, phases of movement may often be recognized where deformation took place under reasonably constant conditions. In particular:

- a) The overall bearing and plunge of anticlinal axes and strike of normal and thrust faults coincides with the intermediate principal stress trajectory  $\sigma_2$ . In shallow deformation another trajectory also is horizontal and perpendicular to  $\sigma_2$ . For anticlines and thrusts the other horizontal trajectory is the principal compression or  $\sigma_1$ .
- b) Deflection of structures, particularly folds, define local or regional boundary conditions for the stress and more pronouncedly the transport field, such as pre-existing material, irregularities (faults, edges of incompetent beds, etc.), or block boundaries of a higher order. This is a geological application of the "de Saint-Venant principle" of mechanics, which states that the domain of influence of an irregularity on the stress field is of a size comparable to that of the irregularity itself.

### 3.1.3 RELATIONSHIP OF VARIOUS PARTS OF A TRANSPORT FIELD

The local vectors of the transport field are assumed to have the direction of  $\sigma_1$  or  $\sigma_3$  (in extensional areas) and a length corresponding to the amount of deformation as established by material balance calculations. A general

field of transport is very complex. Fortunately for shallow geological deformations, several simplifications are usually possible:

- a) Compression and extension (sinks and sources) may often be assigned a geometrically simple distribution, at least at the level of quantitative sophistication called for by the quality of geological and geophysical data. Often their domains are separated, and frequently they are confined, particularly to boundaries of blocks (or plates) of insignificant internal deformation. These block boundaries are, in fact, always diffuse to some extent, even if shown on a map as a line, and sometimes they cannot be defined by direct observation. They often must be inferred from evident differences of movement across a zone of some width (compare p. 3). In other words: block boundaries may sometimes be approximated by first order discontinuities in the vector field of transport, and more often by second or higher order discontinuities. In these cases, there is a finite gradient across the boundary. Thus, the CP may be subdivided into a number of blocks of different orders of importance, and with boundaries of different orders of discontinuity. The same holds for the surroundings of the CP (IDOL - mosaic, Figure 14).
- b) The 3-dimensional field of transport may be separated to a large extent into component 2-dimensional fields that may be modeled on a map view or cross section. Thus, the distribution of sinks (compression in folds and thrusts) and sources (extension particularly across normal faults) in the CP region may be modeled on a map, and the distribution of vertical components of movement may be superposed on cross sections.
- c) The rigid blocks or polygons in a plane 2-dimensional field move by a superposition of translations and rotations. In the general case this leads to an extremely bewildering result. However, there usually is a hierarchy of quantitative importance of both translations and rotations, and a rational analysis demands that the first order ones be dealt with first, that the error between a first order model and observed quantities be estimated, and that this error be



then reduced by superposing second order movements - again an iteration procedure that should be continued only as far as the quality of the information warrants and the occasion demands. With some experience, the first guesses may not be too bad, although generally some trials are necessary. The process should begin with first order translation as it is both easier to model and geometrically simpler to accommodate in nature. Rotations invariably lead to rigid-body incompatibilities in compressional domains which are eased by dilatancy on the one hand, and diffusion of adjustments on the other.

#### 4.1 MODELING EN ECHELON FOLD BELTS

One of the many difficulties in modeling is that of en echelon fold belts such as CLEW. Because of their 3-dimensional complexity and non-linear development (changing material distributions and boundary conditions) little is known about them theoretically. Insight of a largely qualitative and intuitive nature must be sought by comparison with known natural and experimental belts.

Intriguing cross-sectional and plan-view deformational pictures are provided by the sandbox experiments of Emmons (1969) although the boundary conditions of his divided container are not very realistic. The main point that is illustrated is oblique and non-parallel mass transport on warped fault surfaces which anastomose and dissect the sand body into an ever finer mosaic of quasi-rigid blocks ("reticulation"). Due to the complex mass transport, domains of compression are followed closely by domains of extension.

Evidently, mass balance considerations on cross sections are rather inadequate in this situation, and only semi-quantitative estimates are possible.

Comparison with such illustrations as Figure 6 of Harding and Lowell (1979), here redrawn as Figure 5, and Figures 3 and 4 of Emmons (1969), suggest an estimate of depth for the basal shear that drives the en echelon deformation. The compressive deformation is contained in a wedge whose boundary dips at about 45° (a little less in Figures 3 and 4 of Emmons). The depth to basal drive is consequently about half the width of the fold belt. Similar results may be inferred from other publications.

En echelon structures are common because blocks and subblocks of the earth's crust usually move somewhat differentially, and the earth is generally horizontally or subhorizontally layered to some extent with prominent competent and incompetent intervals at various levels.

It follows that en echelon belts of different depths of decollement may be superposed.

In CLEW this is clearly the case. The total width of the belt is 30 - 40 km but the subbelt designated as RAW in Figure 15e consists of brachy-anticlines less than 5 km or even 3 km wide which points to a depth of decollement of less than 2 km or approximately at the base of the Yakima (CR) basalts. There may be local decollement horizons or even gradational decollement intervals at intermediate depths. This is suggested, e.g., by the Selah Butte trend of brachy-anticlines (see Figure 15, Stage 7 and Figure 24).

In addition to variations in the depth of superposed en echelon belts, there is a variation of angle between the axes of individual brachy-anticlines and the average strike of the entire belt. Angles of 30° or 40° are frequent (Wilcox et al., 1973, Figure 9, Figure 11) but angles of less than 20° or even 10° are characteristic of some belts such as the Newport-Inglewood trend (Harding, 1973, Figure 7). Much seems to depend on the relation of the local stress field to local inhomogeneities such as faults, or basins and highs; later en echelon folds tend to have smaller angles (Wilcox et al., 1973, p. 79). For the deep en echelon belt of CLEW the angle is typically a little more than 20° (Yakima Ridge, Rattlesnake Hills) but for RAW it is usually less than 10°. For HOOK it is again 20° to 30°.

While short folds (brachy-anticlines) are typical for oblique shear with a compressive component (oblique-convergent boundary), they are not the only structures but are usually affected by and interfere with a maze of other complex faults (compare Harding, 1973, Figure 7; Harding and Lowell, 1979, Figure 6). In experiments such faults seem to have various origins. In the clay experiments of Wilcox et al. (1973) a pattern of conjugate shears develop (synthetic and antithetic with respect to the master shear, also called Riedel shears and conjugate Riedel shears) and bear the usual Mohr relationship to the strain ellipse. Although often irregular in detail, they are very regular as a set.

In the CP the situation is more complex. Wrench movement in RAW is superposed on that in CLEW, and the Yakima folds



affect a large domain that includes CLEW. Each deformational system may be expected to develop its own set of shears which compete and influence each other mutually. Closely spaced joint and shear patterns criss-crossing the CRB are evident from the air and are well represented on topographic contour maps (e.g. sheet Walla Walla, 1:250'000). Topographic features suggest that RAW is affected by small synthetic Riedel shears similar to those shown by Harding (1973, Figure 7) for the Newport-Inglewood trend. It is possible that the Thrall-Wymer-Selah Butte cross-trend of CLEW developed on an early synthetic Riedel shear that subsequently influenced the main deformation (see Figure 15, Stage 7).

As displacement increases, the faults acquire the complex geometry (3-dimensionally warped, reticulating system) and variable kinematic function typical for mature wrench zones (Emmons, 1969).

In conclusion, it is obvious that in the modeling of en echelon zones drastic simplifications are necessary to keep them manageable.

## 5.1 LOCAL OBSERVATIONS

### 5.1.1 DEFORMATION STYLE AND REHOLOGY

Observation on good outcrops bears out what is known from other areas that have been deformed under small overburden and at low temperature, and agrees with the results of deformation experiments under similar conditions in the laboratory. Basalts, as well as inter-flow sediments deformed in an essentially brittle manner. Several types of brittle failure have been observed, and they are schematically illustrated in Figure 6. They are commonly superposed on each other, and sometimes the sequence of superposition may be demonstrated. Mohr-Coulomb type thrust-faults cut bedding at an angle less than 45 degrees (usually even less than 30 degrees) with little or no rotation of the beds. On the other hand, they often occur within a sequence of rotated or folded beds while still maintaining their angular relationship with bedding; these thrusts were rotated or even folded after they had formed. Such folded thrusts are well documented from many fold belts. Particularly interesting are those that may be observed on Manastash Ridge along Interstate 82 and its surroundings. The main thrust exposed in the roadcut is doubtless the one that emplaced lower Yakima on middle Yakima rocks (Bentley, 1977, Figure 18 and 19). It is cut by minor secondary thrusts and is accompanied by

smaller-scale deformation both in basalts and sediments. Interestingly, the direction of thrusting is from north to south, from north of the Manastash fold through its limb towards the core of the fold. Based on the results of mapping by Bentley (oral communication), the examination of aerial photographs, and inspection from the air, other more or less parallel thrusts of the same general nature are present and are responsible for the peculiar topography of Manastash Ridge in this area. The thickness of the section repeated by the main thrust may be estimated from Bentley's figures at 200 m to 300 m, which on the assumption of an original dip of thrust of 30 degrees (now somewhat distorted) results in a horizontal compression of 350 m to 520 m. The other thrusts are smaller, and together the amount of thrusting prior to folding is estimated at about 700 m. This is considerably more than the subsequent amount of compression by folding which, after Bentley (1977, Figure 9), is less than 300 m.

On the map (Shannon & Wilson, 1978), the strike of the thrust faults intersect the strike of the north limb of this typically asymmetric fold at an angle of 20 degrees to the southeast, which demonstrates that between thrusting and folding, the geometry of the stress field at this locality had changed (compare the data from Emmons, 1969, for changing patterns of deformation in strike-slip zones).

Folding is often considered a ductile process, but this is not so under the conditions present when the CP folds were formed. Beds are usually fractured to some degree, and in the more steeply-dipping parts of anticlinal limbs they are often thoroughly brecciated. The folds have usually sharp, although rounded hinges, and as a rule are monoclines rather than anticlines, features which set them apart from the sinusoidal concentric folds of folding theory and schematical textbook illustrations. The CP type folds are the result of shearing, similar to kink bands, with the shear couple acting on layers of competent beds which are rotated. The optimum dip angle for the hinge planes is about 60 degrees (compare Paterson and Weiss, 1977) rather than the 30 degrees for Mohr-type thrust faulting. When the hinges are ruptured, a steep reverse fault may result and be of the type that has been reported from the base of some monoclines, e.g., Saddle Mountain. Although CP folding was accompanied by fracturing of the beds which implies sudden release of elastic energy, displacements are small and distributed through large volumes of rock. Of the other types of faults observed, the strike-slip faults are particularly noteworthy. They are easily identified when horizontally striated; however, striations along strike-slip

faults of known displacement are not always well developed, and sometimes later movements of insignificant strength overprint them. Any steep fault plane or breccia zone may be taken as suggestive of strike-slip faulting. The amount of strike-slip displacement can usually be determined only by mapping and subsequent kinematic analysis (compare Figure 12).

#### 5.1.2 THE TIME OF DEFORMATION

The folds are composed of elements of different trend for which, in some instances, a time sequence can be inferred. The question arises whether the CP fold system is the result of the superposition of deformations due to entirely different stress systems associated with regionally different orogenic situations. A first inspection shows this to be highly improbable. Intra-Yakima unconformities have been reported from isolated locations, e.g., a pre-Pomona one from the Yakima ridge northeast of Yakima (Bentley, 1977, Figure 15.). These local unconformities are probably due to landslides or tilting of blocks at the time of the basalt flows. Important interflow compression does not seem reflected in the overall structural relief. Generally the entire Yakima-Ellensburg sequence, including the Clemans Formation and probably also the Thorp Formation (though this is less certain because of lack of good outcrops on the ridge flanks), are folded conformably. Changes of deformational style (thrusts/folds) and of the geometry of the stress field (especially locally) are commonplace in the course of one individual orogenic event and are easy to understand on general grounds: Each break in continuity because of early faulting and any change of geometry because of folding, create new boundaries and boundary conditions. Folds must be visualized as growth features with nonlinear development. Superpositions like those described from Manastash ridge are attributed to different states of the same orogenic event. The test for this conclusion, which is based on inspection, is whether or not the essential features of the CP system can be fitted into a unified kinematic model. A layer of the Thorp Formation has been dated as 3.7 my (Bentley, 1977, Table 1). On Craig's Hill in Ellensburg (Bentley, 1977, page 12) the Thorp Formation is overlain unconformably by the Naneum Conglomerate which is composed of coarse basaltic pebbles suggesting the existence at that time of Yakima basalt ridges although the unconformity may be due to scouring by tributary streams that carried pebbles from the Wenatchee Mountains (Bentley, 1977, page 12). Similar basaltic conglomerates or coarse gravels are found on some of the ridges (oral communication by F. Kienle), and were shown to

me on top of the Horse Heaven ridge where it is crossed by the McBee road by S. Farooqui. Unfortunately there is no way to exactly date and correlate these conglomerates. On Craig's Hill, the Naneum Conglomerate is topped by loess which surprisingly shows remanent magnetism, with reversed polarity, and is, therefore, considered older than 750,000 years (R. Bentley, oral communication). On this very tenuous stratigraphic evidence the main part of Yakima basalt deformation north of Yakima took place between about 3 my and 1 my with some deformation continuing into the younger Pleistocene. Microearthquake activity (Washington Public Power Supply System PSAR Amendment 23) would indicate that the system is still active to some extent even at present.

In some places, deformation seems to be somewhat older. A Thorp gravel layer (3-7 my), apparently undeformed, is reported from the flank of Manastash ridge, and faults near Goldendale are bracketed by lavas of 4.5 and 3.5 my, resp. (compare Davis, 1977, page C-24). Perhaps the main movements 10 - 7 my ago on the John Day fault (Robin, 1977; Davis, 1977, page C-24) should be viewed in this perspective: on the whole, Yakima deformation seems to have begun on the south of the Yakima block (page 33 and following, see also Figures 15 and 16) and proceeded to the north, although exceptions to this rule should be expected.

#### 6.1 A QUALITATIVE ASSESSMENT OF CP KINEMATICS BY INSPECTION

For the sort of iterative, quantitative approach to kinematic analysis as outlined in the introduction, an educated guess by inspection must be made for an initial input. An excellent impression of the entire structural system of the CP may be obtained by looking at the plastic relief map (Figure 7). Because of the young age and the slow erosion of the structures in the desert, topographic relief expresses structural relief semiquantitatively. The CP appears to be subdivided into four main regions:

##### Region 1:

The topographically (and structurally) most conspicuous region occupies a belt up to about 40 km wide which is present from about Cle Elum in the northwest to Wallula gap on the Columbia River in the southeast. This Cle Elum-Wallula belt - or CLEW for short - is traditionally considered a part of the larger Olympic-Wallowa lineament (OWL) (Bentley, 1977, page 3). The existence of this lineament, at least in the often-voiced sense as a boundary between oceanic and continental crust, has been questioned

by Davis (1977, Page 53) and for the time being it would appear wiser to confine it to CLEW which not only exists but is clearly the most conspicuous structure of the CP. It is composed of a system of mostly faulted east-southeast-trending folds, or of fold segments deflected in that direction, where the long east to east-northeast-trending folds enter CLEW. This pattern forms a right-lateral en echelon belt. It indicates deep-seated right-lateral shear that drives a deformable sequence of partially decoupled more superficial layers (Emmons, 1969; Wilcox et al., 1973; Harding & Lowell, 1979). The process is easily demonstrated by pasting tissue paper with some sticky fluid to stiff board that had previously been sawed in half, and moving the board along the cut in a horizontal, right-lateral sense. This demonstration helps visualize the process, but should not, of course, be taken as an experiment reproducing mechanical conditions in the earth. As the paper is folded in some places, it must be stretched in other places to maintain material balance. In the CLEW, compression far exceeds any extension that may also be present. Thus, the two most important components of motion are dextral strike-slip along and compression across CLEW.

#### Region 2:

The triangular region southwest of CLEW, bordered on the other two sides roughly by the Columbia River and the eastern margin of the Cascades, is characterized by a series of long, narrow ridges with an impressively regular spacing of 30 km. The ridges, although somewhat undulating, maintain a generally parallel east-northeast trend up to CLEW where they are deflected, sometimes abruptly, to the southeast. These regular ridges mark anticlines that indicate a rather regular stress field with the trajectories of maximum compression trending north-northwest. The kinematic (transport) vector points to the north-northwest as the folds are deflected dextrally at CLEW. Movement with respect to the northeastern region has been to the north-northwest. The regularity of the features implies horizontal translational movement, and the smaller superposed irregularities suggest some degree of superposed rotation. The direction of movement has a component of compression across CLEW, and a component of dextral strike-slip along it, which is consistent with the findings on CLEW itself.

The narrow ridges are superposed on broad, gentle structures that are about 30 km wide and may be parallel to the ridges, or parallel to CLEW. This bimodal distribution of structural width suggests a bimodal distribution in the

thickness of crustal layers involved in the deformation which, in turn, implies a certain amount of decoupling or detachment at two levels (compare Figure 8, 8a, 16). Such a detachment is already intimated by the en echelon fold belt on CLEW (see above). A first guess would be that the narrow features are due to local decollement at the base of the Yakima basalts, and that the wide blocks have a vertical thickness of at least 10 km and possibly as much as 20 km. The overall structural relief suggests that vertical movements are superposed on the compressional, horizontal ones. As is evident from the geologic history as well as geophysical data, CP has been involved in isostatic adjustments to tectono-thermal events since the beginning of the Tertiary (see p. 27-51).

#### Region 3:

The northeastern region, again a triangular area, is bordered on the southwest by CLEW, on the east by a line that trends approximately north from Pasco to the northern margin of the CP, and on the northwest by the margin of CP (for a more detailed argumentation of block boundaries in the IDOL mosaic that contains this region, see p. 22 and following). In many ways it resembles a subdued replica of the southwestern region, inasmuch as some narrow, widely spaced ridges are present, the most conspicuous one being Saddle Mountain. On the average they strike about east-west and are dextrally deflected at CLEW. Badger Mountain, the very small northernmost fold near Wenatchee strikes northwest. On the average, horizontal translational movement to the north seems to predominate.

#### Region 4:

The eastern region comprises the rest of the CP to the east of the northeastern region. It is deformed only slightly and might be considered practically underformed (although in Figures 13, 14 it is subdivided as part of the IDOL block mosaic). This implies that its western boundary is a zone of slight dextral strike-slip which must be dispersed as no fault is readily discernible.

In order to fully define a kinematic model operative in the CP, all of its boundaries and relative motions with respect to surrounding terranes should be defined as well. In Figure 14 and the accompanying tables and explanations, an attempt is made to define an internally consistent kinematic model. Here it should suffice to say that in principle a variety of boundary movements is compatible with the kinematics of the CP itself. For example, a particularly



simple solution interprets the CP deformations to be nested in a nook of an N-S trending strike-slip system: this solution in its most elementary form was proposed in a previous, preliminary draft of this report for want of more precise information (see Figure 1(d) and Davis, 1977, Figure 7); indeed one may maintain that as a rule in scientific synthesis, that solution should be envisaged pro tempore which offers the simplest explanation. In the case of the CP, subsequent information called for a more complex solution which is presented in the conceptual framework of block mosaic kinematics in Figures 14 and 14a. However, in principle, even in this more complex solution, the CP folds are still in a nook of the dextral strike-slip system that characterizes the western boundary region of the North American Plate (Figure 9). In addition, it should be noted that a predecessor of CP compression formed the late Oligocene - early Miocene Kachess-Naches-Blue Mountains-Aldrich Mountain system (Davis, 1977; see Figures 1(a) and 15, Stage 1 of this report). Although known only in fragments, this system bears a resemblance to the early kinematic model (compare Figures 1, 9) inasmuch as it calls for reactivation on the southern part of the Straight Creek fault zone which at Cle Elum bends into CLEW; what happens below the CR basalts is not known, but south of it there was compression with an average N-S direction.

## 7.1 A QUANTIFICATION OF THE KINEMATIC MODEL

Magnitudes of shortening may be obtained by measuring cross-sections according to the method sketched on p. 3-4. Their quality depends on the quality and quantity of the sections available. Both are generally poor. Supplementary information may be obtained from the topographic relief of the ridges. Strike-slip displacement is not quantifiable directly, as no correlatable features are known that have been dissected, but must be inferred from the difference in compression on the two sides of a boundary. Rotations are even harder to quantify and must often be introduced as corrections of errors created by modeling pure translation. This is the procedure followed in this report: First, pure translation will be quantified. Then the more serious deviations from nature will be corrected by rotations where suggested by inspection.

### 7.1.1 THE COMPRESSION OF INDIVIDUAL FOLDS (FIGURE 10)

The quality of the information available may be gathered from Shannon & Wilson (1973), Figure 4, which shows a cross section through the Columbia Hills ridge near its maximum development. All that can be safely said is that





correlative members of the Yakima basalt sequence are displaced vertically by about 500 m. The slope is covered by landslides, and the nature of the structure must be interpreted from insight gained elsewhere. Shown on Figure 4 is a normal fault with extension reduced by drag. If instead it were a monocline with a dip of 60 degrees the compression would be 290 m, if there were a reverse fault dipping 60 degrees the compression would be 290 m also, but if it were a clean-cut Mohr-type thrust dipping 30 degrees the shortening would be 870 m. A thrust fault with 500 m displacement was penetrated by a drillhole according to R. Deacon (personal comm.). East-northeastward the ridge (Alder Ridge) loses relief and gradually disappears near Umatilla, where on a small but clearly discernible north-south-striking faulted ridgelet, a new east-northeast striking small ridge reappears at Sillusi Butte. From the figures in Shannon & Wilson (1973) topographical relief largely corresponds to structural relief. Thus, compression along this trend seems to fluctuate between 0 m and 500 m. The fluctuations must be due to either rotations or transfer of movement to other ridges by distributed shear. On p. 35-36 (comments on Figure 15) the fragmentation of the Columbia Hills structure is discussed. Outcrops do not permit a detailed analysis, and for a first rough quantification, an average of 300 m of shortening along the entire trend would appear reasonable. The Horse Heaven Hills have a relief of only about 1000 feet. Much of their north flank is hidden by landslides, but seems to dip steeply to the north. A 60 degree monocline would give 170 m of shortening, and I assign about 200 m of compression the Horse Heaven Hills in the model. Toppenish Ridge, like Columbia Hills, decreases in relief from west to east, and is a little smaller than Columbia Hills. It should not exceed an average of 200 m of shortening. The western part of the Rattlesnake Hills (Ahtanum Ridge) is more of an anticline than the monoclinical ridges dealt with so far, and it may in some places have as much as 400 m of shortening. East of Union Gap, the Rattlesnake Hills develop into a tilted monocline with a steep north limb with 300 m relief, and only at its deflection point on CLEW does it rapidly increase relief to more than 2000 feet. The new detailed maps by Shannon & Wilson (1978), show that this area is very complex structurally, but for a first approximation to the translational model, an average shortening of 300 m would appear adequate. Yakima Ridge seems more important. At Selah Gap its relief is subdued, as happens wherever the ridges leave CLEW (compare p. 52, 53), but also because it branches out, in a somewhat diffuse way, into the Selah Butte anticline. (For its relation to the most conspicuous anticline of the whole CP fold set, Cleman Mountain, with a

relief of 3000 feet and an overturned southwest limb, see Figures 15, 16). On the average, a shortening of 400 m should be reasonable for Yakima Ridge.

For the ridges following to the north, cross sections do exist, and some may be directly observed in Yakima gorge. They permit more reliable estimates of shortening. Sections through Umtanum Ridge are presented by Bentley (1977, Figure 21 and Figure 25). In the Yakima gorge, at Wymer, Umtanum Ridge is formed by a well exposed, somewhat box-shaped fold with a steeper, faulted north-limb. A shortening of about 700 m may be measured on the section, and the  $Dv/Ds$  method referred to in the introduction gives a rough depth to the decollement of about 1300 m below the Vantage horizon, which is near to the base of the Yakima sequence. At Priest Rapids the shape of the fold forming Umtanum Ridge approaches that of a tipped monocline with a steep north limb that is cut by a reverse fault. Shortening is about 600 m, and an average of about 6 km of the rock column is involved. This figure is, however, a mixture of basement involved in the tilted south limb, and folding above the base of Yakima. Umtanum Ridge is assigned an average compression of 600 m. The structure of Manastash Ridge at Interstate 82 was discussed on p. 9. A series of southward directed thrust faults was subsequently folded into the north limb of a monoclinial structure. The sum of the structures approaches 1000 m of shortening. However, the thrusts cut the monoclinial axis obliquely and shortening is reduced along the ridge both to the east and west. In the east near Badger Gap, Manastash Ridge approaches the Saddle Mountains which follows it to the north and is separated from it by slight topographic relief and the Hansen Creek fault zone (Bentley, 1977, Figure 12). Exposures are poor, the aerial photographs are not very helpful, but mapping by Bentley (1977, Figure 11 and Figure 12) discovered a structural relief that, here, far exceeds topographic relief. If Manastash Ridge is to maintain a level of shortening comparable to that found on Interstate 82, then the Hansen Creek fault must have more of a thrust fault character than assumed by Bentley (1977, Figure 11), which on the information available is quite possible. Before it reaches the Columbia River, the Manastash-Hansen Creek structure swings to the southeast and somehow joins Umtanum Ridge. An average of 800 m of shortening is assumed. Saddle Mountain (Bentley, 1977, Figure 27) is an asymmetrical, somewhat box-shaped anticline with a steeper north limb that is cut by a reverse fault. Its structural relief is 280 m; its measurable shortening is 230 m, and the estimated depth to decollement below Saddle Mountain is 1500 m, again somewhere near the base of the Yakima basalt



group. Saddle Mountain is by far the most important structure of the northeastern region 3, and east of Sentinel Gap its relief begins to diminish until it is hardly recognizable east of Skootenay Lake. The eastern boundary of region 3 would pass between Skootenay Lake and Paradise Flats. West of the Columbia River, at the margin of the Kittitas Valley depression, the Saddle Mountains disintegrate into a series of dextral en echelon brachyanticlines: Boylston, East Kittitas, and Whisky Dick ridges. Thereupon it passes into the structures of the Wenatchee Mountains which are a broad uplift bordered by flexures and somewhat faulted internally. The rest of the little folds of the northeastern region 3 are of insignificant shortening which probably totals less than 200 m.

To summarize, the total translational shortening between the Columbia Hills structure in the south and the Kittitas valley depression in the north may be estimated at 2.8 km, and if the Saddle Mountains-Mission Ridge (Wenatchee Mountains) to the north is added, the total is about 3 km. The information on which these estimates are based is poor except where structures are cut by rivers or highways, but nevertheless the order of magnitude should be correct as structural relief is small and material balance considerations do not permit drastic deviations. Even if a revision on more detailed and reliable data were to increase the figure to 5 km, this would still be small compared to other compressional belts.

These figures, then, are our best and fairest input into the translational part of the iterative procedure to approximate the true kinematics quantitatively. If these NNW-translations are performed on a cut-paper model (see Figure 12 and explanations on page 19) with the further assumption that both CLEW and HOOK are fixed boundaries, discrepancies with nature are obvious. The most glaring discrepancy, noticed immediately by comparison with any geological or topographic map (e.g. Figure 7), is the piling-up of shortening components in the southeastern part of CLEW and the SW part of HOOK by the translational model (oblique convergence, compare Figure 3). There are several possible contributions that help remove this discrepancy, but along CLEW the most important are probably dextral rotations. Their pivots should be somewhere north and west of the southern part of CLEW, if the desired correction is to be achieved. This, fortunately, harmonizes with the generally dextral system of the Pacific NW. Indeed, the dextral couple acting across the Columbia Plateau makes a certain amount of dextral rotation all but inescapable. Discrepancies may be eased also by lateral escape of matter



in adjacent blocks of the incasing block mosaic, and this seems to apply particularly to HOOK, see Figure 14a and p. 40.

For a crude assessment of the magnitude of the rotation, Rattlesnake Hills will be examined as an example (Figure 11). For a first attempt take the pivot at the base of the "R". The southeast trending part of the Rattlesnake Hills should have a shortening component of 200 m perpendicular to strike, according to our tentative translational model. In reality, there is a remarkable axial plunge to the southeast and shortening is reduced to practically nil at the southeast end of Red Mountain, 25 km from the pivot. This reduction is achieved by a clockwise rotation of a little less than  $1/2$  degree. The same rigid rotation adds another 150 m of shortening to the 300 m translational shortening at point 3629, an addition that is probably distributed in the overall complication of the area. By shifting the pivot and introducing other refinements, better results may be obtained, but this is not called for by the quality of the information. By applying such very slight rotations to the other ridges on CLEW, with modifications appropriate for each case, the observed axial plunge of the folds as they cross CLEW is achieved.

To reduce compression normal to CLEW to essentially zero at Wallula Gap in correspondence with observation, a regional rotation must be superposed on the local ones, compare p. 38-40.

Such simple kinematic concepts are best modeled on a transparent sheet of paper (Figure 12). A simplified map of the main structures is drawn, and the paper is cut along a combination of structures assumed to have moved as a kinematic unit. The area (= block; for simplicity usually a polygon) is then moved by the required amounts of translation and rotation, either to scale, or at an exaggerated scale as in Figure 12. The stages of kinematic sequences are added one after the other, and at each stage, a copy is made for record. In this way, a quantitative kinematic sequence model is obtained.

In Figure 12, the sequence is assumed to have proceeded from N to S whereas on p. 32 and following a more complex development is favored, with the ridges forming essentially in the opposite (inverse) order. However, for illustration of concepts and techniques this is irrelevant. The amounts of movement are easily read as (if copied on a blank background) shortening (superpositions) result in light-gray stripes, extensions (where the background is exposed) result





in black stripes (not shown in Figure 12), strike-slip motion appears as displacement of the original margins of the sheet, and rotations both as tapering stripes of shortening and angular misfits on the original margins. It is obvious that by combining the translations with slight rotations, shortening along CLEW can be made to vanish at Wallula Gap. Compare Figure 7.

Such models are useful for visualizing the tectonic consequences of rigid body motions. They do not permit, of course, modeling distributed deformation such as that of Figure 2, or the Columbia Plateau realistically.

### 8.1 THE IDOL BLOCK BELT

For an introduction into the kinematic problems of the terranes encasing CP, see Figure 9. Shown in solid lines is the simplest dextral system which is compatible with the Yakima folds, as shown by Laubscher (1977, Figure 5). The reader was cautioned at the time "that nature must be expected to be much more complex than that. All that the extrapolations imply is that some sort of dextral shear - perhaps widely distributed - should be looked for north of the western margin and south of the eastern margin." Figure 9 illustrates the concept of block mosaic kinematics as a means for such a distribution of motion, in relation to the elementary shear system. The distributed block boundaries are shaded. The block mosaic actually chosen (IDOL) is shown in Figures 13 and 14 and discussed in Tables 1 and 2.

Figures 1, 9, 13, 14 illustrate three important points:

- 1) The dextral motion in the Pacific NW may be distributed in various ways.
- 2) N-S compression sometimes squeezes matter upward into free space, as in the Yakima folds, and sometimes squeezes it sideways to the west, as in some of the surrounding blocks: this requires sinistral as well as dextral block boundaries.
- 3) Depending on the boundary conditions obtained in a certain time interval, comparable stress systems may activate different mosaics. Thus the presumably late Oligocene Naches-Blue Mountains system (see Figure 1(a) and Figure 15, Stage 1) reactivated the southern part of the Straight Creek fault (Kachess Lake fault, Clayton and Miller,



1977) which was subsequently plugged by the Snoqualmie batholith and not activated again to any significant amount by Yakima deformation.

#### 8.1.1 THE IDOL BLOCK BELT (FIGURES 13, 13)

The Yakima block is one of a series of blocks which may be arranged in a belt that constitutes the northern margin of the BR province (Idaho - Olympic belt, or IDOL). Figures 13, 14, and Tables 1 and 2 provide a brief definition and description of the blocks and their boundaries. They are based on the detailed geological and geophysical surveys contained in WPPSS PSAR A 23 and their supplements, complemented by the geological map 1:2,500,000 of the U.S. (USGS, 1974) and the topographical maps 1:250,000 and 1:500,000.

Such blocks and their boundaries are not sharply defined even farther south in BR (Eaton, 1979) where large movements are involved. Here in the IDOL belt, movements are small and structures are often discontinuous, resulting in boundaries that are subject to argument. However, the basic tenet here is that zones of movement, however diffuse, must be part of a continuous and compatible system. In the particular case of IDOL, isolated structures, especially faults which affect Miocene rocks, are considered parts of continuous block boundaries that connect kinematically, however diffusely, with the deformations of the CP.

Table 1 lists the chosen block boundaries and their definitions, and Table 2 is a list of the blocks themselves and their definitions. For ease of reference the elements are given symbols which are also used on the maps.



TABLE 1: The block boundaries of IDOL

Map Symbol	Name	Description	Comments
ON	Olympic-Naches	Faulted Neogene sediments along the Straits of Juan de Fuca. Young block faulting bordering the deep Seattle low in the Puget Sound depression (gravity). Deformed Miocene in the Green River-Naches River domain.	Northwestern part of the Olympic-Wallowa lineament (OWL, Raisz 1945, Bentley 1977, Hammond 1979)
CLEW	Cle Elum-Wallula Gap	Northeastern boundary of main Yakima folds, with dextral deflections and en echelon folds which form a belt 30-40 km wide. Intermittantly faulted.	Central part of OWL, bordering Yakima block and therefore kinematically distinct and topographically prominent.
BL	Boise-La Grande	Begins in the southeast as a prominent boundary fault zone between the western Snake River plain and the Idaho batholith, and then trends as a belt of apparently discontinuous faults through the border zone of the Wallowa mountains and the La Grande depression, into the Vansycle-Walla Walla fault zone, to join CLEW at Wallula Gap.	This is a gross simplification as faulting north of the Snake River plain is very distributed. Nevertheless, it appears that the Wallowa mountains are less faulted than the area to the SW and are therefore kinematically bounded by a distributed zone of motion. Contains the southeastern part of OWL.
NS	North Snake River	Continues BL to the southeast.	
PG	Boise-Payette-Grangeville	Main border zone between CR basalts and Idaho batholith.	Trends towards the Lewis and Clark line (LC, Eaton 1978, USGS Prof. Papers 1100).

2.5-0-22

WNP-2

AMENDMENT NO. 18  
September 1981



2.5-0-23

LC        Lewis and Clark  
          Line

"A 16 to 50 km-wide zone of en echelon right lateral and oblique slip faults marking the northeast limit of Late-Cenozoic basin-range faulting" (Eaton 1979, p. 11). To the west it disappears below the CP basalts but is recognizable as a belt of increased gravity gradient that crosses the basalts towards the Beezley Hills Rock Island Dam, and Wenatchee Mountains. In a vague way it forms the border zone of the CP and the Okanogan Highlands (Smith 1978, Fig. 6.2).

HI        Hite fault zone

The Hite fault is the main structure of the border zone between the CP and the eastern Blue Mountains. Towards the NE it becomes indistinct but as a zone seems to trend into LC. Approximate eastern boundary of thin CP crust.

Comment: The gravity  
picture of the junction  
HI-CLEW is complex.

WM        Wallula Gap-Moses  
          Lake

A prominent belt of steepened gravity gradient. Passes through the eastern limit of Saddle Mountain and Frenchman Hills structures and interferes with LC north of Moses Lake. North of LC there is a belt of rather irregular structures in the CR basalts that trends into the Republic graben of the Okanogan Highlands. The belt is 20 to 30 km wide and composed of several strands, the western of which coincides with the east-end of Gable Mountain, and an axial decay of Saddle Mountains, Frenchman Hills and Beezley Hills.

EK        East Kittitas

A structural belt between the Kittitas Valley and the Columbia River, coincides with a north-trending belt of steep gravity gradient parallel to WM but opposite in sense. The gravity belt extends south as far as the CR west of Umatilla, and may even interfere with the Blue Mountains farther south. However, it has played no important role in CRB deformation south of CLEW. Structurally, EK is characterized on its western border (Kittitas Valley) by a dextral array of en echelon brachyanticlines and some flexures and smaller faults which extend as far north as the western end of the Eocene Chiwaukum graben (Leavenworth fault). Its eastern border is marked by a dextral array of axial flexures

WNP-2

AMENDMENT NO. 18  
September 1981





of Manastash Ridge, Saddle Mountains, and Frenchman Hills structures, as well as some short fault segments; in the north particularly by the steep Rock Island structure (USGS prof. papers 100, 1978); there it interferes with LC, and one strand heads NNW into the Entiat fault (E-border of Chiwaukum graben).

Comments: Seems to be the partly reactivated southern continuation of Chiwaukum graben, compare. The eastern border coincides in part with "Hog Ranch Butte arc" of Mackay.

- |    |                     |   |
|----|---------------------|---|
| SO | Shelton-Olympia     | A belt of steep gravity gradient bordering on the northeast the Shelton-Olympia high of Danes et al (1965). Crosses the southern Puget depression into the Coast Ranges.  |
| SC | South Bend-Chehalis | An EW-trending fault belt affecting marine Mio-Pliocene and coinciding with a pronounced gravity step that limits the Shelton-Olympia high to the south. It joins SO east of Chehalis. From this point eastward the situation is unclear in the Eocene volcanics between the Cowlitz and Nisqually rivers, though an eastward trending gravity step penetrates into the Cascades where it joins apparently discontinuous fault zones W and S of Mount Rainier (WR, RL, HS). |
| TA | Tacoma              | The Tacoma gravity step separates the Kitsap high and the Tacoma low of Dames et al. (1965) and crosses the Puget Sound depression from the Olympic Peninsula into the Cascades where it joins ON and WR.   |
| WR | West Rainier        | A north-trending belt of apparently discontinuous faulting that marks the western border of the Cascades E of Tacoma.   |
| RL | Rainier-Lost Horse  | Summarizes a broad belt of deformation with SE-trending faults and folds that from S of Mt. Rainier passes through the Goat Rocks area towards the lost Horse plateau where it joins HOOK.  |

2.5-0-24

WNP-2

AMENDMENT NO. 18  
September 1981



HS

Hood River-Skate  
Mountain

A belt of N to NNW trending faults and folds joining the Hood River graben at the Columbia River, then passing W of Mount Adams into the faulted region SW of Mt. Rainier where it joins SC and RL.

Comments: apparently one of the important young  $\pm$  NS trending fault zones of the Cascades.

HOOK

Hood River-  
Delley Hollow

Western boundary of the Yakima folds which along this trend are deflected in a sinistral sense. NOT mapped as a continuous fault or fault belt but obviously of great kinematic importance for Yakima deformation.

TN

Tieton-Naches

A north-striking belt of discontinuous small faults that connects HOOK (s. of Tieton Reservoir) with CLEW-ON at the Naches River.

Comments: apparently one of the Cascadian NS trends but of minor importance.

WJ

Willapa Bay-Mt.  
Jefferson

A belt of predominantly SE trending faults and topographic lineaments that crosses the Willamette depression near Portland and joins the important NS faults (SI) of the Cascades near Mt. Jefferson. A continuation of sorts of the Brothers fracture zone (BR) that enters SI about 70 km farther south.

TJ

Tygh-John Day

From the Hood River graben at the Columbia River along a SE trending, gravity step through the SE trending W-end of Tygh Ridge towards the John Day River at about Sutton Mtn. and into the John Day fault. Here it enters the maze of distributed faults of BR where the somewhat arbitrary but kinematically useful HA, AW, SS, WS are defined.

Comments: postulated for gravimetric and kinematic reasons. The Blue Mountains gravity step is interrupted

2.5-0-25

WNP-2

AMENDMENT NO. 18  
September 1981



at the John Day River gap.  
 From there to the NW a  
 NW-trending gravity step  
 first passes through Tygh  
 Ridge and then joins HS at  
 the Columbia River. In this  
 area it gets lost in the  
 Cascades gravity picture.  
 This belt has an old history  
 and has been reactivated  
 repeatedly in various ways.

JS	John Day-Snake River	On the Geological Map of the US (1974) a 100 km-wide belt of closely spaced NW trending faults characterizes the NW end of the Snake River depression. It virtually dies out at AW (one of the justifications for choosing this boundary zone), and north of the La Grande depression is continued only by the field of small faults SE of Wallula Gap. JS is its SW border zone, as BL is its NE one.
HB	Hite-Blue Mountains	Northern border zone of intensive La Grande-Baker faulting.
WW	Wallula-Wallowa	A belt including the Wallula and Milton-Freewater faults.

2.5-0-26

WNP-2

AMENDMENT NO. 18  
 September 1981



Table 2: Blocks of the IDOL Mosaic.

In order to better describe the kinematic and dynamic position of the Yakima block between the North American and Pacific plates, and within its border zone (Basin and Range province, Juan de Fuca plate), the IDOL block mosaic is defined. The block boundaries are the lineaments and border zones defined in Table 1. Except for the Yakima block (8) and the region immediately adjacent to the north no attempt at detailed modeling is made. They are treated in a generalized way only.

Number/Symbol	Name	Comments
1 SD1	Southwestern domain	Contains most of the Oregon Coast Range and Cascades, and the Basin and Range province south of BR. Treated as a reference domain to better define the relative kinematics of IDOL transform mosaic.
2 AM2	Aldrich-Malheur	Dominated in the north by the pre-Tertiary rocks of the Aldrich-Strawberry domain, in the south by the young Newberry-Snake River volcanic depression. This is evidently a complex block with a complex history; nevertheless, the boundary zones here chosen seem to display more movement than the interior of the block, and to set it off against the surrounding blocks.
3 TI3	Turnbill-Ironside	A disturbed block dominated by north-trending faults which distinguish it from its surroundings.
4 OW4	Owyhee	At the junction of the Steens Mtn. and the Western Snake River belts.
5 IB5	Idaho Batholith	
6 WA6	Wallowa	
7 LB7	La Grande-Baker	NW end of western Snake River depression. Broken internally by closely spaced NW-trending faults. Actually a submosaic of distinctive character, except for the northwestern corner domain N of HB which may be separated as PM7a.

2.5-0-27

WNP-2

AMENDMENT NO. 18  
September 1981





Number/Symbol	Name	Comments
7a PM7a	Pendleton-Milton-Freewater	
8 YA8	Yakima	The focus of this study. The northern half is distinctly characterized by the Yakima folds, the southern half by the broad Blue Ridge structure with its pre-Tertiary rocks and a gravity low characteristic of a "continental crust of normal thickness". This is also borne out by the crustal isopachs. Actual folding and important post-CRB folding and faulting are virtually absent in this southern half which thus is the stable hinterland of the Yakima folds. This is important for kinematic-dynamic modeling. Though geologically heterogeneous, the block is a kinematic unit for post-CRB deformation.
9 OC9	Ochoco	Relatively rigid, with only moderate internal faulting according to the Geological Map of the U.S.
10 CO10	Cowlitz	Clearly heterogeneous as it straddles such separate tectonic domains as the Cascades and the Coast Ranges. These, however, apparently are subduction-related units of secondary importance for transform-mosaic kinematics.
11 GH11	Grays Harbor	
12 OP12	Olympic Peninsula	
13 TA13	Tacoma	
14,15	No name	Small blocks within CO10, accommodating deformation around Mt. St. Helens.
16 MA16	Mt. Adams	
17 MR17	Mt. Rainier	

2.5-0-28

WNP-2

AMENDMENT NO. 18  
September 1981

Number/Symbol	Name	Comments
17a BE17a	Bethel Ridge	Has probably played a somewhat separate role in the detailed kinematics W of HOOK.
19 to 22		Small blocks that are relevant only for the detailed kinematics northeast of CLEW.
23 RI23	Ritzville	The virtually undeformed part of CP south of LC.
24 ND24	Northern Domain	Is considered firmly attached to the North American Plate.

2.5-0-29

WNP-2

AMENDMENT NO. 18  
September 1981



### 9.1 THE KINEMATICS OF THE IDOL BLOCK MOSAIC (FIGURE 14)

Each of the blocks defined above is treated as a rigid body and given a translational vector  $T_i$ . To complete the picture, each should be assigned a rotational vector also; analysis reveals the probability of small clockwise rotations (s. p. 18-19 and Figure 12). These, however, seem complexly distributed, and as rotational kinematics is not as apparent it is left out in view of its minor significance.

The following procedure was chosen. YA8 has been studied in some detail, and its  $T_i$  is believed the most reliable. It was used as a starting point. The relative motions across its boundaries were very roughly estimated as to shear, extension, and compression. Proceeding thus from block to block, the vector field shown in Figure 14 was constructed. YA-8 was treated as a single rigid block in Figure 14, whereas in Figure 14?, 15, and 16 only the subcrustal lithosphere is assumed rigid, the crust being detached and deformed (Yakima Ridges; see p. 38, 40).

Here are some arguments and comments about the resulting kinematics.

YA8 is characterized by compressive ridges in its northern half indicative of NNW translations of about 3 km, decreasing northward as shortening is absorbed by each succeeding ridge. For the block boundaries this has varying complications. Along CLEW, the normal component of  $T_i$ , or  $T_n$ , is absorbed by shortening that is periodically relieved or redistributed by rotation (not considered here). Along HOOK  $T_n$  was largely used to push the adjacent block mosaic to the NW. The main effect is right slip along ON with minor shortening across ON.

Turning to the southern boundaries of YA8, they must have permitted transfer of  $T_i$  from the adjacent block unless the transport dynamics was frictional coupling with asthenospheric convection below, which looks unreasonable on regional grounds.

Consequently, the  $T_i$  of OC9 and LB7, and probably also of AM2, TI3 and OW4 have components in the direction of, and as long as,  $T_i$  (YA8) (the total translation of YA8). Furthermore, they have components of relative motion at their boundaries (shear and convergence or divergence) which is estimated by inspection of such maps as the Geological Map of the US (1974) or of Washington Public Power Supply System, 1977, where available. For TJ it consists mostly of dextral shear with probably slight convergence (Tygh Ridge),



for AP it consists of sinistral shear with divergence in an ENE direction. The nature of the component LB7 - YA8 is recognized along HB where most of the extensional faulting of LB7 dies out. However, the transition from compressional tectonics in YA8 to extensional tectonics in LB7 through the intermediate block PM7a requires clockwise rotation of YA8, OC9 and AM2, in addition to the translations shown in Figure 14. The southwestern boundary BF of OC9 and AM2 seems to be one of mainly dextral shear, and  $T_i$  (SD1) permits, by shearing along BF, the movement of both OC9 and YA8 in the required direction. The most prominent zone of boundary divergence is across SI and HS - the essentially NS striking, graben zone of the Cascades which permits EW extension towards the free boundary in the west (compare also Figure 14a).

Quantitatively, all  $T_i$ 's except  $T_i$  (YA8) are educated guesses based on insufficient information. In reality the quantities may be somewhat larger than shown in the Figure; they need not be in order to give a consistent picture that harmonizes with the small deformations mapped in the area.  $T_i$  (SD1) then turns out to be directed to the NW and nearly parallel to IDOL (or BF, WJ, ON, CLEW). IDOL is a kind of megabreccia accommodating dextral shear of about 7 km, distributed over a zone 200 - 400 km wide, or an average shear strain gamma of about 0.02.

As to the average clockwise rotation of YA8 and LB7 around a pivot at the northern tip of YA8, it turns out to be no more than 1/2 degree, corresponding to an extension of 2 km in the northern part of LB7.

The reliability of this attempt at embedding Yakima deformation in the kinematics of a surrounding block mosaic depends on several assumptions which need further study. One difficulty, not sufficiently dealt with, is the 3-dimensional relation between lithospheric and crustal kinematics, compare Figures 14a, 15, and 16.

In Figure 14a this problem is illustrated. According to Figure 16 the master shear of the Yakima folds descends into the deeper lithosphere under the Blue Mountains: this would be the proper location of the northern lithospheric block boundary for Yakima deformation proper. North of it, and disharmoniously underlying the Yakima folds, is another lithospheric block YA-8a, whose NE boundary is CLEW.

The strike of the Yakima ridges gives the direction of relative motion YA-8/YA-8a, but does not contain information on lithospheric motion along CLEW. Assuming on Figure 16f,g

that part of the surface deformation measured in the Yakima gorge is the surficial expression (flower structure) of lithospheric motion along CLEW, the transport vector  $T_i$  (YA-8) of Figure 14 may be reinterpreted and modified as composed of two lithospheric vectors  $T_i$  (YA-8) and  $T_i$  (YA-8a). A modest amount of lithospheric motion parallel to CLEW has been added, which would be insufficient to produce conspicuous transcurrent faults at the surface, being hidden in the overall en echelon fold belt.

The vector field of the block mosaic may then be adjusted to the new  $T_i$  (YA-8) (total), Figure 14a. A considerable extension (pull-apart) results across HOOK and WR-HS.

#### 10.1 DYNAMICS OF A BLOCK MOSAIC

Boundary stresses and resulting relative block movements are sensitive to overall boundary conditions which change with time. A complexly wobbling movement is induced which is typical for smaller-scale fault breccias: they often exhibit superposed striations of diverging directions and, in limestones, stylolites and extension cracks that also vary with place and time. Inasmuch as most of CRB deformation seems to have occurred within a small time interval relative to the total and still active B & R movements it is not easy to place it exactly within developmental history of the B & R. For example, the Picture Gorge dykes and associated extensional features reveal a kinematic and dynamic pattern of early B & R tectonics that differed greatly from that of CRB deformation (compare also Eaton, 1979), whereas present-day tectonics as revealed by earthquake distributions and focal mechanisms are different again: a present-day pivot seems to be in the Yellowstone-Helena region. However, earlier block mosaics are never entirely discarded as inherited distributions of material properties always influence stress and strength distributions, and consequently the distribution of potential faulting, to some extent.

Block boundaries tend to interfere with each other during motion, which results in inactivation of old and activation of new boundaries. However, some composite zones of movement by addition of small branch faults that help to overcome local obstacles, may develop some sort of strain softening.

#### 11.1 MAPS OF KINEMATIC DEVELOPMENT IN 8 STAGES (FIGURE 15)

(Compare the cross-sectional development, Figure 16, and the block mosaic IDOL, Figures 14 and 14a).





### 11.1.1 INITIAL MOVEMENTS AT THE BOUNDARIES OF YAKIMA BLOCK YA-8

#### Stage 1: CLEW

Between the stress concentrators of the La Grande Gap in the southeast (apex of block near Wallula Gap) and of the Kachess-Naches area (bend in the Paleogene Straight Creek fault system near Cle Elum) the CLEW lineament in the CR basalts is nucleated. It initially consisted of broad and gentle dextral en echelon brachyanticlines (short folds) similar to those shown by Hardin and Lowell (1979, Figure 5A). This belt has a width of 30 - 40 km and represents the base of an inverted triangle of deformation that converges downward, with an apex at a depth of 15 - 20 km (wedge boundaries at 45° for simplicity, compare Figure 5). This point coincides with a mechanically weak zone, or a mechanical discontinuity, near the base of the crust. If interpreted according to the Riedel model (compare p. 6-8) of en echelon belts, the discontinuity marks the level of disharmony between a more concentrated wrench fault in a comparatively competent lithosphere slab below and the distributed (diffuse) deformation in the crust above.

The amount of dextral motion in this initial stage was minute ("incipient" to "early stage wrench fault," Harding and Lowell, 1979, Figure 5): a fraction of the measurable total deformation across CLEW, which is not more than 2 km. Due to this initial break across the Columbia Plateau crust and lithosphere, a mechanical discontinuity (boundary) is created which had not necessarily existed before (it cuts across gravity trends and crustal isopachs) of probably Eocene age, see p. 47-48; there is a possibility, however, of an Oligocene Kachess-Naches-Blue Mountains system that had also followed CLEW. Because of the small displacement, this boundary represents no insurmountable obstacle although it makes itself felt during subsequent deformation.

There are various reasons for postulating such an initial break along CLEW, the foremost being that the Yakima folds all terminate against, or are deflected, or otherwise influenced by CLEW which thus must have an earlier origin. A further argument though less cogent is based on the fact that the Yakima block is part of a lithospheric block mosaic (IDOL) At the northern end of the Basin-Range block mosaic, which affects the entire lithosphere. The boundaries of the lithospheric block YA-8, and particularly CLEW and HOOK, were subject to forces exerted by all the surrounding blocks of the mosaic. Crustal decollement on the other hand, is obviously due to driving forces only at the southern



K



September 1981

boundary, the other boundaries playing the role of passive constraints. It would therefore seem reasonable to assume an early development of the lithospheric block boundaries and their obstruction soon after initial motion, probably at the northern tip of the block; this, in turn, increased internal NNW compression to the point of yielding along the weak layer at the base of the crust.

#### 11.1.2 INTERNAL DEFORMATION OF THE YAKIMA BLOCK YA-8

As convergent dextral strike-slip motion along CLEW is increasingly obstructed by interference of other faults (for instance HOOK),  $\sigma_N$  and  $\sigma_E$  (the N and E trending horizontal principal stresses) increase, the latter surpassing  $\sigma_V$  (the vertical principal stress), in magnitude; this is a situation that develops into a thrusting instability at a higher stress level.

The kinematic and dynamic theory thus presented is; first, formation of the Yakima lithospheric block boundaries, and second, internal deformation of the Yakima block at higher stress levels.

The sequence of events during this second internal compressional deformation is depicted in stages 2 - 8. Deformation is assumed to begin in the south and propagate northward for various reasons (compare Figure 16):

1. The most important factor in the sequence of events described below is that the Blue Mountains part of the Yakima block seems to have been the most stable. This correlates with a change in crustal composition according to geophysics (compare Figures 13 and 17), the material interpretation of which is offered on p. 44-46. It probably acts as an indenter type stress concentrator in the map view as well as in the cross-section view (Figure 16); the northward tapering thick crustal wedge is pressed against the CP crust with its presumably weak base. It would appear reasonable to assume that stresses were highest in the south, and there caused the first thrust fault to form.
2. Yakima folds have a tendency to be convex to the north which again suggests they were formed by indentation-type deformation propagating from the south.



September 1981

3. Inactivation of CLEW-OWL calls for activation of breaks, permitting block movements towards the free Juan de Fuca plate boundary farther south (compare Figure 14a).
4. The individual Yakima folds seem to emanate from the brachyanticlines of CLEW, and thus to be related to the same mechanical discontinuity, a decollement level at 15 - 20 km depth. Slip area on this decollement layer increases for northerly structures which thus should be more stable and be initiated only after inactivation of the more southerly ones.

Spacing of the Yakima folds, except for Yakima Ridge anticline, is surprisingly regular (25 - 30 km), and this regularity requires an explanation. There are several possibilities or combinations of possible factors, but the most plausible at this time seems their apparent relationship with the broad brachyanticlines of CLEW. It is therefore proposed that as decollement instability at the base of the crust spread to the north, the pre-existing, periodically arranged brachyanticlines on CLEW, compare Harding and Lowell (1979, Figure 5) and Wilcox et al., (1973, Figure 11), or rather the corresponding deep faults (compare Figure 5), were stress concentrators on the decollement surface from which thrusting spread sideways (similar pre-existing features on HOOK are not evident). The relationship of surface folds and decollement surface is shown in Figures 15 and 16.

#### Stage 2: Columbia Hills Anticline.

The thrust emanating from the base of the Blue Mountains crust compare profiles Figure 16 surfaces almost directly, without significant decollement, at the Columbia Hills fold. The crustal wedge above the thrust is segmented into sub-blocks, indications of which appear on the tectonic maps, but they are even more striking on detailed topographic and gravity maps which correlate in many ways. The structurally lowest sub-blocks are the Dalles and Umatilla sub-blocks. They are separated by the high Condon-Wasco sub-block which occupies a position immediately north of the John Day River gap in the Blue Mountains gravity structure. The Bouguer anomaly gradient forms a belt along the northern foot of the Blue Mountains beginning south of Wallula Gap (at La Grande Gap), and extending WSW to the John Day River. There it becomes irregular, but reforms as a belt again after a short interval, this time striking NW, and is displaced at Tygh Ridge. These



relations, not analysed in greater detail, suggest slightly increased NNW movement west of the Umatilla sub-block, with increased shortening of the Columbia Hills fold (which north of the Umatilla sub-block has only minor shortening).

The average trend of the Yakima structures, generally, and the Columbia Hills anticline, in particular, demonstrate that the direction of principal shortening was to the NNW. The gravity gradient in the Blue Mountains proper, east of the John Day River, is reasonably parallel to this direction and suggests a cross section as shown in Figure 16. This does not hold for the gradient west of the river, and here a certain amount of dextral strike-slip along with compression should be expected. Tectonic behavior should accordingly be more complex, and this is manifested by the Tygh Ridge structure, which is nested within a kink of the pronounced gravity gradient belt, and faces south: although a compressive structure should be formed at this kink, no simple thrusting relation with deep crustal structure is obvious.

The NW trending gravity belt intersects the anomalies due to the Cascades volcanoes, but structurally seems to end at the Hood River graben. The latest fault movements within the graben seem to be younger than the Yakima folds, but as the gravity belts and the HOOK lineament emanating from it to the northeast have strongly influenced the Yakima folds, they must in some way have existed from the very beginning of Yakima deformation.

The Columbia Hills structure is strikingly segmented by cross-structures, particularly in the west. The narrow width of the fold in the Columbia River gorge north of the Dalles calls for a limited amount of shallow decollement approximately at the base of the basalts as shown in the cross section Figure 16. The dextral displacement of some of the sequences shown, for example, by Newcomb (1970) is thought to be due to later movements affecting the western corner of the Yakima block and is not shown at this stage. However, the changes of vergence NE of the Dalles must be a primary, though local, dextral feature. The sinistral apparent displacement near Goldendale is not understood in detail but lies on a sinistral lineament (Horse Thief Point - Goldendale Lineament, or HOG), which has affected all the Yakima ridges in various ways, though less severely than CLEW or HOOK. It seems that this cross-structure is also an early feature, possibly a sub-block boundary associated with W (NW) stretching (see Figure 14a).

It has been mentioned that the sub-blocks of this stage of movement are reflected in the gravity picture which because of the minute amount of movement (about 500 m north of the Dalles, at most 200 m north of Umatilla) must be an inherited feature: it probably influenced the position and shape of the thrust and consequently the deformation of the hanging wall block.

Considerable irregularities affect the Yakima ridges where they enter CLEW, and this is certainly true for the Columbia Hills fold. At Sillusi Butte, near Umatilla, a S-striking fault, associated with folds, trends toward the Blue Mountains though its fate there is unknown. East of it, the fold seems to split up and also increase its compression. Apparently the easternmost part of the slipped domain, like the Western half, moved a little farther than the Umatilla sub-block.

The increased complexity of CLEW is understandable in view of the pre-existing complications along CLEW.

### Stage 3: The Horse Heaven Hills Structure

The Columbia Hills structure was inactivated at a modest level of development; instead the base-crust decollement spread to the north, and a new crustal thrust was nucleated at CLEW and propagated to the WSW. The reasons for this development are open to speculation, and some pertinent conjectures are offered on p. 33.

The hanging wall, or upper plate, of the Horse Heaven Hills thrust again shows subdivision into subblocks which are particularly evident on the topographic maps where domains of different shape and drainage character may be distinguished. However, no sharp fault boundaries have been mapped.

The most prominent irregularities are found: 1) on CLEW, 2) on HOG (or north of the Waco-Condon-subblock of stage 2), and 3) on HOOK.

### Stage 4: Toppenish Ridge

Again the Horse Heaven Hills thrust was inactivated after a displacement of no more than 300 m - barely sufficient to make a dent in the gravity picture - and decollement spread another 30 km to the north. Nucleation of Toppenish Ridge on CLEW is somewhat less plausible because HOG here interferes with CLEW, and Toppenish Ridge proper disappears east of HOG to be replaced, after a sinistral offset, by





Snipe Mountain which somehow deteriorates in the wide bulge of CLEW south of the Rattlesnake Hills structure. The corresponding modest compression of no more than 300 m is here somehow absorbed by a distributed network of minute displacements, but is concentrated again to some degree at the small but pronounced faulted fold trending to the NW from the NW corner of the Horse Heaven Hills structure.

#### Stage 5 Rattlesnake Hills Structure

As the front of crustal decollement approaches the apex of Yakima block, the influence of CLEW and HOG becomes dominant and a pronouncedly arcuate ridge containing numerous irregularities results. There are multiple subparallel SW-striking features that accompany the western part of Athanum Ridge, which is the western part of the Rattlesnake Hills structure.

At Union Gap the structure enters CLEW. Concomitantly to being superposed on a CLEW bulge, it splits up into a number of substructures. These become extremely entangled where they interfere with HOG in addition to CLEW. There seems to be some question as to how much landsliding affects the northeastern corner of Rattlesnake Hill structure but most of the irregularities seem to be structural. Although the apparent displacement along HOG is dextral, the en echelon wrinkles and apparent drag in the Rattlesnake Hills structure immediately west of HOG are sinistral. As the Rattlesnake Hills structure, like other Yakima folds, are strongly influenced by HOG, this latter must have formed at an earlier stage in this area too. All offsets and drags are apparent as the structure developed irregularities from the very beginning. However, there may have been some slight sinistral movement along HOG which is the most prominent subblock boundary.

The Rattlesnake Hills-Wallula Gap (RAW) trend of brachyanticlines and concomitant small faults was superposed on CLEW, which it roughly parallels, at this stage. It is more external than the eastern borders of Toppenish-Horse Heaven Hills stages which fits into a picture of an expanding area of decollement slip. The narrow brachyanticlines are rooted at a shallow level, and there probably is a more concentrated fault structure below the Yakima basalt. It presumably has a limited strike slip and negligible dip-slip displacement. On the other hand, as the whole structure is rooted at a deeper level, the base-crust decollement, reactivation, and accentuation of the broad

CLEW warps occurred simultaneously; resulting in the superposition of the narrow RAW on an accentuated, broad CLEW segment.

#### Stage 6: Yakima Ridge

Yakima Ridge is virtually superposed along its entire length on HOOK and CLEW. Cowiche Mountain-Sedge Ridge on HOOK strikes SW and is immediately adjacent to the west end of Ahtanum Ridge, separated only by a very straight feature along the South Fork of Ahtanum Creek. Yakima Ridge is first interfered with by an appendage of CLEW at the southeast trending east end of Cowiche Mountain. East of Yakima, the ridge enters the main CLEW bulge, enhancing CLEW and breaking it into weakly defined sub-blocks. The east end of Yakima Ridge splits up into a series of east-plunging, narrow en echelon ridges. There is no pronounced obvious eastern border of the slipped area as there is for Rattlesnake Hills, and it seems likely that the eastern border is a broadly distributed zone of deformation further heightening the CLEW warps and possibly becoming in places more concentrated on joining RAW. On the other hand, it is abundantly clear for this stage as well as the following ones that there is a lack of compression across the lateral boundaries (compare p. 18 and 19). For the CLEW slight clockwise rotation has probably reduced compression, but this rotation increases compression on HOOK unless blocks MA-16 and MR-17 simultaneously move away to the NW (Figure 14a).

#### Stage 7: Umtanum Ridge

At this stage decollement begins to transgress the borders of the Yakima block. Most of it is still limited by CLEW; however, the easternmost part - Gable Mountain-Gable Butte - now affects a small domain NE of CLEW (22 in Figure 14). The eastern edge of the area of decollement is not bounded by an observable structure, and it is assumed that a zone of distributed dextral shear joins the east end of Gable Mountain with CLEW (compare p. 43 and following).

Umtanum Ridge, affected by several vicissitudes, follows CLEW to the northwest beyond the HOOK-CLEW join; it transgresses the borders of Yakima block also in the same direction. It is uncertain how much of this movement now again follows OWL (ON; compare Figure 14); it is possible that at least some of it is bounded on the west by a vague NS-lineament (NI in Figure 14), with a small amount of



extension of the decollement beyond HOOK (17a in Figure 14), similar to the small amount of extension (22) beyond CLEW in the Gable Mountain area.

Southeast of Priest Rapids, Umtanum Ridge interferes with HOG where it leaves CLEW. It seems likely that the Umtanum Ridge feature splits up there, one (reduced) part continuing into the Gable Mountain branch, and the other poorly defined part following CLEW to the southeast. One reason for this assumption is the apparent decrease in shortening across Gable Mountain; another reason is the apparent divergence of movement between the Yakima block and the Gable Mountain subblock. This divergence is obvious regionally and may be due to the fact that the component of  $T_1$  (YA-8) normal to CLEW (directed NE) was more important in pushing blocks 18-22 than the total transport vector. This in turn implies simultaneous dextral shearing along CLEW. Stages 8 and following would then not be kinematically independent of State 7.

#### Stage 7a: Umtanum-Manastash

Umtanum and Manastash Ridges are closely associated and in some places are not easily distinguished as separate kinematic units. Both units are therefore treated simultaneously in Figure 15. Manastash Ridge does not appear to cross the Columbia River, instead joining Umtanum Ridge in some way at Priest Rapids. At the northwest end, northwest of Wenas Valley, it has not been possible to separate the Manastash, Umtanum and Cleman Mountain features.

Using this information it would appear that decollement affected all these structures nearly simultaneously, but in a highly uneven way because of the pre-existing irregularities of CLEW, which here interferes with HOOK and HOG. Another possibly important interference is that of CLEW with the East Kittitas belt of Bouguer gravity gradient (EK of Figure 14, see also Figure 24), suggesting crustal inhomogeneities.

This is the most concentrated belt of shortening. It has an estimated 1.5 km of shortening in the Yakima gorge section which is about the same as all the other Yakima ridges taken together. This shortening, according to recent mapping, decreases both towards the Priest Rapids section in the southeast and the Cle Elum section in the northwest. In fact, the first impression is that it is concentrated around the northern tip of the Yakima block. This would require that the Yakima block, at this stage, was further pushed to

the north, creating a comparatively strong frontal shortening, but simultaneously avoiding corresponding shortening at its lateral boundaries (see. p. 38).

#### Stage 8: Saddle Mountain

The Saddle Mountain stage expands the area of decollement farther beyond CLEW to incorporate particularly domains 19 and 21 of Figure 14. While the situation on both sides of the Columbia river gorge is quite clear and measurable shortening is about 230 m (see p. 17). complications are manifest in the East Kittitas zone (EK of Figure 14) in the W and WM (Figure 14) in the E. Distributed dextral shearing is implied in both WM and EK, accentuated in the latter by a series of dextral en echelon brachyanticlines (see p. 17).

A part of the Stage 8 movements to enter the Wenatchee Mountains, beyond the simplified domain shown in Figure 16. At Boylston, one of the branch ridges is deflected to the SW, and this is taken to suggest a quantitatively insignificant branch of Stage 8 motion that joins HOOK via SE end of Cleman Mountain.

Further stages of propagation of decollement to the N could be added (see Figure 14a) but they are insignificant kinematically. However, according to the model they are the youngest and may therefore be the seismically most active ones today.

#### 11.1.3 SUMMARY OF IMPORTANT POINTS IN THE MAP-VIEW KINEMATICS OF THE COLUMBIA PLATEAU

##### 1. Distribution of compression:

Distribution of shortening away from some comparatively rigid indenter is commonplace in tectonics. On a small scale, I have investigated the phenomenon in the Jura (Laubscher, 1980). On a continental scale compare Molnar & Tapponnier (1975). Shortening was comparatively concentrated at the tip of block YA-8a during Stage 7-7a ("Wymer Knot").

##### 2. Lateral extension:

At no stage compression at the lateral boundaries is commensurate with NNW translation. This implies lateral stretching.

### 3. Clockwise rotations:

Particularly Stages 6 and 7 show a decrease of shortening eastward, implying a slight clockwise rotation.

## 12.1 DEVELOPMENT OF THE YAKIMA FOLD SYSTEM, CORSS-SECTIONS (FIGURE 16)

Mapped deformation, the Bouguer gravity map and the regional crustal isopachs (Smith, 1978) are combined for a schematic model of deep deformation (for the development of mechanical conditions at depth see p. 51).

Mapped deformation suggests three levels of localized to regional decollement and decoupling which are supposed to be connected by ramps. Gravity and crustal isopachs in turn suggest these to be:

1. The base of lithosphere (sub-Moho velocities here 8.1), perhaps at 50 - 60 km depth. The thickness of the lithosphere may here be somewhat reduced because of the particular setting of CP in a domain of Eocene to Miocene extension.
2. The basal part of CP crust, appx. 20 km. The mantle  $V_p$  of 8.1 km/sec suggests peridotite and at a depth of 20 km this could be serpentinitized. With a thermal gradient of 250 C/km, the rocks at a depth of 20 km would be in the transition zone serpentinite-peridotite plus water where frictional heat, e.g., could produce a layer of high pore pressure propagating with decollement.
3. The Yakima ridges are relatively narrow wrinkles superposed on wider pedestals due to decollement on the second level. The ridges imply localized decollement at depths of 1 - 3 km, probably at the base of the Yakima sequence which is a mechanical discontinuity. Below this discontinuity strata were deformed and broken before the basalts were extruded (p. 48-49); above the discontinuity there is a layered sequence of alternating competent and incompetent beds of surprising regularity.

### Stage 1:

The Yakima block moves as a lithospheric plate, probably part of a primary IDOL (Figure 14). The underlying





reasoning is presented on p. 32-34. Some aspects of this stage that are particularly relevant for the cross-section are:

- zones of dextral shear with a compressional component (dextral-convergent boundaries) commonly develop broad en echelon folds in a deformable layer before faults of noticeable size break to the surface.
- the broad en echelon folds that compose CLEW may be correlated with concentrated dextral shear below 20 km, which would be in the lithosphere.

Consequently, CLEW in this first stage is represented as a "flower structure" typical for en echelon folds (see Figure 5 and Harding & Lowell, 1979): a lithospheric stem (fault) which in the crust branches out into a broad zone of deformation. The branch faults are small and tend to dissipate towards the surface, thus producing broad, apparently unfaulted brachyanticlines.

#### Stage 2:

The compressive stress level inside the block increases to the breaking point. It is higher in the south towards the active plate boundary. The thicker Blue Mountain crust is stronger than the Yakima crust to the north; the first break therefore emerges as a 30 degrees Mohr-type shear from the northern base of the Blue Mountain crust, probably with a slight amount of decollement at levels 2 and 3. The justification for such a Mohr-type shear is taken from the COCORP results in the Wind River structure (Smithson et al., 1979), and the polygonal shape of the shear surface as a combination of Mohr (ramp) and decollement segments is documented from many parts of the world, e.g., Rich (1934), Rodgers (1949), Charlesworth (1961), Bally et al., (1966), Royse et al., (1975), Roeder and Witherspoon (1978), Laubscher (1973). For nucleation of kink-type near-surface folds see Thompson (1978), Laubscher (1977) (Figure 8 of this report).

#### Stage 3:

Activation of level-2 decollement proceeds to produce the Horse Heaven fold. The question of why the Columbia Hills fold was inactivated in favor of the more distant Horse Heaven fold is delicate: active and resisting forces on the whole boundary of a potential shearing surface play a role, and as faulting proceeds at a finite velocity, the scenario

is one of three-dimensionally competing rate processes with changing alliances. The tectonic picture suggests the following general reasons:

- near-surface deformation is highly frictional in kink-like folds beyond moderate widths and dips. Thrusts which may be lubricated at depth e.g. by pore pressure are resisted by dry friction at the surface.
- the base-crust decollement should be nearly frictionless if it is to succeed over surface deformation of very modest amounts. The de-serpentinization process as envisaged would fit.
- localized activation of the base-crust decollement zone is already present all along CLEW as suggested by the brachyanticlines. It has a tendency to spread laterally into the Yakima block, there to combine with the northward spreading decollement surface at the base of the crust. Within this mechanism also lies the most plausible explanation for the periodicity and location of the Yakima folds: they are localized by the pre-existing, periodic en echelon folds of CLEW that propagated laterally on top of the nascent base-crust decollement.

For Stages 4 and 5 the same explanation holds.

At stage 6 decollement and folding approaches the north tip of the Yakima block. Here the periodicity breaks down because of the proximity of the block boundary whose influence on the tectonics of the Yakima Ridge is documented by surface mapping.

Stage 7:

Although CLEW is a pre-existing boundary slightly impeding further propagation of base-crust decollement, it is a weak obstacle for two reasons:

- Neither geology nor gravity nor crustal isopachs imply any important change of crustal structure across CLEW. For that reason, it was inferred that CLEW is probably not a discontinuity inherited from pre-Oligocene times but rather a newly formed break connecting distant inherited stress concentrators. Although its formation preceded actual Yakima folding it did so by a geologically minute time interval. A first weak discontinuity may have been formed during the Oligocene Kachess-Naches-Blue Mountains compressional phase (see



Figure 1(a) and p. 32). However, its main development as part of the IDOL system is probably due to Stage 1 of late Miocene Yakima tectonics.

- The base of CP crust is a potential decollement horizon beyond CLEW and was interrupted by a very small amount on CLEW.

Stage 7 represents all the beyond-CLEW stages such as Gable Mountain-Gable Butte, Saddle Mountain, Frenchman Hills, etc.

Near the northern end of the particular cross-section chosen, CLEW approaches the northern border of the Yakima basalts and, simultaneously, the domain of thin CP crust. Further northward spreading of decollement is severely restricted.

The North Kittitas flexure (shown on Figure 15, Stage 8) may, in a way, be similar to the Blue Mountains: a deformation due to the end of crustal decollement. I have symbolically represented it as an underthrust wedge common at the front of decollement plates (Habicht, 1944; Laubscher, 1977; Thompson, 1981; Price, 1981).

### 13.1 THE DEVELOPMENT OF CRUSTAL STRUCTURE IN THE CP AND ITS INFLUENCE ON THE DYNAMICS OF YAKIMA DEFORMATION AT DEEP LEVELS

#### 13.1.1 A COMPLETE DEFORMATIONAL SYSTEM CAN BE MODELED, EVEN SCHEMATICALLY, ONLY IF VARIATION WITH DEPTH IS INCLUDED

Information placing some constraints on deep structure is contained;

1. in the aspect of surficial structure as explained on p. 12 and following and p. 40-41.
2. in geophysical information on present-day distribution of some rock properties, particularly gravity, seismology, and geothermics.
3. in overall structural history that gives some rationale for placing present crustal structure into a historical perspective, permitting an educated guess about crustal structure at the time of Yakima deformation.

### 13.1.2 PRESENT-DAY CRUSTAL STRUCTURE IMPLIED BY THE GEOPHYSICAL DATA (COMPARE FIGURES 13, 17)

#### 1. Seismic data

Smith (1978) and Hill (1978) compiled and reviewed much of the seismic information presently available. Directly pertinent for the CP are Figure 7.6 - 7.10 of Hill and Figures 6.2 and 6.3 of Smith.

Figure 6.2 of Smith (compare Figure 13 of this report) shows a crustal thickness of less than 25 km for much of the Columbia Plateau; a corridor of thin crust across the Columbia River structural low in the Cascades, a comparatively steep gradient to a thickness of up to 40 km in the Blue Mountains, and a southeast plunging nose of thick crust (up to more than 50 km) continuing from Vancouver Island across the Juan de Fuca strait and Puget Sound into the Cascades (this particular feature has been challenged by Riddihough, 1979). This picture must be greatly generalized in view of structural and gravity data, but nevertheless it correlates in a striking if overall way with CP tectonics.

Figure 6.3 of Smith shows that the minimum crustal thickness of the CP coincides with a  $V_p$  maximum of 8.1 for the Moho. This in turn implies a comparatively cool upper lithosphere, which correlates with a relative heat flow minimum in the area (Blackwell, 1978; compare p. 49).

Figure 7.6 of Hill gives  $V_p$  and earthquake-frequency data for the Puget Sound region which according to Smith's Figure 6.2 is on the 40 km isopach of the Vancouver Island nose. An earthquake frequency minimum at an intermediate depth of about 15 km at a level of lower crustal velocities (6.7 km/sec), and an almost complete cut-off at 30 - 40 km are remarkable. A low-velocity channel at the base of the crust is another feature of possible importance for crustal mechanics in this area.

Although most of the earthquakes occur above 40 km, some earthquakes, including the largest ones, occur to depths of 80 km, in contrast to shallow-focal depths elsewhere in the conterminous US. No clear relation to structures is reported, but it seems



plausible that they correlate with the Vancouver Island crustal nose. However, the structure of Figure 7.6 is not undisputed because it is based on an assumption of plane layers whereas gravity data (Danes and others, 1965; Weston Geophysical, 1979) implies strong lateral variations.

Figure 7.7 of Hill (compare Figure 20 of this report) shows the crustal structure below the central CP (Pasco basin) with, in the center, an upper 10 km layer of 5.2 km/sec (probably sediments and volcanics), then 15 km of 6.4 km/sec, which is a "granitic velocity", including granitic gneisses. This is the crystalline part of the continental crust, commonly above 30 km thick, here reduced to about 1/2 by a process discussed on p. 49.

In the absence of direct information we may assimilate crustal structure in the Blue Mountains to that given for the western Snake River plain. Figure 17 emphasizes the dramatic changes in crustal composition occurring on the boundaries of the Columbia Plateau.

## 2. Gravity structure

(New Bouguer anomaly map by Weston Geophysical, 1979).

The extent of the seismically defined CP coincides approximately with the domain of moderately negative Bouguer (l.t. -90 mgal) anomalies which in turn approximately coincide with low elevation (and therefore suggest isostatic compensation). The western border zone along HOOK and the Wymer apex of the Yakima block have Bouguer anomalies as low as -100 mgal with an undulating band of steep gradient. Other striking steep gradient belts are along the north slope of the Blue Mountains and, west of the John Day River gap, along the Tygh border - all of which mark zones that seem to have been important for Yakima deformation.

The interior of CP is segmented by a series of more or less pronounced belts of steep gravity gradient. The most striking are the  $\pm$  NS trending belts between the Kittitas depression and the Columbia River (EK of Figure 14), and farther east between Wallula Gap and Moses Lake (WM of Figure 14). They abut against an EW trending belt ending in the west around Wenatchee (LC of Figure 14).

Superposed on these conspicuous features are less pronounced structures, particularly one trending from the Walla Walla belt east of Wallula Gap, towards the Rattlesnake Hills. This coincides with the RAW part of CLEW.

A somewhat more diffused and patchy belt may be recognized in the NW part of CLEW. Superposed on all these features are weak irregularities which generally produce weak wrinkles in the contours and which coincide with the Yakima ridges - they may even be due to correction techniques - and demonstrate the shallow character and insignificance of these ridges in comparison with total crustal structure.

From these gravity data it would appear that crustal structure tends to change in a stepwise fashion, rather than gradually, from the Central Pasco basin towards the surrounding highlands, a feature reminiscent of foundered crustal blocks with a central deep graben and corresponding crustal thinning (Figure 20; compare Ziegler, 1977, Figure 7, Ramberg and Smithson, 1971, Figure 6). This feature evidently must have developed prior to CRB outpour and most plausibly during the climactic volcanic activity in the Eocene (Armstrong, 1978). (Although even older crustal inhomogeneities are implied in the Paleozoic-Mesozoic history of the area, Davis, 1977).

Assigning seismic velocities to rock types is not unique but a plausible picture emerges nonetheless. It may be conjectured that the 5.2 km/sec layer is a volcanic-sedimentary fill in a subsiding graben, and thus is most probably of Eocene age. The Pasco graben strikes north and points to the Republic graben although interrupted and shallowed by the EW striking Wenatchee step (LC). The gravity correlation to structure is somewhat confused not only by the superposition of structures of probably different origin but also by the opposing effects of thickened CRB in the Pasco Basin (positive), thick graben fill (negative) and shallow M (positive) in the graben areas, and will have to be quantitatively modeled for greater certainty (compare the note on p. 50).

Some of the cross-structures modifying or terminating the crustal pull-apart such as the Blue





Ridge or the Wenatchee belt (LC) may have played the role of transform-fault zones bounding and displacing the intra-arc (back-arc?) spreading. Compare this Eocene situation north of the Blue Mountains with the Neogene situation (B & R) south of the Blue Mountains (Pasco Basin similar to Rio Grande Rift; also compare the suggested transform zones with the transform zones of Lawrence, 1976 and Eaton, 1979).

3. Cenozoic Geologic History of the Pacific NW and Crustal Development

The particular crustal structure of the CP, setting it apart from other domains of the North American Cordillera, apparently began in the late Cretaceous (Coney, 1978, page 42). The complex and puzzling set of information that has been published about the Pacific Northwest has engendered a number of sometimes complementary, sometimes conflicting syntheses. In evaluating them I start from the Columbia Plateau and its surroundings, and the vast amounts of detailed information amassed in WPPSS Amendment 23 to the WNP 1/4 PSAR.

A very recent synthesis by Hammond (1979) bears greatly on the problems discussed here. The gist of his thesis is that a Coast Range - Klamath Mountains block (with the Cascade volcanic arc on its back) rifted from the continent along the Olympic-Wallowa Lineament (OWL) and rotated about a pivot in the Olympic Mountains). This rotation supposedly took place between 50 and 15 my bp. Such a large-scale rotation was postulated by Simpson and Cox (1977) on paleomagnetic grounds in the southwestern part of this block, but Beck and Burr (1979) found paleomagnetic evidence for much more modest dextral rotation in the Washington coast ranges and they doubted the rigid rotation postulated by Hammond and Simpson and Cox.

Geological and geophysical evidence in the CP and its surroundings are hard to reconcile with Hammond's rotation. Upper Cretaceous-Eocene continental sedimentation occurred in extensional grabens in pre-Tertiary metamorphic and igneous complexes. These grabens converge towards the N end of the Pasco Basin and have no relation with OWL except at the southwest border of what here is called the Roslyn graben, formed by the Lake

Kachess-Hicks Butte fault system (subsequently compressed in the Naches-Blue Mountains stage not much more than 20 my ago). The Swauk Formation does not transgress this boundary according to recent mapping by Clayton and Miller (1977). Though the environment of sedimentation has been described as a "forearc basin" (Hammond, 1979, page 231), the plate tectonic framework of that time interval is not easily defined in such terms.

This is evident from work of Armstrong (1978) and Coney (1978). Volcanism of that time, the "Challis episode" of Armstrong (see his Figure 12-3) occurs in a belt several hundred kilometers wide, east of the Columbia Plateau. If this wide belt of volcanism is considered an arc, then the grabens north of the Columbia Plateau are intra-arc to back-arc. Armstrong implies that the grabens had once been continuous into the volcanic fields of Idaho, but are now covered by the CR basalts.

Coney (1978, p. 42 and following) provides a plate tectonic frame for this peculiar distributed volcanism. He states that "the simple pattern of a well-defined volcano-plutonic belt of arc affinity along the Pacific margin began to break up in Late Cretaceous time, about the same time that the initial effects of the Laramide orogeny began in the Rocky Mountains foreland" (p. 42). To me this seems a very important tectonic fact: the regional tectonic (and thermo-volcanic) activity was in a state of reorganization during this stage. The prominent event is the development of the Laramide Rocky Mountains, and the grabens of the Columbia Plateau region are in the hinterland of the north end of this eastwards bulging arc. The Late Cretaceous was generally quiet in the Pacific NW, but there was a violent burst of igneous activity in the Eocene.

This general plate tectonic picture harmonizes better with the geological and geophysical information in the CP and its surroundings. Crustal isopachs (Smith, 1978) and detailed gravity (Weston, 1979) fail to support the notion that OWL is the locus of a fundamental change of crustal composition. Although thinning, the crust underlying the CP is non-oceanic, and belts of steep gravity gradient predominantly trend NW and EW without much relation to the trend of OWL.



September 1981

Comparative anatomy of the CP and similar structures from other parts of the world suggest a different picture.

14.1 A COMPARISON OF SUSPECTED EOCENE CP GRABENS WITH  
SIMILAR STRUCTURES ELSEWHERE (FIGURES 18 - 20)

The Upper Cretaceous-Eocene grabens present in the region from the Northern Cascades to the Okanogan Highlands are filled with continental deposits containing coal. Though subsequently compressed to some degree, they were, at the time of formation, extensional features that may be compared with other grabens. The trends of the grabens converge toward the Columbia Plateau but it is not known what happens to them below the basalts. A combination of arguments based on geological-historic, tectonic and geophysical data, and a comparison with other grabens is helpful.

Fan-shaped arrangements of smaller grabens are typical at the end of a larger graben. This pattern has been found to hold for many graben structures the world over by H. Cloos (1939). He has shown, moreover, that the main graben is located, at least during initial stages, in the center of a domal uplift, and that its fan-shaped splitting into smaller grabens occurs where it extends beyond the dome. He was able to reproduce this pattern experimentally. It is also plausible on more theoretical grounds (geometry of stress trajectories in ellipsoidal domal uplifts).

The lenticular mass (cushion) uplifting the dome was interpreted to be a magmatic intrusion at the base of the crust, and this picture has been corroborated by later geophysical investigations in many graben areas (e.g. Ramberg and Smithson, 1971; Ziegler, 1977; Ramberg and Spjeldnaes, 1978; Rhinegraben Research Group for Explosion Seismology, 1974; compare also Cook et al., 1979; Seager and Morton, 1978, Figure 7; Keller et al., 1979, Figure 6 for the Rio Grande rift). Under all these grabens the thickness of the crust is reduced by up to 10 km, and the subcrustal mass has physical properties that depend on the age of the rift. These properties correlate with a plausible cooling history of an intrusive mass, and with isostatic subsidence as inferred from the geological record. The latter is particularly complete and well documented for the North Sea rift system because of the search for oil (Ziegler, 1975, 1977, 1978a, 1978b). It demonstrates that where once there had been a dome due to isostatic uplift by a hot intrusive mass, there later developed a basin because of the cooling of this mass under a thinned-out crust. Whereas subcrustal



velocities in active rifts are typically about 7.4 - 7.8 km/sec (compare Smith, 1978, Figure 6-3) they exceed 8 km/s in subsided rift terrains (Ziegler, 1977, Figure 7).

The rifts in the highlands to the north of the Columbia Plateau have been inactive for about 40 my. The subcrustal velocity under the Columbia Plateau is 8.1 km/sec (Smith, 1978, Figure 6-3), and the central part of the Columbia Plateau has a crustal thickness (l.t. 25 km, Smith, 1978, Figure 6-2) that is about 10 km less than that of the surrounding highlands. The central part of the plateau has subsided with respect to sea level by probably more than 2 km since the initiation of rifting.

All these data combined - the geological record, the tectonics implied in the geometry of the grabens, the geophysical configuration and history - fit the model of an Eocene, central graben, now inactive, in the Pasco basin, centered over a region of thin crust.

This concept deserves consideration when interpreting the detailed gravity maps of Weston (1979). The gravity field reflects the superposition of effects arising from anomalous masses at various depths. The geological history and the resulting distribution of anomalous masses are exceedingly complex in the Columbia Plateau and it will not be possible to unambiguously separate all of their contributions to the gravity field. However, it should be noted that bands of steepened gravity gradients like EK and WM resemble that at the western border of the Oslo Graben (Ramberg and Smithson, 1971, Figure 1) which most probably originated at the base of the crust. The width of the belts (approximately 50 km and more) and the gravity step (50 - 90 - mg in the Oslo graben, 20 - 40 mgal for WM and EK) are of the same order. A rough estimate, neglecting all other contributions, shows that a step of less than 5 km in the Moho could produce the correct gravity effect (Nettleton, 1940, pages 112 and following). The width of the Pasco graben measured between mid-points of WM and EK is about 70 km. This is wider than the Rhine graben at the surface (40 km) but less than its low velocity cushion; it also compares well with the Oslo graben at the base of the crust (85 km) and the Rio Grande Rift (e.g. Reilinger et al., 1979; Kelley, 1979, Figure 1).

The southern end of the Pasco graben is the E-W gravity high extending westward through the Columbia River gap in the Cascades. It might have been an Eocene transform zone (sinistral) but speculation is moot at this time. Small branches of a southern graben fan are possibly the La Grande and John Day River gaps in the Blue Mountains gravity belt.\*

There are several possible mechanisms for this crustal thinning that are not mutually exclusive. Each mechanism may contribute to the total thinning, but by differing amounts.

\*Note: After completion of this report a draft for a report on "Determination of three-dimensional structure of eastern Washington from the joint inversion of gravity and earthquake travel time data" by RØDI et al. (1980) was brought to my attention. The authors point out the considerable freedom that exists in selecting a particular model (especially pp. 114 and following). So far as I can see the geological concepts here developed are compatible with the data used by the authors.

1. The crust is certainly stretched in a horizontal direction as established by the well-known normal faults, although by an order of magnitude too small to account for its geophysically established thinning (the models proposed by Lachenbruch and Sass; 1978, for B & R thinning do contribute little to thinning in the Rhine Graben, the North Sea Graben, and the Oslo Graben).
2. Uplift of the dome causes thinning by erosion; but in none of the examples cited and certainly not in the Rhine Graben, can erosion account for more than 1 or 2 km of crustal thinning.
3. Some process of "subcrustal erosion" can also contribute to crustal thinning. The domes are associated with elevated heat flow due to rising magma and this may conceivably lead to elimination of the lower crust, e.g., by stoping when it is still cool and brittle (Laubscher, 1975) or by lateral flow when it is hot and ductile (Sclater et al., 1979, see also Keen and Barrett, 1981). Such a mechanism could account for considerable thinning with modest stretching. Stretching could provide avenues for creeping masses of crystalline peridotite that might "delaminate" the lower crust and form laccoliths at some intermediate crustal level (compare Bird, 1979).

To summarize, the various avenues of reasoning make it appear plausible for the Columbia Plateau that;

1. It has a reduced thickness of continental crust and is not underlain by oceanic crust.



2. The top of the lithosphere (M) is peridotite, and the base of the seismic (not petrological) crust possibly serpentinite.
3. The nature of the crust does not change across OWL, or CLEW, though its thickness increases stepwise particularly along NW and EW trending steps.
4. The basal boundary conditions for the Yakima deformation are
  - a possible incompetent serpentinite layer at the base of the crust for potential decollement and
  - a stepwise changing level of the decollement surface causing stress concentration.
5. The strength of the potential decollement series is greatest where crustal thickness is greatest, i.e., in the frame surrounding CP.

15.1 DEEP STRUCTURE OF YAKIMA DEFORMATION: A COMPARISON OF CLEW WITH THE ANDES OF VENEZUELA (FIGURES 21 - 24)

Similar to CLEW, the Andes of Venezuela are thought to be the result of dextral strike-slip plus a compressional component (Rod, 1956; Schubert and Sifontes, 1970). Both components are on the order of tens of kilometers, perhaps twenty times those postulated for CLEW. A comparison provides some useful insights.

The overall structure of the Venezuelan Andes, based on surface drilling and geophysical data is given by Wittke (in: Bonini et al., 1977), see Figure 21. It shows a crustal thickness of 30 - 35 km. Apart from the faulting, there is a crustal fold consisting of a central high flanked by depressions. Total amplitude is slightly less than 20 km in the north and 10 km in the south (the structure is not quite symmetrical). The high is more pronounced than the lows; the latter amount to about 8 - 11 km in the north, and about 4 - 6 km in the south. The width of the positive raised part of the structure is about 70 km, or twice the crustal thickness, and the flanking depressions are slightly narrower (50 - 60 km, depending on position on the map).

By comparison CLEW (Figure 22) has an overall width of about 40 km, it is flanked by depressions about 30 km wide; however, because these depressions interfere with structures of comparable relief but different origin, their expression is not well defined (compare Figure 24.) The maximum



( )



structural relief on CLEW is about 1400 m positive and 1600 m negative (Bentley, personal communication) or about a tenth to a twentieth that of the Venezuelan Andes, comparable figures considering the relative amounts of movement in the Andes and along CLEW. CLEW should affect about 20 km of crust in comparison with the Andes, as indeed seems to be the case (Figure 23).

Without pushing the comparison too far, I think it supports the interpretation of the kinematics and deep structure of CLEW presented above. In contrast to the Andes, the minute deformation which competes with similar and stronger crustal structures, is barely visible on the detailed gravity map.

#### 16.1 CONCLUSIONS

Yakima deformation may be modeled qualitatively to semi-quantitatively within the conceptual framework of the IDOL (Idaho-Olympic) block mosaic, which is a submosiac of the Basin and Range province. This province in turn is the product of dextral-convergent interaction between the Pacific and North American Plates.

The IDOL submosiac, a NW trending belt, is the northern border zone of the Basin and Range province, and its structures exhibit the results of distributed dextral-convergent shear along its NW strike, slight dextral rotation, and approximately N-S compression (Yakima ridges) an EW extension or pull-apart (particularly Cascades faults, e.g. Hood River graben). This extension suggests decoupling of the Juan de Fuca subduction zone which should be slightly receding to the W in order to accommodate the B & R masses moving westward.

In the development of the Yakima structure three levels of decollement are apparent: asthenosphere, base of reduced crust, and base of Columbia River basalts. A ramp under the Blue Mountains connects the asthenosphere with the base of CP crust, and shallower ramps branch off the base-crust decollement zone to reach the base of the flood basalts under the Yakima ridges where they produce folding by partial detachment.

The time sequence seems to be:

1. The lithospheric break at the NW-SE trending Cle Elum-Wallula Gap belt (CLEW) with slight dextral convergent displacement and the formation of broad, gentle, periodic en echelon brachyanticlines (NE border zone of Yakima block).

The lithospheric break starting from the Hood River graben in the SW in a northeasterly direction to join CLEW at Cleman Mountain-Kelly Hollow (HOOK). This break is a branch of a general pull-apart zone in the Cascades and is the NW border of the Yakima block.

2. After slight initial motion along its lithospheric boundaries the Yakima block got stuck and internal compression built up to produce the decollement-ramp-fold system of the Yakima ridges, beginning in the south and propagating northward. The first ridges developed within the block boundaries which were used as lateral rails for the decollement sheet; they exhibit the same periodicity as the broad en echelon folds on CLEW and may have been nucleated by them. During later stages decollement spread beyond the block boundaries, guided by Eocene graben tectonics now hidden by the Columbia River basalts. Some motion may still continue today, particularly in the northern folds. The total amount of motion for the last 5 my or so is very small (probably less than 5 km).

The special tectonic behavior of the Columbia Plateau may be correlated with its special crustal structure for which gravity and seismic data combined with regional geologic history suggests an Eocene origin. At that time a graben complex was formed with thermal activity that caused uplift and stretching (thinning) of the crust. After cooling the area subsided, providing the basin for the accumulation of the Yakima basalts. The base of the thin crust may be serpentine which would be suitable for decollement.



17.1 REFERENCES

Angelier, J., and Le Pichon, X., 1980, La Subduction Hellénique et l'expansion tégénne: Reconstitution Cinématique et Interprétation Dynamique: C. Rapport Sommaire, Societe Géologique de France, Fasc. 5, p. 158-161.

Armstrong, R. L., 1978, Cenozoic Igneous History of the U. S. Cordillera From Latitude 42° to 49°N Latitude, in Smith, R. B. and Eaton, G. P., eds., Cenozoic Tectonics and Regional Geophysics of the Western Cordillera: Geological Society of America Memoir 152, p. 265-282.

Bally, A. W., Gordy, P. L. and Stewart, G. A., 1966, Structure, Seismic Data, and Orogenic Evolution of Southern Canadian Rocky Mountains. Bulletin of Canadian Petroleum Geology, v. 14, p. 337-381.

Beck, Myrtle, Jr. and Burr, C. D., 1979, Paleomagnetism and Tectonic Significance of the Goble Volcanic Series, Southwestern Washington. Geology, v. 7, no. 4, p. 175-179.

Bentley, R. D., 1977, Stratigraphy of the Yakima Basalts and Structural Evolution of the Yakima Ridges in the Western Columbia River Plateau: Guide book, Geological Society of America Annual Meeting, Seattle.

Blackwell, D. D., 1978, Heat flow and Energy Loss in the Western United States, in Smith, R. B. and Eaton, G. P., eds., Cenozoic Tectonics and Regional Geophysics of the Western Cordillera: Geological Society of America Memoir 152, p. 175-208.

Bonini, W., Pimstein de Gaete, C., Graterol, V., 1977, Mapa de Anomalías Gravimétricas de Bouguer de la Parte Norte de Venezuela y áreas Vecinas: Republica de Venezuela, Ministerio de Energia y Minas, Direccion de Geologia, Caracas, Scale 1:1,000,000.

Charlesworth, H. A. K., 1961, Some observations on Deformation, Crustal Shortening, and Uplift in the Canadian Rocky Mountains. Journal of the Alberta Society of Petroleum Geologists, v. 9, p. 225-.

Clayton, D. N., and Miller, R., 1977, Geologic Studies of the Southern Continuation of the Straight Creek Fault, Snoqualmie Area, Washington. Shannon and Wilson, Inc.

Cloos, H., 1939, Hebung - Spaltung - Vulkanismus: Geologische Rundschau, v. XXX, Zwischenheft 4A, Ferdinand Enke Verlag, Stuttgart.

Coney, P. J., 1978, Mesozoic - Cenozoic Cordilleran Plate Tectonics, in Smith, R. B. and Eaton, G. P., eds., Cenozoic Tectonics and Regional Geophysics of the Western Cordillera: Geological Society of America Memoir 152, p. 33-50.

Cook, F. A., McCullar, D. B., Decker, E. R., Smithson, S. B., 1979, Crustal Structure and Evolution of the Southern Rio Grande rift, in Riecker, R. E., ed., Rio Grande Rift: Tectonics and Magmatism: American Geophysical Union, Washington, D.C., p. 195-208.

Danes, Z. F., Bonno, M., Brau, E., Gilham, W. D., Hoffman, T. F., Johansen, D., Jones, M. H., Malfait, B., Masten, J., and Teague, G. O., 1965, Geophysical Investigation of the Southern Puget Sound Area, Washington. Journal of Geophysical Research, v. 70, no. 22, p. 5573-5580.

Davis, G. A., 1977, Tectonic Evolution of the Pacific Northwest, Precambrian to Present. WNP-1/4 Preliminary Safety Analysis Report, Amendment 23, Vol. 2A, Subappendix 2RC.

Davis, G. A., Monger, J. W. H., and Burchfiel, B. C., 1978, Mesozoic Construction of the Cordilleran "collage", Central British Columbia to Central California, in Howell, D. G. and McDougall, K. A., eds., Mesozoic Paleogeography of the Western United States: Society of Economic Paleontologists and Mineralogists, Pacific Section, Pacific Coast Paleogeography Symposium no. 2, p. 1-32.

Eaton, G. P., 1979, A Plate-Tectonic Model for Late Cenozoic Crustal Spreading in the Western United States, in Riecker, R. E., ed., Rio Grande Rift: Tectonics and Magmatism: American Geophysical Union, Washington D.C., p. 7-32.

Emmons, R. C., 1969, Strike-slip Rupture Patterns in Sand Models, Tectonophysics, v. 7, no. 1, p. 71-87.

Habicht, K., 1945, Geologische Untersuchungen im Sudlichen Sanktgallisch-appenzellischen Molassegebiet: Beitrage Zur Geologischen Karte der Schweiz, Neue Folge 83.

Hammond, P. E., 1979, A Tectonic Model for Evolution of the Cascade Range, in Amentrout, J. M., Cole, M. R. and Ter Best, Harry, Jr., Cenozoic Paleogeography of the Western United States: Society of Economic Paleontologists and Mineralogists, Pacific Section, Pacific Coast Paleogeography Symposium no. 3, p. 219-237.

Harding, T. P., 1973, Newport-Inglewood Trend, California - An Example of Wrenching Style of Deformation: American Association of Petroleum Geologists Bulletin, v. 57, no. 11, p. 97-116.

Harding, T. P. and Lowell, J. D., 1979, Structure Styles, Their Plate-tectonics Habitats, and Hydrocarbon Traps in Petroleum Provinces: American Association of Petroleum Geologists Bulletin, v. 63, no. 7, p. 1016-1058.

Hildebrand-Mittlefehldt, N., 1979, Deformation Near a Fault Termination, Part I: a Fault in a Day Experiment: Tectonophysics, v. 57, p. 131-150.

Hill, D. P., 1978, Sesimic Evidence for the Structure and Cenozoic Tectonics of the Pacific Coast States, in Smith R. B. and Eaton, G. P., eds., Cenozoic Tectonics and Regional Geophysics of the Western Cordillera: Geological Society of America Memoir 152, p. 145-174.

Keen, C. E. and Barrett, D. L., 1981, Thinned and Subsided Continental Crust on the Rifted Margin of Eastern Canada: Crustal Structure, Thermal Evolution and Subsidence History: Geophysical Journal of the Royal Astronomical Society, v. 65, no. 2, p. 443-466.

Keller, G. R., Braile, L. W., and Schlue, J. W., 1979, Regional Crustal Structure of the Rio Grande Rift From Surface Wave Dispersion Measurements, in Riecker, R. E., ed., Rio Grande Rift: Tectonics and Magmatism: American Geophysical Union, Washington, D.C., p. 115-126.

Kelley, V. C., 1979, Tectonics, Middle Rio Grande Rift, New Mexico, in Riecker, R. E., ed., Rio Grande Rift: Tectonics and Magmatism: American Geophysical Union, Washington, D. C., p. 57-70.

Kienle, C. F., Jr., Bentley, R. D., and Anderson, J. L., 1977, Geologic Reconnaissance of the Cle Elum-Wallula Lineament and Related Structures, Shannon & Wilson, Inc.



Lachenbruch, A. H., and Sass, J. H., 1978, Models of an Extending Lithosphere and Heat Flow in the Basin and Range Province, in Smith, R. B. and Eaton, G. P., eds., *Cenozoic Tectonics and Regional Geophysics of the Western Cordillera*: Geological Society of America Memoir 152, p. 209-250.

Laubscher, H. P., 1965, Ein Kinematisches Modell der Juraufaltung. *Eclogae Geologicae Helveticae*, v. 58, no. 1, p. 232-318.

Laubscher, H. P., 1973, Jura Mountains, in De Jong, K. A. and Scholten, R., eds., *Gravity and Tectonics*: John Wiley & Sons, Inc., New York, N. Y., p. 217-227.

Laubscher, H. P., 1975, Plate Boundaries and Microplates in Alpine History: *American Journal of Science*, no. 275, p. 856-876.

Laubscher, H. P., 1977, Fold Development in the Jura: *Tectonophysics*, v. 37, p. 337-362.

Laubscher, H. P., 1981, The 3D Propagation of D<sup>-</sup>collement in the Jura, in McClay, K. R. and Price, N. J., eds., *Thrust and Nappe Tectonics*, p. 311-318.

Lawrence, R. D., 1976, Strike-slip Faulting Terminates the Basin and Range Province in Oregon: *Geological Society of America Bulletin*, v. 87, no. 6, p. 846-850.

McGill, G. E. and Stromquist, A. W., 1979, The Grabens of Canyon Lands National Park, Utah: *Geometry, Mechanics and Kinematics*.

Newcomb, R. C., 1970, Tectonic Structure of the Main Part of the Basalt of the Columbia River Group, Washington, Oregon, and Idaho: U. S. Geological Survey Miscellaneous Investigations Map I-587, Scale 1:500,000.

Nettleton, L. L., 1940, *Geophysical Prospecting for Oil*, McGraw-Hill Book Co., Inc., New York, N. Y., 444 p.

Paterson, M. S., and Weiss, L. E., 1966, Experimental Deformation and Folding in Phyllite: *Geological Society of America Bulletin*, v. 77, no. 4, p. 343-374.

Price, R. A., 1979, Intracontinental Ductile Crustal Spreading Linking the Fraser River and Northern Rocky Mountain Trench Transform Fault Zones, South-central British Columbia and Northeast Washington: Geological Society of America Abstracts with Programs, v. 11, no. 7, p. 499.

Price, R. A., 1981, The Cordilleran Foreland Thrust and Fold Belt in the Southern Canadian Rocky Mountains, in McClay, K. R. and Price, N. R., Eds., 1981, Thrust and Nappe Tectonics, p. 427-448.

Raisz, E., 1945, The Olympic-Wallowa lineament: American Journal of Science, v. 243-A, p. 479-485.

Ramberg, I. B., and Smithson, S. B., 1971, Gravity Interpretation of the Southern Oslo Graben and Adjacent Precambrian Rocks, Norway, Tectonophysics, v. 11, p. 419-431.

Ramberg, I. B., and Spjeldnaes, N., 1978, The Tectonic History of the Oslo Region, in Ramberg, I. B. and Neumann, E. R., eds., Tectonics and Geophysics of Continental Rifts: NATO Advanced Study Institutes Series, Series C, v. 37, D. Reidel Publishers, Dordrecht, Holland/Hingham, Mass., p. 167.

Reilinger, R. E., Brown, L. D., and Oliver, J. E., 1979, Recent Vertical Crustal Movements from Leveling Observations in the Vicinity of the Rio Grande Rift, in Riecker, R. E., ed., Rio Grande Rift: Tectonics and Magmatism: American Geophysical Union, Washington, D.C., p. 223-236.

Rich, J. L., 1943, Mechanics of Low-angle Overthrust Faulting as Illustrated by Cumberland Thrust-block, Kentucky and Tennessee: American Association of Petroleum Geologists Bulletin, v. 18, p. 1584-1590.

Riddiough, R. P., 1978, The Juan de Fuca Plate: American Geophysical Union Transactions v. 59, no. 9, p. 836-842.

Robyn, T. L., 1977, Geology and Petrology of the Strawberry Volcanics, NE Oregon: Ph.D. Dissertation, University of Oregon, 197 p.

Rod, E., 1956, Strike-slip Faults of Northern Venezuela: American Association of Petroleum Geologists Bulletin, v. 40, p. 457-476.

Rodgers, J. D., 1949, Evolution of Thought on Structure of Middle and Southern Appalachians: American Association of Petroleum Geologists Bulletin, v. 33, p. 1643-1654.

Rodi, W. L., Jordan, T. H., Masso, J. F., and Savino, J. M. 1980, Determination of Three-dimensional Structure of Eastern Washington From Joint Inversion of Gravity and Earthquake Travel Time Data. Report submitted to Weston Geophysical Corporation, Systems, Science and Software Project no. 44094.

Roeder, D., and Witherspoon, W. D., 1978, Palinspastic Map of East Tennessee: American Journal of Science, v. 278, p. 543-550.

Royse, F., Jr., Warner, M. A., and Reese, D. L., 1975, Thrust Belt Structural Geometry and Related Stratigraphic Problems, Wyoming-Idaho-Northern Utah, in Bolyard, D. W., ed., Symposium on Deep Drilling in the Central Rocky Mountains: Rocky Mountain Association of Geologists, p. 41-54.

Schubert, C., and Sifontes, R. C., 1979, Bocano Fault, Venezuelan Andes, Evidence of Post-glacial Movement: Science. v. 170, p. 66-69.

Sclater, J. G., and Christie, P. A. F., 1980, Continental Stretching: an Explanation of the Post-mid-Cretaceous Subsidence of the Central North Sea Basin: Journal of Geophysical Research, v. 85, no. B7, p. 3711-3739.

Seager, W. R., and Morgan, P., 1979, Rio Grande Rift in Southern New Mexico, West Texas, and Northern Chihuahua, in Riecker, R. E., ed., Rio Grande Rift: Tectonics and Magmatism: American Geophysical Union, Washington, D.C., p. 87-106.

Shannon & Wilson, Inc., 1973, Geologic Studies of Columbia River Basalt Structures and Age of Deformation, The Dalles - Umatilla Region, Washington and Oregon: Report to Portland General Electric Company.

Shannon & Wilson, Inc., 1978, WNP 1/4 Preliminary Geologic Map W-2685-39, for Washington Public Power Supply System.

Simpson, R. W. and Cox, A., 1977, Paleomagnetic Evidence for Tectonic Rotation of the Oregon Coast Range: Geology, v. 5, p. 585-589.



Smith, R. B., 1978, Seismicity, Crustal Structure and Intraplate Tectonics of the Interior of the Western Cordillera, in Smith, R. B. and Eaton, G.P., eds., Cenozoic Tectonics and Regional Geophysics of the Western Cordillera: Geological Society of America Memoir 152, p. 111-144.

Smithson, S. B., Brewer, J. A., Kaufman, S. Oliver, J. E., and Hurich, C. A., 1979, Structure of the Laramide Wind River Uplift, Wyoming, from Cocorp Deep Reflection Data and from Gravity Data: Journal of Geophysical Research, v. 84, no. B11, p. 5955-5972.

The Rhinegraben Research Group for Explosion Seismology, 1974, The 1972 Seismic Refraction Experiment in the Rhinegraben - First Results, in Illes, J. H. and Fuchs, K. eds., Approaches to Taphrogenesis: Inter-Union Commission on Geodynamics, Scientific Report no. 8, p. 122-137.

Thompson, R. I., 1981, The Nature and Significance of Large 'Blind' Thrusts Within the Northern Rocky Mountains of Canada, in McClay, K. R. and Price, N. J., eds., Thrust and Nappe Tectonics, p. 449-462.

U. S. Geol. Survey Professional Paper 1100, Geological Survey Research, 1978, p. 68 & 78.

Washington Public Power Supply System, 1977, WNP 1/4 Preliminary Safety Analysis Report, Amendment 23, Vol. 2B, Subappendix 2RH.

Weston Geophysical Research, Inc., 1979, Compilation and Interpretation of Gravity in the Vicinity of the Hanford Area, Washington and Oregon: Interim report for Washington Public Power Supply System.

Wilcox, R. E., Harding, T. P., and Seely, D. R., 1973, Basic Wrench Tectonics: American Association of Petroleum Geologists Bulletin, v. 57, no. 1, p. 74-96.

Ziegler, P. A., 1975, Geologic Evolution of North Sea and its Tectonic Framework, American Association of Petroleum Geologists Bulletin, v. 59, no. 7, p. 1073-1097.

Ziegler, P. A., 1977, Geology and Hydrocarbon Provinces of the North Sea, Geojournal 1.1, p. 7-32.

Ziegler, P. A., 1978a, North Sea Rift and Basin Development, in Ramberg, I.B. and Neumann, E.R., eds., Tectonics and Geophysics of Continental Rifts: Proceedings of the NATO Advanced Study Institute Paleorift Systems with Emphasis on the Permian Oslo Rift, Oslo, July 27-August 5, 1977, NATO Advanced Study Institute Series C, v. 37, p. 249-277.

Ziegler, P. A., 1978b, North-Western Europe: Tectonics and Basin Development: Geologie en Mijnbouw, v. 54, no. 4, p. 589-626.

TABLE 2.5-0-3FIGURE CAPTIONS

Figure 1: The Cenozoic kinematics of the Pacific NW, from Eaton (1979). Elements of Columbia Plateau deformation added.

- (a) Period 30 - 20 my b.p. (up Oligocene). Widespread rifting in the south, associated with compressional tectonics and dextral strike-slip in the north: the Straight Creek-Kachess-Naches-Blue Mountains system (added).
- (b) Period 20 - 10 my b.p. (Lower and Middle Miocene). Main extensional period of B & R. Extension spreads northward into the Columbia Plateau; feeder dykes for the CR basalts (dotted).
- (c) Period 10 - 0 my b.p. Rifting in the B & R continues but main activity is shifted to new zones (e.g. Intermountain Seismic Belt). The pole for dextral rotation and spreading shifts towards the Helena-Yellowstone area.
- (d) and (e) Present: If the Rio Grande rift and the Eastern Snake River plain are accepted as "spreading ridges" or sources of material transport, then a rotation pole somewhere in Manitoba results. Masses drifting away from the ridges move to the Pacific Northwest and there are, dependent on the direction of faults, dextrally compressed. In (d) a former model (see Davis, 1977) for Yakima deformation in this context is shown; it resembles the situation of period (a). In (e), the model developed in this report is sketched: the deformation of the Yakima block (Y, dotted) is embedded in a block mosaic that permits matter moving from the spreading centers to the NW to escape laterally upon the decoupled Juan de Fuca (Cascades) subduction zone by distributed dextral shear. As discussed in the report, dextral shear is associated with pull-apart along some block boundaries and compression along others. Although rigid rotation as envisaged in Figure 1 is considered an oversimplifica-





FIGURE CAPTIONS (Continued)

tion, it nevertheless provides an overall kinematic model. Dynamically, the dextral couple driving rotations is attributed to the dextral plate interaction between the Pacific and North American Plates. However, no detailed analysis is given.

Figure 2: Experimental extensional block mosaic, after McGill and Stromquist (1979). Compare Figure 9.

Distributed shear zones bounding the moving mass are shaded. In the Pacific Northwest, space for the westward moving masses may be provided by a receding Juan de Fuca subduction zone. For another example of a receding subduction see Angelier and Le Pichon (1980; the Cretan arc in the Mediterranean).

Figure 3: Elements of rigid block motion, from Laubscher (1965), map view.

This Figure illustrates the essence of material balance in the map view (a) superposition of translation and rotation; (b) translation with dextral shear boundary on the right and an obliquely convergent, or compressive sinistral, or transpressive sinistral boundary on the left. In the Pacific Northwest, the surroundings of the moving block are composed of other moving blocks (block mosaic) instead of being a fixed reference frame as in Figure 3.

Figure 4: Elements of decollement Kinematics, cross-section, from Laubscher (1965).

Material balance for the simple case of plane deformation of a rectangular mass on a basal decollement horizon.

Figure 5: "Flower-structure" in a wrench fault zone, from Harding and Lowell (1979).

An important aspect of this type of deformation is that the faults branching off from the stem tend to terminate blindly in the subsurface, often at places where an interval is split (M<sub>sp</sub>), with horizons on the two sides of the fault diverging. Kinematically, wedges bounded by the blind thrusts below and bedding parallel slip above are required in order to fill the space provided by the diverging horizons. In three dimensions, the faults are curved and form an anastomosing complex ("reticulation").

FIGURE CAPTIONS (Continued)

Figure 12: A cut-paper kinematic model of rigid-body Yakima tectonics.

The arrow shows the direction of translation. In contrast to Figures 15 and 16 deformation is shown to begin in the north. Amounts of movement exaggerated (about 10 times).

(a) Manastash Umtanum: The CLEW boundary is dextral covergent with respect to translation. In order to eliminate shortening at Wallula gap (right margin) small dextral rotations are added. (b) Yakima, (c) Rattlesnake Hills, (d) Toppenish, Horse Heaven and Columbia Hills.

Figure 14: Kinematics of the IDOL block belt.

Heavy arrows are translational vectors with respect to the North American Plate (NA) of idealized rigid blocks comparing the mosaic (scale in YA-8). Dashed arrows are translational vectors of neighboring blocks. Thin lines are difference vectors. The differences cause boundary zone deformations. (a) Starting point is a 3 km NNW translation of YA-8 with respect to NA, and relative motions with respect to NA are crudely estimated. A divergent transport field results with approximately NS shortening, EW extension, and dextral shear in the western part. The mosaic ought to be refined, but this is not warranted by the data. Improved modifications of this basic pattern would involve rotations of subblocks, individual blocks and block groups (compare Figure 12). (b) As explained in the text, the Yakima folds are believed to be decollement features not involving the lithosphere except south of the Blue Mountains where the fold-thrust-decollement system is believed to ramp through the lithosphere into the asthenosphere. Consequently, the Yakima block is subdivided into a southern lithospheric block YA-8 whose leading edge are the decollement features of the Columbia Plateau, and a northern lithospheric block YA-8a which was not subject to the 3 km NNW translation of YA-8.

Inasmuch as there seems to be some dextral lithosphere motion on CLEW (Figure 15, stage 1), a NW-directed translation of YA-8a is added, and the vectors of the surrounding blocks are adjusted. The amount of dextral lithospheric motion at CLEW is believed not to exceed 2 km in view of the embryonic deformation observed. The difference vectors between YA-8a and the surrounding blocks imply a pull-apart of slightly more than 2 km between HOOK and HS-WR (compare the Hood River graben). It is these pull-apart features that may provide space for the decollement sheet overlying YA-8a to move laterally into.



FIGURE CAPTIONS (Continued)

The cross-hatched boundary zones separate domains of additional 2 km lithospheric NW translation (in the SW) and the groups of blocks not affected by YA-8 compression (YA-8a, MA-16, MR 17, 17a) but instead subjected to pull-apart. This extension across N-S striking faults is characteristic of the Cascades where it provides avenues for magmatic activity: it is more widespread than shown in this simplified model (compare also S I).

The IDOL mosaic is a sub-mosaic (north-western boundary zone) of the BR mosaic and should be adjusted to its constraints. This may require modification particularly of the eastern blocks.

Figure 15: Map view of kinematic development in the western Columbia Plateau (Yakima folds).

For each stage structures formed in the preceding stage are shown in blue, new structures in red (including reactivated lateral boundaries). The main folds and faults are outlined in a simplified fashion, zones of steepening by double lines. Structures taken directly from Shannon & Wilson are in black. The writer has tried to coordinate field observations supplied by Shannon & Wilson (not necessarily their map symbols, which are already an interpretation), topographic and geophysical data for a kinematically plausible interpretation.

Figure 21: A deep crustal section through the Venezuelan Andes (Wittke, 1977).

Similarly to subduction zones, the lithosphere is bent down while the crust is arched up. The crustal high is flanked by marginal basins. The structural interpretation by Wittke does not portray the complex pattern of faulting observed at the surface, nor the kinematics inferred on several lines of evidence (compare Figure 23 with "Flower structure" as in Figure 5).

Figure 22: CLEW, simplified as a small-amplitude crustal fold.

The flanking lows are so shallow that they are barely distinguishable on the background of deformations of comparable or greater intensity (compare Figure 24). The down-fold of M is not observable at the present level of seismic information; it would be on the order of the



FIGURE CAPTIONS (Continued)

kilometer, and would be superposed on irregularities of M on the order of 5 - 10 km due to Eocene crustal thinning and subsequent events.

Figure 23: A superposition of Figures 21 and 22.

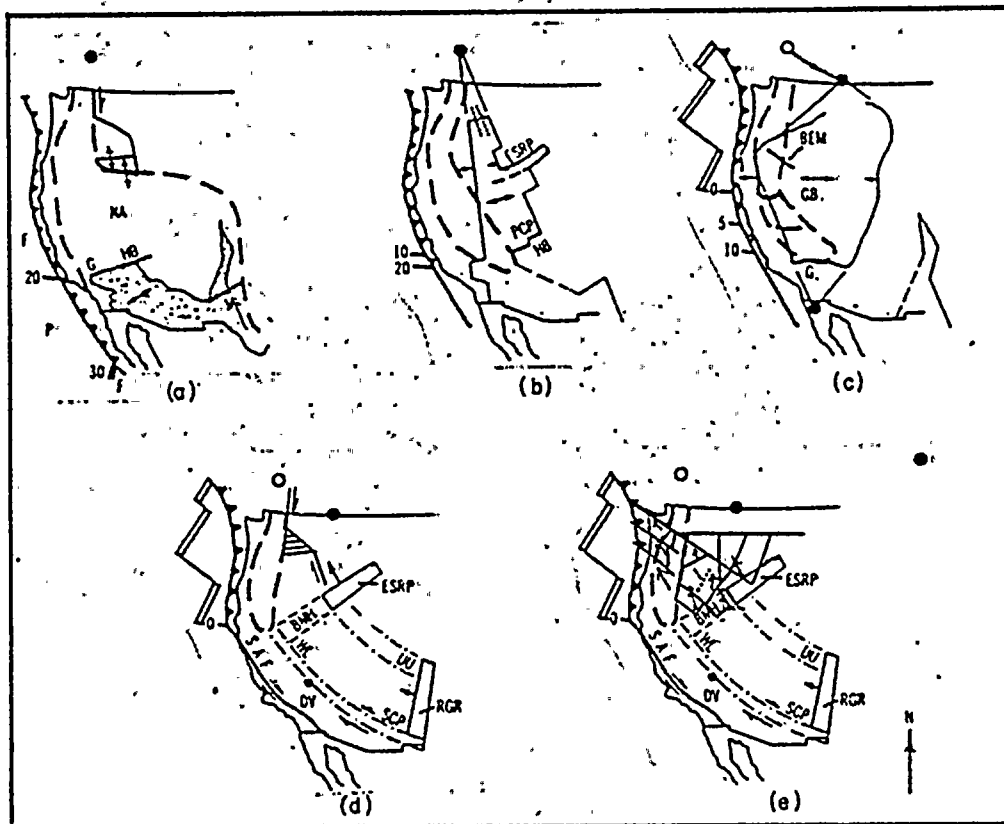
It illustrates the basic geometrical similarity in spite of differences in scale. Flower structure of faulting in Andean crust added.

Figure 24: CLEW crustal upfold and flanking downfolds.

The Yakima ridges become narrow dams where they cross depressed areas on both sides of CLEW. Although these flanking lows are modest features in an area of complex crustal development, they are nonetheless striking enough to demand an explanation.

21



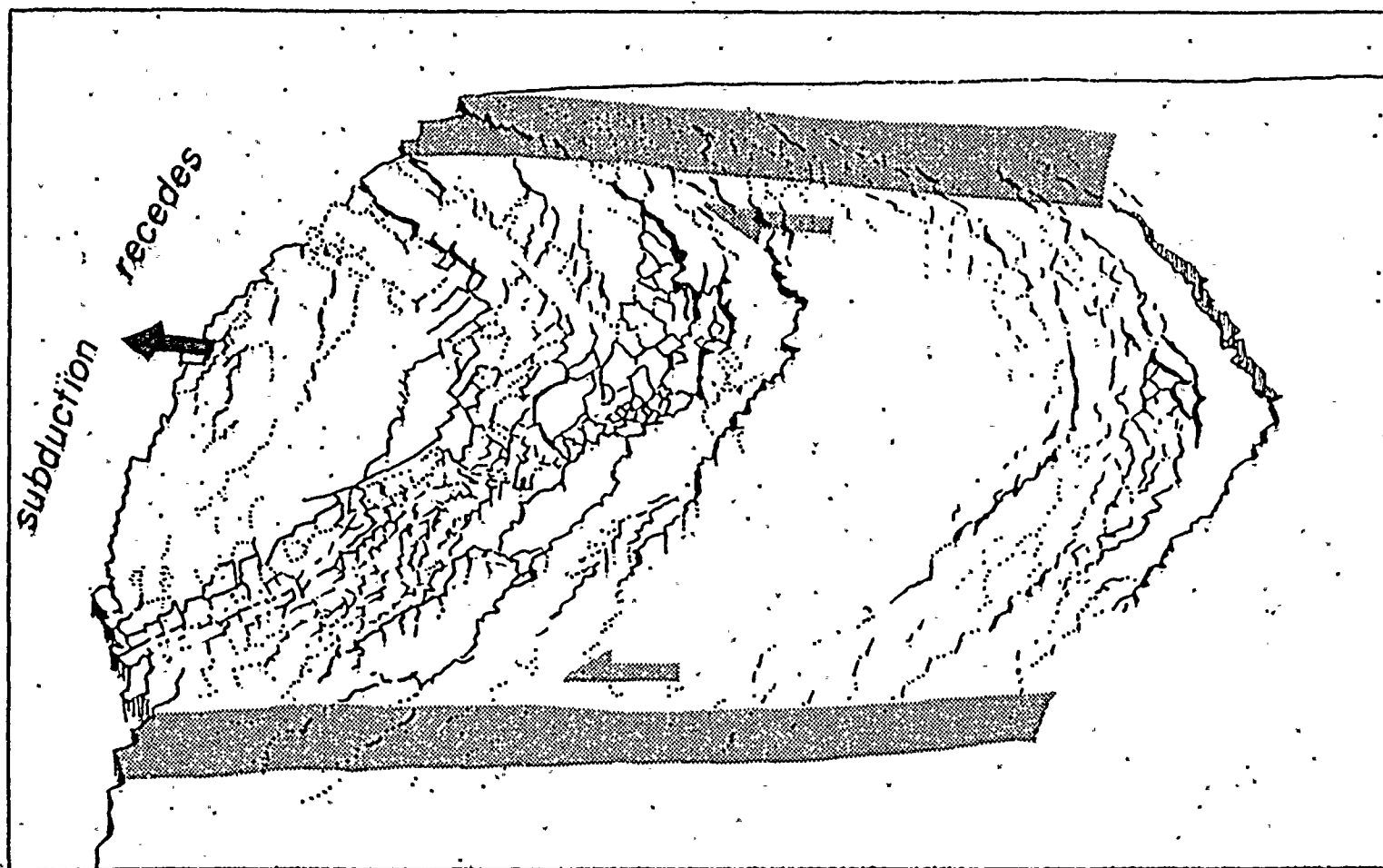


The Cenozoic kinematics of the Pacific NW, from Eaton (1979).  
Elements of Columbia Plateau deformation added.

Figure 1

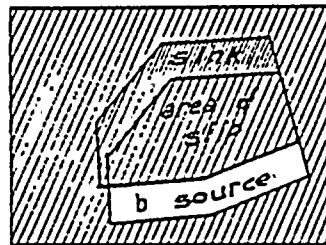
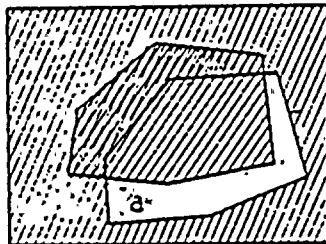






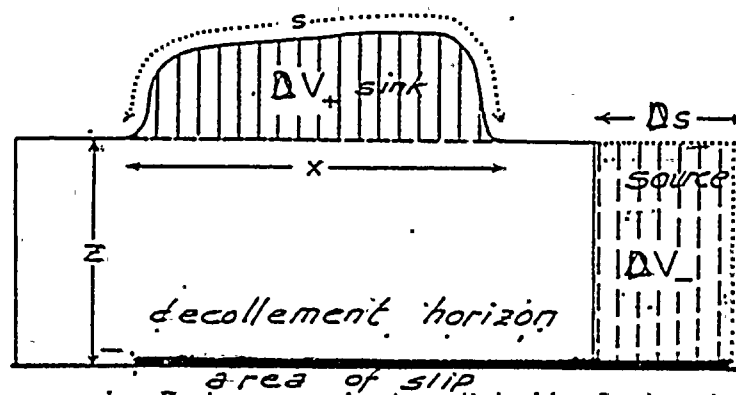
Experimental extensional block mosaic, after McGill and Stromquist (1979). Compare Fig. 9,

Figure 2



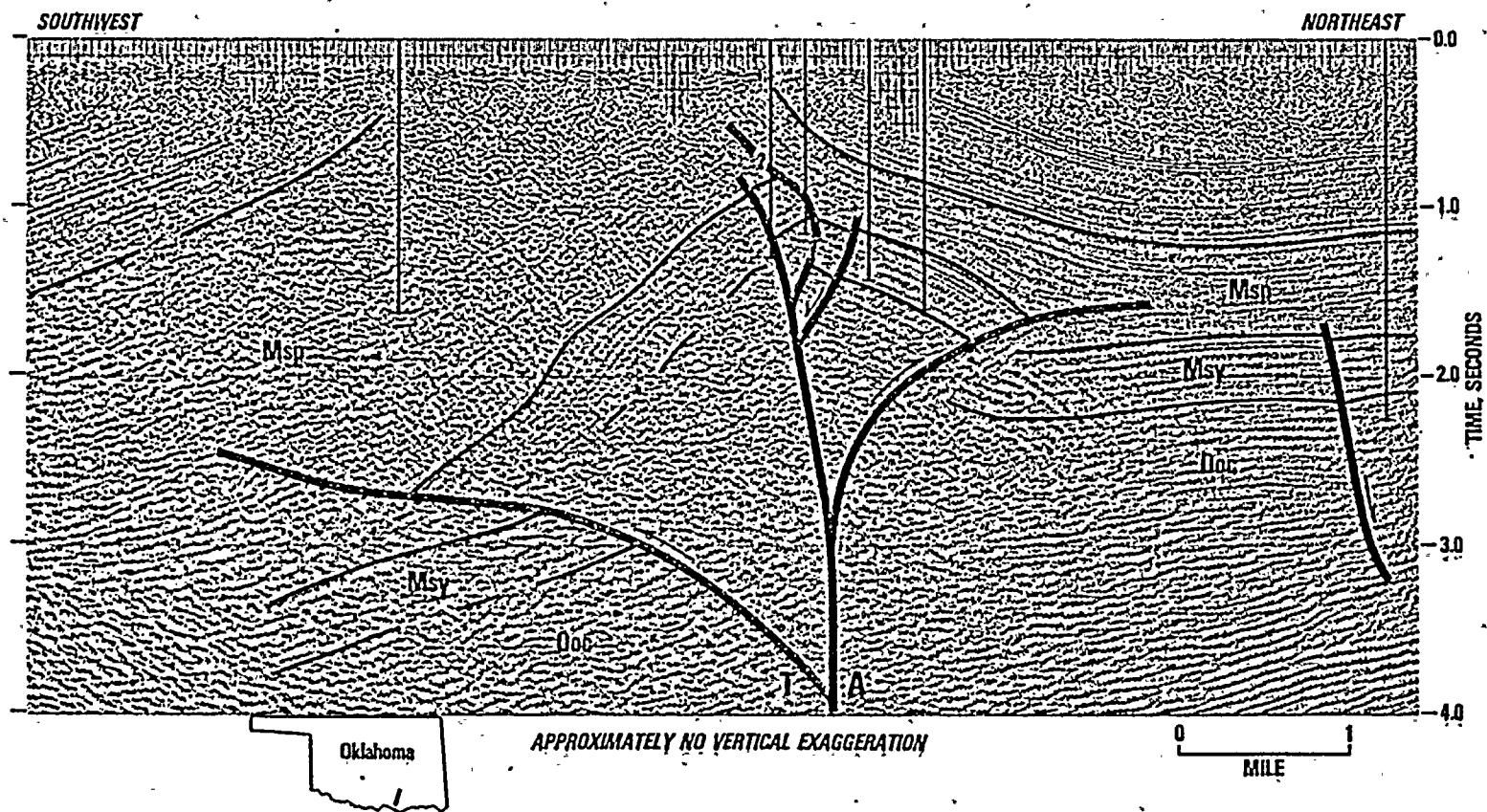
Elements of rigid block motion,  
from Laubscher (1965), map view.  
Figure 2.5 O-3





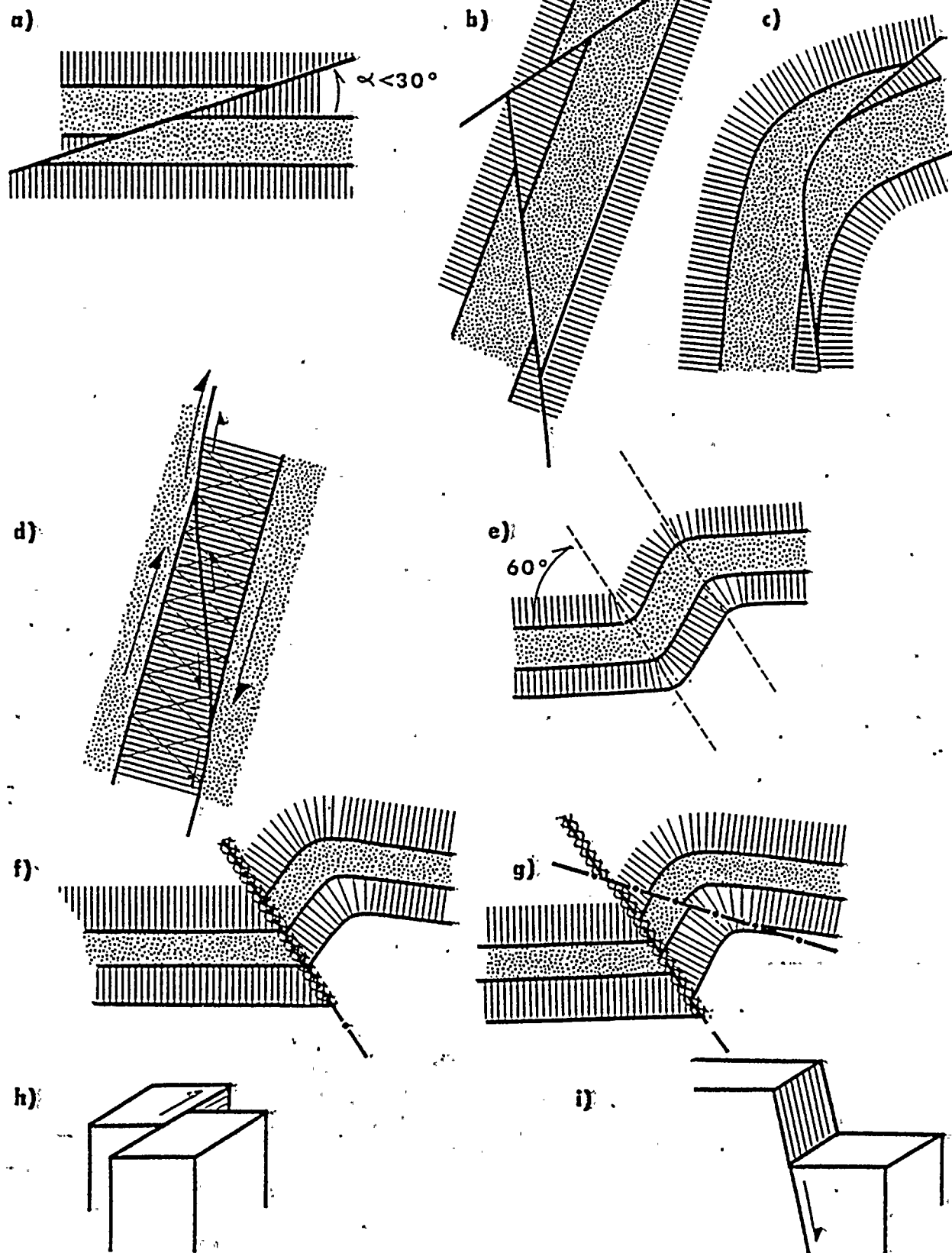
Elements of decollement kinematics,  
cross-section, from Laubscher (1965).  
Figure 2.5 O-4





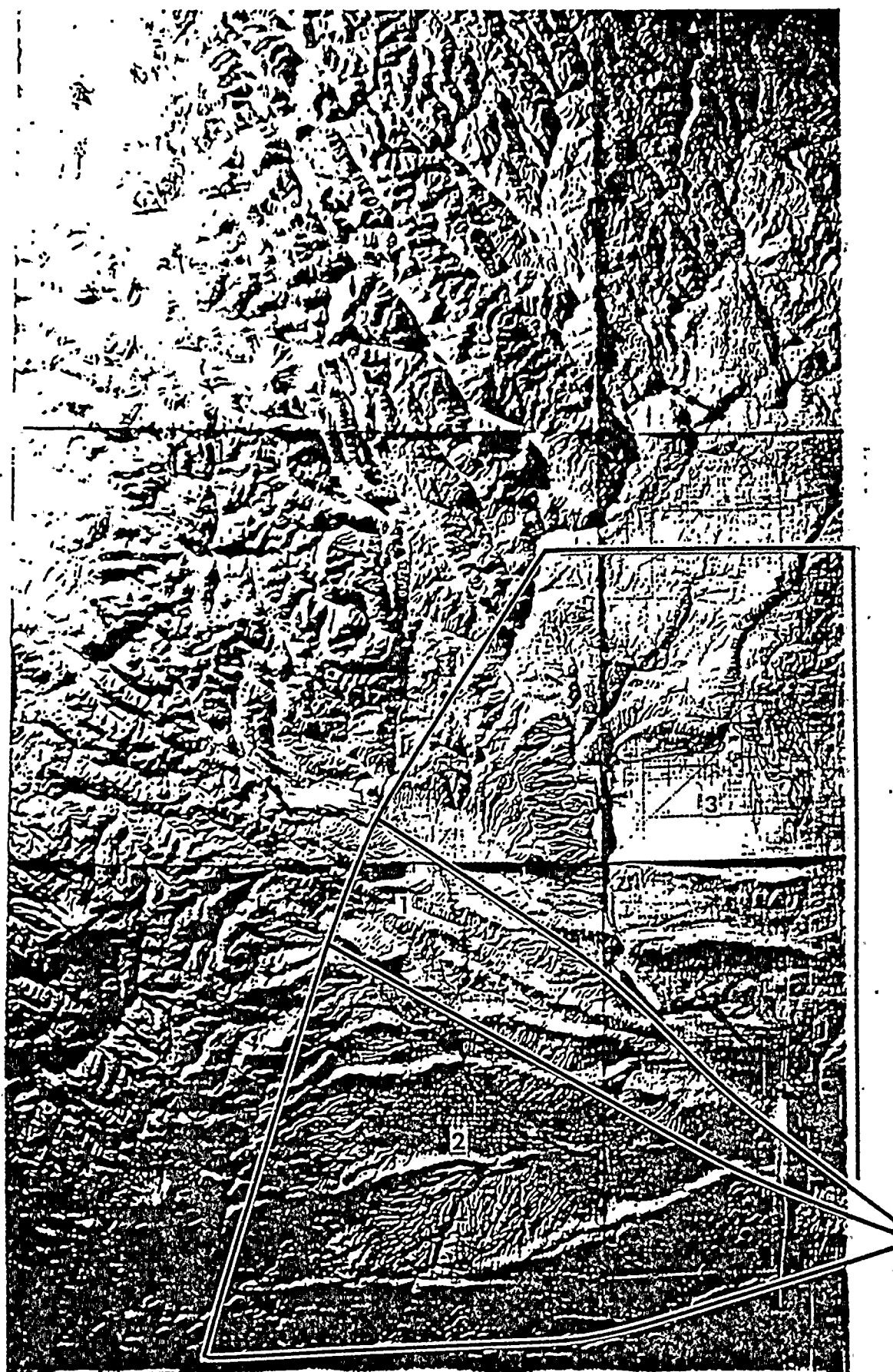
Migrated seismic profile across wrench-fault zone in Ardmore basin of Oklahoma demonstrating flower-structure geometry (adapted from unmigrated interpretation by R. F. Gregory and E. C. Lookabaugh, 1973). *Msp*, Mississippian Springer, *Msy*, Mississippian Sycamore, and *Ooc*, Ordovician Oil Creek reflectors. *T*, displacement toward viewer, *A* away from viewer.

"Flower-structure" in a wrench fault zone, from Harding and Lowell (1979).



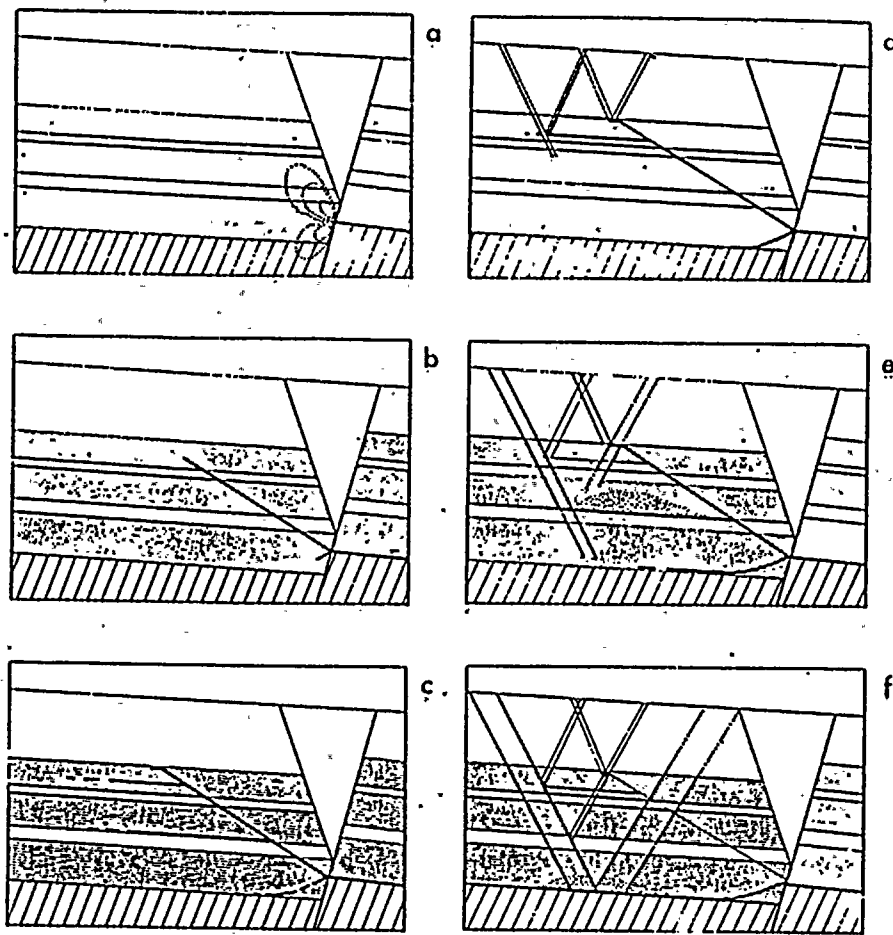
Small-scale structure in the Columbia Plateau Floods.  
Dotted: interflow layers.



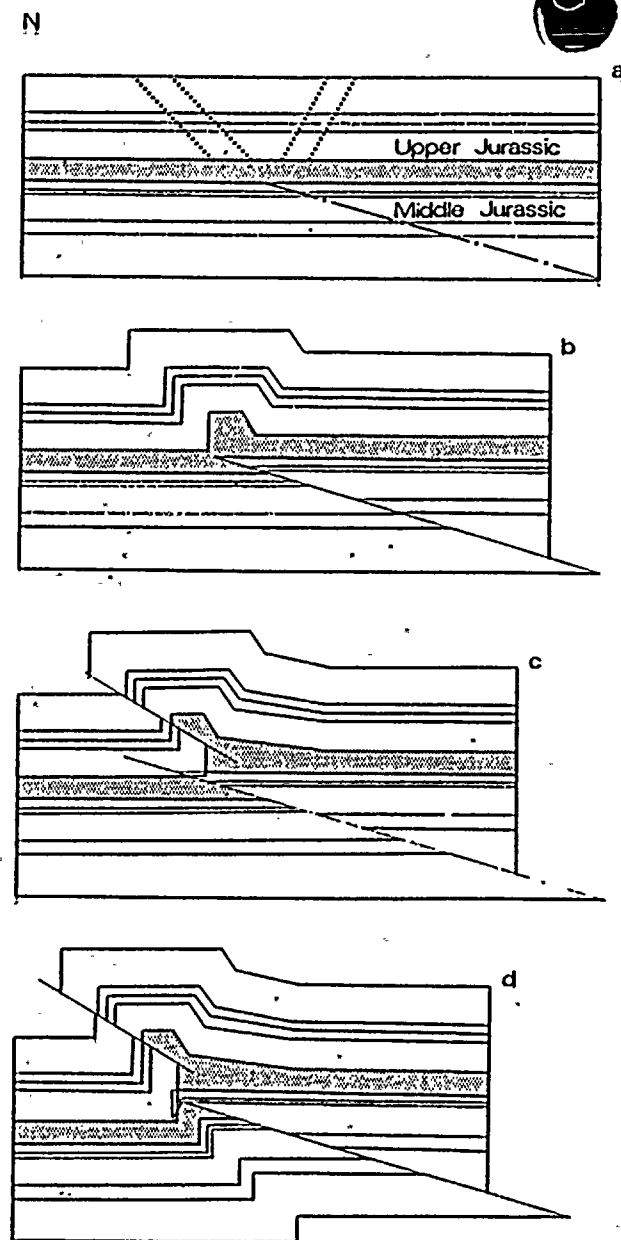


Plastic relief map of the western Columbia Plateau and the adjacent highlands.



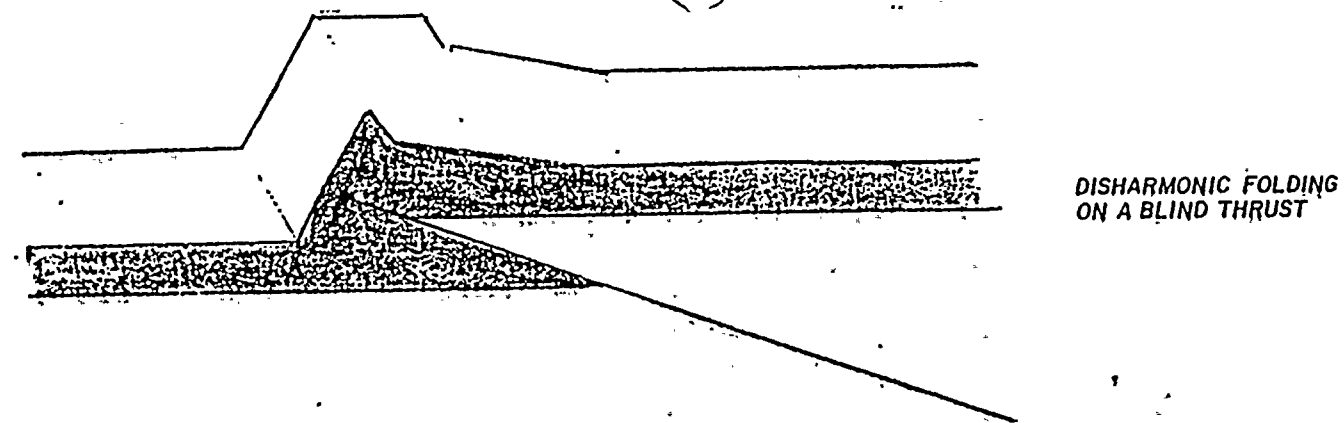


Stages in the spreading of static instabilities, Sprüsel structure. Heavy lines: décollement and thrusting. Double lines: kink bands. The main incompetent intervals are shaded.

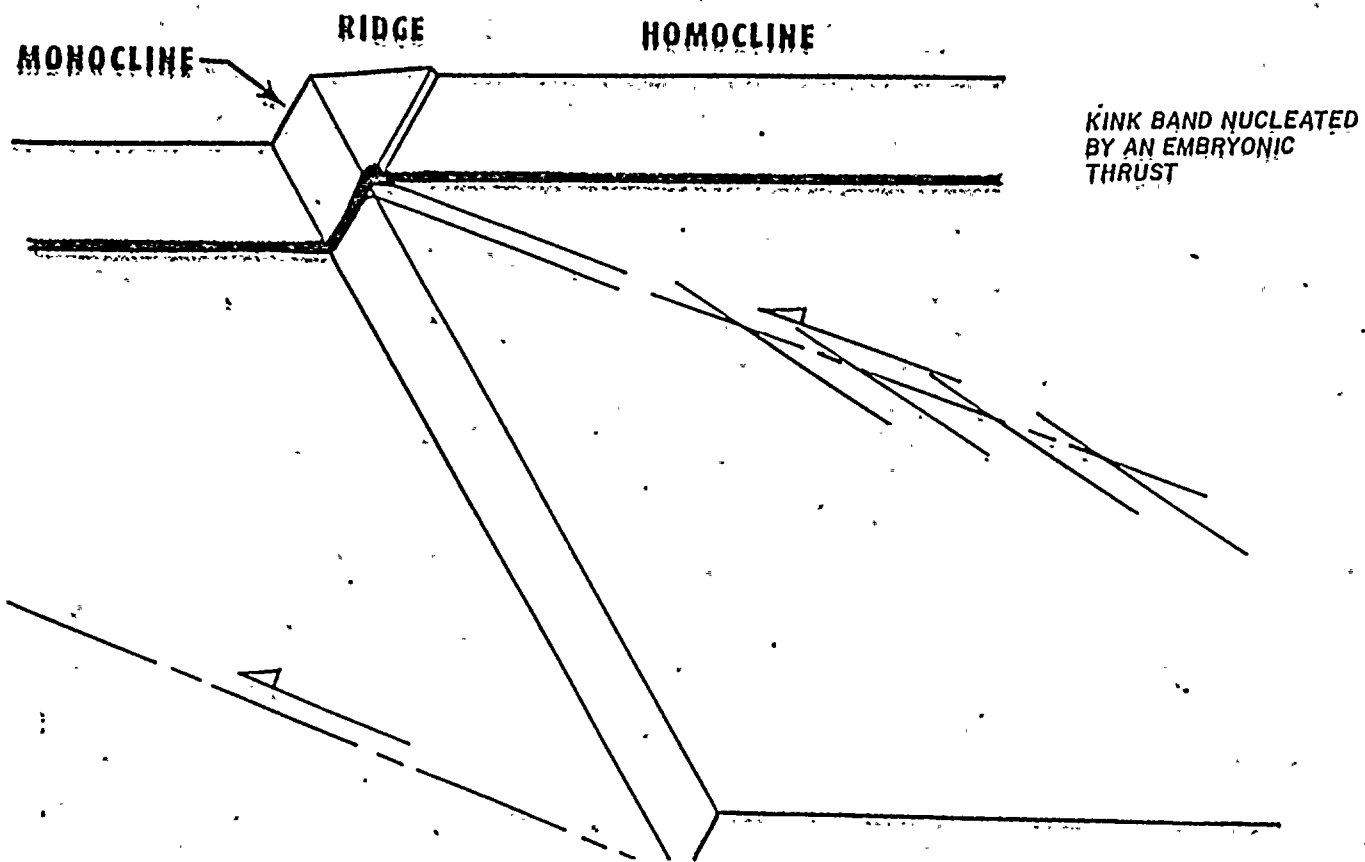


Stages in the development of the Goumois-S anticline.

Decollement, ramps, blind thrusts and kink folds in the Jura, from Laubscher (1977).



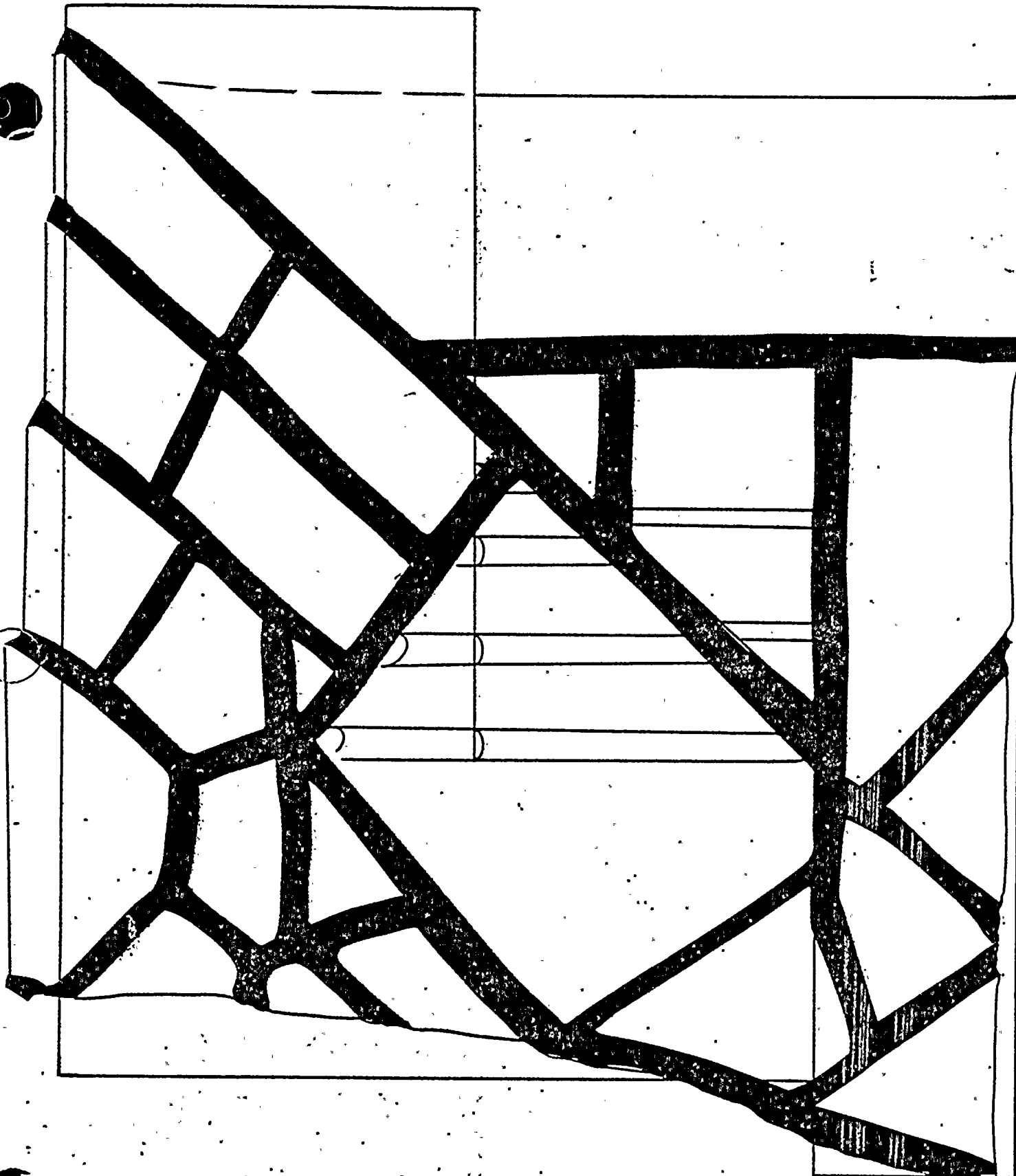
DISHARMONIC FOLDING  
ON A BLIND THRUST



KINK BAND NUCLEATED  
BY AN EMBRYONIC  
THRUST

Possible interpretations of the deep structure of Yakima folds.  
Figure 8a

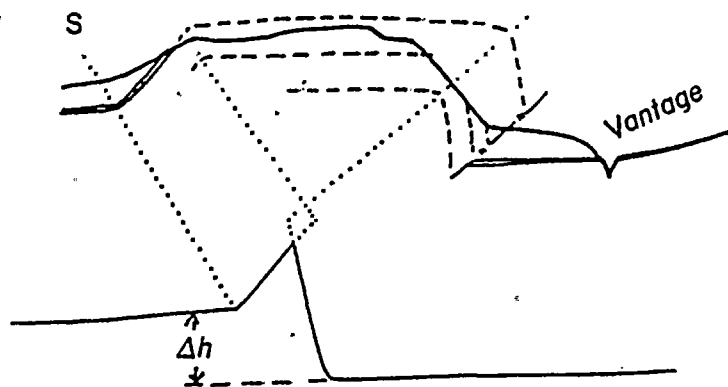




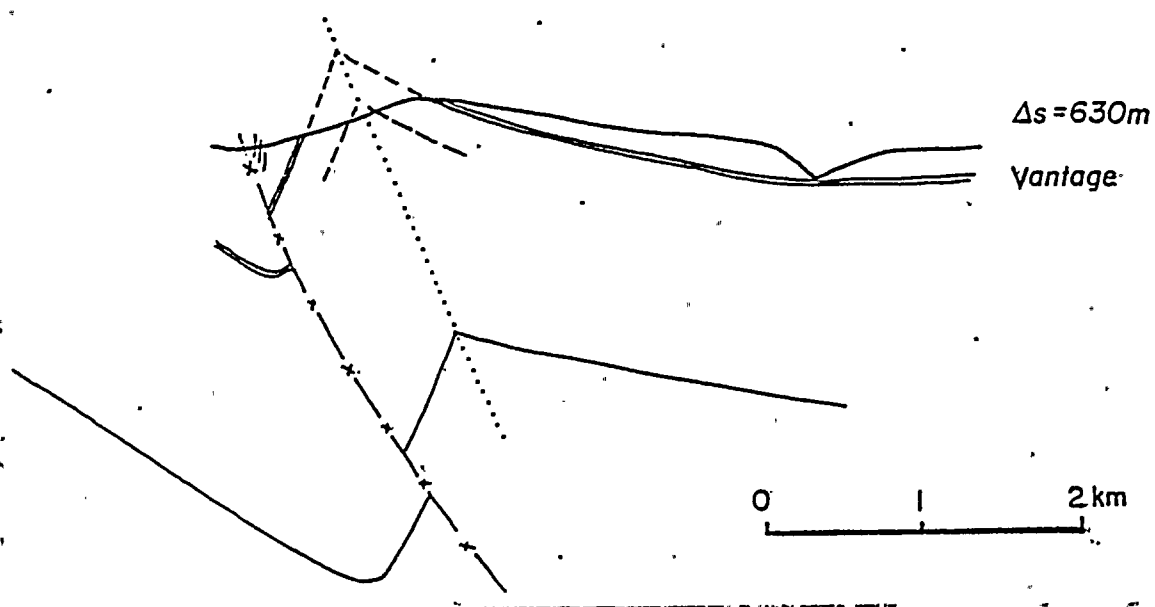
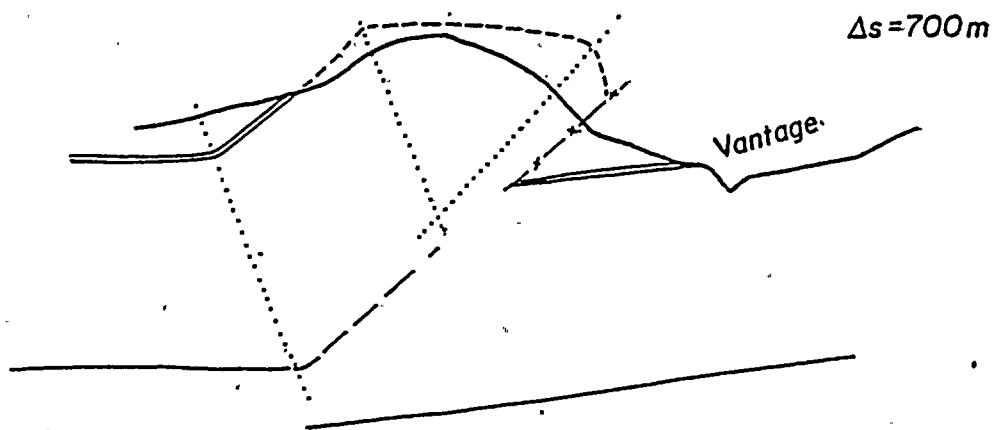
Kinematics of the Columbia Plateau and its surroundings,  
tentative concepts; compare Figs. 1(e), 2, 14.

Figure 9

5010-



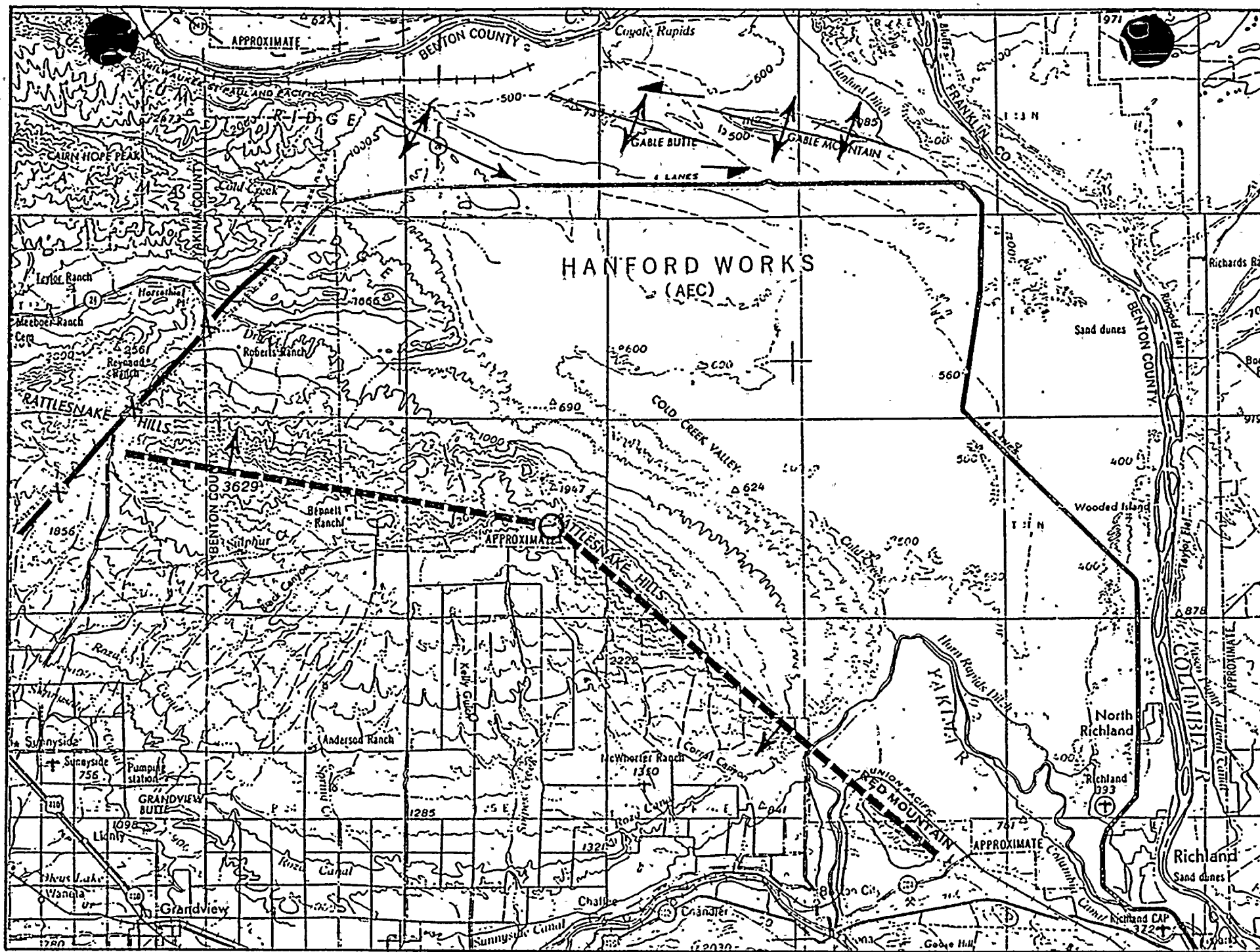
N  
 $\Delta s = 700\text{m}$   
 $\Delta h = 320\text{m}$   
 (ramping on a thrust  
 of  $25^\circ$  dip)



Estimates of compression in Umtanum Ridge, after Bentley (1977).  
 Adjusted from the original which is vertically exaggerated.

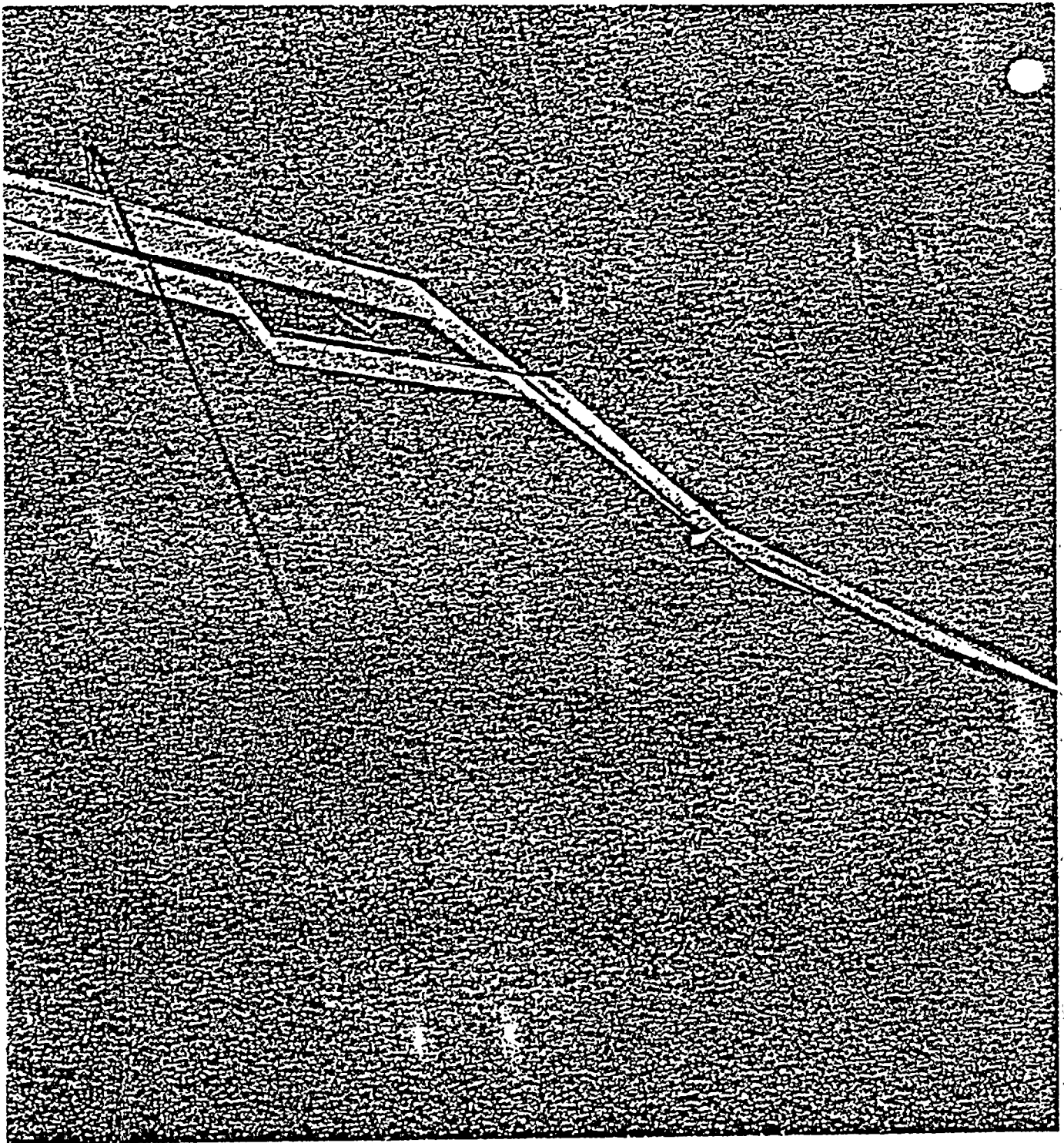






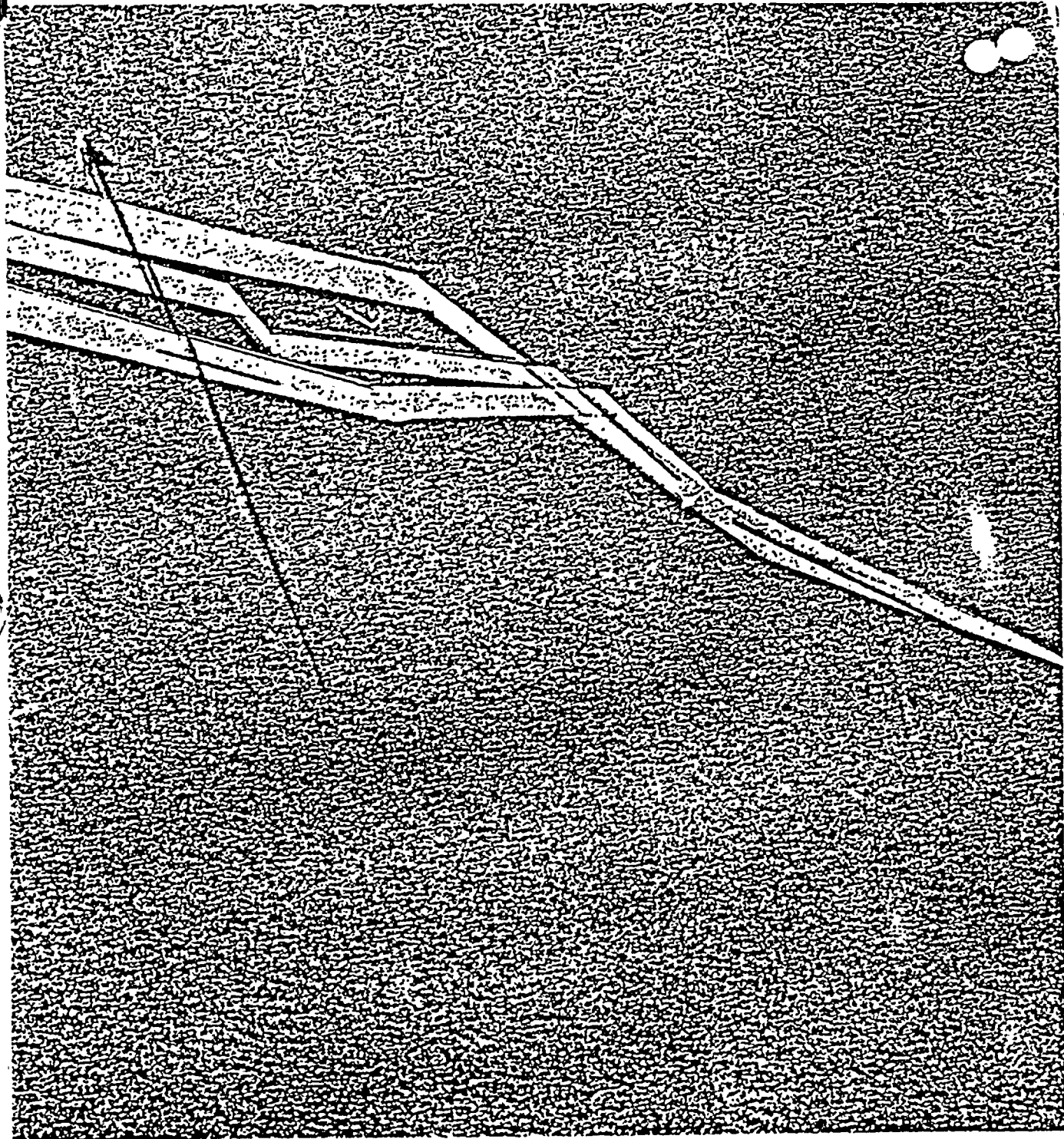
Axial plunge of Rattlesnake Hills.

[Figure 1]

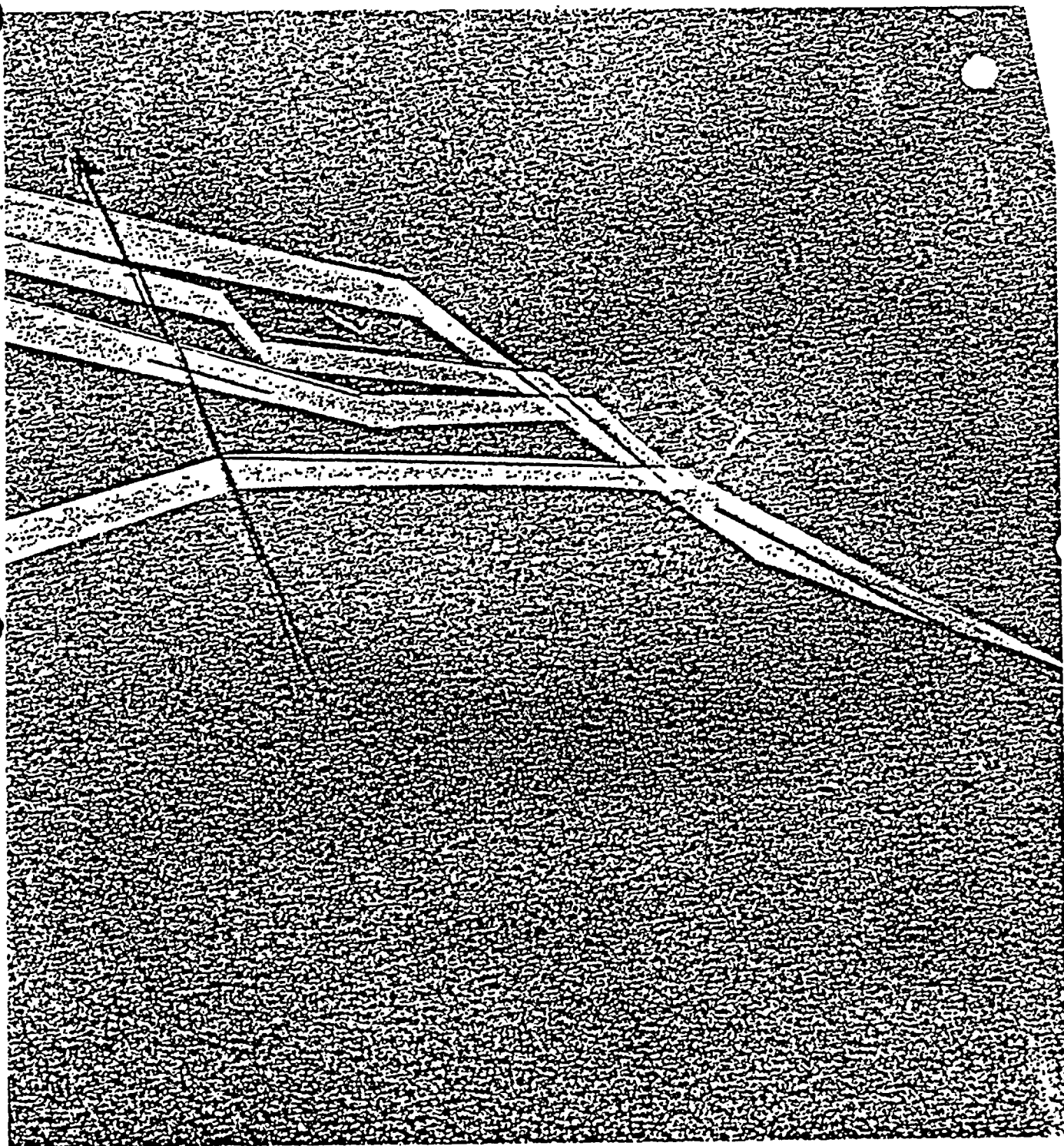


A cut-paper kinematic model of rigid-body Yakima tectonics.  
Figure 12a



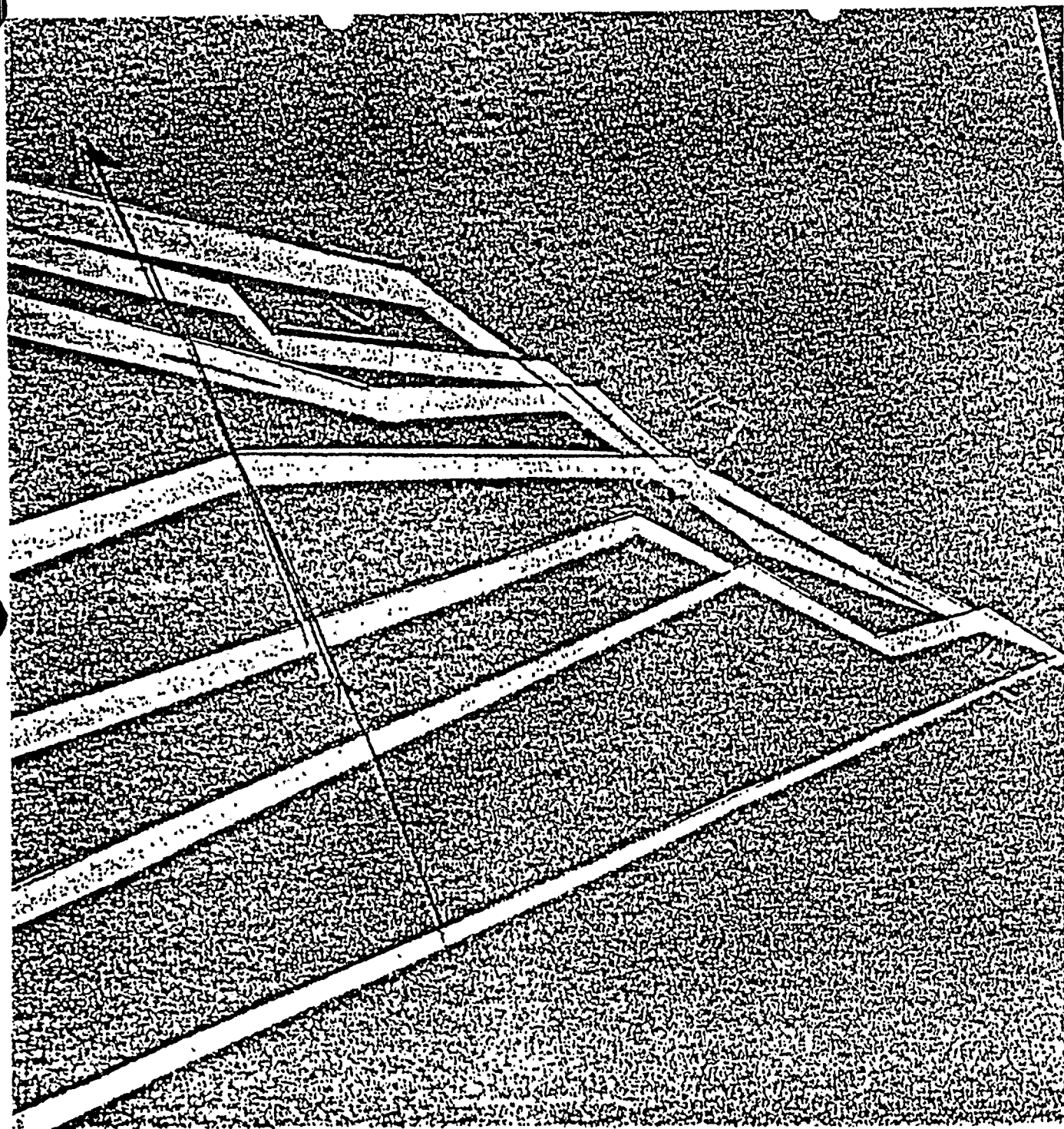


A cut-paper kinematic model of rigid-body Yakima tectonics.  
Figure 12b



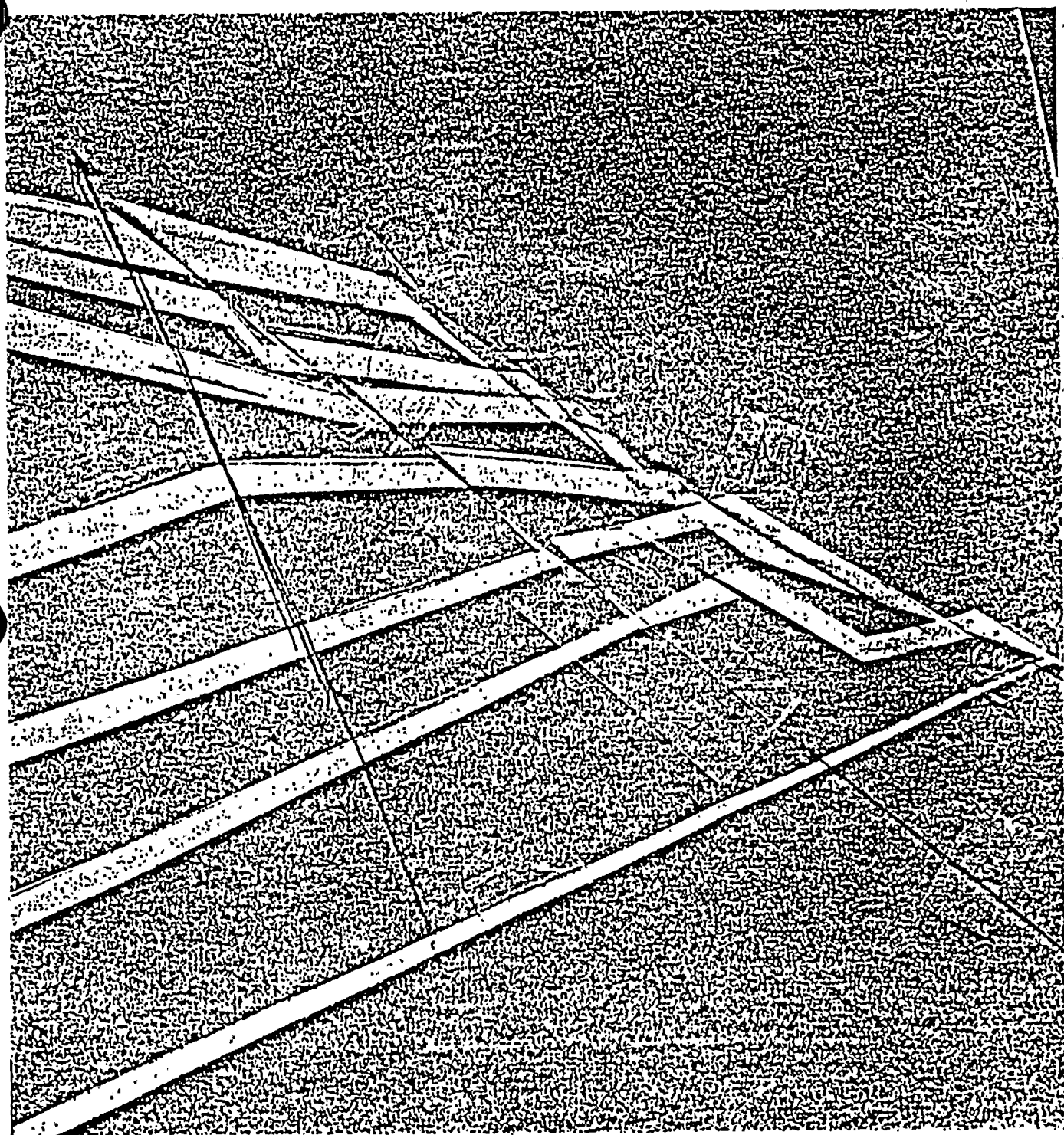
A cut-paper kinematic model of rigid-body Yakima tectonics.  
Figure 12c





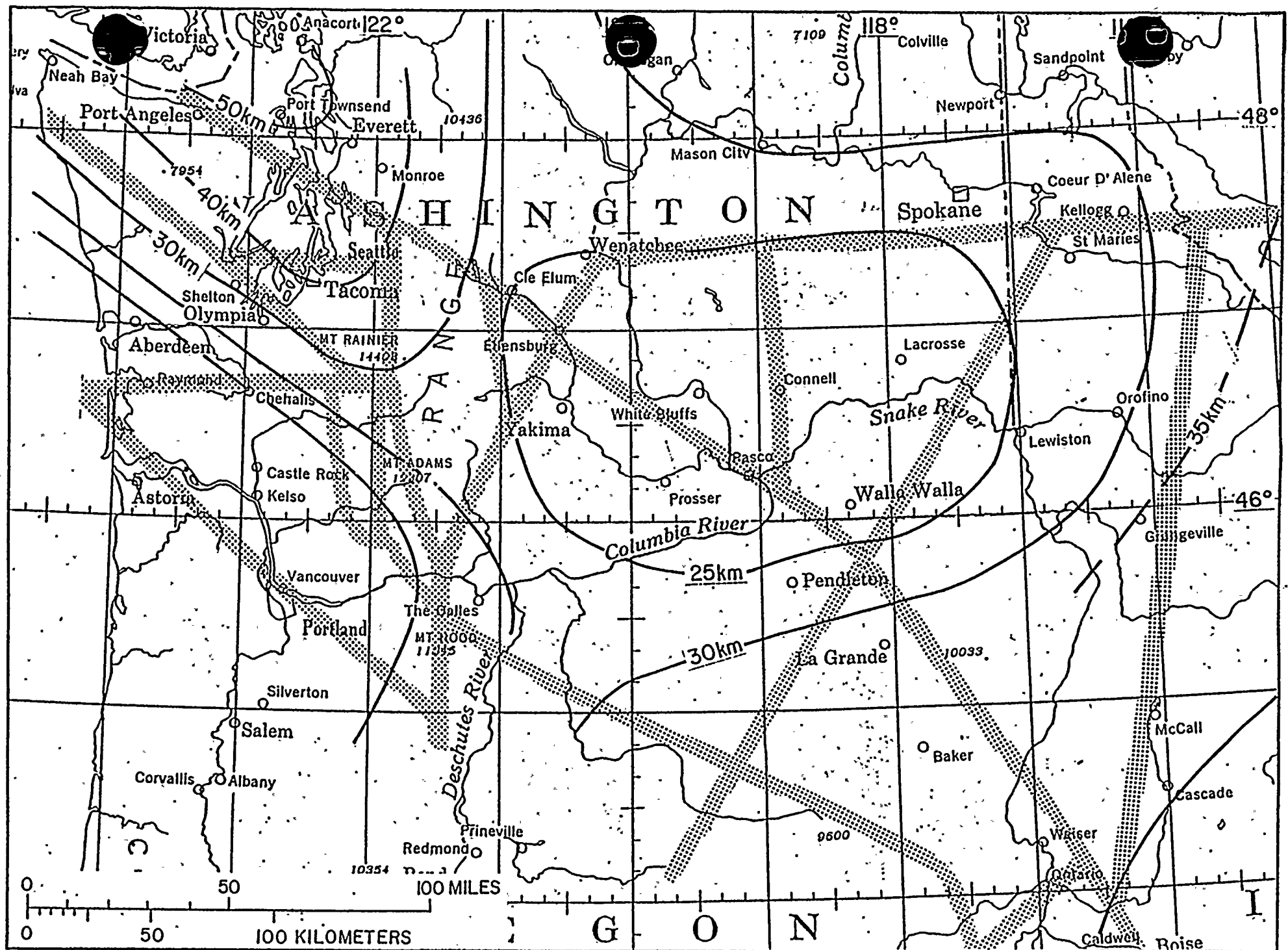
A cut-paper kinematic model of rigid-body Yakima tectonics.  
Figure 12d.





A cut-paper kinematic model of rigid-body Yakima tectonics.  
Figure 12e



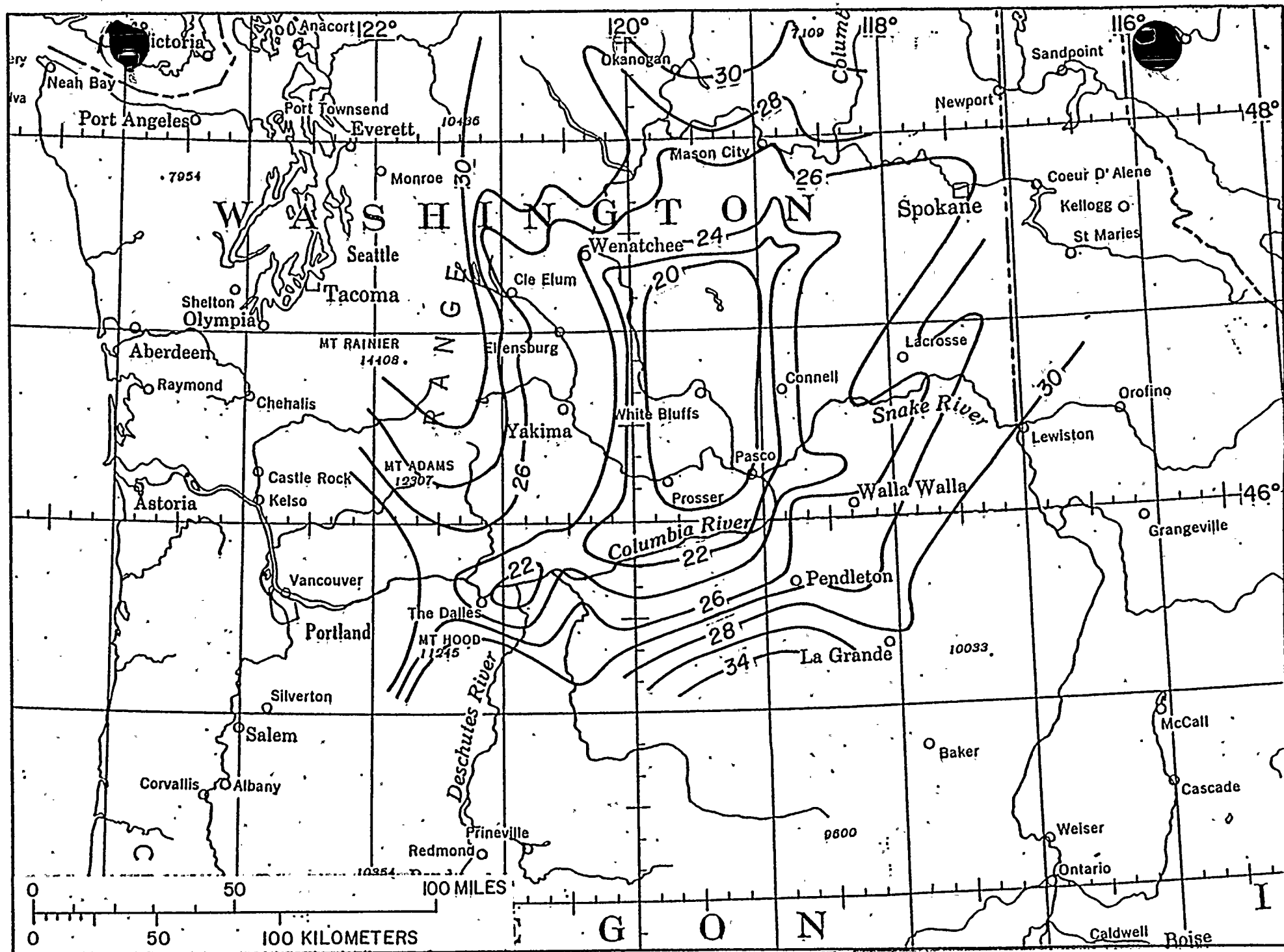


The IDOL block belt and regional crustal isopachs (after Smith 1978). Compare Fig. 17. Figure 13



FIGURES 2.5 O-14 THROUGH 2.5 O-16  
ARE CURRENTLY BEING PRINTED.

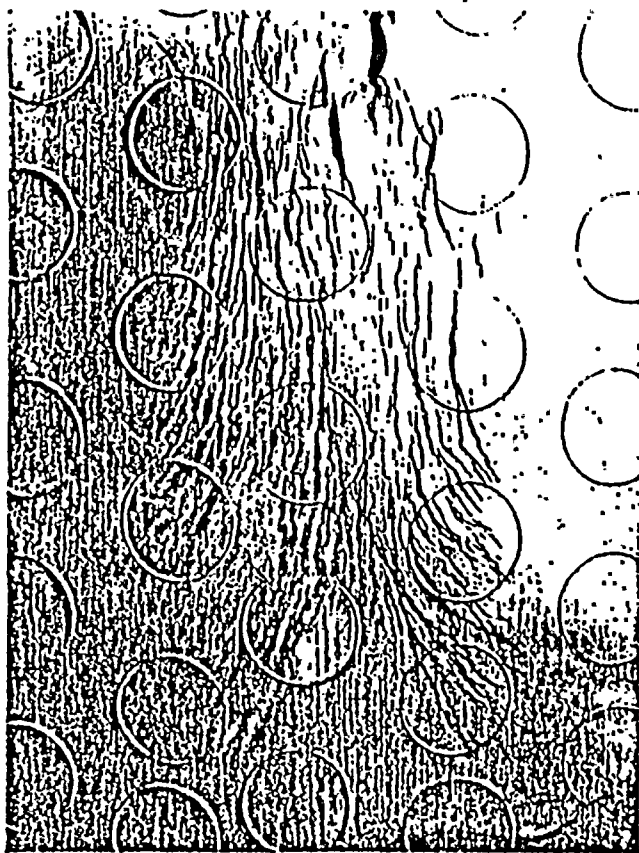




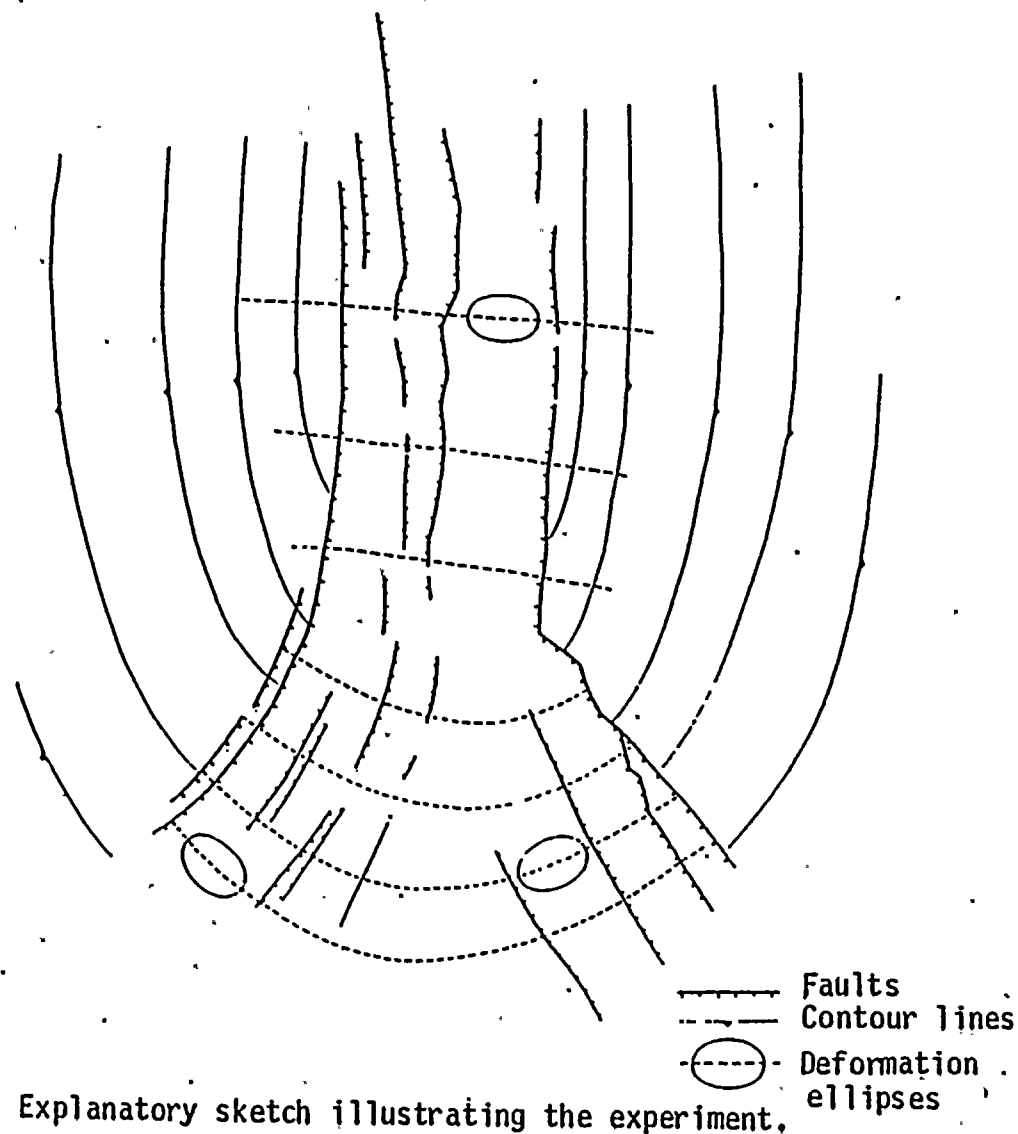
Crustal isopachs of the Columbia Plateau, estimated from seismic and gravity data. Figure 17

FIGURE 2.5 O-18

IS CURRENTLY BEING PRINTED.



Clay experiment of ellipsoidal domal uplift. Originally circular imprints are slightly deformed into ellipses.



Explanatory sketch illustrating the experiment.





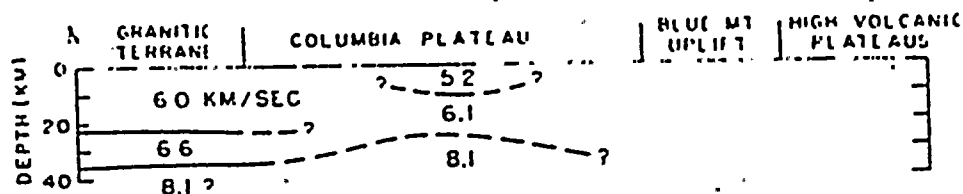
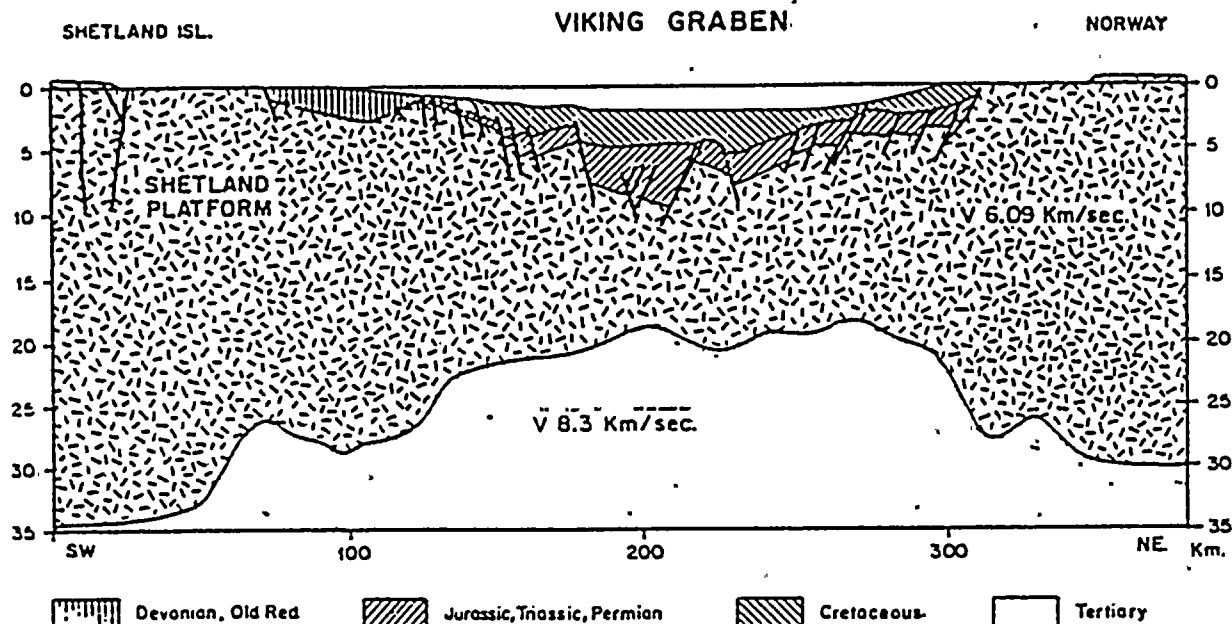


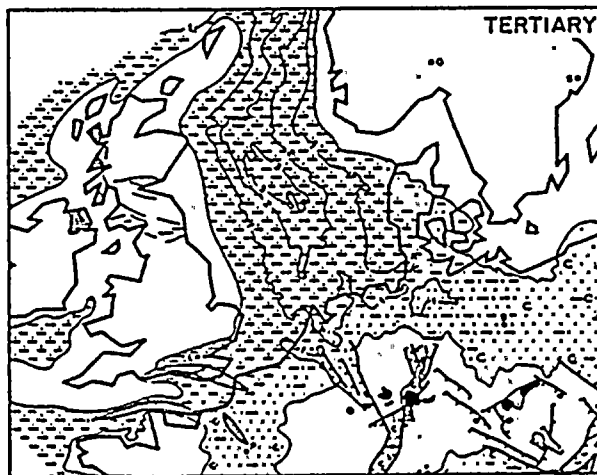
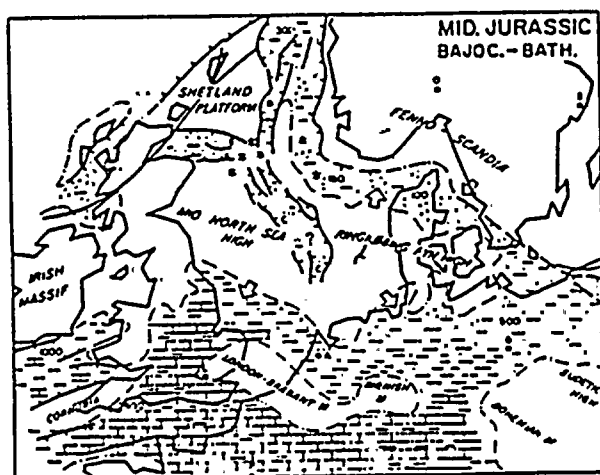
Figure 7-7. Crustal structure of the Columbia Plateau along north-south profile from the Canadian border into east Oregon (see Fig. 7-2). Structure within the Columbia Plateau is constrained by Eaton's analysis of quarry blasts recorded on the Paco Basin seismograph network. (J. P. Eaton, 1976, oral commun.). Upper plot is reduced traveltime curve of first arrivals ( $P_1$ ) on which variations in structure between granitic terrane of northern Washington and Columbia Plateau is based (Hill, 1972). Symbols O and H indicate the two types of instrumentation used to record the data (see Hill, 1972). From Hill (1978)



REFRACTION AND REFLECTION PROFILE ACROSS VIKING GRABEN.  
MODIFIED AFTER SOLLI 1976

Fig 7 Refraction-Reflection section northern North Sea.

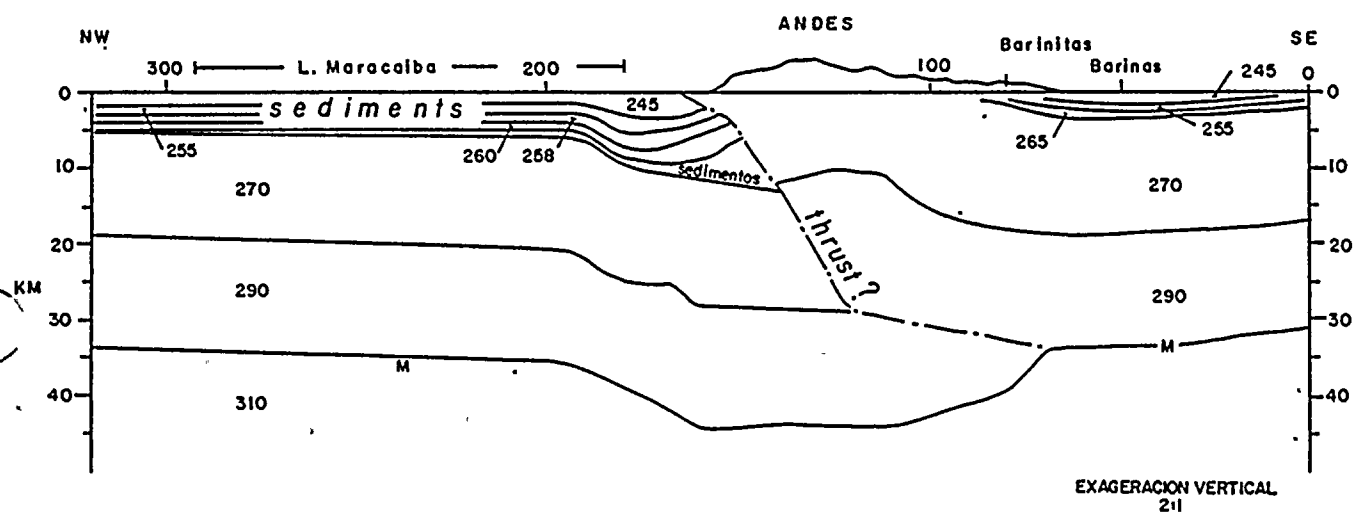
From Ziegler (1977)



Crustal thinning in graben areas (after Hill 1978, Ziegler 1977) and early doming followed by later subsidence (Ziegler 1977).

Figure 20

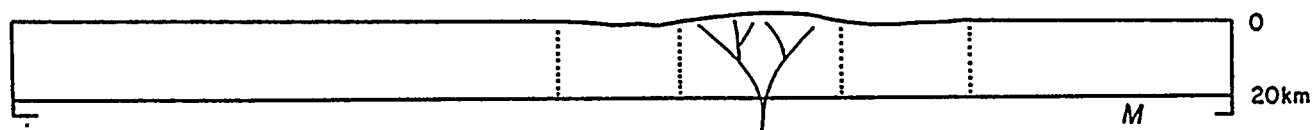




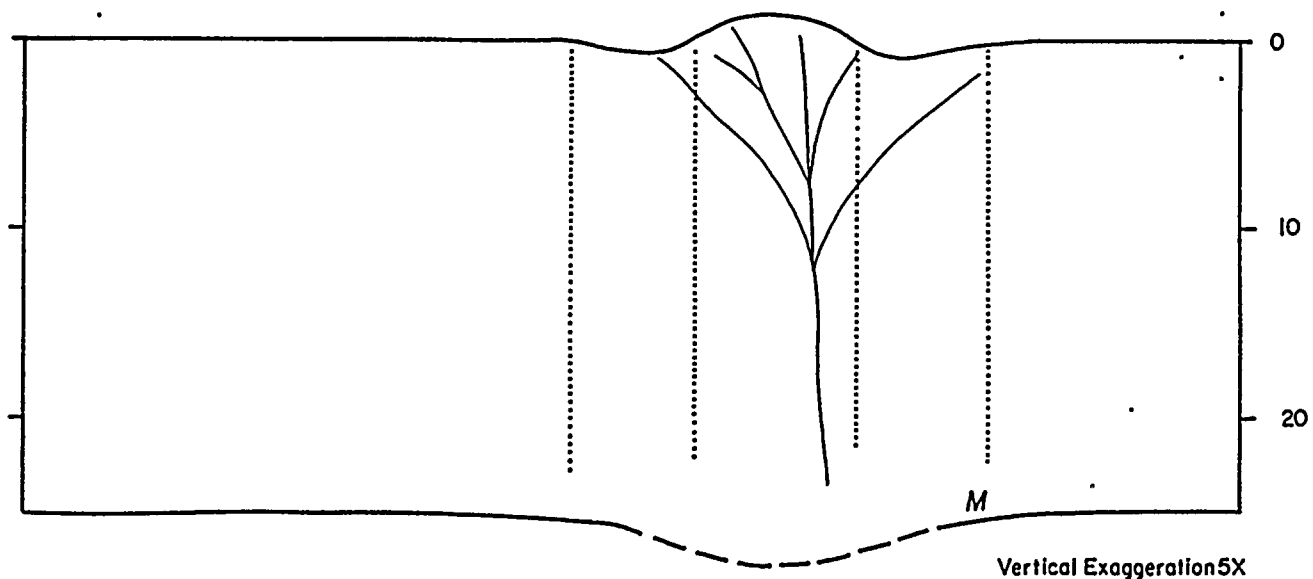
A deep crustal section through the Venezuelan Andes, after Wittke (1977).



CLEW

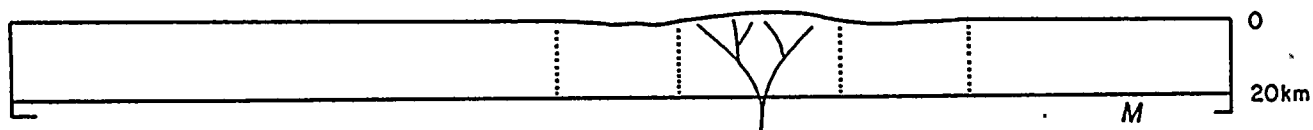


CLEW

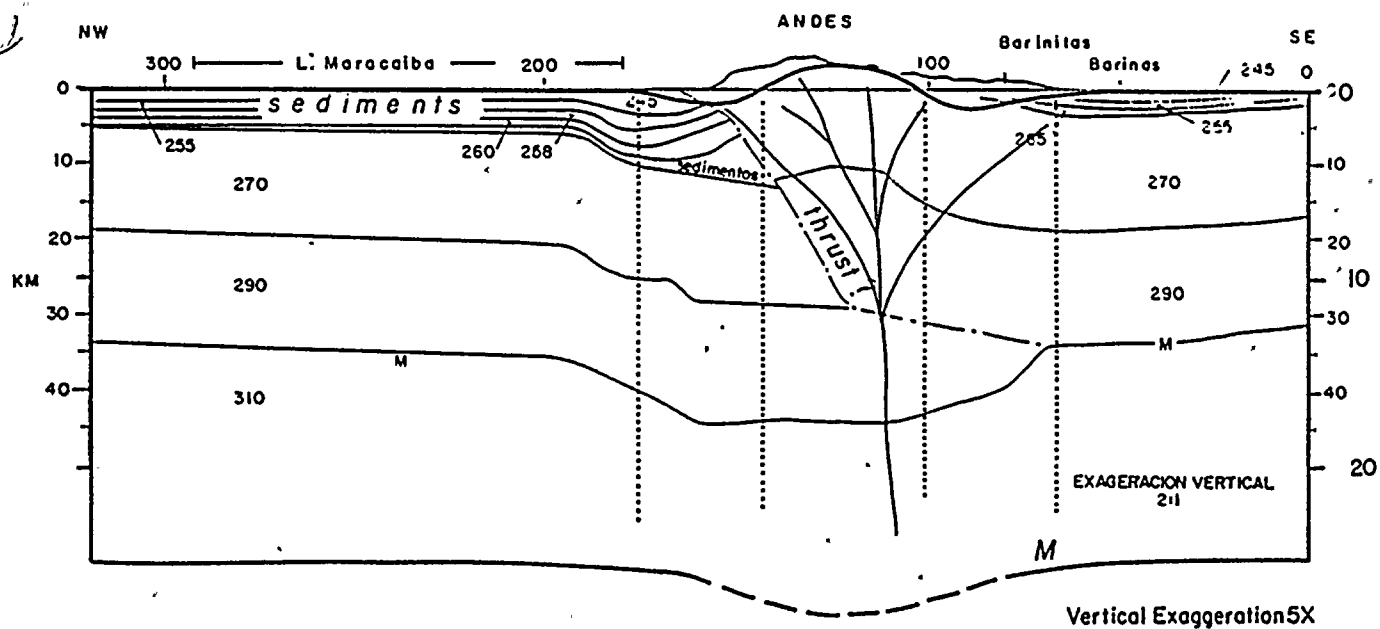


Clew, simplified as a small-amplitude crustal fold.  
Figure 22

CLEW



CLEW



A superposition of Figures 21 and 22.  
Figure 23

FIGURE 2.5 O-24

IS CURRENTLY BEING PRINTED.

